Safety in Mines Research Advisory Committee

Final Project Report

Stope Face Support Systems

A. Daehnke, L.M. Andersen, D. de Beer, G.S. Esterhuizen, F.J. Glisson, M.W. Grodner, T.O. Hagan, E.P. Jaku, J.S. Kuijpers, D.H. Kullmann, A.V. Peake, P.S. Piper, G.B. Quaye, N. Reddy, M.K.C. Roberts, J.K. Schweitzer, R.D. Stewart, T. Wallmach

Research agency: CSIR Mining Technology

Project number: GAP 330

Date: December 1998

Executive Summary

The primary output of SIMRAC Project GAP 330 is the determination of geotechnical areas across the gold and platinum mines to form the basis for future understanding of the rock mass behaviour around reefs where the hangingwall and footwall rock types differ, leading to improved site specific support systems for both static and dynamic loading. Nine sub-outputs contribute towards this objective, and a brief summary of the research methodologies, principal findings and salient conclusions follows.

Geotechnical areas of eight Witwatersrand and two Bushveld orebodies were delineated according to characteristics of the hangingwall and footwall strata. The compiled geotechnical area base maps provide an indication regarding the following rock engineering aspects which influence the performance of local and regional support: stope stability (especially hangingwall stability, fall of ground characteristics and closure rate), attitude and frequency of mining induced fracturing, seismicity, punching of support and pillar strength.

The support usage of the gold and platinum mines is quantified, and support practices categorised according to mine, shaft, reef, production, stoping width and depth. The support usage database is applied to assess the performance of existing support systems by means of appropriate accident analysis. Further work was done to maintain and expand the current accident database. Analysis thereof leads to important insights into the rockfall versus rockburst hazards associated with the various reefs, general and reef specific accident trends since 1990, the relative hazards related to accident location, and quantified fallout thicknesses to set support criteria.

Numerical models were used to investigate mechanisms leading to stope closure and the effect of support stiffness on hangingwall stability and keyblock dislocation. Further analytical models were developed to quantify stable hangingwall spans between adjacent support units. A detailed keyblock stability investigation has given new insights into zones of support influence, stable hangingwall spans, the effect of in-situ compressive hangingwall stresses, as well as various other parameters governing the interaction between support and the rock mass. The work has lead to the formulation of a site specific support design methodology which is based on (i) tributary area concepts to establish support resistance and energy absorption requirements, and (ii) stable hangingwall spans to quantify support spacing.

Extensive underground instrumentation has lead to an improved understanding of deformation mechanisms associated with mining the Carbon Leader Reef. A significant output of the instrumentation site are new insights into wave velocities of fractured hangingwall rock, which were found to be an order of magnitude lower than wave speeds in competent rock. The results have important implications for the quantification and understanding of rock dynamics, closure velocities and the design of effective rockburst resistant support systems. A novel seismic analysis relates the spatial and temporal distribution of seismicity to various geotechnical areas delineating the Vaal Reef.

Three groups of impediments (generic, geotechnical and mining related) to successful implementation of stope support systems were identified and assessed. The performance of 12 widely used elongate support types has been quantified. A rigorous elongate evaluation procedure is proposed, resulting in improved support design by using consistent elongate performance parameters with known support capabilities.

Acknowledgements

The authors would like to express their gratitude towards the Safety in Mines Research Advisory Committee (SIMRAC) for financial support of project GAP 330. The excellent cooperation of the personnel of the gold and platinum mines which have contributed towards this project, specifically Western Deeps Levels, Vaal Reefs and Elandsrand, is gratefully acknowledged.

Finally, the authors are indebted to A.J. Jager, M.K.C. Roberts, Dr T.O. Hagan and Dr S.M. Spottiswoode for their guidance and valuable technical contribution, as well as D. Breitenbach for editing this report.

Table of contents

List of figures

List of tables

Glossary of abbreviations and symbols

Abbreviations

BPM	Big Pebble Marker
DAU	data acquisition unit
DC	direct current
FOG	fall of ground
FW	footwall
GMM	Ground Motion Monitor
HW	hangingwall
PGE	platinum group elements
PSS	Portable Seismic System
RPM	Rustenburg Platinum Mines
UCS	uniaxial compressive strength
USM	Upper Shale Marker
VCR	Ventersdorp Contact Reef
WDL	Western Deep Levels

Symbols

A	tributary area
b	hangingwall beam thickness
E	Young's modulus
E'	effective rock modulus
$F(z)$	probability distribution
G	modulus of rigidity
g	acceleration due to gravity
h	downward hangingwall displacement during rockburst, layer thickness
l	stope span
M	seismic magnitude
M_o	seismic moment
n	sample size
ΔS	differential stress
V_E	volume of elastic convergence
$V_{I, II}$	frictional resistance at abutments
v	peak hangingwall velocity during rockburst
W	keyblock weight
α, β	orientation of hangingwall discontinuities
γ	gamma value
μ	coefficient of friction, population mean
ν	Poisson's ratio
ρ	density
σ	standard deviation
σ_x	compressive hangingwall stresses

Project overview

The Leon commission of Inquiry into Safety and Health in the Mining Industry correctly identified rockfalls and rockbursts as the major influence on the safety record of the South African gold and platinum mining industry. Stope support, with an annual value in excess of R 1,2 billion, is used extensively by the mining industry, in an attempt to stabilise the rockmass and reduce the rock related hazards associated with ore extraction.

Widely varying rock mass conditions and behaviour of the various reefs is attributed to varying rock types, rock strength and type of structures in the hangingwall and footwall. Combinations of these parameters delineate geotechnical areas, where the differing rock mass behaviour makes the support of stopes in any particular geotechnical area site specific.

SIMRAC Project GAP 330, *Stope Face Support System*, is a three-year project, managed and coordinated by the CSIR, Division of Mining Technology. The project aim is to delineate geotechnical areas and, by means of underground investigations and numerical models, gain insights into rock failure modes and the support interaction with a discontinuous rock mass, identify impediments to successful stope support implementation, and quantify the performance of elongates. Specifically, the primary output, as defined in the project proposal, is:

> *The determination of geotechnical areas across the gold and platinum mines will form the basis for future understanding of the rock mass behaviour around reefs where the hangingwall and footwall rock types differ, leading to improved site specific support systems for both static and dynamic loading.*

Nine enabling outputs have contributed towards this objective. These were defined in the project proposal as follows:

1. *Define geotechnical areas across the gold mining industry and the potential for the platinum mines on the basis of differing rock mass behaviour.*
2. *Assess performance of existing support systems within the different geotechnical areas by means of appropriate accident analysis.*
3. *Maintain and expand the current accident database.*
4. *By use of in-situ tests and numerical models, evaluate the rock mass / support interaction in the various geotechnical areas and at different depths.*
5. *Verify models by means of underground observations and measurements, including seismic analysis.*
6. *Further develop the stope support design methodology.*
7. *Identify and assess impediments to successful implementation of stope face support systems.*
8. *Assess the performance of elongate support currently in use in the mining industry.*
9. *Application of keyblock analysis techniques for stope support design.*

The report consists of ten main sections, in which the introduction, research methodology, results and conclusions of each of the enabling outputs is dealt with separately. The final section synthesises the main outcomes and new knowledge gained, and makes recommendations for further research work. For a brief overview and summary of the principal findings of this project, it is recommended that the reader focus his/her attention on the final section. Finally, a list of appendices provides detailed information of numerical and seismic analyses, as well as underground and laboratory measurements.

1 Delineate geotechnical areas on the basis of differing rock mass behaviour

1.1 Introduction

This study provides a detailed review on a variety of geotechnical environments, representing the most comprehensive study of this nature to date. Activities are subdivided into a) define geotechnical areas across the gold mining industry on the basis of differing rock mass behaviour, and b) establish the potential for defining geotechnical areas within the Bushveld Igneous Complex. The complex environments associated with the Witwatersrand and Bushveld mining operations require a careful consideration of geological, rock engineering and mining parameters when assessing the application of certain support types and support strategies. Experience has shown that the successful application of certain support types varies from mine to mine, depending on the characteristics of the footwall, hangingwall and reef horizons. To date the impact of these parameters on support strategies is not well defined.

Previously established geotechnical area maps have also been transformed in order to show hard and soft footwall and hangingwall lithologies by using the UCS of the respective lithologies as the critical parameter. The reefs which were investigated of the Witwatersrand, the Carbon Leader, Vaal Reef, Leader Reef, B-Reef, Big Pebble Marker, Witpan Reef, VS5, Ventersdorp Contact Reef (Figure 1.1.1), and for the Bushveld Complex the UG2 and the Merensky Reef. It was requested by GAPREAG representatives that Free State orebodies which were not referred to in the original proposal should also be investigated. In this report the orebodies are detailed in stratigraphic order.

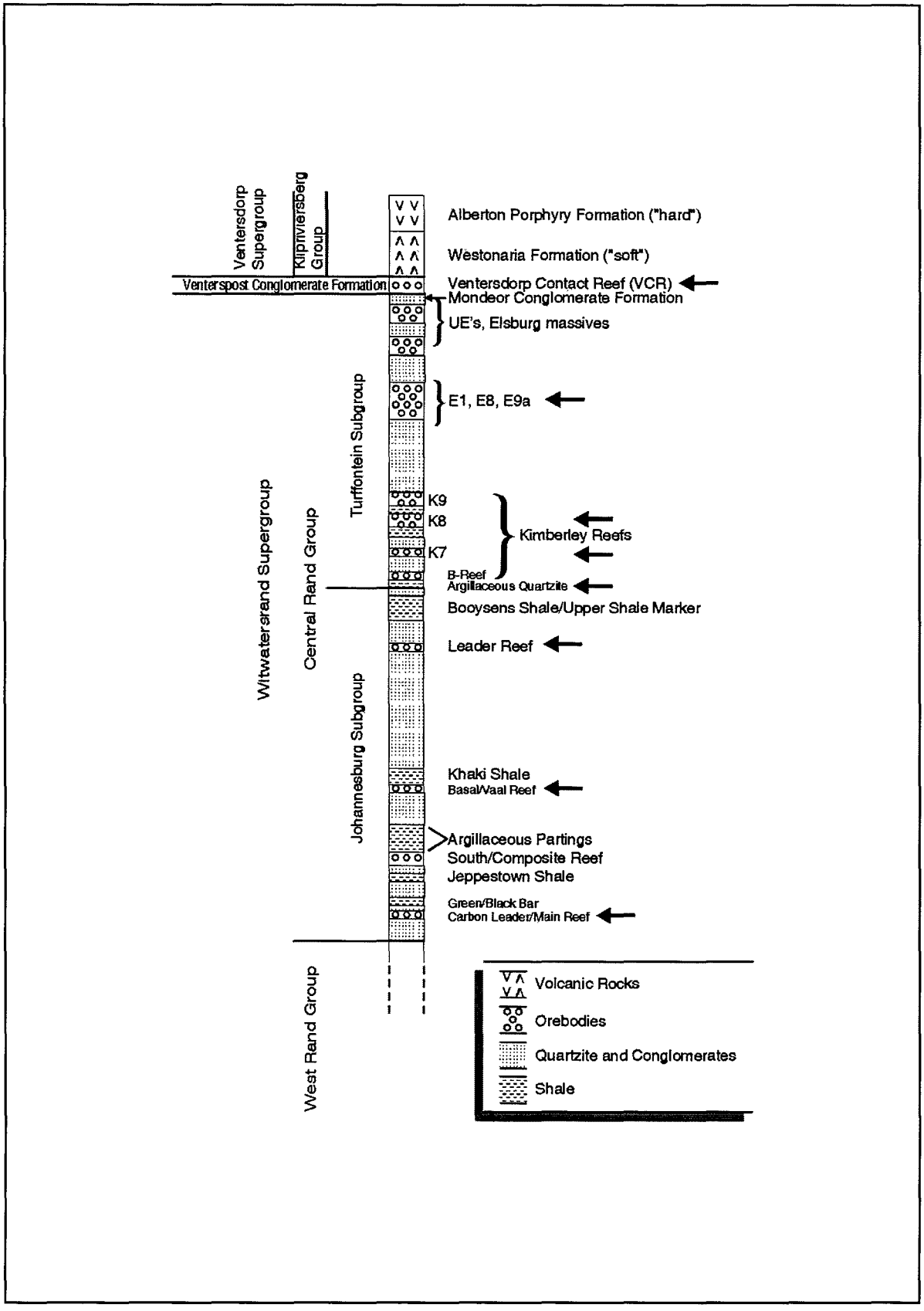

Figure 1.1.1 Idealised stratigraphic profile of the Central Rand Group. Arrows mark orebodies for which the geotechnical environment has been delineated.

1.2 Previous work

The Witwatersrand gold reefs form part of a sequence predominantly comprised of argillaceous and siliceous quartzites, intercalated with shales, grits and conglomerates (e.g. Minter et al., 1986; Antrobus et al., 1986; Engelbrecht et al., 1986; Tucker and Viljoen, 1986) that formed more than 2800 Ma ago. Associated with these sedimentary units are a great variability of rock engineering properties such as uniaxial compressive strength values (UCS), Young's moduli and Poisson's ratios (e.g. Gay and Jager, 1986; Johnson and Schweitzer, 1996; Schweitzer and Johnson, 1997). These variations in rock engineering properties exert significant impact on rock mass behaviour in deep and ultra-deep mining operations (e.g. Potgieter and Roering, 1984; Johnson and Schweitzer, 1996; Roberts et al., 1994, 1997; Schweitzer and Berlenbach 1996, 1997) and are, therefore, also considered during the establishment of geotechnical area maps.

The Bushveld Igneous Complex intruded into sedimentary rocks of the Transvaal Supergroup. It is the world's largest chromitite and platinum depository. An area of approximately 300 000 km^2 is occupied by rocks of the Bushveld Complex, with the total sequence having a thickness of about 15 km. Four units are defined: the Rustenburg Layered Suite, the Rashoop Granophyre Suite (SACS, 1980), and the volcanic suite of the Rooiberg Group (Schweitzer and Hatton, 1995; Hatton and Schweitzer, 1995). The major concern of this study, with regard to the Bushveld Complex, are the platiniferous UG2 and Merensky Reefs of the Rustenburg Layered Suite. The UG2, a chromitite band, has an average width of 1,2 – 1,5 m, and is mined at several mines, which are situated in the western compartment of the Rustenburg Layered Suite. The Merensky Reef is generally mined at a stoping width of 1 m. This orebody is also extracted in the western lobe of the Bushveld Complex and in the eastern (Lebowa Platinum Mine) and Potgietersrus (Potgietersrus Platinum Mine) lobes. More detailed accounts of the previous work will be presented in the following discussions in establishing geotechnical areas for the individual reefs. In summary, however, it is concluded that prior to the beginning of this project concerted efforts of various rock mechanics and geological disciplines have been rare, if not completely absent. This is especially true for the platiniferous orebodies.

1.3 Methodology for defining geotechnical areas

The issue of geotechnical areas has drawn varying opinions from across the South African gold and platinum mining industry. Many mine rock mechanics personnel delineate such areas as to include similar rock mass behaviour or areas where the same support strategies are applicable. The GAP 330 project considers a geotechnical area as an area potentially exhibiting a distinct rock mass behaviour. The GAP 416 project was later assigned the task of establishing a methodology for defining geotechnical areas across the gold and platinum mines so as to provide a common understanding. This methodology is briefly summarized in the following paragraphs.

It is suggested that regional geotechnical areas should be delineated before the onset of mining activities. A recent mining survey revealed that most mine rock mechanics personnel are of the view that a maximum number of 10 geotechnical areas should be defined. Input parameters are either one or various combinations of information about the orebody geometry, depth, stratigraphy, major geological features and regional hydrology. These are collected by means of geophysical techniques, borehole data and historical records considering known areas of similar geological settings. Activities such as the identification of a mining method, mining layout including the need for a type of regional support and mining sequence are then facilitated. Once these decisions are made, it is possible to form an idea about the possible regional, rock mass behaviour. This leads to regional mine design strategies and can be referred to as a regional geotechnical area.

As soon as mining commences, detailed information about the rock mass characteristics are available, falling into the following major categories:

- Orebody information,
- Stratigraphy,
- Discontinuities,
- Stress environment, and
- Production parameters.

GAP416 provides details with respect to further subdivisions of these categories.

The above categories are further subdivided into fixed and variable parameters. The fixed, or geological parameters, refer to those that exist prior to mining activities, whereas the variable parameters involve those imposed on the rock mass by the mining operation.

The above methodology suggests that fixed and variable criteria have to be considered for the compilation of geotechnical areas. This contribution, however, concentrates on the characterisation of the fixed geological parameters, and the term "geotechnical", when applied, is used in this sense. Special attention is given to the rock type assemblage in the close proximity to current and potential excavations. Thus provisional regional geotechnical area maps were compiled for eight Witwatersrand orebodies:

Free State: BPM, Leader Reef, B REEF, VS5 and WITPAN
West Rand / Carletonville / Klerksdorp: VCR
Carletonville: Carbon Leader
Klerksdorp: Vaal Reef

For these, the immediate footwall/hangingwall rock type assemblage and major hangingwall partings and other discontinuities, such as faults, joints and dykes, were delineated. The orebodies of the Orange Free goldfield were selected because they, currently or potentially, will contribute significantly to South Africa's gold production (Table 1.3.1). Orebodies that have been mined extensively, and that are predominantly mined as remnants, such as the Basal Reef, have been excluded.

Once the rock type environment was delineated, the maps were transformed to feature "hard" and "soft" footwall and hangingwall lithologies, using the uniaxial compressive strength (UCS) as a critical geotechnical parameter. This transformation was performed to identify potential areas where footwall and/or hangingwall punching of support may occur.

Table 1.3.1 Production figures given in "mined square metres" for economically important reefs of the Free State (status 1995; B. Northropp, pers. communication, 1995).

MINE	KIMBERLEY'S	ELSBURG'S	BASAL	LEADER	TOTAL
Beatrix	502 279				502 279
Freddies	73 227		661 780	51 367	786 374
Harmony	88 461		160 893	883 069	1 132 423
HJ Joel	155 350				155 350
Loraine	51 099	81 759	207 802		340 660
Pres. Brand	36 218		280 976	92 408	409 602
Pres. Steyn	85 623	46 608	413 845	45 276	591 352
Saaiplaas	57 076		489 398		546 474
St Helena			124 051	9 378	133 429
Unisel			178 316		178 316
W Holdings	1 643		609 354	67 044	678 041
Total	**1 050 976**	**128 367**	**3 126 415**	**1 148 542**	**5 454 300**
Percentage	**19.27**	**2.35**	**57.32**	**21.06**	

1.4 Geotechnical areas

In order to define "hard" and "soft" footwall and hangingwall lithologies, existing uniaxial compressive strength (UCS) values for the various rock types were compiled. Traditionally, shales and argillaceous lithologies are considered as "soft" whereas siliceous quartzites, for example, are regarded as "hard". Based on UCS data from rocks associated with the Ventersdop Contact Reef, which are presented as an example (Table 1.4.1, Figure 1.4.1), a value of approximately 200 MPa is proposed as a cut-off value between "hard" and "soft" lithologies. This also groups the various Ventersdorp lava types into "hard" (Alberton Formation) and "soft" (Westonaria Formation), and classifies the Jeppestown Shales and Mondeor Conglomerates as "soft". Figure 1.4.1 also displays the spread of the various rock strengths with the highest, lowest and average value of the rock strength for a variety of rock types. Although some overlap occurs, the "hard" and "soft" rock types can be grouped into being harder or softer than 200 MPa.

Mining induced fracture patterns may potentially be related to the above classification. Figures 1.4.2a to d show examples of fracture patterns of the four geotechnical areas described above. Note that the predicted inflection points and fracture densities change as a function of rock strength or hardness. In the case of different footwall and hangingwall lithologies (e.g. hard/soft) the inflection points generally lie in the soft lithologies. It is also noteworthy that the fracture densities increase with rock strength.

Regional borehole information, around the Bushveld Complex, is used to pinpoint the potential variability of footwall and hangingwall rock types of the UG2 and Merensky Reef. As the rock type has an essential influence on the rock mass behaviour, it is apparent that this information,

particularly on a more refined local or mine scale, contributes to defining stope support systems requirements and strategies. A detailed description of the individual reefs together with their geotechnical setting and assessment thereof is provided in the relevant subsections.

Table 1.4.1 Average uniaxial compressive strength values with number of measurements in brackets (after Roberts et al., 1997).

MINE	FORMATION	STRIKE DIRECTION	DIP DIRECTIOIN	PERPEND. DIRECTION
DEELKRAAL	Hard Lava DE	241 ± 32 (3)	NO TEST	NO TEST
	Hard Lava DW	252 ± 19 (3)	NO TEST	NO TEST
	Hard Lava	217 ± 40 (3)	237 ± 22 (4)	191 ± (3)
EAST DRIE	Hard Lava ED2	296 ± 51 (3)	171 ± 62 (3)	215 ± 52 (3)
KLOOF	Hard Lava K3	450 ± 234 (3)	577 ± 66 (3)	454 ± 243 (3)
	Hard Lava K8A	206 (1)	N/A	212 ± 30 (3)
	Hard Lava K8B	98 (1)	186 (1)	167 (1)
WEST DRIE	Hard Lava WD3	222 (1)	192 ± 10 (3)	214 (1)
WEST DEEP LEV	Hard Lava WDLHW		233 ± 35 (3)	
KLOOF	Soft Lava K6	174 ± 16 (3)	161 ± 20 (3)	177 ± 11 (3)
EAST DRIE	Soft Lava ED3	150 ± 13 (3)	82 ± 23 (3)	114 ± 27 (3)
LIBANON	Soft Lava LB1	175 ± 56 (3)	176 ± 24 (3)	204 ± 29 (3)
EAST DRIE	Jepp. Shale ED1	119 ± 28 (3)	96 ± 34 (3)	160 ± 23 (3)
WEST DRIE	Jepp. Shale WD1	N/A	153 ± 52 (2)	252 ± 2 (2)
KLOOF	Transit. Shale K2	196 ± 86 (2)	217 ± 50 (3)	203 ± 69 (3)
KLOOF	Booy. Shale K5	128 ± 20 (3)	155 ± 24 (3)	150 ± 45 (3)
LEEUDOORN	Booy. Shale LEE2	119 ± 8 (3)	102 ± 7 (3)	101 ± 24 (3)
LIBANON	Booy. Shale LB2	215 ± 5 (2)	145 (1)	125 (1)
KLOOF	Elsburg Qtz K4	296 ± 8 (3)	250 ± 22 (3)	255 ± 23 (3)
	Elsburg Qtz K7	286 (1)	333 (1)	221 (1)
LEEUDOORN	Elsburg Qtz LEE2	N/A	N/A	225 ± 25 (2)
	Elsburg Qtz LEE5	N/A	221 ± 48 (3)	N/A
WEST DEEP LEV	Elsburg Qtz WDLFW	173 ± 11 (3)		
DEELKRAAL	Mond. Cong. D1	274 (1)	181 (1)	261 ± 6 (2)
	Mond. Cong. D1A	171 ± 28 (2)	151 ± 52 (2)	114 ± 43 (2)

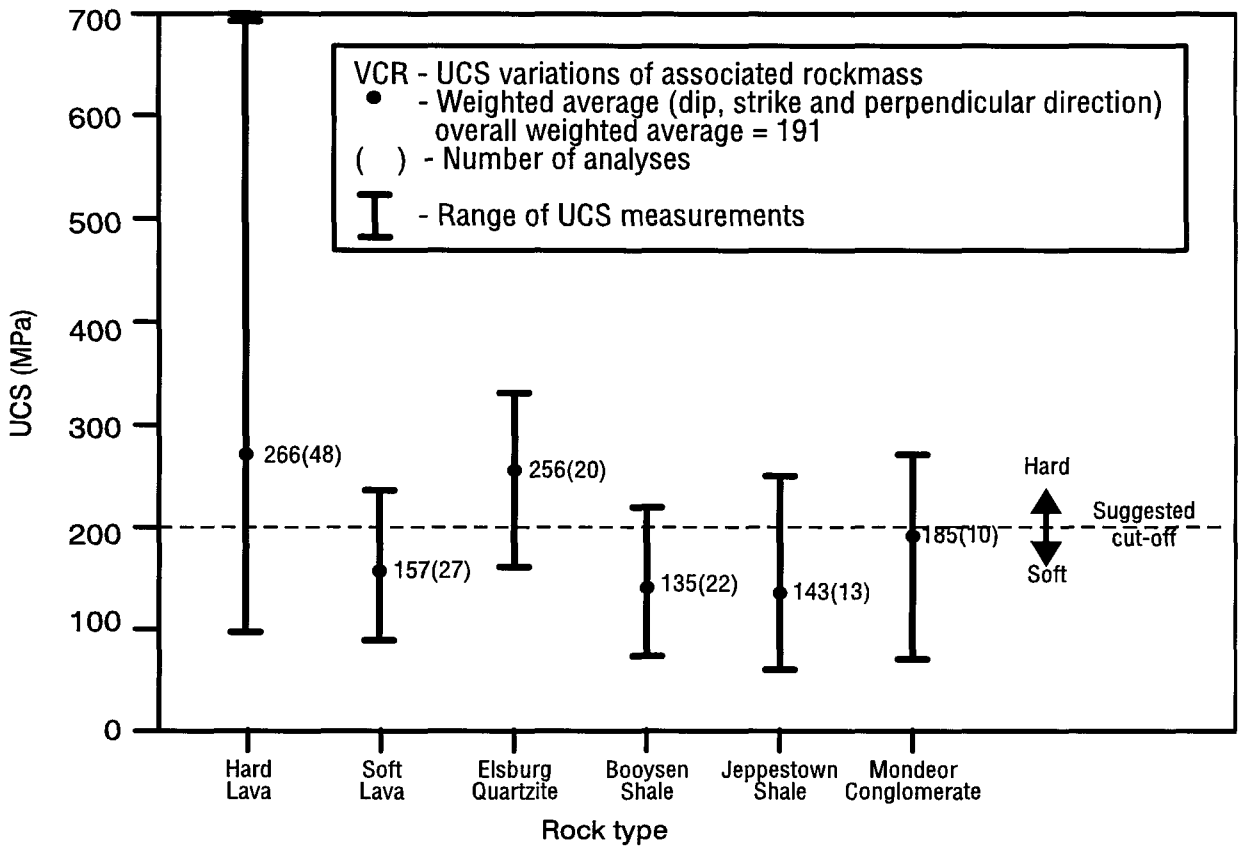

Figure 1.4.1 UCS variations of lithologies associated with the VCR. Data are from Table 1.4.1.

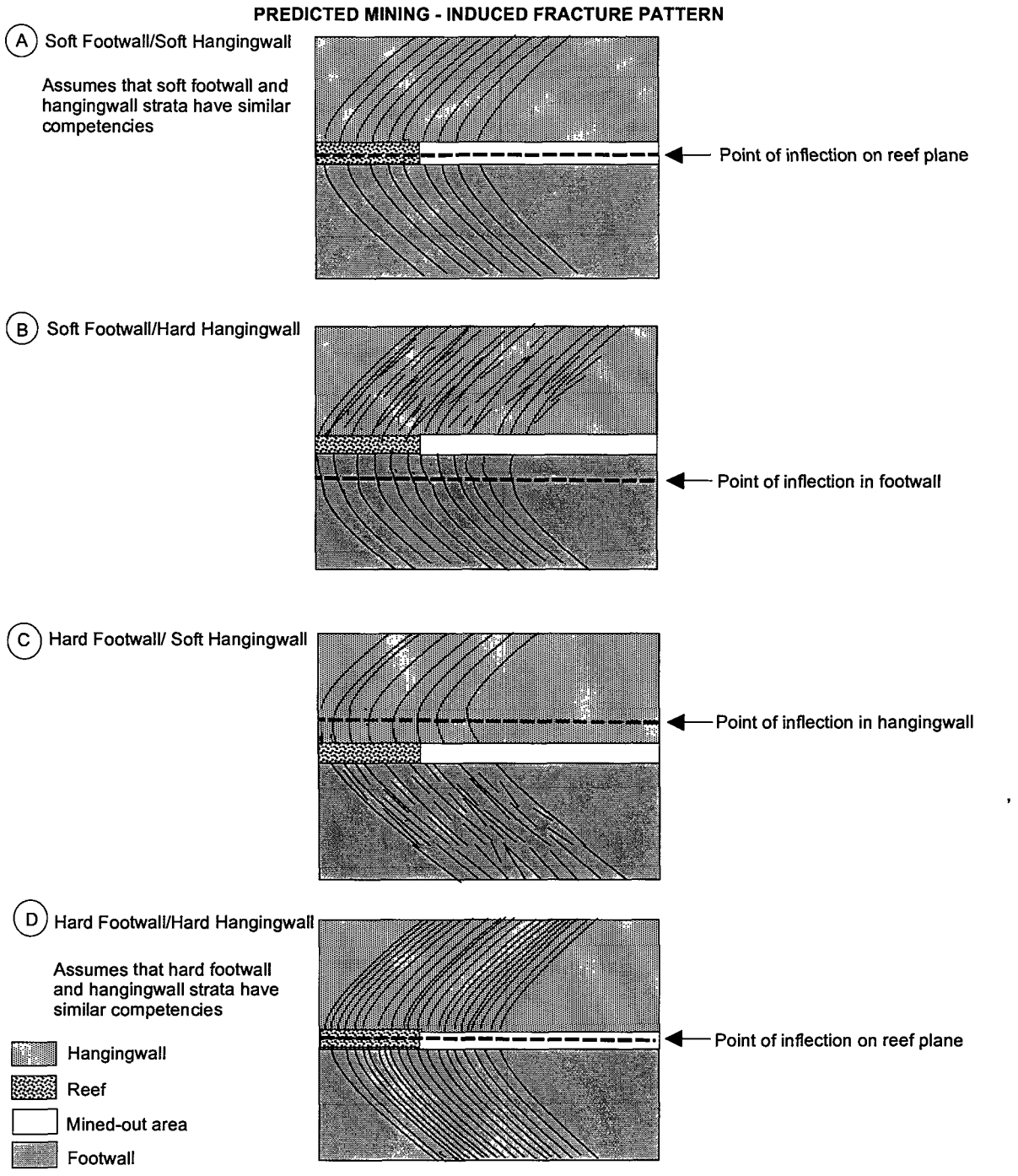

Figures 1.4.2 a-d ***Predicted mining-induced fracture pattern in various footwall and hangingwall lithologies. Note that the point of inflection appears in the soft lithology. The fracture frequency increases with the competency of the rock type.***

1.4.1 Witwatersrand basin

Geological features (see Schweitzer and Johnson, 1997 for a review) significantly influence the rock mass behaviour associated with the economic reef horizons of the Witwatersrand Basin. Features can be classified into primary (e.g. rock type, bedding planes and other sedimentary structures, reef geometry) and secondary structures (e.g. faults, joints, dykes, extension gashes, shear fabrics, metamorphic features). These parameters vary widely, both laterally and vertically, influencing mine safety, support strategies and mine layouts.

Due to the depletion of shallow depth deposits (Sanders et al., 1994; Tainton, 1994), gold producers in South Africa also now consider the mining of ultra deep deposits (i.e. 3500 - 5000 m; Schweitzer and Johnson, 1997). At these depths rockburst related fatalities increase significantly (Gurtunca and Gay, 1993; Roberts et al., 1994) and the influence of geological features on the rockmass behaviour is likely to become even more pronounced. Detailed geological studies of the ore deposits therefore become even more important (Gay and Jager, 1986). For example, rock composition (an argillaceous (soft) vs a siliceous (hard) quartzite) may represent an indicator for burst proneness. Other examples are seismic events and rockbursts which occur due to the change of the prevailing stress field around a dyke or fault, as the result of mining in its proximity (Lightfoot et al., 1996).

1.4.1.1 Johannesburg subgroup

Randfontein Formation

The Randfontein Formation constitutes the lowermost formation of the Central Rand Group (Figure 1.1.1) and the lower half of the Johannesburg Subgroup of the Witwatersrand Supergroup. It rests unconformably on the upper members of the Jeppestown Formation (West Rand Group) and is overlain by the basal conglomerate member of the Krugersdorp Formation. In the Carletonville Goldfield, the Randfontein formation attains a thickness of 550 m. It incorporates the important economic horizons of the Carbon Leader and the Main Reef, of which the former will be considered in the following sections.

A detailed discussion on the geology of the Carletonville Goldfield and its economic reef horizons is provided by Engelbrecht et al. (1986).

The Carbon Leader

Geotechnical Environment of the Carbon Leader

The Carbon Leader (Figure 1.1.1) unconformably overlies a complex quartzite/conglomerate sequence containing multiple partings (Figure 1.4.3). As a general rule the footwall becomes increasingly more argillaceous towards the south (Figure 1.4.4), the deeper areas of mining (Figure 1.4.5). The North Leader subcrops against the Carbon Leader in the most northern part of the goldfield (Figure 1.4.5). Presumably these competency contrasts influence the fracture pattern, but further investigations are required to determine this relationship.

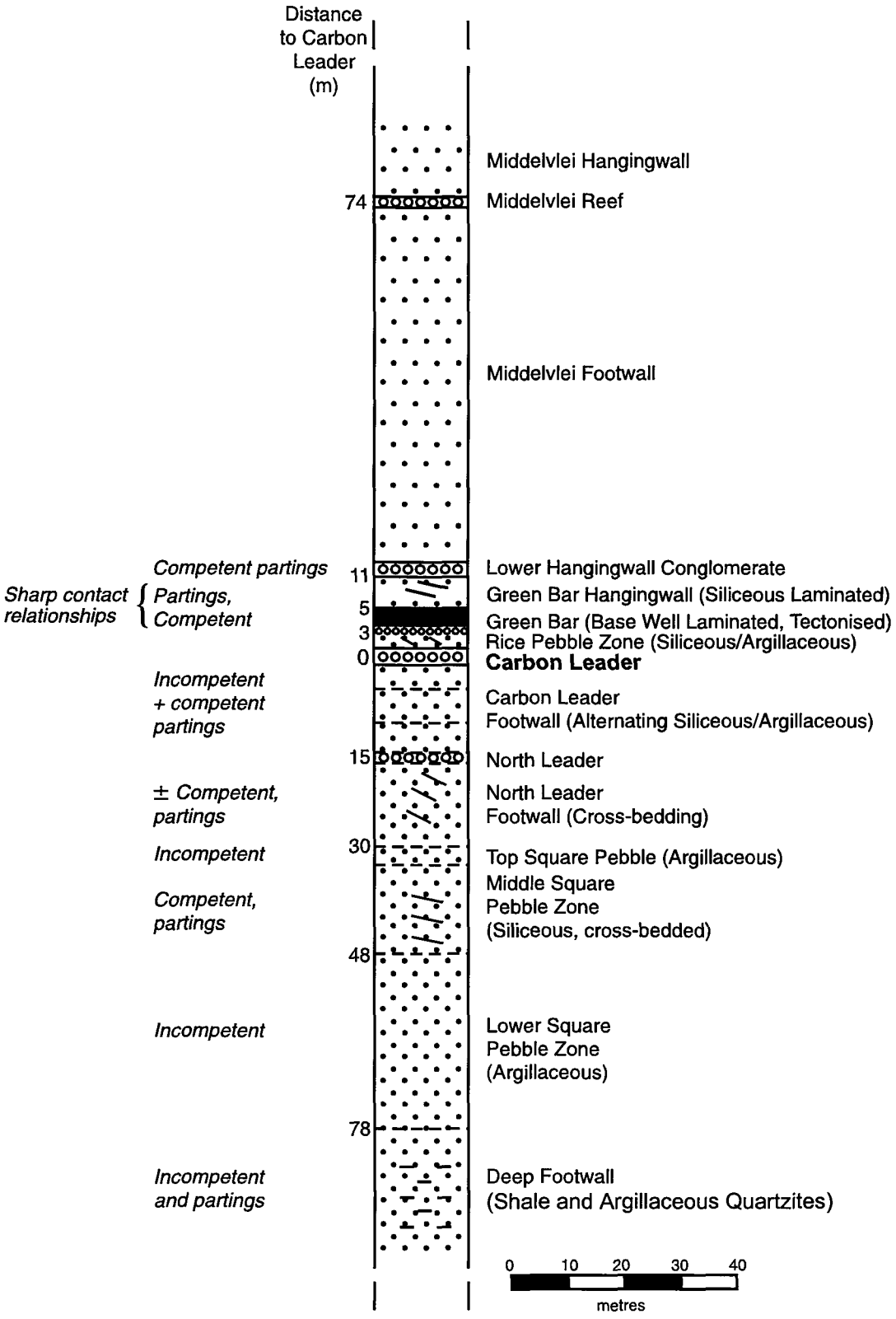

Figure 1.4.3 Stratigraphic column of the Carbon Leader. The various competencies and parting planes of the rock assemblages are indicated.

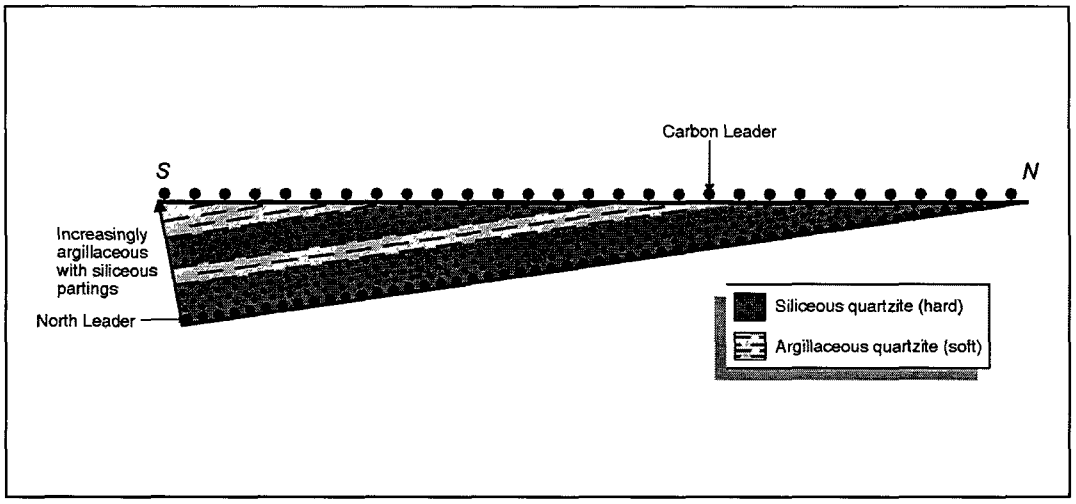

Figure 1.4.4 Schematic section through the footwall of the Carbon Leader showing the increase in argillaceous units towards the south.

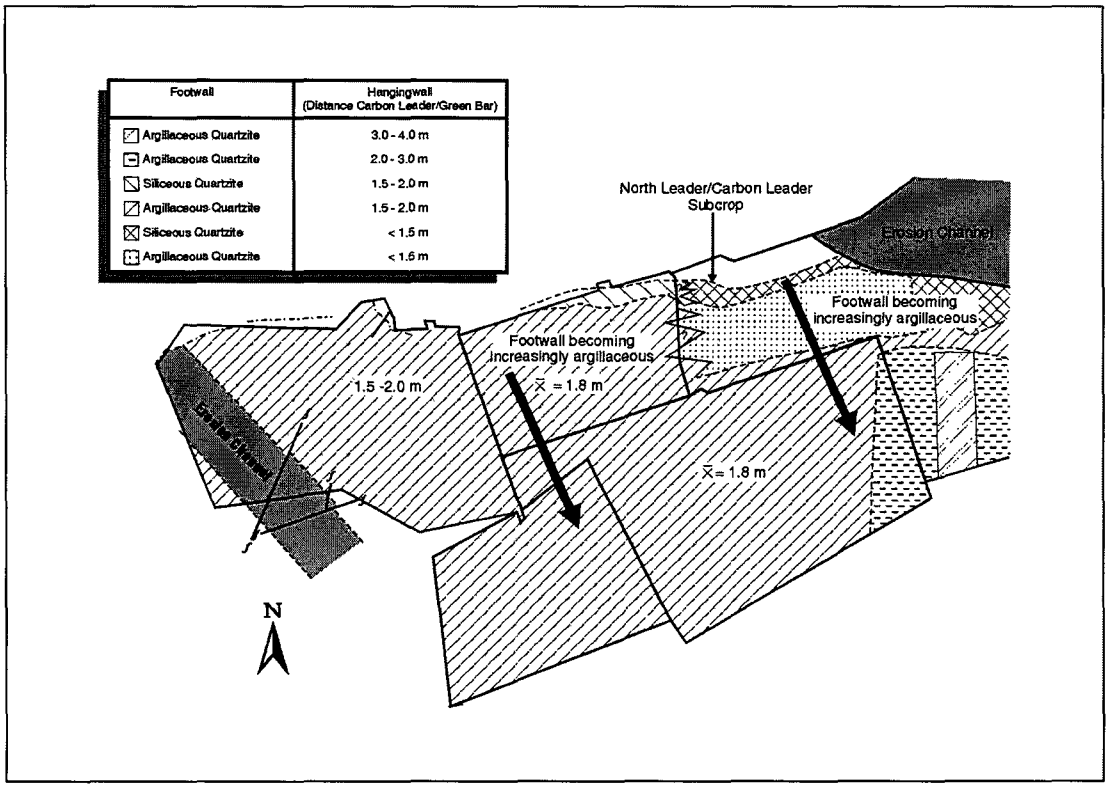

Figure 1.4.5 Geotechnical area map of the Carbon Leader in the Carletonville Goldfield. The North Leader subcrops against the Carbon Leader in the northern part of the goldfield. Note that the footwall of the Carbon Leader becomes increasingly argillaceous towards the southern part of the goldfield. The variable distances between the Carbon Leader and the Green Bar are also indicated.

The Carbon Leader is a narrow conglomerate band or seam, seldom exceeding 10 cm in thickness. On Driefontein Gold Mine borehole intersections, however, indicate thicknesses of > 2 m (Jager, pers. comm., 1997). Generally three facies types are distinguished, i.e. channel reef, transitional reef, and terrace reef. Discontinuous carbon seams are associated with the latter two. The relationship between the Carbon Leader and its footwall units is complex and results in well developed parting planes, which may influence rock mass behaviour.

The Carbon Leader is immediately overlain by a generally competent, medium- to coarse-grained siliceous quartzite (Siliceous Hangingwall Quartzite). In the Carletonville area the thickness of this quartzite varies between 1,4 to 4 m (Engelbrecht et. al., 1986; Figures 1.4.6a and b). The Green Bar, a 1 to 2,5 m thick argillaceous unit overlies the quartzite. Bedding planes are especially prominent in the lower portion of the Green Bar, which grades upwards into more competent, less well-bedded siltstone. The transition from the hard hangingwall quartzite to the softer, well-bedded Green Bar is significant for the rock mass behaviour in two regards.

Firstly, the so-called Rice Pebble Marker, having pronounced parting planes at its base and top, defines the transition. These parting planes, resulting in weak cohesion, control rockfalls and it is suggested that the fall of ground thickness of hangingwall strata is defined by the distance between the stope hangingwall and the base of the Green Bar (Figure 1.4.6). This parting plane has also been observed to be reactivated as a bedding-parallel fault during seismic events. Due to the lack of cohesion between the hangingwall quartzite and the Rice Pebble Marker, the quartzites below this plane will potentially result in rockfalls as soon as the "supporting" reef is mined. The combined thickness of the ejected and stope width corresponds, approximately, with the distance between the footwall of the stopes to the base of the Green Bar, as exemplified for Western Deep Levels in Figure 1.4.6b.

Secondly, the Green Bar has a lower competency than the hangingwall of the Carbon Leader (Gay and Jager, 1986). The mining induced extension fractures dip approximately 70° towards the face in the competent siliceous hangingwall quartzite. However, in some areas (e.g. West Driefontein), however, planar cross-beds are prominent, weakening the rock and resulting in vertical extension fractures (Figure 1.4.7).

The presence of sedimentary partings, expressed as lithological contacts and bedding planes, is more pronounced with the Carbon Leader, when, for example, being compared to the Vaal Reef (discussed below). The increasingly argillaceous nature of the footwall strata towards the deeper areas of Carbon Leader mining suggests that weak parting planes will simultaneously increase in frequency.

A geotechnical area map has been compiled displaying hard/hard, soft/hard, hard/soft and soft/soft footwall/hangingwall relationships (Figure 1.4.8). This methodology is based on the conversion of the above-described siliceous and argillaceous footwall and hangingwall lithologies into "hard" and "soft" , respectively, employing known UCS values.

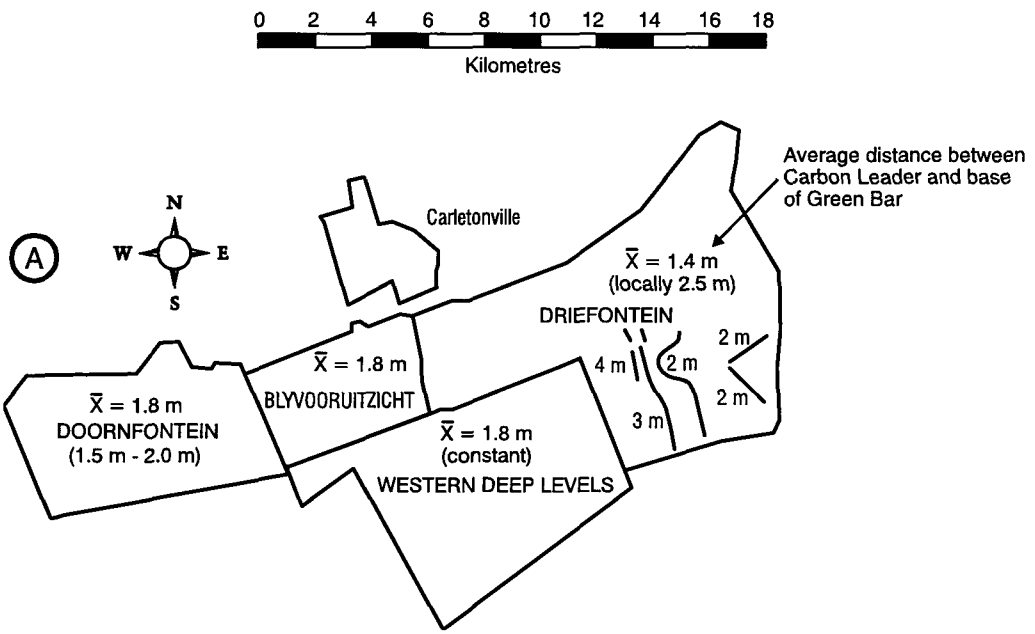

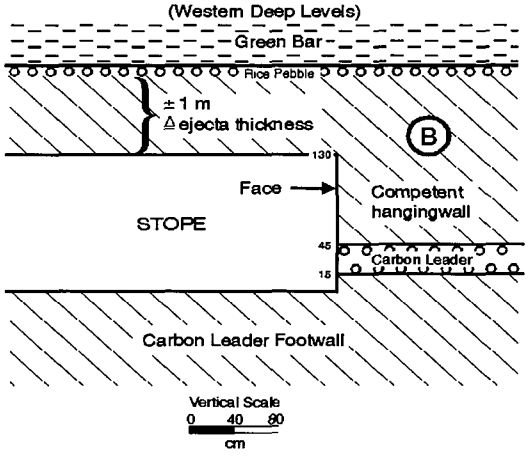

	Doorn-fontein	Blyvoor-uitzicht	WDL	West Drief.	East-Drief.
Stope width and ejecta	2.20 m	2.20 m	2.30 m	2.20 m	2.20 m
Stope width	1.50 m	1.30 m	1.30 m	1.50 m	1.65 m
Ejecta thickness	0.69 m	0.93 m	0.97 m	0.74 m	1.10 m

Figures 1.4.6 a and b Isopach plan indicating the average distance between the Carbon Leader and the base of the Green Bar (A). Also shown is an example of how ejecta thicknesses relate to the rock characteristics (B).

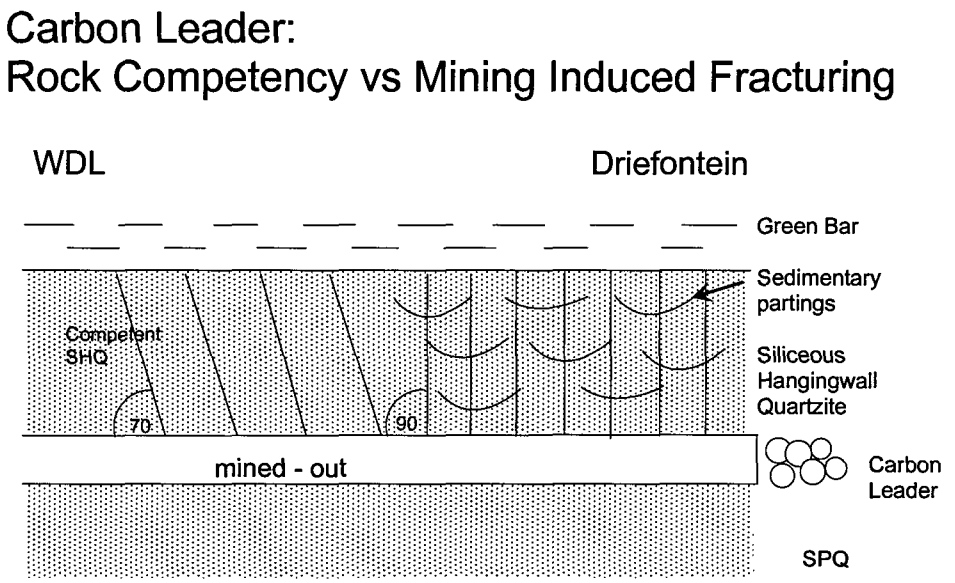

Figure 1.4.7 Variations of mining induced extension fractures in the competent siliceous hangingwall quartzite of the Carbon Leader.

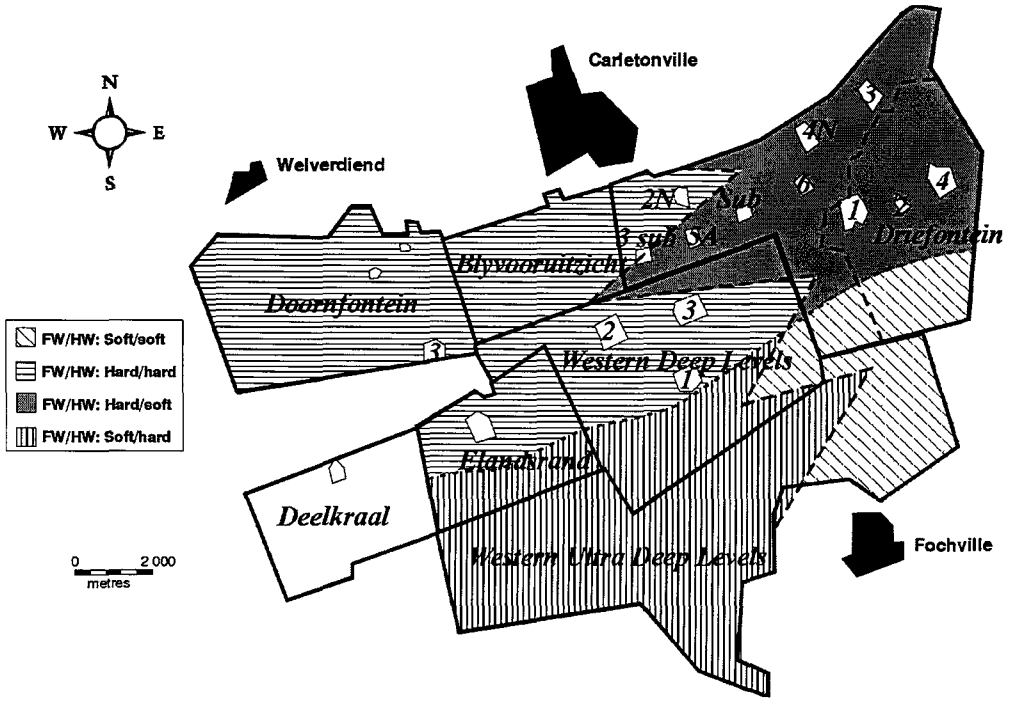

Figure 1.4.8 Redefined geotechnical areas for the Carbon Leader Reef. See text for explanation.

Strathmore Formation

In the Klerksdorp Goldfield , the Johannesburg Subgroup is presented by a sequence of quartzites, conglomerates, and quartz wackes, about 1100 m thick. The succession is present east, south-east, and south of Klerksdorp. The Strathmore Formation forms the uppermost part of the Johannesburg Subgroup (Figure 1.1.1). The Vaal Reef, at the base of the Strathmore Formation, is the most important economic horizon in the area.

The Vaal Reef

Lithologies associated with the Vaal Reef vary significantly (Figure 1.4.9). The sequence consists of argillaceous and siliceous quartzites, intercalated with shale, grits, and conglomerates. Variable rock engineering properties are encountered (Figure 1.4.9). The Vaal Reef overlies the MB5 unconformably. A simplified geological section (Figure 1.4.10) indicates the variability of stratigraphic units, and the low angle unconformity between the Vaal Reef and the underlying units. For a detailed geological description of the Klerksdorp Goldfield see Antrobus et al. (1986). The following discussion considers the geological features of the Vaal Reef and their potential influence on rock mass behaviours.

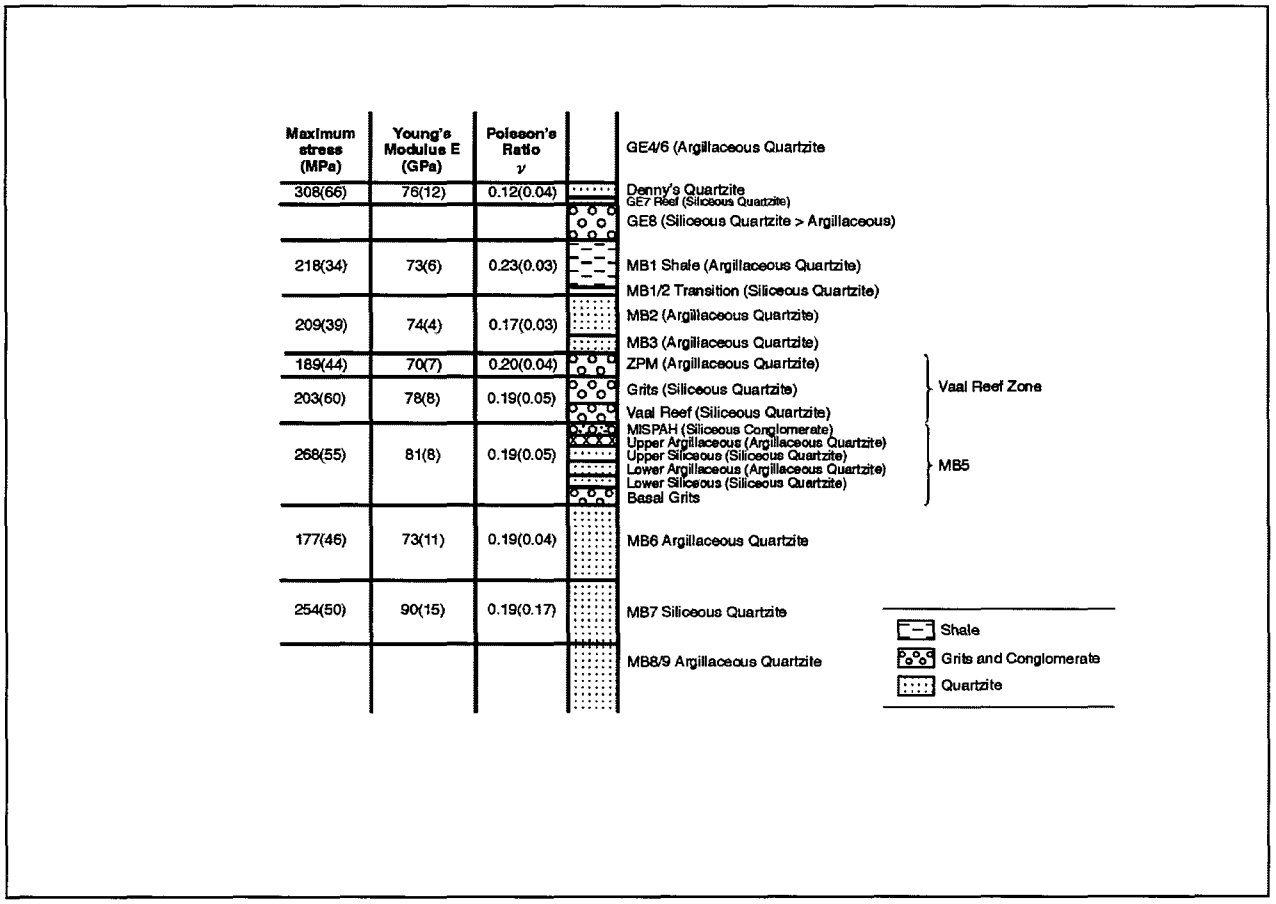

Figure 1.4.9 Simplified stratigraphic column of strata associated with the Vaal Reef. The rock engineering properties are included (after Gay and Jager, 1986). The numbers in brackets refer to the standard deviations. ZPM = Zandpan Marker.

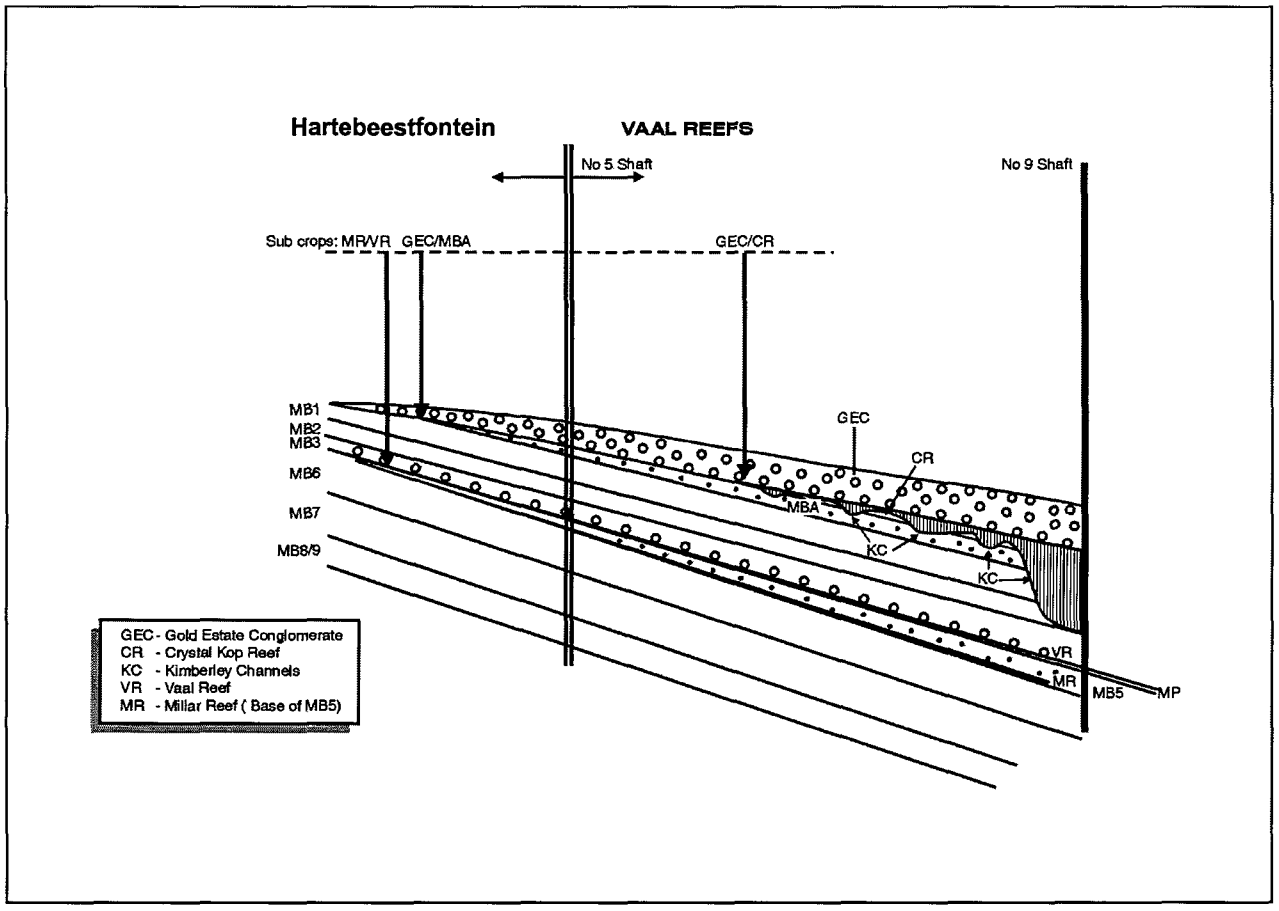

Figure 1.4.10 ***Simplified geological section across Vaal Reefs Gold Mine, indicating the stratigraphic relationships. Note the low angle unconformity between the Vaal Reef and the MB5. Refer to Figure 1.4.11 for position of section line.***

The distribution of the Vaal Reef is related to channel structures. The truncation between the Vaal Reef and its footwall units results in a maximum unconformity angle of 12°. The reef is characteristically a light-grey, pebbly, siliceous quartzite conglomerate, which has a bimodal size-frequency distribution. The thickness of the reef varies from less than 20 cm to over 50 cm and increases towards the southeast of the goldfield.

Immediately overlying the Vaal Reef is a very competent, siliceous (hard) quartzite, with an average thickness of 0,5 m (Figure 1.4.11), containing several bedding partings locally known as the "grey glassy". This quartzite is, in turn, overlain by an argillaceous quartzite (Zandpan or 12 Foot Marker) and a well-defined parting plane separates the two lithologies. Due to the weak cohesion along this plane, it controls the beam thickness and is known to result in unstable hangingwall conditions, deserving special attention when determining support resistance (e.g. Atkins and Keen, 1984; Gay and Jager, 1986; Kullmann et al., 1994).

The Zandpan Marker locally cuts down into the Vaal Reef or its footwall units, resulting in the Vaal Reef being overlain by argillaceous quartzites or being eroded (Figures 1.4.11 and 1.4.12). Areas in which the Zandpan Marker cuts down in stratigraphy, however, are only known on Hartebeesfontein and the northeastern part of Vaal Reefs, but these localities are not well defined (question marks and dashed lines in Figure 1.4.12).

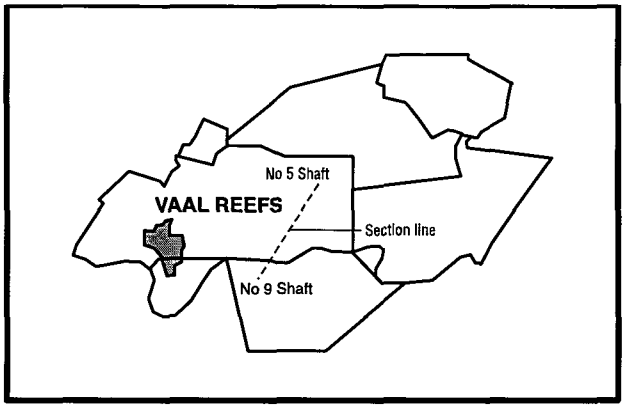

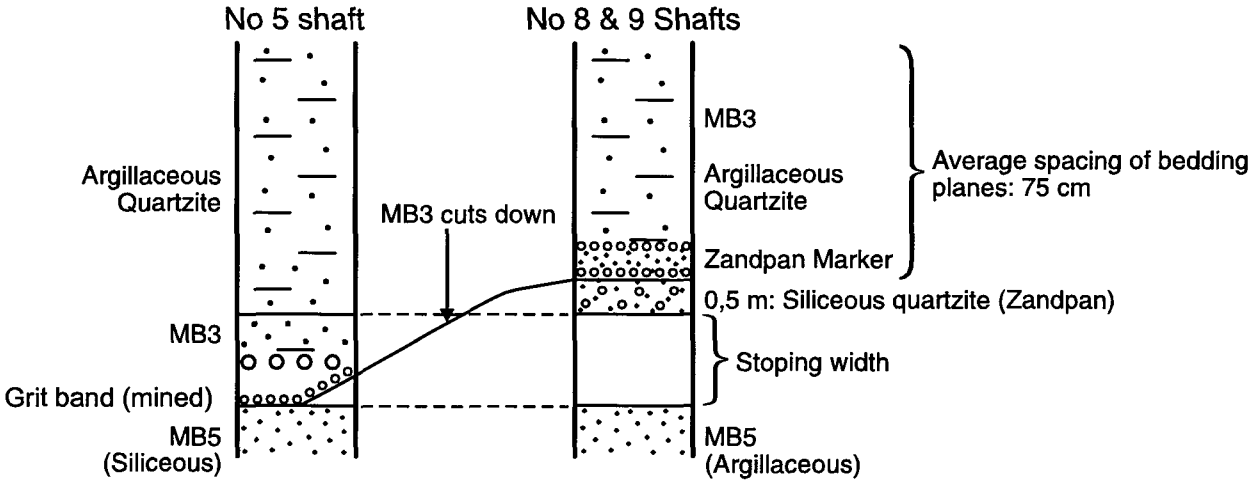

Figure 1.4.11 Schematic section indicating the distribution of the Zandpan Marker. Note that the Zandpan Marker erodes into the Vaal Reef horizon, resulting in varying rock mechanic properties associated with this excavation.

Parting planes also control the cohesion between various hangingwall and footwall units. The significance of the parting plane at the contact between the "grey glassy" and the Zandpan Marker has already been pointed out. Of note also is the variability of parting planes in the MB5 footwall units, which can change in frequency from a spacing width of some 50 cm in the argillaceous quartzites, to 2 m in the siliceous quartzite (Figure 1.4.11). These discontinuities may also influence the rock mass behaviour in development areas.

Superimposition of the Vaal Reef footwall and hangingwall maps result in the definition of seven geotechnical areas (Figure 1.4.12; Table 1.4.2). The geotechnical areas indicate a variety of NE-SE striking footwall units. Only two different hangingwall lithologies however, i.e. the siliceous "grey glassy" and the Zandpan Marker are defined.

The geotechnical area map presented in Figure 1.4.12 was modified in order to show "hard" and "soft" footwall and hangingwall assemblages, based on UCS measurements, which are presented in Figure 1.4.13, using the introduced threshold value of 200 MPa. The classification of the hangingwall and footwall rock types (Table 1.4.2) in "hard" and "soft" results in four geotechnical areas (Figure 1.4.14).

Table 1.4.2 Summary of geotechnical areas defined for the Vaal Reef on the basis of rock type (Figure 1.4.12).

Hangingwall Rock Type	Footwall Rock Type
Siliceous quartzite	Siliceous pebbly conglomerate (Mispah)
Siliceous quartzite	Argillaceous quartzite
Siliceous quartzite	Siliceous quartzite
Siliceous quartzite	Argillaceous quartzite
Siliceous quartzite	Siliceous quartzite
Argillaceous quartzite (Zandpan Marker)	Siliceous quartzite (with grit bands)
Argillaceous quartzite	Argillaceous quartzite

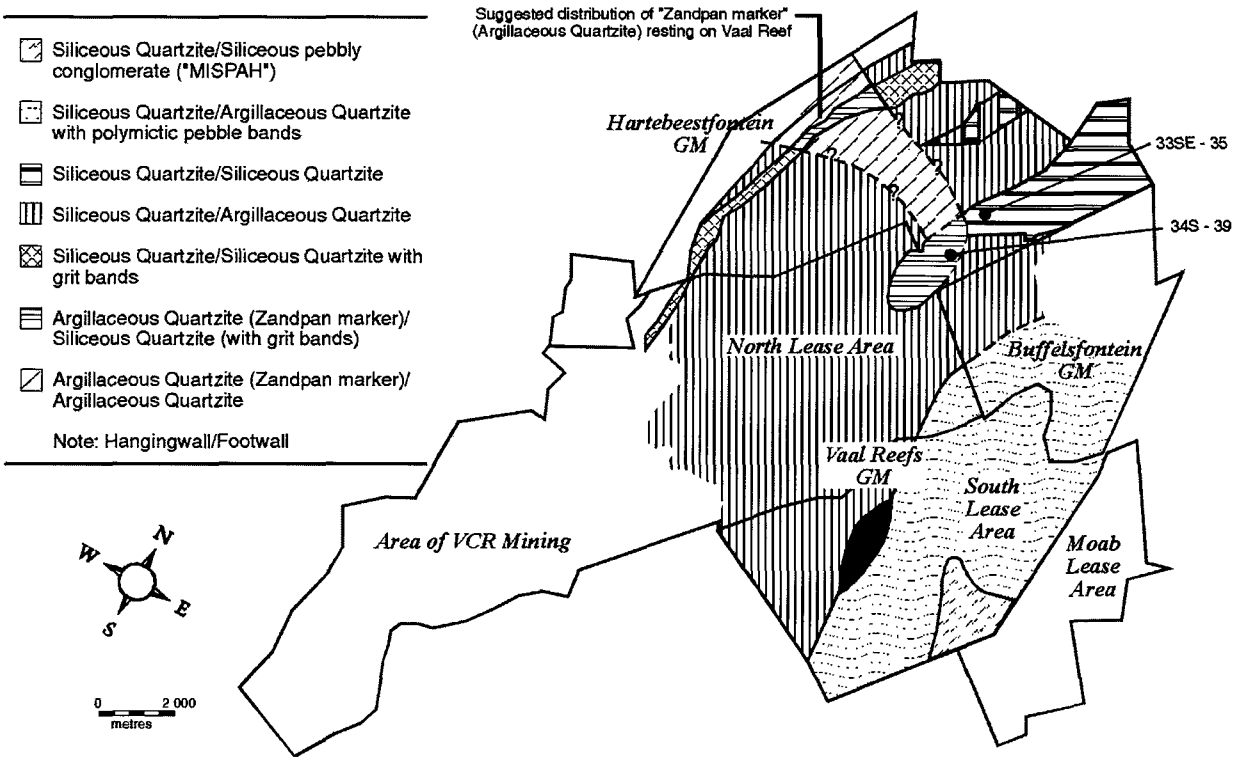

Figure 1.4.12 Geotechnical areas of the Vaal Reef. For explanation see text.

	Lithology No. of samples	σ_1 Std deviation	Young's Modulus (E) Std deviation
①	MB6 2	119.00 8.00	45.0 9.0
②	MB7 2	193.00 1.00	63.7 0.4
③	FW/Qtz 3	212.00 15.64	59.00 9.46
④	HW/Qtz 2	227.5 5.5	62.0 1.0
⑤	HW/Qtz 2	268.85 32.05	81.8 5.4
⑥	F/wall Drive 2	188.40 16.50	74.15 0.75
⑦	HW/Qtz 2	147.67 8.50	50.33 1.70
⑧	Reef 2	118.40 0.40	61.20 1.00
⑨	HW/Qtz 2	189.85 9.25	69.35 2.05
⑩	FW/Qtz	244.80 8.60	78.50 1.90
⑪	FW Parting 6	116.00 1.15	43.67 1.60
⑫	HW Parting 3	154.67 15.17	44.33 2.05
⑬	Reef 6	229.90 28.45	47.67 4.27
⑭	FW/Qtz 3	138.93 6.03	55.67 1.62
⑮	HW/Qtz 5	193.57 16.60	64.39 2.44
⑯	FW/Qtz 3	178.00 12.96	57.67 3.10
⑰	HW/Qtz 1	152.30	71.30
⑱	HW/Qtz 3	208.50 3.70	74.20 2.13
⑲	HW/Qtz 1	219.60	81.30
⑳	HW/Qtz 5	192.26 24.57	74.2 2.12
㉑	HW/Qtz 6	195.30 17.16	59.98 2.08
㉒	HW/Qtz 10	183.53 28.85	62.66 7.14
㉓	FW/Qtz 4	219.9 33.88	66.82 2.94

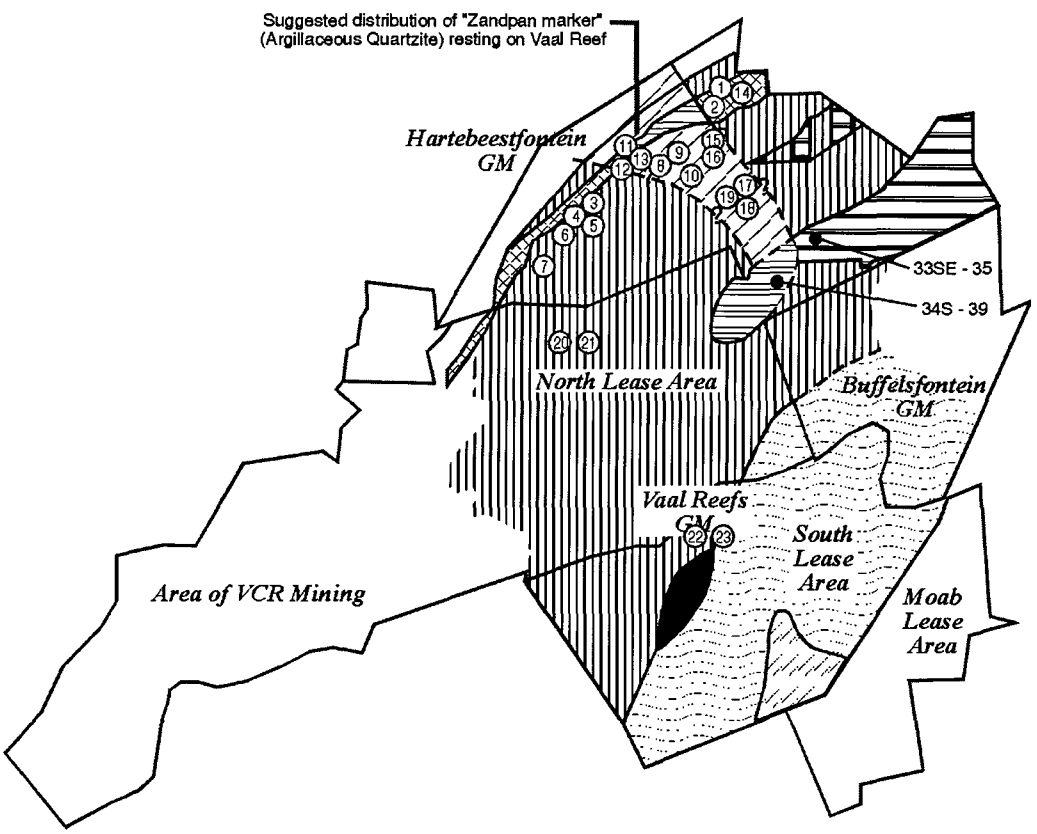

Figure 1.4.13 Various compressive strengths of Vaal Reef hangingwall and footwall units.

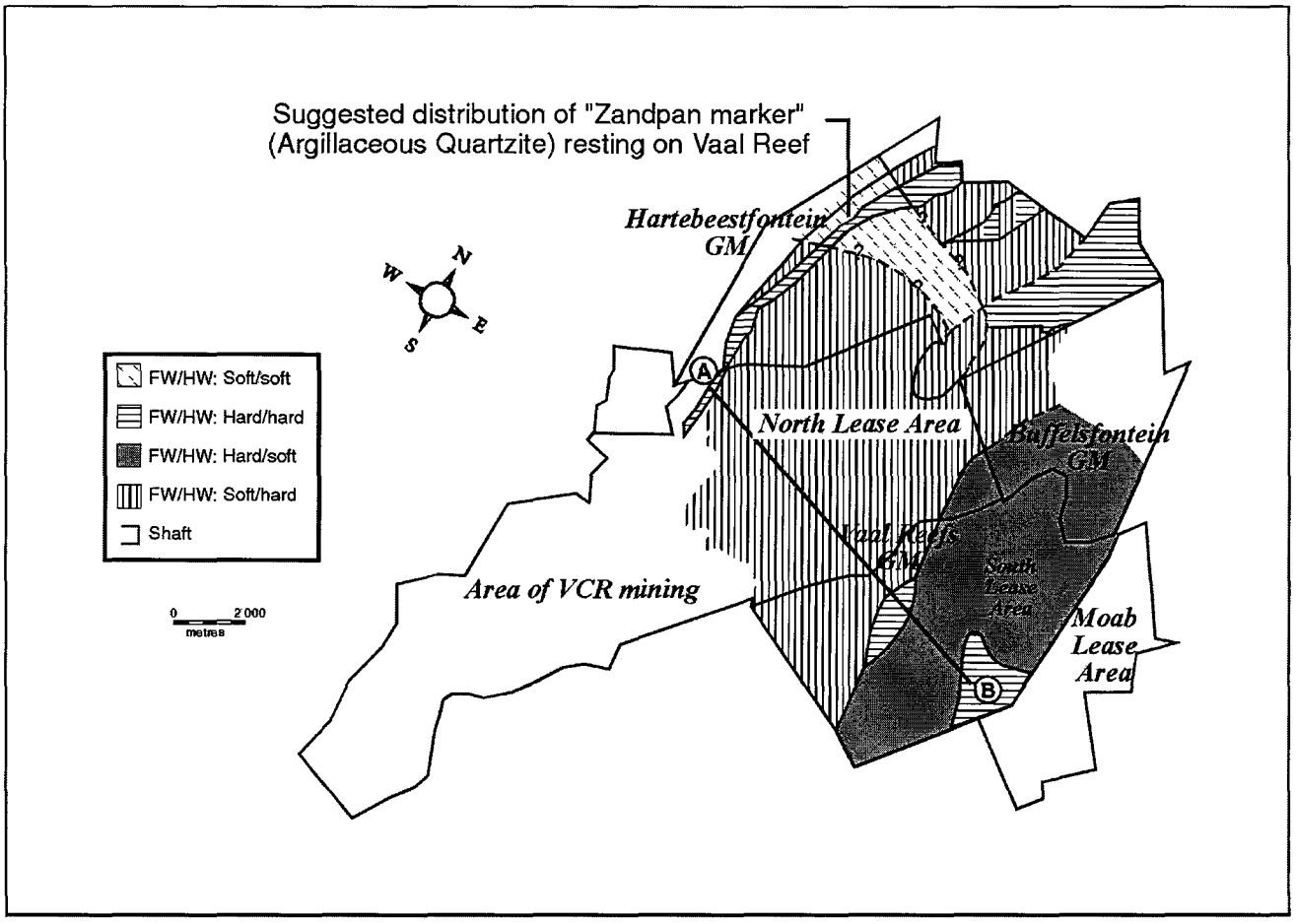

Figure 1.4.14 Redefined geotechnical area map of the Vaal Reef, using UCS values of footwall and hangingwall strata.

1.4.1.2 Turffontein subgroup

The Kimberley Formation forms the lower part of the Turffontein Subgroup (Figure 1.1.1). In the Orange Free State goldfield, it can be subdivided into several members. The members generally have an unconformity at their base, most pronounced in the proximal mining areas. The formation is unconformably overlain by the Eldorado Formation (Elsburg's), which can be clearly distinguished from the underlying Aandenk Member by its predominantly siliceous lithologies.

Geotechnical Environment of the Kimberley Formation

Several orebodies are preserved within the Kimberley succession (Figures 1.4.15, 1.4.16 and 1.4.17). The B-Reef, Big Pebble Marker (BPM) and Witpan (8A) are considered in this study. Orebodies contained within the Kimberley succession are generally situated in argillaceous ("soft") strata, with siliceous ("hard") quartzites and conglomerates representing a minority. The succession is truncated towards the south, where only one Kimberley orebody is preserved, locally termed Sand River-, Kalkoonkrans-, or Beatrix Reef. Of note are locally developed shale channels. These may be developed in the hangingwall and the footwall of orebodies, also truncating the orebody itself. Channel depths and widths are highly variable and these were also considered during the

compilation of the geotechnical areas, due to their impact on rock mass behaviour during stoping and development.

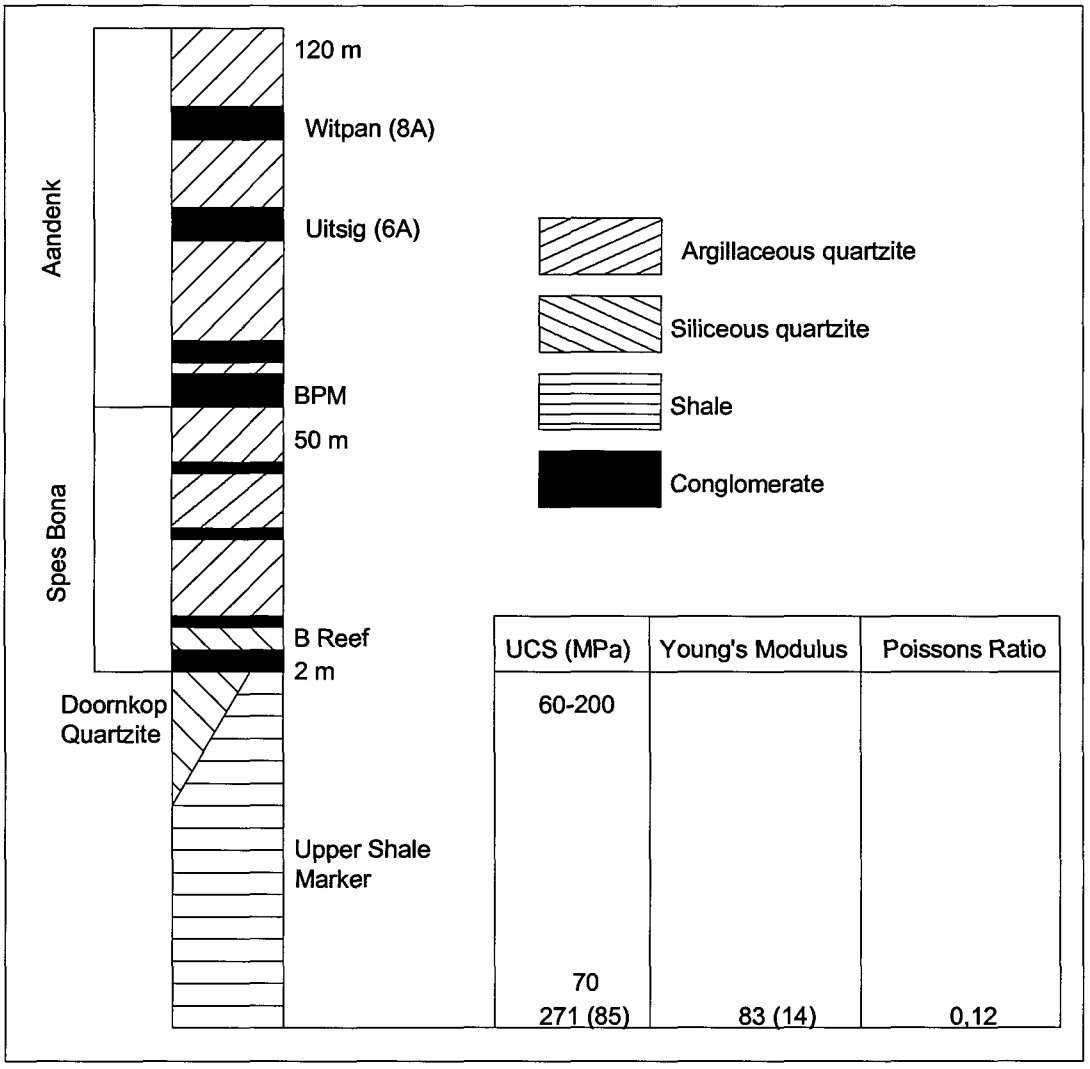

Figure 1.4.15 Generalized stratigraphic section of the Kimberley succesion. Rock engineering properties are shown for the Upper Shale Marker (numbers in brackets are standard deviations).

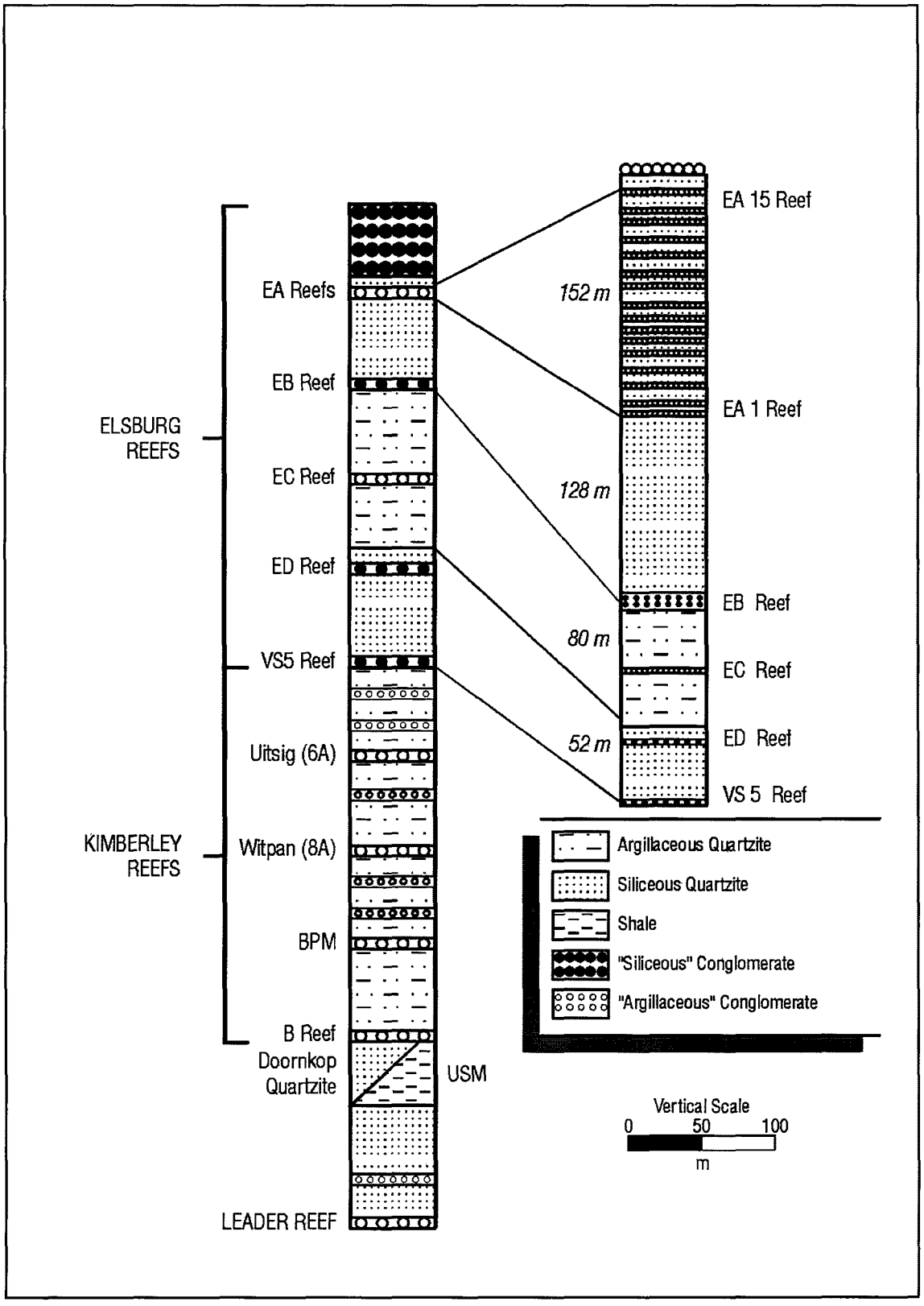

Figure 1.4.16 Generalized stratigraphic column of some of the Free State orebodies. USM = Upper Shale Marker; BPM = Big Pebble Marker

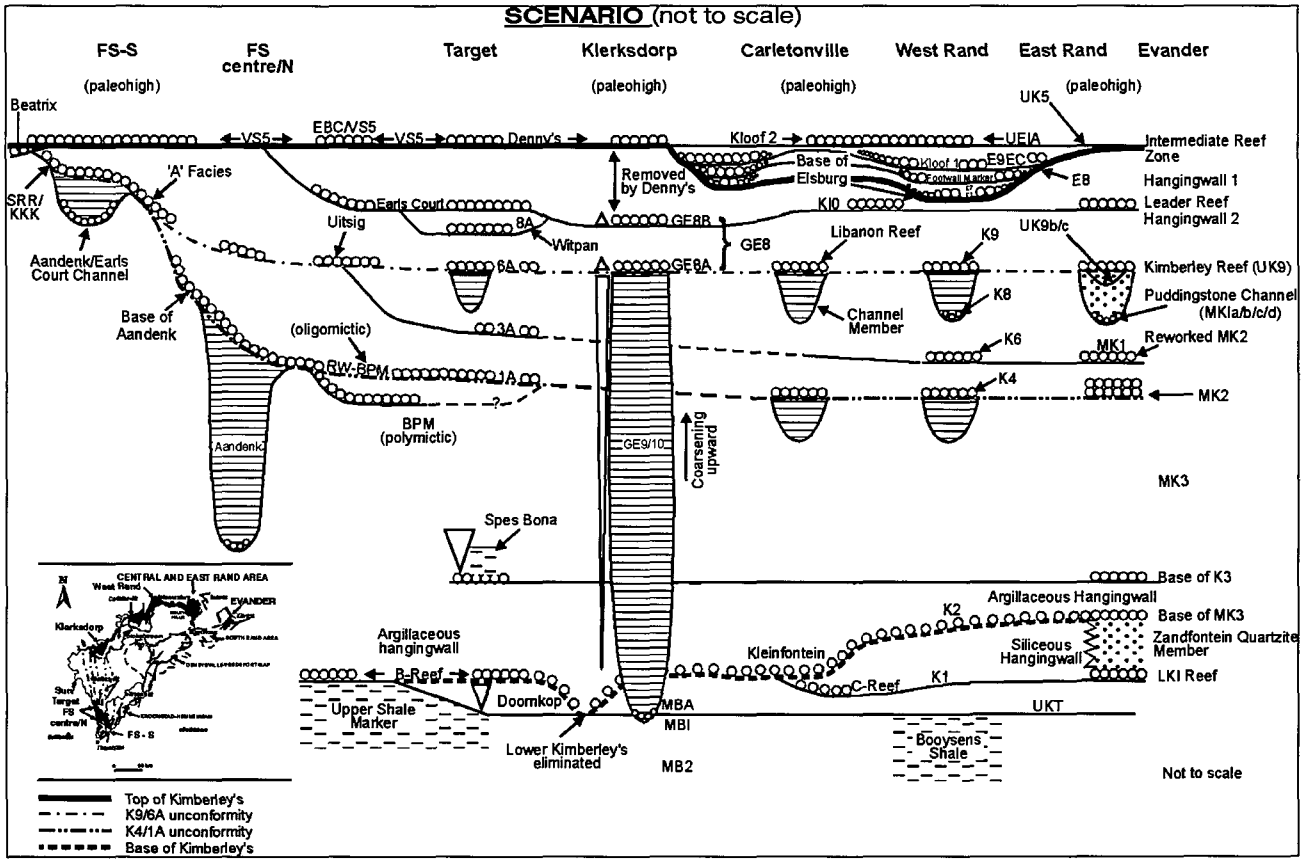

Figure 1.4.17 Regional stratigraphic correlation of the Kimberley succession, (Kimberley Working Group, 1997).

B-Reef

The B-Reef is the basal orebody of the Kimberley succession (Figures 1.4.15 and 1.4.16), and overlies the Upper Shale Marker (which is the Free State equivalent of the Booysens Shale) over large areas. High UCS values may be associated with the Upper Shale Marker (Figure 1.4.15). In a bedding parallel orientation, however, the strengths of laminated shales are generally much lower, due to the low cohesion between the fine shale laminae. Discontinuous, argillaceous partings are present in the argillaceous hangingwall quartzite.

Three, northwest/southeast striking geotechnical areas are delineated (Figure 1.4.18). The B-Reef is predominantly mined in a "soft", argillaceous environment (Table 1.4.3). Footwall partings are prominent in the central portion of the Free State where the shale of the Upper Shale Marker underlies this orebody. The footwall of the B-Reef, prone to bulging, and should be most prominent in the central portion of the area under consideration (Figure 1.4.18). Footwalls of the B-Reef in the northeastern and southwestern portions are siliceous and argillaceous quartzites, respectively.

A redefinition of geotechnical areas, by using "hard" and "soft" footwall and hangingwall lithologies is presented in Figure 1.4.19. Only two distinct geotechnical areas are distinguished. The footwall to the B-Reef is either hard or soft, whereas the hangingwall is always "soft".

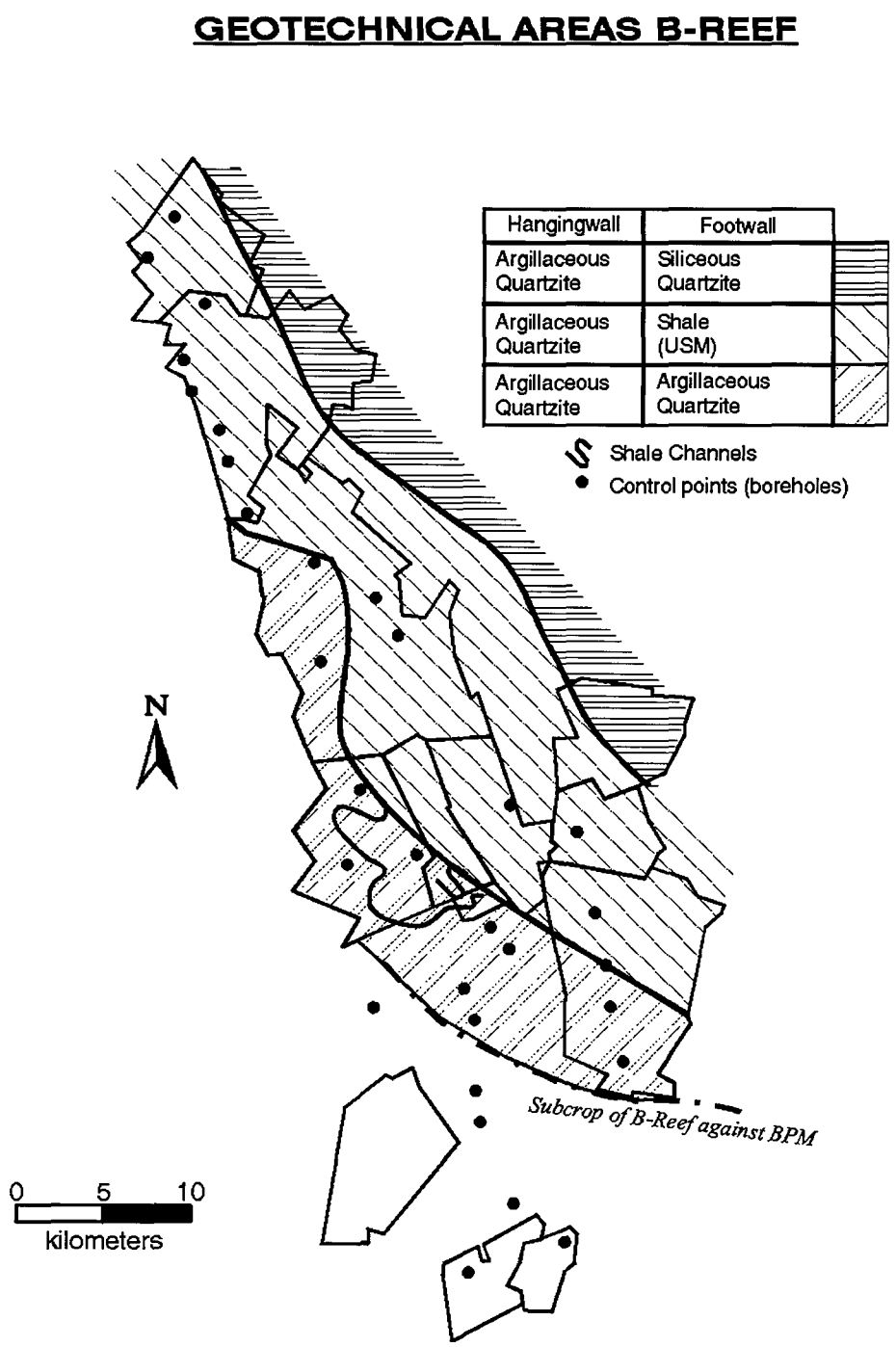

Figure 1.4.18 Geotechnical areas of the B-Reef, as defined on the basis of rock type.

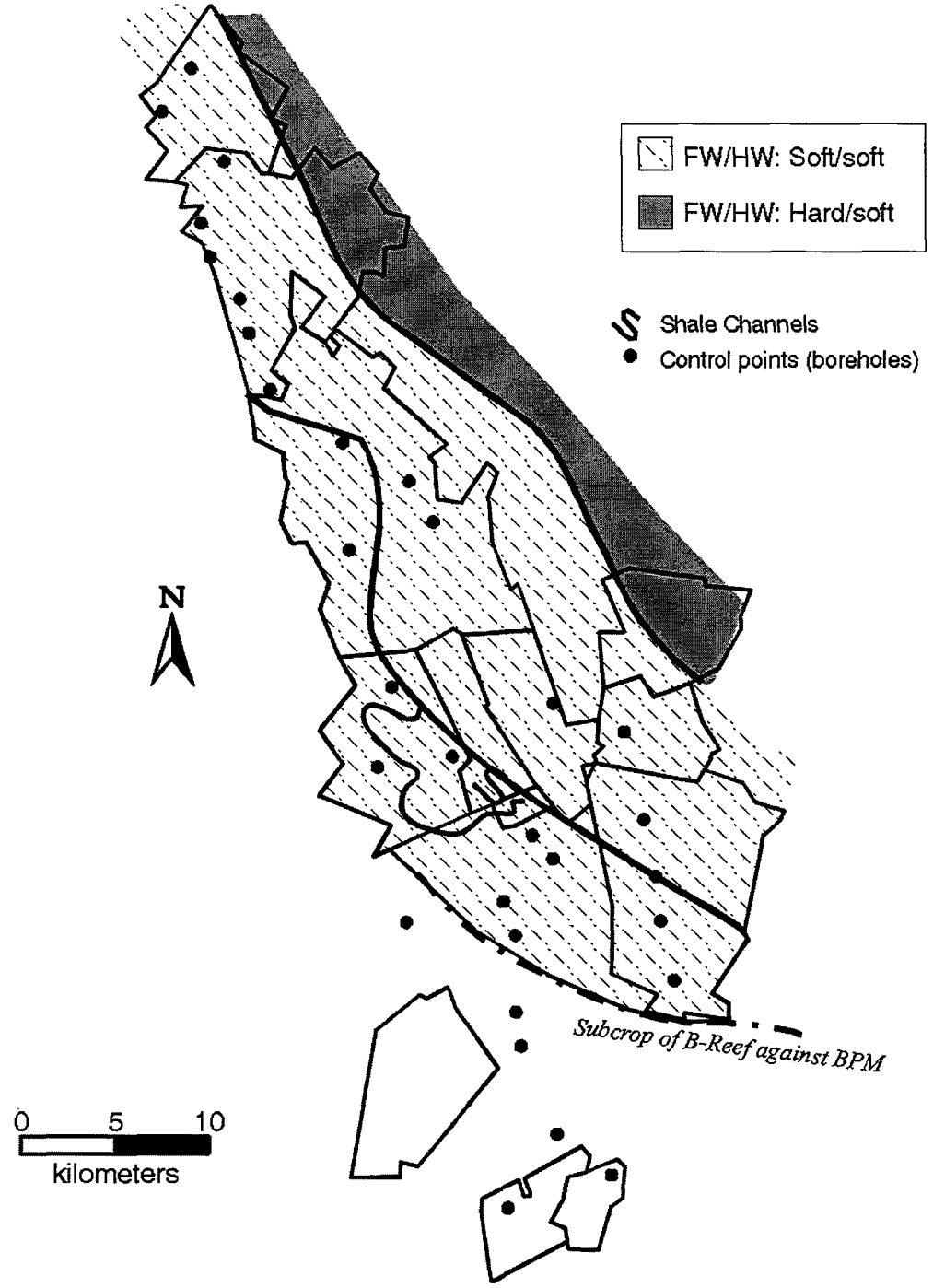

Figure 1.4.19 Redefined geotechnical area map for the B-Reef, employing UCS values.

Table 1.4.3 Summary of the footwall and hangingwall lithologies of the considered Free State orebodies and associated, potential hazards.

Succession	Reef	Footwall	Hangingwall	Type	Potential Problem
	Leader Reef	Argillaceous quartzite	Argillaceous quartzite	S-S	FW ride/bulging Parting plane FOG
Kimberley	B-reef	Argillaceous quartzite	Argillaceous quartzite	S-S	FW ride/bulging Parting plane FOG
		Shale	Argillaceous quartzite	VS-S	FW ride/bulging and punching Parting plane FOG
		Siliceous quartzite	Argillaceous quartzite	H-S	Parting plane FOG
	BPM	Argillaceous quartzite	Siliceous quartzite	S-H	FW ride/bulging Stress fracture FOG
		Argillaceous quartzite	Argillaceous quartzite	S-S	FW ride/bulging Parting plane FOG
		Shale	Argillaceous quartzite	VS-S	FW ride/bulging punching Parting plane FOG
	Witpan	Argillaceous quartzite	Argillaceous quartzite	S-S	FW ride/bulging Parting plane FOG
		Conglomerate	Argillaceous quartzite	H?-S	Parting plane FOG
Elsburg	VS5	Argillaceous conglomerate	Argillaceous quartzite	S-S	FW ride? Parting plane FOG
		Argillaceous quartzite	Siliceous conglomerate	S-H	FW ride/bulging Stress fracture FOG
		Argillaceous quartzite	Siliceous quartzite?	S-H	FW ride/bulging Stress fracture FOG
		Argillaceous quartzite	Argillaceous quartzite	S-H	FW ride/bulging Parting plane FOG
		Argillaceous quartzite	Dolerite Sill?	S-H?	FW ride/bulging Stress fracture FOG

Big Pebble Marker

The Big Pebble Marker (BPM) is, like the B-Reef, predominantly mined in a "soft" environment (Figure 1.4.15; Table 1.4.3). This is due to its predominantly argillaceous footwall and hangingwall. On the BPM however, stoping widths can exceed 2 m, for example as observed at Harmony Gold Mine. As the effects of seismicity are substantially increased with wider widths (Arnold et al., 1994), the increase in reef thickness towards the southeast should also be considered in an assessment of rock mass behaviour.

Three geotechnical areas are delineated for the Big Pebble Marker (Figure 1.4.20). The redefined geotechnical area map, which refers to "soft" and "hard" footwall and hangingwall lithologies, is presented in Figure 1.4.21. There are two geotechnical areas, both of which have a "soft" footwall but have either "hard" or "soft" hangingwall lithologies.

Geotechnical Areas:
Big Pebble Marker (BPM)

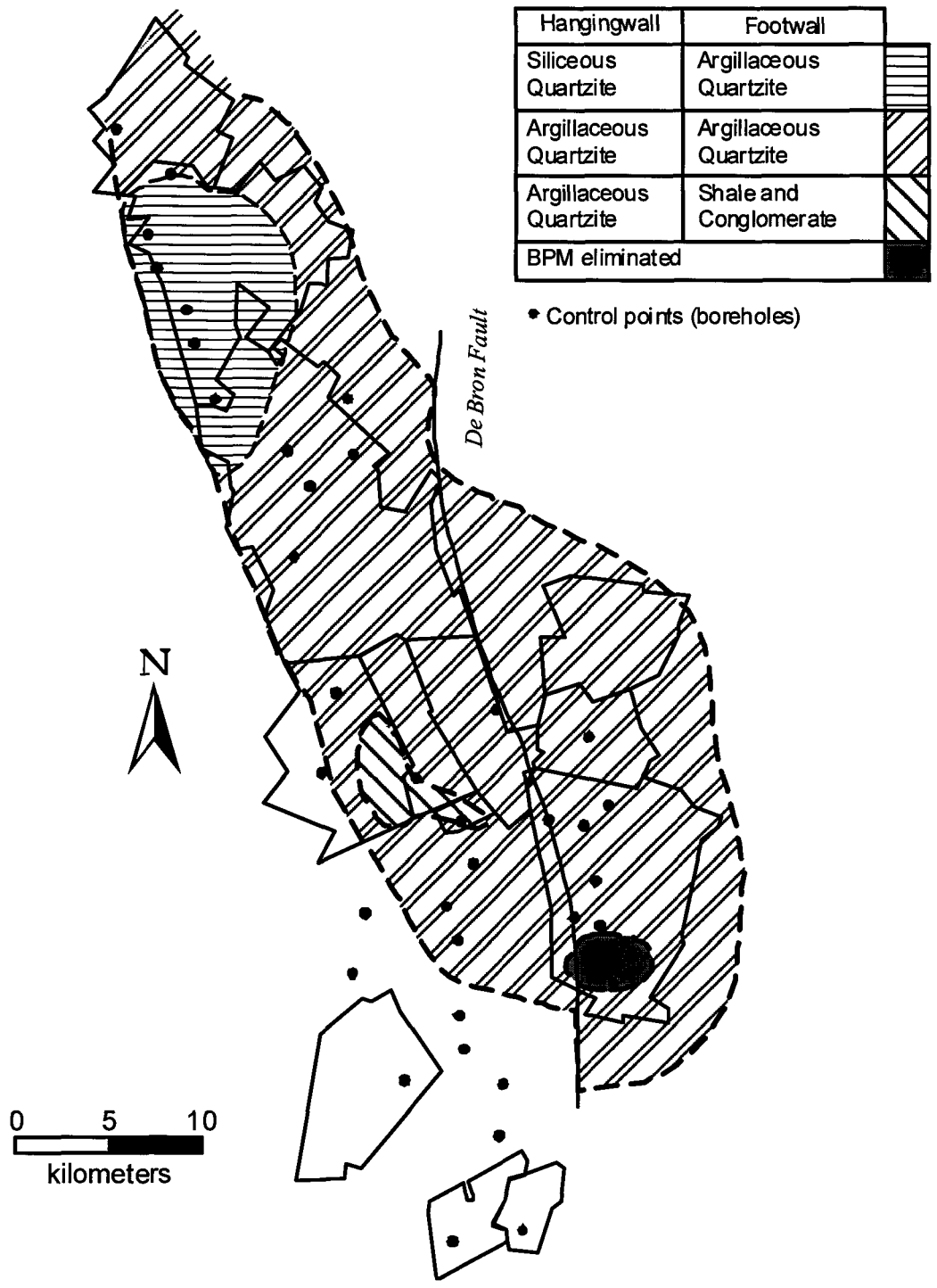

Figure 1.4.20 Big Pebble Marker geotechnical area map as defined by rock type assemblage.

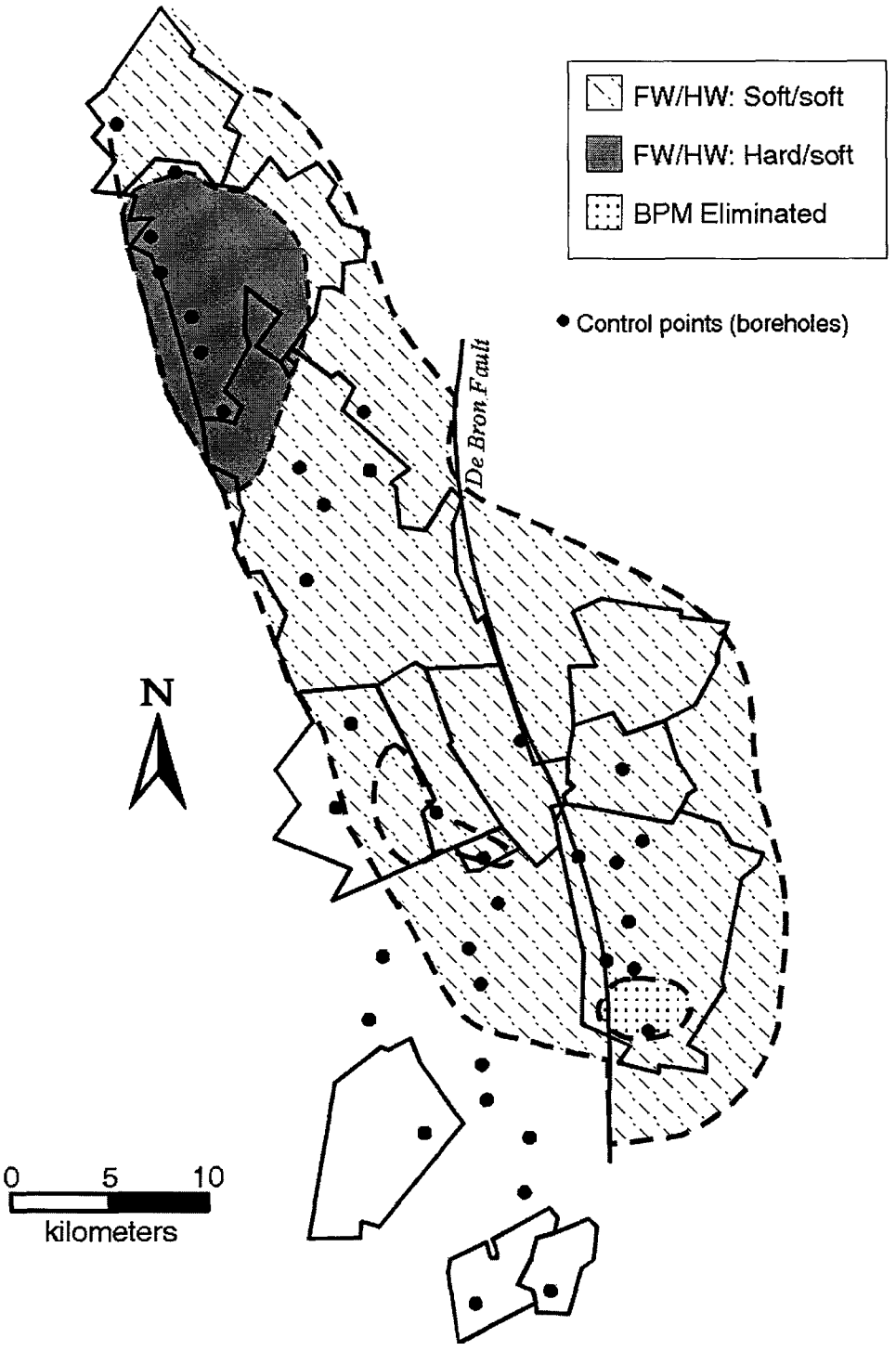

Figure 1.4.21 Map of redefined geotechnical areas of the Big Pebble Marker based on "hard" and "soft" footwall and hangingwall lithologies.

Witpan Reef

Within this reef horizon two geotechnical areas are delineated (Figure 1.4.22), which consider argillaceous quartzites and conglomerates (Table 1.4.3). The area where conglomerate (the Big Pebble Marker) underlies the Witpan is confined to the southern region of the Free State (Harmony area). It has to be established whether the conglomeratic footwall results in a different rock mass behaviour, when compared to the northern argillaceous footwall.

The redefined geotechnical areas based on "hard" and "soft" footwall and hangingwall lithologies are presented in Figure 1.4.23. Only soft/soft footwall/hangingwall relationships are present, according to this classification scheme.

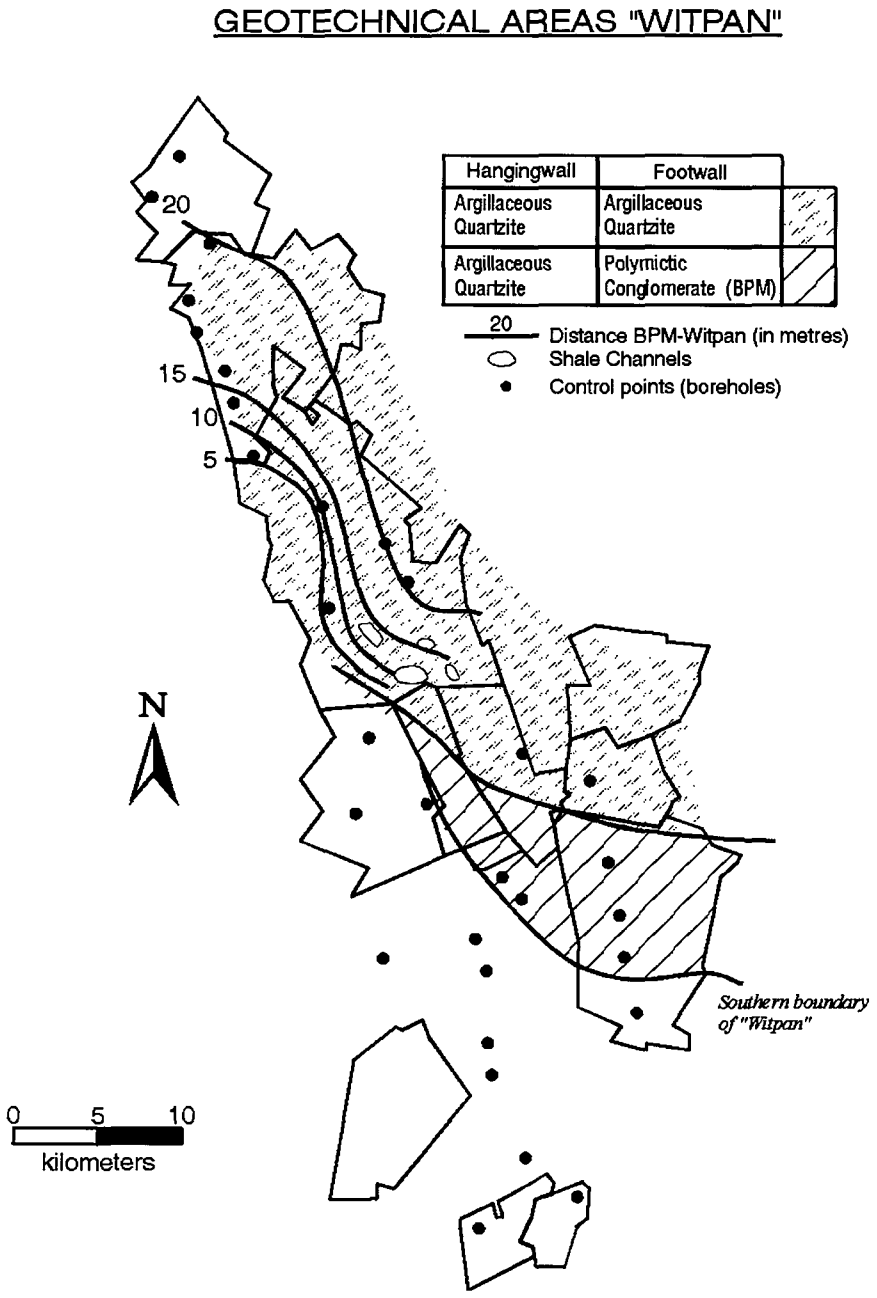

Figure 1.4.22 Geotechnical areas of the Witpan Reef considering rock type assemblages.

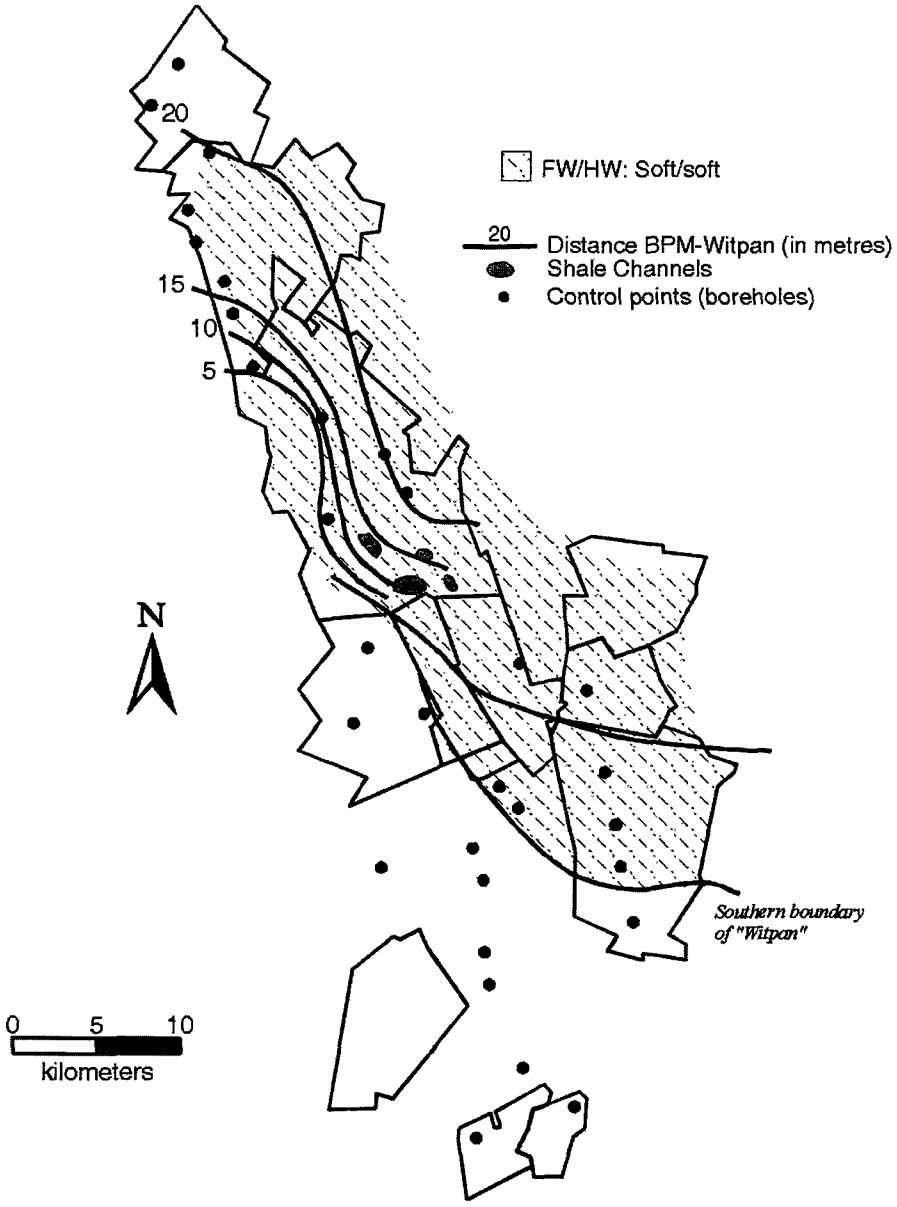

Figure 1.4.23 Map of redefined geotechnical areas of the Witpan Reef based on "hard" and "soft" footwall and hangingwall lithologies. Note contour intervals for Witpan/BPM middling, being important should both reefs be stoped.

Leader Reef

A single geotechnical area is delineated for the Leader Reef over the extent of the Free State area. Both footwall and hangingwall lithologies are represented by argillaceous quartzites (Table 1.4.3; Figure 1.4.24). Siliceous quartzite bands are however, present in the hangingwall of the Leader Reef Zone, where uniaxial compressive strength values can exceed 300 MPa. Also of note is the Khaki Shale which, on average, is encountered some 15 metres into the footwall of the Leader Reef.

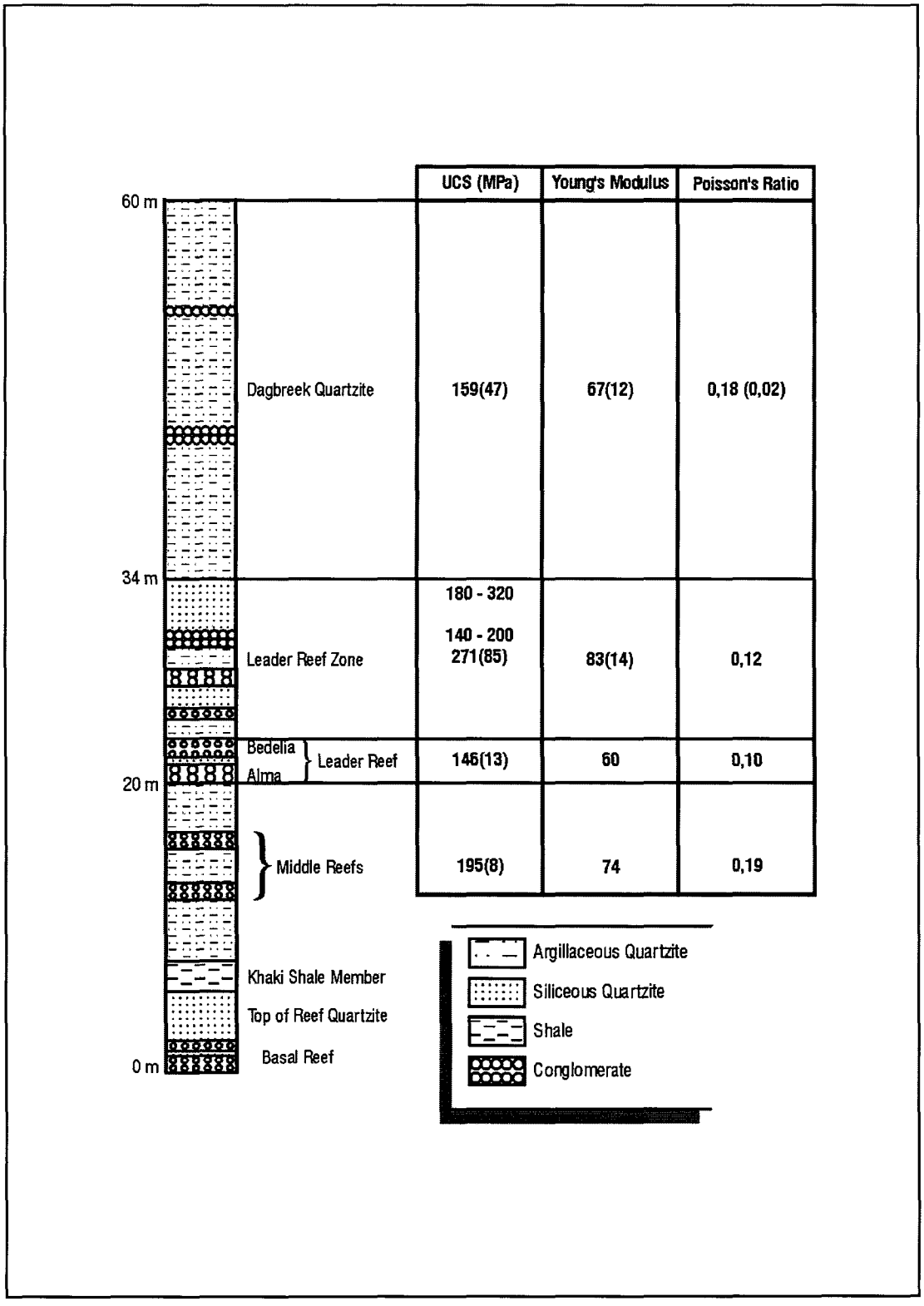

Figure 1.4.24 Generalized stratigraphic column of the succession associated with the Leader Reef. Rock engineering properties of the reef and the immediate hangingwall and footwall are also shown (numbers in brackets are standard deviations).

Elsburg Formation

Orebodies of the Elsburg succession are predominantly preserved in siliceous environments (Figure 1.4.25). The basal VS5 is, however, an unusual Elsburg reef, because it immediately overlies the Kimberley succession.

VS5

Five geotechnical areas are delineated for the VS5 (Figure 1.4.26). Geotechnical areas are comprised of siliceous conglomerates with argillaceous quartzite, and argillaceous footwall and hangingwall quartzites (Table 1.4.3). The remaining three areas occur locally. The geotechnical area defined by a hangingwall sill is situated towards the north of Beatrix and HJ Joel (Figure 1.4.27). The redefined geotechnical areas based on "hard" and "soft" footwall and hangingwall lithologies are presented in Figure 1.4.26. It is obvious that the very central part of the area under consideration has hard/hard footwall/hangingwall relationships. The outermost parts of the area have soft/soft and the area in-between displays soft/hard footwall/hangingwall relationships.

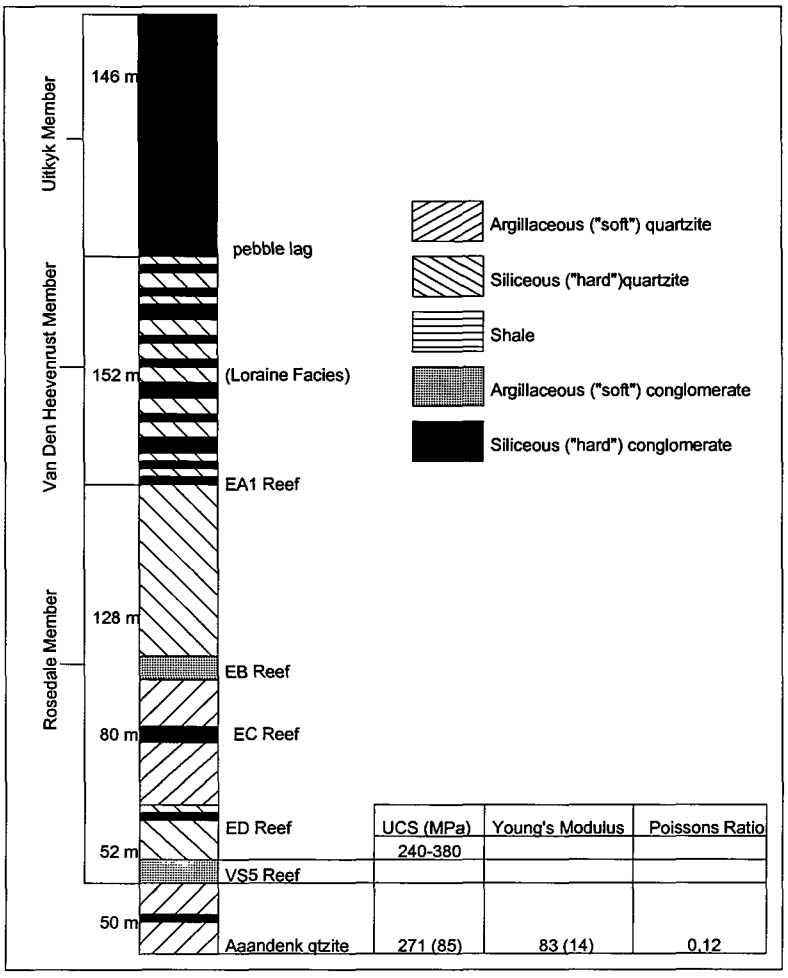

Figure 1.4.25 Generalized stratigraphic column of the Elsburg succession, Free State. Rock engineering properties of the VS5 footwall and hangingwall are also shown.

Geotechnical Areas: VS5

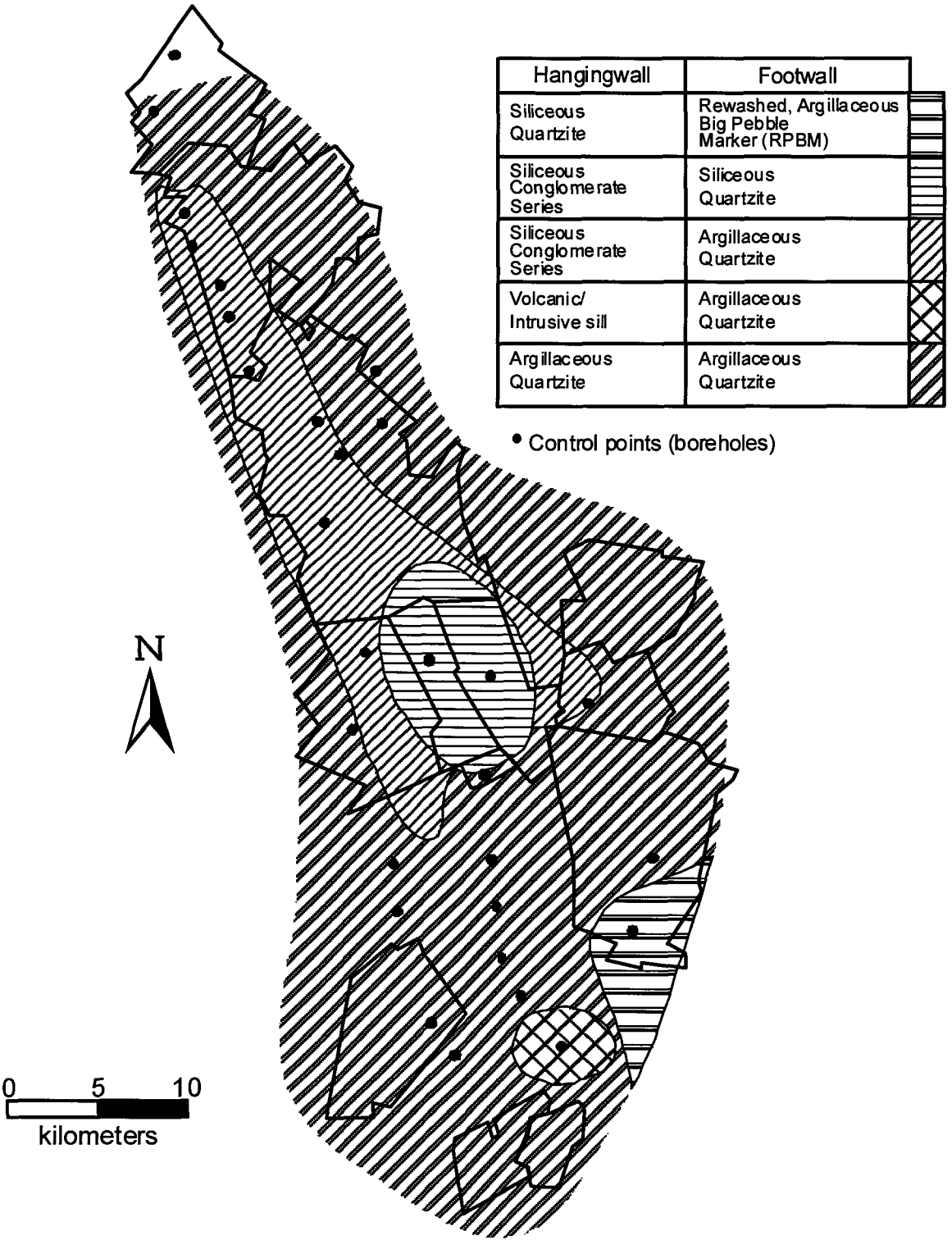

Figure 1.4.26 Geotechnical areas of the VS5 based on various footwall/hangingwall lithologies.

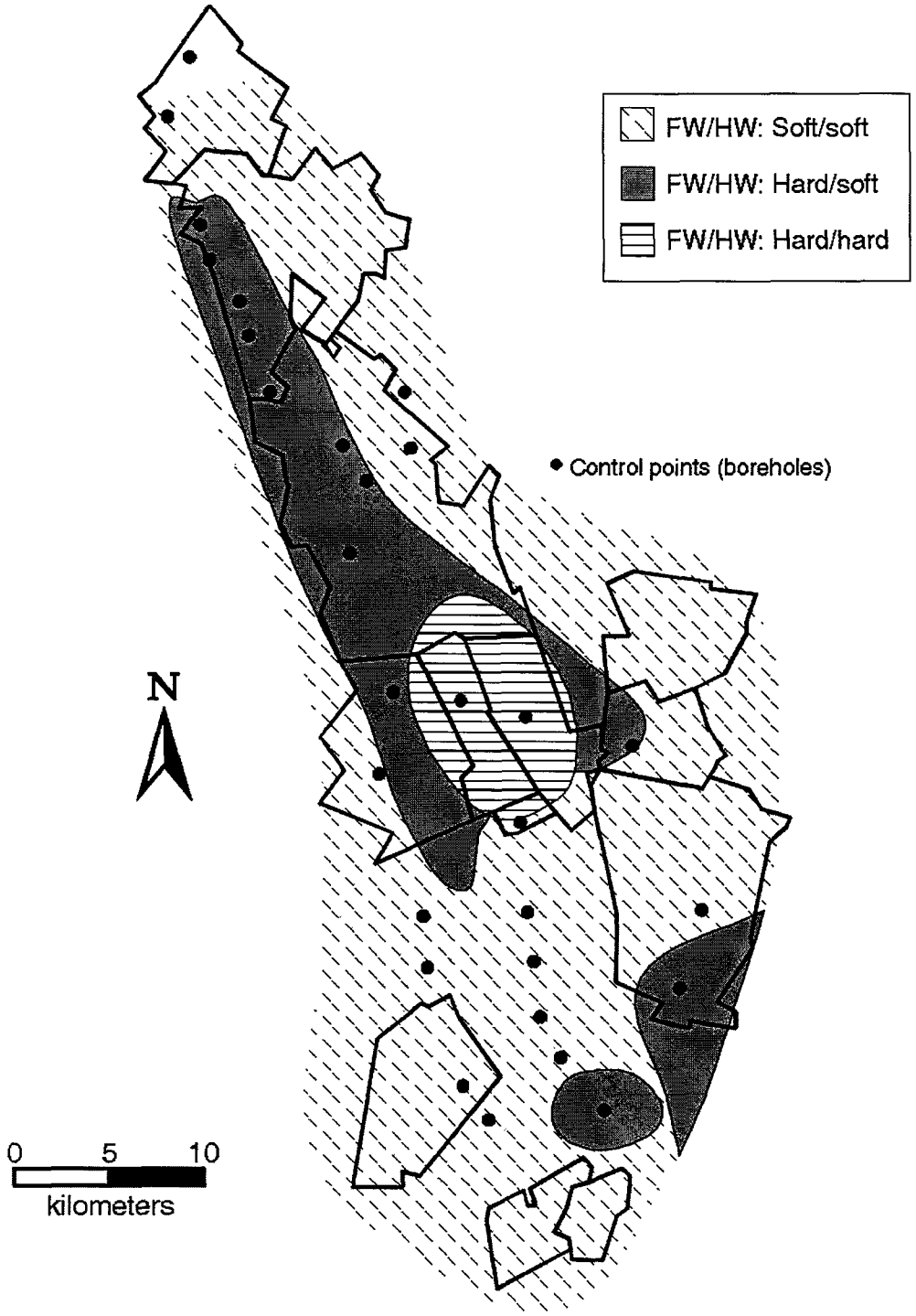

Figure 1.4.27 Map of redefined geotechnical areas of the VS5 based on "hard" and "soft" footwall and hangingwall lithologies.

1.4.1.3 East Driefontein Subgroup

Ventersdorp Contact Reef

The approximately 2800 Ma old (Armstrong et al., 1991) Ventersdorp Contact Reef (VCR) is one of the major South African gold bearing orebodies being mined along the northern and northwestern edge of the Witwatersrand Basin. Its stratigraphic position is shown in Figure 1.1.1. It separates the predominantly sedimentary lithologies of the Witwatersrand from the volcanic Ventersdorp Supergroup (Figure 1.4.28; SACS, 1980).

The geotechnical environment of the VCR was considered in detail by Roberts et al. (1997) and its geotechnical characteristics are briefly summarized here according to Roberts et al. (1997) for completeness, but also because of the re-definition of the geotechnical areas into various hard/soft rock type assemblages.

Superimposing the footwall and hangingwall lithologies results in eleven geotechnical areas (Figure 1.4.29). The approximate coverage of these areas is summarised in Table 1.4.4.

Table 1.4.4 Approximate percentages of geotechnical areas considering siliceous and argillaceous footwall quartzites and conglomerates, and two hangingwall lava types.

Footwall Rock Type	Hangingwall Rock Type	Area Coverage (%)
Siliceous Quartzite	Hard lava	50
Argillaceous Quartzite	Hard lava	20
Siliceous Quartzite	soft lava	10
Siliceous Conglomerate	Hard lava	7
Booysens Shale	Hard lava	5
Argillaceous Quartzite	soft lava	2
Jeppestown Shale	soft lava	2
Argillaceous Conglomerate	hard lava	1
Booysens Shale	soft lava	1
Argillaceous Conglomerate	soft lava	1
Jeppestown Shale	hard lava	1

Further modifications have been made to the above by using the rock strength as a critical parameter to redefine the geotechnical areas (Figures 1.4.1, 1.4.30 and 1.4.31).

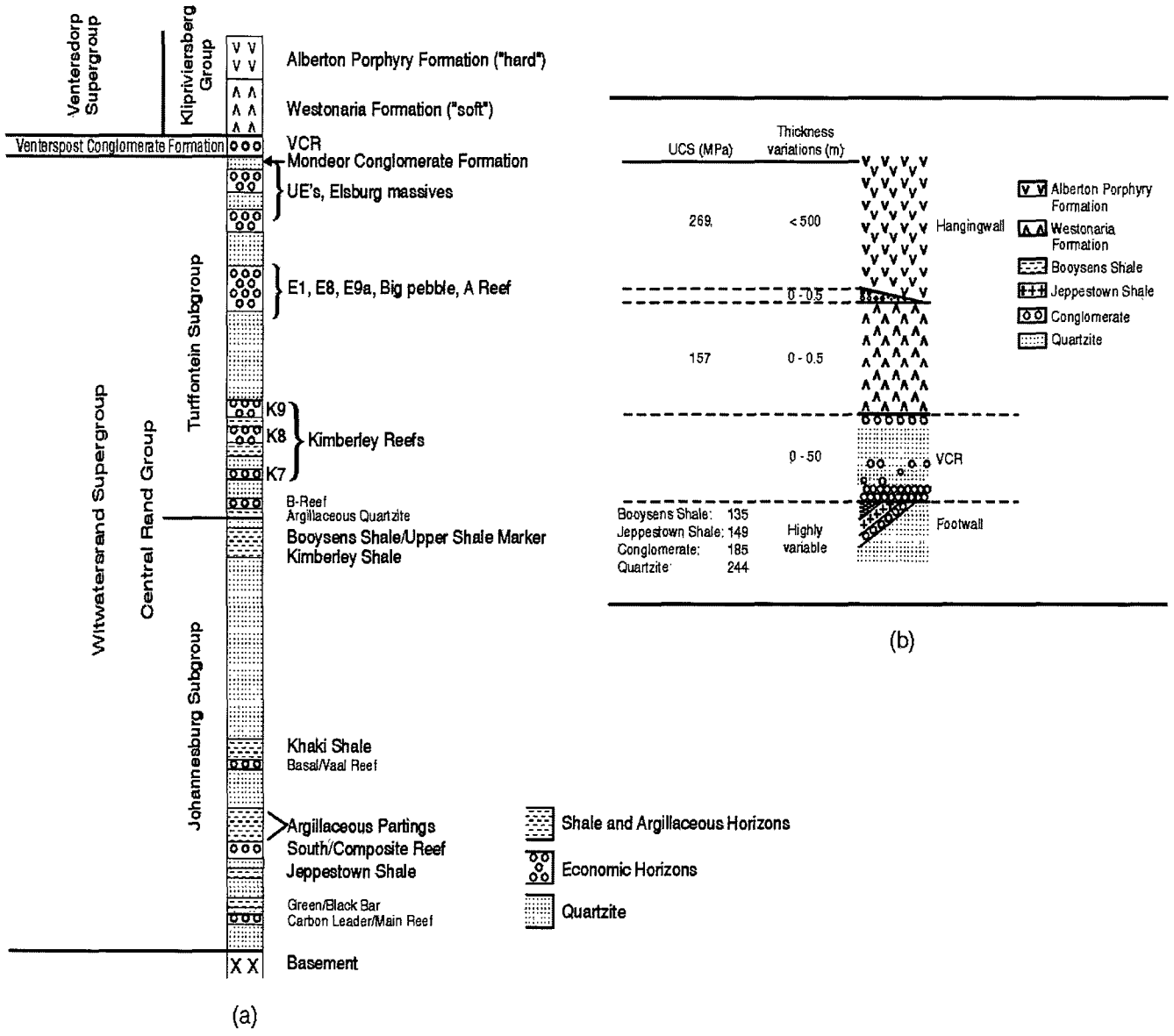

Figure 1.4.28 Stratigraphic position of the Ventersdorp Contact Reef (a). An idealised stratigraphic section through the Ventersdorp Contact Reef and under- and overlying rocks, together with the thickness and uniaxial compressive strength (UCS) variations are also provided (b).

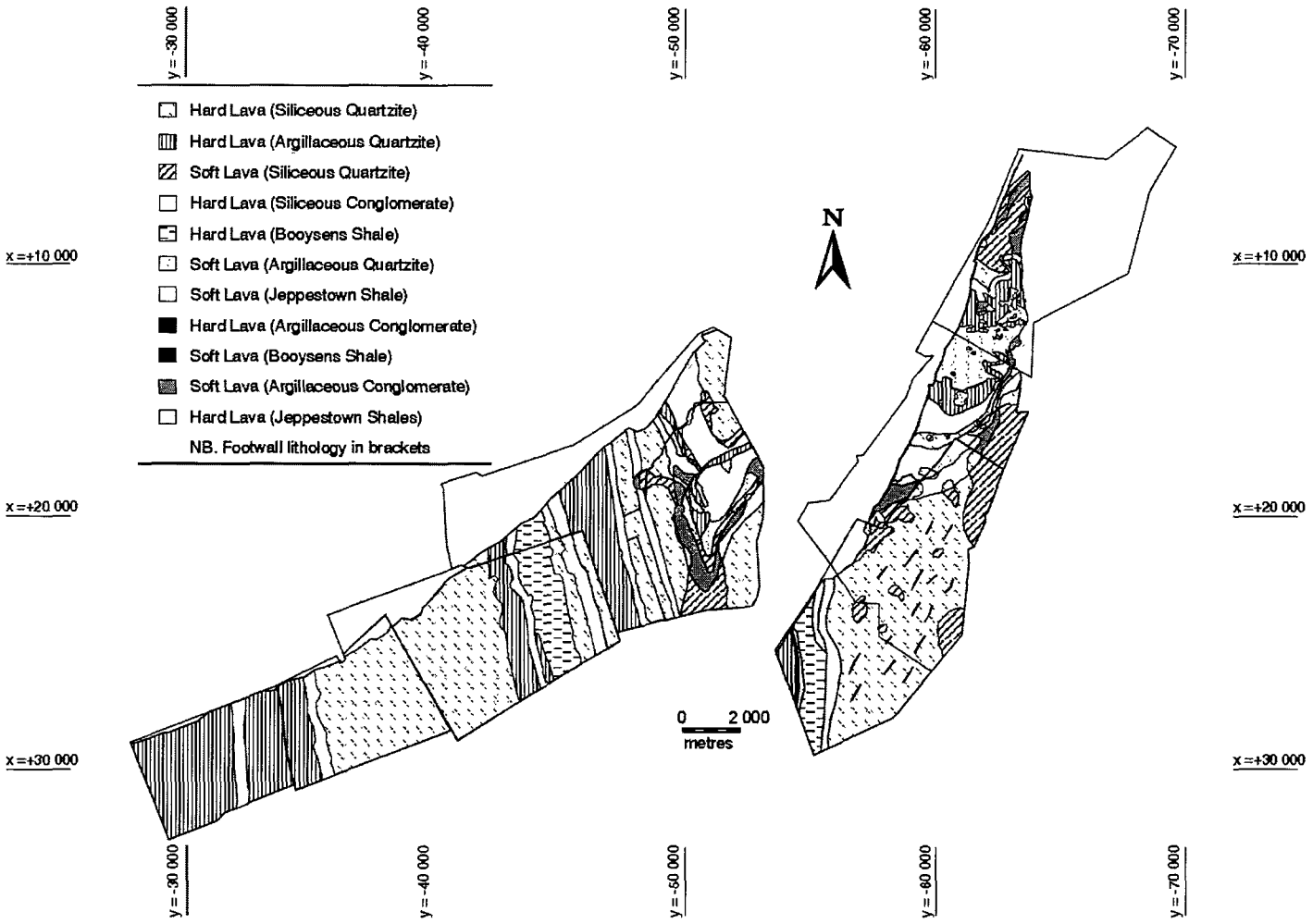

Figure 1.4.29 Geotechnical area map of the Ventersdorp Contact Reef, considering rock type assemblages.

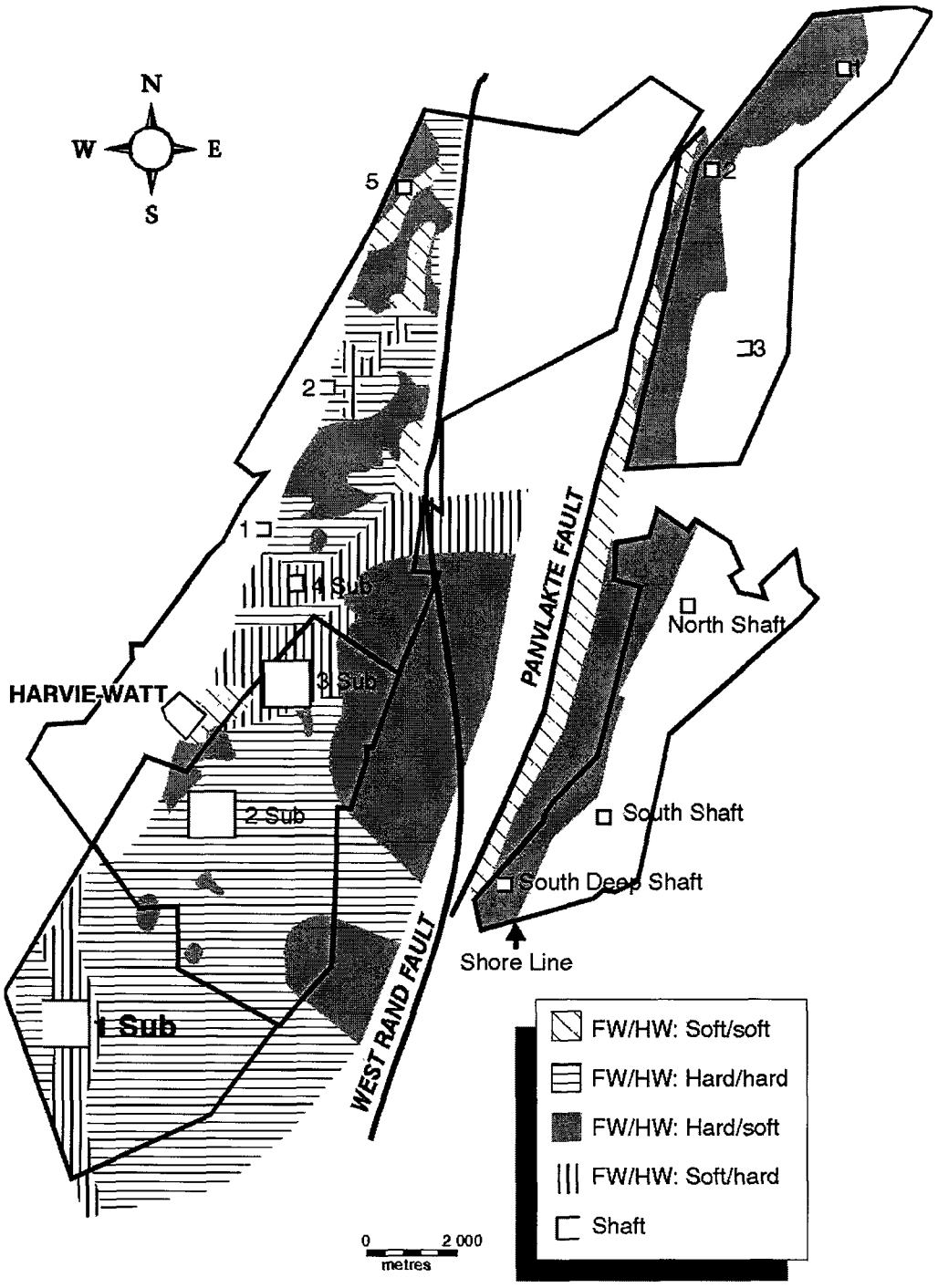

Figure 1.4.30 Redefined geotechnical area map of the Ventersdorp Contact Reef for the West Rand Goldfield, considering rock strengths (see Figure 2.31 for Carletonville Goldfield).

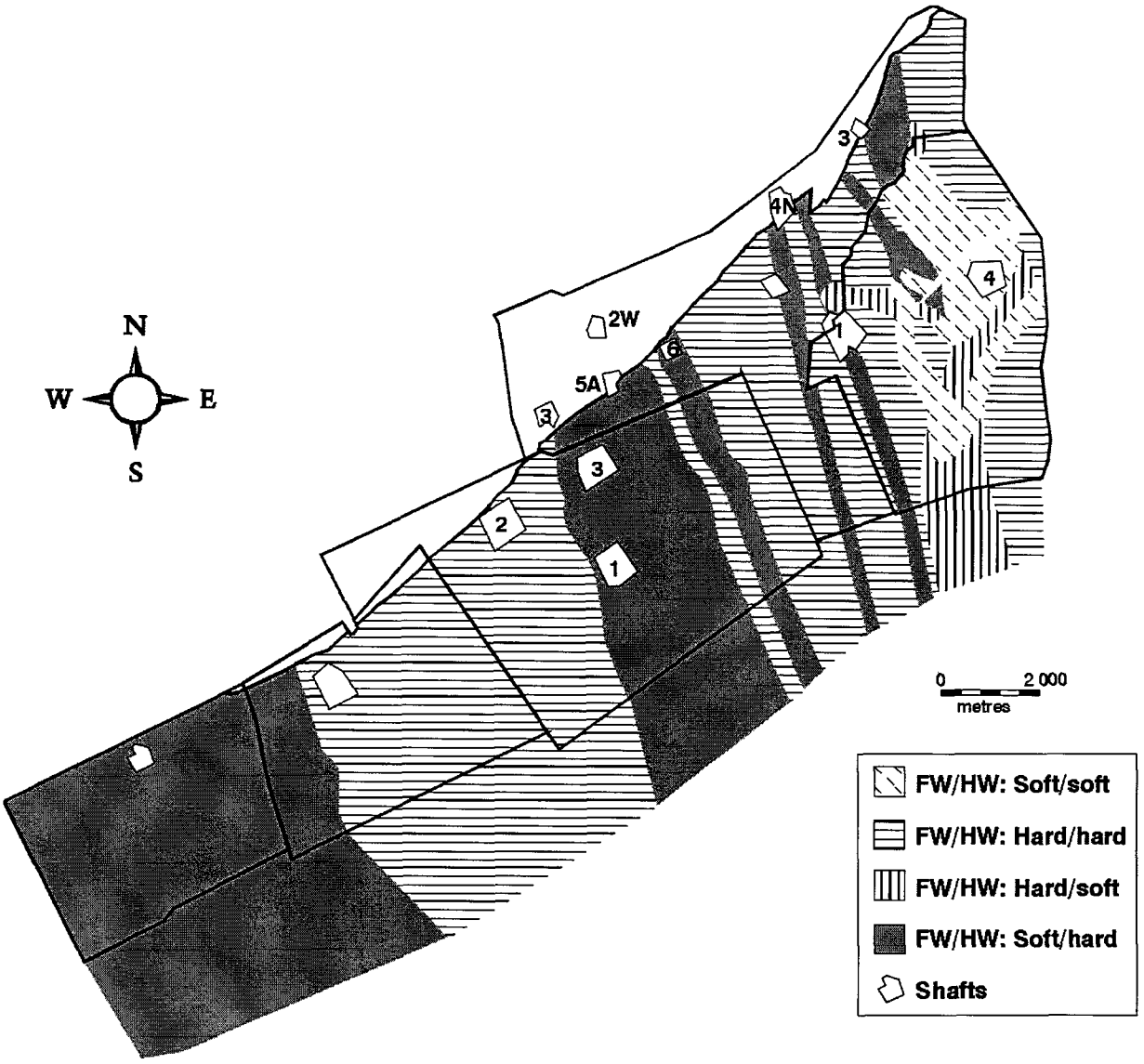

Figure 1.4.31 Redefined geotechnical area map of the Ventersdorp Contact Reef for the Carletonville Goldfield (see Figure 2.30 for West Rand Goldfield).

1.4.1.4 Secondary geological features of rock engineering significance

Secondary geological features such as faults, dykes and joints, where present, may override the rock mass behaviour as expressed by individual geotechnical areas, and, hence, result in a different rock mass behaviour. This could necessitate the delineation of separate distinct geotechnical areas around certain discontinuities.

Faulting and dyke intrusions of many ages are prominent in the orebodies. Fault displacements can amount to several kilometres. Major faulting and dyke intrusion was, however, associated with the Ventersdorp, Bushveld, Pilanesberg and Karoo events. It is considered that seismicity is less pronounced in the Free State, when compared to that of the Carletonville area. This may be attributed to the shallower depths of Free State mining and fault rock characteristics. Our study, in addition, reveals that the majority of the Free State orebodies are mined in "soft" geotechnical environments, and this could be a contributing factor to reduced seismicity.

The structural history of the northern edge of the Witwatersrand Basin was already dealt with by Roberts et al. (1997). This section, therefore, serves to highlight some structural aspects pertinent to the geotechnical environments, as delineated for the Klerksdorp and Free State Goldfields. Average maximum horizontal stresses for these regions are depicted in Figure 1.4.32.

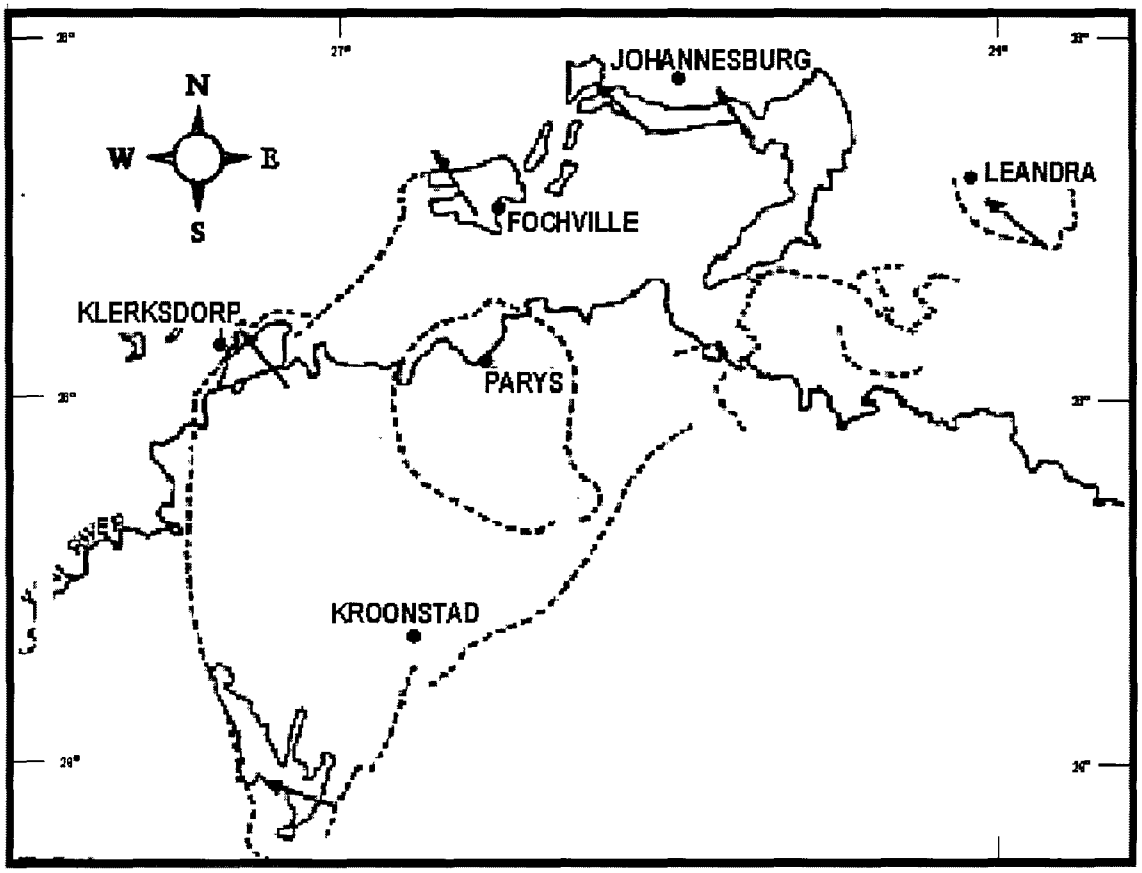

Figure 1.4.32 The orientations of average maximum horizontal stresses in the Witwatersrand Basin (after Gay and Jager, 1986).

Klerksdorp Goldfield

Joints may exert a significant influence on the stability of the excavation, resulting in weak hangingwall conditions (Heunis, 1976). Van der Heever (1982) has shown that the hard, brittle quartzites associated with the Vaal Reef show a higher degree of near vertical jointing, with a more regular spacing than the argillaceous varieties. Joints parallel to the bedding are best developed in the argillaceous units. For example, the frequency of steeply dipping joints in the siliceous MB 7 is 15/100 m, whereas in the argillaceous (MB6) it drops to 10/100m.

Van der Heever (1982) has distinguished three joint sets in the Klerksdorp area (Figure 1.4.33):

Set 1: 345/60° E
Set 2: 065/80° NW
Set 3: Bedding-parallel joints

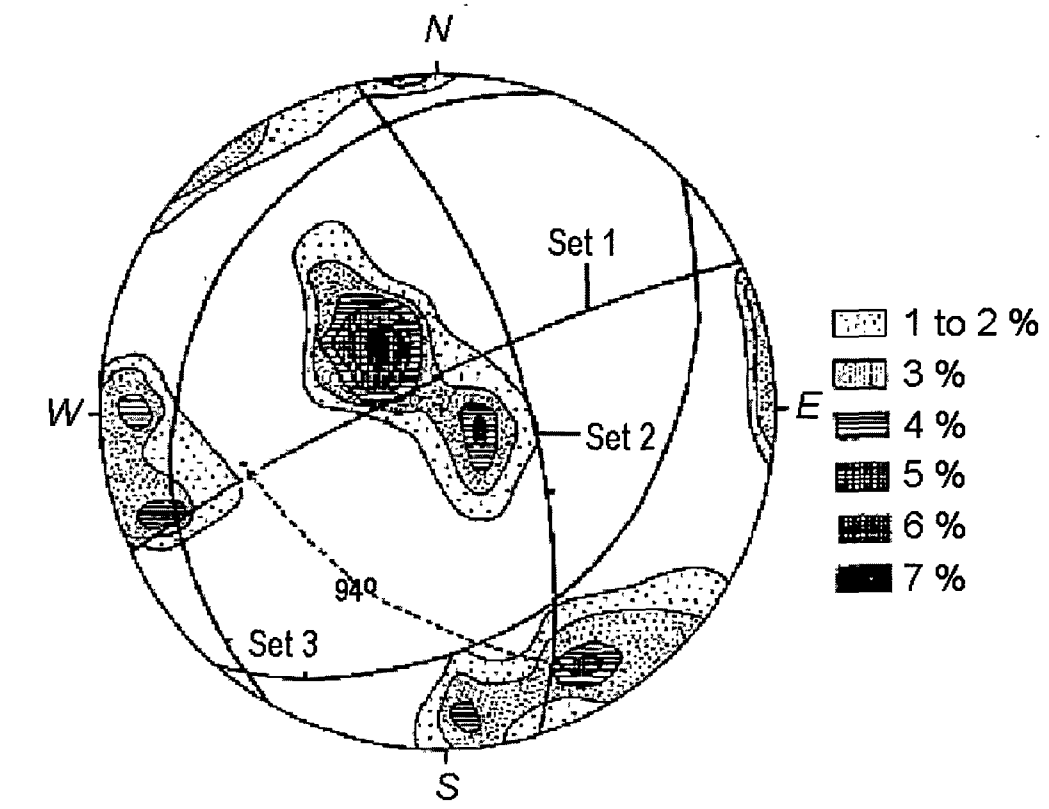

Figure 1.4.33 Joint distribution in the Klerksdorp area, indicating three populations of joints (lower hemisphere equal area projection; after van der Heever, 1982).

The relationship between seismic events and the spacial distribution of joints is not clear, due to the fact that the interval of jointing (1-2 m) is outside the resolution of the seismic location system. Gay and Jager (1986), however, argue that joints are too small to be able to store sufficient energy to precipitate a large seismic event. Quaye (pers. communication, 1996) has shown that where joints intersect with other structures, like bedding-parallel faults and mining induced fractures, in the hangingwall of mining areas, rockfalls may occur as soon as the "supporting" reef is mined. Further investigations are required to study the relationship of such intersecting structures and the Vaal Reef rockmass behaviour.

The regional structure in the Klerksdorp Goldfield is dominated by NE-SW striking faults, with most of the faults being extensional (Figure 1.4.34). Many of the faults are intruded by dykes. Gay and Jager (1986) pointed out that the Klerksdorp and Welkom Goldfields differ from other Witwatersrand goldfields, in that they are cut by major faults with throws of several hundred metres and that the largest magnitude events occur in these two goldfields, with many seismic events located in the vicinity of major faults.

Bedding-parallel faults in the Klerksdorp Goldfield are also often associated with seismic events (van der Heever, 1982). Special attention is drawn to bedding-parallel faults associated with the contact between the Grey-Glassy and the Zandpan Marker (Figure 1.4.11), expressed by slickensides and quartz veins along this contact. Because bedding-parallel faults are assumed to step up in stratigraphy, resulting in the formation of "ramps" (Boyer and Elliot, 1982), they may result in hazardous hangingwall conditions. Detailed structural studies are required to assess the influence of these discontinuities on rockmass behaviour. It is noted that two of the documented joint sets are parallel to major faults, i.e. the NE/SW and the bedding parallel faults (Figures 1.4.33 and 1.4.34).

The structural history in the Klerksdorp Goldfield is, however, not fully elucidated, yet. Of note is a horizontal stress anisotropy in the Klerksdorp area, with the maximum horizontal stress being NW-SE oriented (Figure 1.4.32; Gay and Jager, 1986). This may be due to residual stresses, associated with the earlier depositional, erosional and tectonic histories of the rocks. Where such residual stresses occur, stored within the fault and the immediately adjacent strata, mining-induced stresses may perturb the fault, resulting in a seismic event. Notably, this stress direction coincides with the movement direction of a thrust event in post-Ventersdorp Contact Reef, documented in the Carletonville area (Berlenbach, 1995).

Van der Heever (1982) distinguishes nine different classes of dykes, also suggesting a complex structural and igneous history. Schweitzer and Johnson (1997) suggest that the composition of dykes may influence the proneness to rockburst. For example, siliceous Ventersdorp dykes are proposed to be seismically more active than less competent dykes. A classification of dykes, depending on their ages, orientation and composition would, therefore, aid the assessment of rockmass behaviour associated with the Vaal Reef.

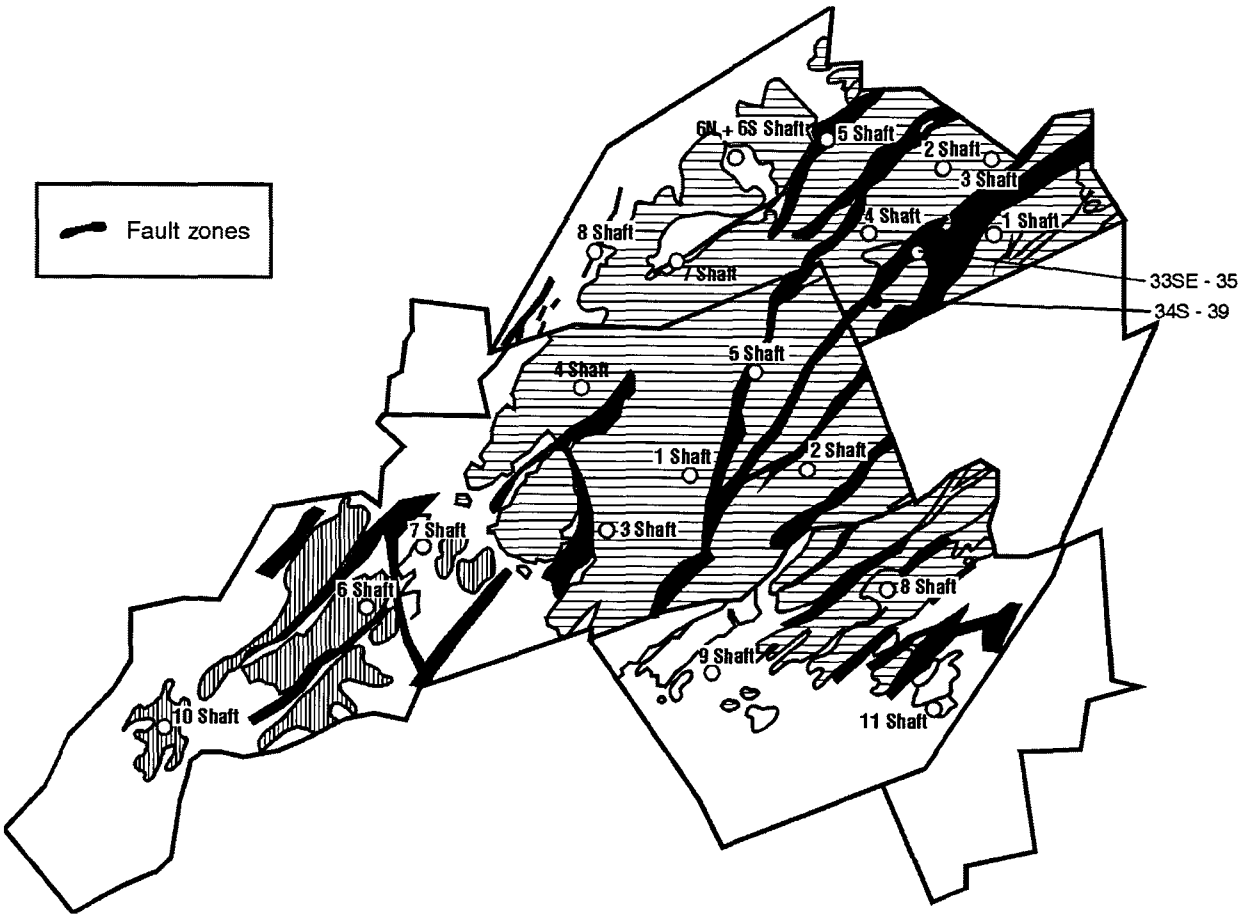

Figure 1.4.34 Major normal faults in the Klerksdorp area. The faults are mainly extensional, but were reactivated during various tectonic events. Also shown are the mined-out areas for the Vaal Reef (horizontal hatching) and the Ventersdorp Contact Reef (vertical hatching).

The Free State Goldfield

The Free State Goldfield is structurally complex (Figure 1.4.35). This is due the long and protracted tectonic history of the area (Rompel, 1995). A brief summary of the tectonic history is given below.

The orebodies of Central Rand Group age were deposited during a syn-sedimentary contractional event, which resulted in the development of a downwarped basin in the front of the orogeny. The auriferous sediments deposited in this basin, hence, have a series of onlapping unconformities, thinning rapidly to the west and south (Figure 1.4.17). This initial shortening event eventually produced thrusting of up to 350 m, as well as overfolding of many of the orebodies. At the end of this phase there was a period of low-angle normal faulting (mainly along the pre-existing thrusts).

The oldest dykes to intrude the strata are tholeiites of the Orkney and Jeanette Formation (Klipriviersberg Group). The dykes were faulted by a strike-slip event that also resulted in folding of the Klipriviersberg lavas. The faults were, in turn, displaced by the major Platberg extension event (including the De Bron, Arrarat and Dagbreek faults). These faults form a complex braided system and are important for fault-loss investigations of many of the reefs. The Platberg age faulting was followed by the extrusion of younger Ventersdorp lavas, which were partially eroded during a period of further contraction. Later ilmenite dykes (probably of Bushveld Complex age) intruded subsequently, to be followed by Karoo age dykes, associated with the break-up of Gondwana

during Jurassic times. Dyke intrusion terminated with several Cretaceous kimberlitic dykes. Recent seismic analyses show a normal dip-slip movement, particularly along the Platberg age faults. Seismicity along the major geological discontinuities appears to be less pronounced in the Free State when compared to the northern edge of the Witwatersrand Basin. It can be speculated that this is because of the shallower depth of mining in the Free State. Mendecki (1997) also suggests that the minimal damage caused during large magnitude events (such as the 1989 Brand earthquake, which was a local magnitude 4.7) may be due to the "soft' nature of the fault rock. In the case of the Brand fault, the fault rock is predominantly pyrophyllite (Mendecki, 1997). We argue that the minimal damage is rather due to the "soft" nature of the rock around the excavation, with the talcaceous fault rock (Mendecki, 1997) being prone to slip.

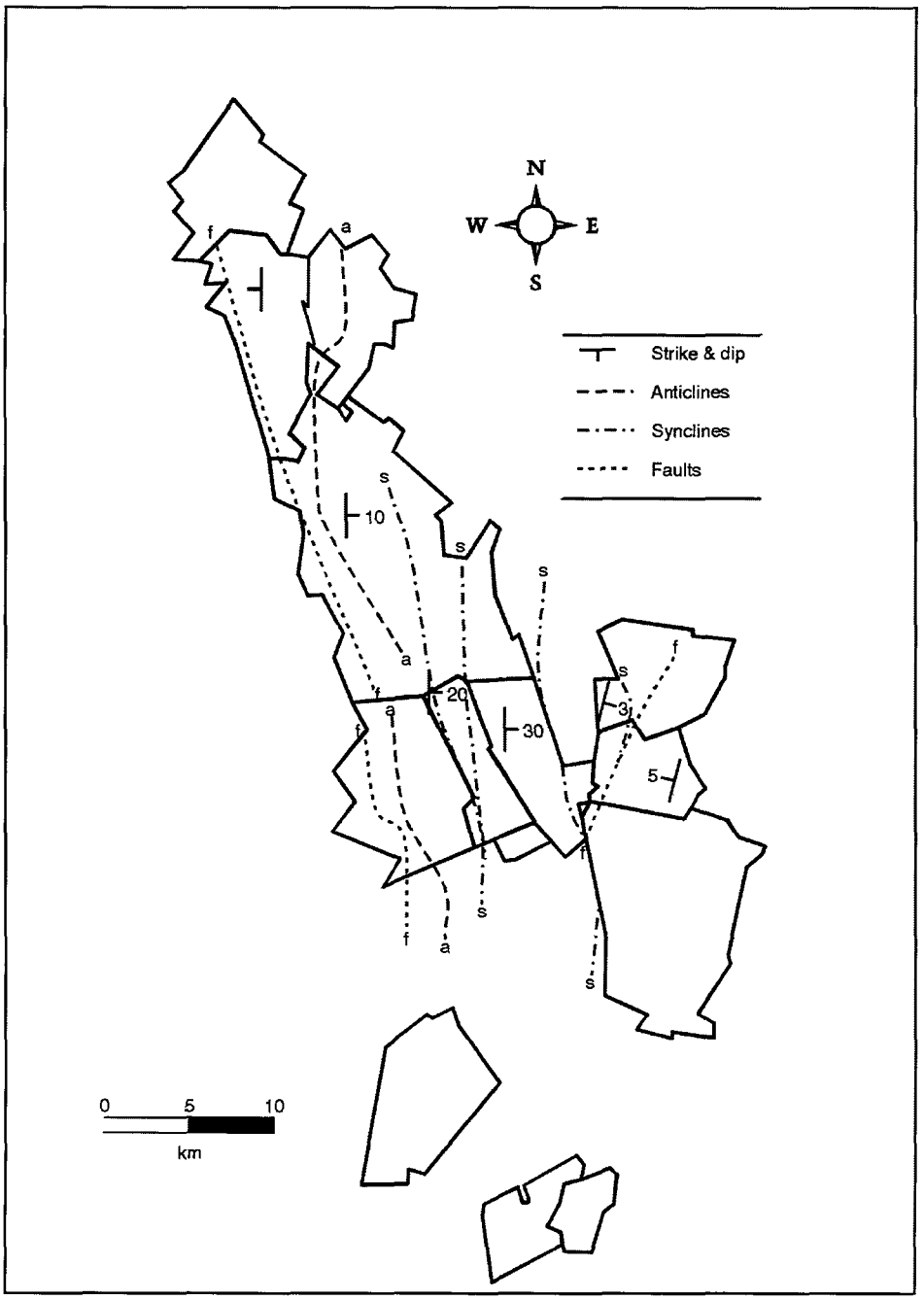

Figure 1.4.35 Major structural features of the Free State Goldfield. Also shown are the outlines of the mine boundaries (after Rompel, 1995).

1.4.2 Potential geotechnical areas, Bushveld Igneous Complex

This study concentrates on the mafic rocks of the Critical Zone of the Rustenburg Layered Suite, which contains various platiniferous and chrome bearing reefs (Figures 1.4.36 to 1.4.39). Rock engineering properties of the strata associated with the Bushveld orebodies are highly variable, even within one rock type. Highest UCS values are, however, generally exhibited by anorthosites (>200 MPa), with mottled and spotted anorthosites generally displaying lower UCS's (160 - 180 MPa). UCS values are highly variable for pyroxenites and vary from 100 to 190 MPa. Norites and melanorites range from about 120 - 170 MPa.

Borehole information on a regional scale around the Bushveld Complex (Figure 1.4.36 and 1.4.37) is used to delineate any variability of footwall and hangingwall rock types to the UG2 and Merensky Reef. As the rock type has an essential influence on the rock mass behaviour, it is apparent that this information, particularly on a more refined local or mine scale, contributes to defining stope support systems requirements and strategies.

One aim of the investigation is to develop a fence diagram around the Bushveld Igneous Complex (eastern and western limbs) to facilitate the identification of the following geotechnical parameters:
a) beam thickness,
b) footwall partings,
c) variability of footwall and hangingwall rock type assemblage, and
d) UG2 and Merensky Reef middling thickness.

From the preliminary results, which are summarized in Figures 1.4.37 and 1.4.38, it is concluded that there exists a very good potential for locally defining geotechnical areas within the Bushveld Igneous Complex, warranting a much more detailed assessment.

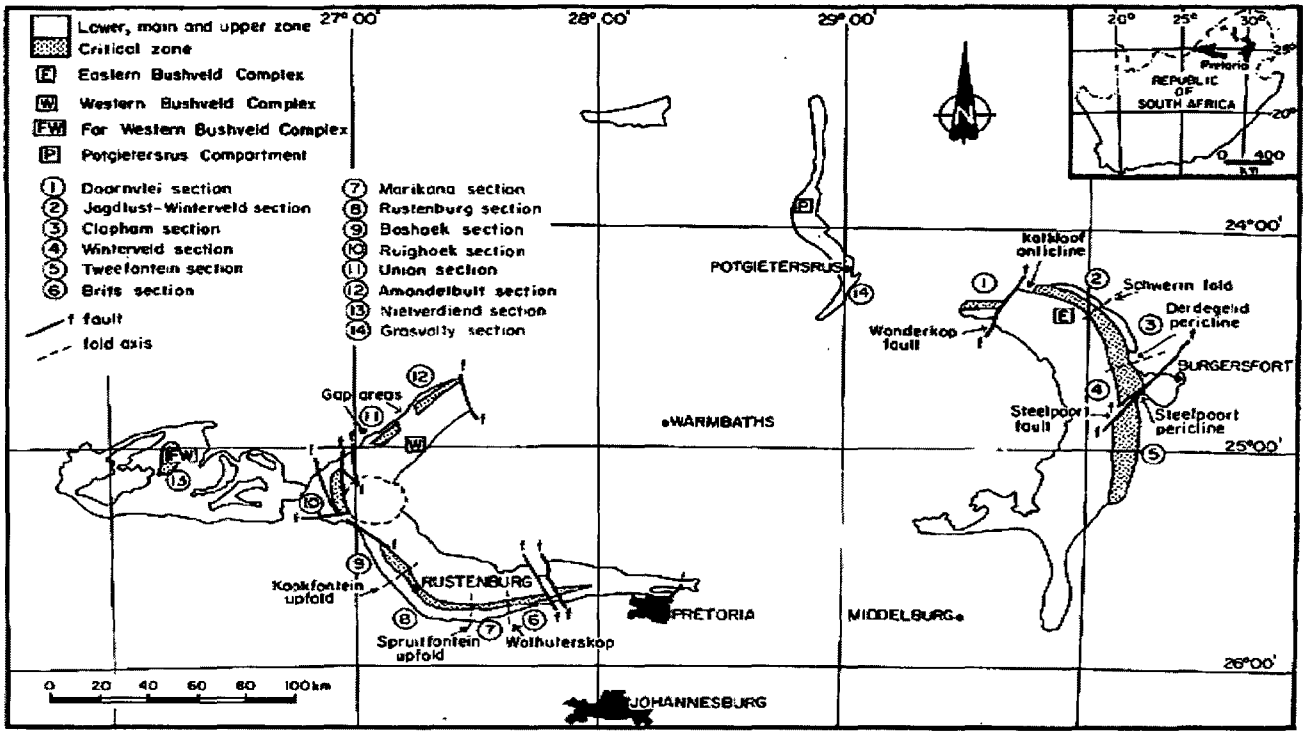

Figure 1.4.36 Outline of the Bushveld Igneous Complex with position of mines and boreholes (Figure 1.4.37).

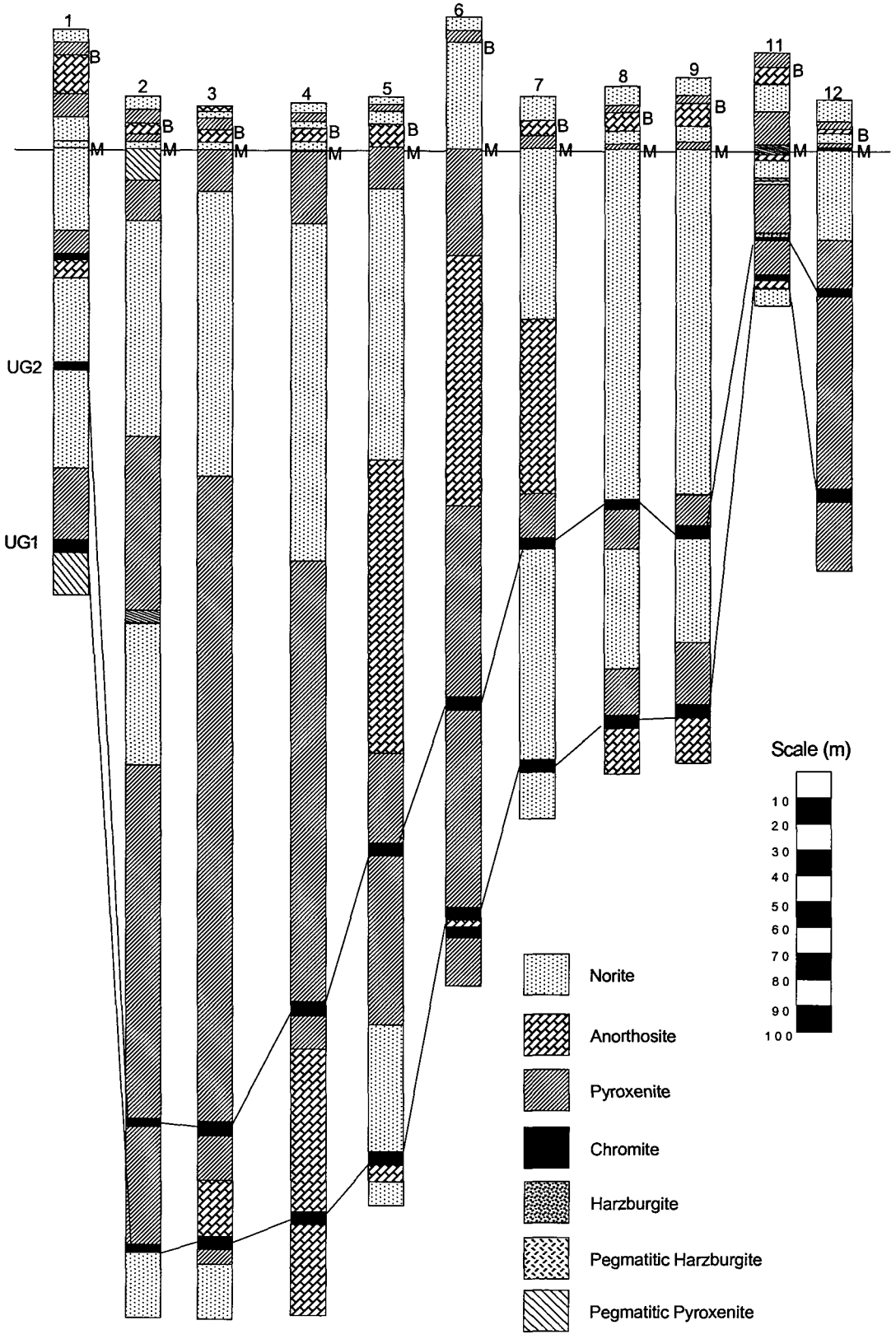

Figure 1.4.37 Boreholes from various localities around the Bushveld Igneous Complex indicated in Figure 1.4.36. Position of various rock types and orebodies are also indicated.

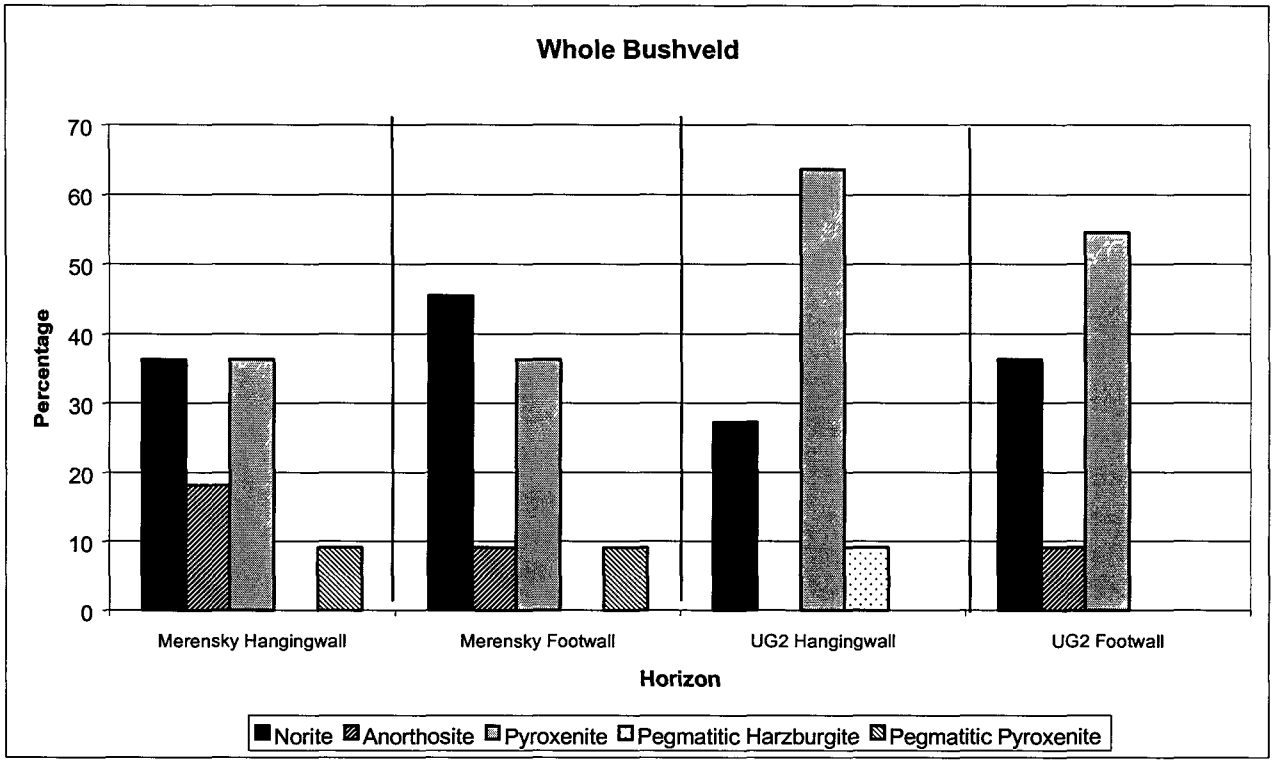

Figure 1.4.38 Different footwall and hangingwall rock types associated with the Merensky Reef and the UG2 (see text for discussion).

UG1 and UG2

The upper group chromitites are of great lateral extent (Figure 1.4.37). They usually consist of two chromitite layers, UG1 and UG2, although in the central sector of the eastern Bushveld Complex layers, UG3 and UG3a, are developed. In addition, thin chromitite layers, present in the overlying Merensky and Bastard Reefs have traditionally been included in discussions of the upper group. The stratigraphy, thicknesses and compositions of the upper group chromitite layers show considerable variations throughout the Bushveld Complex. The high degree of variability invites a detailed analysis of the different footwall and hangingwall lithologies throughout the Rustenburg Layered Suite and their associated rock mass behaviour, potentially resulting in the establishment of geotechnical areas. Due to the high variability of footwall and hangingwall lithologies, the following discussion of the assemblages are only an example. The Rustenburg section on Rustenburg Platinum Mines (RPM) (Figure 1.4.37, Section 8) is chosen as a reference section.

The UG1, the lowermost of the upper chromitite layers is one of the most distinctive and persistent chromitite layers within the Rustenburg Layered Suite (Viljoen and Hieber, 1986). On RPM, the main layer has an average thickness of 70 cm, which can, again, vary considerably. The footwall of the UG1 is anorthosite, followed by pyroxenite, both found within the multiple chromitite layers of the UG1 and in the immediate hangingwall.

The fine to medium-grained pyroxenite passes sharply upwards into an anorthositic norite. The norite continues up to the UG2. Pyroxenite is again encountered above the UG2 chromitite layer, and norite is present above the pyroxenite up to the next unit, the Merensky Reef. Two thin

chromitite layers are developed above and below the Merensky pegmatoid, a pegmatoidal pyroxenite in which platinum-group elements are concentrated.

The UG2 forms the uppermost of the substantial chromitite layers within the Rustenburg Layered Suite and on RPM it lies approximately 140 m below the Merensky Reef. The overlying 8 m of feldspathic pyroxenite contain up to three chromitite layers (three leaders or triplets), each several centimetres thick, within the first 1 m above the main layer. It is noted that lithological contact relationships of the various strata range from sharp to transitional. The sharp contacts are of significance to rock engineering and they are commonly associated with chromitite layers.

From Figure 1.4.37 it can be concluded that 4 footwall/hangingwall rock type assemblages can be distinguished for the UG2. These are: Norite/Norite; Pyroxenite/Pyroxenite; Norite/Pyroxenite; Pyroxenite/Norite. The varying distance of parting planes, such as those caused by the triplets on top of the UG2, also need to be taken into consideration. The relative abundances of the various footwall and hangingwall lithologies are displayed in Figure 1.4.38. Pyroxenite is the most common followed by norite, which is the second most common footwall and hangingwall lithology of the UG2.

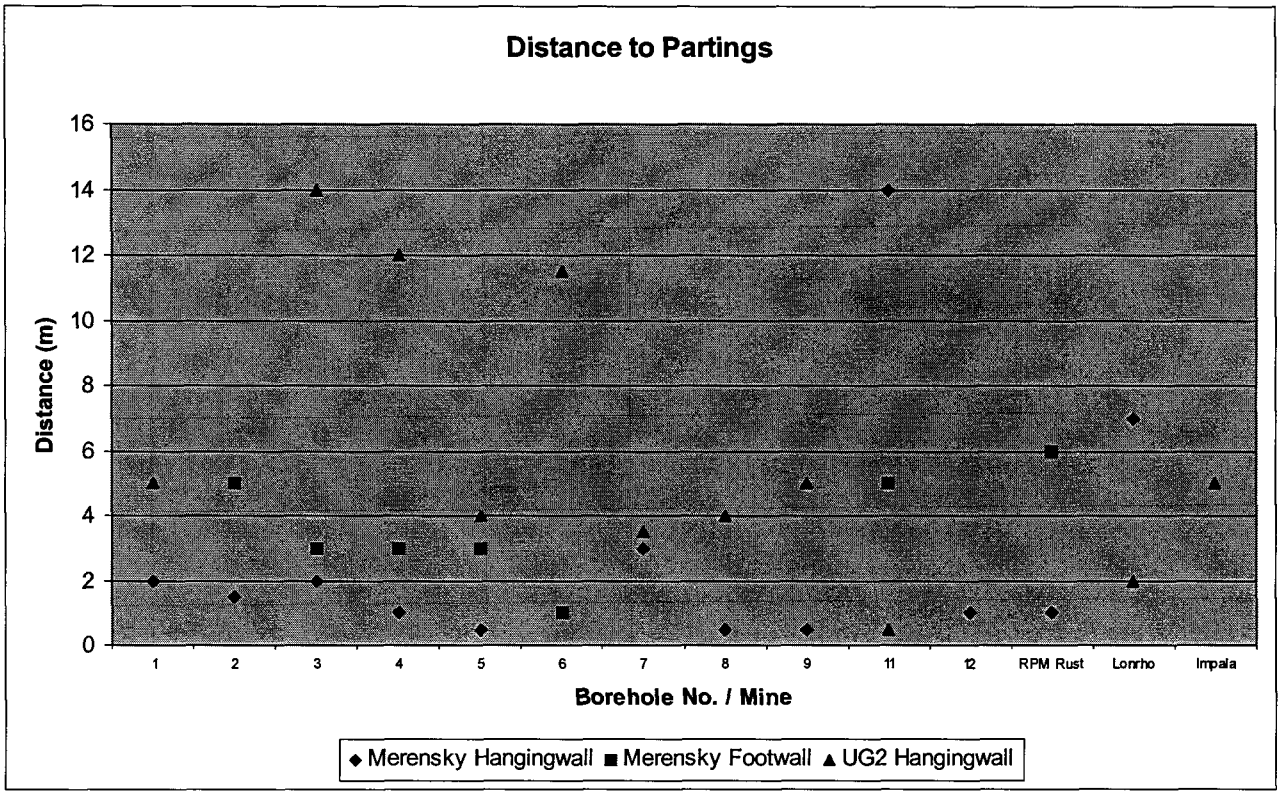

Figure 1.4.39 Distance of partings in footwall and hangingwall of the Merensky Reef and the UG2 (see text for discussion).

Merensky Reef

The Merensky Reef unit, which includes the pyroxenitic Merensky Reef, is remarkable consistent in thickness across the whole Rustenburg Section, varying between 9 and 10 m (Viljoen and Hieber, 1986), unless potholes are encountered. The Merensky Reef unit commences with the pyroxenite layer with associated chromitite layers, and is overlain by a differentiated suite consisting of norite, anorthositic norite, spotted anorthosite and, finally, mottled anorthosite.

The Merensky Reef forms the lowermost part of the basal pyroxenite/chromitite assemblage of the Merensky Reef unit. It commences with a thin, 1 cm thick chromitite layer which rests, in most instances, directly on underlying anorthositic norite. The lower chromitite layer is well defined and is immediately overlain by a pegmatoidal feldspathic pyroxenite, which, for large areas of the Rustenburg Section, averages 25 cm in thickness. A second chromitite band (1 cm thick), occurs at or close to the top of this coarse-grained unit and demarcates the top of the geological entity termed the Merensky Reef. The upper chromitite layer is overlain by a medium-grained poikilitic pyroxenite, the so-called "Merensky pyroxenite". The Merensky Reef is on average, mined at a stoping width of 1 m.

The dominant silicate in the pegmatoidal reef is bronzite, which accounts for 80 per cent by volume of the reef and occurs as closely packed, subhedral to euhedral crystals. The less abundant plagioclase feldspar is intercumulus. Biotite, hornblende and magnetite are accessory minerals. Base-metal sulphides and (PGM) form minor constituents in the spotted anorthosite footwall for several centimetres below the reef in some areas. These tend not to be present in the mottled anorthosite footwall. In order of diminishing abundance, these ore minerals are: pyrrhotite, pentlandite, chalcopyrite, and pyrite (Viljoen and Hieber, 1986). Locally the PGE can show a tendency to become either enriched in the hangingwall pyroxenite or in the spotted anorthosite footwall. This may then result in different mining layouts.

The PGM have their highest concentration in the feldspathic pyroxenite, throughout the Rustenburg Section where values account for about 70 per cent of the total PGE mined. As the greater portion is thinner than the minimum practical stoping width, it is necessary to extract material from above and below the reef mining operations. This has also consequences for the evaluation of rock mass behaviour, since it requires knowledge of the hangingwall and footwall lithologies, their composition (which influences strength of the rock), fabric development (igneous and structural) and the formation of faults and joints in the hangingwall of mining areas, which may control potentially hazardous conditions.

Based on the borehole information presented in Figures 1.4.37 and 1.4.38, six footwall/hangingwall rock type assemblages are distinguished for the Merensky Reef. These are: Norite/Norite; Pegmatitic Pyroxenite/Norite; Pyroxenite/Norite; Pyroxenite/Anorthosite; Norite/Pyroxenite; Norite/Pegmatitic Pyroxenite. Norite is the most abundant footwall lithology for the Merensky Reef. Norite and pyroxenite occur in equal proportions in the hangingwall of the Merensky Reef.

Bastard Reef

The Bastard Reef unit (Figure 1.4.37) shows a similar cyclicity as the Merensky Reef unit, viz. a basal pyroxenite grading upwards into a norite, spotted anorthosite and terminated by very well-developed mottled anorthosite. The whole unit is, however, over 100 m thick, compared to 9 m for the Merensky Reef unit. The lowermost poikilitic pyroxenite constituting the Bastard Reef is frequently marked by a chromitite layer or parting along its base, although this is not developed everywhere. Odd scattered patches of coarser grained and pegmatoidal pyroxenite are developed immediately above the basal contact, and low PGE values are also sometimes encountered at or

close to this contact. The unit culminates in the mottled anorthosite, which also demarcates the top of the Critical Zone of the Rustenburg Layered Suite.

In summary, it can be concluded that the rock assemblages encountered within the various chromitite and platinum orebodies are variable. More importantly, footwall and hangingwall lithologies of the orebodies vary regionally (Figure 1.4.38).

As the various footwall and hangingwall lithologies could exert different rock mass behaviours, it is proposed that the compilation of geotechnical areas, defined by hard and soft footwall/hangingwall assemblages can yield important information for the correct choice of support types and support strategies. Different rock types, in addition, could have distinct joint sets. Relatively hard anorthosite may require a different support type when compared to relatively friable pyroxenite.

Figure 1.4.39 displays the average distances of partings in the footwall and hangingwall of the Merensky Reef and the UG2. It can be stated that the average distance of partings in the hangingwall of the UG2 exceeds the average distance of partings in the Merensky Reef. Partings are, however, common in the hangingwall of both UG2 and Merensky Reef, and occur in the immediate hangingwall up to a distance of 14 m. The highest frequency of partings is encountered within 6 m hangingwall distance to the orebodies.

1.5 Summary and discussion

A literature review reveals that a huge scope exists for multidisciplinary studies that identify and evaluate geotechnical environments as associated with the Witwatersrand and Bushveld ore deposits. Two major types of geotechnical area maps have been compiled for eight Witwatersrand and the two major Bushveld orebodies. These maps were, initially compiled on the basis of rock type, the associated mineral assemblage, and the distance to pronounced partings. Information from exploration boreholes were utilised to predict the geotechnical environment in areas to be potentially mined. Major fault, dyke, joints, and channel features were also documented. Subsequently, the various rock types were correlated with their respective UCS', resulting in maps featuring "hard" and "soft" footwall and hangingwall lithologies. It is proposed that a cut-off value of 200 MPa can be employed to classify strata as either soft or hard. The compilation of the latter type of geotechnical area map aims at evaluating and predicting regional and local support performance, stope stability, and potential seismicity. The importance of the rock type in determining the attitude and frequency of mining induced fracturing is highlighted in Figures 1.5.1 and 1.5.2. Regional support performance addresses factors such as pillar strength and foundation failure or hangingwall punching. Local support performance, especially, considers the footwall and hangingwall punching of support, thereby also identifying areas were the application of headboard is desirable. Stope stability is predominantly predicted through the delineation of soft footwall regions, where footwall bulging may occur, and major hangingwall partings that also control fall of ground characteristics, such as their heights. The delineated competency of the footwall and hangingwall assemblages provides an indication with regard to closure rate and the attitude and frequency of mining-induced fracturing. The above demonstrates that the compiled maps are of immediate, practical importance (also see Table 1.5.1).

Table 1.5.1 Number of geotechnical areas, as per rock type, presence of partings and UCS, for the Witwatersrand and Bushveld orebodies under consideration.

	Number of geotechnical areas (as per rock type)	Number of geotechnical areas (as per UCS)
Merensky Reef	6	-
UG2	4	-
Ventersdorp Contact Reef (VCR)	11	4
VS5	5	3
Witpan (8A)	2	1
Big Pebble Marker (BPM)	3	2
B-Reef	3	2
Leader Reef	1	1
Vaal Reef	7	4
Carbon Leader	6	4

The number of geotechnical areas, whether defined by rock type assemblage, distance to major hangingwall partings, or employing rock competency (Table 1.5.1), also provide an indication of the diversity and complexity that is associated with an individual orebody. Inspection of Table 1.5.1 reveals that the major orebodies of the West Wits Line (i.e. the Carbon Leader and the VCR), and the Vaal Reef of the Klerksdorp Goldfield are characterized by the most complex geological settings. The Free State orebodies under consideration are, in contrast, except for the VS5, located in less diverse environments.

The preliminary assessment of the geotechnical environments associated with the platiniferous UG2 and Merensky Reef reveals that huge potential exists to establish regional geotechnical maps for these orebodies (Table 1.5.1). Rock types and partings seem to be the major factors controlling rock mass behaviour. Additional geotechnical criteria are potholes, domes, faulting, dykes and jointing.

It is concluded that the outlined geotechnical areas define mining regions that potentially require distinct support strategies.

Table 1.5.2 Anticipated rock mass response as predicted for the defined geotechnical environments.

	Footwall soft[1]	Hangingwall Soft[2]	Competent FW/HW assemblage[3]	Incompetent FW/HW assemblage[4]	Pronounced HW partings[5]
Merensky Reef	tbd	tbd	tbd	tbd	✓
UG2	tbd	tbd	tbd	tbd	✓✓
Ventersdorp Contact Reef (hard lava)	(✓)	n/a	✓	n/a	✓
Ventersdorp Contact Reef (soft lava)	(✓)	✓	(✓)	(✓)	✓
VS5	✓	n/a	(✓)	(✓)	(✓)
Witpan (8a)	✓	✓	n/a	✓	✓
Big Pebble Marker	✓	✓	n/a	✓	(✓)
B-Reef	✓✓	✓	n/a	✓	(✓)
Leader Reef	✓	✓	n/a	✓	(✓)
Vaal Reef	(✓)	(✓)	(✓)	minor	✓
Carbon Leader	With increasing depth	n/a	✓	n/a	✓

tbd = to be determined
n/a = not applicable
(✓) = occurs locally
1 = punching of support; pillar foundation failure; footwall bulging/ride
2 = punching of support; pillar stability
3 = relatively high frequency of mining induced fracturing; relative low closure rates; high stress environment (? seismicity)
4 = relatively low frequency of mining induced fracturing; relatively high closure rates
5 = Height of falls of ground controlled by hangingwall parting

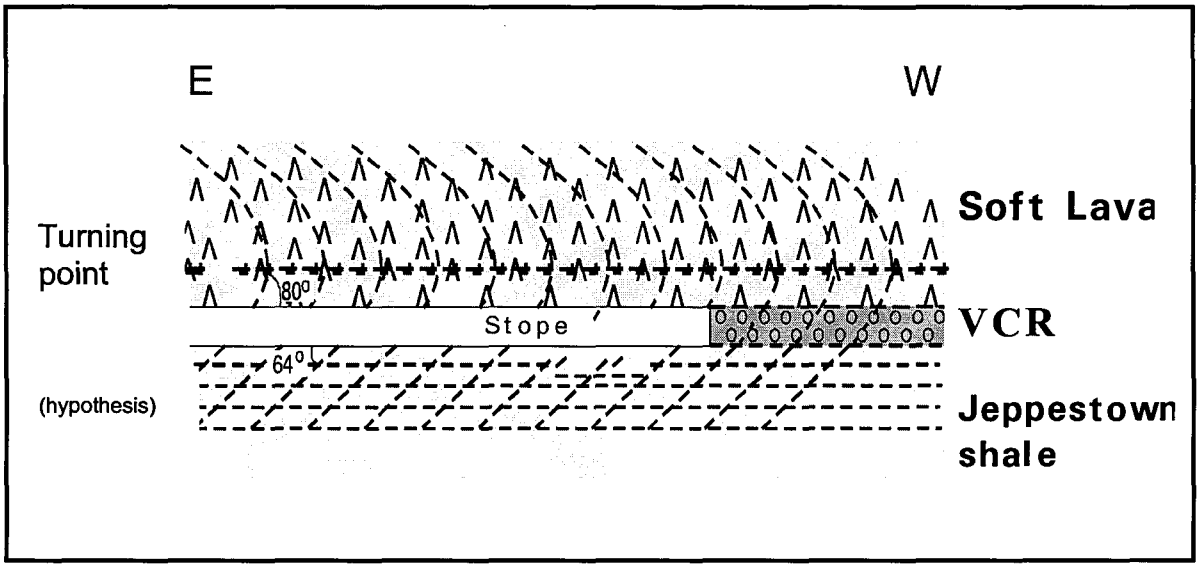

Figure 1.5.1 Attitudes of mining induced stress fracturing at East Driefontein Gold Mine. The point of inflection is interpreted as to occur in the hangingwall of the excavation (after Roberts et al., 1997).

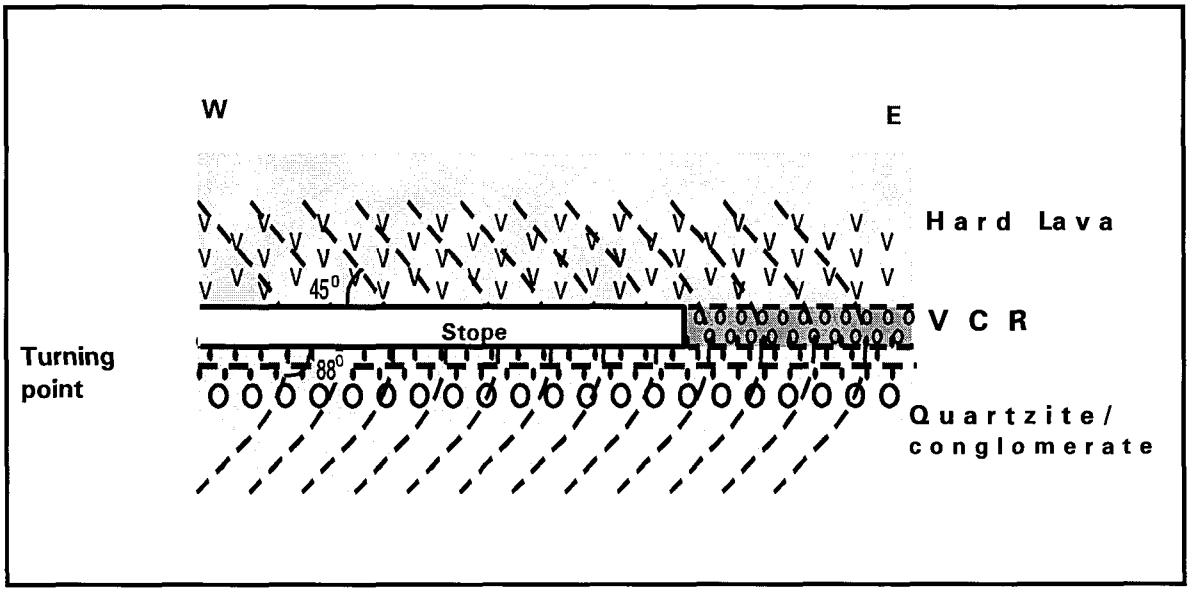

Figure 1.5.2 Attitudes of mining induced stress fracturing at Deelkraal Gold Mine. The point of inflection is interpreted as occurring in the footwall of the excavation (after Roberts et al., 1997).

1.6 Recommendations and suggestions for further studies

This study supports earlier observations that geological parameters have an important impact on rockmass behaviour. It is suggested, however, that the understanding of the relationships between geological features and rockmass behaviour is mostly only empirical, but that the prediction of the rock mechanic behaviour of rocks in specific geotechnical areas is possible. The following major points are recommended as potential, future activities.

a) Geotechnical area maps for the UG2 and Merensky Reef will contribute to the delineation and prediction of areas with varying rock mass behaviour.

b) Future underground studies have to confirm and verify the predictions (see Table 1.5.2) made during this investigation.

c) A base map that shows depth contours, the location of major geological features, and rock types. This information can be gathered from boreholes drilled during the pre-production stage and from historical data from areas of similar geological setting.

d) Thickness contour maps for both hangingwall and footwall strata should be compiled. In addition, dominant joint sets and orientations and mean joint spacing and intensities, associated with each rock type should be documented. This information can be deduced from stratigraphic studies, tapping into experience of both mine geologists and rock mechanics personnel. It is then possible to extrapolate this information from mined out areas to solid ground.

e) Isopach maps showing variations in reef thickness and pay width. This information can also be deduced from boreholes during the pre-production stage of the mine. This facilitates the adoption of correct support strategies that eventually improve support performance.

f) The magnitude and orientation of the principal stresses should be determined. This will help to estimate the k-ratio and in deep mines, the direction of fracturing. Such information influences the correct choice of mining directions.

g) Further investigations are required to quantify the relationship between competency contrast and fracture patterns.

h) Deformation mechanisms associated with the reef horizons are complex, and not well understood, requiring further investigations.

i) Detailed rock engineering property studies could, in the future, define "soft"/"hard" thresholds that are orebody specific. This holds especially true for the UG2 and Merensky Reef.

j) This study highlights the importance of hangingwall partings and their control on stope stability and support performance. A detailed investigation into the behaviour of parting planes will significantly contribute to a better understanding of the relationship between parting characteristics and associated rock mass behaviour.

1.7 References

Antrobus, E.S.A., Brink, W.C.J., Brink, M.C., Caulkin, J., Hutchinson, R.I., Thomas, D.E., Van Graan, J.A., & Viljoen, J.J. , 1986. The Klerksdorp Goldfield. In: Anhaeuser, C.R., and Maske, S. (Editors): Mineral Deposits of Southern Africa, Vol. 1, Geol.Soc.S.Afr., Johannesburg, 549-598.

Armstrong, R.A., Compston, W., Retief, E.A., Williams, I.S., & Welke, H.J., 1991. Zircon ion microprobe studies bearing on the age and evolution of the Witwatersrand triad. Prec. Res. 53, 243-266.

Arnold, D.A., Legg, E.W., & Roberts, M.K.C., 1994. Reducing the unsupported stope span at Hartebeestfontein Gold Mine. XV'th CMMI Congress, Johannesburg, SAIMM, Vol. 1, 159-165.

Atkins, A.R., & Keen, M.A. , 1984. The measurement of rock deformation about excavations in hard rock mining. SANGORN, Monitoring for Safety in Geotechnical Engineering, 47-52.

Berlenbach, J.W. , 1995. Aspects of bedding-parallel faulting associated with the Ventersdorp Contact Reef on the Kloof Gold Mine. S.Afr.J.Geol., 98(4), 335-348.

Boyer, S.E. & Elliot, D., 1982. Thrust systems. Bull.Am.Assoc.Petrol.Geol., 66, 1196-1230.

Engelbrecht, C.J., Baumbach, G.W.S., Matthysen, J.L., & Fletcher, P., 1986. The West Wits Line. In: Anhaeuser, C.R., and Maske, S. (Editors): Mineral Deposits of Southern Africa, Vol. 1, Geol.Soc.S.Afr., Johannesburg, 599-648.

Gay, N., & Jager, A.J., 1986. The influence of geological features on problems of rock mechanics in Witwatersrand Mines. In: Anhaeuser, C.R., and Maske, S. (Editors): Mineral Deposits of Southern Africa, Vol.1, Geol.Soc.S.Afr., 753-772.

Guler, G., 1997. Unpublished MSc. thesis – University of the Witwatersrand, Johannesburg 240 pp.

Gurtunca, R.G., & Gay, N.C., 1993. Rock engineering - implementing the latest developments in improving safety in underground mining operations. Mine Management Forum, Midrand, Johannesburg, 9-10 November, 20 pp.

Heunis, R., 1976. Improvements in the design of seismic location systems and the development of a seismic method for the delineation of geological dykes in mines. M.Sc. Thesis, University of pretoria (unpublished).

Hatton, C.J. & Schweitzer, J.K., 1995. Evidence for synchronous extrusive and intrusive Bushveld magmatism. Journal of African Earth Sciences, 21, 579-594.

Johnson, R.A. & Schweitzer, J.K., 1996. Mining at ultra-depth: Evaluation of alternatives. In: Aubertin et al. (Editors), Rock Mechanics, Balkema, Rotterdam, 359-366.

Kimberley Working Group, 1998. Regional characteristics of the Kimberley succession, with implications for enhanced exploitation and explortion. Consultancy report, CSIR: Miningtek, 32 pp and 60 figures.

Kullmann, D.H., Stewart, R.D., & Lightfoot, N., 1994. Verification of a discontinuum model used to investigate rock mass behaviour around a deep-level stope. SANGORN: Applications of Numerical Modelling in Geotechnical Engineering Symposium, Pretoria, September 1994, 6 pp.

Lightfoot, N., Goldbach, O.D., Kullmann, D.H., & Toper, A.Z., 1996. Rockburst control in the South African deep level gold mining industry. In: Aubertin, M., Hassani, F., and Mitri, H. (Editors): Rock Mechanics Tools and Techniques, Balkema, Rotterdam, 295-303.

Minter, W.E.L., Hill, W.C.N., Kidger, R.J., Kingsley, C.S. & Snowden, P.A., 1986. The Welkom Goldfield. In: Anhaeuser, C.R., and Maske, S. (Editors): Mineral Deposits of Southern Africa, Vol. 1, Geol.Soc.S.Afr., 497-540.

Mendecki, A.J. (Editor), 1997. Seismic Monitoring in Mines. Chapman & Hall, London 262 pp.

Potgieter, G.J. & Roering, C., 1984. The influence of geology on the mechanisms of mining-associated seismicities in the Klerksdorp Goldfield. In: Gay: N.C., Wainwright E.H. (Editors): Proc 1st Int. Congr. Rockburst and Seismicity in Mines, Johannesburg, SAIMM 6: 45-50.

Roberts, M.K.C., Gurtunca, R.G., & Gay, N.C., 1994. Current rock engineering developments to improve safety in South African gold mines. Intern. Symp., New Development in Rock Mechanics and Engineering, Shenyang, China, 6 pp.

Roberts, M.K.C., Eve, R.E., Jager, A.J., Schweitzer, J.K., Guller, G., Quaye, G., Milev, A., Glisson, J. & Kuijpers, J., 1997. SIMRAC Final Project Report (GAP032): Improved support design by an increased understanding of the rock mass behaviour around the Ventersdorp Contact Reef. 94 pp and 346 pp Appendices.

Rompel, A.K.K., 1995. Tectonic History of the Central Welkom Goldfield with particular reference to President Brandt Mine. Unpublished Ph.D. thesis – University of the Witwatersrand, Johannesburg 240 pp.

SACS (South African Committee for Stratigraphy, 1980. Lithostratigraphy of the Republic of South Africa, South West Africa/Namibia, and the Republics of Bophuthatswana, Trankei, Venda. Handbook 8 (Compiler: Kent, L.T.) Geological Survey. South Africa 690 pp.

Sanders, J.W., Rowland, T.W., & Mellody, M., 1994. Formation related gold production from the Central Rand Group and the Ventersdorp Supergroup, South Africa. XV'th CMMI Congress, Johannesburg, SAIMM, 47-53.

Schweitzer, J.K. & Berlenbach, J.W., 1996. Geological controls on rockmass behaviour associated with the platinum and chromite excavations, Rustenburg Layered Suite, Bushveld Igneous Complex: a pilot study. Internal report, CSIR: Miningtek, 45 pp.

Schweitzer, J.K. & Berlenbach, J.W., 1997. Geotechnical environments associated with presently mined Bushveld and Witwatersrand orebodies, and their importance for the application of impact ripping. Internal report, CSIR: Miningtek, 29 pp.

Schweitzer, J.K. & Hatton, C.J. , 1995. Chemical alteration within the volcanic roof rocks of the Bushveld Complex. Economic Geology, 90, 2218-2231.

Schweitzer, J.K. & Johnson, R.A., 1997. Geotechnical classification of deep and ultra-deep Witwatersrand mining areas, South Africa, Mineralium Deposita, 32, 335-348.

Tainton, S., 1994. A review of the Witwatersrand Basin and trends in exploration. XV'th CMMI Congress, SAIMM, Johannsburg, Vol. 3, 19-45.

Tucker, R.F., & Viljoen, R.P., 1986. The geology of the West Rand Goldfields with special reference to the southern limb. In: Anhaeuser, C.R., and Maske, S. (Editiors): Mineral Deposits of Southern Africa, Vol. 1, Geol. Soc. Afr., 649-688.

Van der Heever, P., 1982. The influence of geological structure on seismicity and rockbursts in the Klerksdorp Goldfield. M.Sc. Thesis, Rand Afrikaans University (unpublished).

Viljoen, M.J. & Hieber, R., 1986. The Rustenburg Section of Rustenburg Platinum Mines Limited, with reference to the Merensky Reef. In: Anhaeuser, C.R., and Maske, S. (Editors): Mineral Deposits of Southern Africa, Vol. 1, Geol.Soc.S.Afr., 1107-1134.

2 Assess the use and performance of existing support systems

2.1 Introduction

The Mining Technology Division of the CSIR is involved with a number of research projects for evaluating mine support systems and their effect on rock mass behaviour under both quasi-static and dynamic loading conditions. Although certain information on mine support practices has been obtained in recent years this information is not sufficiently comprehensive for the current project requirements and also does not take the significant support changes that have occurred more recently into consideration.

The information on mine support practices will form the basis of an on-going database of mine support information that will be updated, as new information becomes available. The data are also required to provide further insight into the definition of geotechnical areas, the efficiency of existing support systems from one geotechnical area to another and to form a baseline from which future changes in industry support practices can be compared.

2.2 Scope of the work

The scope of the mine support database is as follows:

- Include stopes but not tunnels or other excavations.
- Include all major gold and platinum mines.
- Where possible, obtain data by reef for each shaft at the above mines.
- Include mining data, rock mechanics data, support types, consumption and costs.
- Distinguish between internal, gully and face area support practices.
- Obtain data for the 1997 calendar year.

2.3 Literature review

A review of the information published in rock mechanics symposia, Association of Mine Managers papers and mining journals established that only very selected information of the type required is available. The most comprehensive summary of mine support practices to date can be found in two reports which were prepared for Miningtek in 1996 by Groundwork Consulting. The first of these two reports is entitled "Permanent Stope Support Usage in South African Gold and Platinum Mines" and provides information on stope support practices by shaft for gold mines and by mine for platinum mines for 1995. The second report, entitled "Stope Support Costs for Gold and Platinum Mines", provides information on stope support costs by shaft for gold mines and by mine for platinum mines for 1995.

One of the key requirements for this current study is to provide mine support information by reef and shaft, as well as to separate support practices by internal, gully and face area support. In the two reports listed above the information was given only by shaft for gold mines and by mine for platinum mines. Furthermore, the separation of data into the internal, gully and face area

sections of the stope was determined theoretically rather than being based on actual information from mines. The other limitations of the previous two reports, in addressing the requirements of this study, are considered to be as follows:

- The data was obtained primarily from suppliers rather than the mines themselves.
- Limited information was provided on important mining parameters such as rates of face advance and mining depths.
- Considerable support changes have taken place since the 1995 survey, particularly in the case of pre-stressed elongates, and these need to be documented.

Accordingly, it was felt that the support information available in the two previous reports and the published literature was not suitable to meet the requirements of this current study and it was necessary to undertake a new study.

2.4 Research methodology

2.4.1 Source of required information

The two main options that exist for obtaining the required data are to obtain the data from the mine support suppliers or from the mines themselves. Previous studies were based primarily on supplier information and this presented three major problems. Firstly, the supplier quantities are usually by mine, seldom by shaft and rarely by reef. Secondly, not all suppliers are prepared to divulge their sales quantities. Thirdly, mine support suppliers are unable to assist with the mining and rock mechanics data required for this survey. Accordingly, it was decided that the only source from where all the required information could be obtained would be from the mines themselves.

It was originally hoped that the information could be obtained by geotechnical area in order to provide additional information for other research projects. There does not, however, appear to be a strong correlation between areas with similar support practices and the delineated geotechnical areas within a shaft. Support practices take factors, other than geotechnical issues, such as historical practices and production requirements as well as rock mass behaviour into consideration. Few mines have support practices documented in such a way that they can determine the support consumption by their newly defined geotechnical areas. Accordingly, it was agreed that it would not be possible to document support practices by geotechnical area and it would, therefore, be done by reef and shaft only.

2.4.2 Data collection process

A number of steps needed to be followed to ensure that individual mines were supportive of the stope support survey, to ensure that approval would be given by management and to ensure that the final information would be as accurate as possible. The process that was followed at each mine, to obtain the required information, is given below:

- Discussions with Group Rock Mechanics Engineers to obtain their support and

permission to contact rock mechanics personnel on their mines,

- Discussions with mine rock mechanics departments to establish availability of data required and, in particular, the availability of the required information by geotechnical area,
- Discussions with mine rock mechanics departments to explain the data required and the data collection forms to be completed upon approval from management,
- Obtain written permission from mine management,
- Request rock mechanics departments to obtain mine support consumption data from their stores and mining data from the survey department and then to complete the forms,
- Collect data from mines,
- Review, analyse and collate data,
- Discuss and resolve discrepancies with mines,
- Collate and document mine support data by shaft and by reef, and
- Prepare final report.

2.4.3 Data collection questionnaire

A double-sided page of explanatory information was discussed and given to the most senior rock engineer at each mine. This contained information relating to the purpose of the survey, the process that was to be followed and the main support groups that should be used on the forms. Each respondent was then given a completed example of the two-sided survey forms, which could be used as a reference document during the data capturing process. Finally, the respondents were provided with sufficient blank forms to complete the information for each reef on each shaft of their mine.

2.4.4 Limitations of the methodology used

Whilst the methodology adopted was considered to be the only feasible means of obtaining the required information, it was accepted that there were still limitations with the approach adopted:

- Some mines were still in the process of defining their geotechnical areas and therefore it was therefore not possible to provide data by this category.
- Staff shortages in certain rock mechanics departments made it very difficult for them to find the time to collect the required information and complete the forms.
- Rock mechanics personnel changes took place during the survey and this resulted in delays in obtaining information.

- In some cases different interpretations were made of the required data resulting in difficulty in making direct comparisons.

- Shaft closures and sales during the survey prevented certain information from being obtained.

- With only one primary source of the data it is difficult to check the accuracy of the data provided other than spotting obvious errors.

2.4.5 Deficiencies in the returned data

In order to provide summaries of industry mining data and support practices it was essential that all questionnaires were submitted prior to the commencement of report writing. Unfortunately, questionnaires were outstanding from 10 mines at the end of the survey despite numerous requests for assistance. It was decided to use data from other sources such as existing databases and supplier information to fill these gaps and to enable industry summaries to be made. Additional information was gathered from these sources so that comprehensive information has been included in the database for mining data and support practices for each major mine, shaft and reef in the gold and platinum mining industry. Where the mining activity on a particular reef was less than 5 per cent of the total centares for the shaft, data for that particular reef has been included with the major reef and both reef names are mentioned in the database.

Whilst it has been possible to obtain the missing mining data and support practices from other sources, this has not been possible in the case of rock mechanics data and information on support consumption and costs. Until such time as reliable data is provided by all mines the summary of support costs and consumption will provided misleading results.

Once all the data had been collated and total industry figures were available it appeared that the data on certain support types might not be completely accurate. Further information on these deficiencies is given below:

2.4.5.1 Hydraulic and mechanical props

The data for hydraulic and mechanical props, by their nature reusable items, was presented either as capital or maintenance costs, never both and sometimes neither. In addition, the capital nature of the purchases, many at once, then none for months, made allocating the capital costs very difficult. There was also no indication of the numbers in use at any one time. Based on the support practices data the overall use of hydraulic props appears high while the use of mechanical props appears low.

2.4.5.2 Backfill

Once all the data had been collected and analysed it appeared that the total quantity of backfill being placed is lower than estimated from other sources. In some questionnaires the quantity of backfill placed has been omitted or apparently under-estimated. One explanation for this is that elongates or packs have been defined as the internal support type and these become buried in the backfill resulting in a certain degree of double-supporting which was not defined in the some responses.

2.4.5.3 Precast packs

The use of precast packs is another area where the total use according to the questionnaire responses is lower than the use estimated from other sources. It is more difficult in this case to estimate at which mines the differences occur.

2.4.5.4 Pack pre-stressing systems

The information supplied, regarding the consumption of pack pre-stressing components, was very incomplete. With some mines gave the number of pre-stressing bags used without the amount of grout, and vice-versa for others. Very seldom was the type of system, weeping or non-weeping, specified.

2.4.5.5 High consumption

In several cases, the specified support practices were not borne out by the actual consumption of support units. For example, in one case the density of profile props was 10. 8 per square metre. In these cases, the other support types theoretically used were analysed and a more equitable division of centares was calculated.

2.4.5.6 Pack losses

A comparison of pack consumption data and support practices from the questionnaire responses reveals considerably more packs are used than the would be expected on the basis of support practices and centares mined. The cause of this discrepancy is attributable to various forms of pack losses. These results are consistent with the findings of a detailed stope support audit conducted at Saaiplaas mine in 1993, where the actual support used exceeded the theoretical support requirements by 20 per cent at two of the shafts and 60 per cent at the largest of the three shafts.

Some of the reasons for the actual pack consumption exceeding the theoretical consumption are as follows :

- Wastage of support units by ordering the incorrect units or as a result of deterioration by storing them on surface too long.
- Loss of support units underground before they are installed or through blast damage.
- Wastage of support units as a result of damage during handling, building larger packs than required, and being used for blocking or other non-pack applications.
- Building packs in off-reef locations such as travelling ways and cross-cuts.
- Double support practices, eg :
  - Packs and backfill,
  - Grout inside skeleton packs, and
  - EPS packs (elongates and skeleton packs).
- Pack reclamation is practised at some mines and this will, to a certain extent, tend to offset the causes of pack losses.

2.5 Results

2.5.1 Description of the database

The database has been created in a Microsoft Excel spreadsheet format.

2.5.1.1 Mines and shafts

The list of mines and shafts in the database are those that were operational during 1997.

Between 1995 and 1997 a number of mines have changed ownership and a number of shafts, particularly in the Free State and Klerksdorp, have changed their names. The names of the mines and shafts that have changed between 1995 and 1997 are given in the table below together with the names that are used at present.

Table 2.5.1.1 Mine and shaft name changes.

1995 NAME	1997 NAME	1998 NAME
Deelkraal 1	Deelkraal 1	Elandsrand Deelkraal
Freddies 1	Freegold 2	Tshepong North
Freddies 10	Western Holdings 10	Matjhabeng Kudu
Freddies 5	Western Holdings 5	Matjhabeng Nyala
Kinross 1	Kinross 1	Evander 7
Kinross 2	Kinross 2	Evander 8
Leslie 1	Leslie 1	Evander 9
President Steyn 3	Freegold 1 West	Bambanani 1 West
President Steyn 4	Freegold 1 East	Bambanani 1 East
Saaiplaas 3	Saaiplaas 3	Harmony S3
Saaiplaas 4	Freegold 3 South	Masimong 3 South
Saaiplaas 5	Freegold 3 North	Masimong 3 North
Unisel	Unisel	Harmony Unisel
Vaal Reefs 1	Vaal Reefs 1	ARM 1
Vaal Reefs 10	Vaal Reefs 10	Vaal River Tau Lekoa
Vaal Reefs 11	Vaal Reefs 11	Vaal River Moab Khotsong
Vaal Reefs 2	Vaal Reefs 2	ARM 2
Vaal Reefs 3	Vaal Reefs 3	ARM 3
Vaal Reefs 4	Vaal Reefs 4	ARM 4
Vaal Reefs 5	Vaal Reefs 5	ARM 5
Vaal Reefs 6 and 7	Vaal Reefs 6 and 7	ARM 6 and 7
Vaal Reefs 8	Vaal Reefs 8	Vaal River Great Noligwa
Vaal Reefs 9	Vaal Reefs 9	Vaal River Kopanang
WAGM North	WAGM North	REGM 4
Western Holdings 2 and 3	Western Holdings 2 and 3	Western Holdings 2 and 3
Western Holdings 4 and 5	Western Holdings 4 and 5	Western Holdings 4 and 5

Western Holdings 7	Western Holdings 9S	Matjhabeng Sable S
Western Holdings 8	Western Holdings 8	Matjhabeng Eland
Western Holdings 9	Western Holdings 9N	Matjhabeng Sable N
Winkelhaak 2 and 2A	Winkelhaak 2 and 2A	Evander 2
Winkelhaak 5	Winkelhaak 5	Evander 5
Winkelhaak 6	Winkelhaak 6	Evander 6

2.5.1.2 Grouping of support products

The many support types used by the industry were grouped into eighteen support groups to facilitate analysis of the data. A description of each group of support products is given in the table below.

Table 2.5.1.2 Description of support product groups.

SUPPORT GROUP		SUPPORT TYPES
1	Mats and slabs	Packs constructed from timber mats or timber slabs with horizontal grain timber only.
2	End-grain packs	Timber packs containing end-grain members, eg Cross-bow, Stratos, C-mat, Apollo, Lexus.
3	Timber composites	Slabs with horizontal grain timber blocks attached.
4	Brick composites	Slabs with bricks attached to the slabs or sandwich packs.
5	Precast packs	eg Durapak, Pambili, Vimbela, Heraklith.
6	Mine poles	Mine poles.
7	Cluster packs	Clusters of mine poles.
8	Elongates	Timber elongates, eg Profile Prop, pencil prop.
9	Pre-stressed elongates	Timber elongates which are pre-stressed, eg Cone prop, Loadmaster, Ebenhaeser, Madoda.
10	Steel props	Permanent steel props, eg RocProp and Sand Prop.
11	Hydraulic props	Rapid yield and slow yield.
12	Mechanical props	eg Camlok, Multimech.
13	Grout packs	RSS grout packs and Elsburg packs.
14	Backfill	Cemented, silicated and un-cemented backfill.
15	Rockbolts	Rockbolts used for permanent support.
16	Caving	Caving in the back areas with no other support.
17	Pack pre-stressing	Weeping, non-weeping, bags and grout
18	Pillars	Pillars for internal support.

2.5.2 Summary of mining related data

In table below the mining data provided in the responses has been summarised by gold, platinum, total industry, region and reef. The average centares per month for gold and platinum mines in 1997 was 1,88 million at a face advance rate of 9,4 metres/month, a stoping width of 1,36 metres, a dip of 17 degrees and a depth of about 1100 metres.

Table 2.5.2.1 Summary of mining data.

	Centares (m^2/month)	Face Adv. (m/month)	Stope width (metres)	Dip (degrees)	Depth (metres)
Gold	1 034 500	7,8	1,50	19,5	1 522
Platinum	845 161	11,4	1,19	14,0	566
Total	**1 879 661**	**9,4**	**1,36**	**17,0**	**1 092**
Region					
Rustenburg	845 161	11,4	1,19	14,0	566
Free State	363 109	11,1	1,86	26,5	1 603
Far West Rand	216 921	7,8	1,39	22,0	1 745
Klerksdorp	209 317	8,4	1,34	17,2	1 799
West Rand	160 147	8,4	1,87	30,0	976
Evander	56 400	9,6	1,22	22,9	1 375
East Rand	28 606	6,9	1,12	21,8	2 173
Reef					
Merensky	511 894	11,0	1,15	13,6	769
UG2	333 267	12,0	1,25	14,4	1 003
Basal	247 111	7,4	1,46	25,1	1 745
VCR	187 743	7,9	1,54	24,1	1 137
Vaal	164 806	8,1	1,24	14,9	1 943
Kimberly	98 300	9,7	1,24	25,0	1 316
Carbon Leader	91 958	7,8	1,25	22,1	2 094
Beatrix	71 242	13,1	1,37	9,0	885
Main	68 551	5,3	1,81	18,5	1 206
UE1A	21 448	5,0	3,50	0,0	800
Composite	17 212	6,8	1,09	20,5	3 090
Leader	16 554	8,0	1,53	14,3	1 376
Elsburg	13 516	9,7	2,00	24,1	1 753
Kalkoenskrans	12 463	6,7	1,40	18,0	2 000
C	5 664	9,6	1,36	21,0	1 950
A	5 292	7,4	1,65	7,0	1 416
B	5 286	11,8	1,24	8,0	1 750
Deelkraal	2 531	8,0	1,17	30,0	1 500
South	2 082	6,0	0,80	25,0	1 500
Black	1 909	7,0	1,04	20,0	588
Kloof	832	8,0	1,57	30,0	2 500

2.5.3 Summary of rock mechanics data

A summary of the rock mechanics data that were received is given in the table below. Not all the required data were received and the summaries have been weighted on the basis of centares for each submission by reef.

Table 2.5.3.1 Summary on rock mechanics data.

	Beam height (metres)	**FOG Area (m^2)**	**Rockfall (kN/m^2)**	**Rockburst (kJ/m^2)**	**Closure rate (mm/metre)**
Gold	0,8	13,2	43	32	13
Platinum	3,4	15,2	47	0	1
Total	**2,1**	**14,2**	**45**	**32**	**6**
Region					
Rustenburg	3,4	15	47	0	1
Free State	0,9	5	31	18	9
West Rand	0,6	4	27	18	10
Far West Rand	1,5	27	45	37	26
Klerksdorp	0,8	34	71	21	12
Evander	0,7	23	23	0	5
East Rand	0,6	2	38	53	11
Reef					
Merensky	6,0	6,7	31	0	1
UG2	1,5	21,3	54	0	1
Basal	1,0	3,9	36	18	16
VCR	1,1	6	53	44	12
Vaal	4,5	15,7	86	21	15
Kimberly	0,6	21,2	24	0	8
Carbon Leader	1,2	2,5	34	32	31
Beatrix	0,8	5,1	25	0	1
Main	0,5	1,1	42	45	7
UE1A	Insufficient Data				
Composite	0,8	1,7	42	53	14
Leader	0,8	5,9	22	18	6
Elsburg	1,2	3,6	35		15
Kalkoenskrans	1,0	4,0	50		8
C	Insufficient Data				
A	0,8	6,1	21	18	14
B	1,8	4,0	47	18	6
Deelkraal	Insufficient Data				
South	Insufficient Data				
Black	0,3	1,3	28		4
Kloof	Insufficient Data				

2.5.4 Summary of permanent support practices

The tables below give the percentage of the centares mines that used various types of support products for permanent support by industry and reef type. Permanent support has been defined as the support behind the sweeping line, excluding the gullies.

Table 2.5.4.1 Permanent support practices by industry.

SUPPORT TYPE	TOTAL	Gold	Platinum
Mats and slabs	31,3	48,1	5,5
Mine poles	15,9	0,3	39,9
Pre-stressed elongates	12,4	6,2	21,9
Elongates	9,1	15,0	0,0
Backfill	6,3	8,9	2,5
Cluster packs	5,6	0,0	14,2
Brick composites	5,5	9,0	0,0
Grout packs	5,2	1,3	11,3
End grain packs	3,0	2,8	3,3
Rockbolts	2,2	2,8	1,4
Caving	1,4	2,3	0,0
Precast packs	0,8	1,3	0,0
Timber composites	0,7	1,1	0,0
Steel props	0,6	0,9	0,0
	100 %	100 %	100 %

Table 2.5.4.2 Permanent support practices by reef type.

SUPPORT TYPE	Basal	Beatrix	Carbon Leader	Kimberly	Main Reef	Merensky	UG2	Vaal Reef	VCR
Mats and slabs	71,0	19,0	0,0	59,0	46,0	4,7	7,0	23,0	16,0
Mine poles	0,0	0,0	0,0	0,0	0,0	40,5	39,3	0,0	1,4
Pre-stressed elongates	1,3	0,0	9,5	0,0	0,0	26,0	13,9	9,1	24,1
Elongates	3,9	0,0	5,1	33,6	21,2	0,0	0,0	7,7	11,2
Backfill	1,6	0,0	58,9	0,0	12,9	3,8	0,0	3,2	21,1
Cluster packs	0,0	0,0	0,0	0,0	0,0	5,7	29,7	0,0	0,0
Brick composites	17,9	0,0	26,5	0,0	3,4	0,0	0,0	10,5	14,0
Grout packs	0,0	0,0	0,0	0,0	16,4	17,3	0,6	0,0	0,0
End grain packs	2,7	74,6	0,0	4,0	0,0	2,0	5,6	7,2	7,1
Rockbolts	0,0	0,0	0,0	3,4	0,0	0,0	3,9	0,0	4,6
Caving	0,0	0,0	0,0	0,0	0,0	0,0	0,0	20,7	0,0
Precast packs	0,0	0,0	0,0	0,0	0,0	0,0	0,0	11,3	0,0
Timber composites	0,0	0,0	0,0	0,0	0,0	0,0	0,0	5,1	0,3
Steel props	1,7	6,4	0,0	0,0	0,0	0,0	0,0	2,2	0,0
	100%	100%	100%	100%	100%	100%	100%	100%	100%

2.5.5 Summary of gully support practices

The tables below give the percentage of the centares mines that used various types of support products for gully support by industry and reef type. Gully support has been defined as the support used on the shoulders of the gully, excluding the use of tendons in the gully hangingwall. Where rockbolts appear in the table below they refer the bolting above the shoulders of the gully.

Table 2.5.5.1 Gully support practices by industry.

SUPPORT TYPE	TOTAL	Gold	Platinum
Mats and slabs	41,2	62,1	9,0
Mine poles	15,6	0,2	39,4
End grain packs	12,3	7,6	19,6
Brick composites	7,3	12,1	0,0
Cluster packs	6,8	0,0	17,4
Grout packs	4,3	2,9	6,4
Timber composites	4,2	6,9	0,0
Pre-stressed elongates	3,2	0,0	8,0
Elongates	1,9	3,1	0,0
Rockbolts	1,8	2,7	0,3
Precast packs	1,4	2,3	0,0
	100 %	100 %	100 %

Table 2.5.5.2 Gully support practices by reef type.

SUPPORT TYPE	Basal	Beatrix	Carbon Leader	Kimberly	Main Reef	Merensky	UG2	Vaal Reef	VCR
Mats and slabs	87,0	36,2	47,6	80,5	62,6	10,0	7,0	33,6	23,9
Mine poles	0,0	0,0	0,0	0,0	0,0	41,4	35,6	0,0	1,4
End grain packs	2,6	0,0	0,0	4,2	5,2	20,5	18,0	25,1	11,9
Brick composites	10,4	6,4	26,5	0,0	3,5	0,0	0,0	21,8	22,1
Cluster packs	0,0	0,0	0,0	0,0	0,0	6,8	36,5	0,0	0,0
Grout packs	0,0	57,5	0,0	0,0	16,4	9,6	0,6	0,0	0,0
Timber composites	0,0	0,0	16,8	0,0	10,5	0,0	0,0	5,1	25,3
Pre-stressed elongates	0,0	0,0	0,0	0,0	0,0	11,6	1,5	0,0	0,0
Elongates	0,0	0,0	0,0	15,3	0,0	0,0	0,0	0,2	11,2
Rockbolts	0,0	0,0	0,0	0,0	0,0	0,0	0,8	0,0	4,1
Precast packs	0,0	0,0	8,4	0,0	1,8	0,0	0,0	14,2	0,0
	100%	100%	100%	100%	100%	100%	100%	100%	100%

2.5.6 Summary of face area support practices

The tables below give the percentage of the centares mined that used various types of support products for face area support by industry and reef type. Face area support has been defined as the support used between the face and the permanent support and consists of permanent, rolling and temporary support.

Table 2.5.6.1 Face area support practices by industry.

SUPPORT TYPE	TOTAL	Gold	Platinum
Mine poles	41,9	33,5	54,8
Hydraulic props	27,1	43,0	2,7
Mechanical props	13,3	9,4	19,3
Pre-stressed elongates	10,8	7,1	16,5
Rockbolts	6,2	5,9	6,7
Steel props	0,7	1,1	0,0
	100 %	100 %	100 %

Table 2.5.6.2 Face area support practices by reef.

SUPPORT TYPE	Basal	Beatrix	Carbon Leader	Kimberly	Main Reef	Merensky	UG2	Vaal Reef	VCR
Mine poles	70,7	23,4	33,6	58,1	31,3	56,3	52,0	27,9	22,3
Hydraulic props	6,2	0,0	13,5	0,0	54,2	3,8	0,6	56,4	56,1
Mechanical props	18,5	70,2	0,0	4,0	14,5	17,8	22,1	3,5	4,2
Pre-stressed elongates	1,4	0,0	53,0	0,0	0,0	17,5	14,7	8,4	13,3
Rockbolts	0,6	6,4	0,0	38,0	0,0	4,5	10,6	0,0	4,1
Steel props	2,7	0,0	0,0	0,0	0,0	0,0	0,0	3,8	0,0
	100%	100%	100%	100%	100%	100%	100%	100%	100%

2.5.7 Summary of permanent support usage and costs

The preliminary summaries of support usage which were made provided misleading results since not all mines had provided data and the data from some other mines appeared not to be comprehensive. In order to estimate the total value of the support market the information for the cost per centare of each support type from the 1995 survey was used. In the table below the product of the area mined on each type of permanent support and the Rands per square metre from the 1995 survey is presented.

Table 2.5.7.1 Summary of permanent stope support costs.

SUPPORT TYPE	TOTAL	Gold	Platinum
	R million / month	R million / month	R million / month
Mats and slabs	35,1	32,6	2,5
Mine poles	0,8	0,1	0,7
Pre-stressed elongates	8,2	2,5	5,7
Elongates	1,8	1,8	0,0
Backfill	10,9	9,4	1,5
Cluster packs	0,8	0,0	0,8
Brick composites	6,1	6,1	0,0
Grout packs	7,7	0,9	6,8
End grain packs	4,0	2,8	1,2
Rockbolts	0,3	0,2	0,1
Precast packs	1,1	1,1	0,0
Timber composites	0,8	0,8	0,0
Steel props	0,6	0,6	0,0
	R 78,2 mill/mth	R 58,9 mill/mth	R 19,3 mill/mth

2.5.8 Changes since the 1995 survey

2.5.8.1 Gold mining industry

The total centares mined per month has reduced by 12 per cent from 1,18 million to 1,03 million square metres per month. The estimated value of the permanent support market, in 1995 terms, has declined from R 80,5 million to R 78,2 million per month. This can be attributed to a reduction in the area mined as well as the increased use of pre-stressed elongates instead of packs and a change from the more expensive end-grain packs to solid mats and slabs.

2.5.8.2 Platinum mining industry

Although there is an apparent reduction in the total centares mined in the platinum industry from 0,90 million to 0,85 million square metres per month, the 1995 data for platinum mines were not considered to be accurate and may well have been overstated. Now that more reliable mining information is available it is more likely that the 1995 mining activity was between 0,80 million and 0,85 million square metres per month and that that actual centares has remained constant or increased slightly in the platinum industry during the past two years.

The estimated value of the permanent support market, in 1995 terms, has increased from R 16,2 million to R 19,3 million per month. The majority of this increase is due to a large increase in the use of pre-stressed elongates or mine poles instead of normal mine poles or hydraulic props.

2.6 Assess the performance of existing support systems by means of accident analysis

An attempt is made to relate the support usage to fatal accidents associated with rockfalls and rockbursts. Detailed information of the support usage on the gold mines is only available for 1995 and 1997, and hence the accident analysis is restricted to a relatively small set of casualty data containing details of rock related fatalities which occurred in 1995 and 1997.

The support types used by the gold mines are grouped according to the following categories:

- Mats and slabs: Packs constructed from timber mats and timber slabs
- End-grain packs: Timber packs containing end-grain members, e.g. Hercules, Apollo, Cross-bow, C-mat
- Composite packs: Brick composites, sandwich packs and timber block composites
- Pre-cast packs: e.g. Durapack
- Grout packs: RSS grout packs and Elsburg packs
- Elongates & steel props: Timber elongates (including pre-stressed varieties) and steel props, e.g. Rocprop
- Rockbolts: Rockbolts used for permanent support
- Backfill: Cemented, silicated and un-cemented backfill

Only permanent support types are investigated, the reason being that the 1995 support usage survey encompassed only permanent support types. It is recommended, however, that futures studies investigate the usage and fatalities associated with temporary support systems, such as hydraulic props and mechanical props (e.g. Camlocks).

The accident database was used to obtain data relating fatalities to support types. Only fatalities within 1,5 m to the nearest support type were considered. Tables 2.6.1 a) and b) list the support usage and fatalities associated with a particular support type. The tables list the support type, the percentage area and the area (in million square metres) supported by the specific support type, the number of fatalities which occurred within 1,5 m of the support type (given for various reefs), and a hazard rating. The hazard rating is defined as the number of fatalities per million square metres supported by the specific support type.

From the hazard rating it is apparent that the fatality database used in this study is too small to make general conclusions regarding the effectiveness associated with a specific support type. For example, in 1995, 4,08 fatalities per million m^2 occurred within 1,5 m of packs constructed from timber mats or slabs. In 1997 the corresponding hazard rating drops to 0,84. The relatively large variance between the 1995 and 1997 data indicates that not sufficient casualty data is used, and the hazard rating is significantly affected by relatively few fatalities. Furthermore, the cause of rockfalls and rockbursts depend on multiple factors, such as mine layout, the geological complexity of the rockmass, depth, support spacing, pillar extraction and remnant mining, and the link to a particular support type is tenuous.

Table 2.6.1 a) Pack support usage and associated fatalities (RB and RF refer to rockburst and rockfall related fatalities, respectively).

Number of fatalities on various reefs:

Support Type	Area covered (% of tot)	Area covered (mill. m²)	VCR		Carbon Leader		Vaal Reef		Basal Reef		Other reefs		Total fatals	Hazard (fatals/ mill. m²)
			RB	*RF*	*RB*	*RF*	*RB*	*RF*	*RB*	*RF*	*RB*	*RF*	*RB+RF*	
Mats and Slabs														
1995	32,9 %	4,654	1	2	3	1	0	0	1	4	2	5	19	4,082
1997	48,0 %	5,959	0	0	0	0	0	0	0	1	0	4	5	0,839
End-grain Packs														
1995	10,8 %	1,528	2	0	4	1	0	1	0	0	0	0	8	5,236
1997	2,8 %	0.348	1	1	0	0	0	0	0	0	2	1	5	14,37
Composite Packs														
1995	16,5 %	2,334	5	3	0	0	0	0	0	1	2	1	12	5,141
1997	10,1 %	1,254	2	3	0	0	0	1	0	1	0	2	9	7,177
Pre-cast Packs														
1995	1,7 %	0,240	0	0	0	0	0	0	0	0	0	0	0	0
1997	1,3 %	0,161	0	0	2	0	0	0	0	1	0	0	3	18,63
Grout Packs														
1995	3,4 %	0,481	0	0	0	0	0	0	0	0	0	3	3	6,237
1997	1,3 %	0,161	0	0	1	0	0	0	0	0	0	0	1	6,211

Number of fatalities in the proximity of packs, but where pack type was unspecified:	1995	1	2	4	1	0	2	2	7	1	3	23	
	1997	6	0	5	0	0	1	0	1	1	4	18	

Table 2.6.1 b) Support usage and associated fatalities.

Number of fatalities on various reefs:

Support Type	Area covered (% of tot)	Area covered (mill. m²)	VCR		Carbon Leader		Vaal Reef		Basal Reef		Other reefs		Total fatals	Hazard (fatals/ mill. m²)
			RB	*RF*	*RB*	*RF*	*RB*	*RF*	*RB*	*RF*	*RB*	*RF*	*RB+RF*	
Elongates & steel props														
1995	18,4 %	2,603	0	0	0	1	0	0	0	0	0	0	1	0,384
1997	22,1 %	2,743	0	1	3	0	0	0	0	1	0	1	6	2,187
Rockbolts														
1995	2,3 %	0,325	0	1	0	0	0	1	0	1	1	4	8	24,62
1997	2,8 %	0,348	1	1	0	0	3	4	0	2	0	2	13	37,36
Backfill														
1995	11,1 %	1,570	1	0	1	0	0	0	0	0	0	0	2	1,274
1997	8,8 %	1,092	0	0	0	0	0	0	0	0	0	0	0	0

2.7 Conclusions and recommendations

In this report an explanation of the source and derivation of the information contained in the industry support database has been given. The information contained in the database has been summarised to provide totals for the industry, as well as individually for gold mines, platinum mines, by region and by reef type. However, the current gaps in the database prevent meaningful summaries being made of mine support costs and consumption in terms of Rands per square metre for different regions and reefs. Once the outstanding information is provided by the industry a summary of this important information can be completed.

Mine support practices are changing on a regular basis. This survey is a snapshot of industry practices during 1997. It is recommended that the database is updated on a yearly basis.

3 Maintain and expand the accident database

3.1 Introduction

A database was developed in order to capture the rockburst and rockfall fatality information for all fatal accidents that have occurred in the South African Gold mining industry since 1990. To date, this database encompasses 1807 fatalities for a period of eight years (i.e. from 1990 to 1997). This information is used as a tool for investigating and identifying problematic areas and reefs, so that research needs and remedial action can be directed. The database also gives insights into fatality trends and their dependence on various parameters, such as locations, reef types, geotechnical areas, depths, rockburst magnitudes ,etc.

This report presents the outcome of the analyses that have been conducted to establish accident statistics and trends. Although each reef type has been analysed individually, priority has been given to four reefs, namely: VCR, Carbon Leader, Vaal Reef and Basal Reef. The data for the remaining reefs, such as Kimberly, Composite, Main, Deelkraal, Elsburg, Kloof, South, Beisa, Middle, Leader and Pyrite Reefs, are accumulated into a category referred to as "other reefs"

In order to set the fatality data into perspective, the production of each reef, in terms of square metres mined, was obtained for individual mines, and the casualty data was normalized and expressed as "fatalities per million square metres mined".

3.2 Previous work

Previous accident analysis showed that rockfalls and rockbursts are the major cause of underground fatalities in the gold and platinum mines. A large number of these occur in the face area at a distance of approximately 2,5 m from the stope face, in front of permanent support. This critical area, between the stope face and the permanent support, is known as a stope face area and is the location where the worker concentration is highest.

In the past, back analysis of collapse dimensions was performed to determine the required support resistance. For rockfall cases, these analysis indicated that about 50 per cent of falls are less than 0,45 m thick, 85 per cent are less than 1,0 m, and the 95 per cent are less than 2,0 m. The thicker falls are usually associated with geological structures such as faults or dykes. As part of the work reported here the fallout thicknesses for rockfall and rockburst cases are updated with more extensive data, and new support resistance and energy absorption criteria for the various reefs are calculated.

Figure 3.2.1 gives an overview of the total fatality distribution for the various reefs categorised according to rockfall and rockburst related fatalities.

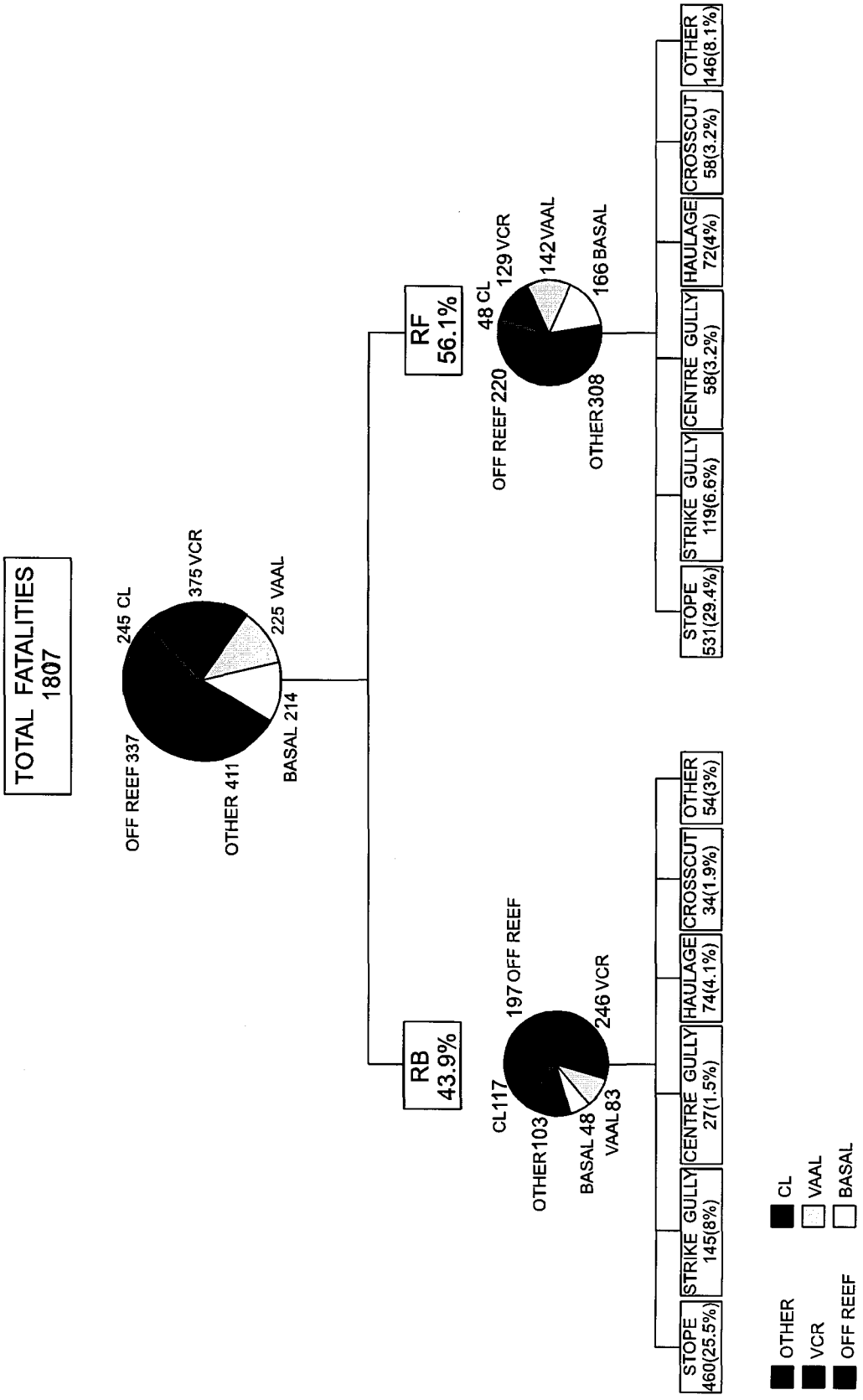

Figure 3.2.1 Overview of the total fatality distribution for the various reefs categorised according to rockfall and rockburst related fatalities for the period 1990 to 1997.

3.3 Breakdown of fatality numbers according to rockburst versus rockfall, location and reef type

The total number of fatalities per year will be presented as follows.

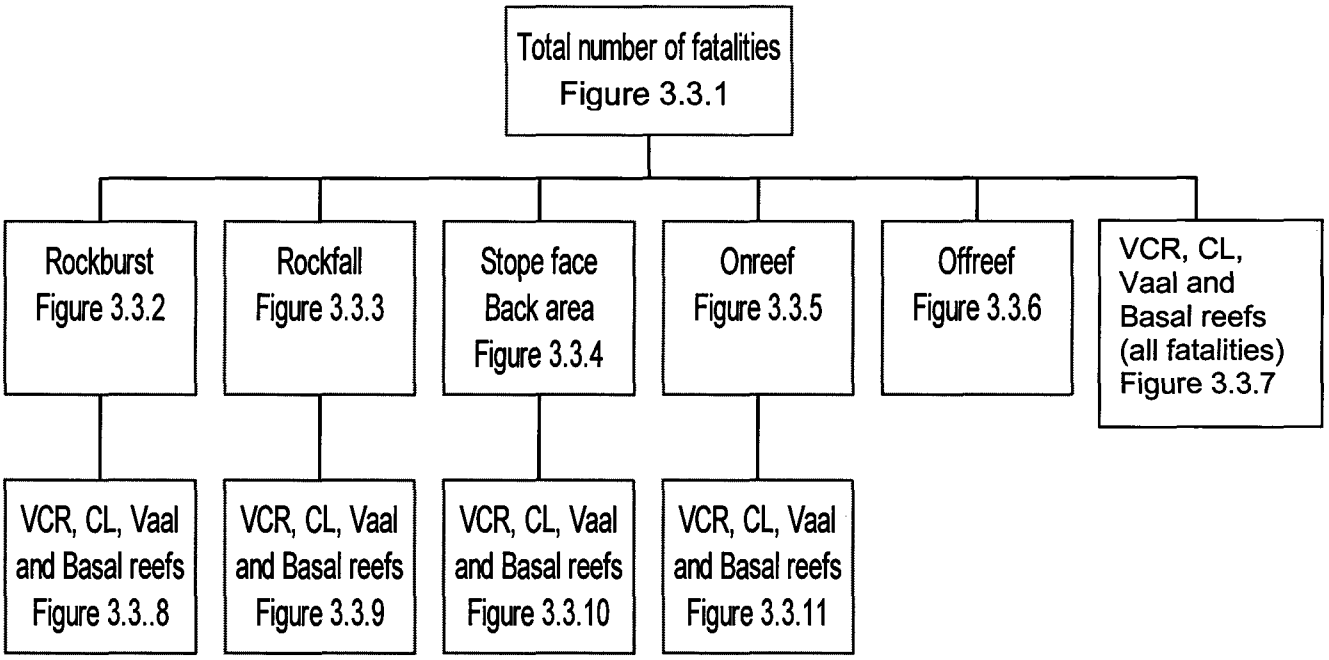

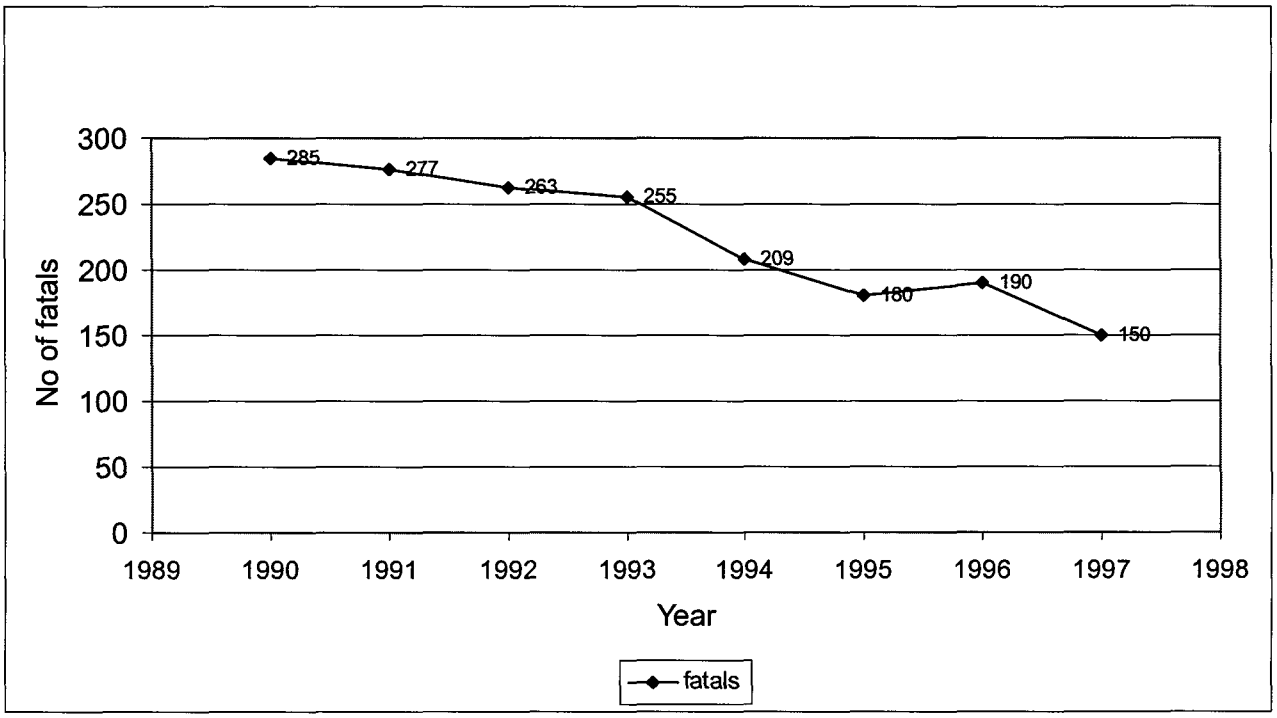

Figure 3.3.1 Total number of fatalities (1990-1997).

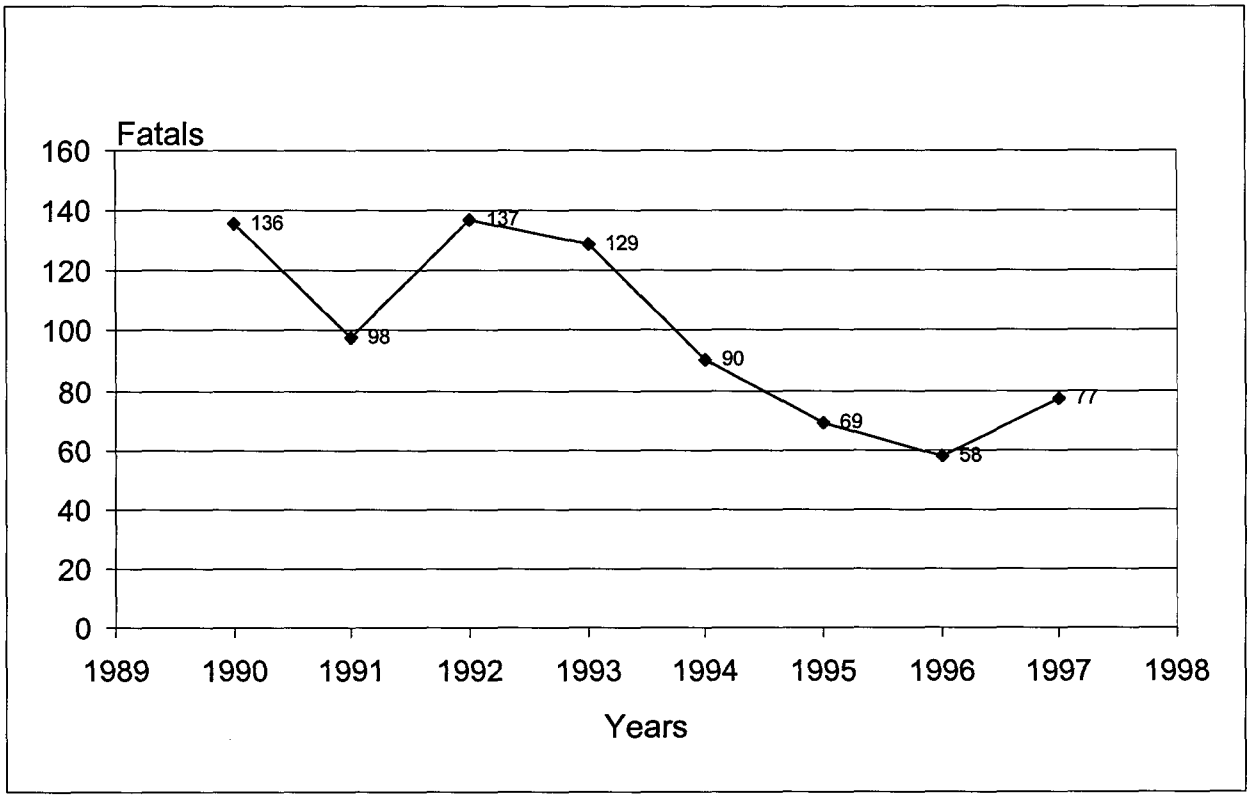

Figure 3.3.2 Rockburst fatalities.

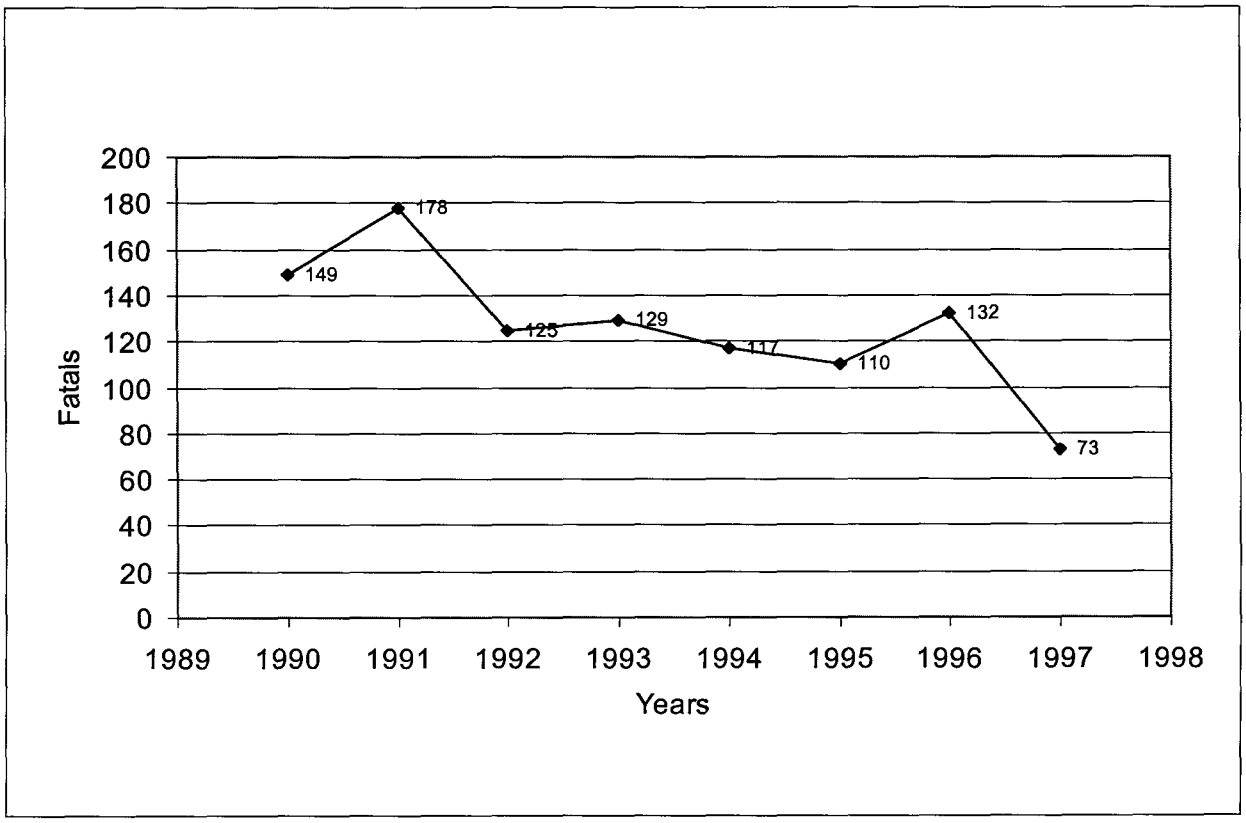

Figure 3.3.3 Rockfall fatalities.

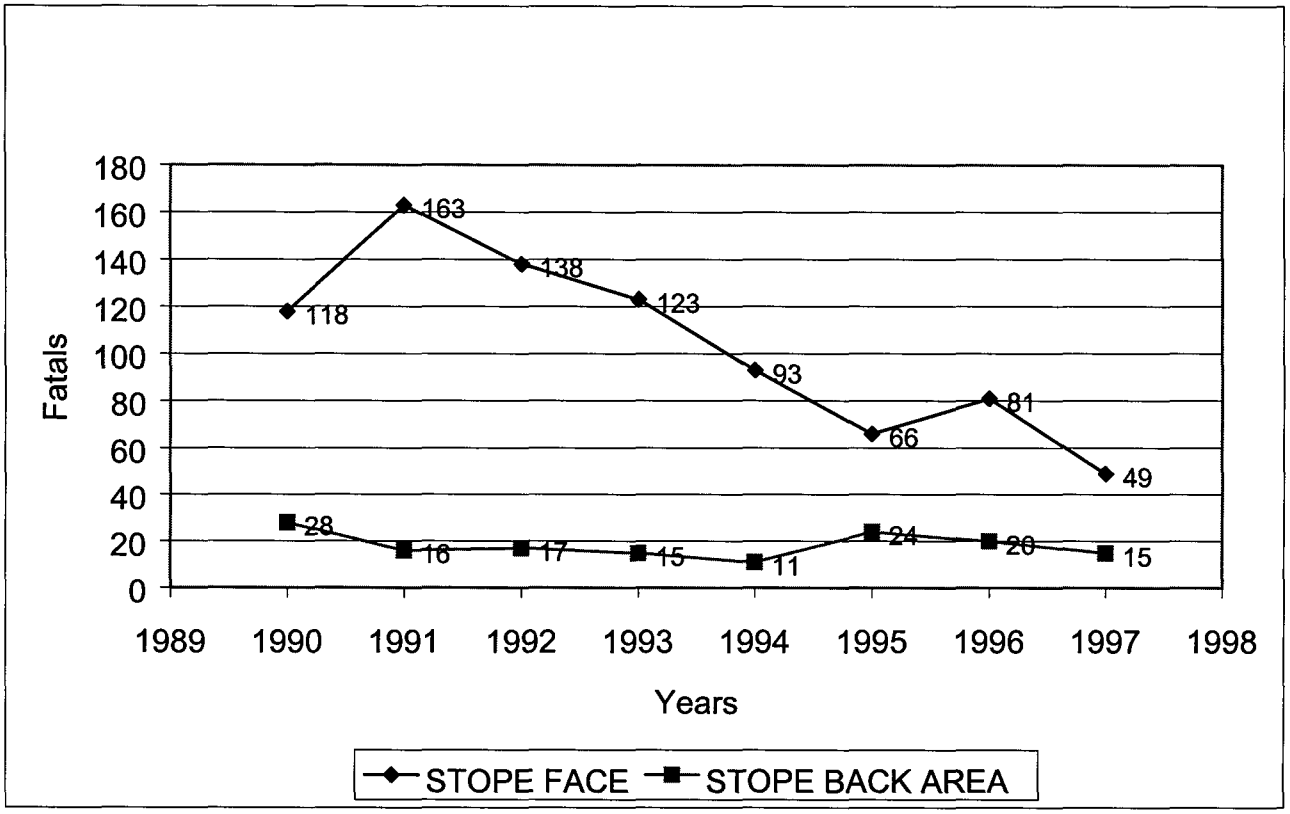

Figure 3.3.4 Stope and back area fatalities.

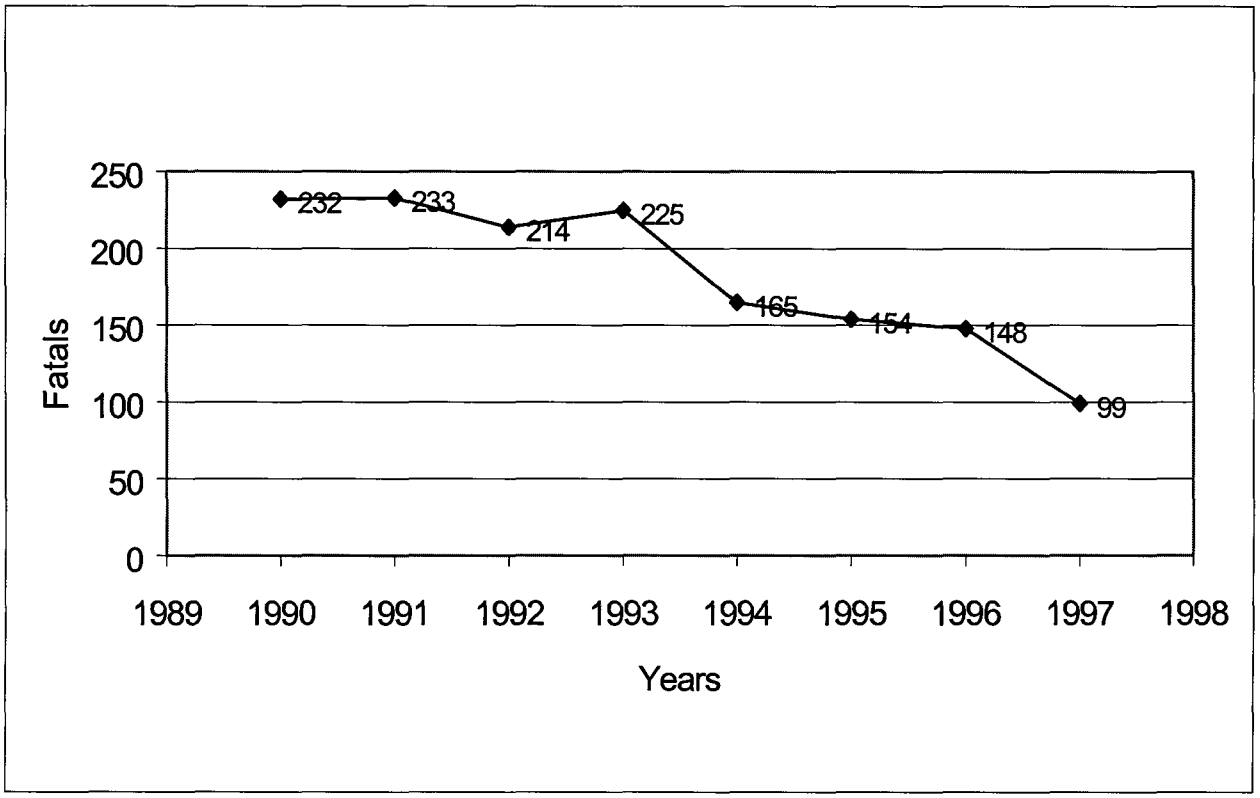

Figure 3.3.5 On reef fatalities.

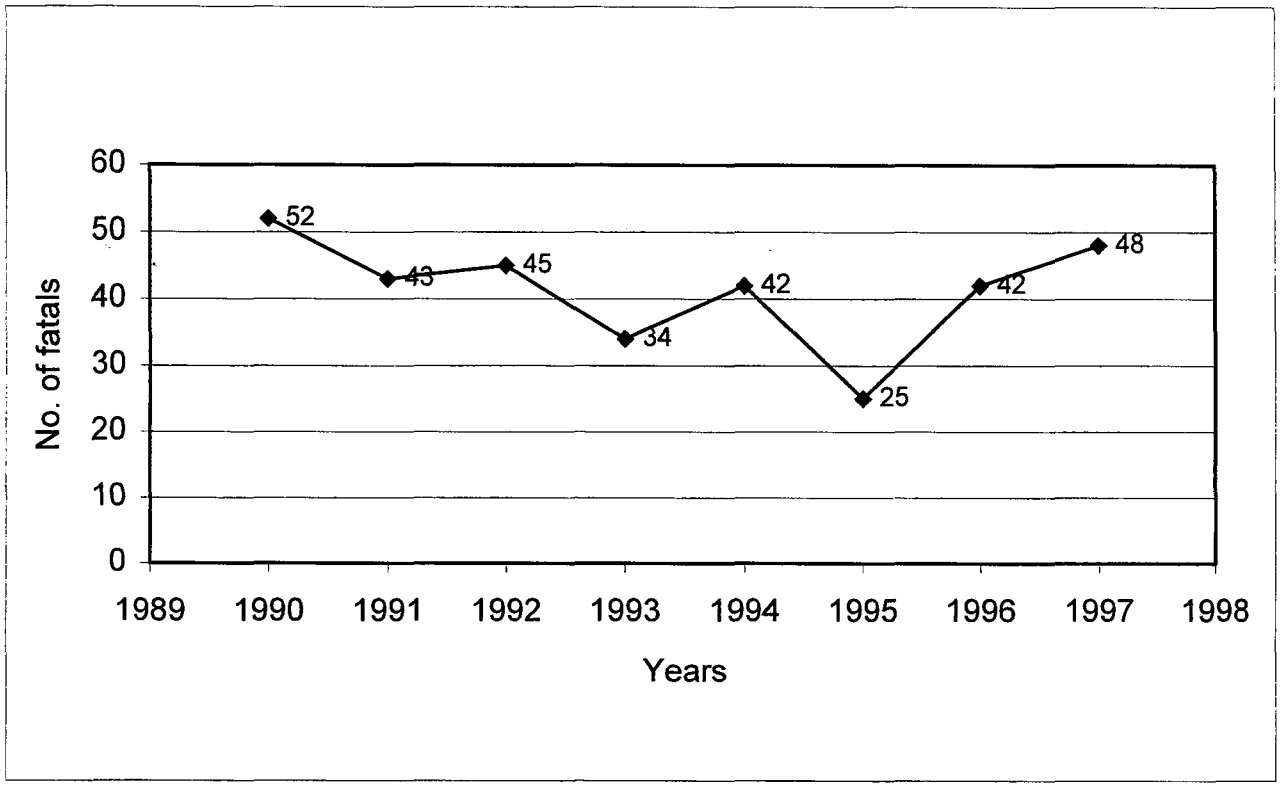

Figure 3.3.6 Off reef fatalities.

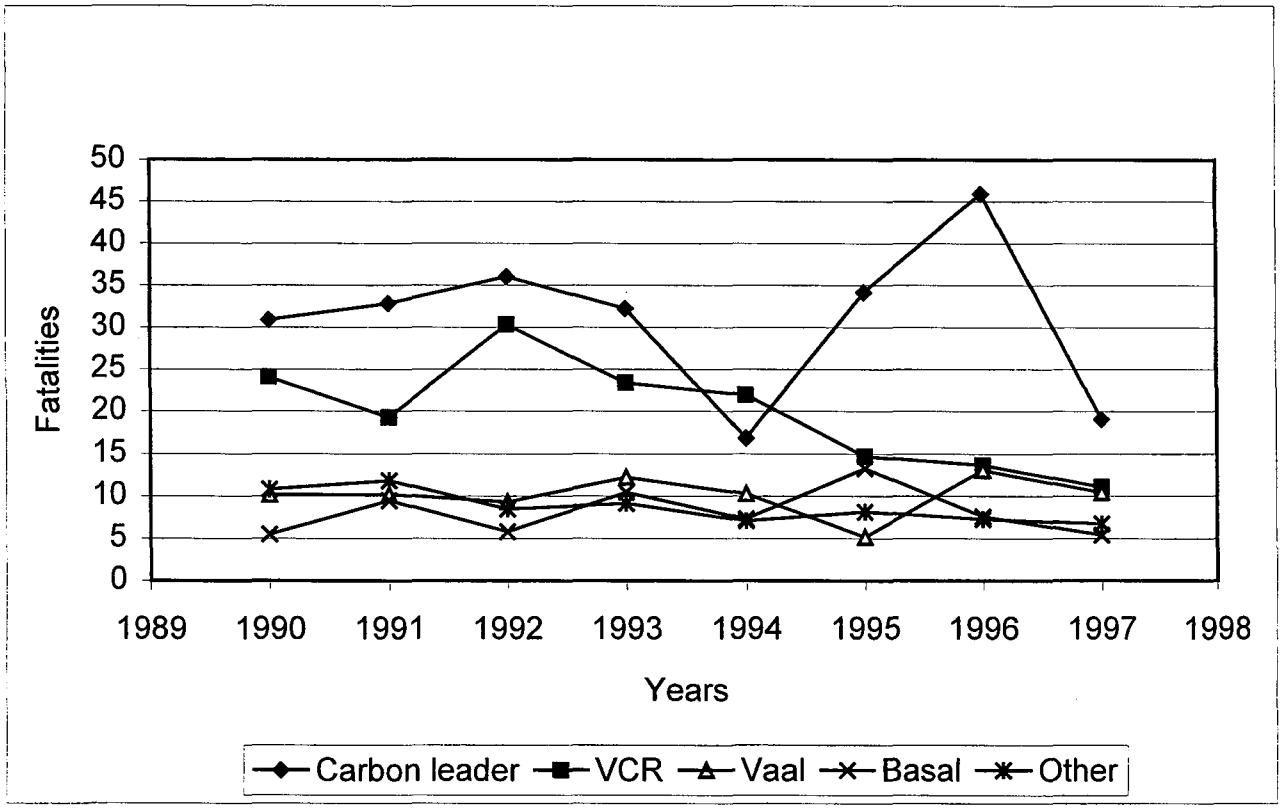

Figure 3.3.7 Fatalities per million square metres mined for various reefs.

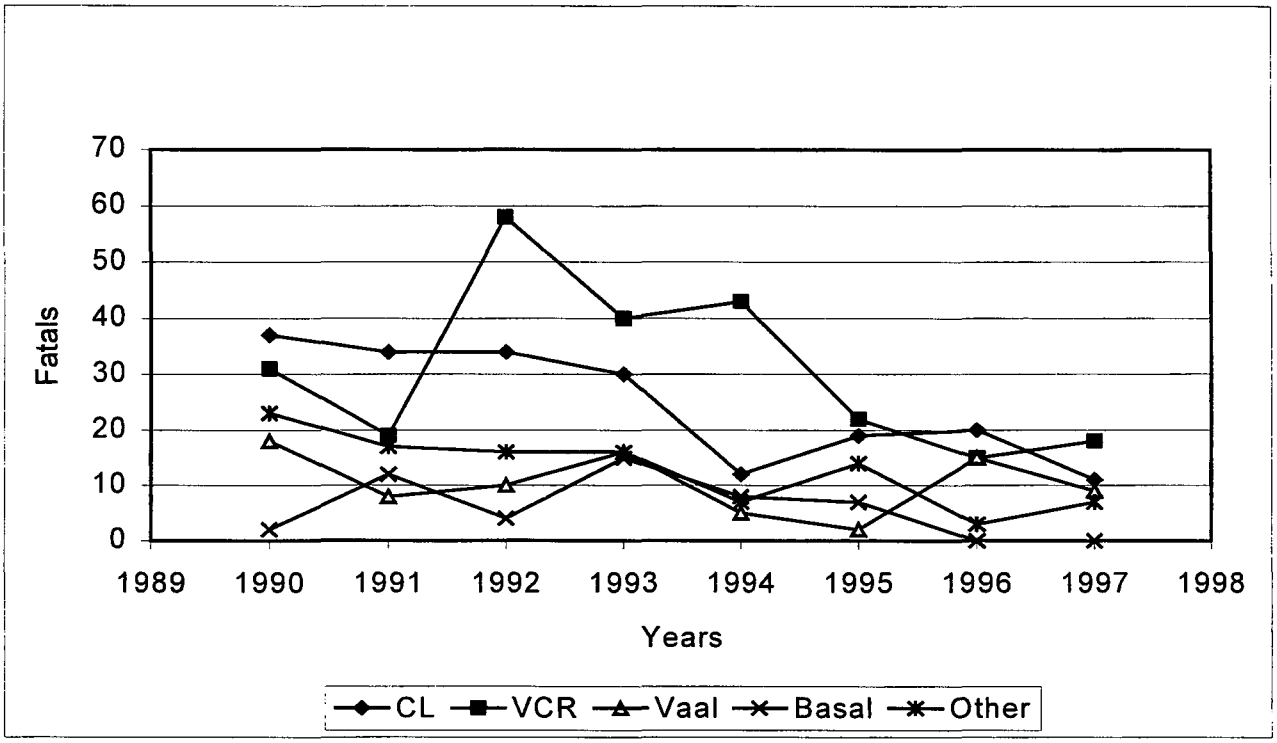

Figure 3.3.8 Rockburst fatalities.

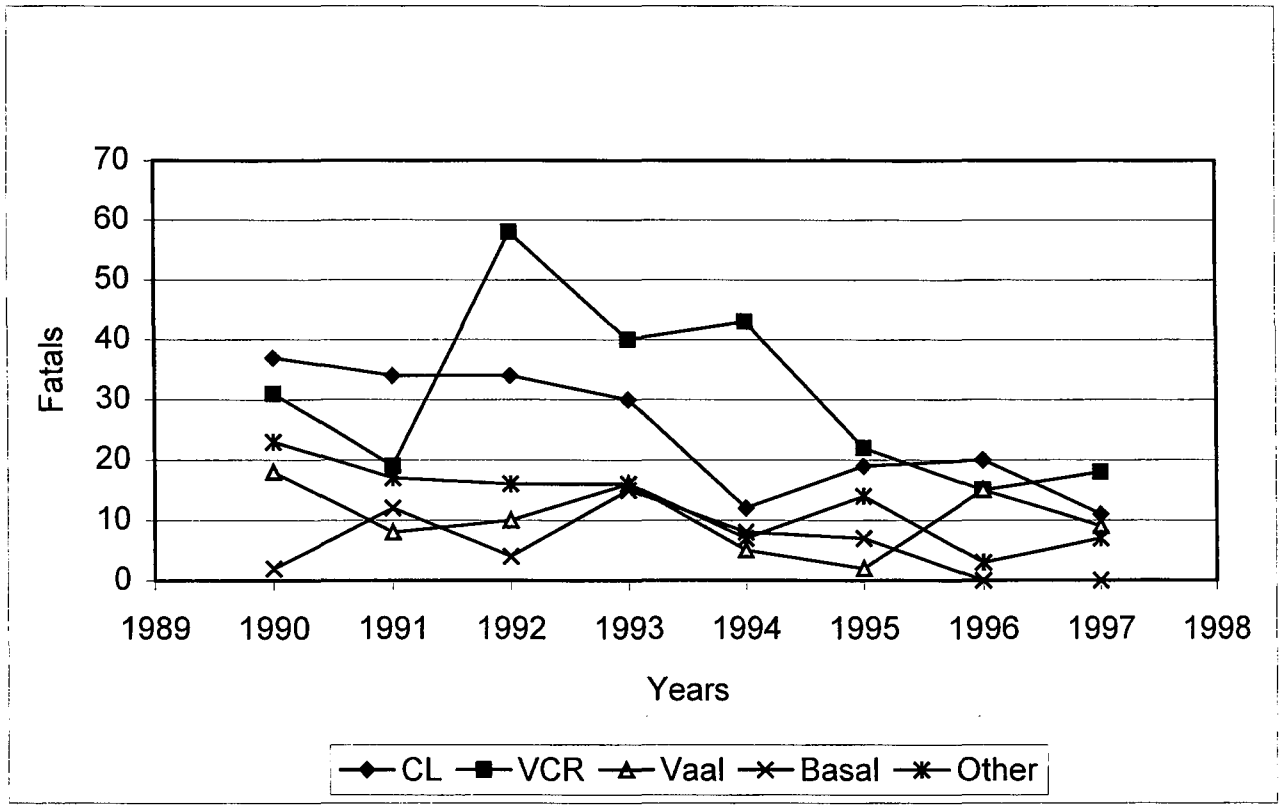

Figure 3.3.9 Rockfall fatalities.

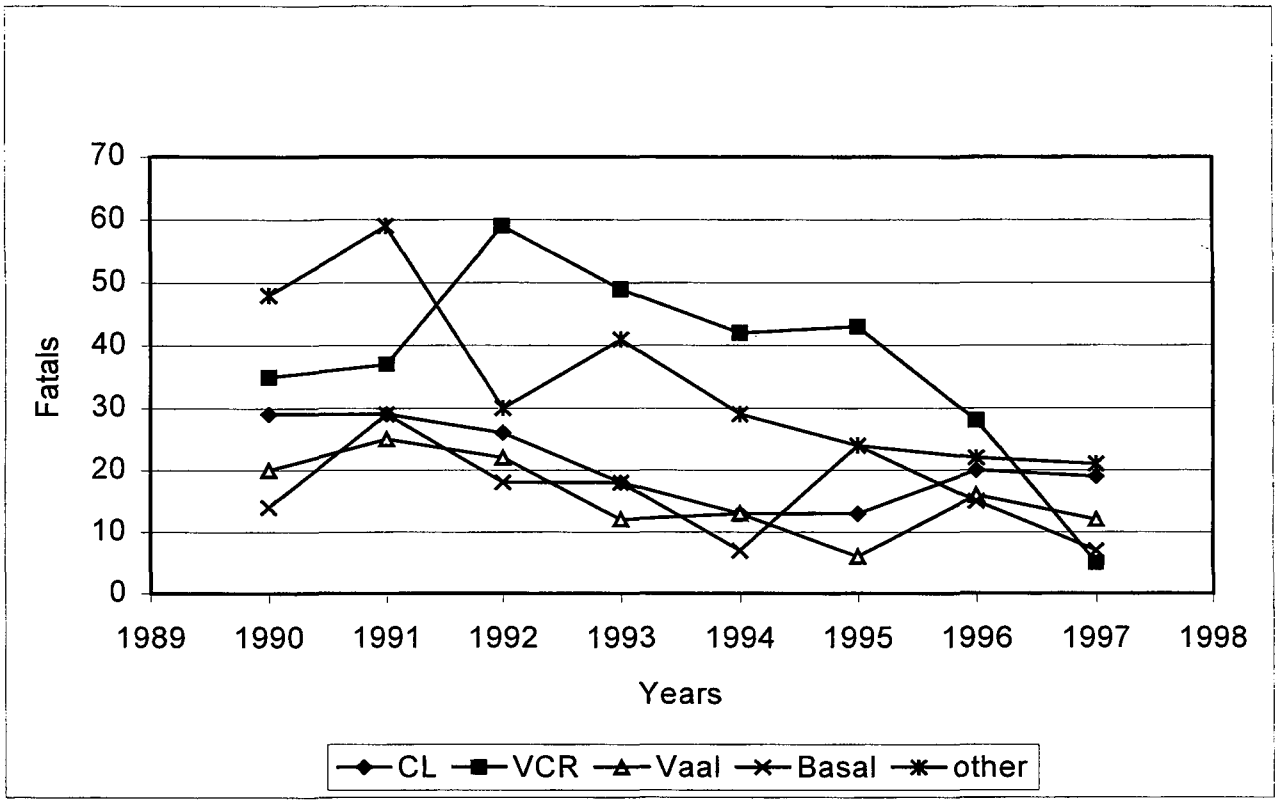

Figure 3.3.10 Stope and back area fatalities by reef.

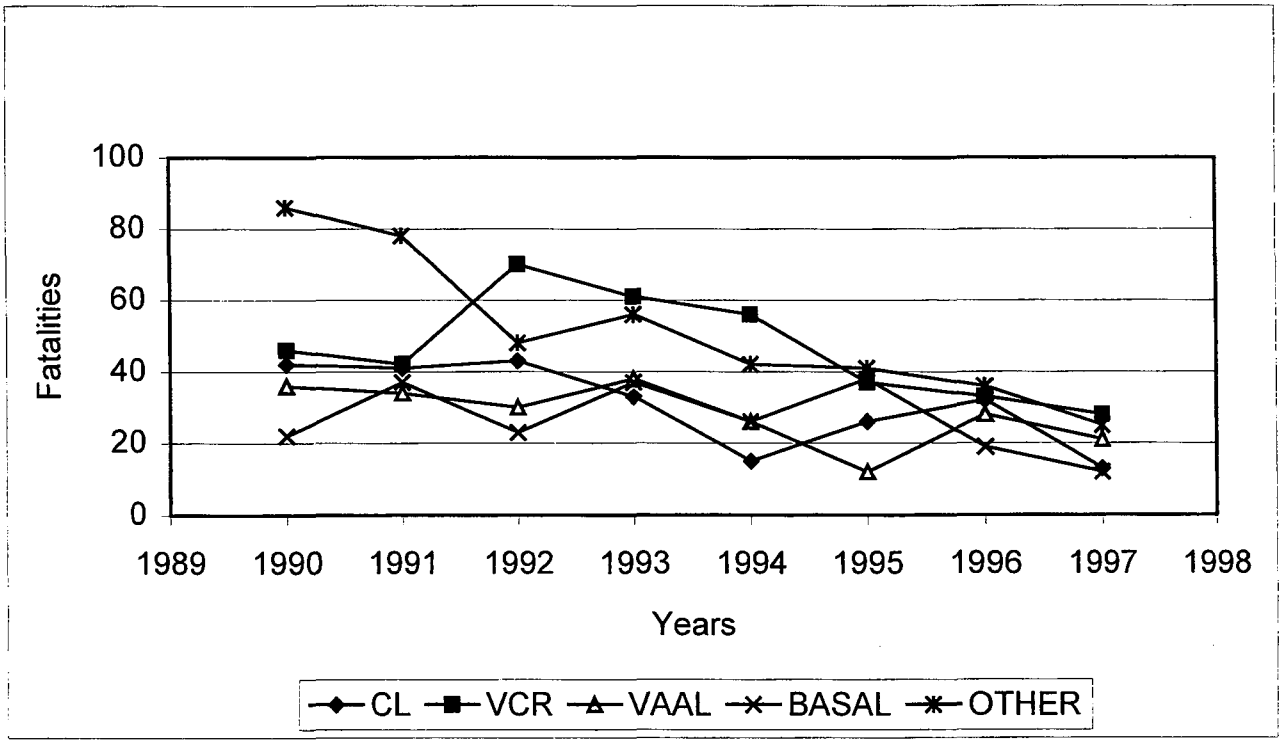

Figure 3.3.11 On-reef fatalities by reef.

3.4 Normalised fatality trends

To compare safety records and gain insights into accident trends, the number of fatalities that occur each year need to be normalised with respect to production data. For the purposes of showing general rock-related safety trends from 1990 to 1997 (Figure 3.4.1), the accident data is normalised with respect to three parameters: (i) square metres mined, (ii) workforce and (iii) gold production. In each case a least squares trend line is fitted to the data, bounded by trend lines indicating 80 per cent confidence envelopes. For example in case (i), fatals normalised with respect to square metres mined, the average decrease is 2,8 per cent per year and, considering the scatter of the data, it can be stated with 80 per cent confidence that the average decrease is between 1,3 per cent and 4,3 per cent per year.

From Figure 3.4.1 it is evident that in all three cases the normalised fatality trends are decreasing. The mean decrease of the three cases is an average 4,5 per cent per year, with an 80 per cent confidence that the average decrease is between 2,9 per cent and 6,2 per cent per year.

Figures 3.4.2 to 3.4.6 illustrate rockburst versus rockfall accident fatality trends normalised with respect to square metres mined for various reef types. From these trends it is apparent that the main factor contributing to the industry average decrease in fatalities, is a decrease in the rockburst related fatalities associated with mining the VCR. The fatality trends of the other reefs remain comparatively constant.

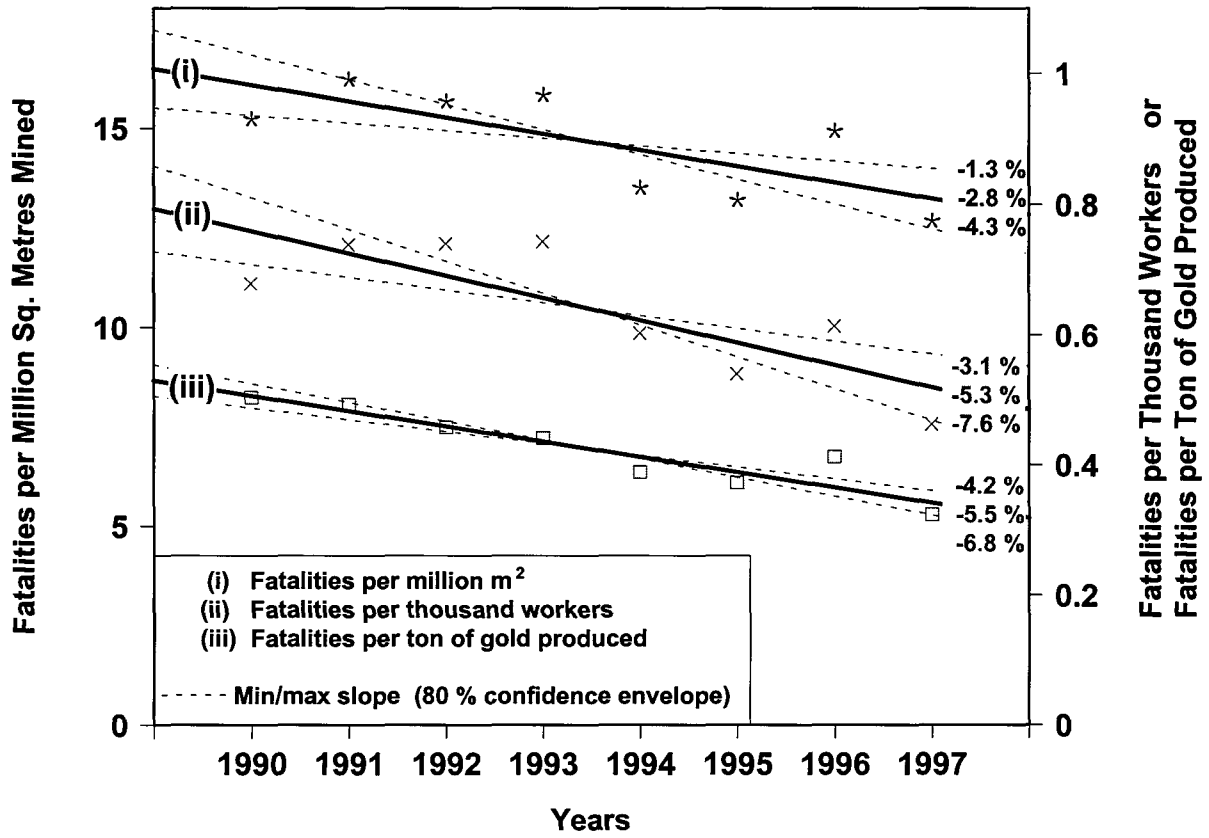

Figure 3.4.1 Total rock related fatalities normalised with respect to square metres mined, number of workers, and ton of gold produced.

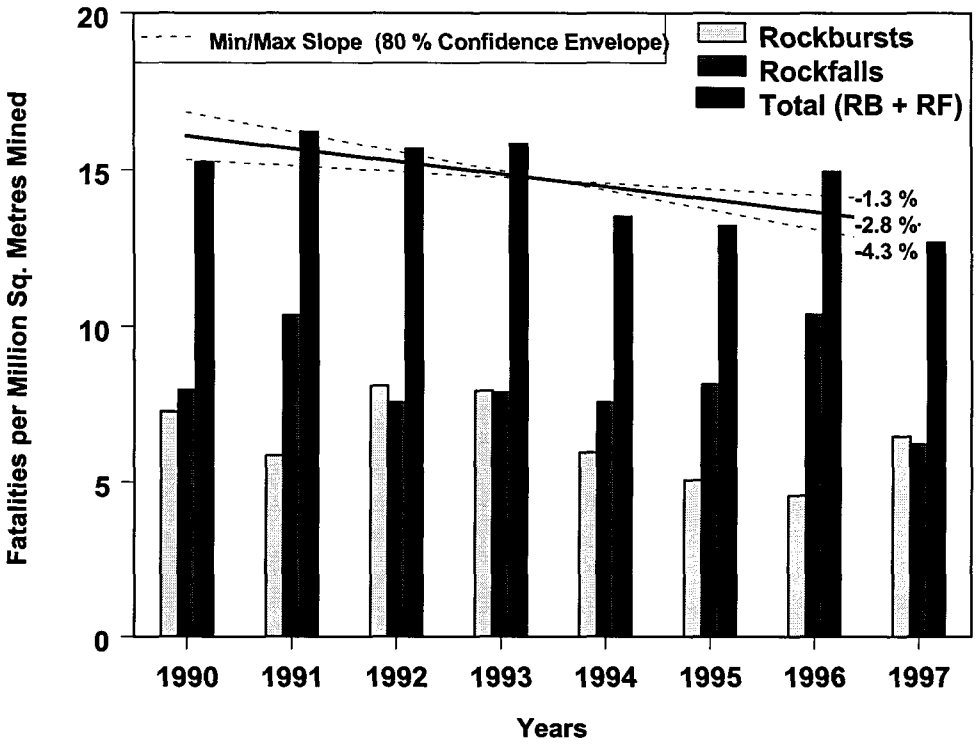

Figure 3.4.2 Total rock related fatalities associated with all reefs.

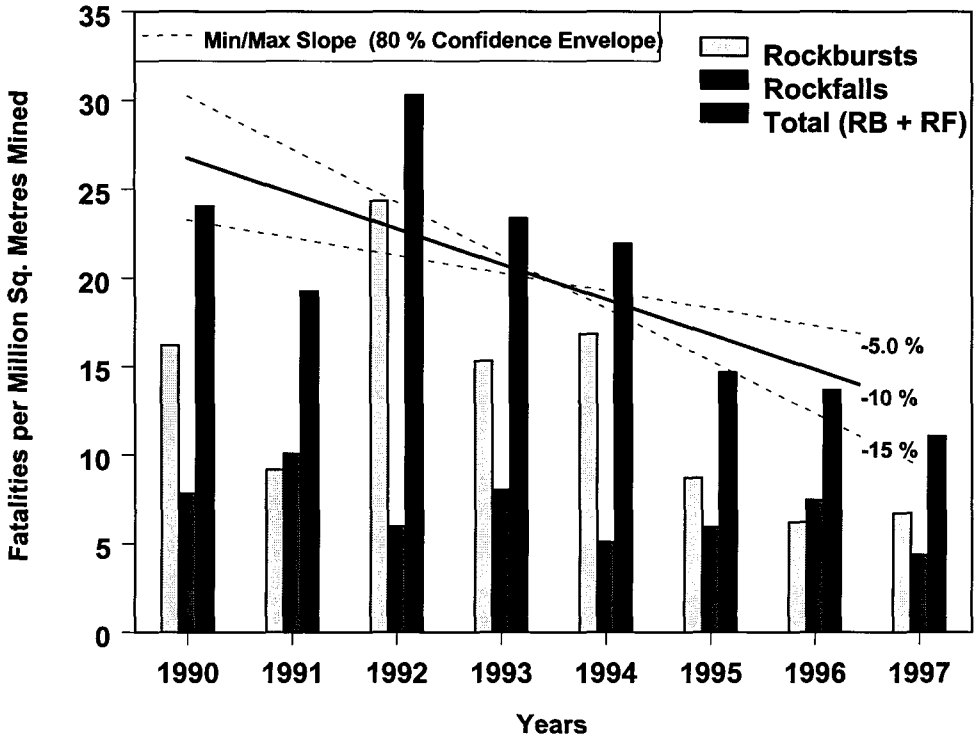

Figure 3.4.3 Total rock related fatalities associated with VCR.

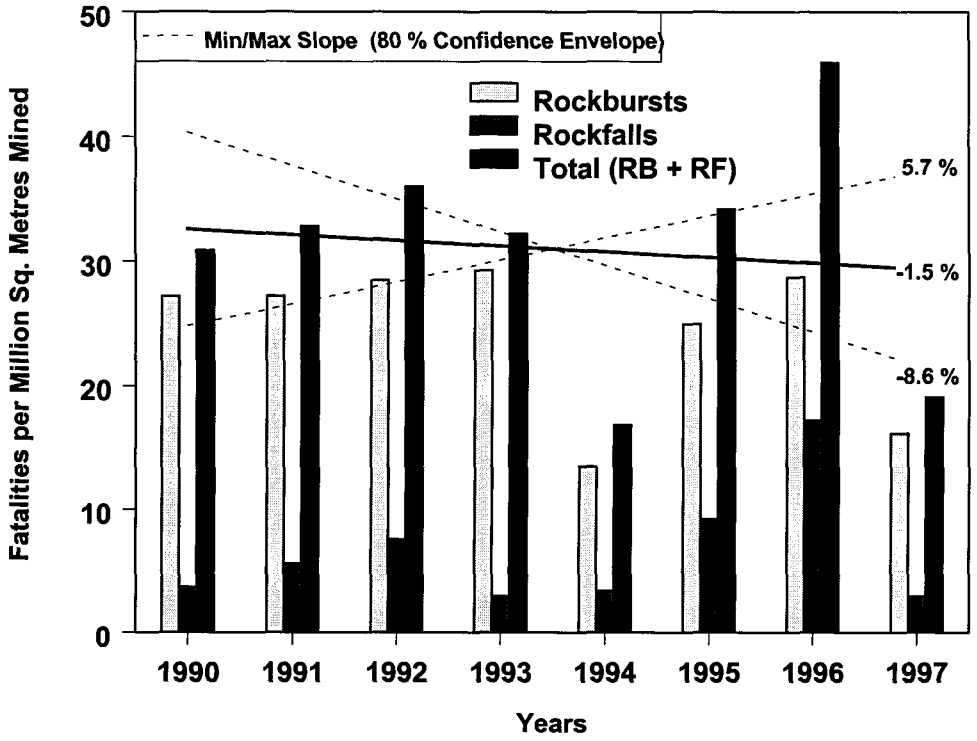

Figure 3.4.4 Total rock related fatalities associated with Carbon Leader Reef.

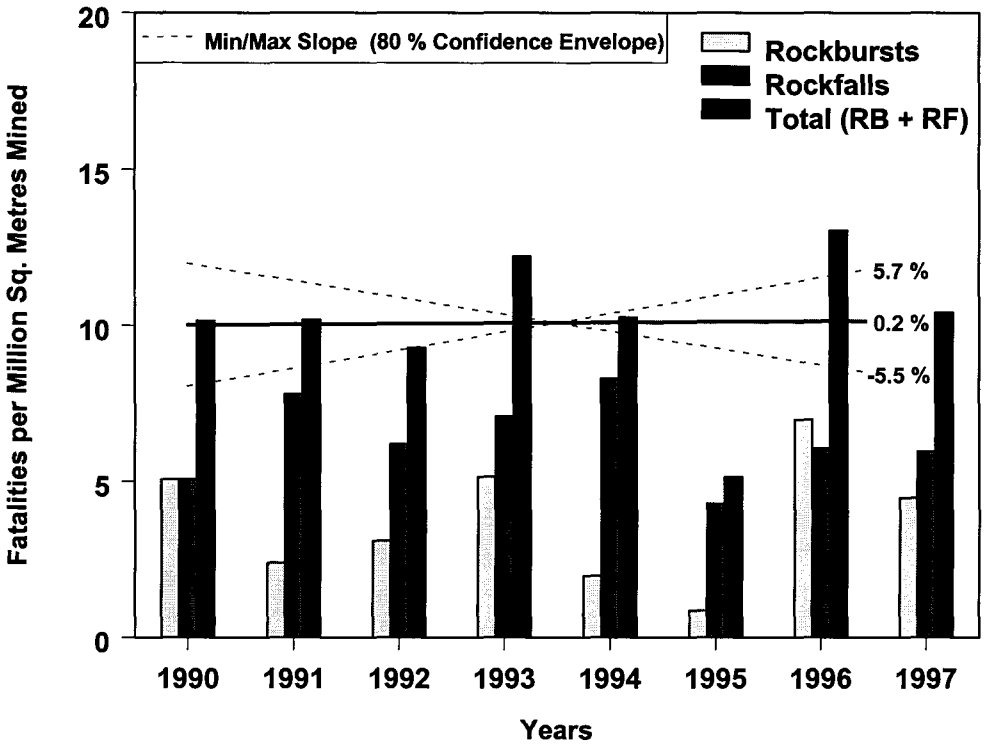

Figure 3.4.5 Total rock related fatalities associated with Vaal Reef.

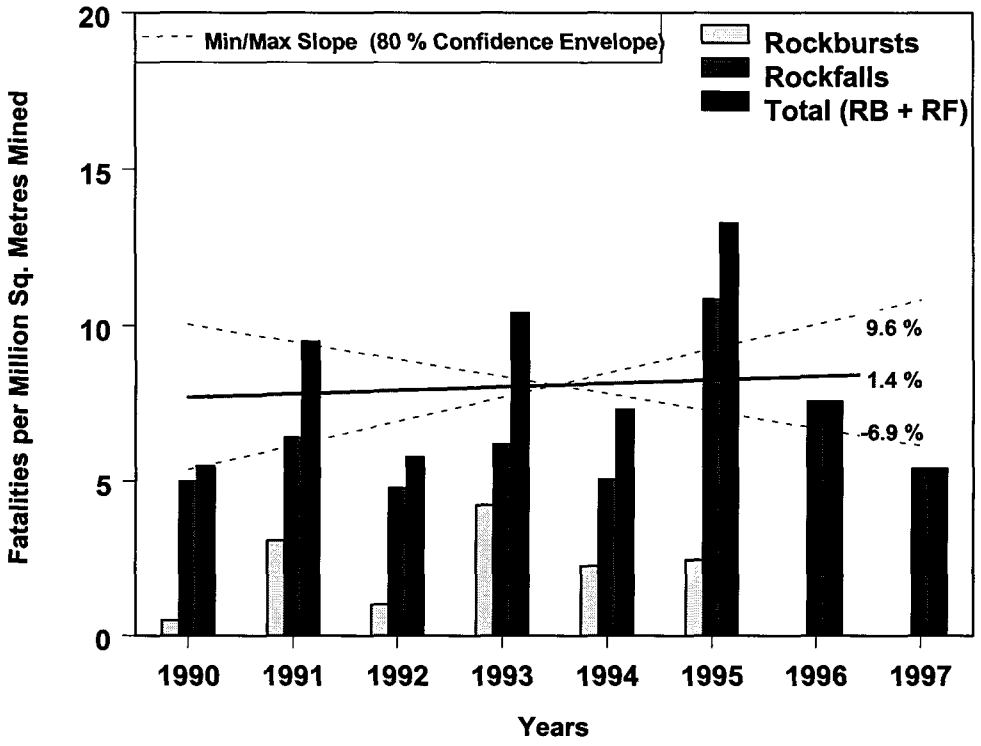

Figure 3.4.6 Total rock related fatalities associated with Basal Reef.

3.5 Fatalities according to location

Figure 3.5.1 shows the percentage of total rock-related fatalities according to location. It is evident that the major problem area is the stope (55 per cent) and particularly the stope face (> 50 per cent), whilst few fatalities are associated with the back areas (< 5 per cent). The strike gully is associated with the second highest number of fatalities (15 per cent). It is notable that, out of the five main hazard areas, the strike gully is the only location where more fatalities occur due to rockbursts, as opposed to rockfalls.

The results of the analyses of 1807 fatals are summarized in the following table, and indicate that the problematic area is the stope face.

Table 3.4.1 Percentage of total rock related fatals according to location, rockburst and rockfall.

	Rockburst (%)	*Rockfall (%)*	*Total (%)*
Stope	*25,4*	*29,4*	*54,8*
Strike gully	*7,9*	*6,6*	*14,5*
Centre gully	*1,4*	*3,2*	*4,6*
Haulage	*4,1*	*4*	*8,1*
Crosscut	*1,9*	*4,8*	*6,7*
Other	*2,8*	*8,2*	*11*
	43,5	*56,2*	*99,7*

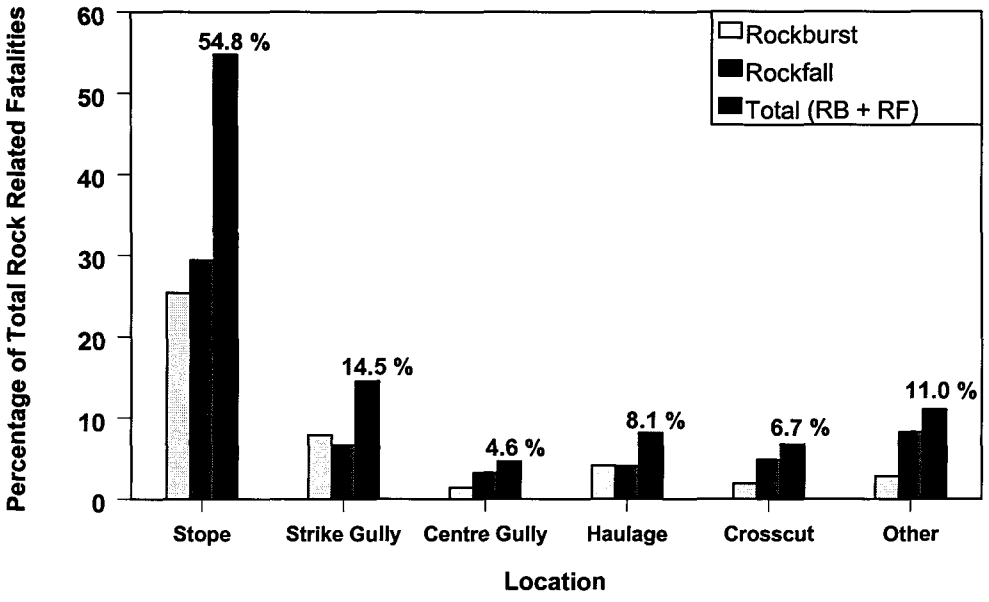

Figure 3.5.1 Fatalities categorised according location.

3.6 Gully related fatalities

A significant number of fatalities occur in gullies (see Figure 3.5.1). In order to gain insights into these fatalities, the gully fatalities are compared to the total number of fatalities. In addition, the strike gully fatalities are compared to the dip gully fatalities for each mining region. The results are shown in Figure 3.6.1 to 3.6.8.

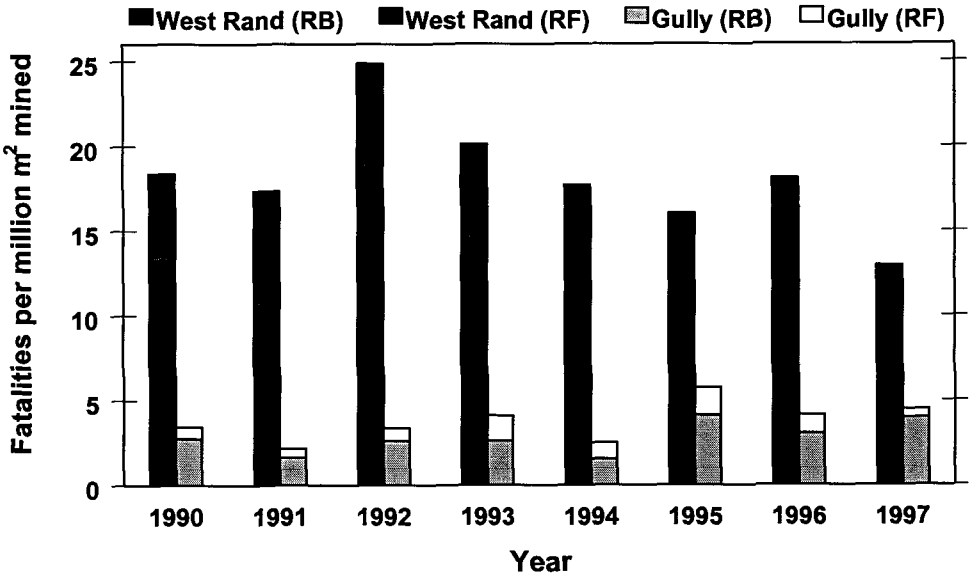

Figure 3.6.1 Total West Rand versus gully rock related fatalities.

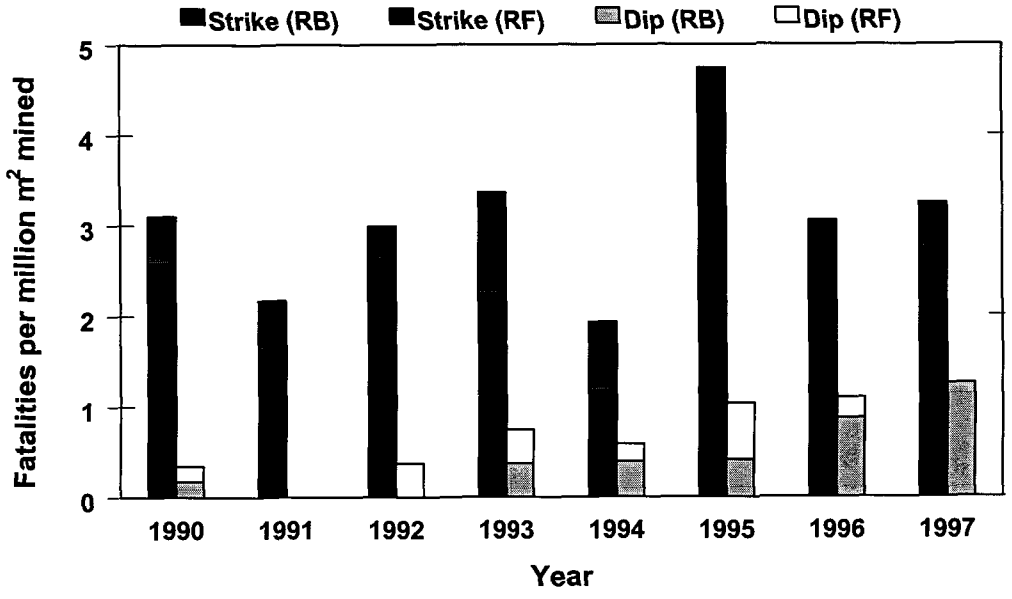

Figure 3.6.2 West Rand strike versus dip gully rock related fatalities.

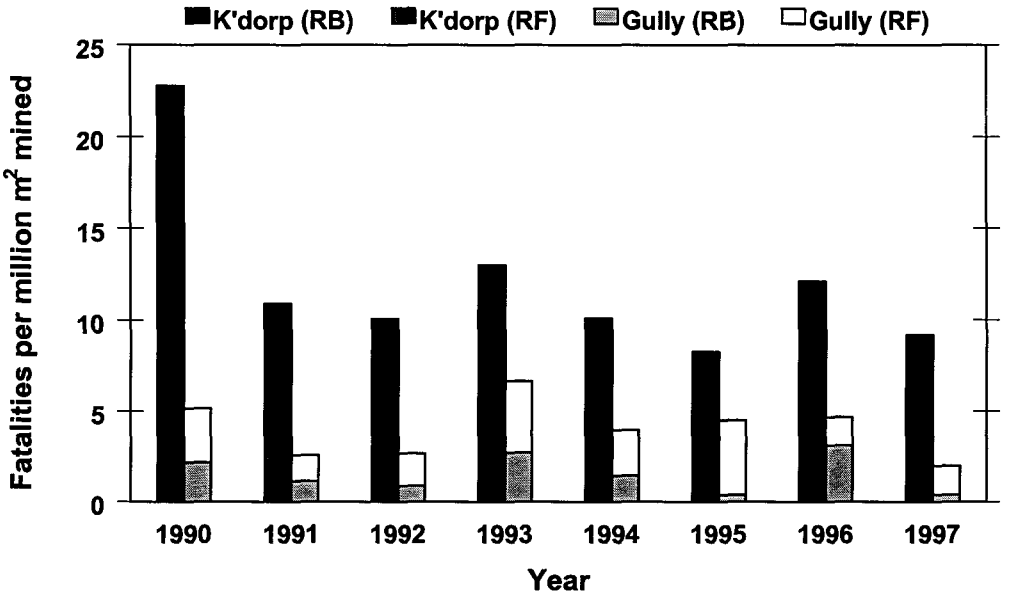

Figure 3.6.3 Total Klerksdorp versus gully rock related fatalities.

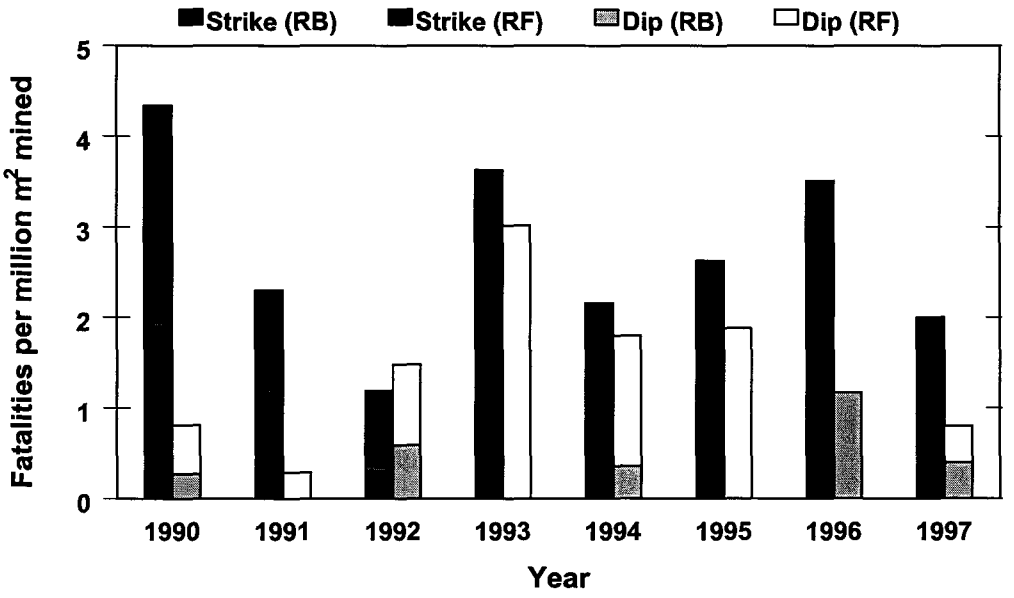

Figure 3.6.4 Klerksdorp strike versus dip gully rock related fatalities.

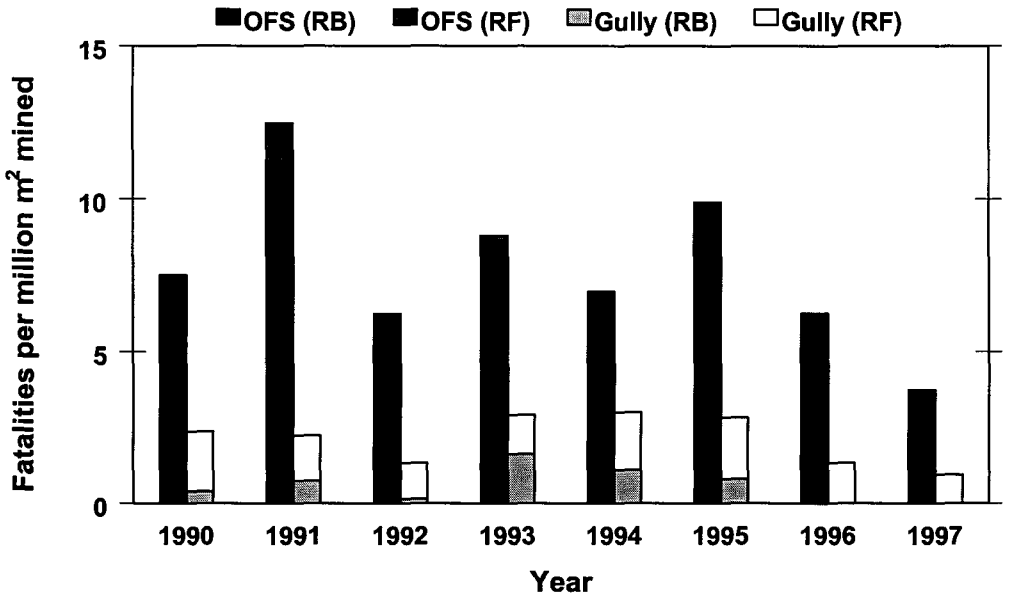

Figure 3.6.5 Total OFS versus gully rock related fatalities.

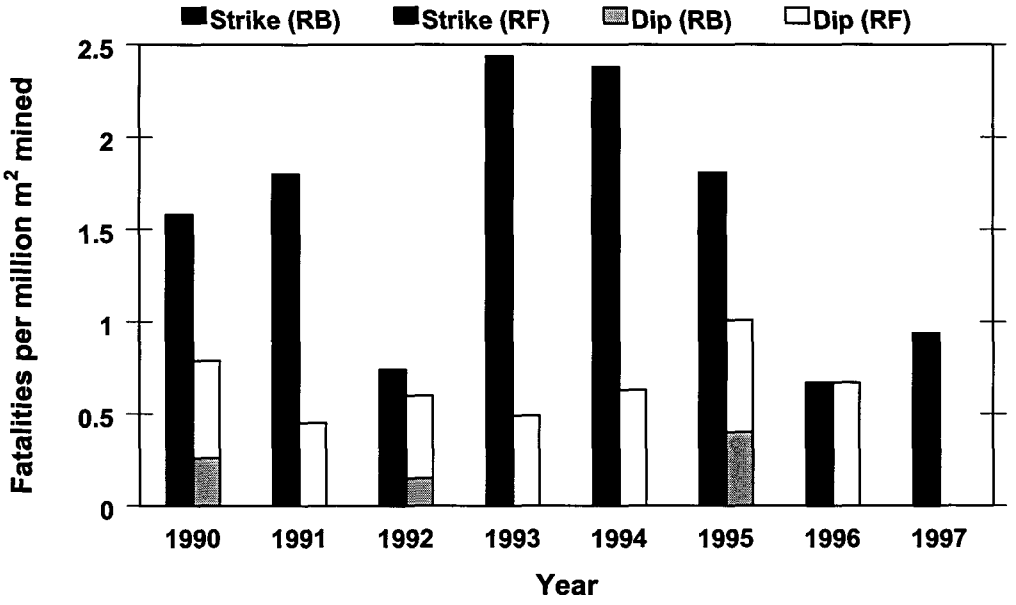

Figure 3.6.6 OFS strike versus dip gully rock related fatalities.

3.7 Rockburst versus rockfall hazard ratings

Further analyses that have been conducted to determine the hazard rating of individual reefs indicate that mining on the **Carbon Leader Reef** is the most hazardous. The comparison of the ratio of rockburst to rockfall fatalities indicates that the major contributing factor is rockbursts (Figure 3.7.1). **VCR** mining is the second most hazardous and, although the ratio is significantly less than that of Carbon Leader, the rockbursts also cause more deaths than rockfalls.

The rest of the reefs have a ratio of less than one, which indicates rockfalls being the major contributor.

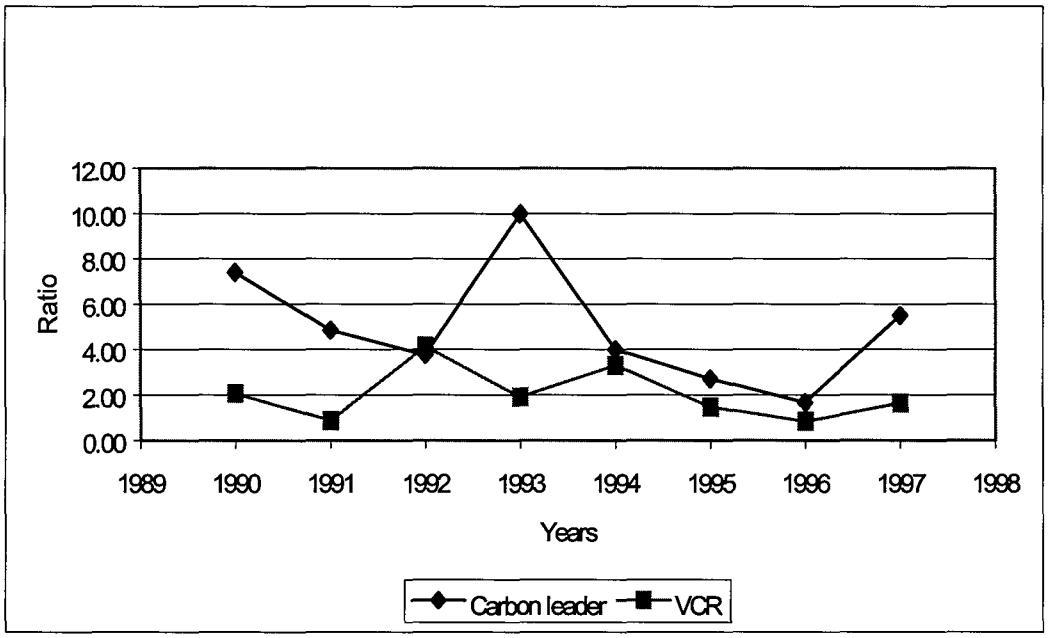

Figure 3.7.1 Ratio of rockburst to rockfall for Carbon Leader Reef and VCR.

3.8 An estimate of support resistance requirements

In order to determine a support resistance criterion that would prevent rockfalls for those areas not subject to seismic events, it is necessary to analyse the fallout thickness. The accident database has been used to derive this data and cumulative percentage fallout thicknesses are shown in Figures 3.8.1 to 3.8.4 for the Carbon Leader Reef, the Ventersdorp Contact Reef, the Vaal Reef and the Basal Reef, respectively.

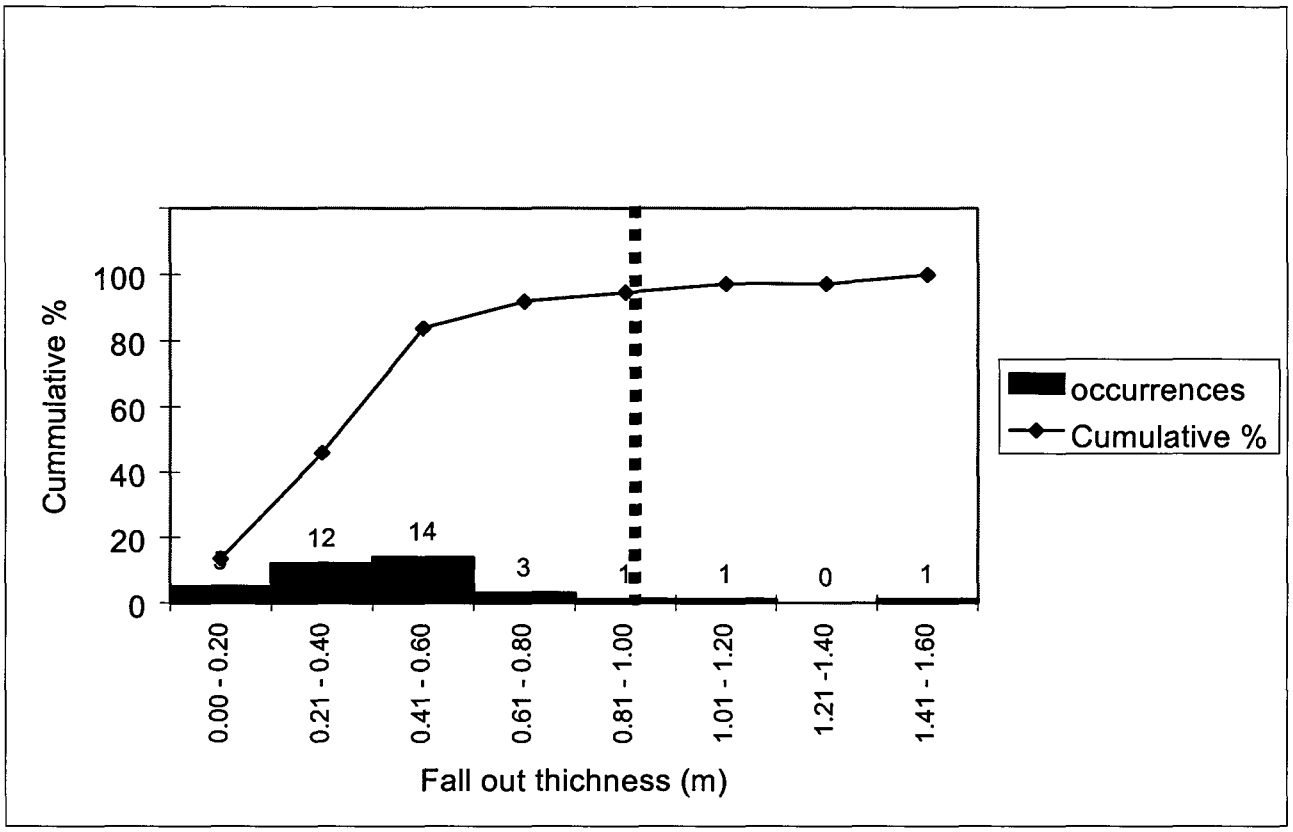

Figure 3.8.1 Cumulative rockfall fallout thickness for the Carbon Leader Reef.

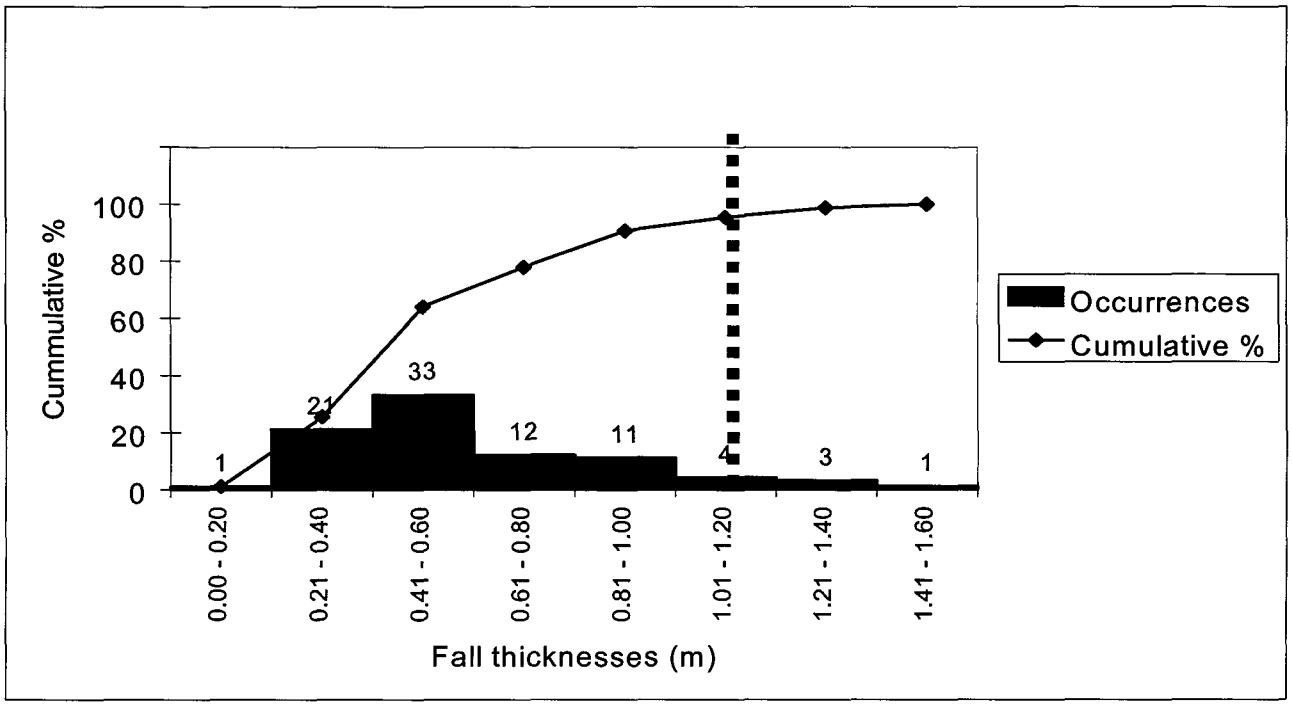

Figure 3.8.2 Cumulative rockfall fallout thickness for the VCR Reef.

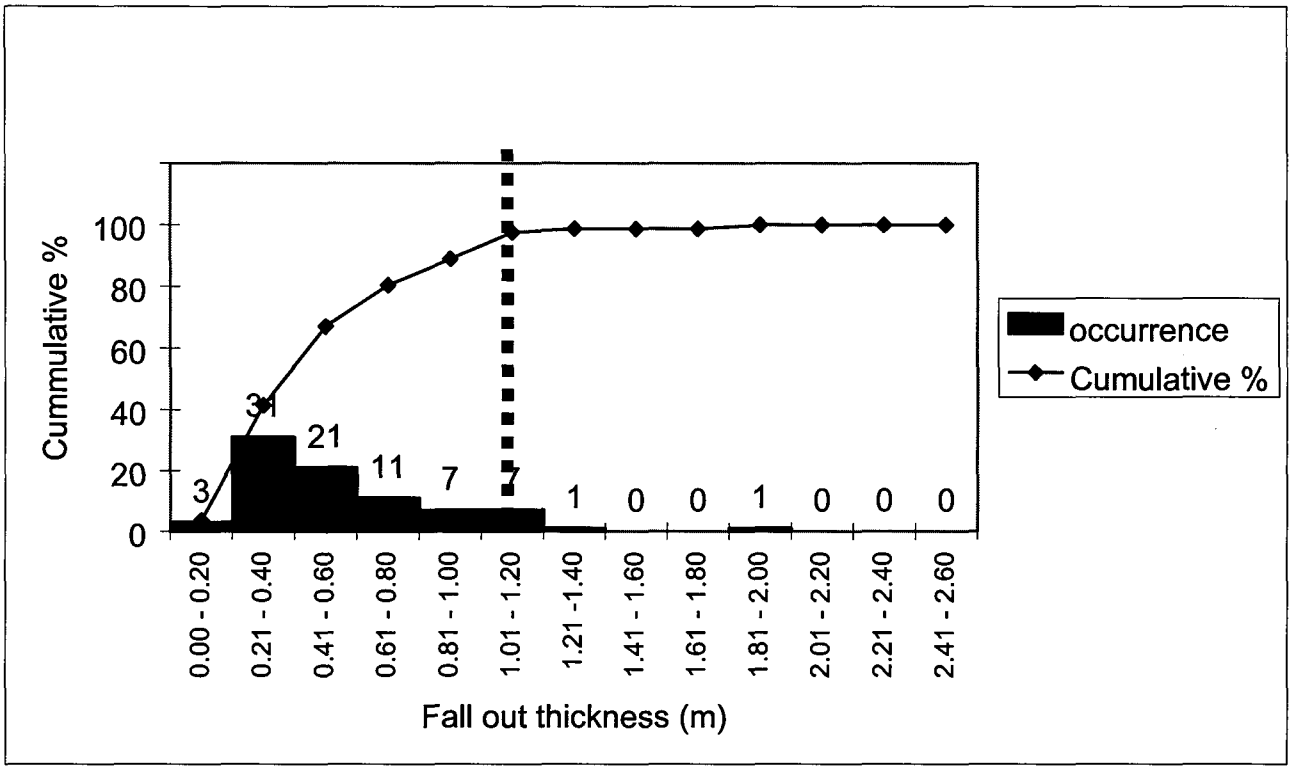

Figure 3.8.3 Cumulative rockfall fallout thickness for the Vaal Reef.

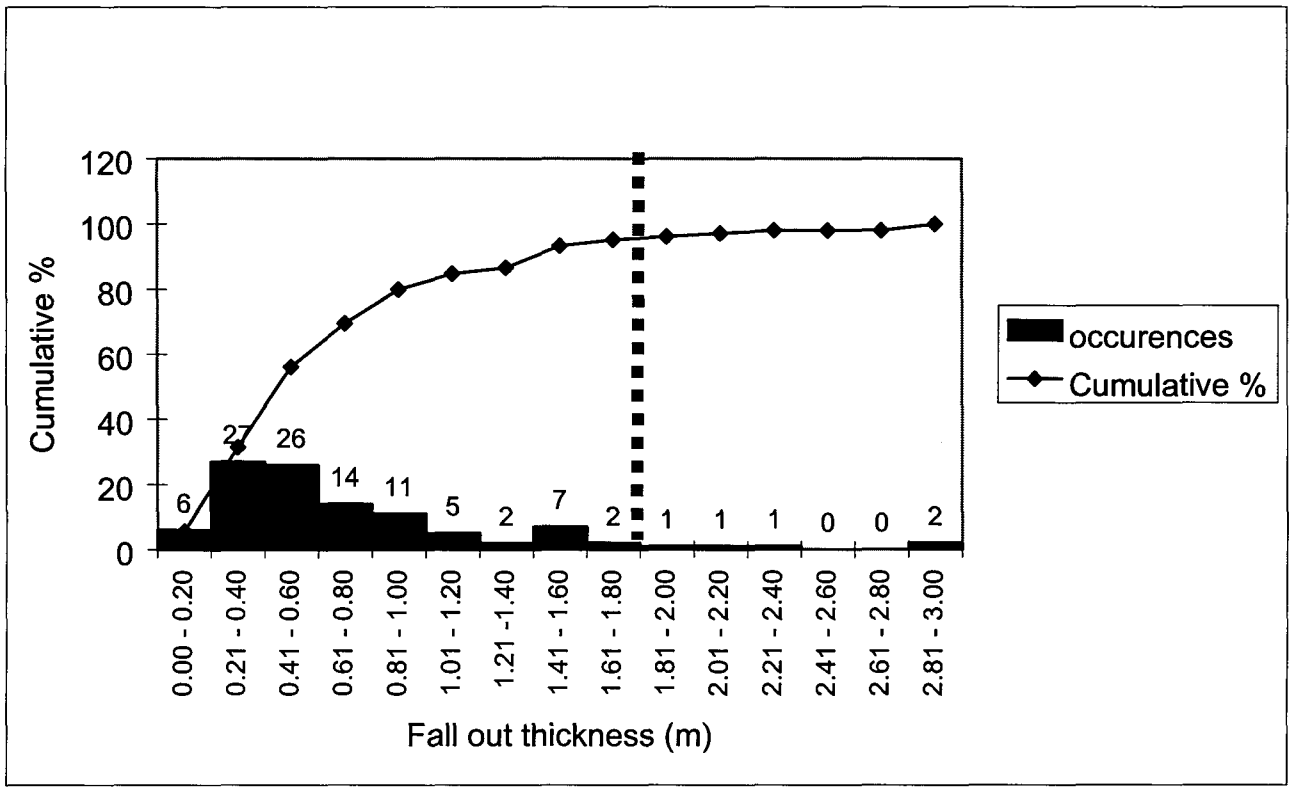

Figure 3.8.4 Cumulative rockfall fallout thickness for the Basal Reef

The criterion requires that the support system should prevent 95 per cent of all fallouts. The table below shows the fallout thickness for the 95 per cent frequency level, i.e. 95 per cent of all falls were the indicated thickness or less. Data is given for (i) occurrences of rockfalls, and (ii) associated number of fatalities. It is evident that the 95 per cent cumulative fallout thicknesses are the same for either case investigated. The table also shows the associated support resistance criteria.

Table 3.8.1 Fallout thickness for the various reefs at 95 per cent frequency level as the support resistance criterion.

95 per cent fallout frequency level (Rockfalls)			
Reef type	**Fatalities**	**Occurrences**	**Support resistance**
Carbon Leader	1,0 m	1,0 m	27,5 kN/m^2
VCR	1,2 m	1,2 m	31,8 kN/m^2
Vaal	1,2 m	1,2 m	31,8 kN/m^2
Basal	1,8 m	1,8 m	47,7 kN/m^2

The support resistance of stope support systems, that have been designed, or are in current use, should be evaluated against the support resistance required for the appropriate reef, given above, to ensure that they exceed the criterion.

3.9 An estimate of energy absorption requirements

The currently used energy absorption criterion of 60 kJ/m^2 has been considered necessary for the stope support to reduce rockburst damage. The basis of this criterion was a support resistance of 200 kN/m^2 which could be displaced through 0,3 m at 3 m/s during a rockburst and in the process absorb 60 kJ/m^2 of energy. The energy absorption ability of support systems used in rockburst prone stopes should, therefore, have met this criterion. In this report, this criterion has been re-evaluated using quantified ejection thicknesses for the four reefs from the accident database. For the purpose of these analyses, the ejection velocity is still considered to be 3 m/s.

Figures 3.9.1 to 3.9.4 show histograms of ejected block thickness from rockbursts as a cumulative percentage of increasing block thickness, measured at the site of fatal accident for the Carbon Leader, the Ventersdorp Contact Reef, the Vaal Reef, and the Basal Reef. The ejection thickness, representing 95 per cent of the cumulative percentage, will be used for the purpose of developing the energy absorption criteria.

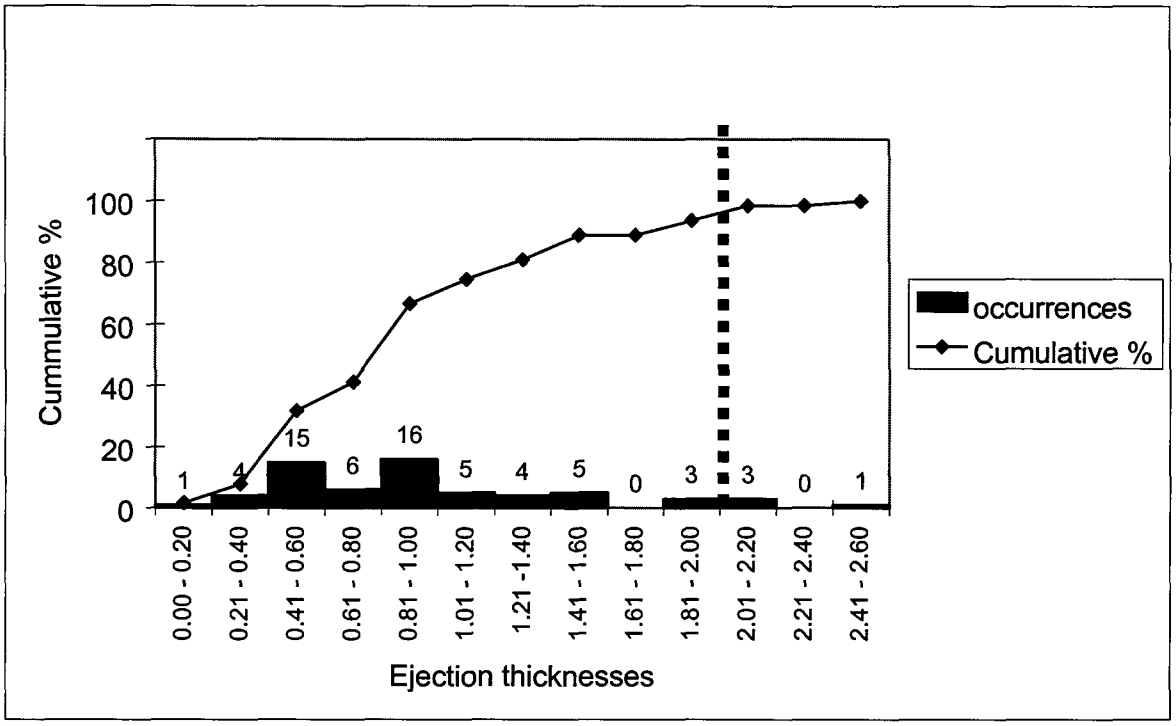

Figure 3.9.1 Cumulative rockburst ejection thicknesses for the Carbon Leader Reef.

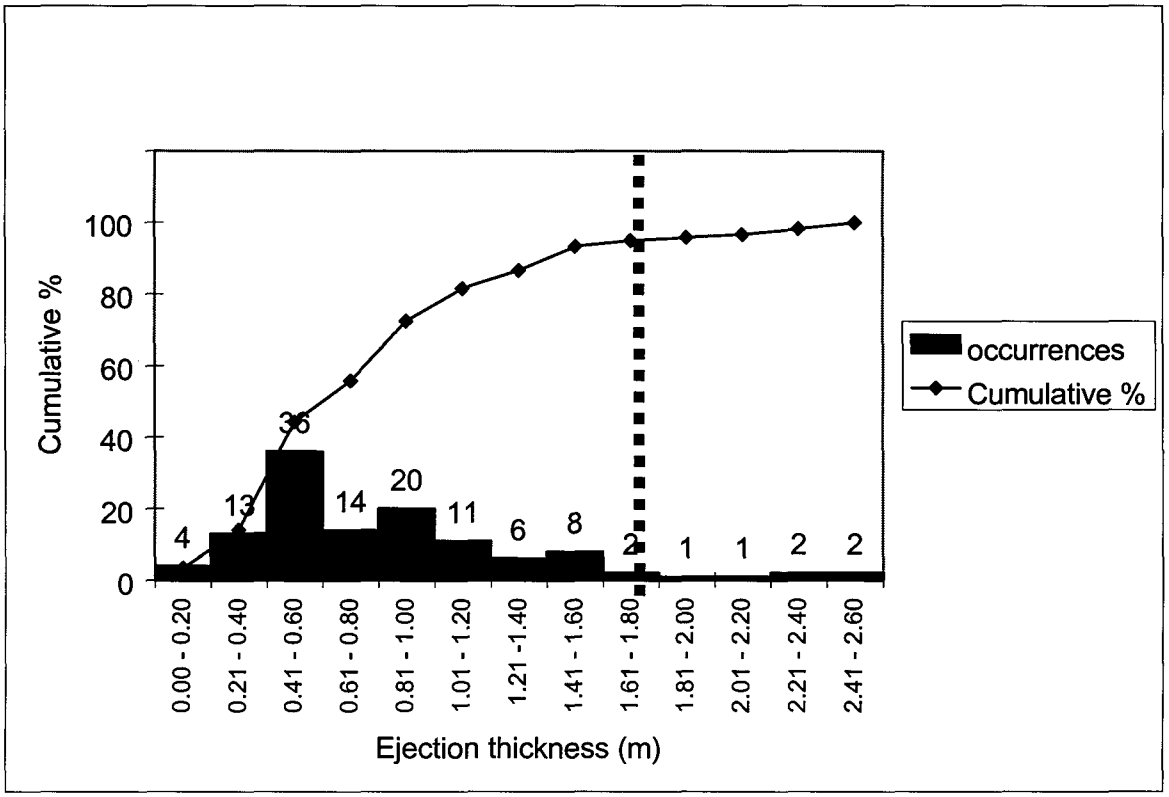

Figure 3.9.2 Cumulative rockburst ejection thicknesses for the Ventersdorp Contact Reef.

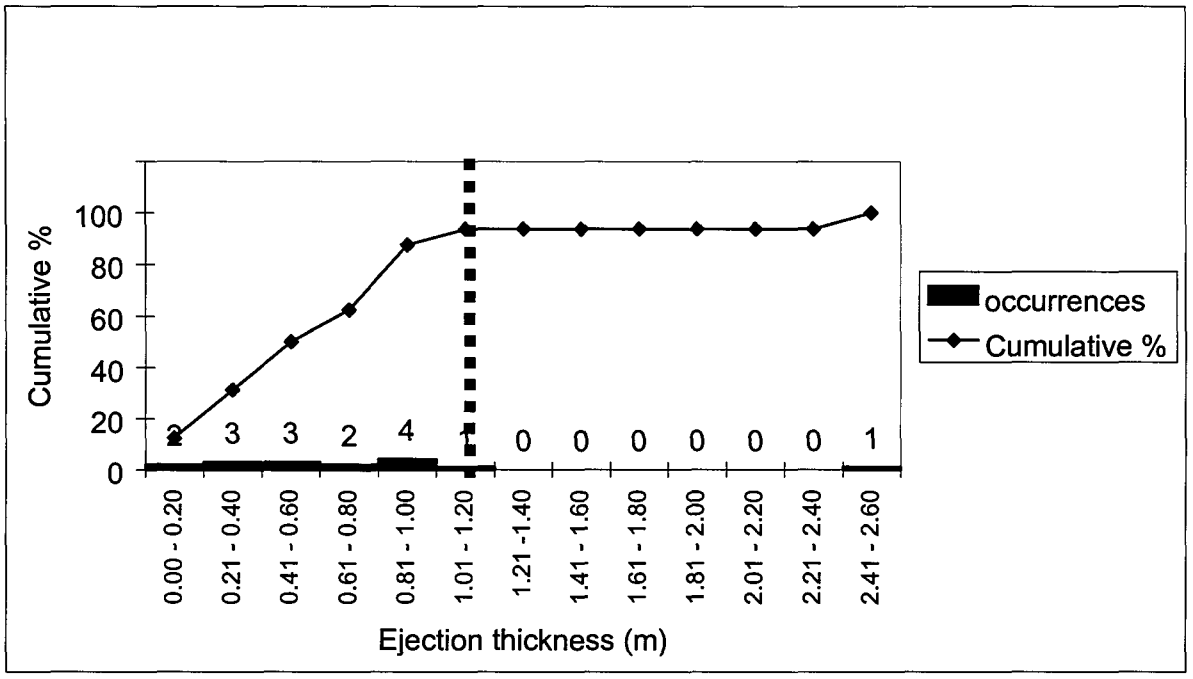

Figure 3.9.3 Cumulative rockburst ejection thicknesses for the Vaal Reef.

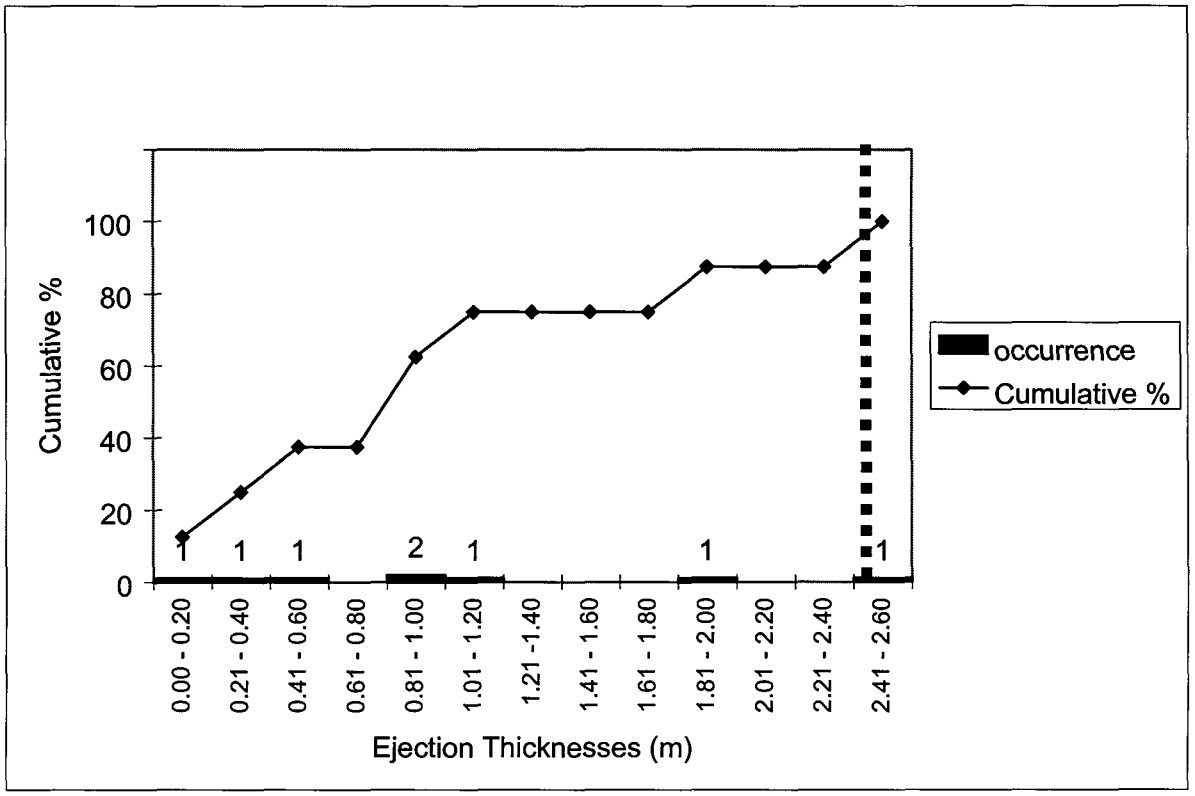

Figure 3.9.4 Cumulative rockburst ejection thicknesses for the Basal Reef.

The actual number of rockbursts used to construct the histograms are 63 for Carbon Leader Reef, in which 104 fatalities occurred; 120 for Ventersdorp Contact Reef, in which 218 fatalities occurred; 16 for Vaal Reef, in which 26 fatalities occurred, and 8 for the Basal Reef, in which 12 fatalities occurred.

The small number of rockbursts and associated fatalities of the Vaal Reef and Basal Reef are due to the fact that rockbursts are relatively uncommon across these reefs. Hence the ejection thickness, determined by means of the relatively sparse data, should be interpreted with care. Further data is required particularly in the case of the Basal Reef, where a single rockburst increases the 95 per cent cumulative ejection thickness to 2,6 m.

Using these block ejection thicknesses, it is possible to calculate a minimum energy absorption requirement per square metre of stope hangingwall that a support system should provide to stabilise the stope hangingwall in 95 per cent of the cases. The velocity of ejection is assumed to be 3 m/s and it is also assumed that the support system has the ability to yield 0,2 m, typical of the yieldability of hydraulic props and yielding timber props.

Therefore: Energy absorption criterion = $1/2mv^2 + mgh$

Where:
m = 2700 kg * ejection thickness
v = 3.0 m/s
h = 0,2m
g = 9,81
Eac is the energy absorption criterion

The energy absorption criterion is detailed for specific reefs in Table 3.9.1.

The energy absorption ability of stope support system that have been designed, or are in current use, should be evaluated against the energy absorption requirement or Eac for the appropriate reef, to ensure that they exceed the criterion.

Table 3.9.1 Ejection thicknesses for the various reefs at 95 per cent frequency level and the associated energy absorption criteria.

95 per cent ejection thickness frequency (Rockbursts)			
Reef type	**Fatalities**	**Occurrences**	**Energy absorption criteria**
Carbon Leader	2,2	2,2	38,4 kJ/m^2
VCR	1,8	1,8	31,4 kJ/m^2
Vaal	1,2	1,2	20,9 kJ/m^2
Basal	2,6	2,6	45,4 kJ/m^2

3.10 Fatality distribution in terms of distance from the stope face

In order to determine the distance from the stope face at which falls are likely to happen and injure people, the distances of the fatalities from the face were analysed for each reef for the period 1990 to 1997. These analyses were done on the fatalities that occurred on the stope face and stope back areas. This information was then normalized to the production in square metres. The results are illustrated in Figure 3.10.1 to 3.10.8.

From the results it is evident that, with exception of Vaal Reef and Basal Reef rockbursts, most fatalities occur between 1 m to 2,5 m behind the face. Further accident enquiry observations revealed that a significant percentage of all rockfall fatalities are associated with early examination and barring during the re-entry period. In most cases, the temporary support (such as minepoles or camlock props) in this region are being removed at the end of each shift before the blasting process. This causes the workers to be exposed to an unsupported hangingwall beam and exacerbates the rockfall hazard during re- entry.

The distance in which most rockburst fatalities occur on the Vaal Reef is approximately 3 m to 4 m from the stope face. This suggests the shakedown phenomenon during rockbursts is more problematic, as opposed to the face burst problem.

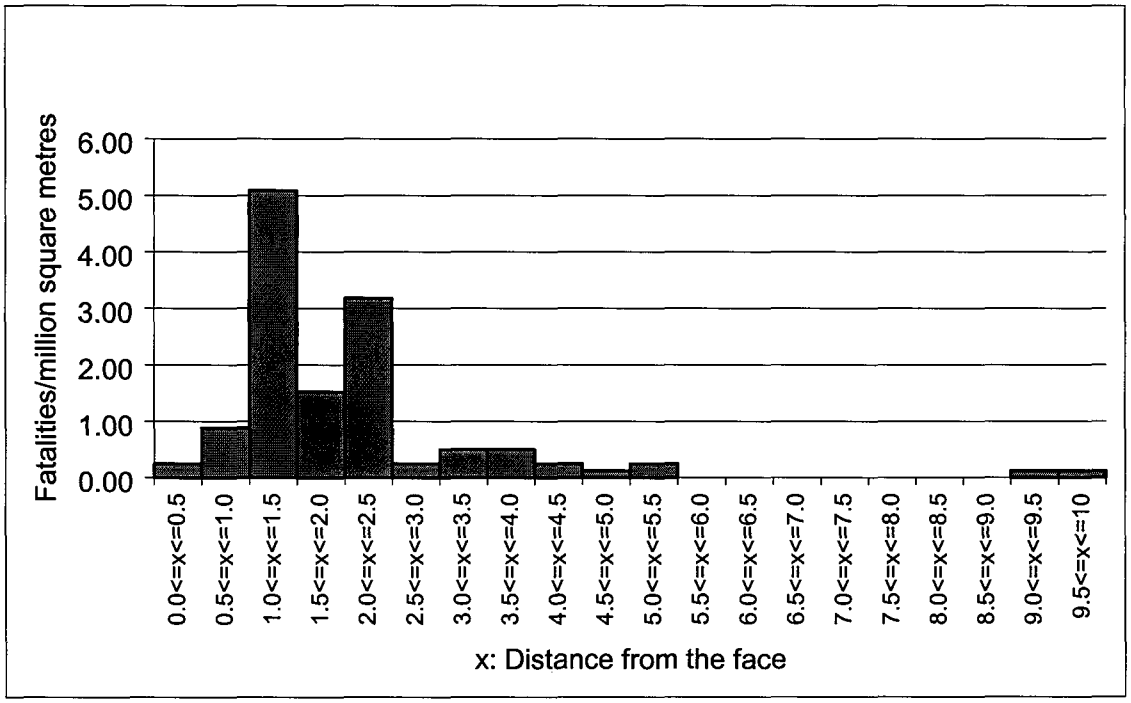

Figure 3.10.1 Distance of fatalities from the stope face for Carbon Leader rockbursts.

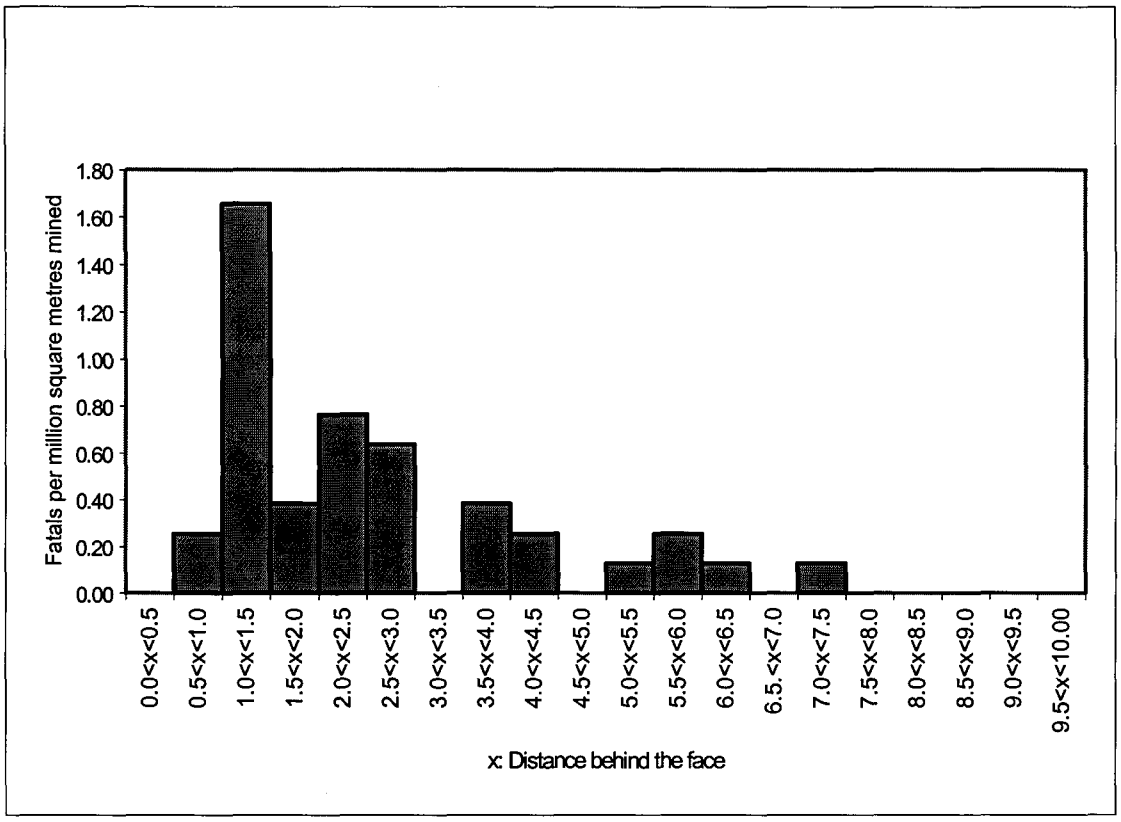

Figure 3.10.2 Distance of fatalities from the stope face for Carbon Leader rockfalls.

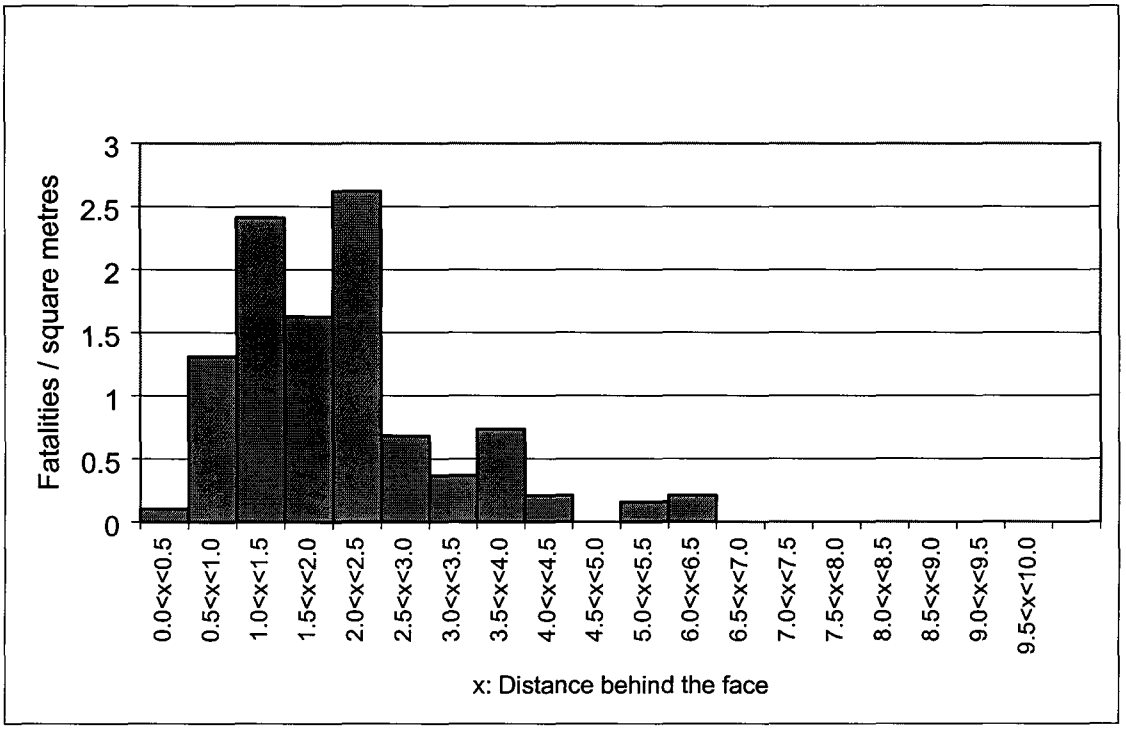

Figure 3.10.3 Distance of fatalities from the stope face for VCR rockbursts.

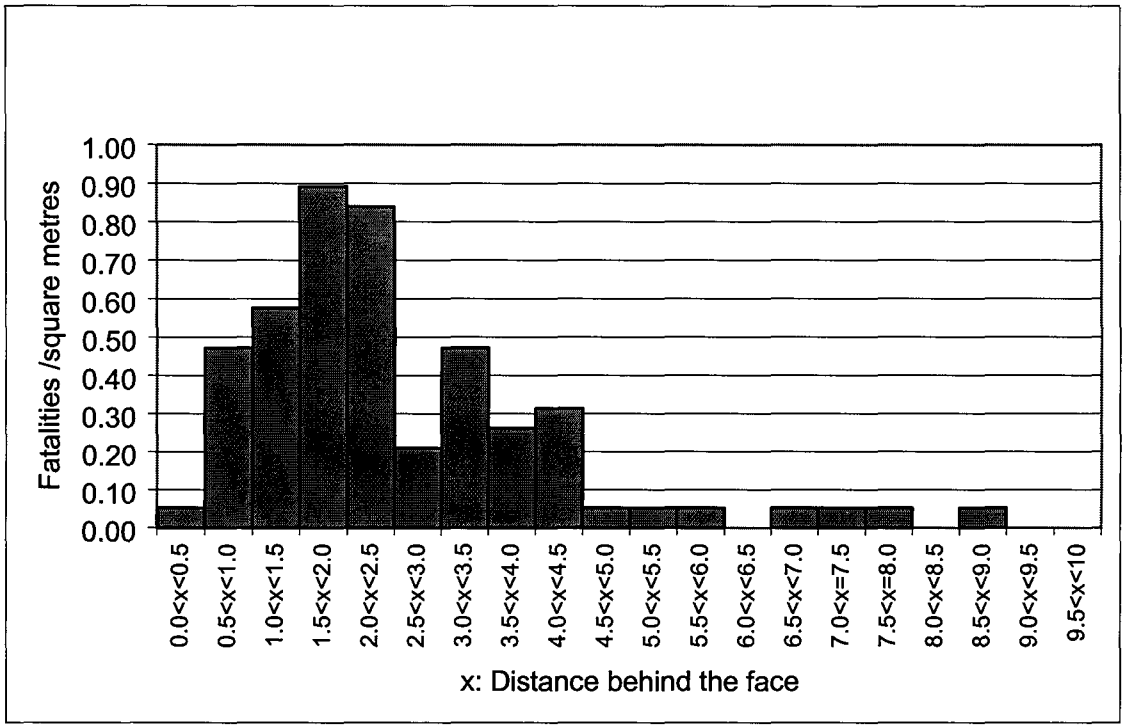

Figure 3.10.4 Distance of fatalities from the stope face for VCR rockfalls.

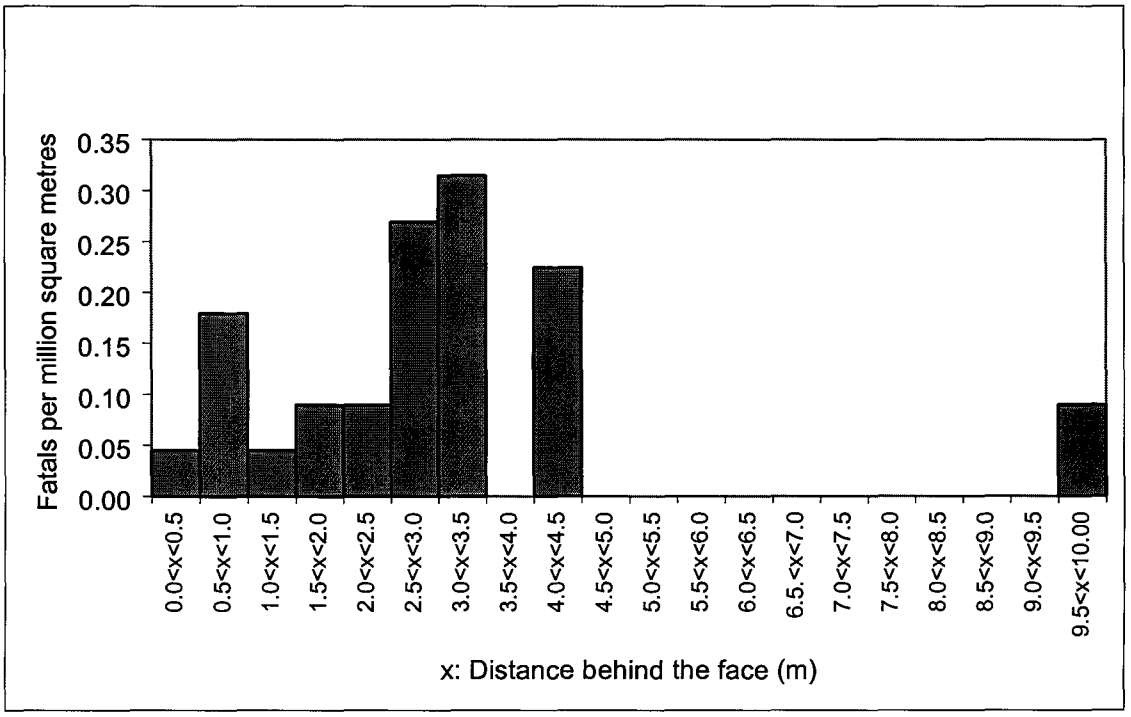

Figure 3.10.5 Distance of fatalities from the stope face for Vaal Reef rockbursts.

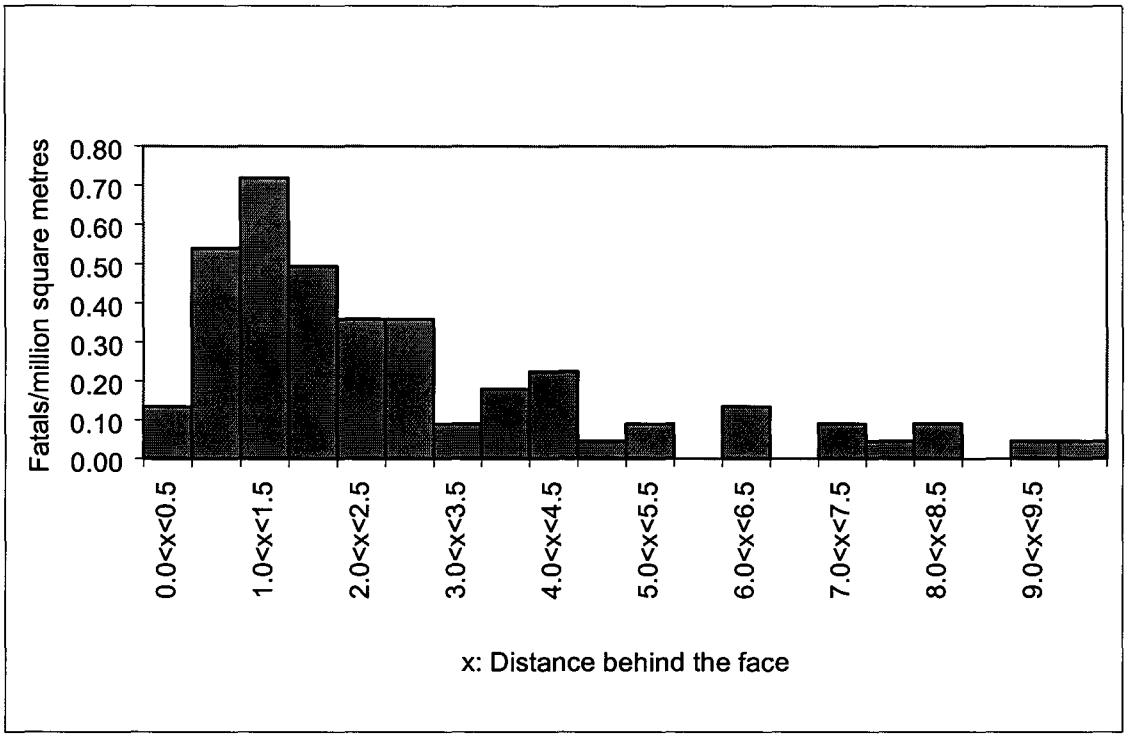

Figure 3.10.6 Distance of fatalities from the stope face for Vaal Reef rockfalls.

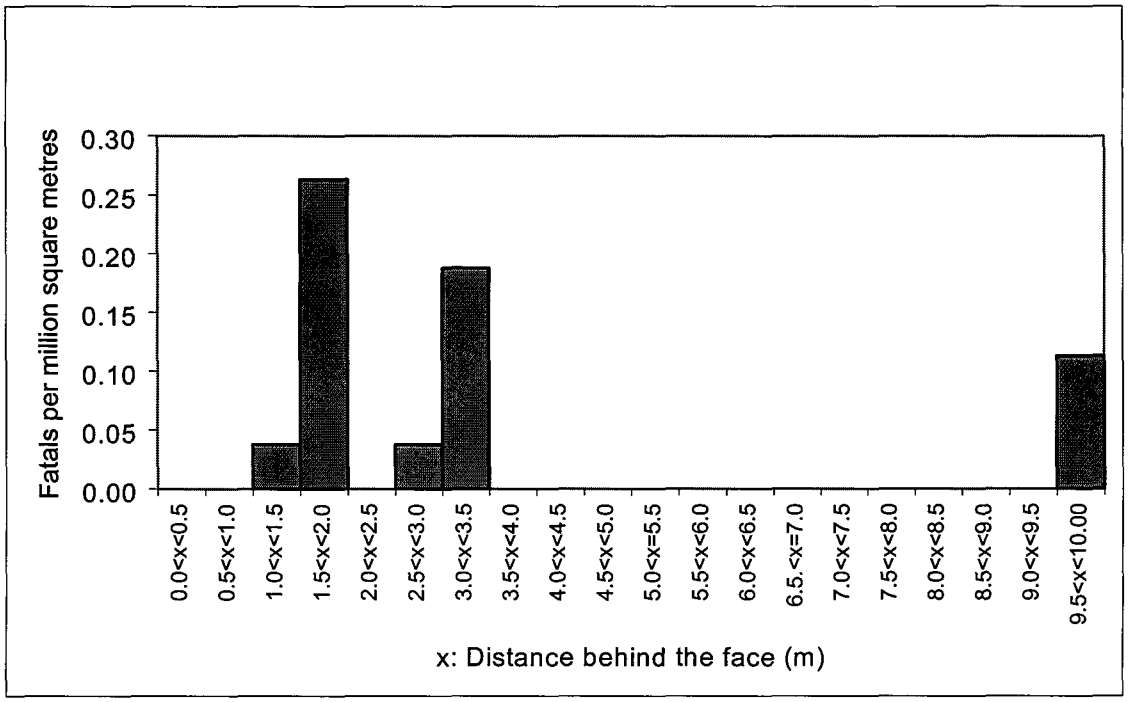

Figure 3.10.7 Distance of fatalities from the stope face for Basal Reef rockbursts.

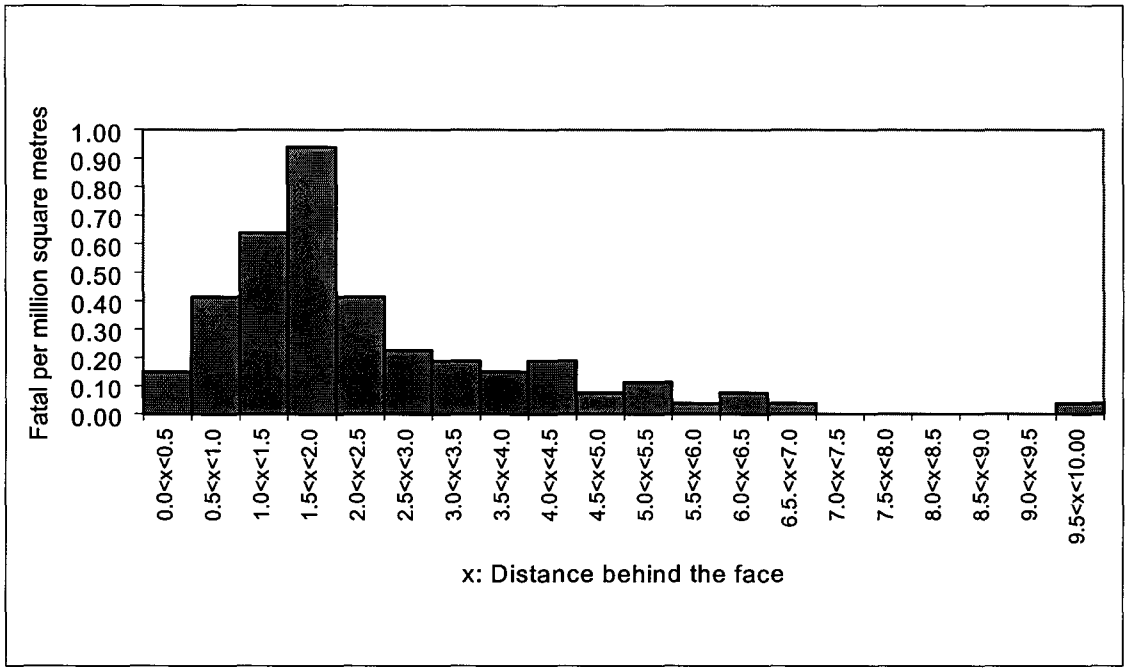

Figure 3.10.8 Distance of fatalities from the stope face for Basal Reef rockfalls.

3.11 Area mined

The area mined has decreased from 18,7 million m^2 in 1990 to 11,7 million m^2 in 1997. This represents a 32 per cent drop over the period. Figure 3.11.1 shows the decline in total annual area mined during the period 1990 to 1997.

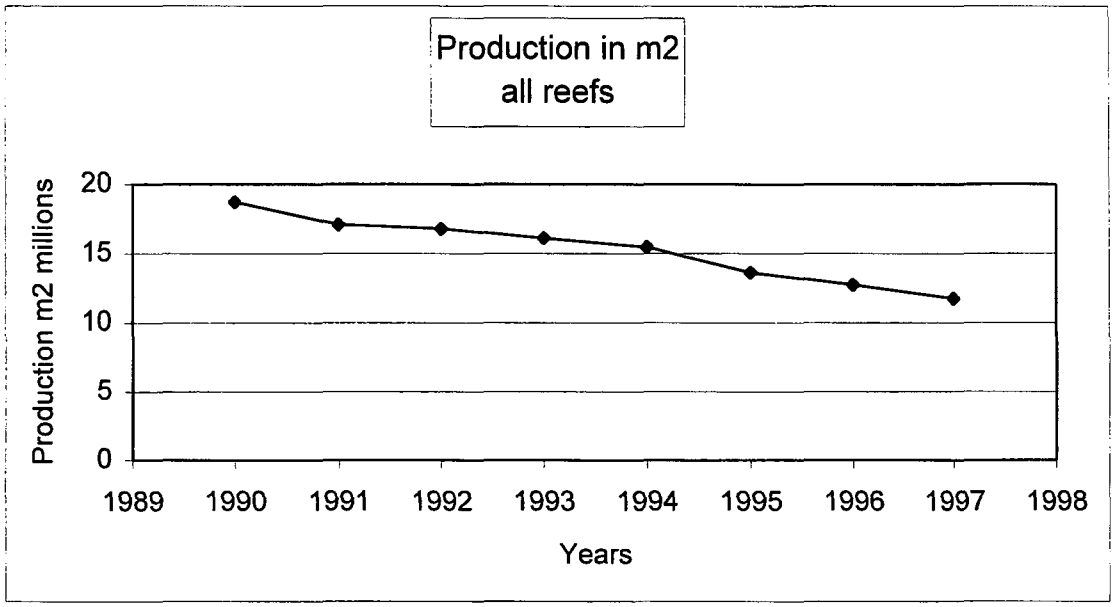

Figure 3.11.1 Total annual area mined since 1990

Figure 3.11.2 shows the annual area mined on each reef. With the exception of the VCR, the production of the reefs has continually declined over this period. The VCR has increased from 1,9 million m^2 to 2,5 million m^2.

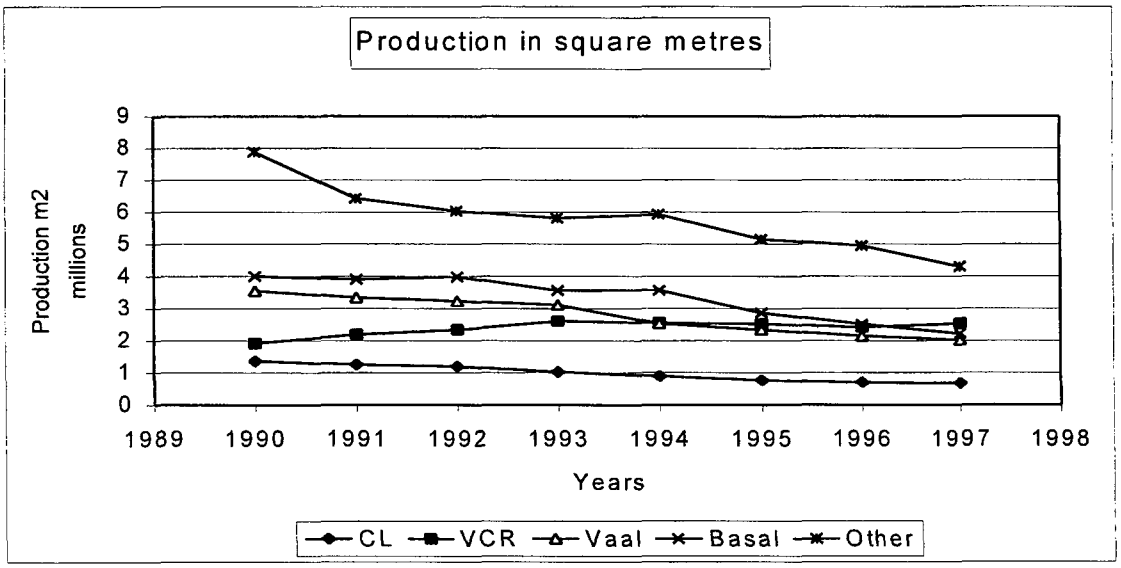

Figure 3.11.2 Production trend for each reef since 1990

In 1990, these reefs represented some 58 per cent of the total production. Currently, they account for 63 per cent of the total production, where the individual reefs (i.e. Carbon Leader, VCR, Vaal and Basal Reef) contributed 6,4 per cent, 15,6 per cent, 18,2 per cent, and 21,7 per cent of the overall production, respectively (see Table 3.11.1).

Table 3.11.1 Production details of the various reefs.

production by reef	CL	VCR	VAAL	BASAL	OTHER	total
1990	1359808	1913428	3544561	4007962	7876821	18702580
1991	1248262	2180600	3336600	3897719	6418648	17081829
1992	1193295	2341386	3230960	3981537	6034812	16781990
1993	1024088	2610063	3111194	3552239	5809975	16107559
1994	890071	2550641	2531044	3557937	5936886	15466579
1995	760494	2522042	2335101	2860525	5157305	13635467
1996	696721	2412459	2146670	2509330	4953412	12718592
1997	681500	2529551	2013602	2220181	4304870	11749704
total production	7854239	19060170	22249732	26587430	46492729	**122244300**
Percentage of the total	6.4	15.6	18.2	21.7	38.0	**100**

3.12 Distribution of the Carbon Leader Reef fatalities

The location of the fatalities that have occurred on the Carbon Leader Reef for the period from 1994 to 1997 are plotted on plans related to the following parameters: (i) geological structures, (ii) geotechnical areas, and (iii) the distance from the Green Bar to the hangingwall skin of the stope.

The aim of this study was to investigate:

- The fatality occurrence from a geotechnical point of view, including the distance from the Green Bar to the hangingwall.

- The impact of geological structures in respect to faults and dykes.

Figure 3.12.1 and 3.12.2 show the results thereof. Table 3.12.1 summarizes the results with respect to the geological structures.

Table 3.12.1 Number of fatalities associated with geological structures.

	Number of events				Total no. of fatalities
	Rockburst		Rockfall		
	on structure	close to structure	on structure	close to structure	
1 fatality	17	3	4	1	25
2 fatalities	3	0	1	0	8
3 fatalities	1	0	0	0	3
4 fatalities	1	0	0	0	4
	22	3	5	1	40

From the above table, it is evident that 88 per cent of rockburst incidents have occurred on the geological structures (that is fault and dykes). It also appears that out of six rockfall incidents, four of them occurred on the structures. Thus, from this preliminary study, it can be concluded that geological structures are a major safety hazard. It is, however, recommended to conduct further studies of the spatial distribution of rock related fatalities to gain further insights into the role and impact of specific types of structures, e.g. rolls, dykes and faults.

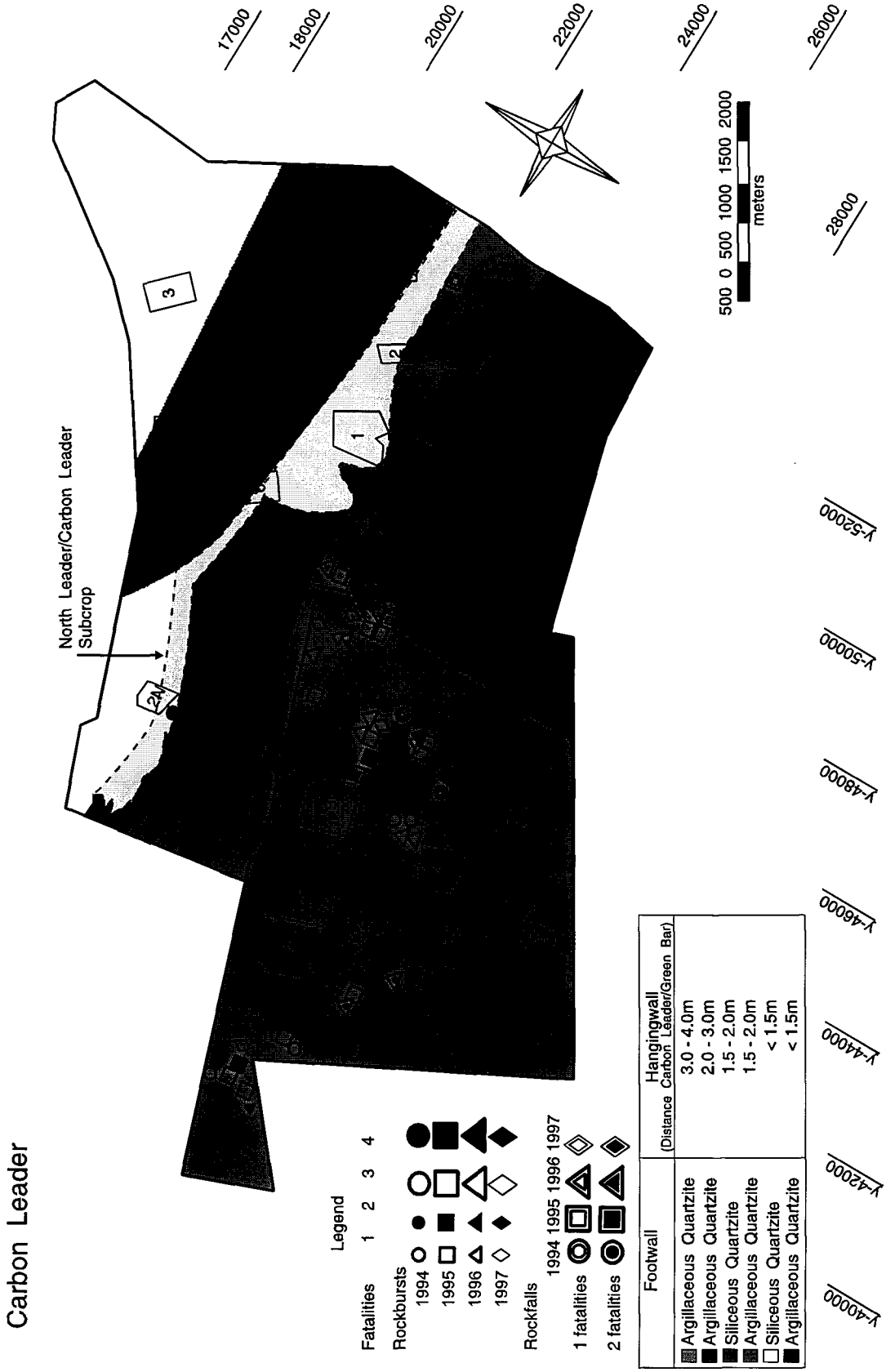

Figure 3.12.1 Distribution of fatalities associated with mining the Carbon Leader Reef superimposed on the geotechnical area classification.

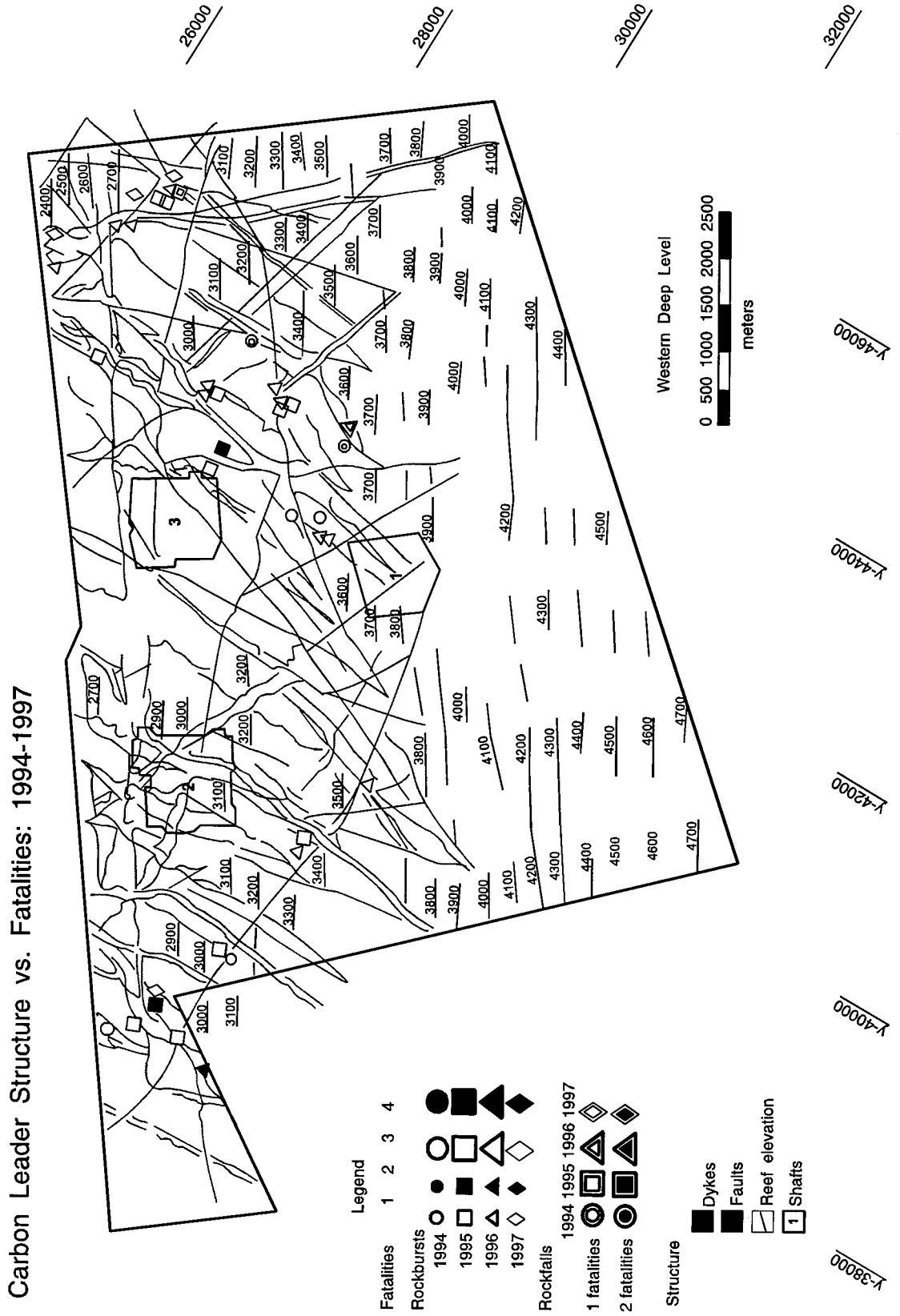

Figure 3.12.2 Distribution of fatalities associated with mining the Carbon Leader Reef superimposed on the structural geology map.

3.13 Conclusions

Rock mass instabilities continue to be the single largest cause contributing towards the toll of injuries and fatalities suffered by the workforce during deep-level mining operations in South Africa. The database contains detailed information of all rockfall and rockburst related fatal accidents since 1990 and, inclusive of the 1997 data, encompasses 1807 fatalities.

The objective of this work is to maintain and expand the accident database, and, furthermore, to review rock related fatality statistics and trends, which are associated with South African deep level gold mining since 1990. The output of the work is the identification of potentially hazardous reefs and workplaces to assist in focusing on problem areas and directing research needs. Specifically, based on the findings of this work, the following conclusions can be drawn:

- Of the total number of rock related fatalities associated with the gold mining industry, 56 per cent are due to rockfalls, while 44 per cent are due to rockbursts.

- The reef associated with the most fatalities is the Ventersdorp Contact Reef (375 since 1990). However, normalised with respect to square metres mined, the Carbon Leader Reef is the most dangerous reef to mine, with a particularly large proportion of rockburst related fatalities.

- Normalised data for all reefs indicates a mean annual decrease in rock related fatalities of 4,5 per cent per annum. The predominant reason for the decline in fatalities is a significant decrease in the rockburst related fatalities associated with mining the Ventersdorp Contact Reef (VCR). The number of rock related fatalities of the Carbon Leader, Vaal and Basal Reef have not shown a clear upward or downward trend since 1990.

  It is strongly recommended that additional work be conducted to establish the cause and origin of the decrease in VCR rockburst fatalities, and to employ similar measures, if appropriate, on the remaining reefs.

- Most fatalities occur in the stope (55 per cent), and particularly in the immediate face area (± 50 per cent). The second most hazardous area is the strike gully, where approximately 15 per cent of all fatalities occur.

- The accident database is used to determine fallout thicknesses for the various reefs as a reference against which similar analyses for various geotechnical areas carried out on the mines can be compared. This data is used to determine support resistance and energy absorption requirements to design suitable rockfall and rockburst resistant support systems, respectively.

- With the exception of Vaal Reef and Basal Reef rockbursts, it is shown that most fatalities occur between 1,0 and 2,5 m behind the stope face. This highlights the inadequacy of temporary support systems or their implementation in the immediate face area, and it is recommended to initiate research work to further elucidate this problem.

- Preliminary work dealing with the spatial distribution of fatalities across the Carbon Leader Reef has emphasised the safety hazard associated with geological structures. Further work is required to quantify the spatial distributions of fatalities across other reefs.

4 Interaction between rock mass and support

4.1 Introduction

The immediate hangingwall of the Carbon Leader reef consists of a quartzite layer with a thickness varying between 0,5 and 2,5 m. This quartzite layer is not homogeneous, but typically contains weak inclusions, such as argillaceous layers deposited in flow channels together with mining induced fractures (Figure 4.1.1). Deformations across the argillaceous layers are often observed.

The interface between the quartzite layer and the adjacent layer of Green Bar consists of the so called "rice pebble zone" on top of the quartzite layer and pockets of densely laminated Green Bar at the bottom of the Green Bar layer. This interface is *not* planar, but undulating as shown in Figure 4.1.1. The interface is considered to offer a relatively low resistance to separation.

The Green Bar itself is laminated and the direction of lamination is approximately parallel to the bedding. The laminations can be expected to cause a local reduction in shear strength, but such a possible effect has not yet been analysed.

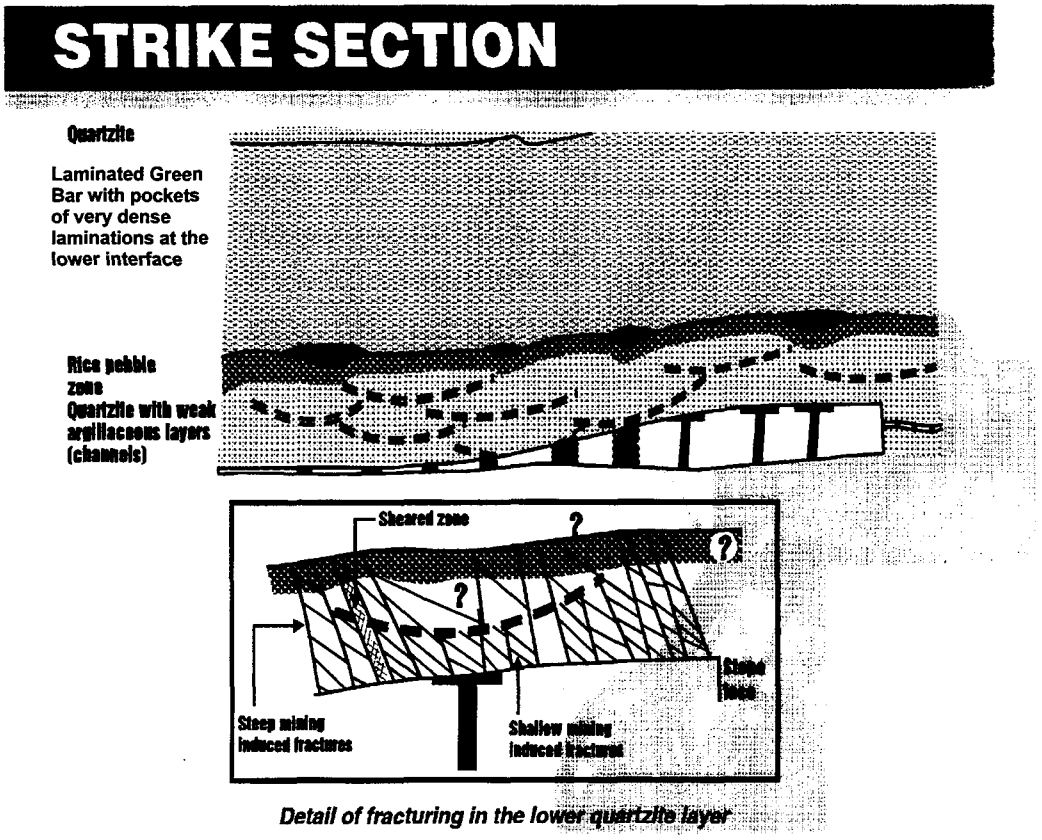

Figure 4.1.1a Sketch of a strike section along the Carbon Leader Reef.

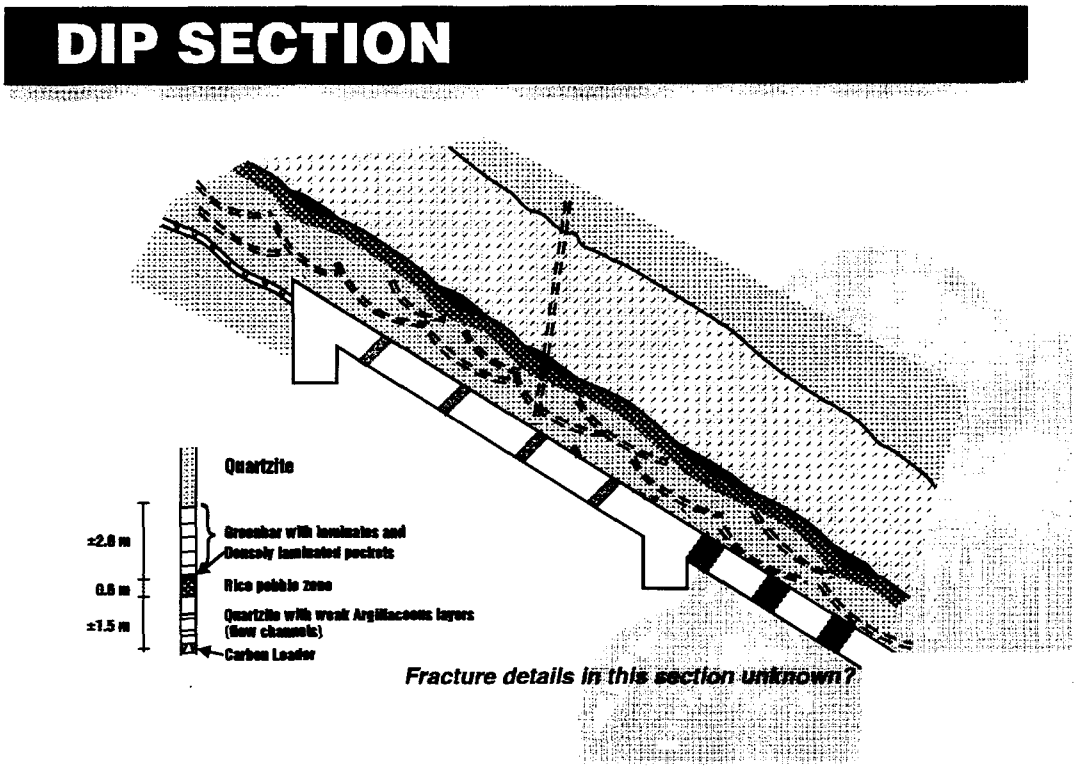

Figure 4.1.1b Sketch of a dip section along the Carbon Leader Reef.

The conceptual model, which aims to analyse the influence of local support, is based on these geotechnical observations. The most important structure, from a mechanical point of view, is the quartzite layer with its flow channels and fractures. It is this layer that is potentially unstable and requires artificial support in order to prevent rockfalls and associated instabilities.

The in situ observations were carried out in the stope. As a consequence only those deformations which occurred behind the stope face could be monitored. While the failure processes can be expected to occur in and above the abutments, due to high stress concentrations, the majority of the inelastic deformations can also be expected to be initiated there. As a consequence, these deformations cannot directly be recorded in the stope itself and are not captured in the in situ data.

Time effects are not explicitly taken into account in the numerical models. The simulations, therefore, represent an immediate response to mining and do not cater for time delays, which cause continuous deformation (closure) in a typical deep level mining environment. The *mechanism* of deformation and the final values of deformation and stress do not necessarily have to be affected by such time effects. The models are, therefore, useful in calibrating in situ deformation mechanisms.

In the conceptual model both the quartzite layer and the Green Bar layer are explicitly represented, as they are perceived to contribute the majority of the inelastic deformations. In the numerical model these structures are represented by a stack of beams. As the aim of this study is to investigate the interaction between local support and the immediate hangingwall, both global and local effects of these beams are investigated.

4.2 Previous work

Inelastic deformations and unstable conditions around deep level stopes have been recognised for a long time. It was realised in the sixties that such inelastic deformations and associated conditions were limited to the immediate surroundings of the excavation only and that the remainder of the rockmass could be considered elastic. (Cook et. al., 1966; Salamon, 1963). Subsequently research efforts (Leeman, 1958; Kersten, 1969; Roering, 1979; etc.) were concentrated on the behaviour of the area surrounding deep level longwall stopes and a conceptual model was proposed by Adams and Jager (1980). This conceptual model is mainly based on the formation and action of mining induced shear and extension fractures, as well as the presence of so called "bedding planes".

Brummer (1987) and Legge (1984) more or less confirmed the conceptual model, with aid of their detailed in situ observations. The action ahead of a typical stope face is believed to result in an effective horizontal dilation towards the stope. These movements are associated with the induction of horizontal compressive stresses in the immediate hangingwall, which, in turn, are considered a stabilising factor. Herrmann (1987) investigated the effect of the horizontal compressive stresses in the immediate hangingwall by cutting a slot parallel to the dip direction into the hangingwall. The fracture orientation was affected by this slot with extension fractures assuming a steeper orientation. He attributed this to an effective decrease in horizontal confinement due to the presence of the slot.

The action ahead of the stope face has also been represented in numerical models. One approach has been the explicit representation of assumed fracture patterns (Lightfoot, 1996; Eve, 1996). The resulting deformations and stress distributions are directly related to the selected fracture pattern and the associated parameters. While it can be expected that the results are sensitive, with respect to geometry and parameters, this sensitivity has not been assessed. Another approach has been the assumption of a homogeneous rockmass with a particular micro structure (Napier and Pierce, 1995; Sellers, 1996; Handley, 1995; Kuijpers, 1998). This last approach allows the formation of mining induced fracturing to take place in a "natural" fashion. The choice of the micro structure and associated parameters, however, influences the results in a similar manner as the explicit models and sensitivity, with respect to these factors, has also not been assessed.

4.3 Research methodology

In order to obtain a relatively objective and sufficiently simple model, which incorporates most of the observed behaviour, it was decided to concentrate on the mechanism of layered rockmass. One of the major considerations leading to this choice was the apparent lack of shear fractures at the present site (see also Figures 4.1.1). From the observations it appears that explicit layers, which may or may not contain steep extension fractures, represent the environment adequately. The effect of bedding planes on stress distribution and associated fracture formation has been addressed previously (Napier and Ozbay, 1993; Kuijpers, 1998; Sellers, 1997) and the effect of support pressure and resulting deformations has also been investigated (Kuijpers, 1998), but these efforts have not led to conclusive results with respect to support requirements.

The analyses presented here concentrate on parameters such as layer thickness, interface friction and dilation (undulation), support pressure, stability of the hangingwall beam etc.
The numerical simulations are split into two main categories, namely:

1. global models which focus on the behaviour of these layers around a simulated stope environment, and
2. local models that concentrate on the interaction between individual support units and neighbouring parts of the immediate hangingwall.

The global models provide data such as closure, bedding plane slip and separation, stresses in individual layers, and the effects of support pressure on those parameters. The local models address, in more detail, the interaction between an individual support unit and the associated part of the hangingwall beam. The stability of that part of the hangingwall beam can be assessed with respect to parameters such as support force, hangingwall stress, and bedding plane separation.

Local models can be subdivided into two categories, namely:

1. models which represent a densely fractured rockmass with a wide variety of fracture orientations, and
2. models which represent the discrete nature of a particular fractured rockmass.

In the first category it is assumed that the effective fragment sizes are too small to be of practical relevance. The material behaviour can, therefore, be represented by a simplified model, in which the effect of individual fractures is smeared and not explicitly captured. The parameters used for this model are referred to as smeared, effective parameters, as they represent the behaviour of the rockmass, rather than the behaviour of individual discontinuities.

In the second category the behaviour of individual discontinuities manifests itself directly on a larger scale, which may be of practical relevance and these discontinuities are therefore explicitly represented.

4.4 Discussion of results

4.4.1 Conceptual model

The conceptual model used here is a two dimensional model in which the layering is explicitly represented by a stack of beams. A typical section is taken along strike and mining activity is represented by effectively simulating the excavation process in a stepwise fashion. In order to account for the influence of the dip direction, a two dimensional model of a section along dip has also been investigated. By incorporating the results of this last model, a more realistic representation of a longwall stope can be obtained.

A typical result from a strike section model shows the activation of slip between individual beams (=layers) near the abutments of the longwall stope (Figure 4.4.1). The effective friction between these beams determines the exact location of action; a relatively low frictional resistance allows mobilisation of slip ahead of the stope face, while a relatively high frictional resistance would limit the mobilisation of slip to areas behind the stope face directly below and above the excavation. In the numerical models it is assumed that the interfaces between the beams or layers only offer frictional resistance. In reality there may be adhesion across these interfaces, but as long as the cohesive strength is relatively low, compared to the rock mass strength, breakage of the interfaces will occur at similar locations as indicated in Figure 4.4.1

For practical purposes the cohesive strength between individual beams has been set to zero. This results in the mobilisation of a maximum amount of beams and is, thus, a conservative estimate. The resulting stress redistribution can lead to fracture formation from the activated interfaces. This has already been demonstrated by Napier and Hildyard (1992).

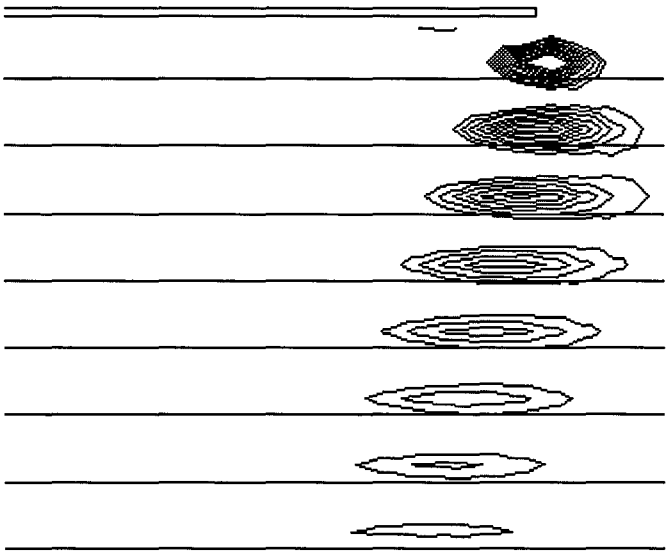

Figure 4.4.1 Areas of slip mobilisation in the layered model (Quarter symmetry; DIGS).

The purpose of the model is to demonstrate the effect of the parameters associated with layered rock such as layer thickness, layer profile, inter layer friction etc. One of the major obstacles associated with this type of analysis is the apparent challenge which it presents to numerical representations. Figures 4.4.2 and 4.4.3 show the results of an analysis of a single beam with a varying width to height ratio. The beam is clamped on both sides and is subjected to a uniformly distributed load (gravitational loading). Both the analytical and numerical (FLAC & DIGS) results are shown in this graph. It is obvious that the numerical results deviate substantially from the analytical solution once critical width to height ratios are exceeded. This type of result is not unique to a particular computer programme and similar problems can be expected with other programs as well (Kuijpers,1998).

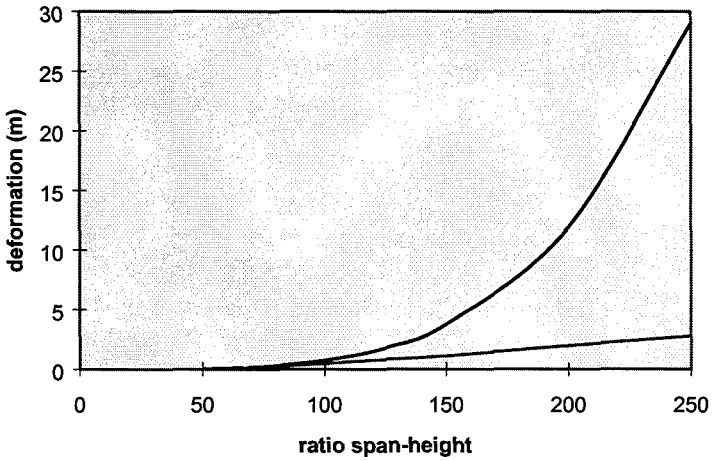

Figure 4.4.2 Mid span deformation versus slenderness (length/height) of a single beam with a height of 800mm and an Elasticity Modulus of 70GPa. Theoretical (upper curve) versus FLAC (lower curve) results.

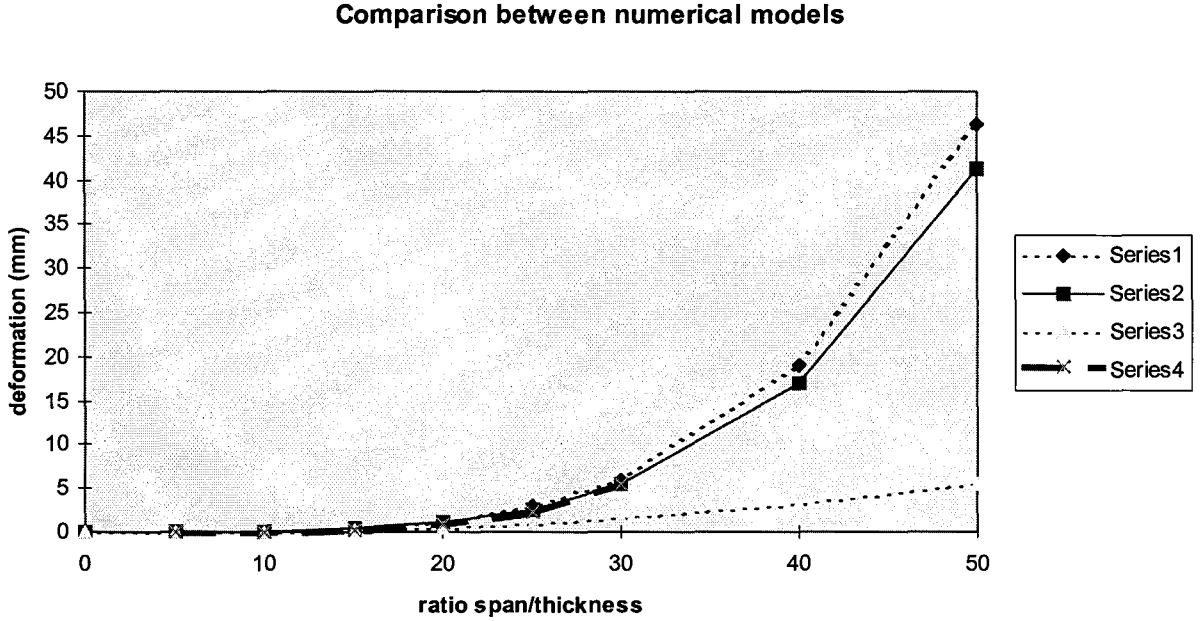

Figure 4.4.3 Mid span deformation versus slenderness (span/thickness) of a single beam with a height of 800mm and an Elasticity Modulus of 70GPa.
Series 1: theoretical
Series 2: FLAC
Series 3: DIGS normal grid (reasonable convergence)
Series 4: DIGS fine grid (no convergence for large slenderness values)

In a typical longwall stope environment where stope spans can easily exceed 50 metres and the layer thickness can be as small as a few centimetres, if flow channels are taken into account, the span to height ratio may be too large to allow for realistic numerical representation. A model of multiple layers can be expected to suffer from similar problems as the single beam model. It is because of these shortcomings that no attempt has been made to simulate extremely slender beams/layers and the models have been limited to a width to height ratio of around 50.

In the following the mechanisms associated with interlayer slip and the effect on in stope deformations are discussed. A distinction can be made between two separate mechanisms.
The first one is a gravitational mechanism which causes an individual layer to deform according to:

$$\delta = \frac{1}{EI}(Q_0 x + \frac{1}{2} M_0 x^2 - \frac{1}{12} q l x^3 + \frac{1}{24} q x^4) \qquad (4.4.1)$$

whereby M_0 and Q_0 are the boundary conditions for the moment and rotation respectively and q represents the uniform load (weight in this case).

As the weight is directly related to the height of the beam, $Q_0 = 0$ (clamped) and $I = \frac{h^3}{12}$, equation 4.4.1 can be simplified to:

$$\delta = \frac{\rho}{12Eh^2}(\frac{l^2}{2} x^2 - l x^3 + \frac{1}{2} x^4) \qquad (4.4.2)$$

This function is graphically displayed in Figures 4.4.2 and 4.4.3, and from equation 4.4.2 it can be appreciated that the relation between the deformation and the slenderness of the beam is of a quadratic nature (h^2) and that the relation between the deformation and the span of the opening is of a fourth order (x^4).

The second mechanism is not always recognised, although it plays a fundamental role around openings in a highly stressed layered medium. This mechanism can be visualised by comparing the shear stresses along a particular interface, without and with the occurrence of slip, along that interface. In the first case slip is prevented by the presence of relatively high shear stresses, which can be transmitted across such an interface, if the cohesive strength would be sufficient. In the second case the shear stresses that are transmitted across the interface are limited by the frictional resistance across the interface. Slip occurs if these limited shear stresses are less then the shear stresses required to prevent slip. The difference between these two shear stresses can be considered as a driving stress causing additional deformation of the affected layers.

If this differential stress is termed ΔS, then the moment which it induces in a layer of height h is $\Delta S(\frac{h}{2})$

The deformation induced by this moment in an associated layer at mid span is expressed by:

$$\delta = \frac{C}{EI}.\Delta S h l^2 \qquad (4.4.3)$$

whereby the constant C is dependant on the exact boundary conditions.

From equation 4.4.3 it can be noticed that the relation between the deformation and slenderness of the beam is also of a quadratic nature, while the relation between the deformation and span is most likely of a third order (l^3), as the differential stress ΔS can be expected to be linearly related to the span l ($\Delta S = Cl$). It is for this reason that the deformation, which is associated with relatively small spans, is dominated by the second mechanism, while the first mechanism becomes dominant with relatively large spans.

In order to demonstrate the effect of both mechanisms, numerical simulations of an expanding stope with a single layer, both below and above the stope, have been performed, with and without gravitational forces. The results, which are shown in Figure 4.4.4, clearly demonstrate how relatively small spans are mainly affected by the second mechanism of limited shear resistance near the abutments. No distinction can be made between hanging- and footwall deformations in this case, as the mechanism causes equal deformations towards the opening. The first mechanism of gravitational deformations causes both the hanging- and footwall layer to deform downwards. Mechanism one and two are, therefore, supplementary in the hangingwall, but cause opposite deformations in the footwall. With increasing span (equivalent to slenderness of the beams) the first mechanism will dominate, while the second mechanism becomes irrelevant.

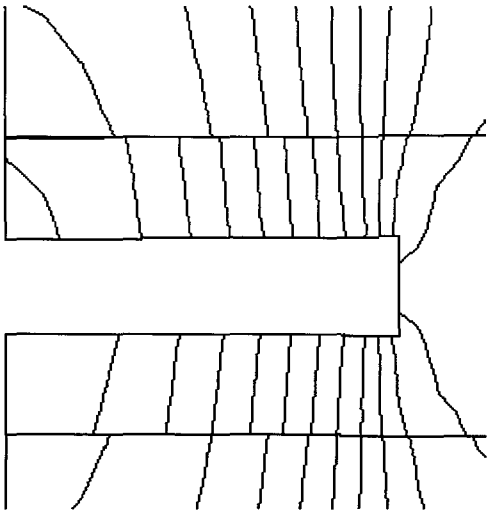

a) Half span =10 m; gravity active both mechanisms active

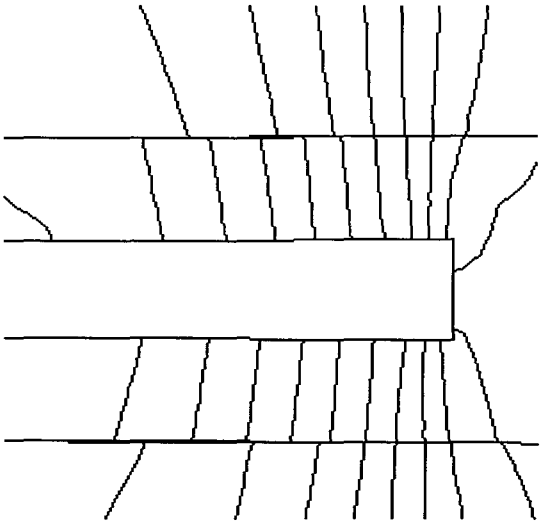

b) Half span =10 m; only second mechanism active

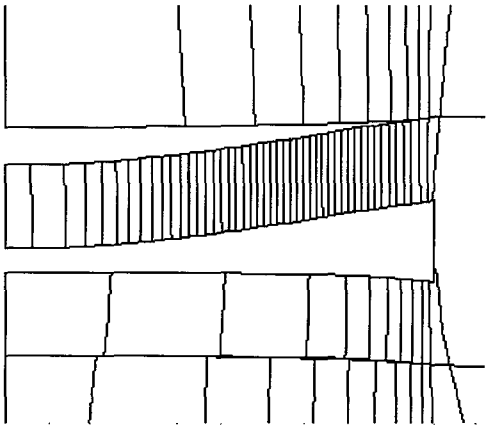

c) Half span = 50 m; gravity active (combination of the first and second mechanism)

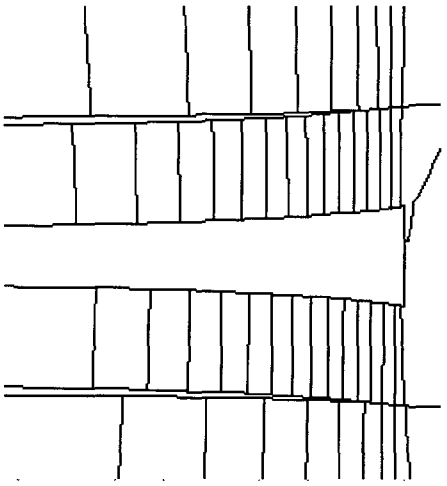

d) Half span = 50 m; no gravity (second mechanism only)

Figure 4.4.4 Behaviour of two single layers around an expanding stope with and without gravity; half symmetry is used and vertical deformation contours are shown (FLAC).
layer thickness = 0,8m and the vertical scale is enlarged.

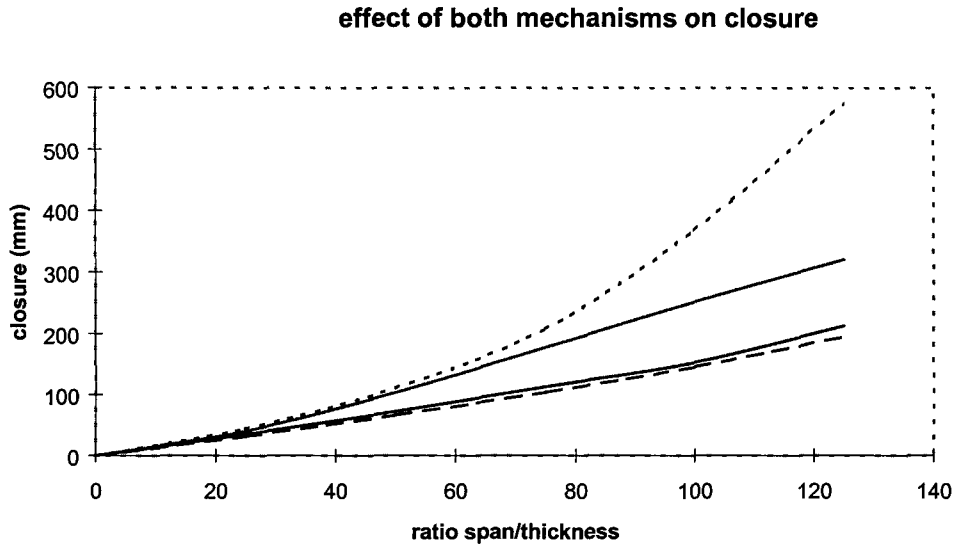

Figure 4.4.5 Summary of the results of the previous FLAC analyses:

top: stope closure with gravity
directly below: stope closure without gravity
next: (elastic) closure of the solid (excluding the layers) with gravity
bottom: (elastic) closure of the solid (excluding the layers) and without gravity.

Figure 4.4.5 combines all results of the FLAC simulations with a single layer in both hanging- and footwall. It is of interest to note that gravity has a marginal effect on the solid rockmass, but has a marked influence on the deformation of the layers itself.

Inelastic closure is completely associated with the deformation of the layers in this case. Figure 4.4.5 clearly demonstrates how the contribution of the inelastic closure to the total closure increases exponentially with increasing ratio of span to layer thickness.

Although equation 4.4.3 provides some general insight in the second mechanism, it is of practical value to obtain exact values for the deformations associated with this mechanism. In order to do so numerical simulations had to be performed, as a closed formed analytical solution is not available and equation 4.4.3 is only an approximation.

While Figure 4.4.4 demonstrates the potential effect of both mechanisms, it does not provide a complete overview of the magnitude of the associated deformations. Besides "conventional" parameters such as friction, layer thickness and span, the effect of the second mechanism is also influenced by an additional parameter, namely the surface roughness or undulation of the interface between individual layers. This undulation can explicitly be represented by mapping and reproducing the exact geometry of the interfaces. As such information is, however, not available, it has been decided to represent this effect indirectly, through a dilation angle. Figure 4.4.6 shows how such a dilation angle can be related to the surface roughness of a particular interface.

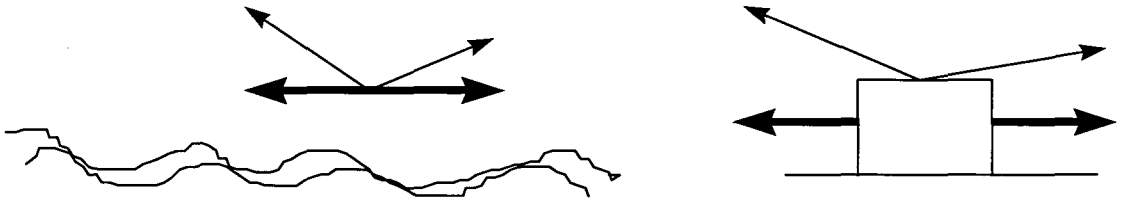

UNDULATING SURFACES DILATION MODEL

Figure 4.4.6 Dilation angle representing the undulation of the layering.

In order to calibrate the model a parameter study has been done with DIGS. Parameters which have been investigated are friction, dilation, slenderness, effect of mining steps, and gravity. The in-situ stresses assumed for this model are 60 MPa vertical and 30 MPa horizontal. The results are listed in the appendix and are also shown in the following graphs and figures.

Figure 4.4.7 shows a typical result of such a numerical simulation.

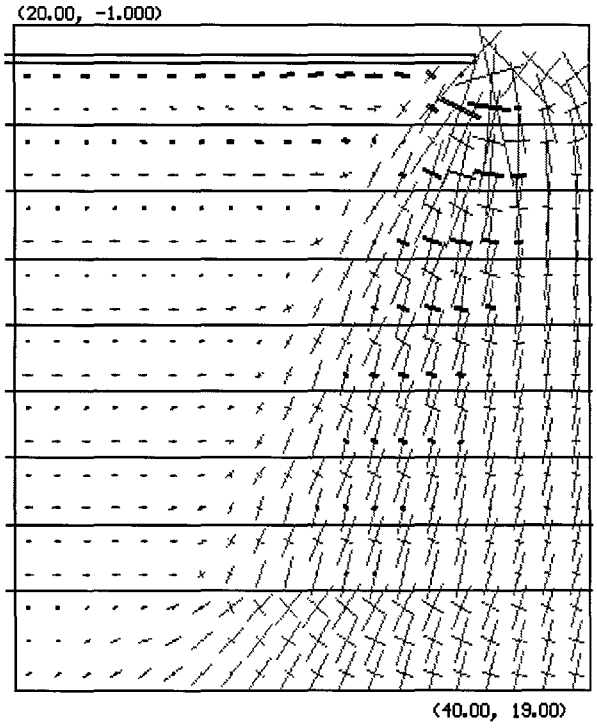

Figure 4.4.7 Typical result of one of the numerical models; friction angle = 15°; dilation angle = 30°; stope span = 72 m; layer thickness = 2 m; 8 layers.

Figure 4.4.7 shows the stress distribution around the quarter symmetric area of a longwall stope. Mining is from left to right and it is obvious how tensile stresses (black lines) are induced near the bedding planes. Relative slip across these bedding planes causes the induction of these tensile stresses. This slip, in combination with dilation, will be shown to have a major effect on inelastic closure.

In Figure 4.4.8 the effect of slip across the bedding planes can be seen to have a large influence on the stope closure. This effect becomes especially evident if the relative slip across the bedding planes is associated with dilation. As has been argued before, such a possibility can be assumed if the bedding plane surfaces are undulating.

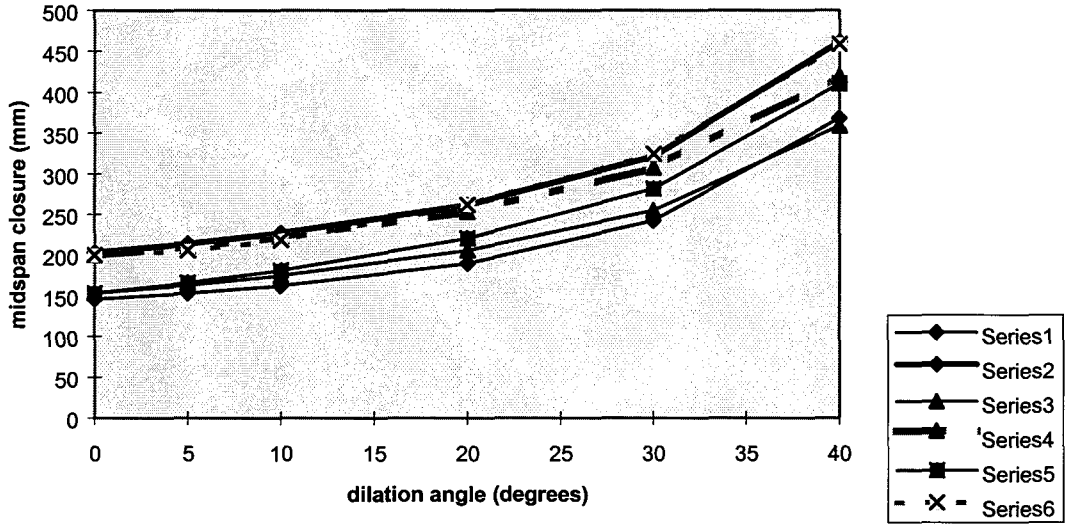

Figure 4.4.8 Effect of dilation angle on closure.
Final stope span = 72 m; layer thickness 2 m; 8 layers
friction coefficient across bedding planes = 0,268 ($\tan 15^{o}$)
Series 1: no gravity; single mining step
Series 2: gravity; single mining step
Series 3: no gravity; 18 mining steps
Series 4: gravity; 18 mining steps
Series 5: no gravity; 18 mining steps; dilation upon reversal of slip
Series 6: gravity; 18 mining; dilation upon reversal of slip

In Figure 4.4.8 the relation between the dilation along the bedding planes and the vertical deformation of the stope at mid span is shown. In the simulations representing multiple mining steps, a reversal of slip across bedding planes takes place once they become "undermined". In series 5 and 6 in Figure 4.4.8 this reversed slip is associated with a dilation angle, that is equal to the dilation angle which is associated with the initial slip direction.

From Figure 4.4.8 it becomes clear that the dilation angle along bedding planes is a major factor controlling the deformation of the strata into the stope. It is also clear that gravity (series 2, 4 and 6) accounts for a certain portion of the deformation. The difference between the results of single and multiple mining steps is marginal. This can be observed by comparing series 1 with series 3 and 5, and series 2 with series 4 and 6. The incorporation of a reverse dilation angle does have an effect, but this effect only becomes pronounced at relatively large angles.

While figure 4.4.8 only shows the results for a particular geometry with 8 layers of 2m thickness and a stope span of 72m, it allows the identification of a mechanism which can be associated with inelastic closure around longwall stope in layered strata.

When the results of the numerical simulations are examined in more detail, it appears that the dilation, which is initiated near the abutments, causes separation of the affected bedding planes over the whole span of the stope. In other words, the bedding planes are wedged open near the abutments and as no resistance is encountered above and below the open stope, such separation is not restrained there.

The fact that mining steps hardly have an influence on the results can be explained from this behaviour as bed separation can be induced over the full stope span by a single wedging force near the abutments only. It is therefor not necessary for the dilatation to be locked into the strata at various mining steps in order to affect the closure at mid span.

The support may offer resistance against bedding plane separation, but no attempt has been made to include this effect in these numerical simulations. As has been explained before, the numerical models are incapable of dealing with relatively slender beams and the selected models contain therefore unrealistically thick layers. The support resistance against the deformation of such thick layers would be of no influence.

Figure 4.4.9 shows the results for a single bedding plane with gravity compared to the results for 8 layers as shown in series 2 in Figure 4.4.8

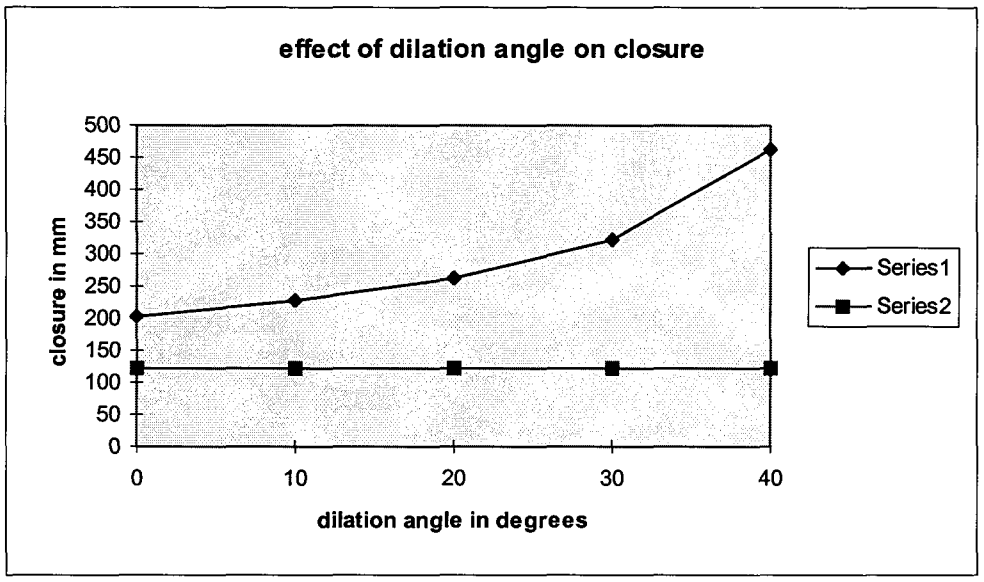

Figure 4.4.9 Comparison between a single layer and multiple layers stope span = 72m; layer thickness = 2m. Series 1: 8 layers; single mining step Series 2: 1 layer; single mining step

Figure 4.4.9 clearly demonstrates that the effect of dilation across bedding planes is not obvious in the case of a single layer, but requires the activation of multiple layers. It is therefor of importance to establish how many bedding planes are activated in a realistic scenario. Unfortunately such information is not available at present. Such information is essential as it enables differentiation between various geotechnical areas.

By including a cohesive resistance or strength across the bedding planes, the model can be used to investigate the influence of applied stresses or loading. This would indirectly relate to the depth of the excavation. Unfortunately no values are available to calibrate such a cohesive resistance and therefore a conservative estimate of zero strength has been assumed.

The effect of layer thickness has also been investigated, but only for the case of a single layer. Figure 4.4.10 shows the results for such a case in which the layer thickness has been varied, gravity has been included and zero dilation has been assumed. The stope span of 72m has been simulated in a single mining step. The effect of the coefficient of friction across the bedding planes has also been addressed here.

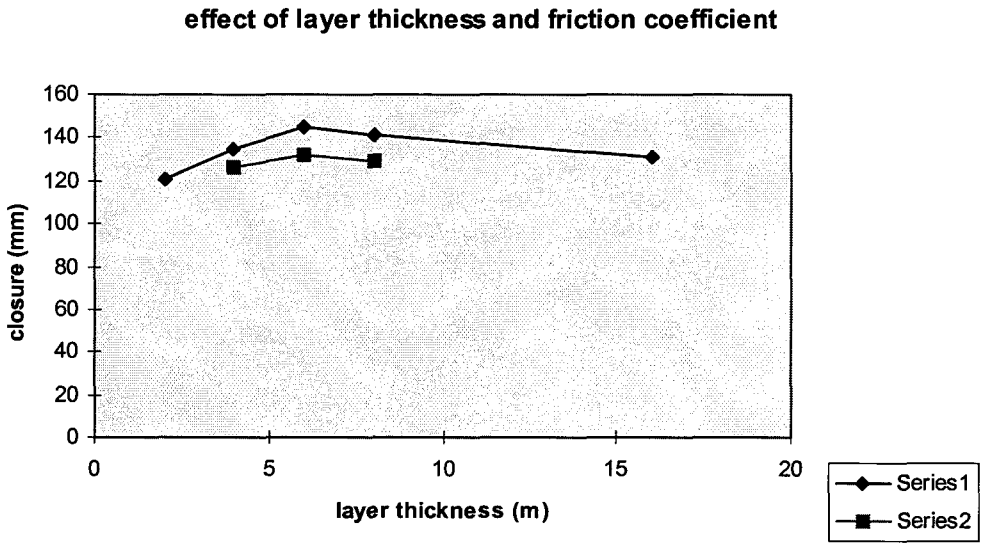

Figure 4.4.10 Single layer of varying height.
Series 1: coefficient of friction across bedding plane = 0.268 $(\tan 15^{o})$
Series 2: coefficient of friction across bedding plane = 0.577 $(\tan 30^{o})$

Figure 4.4.10 shows that an increase in frictional resistance leads to a decrease in deformation as the amount of slip across the bedding planes is obviously reduced. Of more interest is the fact that a layer thickness of approximately 6m. results in a maximum amount of closure in this particular case. This must be related to the amount of slip which can be generated across the bedding plane. The stress distribution around the abutment of the stope results in areas within which slip can occur (ESS envelopes). The shape of these areas dictates the potential for movement along the bedding planes at a particular location. Apparently this potential is at a maximum at a distance of approximately 6 meters from the stope in this particular case.

As has been indicated previously, the dip of the strata needs to be taken into account in order to obtain a more realistic representation of the underground situation. Figure 4.4.11 shows the result of a model of a section along dip.

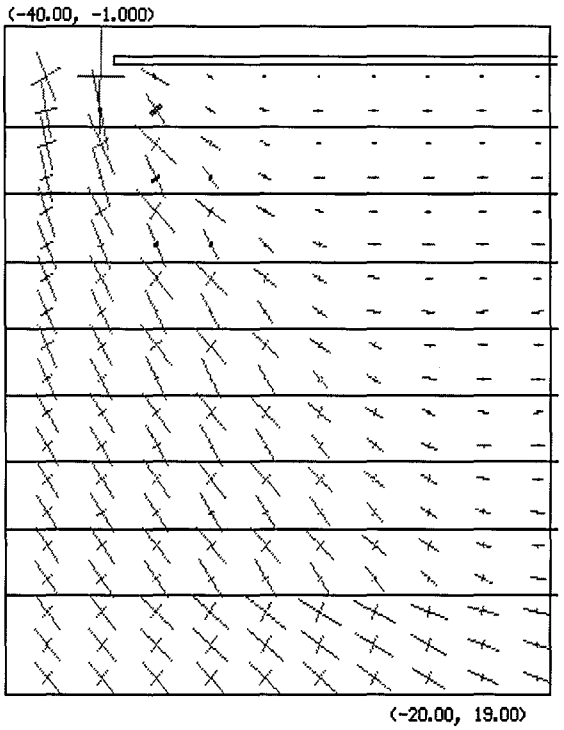

a) Updip footwall (equivalent to downdip hangingwall)

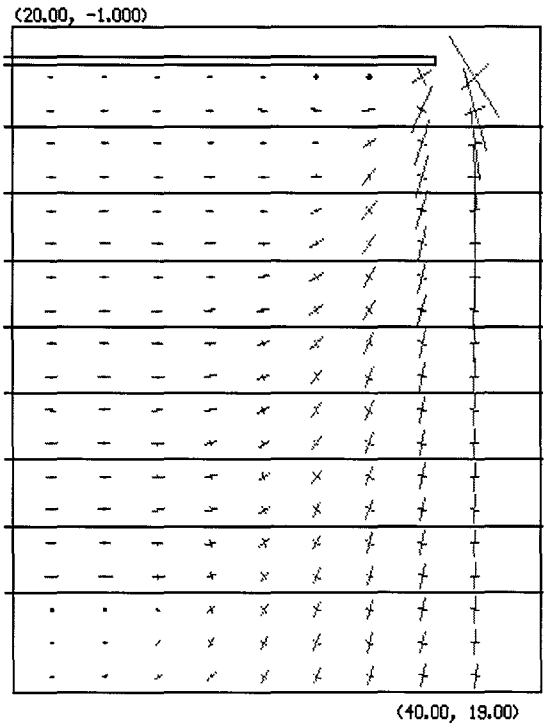

b) Down dip footwall (equivalent to up dip hangingwall)

Figure 4.4.11 Typical numerical results from a simulation in which the stress field is not normal to the strata (45° ***inclination).***
Stope span = 72m; friction angle = 15° ***; dilation angle =*** 20°

Figure 4.4.11 shows how the down- and up-dip sides differ when the strata is dipping or, alternatively, when the stress field is rotated. Figure 4.4.11a indicates that the down dip hangingwall is far more unstable than its up dip counterpart, due to the orientation of the stresses with respect to the bedding planes. Bedding plane slip and associated tensile stresses and subsequent fracturing are far more likely to occur in the down dip hangingwall. Of interest is also the closure which occurs in this particular case. A value of 111.68 mm. is computed, which compares to 220.86 mm. for the case in which the dip is zero and the stresses are perpendicular to the stope horizon. It is not immediately clear what controls the magnitude of this reduction, but this aspect requires further investigation.

4.4.2 Failure of the Green Bar

A relatively weak layer of Green Bar, which in most areas of the Carbon Leader Reef separates the immediate hangingwall from the surrounding rockmass, appears to be the cause of instability in many rock related accidents. Failure of the immediate hangingwall is often related with a massive break-out of the overlying Green Bar layer. In an initial attempt to model this behaviour it was assumed that the Green Bar is much weaker than the surrounding rock, and that only the failure of the Green Bar and the immediate hangingwall are of relevance to this problem. In the example shown in Figure 4.4.12, a cohesive strength of 20MPa and a friction angle of 10 degrees have been assumed for the Green Bar. The hangingwall has been given a limited tensile strength, but its compressive strength was assumed to be unlimited as the relatively weak Green Bar layer effectively shields the hangingwall from high stresses. Results of initial computer simulations (FLAC) showed a mechanism in which the Green Bar is subjected to failure and associated deformations in the following sequence:

- Ahead of the stope face the layer of Green Bar is being plastically deformed between two layers of solid rock, due to excessive shear stresses.
- The plastic deformations effectively result in a squeezing process in which horizontal dilation of the Green Bar layer towards the direction of the stope is initiated.
- When this horizontal deformation in its turn induces horizontal stresses which exceed the strength of the Green Bar, vertical dilation of the Green Bar layer above the immediate hangingwall just behind the stope face will take place.
- Depending on the flexibility, (tensile) strength and the support conditions of the immediate hangingwall, the Green Bar may be pushed through this hangingwall beam (plate), or a stable equilibrium may be obtained.
- If the vertically dilating Green Bar breaks through the hangingwall beam, a reduction in resistance against the plastic deformation mechanism occurs and additional failure may subsequently take place in a violent fashion due to the brittle failure of the hangingwall which provides confinement to the yielding Green Bar.

A typical result of a numerical simulation with FLAC is shown in Figure 4.4.12, where it can be observed how the hangingwall beam near the stope face is deformed (and stressed) by a layer of Green Bar which is being squeezed away from the area ahead of the stope face. It should be emphasised here that the mechanism is especially sensitive to the effective frictional resistance within the Green Bar layer. Further analyses of this mechanism should therefore be substantiated by appropriate parameters which need to be obtained for this material and its interface with the surrounding rockmass. The mechanism appears to be especially powerful for relatively low (effective) friction angles and this property should therefore be thoroughly investigated.

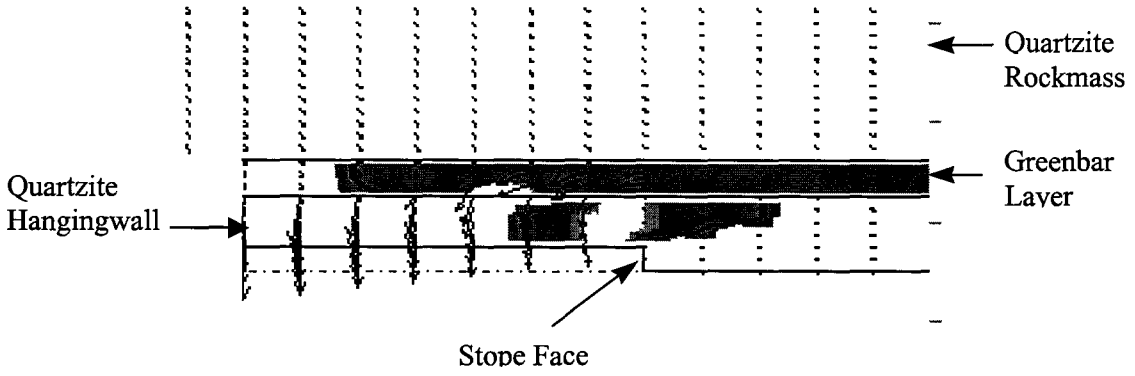

Figure 4.4.12 Deformations induced by 'squeezing' of Green Bar around the abutment of a longwall stope; the layer of Green Bar is located immediately above the hangingwall beam, which in turn fails in tension (failed area is shaded).

Based on in situ observations and the results of preliminary numerical modelling shown in Figure 4.4.12, it appears that the mechanism controlling this unstable behaviour is not merely a passive one, in which a well defined hangingwall beam is being dislodged by gravitational or seismically induced forces, but that the Green Bar layer itself may play an active role in destabilising the underlying hangingwall beam by effectively forcing this beam into the excavation. The proposed mechanism is sketched in Figure 4.4.13 and basically consists of two main stages.

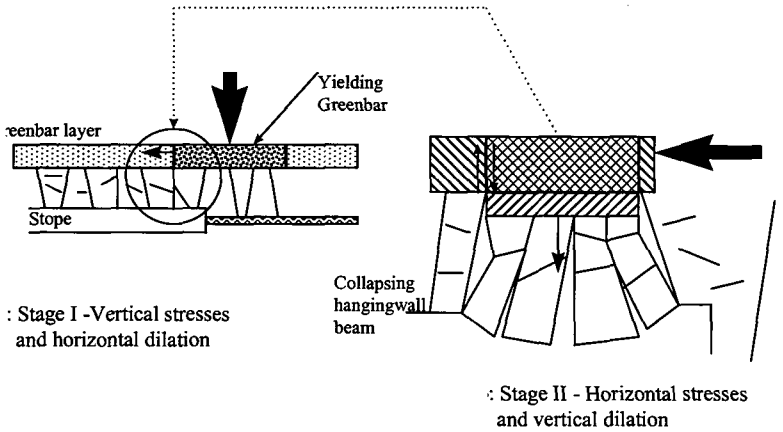

Figure 4.4.13 Mechanism associated with Green Bar failure and hangingwall collapse.

Stage I in Figure 4.4.13 involves the failure of Green Bar near the current stope face due to excessive vertical stresses. Associated with this failure is a post-failure deformation which includes horizontal dilation of the Green Bar material towards the excavation (Figure 4.4.13a). Stage II in Figure 4.4.13 is associated with the induction of *excessive* horizontal stresses due to the horizontal dilation from stage I. The limited horizontal resistance of the Green Bar material is partly explained by its anisotropic properties and partly by its post-failure behaviour. Both need to be quantified by appropriate laboratory tests in order to analyse this mechanism. The failure of the Green Bar due to excessive horizontal stresses will result in vertical dilation of the material towards the excavation (Figure 1b). This vertical dilation forces the quartzite hangingwall beam to bulge into the mined out area and, depending on the combined strength and stiffness of this beam and the support structure, this beam may or may not collapse.

Collapse of this beam would have an immediate effect on the effective horizontal strength/resistance of the Green Bar material as vertical confinement is provided by this beam. As the horizontal strength/resistance in its turn controls the resistance against vertical stresses in a similar way, it is possible that failure of the immediate hangingwall beam may result in a (substantial) reduction in vertical resistance which may cause violent energy release.

From the initial numerical models it appears that the mechanism is mainly controlled by the vertical and horizontal strength/resistance of the Green Bar, by the effective friction angle after failure of the Green Bar and/or the effective friction angle along the interface between the Green Bar and the surrounding rockmass. The horizontal dilation of stage I and the vertical dilation of stage II are also very important parameters which need to be quantified.

Practical solutions to prevent the collapse of the immediate hangingwall by excessive vertical dilation are:

1. Support of the hangingwall beam in such a way that a collapse is impossible and vertical deformations can be accommodated.
2. Allow the Green Bar to dilate through the hangingwall beam at a location where this can be accommodated (e.g. back area)

This last approach would require the cutting of a slot and most likely a reduced form of support as described under 1.

Any further analyses need to be supported by appropriate laboratory tests which allow the determination of the *post failure* properties of the Green Bar in particular and which also provide the effective friction angle along the interface between the Green Bar and the overlying strata. Different geotechnical areas can in this way be assessed.

4.5 Local support considerations

4.5.1 Introduction

Currently, individual support units are designed to resist vertical deformations and vertically applied loads, which are assumed to be uniformly distributed over an area affected by a particular support unit. This design methodology addresses the stability of (stope) hanging-walls by ensuring that the distributed load-bearing capacity of individual support units is sufficient to prevent the ejection of a potentially unstable hanging-wall which is supported by such units. Empirical parameters relating to ejection velocities and associated hanging-wall dimensions are used to determine the efficiency of individual support units. As these parameters have been established over a long period of time, they are generally accepted as sufficient, even for worse case scenario's, although it could be questioned if the values which are currently being used might be relaxed and varied according to variations in so-called "geo-technical" conditions, mining lay-outs, geological conditions, etc. It may be expected that continuing research will ultimately lead to more realistic design criteria and associated parameters.

This contribution however is not concerned with the design criteria related to uniformly distributed vertical deformations and loads. For the purpose of this work those design criteria are assumed to be satisfied, although it is realised that a large amount of work is required in order to define more realistic design criteria and parameters.

In the following some major causes of unstable hanging-wall behaviour, which occur despite the fact that the current support design criteria have been met, are discussed and briefly analysed. All these cases have been associated with the occurrence of fatalities and can be related to *local* instabilities.

4.5.2 Local stability

Local stability is defined here in terms of relatively small areas of the hangingwall with dimensions ranging from decimetres to a few metres. While it is assumed that the global stability of a hangingwall is ensured by providing sufficient total vertical support capacity, parts of the hangingwall may become unstable as the effect of the support may not be transmitted to these areas. Two main classes of unstable behaviour, which can both be associated with *local* instability, are identified here and specific cases which are directly associated with a large percentage of rock related accidents have been selected to illustrate the problem. All cases are related to unstable local hanging-wall conditions for which current support systems are not designed and for which no design criteria are available yet.

4.5.2.1 Non axial deformations

Many rock related accidents can be associated with the inability of individual support units to resist or accommodate horizontal deformations (40% of fatalities in the Orange Fee State gold mines in 1996 for instance; Glisson, 1997). In such situations horizontal movements can easily lead to toppling and/or buckling of support units with a subsequent loss of support resistance and increased potential for rock falls (Figure 4.5.1).

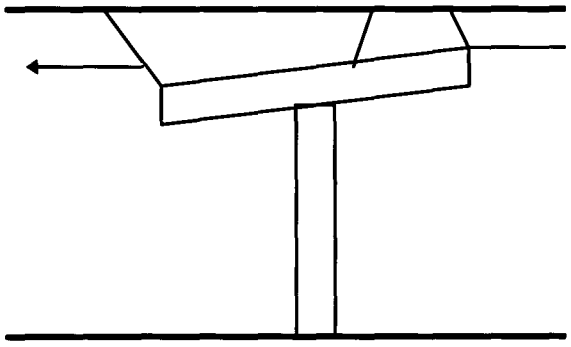

Figure 4.5.1 Horizontal movement of hangingwall blocks not resisted nor accommodated by the support unit

Analyses with the computer programme FLAC demonstrated that after a limited amount of horizontal movement the support resistance disappears rapidly. These analyses were based on the observed axial load-deformation characteristics of conventional timber sticks and headboards and clearly showed that such support units are inadequate under circumstances which involve (large) horizontal deformations.

Such horizontal movements are normally associated with differential movements between hanging and footwall parallel to the stope plane, but they can also be related to local deformations caused by gravity and other mechanisms. Figure 1a to 1c show the basic problem: with increasing horizontal deformation (horizontal axis in Figure 1b and 1c) the support unit is subjected to increasing (induced) vertical stresses as rotation of the support unit cannot take place freely. These vertical stresses (vertical axis) exceed the strength of the unit after a certain amount of horizontal deformation and the support unit looses its load resisting capacity. The fact that the rotated support unit may eventually topple has not been explicitly analysed here, but can obviously only make matters worse.

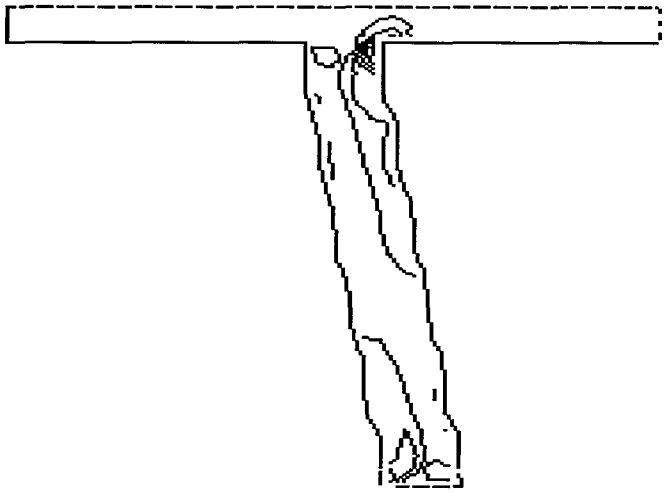

a) Horizontal deformation of timber stick and (slender) head board

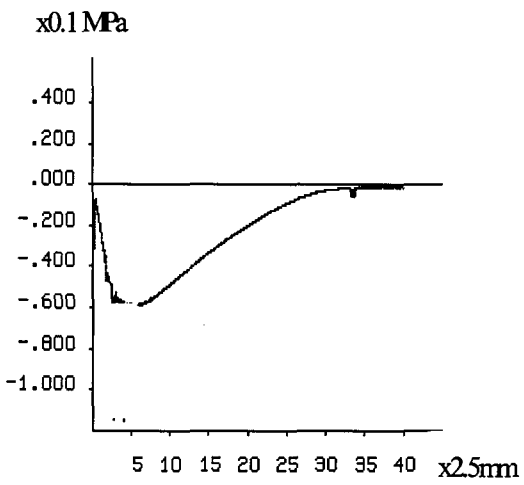

b) Horizontal resistance with increasing horizontal deformation

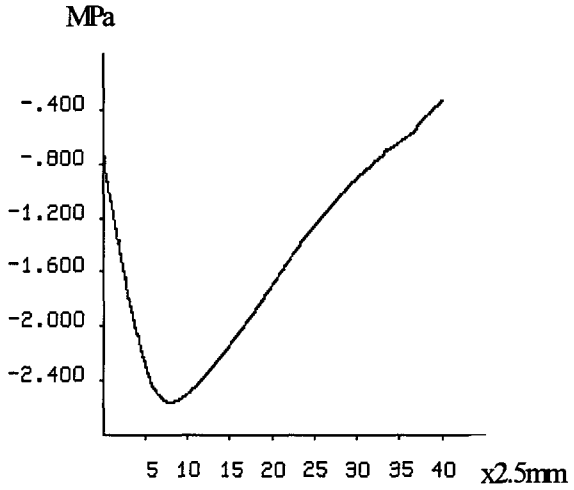

c) Development of axial stresses during horizontal deformation

Figure 4.5.2 FLAC results of a timber support simulation.

Improvements, such as larger headboards and better connections between headboard and stick, only resulted in marginal increases in support resistance against these horizontal (non-axial) deformations and do not lead to a satisfactorily solution. An example of such an "improvement" is shown in Figure 4.5.3.

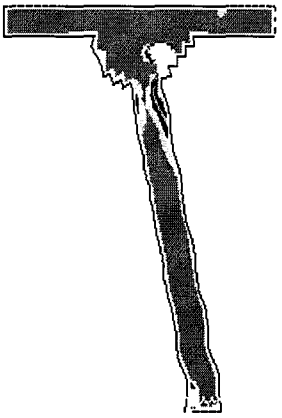

a) Horizontal deformation of timber prop and (large) headboard

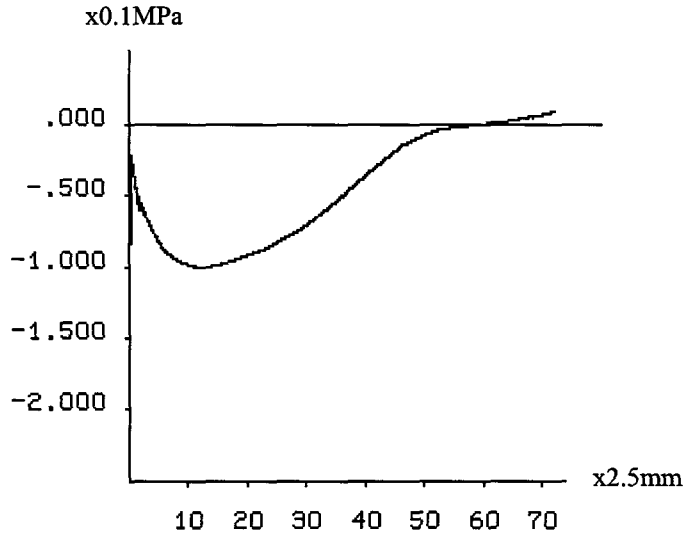

b) Horizontal resistance with increasing horizontal deformation

Figure 4.5.3 Results of a simulation of a timber prop with a relatively large head board (FLAC)

These examples merely demonstrate a potential mechanism which could negatively affect support performance. Quantitative results will be sensitive to selected boundary conditions and the detailed structure of the support unit itself, but a similar mechanism will be operative. Individual support units are not designed to absorb, accommodate, or resist deformations in non-axial directions. Under conditions of relative lateral movement between hanging- and footwall (ride) and also in cases where the hangingwall (and/or footwall) cannot be assumed to be coherent and unconditionally stable, additional support functions are required.

Potential solutions may be found in alternatives such as bracing of the support units, either by tie-downs or by linking individual units. Support units could also be designed in such a way that horizontal deformations are not resisted, but rather accommodated, for instance by friction-less inserts between headboard and hangingwall and by free rotating joints at the unit ends. Support may also be designed as a more integrated system, in such a way that all support requirements are catered for. Resistance against non-axial deformations is one of the additional requirements, but maintenance of the integrity of that part of the hangingwall which is not

directly supported, is another, extremely important requirement, which is currently not addressed in support design.

Figure 4.5.4 shows a possible bracing configuration. Horizontal movements could in such a set-up more easily be restrained and toppling and even buckling could be prevented. In this alternative individual support units are effectively tied down to the lower parts of neighbouring support units and horizontal resistance is provided by tensile forces in these tie-downs.

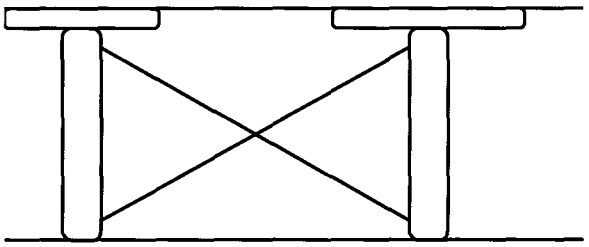

Figure 4.5.4 Bracing by tie-downs for horizontal stability.

A similar alternative providing horizontal resistance is shown in Figure 4.5.5, where the bracing is located in the hanging wall only. Individual support units are connected to neighbouring units without occupying space in the mine opening itself. Instabilities induced at individual support units are transferred to neighbouring units which can offer resistance if the cause of instability can be assumed to be exceptional and therefor restricted to a limited number of units only. An additional advantage of this last alternative is the provision of areal support by the bracing near the hangingwall which could prevent unstable behaviour of the area in between the main support units. This type of instability will be further discussed under Class II. Other alternatives can obviously be created and designed, but the requirement for any practical solution is the capability to resist and/or accommodate horizontal deformation in such a way that the load-bearing capacity of the support will remain sufficient.

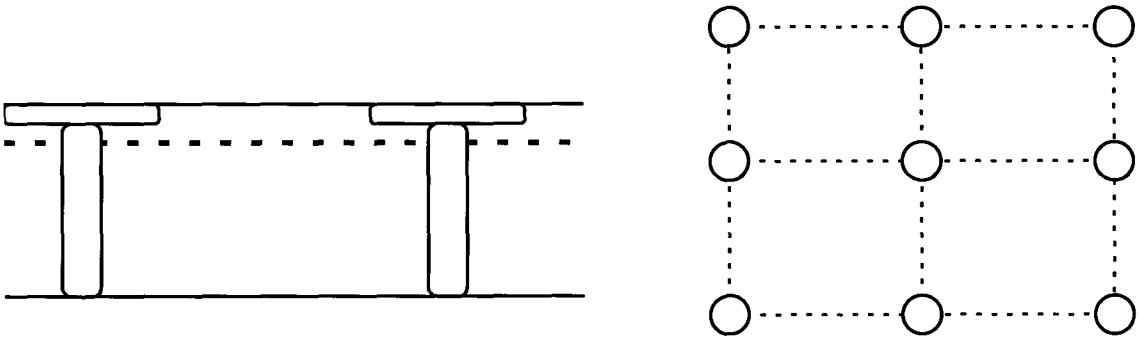

Section of the bracing near the hangingwall

Plan view of horizontal bracing

Figure 4.5.5 Bracing close to the hangingwall.

In order to demonstrate the problem of non axial deformation two more practical examples are given:

1. In areas containing so-called "rolls", which are typically associated with thrust folding, stopes are excavated in such a way as to negotiate such a roll (Figure 4.5.6)
2. Areas which are subject to large amounts of ride (Figure 4.5.7)

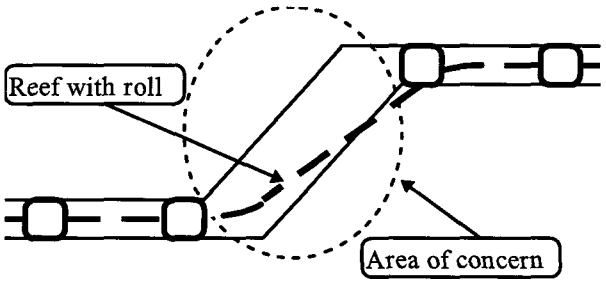

Figure 4.5.6 No appropriate support available for the steeply inclined part of the stope.

The large majority of all rock related accidents in goldmines which contain these so-called reef rolls (Ventersdorp Contact Reef lava deposits) occur in the steep part of the stopes, which is indicated in Figure 4.5.6 due to a combination of factors. One of the main problems is the fact that support units are not designed for these circumstances and design criteria are absent. Current support units are inadequate because they either have to accommodate large amounts of stope parallel deformations, or they have to be installed in such a way that their stability is questionable as well (Figure 4.5.7).

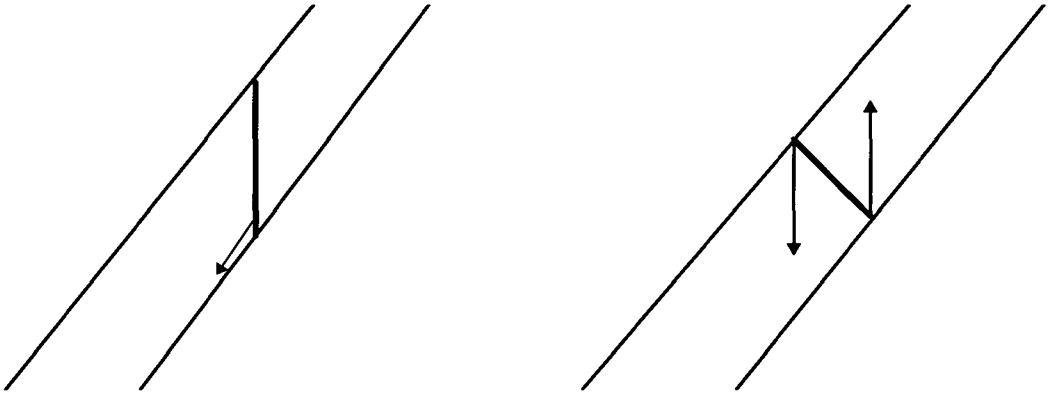

a) stope parallel deformations have to be accommodated

b) support units may loose 'grip'

Figure 4.5.7 accommodation of stope parallel deformations (ride) is not considered.

Alternatives to the bracing concept could involve roof-bolting or completely new support technologies such as inflatable bags (Wojno, 1997).

4.5.2.2. Effective hangingwall strength

In current support design, spacing between individual support units is a parameter which is not directly considered. Spacing can be related to the percentage of direct coverage which is provided by the support system. Coverage is presently *not* considered as a parameter in support design, but this may prove to be a serious short coming.

Using data from fatal accident statistics (Table 4.5.1), it is clear that the main cause of such accidents is *not* the failure of individual support units.

Table 4.5.1 Complete survey of 1990-1996 accident statistics; Behaviour of individual support units during fatal accidents.

AVERAGE 1990-1996	ROCK BURSTS	ROCK FALLS
FATALITIES	102	175
FAILED SUPPORT UNITS	30	8
TOPPLED, KICKED-OUT UNITS	120	35

Although it is generally accepted that the immediate hangingwall in between support units is potentially unstable, this potential is not quantified and it is also ignored as a support design criterion. Current support systems rely directly on the coherence of the exposed hangingwall to resist gravitationally induced stresses. Such a reliance is highly dangerous when the coherence of the exposed hangingwall is limited, as can be expected in a highly fractured and fragmented environment.

In order to quantify the coherence of the immediate hangingwall in situ, it has been proposed to perform pull-out tests. Such tests should provide data with respect to the resistance against pull-out forces, as well as information with regard to the actual geometry of potentially removed volumes of hangingwall. Both resistance and geometry can be related to an effective hangingwall strength, which, in turn, can be related to a "self supporting" capacity as shown in Figure 4.5.8.

.

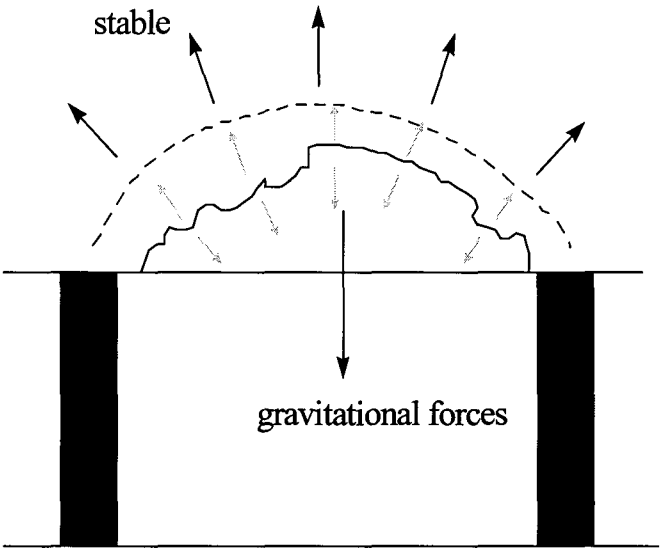

Figure 4.5.8 Compression arch between support units and the suspension of rock between these units.

An increase in support spacing results in the potential for larger volumes of rock to become detached. The bounding surface of that volume obviously also expands, but the ratio between the volume (mass) and the bounding surface is not constant. This ratio, which is a measurement of the average stress acting along that surface, is linearly related to the support spacing, provided the shape of the volume does not change. In that case the average stresses increase linearly with increasing support spacing and the effective hangingwall strength thus determines the critical support spacing underneath a particular hangingwall.

Figure 4.5.9 shows the relation between the critical joint strength and the support spacing due to gravitational loading. This is the static case in which no seismic accelerations are induced.

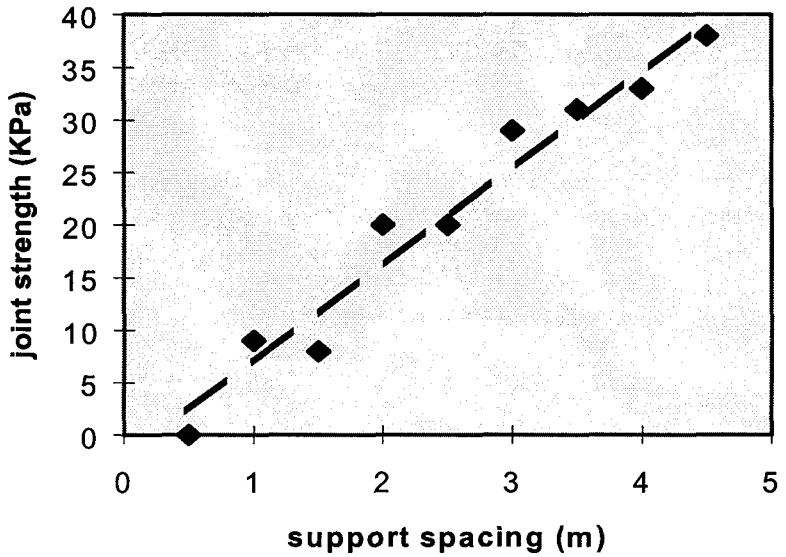

Figure 4.5.9 Relation between critical joint strength and support spacing due to gravitational loading (static).

While the current design of individual support units ensures an adequate performance of such units even under rockburst conditions, this does not guarantee the stability of the complete

stope hangingwalls under the same conditions. Figure 4.5.10 illustrates a problem which is applicable to the overwhelming majority of all rock related accidents. (table 4.5.1)

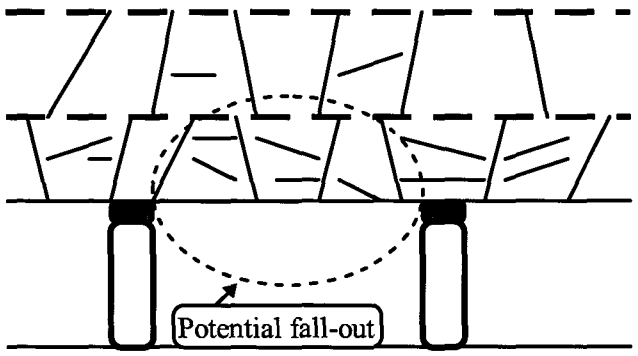

Figure 4.5.10 Typical instability problem associated with absence of any form of support between the main support units.

Although this issue has been raised previously (1996 SIMRAC report GAP032, for instance), it hasn't been emphasised sufficiently that the current support design does not address the stability of the area in between individual support units at all. This renders the support design incomplete as the inherent assumption of a uniformly distributed support resistance is invalid in most practical cases. This fact is clearly demonstrated in situations whereby the hangingwall between intact support units has been ejected. The support resistance has apparently not been transmitted to that part of the hangingwall which is not directly influenced by the individual support units. Simple numerical models demonstrate that such a behaviour is related to the potential unstable behaviour of the area underneath a compression arch between individual support units. (Figure 4.5.11).

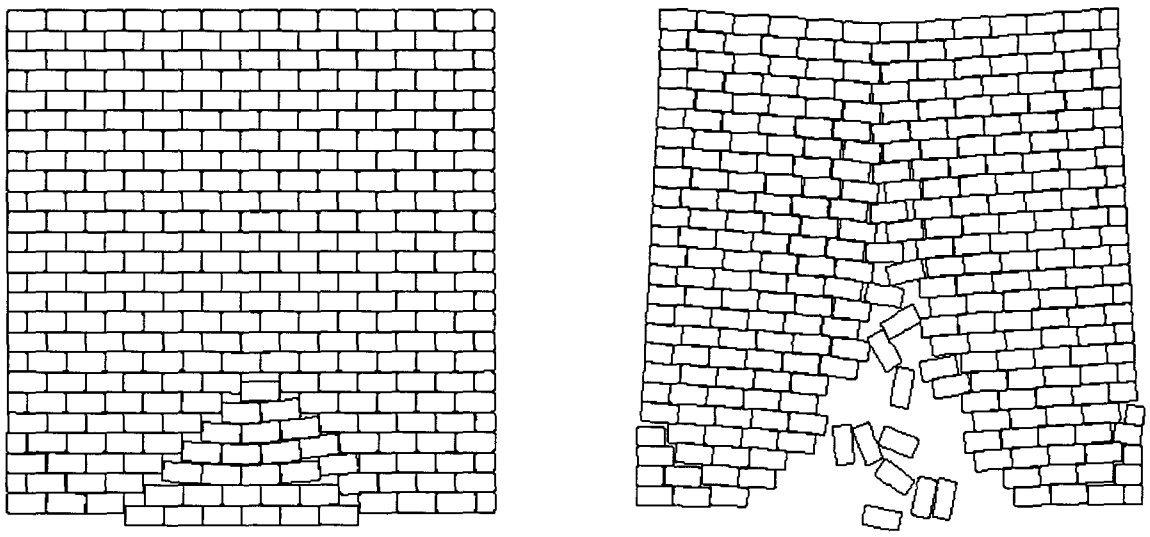

Figure 4.5.11 Scenarios of local instability of hangingwall between main support units.

No support requirements are presently available for this potentially unstable part of the hangingwall, while the majority of fatalities can directly be associated with this form of instability (see rockburst task group reports for instance). The spacing between individual support units will obviously affect the requirements for the support of the hangingwall in between these units (areal support), in the sense that a variation in support spacing will lead to a variation in (areal) support requirements, but a total absence of areal support can only. As such a requirement

appears to be impractical for deep level mining scenarios, were intense fracturing and jointing most often results in the potential for relatively small block sizes, areal support requirements should be given urgent consideration.

While such an additional support requirement is justified here on the basis of physical and mechanical considerations and should lead to improved hangingwall control and a substantial reduction in rock related accidents, it is obvious that additional costs will be incurred. This negative aspect could however be offset by a more efficient design of the individual support units once more realistic data with respect to their design criteria becomes available from appropriate underground monitoring. This may lead to a substantial reduction in costs of individual support units as present design parameters may lead to excessive support requirements.

4.5.2.3 Effect of bedding plane separation on support performance and stability

The undulating nature of bedding planes has been shown to cause additional closure and bedding plane separation on a stope span scale. On a smaller scale separation across an undulating bedding plane can be expected to be associated with local variations in the magnitude of separation. Upon compacting, due to support pressure or as a result of complete closure, a situation can arise in which certain areas of two neighbouring layers are in contact, while other areas of such layers remain separated by varying distances. Such conditions are typically observed underground and it is thus of practical relevance to investigate the support interaction in such a case.

In order to analyse the interaction between individual support units and the immediate hangingwall, a simplified model has been used. This model represents a single horizontal layer containing two steep joints (fractures). A support unit is assumed to act underneath the block which is bounded by the two fractures and various boundary conditions and geometry variations have been analysed. The following figures show the various results of the (FLAC) models which have been used.

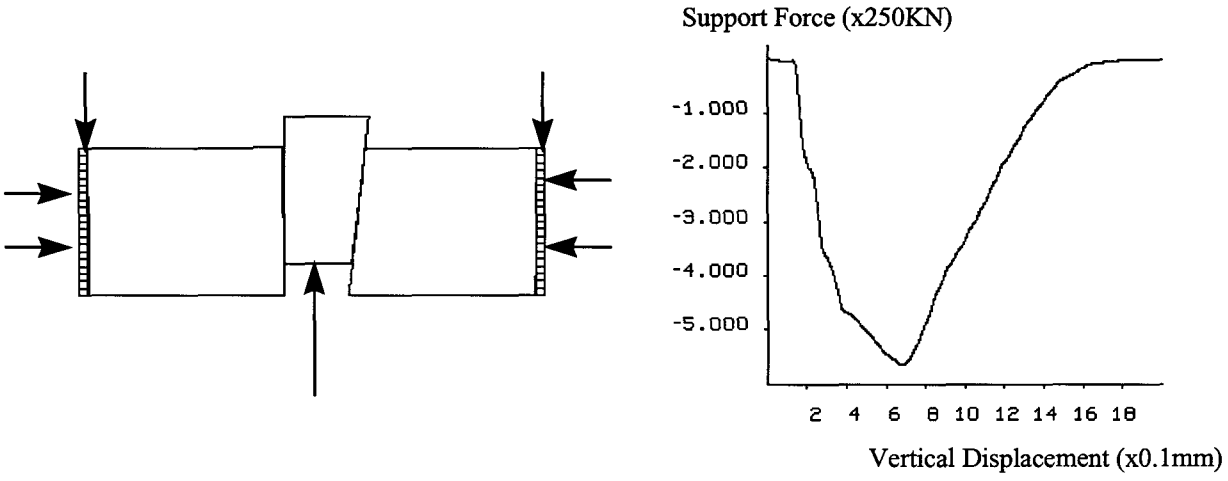

a) magnified deformation ***b) support response***

Figure 4.5.12 Squat beam; fixed boundaries; rigid blocks; unstable.

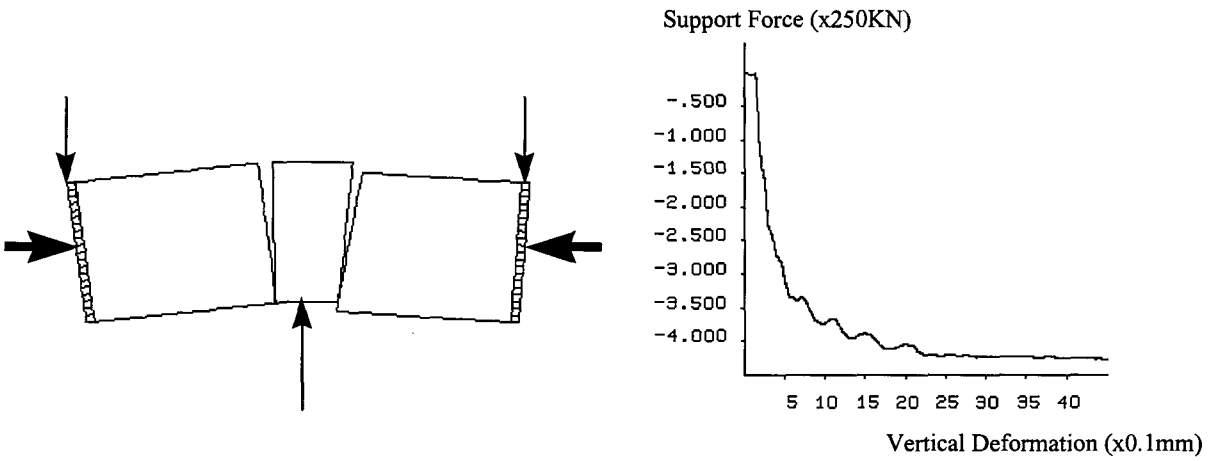

a) magnified deformation ***b) support response***

Figure 4.5.13 Squat beam; pressurised boundaries; rigid blocks; yielding.

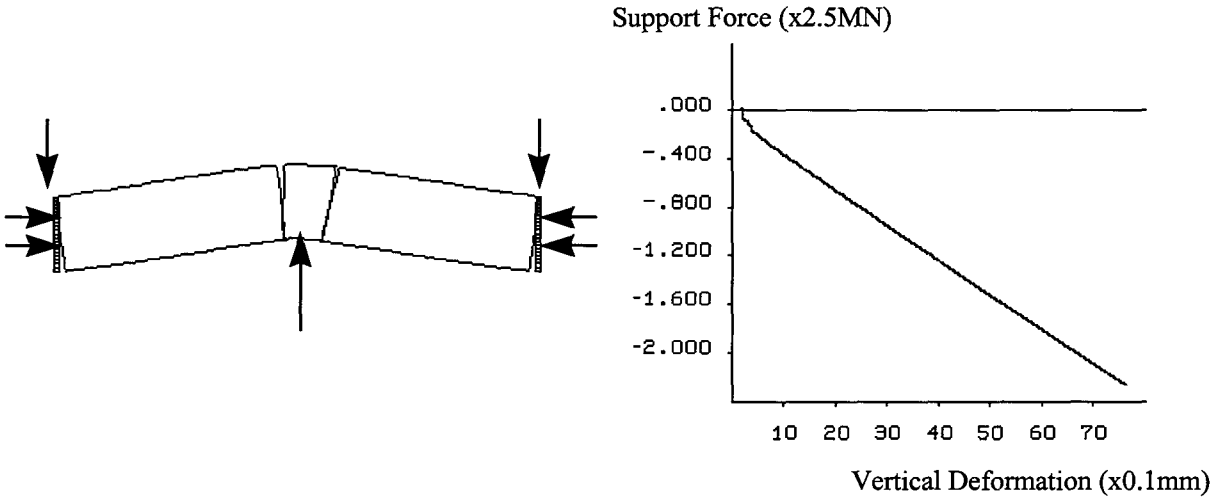

a) magnified deformation ***b) support response***

Figure 4.5.14 Slender beam; fixed boundaries; rigid blocks; stable.

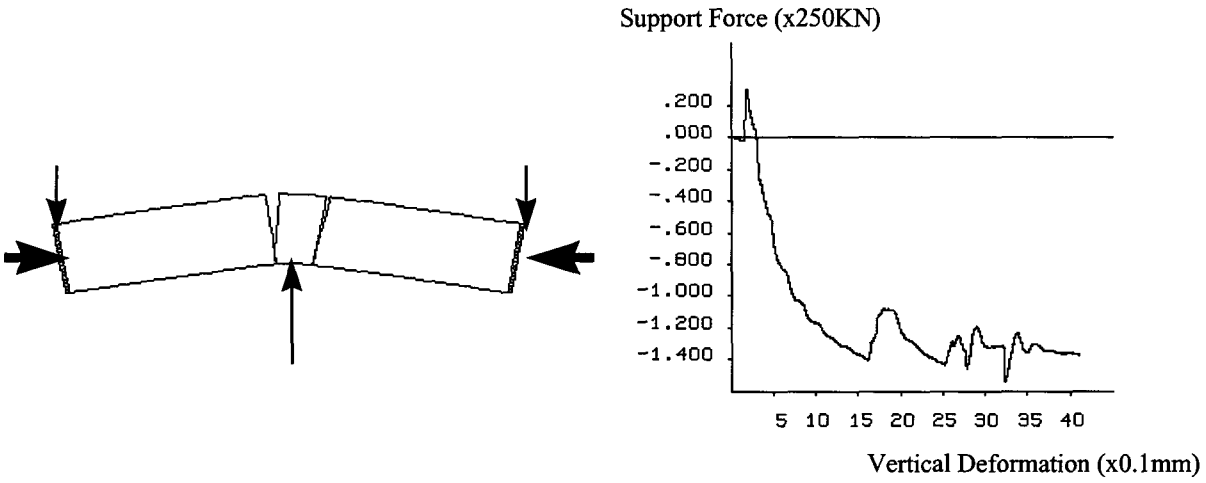

a) magnified deformation ***b) support response***

Figure 4.5.15 Slender beam; pressurised boundaries; rigid blocks; yielding.

The simulations in Figure 4.5.12 to 4.5.15 demonstrate how a variety of potential support hangingwall interactions are possible. Local boundary conditions will depend on fracture geometry, rock strength, detailed geology, etc. The results show a variation between unconditionally stable behaviour and conditionally unstable behaviour. The practical implication of these results is that they represent the potential for support induced instability.

It is possible for an individual support unit, under the right circumstances, to punch part of the immediate hangingwall out of its original position. Figure 4.5.12 shows the most dramatic scenario in which such an action is followed by a complete loss of the support function. The practical consequence of such a situation may involve loss of stability in the surrounding hangingwall and subsequent hangingwall collapse.

A more moderate scenario is shown in Figure 4.5.13 and 4.5.15. While part of the hangingwall is being dislodged as well in those simulations, this is not associated with a loss of support resistance. The constant horizontal stress, which is assumed to be present in those cases, ensures a yielding response resulting in a limited support resistance.

In cases such as those described above it would be undesirable to design for a support resistance which exceeds the failure strength (Figure 4.5.12) or the yield strength (4.5.13 & 4.5.15) associated with particular hangingwall conditions. Although the in situ measurement of such a yield strength is not a common practice, such measurement have been performed in the past and demonstrated the likelihood of similar behaviour around stopes in the Carbon Leader. (Herrmann, 1987)

4.6 Conclusions and recommendations

It follows from the conceptual numerical model that a substantial amount of inelastic closure may be associated with the presence of stope parallel bedding planes. The main parameter controlling this inelastic closure is the effective dilation associated with the slip across these bedding planes. This dilation appears to be cumulative; in other words the number of active bedding planes affects the total closure to a very large extent. Slip and associated dilation is

initiated near the abutments and causes bedding plane separation over the full stope length. This observation is of particular interest as it may explain observed bedding plane separation in extensometers.

This particular mechanism of bedding plane separation may also explain the observations of Gürtunca et. al. (1990) in which is was observed that, up to a pressure of approximately 1 MPa in the supporting backfill, no differential movement was observed in the hangingwall across a strike gully, while higher pressures induced a differential between the deformation of the hangingwall above the unsupported gully and the deformation of the hangingwall in direct contact with the pressurised backfill.

It is suggested here that closure of the bedding planes requires a certain pressure; this pressure obviously depends on the layer thickness and possible other secondary parameters. Closure of all separated layers would clearly require increased pressures and it is thus has also been observed by Gürtunca et. al. (1990) who note that at stresses above 3,5 MPa no additional differential closure is developing between the hanging wall above the unsupported gully and the hangingwall subjected to the backfill pressure.

Herrmann (1987) observed that local support did not affect the (inelastic) closure in a longwall stope. Unfortunately it was not possible to investigate the support interaction as unrealistically thick layers had to be represented due to numerical constraints. The slenderness of the beams had to be limited in order to obtain reliable results. This is a universal problem and affects all traditional numerical models. A cure is not obvious, but the problem needs to be addressed.

Associated with the issue of bed separation is a particular stability problem associated with local support. A variety of situations may be encountered, depending on support strength and boundary conditions. The support may cause an instability and become completely ineffective; the support may cause a yielding response in the immediate hangingwall and thus be conditionally stable and the support may be unconditionally stable. It is important to realise that the first to cases are realistic scenario's which may induce hangingwall instabilities. If the support strength exceeds levels which may induce sliding across certain fractures in the immediate hangingwall, instability is possible.

Individual support units do not necessarily form a support *system* unless the rockmass itself contributes to the load bearing capacity. Such a capacity is in fact indirectly assumed if the rock surface is not completely covered by support. While the contribution of the rockmass to the support system is difficult to quantify, it is clear from many rock related accidents that the inability of the rockmass to bridge the span between individual support units is one of the main reasons for (local) instabilities and the consequences thereof. Under such circumstances the rockmass requires additional support in order to *assist* it in bridging the gap between the (main) support units.

Although a reduction of the support spacing will obviously increase the ability of the rockmass to bridge the (smaller) gaps, it may be far more efficient and cost effective to increase the load bearing capacity of the rockmass itself by providing it with some form of (areal) support. The only function of the areal support would be to assist the rockmass in bridging the distance between the main support units, so that these in their turn can be designed more efficiently for that function for which they should be designed, namely to prevent the immediate stope hangingwall from detaching itself from the surrounding rockmass, thus causing global instability. (the current support design methodology is assuming exactly that same function, without considering local stability).

Although the main units should not have to be designed to provide local stability, such stability needs to be ensured either by the rockmass itself or by a combination of that rockmass and some form of appropriate and effective reinforcement.

The need for some form of secondary support is identified by the previous considerations. The exact requirements for such support depends completely on the rockmass under considerations. In cases of a very competent hangingwall no secondary support may be required, while in cases of a highly fragmented hangingwall, only a very limited contribution towards load bearing capacity can be expected from the rockmass itself. In order to address this issue, which has an immediate and direct effect on the safety and efficiency of (stope) support systems, serious effort has to be directed towards identifying areal support requirements for different conditions. Individual support units do not fulfil all support requirements, they are only designed to resist axial deformations, which may not be sufficient in many applications.

As a practical means to ascertain a critical support spacing, the concept of effective hangingwall strength has been introduced.

Other local instability problems have been discussed as well. Most of them can be related to the inability of individual support units to resist non axial loading.

4.7 References

Adams, G.R., Jager A.J. & Roering, C. 1981. Investigation of rock fracture around deep level gold mine stopes. *Proceedings of the 22nd U.S. Symposium on Rock Mechanics.* Boston, M.I.T., p. 213-218.

Brummer, R.K. 1987. Fracturing and deformation at the edges of tabular gold mining excavations and development of a numerical model describing such phenomena. *PhD Thesis.* Johannesburg: Rand Afrikaans University.

Cook, N.G.W., Hoek, E., Pretorius, J.P.G. & Salamon, M.D.G. 1966. Rock Mechanics applied to the study of rock bursts. *J. S. Afr. Inst. Min. Metall.* Vol. 66, p. 436-528.

Eve, R.A. 1996. *SIMRAC Final Project Report GAP032.* Pretoria: Department of Minerals and Energy.

Gürtunca, R.G., Squelch, A.P. & Gonlag, M.D. 1990. Results of a backfill monitoring program at harmony gold mine, 3 shaft, 27/18b stope. *COMRO internal note no. R04/90.* Johannesburg: Chamber of Mines Research Organisation.

Glisson, J. 1997. *Private communication.*

Handley, M.F. 1995. An investigation into the constitutive behaviour of brittle granular media by numerical experiment. *PhD Thesis.* Minneapolis: University of Minnesota.

Herrmann, D.A. 1987. Fracture control in the hangingwall and the interaction between the support system and the overlying strata. *M.Sc. Dissertation.* Johannesburg: University of the Witwatersrand.

Kersten, R.W.O. 1964. Report on Chamber of Mines Project 111/64/10108. Johannesburg: Chamber of Mines Research Organisation.

Kuijpers, J.S. 1998. Identification of inelastic deformation mechanisms around deep level mining stopes and their application to improvements of mining techniques. *PhD Thesis.* Johannesburg: University of the Witwatersrand.

Leeman, E.R. 1960. Some underground observations relating to the extent of the fracture zone around excavations in some central Rand Mines. *Papers & Discussions, Association of Mine Managers of South Africa.* Vol. 1958-1959, p. 385-404.

Legge, N.B. 1984). Rock deformation in the vicinity of deep gold mine longwall stopes and its relation to fracture. *PhD Thesis.* Cardiff: University College.

Lightfoot, N., Goldbach, O.D. Kullmann, D.H. & Toper, A.Z. 1996. Rockburst control in the South African deep level gold mining industry. *Proceedings of the 2nd North American Rock Mechanics Symposium.* Canada, p. 295-303.

Napier, J.A.L. & Hildyard, M.W. 1992. Simulation of fracture growth around openings in highly stressed , brittle rock. *J. S. Afr. Inst. Min. Metall* . Vol. 92, No. 6, p. 159-168.

Napier, J.A.L. & Pierce, A. 1995. Simulation of extensive fracture formation and interaction in brittle materials. *Proceedings of the Mechanics of Faulted and Jointed Rock.* Vienna, p. 63-67.

Salamon, M.D.G. 1963. Elastic analysis of displacements and stresses induced by the mining of seam or reef deposits. *J. S. Afr. Inst. Min. Metall.* Vol. 64, part I, p. 128-149.

Sellers, E.J. 1997 A tessellation approach for the simulation of the fracture zone around a stope. *Proceeding of SARES97.* Johannesburg: p. 143-154.

Roering, C. 1979 *Annual report for the Chamber of Mines of South Africa in fulfilment of research grant GTIP04.* Johannesburg: Rand Afrikaans University.

Wojno, L. 1997. *Private communication.*

5 Underground observations and seismic analysis within various geotechnical areas

5.1 Underground observations and measurements

5.1.1 Introduction

5.1.1.1 Objectives

Enabling output 5 involves the provision of data for the verification of numerical models by means of underground observations, measurements and seismic analysis. The objective is to gather and analyse data about the fractured stope hangingwall in order to devise a conceptual model, which would be used for back analysis by numerical modelling.

The hangingwall is characterised in terms of various parameters, a synthesis of which will be used to propose the conceptual model. These include the nature of fracturing, fracture zone characteristics, time-dependent behaviour of the fracture zone and behaviour during dynamic loading.

5.1.1.2 Outline of Chapter 5

This chapter is arranged around the objectives described above. Section two covers results of the literature search. Section three describes the research methodologies used and section four discusses the results of the study. Section five describes the conceptual model.

Appendices contain information on the instrumentation used and detailed results.

5.1.1.3 Choice of test site

Two underground sites were visited in order to select a suitable stope for the in-stope monitoring programme:

87-61E longwall on WDL South Mine
The first site was the 87-61E longwall on WDL South Mine. This longwall consisted of four panels breast-mining the VCR. Entry time from surface to the site was good (less than 30 minutes) and seismically active dykes nearby ensured that the stope would be subjected to dynamic loading. Two panels displayed few joints and a smooth hangingwall, whereas the other two panels displayed intense fracturing, a blocky hangingwall and geological structures including reef rolls and two faults.

Because of the increased complexity of the hangingwall in the latter two panels, it was felt that these should be suitable as the site for the in-stope monitoring programme. This stope, however, was a VCR stope which has been studied in detail in a previous project, GAP 102. We therefore visited a second site on WDL East Mine.

91 E1/93 E4 panels on WDL East Mine
At this site (Figure 5.1.1.1) the Carbon Leader Reef is being mined on breast by a conventional 25 m long panel. Until recently the stope used backfill as permanent support and Camlok props as temporary face area support. Permanent support had been replaced with elongates (initially cone props with a later switch to Madodas and then Ebenhaesers) and packs without backfill. Entry time to the site was poor (approx. 90 minutes), but the nature of the hangingwall displayed ideal conditions for in-stope monitoring. Seismically active dykes close by ensured that the stope would experience dynamic loading. This second site was chosen as the research stope for the underground hangingwall fracture-zone monitoring programme.

The panels are situated at a depth of approximately 2500 m below surface. Panels 91 E1 and 93 E4 were examined. An argillaceous quartzite footwall, a siliceous quartzite hangingwall and a Carbon Leader to Green Bar parting of 1,5-2,0 m characterise the geotechnical area.

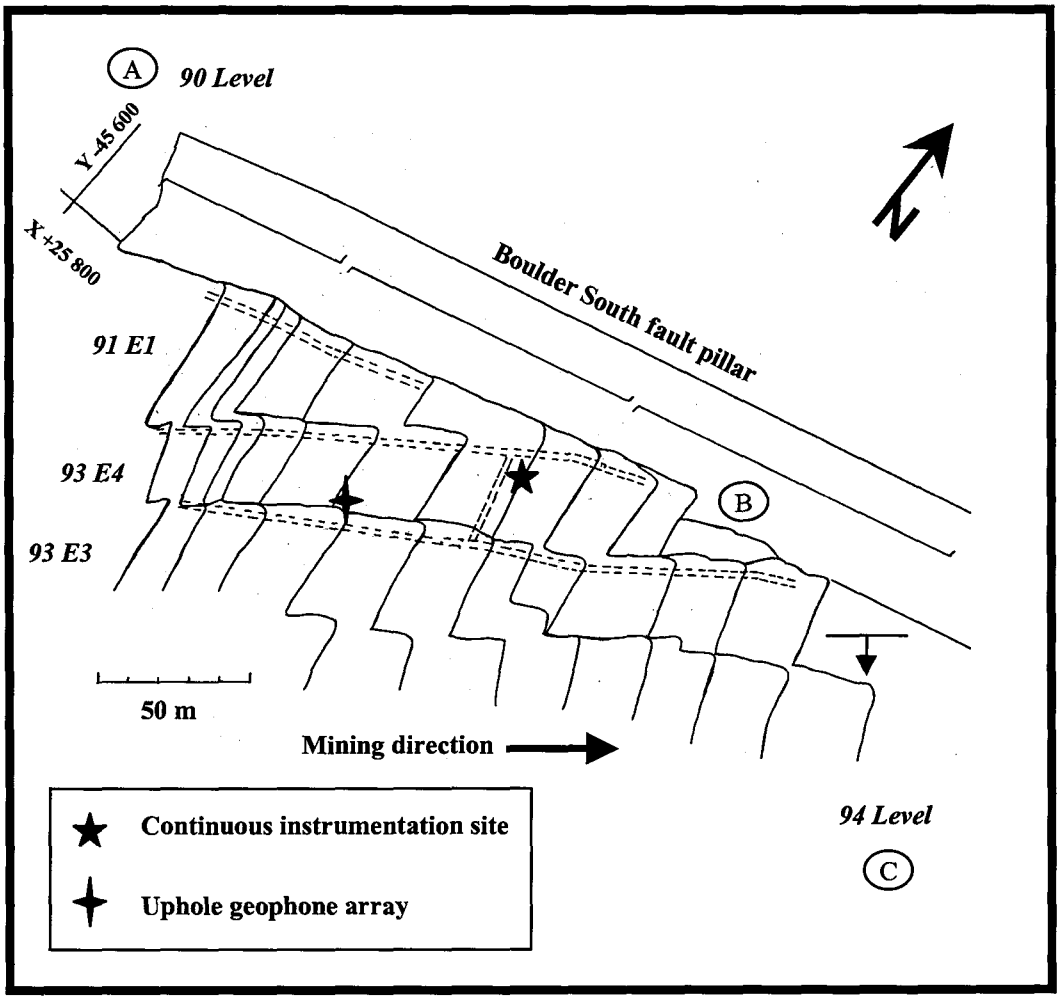

Figure 5.1.1.1 Locality plan of site (Positions 'A' through 'C' are discussed in the text in Section 5.1.4.7).

5.1.1.4 Site establishment

Considerable effort has gone into establishing the site for the monitoring programme. As mentioned above, the mine initially changed the support from backfill to a cone prop/pack support system (see Figure 5.1.1.2), thus allowing a conventionally supported panel to be instrumented, as well as allowing hangingwall behaviour in the back area to be monitored. The elongate support system was later changed to Madoda/packs with pack breaker lines installed every 8 m along dip (similar to that shown in Figure 5.1.1.2). Most recently, the support system comprises Ebenhaeser props with diagonally placed in-panel pack breaker lines (see Figure 5.1.1.3).

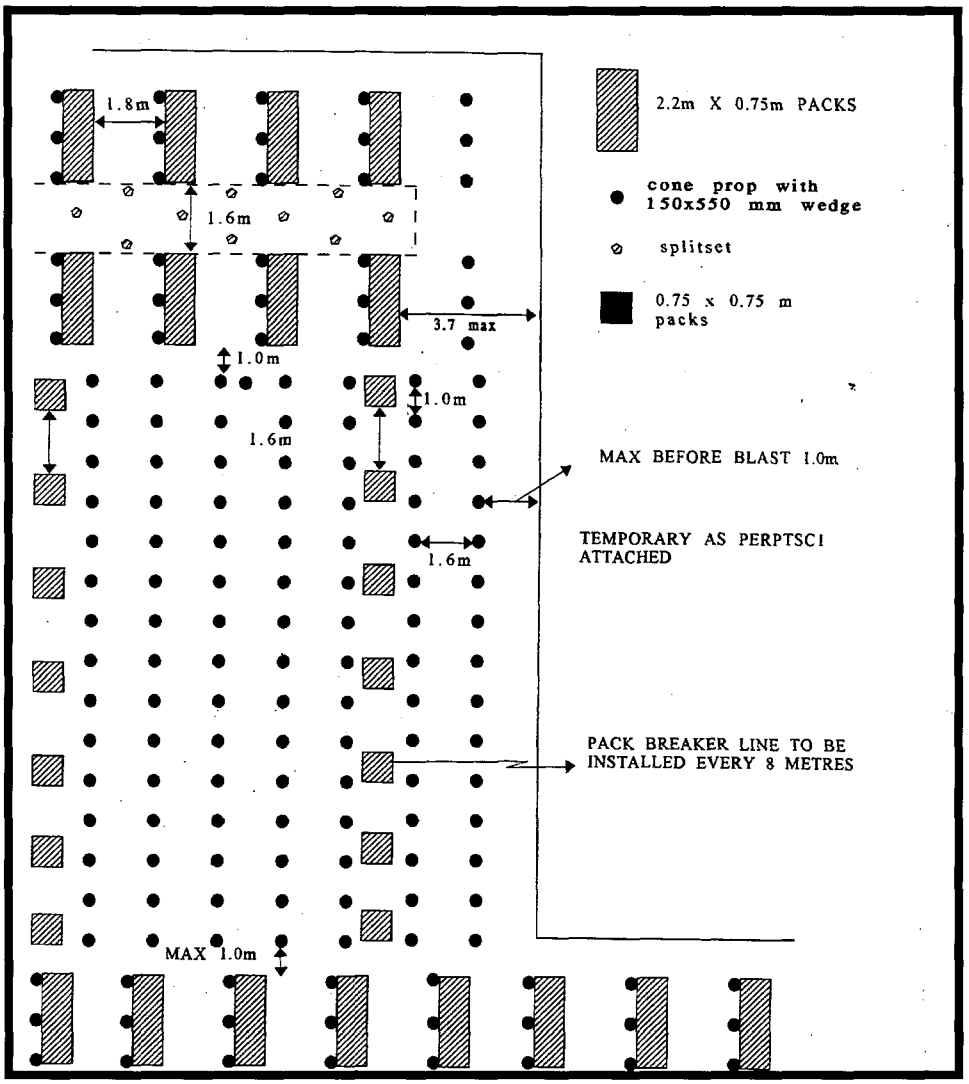

Figure 5.1.1.2 Elongate support in 91E1/93E4 panels.

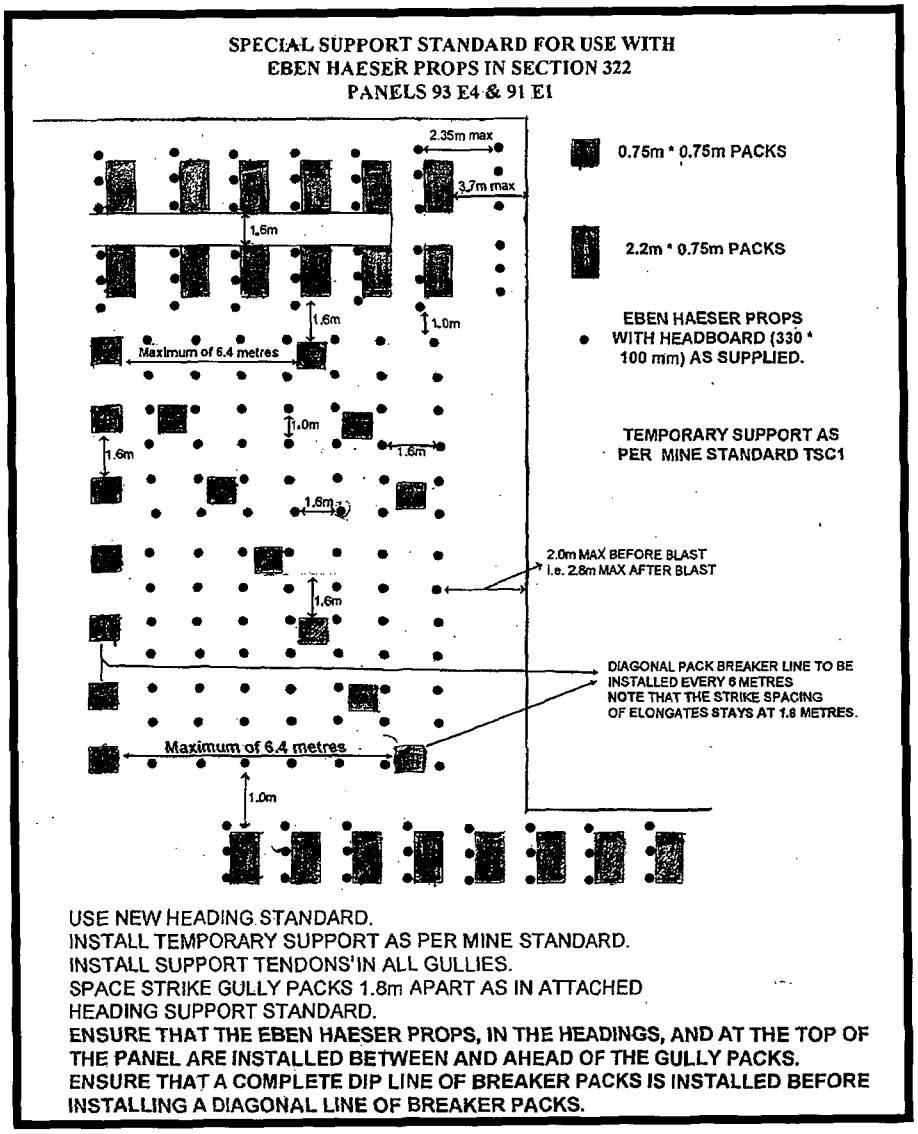

Figure 5.1.1.3 Revised support strategy.

5.1.2 Literature survey

A major output of this study is the proposal of a conceptual model to be used for back analysis in numerical modelling. The literature survey was therefore directed at past studies based on the Carbon Leader.

Hagan (1980) conducted a study of mining-induced fracturing and instability on a deep level Carbon Leader longwall stope with variable lag lengths. The results and conclusions are outlined. The dominant joint set is a highly persistent north-north-east trending set. Major geological discontinuities are not a common factor affecting hangingwall instability. The frequency of fracturing is reduced by lithological differences across well-defined parting planes. The interaction of joints, bedding planes and minor faults with mining-induced fracturing results in hangingwall instability.

Legge (1984) conducted a detailed study on rock deformation on deep level Carbon Leader longwall stopes with the emphasis on fracturing. The major findings are outlined. Strain softening behaviour in the confined area ahead of a stope face results in the formation of shear fractures as the face advances, each separated by a relatively solid portion of rock. Significant lateral movement may be expected along parting planes. Factors affecting this movement include slip along fractures which may displace the parting plane, friction due to natural

asperities and undulations along the parting plane, frequency of occurrence of parting planes, stiffness and density of support and buckling and caving of strata into the stope. A repeatable pattern of fracturing occurs as the stope is advanced and the zone of fractured rock adopts a consistent form.

Brummer (1987) studied the nature and fracture mechanisms around deep level Carbon Leader stopes. High edge stresses induced by mining results in the formation of fractures in a manner that relieves vertical stress. In the fracture zone, the reef shortens vertically but dilates horizontally. Parting planes appear to exert a strong controlling influence on the deformation processes that occur near the edges of tabular excavations.

5.1.2.1 Seismic measurements

Goldbach (1990) analysed seismic data recorded by a downhole geophone array installed in a 15 m long borehole drilled into the sidewall of an underground tunnel in a deep level South African gold mine in an attempt to characterise the effect of the fracture zone on ground motion at that location. A reduction in the propagation velocities of seismic waves passing through the fracture zone, as well as an amplification of the P-wave first pulses was reported. A site effect, in the form of spectral amplification within certain frequency bands, was interpreted as being the result of energy trapping in the fracture zone. An eight-fold increase in attenuation for frequencies above 500 Hz was found in association with the fracture zone.

Durrheim *et al* (1996) made measurements of the effect of seismic shaking on the fractured rock surrounding an excavation at a site where a remnant pillar was being extracted on Carbon Leader Reef some 1900 m below surface. An increase in the duration of shaking and an amplification of peak ground velocities and accelerations compared with the ground motion in solid rock were found. These effects were attributed to the trapping of energy in the fractured rock surrounding the highly stressed excavation. Site-specific resonances at frequencies above the corner frequencies of the recorded seismic events were observed.

5.1.3 Research methodology

An in-stope monitoring programme was devised with the aim of characterising the hangingwall of the conventionally supported stope.

5.1.3.1 Closure-ride measurements

Manual closure-ride stations were installed at the top and bottom of panels between gully support units. The stations were installed as close to the face as possible and new stations were installed as soon as the station to face distance exceeded 15 m. The stations were monitored on a daily basis with a typically 24 hour interval between readings. Distance to face was also measured. This is regarded as long term measurements by Toper et al (1998:35).

The four-peg method of installation, as discussed by Piper and Gurtunca (1987) was used. The closure measured using this technique is due to time-dependent behaviour, as well as elastic and inelastic effects as the face moves away from the station. Software based on a Microsoft Excel spreadsheet devised by Toper was used to calculate the closure and ride from the data.

5.1.3.2 Hangingwall profiles

Hangingwall profiles were measured in strike gullies in previously backfilled areas and conventionally supported areas. Grodner (1996) discusses the methods employed.

Hangingwall profiles are used to quantify hangingwall conditions in order to compare conditions at various localities. Factors affecting hangingwall conditions may be identified and their influence determined.

The measurements are taken periodically (every 2 cm) along a tape stretched over the required distance. Distance from the tape to the hangingwall is measured. Corrections are made for tape orientation and hangingwall orientation. The data is entered into a spreadsheet. The results obtained include profile lengths, average gradient, and average of the absolute deviation from the mean.

5.1.3.3 Quasi-static instrumentation

Continuous monitoring instrumentation was used to characterise the behaviour of the stope hangingwall.

The layout for the in-panel instruments that were monitored electronically on a continuous data-logging basis is shown in Figure 5.1.3.1. Extensometers measured the inelastic deformation in the hangingwall at 0,5 m, 1,0 m and 2,0 m depth. Closure meters measured stope closure at the site.

Tiltmeters, capable of detecting bi-directional tilting of 20° to an accuracy of 0.001° in two mutually perpendicular directions, were installed on the footwall and hangingwall. A crack gauge, capable of detecting both crack opening and closing, was installed across a fault. Doorstopper strain gauges measured the local stress changes of the hangingwall skin.

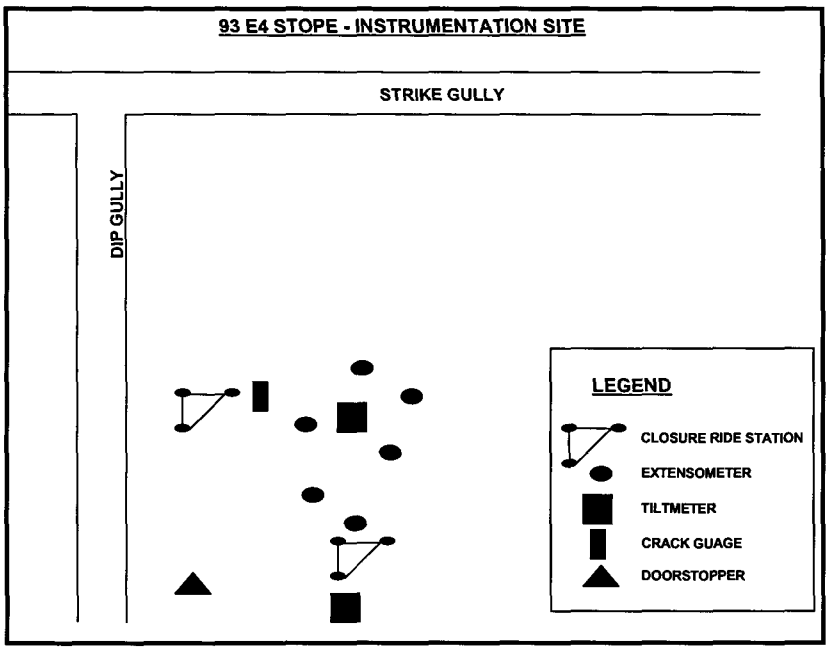

Figure 5.1.3.1 Layout of continuous monitoring instrumentation.

5.1.3.4 Seismic instrumentation

Vertical variations in seismic ground motion, with increasing depth into the hangingwall, were measured via a vertically oriented co-linear triaxial geophone array (Figure 5.1.1.1). The separation between adjacent triaxial geophones in the array was 2 m.

The deployment of five triaxial geophones, up a single 11 m long hole, as a co-linear array required a novel design to be devised. M & M Systems manufactured this array. The necessary Portable Seismic System (PSS) hardware (DAU, outstations, termination box, DC power supply, PC), that the geophone array used to record the seismic ground motion, was also obtained. A site for the 11 m up-hole, into which the co-linear array was to be installed, was chosen in the strike gully at the down-dip end of panel 93E4. The footwall was lifted in order to accommodate the outstations. A DAU room was established on 91 level. This room had a clean concrete floor, was well ventilated, had been fenced off and power was available. A single 20-pair cable was installed from the outstations in the stope to the DAU room; this was a distance of about 600 m.

A special steel-armoured cable with a non-toxic sleeve is required to meet the mine's safety regulations and a kilometre of such a cable was bought for this purpose.

Drilling of the geophone hole was completed by mid-December 1997. Unfortunately, the hole – planned to be 11 m long – was drilled to just 10 m. As a result, the bottom-most triaxial component of the assemblage was installed just 0,5 m into the hangingwall (Figure 5.1.3.2a). Difficulties were experienced with the grouting of the geophones into the hole, due to the highly fractured nature of the rock mass surrounding the hole. Owing to various complications which arose during the drilling of the hole, the array was more than 50 m behind the 93E4 face by the time the seismic system was commissioned and operational.

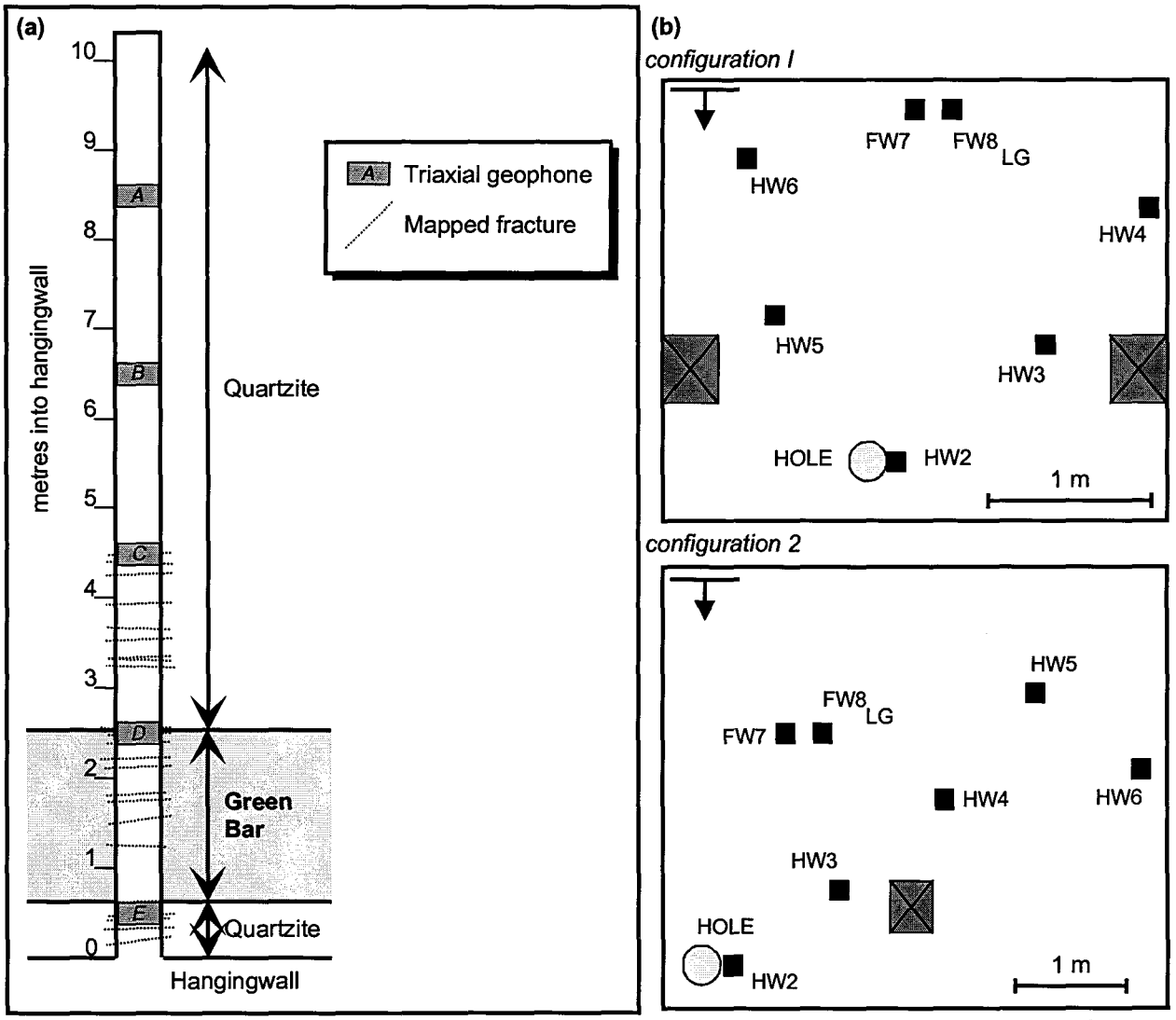

Figure 5.1.3.2 (a) Vertical section showing positions of sensors in uphole geophone array. Mapped positions of Green Bar and fracturing around hole are also indicated. (b) Schematic (scale is approximate) of positions of GMM sensors (e.g. 'HW2') with respect to hole in plan ('FW7' and 'FW8' were positioned on the footwall).

A new generation eight-channel Ground Motion Monitor (GMM) was obtained via GAP 530. This was used to measure horizontal variations in seismic shaking across the skin of the stope hangingwall, via an array of uniaxial vertical geophones installed at various points on the rock face, in the immediate vicinity of the hole (Figure 5.1.3.2b).

The PSS and GMM arrays were connected via a common geophone channel to allow for the comparison of the data sets and the identification of common recorded seismic events. A computer program was written to identify the common events on the basis of high correlation of

the common signals and then combine the data files, after correcting for offsets in the data and for differing sampling rates.

The combined data set was analysed and interpreted in partnership with GAP 530. This analysis included the investigation of the variation in spectral response of the rock mass in three dimensions and in time, as well as the assessment of the velocity variations of the rock mass in the vicinity of the three-dimensional array. The analysis and interpretation of the data was expected to lead to improved understanding of the behaviour of the stope hangingwall in response to seismic excitation, laterally and with depth into the hangingwall, and of the changes in the rock mass with time and distance from the stope faces.

5.1.4 Discussion of results

5.1.4.1 Site description

A representative stratigraphic column is presented in Figure 5.1.4.1. The footwall consists of a green-grey, poorly sorted, very coarse grained, and immature quartzite. Glassy, cleaner quartzites occur locally. Persistent, argillaceous parting planes are up to 20 mm thick and strongly laminated. Impersistent, argillaceous parting planes are 20-30 cm apart and up to 4 mm thick and are also strongly laminated. The thicker argillaceous parting planes have smooth, shiny bottom contacts indicating movement along the planes. A 5-10 cm thick medium pebble conglomerate occurs approximately 50 cm below the Carbon Leader, and another similar conglomerate up to 170 cm below the Carbon Leader.

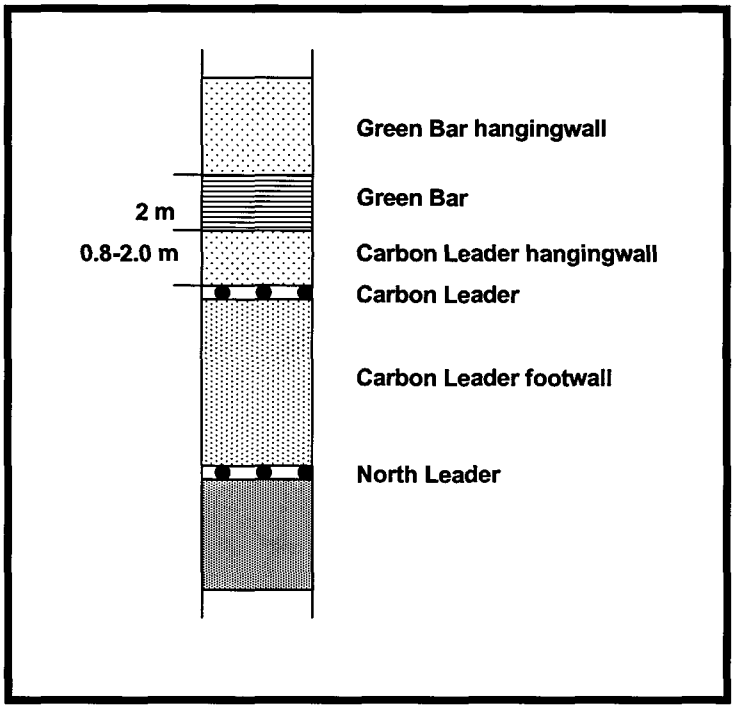

Figure 5.1.4.1 Stratigraphic column of the Carbon Leader.

The Carbon Leader is a narrow conglomerate up to 12 cm in thickness. It has an erosive base, often eliminating the argillite parting directly below it.

The Carbon Leader is immediately overlain by a very coarse grained, light grey siliceous quartzite, up to 200 cm thick. Glassy, more mature quartzites occur locally. Argillaceous parting planes less than 1 mm thick occur above the glassy quartzites. The Rice Pebble Marker overlies the hangingwall quartzites. This is a gritty, immature quartzite up to 30 cm thick with numerous argillaceous parting planes.

The Green Bar, an argillaceous unit up to 2,5 m thick, overlies the Rice Pebble Marker. The Green Bar lies at an average of 2,0 m above the Carbon Leader. Local tectonic undulations and erosional features may reduce the quartzite parting to 1,2 m. The base of the Green Bar is characterised by a smooth, polished, tectonised undulating surface. A well-bedded, often pyritic siltstone occurs at the base, grading into a less well-bedded chloritoid shale. Fault gouge and vein quartz may occur locally on the bottom contact.

5.1.4.2 Discontinuity mapping

The term discontinuity includes natural geological features such as joints, faults, bedding and parting planes and fractures created by mining activity.

Joints are those discontinuities exhibiting no discernible displacement. They may contain infillings of vein quartz and/or chlorite. Faults are those discontinuities that exhibit visible displacement across the discontinuity plane. Movement may be a few millimetres to tens of metres and is indicated by fault gouge, mylonitic material, comminuted rock material or slickensides. Bedding or parting planes include those discontinuities that are parallel or sub-parallel to the reef plane. Mining-induced fractures are discrete breaks in the rock mass along which movement may or may not occur and are accompanied by the optional occurrence of infilling.

Jointing
Three major joint sets occur, as illustrated in Figure 5.1.4.2. The north-north-east trending set is the dominant one, followed by an east-west trending set and the north-west trending set.

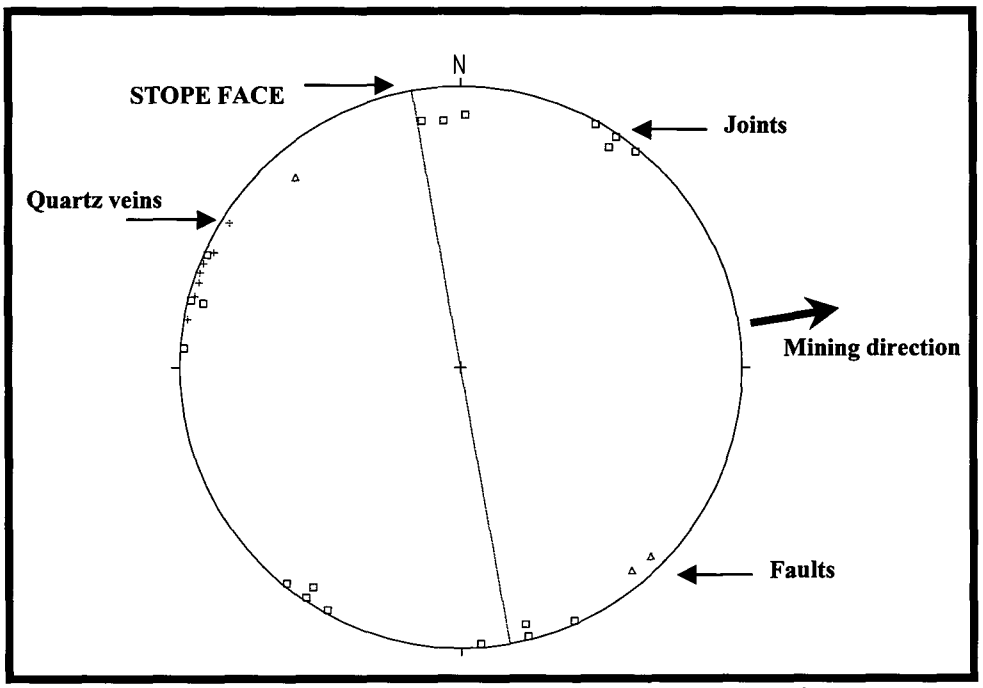

Figure 5.1.4.2 Lower hemisphere, equal area pole plot of discontinuities.

The north-north-east set dips steeply to the east. These joints are generally closed with less than 1 mm black chlorite and rare vein quartz infilling. They occur as persistent (greater than 10 m) regularly spaced smooth planes. Spacing varies between 0,5 to 2,0 m. The east-west trending joints are closed and contain a black, chlorite veneer. They are persistent, smooth and spaced 1,0 to 2,5 m apart.

The north-west trending set is sub-parallel to the mining direction. They are closed, smooth joints with a red-brown oxidised pyrite stain. They appear less persistent, probably because they are difficult to distinguish.

Extension gashes welded with vein quartz trend in a north to north-north-westerly direction and are near vertical. They extend for up to 1 m and are 1 to 3 cm thick.

Faulting
Faults strike north-east, sub-parallel to the dominant joint set. The faults are all normal with throws of less than 1 m and dip steeply to the south. The fault planes usually contain fault gouge, vein quartz and slickensides, the latter indicating lateral movement.

Bedding and parting planes
These planes are generally defined by a change in lithology, grain size or by sedimentary structures. The hangingwall, although a clean siliceous quartzite, contains argillaceous laminations, which define bedding planes.

Planar beds are common with planar and trough cross beds occurring locally. The former extends for up to 10 m along dip, whereas trough cross beds are about 2 m wide. The argillite along these beds are sometimes polished or striated, indicating lateral movement along the beds. Areas with planar beds tend to form a smoother hangingwall than areas containing trough cross beds.

A well-defined argillaceous bed locally defines the base of the Rice Pebble Marker (found below the Green Bar). The base also occurs as a welded plane with a thin argillite veneer. This variation may be due to sedimentological control, as well as selective bedding parallel movement along the plane.

Mining-induced fracturing
Mining-induced fractures have been grouped into extension and shear fractures and are illustrated in Figure 5.1.4.3.

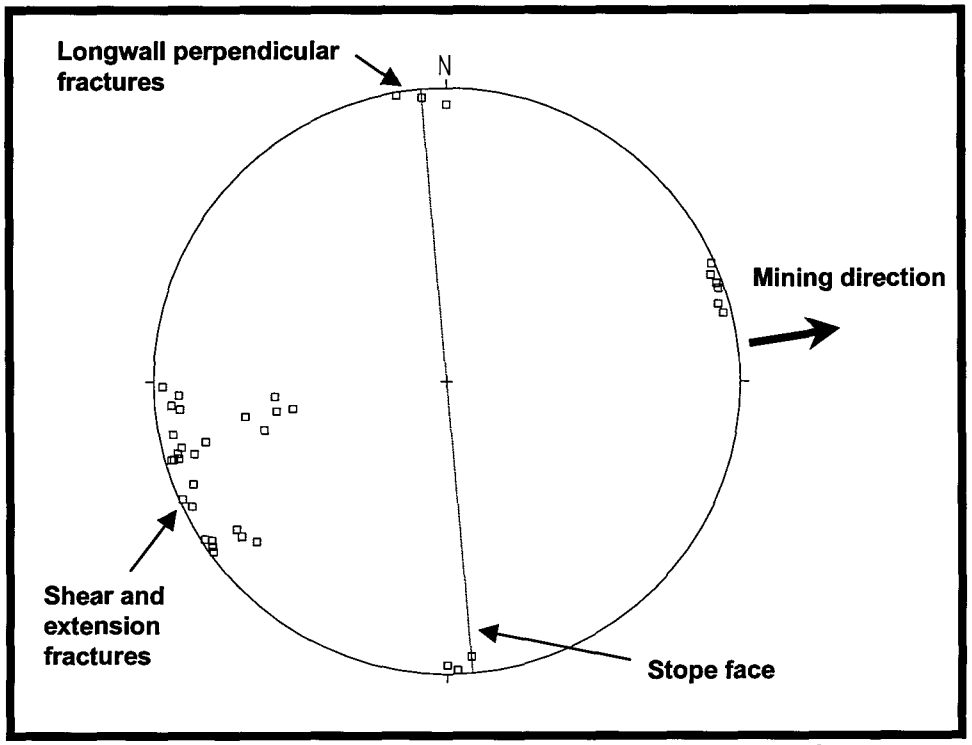

Figure 5.1.4.3 Lower hemisphere, equal area pole plot of mining-induced fractures.

Shear fractures occur as zones of intensely fractured rock up to 15 cm wide, along which some displacement has occurred. The zone defines an irregular profile on the hangingwall. Spacing of the shear fractures varies between 1,6 and 2,0 m. The zones are almost perpendicular to the hangingwall, with individual fractures dipping steeply towards or away from the face, and are

persistent along dip. The fracture surfaces contain white, powdery gouge or have a white, dusty appearance. Orientations range from face parallel to up to 20° away from the face. The face oblique fractures may be similar to the longwall parallel fractures described by Hagan (1980:31).

Extension fractures occur as discrete, persistent fractures. Dips are steep (70°-85°), but generally less than those of the shear fractures. Orientation is generally face parallel. Spacing increases near shear fractures and faults typically 2-10 cm apart. Between shear fractures spacing is 15-25 cm. Extension fractures do not pass through shear fractures. Coalescing of the fractures as they approach a fault, is often seen.

Shallow dipping extension fractures occur locally, especially where bedding is pronounced. Orientation is face parallel and dips vary from 45° to 60°. They are impersistent as trace lengths are generally less than 3 m. Termination against steep extension fractures, shear fractures and bedding is common. These fractures are clearly seen where falls of ground expose the hangingwall strata. Their local occurrence may be related to well-developed bedding.

Fractures perpendicular to the stope face occur at the bottom of panels, parallel to inter-panel sidings. They are steeply dipping in a downdip direction and are closely spaced, resulting in an intensely fractured hangingwall.

Shear fractures that develop oblique to the face sometimes propagate along joint traces. They may locally cross a joint and follow the joint trace for up to a metre.

5.1.4.3 Hangingwall profiles

Profiles of the hangingwall were measured at various localities to characterise hangingwall conditions and to quantify the quality of ground conditions. The results presented here are a comparison of profiles captured in backfilled areas and conventionally supported areas.

Profile lengths
Results for profile lengths and average gradient are illustrated in Figure 5.1.4.4.

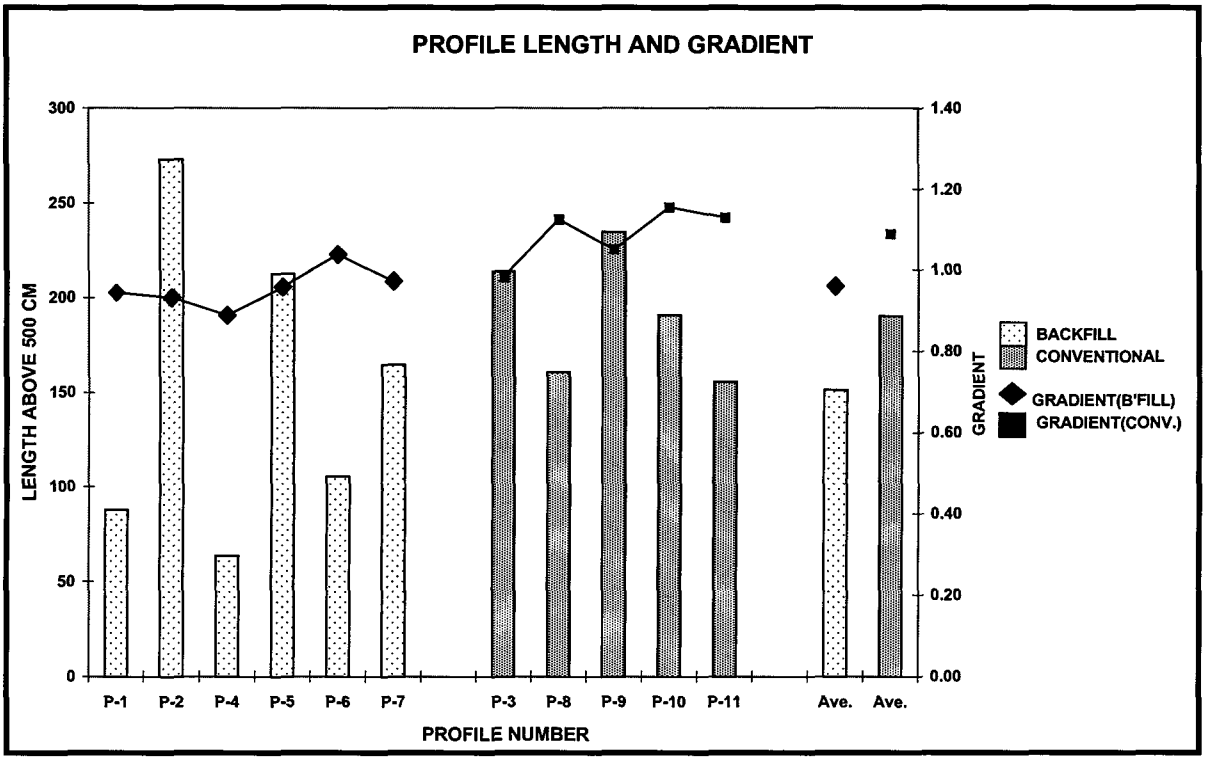

Figure 5.1.4.4 Profile lengths and average gradient.

The total length of each profile was measured and the straight-line length of 500 cm was subtracted from this value. The average extra profile length (over 500 cm) for backfilled areas was 151 cm with a variance of 58,9 cm at 95 per cent confidence, and for conventional areas 190,1 cm with a variance of 26,6 cm. Assuming the shorter the length of the profile, the smoother the hangingwall, it is seen that backfilled areas have a smoother hangingwall than conventionally supported areas.

P-2 has a very high profile length due to a large fall of ground at that location. The profile for P-2 is, however, less rough resulting in a relatively `lower gradient.

Average gradient
The greater the difference in heights between adjacent points on a profile, the less smooth that profile. A measurement of the change in gradient between points along a profile would give a good indication of the roughness of that profile. The average gradient for backfilled areas is 0,96 while conventionally supported areas have a steeper gradient of 1,09.

Average of absolute deviations from the mean
This function measures the amount of variation in a data set. Results are illustrated in Figure 5.1.4.5. Backfilled areas have a value of 9,30 while conventionally supported areas have a slightly higher deviation of 10,88.

Overall indications are that the roughness of the hangingwall in the conventionally supported areas is higher and, consequently, the quality of the hangingwall may be lower. Parting planes were not seen to influence the results to any extent. Profiles were measured in strike gullies where the influence of parting planes would not be obvious. The occurrence of parting planes is a local feature with lateral variation and, consequently, areas where profiles were measured may not have exhibited parting planes.

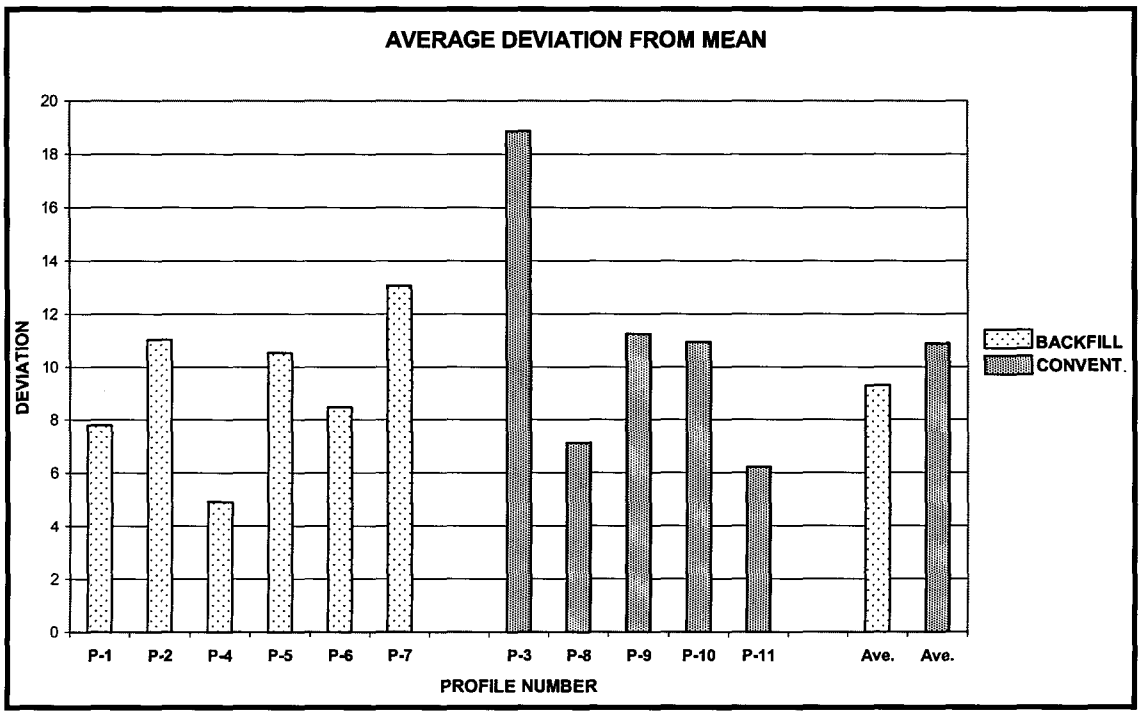

Figure 5.1.4.5 Average absolute deviation from the mean.

5.1.4.4 Closure-ride data

Comparison between closure data for different geotechnical areas
Results are compared for sites at Western Deep Levels, West Driefontein and Vaal Reefs. The site at Western Deep Levels has already been described in detail.

The site at West Driefontein (Carbon Leader) was situated at 6 shaft, 34-35 crosscut on 34 level. Panels three, four, five and six were monitored. The depth below surface was between 2329 m and 2387 m. The geotechnical area is defined by a soft quartzite hangingwall and hard quartzite footwall and a Green Bar to Carbon Leader distance of 2 - 3 m. Thickness of the Green Bar is 2,8 m. Support used is backfill and Madoda props. The average stoping width was 1,2 m.

The site at Vaal Reefs (Vaal Reef) was situated at 11 shaft (accessed via 8 shaft) on the 73-48 line. Panels 14, 15, 16, 17, and 18 were monitored. The depth below surface was between 2117 m and 2164 m. The geotechnical area is defined by a hard quartzite footwall and hangingwall. Support used is 1,8 m Rocprops alternating with packs. The average stoping width was 2 m.

The results are tabulated below:

Table 5.1.4.1 Results of closure monitoring at different sites.

LOCALITY	REEF	MAXIMUM DEPTH (m) (below surface)	AVERAGE CLOSURE (mm/day)	AVERAGE CLOSURE (mm/m)	AVERAGE FACE ADVANCE (m/month)
W.D.L. EAST	Carbon Leader	2599	5.60	16.8	10.0
WEST DRIE.	Carbon Leader	2387	3.49	13.4	7.6
VAAL REEFS	Vaal Reef	2164	4.33	27.9	4.9

The comparatively low figures for West Driefontein can be attributed to the use of backfill. The high closure per metre face advance at Vaal Reefs may be attributed to inelastic dilation along well-defined bedding planes in the hangingwall and the slow rate of face advance.

Closure results for Western Deep Levels East
Results for the monitoring site at Western Deep Levels are discussed in more detail. Results are tabulated in Table 5.1.4.2. 'Panel standing' indicates that the panel stood for longer than seven days. 'Seismic event' indicates stations that were affected by a seismic event that resulted in a significantly higher closure on a particular day.

The average closure per day is 5,60 mm/day. Closure rates per day vary from 1,75 mm/day to 19,56 mm/day. This high range is due to panels standing for long periods, seismic events and the presence of loose hangingwall blocks at some stations. The average closure per metre face advance is 16,8 mm/m. Closure rates per metre face advance vary from 0 to 46 mm/m. The large range may also be due to the effect of the factors mentioned above, as well as inelastic dilation.

Panels standing for longer than seven days were subject to closure rates of between 1,88 and 7,00 mm/day. An average closure rate of 2,00 mm/day can be expected for standing panels. Station 111, where 7,00 mm/day was measured, was located within 2 m of a fault striking north-east and dipping 80° south-east. The fault may have affected the hangingwall resulting in dilation along bedding planes and sliding along the fault plane. Closure rates for standing panels are partly due to dilation along well-defined bedding planes in the hangingwall and blasting in adjacent panels. Closure during non-blasting periods may account for up to 46 per cent of the total closure experienced at a station.

Closure rates are linear and higher for station distances up to 13 m behind the stope face. Thereafter the closure rate is lower. Ebenhaeser support units used in this area should be able

to accommodate these closure rates up to a distance of 13 m behind the face. Closures of 25 mm/day were measured after a seismic event.

Table 5.1.4.2 Closure results for Western Deep Levels East site.

STATION	CLOSURE (mm/day)	CLOSURE mm/m	DISTANCE FROM FACE	FACE ADV. (m/month)	DIST. ADV. (m)	COMMENTS
412	4.11	17.36	6.00	7.10	23.90	Panel standing
422	5.83	0.00	7.10	0.00	0.00	Panel standing, seismic event
432	7.00	18.37	2.80	11.43	20.20	Seismic event
442	19.56	46.03	3.40	12.75	6.80	Hangingwall block loose
452	8.77	33.86	3.50	7.77	5.70	Panel standing, seismic event
472	9.47	20.00	2.80	14.21	16.10	Seismic event
411	2.62	12.13	4.30	6.48	21.60	Panel standing
421	5.69	43.58	4.20	3.80	8.10	Panel standing
431	3.76	11.67	9.80	9.66	13.20	
451	4.73	10.35	3.50	13.70	20.10	
461	5.66	11.52	3.00	14.05	17.80	
471	6.17	9.66	2.60	19.17	14.70	
491	3.72	9.88	3.10	10.69	25.30	
111	4.03	26.12	2.4	4.63	16.5	Panel standing
121	3.29	15.19	3.2	6.51	20.6	Panel standing
131	3.86	12.16	3.7	9.51	22.2	
141	2.93	7.70	4.2	11.40	15.2	Panel standing
161	6.74	11.52	2.8	17.56	15.8	
112	3.29	22.14	2.8	4.46	15.9	Panel standing
122	3.21	16.1	2.2	6.0	19.6	Panel standing
132	1.75	9.7	3	5.4	19.7	Panel standing
142	2.76	7.3	5.6	12.3	9.4	
152	6.75	13.7	2.2	15.2	17.7	Seismic event
4101(N)	4.44	11.1	8.4	12.0	10.8	
4111	7.51	21.1	2.2	10.7	16.7	Seismic event
4112	4.55	11.8	2.8	11.6	18.1	
4121	4.77	18.6	3.1	7.7	14.6	
4101	6.36	14.9	2.8	12.8	4.7	
4122	9.59	25.1	2.4	11.5	8.4	Seismic event
4131	4.32	12.6	3.8	10.3	12.7	
4132	6.59	17.9	2.4	11.0	8.1	
AVERAGE	5.61	16.7		10.0		

5.1.4.5 Quasi-static data

The closure meters and the extensometers were either damaged or became loose during the measuring period and as a result no useable data was obtained.

Crack gauge
The crack gauge was installed across a north-easterly trending fault to measure relative convergence or divergence across the discontinuity. Increases in readings indicate opening or divergence and a decrease in readings indicates closing or convergence.

Figure 5.1.4.6 illustrates the behaviour of the discontinuity over the monitoring period. The discontinuity opens to slightly over 1 mm and then closes up by 7 mm. Dotted lines indicate that no data is available.

Figure 5.1.4.7 illustrates behaviour of the discontinuity during blasting and a seismic event. The discontinuity generally closes during blasting but opens during a seismic event. For smaller seismic events, a reversal in the behaviour occurs. When opening, the discontinuity will close and vice versa during seismic events.

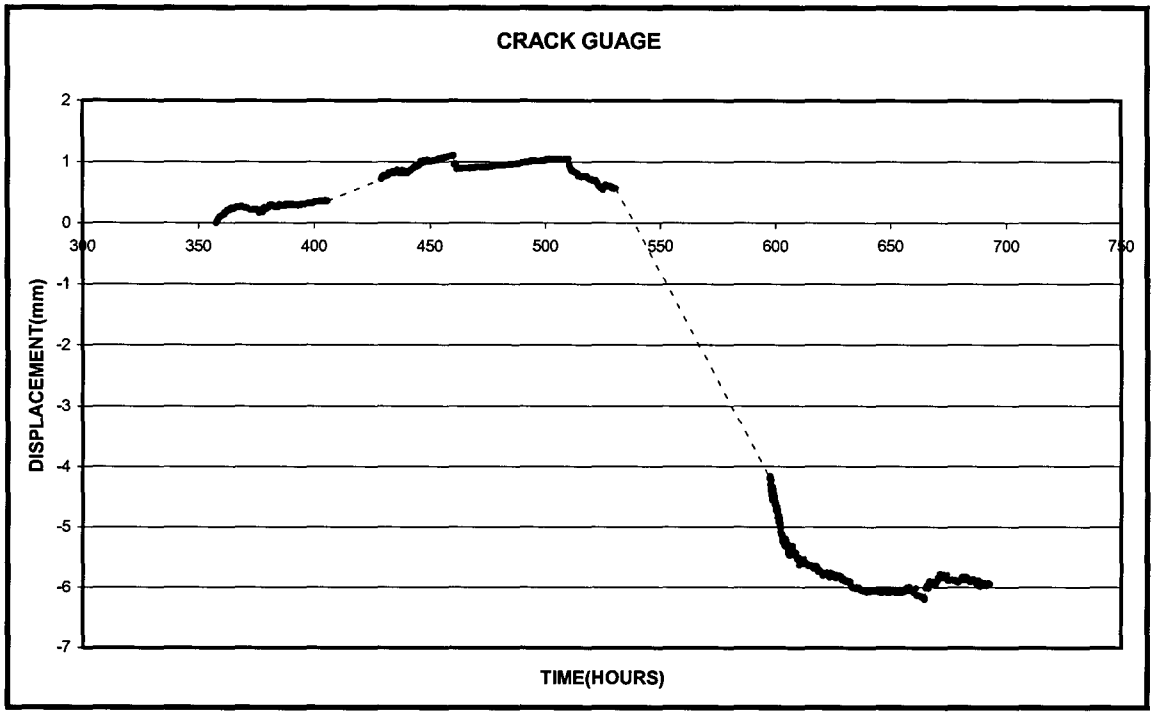

Figure 5.1.4.6 Results for the crack gauge.

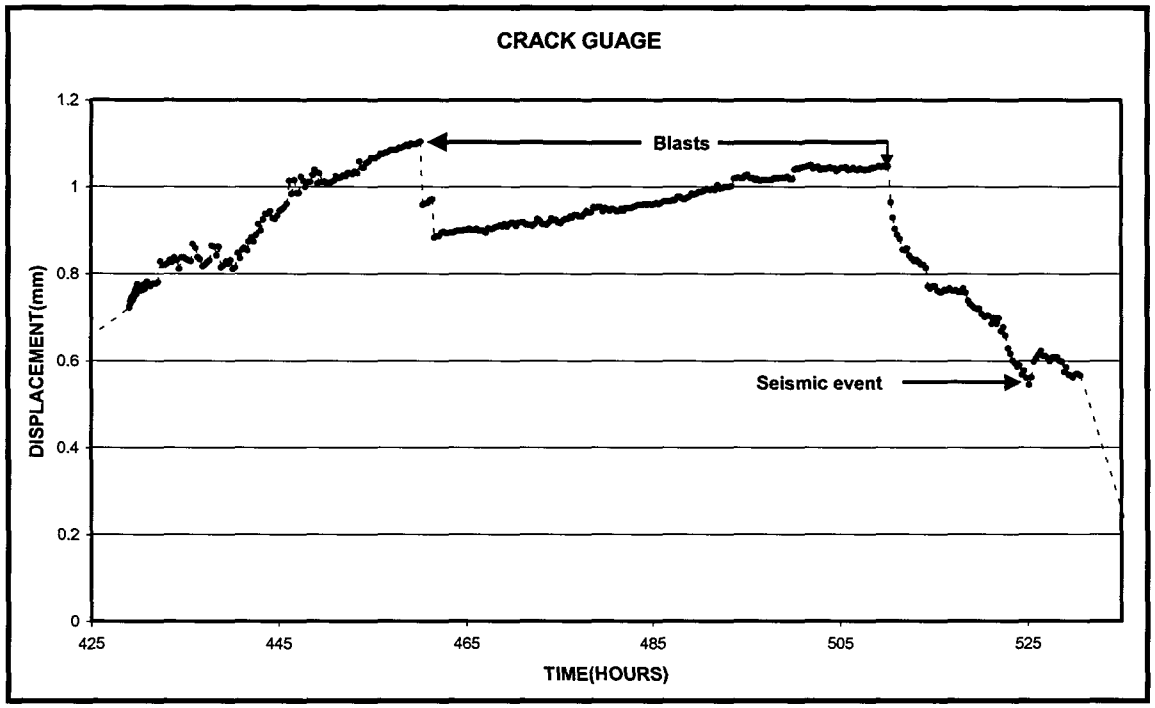

Figure 5.1.4.7 Dynamic behaviour of crack gauge.

Tiltmeter

Tiltmeters attached to the hangingwall and footwall were used to measure tilt in two directions, along strike and dip. The X sensor measures tilt along dip and the Y sensor along strike, where an increase in dip above horizontal is positive and a decrease below horizontal is negative. The

tiltmeter represents behaviour of the block to which it is attached and not necessarily for the rock mass as a whole due to fracturing and other discontinuities. The initial readings commenced when the face was 17 m away and stopped when the face was 33 m away.

Figure 5.1.4.8 illustrates tilt of the footwall for the monitoring period. Along strike, the footwall initially tilts down towards the back area followed by tilting up towards the face. Along dip, the footwall tilts downward in the downdip direction and at around 824 hours it begins to tilt upwards. Tilt along strike is greater than along dip.

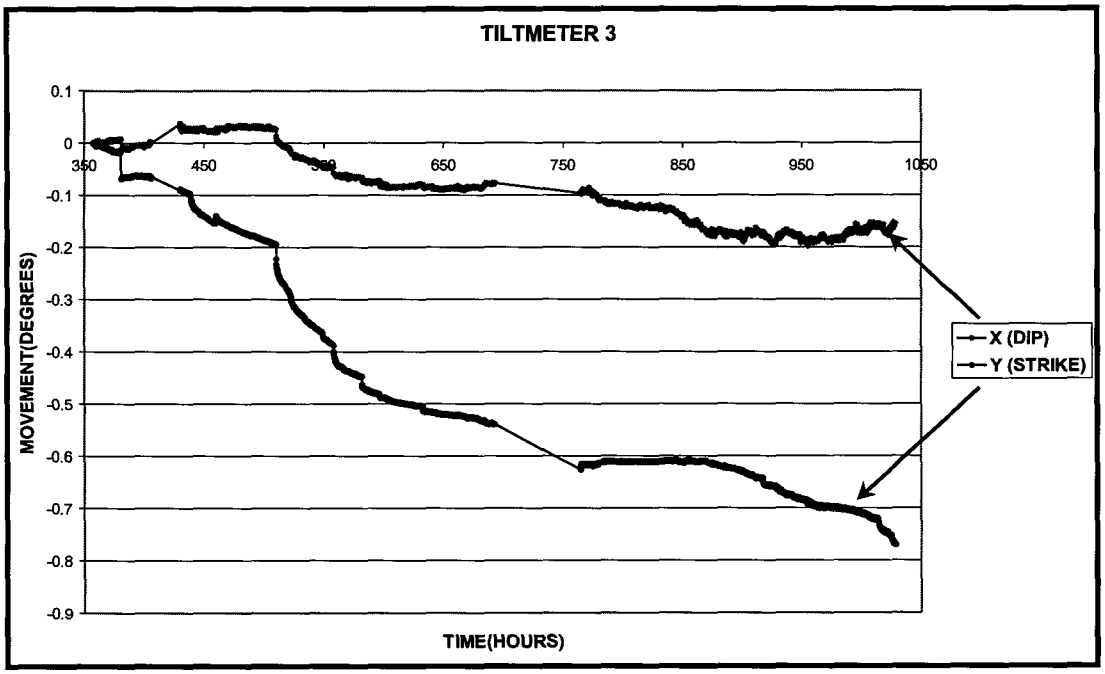

Figure 5.1.4.8 Tiltmeter results for the footwall.

Figure 5.1.4.9 illustrates the tilt of the hangingwall during the monitoring period. The hangingwall tilts downward in a downdip direction until 818 hours, where it begins to tilt upwards. Tilt along strike is initially downward towards the face until 467 hours, where it begins to tilt upwards. Amount of tilt along dip is initially higher and decreases with time, whereas along strike the amount of tilt increases with time.

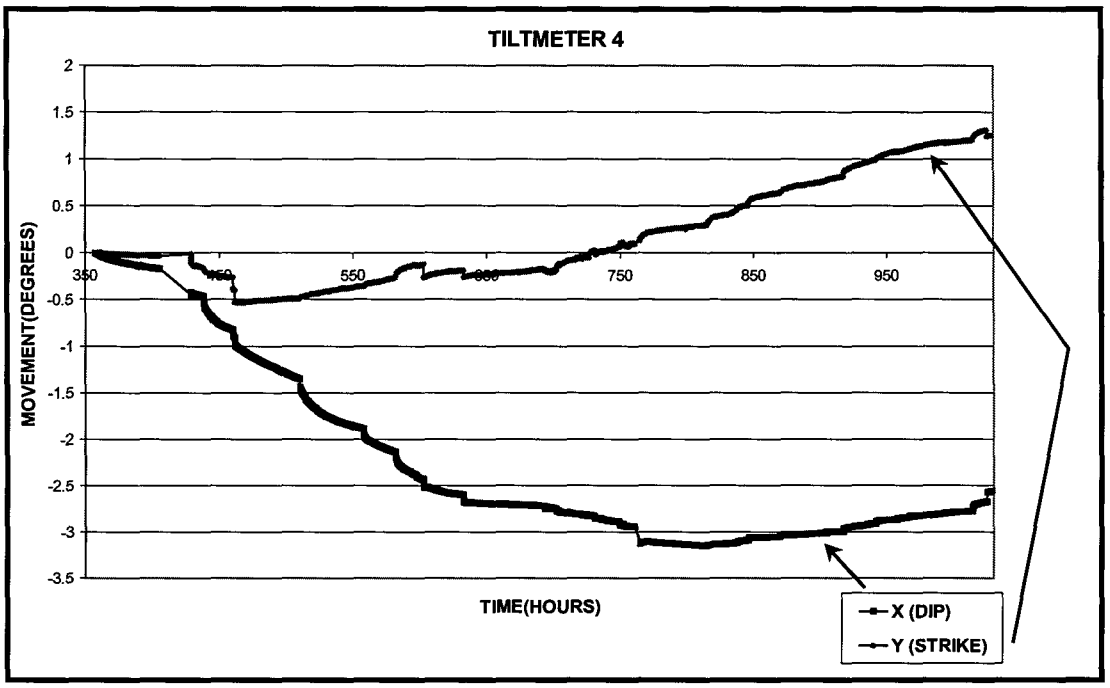

Figure 5.1.4.9 Tiltmeter results for the hangingwall.

The dynamic behaviour of the hangingwall tiltmeter is illustrated in Figure 5.1.4.10. During this period, the face advanced from 20 m to 26 m. Tilt along dip increases after a blast, whereas a much smaller corresponding increase occurs along strike. A seismic event appears to have no effect on the tilt along dip and a very minor influence on the tilt along strike.

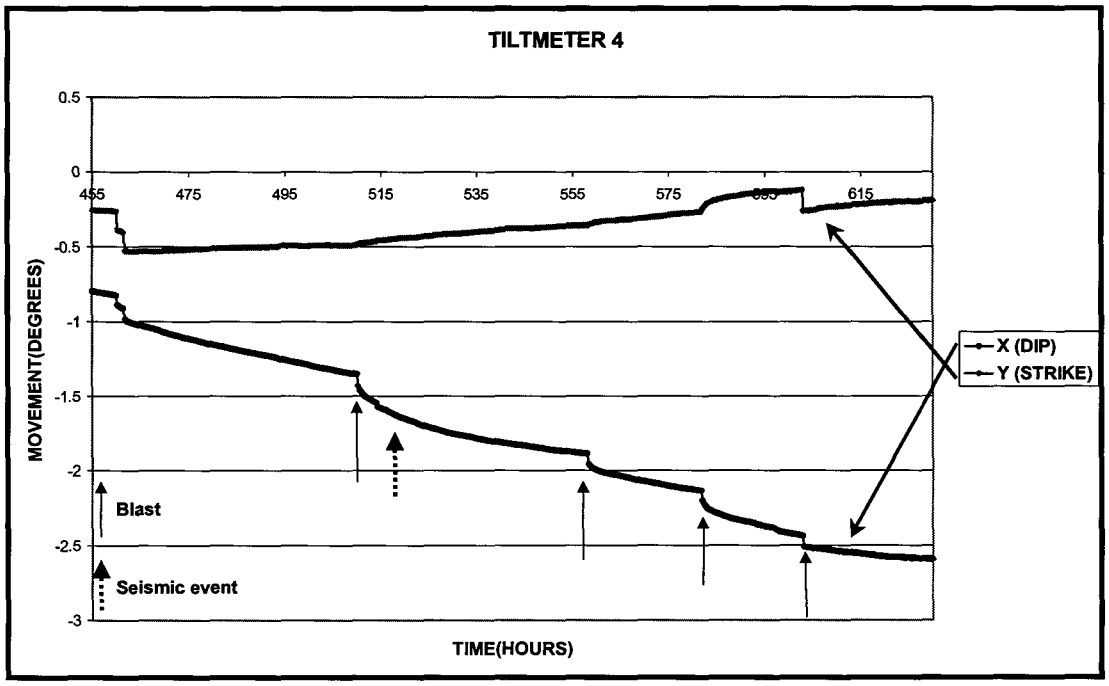

Figure 5.1.4.10 Dynamic behaviour of hangingwall tiltmeter.

5.1.4.6 Falls of ground

Post falls of ground inspections were conducted whenever accessible falls of ground were found. Dimensions of the blocks and their bounding surfaces were measured in order to determine characteristic discontinuities leading to falls of ground and critical block sizes.

Argillaceous bedding planes define the upper bounding surfaces of blocks. These planes are often polished and smooth due to bedding parallel movement. The upper bounding surface was seen to transgress bedding planes where the bedding density was higher (beds were 10 to 15 cm apart). Falls to the Green Bar occurred in strike gullies and on the downthrow side of faults. The base of the Green Bar defines the upper bounding surface here. This is a well defined plane, polished and slickensided with vein quartz and fault gouge infilling. Portions of the Green Bar may also fall locally, especially where the lithology is highly laminated.

Steeply dipping mining-induced fractures define the blocks along dip. Joints and new tensile fractures define the blocks along strike. Fault-bound blocks extend along the fault for up to 5 m. Falls in strike gullies also propagate along the gully.

The average size of blocks (where Green Bar is not exposed) is 100 x 100 x 80 cm. The maximum height of blocks, where the Green Bar is exposed, is 1,5 m. Falls generally occur between support units in the stope and between packs in the strike gullies.

Extension gashes do not appear to influence falls of ground, probably due to their welding by vein quartz.

5.1.4.7 Seismic investigation

Between mid-December 1997 and the beginning of July 1998, over 3 500 seismic events were recorded by the Portable Seismic System (PSS) uphole array. During this period, the closest stope faces (93E4) advanced from 60 m to 140 m away from the recording site, while the faces at the bottom of the stope (94E1) advanced from a distance of 250 m to 300 m. In late June 1998, a large seismic event close to the site damaged the hangingwall around the geophones, even exposing the bottom triaxial geophone assemblage. Shortly thereafter, the data PC failed and data collection was terminated. Most of the data set comprised recordings of face blasts and associated seismicity, but mining-induced seismicity from further afield was also recorded. Blast events were recorded from faces to the west of the site (90 Level and above – see Figure 5.1.1.1), as well as from faces to the east and south east (93 and 94 Levels). Mining-induced seismicity was also recorded from the Boulder South fault to the north (Figure 5.1.1.1).

The Ground Motion Monitor (GMM) does not record data continuously, but in batches for a few weeks at a time (determined by the battery life and robustness of the components). Some 521 common events were identified as having been recorded by both the PSS and the GMM, and the data files were combined for joint assessment. All detailed analysis was conducted using the combined data.

Data groups

The situation of the sensors in the project array meant that source locations could not be determined with any confidence: the seismic energy travelled along raypaths which were significantly refracted by the highly fractured rock mass in the vicinity of the mining excavations. Seismic data recorded by the mine's seismic network were provided by the mine and were used for determining the locations of some of the larger events recorded by the project arrays.

Some repeatable characteristics which had been observed in the PSS waveforms – notably, the apparent azimuth angles between source and receiver derived from the known polarisation characteristics of the P-wave first arrivals – were used to group the data into various clusters. The mine's data were then used to associate the clusters with specific source regions (e.g. the 93 Level stope faces to the north east of the recording site, which were steadily advancing away from the site during the period of recording).

It was found that data recorded from seismic events on *90 Level* (to the *west* of the site – 'A' in Figure 5.1.1.1) tended to have a dominant P-wave amplitude on the east-west horizontal component. Travel times for these seismic waves tended to be shorter than expected from the

assumed rock mass velocities. The waves recorded on the geophones closer to the hangingwall surface arrived with a noticeable delay, compared with those further into the hangingwall.

Data recorded from seismic events on *93 Level* (to the *north east* of the site – associated with stope faces closest to the site: 'B' in Figure 5.1.1.1) tended to have similar P-wave amplitudes on both the north-south and east-west horizontal components. Travel times tended to be more or less consistent with those expected from the typical seismic velocities for the rock mass. There was generally negligible delay in arrival of the waves at the geophones at various depths into the hangingwall.

Data recorded from seismic events on *94 Level* (to the *east* of the site, at similar distances as those for the 90 Level events – 'C' in Figure 5.1.1.1) tended to have a dominant P-wave amplitude on the north-south horizontal component. Travel times for these waves tended to be noticeably longer than expected. There was typically no measurable delay in arrival of the waves at the geophones at various depths into the hangingwall.

Comparison of the velocity spectra recorded for similar events (similar magnitude events at similar distances) revealed that the seismic waves from the east ('C' in Figure 5.1.1.1) suffered much higher attenuation at all frequencies than those from the west ('A' in Figure 5.1.1.1). This observation – coupled with that of the lower apparent velocities for raypaths from the east – indicates that the waves from the east were traversing more highly fractured rock (the hangingwall of the excavation) compared with those from the west (for which at least some of the travel was through more competent rock ahead of the advancing faces). The high-frequency fall-off in amplitude (above the corner frequency) was steeper for the waves from the west: at the highest frequencies, the amplitudes were similar, but the waves retained higher frequencies at the recording site than those from the east.

It was found that the most well-developed clusters were associated with the 93 Level stope faces to the north east of the site. These data were divided into groups on the basis of events occurring during sufficiently short time intervals (a few weeks) that the source can be assumed constant for each cluster. The data were then examined to determine whether any significant changes had occurred in the state of the rock mass in the vicinity of the site during the recording period.

Waveform study

Unfortunately, it seems that the grouting around the top triaxial geophones ('A' in Figure 5.1.3.2a) did not take hold, as the signals recorded from these geophones were dominated by a mono-frequency 'ringing' characteristic, so that these geophones had to be excluded from any analysis. Figure 5.1.4.11 shows the waveforms recorded via the other four triaxial geophones from an M0,1 event at about 100 m distance. Changes in the appearance of the waveforms from top to bottom through the array are evident.

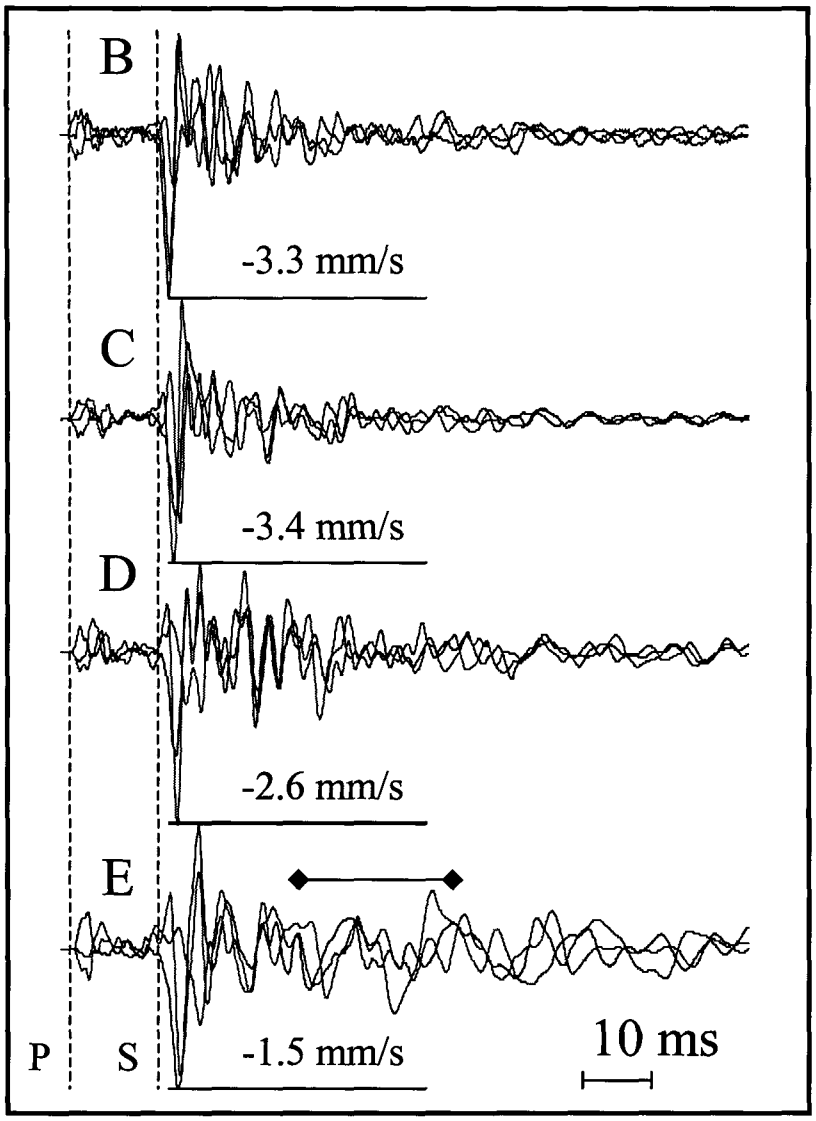

Figure 5.1.4.11 Waveforms recorded by the triaxial uphole array from an M0,1 seismic event which occurred on 16 January 1998 (00:04:36) at about 100 m distance. 'B' through 'E' refer to the geophones positioned as indicated in Figure 5.1.3.2a

From Figure 5.1.4.11, it can be seen that there is a general increase in the complexity of the signals from top to bottom. This is accompanied by an increase in duration of the coda waves (the waves recorded after the P- and S-phase body wave packages, consisting of a mix of surface waves and scattered body waves). These effects are indicative of energy trapping within the fracture zone close to the excavation. One other interesting feature is indicated in the figure by the horizontal line above the waveforms for 'E'. The low frequency, high amplitude pulse was commonly observed in the data from the bottom-most geophones in the hole, for events from various azimuths and at various distances. Clearly, this is some fundamental mode of response of the hangingwall closest to the excavation; it is not well understood, at this stage, but could be related to the passage of surface waves through the very low velocity zone created by the fractured rock.

The frequency-domain spectra averaged for five events recorded from similar distances and azimuths (to the west of the site) within a few days of one another are shown in Figure 5.1.4.12. The spectra shown in Figure 5.1.4.12a are for the uphole vertical geophones from 'B' through 'E' (Figure 5.1.3.2a), while those in Figure 5.1.4.12b are for the GMM vertical geophones attached to the hangingwall of the excavation.

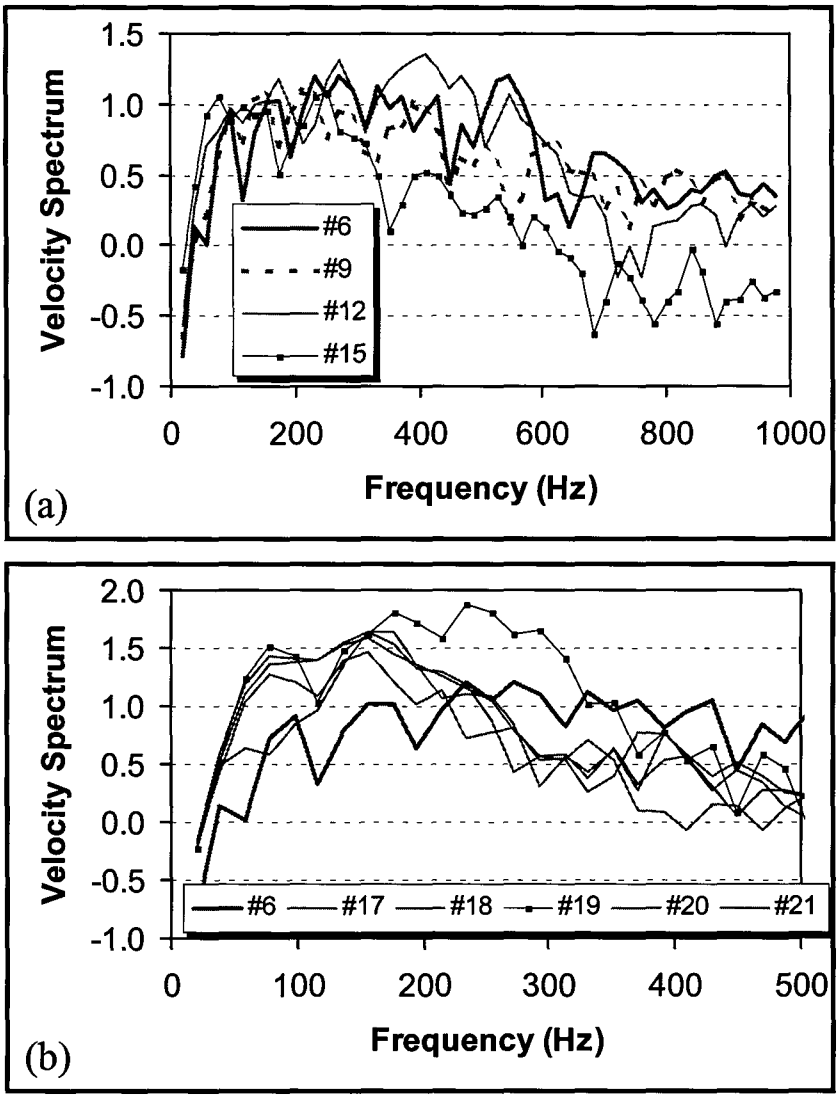

Figure 5.1.4.12 Log(Velocity) spectrum data averaged over five similar events (a) for vertical geophones in the uphole array (geophone '#6' is at the top, while '#15' is at the bottom of the hole) (b) for vertical geophones attached to the hangingwall (geophone '#17' is 'HW2' in Figure 5.1.3.2b, '#18' is 'HW3', etc); '#17', '#18', '#20', and '#21' exhibit very similar behaviour to one another

At low frequencies (< 100 Hz), there is an amplification of the signals from top to bottom evident in Figure 5.1.4.12a. Above 300 Hz, the signal for the bottom-most geophone loses amplitude markedly, indicative of significant high-frequency attenuation by the fractured rock mass close to the excavation. The signal for '#12' (positioned on the top Green Bar contact) exhibits noticeable resonance (increased amplitude) between 300 and 500 Hz. At higher frequencies, the amplitude of the '#12' signal is below those of the geophones above it, consistent with its position in rock that is more fractured than that higher up, but not as fractured as that beneath it. The signals for '#6' and '#9' are generally similar to each other, as these geophones are in less fractured ground (though still not in solid rock) and not close to major interfaces.

At low frequencies (< 250 Hz), there is an amplification of the signals recorded from sensors on the hangingwall compared with those deeper into the rock mass ('#6') evident in Figure 5.1.4.12b. While the spectra for the other GMM waveforms are similar to one another in amplitude and shape, that for '#19' ('HW4' in Figure 5.1.3.2b) displays a clear additional resonance (amplification between 150 and 350 Hz). The amplitudes for '#6' fall off more slowly (less high-frequency attenuation in less fractured ground) than those for the GMM waveforms, so that '#6' has greater amplitude at higher frequencies.

An attempt was made to detect time-dependent behaviour in the rock mass response from changes in the waveform characteristics as the stope faces advanced away from the recording site. To this end, clusters of recorded blast events from a single set of stope faces (on 93 Level, to the north east of the site) were identified in the data set and sub-divided into three distinct time periods: 1 – events recorded during March and April 1998, 2 – events recorded during May 1998, and 3 – events recorded during June 1998. The frequency-domain velocity spectra were then examined to find differences between signals from different geophones and differences for any given geophone with time. The averaged spectra are shown in Figure 5.1.4.13 and are discussed below. The reduced frequency band for the GMM spectra ('#17' and above) is consistent with the lower sampling rate for these data.

The spectra for **'#6'** (near the top of the hole) continue to increase in amplitude above the corner frequency, indicating that the waveforms had suffered less high-frequency attenuation while travelling from these closer, higher-frequency sources (compare with Figure 5.1.4.12a). The spectra have very similar shapes for the three time periods, with somewhat more high-frequency attenuation (> 500 Hz) at later times, suggesting some degradation in rock mass condition with time, or an increased attenuation of higher frequencies as the distance to the stope faces increased.

The spectra for **'#9'** (below '#6' in the hole) are flat above the corner frequency, indicating a greater degree of high-frequency attenuation associated with somewhat more fractured ground than was the case for '#6'. The spectra have very similar shapes for the three time periods, with more high-frequency attenuation at later times. The spectra for **'#12'** (below '#9' in the hole, close to the top Green Bar contact) have higher amplitudes across a broad range of frequencies than those for '#9', even though '#12' was positioned in more fractured ground. Evidently, the presence of the Green Bar interface has an amplifying effect on the seismic waves travelling from the stope faces. The spectra have very similar shapes for the three time periods, with no significant time-dependent effect being apparent.

The spectra for **'#15'** (below '#12' in the hole, close to the bottom Green Bar contact and about 0,5 m into the hangingwall) exhibit significant attenuation compared with those for '#12' and fall off above the corner frequency. The highly fractured rock close to the excavation evidently absorbed the high-frequency energy more than was the case for the rock higher up. The spectra have very similar shapes for the three time periods, with more high-frequency attenuation at later times. The spectra for **'#17'** and **'#18'** (on the hangingwall: 'HW2' and 'HW3' in Figure 5.1.3.2b, respectively) have similar characteristics to those from '#15', in close proximity and just 0,5 m above them.

The spectra for **'#19'** ('HW4' in Figure 5.1.3.2b) are very different from those for '#17' and '#18' (even though '#19' was positioned less than a metre from '#18'), exhibiting significant amplification between 150 and 350 Hz. This resonance is clearly a local site effect affecting just the immediate vicinity of this geophone.

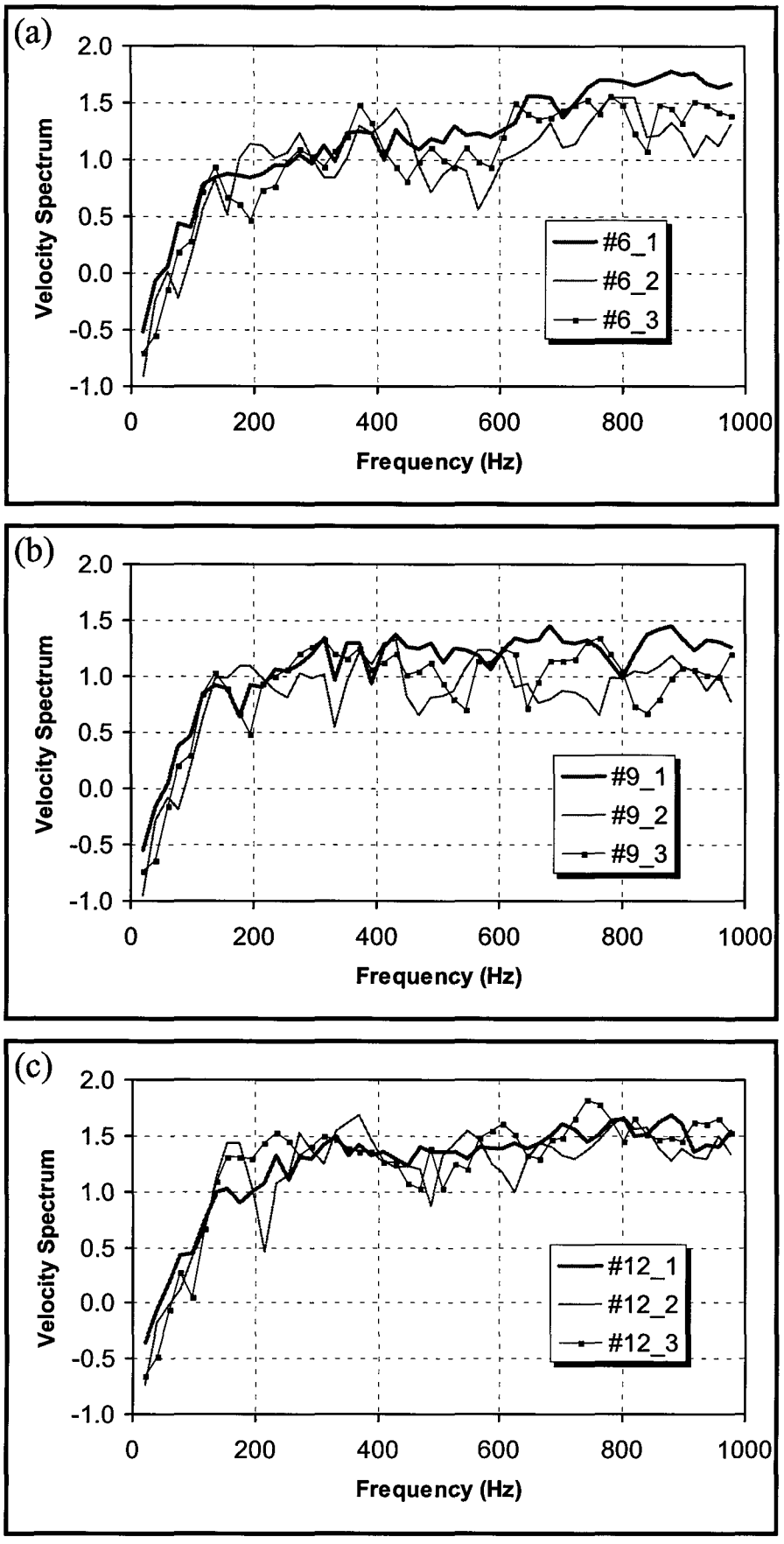

Figure 5.1.4.13 Log(Velocity) spectra recorded at vertical geophones from blast sources at a single group of stope faces (nomenclature: #G_T – averaged spectra for events recorded at geophone G during time period T, as explained in the text)

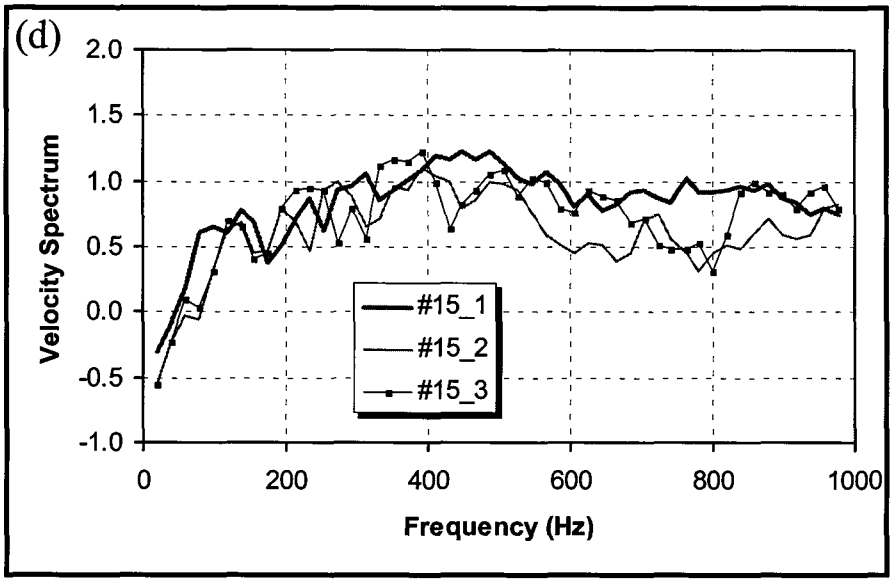

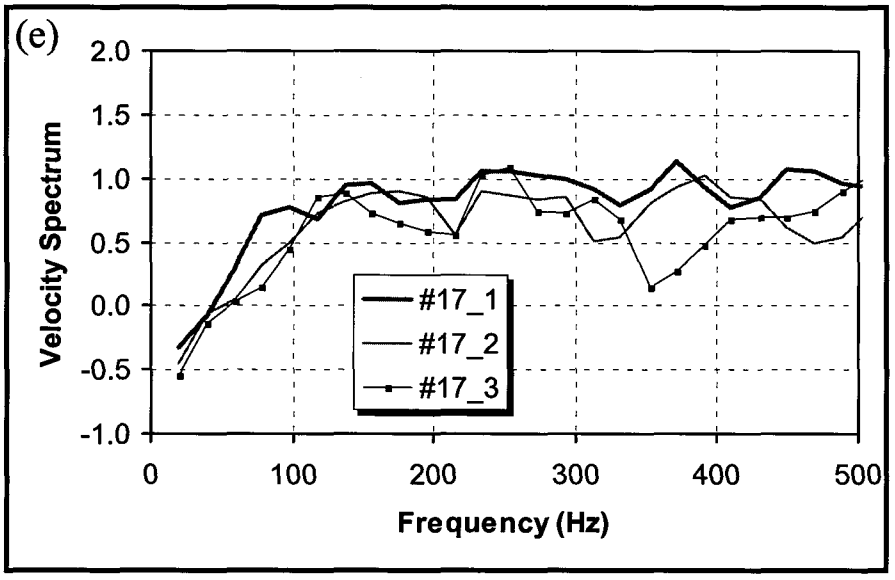

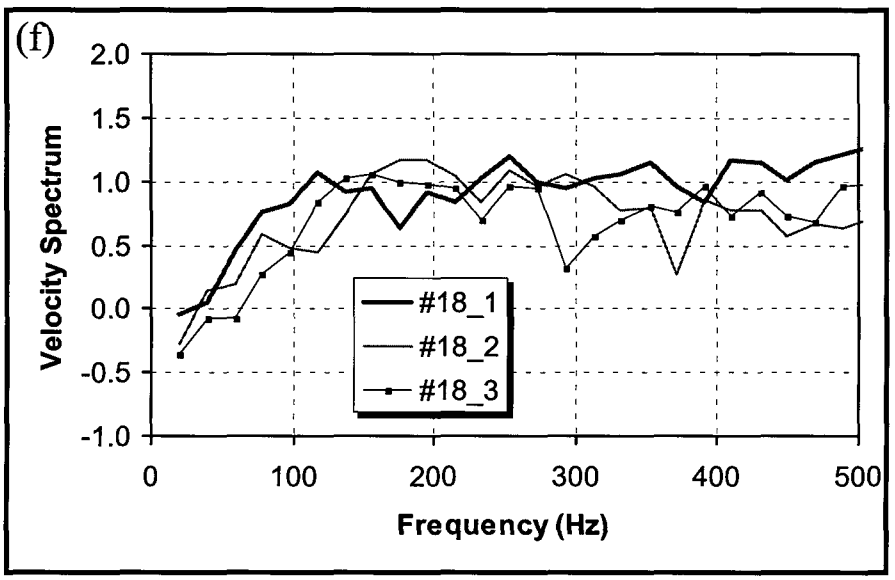

Figure 5.1.4.13 (continued 1) Log(Velocity) spectra recorded at vertical geophones from blast sources at a single group of stope faces

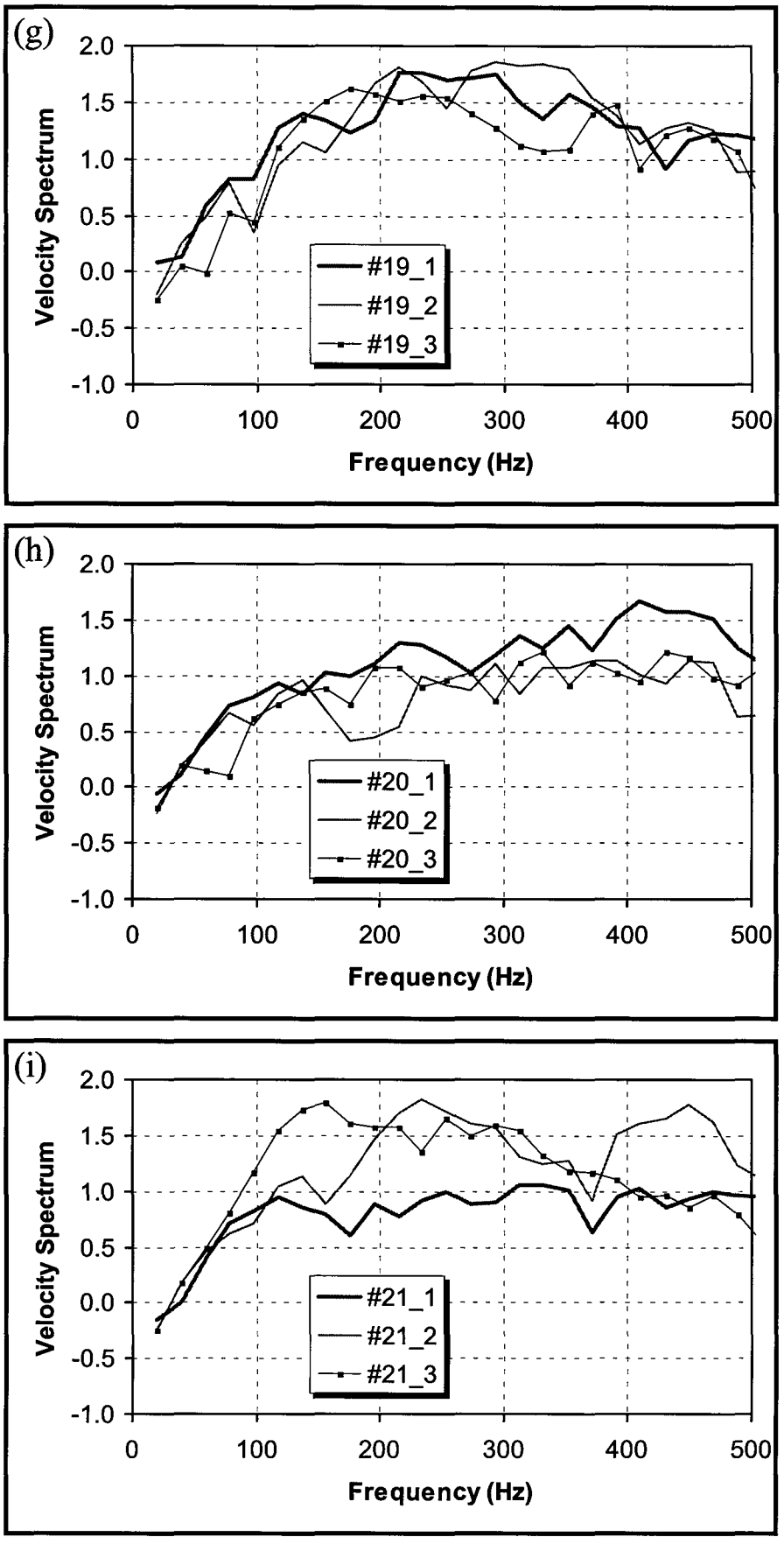

Figure 5.1.4.13 (continued 2) Log(Velocity) spectra recorded at vertical geophones from blast sources at a single group of stope faces

The spectra for **'#20'** and **'#21'** ('HW5' and 'HW6' in Figure 5.1.3.2b, respectively) can be misleading: these geophones were in the 'configuration 1' positions during the first time period,

but in the 'configuration 2' positions during the second and third time periods. The rock mass response at the second position for '#21' clearly had significant site effect. The differences in appearance of the spectra between the second and third time periods may be indicative of a local change in the rock mass condition in the vicinity of that geophone with time.

Velocity study

S. Spottiswoode developed a model on the basis of which the passage of plane waves through the three-dimensional array could be analysed in terms of local velocities and propagation directions. For any pair of geophones, the velocity of propagation V of an arbitrarily oriented plane wave past both geophones (in the plane of the geophones) can be determined from the apparent velocities V_x and V_y, in the X and Y directions, respectively (see Figure 5.1.4.14a). The component velocities V_x and V_y can be determined from the travel-time between the geophones (e.g. T_x in Figure 5.1.4.14b) and the difference in their X and/or Y position co-ordinates.

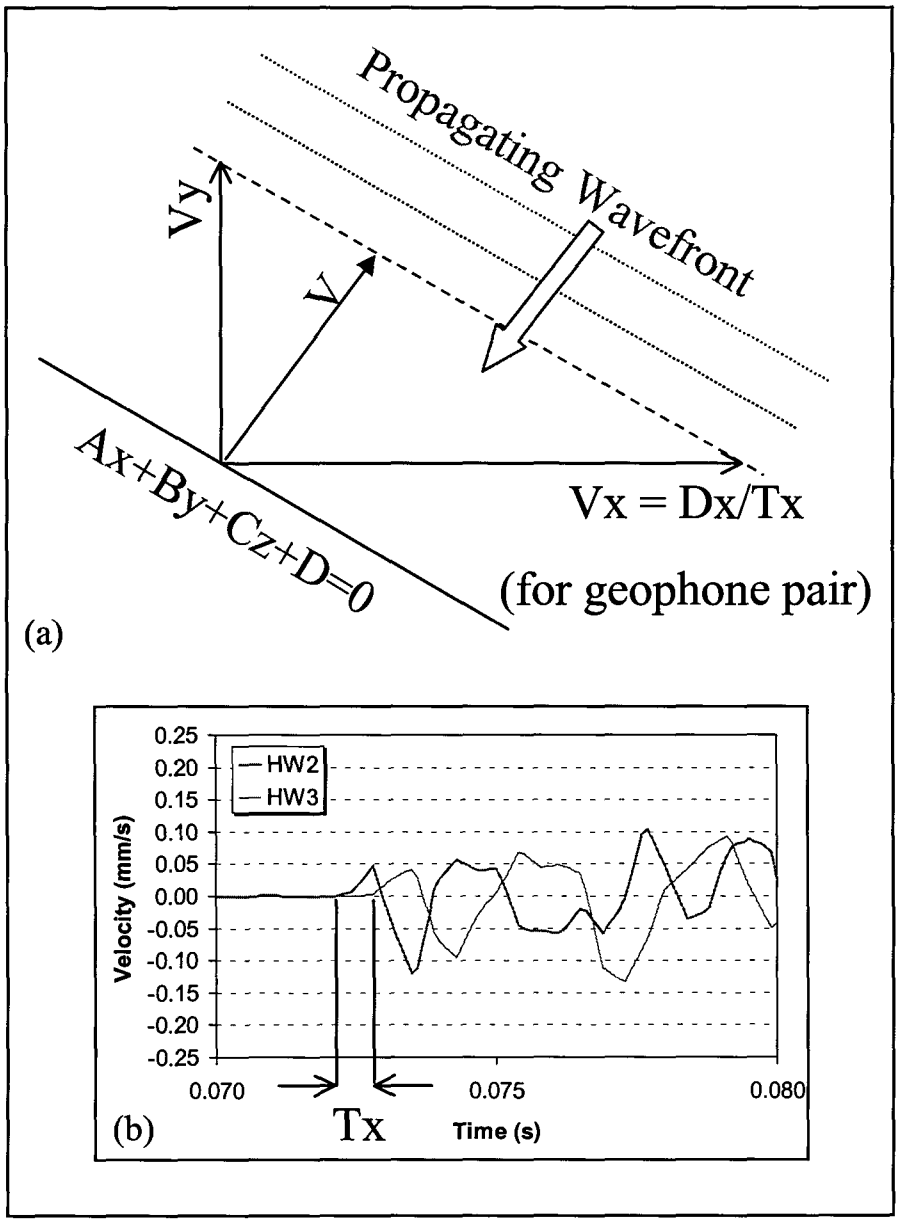

Figure 5.1.4.14 (a) Determination of velocity for a plane wave passing by a pair of spatially separated geophones
(b) Example of difference in recorded arrival-times at a pair of spatially separated geophones

The analysis can be extended to three dimensions by including another geophone (not in the plane of the first two geophones) in the calculations. Velocities of coda wave phases can be

determined by cross-correlating windows of waveform data at later times in the recorded signal to determine time lags between traces. The results of the analysis are summarised in Tables 5.1.4.3 and 5.1.4.4, below.

Table 5.1.4.3 Velocities of plane wave propagation determined for vertical geophones in uphole array

Channel	Median velocity (m/s)	Deviation (m/s)	Direction [1]
6	599	87	0,14
9	540	164	0,66
12	679	88	0,52
15	542	24	0,87

[1] Direction of 0 is for horizontal propagation, 1 is for vertical propagation

The velocities derived from the analysis (Table 5.1.4.3) are significantly lower than seismic wave velocities measured in solid rock. The lack of a vertical gradient in velocity results from the consideration of a number of geophones on the hangingwall (the velocity quoted for each channel in Table 5.1.4.3 was derived from the application of the analysis to that geophone in combination with all geophones below it). The median directions suggest a predominantly vertical propagation for waves in the fractured rock, indicating energy trapping in the fracture zone. The more horizontal direction for the top geophone (6) might correspond with the passage of seismic waves past the recording site in the less fractured ground higher up, before the energy is refracted into the lower velocity regions lower down.

Table 5.1.4.4 Velocities of plane wave propagation determined for various windows in waveform data

Window position	Median velocity (m/s)	Deviation	Direction [1]
P	648	103	0,68
P + 3,2 ms	571	87	0,73
P + 6,4 ms	542	67	0,67
P + 9,6 ms	513	73	0,67

[1] Direction of 0 is for horizontal propagation, 1 is for vertical propagation

Table 5.1.4.4 compares the velocities determined for windows positioned at 3,2 ms intervals along the waveform. At later times, the median velocity is lower, consistent with the arrival of lower velocity shear and surface waves after the initial compressional waves from the source.

In addition to the analysis reported above, the local seismic wave velocities were also measured more directly, by stimulating the bottom of the hole and recording the arrivals at the vertical geophones in the hole. The results are given in Table 5.1.4.5.

Table 5.1.4.5 Results of direct interval velocity measurements for uphole array

Channel [1]	2 m Interval velocity (m/s)	4 m Interval velocity (m/s)	6 m Interval velocity (m/s)
6	–	–	–
9	1 125	–	–
12	596	778	–
15	403	478	584

[1] Velocities are expressed in terms of the spatial interval above the channel indicated

A vertical gradient of upwardly increasing velocity is evident from Table 5.1.4.5. The velocity measured between the bottom and top of the hole (6 m interval) is in good agreement with velocities derived from the plane-wave analysis.

The low velocities determined for the local rock mass in the vicinity of the recording site can be reconciled via the relationship of Young's modulus to joint stiffness and joint spacing. A velocity of 600 m/s is 1/6 of the shear wave velocity in solid rock, which corresponds to a 36-fold

reduction in modulus (i.e. a reduction from 70 GPa to 1 900 MPa). Bandis *et al* (1983) proposed a joint stiffness of 40 MPa/mm, so that a modulus of 1 900 MPa would imply a fracture spacing of about 50 mm, which seems reasonable for the site under consideration. Given that Bandis derived the joint stiffness figure under laboratory conditions, the stiffness for the rock mass taken as a whole (with multiple joints oriented in various directions) could well be lower, with a corresponding increase in the joint spacing being inferred.

The seismic waves propagating outwards from the source of a seismic event would radiate at approximately equal velocities in three dimensions while travelling through intact rock. The fracture zone in the hangingwall of an excavation is a two-dimensional low velocity zone: upon impinging on this zone, the seismic waves are trapped in a wave guide and radiate further in two dimensions, with attendant decreased energy loss (Figure 5.1.4.15). This mechanism, combined with the energy trapping resulting from multiple reflections within the fracture zone, is a possible explanation for the amplification in seismic wave amplitudes observed in the fracture zone.

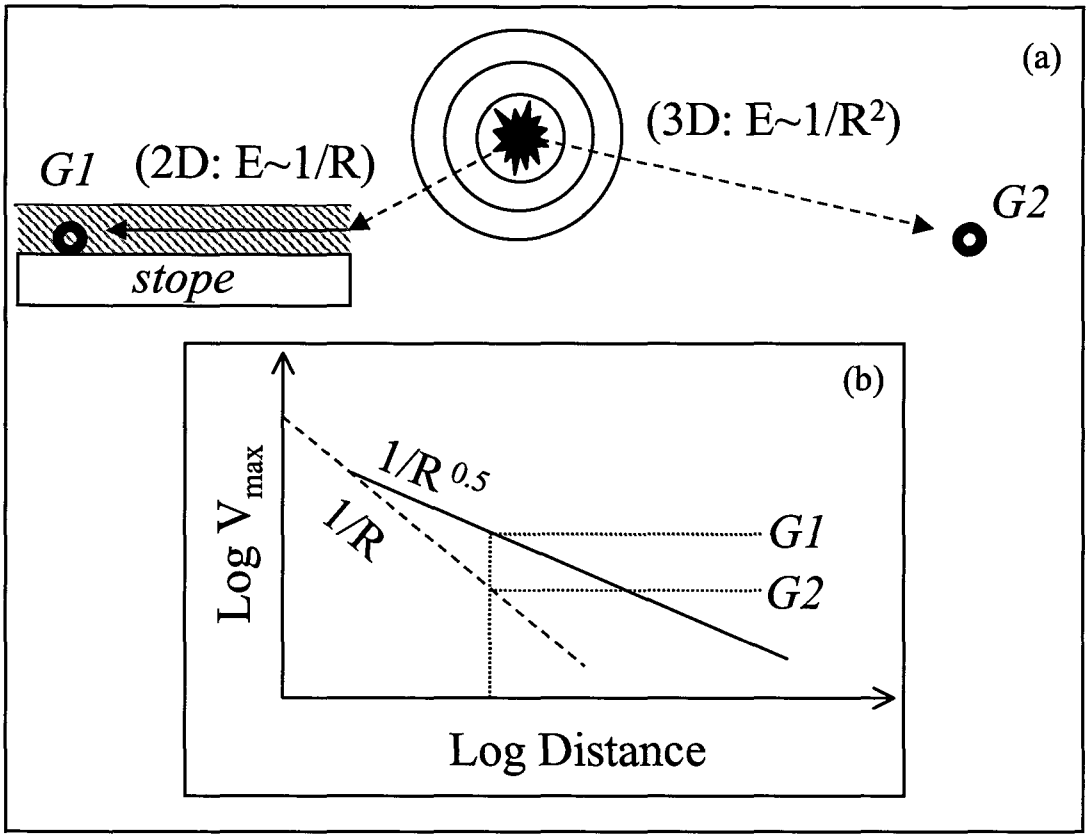

Figure 5.1.4.15 Seismic waves propagating outwards from a source lose energy at a reduced rate when travelling in a two-dimensional wave guide. Seismic waves recorded at 'G1' (in the hangingwall of an excavation) have higher amplitudes than those recorded at 'G2' (in solid rock)

5.1.5 Conclusions

5.1.5.1 The conceptual model

Based on observations and measurements a conceptual model is proposed with particular attention to aspects important to numerical modelling.

The hangingwall quartzites of the Carbon Leader vary in thickness from 0,8 to 2,0 m, the average being 1,8 m. The variation in thickness is due to the erosive nature of an event prior or during initial Green Bar deposition. The quartzite is inhomogeneous as a result of various types of bedding. The type and orientation of the bedding planes are determined by sedimentological

controls during deposition. Planar beds, planar cross beds and trough cross beds occur together with apparently massive quartzite. Finely laminated, often pyritic argillaceous layers define the bedding planes. The soft and platy nature of the clay minerals comprising the argillite allows for relatively easy lateral movement.

The Rice Pebble Marker, situated immediately below the Green Bar, has an average thickness of 30 cm. This unit has a higher argillaceous content than the underlying quartzites and is less siliceous. Lateral variation during deposition results in more massive quartzites grading laterally into planar-bedded quartzites. A well-developed parting plane defines the contact with the underlying strata, although a welded contact was noted locally. Steep extension fractures are seen to terminate against bedding planes near the base of this unit.

The contact between the Rice Pebble Marker and the Green Bar is a well defined, undulating interface, often polished and striated, as well as containing fault gouge and vein quartz. Lower resistance may be offered to separation and lateral movement due to the nature of the interface. A finer grained, more strongly laminated shale fills the troughs of the undulations. A parting plane separates the finer grained shale from the coarser, more massive shale. This parting plane also shows signs of lateral movement and may also offer lower resistance to separation and lateral movement.

Behaviour of the footwall and hangingwall change during blasting periods. These movements are, however, too complex to be modelled numerically with current software.

5.1.5.2 Seismic observations

The complex waveforms recorded closer to the excavation (compared with the simpler waveforms recorded deeper in the rock mass) indicate energy trapping in the fractured rock in the hangingwall of the excavation. Perhaps because the recording of seismic waves started only after the nearest stope faces were more than 50 m from the recording site (thus, after most of the deformation associated with the removal of material from the rock face had presumably already taken place), there does not appear to have been significant degradation of the condition of the rock mass in the hangingwall around the recording site during the period of observation. However, marked local variations (i.e. site effect) in the response of the rock mass to seismic excitation were clearly evident, even on the scale of a few metres or less, in both the horizontal and vertical directions. The presence of the Green Bar in the hangingwall appears to have had a marked effect on the rock mass response locally.

The wave velocities for seismic energy sweeping through the three-dimensional array are very low (compared with those measured in solid rock). The implications for joint stiffness are especially important in the context of the modelling of static and dynamic deformation of the rock mass in the vicinity of stoping.

5.1.6 References

Bandis, S. C., Lumsden, A. C. & Barton, N. R. 1983. Fundamentals of rock joint deformation. *Int. J. Rock Mech. Min. Sci. & Geomech. Abstr.*, 20(6): 249-268.

Brummer, R. K. 1987. Fracturing and deformation at the edges of tabular gold mining excavations and the development of a numerical model describing such phenomena. *D.Eng. Dissertation.* Johannesburg: Rand Afrikaans University., 204p.

Durrheim, R. J., Kullmann, D. H., Stewart, R. D. & Cichowicz, A. 1996. Seismic excitation of the rock mass surrounding an excavation in highly stressed ground. *Proceedings of the 2nd North American Rock Mechanics Symposium: NARMS'96.* Montreal, 19-21 June. Rotterdam: Balkema, p. 389-394.

Goldbach, O. D. 1990. The use of seismogram waveforms to characterize the fracture zone around a mine excavation. *M.Sc. Dissertation.* Johannesburg: University of the Witwatersrand., 178p.

Grodner, M. 1996. Notes on hangingwall profiles measured at WDLS preconditioning site. *Miningtek internal note.* Johannesburg., 14p.

Hagan, T. O. 1980. A photogrammetric study of mining-induced fracture phenomena and instability on a deep level longwall stope face with variable lag lengths. *M.Sc. Dissertation.* Johannesburg: Rand Afrikaans University., 55p.

Legge, N. B. 1984. Rock deformation in the vicinity of deep gold mine longwall stopes and its relation to fractures. *Ph.D. Dissertation.* Cardiff: University College, Cardiff., 284p.

Toper, A. Z., Stewart, R. D. , Kullmann, D. H., Grodner, M., Lightfoot, N., Janse van Rensburg, A. L. & Longmore, P. J. 1998. Develop and implement preconditioning techniques to control face ejection rockbursts for safer mining in seismically hazardous areas. *SIMRAC Final Project Report GAP 336.* Johannesburg: CSIR: Miningtek., 110p.

5.2 Study of seismicity associated with mining of the Vaal Reef

5.2.1 Introduction

The aim of this study is to determine whether or not a correlation exists between the seismicity and the geotechnical classifications of the Klerksdorp Goldfield. The gamma (γ) parameter is used to quantify the effect of stress and mining method on seismicity. The analysis has been completed for selected areas at Vaal Reefs G.M. (areas near to and surrounding 1#, 2#, 5#, 8#, 9# and 11#) and for Hartebeestfontein G.M.

The entire area of mining is divided into seismogenic volumes using the seismic event location distribution, mining geometry and local geology. The γ_E and γ_R parameters are computed for each of these volumes for the individual yearly mining steps, as well as for the entire period of mining (in this study, 1990 – 1995). A comparative analysis is carried out where the magnitude of these parameters is studied with regard to the geotechnical areas present in the particular seismogenic volume.

The two quantities γ_E and γ_R highlight the differences in seismic source contribution to the cumulative seismic moment. The magnitude of γ_E provides insight into the 'structural activity' of the area (i.e. contribution of large magnitude events generated by movement/slip on geological structures such as faults and dykes). In contrast, by damping the large magnitude events during the calculation of γ_R, the effect of the movement on large-scale structural features is diminished. The magnitude of γ_R therefore provides an indication of the mining induced seismicity of the geotechnical areas as a function of rock type and rock mass properties. To reiterate, the magnitude of γ_E represents the amount of energy released due to the structural activity of the area, whereas γ_R may be related to the propensity of the rock mass itself to dissipate energy seismically.

5.2.2 Literature search/evaluation

Seismicity induced by mining is usually defined as the appearance of seismic events caused by rock failures resulting from changes in the stress field in the rock mass near mining excavations. In general, seismicity in deep mines is affected by factors such as depth, production, mining geometry, geologic structure, and geological discontinuities.

In the following sections, the relationships found to exist between geological features (such as faults, dykes and rock type), mining method and seismicity are summarised in a general sense, and then in some detail with reference to the Vaal Reef. The parameters used to quantify the effect of mining induced stresses and excavation method on the seismicity of an area are given in the latter part of this section.

5.2.2.1 Relationship between geological features, mining method and seismicity

Several researchers (Schweitzer & Johnson, 1997; Potgieter & Roering, 1984) propose a close link between seismicity, geological characteristics and mining methods. Seismic tremors may result from a combination of mine layout and associated geological features, also resulting in different pillar failure mechanisms and different degrees of damage to the excavation (Lenhardt, 1990; Lenhardt & Hagan, 1990).

It is predicted that as mining proceeds to greater depths, the number and magnitude of seismic events will also increase (Lenhardt, 1989; Gay *et al.*, 1995a) resulting in a relatively higher number of rockburst related fatalities (Gurtunca & Gay, 1993; Roberts *et al.*, 1993, 1994).

Differences in seismicity have been observed for the Klerksdorp and Carletonville gold fields and are attributed to different mining methods, different degrees of geological disturbance, and different rock type and assemblages (Gay, 1986; Gay & Jager, 1986b; Gay, 1993). Spottiswoode (1986) highlights the close inter-relationship between mining geometry, seismicity and fault properties for the Klerksdorp gold field. In general, two distinct classes of seismic events are distinguished, and these are related to fault slip and unstable fracturing of intact rock (Joughin & Jager, 1983; Brummer, 1988).

Lithological variation of the Vaal Reef

The lithologies associated with the Vaal Reef show a wide variety in composition and other geological properties (Piper, 1997). These variances are particularly important where competent (siliceous) quartzites vary laterally with incompetent (argillaceous) quartzites. Such transitions were observed in the footwall and hangingwall units of the Vaal Reef horizon.

Piper (1997) mentions that the parting planes in the hangingwall of the Vaal Reef (Zandpan Marker) influence the rock mass behaviour. The parting planes occur only a few decimetres to metres into the hangingwall of the mining areas and may result in rock falls as soon as the supporting reef is mined.

His study also suggests that the composition and orientation of dykes and faults may influence the proneness to seismic activity. An interesting phenomenon reported by Piper is that the tectonically reactivated dykes associated with friction melts (pseudotachylytes) are seismically more active than those which are not reactivated.

Faults and dykes associated with the Vaal Reef

The regional structure in the Klerksdorp goldfield is dominated by NE-SW striking faults most of which are extensional (Berlenbach & Schweitzer, 1997). Dykes intrude most of the faults. According to van der Heever (1982) bedding–parallel faults in the Klerksdorp goldfield are often associated with the contact between the Grey-Glassy and the Zandpan Marker, which is indicated by slickensides and quartz veins along this contact. Bedding-parallel faults are assumed to 'step-up' in stratigraphy, resulting in the formation of 'ramp' structures (Boyer & Elliot, 1982 cited in Berlenbach & Schweitzer, 1997). This may result in hazardous hangingwall conditions.

Gay & Jager (1986) observed a horizontal stress anisotropy in the Klerksdorp area, with the maximum horizontal stress oriented in a NW-SE direction. This is thought to be due to the residual stresses associated with the earlier depositional, erosional, and tectonic history of the rocks. Seismic events may result from mining induced stresses causing perturbations in the residual stress field stored within the fault and in the immediately adjacent strata.

Schweitzer & Johnson (1997) suggest that the composition of dykes may influence the proneness to rockburst. For example, siliceous Ventersdorp dykes are proposed to be seismically more active that the less competent dykes.

5.2.2.2 Seismic parameters

Seismic activity of an area may be quantified using the linear relationship between seismicity and elastic convergence (McGarr, 1976). The parameter used to quantify the seismic activity is referred to as the ratio γ_E, expressed as:

$$\gamma_E = \frac{\sum M_o}{G\Delta V_E} \qquad \gamma_E \text{ varies between 0 and 1.} \tag{5.2.2.1}$$

where:

$\sum M_o$ Cumulative seismic moment calculated from the magnitude using the Hanks-Kanamori relationship, $M_o = 10^{1.5M+9.1}$.

G Average modulus of rigidity of the rock types involved.

ΔV_E Change in the volume of elastic convergence due to mining in period being analysed.

Because the seismic moment has a logarithmic nature, the cumulative seismic moment can be dominated by a few large magnitude events. To overcome this effect, a supplementary parameter (referred to as γ_R) is introduced, where less weight is placed on the largest events (Milev & Spottiswoode, 1997). This parameter is defined in terms of the number of rockburst fatalities as a function of magnitude.

Milev & Spottiswoode (1997) plotted the ratio of the number of fatalities (62 in total) due to rockbursts during 1990 and 1991 to the number of seismic events recorded by the national network of the South African Geological Survey, expressed in 0.5 magnitude unit bins. The minimum magnitude threshold of the seismic data was $M \approx 2.0$. The number of smaller events was estimated using b = 1.0 where $LogN = a - bM$ is the standard magnitude-frequency relationship.

The relationship between the magnitude and number of fatalities, derived from Figure 5.2.2.1 is expressed by Milev & Spottiswoode (1997) as

$$\gamma_E \; R = 10^{M-4.25} \tag{5.2.2.2}$$

Milev & Spottiswoode (1997) define γ_R as:

$$\gamma_R = \frac{\sum R}{G\Delta V_E} \tag{5.2.2.3}$$

where:

$\sum R$ Expected number of fatalities per corresponding seismogenic volume.

G Average modulus of rigidity of the rock types involved.

ΔV_E Change in the volume of elastic convergence due to mining in period being analysed.

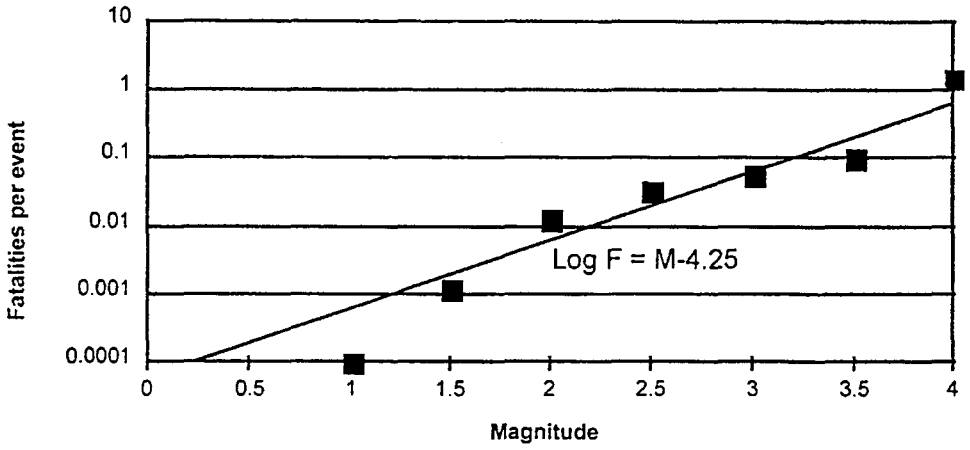

Figure 5.2.2.1 ***The number of fatalities as a function of magnitude in the Carletonville area during 1990 and 1991. A total of 62 fatalities for a workforce of some 100 000 miners were attributed to rockbursts (from Milev & Spottiswoode, 1997).***

5.2.3 Research methodology

5.2.3.1 Methodology outline

The flow chart in Figure 5.2.3.1 summarises the steps taken to calculate γ_E and γ_R. The yearly face advances are digitised from 1:1000 mine plans. The 1:5000 plans (provided by Vaal Reefs G.M. and Hartebeestfontein G.M. on request) proved to be extremely useful, enabling better management of the numerous 1:1000 sheets. The digitised area is then divided into a number of 'coarse windows', which are then merged into one large window. The volume of elastic convergence (ΔV_E) and a weighting factor (ΣR) are computed using MINFFT, a program that uses MINSIM-D inputs for different mining steps and has a solution procedure based on the Fast Fourier transform. Seismogenic volumes are defined using MINAVS, a seismic and modelling output data visualisation program. A smoothing routine, MINCON, is used to contour the seismic data and modelling output. MINFOUT is then used to generate a summary file, containing the seismic moment, convergence values and weighting factor for each mining step, within each seismogenic volume.

5.2.3.2 Improvements/modifications to the methodology

Since the start of the seismic analysis, the methodology has undergone a number of modifications and improvements. The most significant changes are:

1. The development of MINCON, a FORTRAN program written by Dr SM Spottiswoode. The smoothing routine fits a Gaussian curve to the data (seismic data and modelling output). The smoothed ERR and seismic event number densities are particularly useful in defining the seismogenic volumes and have enhanced the interpretation.

2. The development of MINAVS (written by Mr J Maccalari in collaboration with Dr SM Spottiswoode), a software package designed to display both seismicity data and modelling parameters (such as elastic convergence, ERR, vertical stresses etc.) for chosen mining steps. This tool has cut down on the number of intermediate steps involved in the calculation of the gamma values, significantly speeding up the process. MINAVS has powerful visualisation capabilities and allows the display of quantities such as smoothed event number densities, smoothed ERR etc. (Figure 5.2.3.2)

3. MINFOUT, a FORTRAN program written by Dr SM Spottiswoode, was modified to use the areas defined in MINAVS. The program generates a summary file of the seismic parameters and modelling parameters for same area, i.e. the cumulative seismic moment and the volumetric moment are calculated for exactly the same area. This is a substantial improvement, increasing the accuracy of the calculation and decreasing the time taken over the task. Previously, the areas defined in ANALYSE, were redefined in MF, attempting to demarcate the same area.

4. In the initial stages of the project, the entire area of mining was divided into seismogenic volumes on the basis of the event location pattern, mining steps and local geology, and parameters γ_E and γ_R calculated for each volume. Each of the seismogenic volumes was then further subdivided into smaller areas located over sites of active mining in an attempt to monitor parameter variation on a more local scale. However, no meaningful insights were gained from this subdivision, and the seismic parameters were found to be dependent on the size and shape of polygon used to define the small seismogenic volumes.

5. An alternative approach is introduced, where γ_E and γ_R are computed for each mining step (in contrast to the previous approach where cumulative γ_E and γ_R are computed for all mining steps within a particular time period). This proved to be extremely useful, because the change in the seismic parameters with time (i.e. for each yearly mining step) for a particular seismogenic volume can be studied.

6. During the analysis of Hartebeestfontein G.M. it was found that in a number of modifications to MINFFT (MINSIM solution procedure based on the Fourier transform) were necessary to account for the complex structural geology. Numerous faults and dykes crosscut the area, and as a result, the strike and dip of the orebody is highly variable. The original version of MINFFT was based on an average strike and dip for the reef. A different approach is now being taken, where the local structure (strike and dip) is taken into account. The reef is modelled as a 'floppy blanket' and the local dip is used in the computations (Figure 5.2.3.3).

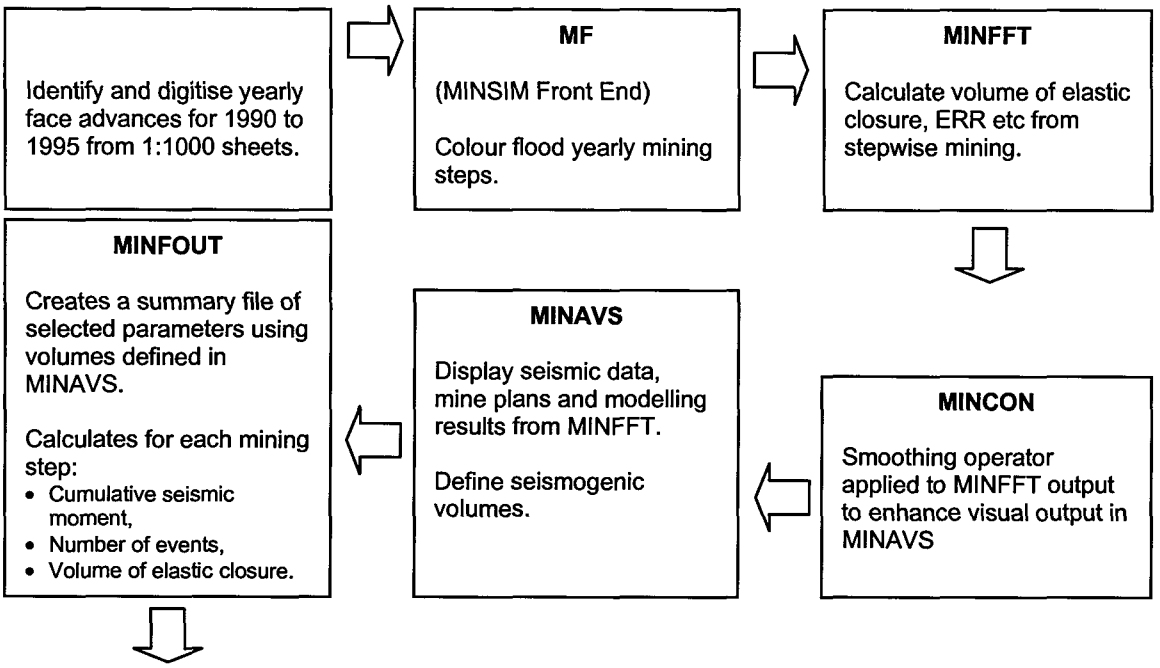

Calculations

- γ_E is the ratio of the cumulative seismic moment to the volume of elastic convergence (McGarr, 1976). Computed for each mining step.
- γ_R is the ratio of the total number of expected fatalities per corresponding seismogenic volume to the volume of elastic convergence (Milev and Spottiswoode, 1997). Computed for each mining step.

$$\gamma_E = \frac{\sum M_o}{G\Delta V_E} \qquad \gamma_R = \frac{\sum R}{G\Delta V_E} \cdot 10^{14}$$

where:

$\sum M_o$	Cumulative seismic moment calculated from the magnitude using the Hanks-Kanamori relationship.
G	Average modulus of rigidity of the rocks involved (Quartzite: 30.1 GPa).
ΔV_E	Volume of elastic closure due to mining during time period being analysed.
$\sum R$	Expected number of fatalities per corresponding seismogenic volume, where $R = 10^{M-4.25}$

Figure 5.2.3.1 Flowchart of the computation sequence used to calculate γ_E and γ_R parameter.

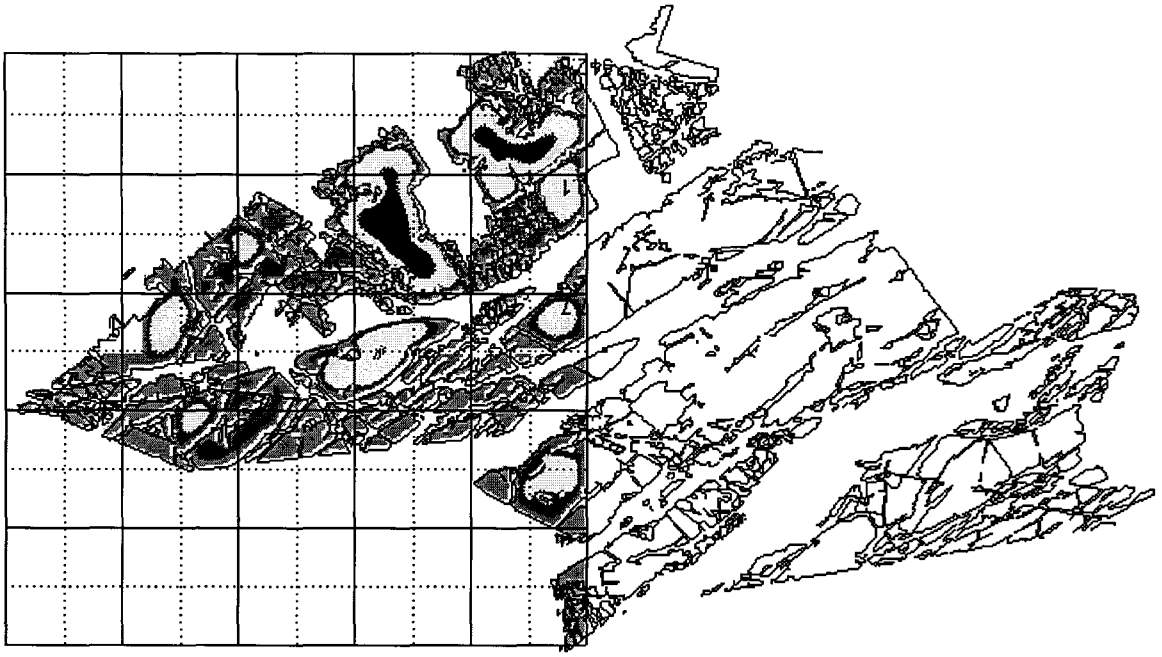

Figure 5.2.3.2 Example of output from MINFFT viewed in MINAVS for western processing strip of Hartebeestfontein G.M. Parameter viewed is elastic convergence computed for 1995 mining step.

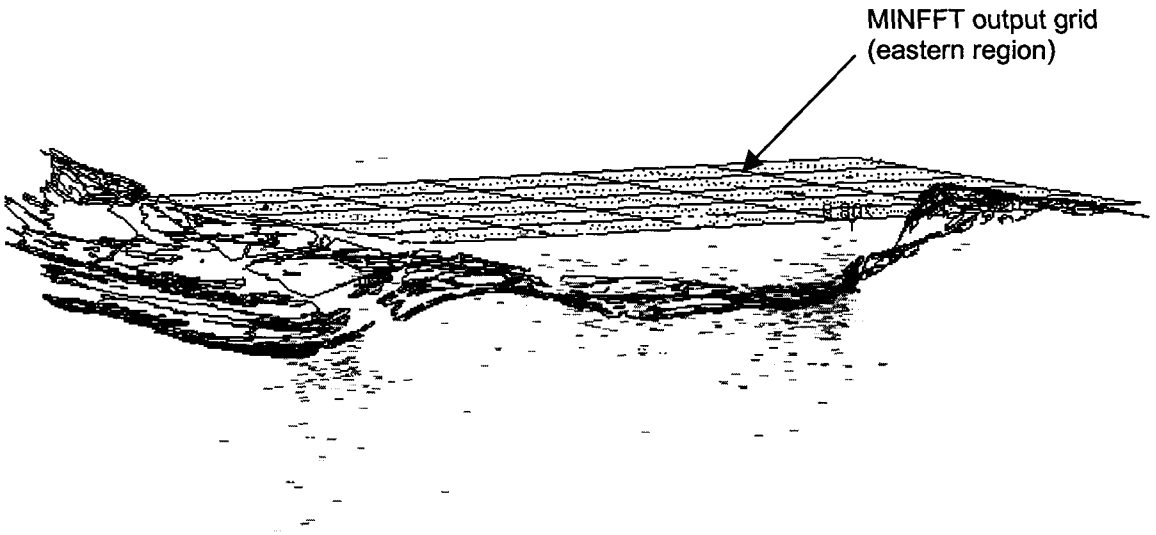

Figure 5.2.3.3 Cross section (northerly direction) of Hartebeestfontein G.M viewed in MINAVS. Digitised mine plan is draped over the depth contours of the Vaal Reef. MINFFT output grid and spatial distribution of seismic events for the eastern region is shown.

5.2.3.3 Definition of seismogenic volumes

In the initial stages of the project, two types/scales of seismogenic volumes were defined on the basis of the seismic event distribution, mining geometry and local geology:

- Large seismogenic volumes (labelled Areas 1, 2 etc.) which included seismicity at the stope face as well as events in the back areas.
- Smaller sub-volumes located directly over the regions of active mining.

The intent behind defining sub-volumes was to zoom into areas of active mining thereby avoiding (as far as possible) the structural contribution to the seismicity. It was found, however, that parameter variation with the sub-volumes was excessive and added no new insights to the analysis. The accuracy of γ_E and γ_R computed for the sub-volumes is limited by location accuracy.

Towards the later stages of the project, an alternative approach was taken where:

- γ_E and γ_R are computed for a particular seismogenic volume for all mining steps within a given time period during which mining takes place (in this study, between 1990 – 1995).
- γ_E and γ_R are computed for a particular seismogenic volume for each mining step on a yearly basis (i.e. for the 1990 mining step, 1991 mining step etc.). This proved to be extremely useful, because the change in the seismic parameters (ΣM_o, γ_R etc.) with time for a particular seismogenic volume could be studied. In this approach, only the large seismogenic volumes are defined, and the parameter variation is analysed with respect to time rather than space.

The seismogenic volumes were defined according to event distribution, local geology and attempted where possible to follow the boundaries of the geotechnical classifications of the Vaal Reef (according to Berlenbach & Schweitzer, 1997). The volumes were labelled Area 1, Area 2 etc.

5.2.3.4 Interpretation of γ_E and γ_R

γ_E represents the level of seismic activity due to mining, and therefore provides an indication of the seismic hazard. High (~1) values of γ_E imply higher seismic hazard and more difficult mining conditions. Low values of γ_E imply less difficult mining conditions. Quantifying the seismic hazard by use of γ_E could have important support implications.

In addition to this general γ_E interpretation, the two quantities γ_E and γ_R highlight the differences in seismic source contribution to the cumulative seismic moment. In general, mining activities induce a large number of small magnitude events (M < 2.0) whereas the events associated with movement on structural features, such as faults and dykes, are considerably fewer in numbers and larger in magnitude. As the γ_E parameter is more sensitive to the effect of large magnitude structurally induced events, the magnitude of this parameter will be an indication of the structural 'activity' in the area. Damping the effect of the large magnitude events in the calculation of γ_R by introduction of a weighting factor, subdues the structural contribution, and therefore indicates the seismic hazard due to mining in a particular geotechnical area.

In this report, despite the fact that the weighting factor was determined empirically, this is considered to be purely a mathematical technique designed to downgrade the dominating effect of the large magnitude events. The computed γ_R values are used to give an indication of the seismic activity due to mining, not as an estimation of expected number of fatalities per seismogenic volume.

5.2.4 Discussion of results

5.2.4.1 Study areas

Table 5.2.4.1 summarises the areas for which the seismic parameters (γ_E and γ_R) were computed during the course of this project. The areas studied are those where the Vaal Reef is currently being mined, and are shown schematically in Figure 5.2.4.1.

Three areas within Vaal Reefs G.M. were studied, each of which were split into a number of 'processing strips'. The 2# area was divided into two strips for numerical modelling, an area to the west (bordering on 1#) and an eastern area. The second area located in the vicinity of 5# was processed using one strip. The third area surrounding 8#, 9# and 11# was divided into three processing strips, labelled according to the nearest shaft in the strip.

Hartebeestfontein G.M. was processed using two strips. The eastern strip encompasses 1#, 2#, 3#, 4# and 5#, and the strip to the west encloses 6#, 7# and 8#.

Table 5.2.4.1 Study areas.

Mine	Study area	Number of processing strips	Strip name
Vaal Reefs G.M.	2#	2	2 # East, 2# West
	5#	1	5#
	8#, 9#, 11#	3	9#, 8#, 11#
Hartebeestfontein G.M.	1#, 2#, 3#, 4#, 5#, 6# (N & S), 7#, 8#	2	Hartebeestfontein East (1#, 2#, 3#, 4#, 5#) Hartebeestfontein West (6# (N & S), 7#, 8#)

5.2.4.2 Geotechnical classes

Refer to Figure 5.2.4.2 for a schematic representation of the geotechnical classes and location of the study areas. For brevity the defined geotechnical classes are numbered (e.g. 'class 1' refers to the geotechnical area where siliceous quartzite in the hangingwall overlies siliceous pebbly conglomerate in the footwall) according to Table 5.2.4.2.

Superimposition of the footwall and hangingwall maps resulted in the definition of geotechnical areas for the Vaal Reef in the Klerksdorp goldfield (Berlenbach & Schweitzer, 1997). These researchers define five different footwall lithologies, ranging from argillaceous quartzite to siliceous quartzite (where the classification depends on the presence of grit bands etc.). Only two different hangingwall lithologies are identified, i.e. the Grey-Glassy (siliceous quartzite) and the Zandpan Marker (argillaceous quartzite). Combinations of the various footwall and hangingwall lithologies result in the definition of seven geotechnical areas, summarised in Table 5.2.4.2.

The hangingwall/footwall combinations will influence the rock engineering properties of the various defined geotechnical areas. It is well known that competency contrasts influence fracture patterns (Berlenbach & Schweitzer, 1997). The various competencies for the Grey-Glassy and the Zandpan Marker are thought to result in different fracture patterns, which may impact on rock mass behaviour. Areas of particular importance in this regard are where the Zandpan Marker cuts down on the Vaal Reef (classes 6 and 7).

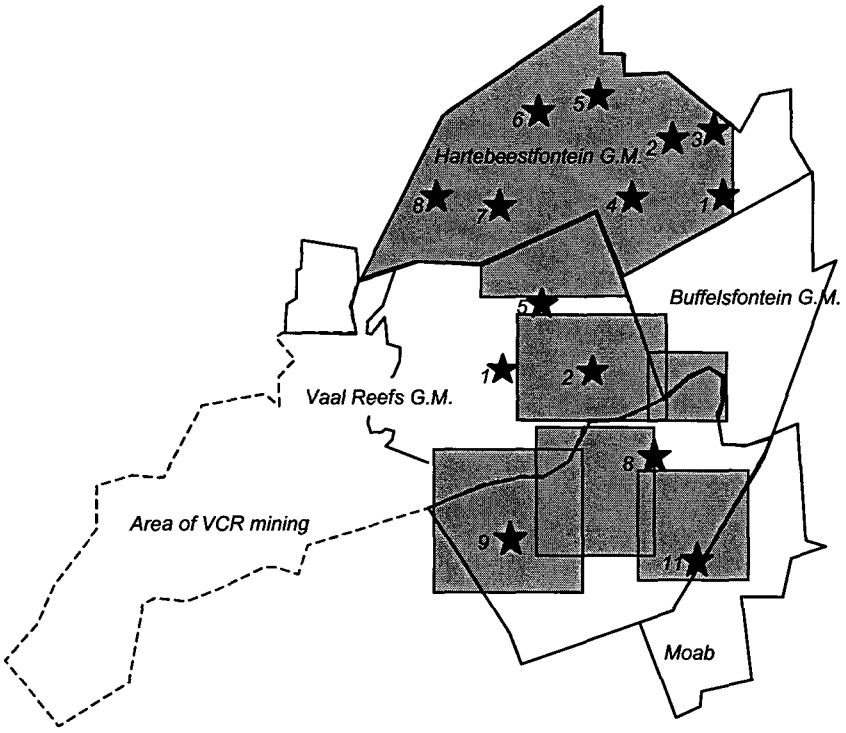

Figure 5.2.4.1 Study areas defined for the Vaal Reef within Vaal Reefs G.M. and Hartebeestfontein G.M.

Table 5.2.4.2 Geotechnical classes defined for the Vaal Reef.

Class	Hangingwall rock type	Footwall rock type
1	Siliceous quartzite (grey-glassy)	Siliceous pebbly conglomerate (MISPAH)
2	Siliceous quartzite (grey-glassy)	Argillaceous quartzite with pebble bands
3	Siliceous quartzite (grey-glassy)	Siliceous quartzite
4	Siliceous quartzite (grey-glassy)	Argillaceous quartzite
5	Siliceous quartzite (grey-glassy)	Siliceous quartzite with grit bands
6	Argillaceous quartzite (Zandpan marker)	Siliceous quartzite with grit bands
7	Argillaceous quartzite (Zandpan marker)	Argillaceous quartzite

Hangingwall units

Immediately overlying the Vaal Reef is a very competent siliceous quartzite (locally known as the Grey-Glassy) with an average thickness of 0,5m (Berlenbach & Schweitzer, 1997). The Grey-Glassy is generally stoped out, and is in turn overlain by an argillaceous quartzite (the

Zandpan or 12 Foot Marker) which forms the base of the Zandpan Member, an 80m thick coarse-grained quartzite package. The Grey-Glassy and the Zandpan Marker are separated by a well-defined parting plane (Berlenbach & Schweitzer, 1997).

According to Berlenbach & Schweitzer (1997) the Zandpan Marker can locally cut down into the Vaal Reef or its footwall units, resulting in the Vaal Reef being overlain by argillaceous quartzites or being eroded. Areas in which the Zandpan Marker cuts down in stratigraphy are, however, only known at Hartebeestfontein G.M and the northeastern part of Vaal Reefs G.M. (5# area) but these localities are not well defined (see question marks and dashed lines in Figure 5.2.4.2).

Footwall units

The Vaal Reef unconformably overlies the MB5 zone, which consists of an alternating argillaceous and siliceous quartzite sequence. The MB5 quartzite becomes progressively more argillaceous in a southeasterly direction. From bottom to top, the MB5 zone comprises the following units:

- a lower siliceous quartzite,
- a lower argillaceous quartzite,
- an upper siliceous quartzite forming localised lenses within the stratigraphy,
- an upper argillaceous quartzite, and
- a siliceous quartzite grit band (MISPAH).

Although Figure 5.2.4.2 indicates that the southern part of 11# intersects class 1, the MISPAH only forms the footwall to the Vaal Reef in an extended area in the Moab lease area (Berlenbach & Schweitzer, 1997; Gilroy *et al.*, 1994).

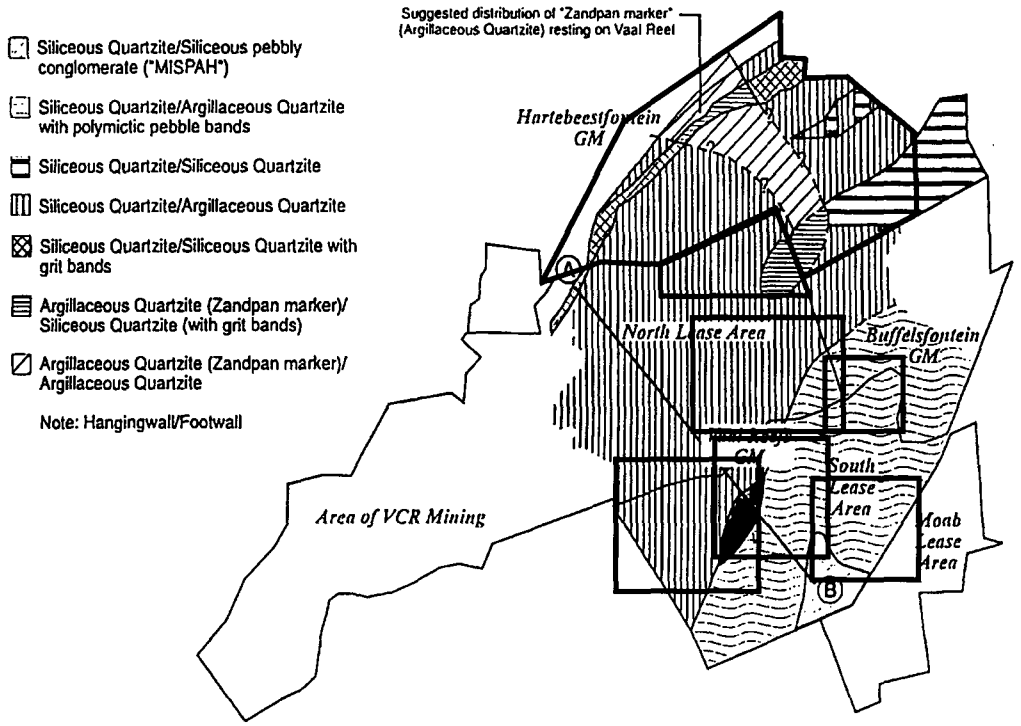

Figure 5.2.4.2 Geotechnical areas defined for the Vaal Reef in the Klerksdorp goldfield (from Berlenbach & Schweitzer, 1997).

Parting planes

Parting planes may control the cohesion between the hangingwall and footwall units, and as a result, may influence the behaviour of the rock mass. Two observations mentioned by Berlenbach & Schweitzer (1997) regarding these planes are as follows:

- A significant parting plane exists in the contact between the Grey-Glassy and the Zandpan Marker. Weak cohesion along this plane is thought to control the beam thickness and is known to result in unstable hangingwall conditions (Kullman *et al.*, 1994).

- There is variability in parting planes in the MB5 footwall units, which can change in frequency from a spacing of some 50cm in the argillaceous quartzite, to 2m spacing in the siliceous quartzites.

Although argillaceous quartzite is present in both geotechnical classes 2 and 4, their rock mass properties could differ due to the presence of parting planes associated with polymictic pebble bands in class 2 (Berlenbach & Schweitzer, 1997).

5.2.4.3 Seismicity

Some general qualitative observations are presented before the seismicity of the Vaal Reef is quantified (by means of the γ_E and γ_R parameter) according to the methodology described in section 5.2.3.

Two broad types of mine tremors are recognised in this study. Firstly, mine tremors directly connected with mining operations i.e. those associated with the formation of fractures at stope faces as a result of mine-induced stress release. Secondly, seismic events associated with movement on major geological discontinuities resulting from the interaction between mine-induced and residual tectonic stresses in the area.

Seismic events at the stope face

In general there is a high event number distribution in the Klerksdorp goldfield in areas undergoing active mining. These tremors can be directly connected to mining operations and tend to be of low to medium magnitude. These events are thought to be associated with the formation of fractures at stope faces as a result of mine-induced stress release. The number of these 'stope-face' events is generally a function of the mining activity (in this study, given by the area or volume mined per mining step). These tremors occur in the vicinity of the mining face, or on some pre-existing zone of weakness near the face.

Seismic events associated with geological discontinuities

A second population of seismic events is recognised in the Klerksdorp goldfield. Studies of the event distribution show that the larger events generally are located in the vicinity of the major fault zones. The Klerksdorp goldfield is crosscut by numerous NE-SW striking faults, some of which have throws of several hundred metres. The large seismic events are associated with movement on major geological discontinuities, resulting from the interaction between mine-induced and residual tectonic stresses in the area. These events cannot always be pinpointed to any specific area of mining, but appear to be triggered by mining operations.

An example: The seismic events of Vaal Reefs G.M. 2# are located over currently mined areas, but there is an added contribution due to a high amount of seismicity occurring over fault zones, dykes and in the back areas. This is particularly apparent in the area to the east of 2# (bordering on 5#) where seismic events cluster on the Clemcor dyke.

5.2.4.4 Seismic parameters computed for Vaal Reefs G.M.

Four geotechnical classes occur at Vaal Reefs G.M. (Figure 5.2.4.2). The area was divided into six strips for processing and a total of 31 seismogenic volumes were defined. The volumes were delineated according to the geotechnical classifications, event distribution and mining geometry.

Spatial parameter variation

Vaal Reefs G.M. 2 Shaft area

The area surrounding Vaal Reefs G.M. 2# was processed in two strips (Figure 5.2.4.3) and seven seismogenic volumes were defined (Figure 5.2.4.4). Table 5.2.4.3 summarises the various quantities output from the numerical modelling (area mined, volume of elastic convergence ΔV_E for each mining step) and computed from the seismicity (cumulative seismic moment ΣM_o, expected number of fatalities per seismogenic volume ΣR, number of events per mining step and maximum event magnitude). Using equations 5.2.3.1 and 5.2.3.2 the parameters γ_E and γ_R are computed for each seismogenic volume. These parameters are computed for the entire period of mining (Table 5.2.4.3) and for each mining step (Table 5.2.4.4). Figures 5.2.4.5 and 5.2.4.6 provide a diagrammatic representation of γ_E and γ_R computed for the seven seismogenic volumes for the period of mining from 1990 to 1995.

The γ_E values for all areas (except areas 1 and 3) are high, ranging from 0.7 to 1.21. In contrast to the γ_E values, the γ_R values are low, ranging between 0.05 and 0.33.

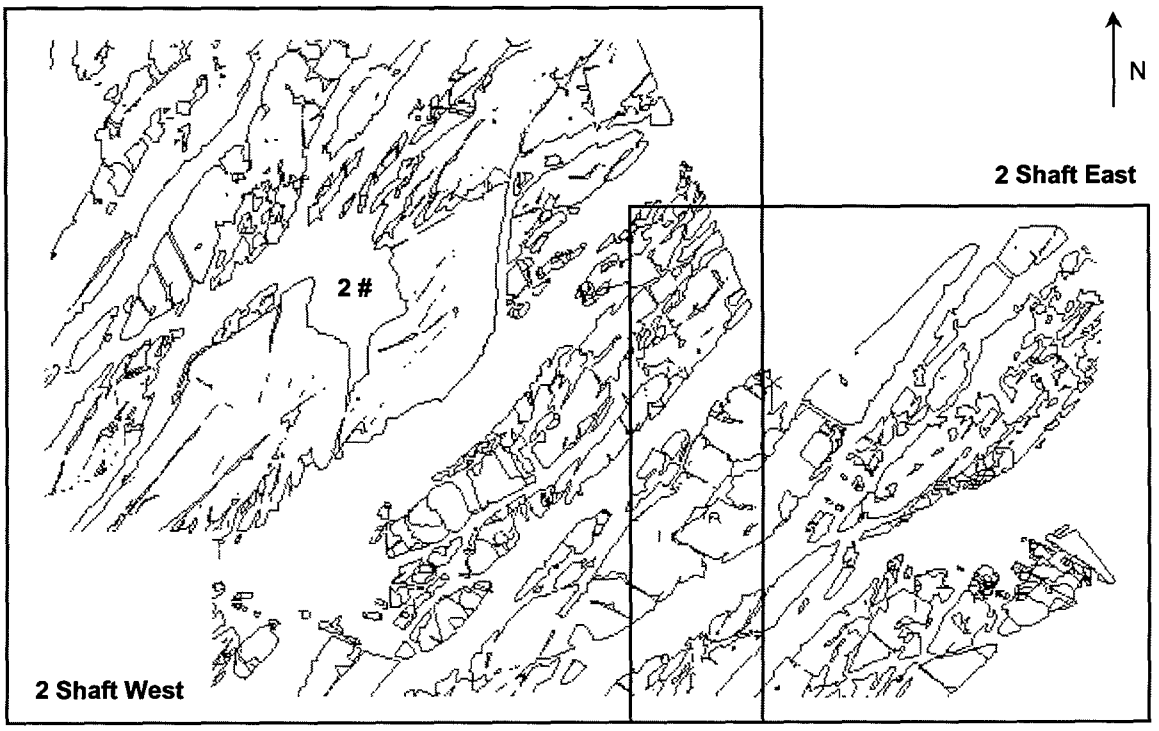

Figure 5.2.4.3 MINFFT processing strips for Vaal Reefs G.M. 2 Shaft area.

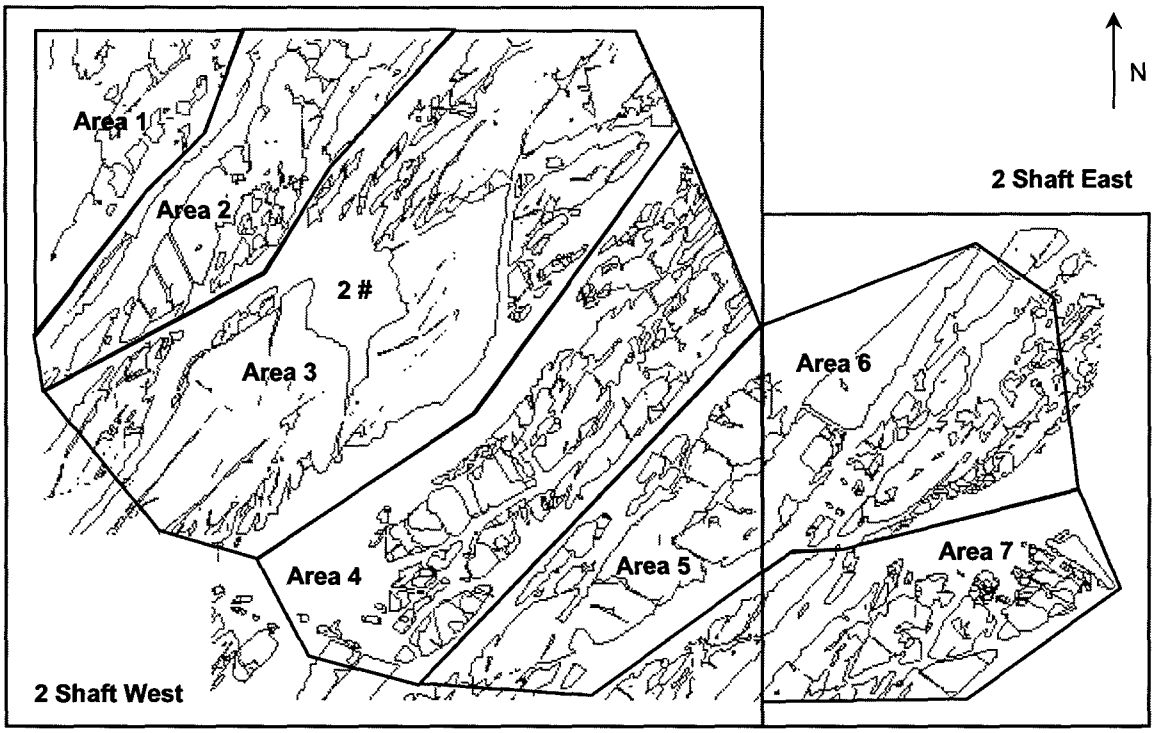

Figure 5.2.4.4 Seismogenic volumes defined for Vaal Reefs G.M. 2 Shaft area.

Table 5.2.4.3 Seismic parameters for Vaal Reefs G.M. 2 Shaft area.

Seismogenic Volume	Time Period	Area Mined m^2	ΔV_E m^3	Number Events	ΣR	ΣM_o N.m	Maximum Magnitude	γ_E	γ_R
2 Shaft Area									
Area 1	90 - 95	27216	10694	86	0.151	4.65E+13	2.9	0.14	0.05
Area 2	90 - 95	70632	20351	111	0.586	4.47E+14	3.5	0.73	0.10
Area 3	90 - 95	279612	85601	275	0.696	1.91E+14	3.2	0.07	0.03
Area 4	90 - 95	196344	59111	837	3.357	1.57E+15	3.4	0.88	0.19
Area 5	90 - 95	55404	15400	97	0.481	3.24E+14	3.5	0.70	0.10
Area 6	90 - 95	77760	27005	503	2.683	7.62E+14	3.4	0.94	0.33
Area 7	90 - 95	46980	15712	132	0.802	5.71E+14	3.6	1.21	0.17

Table 5.2.4.4 Seismic parameters for Vaal Reefs G.M. 2 Shaft area.

Seismogenic Volume	Mining Step	Area Mined m^2	ΔV_E m^3	Number Events	ΣR	ΣM_o N.m	Maximum Magnitude	γ_E	γ_R
2 Shaft Area									
Area 1	1990	6804	2858	2	0.007	1.1E+12	2	0.01	0.01
	1991	5184	2836	14	0.028	1.6E+11	2.2	0.00	0.03
	1992	6804	1885	19	0.026	5.8E+12	2.2	0.10	0.05
	1993	5508	2253	14	0.052	2.9E+13	2.9	0.43	0.08
	1994	2592	741	25	0.018	3.2E+12	2.2	0.14	0.08
	1995	324	122	12	0.02	7.20E+12	2.5	1.96	0.54
Area 2	1990	14580	4899	9	0.057	9.2E+12	2.6	0.06	0.04
	1991	13932	5838	28	0.03	4.4E+12	2.1	0.03	0.02
	1992	15552	4028	36	0.155	7.3E+13	3	0.60	0.13
	1993	9072	2622	21	0.069	3.2E+13	2.9	0.41	0.09
	1994	12960	2035	9	0.093	6.8E+13	3	1.11	0.15
	1995	4536	930	8	0.182	2.6E+14	3.5	9.29	0.65
Area 3	1990	62532	27514	20	0.218	2.70E+12	3.2	0.00	0.03
	1991	69012	21463	58	0.066	6.9E+11	2.5	0.00	0.01
	1992	60588	16601	68	0.267	1.6E+14	3.2	0.32	0.05
	1993	45036	11394	58	0.082	1.7E+13	2.3	0.05	0.02
	1994	17172	4156	40	0.049	9E+12	2.1	0.07	0.04
	1995	25272	4473	31	0.014	1.4E+12	1.8	0.01	0.01
Area 4	1990	36288	16874	51	0.689	3.90E+14	3.3	0.77	0.14
	1991	56700	16840	151	0.635	6E+13	3.3	0.12	0.13
	1992	23004	8350	168	0.419	1.8E+14	3.1	0.72	0.17
	1993	41472	9912	144	0.5	3.1E+14	3.4	1.04	0.17
	1994	30780	5263	204	0.816	5.2E+14	3.3	3.28	0.52
	1995	8100	1871	119	0.298	1.1E+14	2.9	1.95	0.53
Area 5	1990	22356	6304	7	0.053	8.40E+12	2.6	0.04	0.03
	1991	9072	2703	19	0.035	1.2E+12	2.2	0.01	0.04
	1992	10044	2531	12	0.04	1.4E+13	2.6	0.18	0.05
	1993	8100	2454	32	0.232	2.4E+14	3.5	3.25	0.31
	1994	4860	1123	19	0.107	5.6E+13	3	1.66	0.32
	1995	972	284	8	0.014	4.2E+12	2.3	0.49	0.16
Area 6	1990	31428	9303	63	0.568	7.9E+13	3.3	0.28	0.20
	1991	20736	8377	162	0.855	8.3E+13	3	0.33	0.34
	1992	10044	4560	74	0.372	1.2E+14	2.8	0.87	0.27
	1993	5508	1542	68	0.319	1.7E+14	3.1	3.66	0.69
	1994	9396	2838	68	0.233	8E+13	2.8	0.94	0.27
	1995	648	385	68	0.336	2.3E+14	3.4	19.85	2.90
Area 7	1990	17496	5231	10	0.045	5.6E+11	2.4	0.00	0.03
	1991	12312	4888	21	0.161	2.6E+13	2.8	0.18	0.11
	1992	6480	2579	18	0.177	1.1E+14	3.1	1.42	0.23
	1993	5508	1151	17	0.266	3.8E+14	3.6	10.97	0.77
	1994	4860	1667	15	0.03	6.4E+12	2.3	0.13	0.06
	1995	324	196	51	0.123	4.8E+13	2.9	8.14	2.08

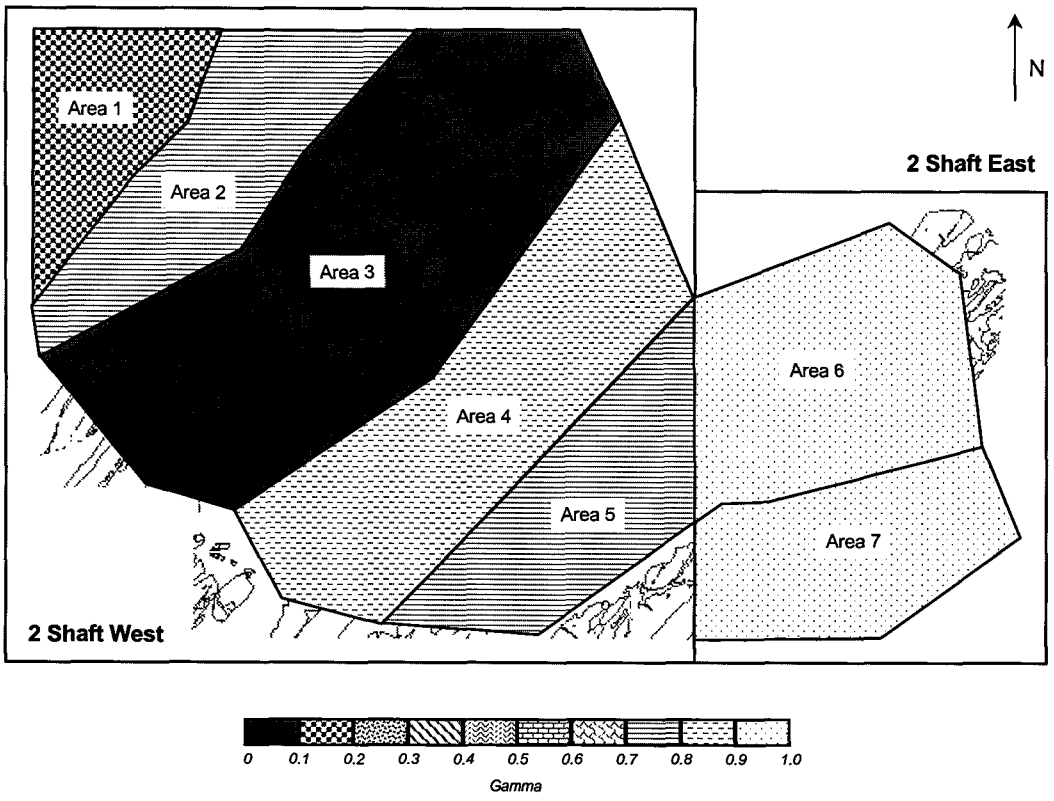

Figure 5.2.4.5 γ_E ***computed for Vaal Reefs G.M. 2 Shaft area.***

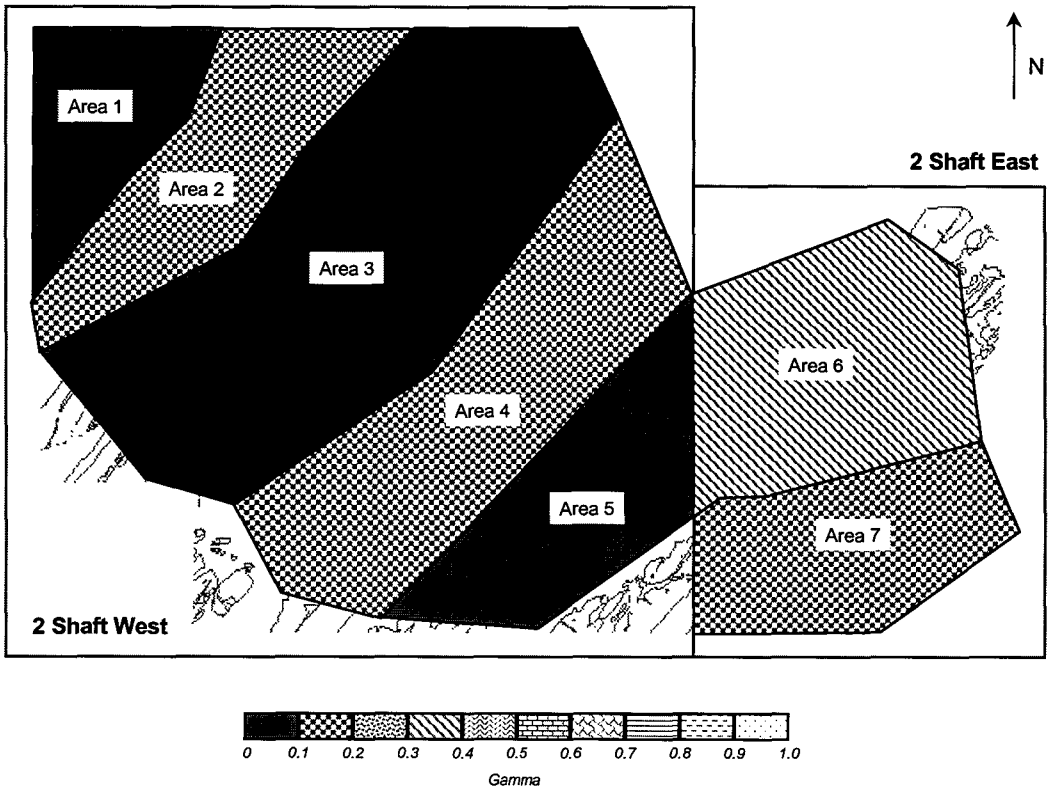

Figure 5.2.4.6 γ_R ***computed for Vaal Reefs G.M. 2 Shaft area.***

Vaal Reefs G.M. 5 Shaft area

The area surrounding Vaal Reefs G.M. 5# was processed in one strip and five seismogenic volumes were defined (Figure 5.2.4.7). Tables 5.2.4.5 and 5.2.4.6 summarise seismic and modelling parameters computed for each of the seismogenic volumes for the 1990 – 1995 mining period, and for each mining step, respectively.

Figures 5.2.4.8 and 5.2.4.9 illustrate the spatial variation of γ_E and γ_R diagrammatically. The γ_E values for four of the five seismogenic volumes are moderate and range from 0.37 to 0.61. The excessively high γ_E of 1.45 (area 5) could be as a result of mining occurring on the boundary between Vaal Reefs G.M. and Hartebeestfontein G.M. The corresponding γ_R values are predominantly low, ranging between 0.17 and 0.23, with an outlier of 0.55 for area 5.

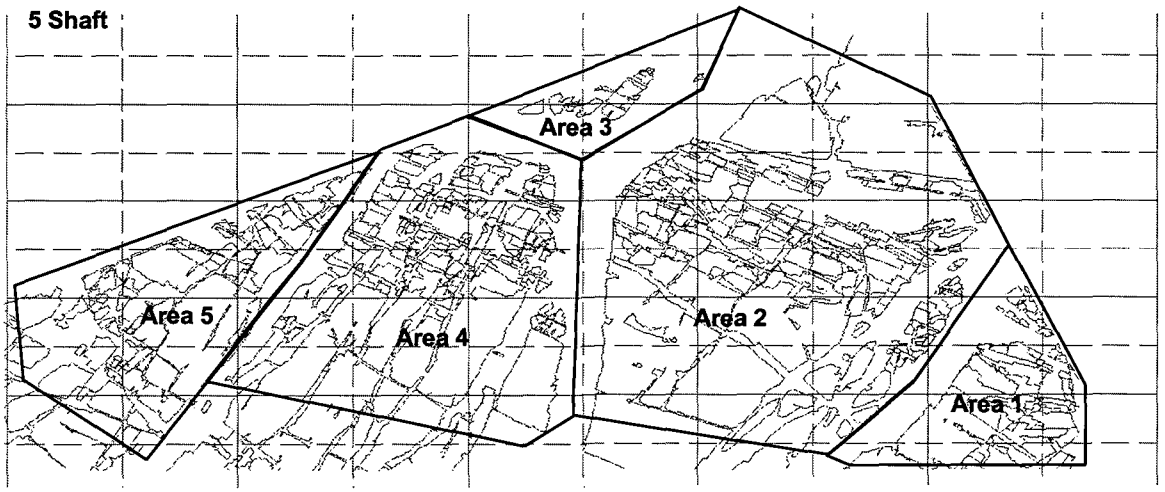

Figure 5.2.4.7 Seismogenic volumes defined for Vaal Reefs G.M. 5 Shaft area.

Table 5.2.4.5 Seismic parameters for Vaal Reefs G.M. 5 Shaft area.

Seismogenic Volume	Time Period	Area Mined m^2	ΔV_E m^3	Number Events	ΣR	ΣM_o N.m	Maximum Magnitude	γ_E	γ_R
5 Shaft Area									
Area 1	90 - 95	87400	26112	1325	1.528	2.94E+14	2.8	0.37	0.19
Area 2	90 - 95	330600	93307	8330	5.27	1.702E+15	3.8	0.61	0.19
Area 3	90 - 95	28200	3714	1120	0.26	5.034E+13	2.8	0.45	0.23
Area 4	90 - 95	157200	43334	2475	2.26	7.84E+14	3.2	0.60	0.17
Area 5	90 - 92	27900	9313	506	1.54	4.06E+14	3.3	1.45	0.55

Table 5.2.4.6 Seismic parameters for Vaal Reefs G.M. 5 Shaft area.

Seismogenic Volume	Mining Step	Area Mined m^2	ΔV_E m^3	Number Events	ΣR	ΣM_o N.m	Maximum Magnitude	γ_E	γ_R
5 Shaft Area									
Area 1	1990	24100	4386	48	0.142	2.2E+13	2.6	0.17	0.11
	1991	25400	8992	236	0.301	2.3E+13	2.4	0.08	0.11
	1992	22500	6840	270	0.332	7.8E+13	2.8	0.38	0.16
	1993	6200	2269	278	0.244	5.2E+13	2.7	0.76	0.36
	1994	7800	2980	267	0.286	6.9E+13	2.5	0.77	0.32
	1995	1400	645	226	0.223	5E+13	2.7	2.57	1.15
Area 2	1990	76300	24111	139	1.072	4.2E+13	3.8	0.06	0.15
	1991	59400	18711	580	1.021	5.1E+14	3.7	0.91	0.18
	1992	69400	12700	892	0.612	1.9E+14	2.9	0.50	0.16
	1993	70900	17867	2241	0.882	3.4E+14	3.2	0.63	0.16
	1994	51300	18519	2466	0.922	4.1E+14	3.4	0.74	0.17
	1995	3300	1399	2012	0.761	2.1E+14	2.9	4.99	1.81
Area 3	1990	100	141	3	0.029	3E+10	2.7	0.01	0.68
	1991	100	105	12	0.059	1E+11	2.7	0.03	1.87
	1992	900	127	31	0.003	1.3E+11	1.2	0.03	0.08
	1993	10800	1339	83	0.004	1.1E+11	0.5	0.00	0.01
	1994	15300	1775	417	0.049	1.1E+13	2.5	0.21	0.09
	1995	1000	227	574	0.117	3.9E+13	2.8	5.71	1.71
Area 4	1990	32400	13705	61	0.303	8.2E+13	2.9	0.20	0.07
	1991	29900	6369	300	0.74	2.7E+14	3.2	1.41	0.39
	1992	36200	6661	304	0.378	1.2E+14	3	0.60	0.19
	1993	26600	8033	417	0.506	2.3E+14	3.2	0.95	0.21
	1994	20700	5237	800	0.212	5.7E+13	2.8	0.36	0.13
	1995	11400	3329	593	0.125	2.5E+13	2.6	0.25	0.12
Area 5	1990	11100	2220	64	0.396	7.5E+13	3.1	1.12	0.59
	1991	9100	2594	192	0.532	7.1E+13	3	0.91	0.68
	1992	7400	4499	250	0.615	2.6E+14	3.3	1.92	0.45

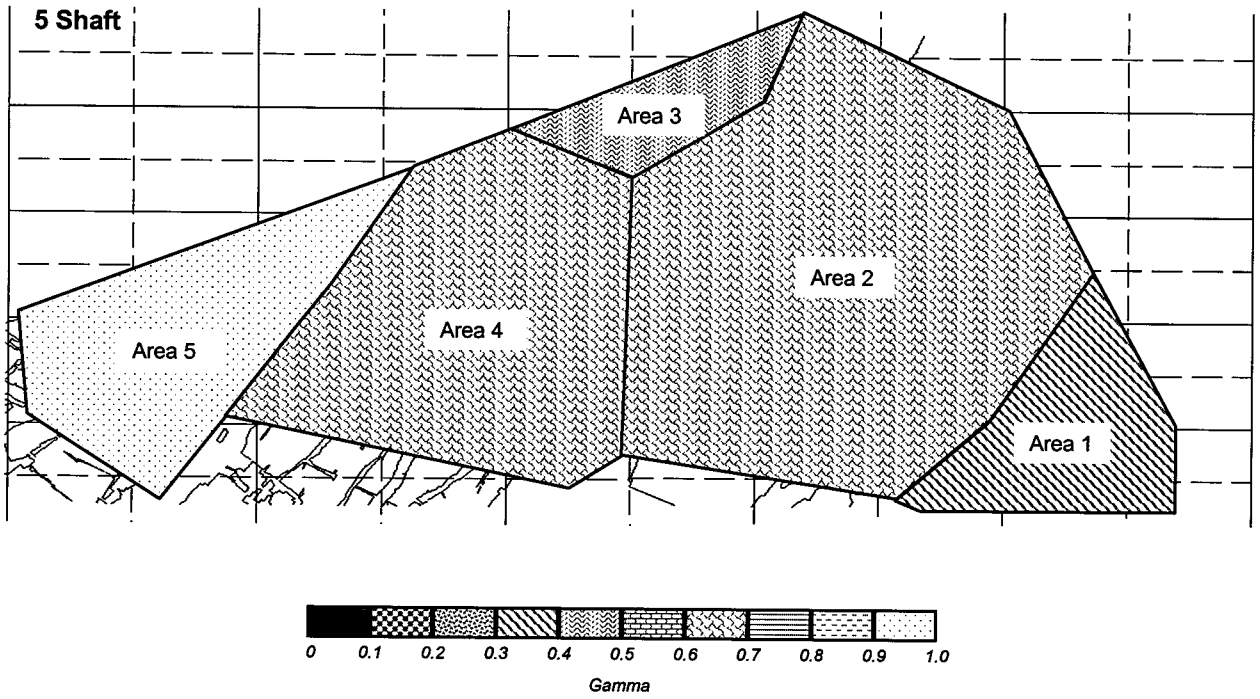

Figure 5.2.4.8 ***γ_E computed for Vaal Reefs G.M. 5 Shaft area.***

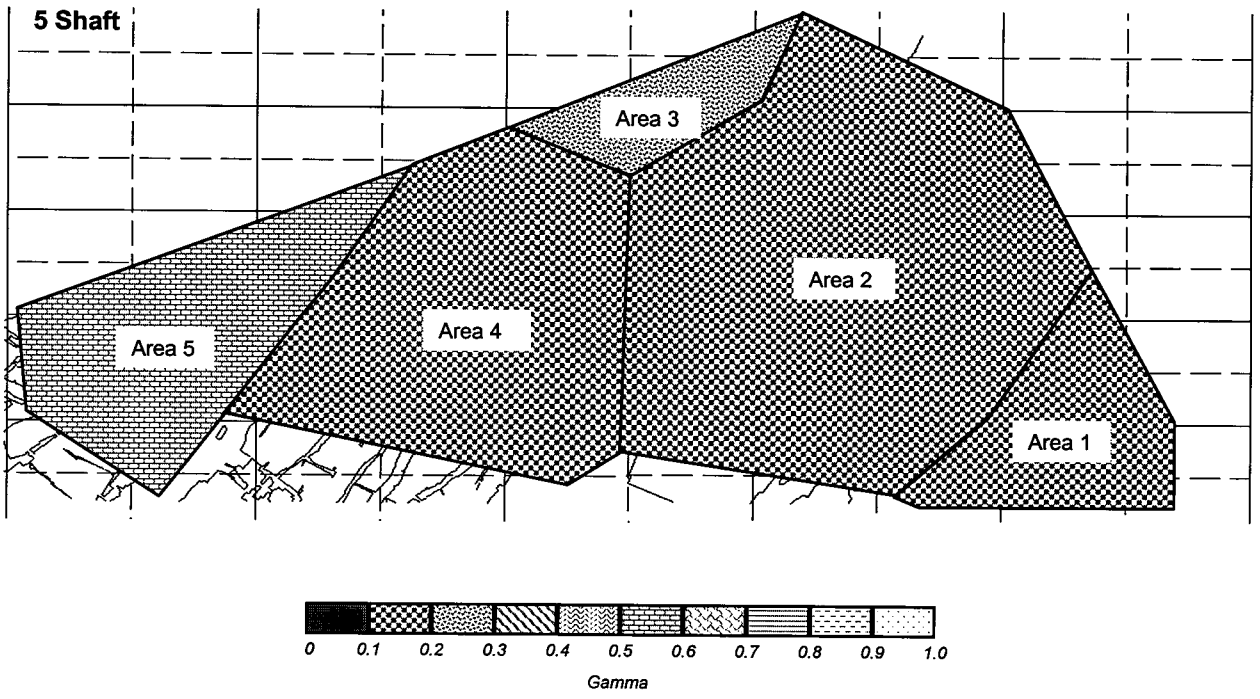

Figure 5.2.4.9 ***γ_R computed for Vaal Reefs G.M. 5 Shaft area.***

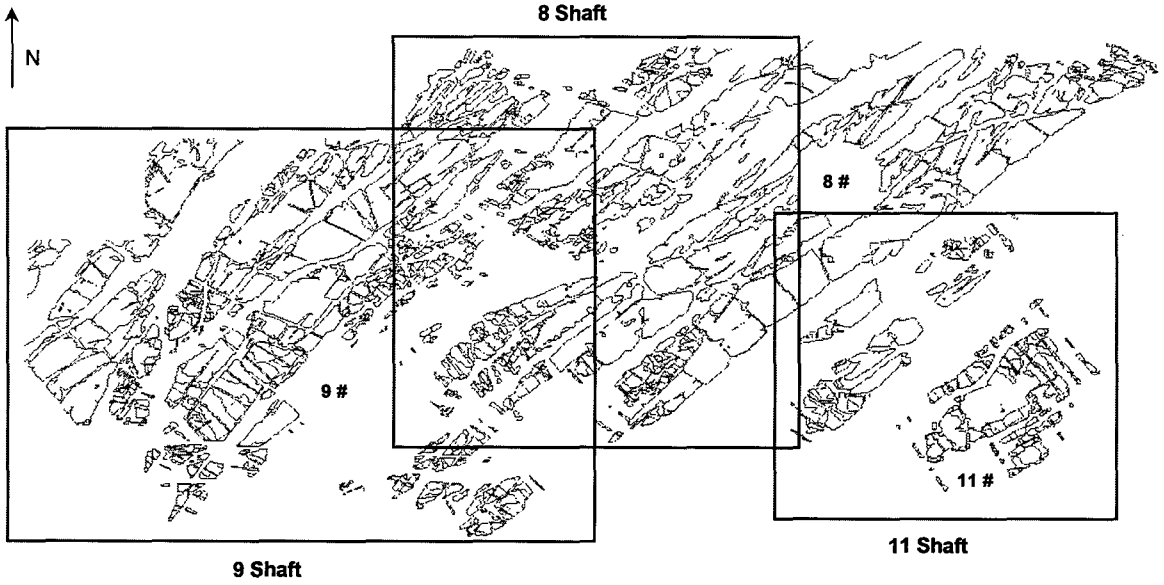

Figure 5.2.4.10 MINFFT processing strips for areas surrounding Vaal Reefs G.M. 8, 9 and 11 Shaft.

Vaal Reefs G.M. 8 Shaft area

The area to the south of Vaal Reefs G.M. 5#, encompassing 8#, 9# and 11# was processed in three strips (Figure 5.2.4.10).

Six seismogenic volumes were defined in the Vaal Reefs 8# area (Figure 5.2.4.11). Tables 5.2.4.7 and 5.2.4.8 summarise the seismic and modelling parameters computed for each of the seismogenic volumes for the 1990 – 1993 mining period, and for each mining step, respectively. Figures 5.2.4.12 and 5.2.4.13 illustrate γ_E and γ_R diagrammatically.

The γ_E values of four of the six seismogenic volumes (areas 3 to 6) are low ranging from 0.02 to 0.28. This parameter increases towards the southeastern corner, reaching a high of 1.49 in area 1. The γ_R values are predominantly low, ranging between 0.02 and 0.24, increasing to an amount of 0.42 for area 1.

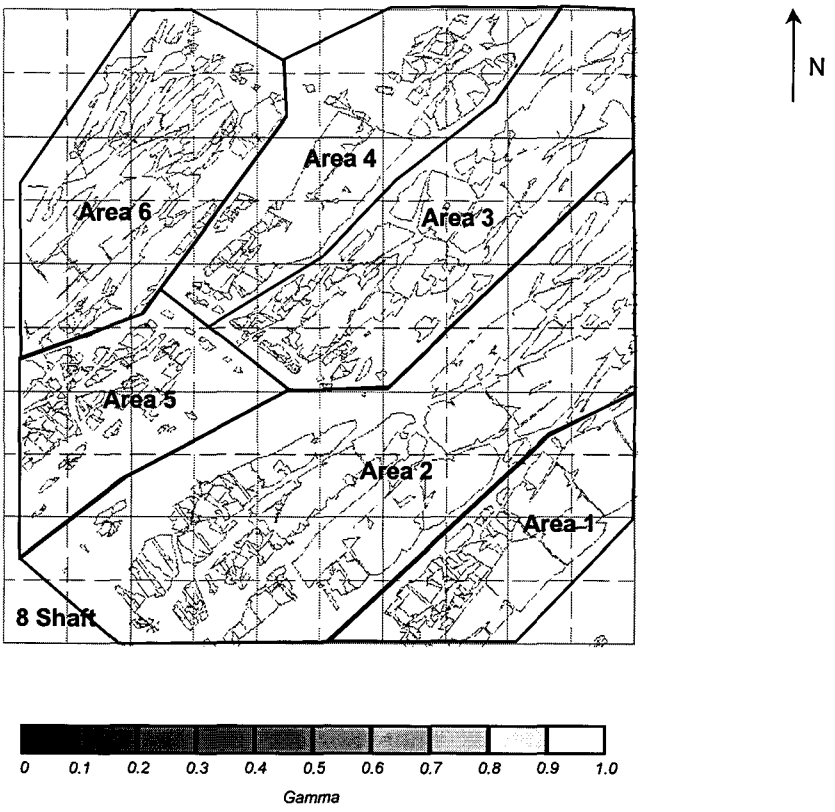

Figure 5.2.4.11 Seismogenic volumes defined for Vaal Reefs G.M. 8 Shaft area.

Table 5.2.4.7 Seismic parameters for Vaal Reefs G.M. 8 Shaft area.

Seismogenic Volume	Time Period	Area Mined m^2	ΔV_E m^3	Number Events	ΣR	ΣM_o N.m	Maximum Magnitude	γ_E	γ_R
8 Shaft Area									
Area 1	90 - 93	30184	6167	162	0.777	2.77E+14	3.1	1.49	0.42
Area 2	90 - 93	95256	18621	275	1.353	2.43E+14	3.9	0.43	0.24
Area 3	91 - 93	16660	3450	64	0.024	2.31E+12	1.8	0.02	0.02
Area 4	90 - 93	119560	21803	222	0.522	1.81E+14	3.1	0.28	0.08
Area 5	90 - 93	55272	12115	78	0.29	1.04E+14	3.1	0.28	0.08
Area 6	90 - 93	84476	16561	87	0.394	2.04E+13	3.4	0.04	0.08

Table 5.2.4.8 Seismic parameters for Vaal Reefs G.M. 8 Shaft area.

Seismogenic Volume	Mining Step	Area Mined m^2	ΔV_E m^3	Number Events	ΣR	ΣM_o N.m	Maximum Magnitude	γ_E	γ_R
8 Shaft Area									
Area 1	1990	7644	1980	23	0.258	1.1E+14	3	1.85	0.43
	1991	13132	2035	56	0.241	3.8E+13	2.9	0.62	0.39
	1992	6272	1606	50	0.235	1.2E+14	3.1	2.48	0.49
	1993	3136	546	33	0.043	9.1E+12	2.3	0.55	0.26
Area 2	1990	22540	6041	48	0.622	1.1E+13	3.9	0.06	0.34
	1991	28224	4318	115	0.483	8.9E+13	3.1	0.68	0.37
	1992	27048	5139	77	0.23	1.4E+14	3.2	0.91	0.15
	1993	17444	3122	35	0.018	2.5E+12	2.1	0.03	0.02
Area 3	1991	7644	1575	4	0.005	4.0E+11	1.7	0.01	0.01
	1992	5880	1170	18	0.015	1.5E+12	1.8	0.04	0.04
	1993	3136	706	42	0.004	4.1E+11	1.6	0.02	0.02
Area 4	1990	26656	5464	15	0.113	9.8E+12	3	0.06	0.07
	1991	41356	6038	71	0.095	3.9E+12	2.4	0.02	0.05
	1992	31948	6773	91	0.183	9.5E+13	3.1	0.47	0.09
	1993	19600	3528	45	0.131	7.2E+13	3.1	0.68	0.12
Area 5	1990	25088	5720	5	0.01	1.5E+12	1.9	0.01	0.01
	1991	12152	2771	35	0.167	7E+13	3.1	0.84	0.20
	1992	11956	2403	34	0.08	1.8E+13	2.4	0.25	0.11
	1993	6076	1221	4	0.033	1.4E+13	2.7	0.38	0.09
Area 6	1990	29988	7047	8	0.017	5.4E+11	1.9	0.00	0.01
	1991	22540	3651	39	0.298	1.9E+12	3.4	0.02	0.27
	1992	18816	3669	28	0.064	1.6E+13	2.5	0.14	0.06
	1993	13132	2193	12	0.015	2E+12	1.9	0.03	0.02

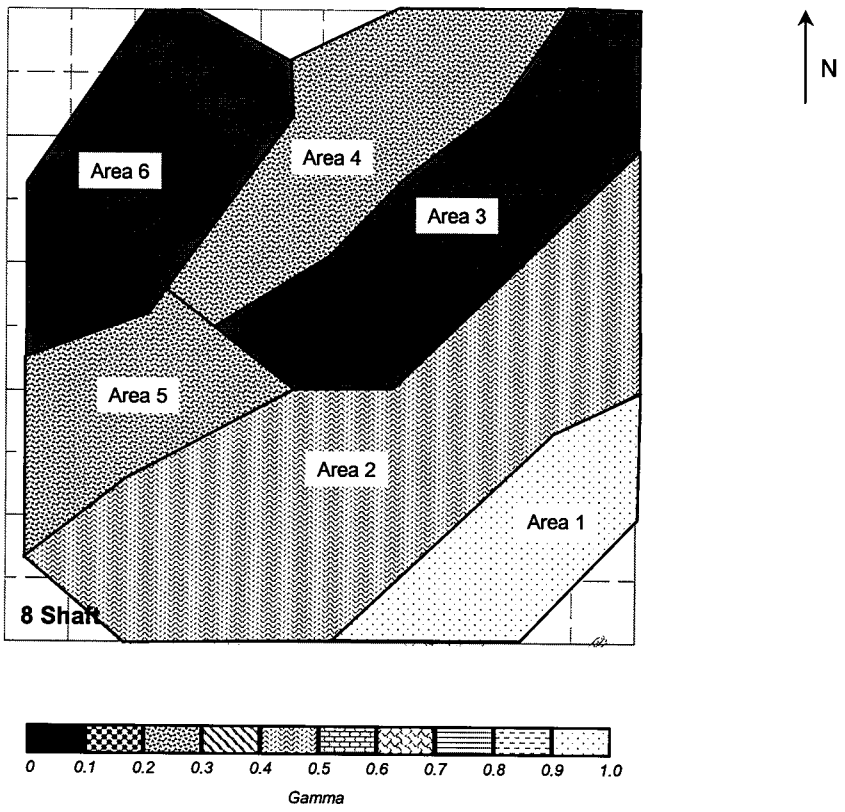

Figure 5.2.4.12 γ_E computed for Vaal Reefs G.M. 8 Shaft area.

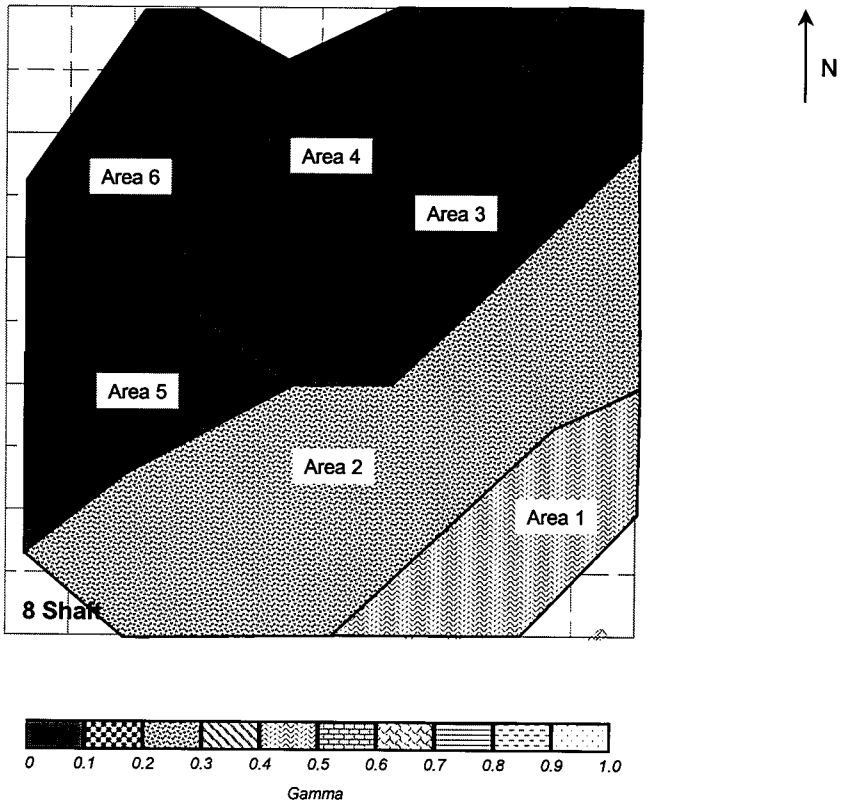

Figure 5.2.4.13 γ_R computed for Vaal Reefs G.M. 8 Shaft area.

Vaal Reefs G.M. 9 Shaft area

This area was divided into ten seismogenic volumes (Figure 5.2.4.14). The modelling and seismic parameters computed for each of the volumes for the 1990 – 1995 mining period, and for each mining step are given in Tables 5.2.4.9 and 5.2.4.10, respectively. The variation in γ_E and γ_R is shown diagrammatically in Figures 5.2.4.15 and 5.2.4.16.

The γ_E values of six of the ten seismogenic volumes (areas 1,2,3,4,7 and 8) are low, ranging from 0.01 to 0.30. The remaining areas show γ_E values ranging from moderate (0.64) to very high (1.34). The γ_R values of all ten seismogenic volumes are low, varying from 0.01 to 0.26.

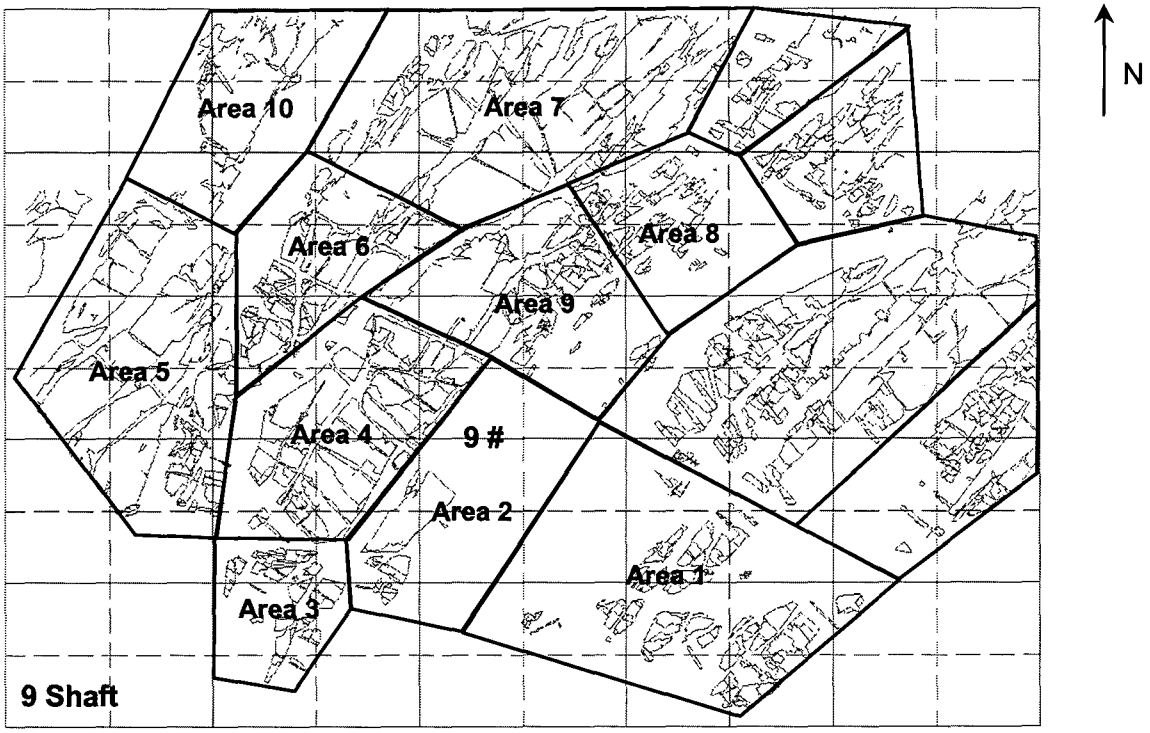

Figure 5.2.4.14 Seismogenic volumes defined for Vaal Reefs G.M. 9 Shaft area.

Table 5.2.4.9 Seismic parameters for Vaal Reefs G.M. 9 Shaft area.

Seismogenic Volume	Time Period	Area Mined m^2	ΔV_E m^3	Number Events	ΣR	ΣM_o N.m	Maximum Magnitude	γ_E	γ_R
9 Shaft Area									
Area 1	91 - 95	77571	23927	249	0.084	1.28E+13	2.5	0.02	0.01
Area 2	91 - 95	32955	28358	39	0.047	1.06E+13	2.4	0.01	0.01
Area 3	93 - 95	23491	14195	35	0.041	2.05E+13	2.8	0.05	0.01
Area 4	91 - 95	79937	52477	378	0.935	4.74E+14	3.4	0.30	0.06
Area 5	91 - 95	11154	2040	46	0.157	7.12E+13	3.1	1.16	0.26
Area 6	90 - 95	31603	17099	197	1.058	5.56E+14	3.4	1.08	0.21
Area 7	90 - 95	39377	24081	138	0.295	4.08E+13	3	0.06	0.04
Area 8	90 - 95	44954	18180	276	0.151	4.00E+13	2.8	0.07	0.03
Area 9	90 - 95	42419	12420	243	0.857	5.02E+14	3.3	1.34	0.23
Area 10	90 - 95	53742	12273	150	0.658	2.38E+14	3.3	0.64	0.18

Table 5.2.4.10 Seismic parameters for Vaal Reefs G.M. 9 Shaft area.

Seismogenic Volume	Mining Step	Area Mined m^2	ΔV_E m^3	Number Events	ΣR	ΣM_o N.m	Maximum Magnitude	γ_E	γ_R
9 Shaft Area									
Area 1	1991	17238	3461	5	0.007	2.4E+11	1.7	0.00	0.01
	1992	11492	5366	20	0.016	1.6E+12	1.8	0.01	0.01
	1993	32617	6549	180	0.012	6.6E+11	1.6	0.00	0.01
	1994	13013	7710	19	0.007	7.7E+11	1.7	0.00	0.00
	1995	3211	841	25	0.042	9.5E+12	2.5	0.38	0.17
Area 2	1991	19097	8495	3	0.008	1.3E+12	2	0.01	0.00
	1992	11830	15385	6	0.018	5.9E+12	2.4	0.01	0.00
	1993	1183	3609	15	0.004	2.9E+11	1.2	0.00	0.00
	1994	676	678	11	0.012	1.9E+12	2.1	0.09	0.06
	1995	169	191	4	0.005	1.2E+12	1.9	0.21	0.09
Area 3	1993	13858	9839	10	0.001	6.2E+10	1.1	0.00	0.00
	1994	6591	3915	5	0.003	4.7E+11	1.7	0.00	0.00
	1995	3042	441	20	0.037	2E+13	2.8	1.51	0.28
Area 4	1991	23660	7074	11	0.139	1.3E+14	3.3	0.61	0.07
	1992	25181	18483	45	0.109	2.8E+13	2.6	0.05	0.02
	1993	14872	17817	203	0.463	2.6E+14	3.4	0.48	0.09
	1994	15379	8489	93	0.127	2.3E+13	2.4	0.09	0.05
	1995	845	614	26	0.097	3.3E+13	2.8	1.78	0.52
Area 5	1991	3887	601	9	0.025	4.1E+12	2.3	0.23	0.14
	1992	4225	675	9	0.008	6.6E+11	1.5	0.03	0.04
	1993	2197	547	10	0.087	5.9E+13	3.1	3.58	0.53
	1994	676	161	5	0.004	3.7E+11	1.3	0.08	0.08
	1995	169	56	13	0.033	7.1E+12	2.4	4.21	1.96
Area 6	1990	11661	6720	8	0.168	6.7E+12	3.4	0.03	0.08
	1991	9464	5059	42	0.181	2.2E+13	3	0.14	0.12
	1992	5239	2463	91	0.154	2.7E+13	2.3	0.36	0.21
	1993	3211	1920	30	0.364	3.5E+14	3.4	6.06	0.63
	1994	1690	656	18	0.185	1.5E+14	3.3	7.60	0.94
	1995	338	281	8	0.006	6.6E+11	1.5	0.08	0.07
Area 7	1990	13013	5297	20	0.055	8.8E+12	2.4	0.06	0.03
	1991	6253	3974	29	0.105	3.8E+12	3	0.03	0.09
	1992	4056	2768	29	0.069	1.7E+13	2.5	0.20	0.08
	1993	9464	4233	31	0.025	3.4E+12	2.1	0.03	0.02
	1994	5746	6692	24	0.035	7.1E+12	2.3	0.04	0.02
	1995	845	1117	5	0.006	6.6E+11	1.8	0.02	0.02
Area 8	1990	9971	3254	3	0.013	2.8E+12	2.1	0.03	0.01
	1991	7774	4488	17	0.054	2.1E+13	2.8	0.16	0.04
	1992	6591	3348	15	0.03	5.8E+12	2.2	0.06	0.03
	1993	10647	2308	204	0.015	1.5E+12	1.8	0.02	0.02
	1994	8112	4110	25	0.027	5.9E+12	2.2	0.05	0.02
	1995	1859	672	12	0.012	3E+12	2.2	0.15	0.06
Area 9	1990	17238	7094	7	0.033	8.1E+12	2.5	0.04	0.02
	1991	8281	2721	58	0.559	3.7E+14	3.3	4.52	0.68
	1992	11154	1246	36	0.096	3.2E+13	2.8	0.85	0.26
	1993	3380	1013	95	0.137	8.7E+13	3.1	2.85	0.45
	1994	1521	279	33	0.014	1.6E+12	1.8	0.19	0.17
	1995	845	67	14	0.018	3E+12	2	1.49	0.89
Area 10	1990	10816	2661	3	0.039	2.1E+12	2.7	0.03	0.05
	1991	14196	2825	51	0.171	1.8E+13	2.6	0.21	0.20
	1992	15717	2923	22	0.248	1.7E+14	3.3	1.93	0.28
	1993	5577	2136	28	0.079	2.1E+13	2.4	0.33	0.12
	1994	5915	1396	32	0.077	1.7E+13	2.3	0.40	0.18
	1995	1521	332	14	0.044	1E+13	2.2	1.00	0.44

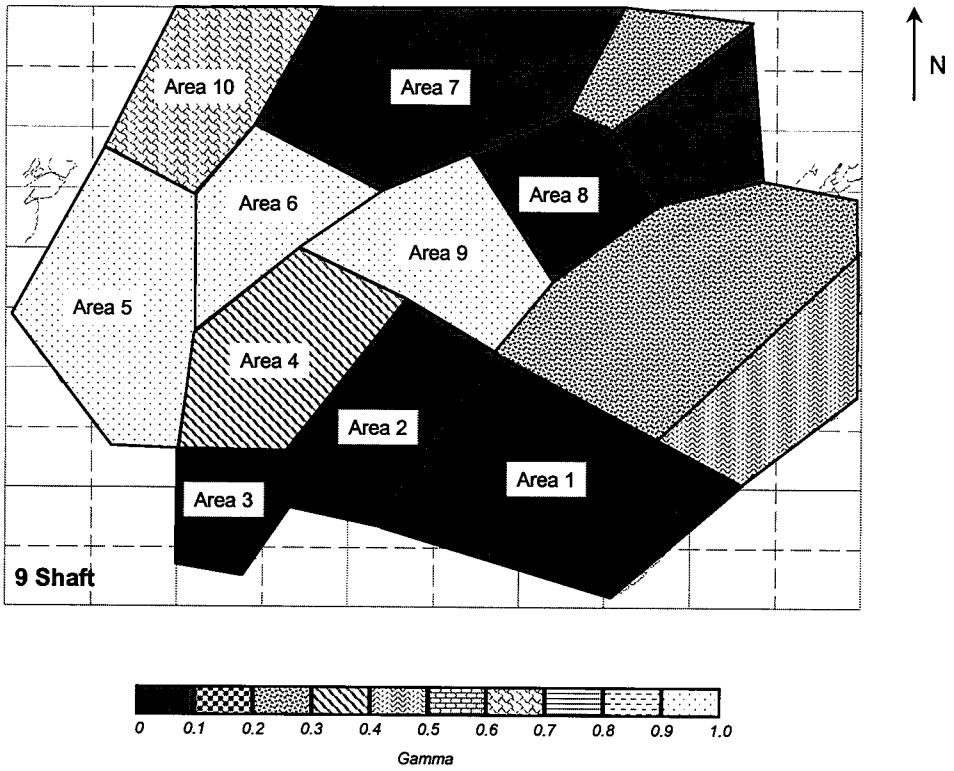

Figure 5.2.4.15 γ_E ***computed for Vaal Reefs G.M. 9 Shaft area (unlabelled areas belong to 8 Shaft).***

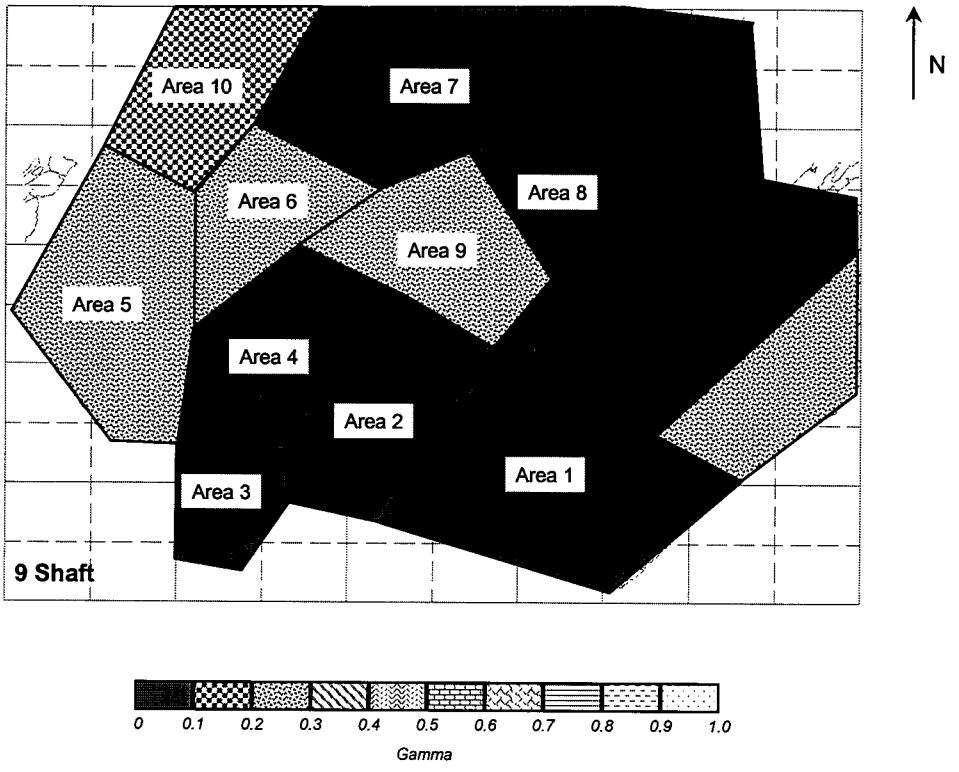

Figure 5.2.4.16 γ_R ***computed for Vaal Reefs G.M. 9 Shaft area (unlabelled areas belong to 8 Shaft).***

Vaal Reefs G.M. 11 Shaft area

This area was divided into three seismogenic volumes (Figure 5.2.4.17). The modelling and seismic parameters computed for each of the volumes for the 1990 – 1995 mining period, and for each mining step are given in Tables 5.2.4.11 and 5.2.4.12, respectively. The variation in γ_E and γ_R is shown diagrammatically in Figures 5.2.4.18 and 5.2.4.19.

The γ_E of two of the three seismogenic volumes are low (0.01 – 0.14). Area 1 shows a moderate γ_E value of 0.48. The γ_R values of three seismogenic volumes are very low, varying from 0.01 to 0.11.

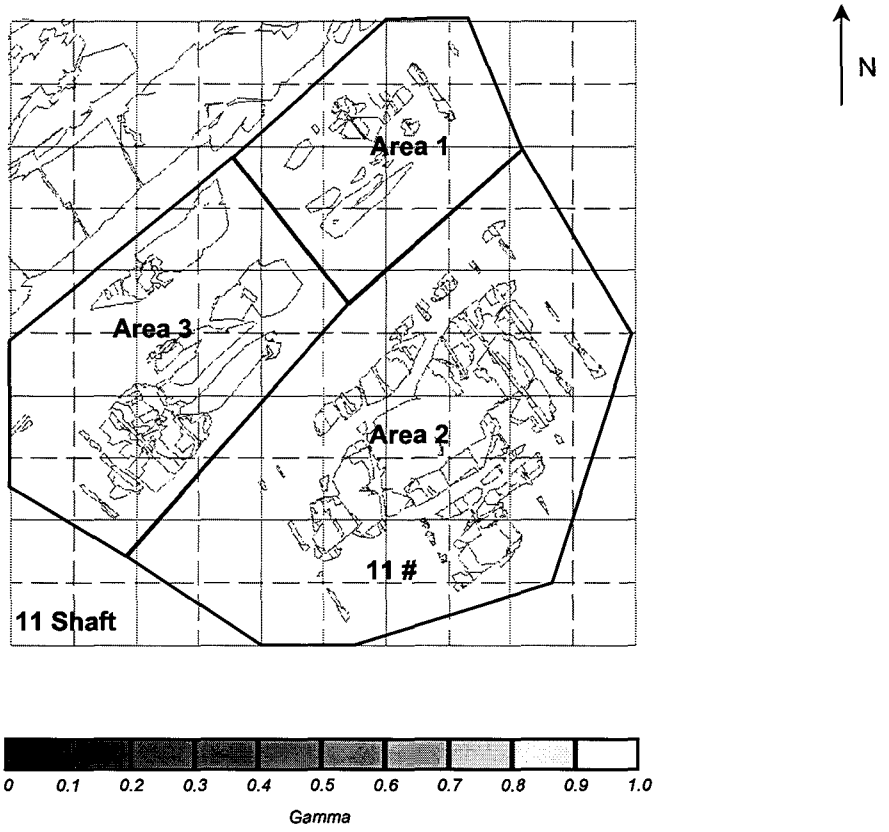

Figure 5.2.4.17 Seismogenic volumes defined for Vaal Reefs G.M. 11 Shaft area.

Table 5.2.4.11 Seismic parameters for Vaal Reefs G.M. 11 Shaft area.

Seismogenic Volume	Time Period	Area Mined m^2	ΔV_E m^3	Number Events	ΣR	ΣM_o N.m	Maximum Magnitude	γ_E	γ_R
11 Shaft Area									
Area 1	90 - 95	34272	4270	67	0.138	6.209E+13	2.9	0.48	0.11
Area 2	90 - 95	309168	90260	1499	1.157	3.832E+14	3.1	0.14	0.04
Area 3	90 - 95	179712	36377	198	0.119	6.38E+12	3	0.01	0.01

Table 5.2.4.12 Seismic parameters for Vaal Reefs G.M. 11 Shaft area.

Seismogenic Volume	Mining Step	Area Mined m^2	ΔV_E m^3	Number Events	ΣR	ΣM_o N.m	Maximum Magnitude	γ_E	γ_R
11 Shaft Area									
Area 1	1990	432	97	5	0.009	2.50E+12	2.2	0.86	0.31
	1991	1296	54	7	0.008	1.30E+12	2	0.79	0.49
	1992	4176	668	9	0.005	3.70E+11	1.5	0.02	0.02
	1993	8064	1081	21	0.003	1.50E+11	1.1	0.00	0.01
	1994	8352	1295	16	0.106	5.70E+13	2.9	1.46	0.27
	1995	11952	1076	9	0.007	7.70E+11	1.6	0.02	0.02
Area 2	1990	19728	15743	11	0.102	7.40E+13	3.1	0.16	0.02
	1991	47232	18987	29	0.128	8.20E+12	2.6	0.01	0.02
	1992	59328	16730	121	0.172	6.70E+13	3	0.13	0.03
	1993	85536	18048	832	0.208	7.20E+13	3.1	0.13	0.04
	1994	63216	14540	184	0.143	4.20E+13	2.8	0.10	0.03
	1995	34128	6211	322	0.404	1.20E+14	2.8	0.64	0.22
Area 3	1990	29664	3560	5	0.002	1.00E+11	1.5	0.00	0.00
	1991	31104	5412	12	0.063	1.20E+11	3	0.00	0.04
	1992	42624	8951	25	0.007	3.50E+11	1.2	0.00	0.00
	1993	24048	6613	105	0.025	2.00E+12	1.8	0.01	0.01
	1994	27648	4700	20	0.006	4.10E+11	1.4	0.00	0.00
	1995	24624	7141	31	0.016	3.40E+12	2.3	0.02	0.01

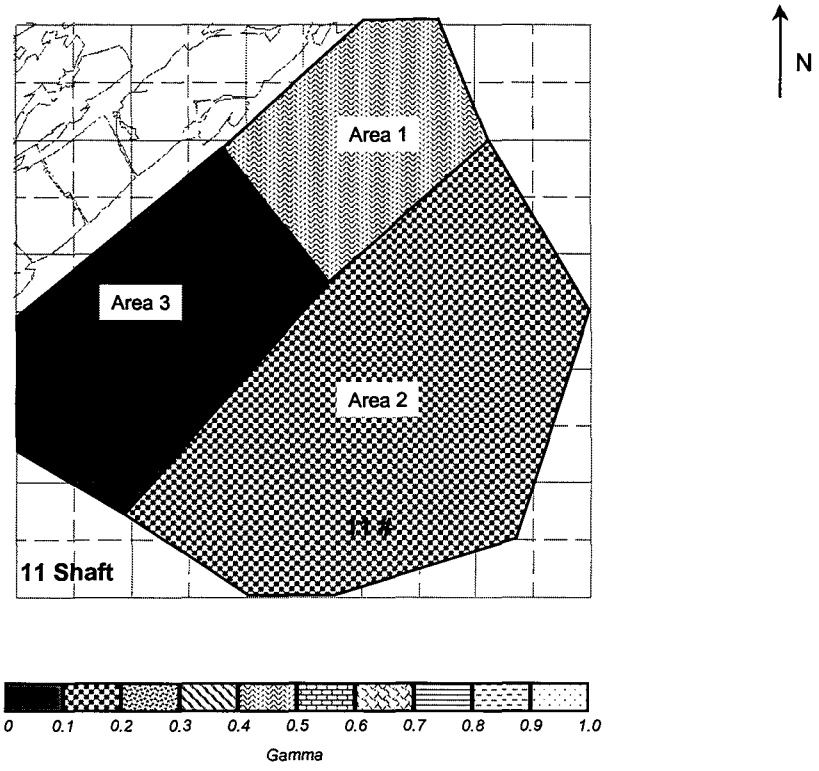

Figure 5.2.4.18 γ_E computed for Vaal Reefs G.M. 11 Shaft area.

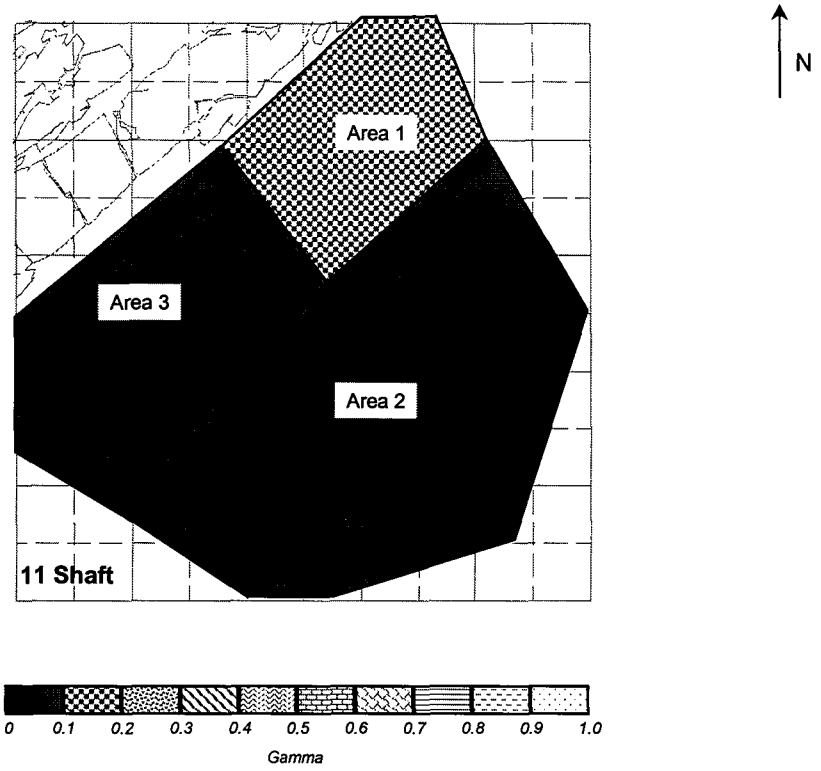

Figure 5.2.4.19 γ_R computed for Vaal Reefs G.M. 11 Shaft area.

Temporal parameter variation

The analysis of the change in seismic parameters with time is a recently developed innovation. In this approach, the parameters computed for each particular mining step (such as γ_E , γ_R, the total seismic moment for all events that occurred during that mining step and area mined during the time period) are plotted with respect to time (i.e. each yearly mining step). In the examples given, the γ_E parameter is not plotted because the same trends shown by γ_R are evident but are more extreme.

Vaal Reefs G.M. 2 shaft area

Some interesting correlations are evident when the parameters are studied with regard to time (i.e. mining step). The variation in the area mined, seismic moment and γ_R parameter with mining step is shown in Figures 5.2.4.20 and 5.2.4.21 for geotechnical classes 4 and 2, respectively.

In Figure 5.2.4.20, an increase in the area mined in 1991 correlates with a decrease in the cumulative seismic moment. Between 1992 and 1995, the area mined decreases steadily, and is accompanied by an increase in the seismic moment and increase in γ_R.

Figure 5.2.4.21 shows similar but more pronounced trends. There is a substantial increase in the cumulative seismic moment for the 1993 mining step when the area mined is decreased. In 1995, the large increase in the γ_R value results from the small area mined and low corresponding elastic convergence.

The above trends are illustrated in Figure 5.2.4.22, where the cumulative seismic moment (computed for each mining step) is plotted against the difference in the area mined (between successive mining steps) for both geotechnical classes in the area.

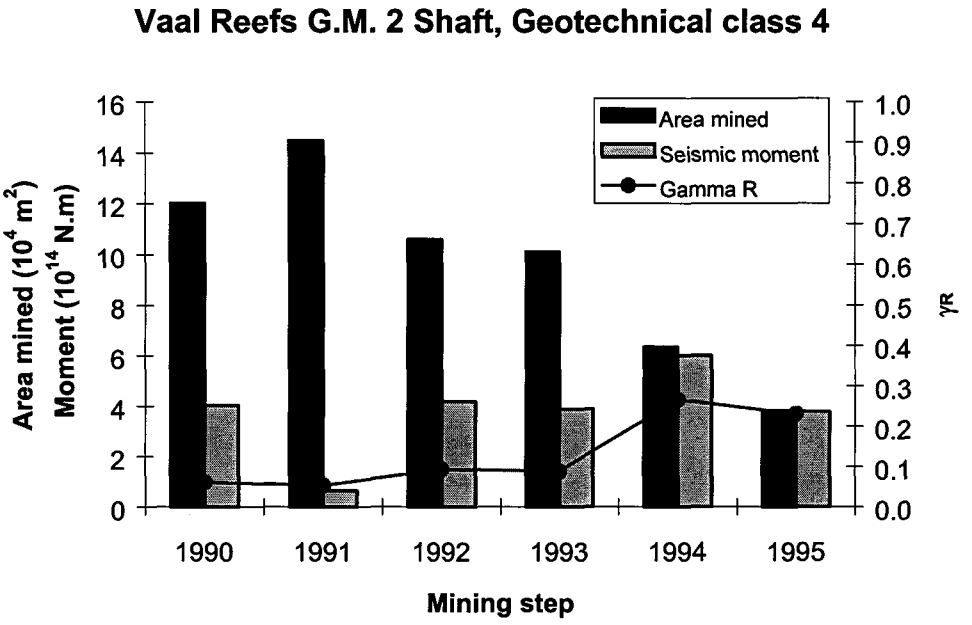

Figure 5.2.4.20 Variation of area mined, seismic moment and γ_R with mining step for Class 4 geotechnical area, Vaal Reefs G.M. 2 Shaft area.

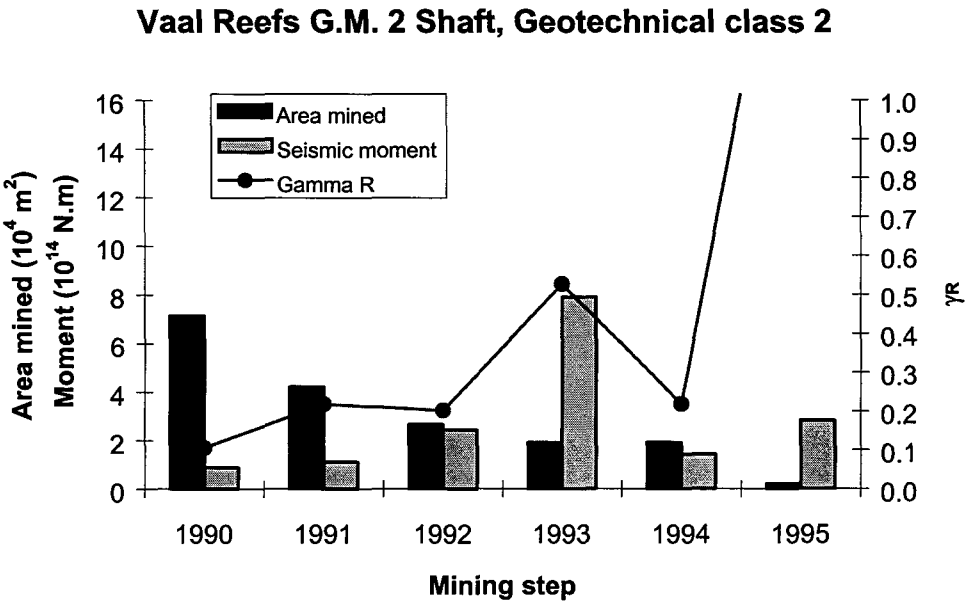

Figure 5.2.4.21 Variation of area mined, seismic moment and γ_R with mining step for Class 2 geotechnical area, Vaal Reefs G.M. 2 Shaft area.

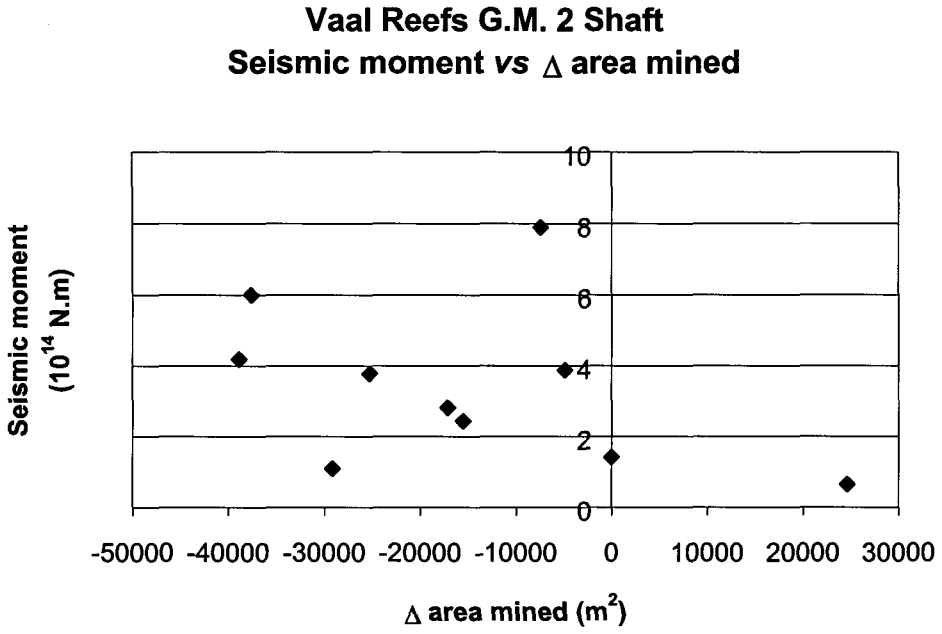

Figure 5.2.4.22 Graph of cumulative seismic moment (for each mining step) plotted against the difference in area mined (between successive mining steps) for Vaal Reefs G.M. 2 Shaft area.

Vaal Reefs 5 Shaft area

The variation in the area mined, seismic moment and γ_R parameter with mining step is shown in Figures 5.2.4.23 and 5.2.4.24 for geotechnical classes 4 and 6, respectively.

γ_R shows similar trends in Figures 5.2.4.23 and 5.2.4.24. When a large area is mined (between 1990–1994 and 1990–1992 in Figures 5.2.4.23 and 5.2.4.24, respectively) the γ_R values tends to be low. The increase in this parameter in 1995, in both cases, correlates with a sudden decrease in area mined. In both Figures, the lowest cumulative seismic moment of all the mining steps is found in the time period when the largest area of mining occurs (1990).

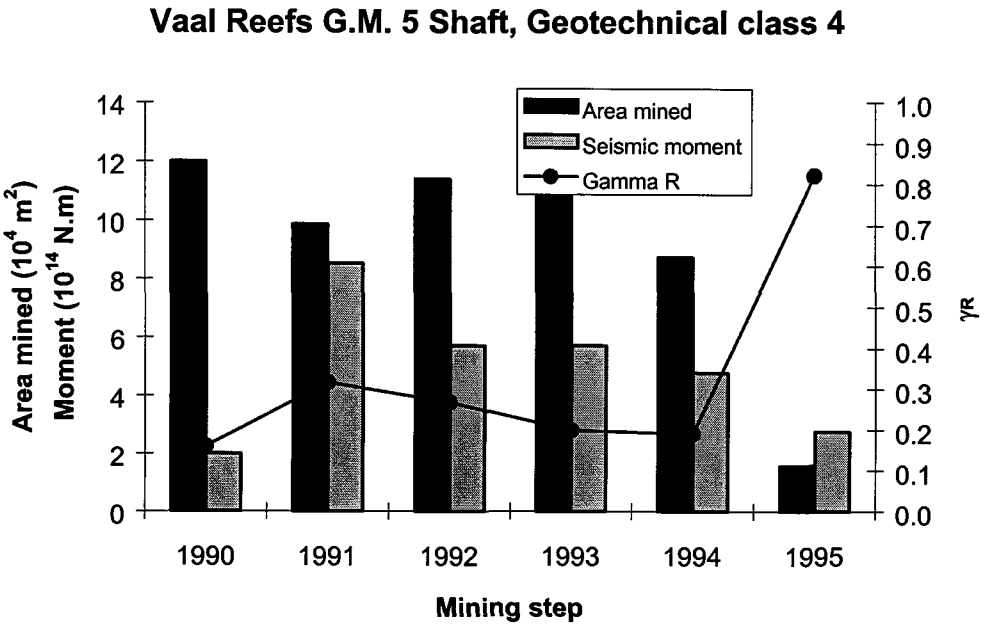

Figure 5.2.4.23 Variation of area mined, seismic moment and γ_R with mining step for Class 4 geotechnical area, Vaal Reefs G.M. 5 Shaft area.

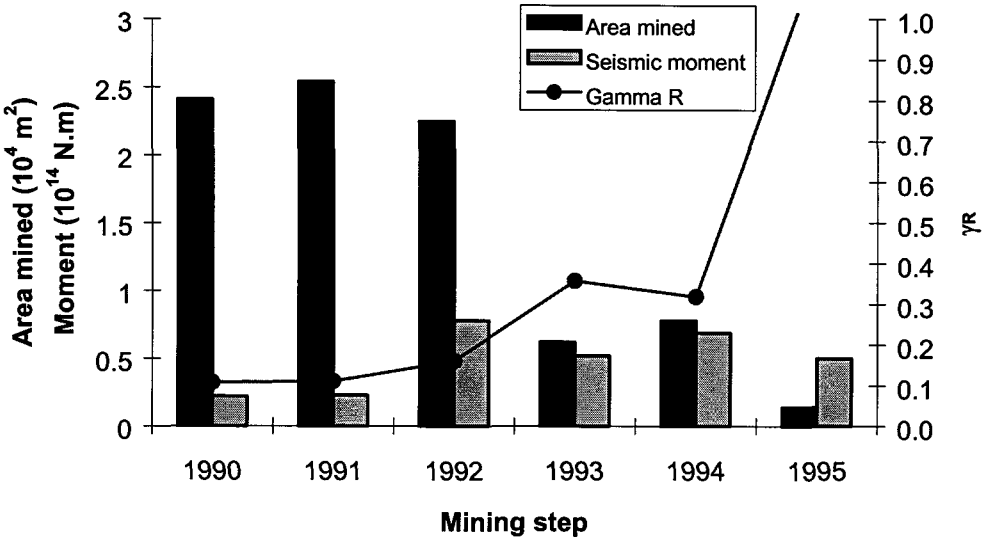

Figure 5.2.4.24 Variation of area mined, seismic moment and γ_R with mining step for Class 6 geotechnical area, Vaal Reefs G.M. 5 Shaft area.

Vaal Reefs 8 Shaft area

The parameter variation with time (mining step) for each geotechnical class is shown in Figures 5.2.4.25, 5.2.4.26 and 5.2.4.27 respectively. A decreasing general trend for γ_R accompanying a decrease in the area mined is evident in Figures 5.2.4.25 and 5.2.4.26. A slightly different trend is shown in Figure 5.2.4.27, where there is a slight increase in the γ_R value with a decrease in the mining area.

The decrease in the area mined for the time period 1990 – 1991 (Figure 5.2.4.26) and 1992 – 1993 (Figure 5.2.4.27) correlates with an increase in the cumulative seismic moment. This trend was also noted in the analysis of Vaal Reefs G.M. 2# and surrounds.

Vaal Reefs G.M. 9 Shaft

Only one geotechnical class (class 4) is present in the study area. Figure 5.2.4.28 shows the variation in parameters with mining step for geotechnical class 4. As observed in the case studies discussed so far, the lowest cumulative seismic moment of all the mining steps occurs during the time step where the largest area is mined (in this example, 1990). During the first three mining steps, an increase in the cumulative seismic moment correlates with a decrease in the area mined. There is a general decrease in area mined from 1990 to 1995, which is accompanied by an increase in the γ_R parameter.

Vaal Reefs G.M. 11 Shaft area

Only one geotechnical class (class 2) is present in the 11# study area. The variation in parameters with mining step is shown in Figure 5.2.4.29. Unlike the other areas studied thus far, there is an increase in the area mined from 1990 to 1993. γ_R remains more or less constant for this period. This parameter increases in 1994 and 1995, as the area mined decreases.

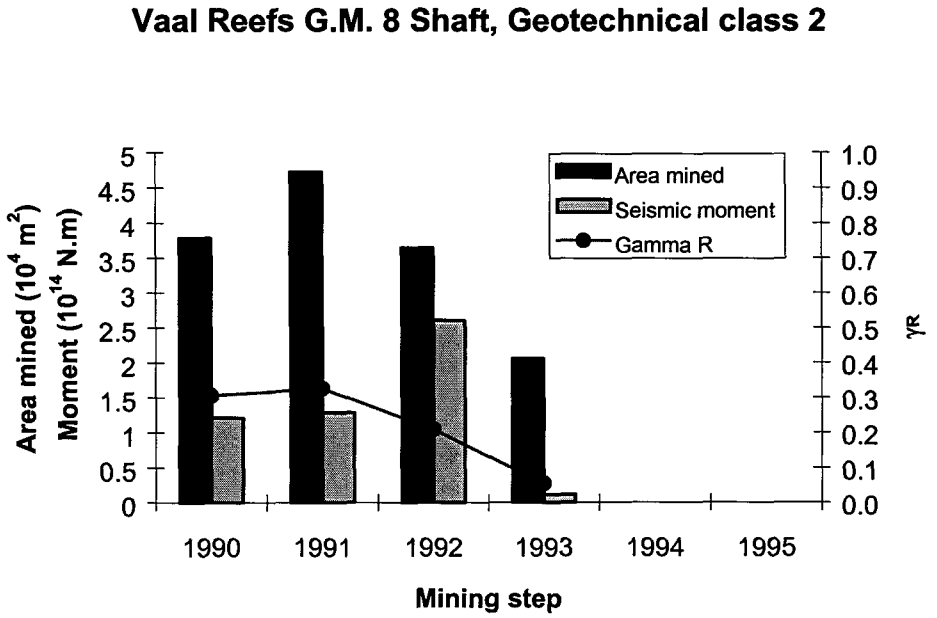

Figure 5.2.4.25 Variation of area mined, seismic moment and γ_R with mining step for Class 2 geotechnical area, Vaal Reefs G.M. 8 Shaft area.

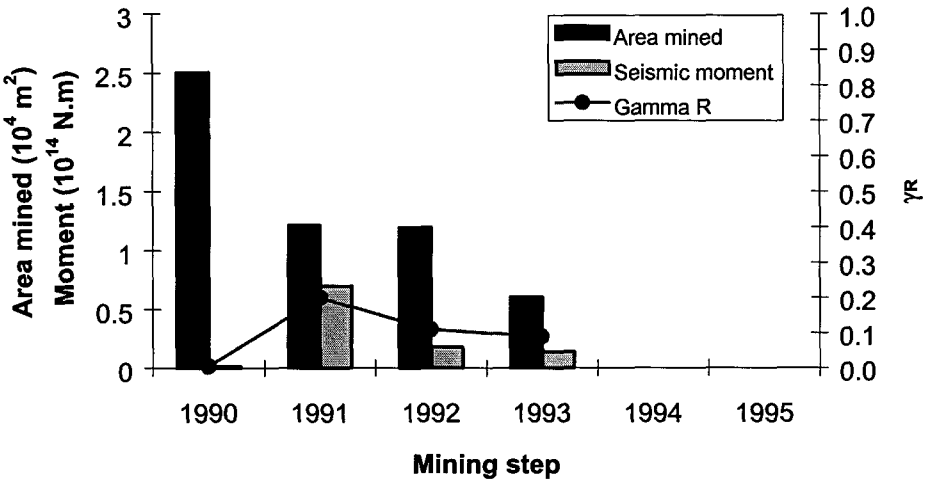

Figure 5.2.4.26 Variation of area mined, seismic moment and γ_R with mining step for Class 6 geotechnical area, Vaal Reefs G.M. 8 Shaft area.

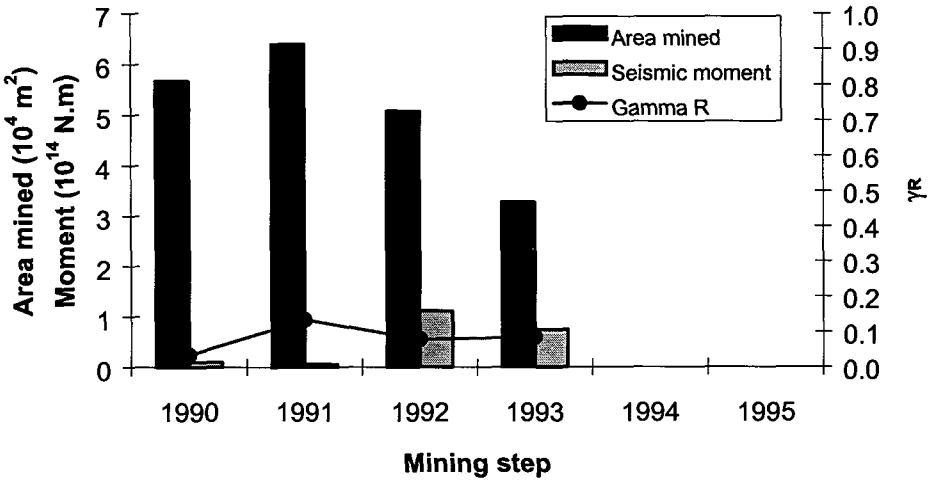

Figure 5.2.4.27 Variation of area mined, seismic moment and γ_R with mining step for Class 4 geotechnical area, Vaal Reefs G.M. 8 Shaft area.

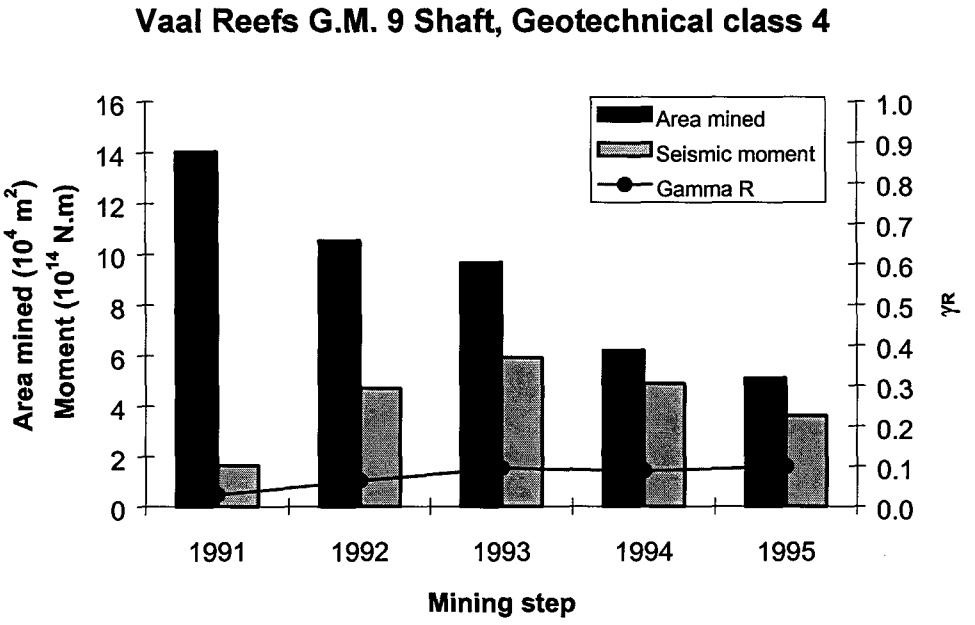

Figure 5.2.4.28 Variation of area mined, seismic moment and γ_R with mining step for Class 4 geotechnical area, Vaal Reefs G.M. 9 Shaft area.

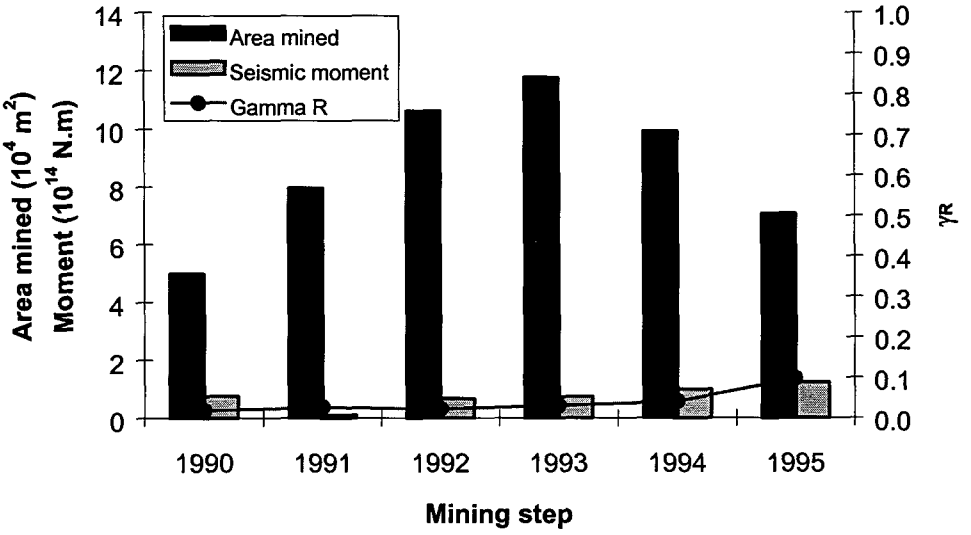

Figure 5.2.4.29 Variation of area mined, seismic moment and γ_R with mining step for Class 2 geotechnical area, Vaal Reefs G.M. 11 Shaft area.

5.2.4.5 Seismic parameters computed for Hartebeestfontein G.M.

Five geotechnical classes are present at Hartebeestfontein G.M (Figure 5.2.4.30). The area was divided into two strips for processing (Figure 5.2.4.31) and a total of 15 seismogenic volumes were defined (Figure 5.2.4.32). The volumes were delineated as far as possible according to the geotechnical classifications, event distribution and mining geometry.

Spatial parameter variation

To facilitate interpretation of the results, the seismogenic volumes are grouped according to the geotechnical classes present (Table 5.2.4.13). This grouping is used during the discussion of the results. Table 5.2.4.14 summarises the various quantities output from the numerical modelling and seismic analysis computed for the entire period of mining (1990 – 1995). Tables 5.2.4.15 and 5.2.4.16 summarise the parameters computed for each mining step. Figures 5.2.4.33 and 5.2.4.34 provide a diagrammatic representation of γ_E and γ_R computed for the seismogenic volumes.

Table 5.2.4.13 Geotechnical classes present in seismogenic volumes defined for Hartebeestfontein G.M.

Seismogenic volumes	Geotechnical classes
Areas 1, 2 and 14	Class 4 , class 5
Areas 3, 4, 7 and 15	Class 7
Areas 5, 6, 11 and 13	Class 4
Areas 8 and 9	Class 4, class 6
Area 10	Class 3
Area 12	Class 3, class 4

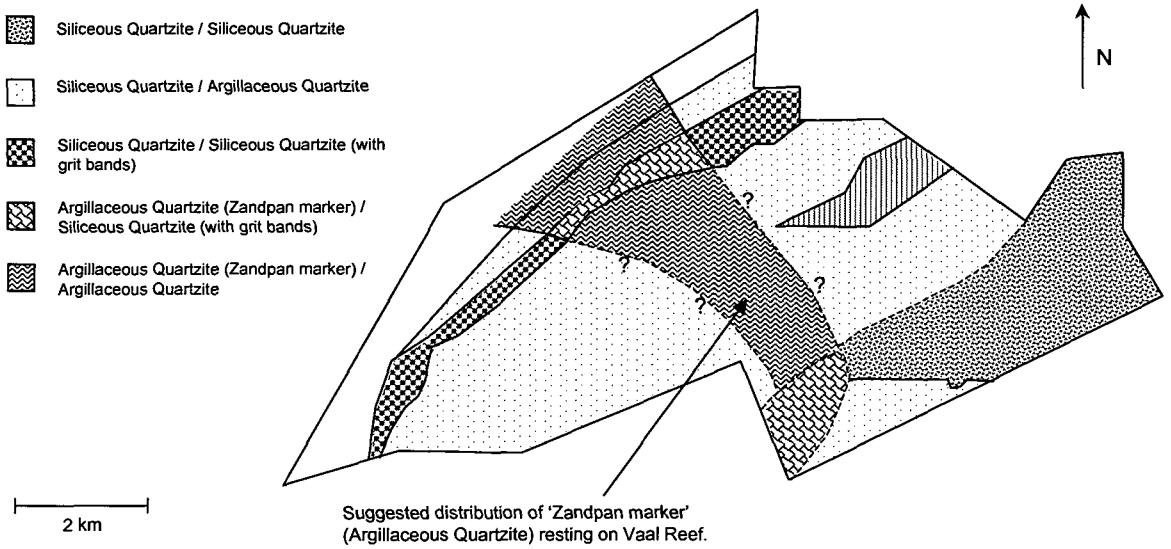

Figure 5.2.4.30 Geotechnical areas defined for the Vaal Reef at Hartebeestfontein G.M.

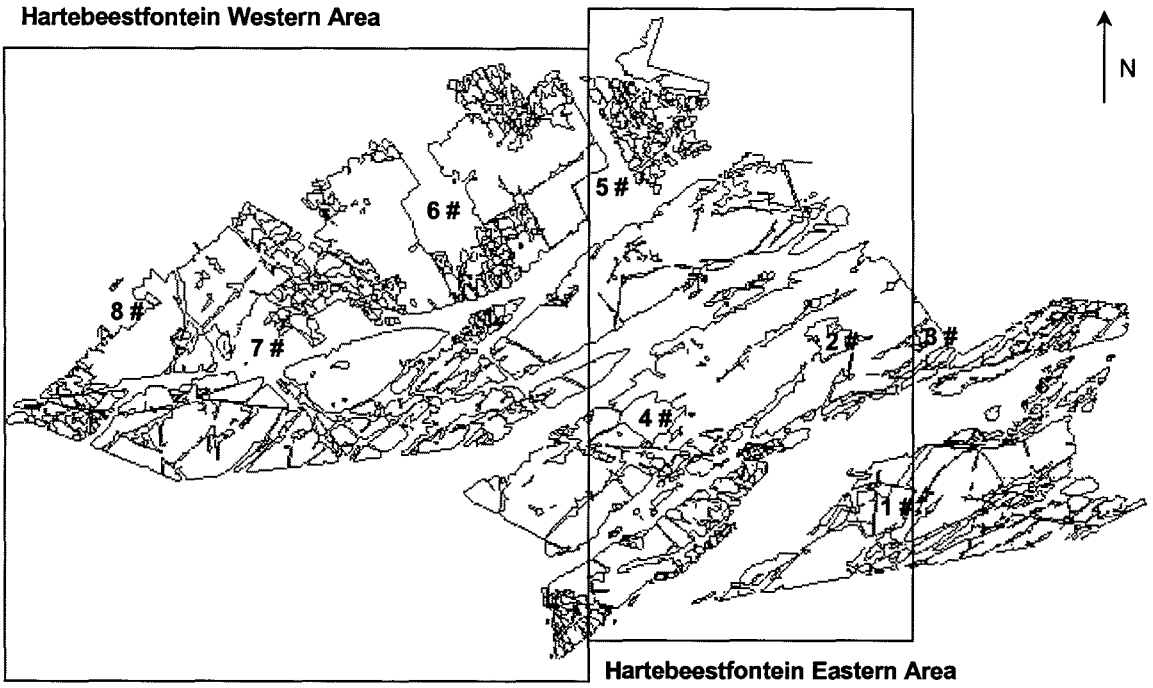

Figure 5.2.4.31 MINFFT processing strips for Hartebeestfontein G.M.

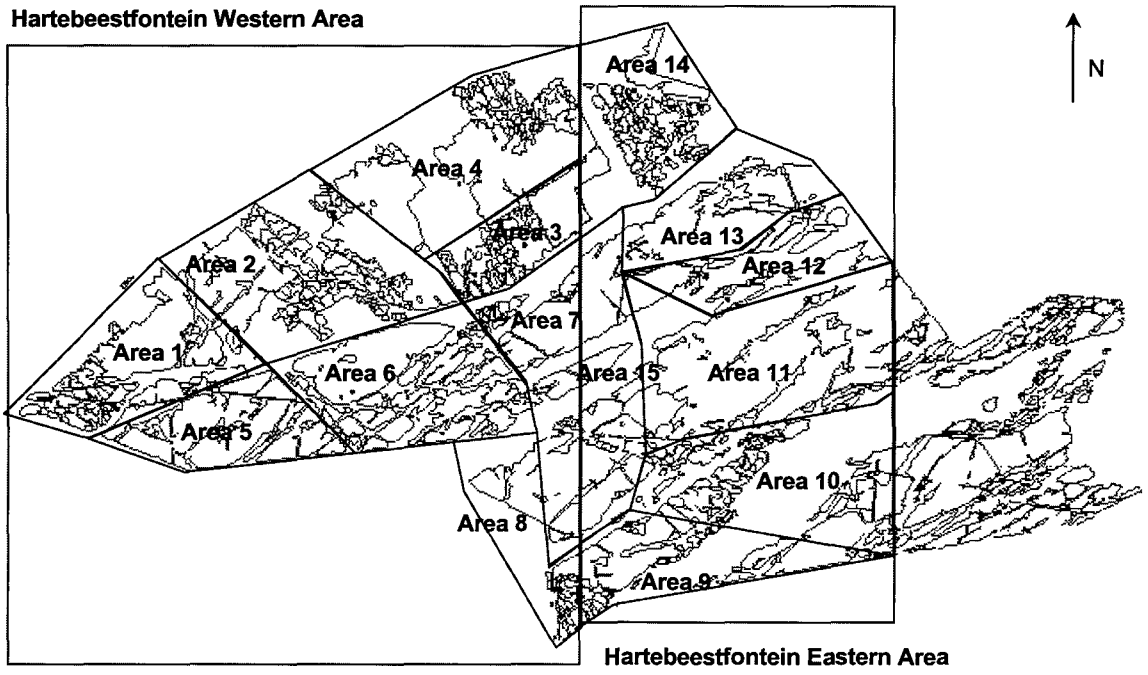

Figure 5.2.4.32 Seismogenic volumes defined for Hartebeestfontein G.M.

Table 5.2.4.14 Seismic parameters computed for Hartebeestfontein G.M.

Seismogenic Volume	Time Period	Area Mined m^2	ΔV_E m^3	Number Events	ΣR	ΣM_o N.m	Maximum Magnitude	γ_E	γ_R
Hartebeestfontein G.M.									
Area 1	90 - 95	221480	85389	1711	5.836	1.1E+15	4.01	0.41	0.23
Area 2	90 - 95	781648	359868	2989	6.792	7.3E+14	3.82	0.07	0.06
Area 3	90 - 95	248332	127613	3129	6.019	9.6E+14	4.11	0.25	0.16
Area 4	90 - 95	136024	82407	901	1.604	1.2E+14	3.12	0.05	0.06
Area 5	90 - 95	71540	28960	599	1.981	2.2E+14	3.71	0.25	0.23
Area 6	90 - 95	344176	86322	787	3.132	2.9E+14	3.61	0.11	0.12
Area 7	90 - 95	124264	53211	1072	4.014	7.6E+14	4.11	0.48	0.25
Area 8	90 - 95	27440	10785	1025	2.887	3.4E+14	3.6	1.05	0.89
Area 9	90 - 92	28616	6095	262	2.279	2.8E+14	3.84	1.52	1.24
Area 10	90 - 95	36260	13553	509	2.846	3.5E+14	3.66	0.85	0.70
Area 11	90 - 95	287532	90616	668	2.023	1.7E+14	3.2	0.06	0.07
Area 12	90 - 95	94276	19881	182	1.482	2.2E+14	3.84	0.37	0.25
Area 13	90 - 95	43904	23781	454	1.222	9.4E+13	3.09	0.13	0.17
Area 14	90 - 95	8820	15149	275	0.77	8.5E+13	3.25	0.19	0.17
Area 15	90 - 95	137788	42370	805	4.765	9.9E+14	4.25	0.78	0.37

Table 5.2.4.15 Seismic parameters computed for Hartebeestfontein G.M.

Seismogenic Volume	Mining Step	Area Mined m^2	ΔV_E m^3	Number Events	ΣR	ΣM_o N.m	Maximum Magnitude	γ_E	γ_R
Hartebeestfontein G.M.									
Area 1	1990	62916	23216	14	0.327	5.1E+13	3.71	0.07	0.05
	1991	70364	25683	129	1.122	1.8E+14	3.74	0.23	0.15
	1992	35280	16899	295	0.907	1.7E+14	3.73	0.33	0.18
	1993	27048	8168	1082	1.768	2.7E+14	3.36	1.10	0.72
	1994	10780	5476	88	1.16	3.0E+14	4.01	1.82	0.70
	1995	15092	5946	103	0.552	8.2E+13	3.43	0.46	0.31
Area 2	1990	98196	86707	90	0.376	8.4E+12	3.33	0.00	0.01
	1991	100156	54685	395	1.591	1.5E+14	3.82	0.09	0.10
	1992	167384	62267	735	1.758	2.0E+14	3.45	0.11	0.09
	1993	149156	50564	768	1.072	1.2E+14	3.56	0.08	0.07
	1994	121912	44376	405	0.842	9.3E+13	3.28	0.07	0.06
	1995	144844	61269	596	1.153	1.6E+14	3.63	0.09	0.06
Area 3	1990	67228	37715	72	1.603	5.5E+14	4.11	0.48	0.14
	1991	41160	22844	330	0.841	3.5E+13	3.27	0.05	0.12
	1992	48804	26647	771	1.355	1.3E+14	3.24	0.16	0.17
	1993	32144	15461	1059	1.409	1.8E+14	3.78	0.39	0.30
	1994	36652	16054	493	0.388	2.5E+13	3.05	0.05	0.08
	1995	22344	8893	404	0.423	3.7E+13	3.16	0.14	0.16
Area 4	1990	1764	10199	47	0.111	5.8E+12	2.52	0.02	0.04
	1991	38220	22473	175	0.33	4.5E+12	2.93	0.01	0.05
	1992	23128	16560	240	0.361	3.1E+13	3.12	0.06	0.07
	1993	11760	8397	203	0.386	4.2E+13	3.04	0.17	0.15
	1994	26068	11235	169	0.246	2.0E+13	2.81	0.06	0.07
	1995	35084	13542	67	0.17	1.9E+13	3.01	0.05	0.04
Area 5	1990	18816	6586	22	0.593	6.4E+13	3.71	0.32	0.30
	1991	20188	7429	121	0.247	1.1E+13	3.09	0.05	0.11
	1992	16464	7030	156	0.51	5.8E+13	3.41	0.27	0.24
	1993	11564	3215	111	0.158	1.5E+13	2.86	0.16	0.16
	1994	3136	2399	128	0.417	6.7E+13	3.51	0.93	0.58
	1995	1372	2301	61	0.056	3.3E+12	2.48	0.05	0.08
Area 6	1990	33124	11759	49	1.03	3.9E+13	3.61	0.11	0.29
	1991	62720	14990	120	0.479	9.3E+12	3.44	0.02	0.11
	1992	76244	21120	155	0.762	1.1E+14	3.43	0.17	0.12
	1993	22932	6903	136	0.495	9.2E+13	3.55	0.44	0.24
	1994	53508	8882	88	0.111	1.0E+13	2.79	0.04	0.04
	1995	95648	22669	239	0.255	2.8E+13	2.9	0.04	0.04
Area 7	1990	16268	12608	36	1.251	3.9E+14	4.11	1.03	0.33
	1991	15680	4798	134	0.281	4.0E+12	3.38	0.03	0.19
	1992	23324	15510	191	0.427	6.7E+13	3.61	0.14	0.09
	1993	20188	9347	220	0.615	9.1E+13	3.64	0.32	0.22
	1994	9408	2832	234	0.822	1.2E+14	3.45	1.41	0.96
	1995	39396	8116	257	0.618	9.2E+13	3.66	0.38	0.25
Area 8	1990	1960	2328	20	0.45	6.8E+13	3.6	0.97	0.64
	1991	2744	1995	99	0.44	2.2E+13	3.21	0.37	0.73
	1992	1372	731	115	0.795	1.0E+14	3.4	4.54	3.61
	1993	10388	1828	176	0.13	1.0E+13	2.6	0.18	0.24
	1994	7448	1542	321	0.679	9.1E+13	3.42	1.96	1.46
	1995	3528	2360	294	0.393	4.9E+13	3.18	0.69	0.55

Table 5.2.4.16 Seismic parameters computed for Hartebeestfontein G.M.

Seismogenic Volume	Mining Step	Area Mined m^2	ΔV_E m^3	Number Events	ΣR	ΣM_o N.m	Maximum Magnitude	γ_E	γ_R
Hartebeestfontein G.M.									
Area 9	1990	13720	2168	46	0.562	3.7E+13	3.24	0.57	0.86
	1991	14112	3570	104	0.862	4.2E+13	3.73	0.39	0.80
	1992	784	357	112	0.855	2.0E+14	3.84	18.63	7.96
	1993			115	0.59	1.2E+14	3.6		
	1994			41	0.095	1.1E+13	2.71		
	1995			78	0.789	1.8E+14	3.77		
Area 10	1990	9996	2979	14	0.466	9.2E+13	3.66	1.03	0.52
	1991	2352	1272	51	0.524	1.1E+13	3.64	0.29	1.37
	1992	6860	2092	106	0.252	2.3E+13	2.83	0.37	0.40
	1993	7252	3931	137	0.643	9.6E+13	3.48	0.81	0.54
	1994	2352	814	64	0.237	3.1E+13	2.97	1.27	0.97
	1995	7448	2465	137	0.724	9.5E+13	3.38	1.28	0.98
Area 11	1990	66052	17834	15	0.109	3.0E+12	2.96	0.01	0.02
	1991	65268	22452	67	0.298	1.3E+13	3.11	0.02	0.04
	1992	44688	14792	60	0.15	1.6E+13	2.91	0.04	0.03
	1993	53704	16917	126	0.322	2.6E+13	2.78	0.05	0.06
	1994	35084	10209	160	0.366	3.0E+13	2.65	0.10	0.12
	1995	22736	8412	240	0.778	8.0E+13	3.2	0.32	0.31
Area 12	1990	3332	1979	4	0.03	4.5E+11	2.62	0.01	0.05
	1991	7448	2443	23	0.159	1.0E+13	2.94	0.14	0.22
	1992	32928	5400	24	0.065	4.7E+12	2.67	0.03	0.04
	1993	21364	4337	56	0.424	7.1E+13	3.36	0.54	0.32
	1994	8820	2725	40	0.65	1.2E+14	3.84	1.46	0.79
	1995	20384	2996	35	0.154	1.5E+13	2.68	0.17	0.17
Area 13	1990	6860	5680	10	0.023	1.5E+12	2.29	0.01	0.01
	1991	9604	3573	36	0.158	4.0E+12	2.91	0.04	0.15
	1992	6860	3307	55	0.19	2.2E+13	3.09	0.22	0.19
	1993	8428	5369	58	0.119	8.9E+12	2.76	0.06	0.07
	1994	7252	4329	146	0.293	2.2E+13	2.7	0.17	0.22
	1995	4900	1524	149	0.439	3.6E+13	2.79	0.78	0.96
Area 14	1990	3136	4786	16	0.105	1.1E+13	2.94	0.08	0.07
	1991	2352	3657	29	0.027	8.2E+11	1.93	0.01	0.02
	1992	784	1083	38	0.152	1.2E+13	2.72	0.37	0.47
	1993	1176	2246	69	0.167	1.6E+13	3.01	0.24	0.25
	1994	980	1602	74	0.097	7.9E+12	2.76	0.16	0.20
	1995	392	1775	49	0.222	3.7E+13	3.25	0.69	0.42
Area 15	1990	30380	8567	51	0.511	8.4E+13	3.6	0.33	0.20
	1991	20384	8419	174	0.456	4.2E+13	3.41	0.17	0.18
	1992	23324	7510	140	0.502	5.6E+13	3.15	0.25	0.22
	1993	33908	9596	125	1.394	3.3E+14	3.87	1.14	0.48
	1994	15288	4158	111	0.524	8.0E+13	3.47	0.64	0.42
	1995	14504	4119	204	1.378	4.0E+14	4.25	3.23	1.11

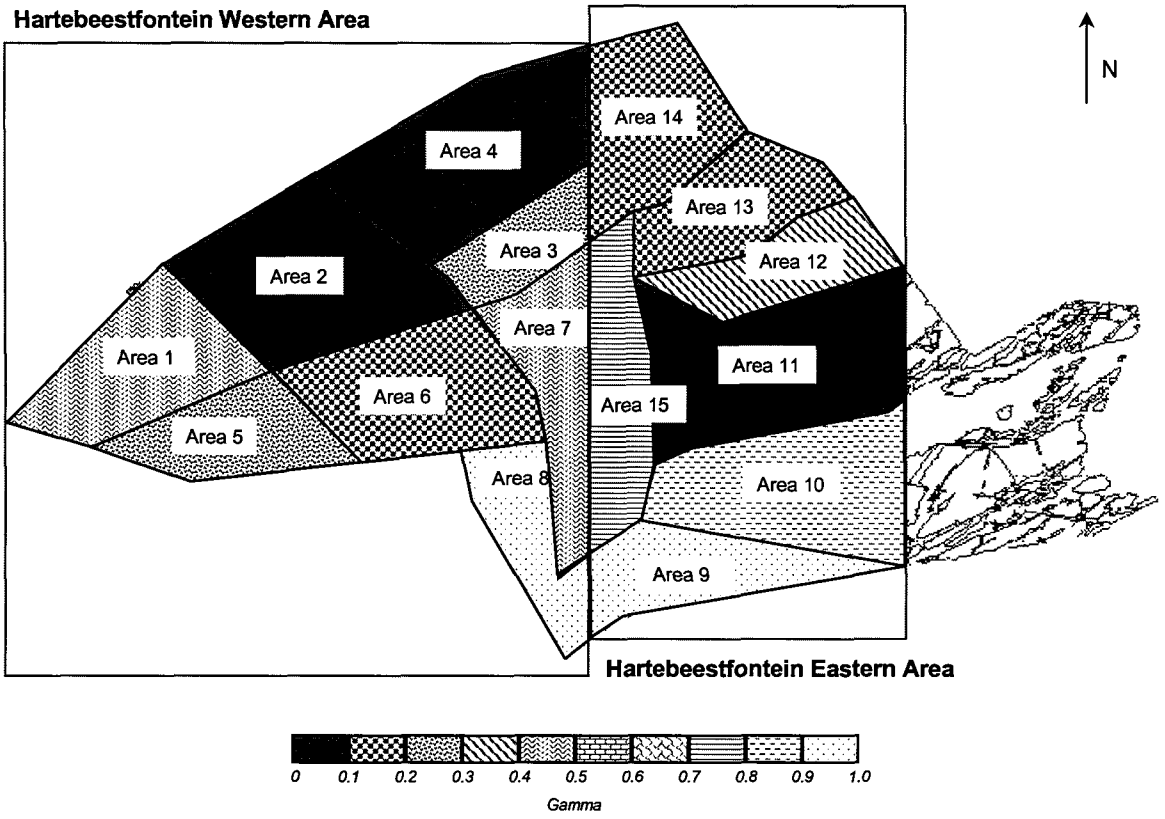

Figure 5.2.4.33 γ_E ***computed for Hartebeestfontein G.M.***

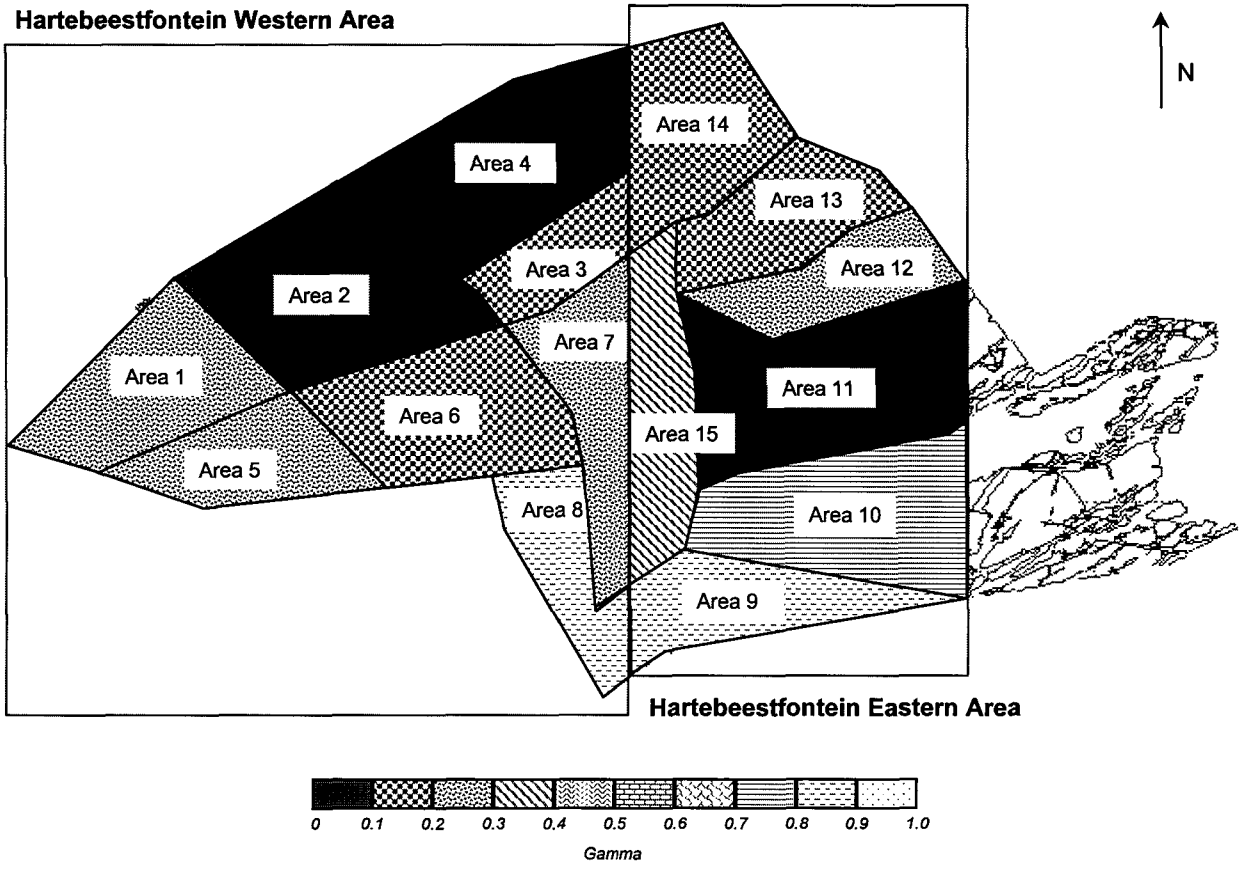

Figure 5.2.4.34 γ_R ***computed for Hartebeestfontein G.M.***

Areas 1, 2 and 14

These three seismogenic volumes (areas 1, 2 and 14) lie mostly within geotechnical class 4. Class 5 occurs on the outer edge of the basin, along the northern edges of the areas. The γ_E parameter for area 1 is moderate (0.41) and low for the remaining two areas (0.07 and 0.19). γ_R for all three areas is low, ranging from 0.06 to 0.23.

Areas 3, 4, 7 and 15

These areas are situated within geotechnical class 7. The γ_E parameter for areas 3 and 4 is low (0.05 – 0.25), while areas 7 and 15 show this parameter to vary from moderate values (0.48) to high (0.78). The γ_R parameter for all areas is low, ranging from 0.06 to 0.37.

Areas 5, 6, 11 and 13

Four seismogenic volumes are situated within geotechnical class 4. Both γ_E and γ_R, for all four areas, are low varying from 0.06 – 0.25 and 0.07 – 0.23, respectively.

Areas 8 and 9

Areas 8 and 9 are located within geotechnical classes 4 and 6. The γ_E parameter is very high for both areas, ranging from 1.05 to 1.52. γ_R is also high and varies from 0.89 to 1.14. Both of these areas are situated on the boundary between Vaal Reefs G.M. and Hartebeestfontein G.M.

Area 10

Area 10 is situated within geotechnical class 3. Both γ_E and γ_R are high, having values of 0.85 and 0.7, respectively.

Area 12

Area 12 is located in geotechnical classes 3 and 4. Both γ_E and γ_R are low, having values of 0.37 and 0.25, respectively.

Temporal parameter variation

Graphs showing the variation of the seismic moment, mining area and γ_R with mining step are plotted for each of the 15 seismogenic volumes. For brevity, each of these graphs is not included in the text, but in Appendix C (Figures C-1 to C-15). The main trends are summarised in the first part of this section.

In the latter part of this section, summary graphs are compiled showing the parameter variation for a particular geotechnical class, i.e. the contributions to the seismic moment and area mined from all seismogenic volumes, defined within a particular geotechnical class, are used to compute the γ_R parameter. These graphs are given in the appendix (Figures C-16 to C-20).

Parameter variation for each seismogenic volume

The main trends evident in Figures C-1 to C-15 are summarised as follows:

- A decrease in the area mined is accompanied by an increase in the cumulative seismic moment and γ_R. This inverse relationship is illustrated very clearly in the following

seismogenic volumes: area 1 (1991 – 1994), area 4 (1991 – 1995), area 11 (1990 – 1995), area 12 (1992 – 1995), and area 15 (1993 – 1995).

- A similar inverse relationship, although not as clear as the examples given above, may be observed in: area 5 (1990 – 1994), area 6 (1990 – 1995) and area 13 (1991-1995).

- The highest cumulative seismic moment of all times steps associated with the lowest area mined. This inverse relationship is well illustrated in: area 7 (1990, 1995), area 8 (1992, 1993) and area 15 (1995).

- Large cumulative seismic moment observed after the cessation of mining. In the case of area 9, large cumulative seismic moments occur after mining activities, cease for that particular seismogenic volume, after 1992.

Parameter variation with geotechnical area

Figures C-16 to C-20 show the variation in seismic moment, area mined and γ_R with geotechnical class. These graphs are included for completion purposes, but did not lead to any new insights.

5.2.4.6 Discussion

To simplify the task of comparing γ_E and γ_R values computed for all the study areas thus far, while considering the geotechnical classifications, it was necessary to identify the general trend of each study area as a whole. This simplification obviously adds a certain amount of subjectivity to the interpretation. Qualitative terms such as high, low, poor etc. are used (Figure 5.2.4.35).

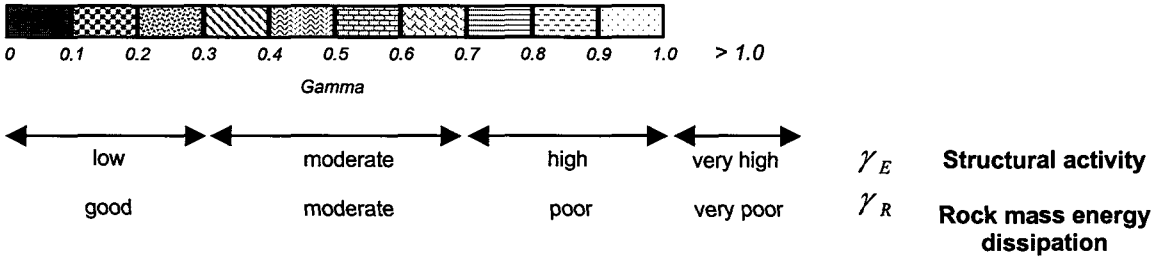

Figure 5.2.4.35 Qualitative gamma scale.

The magnitude of the γ_E value for the seismogenic volumes was used to quantify the structural activity (movement on faults and dykes etc.) present. For example, high γ_E (when γ_E ~ 1) implies high structural activity due to active faulting.

The γ_R parameter was used to evaluate the ability of the rock mass itself to dissipate energy on a smaller scale, due to the properties of the lithology and presence of small scale structures (such as partings associated with bedding planes or pebble bands) within the rock mass. Low γ_R would imply efficient energy dissipation, and therefore the release of strain energy within the rock mass itself.

The results for Vaal Reefs G.M. and Hartebeestfontein G.M using this qualitative approach are summarised in Tables 5.2.4.17 and 5.2.4.18, respectively.

Table 5.2.4.17 Qualitative summary of γ_E and γ_R parameters computed for Vaal Reefs G.M.

Seismogenic volume	Geotechnical class	γ_E	Structural activity	γ_R	Rock mass energy dissipation
Vaal Reefs 2#					
1	4	0.14	low	0.05	good
2	4	0.73	high	0.10	good
3	4	0.07	low	0.03	good
4	2	0.88	high	0.19	good
5	2	0.70	high	0.10	good
6	2	0.94	high	0.33	moderate
7	2	1.21	very high	0.17	good
Vaal Reefs 5#					
1	6	0.37	moderate	0.19	good
2	4	0.61	moderate	0.19	good
3	4	0.45	moderate	0.23	good
4	4	0.60	moderate	0.17	good
5	4	1.45	very high	0.55	moderate
Vaal Reefs 8#					
1	1	1.49	very high	0.42	moderate
2	2	0.43	moderate	0.24	good
3	2	0.02	low	0.02	good
4	4	0.28	low	0.08	good
5	3	0.28	low	0.08	good
6	4	0.04	low	0.08	good
Vaal Reefs 9#					
1	4	0.02	low	0.01	good
2	4	0.01	low	0.01	good
3	4	0.05	low	0.01	good
4	4	0.30	low	0.06	good
5	4	1.16	very high	0.26	good
6	4	1.08	very high	0.21	good
7	4	0.06	low	0.04	good
8	4	0.07	low	0.03	good
9	4	1.34	very high	0.23	good
10	4	0.64	moderate	0.18	good
Vaal Reefs 11#					
1	2	0.48	moderate	0.11	good
2	2	0.14	low	0.04	good
3	2	0.01	low	0.01	good

Table 5.2.4.18 Qualitative summary of γ_E and γ_R parameters computed for Hartebeestfontein G.M.

Seismogenic volume	Geotechnical class	γ_E	Structural activity	γ_R	Rock mass energy dissipation
Hartebeestfontein					
1	4 & 5	0.41	moderate	0.23	good
2	4 & 5	0.07	low	0.06	good
14	4 & 5	0.19	low	0.17	good
3	7	0.25	low	0.16	good
4	7	0.05	low	0.06	good
7	7	0.48	moderate	0.25	good
15	7	0.78	high	0.37	moderate
5	4	0.25	low	0.23	good
6	4	0.11	low	0.12	good
11	4	0.06	low	0.07	good
13	4	0.13	low	0.17	good
8	4 & 6	1.05	very high	0.89	poor
9	4 & 6	1.52	very high	1.24	very poor
10	3	0.85	high	0.70	poor
12	3 & 4	0.37	moderate	0.25	good

Spatial variation of parameters with geotechnical area

Vaal Reefs G.M. 2 Shaft area

The regions studied in the Vaal Reefs 2 # area lie within two geotechnical classes (class 2 and 4), both of which have siliceous quartzite in the hangingwall and argillaceous quartzite in the footwall (in class 2, pebble bands are associated with the argillaceous quartzite).

γ_E in excess of 1 implies that there is a source of seismic energy, in addition to the seismicity generated by mining. The high seismic activity of particular seismogenic volumes of Vaal Reefs G.M. 2# is attributed to displacement on the numerous intersecting faults and dykes (in particular, back area seismic activity on the Clemcor Dyke). In addition, the competent siliceous quartzite, occurring in the hangingwall of both geotechnical classes is capable of storing high stain energies and is potentially more seismically active (McGarr, 1971, van der Heever, 1982).

The γ_R in this area are low implying efficient release of strain energy within the rock mass. The relatively incompetent lithology in the footwall (the argillaceous quartzite) allows efficient energy dissipation. This effect is enhanced by small-scale slip along the parting planes associated with the pebble bands found in the argillaceous quartzite in the footwall.

Vaal Reefs G.M. 8 Shaft and 11 Shaft area

These areas are located predominantly within geotechnical class 2, which consists of siliceous quartzite in the hangingwall, overlying argillaceous quartzite containing polymictic pebble bands in the footwall. Associated with the pebble bands in the argillaceous quartzite are parting planes. Also present, but less widespread are geotechnical classes 3 and 4, both of which have

siliceous quartzite in the hangingwall, but either siliceous (class 3) or argillaceous (class 4) in the footwall.

The low γ_E of all seismogenic volumes (with the exception of Vaal Reefs G.M. 8#, area 1) indicates a low level of seismic activity, with a low structural contribution to the cumulative moment due to faulting. The γ_R is also low, implying efficient energy dissipation by the rock mass.

The low γ_E and γ_R is attributed to the relatively incompetent argillaceous quartzites of classes 2 and 4 in the footwall that are not capable of storing excessive strain energy, and to small-scale slip along the parting planes associated with the pebble bands.

The very high γ_E and moderate γ_R of area 1 (8#) could be due to the influence of geotechnical class 1, the so-called 'MISPAH' where competent lithologies are present in both hangingwall and footwall (siliceous quartzite overlies siliceous pebbly conglomerate in the footwall).

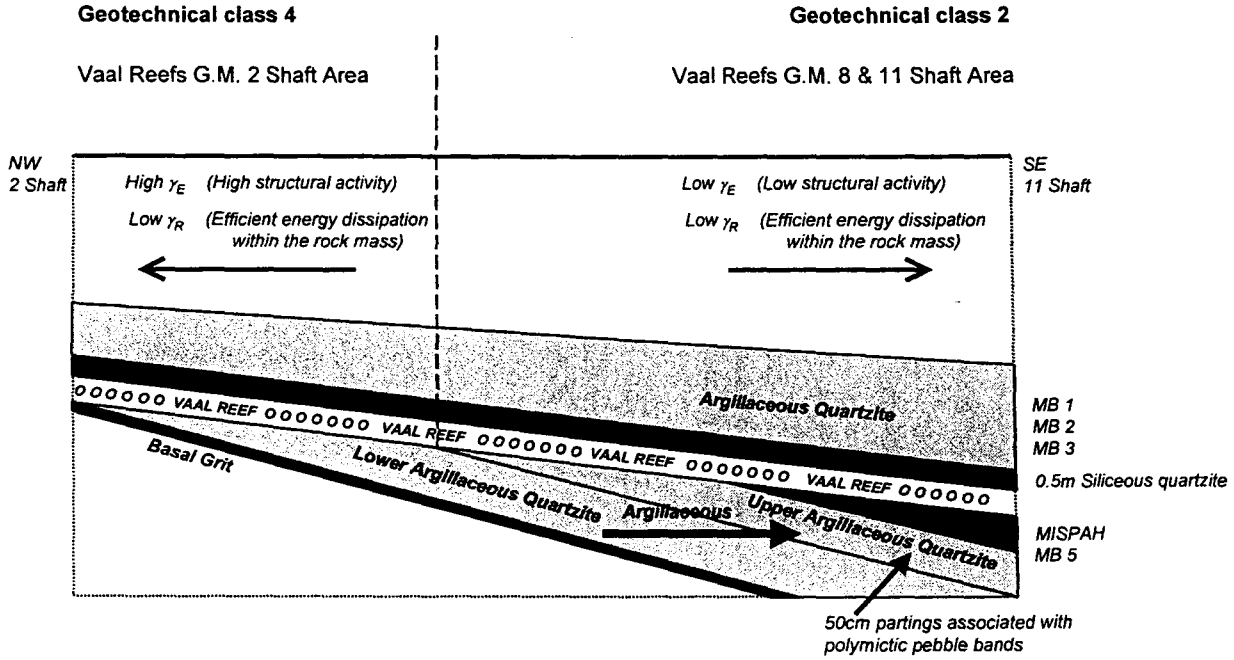

Figure 5.2.4.36 Schematic section showing the variation of γ_E and γ_R with geotechnical class at Vaal Reefs G.M.

Vaal Reefs G.M. 9 Shaft area

This area lies entirely within geotechnical class 4 consisting of siliceous quartzite in the hangingwall, overlying argillaceous quartzite in the footwall.

The γ_E parameter is variable, indicating that different seismogenic volumes have differing degrees of structural activity. The high γ_E indicate that the large-scale geological features in the area (faults and dykes) have a large contribution to the overall seismicity. In addition, as mentioned before, the competent siliceous quartzite in the hangingwall stores high stain energies and is potentially more seismically active.

In contrast to the variable structural activity of the area, the γ_R values are all low, indicating efficient dissipation of strain energy on small scale structures present in the relatively less competent argillaceous quartzite in the footwall.

A schematic cross-section (Figure 5.2.4.36) was drawn from Vaal Reefs G.M. 2#, through the 8# area, ending at 11# (from NW to SE, along dip of the Vaal Reef) to illustrate the variation of the γ_E and γ_R parameters with geotechnical area.

Hartebeestfontein G.M. geotechnical class 3 (Area 10)

In the discussion relating to Vaal Reefs G.M., the spatial parameter variation is discussed with regard to processing strip, each of which were named after the nearest shaft in the area. In this section, however, the variation is discussed according to a particular geotechnical class.

In geotechnical class 3 siliceous quartzite is present in both the hangingwall and footwall. Both the γ_E and γ_R computed for this area are high and are attributed to structural activity on the large scale geological features (faults and dykes) which contributes substantially to the overall seismicity. The competent siliceous quartzite in both hangingwall and footwall is capable of storing high strain energies and is therefore potentially more seismically active. As a result, the energy dissipation within the rock mass itself is poor.

Hartebeestfontein G.M. geotechnical class 4 (Areas 5, 6, 11 and 13)

This geotechnical class is widespread in the Hartebeestfontein gold mining district. In this class, siliceous quartzite occurs in the hangingwall overlying an argillaceous quartzite in the footwall.

Both γ_E and γ_R are low, indicating that the geological features present in the area contribute little to the level of seismic activity, and that a relatively incompetent lithology is present, which is not capable of storing excessive strain energy. This effect is attributed to the presence of the argillaceous quartzite in the footwall.

Hartebeestfontein G.M. geotechnical class 3 and 4 (Area 12)

Area 12 is situated in a geotechnical class where siliceous quartzite in the hangingwall overlies intercalated siliceous and argillaceous quartzite the footwall.

γ_E is moderate, implying a moderate level of structural activity in the area. This is possibly a result of higher structural activity in the areas where siliceous quartzite occurs in both the hangingwall and footwall.

γ_R is low, and implying efficient energy dissipation within the rock mass, which occurs where argillaceous quartzite is present in the footwall.

Hartebeestfontein G.M. geotechnical classes 4 and 5 (Areas 1, 2 and 14)

These areas span two geotechnical classes, where siliceous quartzite occurs in the hangingwall, and either argillaceous quartzite (class 4) or siliceous quartzite with grit bands (class 5) occurs in the footwall.

The structural activity was found to be variable, ranging from low to moderate, and is probably a result of the build up of strain energy in the areas where competent siliceous quartzite occurs in both hangingwall and footwall. The rock mass energy dissipation is good, implying efficient release of strain energy on a small scale.

Hartebeestfontein G.M. geotechnical classes 4 and 6 (Areas 8 and 9)

In geotechnical class 6, the Zandpan Marker cuts down locally into the Vaal Reef, resulting in the reef being overlain by argillaceous quartzite. Siliceous quartzite (with grit bands) occurs in the footwall.

The γ_E and γ_R computed for both areas where this class occurs are very high, indicating high structural activity and poor strain energy dissipation within the rock mass, respectively. Since the γ_E and γ_R computed for other areas occurring at Hartebeestfontein G.M. within class 4 are low to moderate, the excessively high values of this parameter are attributed to the presence of the Kromdraai fault zone.

Hartebeestfontein G.M. geotechnical class 7 (Areas 3, 4, 7 and 15)

This geotechnical class differs from all the classes discussed thus far, as argillaceous quartzite is present in both the hangingwall and footwall. The extent of the Zandpan marker, however, is not fully known, and the seismogenic volumes defined to encompass the Zandpan marker are therefore subject to error. In addition, towards the northern extent of the basin, class 5 (siliceous quartzite overlying siliceous quartzite with grit bands in the footwall) crosscuts the Zandpan Marker.

The γ_E values indicate variable structural activity, ranging from low to high. A low structural activity would be expected for geotechnical classes such as class 7, where incompetent lithologies are present in both hangingwall and footwall. The high structural activity is thought to be due to the influence of geotechnical class 3 (siliceous quartzite in both hangingwall and footwall) that occurs to the east of the suggested distribution of the Zandpan marker. This result implies that the Zandpan Marker is less extensive than originally thought.

The γ_R values, with an exception of where class 3 is thought to occur, are low, implying efficient energy dissipation by the rock mass. This effect is attributed to the incompetent argillaceous quartzite in both hangingwall and footwall.

A schematic cross-section (Figure 5.2.4.37) was drawn from west (8#) to east (1#) across Hartebeestfontein G.M. to illustrate the variation of the γ_E and γ_R parameters with geotechnical area.

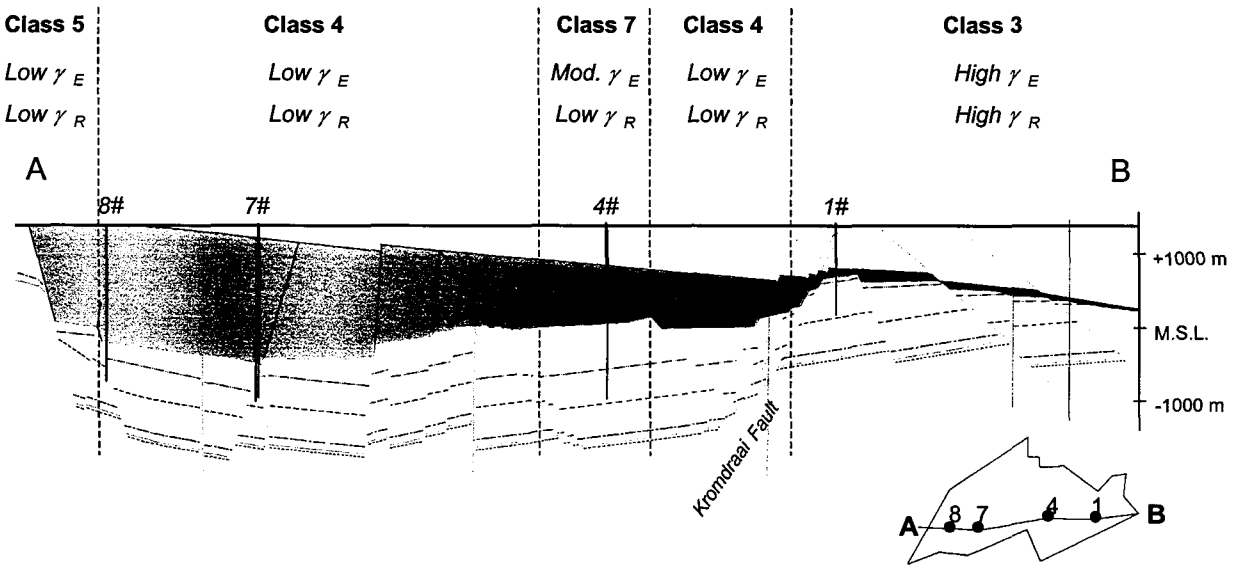

Figure 5.2.4.37 Schematic section showing the variation of γ_E and γ_R with geotechnical class at Hartebeestfontein G.M.

Temporal variation of parameters

The following comments are based on the trends shown in the graphs where the seismic parameters and area mined are plotted for each mining step.

Two phenomena are noted in these studies and are summarised as follows:

- An inverse relationship was observed to exist between the cumulative seismic moment of a particular mining step and area mined during that step,
- The largest cumulative seismic moment was often associated with the mining step where the least area of mining had occurred.

These phenomena were observed in a number of seismogenic volumes defined at Vaal Reefs G.M. and at Hartebeestfontein G.M. The relationship between the seismicity and mining may be explained by the existence of two populations of seismic events observed in this study, which have different contributions to the seismic moment.

The first population comprises low magnitude seismic events, which have a relatively low contribution to the cumulative seismic moment of a particular seismogenic volume. These events occur in the vicinity of the stope face and are thought to be directly associated with mining operations. The stope face events are associated with the formation of fractures that occur as a result of mine-induced stress release.

A second event population of larger magnitude events is recognised which contributes significantly to the cumulative seismic moment. These events are associated with movement on major geological discontinuities resulting from the interaction of mine-induced and residual tectonic stresses in the area.

It is thought that the large seismic events, which occur on large geological features are triggered by sudden changes (in the cases studied so far, a decrease) in the rate of mining. This could also be a result of a time effect, related to changes in the stress field on a mine-wide scale.

5.2.5 Conclusions and recommendations

Studies of the seismicity of the Vaal Reef (spatial and temporal distribution of seismic events, and computation of γ_E and γ_R computed for selected seismogenic volumes) indicate that:

- Two populations of seismic events are evident: (1) low magnitude tremors associated with the formation of fractures at stope faces as a result of mine-induced stress release, and (2) larger events associated with major geological discontinuities resulting from the interaction between mine induced and residual tectonic stresses in the area. These events cannot always be pinpointed to any specific area of mining but appear to be triggered by mining operations.

- The numerous faults and dykes crosscutting the Klerksdorp goldfield have a marked effect on the seismicity. High γ_E indicating structural activity was found at selected areas at Vaal Reefs G.M. 2 and 9 shaft (siliceous quartzite in the hangingwall overlying argillaceous quartzite with/without pebble bands in the footwall) and at Vaal Reefs G.M. 8 shaft (siliceous quartzite overlying siliceous pebbly conglomerate in the footwall). At Hartebeestfontein G.M., very high γ_E were computed for seismogenic volumes located in areas where the Zandpan marker cuts down on the Vaal Reef (argillaceous quartzite in the hangingwall overlying siliceous quartzite with grit bands in the footwall) in the vicinity of the Kromdraai fault zone. High γ_E occurred at Hartebeestfontein G.M. where siliceous quartzite occurred in both the hangingwall and footwall, also in the vicinity of the Kromdraai fault.

- Correlation between the seismic parameters and geotechnical area is only evident where there is (1) a relatively large contrast in quartzite competency e.g. where the Zandpan marker (argillaceous quartzite) cuts down on the Vaal Reef at Hartebeestfontein G.M., or (2) where competent siliceous quartzite occurs in both hangingwall and footwall, allowing the build up of strain energy within the rock mass.

- A decrease in the area mined for a particular mining step is often accompanied by an increase in the cumulative seismic moment for that step. It is thought that the large magnitude seismic events, which occur on major geological discontinuities, could be triggered by sudden changes in the rate of mining. This is a preliminary conclusion, and needs further investigation.

It is recommended that:

- Future studies of this nature are carried out in geotechnical areas where there is a marked competency contrast in hangingwall and footwall lithology. To overcome the subjectivity of the definition of the seismogenic volumes, it is suggested that the seismic parameters (γ_E and γ_R and $\sum M_o$) are contoured over the entire area of study, rather than computed for discrete volumes.

- The preliminary studies of the temporal variation of the seismic parameters with mining step have revealed some interesting results (i.e. the increase in cumulative seismic moment for a particular mining step with a decrease in the area mined; the correlation of high seismic moment with small area mined and *vice versa*). Further work investigating the potential triggering mechanisms could give some insights into where/when these phenomena occur. Such mechanisms could be the orientation of the geological features with respect to the regional stress field, time effects, rate of mining and mining geometry, and possibly the dewatering of the areas undergoing mining.

5.2.6 References

Berlenbach, J.W. & Schweitzer, J.K. 1997. SIMRAC Interim Report (GAP330): Geotechnical environments associated with the auriferous Vaal Reef and Carbon Leader, Witwatersrand Basin, South Africa.

Boyer, S.E. & Elliot, D. 1982. Thrust systems. *Bulletin of American Association of Petroleum Geology.* 65: p. 1196 - 1230.

Brummer, R.K. 1988. Active method to combat the rockburst hazard in South African gold mines. *CARE '88, Conference Applied Rock Engineering.* Newcastle upon Tyne, London, p. 35 – 43.

Gay, N.C. 1986. Mining in the vicinity of geological structures – evaluation of the problem. *Mining in the vicinity of geological and hazardous structures.* SAIMM Colloquium, 4 June, 32pp.

Gay, N.C. & Jager, A.J. 1986a. The effects of geology on the design and support of deep gold mines. *Extended abstracts, Geocongress '86,* 21st Biennial Congress of the Geological Society of Southern Africa, Johannesburg, p. 219 – 224.

Gay, N.C. & Jager, A.J. 1986b. The influence of geological features on problems of rock mechanics in Witwatersrand mines. (In: Anhaeusser, C.R. & Maske, S. *Mineral deposits of Southern Africa.* Geological Society of Southern Africa, p. 753 – 772).

Gay, N.C. 1993. Mining in the vicinity of geological structures – an analysis of mining induced seismicity and associated rock bursts in two South African mines. (In: Young, R.P. *Rockbursts and seismicity in mines.* Balkema: Rotterdam, p. 57 – 62).

Gay, N.C., Jager, A.J. Ryder, J.A. & Spottiswoode, S.M. 1995a. Rock engineering strategies to meet the safety and production needs of the South African mining industry in the 21st century. *Journal of the South African Institute for Mining & Metallurgy,* p. 115 –136.

Gilroy, J.A. C., Joubert, P. & van Wyk, J.J. 1994. The planning and implementation of No. 11 Shaft at Vaal Reefs. XVth CMMI Congress, Johannesburg: SAIMM, 1: p. 55 – 69.

Gurtunca, R.G. & Gay, N.C. 1993. Rock Engineering – implementing the latest developments in improving safety in underground mining operations. *Mine Management Forum,* Midrand, 9 – 10 November, Johannesburg, 20 pp.

Joughin, N.C. & Jager, A.J. 1983. Fracture of rock at stope faces in South African gold mines. *Symposium on Rockbursts.* October, London: IMM, p. 53 – 66.

Kullman, D.H., Stewart, R.D. & Lightfoot, N. 1994. Verification of a discontinuum model used to investigate rock mass behaviour around a deep-level stope. *Applications of Numerical Modelling in Geotechnical Engineering Symposium,* September, Pretoria: SANGORN, 6 pp.

Lenhardt, W.A. 1989. Seismic event characteristics in a deep level mining environment. *International Symposium in Rock Mechanics and Rock Physics at great depth,* Pau, France, p. 727 – 732.

Lenhardt, W.A. 1990. Damage studies at a deep level African gold mine. (In: Fairhurst, C. *Rockbursts and seismicity in mines.* Balkema: Rotterdam, p. 391 – 393).

Lenhardt, W.A. & Hagan, T.O. 1990. Observations and possible mechanisms of pillar-associated seismicity at great depth. *Technical challenges in deep level mining.* Johannesburg: SAIMM, p. 1183 – 1194.

McGarr, A. 1971. Stable deformation of rock near deep-level tabular excavations. *Journal of Geophysical Research*, 74: p. 7088 – 7106.

McGarr, A. 1976. Seismic moment and volume changes. *Journal of Geophysical Research*, 84: p. 2348 – 2350.

McGarr, A., Spottiswoode, S.M. & Gay, N.C. 1975. Relationship of mine tremors to induced stresses and to rock properties in the focal region. *Bulletin of the Seismological Society of America*, 65: p. 981 – 993.

Milev, A. & Spottiswoode, S.M. 1997. Integrated seismicity around deep-level stopes in South Africa. *International Journal of Rock Mechanics and Mining Science*. 34.

Piper, P. 1997. SIMRAC Interim Report (GAP330): Delineating geotechnical areas on the basis of support usage.

Potgieter, G.J. & Roering, C. 1984. The influence of geology on the mechanisms of mining-associated seismicity in the Klerksdorp goldfield. (In: Gay, N.C., Wainwright, E.H. *Proceedings of the 1st International Congress in Rockbursts and Seismicity in Mines*. Johannesburg: SAIMM, p. 45 – 60).

Roberts, M.K.C., Gay, N.C. & Jager, A.J. 1993. Implementation of new and improved support technology on mines to make mining safer and more cost effective. *25th International Conference on Safety in Mines Research Institutes*. Pretoria, September, p.1 – 5.

Roberts, M.K.C., Gurtunca, R.G., & Gay, N.C. 1994. Current rock engineering developments to improve safety in South African mines. *International Symposium on New Developments in Rock Mechanics and Engineering*. Shenyang, China, 6 pp.

Schweitzer, J.K. & Johnson, R.A. 1997. Geotechnical classifications of deep and ultra-deep Witwatersrand mining areas, South Africa. *Mineralium Deposita*, 126: p. 1 – 14.

Spottiswoode, S.M. 1986. Use of seismicity to qualify hazardous structures. *Colloquium: Mining in the vicinity of geological and hazardous structures*, 4 June, Mintek, Johannesburg, 30 pp.

Rorke, A.J. & Roering, C. 1984. Source mechanism studies of mine-induced seismic events in a deep-level gold mine. (In: Gay, N.C., Wainwright, E.H. *Proceedings of the 1st International Congress in Rockbursts and Seismicity in Mines*. Johannesburg: SAIMM, p. 51 – 55).

Van Aswegen, G. 1990. Fault stability in SA gold mines. (In: Rossmanith, H.P. *Mechanics of Jointed and Faulted Rock*. Balkema: Rotterdam, p. 717 – 725.

Van der Heever, P. 1982. The influence of geological structure on seismicity and rockbursts in the Klerksdorp goldfield. M.Sc. Thesis. Johannesburg: RAU.

6 Further developments of the stope support design methodology

6.1 Introduction

Rock mass instabilities are the single largest cause that contributes to the toll of injuries and fatalities suffered by the workforce during gold and platinum mining operations in South Africa. Approximately half of the number of fatalities are associated with rockfalls, whilst the remainder are a consequence of the failure of dynamically loaded rock during seismic events and rockbursts.

Stope support systems, consisting of combinations of props and packs, are used to stabilise the rock mass surrounding the mining excavation and reduce the risk of rockfalls and rockbursts. In South African gold and platinum mines, the methodology currently used to design stope support is based upon the tributary area concept, and does not adequately address the fact that the rock being supported may be fractured and jointed. Due to the complexities associated with the behaviour of a discontinuous rock mass, the interaction of the support system with a fractured and jointed rock mass is poorly understood. Relatively little progress has been made in quantifying the effect of support spacing on the rock mass stability, and, typically, it is the responsibility of the rock engineer to estimate support spacing based upon past experience. The many casualties resulting from falls of ground between support units is testimony to deficiencies in this method. In order to improve safety and continue mining at increasing depth, it is important to understand the mechanisms of the support – rock interaction, the zones of support influence, and the role of rock mass discontinuities.

The objective is to formulate a basis for quantifying support mechanisms, and, more specifically, to gain insights into the influence of rock discontinuities such as joints, fractures and bedding planes on stable spans. Instabilities generally initiate at discontinuities, which are shown to be of prime importance when spacing support units. An attempt is made to evaluate the interaction of the support with a discontinuous rock mass, with a view to developing a support system design methodology that maximises support spacing, whilst maintaining a stable hangingwall span between support units. The methodology addresses hangingwall stability problems due to both quasi-static (rockfall) and dynamic (rockburst) failure. Due to the widely varying rock mass conditions and the behaviour of the reefs extracted by the gold and platinum mines, the methodology needs to take into account both the local geological conditions and rock types, as well as the spacing and orientation of the various discontinuities.

The ultimate output of this work is a design tool for the gold and platinum mining industry to assist the rock mechanics engineer in improving support design, with particular emphasis on optimised support spacing and support performance requirements for static and dynamic conditions.

6.2 Review of rock mass discontinuities

The behaviour and deformation of the rock mass surrounding stopes is influenced by mining induced and geological discontinuities. Hence, in order to gain insights into the support – rock mass interaction, an understanding of typical rock mass discontinuities is required. Investigations into mining induced stress fractures in intermediate and deep level gold mine stopes have revealed that two main types of fractures are present in the hangingwall (Adams et al., 1981) and are recognised to occur in at least four sets, based on their orientation.

- *Shear Fractures*: These fractures are associated with highly stressed rock, and thus are found in intermediate and deep level mines. It is estimated that the fractures initiate 6 to 8 m ahead of the advancing stope face and separate the rock into blocks of relatively intact material. They are oriented approximately parallel to the stope face and are regularly spaced at intervals of 1 to 3 m. Shear fractures usually occur in conjugate pairs in the hanging- and footwall, and typically reveal distinct signs of shear movement. Their dip in the hangingwall is generally towards the back area at angles of 60 to 70 degrees (Jager, 1998; Esterhuizen, 1998).

- *Extension Fractures*: These fractures initiate ahead of the stope face and are smaller than shear fractures. They form after shear fractures have propagated and are generally truncated by parting planes. Extension fractures normally do not exhibit relative movement parallel to the fracture surface and are typically oriented parallel to the stope face. They are commonly spaced at intervals of 10 cm, with lower and upper limits of 5 to 50 cm, respectively. The strike length is typically 3 m, where lower and upper limits of 0,4 and 6 m have been observed (Esterhuizen, 1998). Extension fractures normally dip between 60 and 90 degrees, where the direction of dip (i.e. towards or away from the stope face) can be influenced by the hanging- and footwall rock types (Roberts, 1995)

Most gold reef extraction takes place in bedded quartzites. Reef parallel bedding planes typically represent weak interfaces between adjacent strata, and provide little cohesion and low frictional resistance. Bedding planes are generally spaced at 0,2 to 2,0 m intervals. The rock fallout height is commonly governed by the position of bedding planes.

The three most prevalent discontinuity types, extension fractures, shear fractures and bedding planes, are illustrated in Figure 6.2.1. Their influence on the rock mass behaviour and stability is considered in this study, and an attempt is made to quantify their effect on support spacing and rock mass stability under static and dynamic conditions.

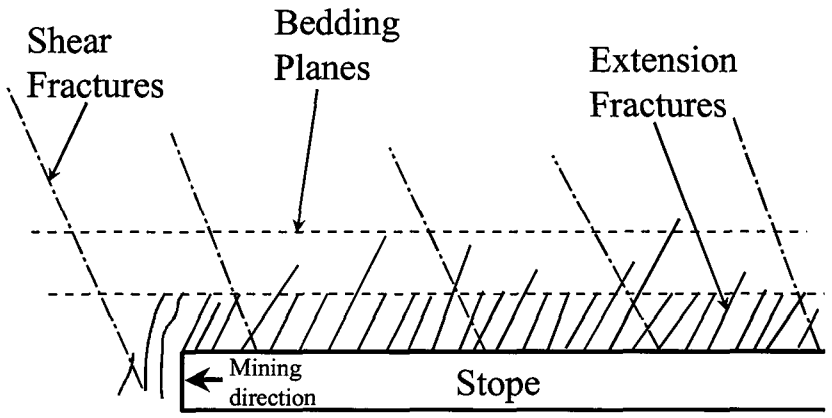

Figure 6.2.1 Simplified schematic showing the three most prevalent discontinuity types in intermediate and deep level mines.

6.3 Research methodology

6.3.1 Numerical simulations of support interaction with a discontinuous rock mass

The finite-discrete element program ELFEN (Rockfield, 1996) was used as a tool to investigate the interaction of support units with a discontinuous rock mass. Various ELFEN models were constructed, incorporating several discontinuity types. The aim of the numerical models was to obtain qualitative insights into the stress trajectories arising due to the load transfer from the support elements to the discontinuous hangingwall rock.

The ELFEN simulations model a fractured hangingwall beam discretised by closely spaced extension fractures. In intermediate and deep level mines, the extension fractures are typically oriented face parallel, where the fracture length in the dip direction is generally much longer than the fracture spacing in the strike direction. Hence, it is considered reasonable to model a section of the hangingwall along the strike direction in two dimensions and assume plane strain conditions in the out-of-plane (dip) direction. The fracture surfaces were modelled with no cohesion and a friction angle of 40 degrees.

The boundary conditions along the top of the numerical models were a uniformly applied load. In practice the hangingwall beam is not loaded uniformly, with local bedding plane separation and undulation, and the influence of the face and back area, leading to irregular hangingwall loading. The aim of the simulations conducted here, however, was to gain general qualitative insights into the stress distribution within a discontinuous hangingwall beam, and thus the loading conditions are simplified to a uniformly applied load.

The hangingwall is assumed to be confined at both ends, i.e. at the face and back area. The assumption of hangingwall confinement, as well as compressive hangingwall stresses, is further described at a later stage.

Figure 6.3.1 shows the principal stress distribution associated with two prop like support elements loaded by a hangingwall slab discretised into blocks by closely spaced vertical fractures. It is evident that the stresses are transmitted from the support units, through the long axis of the blocks defined by the vertical discontinuities, into the more competent (in this case non-fractured) medium above the bedding plane. In this case, small clamping stresses are generated as a consequence of the Poisson effect to act on the vertical slabs between the support units.

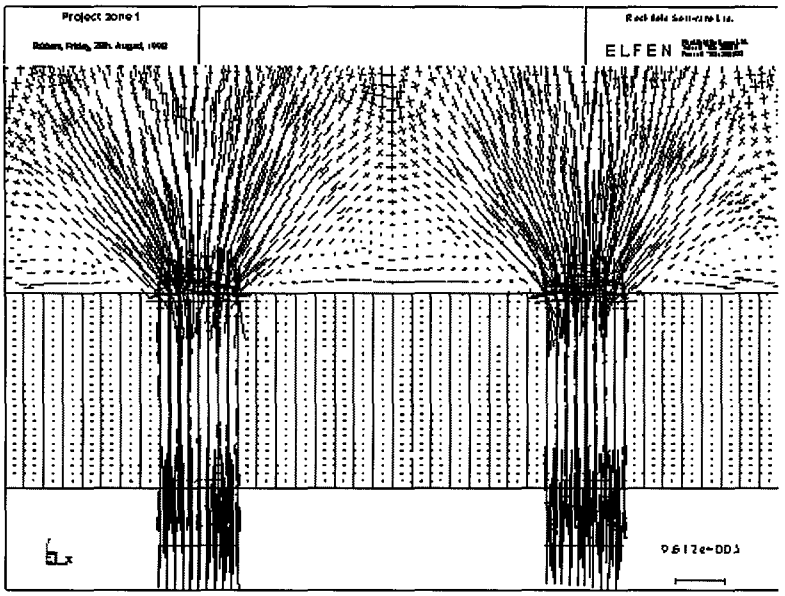

Figure 6.3.1 Stress distribution associated with a discontinuous hangingwall interacting with two support units.

In the case of a hangingwall discretised by dipping extension fractures in conjunction with a discontinuity simulating a shear fracture, the stress trajectories follow the paths shown in Figure 6.3.2. As noted before, the stresses seem to be transmitted mainly parallel to the discontinuities, through the fractured layer into the competent layer above the bedding plane. Again, very low clamping stresses act on the slabs between the support units.

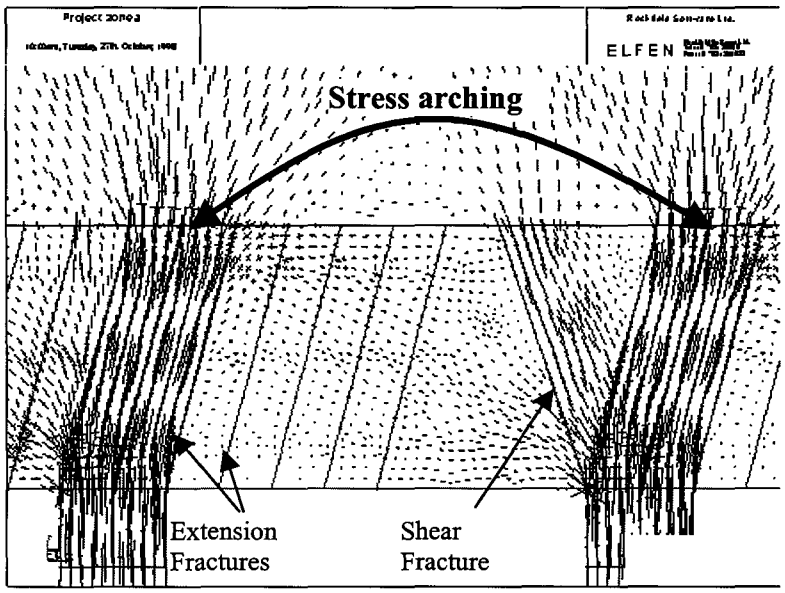

Figure 6.3.2 Stress transfer through a hangingwall beam discretised by discontinuities modelling extension and shear fractures.

In intermediate and deep mines, fracturing ahead of the stope face induces rock dilation, leading to compressive hangingwall stresses parallel to the skin of the excavation (Jager and

Roberts, 1986). The compressive stresses can only be maintained if the hangingwall beam is continuous, i.e. if the hangingwall is confined at both ends. This is generally the case in intermediate and deep gold mines, with compressive hangingwall stresses contributing significantly towards the rock mass stability. Figure 6.3.3 shows the stress distribution associated with a model loaded in the vertical and horizontal direction. The magnitude of the horizontal stress is 1 MPa, whilst the total load carried by each support unit is 200 kN; these are typical load magnitudes as measured underground. Although the stress distribution is complicated by the addition of the horizontal stresses, the basic stress field consists of the superposition of the vertical and horizontal stress components. Stress arching in the competent layer is evident (shown in Figure 6.3.3), leading to the conclusion that most of the stress generated by the support units follows a path parallel to the discontinuities, as observed in Figure 6.3.3. However, the horizontal stresses generated by dilation of the fracture zone ahead of the stope face provide significant clamping forces to the rock structures between support units.

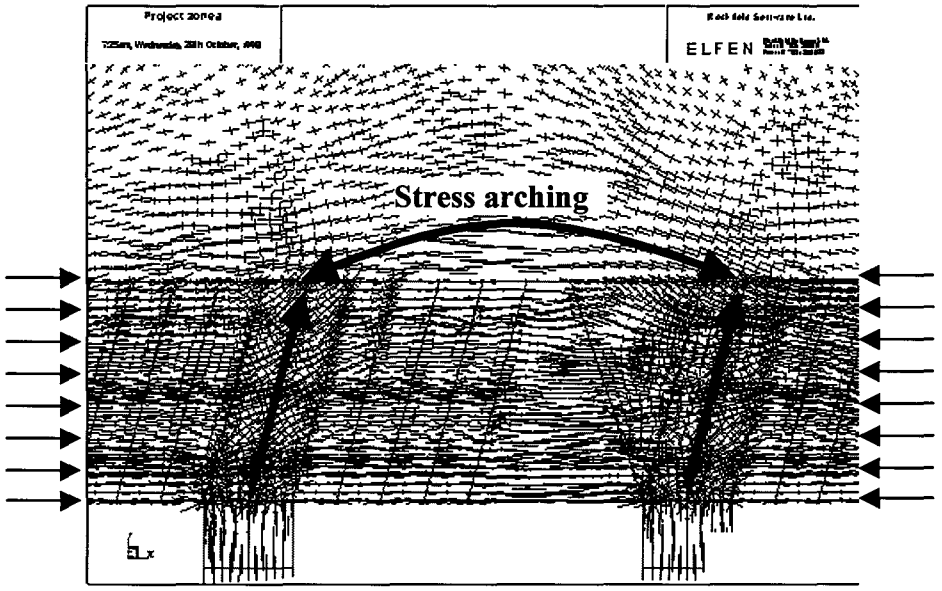

Figure 6.3.3 Vertical and horizontal loading of a discontinuous hangingwall beam.

To summarise, simplified numerical models representing a discontinuous hangingwall beam, discretised by extension fractures, a shear fracture and a bedding plane, have shown that the load carried by support units is generally transmitted in a direction parallel to the fracture orientations. Comparatively little stress is transmitted across the fractures, and the hangingwall rock between adjacent support units is essentially unstressed. When the hangingwall is clamped by compressive stresses acting parallel to excavation surface, the resulting stress field can be approximated by the linear superposition of horizontal and vertical loading, i.e. the majority of the stress induced by the loaded support units continues to be transmitted parallel to fracture surfaces.

Hence, in subsequent results given in the following sections, the compressive stresses induced by support units are assumed to be transmitted parallel to the fracture surfaces. Support units do not directly stress the hangingwall rock between adjacent support units, and hangingwall stability in this region is governed by compressive in-situ stresses and the buckling potential of the hangingwall beam.

A central assumption implicit in this work is that the hangingwall rock is confined. As described earlier, in intermediate and deep level mines fracturing ahead of the stope face leads to rock dilation, thereby causing compressive horizontal stresses in the stope hangingwall. Squelch (1994) measured maximum compressive hangingwall stresses of 1 to 10 MPa at depths of 0,7 to 2,2 m into the hangingwall. The horizontal stresses clamp the fractured rock together and, depending on the orientation of fractures, can significantly improve the structural integrity and stability of the hangingwall (Jager and Roberts, 1986).

Herrmann (1987) found that, in stopes with back area caving, stress relaxation occurred in the lower layers of the hangingwall, and noted the importance of rock confinement to maintain compressive hangingwall stresses. Rockfalls and caving in the back area generally lead to reduced hangingwall confinement. Compressive hangingwall stresses can, however, still be maintained when the lateral hangingwall movement is restricted due to frictional resistance generated at bedding plane interfaces.

As an example of this mechanism, consider the stope shown in Figure 6.3.4. The elongates and packs shown in Figure 6.3.4 are assumed to be carrying a load of 200 kN and 400 kN, respectively. Thus, in order to estimate the horizontal compressive stress, which can be maintained between the face and the two rows of elongates, the total load carried by the second elongate and the two packs is determined as 200 kN + 400 kN + 400 kN = 1000 kN. The self weight of the rock between the second elongate and the packs is 160 kN (assuming a centre to centre support spacing of 3 m and a bedding height of 1 m). Thus the effective clamping force pinning the hangingwall to the bedding plane is 1000 kN – 160 kN = 840 kN. If the bedding plane has an apparent friction angle of 40°, the maximum horizontal force that can be maintained is: (tan 40°) x 840 kN $\approx$ 700 kN, or, converting to stress, 0,7 MPa. Thus it is shown that, even with caving and rockfalls in the back area, reasonably high compressive hangingwall stresses can be maintained.

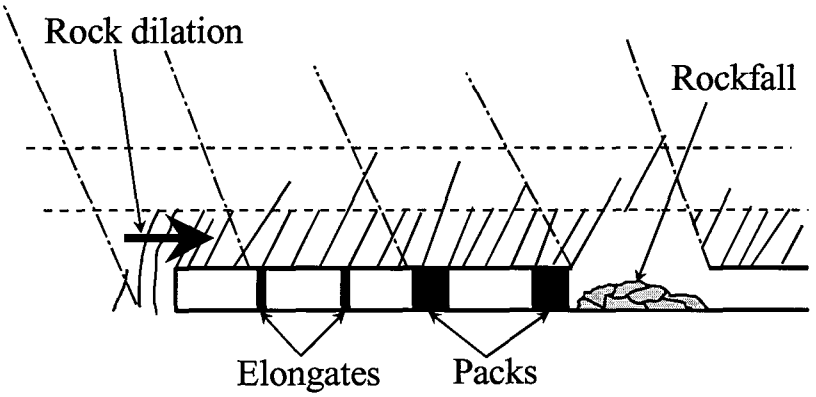

Figure 6.3.4 Stope with a back area rockfall lading to reduced hangingwall confinement.

6.3.2 Quantifying stable hangingwall spans between support units

The qualitative insights gained from the numerical simulations are used to develop a simplified conceptual model describing the rock mass stability and quantifying stable spans between adjacent support units. The model is suitable to apply in a support design methodology to optimise support spacing while maintaining high levels of safety. Details of the procedure of the proposed support design methodology are given in Sections 6.4 and 6.5 for rockfall and rockburst cases, respectively.

Two failure mechanisms are considered, namely instabilities due to (i) beam buckling and (ii) shear failure due to slip at the abutments.

6.3.2.1 Hangingwall beam buckling

The design procedure followed here is based on that developed by Evans (1941), and subsequently modified and extended by Beer and Meek (1982), Brady and Brown (1985), and Hutchinson and Diederichs (1996). The solution technique, which is based on the Voussoir beam, follows the intuitive idea that in a discontinuous hangingwall beam the central transverse crack determines the deformational behaviour (Figure 6.3.5). In the buckling mode the beam becomes unstable to form a 'snap-through' mechanism.

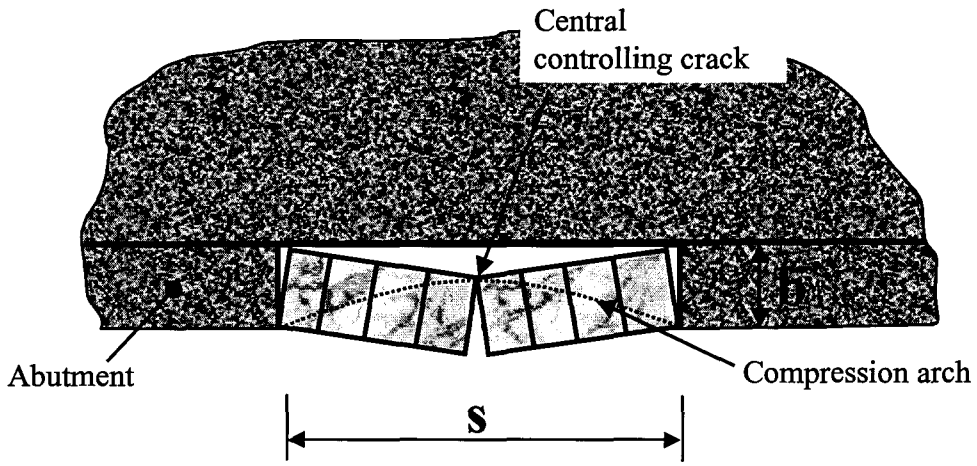

Figure 6.3.5 Voussoir beam geometry for hangingwall beam analysis.

In analysing the stability of the Voussoir beam the following assumptions are made:

- As the beam deflects, a parabolic compression arch develops in the beam.
- Deflection of the beam occurs before slippage at the abutments. Stability against slippage (see Section 6.3.2.2) is determined after the compression arch develops.
- The abutments are stiff, i.e. they do not deform under the arching stress. Each abutment is subjected to the same distributed load as the ends of the beam, however the loaded area is small compared to the beam span. Elastic compression of the abutments will therefore be small compared with the beam compression and may be neglected (Brady and Brown, 1985).

The Voussoir beam problem is statically indeterminate, i.e. no explicit solution is available and an iterative process is followed to determine the beam equilibrium position. The solution procedure is given in texts such as Brady and Brown (1985), Hutchinson and Diederichs (1996) and is not repeated here.

Previously documented results of this solution have used an absolute snap-through limit, which is the limit of stable deflection according to the mathematical formulation. This limit is extremely sensitive to beam thickness, a difficult parameter to accurately and reliably estimate, and one

which may change as deflection and layer separation occurs. Hutchinson and Diederichs (1996) recommend a design snap-through limit that is reached when the mid-span deflections reach 10 per cent of the beam thickness. Beyond this deflection, small differences in thickness have an unacceptably large influence on stability and the beam is considered unstable.

Taking Hutchinson and Diederichs's (1996) design snap-through limit into account (max. 10 per cent beam deflection at mid-span), the span versus minimum beam thickness is given in Figure 6.3.6. The snap-through limits are given for various values of in-situ rock mass elasticity modulus (E`) parallel to the excavation surface. The in-situ rock mass modulus is predominantly governed by the stiffness of the rock mass discontinuities, and is considerably lower than the stiffness of solid rock, which is characterised by Young's modulus. As is apparent from Figure 6.3.6, the relationship between span and beam thickness is highly dependent on the in-situ rock mass elasticity modulus parallel to the excavation surface.

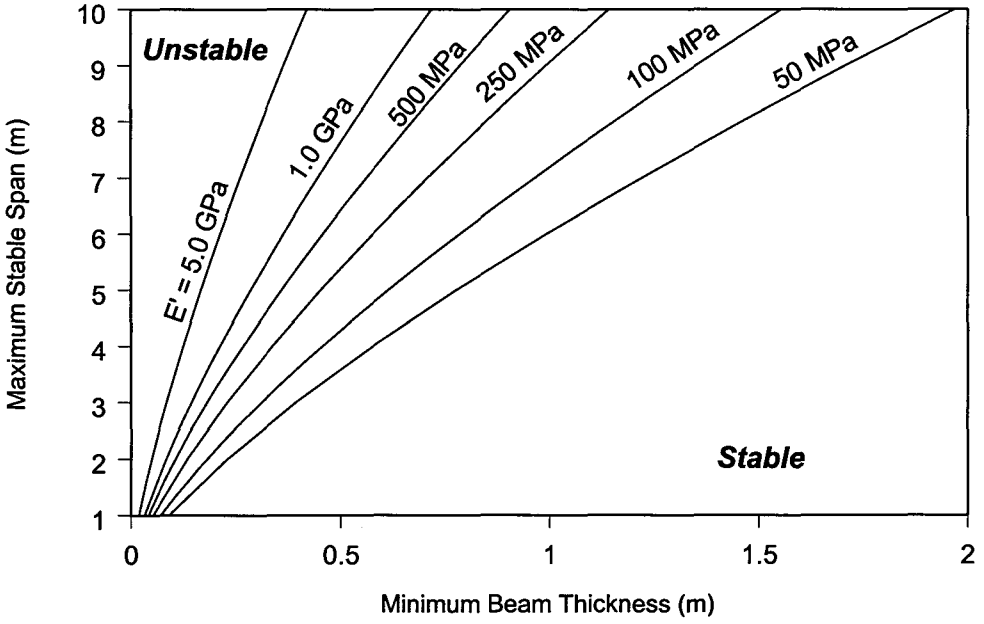

Figure 6.3.6 Span versus minimum beam thickness at 10 per cent beam deflection for various values of in-situ rock mass modulus (E`).

Bandis et al. (1983) made use of experimental data to establish a relationship between normal joint stiffness and normal stress for well interlocked joints in various rock types (Figure 6.3.7). The joint stiffness is found to increase with increasing normal stress. For rock mass discontinuities in a typical gold or platinum hangingwall, where the compressive hangingwall stresses are generally less than 5 MPa, a discontinuity stiffness of 40 MPa/mm is assumed for the purposes of this study. It is recognised, however, that further in-situ discontinuity stiffness measurements are required to obtain more accurate and representative stiffness data.

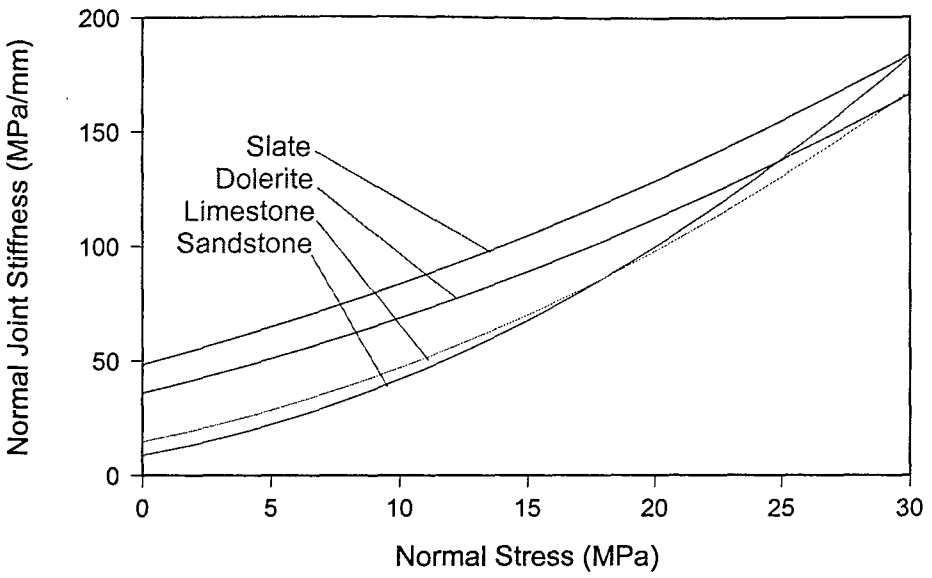

Figure 6.3.7 Normal joint stiffness for well interlocked joint examples in various rock types (after Bandis et al., 1983).

The joint stiffness is incorporated in the buckling analysis procedure. To simplify the analysis, and considering the comparatively minor variations in stiffness for compressive hangingwall stresses ranging from 0 to 5 MPa, the stiffness is assumed to be independent of normal stress, i.e. the joint stiffness is kept constant at 40 MPa/mm, irrespective of the compressive stresses acting within the hangingwall beam.

The effective rock modulus (E`) is calculated by multiplying the normal joint stiffness by the lateral deformation (arch shortening) during beam deflection. It is thus assumed that lateral hangingwall deformation occurs at the discontinuities only and that the rock between adjacent discontinuities does not deform. This is a realistic assumption, as the Young's modulus of the intact rock is much higher than the effective joint modulus.

Multiple discontinuities act as springs in series and each discontinuity is compressed equally. Span versus thickness relations shown in Figure 6.3.8 give the stability envelopes of hangingwall beams with 3 joints, as well as 1, 3, 5 and 10 joints per metre of hangingwall length. The analysis is modelled with a minimum of three discontinuities to facilitate deformation in the buckling mode. Thus, in the case of a hangingwall discretised by 1 joint per metre, the beam can only fail in the buckling mode when the span exceeds 3 m.

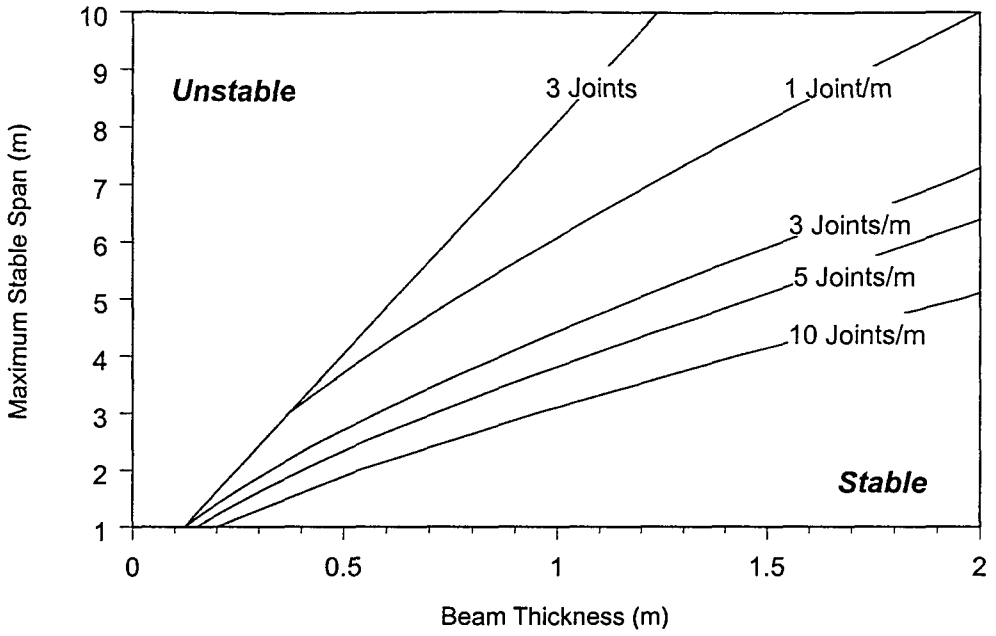

Figure 6.3.8 Buckling stability envelopes of a discontinuous hangingwall beam.

As the beam deflects, the arch stresses are transmitted through the beam edges to the abutments. The maximum abutment stresses versus span for various beam thicknesses are given in Figure 6.3.9 (given for the case of 5 joints per metre). It is evident that the maximum abutment stress for typical beam thicknesses encountered in South African mines is approximately 0,4 – 0,5 MPa for spans ranging from 2,5 to 6,0 m. However, these are local stresses, and, when averaged along the beam thickness, the mean compressive stresses induced by block rotation in the buckling mode are considerable lower in magnitude.

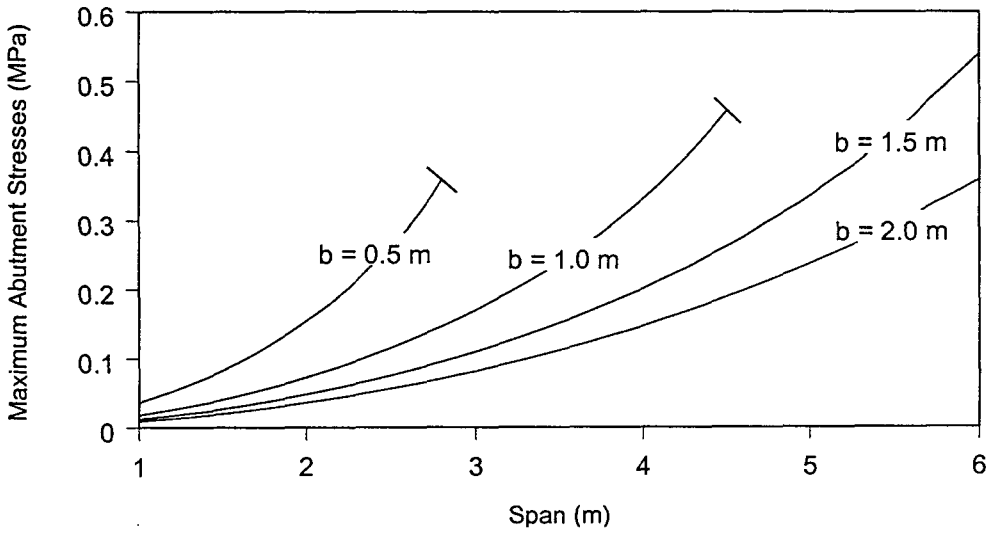

Figure 6.3.9 Maximum abutment stresses versus span for various beam thicknesses.

6.3.2.2 Shear failure by slip at the abutments

The second failure mechanism considered in this study is shear failure by slip at the abutments. Figure 6.3.10 shows a simplified schematic indicating the main parameters governing the stability of hangingwall keyblocks prone to shear failure, where W is the block weight, b is the beam thickness, s is the span between adjacent support units, α and β are angles of extension and shear fractures, and σ_x is the magnitude of compressive hangingwall stress. The hangingwall stresses are generated by two mechanisms, namely:

- In intermediate and deep level mines, the rock dilation associated with fracturing immediately ahead of the stope face generates compressive stresses parallel to the excavation surface.
- The block rotation associated with the 'snap-though' failure mechanisms described in Section 6.3.2.1 generates compressive hangingwall stresses.

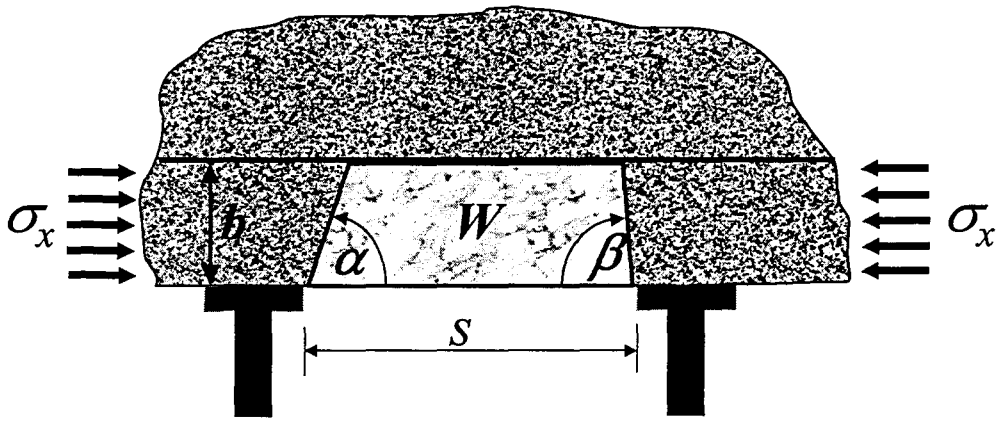

Figure 6.3.10 Keyblock instability due to shear failure at the abutments.

The discontinuities, which represent mining induced fractures, are assumed to have zero cohesion on the inclined contact surfaces. Hence, for the keyblock to be stable, the lateral thrust at the abutments due to in-situ compressive hangingwall stresses must mobilise a frictional resistance sufficient to provide the abutment shear force. The frictional resistance for either side of the keyblock can be calculated using the following expressions:

$$V_I = \sigma_x\, b\left(\frac{\mu\sin\alpha - \cos\alpha}{\sin\alpha + \mu\cos\alpha}\right) \qquad V_{II} = \sigma_x\, b\left(\frac{\mu\sin\beta - \cos\beta}{\sin\beta + \mu\cos\beta}\right) \tag{6.3.1}$$

The coefficient of friction, μ, is an important parameter governing the resistance to shear. Typically, discontinuity types encountered underground have closely matched surfaces, this particularly being the case with mining induced fractures. The associated apparent friction angle can be relatively high, and friction angles of 30 to 50 degrees are considered realistic.

The keyblock is considered unstable when $W > V_I + V_{II}$. If the frictional resistance exceeds the weight of the hangingwall block ($V_I + V_{II} > W$), stability is only ensured if:

- $V_I > ½\,W$ and $V_{II} > ½\,W$ (Figure 6.3.11 a and b), or
- $V_I > ½\,W$ or $V_{II} > ½\,W$ and the angle of the opposing discontinuity prevents any rotation (Figure 6.3.11 c and d). Thus, if the frictional resistance on either discontinuity is less than

half the keyblock weight, the keyblock is stable only on condition that kinematically no block rotation is possible.

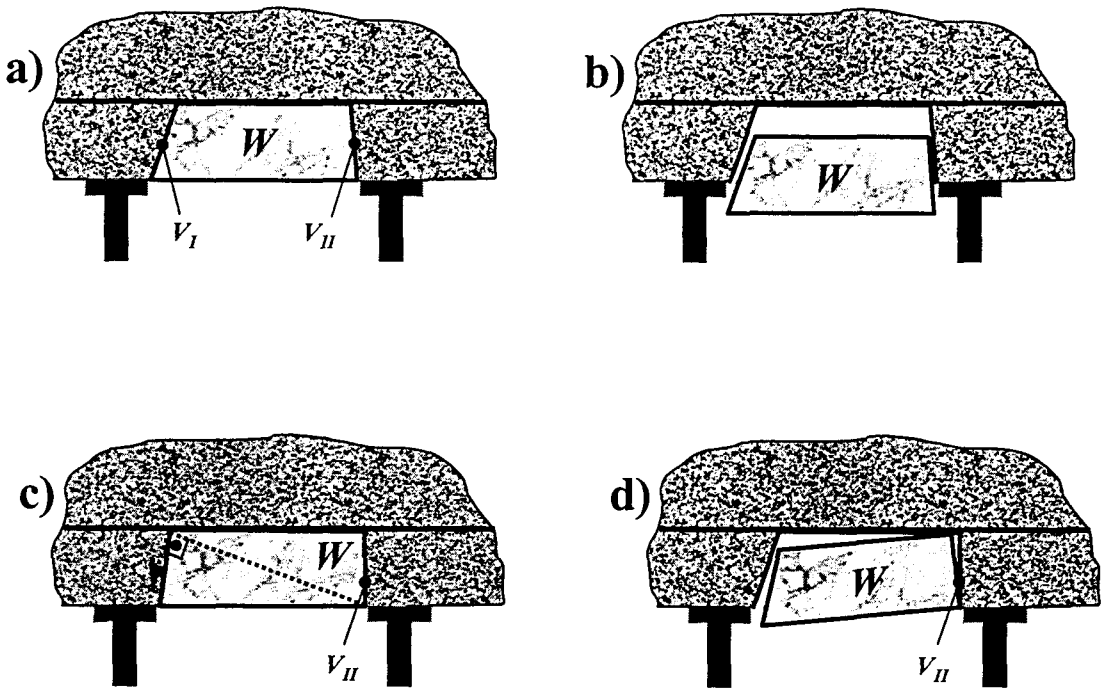

Figure 6.3.11 Schematic diagrams showing possible failure modes due to shear at discontinuity interfaces:

- ***a) Keyblock is stable as V_I > ½ W and V_{II} > ½ W.***
- ***b) Keyblock shear failure as V_I < ½ W and V_{II} < ½ W.***
- ***c) Although V_I < ½ W, the keyblock is stable as V_{II} > ½ W and no block rotation is possible.***
- ***d) Keyblock is unstable as V_I < ½ W and block rotation is kinematically possible (V_{II} > ½ W).***

6.4 Rockfall support design methodology

A methodology is proposed to evaluate the suitability, in terms of loading requirements and spacing, of a given support system to effectively cater for rockfall conditions. The support system evaluation consists of two phases, namely:

1. Tributary area theory is applied to determine if the load requirements of the support system are met.

2. The support spacing and stable spans between adjacent support units are verified by investigating the possibility of failure due to the two predominant failure mechanisms outlined in Sections 6.3.2.1 and 6.3.2.2, i.e. (i) beam buckling, or (ii) shear failure due to slip at the abutments.

The following assumptions are made with regard to the design methodology:

- The rock mass fall-out thickness is determined by the position of prominent bedding planes and/or back analyses of previous rockfall accidents. Work by Roberts (1995) has shown that the fall-out thickness is reef dependent, and varies between 1,0, 1,2 and 1,4 m for the Carbon Leader, Vaal and Ventersdorp Contact Reef, respectively.

- The hangingwall rock mass is discretised by face parallel extension and shear fractures. At this stage no attempt has been made to include discontinuities of geological origin; unlike mining induced fractures, these are generally not face parallel and need to be considered in future work involving three dimensional modelling.

- The loading requirements due to tributary area load distributions are calculated based on a two dimensional plan view of the stope and associated support system (Figure 6.4.1 a).

- To calculate maximum stable spans and prevent hangingwall failure, due to buckling or shear failure, the cross-section (plane strain is assumed) of the hangingwall rock is taken along the strike direction, i.e. face perpendicular (Figure 6.4.1 b).

- Deflection of the beam occurs before shear failure at the discontinuity interfaces. Stability against slippage is determined after the compression arch has developed in buckling mode.

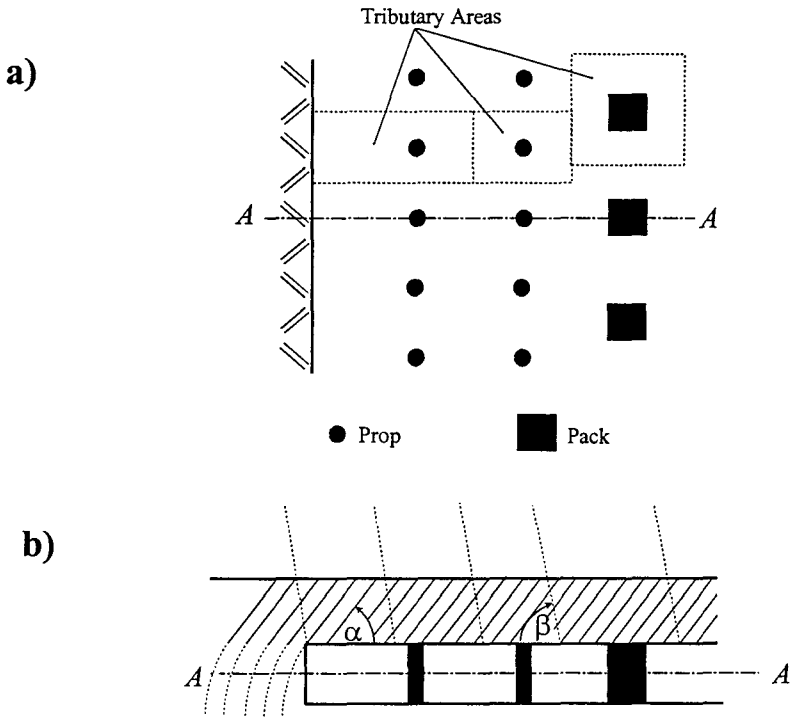

Figure 6.4.1 a) Plan view applied for tributary area load requirements (top), and b) face perpendicular cross-section used to determine maximum stable hangingwall spans in strike direction (bottom).

The solution procedure can readily be coded in the form of a computer program to facilitate the rapid and convenient evaluation of various support systems and associated spacing of support units. Figure 6.4.2 shows a flow chart of the procedure of support system evaluation for rockfall conditions.

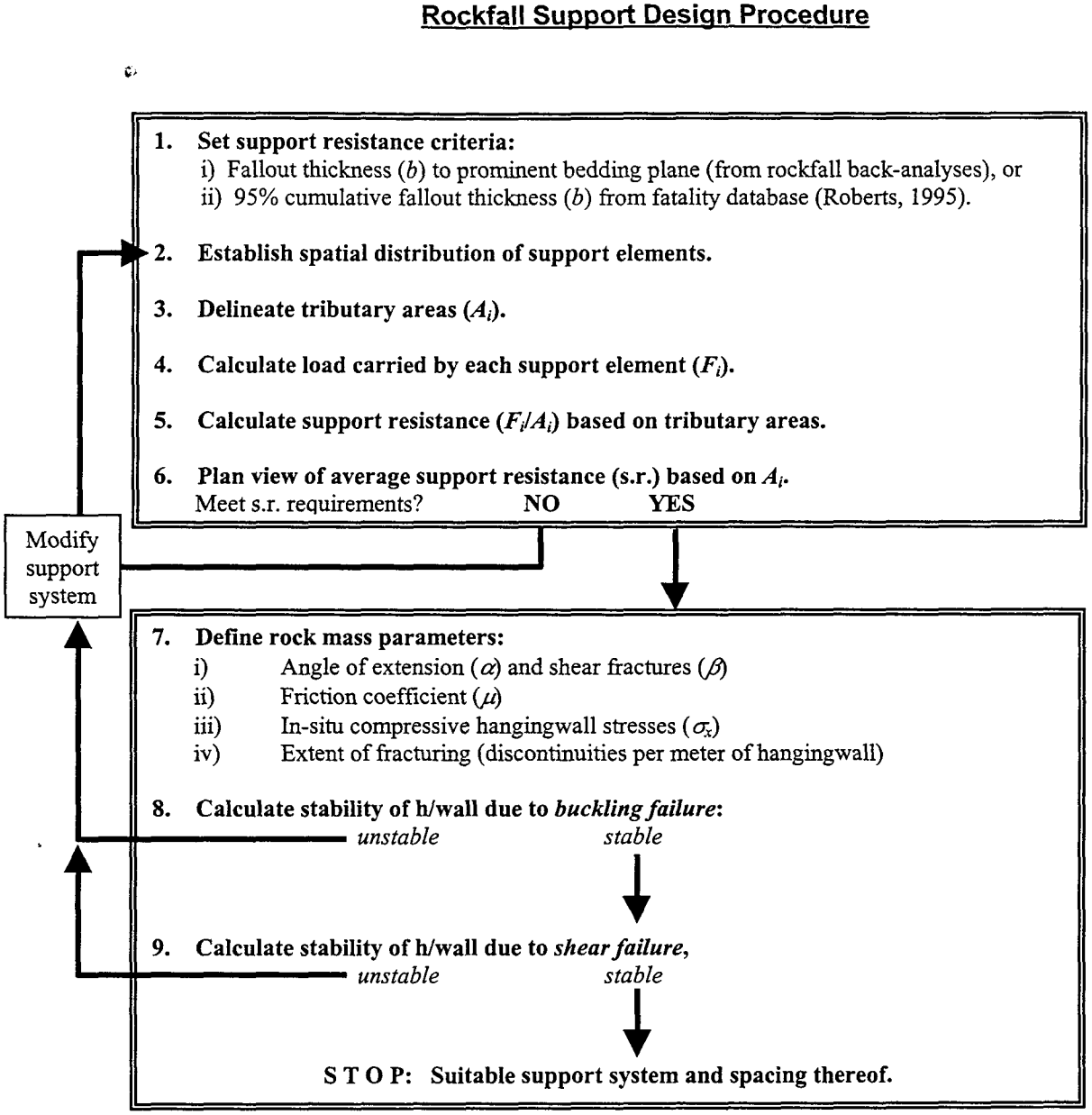

Figure 6.4.2 Rockfall support design procedure.

The parameters governing the maximum stable hangingwall span are the discontinuity angles (α and β), bedding height (b), friction coefficient (μ), and hangingwall clamping stresses (σ_x). The influence of the above-mentioned parameters on the stable span length is investigated.

The maximum span was determined using the proposed rockfall design methodology for an intermediate depth mine with five fractures per metre of hangingwall. Failure due to buckling, as well as shear at the discontinuity surfaces, is taken into account. Compressive stresses at the abutments, due to deformation in the buckling mode, are added to the in-situ hangingwall stresses, due to fracturing ahead of the stope face.

The limiting equilibrium of the keyblock is governed by one of two failure mechanisms: (i) shear failure due to slip at the abutments and/or block rotation, and (ii) buckling failure. Figure 6.4.3

gives stability envelopes for the hangingwall at limiting equilibrium for σ_x = 1,0 MPa, b = 2,0 m and μ = tan 40°. Three prominent stability zones can be identified:

1. **Zone I:** At these discontinuity angle combinations, no shear resistance is active, i.e. all keyblocks, irrespective of span size, are unstable. According to Equations (1), the transition from Zone I to Zone II (when shear resistance becomes active) occurs when $V_I = -V_{II}$. For the friction angle applied here (μ = tan 40°), it can be shown that shear resistance becomes active when $\alpha + \beta > 100°$. Generally, shear resistance is active when the sum of the two discontinuity angles ($\alpha + \beta$) exceeds a constant angle, the magnitude of which is linearly related to the friction angle. Figure 16 gives the minimum angle of $\alpha + \beta$ versus friction angle.

2. **Zone II:** Here the failure mechanism is predominantly shear failure of one of the discontinuity interfaces, leading to instability due to block rotation. Note that for the parameters displayed in Figure 6.4.3 the maximum stable span in Zone II is approximately 3 m, which is in accordance with stable spans as observed underground.

3. **Zone III:** In Zone III the shear resistance increases rapidly. The angles of both discontinuities are greater than 50° and the keyblock is effectively clamped by in-situ compressive hangingwall stresses. The maximum stable span is governed by the buckling resistance, and for the parameters shown in Figure 6.4.3 the maximum stable span is 6 m.

Figure 6.4.4 shows the influence of hangingwall beam thickness (b) on the maximum stable span at limiting equilibrium for various angles of discontinuities. It is apparent that the maximum stable span decreases with decreasing beam thickness.

The effect of compressive hangingwall stresses on the maximum stable span is given in Figure 6.4.5. It is evident that reduced compressive stresses decrease the stability and associated stable span lengths between adjacent support units. In particular, as the compressive stresses are reduced from σ_x = 0,1 MPa to 0,01 MPa, the stable hangingwall span is considerably reduced from a maximum of 4 m (σ_x = 0,1 MPa) to 1 m (σ_x = 0,01 MPa).

In shallow mines less fracturing occurs ahead of the stope face and hence, although generally less rock dilation occurs and the compressive hangingwall stresses are low in magnitude, the hangingwall rock is more competent, allowing increased span lengths. The methodology proposed here is particularly suited for comparatively densely fractured hangingwall rock, as typically encountered in intermediate and deep level mines. In shallow mines the rock engineer needs to assess the spacing of discontinuities and base the maximum stable span on typical block sizes.

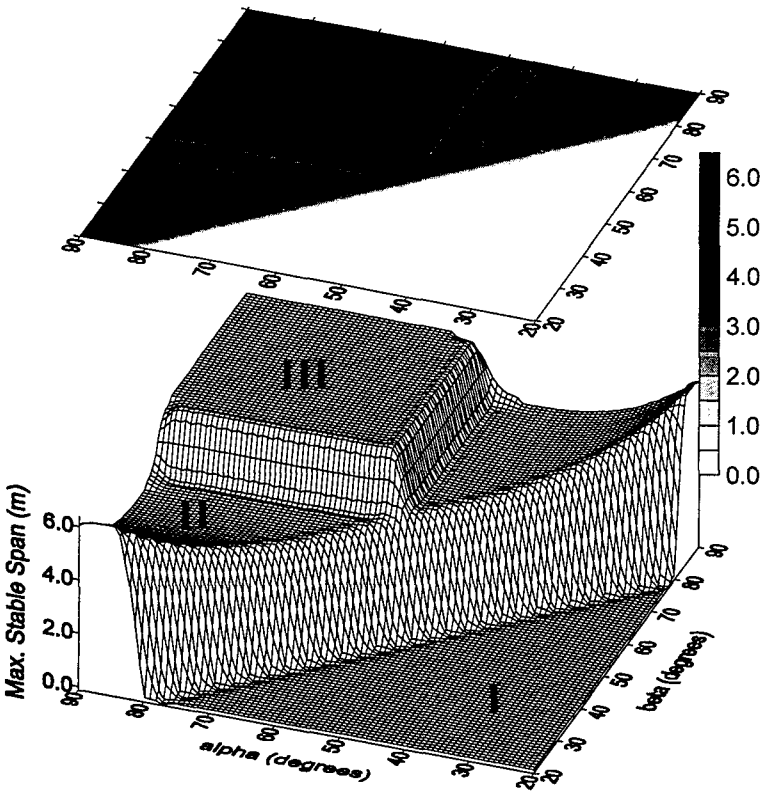

Figure 6.4.3 Maximum stable span versus discontinuity angles for σ_x = 1,0 MPa, b = 2,0 m and μ = tan 40°.

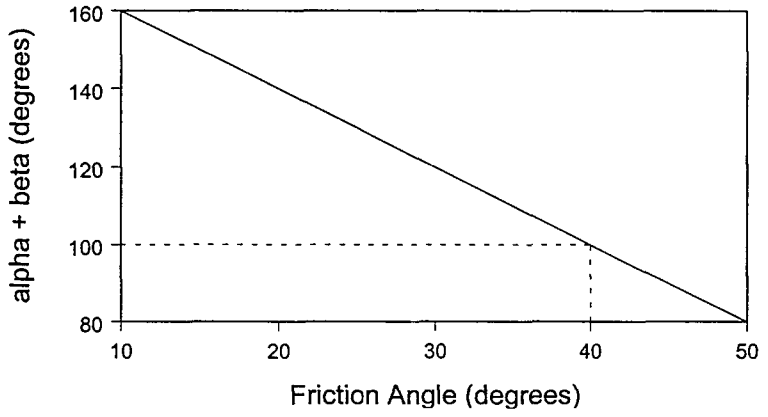

Figure 6.4.4 Values of $\alpha + \beta$ versus friction angle to generate positive shear resistance.

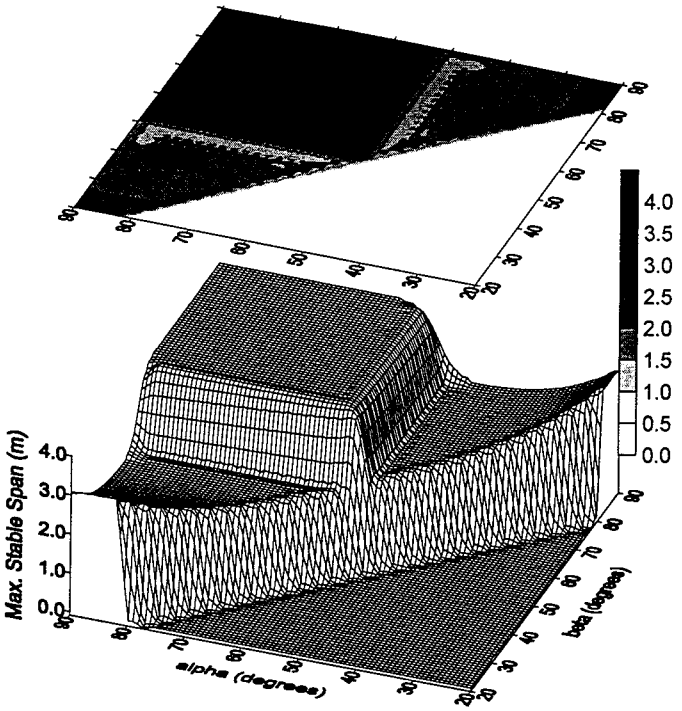

σ_x = 1,0 MPa, b = 1,0 m and μ = tan 40°

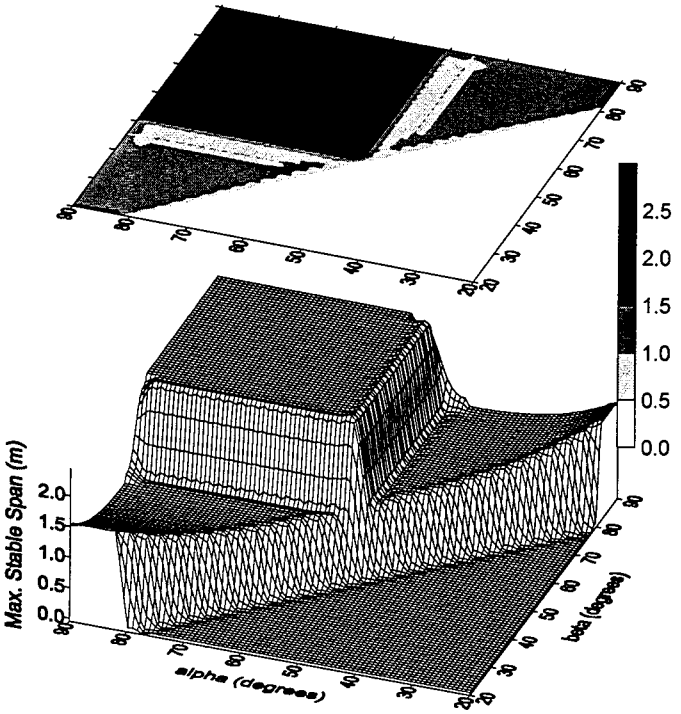

σ_x = 1,0 MPa, b = 0,5 m and μ = tan 40°

Figure 6.4.5 Effect of reduced hangingwall beam thickness (b).

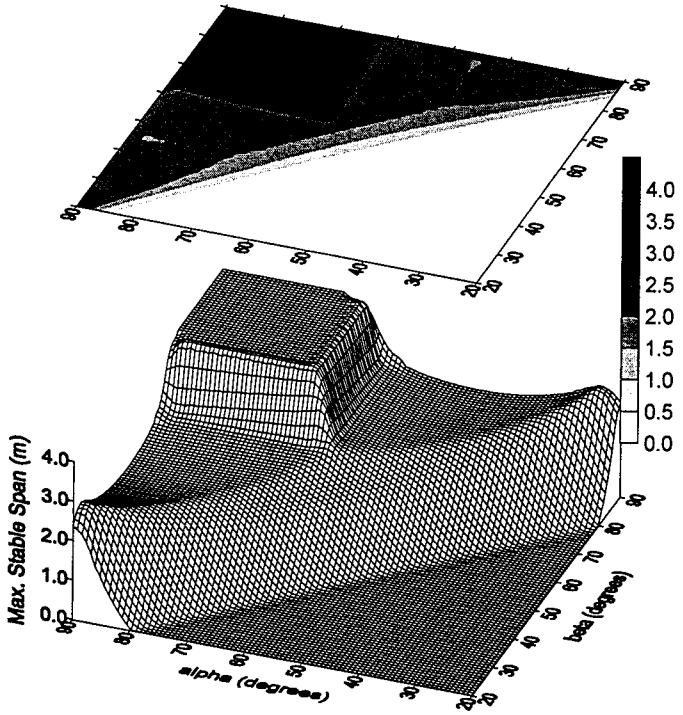

σ_x = 0,1 MPa, b = 1,0 m and μ = tan 40°

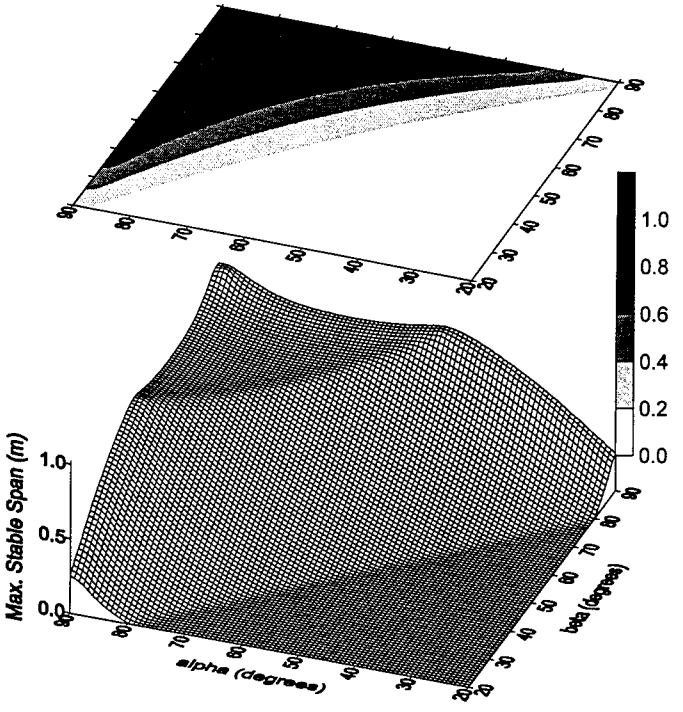

σ_x = 0,01 MPa, b = 1,0 m and μ = tan 40°

Figure 6.4.6 Effect of reduced hangingwall compressive stresses (σ_x).

6.5 Rockburst support design methodology

In seismic and rockburst prone mines, sudden fault rupture or the explosive failure of highly strained rock leads to energy being radiated in the form of stress waves. The stress waves interact with mining excavations, leading to interface and surface waves, energy channeling and wave focussing (Daehnke, 1997). The rock is subjected to rapid accelerations, resulting in rock fabric failure, keyblock ejection and stope closure. The most widely used support criterion used in rockburst prone mines is based on work by Wagner (1982), which takes the kinetic and potential energy of keyblocks into account. Underground observations, rockbursts back analyses and numerical simulations have indicated that hangingwall blocks can be accelerated to velocities of up to 3 m/s. The criteria for effective support systems are thus to absorb the kinetic and potential energy associated with the hangingwall moving with an initial velocity of 3 m/s. Previously (Roberts, 1995), it was assumed that during a rockburst the hangingwall must be brought to rest within 0,2 m of downward movement, i.e. the total energy that had to be absorbed by the support system (per m^2) being:

$$E = \frac{1}{2}mv^2 + mgh \tag{6.5.1}$$

where E is the total energy to be absorbed by the support system, m is the mass of the hangingwall (dependent on fallout height), v is the initial hangingwall velocity (taken as 3 m/s) and h is the maximum allowed downward hangingwall displacement (taken as 0,2 m).

In the design methodology proposed here, the hangingwall is assumed to have an initial velocity of 3 m/s, however the displacement is determined from the energy absorption capabilities of the support unit (Figure 6.5.1 and Equation 6.5.2). Thus the total hangingwall displacement, up to the point in time when dynamic movement ceases, is greater for a support system providing less support resistance, whilst a high load support system will arrest the hangingwall within a shorter distance. In the first case the hangingwall deceleration is reduced, but the potential energy component, which needs to be absorbed by the support system, is increased. In the second case the hangingwall deceleration is higher, with the potential energy component being decreased.

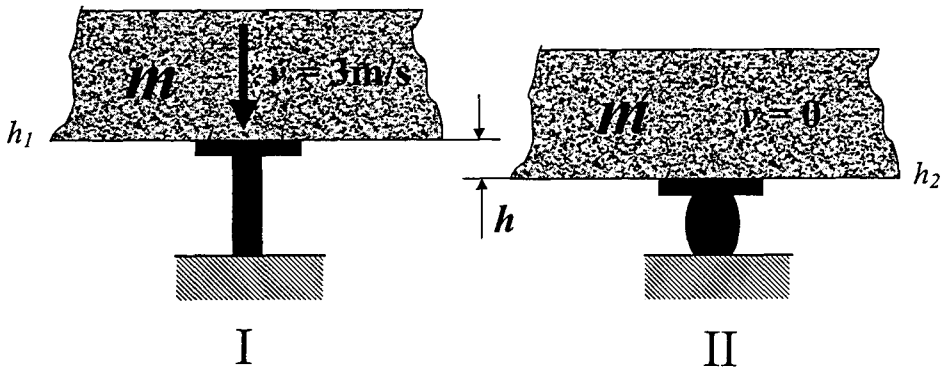

$$\int_{h_1}^{h_2} F(x)\,dx = \frac{1}{2}mv^2 + mg(h_2 - h_1) \text{ , where } h = h_2 - h_1. \tag{6.5.2}$$

Figure 6.5.1 Conceptual model of dynamic hangingwall displacement and associated energy absorption requirements of the support system.

To illustrate the loading requirements of a support unit during a dynamic event, assume that a support unit, with force deformation characteristics as shown in Figure 6.5.2, is installed

underground. Due to pre-stressing and stope convergence, the unit is quasi statically deformed up to point h_1; thereafter a rockburst occurs and the unit is rapidly compressed up to point h_2. The total energy, that is required to arrest the hangingwall, is shown by the hashed area of the graph in Figure 6.5.2. For the support system to meet the rockburst loading requirements, the following criteria apply:

1. The total dynamic hangingwall displacement (h) should not exceed 0,3 m. It is postulated that, if the hangingwall is displaced in excess of 0,3 m, the differential downward displacement between the face and support units, as well as between different support unit types of varying stiffness, could compromise the post-rockburst hangingwall integrity, leading to a heavily fractured hangingwall with low structural strength. Further work needs to be done to provide a more appropriate maximum value of h. In this preliminary study, however, a maximum value of h = 0,3 m is considered realistic and suitable for current support system design.

2. To ensure post-rockburst stability, the load carried by the support unit after the rockburst, i.e. $F(h_2)$, should exceed the deadweight of the keyblock.

3. The stoping width minus h_2 should exceed 0,6 m to ensure sufficient post-rockburst stoping width to allow movement of and prevent injury to mine personnel.

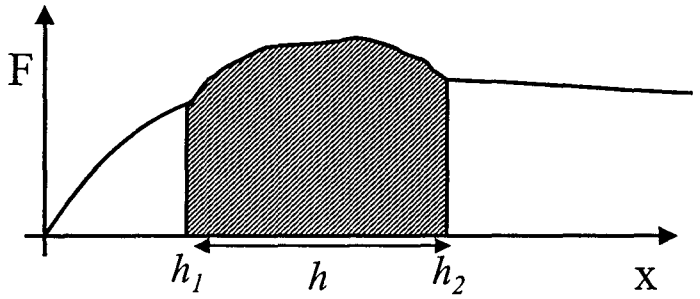

Figure 6.5.2 Quasi static and dynamic force-deformation behaviour of a support unit prior and during a rockburst.

Having calculated h using Equation 6.5.2, the local hangingwall deceleration can be determined from the equations of motions (assuming linear deceleration from v = 3 m/s).

$$a = \frac{v^2}{2h} \tag{6.5.3}$$

Taking the acceleration due to gravity into account, the effective hangingwall weight is calculated using Equation 6.5.4.

$$W_{eff} = m\left(g + \frac{v^2}{2h}\right) \tag{6.5.4}$$

The rockburst support design procedure follows a scheme similar to the rockfall support design methodology, and the assumptions made in the rockfall case also hold for the rockburst case. The main difference between the two design procedures is that in the rockburst case the effective hangingwall weight (Equation 6.5.4) is used, as opposed to $W = m\,g$ for the rockfall case. Figure 6.5.3 gives salient features of the rockburst support design procedure.

The effect of dynamic hangingwall displacement (h) is shown in Figure 6.5.4. Reduced displacement implies higher hangingwall deceleration and associated higher effective weight. This affects the hangingwall stability primarily in the buckling mode and reduced stable spans are evident.

Rockburst Support Design Procedure

1. **Set support resistance criteria:**
   i) Fallout thickness (b) to prominent bedding plane (from rockfall back-analyses), or
   ii) 95% cumulative fallout thickness (b) from fatality database (Roberts, 1995).
2. **Establish spatial distribution of support elements.**
3. **Delineate tributary areas (A_i).**
4. **Calculate load carried by each support element (F_i).**
5. **Calculate support resistance (F_i/A_i) based on tributary areas.**
6. **Calculate hangingwall displacement ($h_i = h_1 - h_2$) for each tributary area.**

$$\int_{h_2}^{h_1} F_i / A_i \, dh = \frac{1}{2} m v^2 + mg(h_1 - h_2)$$

7. **Plan view of average h_i based on A_i.**
   Energy absorption (e.a.) requirement are met if:
   i) $h_i < 0.3$ m
   ii) $F_i(h_2) > A_i \rho g b$
   iii) (Stoping Width $- h_2$) > 0.6 m

   Meet e.a. requirements? **NO** **YES**

Modify support system

8. **Define rock mass parameters.**
9. **Calculate effective hangingwall weight:**

$$W_{eff} = A_i \rho g b \left(g + \frac{v^2}{2h_i} \right)$$

10. **Calculate stability of h/wall due to buckling failure:**
    unstable *stable*
11. **Calculate stability of h/wall due to shear failure,**
    unstable *stable*

S T O P: Suitable support system and spacing thereof.

Figure 6.5.3 Flow chart showing features of the rockburst support design methodology.

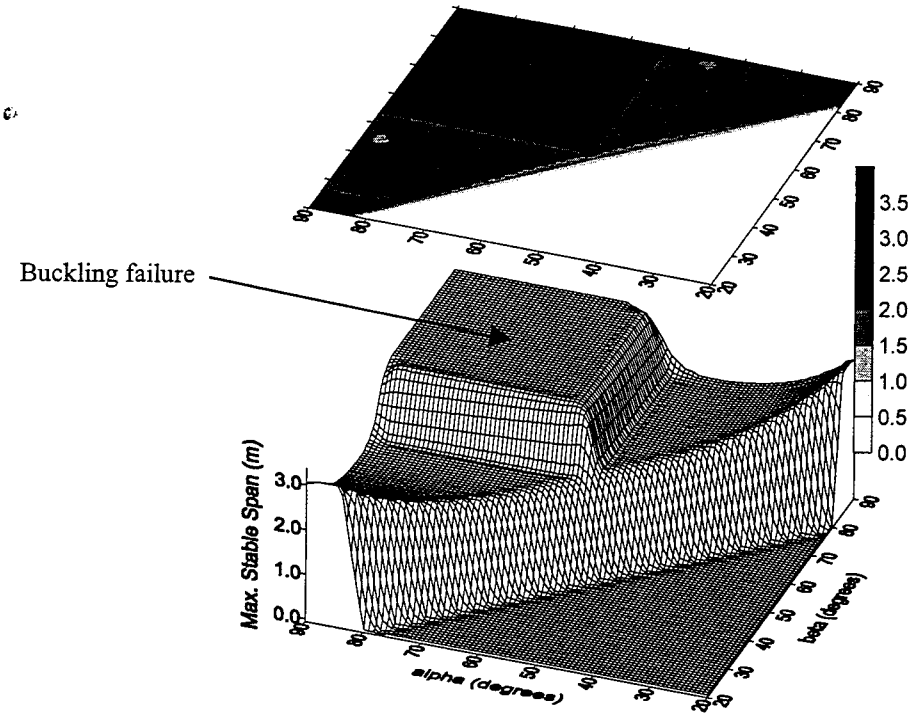

h = 0,3 m, σ_x = 1,0 MPa, b = 1,0 m and μ = tan 40°

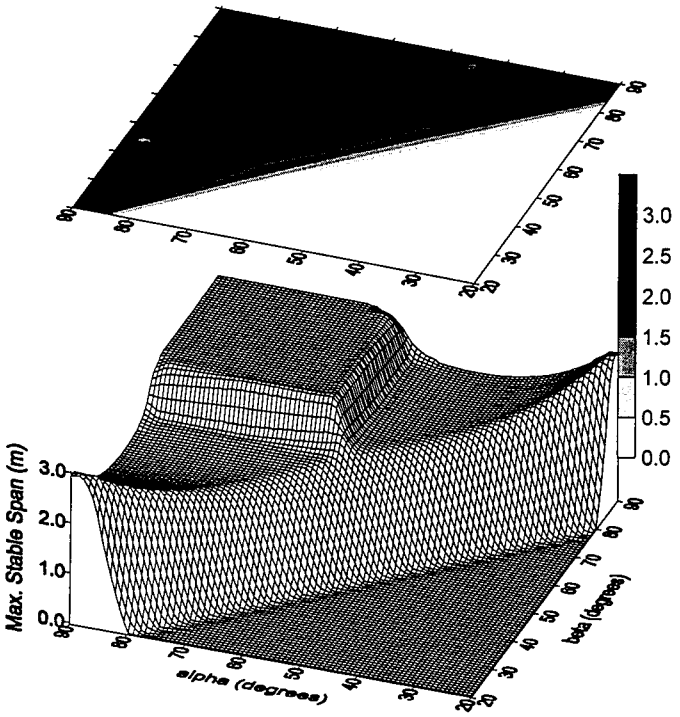

h = 0,1 m, σ_x = 1,0 MPa, b = 1,0 m and μ = tan 40°

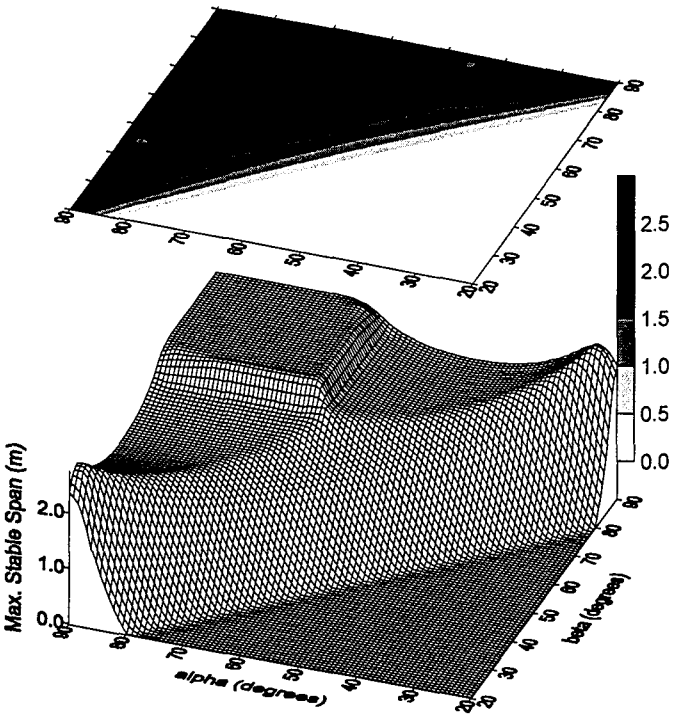

h = 0,05 m, σ_x = 1,0 MPa, b = 1,0 m and μ = tan 40°

Figure 21: Output of the rockburst support design methodology; effect of various hangingwall arrest distances (h).

6.6 Conclusions

The current methodology to design stope support systems in South African gold and platinum mines is based upon the tributary area concept. The discontinuous nature of the hangingwall rock is not adequately addressed and mechanisms leading to rock mass failures between adjacent support units are poorly understood. The work reported here aims to formulate a basis for quantifying support mechanisms and gain insights into the influence of rock discontinuities on stable hangingwall spans.

Numerical models are used to qualitatively investigate the stress transfer from the support units to the discontinuous hangingwall. Stable hangingwall spans are quantified by considering two failure mechanisms, namely (i) beam buckling, and (ii) shear failure due to slip at the abutments. The output of the proposed design methodology is appropriate site specific support spacing, based on discontinuity spacing and orientation. The method is particularly suited to mines at intermediate and great depth, where, typically, the hangingwall is highly discontinuous due to face parallel mining induced fractures. Results of parametric studies show that with increasing in-situ compressive hangingwall stress, beam thickness and friction angle, hangingwall stability is increased, leading to wider stable hangingwall spans between adjacent support units.

A methodology to evaluate support systems catering for rockfall and rockburst conditions is proposed. The method consists of two stages: (i) a tributary area analysis determines the general support resistance requirements for the support system as a whole, and (ii) a stability analysis considering failure due to beam buckling and shear at the beam abutments gives maximum spacing of individual support units.

The methodology is particularly suited to mines in intermediate and great depth. Although the method can give valuable insights into support requirements in shallow mines, additional input, in terms of past experience and engineering judgement, is required from the rock engineer to determine typical block sizes and the support thereof.

The support design method gives insights into spacing and associated stable hangingwall spans in the strike direction only. Due to the face parallel mining induced fracture orientation in intermediate and deep level mines, the hangingwall rock is generally less prone to failure between two support units in dip direction, compared to failure between units in strike direction. Further work dealing with the probability of hangingwall instabilities on strike versus dip directions is given in Section 9.

It is recommended that additional work be conducted to quantify the effect of arbitrarily oriented discontinuities of geological origin on support spacing in strike and dip directions. Further work could re-address the influence of the modified hangingwall stress distribution due to loading by the stope face, support units and backfill. Particularly in the case of shallow dipping fractures, stresses transmitted across discontinuities could stabilise the hangingwall, leading to wider permissible spans.

Parametric evaluations of the proposed support design methodology show that, for most discontinuities observed underground, i.e. dipping between 50° and 90°, the design procedure provides realistic stable spans, which agree with current mining practice and post rockfall/rockburst underground observations and back analyses. It is essential, however, to conduct further back analyses in order to calibrate and verify the design method.

6.7 References

Adams, G.R., Jager, A.J. & Roering, C. 1981. Investigations of the rock fracture around deep-level gold mine stopes. 22nd U.S. Symposium on Rock Mechanics, Massachusetts Inst. of Technology, June 28-July 2.

Bandis, S.C., Lumsden, A.C. & Barton, N.R. 1983. Fundamentals of rock joint deformation. Int. J. Rock Mech. Min. Sci. & Geomech. Abstr. 20(6), pp. 249 – 268.

Beer, G. & Meek, J.L. 1982. Design curves for roofs and hangingwalls in bedded rock based on voussoir beam and plate solutions. Trans Instn Min. Metall. 91. pp. A18 – 22.

Brady, B.H.G. & Brown, E.T. 1985. Rock Mechanics for Underground Mining. George Allen & Unwin, pp. 214 – 218.

Daehnke, A. 1997. Stress wave and fracture propagation in rock. Ph.D. Thesis, Vienna University of Technology.

Esterhuizen, E. 1998. Improved support design through a keyblock approach. Interim Report for SIMRAC Project GAP 330, Stope face support systems, prepared by CSIR Mining Technology and University of Pretoria, pp. 1 – 83.

Evans, W.H. 1941. The strength of undermined strata. Trans Instn Min. Metall. 50, pp. 475 – 532.

Herrmann, D.A. 1987. Fracture control in the hangingwall and the interaction between the support system and the overlying strata. M.Sc. Dissertation, University of Witwatersrand, Johannesburg.

Hutchinson, D.J. & Diederichs, M.S. 1996. Cablebolting in Underground Mines. BiTech Publishers, pp. 265 – 269.

Jager, A.J. 1998. Personal communication on the structure of discontinuous hangingwalls in deep level mines. CSIR: Division of Mining Technology, Carlow Road, Auckland Park, Johannesburg, 2000.

Jager, A.J. & Roberts, M.K.C. 1986. Support systems in productive excavations. Gold 100. Proc. of the Int. Conf. on Gold. Vol 1: Gold Mining Technology. SAIMM, Johannesburg, pp. 289 – 300.

Roberts, M.K.C. 1995. Stope and gully support. Final Report for SIMRAC Project GAP 032, CSIR Mining Technology, pp. 1 – 45.

Rockfield, 1996. ELFEN User Manual, Version 2.6, University College of Swansea.

Squelch, A.P. 1994. The determination of the influence of backfill on rockfalls in South African gold mines. M.Sc. Dissertation, University of Witwatersrand, Johannesburg.

Wagner, H. 1982. Support requirements for rockburst conditions. Proc. of the 1st Int. Cong. on Rockbursts and Seismicity in Mines, SAIMM, eds. N.C. Gay and E.H. Wainwright, Johannesburg, pp. 209 – 218.

7 Identification and assessment of impediments to successful implementation of stope support systems

7.1 Introduction

Stope face support systems have a direct impact on the safety hazard to which the workforce is exposed. Stope support also accounts for ± 23 per cent of direct stoping costs and ± 11 per cent of total working costs. Improved understanding of stope support systems and the behaviour of the rock surrounding excavations has steadily led to the development of improved support design and layouts to address the safety hazard. There are concerns, however, that these potential benefits will not be achieved if support systems are not properly implemented. There is the additional concern that large amounts of money will also be wasted. This report is therefore an assessment of the types of environmental, human and technical problems that can impede successful implementation. Specifically, the three main objectives of this work are as follows:

1 Identify and assess impediments to the successful implementation of stope face support systems within each geotechnical area.

2 Assess how modifications to the mining/support cycle and modification of the mining methods could assist implementation of improved support systems within each geotechnical area.

3 Identify geotechnical areas where rockbolting would be an appropriate support system.

7.2 Literature survey

As this enabling output focuses on impediments to the successful implementation of stope face support systems, the literature search sought out earlier studies on the implementation of other technologies in the stope environment.

The survey involved an electronic search of Chamber of Mines Research Organization and CSIR: Miningtek research reports, the GAP 330 progress report (Hagan and Daehnke, 1997) prepared for SIMRAC (12/97), as well as papers presented to the Association of Mine Managers and the South African Institute of Mining and Metallurgy (SAIMM) over the period from 1988 to early 1999. From similar studies it was hoped to learn from the types of impediment encountered with the implementation of other stope technologies, for example trackless equipment, millisecond blast initiation systems, rapid yielding hydraulic props, and hydraulic rockdrills. It was intended that this information be used as a basis for development of the task methodology, as well as an indication on how identified impediments might be best assessed.

In summary, the literature review had the following objectives:

- to learn from the work undertaken during the previous two years of the project and to establish whether any geotechnical area related impediments had been identified,
- to identify possible examples of similar studies to identify and assess impediments to the introduction of other stope technologies,
- to assist with the development of an appropriate methodology to approach this task, i.e. the formulation of questions requiring answers,
- to consider methods for assessing identified impediments, and
- to enable sub-division of the problem.

7.2.1 Findings of the literature search

A number of papers and reports were identified that presented case studies on the types of problems encountered when introducing new technology into mines. They tended, however, to focus on the mechanics of the process and devoted limited attention to specific problems of implementation. A number of references were identified that dealt with stope support systems and the issues of cost, technical problems and human factors, were, however, identified. Two papers, in particular, were identified that discussed the issue of implementation.

Roberts et al. (1993) list nine recommendations to be considered when introducing a new support type; these are reproduced in Section 7.9.1. In another paper Gürtunca and Gay (1993) emphasise the dual roles of technology (support) champions to drive implementation and the training of mine personnel to understand the motivation for the selection of a particular support system.

Among the papers presented to the Association of Mine Managers there are several that deal with specific projects on individual mines. Amongst these is a paper by Handley (1994-1996) that refers to the softness of the shale footwall, a relative reduction in seismic frequency, and the cost of mat packs motivating a decision to move to yielding timber elongates in the eastern portion of Western Deep Levels (South) mine. Handley also refers to a series of "disastrous" rock-related accidents in which jointing, face shape and support strategies played a role and which, eventually, led to a re-evaluation of mining layouts. In an associated paper MacFarlane (1994-1996) states that joint orientation may "override previously held criteria and highlight the need for a revised system of mining", although he does comment that this conclusion is very site specific.

7.3 Methodology

Initially it was anticipated that one of the outputs of past work on project GAP 330 would be an assessment of the different geotechnical areas with the recommended support systems. This was considered a prerequisite to the identification of impediments to the implementation of support systems on mines. In the absence of such information, however, an alternate approach had to be considered.

One of the primary issues considered was the meaning of the phrase "successful implementation" when applied to stope support systems. For the purpose of this project the phrase is taken to mean that a stope support system is installed in such a manner that it performs at the designed level, utilizing the optimum level of resources.

A questionnaire was prepared, to collect information from individual mines, on their experience concerning the introduction of new or improved support systems or significant changes to their support strategy. Following initial meetings with mines it was evident the questionnaire needed some modification, while the focus on establishing clear links between geotechnical features, the support system used and the impediments was correct. The questionnaire formed the basis of the information gathering exercise. Feedback on the proposed approach was obtained from discussions with members of the project team. In essence, the adopted approach attempted to consider a range of issues impacting on the implementation of support systems. The following list (in no specific order) represents a selection of some of the issues considered during formulation of the methodology.

> How do geotechnical conditions impact on mining, and if so, which features are the most important, e.g. stope width, closure, dip etc.?
>
> Are the impediments more related to mining factors, e.g. face advance rates, work practices, competence, skills, layout or the mining method?

Is it the reef type that is important or is it a function of whether the hangingwall/ footwall combination is hard or soft, whether the reef is deep or shallow, whether it is steep or flat dipping?

What are the links between these (geotechnical) factors and implementation of support systems?

How important are the impediments (relative to one another), and in what way do they impact on implementation?

Are all impediments generic or are there those which relate to a specific reef or condition (e.g. depth)?

What are the more common support combinations, is there anything particularly problematic about their use on a particular reef, under certain conditions, or on a particular mine?

If this is the current situation, what of the future and what must be done to ameliorate the problems, if not eliminate them?

Are there trends or differences that can be identified between gold and platinum?

7.4 Stope face support systems

Before turning to the identification of impediments to the successful implementation of stope face support systems, it is appropriate to consider the types of support in use and possible future trends. In this exercise it must be noted that the primary functions of a support system are to provide:

- the optimum areal coverage and adequate protection from localized falls of ground, and
- the designed support resistance (normally provided by the permanent support).

In addition the support system may fulfill other functions, for example:

- maintain its integrity during and after the blast,
- provide support for the suspension of blast barricades, winch signaling systems, ventilation curtains and pipes (not cables), and,
- of necessity, as support types, backfill and stabilizing pillars will form part of the mine's ventilation planning and distribution network.

7.4.1 Current stope support systems

Table 7.4.1 is a detailed list of both temporary and permanent stope support types. On both gold and platinum mines stope supports are invariably installed in combination, i.e. a *temporary* support with a *permanent* support, as indicated in Table 7.4.1. The table gives an indication of the wide variety of support options available to the engineer for narrow reef support systems, as well as the low level of industry standardization. This latter point suggests that workforce training can be a significant impediment to successful implementation.

7.4.2 Temporary support

As the term implies, temporary supports are the first supports to be installed in the face and before installation of permanent support. For example, they are installed in the face area after a blast or at any time during the shift, when it may be deemed necessary due to bad ground conditions. Temporary support is either removed before the blast and stored for re-use or, as is often the case

with mine poles, knocked out by the blast.

7.4.3 Permanent support

Permanent supports are designed to remain in position and be effective for extended periods, and are not removed prior to the blast. They are designed to provide the necessary resistance and areal support under prevailing conditions.

Table 7.4.1 Temporary and permanent support types.

MINING METHOD	TEMPORARY SUPPORT	PERMANENT SUPPORT		ATTACHMENTS
Narrow reef Stoping	Mine poles#	Mats and slabs	Steel props	Headboards
	Mechanical props#	End-grain composite packs	Grout packs	Extensions
	Face sprags#	Brick composites	Backfill	Foot pieces
		Precast packs	Rock bolts#	Load spreaders
		Mine poles#	Caving	
		Cluster packs	Pillars	
		Elongates#	Hydraulic props#	
		Pre-stressed elongates	Pack pre-stressing	* pre-conditioning
Wide reef stoping	Roofbolts	Roofbolts	Backfill	

* Note: Pre-conditioning of the stope face before a blast by the firing of holes drilled in the footwall of the face is not a true support system. Its use, however, is expected to become more widespread in the future, as it has been shown to significantly reduce the frequency and severity of seismic events in areas of high stress. As a result it reduces the support resistance required from the permanent support system. Those supports indicated by a "# " are normally found in the stope face area.

In any given stope we would expect to find both types of support, as a stope face support system comprises a combination of both temporary and permanent support types. Occasions do arise where a temporary support will be coupled with two permanent support types, for example in the case of backfill, packs, or elongates being employed together with stabilizing pillars.

7.4.3.1 Future stope face support trends

Future projections are that gold mines will need to access deeper and deeper reefs to maintain gold output. On platinum mines, the situation is believed to be similar, as the shallower Merensky Reef reserves are steadily being depleted, necessitating greater output from the deeper UG2 reef.

In their paper on implementing the latest developments in improving safety in underground mines Gürtunca and Gay (1993) refer to the use of lightweight (rapid-yielding) hydraulic props, an improved 3 m/s rockburst prop and headboard system, backfill systems for local support, concrete pillars to replace stabilizing pillars, and pre-condition blasting as some of the support technologies developed for deeper stopes. It is anticipated that the use of these types of support systems, particularly the use of hydraulic props installed and maintained by contractors, will increase steadily in the future, and that the trend towards the design of improved regional, as well as local support systems, will continue.

7.4.3.2 Common support practices

Support practices can vary considerably between different shaft sections on the same mine and more widely still between different mines. This is an indication of the many differences in the mining environment caused by a combination of regional and local conditions, geotechnical factors, mine layout, and rate of extraction. These issues are considered in the next section under generic impediments.

7.5 Identify and assess impediments to the successful implementation of stope face support systems within each geotechnical area

The stope face is defined as the area lying between the advancing stope face and 10 m back from the face in which drilling, blasting, cleaning, and supporting activities take place. This area incorporates both temporary and permanent supports, as it is the permanent support that influences local and regional ground behaviour. Permanent supports have the potential to obstruct transport and cleaning systems, and require special attention at the interface with gullies and therefore must be correctly aligned and installed.

Table 7.5.1 lists three categories into which the majority of impediments to successful support implementation fall. This division is somewhat arbitrary, as it can be argued that many impediments are generic to stope support systems, and not to a particular reef or geotechnical area. The main objective, however, of the division is to clarify the position as much as possible, by grouping together what appear to be common impediments.

Table 7.5.1 Impediments to the implementation of stope support systems

GROUP	IMPEDIMENT
1	Generic
2	Geotechnical
3	Mining process

7.5.1 Generic impediments

This section considers the principle impediments identified, and are considered generic to all stope support systems and, in varying degrees, to support systems on both narrow and wide reef stopes on both gold and platinum mines. Key generic impediments are:

7.5.1 Support cost
7.5.2 Support performance
7.5.3 Infrastructure
7.5.4 Human behaviour
7.5.5 Management systems

This section summarises each impediment and the manner in which it impacts on the implementation process.

7.5.1.1 Support cost

Cost becomes an impediment to the successful implementation of a support system when it appears to represent a disproportionate share of the overall stoping cost. As reported by Piper (1997) stope support costs vary widely. In his example he showed that support costs on gold mines range from R38/m^2 to R166/m^2 with an average cost of R72/m^2 (1995 figures). On platinum mines, stope support costs range from R11/m^2 to R74/m^2, with an average cost of R19/m^2. As support costs represent 8-10 per cent of stope input costs, mines expend considerable effort on keeping them as low as practically possible. In a sensitivity analysis Piper again demonstrates the impact of stope width on support costs; (in his example, a reduction in stope width of 20 per cent equates to a cost saving of 22,8 per cent). This underlines what has long been recognised of course, that is that good drilling and blasting practice can help contain support costs.

7.5.1.2 Support performance

The phrase "successful implementation" requires that, once installed, the support functions as designed, fulfills a role in creating the regional work environment, and locally controls falls of ground. Implicit in this statement is that the support be correctly installed, in the correct position and, in the case of permanent supports, stressed to the desired level. Furthermore, "successful implementation" refers to a support system, rather than individual units, which necessitates that the correct installation procedure be duplicated time and again.

It is suggested that, to install a support system, so that it constantly achieves the optimum performance level, is extremely difficult under average working conditions and production demands. The reason being that a stope is a dynamic environment, changing constantly as a result of the mining process. The successful implementation of the support system, therefore, requires considerable skill, experience and on-going supervision.

A further point is that only pre-stressed supports, for example rapid yielding hydraulic props and cementitious packs, provide the operator with a visible indicator of correct installation. Less sophisticated support types depend on operator skill, experience and adherence to good installation practices.

7.5.1.3 Infrastructure

The term infrastructure defines the policies, equipment, systems and procedures required to ensure that the correct support types are purchased and delivered to the right working stopes at the appropriate time. Infrastructure is not considered an impediment but it must be stated that the provision of the right infrastructure will form an integral role in implementation, especially when changing from one support system to another.

7.5.1.4 Human behaviour

The successful implementation of a support system also depends heavily upon the skills, experience and motivation of the workforce. It is generally recognised that supervisors and workers must want to implement the system, otherwise it will invariably fail to meet expectations. This section considers a number of issues believed to influence worker attitudes towards support systems. This is not intended as a technical review but rather as a commentary, raising issues primarily because of the potentially restrictive effect that they can have on the implementation of support systems, irrespective of geotechnical area.

Support mass
The average stope width of Witwatersrand gold reefs is between 1,2 m - 1,8 m, although there are some notable exceptions such as the Upper Elsburgs (U_{E1} to U_{E2}) at Randfontein Estates Gold

Mine Cooke III section, where the total reef "package" may be as much as 24 m thick. There are also areas of the Ventersdorp Contact Reef, for example at Western Deep Levels South that exceed 4,0 m and the Kimberley reefs at South Deep and Target. The average stoping width on the Merensky platinum reef is 1,0 m and on the UG2 reef 1,5 m. In general though, most stopes are narrow.

The mono-rope winch was introduced to the gold mining industry in the early 1970's. Despite many attempts to develop mechanical support handling and installation systems to operate in narrow stope widths, none has proved successful. Within the stope horizon support handling and installation, therefore, still remain essentially manual activities. As a result, the mass of individual supports, and the ease with which they can be transported and installed, are important issues among the workers who perform these tasks.

At the same time a number of tools have been introduced to facilitate support installation. These include mechanical saws to cut mine poles to size and pack stressing systems which, in effect, replace the blocking/ wedging process used previously. There is a twofold advantage to pre-stressing systems, as they advance the time when the pack becomes "active" and, hence, provide the desired support resistance.

Support mass is a complaint associated particularly with rapid yielding hydraulic props and ultimately led to the development of a second generation of lighter props. This latter development is believed, however, to have only partially solved the problem, as rapid yielding props are still considered to be "too heavy" on many mines. The response to this ongoing complaint has differed between mines with some withdrawing rapid yielding hydraulic props and others sub-contracting the work to contractors. Other mines appear to have few problems and continue as previously, i.e. with their own workforce responsible for prop installation.

Coupled to the issue of prop installation and potential losses, as a result of props "punching" into the hanging-or footwall or "freezing" is the issue of prop maintenance. As a service function prop maintenance has also felt the impact of ongoing attempts to improve productivity. Concern over the possible impact of inadequate maintenance has prompted some mines to sub-contract prop installation and maintenance.

Installation and removal of support

A related issue is the concern expressed by several mines about the increased reluctance of workers to use supports of a type that must be installed and later removed, only to be re-installed again after the blast. This applies to mechanical props that are widely used as temporary face supports, as well as to rapid yielding hydraulic props. There are therefore two main concerns; the first is the safety of the process and the second is the additional work involved. [Note: in the period between 1990 and 1997 a total of 120 workers were killed on gold mines while installing or removing supports (Glisson, 1998)]. One mine indicated dissatisfaction with the procedure for mechanical prop removal, citing, as an occasional problem, that when the props are to be removed from the face at the end of the shift for storage, the support crew has often knocked off.

The role of human behaviour in accidents in the mining industry has surfaced consistently in recent industry studies. Human behaviour was also mentioned here as an underlying cause of poor support implementation. While it is not the intention to enter into further discussion here, worker motivation is considered to be vital to successful support implementation. It is equally well recognised that the implementation of mining technology, in general, benefits from the presence of a "champion" to drive the process.

A further impediment to successful implementation in narrow reef stopes is heavy physical work. Another factor to consider is that as mining depth increases, the influence of geological features on the stope environment increases commensurately. Depth is the most important criterion because of its influence on seismicity and rockfalls, increasing the need for greater support resistance and better areal coverage. Greater support resistance is provided by introducing stronger, and, generally heavier, support systems and reduced support spacing. In turn, improved

areal coverage is provided by the use of headboards or load spreaders. The aggregate effect of these changes is an increased work load, and when depth is compounded by other geological conditions such as soft or friable hanging or footwall rock types, the effort required is further increased. This suggests that efforts need to continue to find some means of handling heavy and awkward supports in the confines of a narrow stope.

In marked contrast to narrow reef stopes, the implementation of support systems on wide reef stopes is simplified. The width permits the use of mechanical drilling and bolting equipment as, for example, at Randfontein Estates GM. This mine has also developed a method of placing backfill that largely eliminates the need to manually construct backfill paddocks. However, where props or packs are used the units are heavier and more difficult to manoeuvre. Steep dips also impose particular problems.

The implementation of a support system requires workers to construct or install supports to a prescribed pattern. Successful implementation is, therefore, influenced by the various working heights and the varying levels of temperature and humidity. Important human constraints are predominantly related to the capacity to perform both physically and mentally under these conditions, whereas work constraints relate to the task and physical environment. These two groups are summarised in Table 7.5.1.4 below.

Table 7.5.1.4 Criteria important to support implementation.

Human constraint	**Requirement**	**Work constraint**	**Requirement**
Knowledge	Why support is required; important to understanding and motivation	Degree of difficulty (of task)	Amount of physical effort required; - also related to working height.
Discipline	To install support correctly every time	Degree of complexity (of task)	Not too complex (normally)
Physical capacity	A physiological requirement	Availability of technology	Reasonable environmental conditions

While Table 7.5.1.4 summarises what are believed to be important factors, it does not provide a simple solution to the problem of combining all of them successfully, to achieve the desired result, namely proper support implementation. The only reasonable solution appears to lie with greater use of technology to replace the more physical aspects of the work.

7.5.1.5 Management systems

Management systems apply the necessary controls over the implementation process. Interviews indicate that the provision, organisation and handling of shaft schedules, support transport vehicles (e.g. timber cars), support distribution network and delivery system is not considered a major impediment to implementation. As with infrastructure, however, it is important to keep in mind management systems when developing a support implementation plan.

Summary

This section considers generic impediments to the successful implementation of stope support systems. The choice of which impediment is more important, depends to some degree upon the individual mine's experience. In the implementation of stope face support systems, management considers support cost and performance to be the two biggest impediments, while infrastructure and management systems are considered to be relatively minor issues. This applies to both narrow

and wide reef conditions. Even if this is accepted, it still, however, raises the question as to why the belief persists that many support systems are not properly implemented. In narrow reef stopes one answer would appear to lie with worker concerns over support mass, ergonomics of support design and difficult working conditions. The installation of stope support is still a highly manual activity and it is inevitable that human performance should be questioned when trying to identify impediments. Although the issues of skills, knowledge and motivation drew comments from mines, not one of these was put forward as the principle reason for the poor implementation of a support system.

7.5.2 GEOTECHNICAL IMPEDIMENTS

The following section considers impediments to the successful implementation of stope face support systems consequent upon identified geotechnical criteria. For example, rock type assemblage, stope geometry, closure, partings, joints, depth and rolls. The principle objective being to establish a link between identified geotechnical areas, common support systems and identified impediments that arise because a support type or system is used in a particular geotechnical area.

SIMRAC project GAP 416 (Güler et al., 1998) defines a geotechnical area as an area exhibiting specific rock mass behaviour and associated hazards in response to mining activities where the same rock engineering strategies may be applied. In project GAP 416 it is suggested that the fixed (geotechnical) parameters may dictate a basic rock mass response, but that mining practice may modify ground conditions. Figure 7.5.2 has been adapted from GAP 416 and depicts the fixed parameters that existed prior to mining and the variable parameters imposed by the mining operation. This section of the report considers the fixed criteria to the right of the central vertical line in Figure 7.5.2.

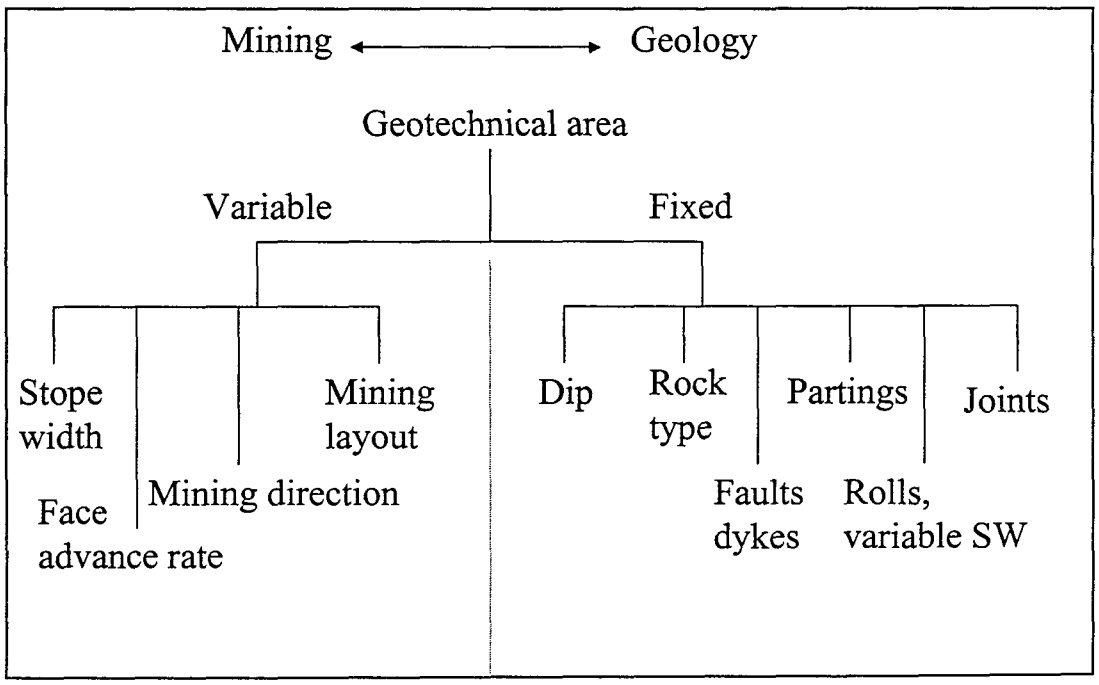

Figure 7.5.2 Diagrammatic representation of division between fixed and variable parameters (after Güler) SIMRAC project GAP 416.

7.5.2.1 Rock type (soft/hard)

Rock type refers to the degree of hardness of the hanging- and footwall rock types with an arbitrary division between soft and hard being made at a UCS of 200 MPa. A soft rock type generally means

that the hangingwall beam is more easily fractured, and more laborious to examine and prepare before support is installed, as well as more likely to break and fall. As depth increases and greater support resistance is required, a soft rock type necessitates the use of some form of load spreader or headboard to distribute the load created by support resistance over a greater area to prevent punching of a soft hanging- or footwall. Load spreaders are commonly used for this purpose, as in certain areas at Hartebeestfontein GM. Load spreaders can either be constructed from a simple slab lagging, or "one-one", or manufactured to suit a particular prop design. Despite being somewhat cumbersome, load spreaders are not regarded as an impediment.

A soft or weak hangingwall always presents an increased safety risk, so more time must be allocated to a proper examination of the hangingwall. A weak hangingwall can also require a reduction in support spacing and additional supports such as "train" packs or support clusters.

7.5.2.2 Orebody geometry (rolls) and variable stope width

A roll in the reef plane larger than the stoping width is difficult to mine, especially if it is unexpected. A roll breaks the support pattern and its negotiation invariably results in a wider stope width and the formation of a brow that must be supported on both sides at least. Where the hangingwall rock type is soft, installing support is often a time consuming process.

7.5.2.3 Faults and dykes

Unless they are small i.e. < 1 m, faults and dykes also break the support pattern and slow the mining rate on the panel where they are intersected. Depending on the depth, bracket pillars may be required along the intrusion to protect adjacent workings. In concentrated mining layouts, for example longwalls, the negotiation of faults and dykes has proved to be a particular problem. This has led to a decision on many mines to change to a more flexible layout, for example the sequential grid layout as practised at Elandsrand GM.

7.5.2.4 Hangingwall partings

Hangingwall partings, especially thin partings and those that have separated from the overlying strata, present a major safety hazard. Special care is required during examination, as well as in the installation of temporary and permanent support, and areal support is desirable. On some mines, notably Evander, St Helena, Saaiplaas and Western Platinum mines, hangingwall partings are secured by rock bolts. This is discussed in greater detail in a later section.

7.5.2.5 Joints

The effect of jointing is to weaken the hangingwall strata and the standard approach is to install temporary and permanent supports with headboards. The headboards should be aligned perpendicularly to the joint direction. Occasionally this is awkward, for example when backfill is used together with rapid yielding hydraulic props. Unless care is exercised and the prop moved timeously, the headboard can become trapped by the backfill.

The above findings are summarised in Table 7.5.2 which plots geotechnical parameters against examples of common impediments to support implementation.

Table 7.5.2 Assessment of geotechnical parameters and common impediments.

	IMPEDIMENT																	
GEO –TECHNICAL PARAMETER	examination & barring	Alignment - positioning of headboard	Clamping/ holding extensions in place	Correct/ sufficient support available	"punching"	Drilling	Cleaning	Freezing	Positioning of filler valve	Installation of gate stulls	Danger of slipping or falling/ falling material	Effective blocking against hangingwall	Props "roll" out	Not always properly mined	Insufficient allowance made for "travel"	Poor recognition of changes in ground conditions	General difficulty in installation	Transport of support units (in stope)
Soft h/wall	•				•			•						•			•	
Rolls, var. SW	•		•	•													•	
Hard h/wall																		
Soft footwall					•		•	•									•	
Joints	•	•																
Dip > 30^0										•	•							•
Hard footwall																		
Closure < 5 mm/m														•				
6 – 40 mm/m																		
> 40 mm/m															•			
Dip < 35^0																•		
> 35^0											•						•	
SW < 1,0 m							•								•		•	•
1,0 - 1,8 m						•												•
> 2,5 m			•											•				
Mining induced fractures		•																
Parting planes	•																	
Non-axial loads													•					
Potholes/Domes																•		

Summary

Table 7.5.2 is a qualitative assessment and ranks geotechnical criteria in terms of the type of impediment incurred. On gold mines, a soft hangingwall, rolls and variable stope widths, soft footwall and joints represent important geotechnical impediments. On platinum mines poor recognition of changes in ground conditions and props "rolling out" are important issues.

Even if the geotechnical environment is fixed, there are still practical limitations regarding control of the stoping environment. Successful implementation is therefore a function of skill, knowledge and ability. The use of technology in narrow reef stopes is constrained by the geometry, although it clearly has a role in trackless and wide reef stopes.

Table 7.5.3 presents an assessment of geotechnical criteria, common support systems and impediments in terms of skill level, discipline and technology. The indication is that skill and discipline feature strongly when implementing a support system where there are variations in stope width (rolls) and where jointing and soft (friable) hangingwall occur. Examples of geotechnical areas where technology could assist include areas where rolls are prevalent, where there are moderate to steep dips, backfill placement in shallow dip conditions, and in soft hangingwall conditions. Furthermore, it is believed that technology can provide suitable areal support, as well as a means of drilling roofbolts holes in narrow stopes.

***Table 7.5.3 Summary of geotechnical criteria, support type, impediment and requirement for skill, discipline* or technology.**

Geotechnical criteria	Support system	Impediment	Skill	Discipline	Other, e.g. Technology
Reef rolls	All supports	Depending upon frequency and size of rolls, many different support heights must be installed	•	•	•
Jointing	Mine poles, props + headboards	Ensuring headboards are aligned perpendicular to jointing	•	•	
Dip	Mine poles, props	Installation perpendicular to dip	•	•	
Soft hanging	Mat packs	Proper blocking against the hangingwall. Pre-stressing an option at additional cost.	•	•	
Dip	Props, elongates + extensions	Extensions can reduce support effectiveness; cause injuries			•
Shallow dip	Backfill	Partial hangingwall contact. Full contact may never occur			•
Soft hanging	Props, packs, elongates	Hanging falls out between supports, even with headboards. Increased areal support.			•
Soft footwall	Props, elongates, poles	Punching of footwall. Loss of props if proper care is not exercised		•	
High closure	props, elongates	Limited yield. Require sufficient "travel" to accommodate closure.		•	
" " "	Timber poles	Limited yield. Break and need to be replaced		•	
" " "	all	Sweepings can be lost		•	
Depth	All	Increased levels of mining induced fracturing and seismicity			•
Parting planes (bedding?)	props + packs + roofbolts props + caving	(Gold) Difficult at SW < 1,5 m; drilling of additional holes required; Cave can overrun second line of props (Platinum) see Section 7.8.			•
All	rapid yielding hydraulic props + backfill	Positioning of prop filler valves away from backfill		•	

7.5.3 Mining Impediments

The mining cycle refers to a group of sequential and parallel activities that have, as their overall objective, the excavation of the reef. The activities all take place within the reef horizon although they are dependant upon or influenced by other activities, resources and outside events. The stoping cycle has three distinct stages; namely drilling/ blasting (rockbreaking), cleaning and, supporting. It is the interaction, or more importantly, the interference that occurs between these stages that has a significant influence on the successful implementation of any support system. These issues are considered in the following section.

7.5.3.1 The rockbreaking process

Rockbreaking is a batch process and has a direct impact on rock conditions in the stope, the stope width, face advance, damage to supports, and the cleaning cycle. The rate of face advance also has a direct impact on the rate at which all other activities must be performed. In turn, the drilling of face holes is dependant upon the timely and proper installation of temporary supports in the immediate face area. As the blast requires workers to evacuate the stope well before blasting time, blasting also places a time constraint on all other activities.

Explosives are the primary rockbreaking tool used to mine the reef in the gold and platinum mine stopes. The blast is violent and ejects rock from the face at high velocity, much of which strikes supports, removing some temporary supports completely and skewing or damaging permanent supports. The blasting process is, therefore, a significant impediment to implementation and, where practicable, supports are built to withstand or, at least absorb, the violence of the blast. In addition to removing and damaging supports, the blast also generates fractures, further weakening the rock surrounding the stope. For example, where there is no clear hangingwall parting, the blast creates its own, leaving behind a rough and uneven surface that can compound problems created by soft hangingwall conditions.

The blast will frequently knock out temporary supports not withdrawn beforehand and on the following drilling shift these supports must be replaced. The loss of support and mining induced fracturing create an unsafe condition that must be remedied on the following shift. The absence of individual supports from the pattern will also degrade overall support resistance, even if only marginally, but could be significant locally particularly with respect to unsupported spans.

7.5.3.2 Drilling and supporting

Ideally the immediate face support should provide areal coverage to the workforce (face to first line of permanent support) and, as with all supports, be placed in a uniform pattern. A reduction in support spacing in the immediate face area creates interference with other activities, particularly drilling. In practice occasions do arise when, either the support will be moved to a position where it does not interfere with the drilling process, or, alternatively, the drilling process will be compromised either by changing the drill angle or shifting the collaring position. In the first case the action degrades the support system, while in the latter it degrades the drilling process.

Support installation normally takes place during the drilling shift and together with other ancillary stope activities, for example sweeping. The installation of temporary support prior to drilling and failure to complete installation of permanent support before blasting time is recognised as a significant problem.

If the required manpower resources and the correct supports are available, the time required to install a support system can be estimated fairly accurately. Given these resources the result should be a successfully installed support system and, over time, a system that can be said to have been successfully implemented. Obviously, the reverse is also true. Resources include a properly trained, skilled and motivated workforce, and sufficient quantities of the correct support, and the correct tools,

and transport systems to ensure their timely delivery.

7.5.3.3 Cleaning

Scrapers and/ or high pressure water jets are commonly used to clean broken rock from the stope face after the blast. Depending upon the proximity of the supports to the face and the straightness of the panel, the scraper scoop or ropes can strike and damage supports. Again the overall effect will be to downgrade support quality, as well as slow the cleaning process. Broken rock left lying on the footwall also interferes with support installation, as it creates a cushion between the rock surface and the support.

Sweeping in the back of the working area often uses scrapers to remove the swept rock. This requires that the strike support spacing is sufficient to accommodate the scraper. This often violates the requirements of optimum support design for strike spacing to be less than the dip spacing. This is a serious impediment to optimum implementation of support.

7.5.3.4 Stope width

Problems relating to the handling of heavy supports in a confined space were discussed in a previous section. Narrow stope widths however, also present other impediments, for example, restricting worker movement and the ease with which a support can be installed. Movement is further made more difficult in flat dipping stopes.

Narrow stope widths (< 1 m) also make installation and maintenance of in-stope support transport systems difficult and, where there is a high rate of closure, the transport system must be moved regularly to avoid being trapped. In stopes with a high rate of closure a separate gully for the transport of supports is a preferred option.

In certain areas rock bolting is used as a supplementary face support system. One of the problems hampering the wider use of bolting is that in stope widths of < 1,2 m current rockdrills cannot be easily positioned to drill holes perpendicular to the hangingwall strata.

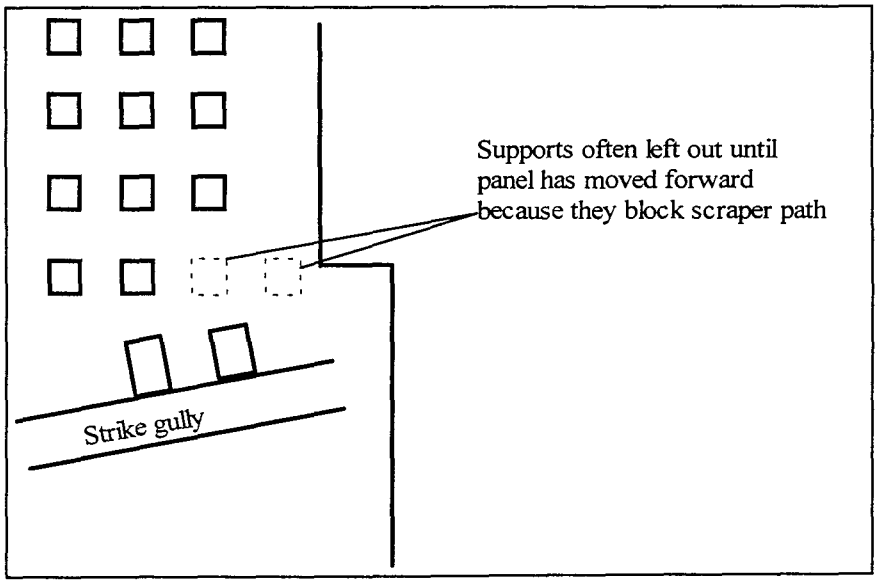

Figure 7.5.3.4 A common example of interference to the face scraper caused by support (pack) positions above gully.

Supports positioned at the intersection of the stope panel and its strike gully invariably seem to interfere with the cleaning process (Figure 7.5.3.4). Although undesirable, occasions arise when the panel is advanced by a further 1-2 blasts before permanent support is installed.

The nature of the cleaning process effectively prevents the simultaneous performance of other activities and, as a result it is often performed on a different shift to drilling/ blasting and supporting. However, delays in setting up the cleaning process for example, as a result of missing scraper rig holes, broken scraper ropes etc., often result in the face being only partially cleaned during the shift. The remaining rock must be removed on the following shift and this reduces the time available for support (and other) activities.

Large falls of ground (F.O.G.s) or generally poor ground conditions require additional support to be installed, often in difficult conditions. Flexibility is required in labour allocation to cater for such situations, otherwise the affected panel will have reduced face advance resulting in poor face shapes exacerbating the situation.

7.5.3.5 Face advance rate

On gold mines attempts to improve productivity have seen the focus shift to a reduction in total face length mined and a corresponding increase in face advance. Many mines, for example, now plan to blast each stope panel every day. Mines, that previously achieved a face advance of 5 m per month, now achieve a rate 2,5 to 3 times this figure. If overall productivity (measured in m^2/ worker) increases, it implies that the productivity of each activity has similarly increased. Unless correctly managed these two important objectives, namely increased face advance and improved support (better areal, and local support), have the potential to interfere with one another. The situation on platinum mines is slightly different where manpower productivity is already between 1 1/2 to 2 times that commonly achieved on gold mines.

A daily blast requires that each stope panel is drilled, blasted, cleaned and supported once every 24 hours. It is also common practice to drill, support and blast a panel on one shift and to clean the face on a second shift (night). The primary reasons for this work arrangement are the incompatibility of the cleaning process with other activities, as well as the significant constraints imposed by blasting. In effect the support rate (the rate at which support must be installed) also increases with the face advance rate. The issues that need to be addressed are whether this support rate is attainable in practice and, if not, what can be done to ensure that it can be achieved. There are no figures to show what the effect of increased face advance is on support implementation. This objective is, however, not believed to have altered the following prerequisites to success:

- time allocated vs actual time available to perform the work,
- minimal interference with other activities,
- the tools and equipment to perform the work,
- the necessary skills and knowledge and, in terms of layouts, adequate stope access and effective transport systems, and
- creating an environment in which support installation becomes a routine operation,
- human resource allocation adequate to complete the installation.

7.5.3.6 Time

Although time was not raised as a constraint it is necessary for the proper installation of supports, as, under ideal conditions, support installation should be a systematic process. Unfortunately such conditions occur only occasionally in the dynamic situation of a working stope and work content varies from shift to shift. Manpower is allocated according to standard rates of work, with work load and worker complements generally fixed at one level for several months at a time.

7.5.3.7 Stope access

Stope access is not considered to be a significant impediment to implementation. It is, however, generally recognised that improved stope access results from the introduction of trackless vehicles and that trackless vehicles facilitate the transport of supports. The recognised benefit of special access ways must therefore be balanced against cost. Impediments stemming from the mining cycle are summarised in Table 7.5.3

Table 7.5.3 Mining related Impediments.

CYCLE ACTIVITY	IMPEDIMENT
Rockbreaking	Batch process, stope width control, support damage, cleaning cycle.
Drilling and supporting	Areal coverage; inter support distance, interference with drilling; delays caused to drilling by friable/ soft hanging; inadequate human resource allocation for deteriorated conditions
Cleaning	Scraper scoops damaging or removing supports, poor cleaning of broken rock, hazards created by scoop and ropes. Sweeping interferes with optimum support spacing
Face advance rate	Potential for a reduction in time available to install support correctly
Stope access	Blocked or lengthy access ways

This section illustrates how the mining process can seriously downgrade the successful implementation of stope face support systems. The major impediment is the blasting process as this damages and weakens supports, as well as also producing other negative side effects. One such effect is that the work environment changes with every blast and workers must constantly adapt to the changed conditions. Proper management of events within the stope itself would appear to be a key element in minimising the downgrading effects caused by mining related impediments.

7.6 Modifications to the mining/support cycle

7.6.1 The mining cycle

The first part of this section considers whether changes to the mining or support cycle are possible in order to facilitate implementation of improved support systems within each geotechnical area. The second part considers possible changes to mining methods to achieve the same objective.

Apart from disruptions caused by the blast the process of support installation is not wholly compatible with the activities of drilling and cleaning. The left hand column in Figure 7.6.1 represents a three day cycle, with each activity performed on a separate day (shift). Today, this cycle has been replaced by the two shift cycle (normally day and night), which is shown in the middle column. In a two shift cycle drilling, supporting and blasting occur on the same shift, and the broken rock is cleaned on a separate shift, normally night, while the third shift is idle. If all three shifts were utilised, the shift following the blast would be shorter by 2/3 hours for re-entry, making it ineffective. There would probably be additional problems, such as adequate supervision. Other options, for example a 4 x 6 hour shift cycle

have been considered, but this does not alter the fundamentals. Figure 7.6.1 indicates how limited the cycle options are within the present mining methods. Although the option of modifying activities within the cycle was considered, it also produced no workable alternatives.

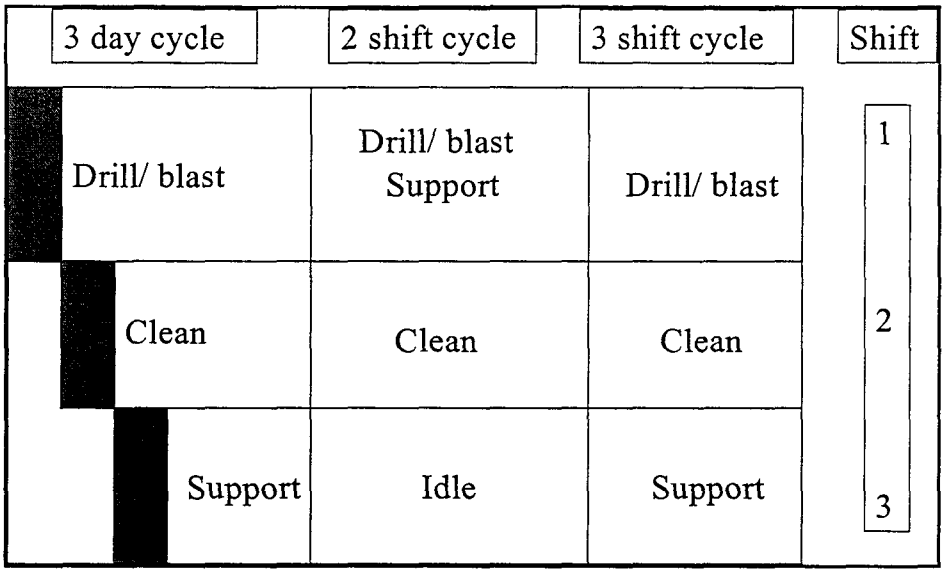

Figure 7.6.1 Shift options for mining and support activities.

Non-explosive mining systems or a continuous blasting system (i.e. not a batch process) offer the potential for significant change. Semi-mechanisation of either the mining or supporting process, for example a remotely operated stope drill rig, still offers potential, as the immediate face area could then be supported without interfering with drilling of the face. Unfortunately, although a number of narrow reef drill rigs have been developed, none has so far proved to be widely successful. Other possibilities to alter the cycle by changing the sequence of activities have been considered, but no realistic options have been identified.

As stope width increases to the point where mechanised equipment can be used, e.g. drill rigs, the problem of interference becomes significantly less. For example, drill rigs can be operated remotely with the operator standing away from the face under supported hangingwall. The rig is also available to drill roofbolts.

The Support Cycle

The support cycle has three basic stages; transport of the supports into the stope, preparation of the area, and support installation. In narrow reef stopes proper access ways and a mono winch will ensure delivery of supports to the face. In trackless narrow reef and wide reef stopes this problem is virtually eliminated.

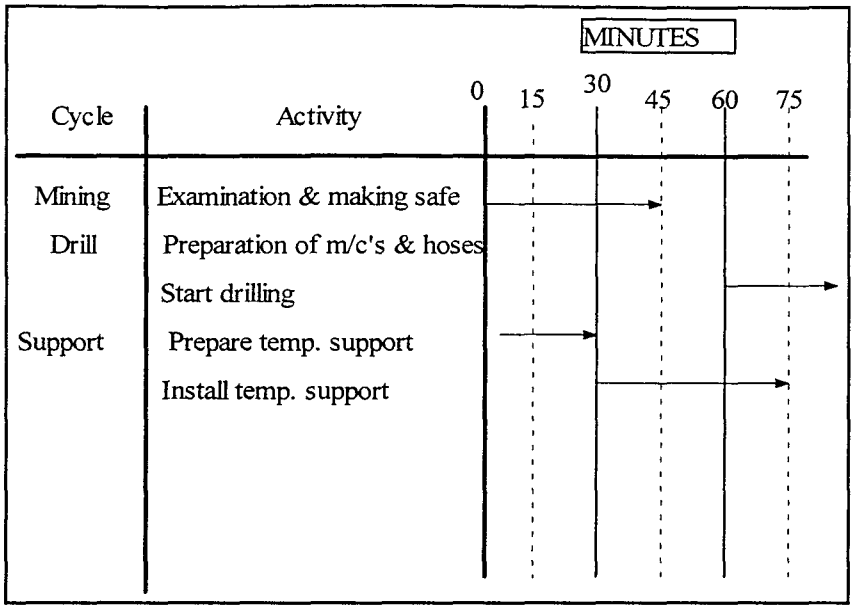

Figure 7.6.2 Sequence of activities at start of drilling/supporting shift.

Figure 7.6.2 represents the activities at the start of the drilling/supporting/blasting shift and its purpose is to highlight the period of intense activity in the immediate face area. It shows that interference between the examination process, the installation of temporary support in the immediate face area, and the drilling cycle lasts for an estimated 1 to 1 1/2 hours. In the light of the importance of the tasks performed, this period of time does not appear to be unreasonable. After this the support team moves out of the immediate face area to concentrate on other tasks, e.g. installation of permanent supports. Depending on the type of support the support team may not need to enter the immediate face area again on that shift other than, perhaps, to remove props prior to the blast.

In order to provide more time to drill and support the stope, attempts have been made to start the cleaning cycle immediately after the blast using automatic winches. These efforts are understood to have been unsuccessful, as the winch control system was not sufficiently responsive in successfully negotiating a path through the broken rock without fouling the face, large rocks or supports.

7.7 Modifications of mining methods to assist implementation of stope face support systems

For both gold and platinum mines there are three common mining methods, namely narrow reef conventional stoping, narrow reef trackless stoping and, thirdly, wide reef trackless stoping. Today the predominant method remains narrow reef conventional stoping, although the other two methods continue to prove successful under certain conditions on both gold and platinum mines. In the narrow reef mining method the full face cut is blasted. One variation is to blast a waste cut into the mined out area as support, and then to mine the reef. This method is presently being evaluated on a trial basis at Vaal River Operations.

Table 7.7.1 presents a comparison of the three mining methods in terms of the method used to drill, clean the face, clean the gully, transport support, support type, and to install the support.

Table 7.7.1 Comparison of three mining methods

Mining method	Drilling	Face cleaning	Gully cleaning	Transport	Support type		Support installation
					Temp.	Perm.	
Narrow reef conventional	Hand held pneumatic drills	Scraper &/or water jets	Scraper	Mono-rope, scraper, manual	Props, poles, ryhp's*	Packs, elongates, backfill	Manual, pre-stressed supports
Narrow reef trackless			LHD	LHD	as above	as above	
Wide reef trackless	As above or drill rigs	LHD#	LHD	LHD	Roofbolts	Backfill, pillars	Drill rigs + bolter

NB. * rapid yielding hydraulic props. # Load-haul-dump truck.

Table 7.7.1 shows that the principle difference between the basic narrow reef mining method and the other two is the use of an LHD to transport rock and support materials. In the wide reef method, the introduction of drill rigs and roofbolters brings an additional advantage to the support process.

As already discussed the implementation of a support system relies very much on the skill and abilities of those who install the supports. Their work is facilitated by the introduction of mechanised equipment, for example an LHD, although there is no guarantee that the use of mechanised handling systems will lead to successful implementation. Experience shows that a decision to use trackless equipment in narrow reef stopes is not always a success, and that other factors such as cost are equally important.

Explosive rockbreaking is restrictive and presents difficulties when trying to consider the possible alternatives that would improve the manner in which support is installed. Although time to complete the installation of the support was not raised as a particular issue, the practice of using blast barricades is one method of containing rock against the face, thereby reducing cleaning time.

Other than the use of barricades the possibility of modifying the mining method to improve implementation appears limited.

7.8 Rockbolts as a stope support system

Roofbolting of the hangingwall in the immediate face area has several advantages over more conventional supports. These include:

- clamping of hangingwall partings,
- keeping the area clear between the last line of permanent support and the face for other activities e.g. drilling of the face and cleaning of broken rock,
- if drilled right up to the face, roofbolts offer immediate support directly after the blast and provide additional protection to re-entry crews, and
- offer the potential for a cost effective replacement of temporary supports.

Rockbolting of the hangingwall is practised on different mines across the Witwatersrand from Evander GM (Kinross) in the east, to Beatrix GM in the Free State. To varying degrees, it is also practised on platinum mines in the Bushveld Complex, for example on the UG2 reef at Western

Platinum Mines. The different regions where rockbolting of the hangingwall is practised have been evaluated to determine the common geotechnical criteria. The common criteria are:

(1) Limited mining induced fracturing,
(2) Working depth < 1500 m and very often < 1000 m below surface,
(3) The presence of a pronounced hangingwall parting within 0,9 m from the stope hangingwall,
(4) Competent hangingwall rock type, and
(5) Stope width > 1,2 m (preferred).

These are summarised in Figure 7.8

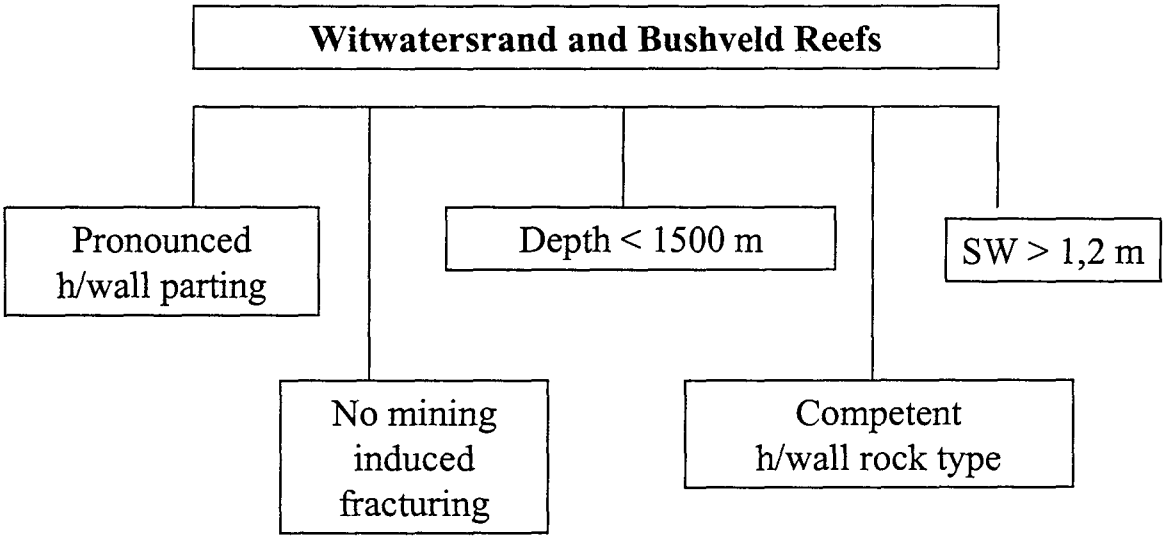

Figure 7.8 Geotechnical criteria as present in current areas of roofbolting.

7.8.1 Mining induced fracturing

Mining induced fracturing aids the break up of the hangingwall. Once the hangingwall becomes "blocky" rockbolts are only able to provide a locking mechanism over a limited area. In the Witwatersrand Basin, mining-induced fracturing is, as a rough rule of thumb, encountered at mining depths exceeding 1000 m. The intensity and attitude of fracturing is also related to the rock type as associated with the excavation, with lithologies, having high uniaxial compressive strengths (UCS), being most intensely fractured. This fact could counteract the application of roofbolting at greater depths. It is noted that mining induced fracturing appears to be absent when mining the UG2 or the Merensky Reef, even at greater (± 2000 m) depth, as is performed at Northam. This enhances the competency of the hangingwall strata.

7.8.2 Working depth

Many of the mines identified e.g. Kinross (Evander GM), Randfontein Estates, Beatrix and Western Platinum use rockbolts at shallow depths, at often less than 1000 m, i.e. in areas where mining induced fracturing is absent.

7.8.3 Pronounced hangingwall parting

On some mines, for example Western Platinum, Beatrix and Kinross, the presence of a pronounced hangingwall parting is an important factor in the decision to use rockbolts.

Roofbolting appears to commonly be practised when mining orebodies of the Kimberley succession, for example at Beatrix or Evander. At both mines, an argillaceous parting, which parts with ease, is positioned about 0,3 to 0,7 m into the hangingwall. This parting is clamped when applying roofbolting, thereby avoiding beam failure.

Roofbolting is also applied at Vaal River Operations, in areas where the Ventersdorp Contact Reef (VCR) is mined (e.g. No. 10 Shaft). Here, a pronounced, undulating bedding plane fault (Figure 7.8.3) is often situated along the VCR/hangingwall contact. Amplitudes of the undulating plane are about 1 m. The fault plane is marked by quartz-veining and possesses very low cohesion with the under- and overlying strata, thereby causing fall of grounds and dilution of grade.

Long 1,2 m split sets are used widely when mining the UG2. This is mainly due to the presence of pronounced, easily parting chromitite stringers in the hangingwall. Especially persistent and hazardous are three chromitite bands, termed the 'Three Leaders' or 'Triplets'. The distance of these to the excavation range from < 0,5 m to 16 m, thereby also determining support resistance requirements.

7.8.4 Competent hangingwall rock type

The effectiveness of rockbolts as a support diminishes rapidly if the hangingwall is weak or friable. It is estimated that the UCS of the hangingwall rock should not be less than 180 MPa for the Witwatersrand. Competency is also controlled by the intensity of the mining induced fracturing (see 7.8.1).

7.8.5 Stope width

Apart from geotechnical criteria adequate stope width is the major factor restricting greater use of rockbolts in stopes. Using current rockdrill technology a minimum of >1 m is required, if the hole is to be drilled at an angle approximately perpendicular to the rock strata. A low stope width also reduces the length of hole that can be drilled, effectively limiting the length of bolt to the stope width.

It is re-emphasized that stoping widths appear to be one of the major criteria for roofbolting. At Beatrix, for example, 3 m long roofbolts are the only support where stoping widths exceed 3 m.

A good example where stoping widths control the application of roofbolts is shown by the Merensky Reef and UG2. As mentioned previously (see 7.8.3), roofbolting is widely used on the UG2, where stoping widths are generally about 1,5 m. Here, split sets are utilised to clamp chromitite stringers in the hangingwall. Partings are also present in the Merensky Reef hangingwall, but roofbolting is absent at stoping widths of about 1 m, whereas bolts are used at greater stoping widths, as is the case at Eastern Platinum Mine.

7.8.6 Rockbolt application

On some mines rockbolts are used as a supplementary face area support by drilling rockbolts right up to the face. The type of rockbolt used most commonly is a pretensioned end anchored rock stud with a bearing plate. Split sets are also used on some mines. For example at Evander rockbolts are used in addition to mechanical props, which are removed before the blast. After the blast the cleaning shift is able to enter an area that is already supported to within 1,0 m of the face, thereby reducing the rockfall hazard. In other applications, the intention is to replace temporary supports with rockbolts, thereby freeing up access in the face area, for example Western Platinum Mines.

7.8.7 Cost implications

Obviously there is a cost involved for drilling the additional holes and for the rockbolts. At some mines, for example Vaal River Operations, rockbolts are under consideration as a potential support system, although it is anticipated that there will be a direct increase in costs and effort. There are also questions around the amount of time it will take to drill the necessary holes.

Summary

The potential benefits of hangingwall rockbolts in stopes include improved access to the stope face for other activities, a potentially reduced safety risk for re-entry after the blast, an active support system close to the face, and, ideally, a replacement for existing temporary support systems. On this latter point, however, mines are naturally very cautious. There are geotechnical areas on many reefs where rockbolts can be used, provided that the stoping width is adequate, and that the hangingwall is competent and contains one or more pronounced partings.

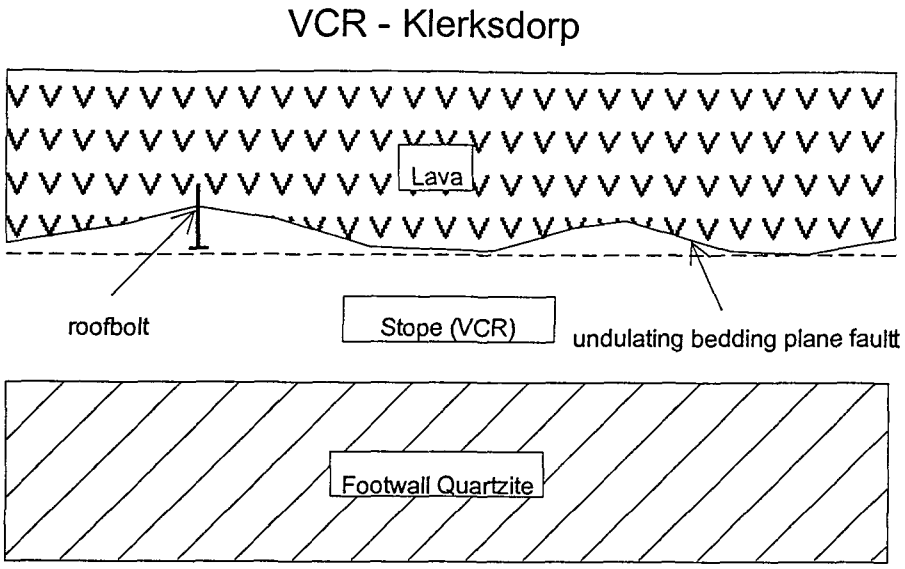

Figure 7.8.3: Roofbolting of undulating bedding fault, VCR, Klerksdorp

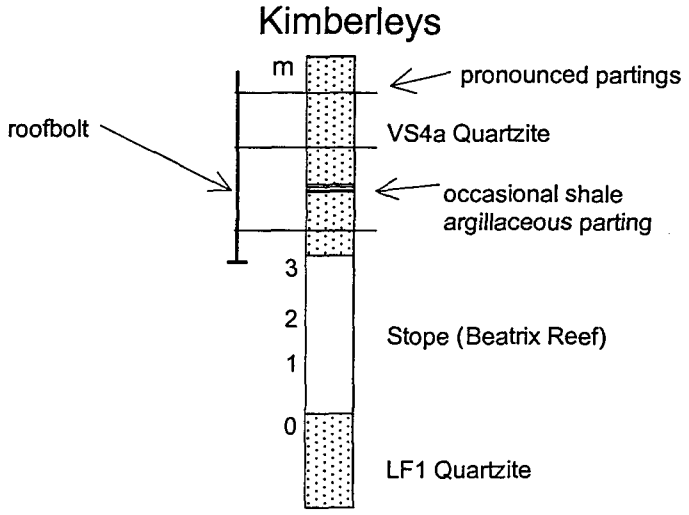

Figure 7.8.4: Roofbolting as associated with high stoping widths of the Kimberley orebody.

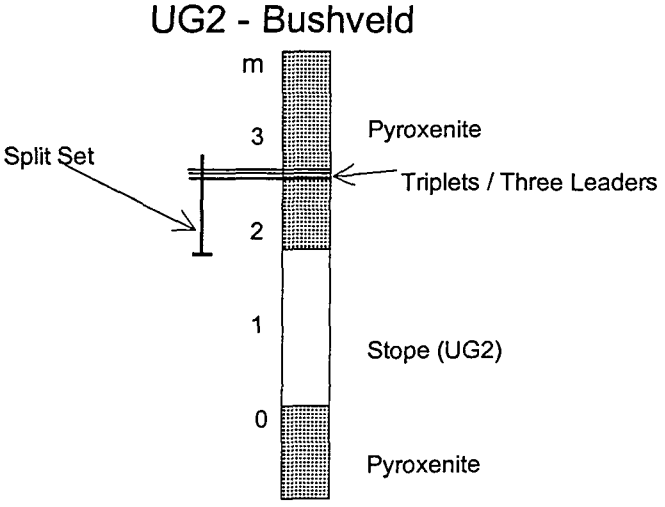

Figure 7.8.5: Geological section through UG2, Bushveld Complex, indicating application of split sets.

7.9 Concluding remarks and recommendations

The phrase "successful implementation" is given earlier in the report as meaning that a stope support system is installed in such a manner that it performs at the designed level, using the optimum level of resources. On the understanding that the geotechnical criteria determine the stope support system, the objective of this enabling output has been to identify the impediments associated with the installation of supports within each geotechnical area. Unfortunately it has not been possible to establish such a link, principally because the choice of support system is governed by factors such as depth, mining method, and mining layout, in addition to geotechnical criteria. The impediments to correct implementation are many and diverse, ranging from stope width to human behaviour and rock type and are often generic covering several types of geotechnical areas.

Correct implementation therefore requires a blend of human skill in many areas (not just support installation) and technology (the support) under difficult working conditions. Human involvement in the implementation process is clearly a concern, e.g. motivation. Other issues, however, such as the rockbreaking process, are probably equally detrimental to proper implementation.

The work also identified several generic, human and mining related impediments. This finding is borne out by a closer examination of the mining cycle and methods that highlight the limitations created by the explosive rockbreaking process to support implementation. Alternative methods to scraping, such as water jetting, should be employed to clear sweepings and thus enable closer strike spacing of support units which is necessary in the presence of face parallel fracturing.

Flexibility in the number of people allocated to support crews to accommodate changes in stope conditions and hence work load needs to be investigated.

Rockbolts are used as a stope support on gold mines from Evander to the southern Free State, as well as on the UG2 reef of the Bushveld Complex. Their use has been considered by many different mines at various times. The report shows that the potential exists for increased use of rockbolts in stopes, provided that minimum geotechnical criteria are met, as there appears to be no restriction simply on the basis of reef mined. It is recognised, however, that the ability to drill the desired length of hole to contain the right length of rockbolt remains a major barrier.

In narrow reef stopes the combination of explosive rockbreaking, variable and confined working environment, and heavy supports conflict with human (manual) efforts to successful implement support systems. Some of these problems do, however, diminish as stope widths increase, but are increased as environmental conditions deteriorate.

In the long term, solutions may be found in non-explosive mining systems and mechanical handling of support systems. Although, as mines go deeper, supports, or support densities, are expected to increase, further adding to the physical effort required in narrow stopes. One recommendation is for mines to continue with their training and re-enforcement practices. Research should re-consider alternatives to current technologies or systems to provide areal support at the required density. A system for drilling roofbolts in narrow stopes would also help address problems of face access and workforce safety upon re-entry.

7.9.1 Strategy for the implementation of stope support systems

1. The responsibility for the successful introduction of a product should be allocated to an appropriate person or team of people who are enthusiastic and strongly motivated to ensure that the maximum benefit accrues to the mine from the product.

2. The implementation team should be fully conversant with the product and must understand what it can achieve and why, how it operates, what the minimum maintenance requirements are, and also be familiar with procedures, even those that might appear to be insignificant, but are in fact

essential to the successful application of the product. The ideal people for mine personnel to interact with to obtain the necessary understanding of the product are the original researchers, the manufacturers and the persons involved in the field trials. These persons have experienced the development of the product, have modified it and know its strengths and weaknesses, and their advice and recommendations need to be applied strictly during the initial installations of the new product.

3. A standard practice for the application of the product should be prepared in conjunction with the suppliers. In addition, a training schedule should be drawn up and a training manual provided.

4. If appropriate to the product, a training stope or a development end should be established on the mine. All persons working in this stope should be made to understand that they are trainers and not a production team and should react accordingly when crews come to the working place for training. All personnel who will be responsible for, or who will use the new product, should pass through this working place. Recognition should be given to those who become proficient in the use of the product, and those who cannot learn to use the product should be prevented from doing so.

5. Follow through training teams should be available to crews who have passed through the training stope and are implementing the product in their production section. These teams should remain with the new users until they are satisfied that they are implementing the product correctly.

6. Audit personnel should visit sections where the new product has been introduced, initially at frequent intervals, and recommend extra training where necessary. Thereafter, the visits should occur at greater intervals and eventually on an ad hoc basis.

7. New recruits to the mine should be given an abbreviated training on the product once it is well established on the mine, followed by on the job peer training.

8. A maintenance schedule for equipment is required, particularly for support units such as hydraulic props. This would involve routine withdrawal for servicing and subsequent testing.

9. Any proposed modifications should be discussed with developers or suppliers to gain from their experience. Only after considerable experience with a product should attempts to introduce modifications to the product or to the application procedures be made. This is not to stifle innovation but rather to prevent repetition of mistakes, which may have been made during field trials or by other more experienced users.

The cost of an effective implementation strategy is by no means trivial. However the cost of incorrect implementation will be significantly greater since, not only is the material cost of the product wasted, but the safety and related economic benefits do not accrue to the mine.

7.10 References

Glisson F. J. 1998. Personal communication on the number of fatal accidents in the South African gold mining industry that occurred when installing or removing props.

Güler, G. et al, 1998. Establish a methodology for defining geotechnical areas within South African platinum and gold stoping horizons. SIMRAC Project GAP 416, final report 31 December.

Gürtunca, R. G. & Gay, N. C. 1993. Rock Engineering - Implementing the latest developments in Improving safety in underground mining operations. Mine Management Forum; Midrand, Johannesburg, 9-10 November.

Hagan, T. O. & Daehnke, A. 1997. Stope face support systems. Annual SIMRAC project progress report GAP 330. 31 December.

Handley, M. F. 1994-1996. Mining strategies for the Ventersdorp Contact Reef at Depth. Stope and development support strategies. Proceedings of the Association of Mine Managers of South Africa.

MacFarlane, A. S. 1994-1996. Mining strategies for the Ventersdorp Contact Reef at Depth. Summary and conclusions: Managing the risk and developing future strategies. Proceedings of the Association of Mine Managers of South Africa.

Piper, P. S. 1997. Stope support costs for gold and platinum mines. Consultancy report as part of SIMRAC Interim project report GAP 330. Groundwork Innovative Project Management CC. 28 February.

Roberts, M. K. C., Gay, N. C. & Jager, A. J. 1993. Implementation of new and improved support technology on mines to make mining safer and more cost effective. 5th International Conference of Safety in Mines Research Institutes. Pretoria, September, pp 1-5.

8 Assessment of elongate performance

8.1 Laboratory and underground evaluation

8.1.1 Introduction

The South African gold mining industry has, for quite some time, recognized the need for a type of support that was easy and quick to install, light weight, and would also offer the required protection against seismic events and falls of ground. In the early days, and at shallow mining depths, timber poles were used with a wood wedge as a means of securing and pre-stressing the support. As mining depths increased to over 1500 m it become apparent that the performance of this type of support was not suitable for mining conditions where stope convergence rates were 10 millimetres per day or more. From this evolved many new types of mine support props, designed to yield 300 millimetres or more, while maintaining an acceptable yield force. The first units developed to this specification were hydraulic props that could yield at one metre per second to accommodate dynamic loading associated with rockbursts. These were followed by timber props, engineered to yield, that have evolved to the present pre-stressable units. Numerous designs of the earlier elongates were patented but only a few were widely used in the mines. These were characterised by their ability to provide the basic functions of efficient protection for the workers and ease of installation at an acceptable cost.

An interim testing procedure has been developed to provide information on the variability of different support units. This information will be used to develop a standard testing procedure for all elongate support units to provide for each support type standard performance curves. These curves will be used in the generally accepted support design methodology and will, with a high degree of certainty, establish the minimum support capabilities of particular support types. The test procedure is described and examples of the results of two elongate types are presented. The significant difference between laboratory results and results obtained from monitoring props installed underground is highlighted.

8.1.2 Testing of elongate support

CSIR Mining Technology (1998) has, for the last two years, embarked on an extensive SIMRAC commissioned testing programme. The objective of this programme is to evaluate currently used types of elongates.

The testing procedure currently consists of twenty-four tests as described below:

- Five rapid displacement tests at a rate of 3.0 m/s – the units are initially compressed slowly for 50 mm then subjected to 3.0 m/s for at least 200 mm and the test completed at the slow rate until failure
- Ten slow displacement tests at a rate of 15 mm/minute
- One test at a deformation rate of 150 mm/min
- One test at 15 mm/min on a 10° inclined platen
- One test at 15 mm/min on a 20 mm stepped platen
- One test at 15 mm/min on a 50 mm stepped platen
- One slow test at a deformation rate of 10 mm/day

- One creep test for seven days
- Three underground tests

The results of these tests are then subjected to statistical analysis (described in Section 8.2) to provide performance curves for support system design. A consistency indicator at various degrees of confidence is calculated, as well as energy absorption curves.

Twelve of the most widely used elongate types by the gold and platinum mining industry were evaluated according to the testing procedure. Detailed results of all the tests are given in Appendix D. As an example of these test results, the force versus deformation curves of only a few elongate types are given here.

Figures 8.1.1 and 8.1.2 display the comparisons between the average results of several types of elongates for the testing rates as indicated.

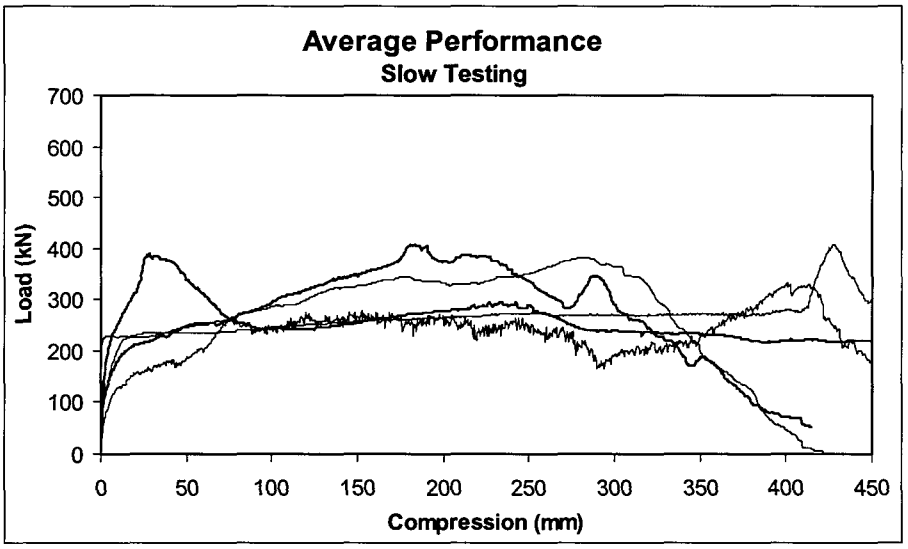

Figure 8.1.1 Comparison of the average performance for several elongate types at a rate of 15 mm/min.

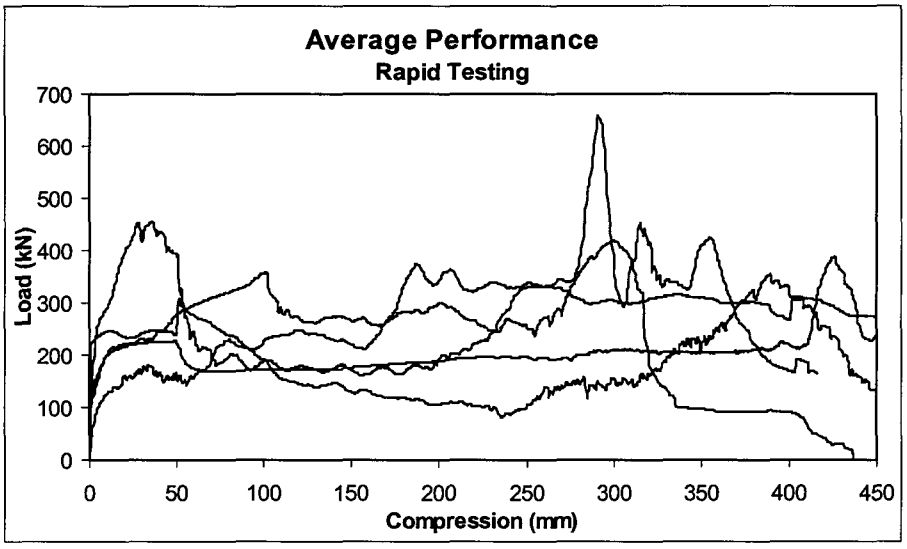

Figure 8.1.2 Comparison of the average performance for the same elongate types as presented in Figure 8.1.1, when tested at a rate of 3,0 m/s.

As an example of further test results, consider the Rocprop force versus deformation curves given in Figures 8.1.3 a) – d). The data is given for slow and fast laboratory tests.

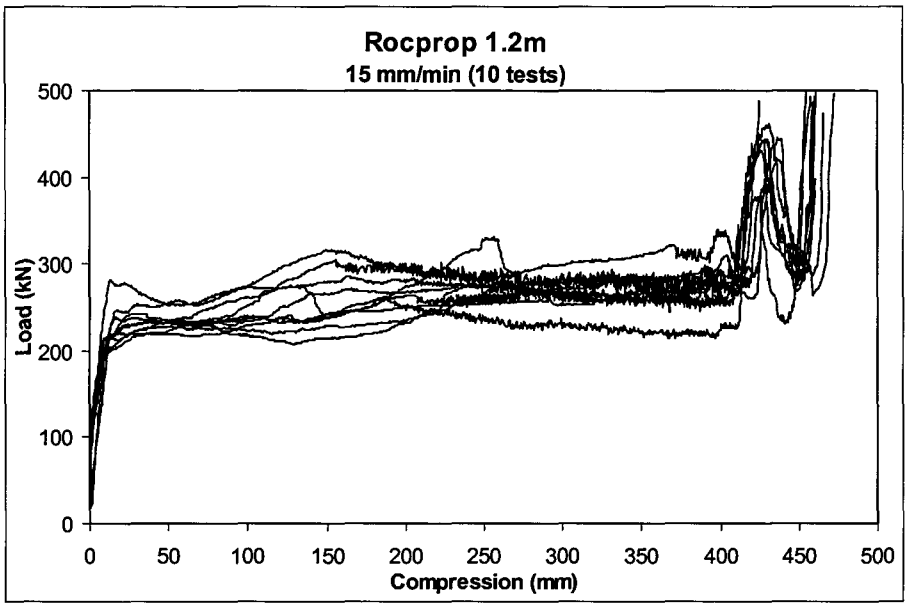

Figure 8.1.3 a) Test results of Rocprop compressed at 15 mm/min.

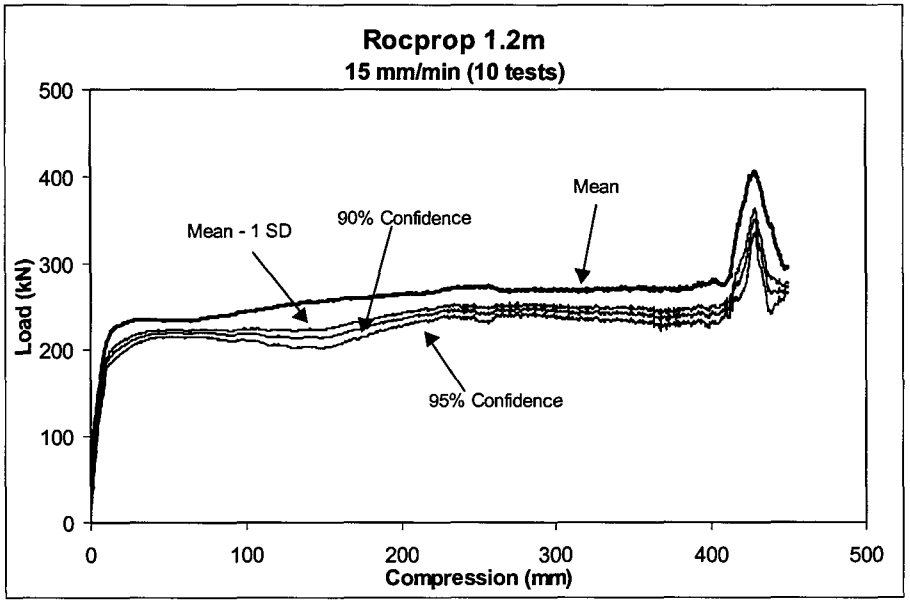

Figure 8.1.3 b) Results of statistical analysis on Rocprop performance data (15 mm/min).

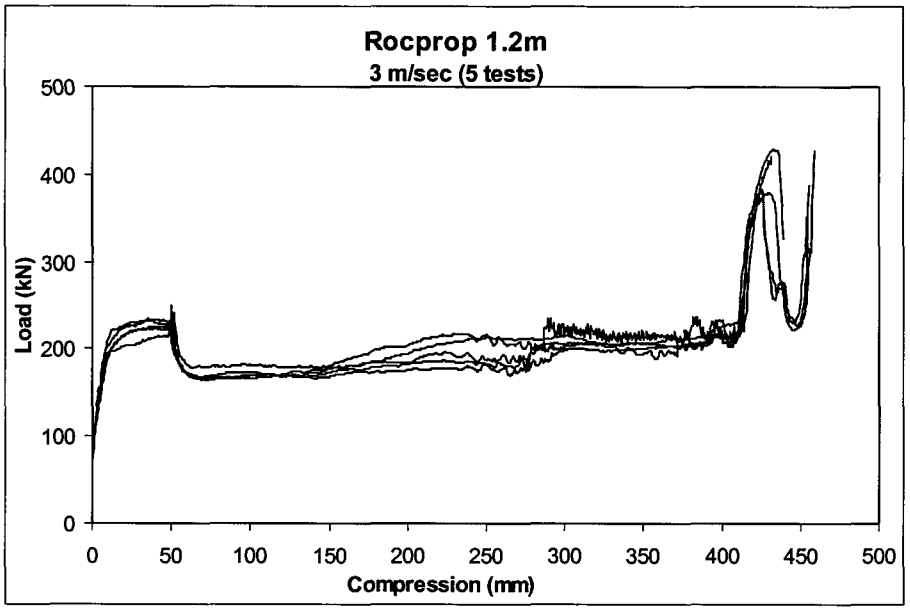

Figure 8.1.3 c) Test results of Rocprop compressed at 3 m/s.

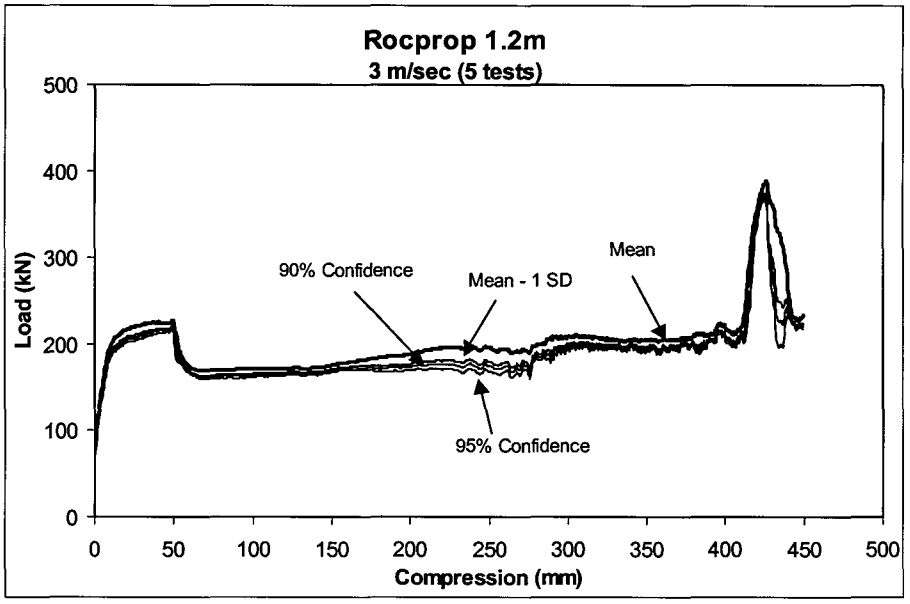

Figure 8.1.3 d) Results of statistical analysis on Rocprop performance data (3 m/s).

Laboratory data of pre-stressed Pencil Props are given as force versus deformation curves in Figures 8.1.4 a) – d). The data is given for slow and fast laboratory tests.

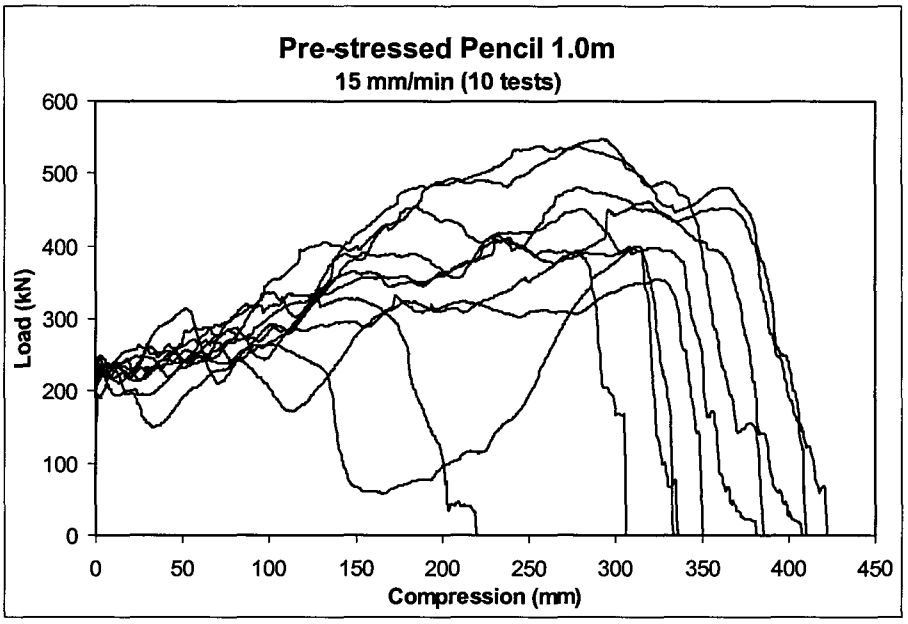

Figure 8.1.4 a) Test results of Pencil Prop compressed at 15 mm/min.

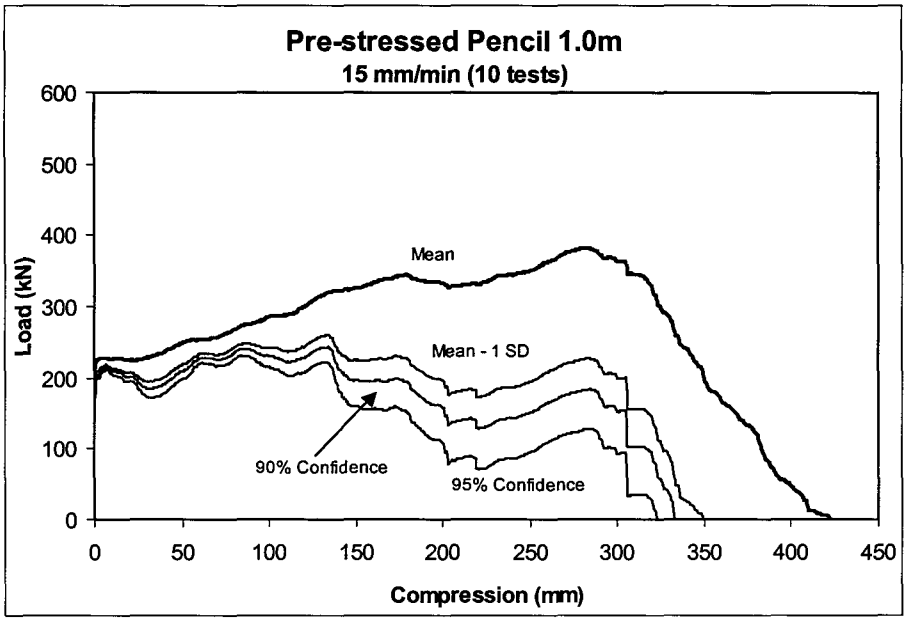

Figure 8.1.4 b) Results of statistical analysis on Pencil Prop performance data (15 mm/min).

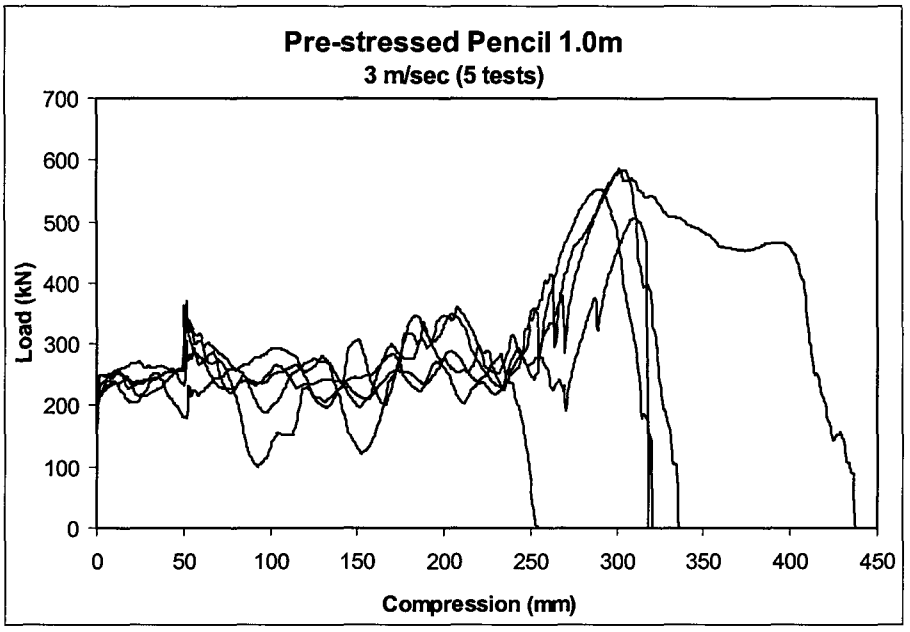

Figure 8.1.4 c) Test results of Pencil Prop compressed at 3 m/s.

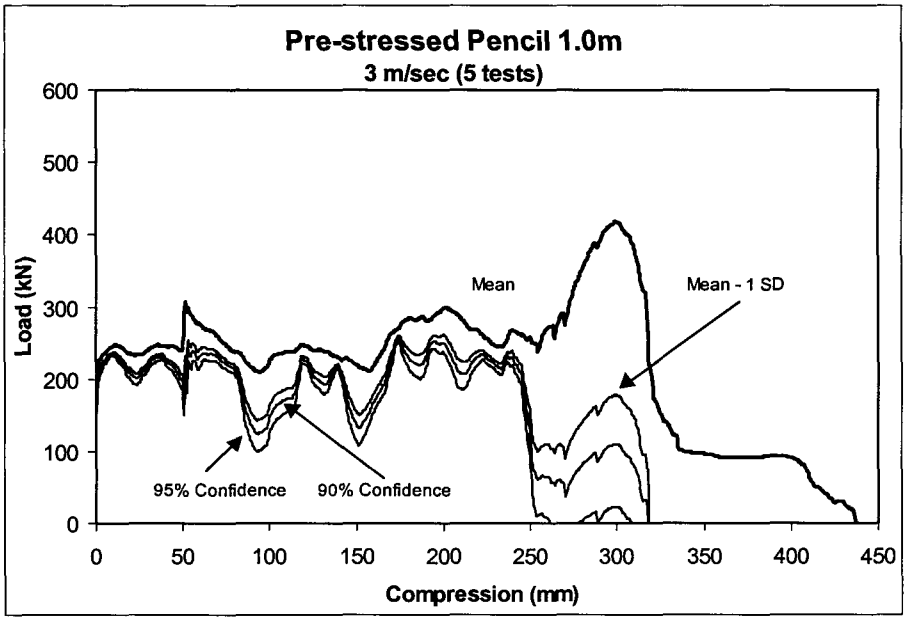

Figure 8.1.4 d) Results of statistical analysis on Pencil Prop performance data (3 m/s).

8.1.2.1 Performance variability

Due to the variety of materials used and the degree of engineering in the construction of each elongate, the variability of performance between different specimens of each type tested is, in itself, a point to take into consideration. The Rocprop elongate, for example, is a well engineered all steel prop, which displays remarkable consistency of performance, see Figure 8.1.3.

The Pencil Prop is a timber-based unit with a separate pre-stressing device and some machining to try and control the yielding behaviour (Figure 8.1.4). Being a basic prop, with timber as its main constituent, it exhibits a greater degree of variability in its performance, as can be seen in Figures 8.1.4. A statistical analysis is proposed (Section 8.2) to take into account the variability of the elongate performance.

8.1.2.2 Rate dependency

Friction based yield units (e.g. the Rocprop) typically exhibit lower loads, as the rate of testing increases. This is clearly seen in Figure 8.1.5. This rate dependency is not followed when timber is combined with an engineered yielding unit, as can be seen in Figure 8.1.6.

There is little indication that testing rates between 15 mm per minute and 50 mm per minute have a noticeable effect on the support performance. The mechanism of timber creep is negated at these loading rates.

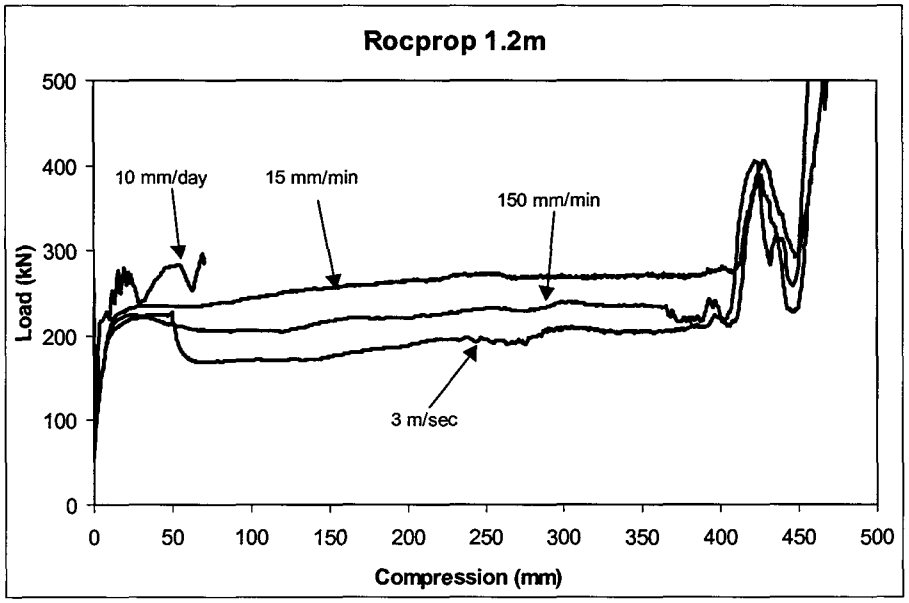

Figure 8.1.5 Rate dependent performance of a Rocprop comparing average performance curves at the respective testing rates.

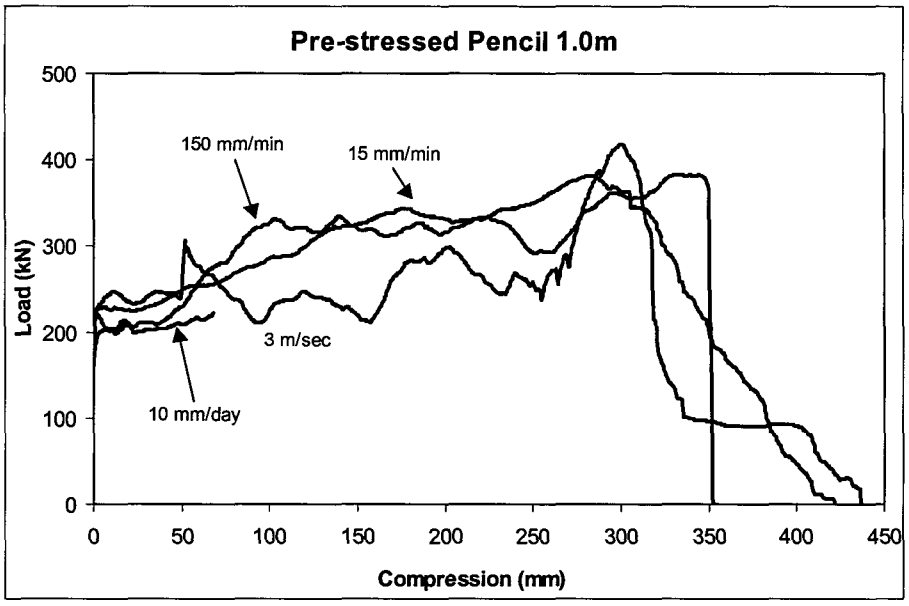

Figure 8.1.6 Rate dependent performance of a pre-stressed Pencil Prop comparing average performance curves at the respective testing rates.

8.1.2.3 Energy absorption capacity

The energy absorption capacities of elongate support, calculated from their performance curves noted in Figures 8.1.3 a) and 8.1.4 b), at a 90 per cent confidence level, are shown in Figure 8.1.7

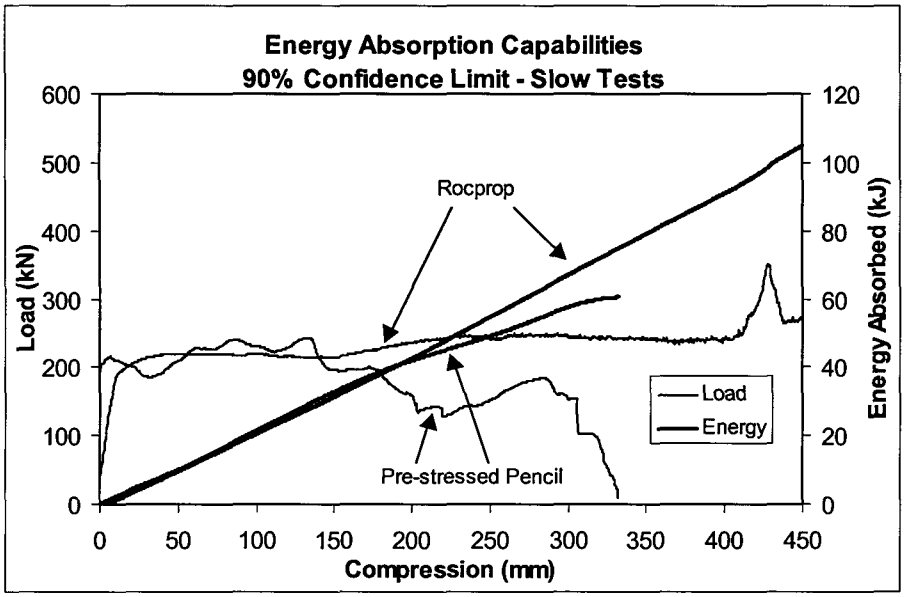

Figure 8.1.7 Energy absorption capacities of two types of elongate at a 90 per cent confidence level.

8.1.2.4 Evaluation of underground elongate performance

The details of the site where the elongates where evaluated are as follows:

WESTERN DEEP LEVELS EAST MINE
93 EAST 4 PANEL
CARBON LEADER REEF
DEPTH: 2689 m

At the above site the following elongates were tested:

(a) Madoda Prop
(b) Ebenhaeser
(c) Ebenhaeser Mark1
(d) Rock Prop
(e) Cone Prop
(f) Profile Prop
(g) Disc Prop
(h) Load Master
(i) Pencil
(j) Gum Poles

Instrumentation used for the testing of elongates was as follows:

(a) Direct closure
(b) Closure Ride Station
(c) 50 ton Load cells

The load cells had a gauge marked from 0 – 25 MPa. Each load cell was calibrated separately and the results were averaging 1,8 t per 1 MPa pressure. Therefore, if a reading of 10 MPa was showing on gauge, a load of 18 tons would actually be applied on the load cell.

Direct closure was taken by installing in the hangingwall and footwall a raw bolt with chain links attached. By using a spring loaded vernier and measuring chain, the closure was measured once per day.

Closure ride stations were installed in each area where elongates were installed and also measured on daily bases. Therefore the following data was recorded on daily basis.

(a) Load cell readings
(b) Direct closure readings
(c) Closure rides station readings

All the above information was brought back to CSIR Miningtek and analysed. Between the 5th October 1998 and 8th October 1998, thirty three elongates were installed in 93 East 4 Panel and a daily reading taken and logged. Unfortunately, on the night of the 25th October 1998, a seismic event of a magnitude of 2,5 occurred. As a consequence of the seismic event, the following occurred:

a) A large number of elongates moved sideways on the load cells and some even off the load cells.
b) The load cell's gauges moved through 360°, thereby damaging the gauge and resulting in inaccurate further gauge readings.

The site itself was very badly damaged as rocks from the hanging wall and face covered the bottom third of all elongates, and had to be cleared for damage to be estimated.

The following photographs give a qualitative overview of various elongate failure mechanisms, as well as an indication of the rockburst damage.

Figure 8.1.8 a) Buckling at bottom section of Rocprop.

Figure 8.1.8 b) Bottom of Rocprop starting to buckle.

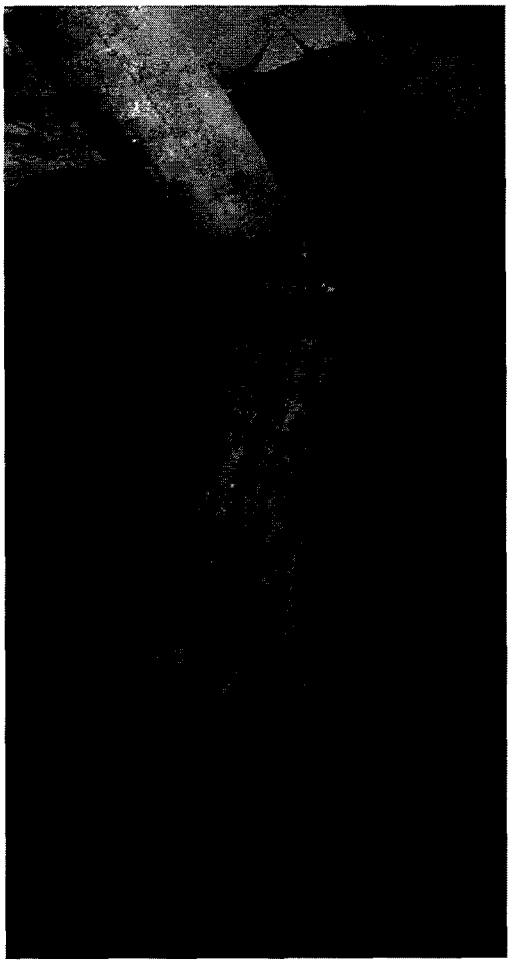

Figure: 8.1.8 c) Rocprop buckling due to over-extension when installed.

Figure: 8.1.8 d) Rocprops installed correctly.

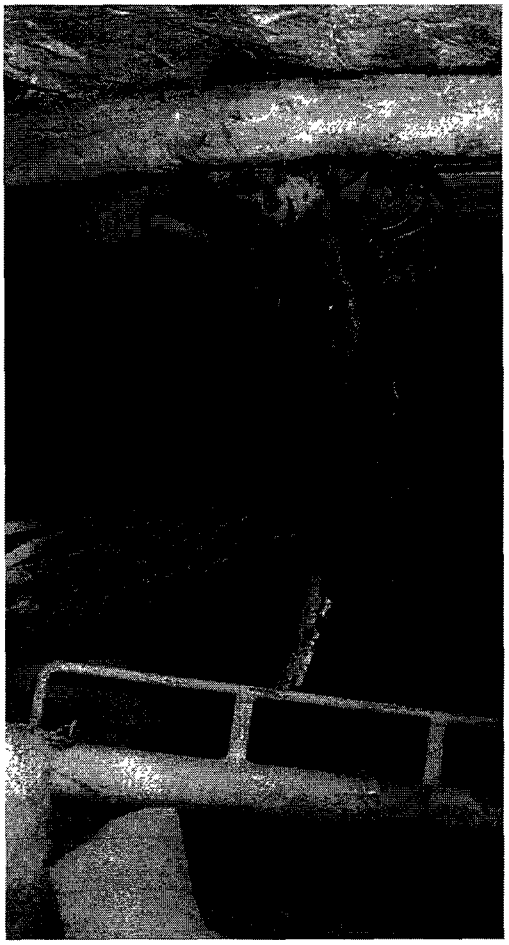

Figure 8.1.8 e) Rocprop failure after stope back-break.

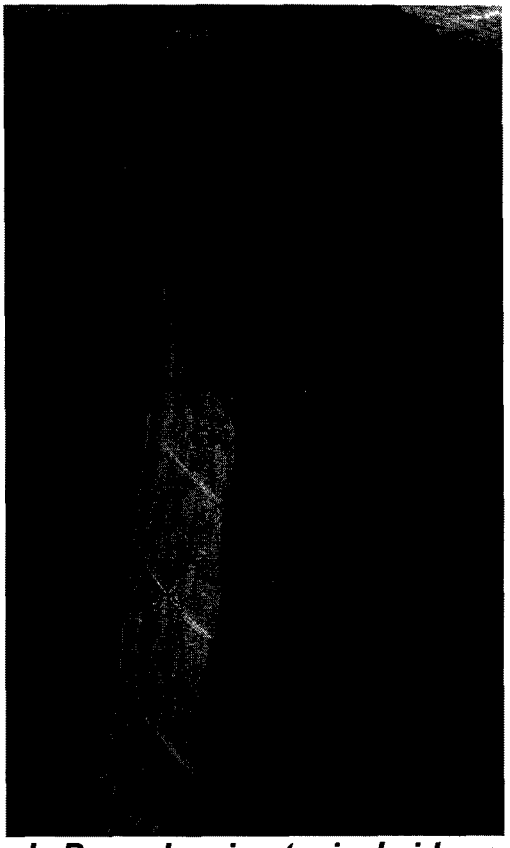

Figure 8.1.9 a) Madoda Prop showing typical sideways movement of pre-stressing device.

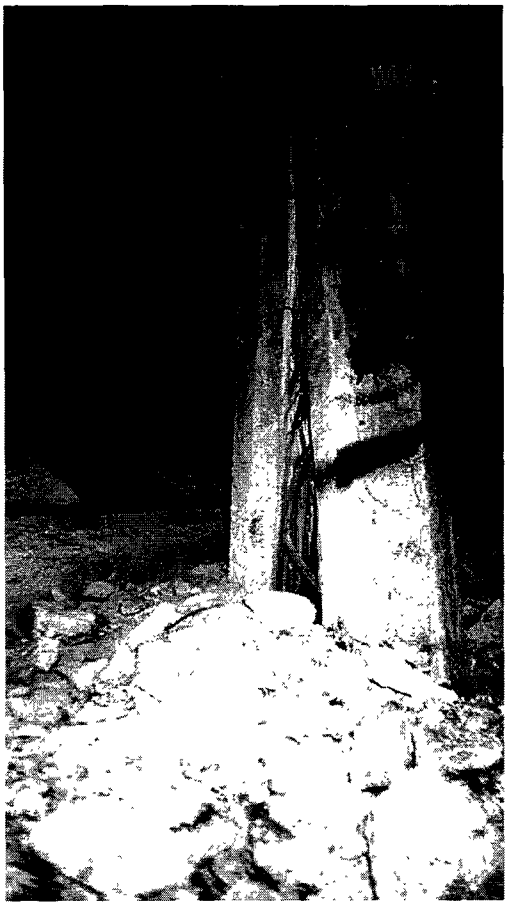

Figure 8.1.9 b) Madoda Prop starting to split.

Figure 8.1.9 c) Madoda Prop split into three.

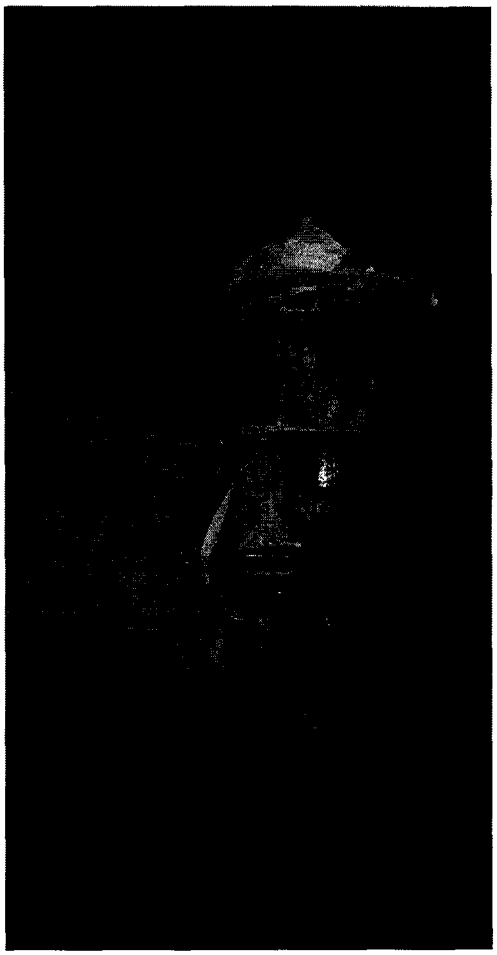

Figure 8.1.10 a) Correctly installed Ebenhaeser MK1.

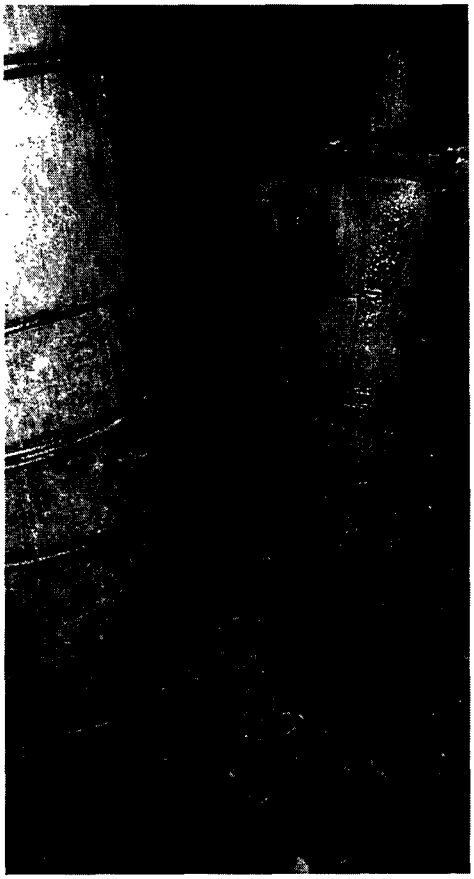

Figure 8.1.10 b) Ebenhaeser; note how top is starting to split.

Figure 8.1.11 a) Turned Profile Prop, note brushing of prop top.

Figure 8.1.11 b) Split turned Profile Prop.

Figure 8.1.12 a) Octagonal Profile Prop; note brushing of prop top.

Figure 8.1.12 b) Octagonal Profile Prop taking load; body of prop splitting.

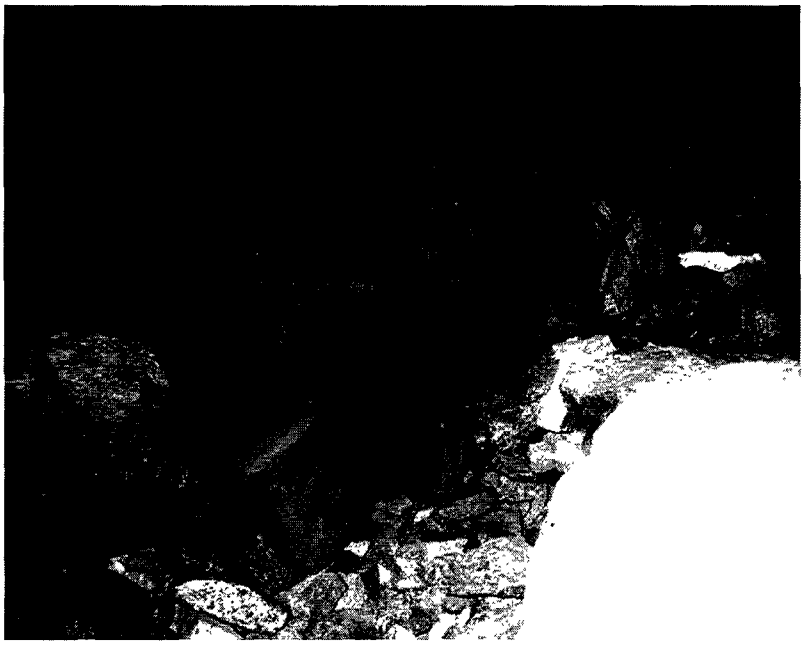

Figure 8.1.13 a) Cone Prop taking load; note how concrete cone is forced upwards into prop and how foot of the prop is splitting.

Figure 8.1.13 b) Cone Prop foot completely split and sideways movement on load cell.

Figure 8.1.14 a) Correctly installed Loadmaster.

Figure 8.1.14 b) Loadmaster; note failure mechanism of foot of prop.

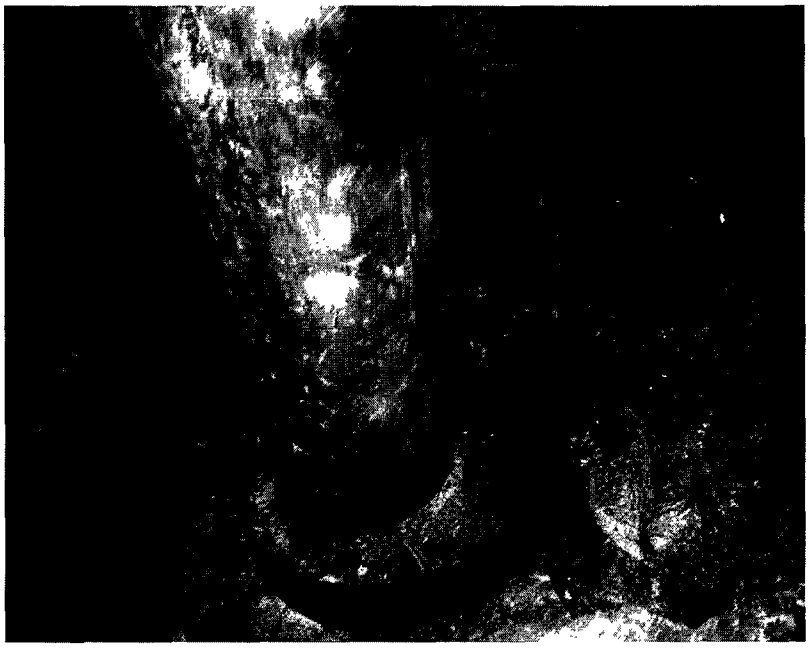

Figure 8.1.15 a) Gum pole on load cell; note how foot of gum pole is starting to brush.

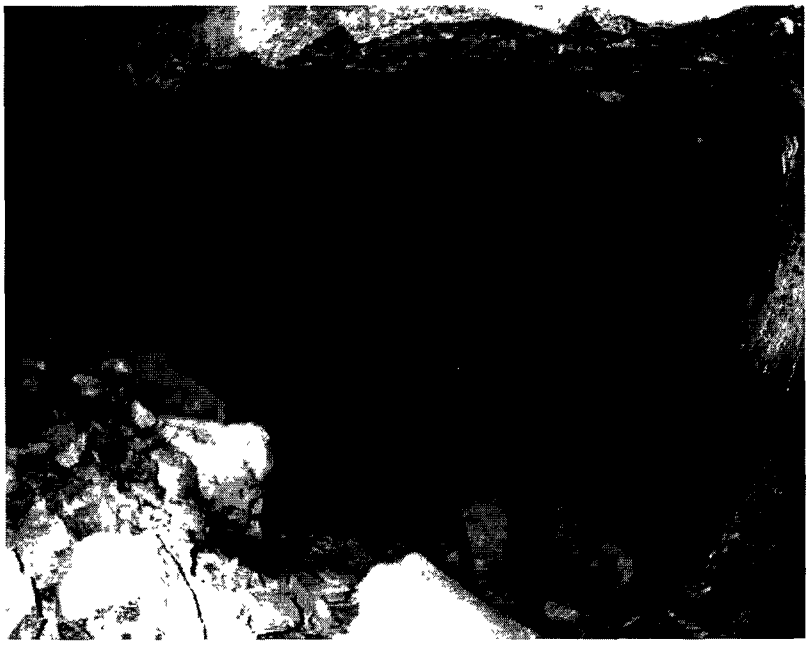

Figure 8.1.15 b) Gum pole; note how top of prop buckled during seismic event.

Figure 8.1.16 a) General photograph of prop failure due to seismic event.

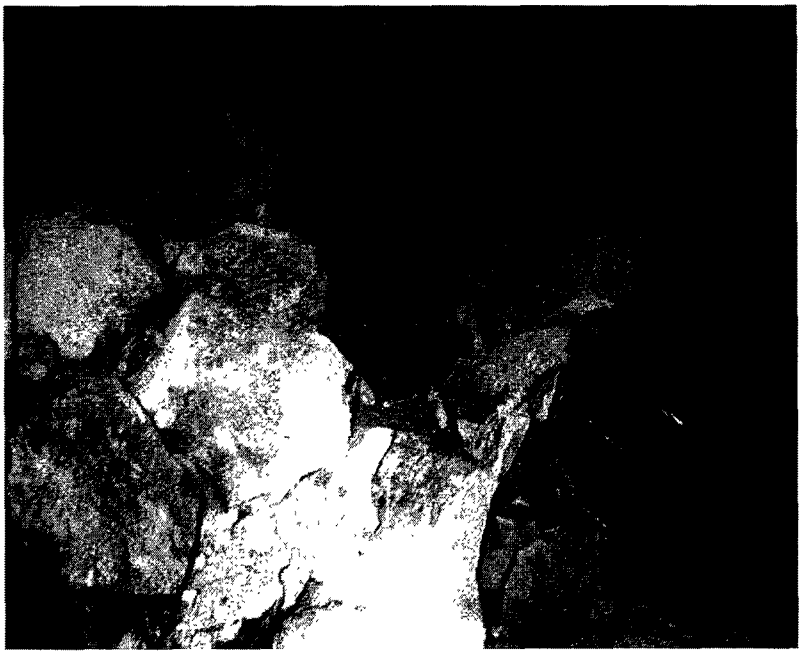

Figure 8.1.16 b) General photograph of how elongates were covered with rock after seismic event.

8.1.2.5 Comparison of underground and laboratory performance

Figures 8.1.17 and 8.1.18 indicate the results obtained from the in situ tests and are compared to the equivalent laboratory results. The difference in performance needs to be taken into account by applying an underground correction factor. This factor takes into account underground considerations, such as poor support installation, slow convergence rates and high humidity / temperature as well as timber creep, all of which have been shown to significantly influence support performance (Roberts *et al.*, 1987). Underground field tests were conducted to establish appropriate correction factors for each type of unit.

The results from the underground trials indicate lower initial performance than that recorded in the laboratory. Overall performance values are similar to those obtained in the laboratory.

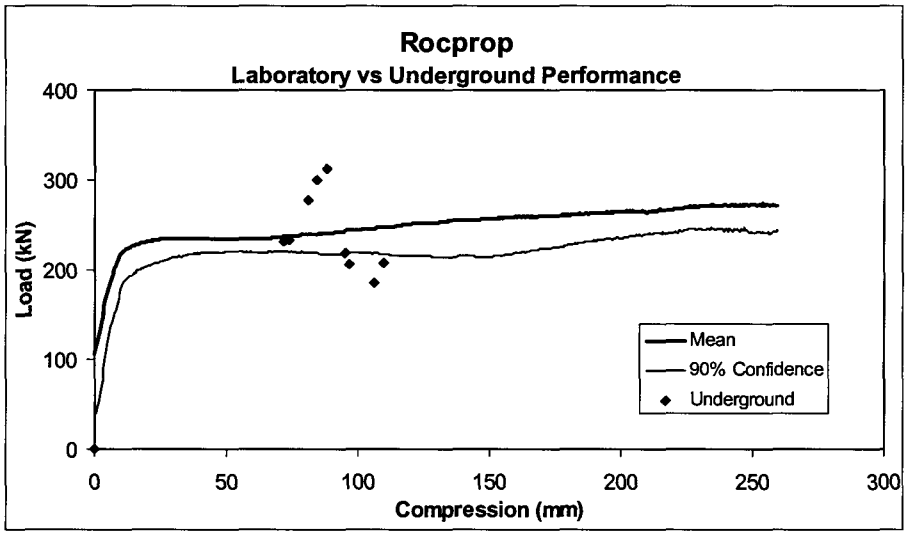

Figure 8.1.17 Comparison of laboratory slow test results (90 per cent confidence) with underground performance for Rocprops.

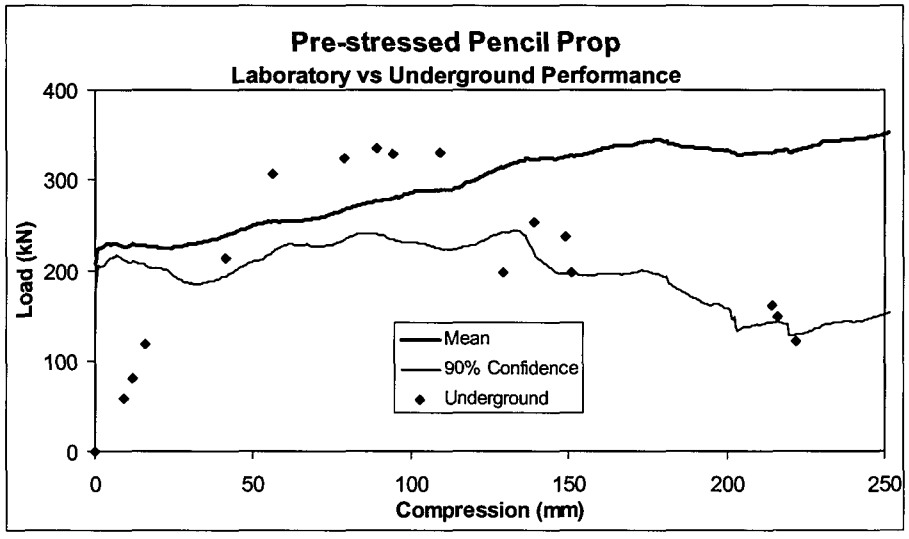

Figure 8.1.18 Comparison of laboratory slow test results (90 per cent confidence) with underground performance for pre-stressed Pencil Props.

8.1.2.6 Stepped and inclined platen tests

These tests were devised to simulate (at least in part) underground installations by evaluating the effects of eccentric loading on the support units. The eccentric loading of support units is a common occurrence underground and has been recognised as a factor adversely affecting the performance of the support units. Three different loading plates were used, of which two were step platens of 20 and 50 mm and the third was an inclined platen of 10 degrees. A limited number of tests have been conducted in this way to determine the validity of the assumption that eccentric loading could compromise the performance of the support units and promote buckling type failure.

The information obtained to date indicates that this type of eccentric loading may compromise the performance of some units. Due to the limited number of tests conducted, no definite conclusions can be made. However, the results indicate that more of these tests will be required to establish each unit's susceptibility to buckling.

The design of the platens was not ideal, as certain units have base plates that have a tendency to slip on the smooth inclined plate. This resulted in poor performance of the unit tested. A more suitable design, that could overcome this problem and be more representative of actual underground conditions, has been proposed.

8.1.3 Conclusions

The objective of these tests was to provide a standard testing procedure for all elongate support types. This procedure will provide officially accepted performance curves for each support type, which will in turn be used in the design of support systems.

Following the acceptance of the standard test procedure, support manufacturers will be required to conduct routine quality assurance testing of their support units which will indicate the performance of their production line product. These results can then be compared to the original performance testing results. This will provide a degree of confidence that the design performance criteria are being met.

8.1.4 Recommendations

The testing procedure for elongate supports will be required to fulfill certain basic requirements, namely:

- Provide initial performance design curves for inclusion in the SDA.
- Establish critical performance limits e.g. buckling potential.
- Provide for a quality assurance reference for individual units.

With this in mind the following testing procedure is recommended.

Three categories of mines should be established.
1. Mines with little (< 2 mm/day) to no convergence.
2. Mines with convergence in excess of 2 mm/day but not seismically active.
3. Mines with convergence in excess of 2 mm/day and seismically active.

This will provide for relevant testing to be conducted for the product's actual application. Mines that do not experience seismicity will not require dynamic testing to be conducted on their support units. Where a particular support unit is applicable to all mines, it will be required to be evaluated over the full spectrum of tests.

A total of 27 units will be required for the full test programme.
This programme is defined as follows:

1. Five rapid displacement tests at 3 m per second for 200 mm. The loading rate to be 30 mm per minute prior to and subsequent to the rapid displacement. Initial displacement to be 50 mm before initiation of the rapid displacement. The unit will be tested to destruction or a minimum of 400 mm.

2. Ten slow tests at a loading rate of 30 mm per minute. The unit will be tested to destruction or a minimum of 400 mm.

3. Three slow tests at a loading rate of 30 mm per minute on a 10 degree grooved platen. The unit will be tested to destruction or a minimum of 400 mm.

4. Two creep tests. Units with pre-stressing devices will be set at 200 kN. Units with no pre-stressing devices will be set at 80 kN. The units will be loaded by the initial compression and their load shedding monitored for a period of seven days.

5. Two slow tests at a loading rate of 10 mm per day for a period of seven days.

6. Five underground tests making use of suitable load cells and convergence measurement devices.

This procedure covers the requirements of all mines as stated above. For mines with convergence in excess of 2 mm/day, no creep tests (test 4 as above) are necessary. Units that are not designed for seismically active areas will not be subjected to rapid displacement testing (test 1 as above).

The laboratory test results showed that, in general, for the same support type the performance of the longer units (1,6 m) was similar to the shorter units (1,0 – 1,2 m). During laboratory compression tests, the deformation occurs predominantly in the yielding portion of the support units, which is identical in the longer and shorter units. The parallel platens of the loading press ensure axial loading, and relatively little failure due to prop buckling occurs. However, in the underground environment the uneven hangingwall and footwall can induce non-axial loading, and the resulting bending moments can lead to buckling failure. The longer support units, in particular, are more prone to buckling failure, and hence their loading capabilities are reduced compared with the shorter units. Further details of the effect of the support unit length on support performance are given in Appendix D.

8.2 Addressing the variability of elongate support performance

8.2.1 Introduction

Elongates, most of which are timber based, are being extensively used in the gold and platinum mines for stope support. The elongates are often used in conjunction with rapid yield hydraulic props, but in some cases pre-stressable, yielding types have replaced the latter as face area support in seismically active mines. Support resistance and energy absorption calculations have revealed that the pre-stressable, yielding varieties may be acceptable under seismic conditions, apparently offering both safety and production advantages over an inefficiently organised or resourced hydraulic prop management system.

Some concern has been expressed, however, that the performance characteristics and consistency of this type of support have not been fully evaluated.

As part of the work conducted under SIMRAC project GAP 330, a provisional test procedure has been proposed to provide a systematic approach to the performance evaluation of the capabilities of elongates. The test procedure entails various laboratory and underground compression tests of the support units, with emphasis placed on repeated tests using units of the same type to investigate performance variability and obtain a statistical distribution of the load versus deformation curves. Whilst it is recognised that this number of tests is comparatively small, particularly to facilitate an accurate statistical data analysis and interpretation, the number of tests are deemed adequate to give important insights into the performance variability associated with various elongate types, and to establish elongate design curves suitable for use in the mining environment.

The objective of the work reported here is to propose a statistical analysis to interpret the results obtained by the above mentioned test procedure. The analysis makes use of data from repeated tests using units of the same type, and attempts to quantify the effect of the inherent strength variability associated with support systems. Although the statistical analysis is demonstrated using elongate performance data, the statistical method is suitable to quantify the variability of any type of support data.

The ultimate output is to enable mine personnel to select units suitable for their particular requirements and engineer support systems, with a high degree of confidence of meeting support resistance and energy absorption criteria. The statistical analysis aims towards ensuring that any major variations in support consistency will not compromise rock mass stability, and hence underground safety.

8.2.2 Statistical methods applied to elongate performance data

Variations in material properties and manufacturing tolerances result in individual support units of the same type having different support capabilities. The variation of support performance can be characterised by the mean μ, standard deviation σ and a probability distribution. The probability distribution is defined by a distribution function, and various functions (e.g. normal, log-normal, gamma, beta and Weibull distributions) have been used to describe and characterise different types of data (Miller and Freund, 1985). Among these, the normal probability function is by far the most widely used. It was first studied in the eighteenth century when scientists observed a high degree of regularity in the measurement of errors. They found that the distributions they observed were closely approximated by a continuous distribution, which they referred to as the normal curve of errors, attributed to the laws of chance. The bell-shaped graph of the normal probability distribution is shown in Figure 8.2.1.

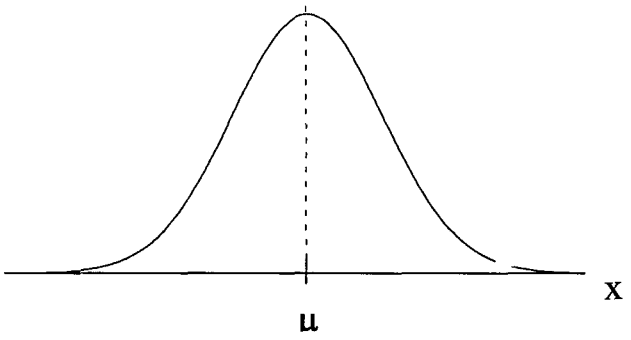

Figure 8.2.1 Graph of a normal probability distribution.

For the purpose of the statistical evaluation of elongate performance, a normal distribution of support performance is assumed. The validity of this assumption is qualitatively demonstrated in Figure 8.2.2, which, as an example, shows the distribution of variability of a Rocprop elongate. The distribution is calculated by considering the load-deformation data of ten laboratory compression tests conducted at a deformation rate of 15 mm/min. The units were compressed over a distance of 450 mm. To obtain the distribution of performance variability, the load generated by the elongate, as measured by the laboratory equipment, was normalised with respect to the mean of the ten compression tests. This was repeated for all ten tests at deformation intervals of 0,5 mm. A histogram is drawn (see Figure 8.2.2), grouping the normalised load data into one per cent variability intervals. The normal distribution is calculated from the average standard deviation normalised relative to the mean load at 0,5 mm deformation intervals. From Figure 8.2.2 it is apparent that a normal distribution approximates the scatter of support performance reasonably well, and is hence a suitable distribution to formulate statistical interpretations, particularly since comparatively little support performance data currently exists. Once the database has been extended, the assumption of a normal distribution can be re-evaluated, and if necessary an alternative probability distribution can be used to represent the scatter of support capabilities more accurately.

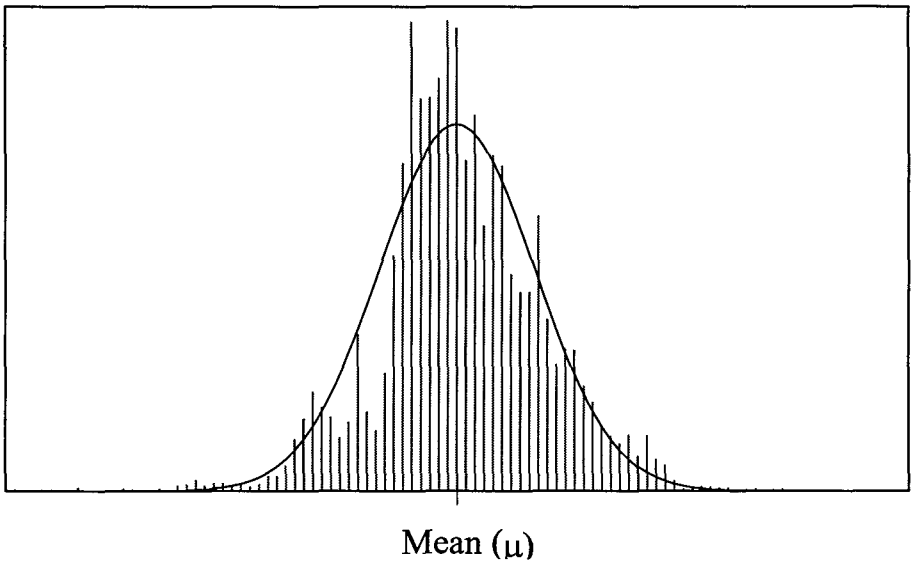

Figure 8.2.2 Histogram of the variability of support performance of a Rocprop elongate versus the normal probability distribution.

8.2.2.1 Evaluating data represented by a normal distribution

The equation of the normal probability distribution, the graph of which is shown in Figure 8.2.1, is

$$y = \frac{1}{\sigma\sqrt{2\pi}} e^{-\frac{1}{2}\left(\frac{x-\mu}{\sigma}\right)^2} \qquad -\infty < x < \infty \ , \tag{8.2.1}$$

where μ and σ are the population mean and standard deviation, respectively (i.e. the mean and standard deviation of, for example, the reaction force at a given displacement of the tested support units), and x is the sample value (reaction force at a given displacement) of the installed support unit. The *population* mean and standard deviation is used to describe the performance of support units evaluated by means of laboratory and underground compression tests, whereas the *sample* data is defined as the actual performance of underground installed support systems (Figure 8.2.3).

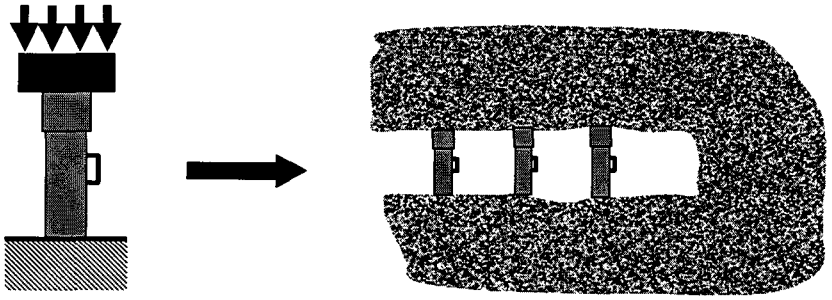

Population data determined by multiple laboratory tests => μ, σ.

Support design makes use of **sample** data (x), i.e. performance of installed support units.

Figure 8.2.3 Schematic illustrating the difference between population and sample data.

The total area under the curve represented by Equation (8.2.1) is equal to 1,0 or 100 per cent, and is used for probability calculations (see Equation 8.2.2, where $F(z)$ is the probability). Since the normal probability distribution cannot be integrated in closed form between every pair of limits a and b, probabilities relating to normal distributions are usually obtained from special tables, such as provided by Miller and Freund (1985).

$$F(z) = \frac{1}{\sqrt{2\pi}} \int_z^{\infty} e^{-\frac{1}{2}t^2} dt \ . \tag{8.2.2}$$

In order to engineer support systems with a high degree of confidence of meeting support resistance and/or energy absorption requirements, performance curves characterising the load versus deformation behaviour should be established for each support type used by the mining industry. A performance curve representing some lower limit of the support capability will ensure that a high percentage of units would meet or exceed this prescribed limit. In Figure 8.2.4, the shaded area represents the percentage of units exceeding the performance specification, whilst the unshaded area to the left should be minimised, as these units would fall below the specification.

In the work presented here, the lower limit of elongate performance is of relevance. To date, relatively little work has been done on the effect of comparatively high elongate loads on the

hangingwall rock mass stability, and hence no upper bound for elongate loads is stipulated. Once further understanding of the support – rock mass interaction is gained, the validity of lower *and* upper performance limits can be re-appraised.

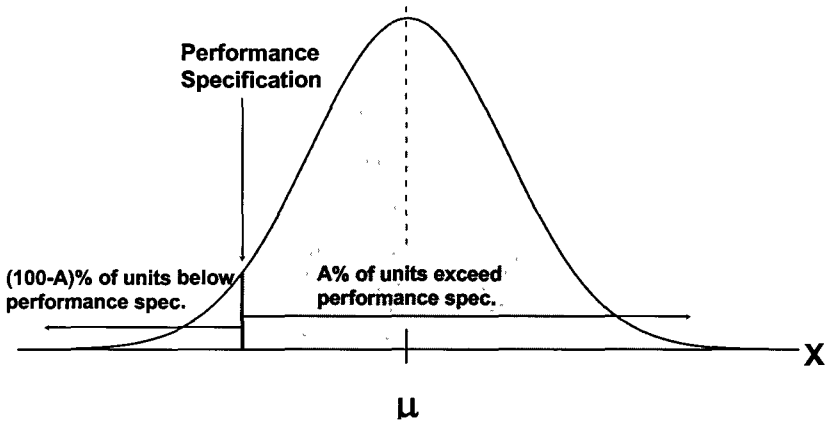

Figure 8.2.4 Probability density function sectioned according to performance specification.

The percentage of units exceeding the performance specification (i.e. the probability of the sample exceeding the performance specification) is a function of the population mean and standard deviation. Furthermore, if multiple support units are installed and the mean performance is of relevance, as opposed to the performance of a single unit, the probability is dependent on the sample number. This relationship can be expressed by the central limit theorem (Miller and Freund, 1985):

$$z = \frac{\bar{x} - \mu}{\sigma / \sqrt{n}} \quad , \tag{8.2.3}$$

where the mean $\bar{x}$ of a random sample of size n is taken from a population having the mean μ and the standard deviation σ.

It is instructive to re-arrange Equation (8.2.3) as follows:

$$\bar{x} = \mu - \alpha\sigma \quad \text{where} \quad \alpha = \frac{-z}{\sqrt{n}} \quad , \tag{8.2.4}$$

i.e., the mean sample performance $\bar{x}$ is a function of the population mean μ and standard deviation σ, as well as a factor α, which depends on (i) the probability z of exceeding the sample performance and (ii) the sample size n. The probability of exceeding the sample performance for various values of α is given in Figure 8.2.5.

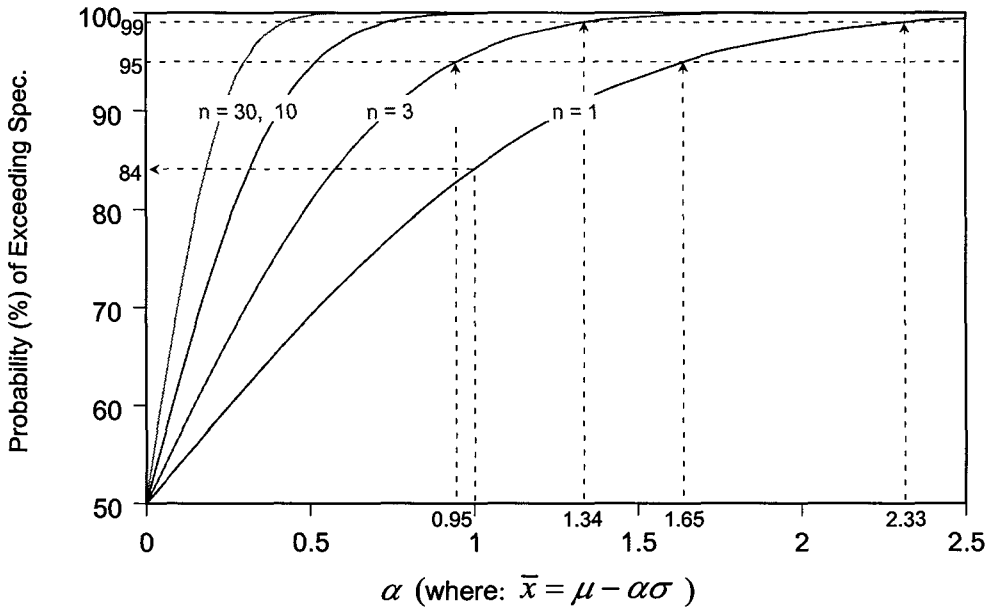

Figure 8.2.5 Probability of exceeding sample performance for various values of α and n.

Previously, as an initial guideline to evaluate support units, it was suggested that, in order to design support systems conservatively (accounting for the variability of support capabilities), the design force-deformation curve $\bar{x}$ of a support type should be the mean μ less one standard deviation σ, i.e. $\bar{x} = \mu - 1.0\sigma$. Substituting $\bar{x} = \mu - 1.0\sigma$ in Equation (8.2.4) it is found that $z = -\sqrt{n}$, that is the probability $F(z)$ of exceeding the mean design curve $\bar{x} = \mu - 1.0\sigma$, depends only on the size n of the random sample taken from a population having the mean μ and the standard deviation σ. This is evident from Figure 8.2.5, where it is shown that, if $n = 1$ and $\bar{x} = \mu - 1.0\sigma$, the probability of exceeding the performance specification is 84 per cent. For $n = 3$ or 30 the probability of exceeding the performance specification increases by $F(z) = 95{,}8$ per cent or 99,9 per cent, respectively.

In other words, the probability of a single support unit meeting the performance requirements is 84 per cent, whereas the probability of the mean of 30 support units exceeding the design specification is 99,9 per cent. Thus, by choosing a design curve calculated by $\bar{x} = \mu - 1.0\sigma$, the design specification for a single support unit is probably not conservative enough (84 per cent), whereas the specification for the mean of a system of, for example, 30 units is too conservative (99,9 per cent), as correctly pointed out by Handley (1998).

From a support design point of view, it is convenient to design for a constant confidence level (say 90 per cent, 95 per cent or 99 per cent), irrespective of the number of units comprising the support system. Hence, the extent to which the mean of a suite of tests is downgraded to give a design force versus displacement curve is variable, depending of the number of support units comprising the system or part of the system which is considered relevant. Table 8.2.1 shows relationships between $\bar{x}$, μ and σ for probability levels of 90 per cent, 95 per cent and 99 per cent of meeting the performance specification, and for n = 1, 3, 10 and 30. The relationships for n = 1 and 3, and $F(z)$ = 95 per cent and 99 per cent, are indicated graphically in Figure 8.2.5.

The sample size (n) is chosen according to ground conditions, which dictate the interaction of multiple units as a system, as opposed to single units acting in isolation. Further details of the parameters influencing sample size, as well as recommendations thereof, are given in Section 8.2.4.

Table 8.2.1 Relating $\bar{x}$, μ and σ for probability levels of 90 per cent, 95 per cent and 99 per cent, and n = 1, 3, 10 and 30.

	Probability of exceeding performance specification		
	90 %	**95 %**	**99 %**
***n* = 1**	$\bar{x} = \mu - 1.282\sigma$	$\bar{x} = \mu - 1.645\sigma$	$\bar{x} = \mu - 2.326\sigma$
***n* = 3**	$\bar{x} = \mu - 0.740\sigma$	$\bar{x} = \mu - 0.950\sigma$	$\bar{x} = \mu - 1.343\sigma$
***n* = 10**	$\bar{x} = \mu - 0.405\sigma$	$\bar{x} = \mu - 0.520\sigma$	$\bar{x} = \mu - 0.736\sigma$
***n* = 30**	$\bar{x} = \mu - 0.234\sigma$	$\bar{x} = \mu - 0.300\sigma$	$\bar{x} = \mu - 0.425\sigma$

8.2.3 Statistical analysis of actual support data

The following examples, using actual support test data, serve as a guide to illustrate the applicability of the statistical method. In all cases, the support data used was obtained by CSIR Mining Technology's laboratory elongate testing programme

8.2.3.1 Rocprop: quasi-static loading

As part of the elongate testing programme, ten 1,2 m Rocprop units were compressed at a constant displacement rate of 15 mm/min. The resulting force-deformation curves are shown in Figure 8.2.6. The ten units display comparatively consistent behaviour and, after an initial rapid load increase, the load carrying capacity remains between 200 and 300 kN for the main duration of the test.

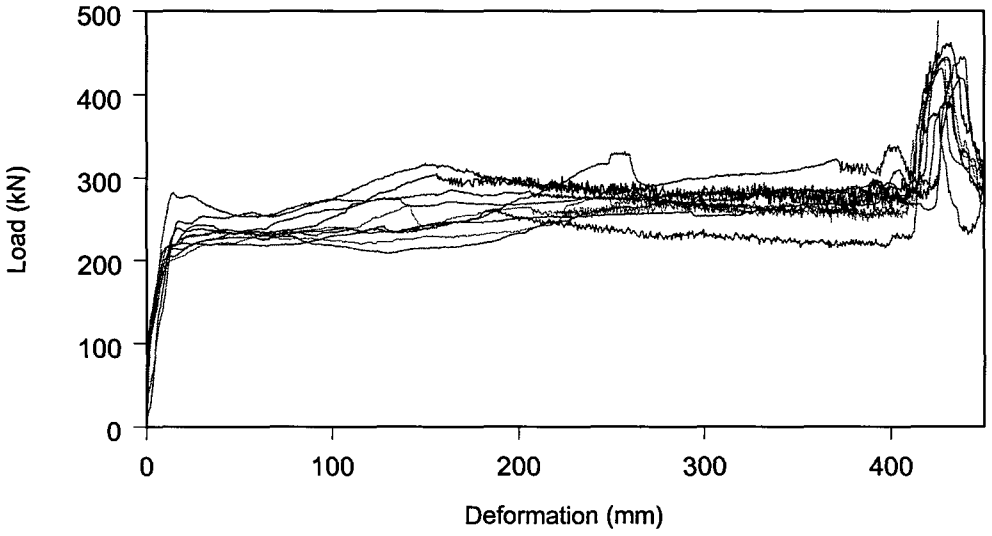

Figure 8.2.6 Force-deformation profiles of ten 1,2 m Rocprops; 15 mm/min deformation rate.

The statistical analysis described previously is used to establish performance curves for various probabilities of exceeding the support load bearing capabilities. The mean μ and standard

deviation σ of the force transmitted by the elongate are calculated for the ten compression tests at various values of deformation (0→450 mm, at deformation intervals of 0,5 mm). Inserting μ and σ in Equation (8.2.4), the parameter $\bar{x}$ can be calculated at deformation intervals of 0,5 mm, resulting in a force-deformation curve of reduced amplitude, which is referred to here as the performance curve.

Figure 8.2.7 gives Rocprop performance curves for 90 per cent, 95 per cent and 99 per cent probabilities of exceeding the support capabilities. Also shown is the mean μ of the ten Rocprop tests, as well as the performance curve calculated by the mean minus one standard deviation $\bar{x} = \mu - 1.0\sigma$, which previously was shown to represent a probability of 84 per cent. The curves shown in Figure 8.2.7 are calculated assuming n = 1, i.e. a single Rocprop unit acting independently of the surrounding support.

The performance curves shown in Figure 8.2.7 are applicable if the support capability of a single unit is of importance. In some instances, however, the average support capability of multiple units is of interest. In this case, the performance curves shown in Figure 8.2.8 are applicable, which are given for n = 1, 3, 10, 30 and ∞, and a probability of 95 per cent of exceeding the average support capability. As intuitively obvious, in the limit, i.e. n = ∞, the performance curve equals the mean μ.

To reiterate, for a fixed probability (of the average support capability of multiple units exceeding the performance curve), the performance curve approaches the mean as the number of units increases. Conversely, for a fixed performance curve, the probability of exceeding the support capability increases with increasing number of support units.

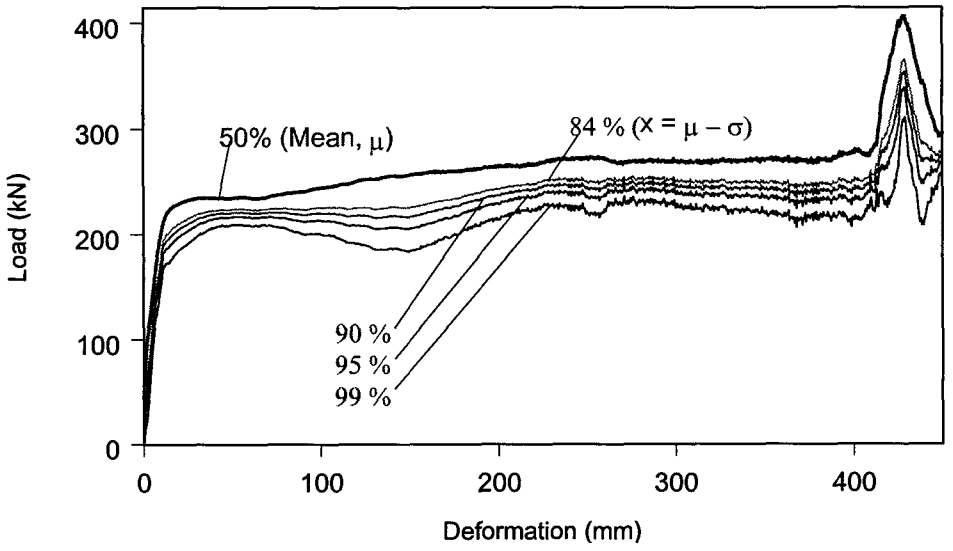

Figure 8.2.7 Probability of a single Rocprop support unit exceeding the performance curve.

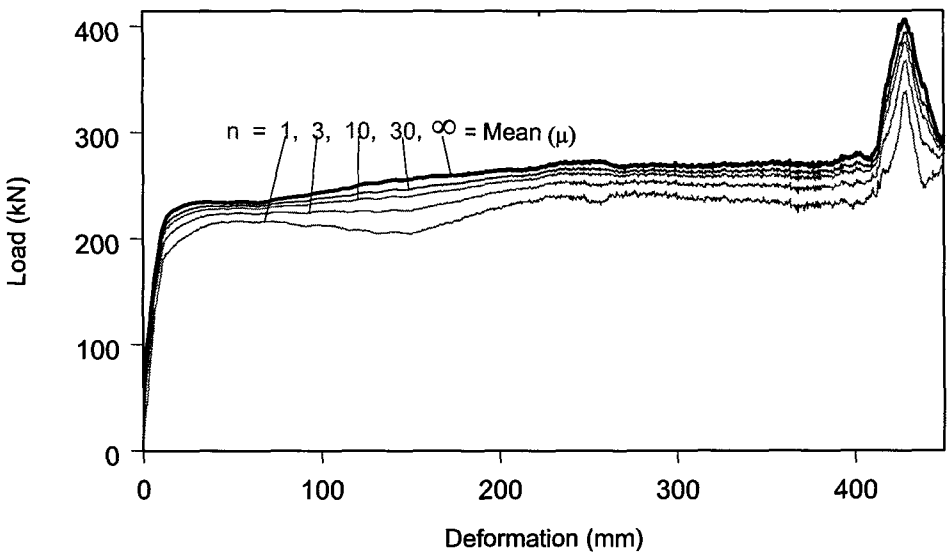

Figure 8.2.8 Performance curves for a support system comprising n = 1, 3, 10, 30 and ∞ Rocprop support units (95 per cent probability of exceeding performance curve).

8.2.3.2 Rocprop: dynamic loading

According to the elongate test procedure, support units used in seismically active areas are evaluated by means of rapid compression tests. Load versus deformation laboratory test data for 1,2 m long Rocprops is given in Figure 8.2.9. The Rocprops are initially loaded at a low deformation rate of 15 mm/minute up to 50 mm deformation, then rapidly at 3 m/s up to 300 mm total deformation, followed by a 15 mm/minute loading rate for the remainder of the test. The Rocprop yielding mechanism is based on frictional resistance and hence, due to lower dynamic compared to static friction coefficients, the load decreases during dynamic loading. The statistical evaluation for this data is given in Figure 8.2.10, which shows Rocprop performance curves for seismic conditions at various probability levels.

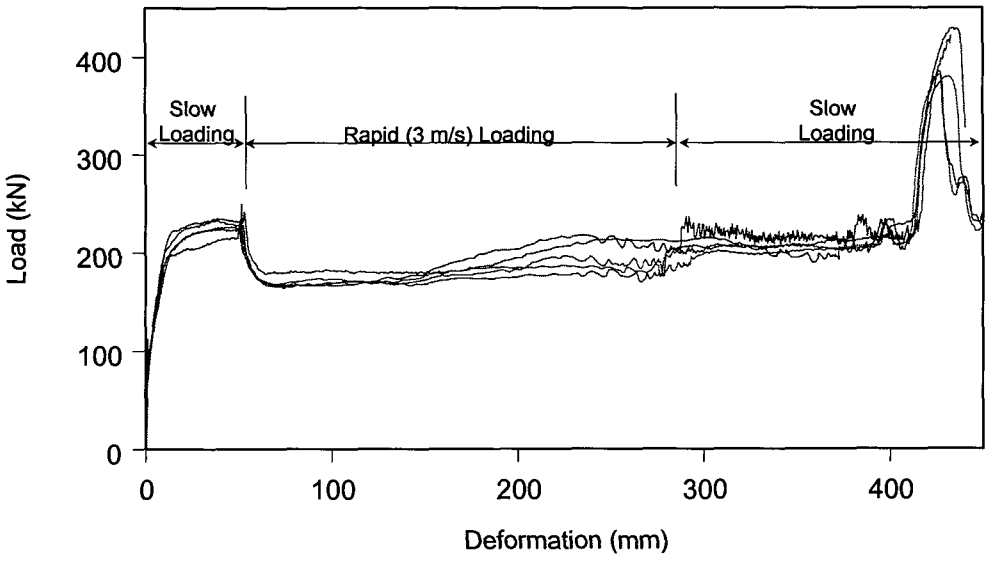

Figure 8.2.9 Force-deformation curves of five 1,2 m Rocprops; 3 m/s deformation rate.

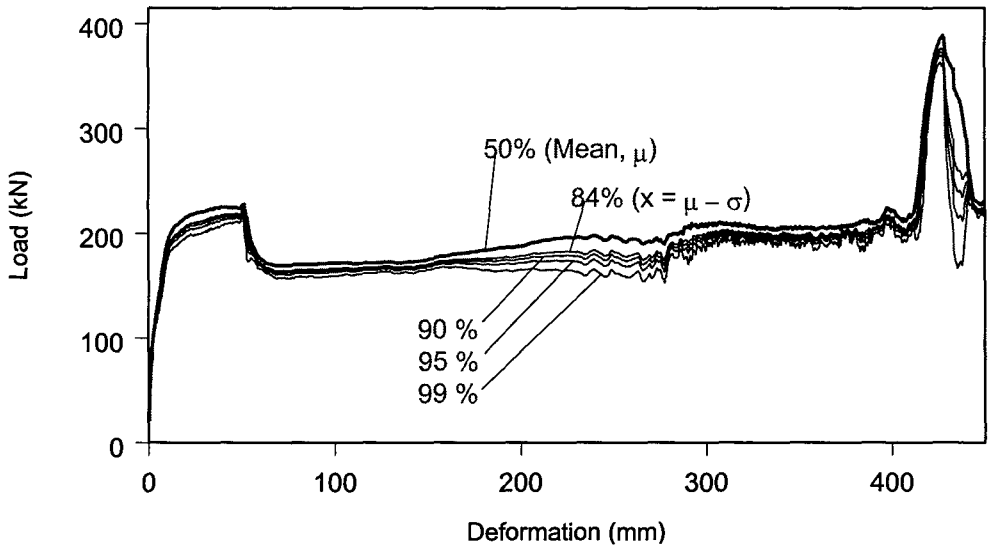

Figure 8.2.10 Probability of a single Rocprop support unit exceeding the seismic performance curve.

8.2.3.3 Loadmaster: quasi-static loading

As a further example of the elongate data analysis, the load versus deformation curves of the Loadmaster support unit are investigated. Figure 8.2.11 shows the ten curves of the slow (15 mm/minute) compression tests. It is evident that the behaviour of the Loadmaster is not as consistent as the Rocprop, and the scatter of the load-deformation data is increased. The statistical analysis of the Loadmaster data is shown in Figure 8.2.12, giving performance curves for various probability values.

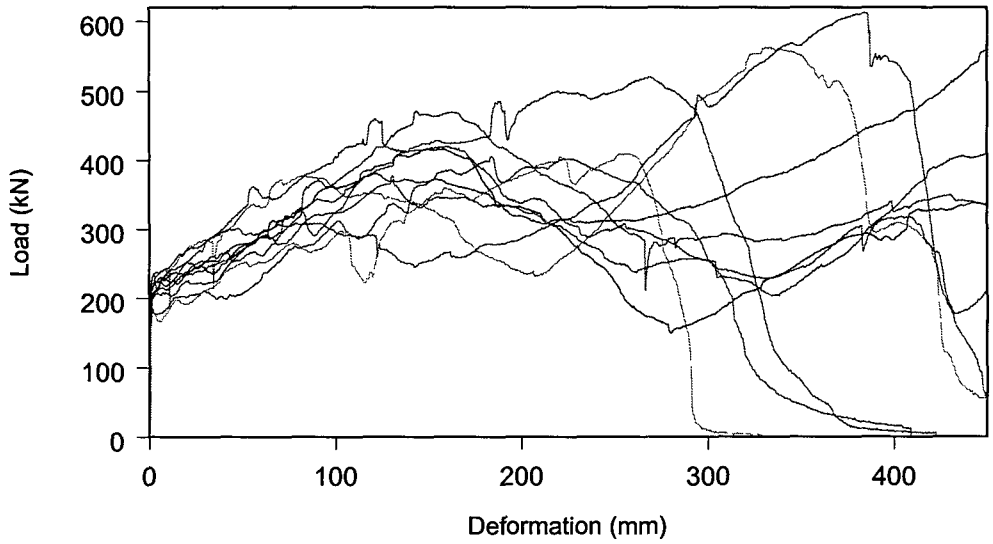

Figure 8.2.11 Force-deformation profiles of ten 1,6 m Loadmaster units; 15 mm/min deformation rate.

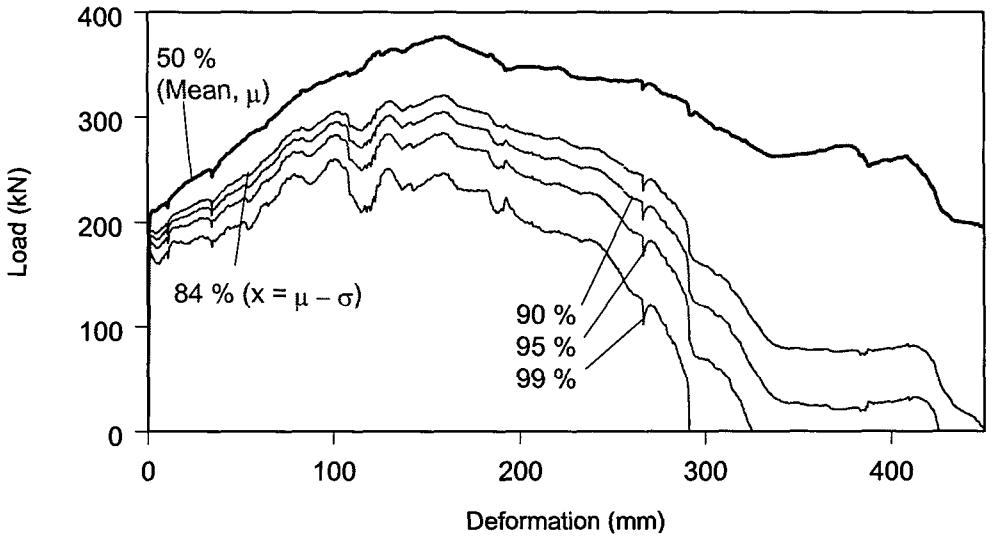

Figure 8.2.12 Probability of a single Loadmaster support unit exceeding the performance curves.

8.2.3.4 Loadmaster: dynamic loading

Results of high loading rate compression tests are shown in Figure 8.2.13, whilst Figure 8.2.14 shows performance curves for various probabilities of exceeding the seismic performance curves.

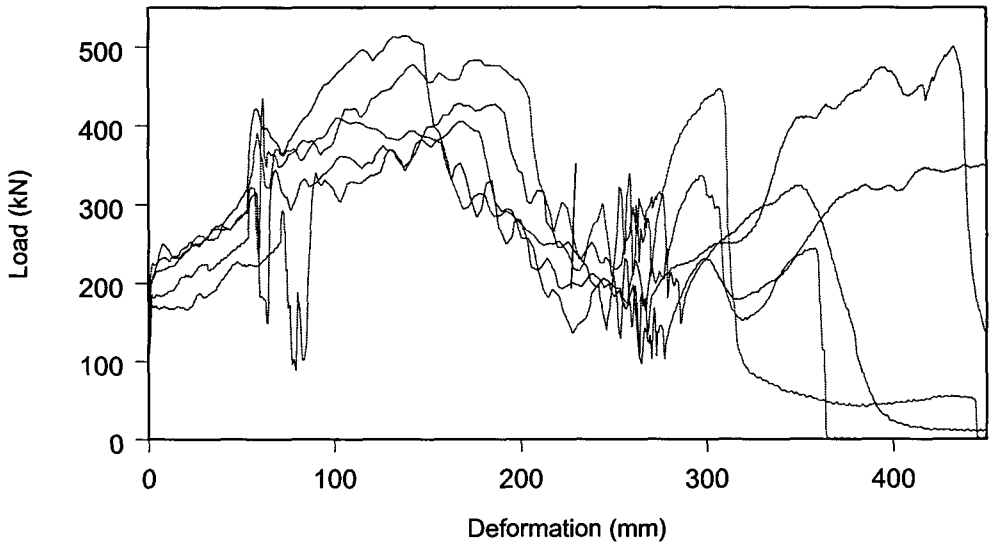

Figure 8.2.13 Force-deformation profiles of five 1,6 m Loadmaster units; 3 m/s deformation rate.

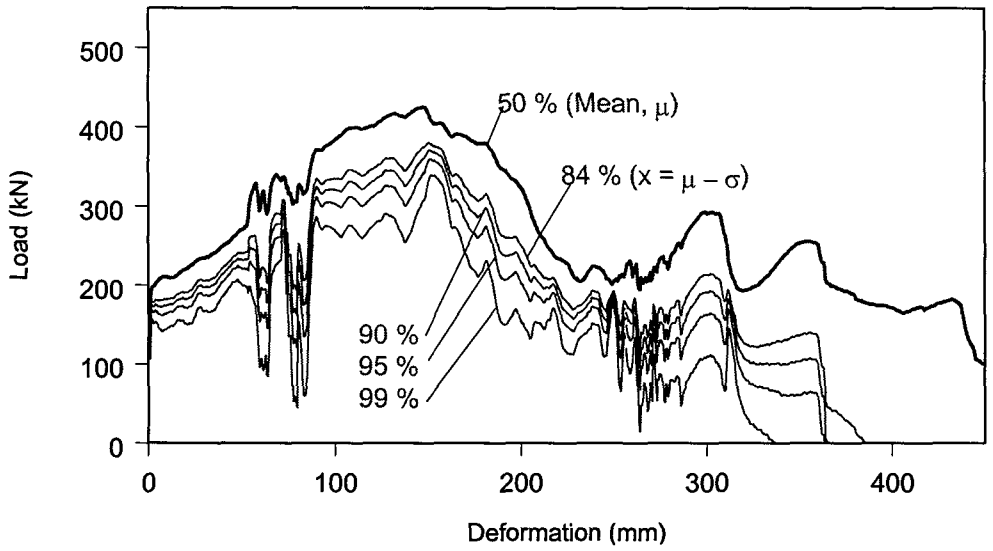

Figure 8.2.14 Probability of a single Loadmaster support unit exceeding the seismic performance curves.

8.2.4 Impact of the statistical analysis on support spacing

The proposed statistical analysis aims to improve support design and reduce rock-related hazards by taking into account and quantifying the inherent variability associated with elongate performance. To this end, force-deformation curves are downgraded to ensure a high probability of installed units exceeding the performance curve. The aim of this section is to investigate the consequences of the modified load-deformation curve on support system design and support spacing.

For purposes of illustrating the average effect of load-deformation curve down-grading, the average load carrying capability of the support unit is calculated up to a deformation of 300 mm (Figure 8.2.15 a). The energy, which can be absorbed by the unit, is calculated during dynamic deformation between 50 mm and 250 mm compression (Figure 8.2.15 b). It is emphasised that the assumption of constant average load and energy absorption between 50 mm and 250 mm is not suitable for actual support system design, and is only used here to demonstrate the average effect of curve downgrading. Actual support design should make use of the methodology proposed by Roberts (1995).

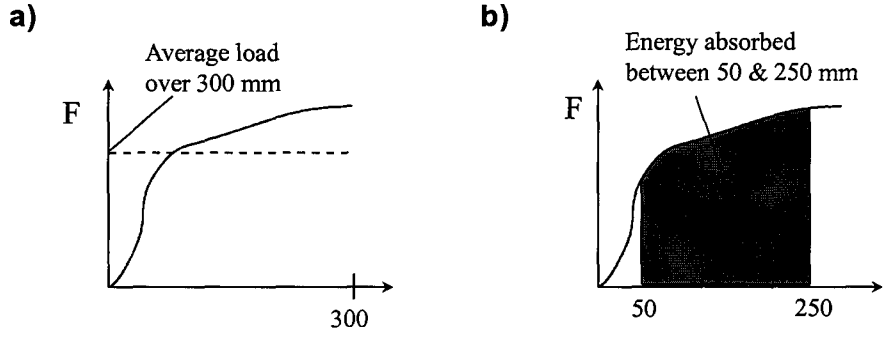

Figure 8.2.15 a) Average load carrying capability up to a deformation of 300 mm, and b) energy absorption between 50 mm and 250 mm deformation.

Table 8.2.2 lists the average support load (of relevance in non-seismic applications, i.e. rockfalls), as well as energy absorption capabilities (seismic applications, i.e. rockbursts), of various support types. The data is given for the mean of the laboratory tests, as well as for downgraded curves, representing the 90 per cent, 95 per cent and 99 per cent performance specifications.

Table 8.2.2 Average support load and energy absorption capability of four elongate types (n = 1, probability F(z) = 90 per cent, 95 per cent and 99 per cent).

	Mean (μ)	90 %	95 %	99 %
1,2 m Rocprop				
Average support load	250 kN	224 kN	217 kN	203 kN
Energy absorption capability	36 kJ	34 kJ	33 kJ	32 kJ
1,6 m Loadmaster				
Average support load	322 kN	250 kN	230 kN	192 kN
Energy absorption capability	67 kJ	52 kJ	47 kJ	39 kJ
1,6 m Ebenhaeser				
Average support load	332 kN	257 kN	236 kN	197 kN
Energy absorption capability	55 kJ	46 kJ	44 kJ	39 kJ
1,6 m Cone Prop				
Average support load	242kN	190 kN	175 kN	148 kN
Energy absorption capability	29 kJ	24 kJ	22 kJ	19 kJ

To demonstrate the effect of curve down-grading on support spacing, the maximum tributary area per support unit, versus fallout height, is determined. The curves are calculated by equating the load carrying and energy absorption capability to the weight and total energy (Wagner, 1982) of the rock mass for rockfall and rockburst conditions, respectively:

Rockfall: $F = \rho b A g$ Rockburst: $E = \rho b A \left(\frac{v^2}{2} + g h \right)$

where: F = average support unit load
ρ = rock density (2700 kg/m^3)
b = fallout height (m)
A = tributary area (m^2)
g = 9,8 m/s^2
E = energy absorbed by support
v = max. h/wall velocity (3 m/s)
h = h/wall displacement (0,2 m)

The tributary area (A) is solved as a function of fallout height (b) and plotted in Figures 8.2.16 a) to 8.2.16 d) for four elongate types at various probabilities of exceeding the design curve. When designing support systems and the spacing thereof, it is essential to consider additional parameters influencing the rock mass stability, that are not considered here. Examples of these are local geological features and discontinuities, mining induced fracturing, mining depth, rockfall and seismic history, support unit interaction with rock mass and each

other, and areal support coverage. These parameters significantly influence the stable hangingwall span between support units, and need to be considered in addition to tributary area rockfall and rockburst criteria.

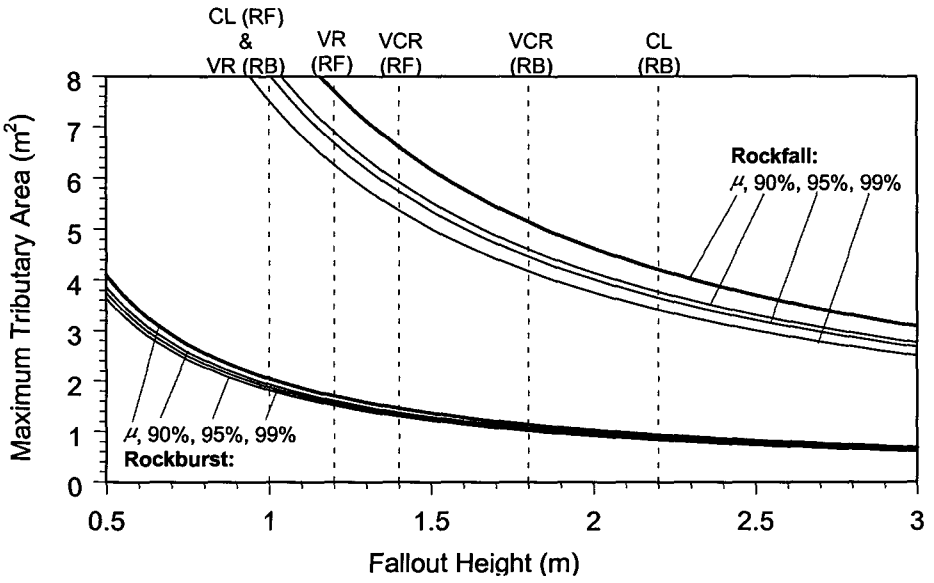

a): 1,2 m Rocprop

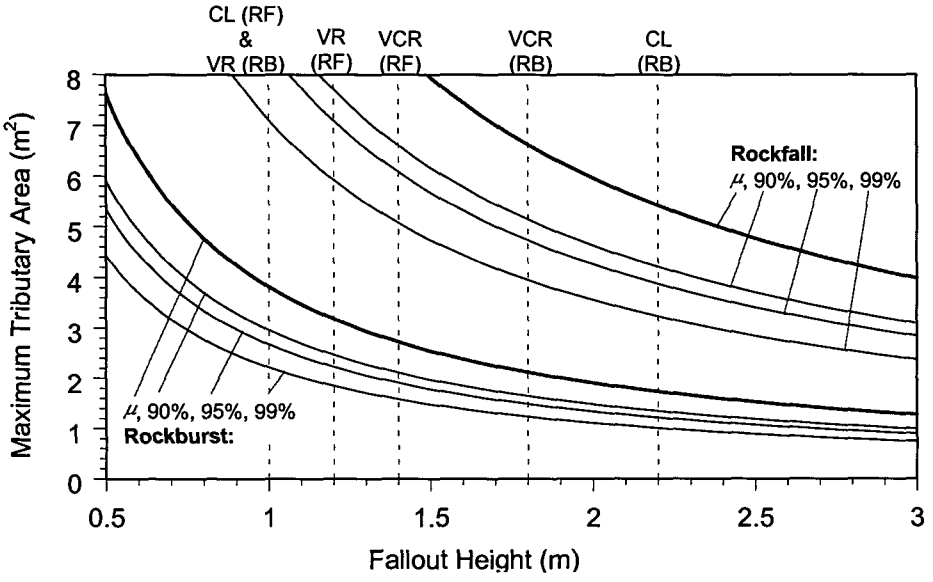

b): 1,6 m Loadmaster

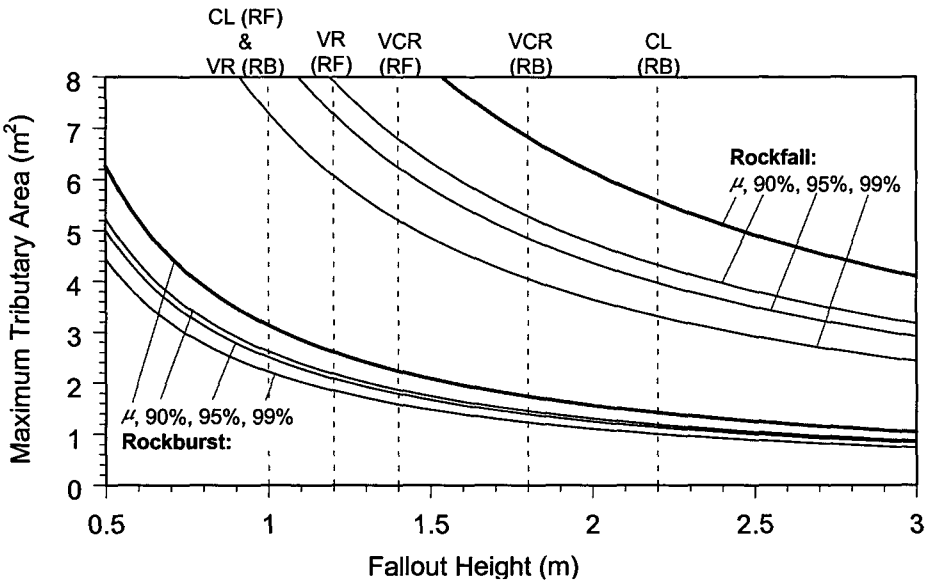

c): 1,6 m Ebenhaeser

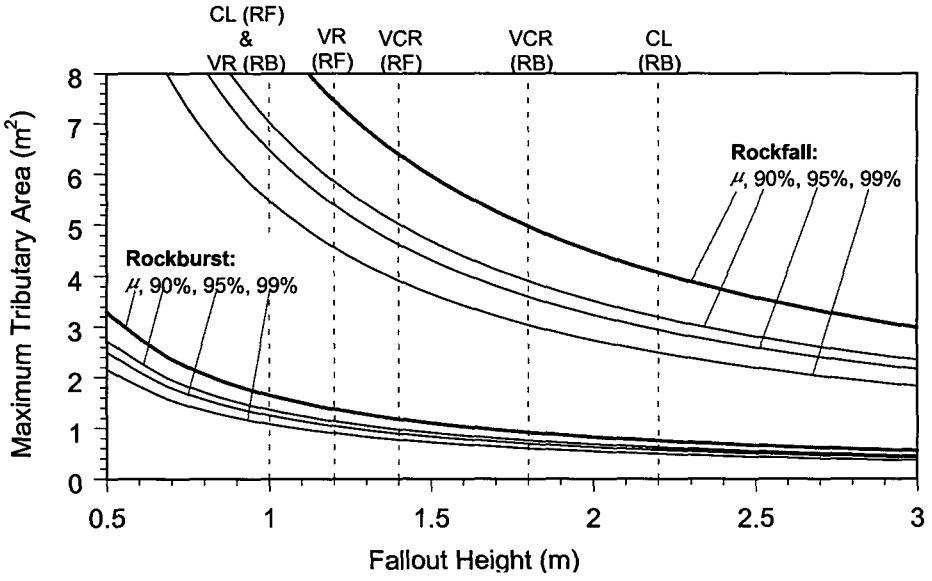

d): 1,6 m Cone Prop

Figures 8.2.16 Maximum tributary area for various elongate types in rockfall (RF) and rockburst (RB) conditions. Also shown are the fallout height criteria (Roberts, 1995) as determined from accident back analyses for the VCR, Vaal Reef (VR) and Carbon Leader Reef (CL).

From Figures 8.2.16 a) to 8.2.16 d) the influence of curve down-grading on support spacing can be estimated. For example, when designing for rockburst conditions on the Carbon Leader Reef using Rocprops, the tributary area is 2,05 m^2, 1,94 m^2, 1,88 m^2 and 1,82 m^2 when using the mean (μ), 90 per cent, 95 per cent and 99 per cent probability curves, respectively. In the case of the Loadmaster the tributary areas are 3,82 m^2, 2,96 m^2, 2,68 m^2 and 2,22 m^2, respectively. The tributary areas associated with the comparatively consistent Rocprop are reduced by 11 per cent when using the 99 per cent probability curve as opposed to the mean; similarly, in the case of the more variable Loadmaster, the tributary areas are reduced by 42 per cent. A

comparatively high level of adjustment does not necessarily imply poor support performance, as the resulting performance curve might be high enough to ensure the elongate meets the required support resistance or energy absorption criteria. Table 8.2.3 lists the percentage reductions in tributary area and support spacing of the four elongate types.

Table 8.2.3 Percentage reductions in tributary area and support spacing (in brackets) due to down-grading of performance curves from the mean value.

	90 %	95 %	99 %
1,2 m Rocprop			
Rockfall	10,4 % (5,3 %)	13,2 % (6,8 %)	18,8 % (9,9 %)
Rockburst	5,6 % (2,8 %)	8,3 % (4,3 %)	11,1 % (5,7 %)
1,6 m Loadmaster			
Rockfall	22,4 % (11,9 %)	28,6 % (15,5 %)	40,4 % (22,8 %)
Rockburst	22,4 % (11,9 %)	29,9 % (16,2 %)	41,8 % (23,7 %)
1,6 m Ebenhaeser			
Rockfall	22,6 % (12,0 %)	28,9 % (15,7 %)	40,7 % (23,0 %)
Rockburst	16,4 % (8,5 %)	20,0 % (10,6 %)	29,1 % (15,8 %)
1,6 m Cone Prop			
Rockfall	21,5 % (11,4 %)	27,7 % (15,0 %)	38,8 % (21,8 %)
Rockburst	17,2 % (9,0 %)	24,1 % (12,9 %)	34,5 % (19,1 %)

From the percentage reductions shown in Table 8.2.3, it can be shown that the average decrease in support spacing designed for rockfall conditions is 10,2 per cent, 13,3 per cent and 19,4 per cent for 90 per cent, 95 per cent and 99 per cent probability design curves, respectively. For rockburst support systems the average decrease in support spacing is 8,1 per cent, 11,0 per cent and 16,1 per cent for 90 per cent, 95 per cent and 99 per cent probability design curves, respectively. Thus, by applying the statistical data analysis and ensuring a comparatively high probability (90 per cent or 95 per cent) of exceeding the support performance curve, the support spacing needs to be modified within acceptable limits, i.e. no major changes in support spacing and associated costs are required.

Current gold and platinum mining support practice is to install a system of multiple elongates in the mining excavation. In most cases, however, falls of ground occur in a local area only, and individual support units are highly stressed and prone to failure. Thus, from a conservative design point of view, the statistical analysis should only consider the probability of failure of a single support unit, i.e. $n = 1$. This is particularly the case in intermediate- and deep-level mining operations, where the zone of support influence in a highly discontinuous rock mass has been shown to be confined to the immediate vicinity of the support unit, and comparatively little support interaction between adjacent support units take place (Daehnke and Roberts, 1998). In shallow mining operations the rock mass is less highly fractured, and, in many cases, multiple units support comparatively competent large blocks of rock. In this case the average support performance of multiple units is of relevance, and a value of $n > 1$ could be chosen.

Future support systems incorporating, for example, bar links between individual elongate units, will provide integrated areal coverage. This will reduce the dependence on individual units and the design specification will be calculated according to the average support capability of multiple units. This would result in a slightly less conservative performance curve, whilst maintaining a similar probability of exceeding the performance specification.

8.2.5 Conclusions and recommendations

The work presented here has demonstrated a statistical methodology to address the variability of elongate support performance. The analysis is based on a normal distribution, taking into account probabilities of exceeding statistically downgraded performance curves, as well as the influence of multiple support units on the average support load bearing capability. As an example of the applicability of the statistical methodology, the quasi-static and dynamic performance of various elongate types is investigated. By means of example evaluations based on the performance of actual elongates, it is shown that, in order to meet the 90 per cent or 95 per cent probability curve, the design curve is adjusted within reasonable limits. Based upon these findings, the following conclusions and recommendations are reached:

1. It is recommended to use support performance curves that ensure a high probability, i.e. 90 per cent (if n = 1: $x = \mu - 1{,}282\sigma$) or 95 per cent (if n = 1: $x = \mu - 1{,}645\sigma$), of exceeding the support capability. This specification aims towards high levels of safety, whilst rationalising the support costs and practical difficulties associated with installing high-density support systems.

2. The rock engineer needs to assess the degree of interaction between adjacent support units, and choose the appropriate sample size (n). In deep and intermediate mines n = 1 in most cases, whereas in shallow mines the sample size can typically range from n = 2 to n = 5. Until further expertise is developed in quantifying zones of support influence, it is not recommended to use n > 5.

3. It is recommended to use the appropriate performance curves when designing support systems for seismic and non-seismic applications. In some cases the support bearing capacity of elongates increases during dynamic loading, whilst in certain cases the loading capacity decreases. Thus a single correction factor for various elongate types loaded under quasi-static and dynamic loading conditions is not applicable, and separate performance curves, based on laboratory and in-situ tests, are required.

4. Additional safety factors should be incorporated when calculating the performance curves. These factors take into account underground considerations, such as poor support installation, slow convergence rates and high humidity/temperature, which have been shown to significantly influence support performance (Roberts *et al.*, 1987). Currently, underground field tests are conducted to establish appropriate correction factors, and these will be incorporated in the performance curve calculation as soon as sufficient underground data is available.

To advance support system design and continue mining at ever-increasing depths with reduced rock-related risk, design methodologies need to be based upon sound engineering principles. A probabilistic approach is particularly suited to quantitatively assess rock mass behaviour and support performance. Although many aspects of the interaction of support with the hanging and footwall rock mass are poorly defined and understood (e.g. the ubiquitous use of the 3 m/s hangingwall velocity parameter criterion across the various geotechnical areas), it is nevertheless necessary to quantify comparatively straightforward design parameters, such as the inherent variability of support systems.

8.3 Preliminary assessment of elongate pre-stressing devices

Elongates can be divided into two distinct types: those where the pre-stress mechanism is an integral part of the elongate, and those where the elongate is not sold with a pre-stress unit. Many of the latter units are installed on their own and others with separate pre-stress devices.

The pre-stress pots are used on products such as poles, pencil sticks, profile props, cone props, disc props, yield masters, high yield, shredder, timber splitter, etc. These systems would then be used in the same manner as other pre-stressed elongates (installed behind hydraulic props or directly on the face as the first line of support). The market for these units is considerable with monthly sales exceeding 100 000 units from at least seven manufacturers.

Since these devices can be purchased separately from elongates and can be mixed to the user's preference, the pre-stress units need to be evaluated individually. Tests conducted on various units indicate a wide range of performances, both in terms of creep and burst pressure. This is due to the various designs and construction techniques employed by the manufacturers. The thickness of steel plate of the various components can also significantly affect product performance. In order to prevent products from being marketed without adequately evaluating performance, a uniform testing procedure needs to be implemented so that the user is able to make informed decisions for support system design. Figure 8.3.1 gives typical seven day creep results for five different pre-stress devices with results summarised below.

Table 8.3.1 Creep characteristics of various pre-stressing devices.

Device	Initial Load (kN)	Final Load (kN)	% Creep
A	205	193	6
B	195	118	39
C*	200	78	61
D	219	180	18
E	230	208	10

*unit removed after 4 days

A significant proportion of this creep takes place in the first few hours. The table below indicates the load loss after only two hours following installation is at least 25 per cent of that obtained after seven days.

Table 8.3.2 Load shedding of various pre-stressing devices.

Device	Load Loss 7 days (kN)	Load Loss 2 hours (kN)	%
A	12	6	50
B	77	20	26
C	122	32	26
D	39	13	33
E	22	13	59

The implication of this load loss is significant for mining environments of low convergence rates. As elongates need to be evaluated for creep, so do the pre-stress devices that are used in conjunction with these units. It was initially thought that time dependent behaviour was governed solely by timber units, but the high pressures within the pre-stress devices (typically in

the order of 8 to 15 MPa) will also cause these units to creep, even at room temperature. As the units expand while pre-loading the elongates, the resulting shape of these units may not be stable at the required pressures and, therefore, continue to deform until an equilibrium between shape and pressure has been obtained.

Intermediate and deep-level stopes are subjected to convergence of at least a few millimetres per day and, as a result, the creep of the support unit (pre-stress device and elongate) should stabilise after the first day. However, the load loss could still be in the order of 10 to 15 per cent, which may only be recovered after several days (depending on the support system and stope conditions). This fact cannot be ignored in the design of support systems (and of course applies to all pre-stressed elongates).

Since many of the elongates used today consist of unturned timber and the fact that the pre-stress devices could be installed on a variety of elongates, the deformation that the devices would undergo could vary considerably. Since most timber poles need to be cut to size for installation, the pre-stress units must also be able to provide a certain degree of lift in order to facilitate installation. These variables would result in the pre-stressing devices taking a different shape following installation, and therefore making it susceptible to a varying degree of creep.

A suggested creep testing procedure for pre-stress units would be as follows:

1. *In a rigid frame, install the pre-stressing device on an insert of a diameter equal to the recommended diameter of elongate.*
2. *Inflate the device to fill a 5 mm gap and pressurise the device to obtain the required pre-load.*
3. *Repeat the above tests using an insert of a diameter 20 mm smaller than above.*
4. *Repeat the above two scenarios this time to fill a gap of the maximum lift recommended for that unit.*

Two tests for each of the four scenarios should be conducted for a period of seven days or until the load loss is less than one per cent (of the original load) over 24 hours, whichever is less. For most units, the required testing period would be four days.

Burst pressure tests also need to be conducted to ensure compatibility with the elongate. The elongate should be allowed to yield without fear of the sudden loss of support resistance, due to the bursting of the pre-stress device.

A suggested burst testing procedure for pre-stress units would be as follows:

1. *In a test frame, install the pre-stressing device on an insert of a diameter equal to the recommended diameter of elongate.*
2. *Inflate the device to the maximum recommended lift.*
3. *Pressurise the device to obtain the required pre-load.*
4. *Slowly compress the device (at 1 mm/sec) to failure or 700 kN, whichever is less.*
5. *A minimum of five units of the same type are to be tested.*

The performance information obtained from these units would have to be incorporated with that from the elongate used to determine the system performance.

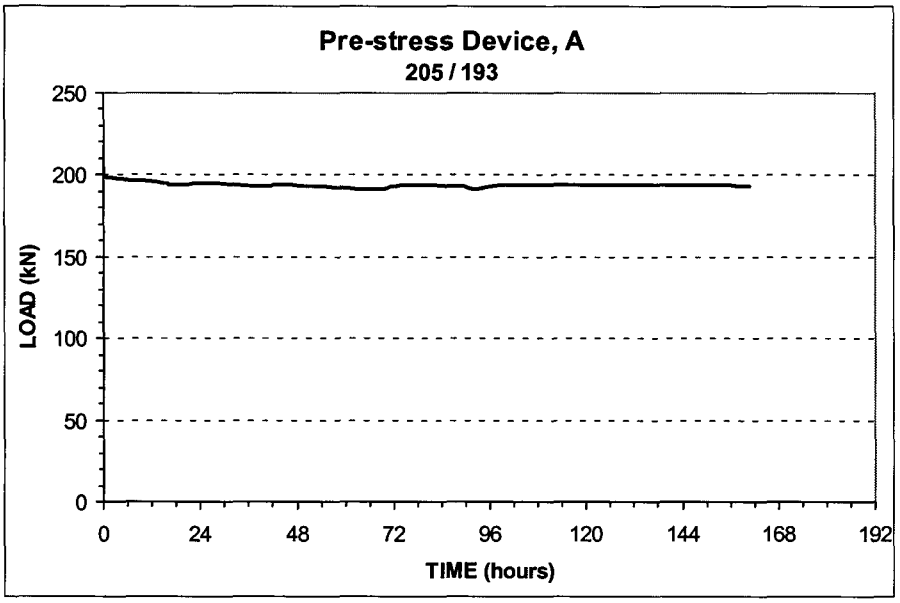
Pre-stress Device, A
205 / 193
LOAD (kN)
250
200
150
100
50
0
0
24
48
72
96
120
144
168
192
TIME (hours)

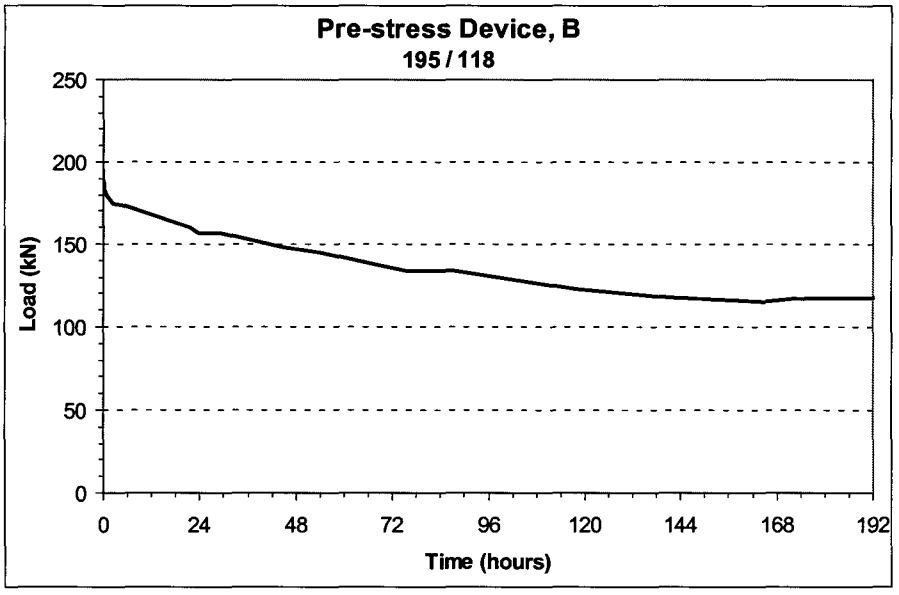
Pre-stress Device, B
195 / 118
Load (kN)
250
200
150
100
50
0
0
24
48
72
96
120
144
168
192
Time (hours)

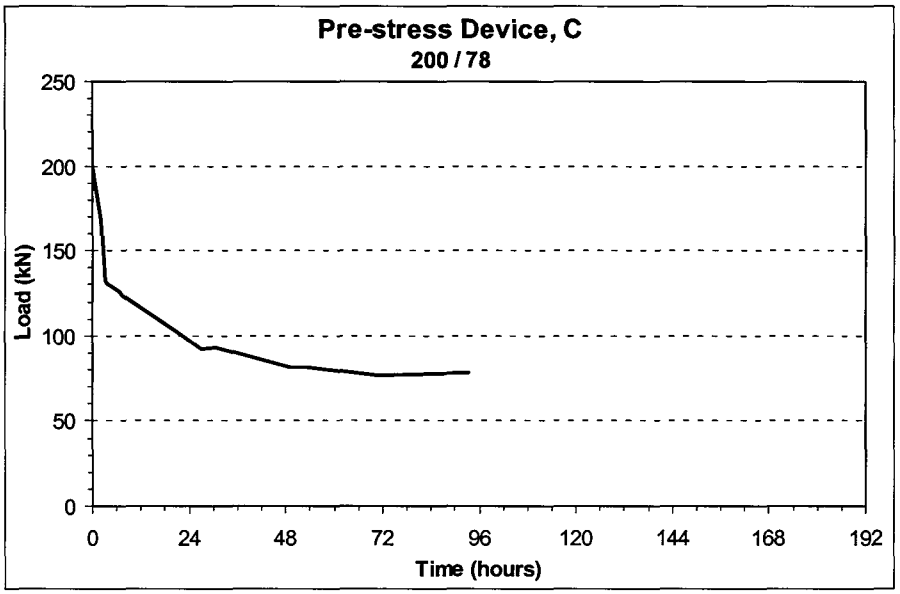
Pre-stress Device, C
200 / 78
Load (kN)
250
200
150
100
50
0
0
24
48
72
96
120
144
168
192
Time (hours)

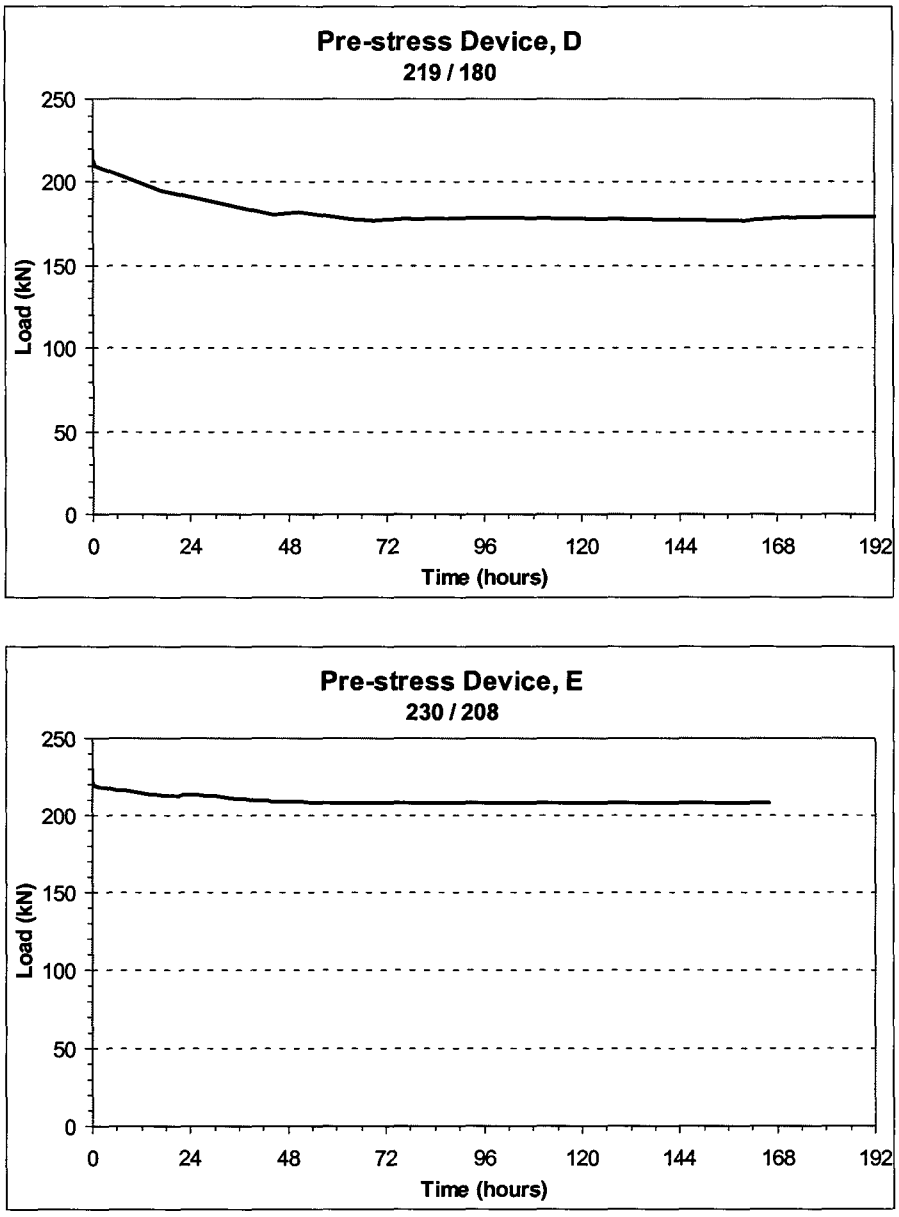

Figure 8.3.1 Load shedding characteristics of various pre-stressing devices.

8.4 References

Daehnke, A. & Roberts, M.K.C. 1998. Quantifying zones of support influence and stable hangingwall spans between support units. To be published: J. S. Afr. Inst. Min. Metall.

Handley, M.F. 1998. Personal communication, Regional Head of Rock Mechanics, Western Deep Levels.

Miller, I. & Freund, J.E. 1985. Probability and statistics for engineers. Third Edition, Prentice-Hall Int.

Roberts, M.K.C., Jager, A.J. & Riemann, K.P. 1987. The performance characteristics of timber props. COMRO Res. Report NO. 35/87.

Roberts, M.K.C. 1995. Stope and gully support. SIMRAC Project GAP 032, Final Project Report.

Wagner, H. 1982. Support requirements for rockburst conditions. Proc. of the 1st Int. Cong. on Rockbursts and Seismicity in Mines, SAIMM, eds. N.C. Gay and E.H. Wainwright, Johannesburg, pp. 209-218.

9 Improved support design through a keyblock approach

9.1 Introduction

9.1.1 Background

Stope support design for deep gold mines in the past was largely based on support resistance and energy absorption criteria. These methods do not take into consideration the fact that the hangingwall of a stope is often highly fractured and may contain geological planes of weakness (referred to as joints in the following sections of this report). The fractures and joints often combine to form blocks in the hangingwall that are free to fall into the workings. If these blocks are not supported, fall of ground accidents may result. The large number of fall of ground accidents, which occur in the face area of stopes and between support units, is evidence of the importance of these features in hangingwall stability. The importance of planes of weakness in support design was recognised in the guidelines for the preparation of codes of practice for the prevention of fall of ground accidents (Department of Mineral and Energy, 1996) where it was stated that "*The spacing of significant discontinuities must be considered in the design of support unit spacings*". This requirement implies that site specific support design should be carried out, taking into consideration the local geology and stress fracturing. Techniques, that are suitable for rock engineers to assess the effects of joints and stress fractures on the stability of excavations are, however, not readily available.

A methodology to allow the site specific evaluation of the effects of joints and stress fractures on stope stability was required. The keyblock method (Goodman & Shi, 1980) was seen as potentially suitable for assessing the effects of jointing and stress fractures on hangingwall stability. A commercially available program, JBlock© (Esterhuizen, 1996), that makes use of the keyblock method was seen as suitable for this type of analysis. The GAPREAG Committee requested that the research presented here be conducted to establish whether the keyblock approach in the JBlock program could result in improved site specific support design.

9.1.2 Statement of the problem

The root problem that led to this research is the large number of fall of ground accidents that take place in the face area and in between support units owing to the existence of stress fractures and joints in the hangingwall of gold mine stopes. The lack of suitable techniques for the site specific evaluation of the effect of joints and stress fractures on stope hangingwall stability resulted in this research being conducted.

9.1.3 Objectives

The overall objective of this research was to develop a methodology so that the keyblock method could be used to account for site specific joint and fracture data in support design. Since this type of analysis is novel to stope support design, an improved understanding of the interaction between stope support units and unstable blocks of rock in the hangingwall was expected. In meeting the overall objectives, the following secondary objectives were set:

- Quantify the stress fractures and joints in gold mine stopes.
- Determine the relationships between support units and falls of ground in actual stopes.
- Determine whether the keyblock software is able to simulate realistic block size distributions.
- Determine how different support layouts and geotechnical parameters affect the stability of keyblocks in the hangingwall of stopes.
- Develop a methodology that will allow the keyblock method to be used in support design.

9.1.4 Overall methodology

The research was carried out by largely relying on previous research outputs and accident statistics to provide field data for the analyses. Large numbers of keyblock simulations were carried out to understand the interaction of support and geotechnical parameters on instability in the hangingwall of stopes. The results were used to propose a methodology for support design. Details of the methodology are presented in Section 9.3.

9.1.5 Scope of research

The research entailed the following activities:

- A literature survey of all relevant previous research, presented in Section 9.2 of this report.
- An analysis of fall of ground accidents in stopes using the CSIR Miningtek accident database, as well as a detailed evaluation of 189 fall of ground accident reports. These results are presented in Section 9.4.1
- Collation of joint data from previous research so that statistics on typical jointing and stress fracture distributions could be obtained as input to the keyblock software.
- Evaluation of the keyblock software against the accident data to verify block size distributions. The results are presented in Section 9.4.3.
- Application of the keyblock software to analyse numerous combinations of geotechnical parameters and stope support layout so that relationships and trends may be identified. In terms of support parameters aspects such as support spacing, type and pattern were evaluated. Geotechnical parameters such as joint dip, spacing and orientation, as well as dynamic loading and clamping stresses, were evaluated. The results of these analyses are presented in Sections 9.4.4 and 9.4.5.
- A methodology, which may be followed in evaluating site specific geotechnical parameters, is proposed. This methodology is demonstrated in a case study, as presented in Section 9.4.

The conclusions of the research are presented in Section 9.5, together with recommendations for further work.

9.2 Literature survey

A study of the literature regarding stress fractures and geological discontinuities in deep gold mine stopes was carried out. The study focused mainly on publications by the Chamber of Mines Research Organisation (COMRO) and CSIR Mining Technology. Literature on the keyblock method was studied only briefly to explain the analysis techniques used in the JBlock software. The findings of the survey are summarised in this section.

9.2.1 Discontinuity types

Discontinuities in stope hangingwalls at depth may be described as stress fractures and geological discontinuities. The stress fractures are dominant in terms of frequency and length and typically strike parallel to the stope face. Geological discontinuities may be joints, minor faults, and dykes or bedding related features. The geological discontinuities may strike at any orientation relative to the mining direction.

9.2.2 Types of stress fractures

Investigations into stress fractures in deep gold mine stopes have revealed that two main types of fractures are present in the hangingwall (Adams, Jager & Roering, 1981).

- Class 1: Fractures that exhibit no relative movement parallel to the fracture surface; they are typically parallel to the stope face and are described as extension fractures.
- Class 2: Fractures that reveal distinct signs of movement and may be described as shear fractures.

The description of the actual fracture sets in the hangingwall as identified by Gay and Jager (1986) was used in further analysis. Five distinct sets of fractures were identified as follows:

- Type 1: Extension fractures formed ahead of the face that occur in zones of about 1,5 m in width and are parallel to the face, spaced about 60 mm apart. The fractured zones are about 1,1 m apart. Fracturing may extend up to 40 m into the hangingwall and footwall.
- Type 2: Extension fractures formed in the blocks of unfractured rock between zones of type 1 fractures. They may curve around the stope face to dip at 45° in the hangingwall and footwall.
- Type 3: Sporadic shallow dipping fractures bounded by fractures of types 1 and 2. These fractures occur in the solid blocks found between fractures of type 1 and 2. They dip between 20° and 40° and occur sporadically in areas of a few to tens of square metres. Where they occur, they greatly reduce the stability of the hangingwall.
- Type 4: Irregular fractures that develop in the plane of the bedding. Their length seldom exceeds 2 m. They are usually found in highly stressed ground which is rockburst prone.
- Type 5: Shear fractures which occur at 1 m to 3 m spacing, that may be described as mining induced normal faults with movement of up to 200 mm. Their dip in the hangingwall is predominantly towards the mined out area at angles of 60° to 70°.

Fracturing of the rock is a highly complex process and all the fracture types may not develop in a stope. During a large seismic event, additional fractures may form (Joughin & Jager, 1983). Geological discontinuities have a significant effect on the formation of stress fractures (Adams, 1995). They form potential initiation points for stress fractures and affect the orientation of stress fractures.

9.2.3 Geological discontinuities

The literature reviewed did not find detailed descriptions of the geotechnical properties of the natural discontinuities. It was noted that discontinuities have an effect on fracture formation and hangingwall stability, but no description of the properties of the discontinuities could be found. The following paragraphs summarise the available information.

Most gold reef extraction takes place under bedded quartzites. The bedding of the quartzite has a major influence on the stability of the hangingwall, when combined with stress fractures (Eve, Mitchell & Sellers 1992;Jager & Turner, 1986; Adams ,1995).

Van der Heever (1982) describes three sets of discontinuities in the Klerksdorp area. Two are steeply dipping and the third is bedding jointing. The strike of the steep sets are approximately along the strike and the dip of the reef. Frequency of joints was noted to be between 15/100 m in hard brittle quartzites and 10/100 m in argillaceous quartzites.

In the Carbon Leader Reef in the Carletonville area, it is reported that quartz filled extension gashes exist that strike approximately north-south in the hangingwall, with secondary jointing crossing these (Hagan, 1996).

At an experimental site in the Carbon Leader Reef at Western Deep Levels it was found that quartz veins existed that strike NNE, with minor faults striking at ENE (Hagan,1996). The quartz veins are welded and do not generally affect the hangingwall stability. The faults are planes of weakness and the hangingwall may fallout at their localities.

9.2.4 The keyblock method

A keyblock is defined as a block that can be removed or fall from a rock face without breaking intact rock. The keyblock method (Goodman and Shi, 1981) identifies potential keyblocks in exposed rock faces. The principle is that non-keyblocks are locked in place until the keyblocks are removed. In principle, support effectiveness is determined by the number of keyblocks that

are held in place by the support. In theory it is only necessary to support the keyblocks, then the remainder of the rock mass will be unable to fail.

The keyblock method, proposed by Goodman and Shi, makes use of analytical geometry to identify keyblocks from jointing and excavation data. The method automatically identifies removable blocks formed, when an excavation surface cuts through a rock mass. The weight, sliding direction, and required support force to stabilise keyblocks may be calculated. The method assumes that the blocks are rigid and joints are continuous. Failure is possible by sliding or block release (drop out) only. Block rotation is not considered. External stresses are not considered.

9.2.5 Keyblock approach used in JBlock©

In deep gold mines, large excavation surfaces are created daily, and it is neither practical nor economical to map each exposed discontinuity and conduct an analysis of potential keyblocks. Instead, support systems are developed to reduce the probability of rockfalls occurring to acceptable levels. It was recognised that rock engineers require a tool to allow them to evaluate the type and frequency of keyblocks that may form and the effect of support systems on the probability of failure of the keyblocks (Esterhuizen and Akermann, 1998).

The JBlock software (Esterhuizen, 1996) was developed to generate three-dimensional rock blocks at an excavation surface from discontinuity statistics. Each generated block is tested to establish whether it is a keyblock. Each keyblock is tested whether it is able to fail by considering external loading and sliding friction. Finally the potential interaction of the keyblock with installed support is tested. The program allows many thousands of blocks to be generated and tested against different support patterns and excavation orientations. The probability of the failure of keyblocks of different sizes is determined, and the spatial distribution of potential failures is shown, allowing the rock engineer to optimise support and excavation layouts.

9.2.6 Discussion

The results of the literature survey were used to develop models of typical jointing and stress fractures in gold mine stopes. These models were analysed for various combinations of geotechnical parameters and support layouts. The literature survey showed that although many fractures have been mapped in gold mine stopes in the past, the mapping has seldom been carried out following standard scan line mapping techniques. The geotechnical parameters such as roughness, continuity and infilling was absent from most of the data.

9.3 Methodology

9.3.1 Data from previous research

In the project proposal it was recognised that vast amounts of research had been done in the past regarding stress fractures in gold mines and that this source of data would provide the input for the keyblock studies. It was also recognised that the SAMRASS accident database and the CSIR Mining Technology database on fall of ground accidents was available to provide information on dimensions of falls of ground and support data. The intention was therefore not to conduct any further field work, but to rely on the existing data. A literature survey was carried out and, as explained in Section 9.2.6, although large volumes of data existed, the geotechnical content was limited. It was necessary to resort to other methods, using the existing information, to obtain the required inputs.

9.3.2 Data for keyblock analysis and calibration

The first part of the project was aimed at obtaining distributions of jointing and stress fracture properties for input into the JBlock program. This was achieved by collating results of previous studies, interviewing researchers and obtaining additional data from current research. As a result a set of typical data were compiled to use in the further analyses.

It was recognised that the JBlock software would have to be calibrated against actual keyblock sizes, to see if it generates realistic block dimensions. The approach followed here was that large amounts of data on rockfall dimensions existed in the accident files of the Department of Minerals and Energy. In addition, these data had been compiled in the accident database of CSIR Mining Technology. Since more information was required than taken up in the database, a further study of 189 accident reports was carried out. The main purpose of the additional study was to determine how rockfalls are related to the support units and what hazards are related to falls of ground, in terms of injuries and fatal accidents. The database provided good information on block dimensions, and this was used as a basis for comparing the keyblock software results. In these comparisons, a number of "typical" geotechnical data sets were evaluated using the JBlock software and the generated block sizes were compared to the block sizes reported in the accident reports.

9.3.3 Evaluation of support and geotechnical parameters

The main part of the research entailed analyses of different combinations of support and geotechnical parameters. The objective was to establish which parameters had an overriding influence on keyblock instability. Since this type of analysis had not been done before, it was also intended to provide new insights into the interaction between keyblocks and support systems.

Relationships between the geotechnical parameters such as joint frequency, joint dip, joint strike, number of joint sets and keyblock stability were evaluated. The analyses were repeated to establish the effect of external influences, such as clamping stresses and dynamic loading. The results were expressed either as failure probabilities or hazard. The hazard was defined as the number of persons who could be involved (injured or killed) should the keyblocks fail. The relationship between keyblock size and hazard was obtained from the accident data. This provided output that was directly related to safety in the workplace.

Methods were developed in which the JBlock software could be used to evaluate different support cycles, support patterns and support types, so that the results of different runs could be compared. Analyses were carried out to evaluate aspects such as support density, area of influence of support and support cycles. It was considered important that the rock engineers would be able to evaluate keyblock stability on a comparative basis for different support or geotechnical scenarios.

9.3.4 Development of a design methodology to account for keyblock failure

Initially it was proposed that the results of the keyblock analyses should be incorporated into the updated SDA software. The large number of variables, however, made it difficult to provide a set of rules that would be applicable in all conditions. It was also found that in most cases, where the discontinuities in the hangingwall of the stopes are steeply dipping and clamping stresses exist, keyblock failure does not represent a hazard. It is only when shallow dipping discontinuities exist or clamping stresses are absent that keyblock failure becomes a problem. It was therefore decided that the SDA should warn users of potential keyblock instability, if appropriate. A methodology of conducting a keyblock analysis was prepared, to allow rock engineers to carry out such an analysis if required.

9.4 Results

9.4.1 Analysis of fall of ground accidents

A total of 186 fall of ground accidents in stopes in the Carletonville district were evaluated to determine the mode of failure of supports, the location of falls relative to the support units, and the risk associated with falls of different sizes. Accident reports were collected from the Department of Minerals and Energy (DME). The data were evaluated and the results used as a guide to calibrate the keyblock analysis results and to determine the risk associated with falls of different sizes.

9.4.1.1 Mode of failure of supports

A study of the mode of failure of the supports showed that the 59 per cent of falls of ground were associated with temporary supports that were dislodged. A further 17 per cent were attributed to permanent supports that had dislodged, shown in Figure 9.4.1.1-1. A further interesting result is that failure of the temporary and tendon support units only accounted for 24 per cent of the accidents. No failure of permanent supports was reported. This result clearly shows that support units require some form of lateral constraint to prevent them being toppled over.

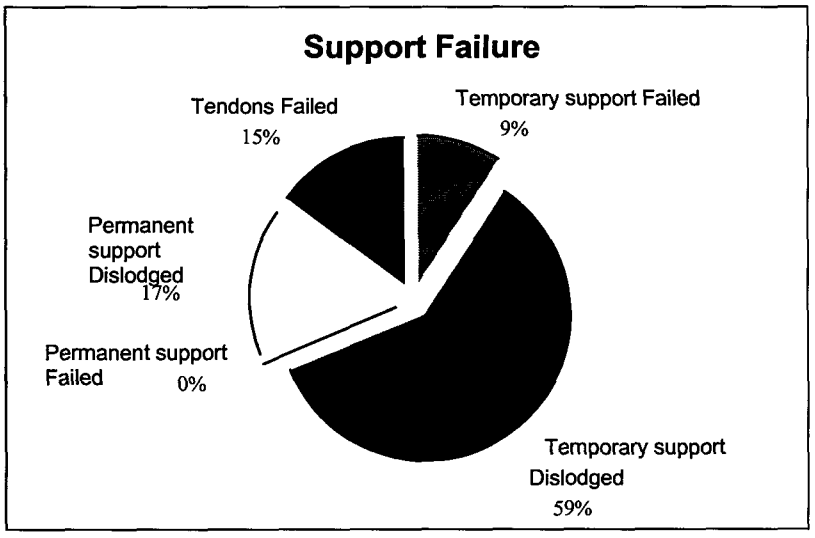

Figure 9.4.1.1-1 Modes of support failure.

9.4.1.2 Location of falls relative to support units

Of particular interest was the location of falls of ground relative to the support units. The results are shown in Figure 9.4.1.2-1, where it can be seen that the largest proportion (44 per cent) of falls of ground occur in the face area. These falls occurred in the absence of any support. Falls in the face area represent a high risk, as most mining activities occur at the face. Falls between permanent and temporary supports account for 13 per cent of all falls, while falls involving the failure or dislodgement of support units represent the remaining 43 per cent.

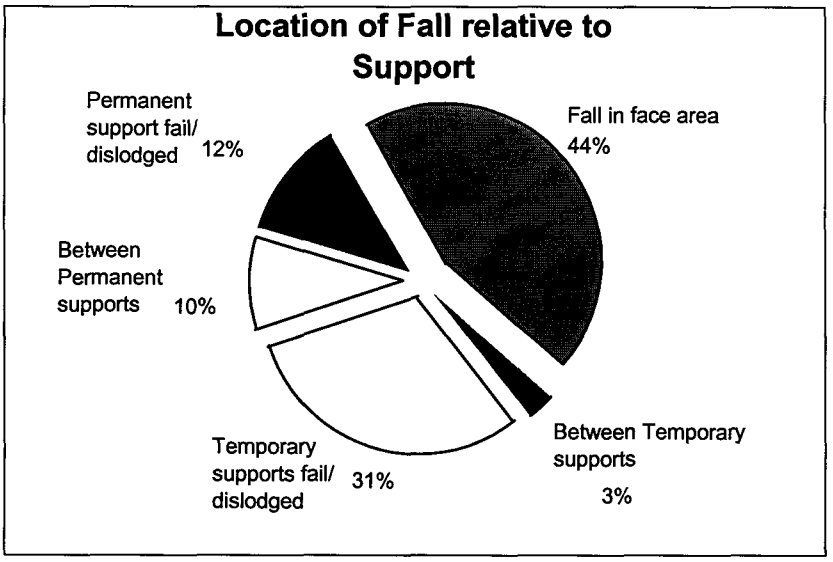

Figure 9.4.1.2-1 Location of falls relative to supports.

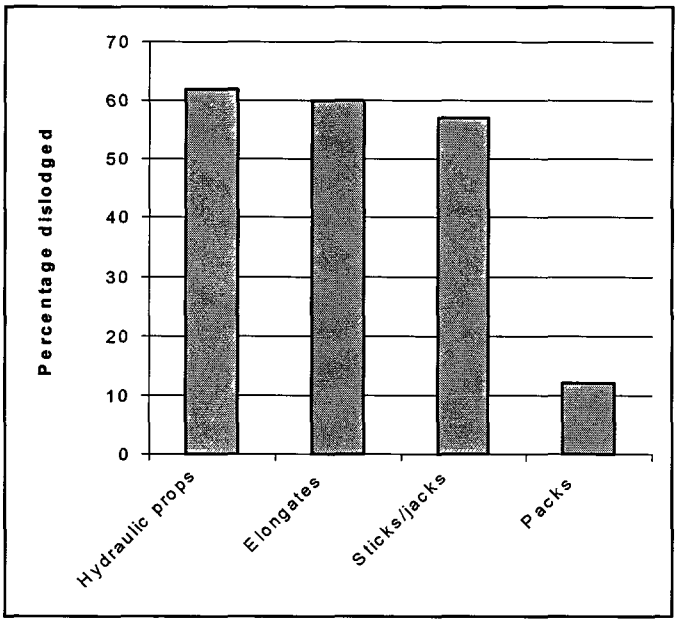

Figure 9.4.1.2-2 Percentage of supports of each type that failed by being dislodged as a percentage of all supports of that type involved in fall of ground accidents.

Further evaluation of the dislodgement of supports showed that elongate type supports were the most likely to dislodge. The results showed that if hydraulic props, stick, jacks and elongate supports are involved in a fall of ground accident, the likelihood that they will be dislodged is approximately 60 per cent, as shown in Figure 9.4.1.2-2. The traditional pack type support is clearly not susceptible to this type of failure.

9.4.1.3 Shape of falls of ground

Support is installed in rows that are parallel to the face. In addition, the majority of stress fractures are also parallel to the stope face. The expectation is that the falls of ground would be longer in the direction parallel to the face than perpendicular to the face. The dimensions of the falls in the direction parallel to the face was taken as the "length" of the fall, while the dimension perpendicular to the face was taken as the "width" of the fall. The ratio of length to width of the

falls is shown in Figure 9.4.1.5-1, where it can be seen that most of the falls had ratios in excess of unity, and the trend increases as the fall size increases. This implies that larger falls are "longer" than smaller falls. The dominant role of face parallel fractures on falls of ground is confirmed by this result.

9.4.1.4 Hazard associated with fall size

The keyblock analysis method produces potentially unstable blocks of different dimensions. If these blocks are shown to be unstable, the hazard associated with each block is required to add meaning to the results. It was, therefore, necessary to establish the number of persons affected by each fall of ground to obtain a relationship between the fall size and the hazard (expressed as persons affected per fall). The results are shown in Figure 9.4.1.5-2. Note that the horizontal axis is logarithmic. The relationship between the fall size and the hazard was used to calculate the hazard in the keyblock analysis program.

9.4.1.5 Conclusions of fall of ground study

The study showed that failure of supports, either through being dislodged or mechanical failure, was associated with 43 per cent of all fall of ground accidents studied. The remaining 57 per cent of the failures did not involve support units, and were either in the face area, or failed between supports. The dislodgement of support units was the main cause of supports not fulfilling their function. Elongate support types were the most susceptible to failing by dislodgement. The well known fact that a large number of accidents occur in the face area, in the absence of support, is confirmed by this study. It is not clear, however, what proportion of the 43 per cent dislodged or failed supports were the cause of the fall of ground or merely a consequence of the instability induced by the fallout between support units.

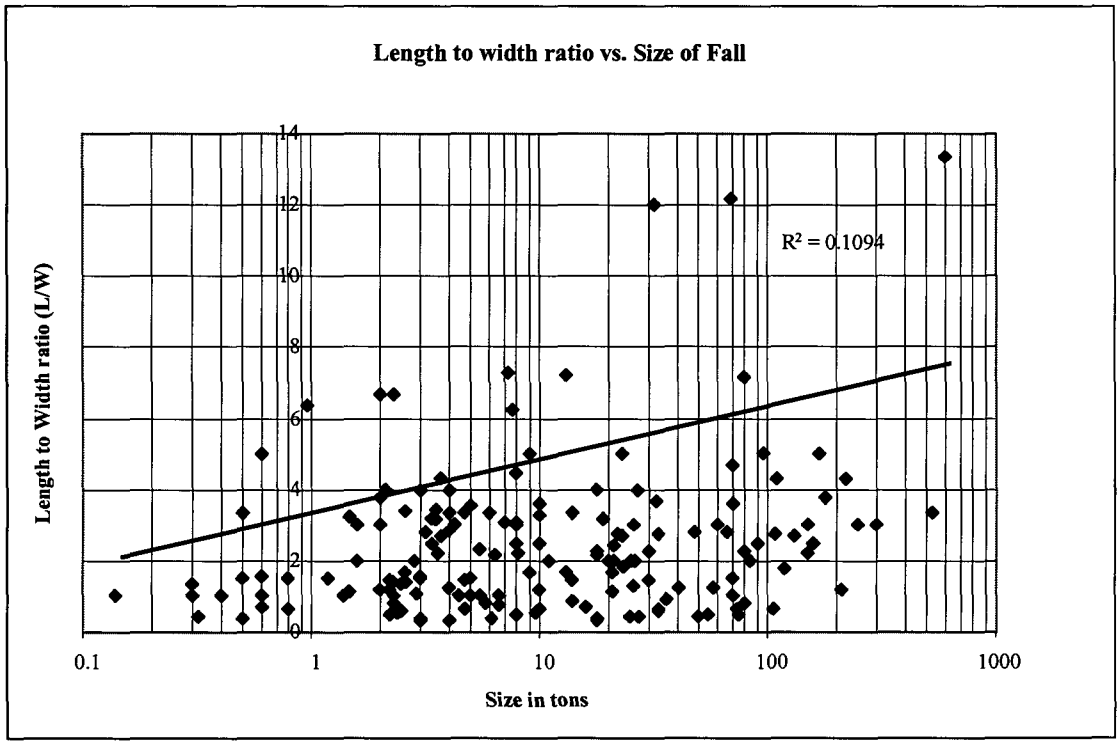

Figure 9.4.1.5-1 Aspect ratio of falls of ground from accident statistics.

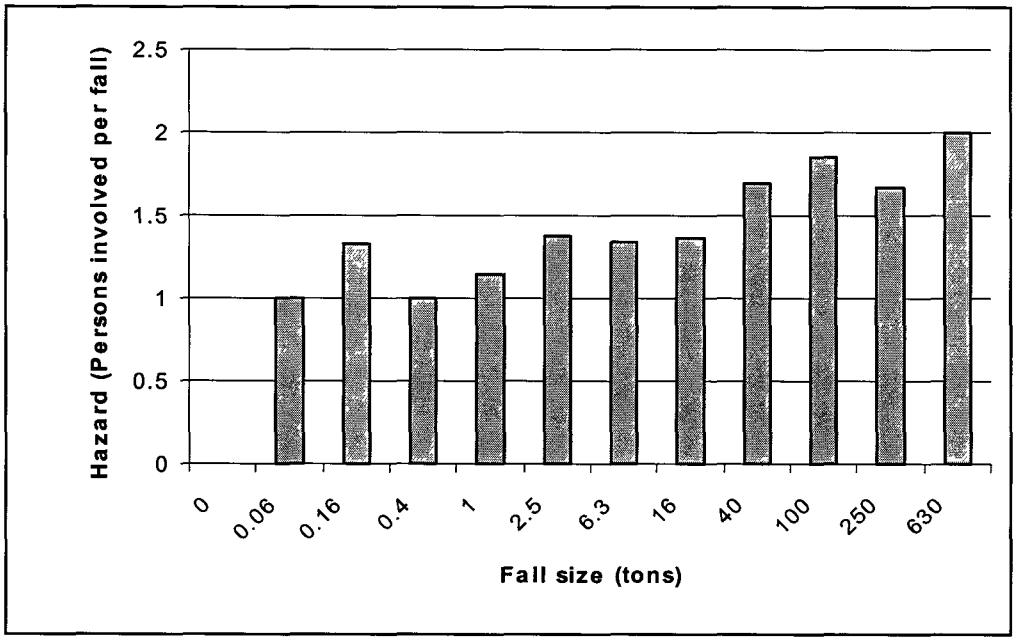

Figure 9.4.1.5-2 Hazard associated with falls of ground of different dimension.

The hazard associated with the falls of different sizes showed that the hazard (expressed as persons affected per fall) did not increase rapidly with fall size. The hazard doubles for approximately an increase of three orders of magnitude in size.

9.4.2 Keyblock data from accident statistics

The results of keyblock analyses need to be verified against actual keyblock failures in underground workings. The only source of data, that is readily available, in which rockfall sizes are presented, are the accident reports of the Department of Minerals and Energy. Data from the accident reports have been collated into an accident database at CSIR Mining Technology. A further source of information is the actual accident reports.

9.4.2.1 Evaluation of accident database

Data on falls of ground, that resulted in fatal accidents, were compiled to obtain the dimensions of each fall of ground. The objective was to provide information for calibration of keyblock analysis results and to determine whether there were differences between the different reefs being mined.

9.4.2.2 Fall dimensions

From the analysis it was found that there is little difference between the rockfall dimensions in the different reefs, in spite of the different depths, hangingwall composition and support types. The average dimensions of falls in the different reefs are as follows.

Table 9.4.2.2-1 Average dimension of rockfalls.

Reef	Average height	Average Length	Average Width
Basal Reef	0,81	4,05	3,03
Carbon Leader Reef	0,89	8,87	4,62
Vaal Reef	0,74	4,08	2,64
VCR	0,84	5,86	3,32

A simulated result of the volume of falls was derived from the product of the length, width and height of falls. Note that the volume exaggerates the importance of larger falls. These results are summarised in Table 9.4.2.2-2, which show that the Carbon Leader Reef and the VCR have resulted in the largest fall volumes. These reefs are mined at greater depths than the Vaal Reef and the Basal Reef, which may explain the difference.

Table 9.4.2.2-2 Calculated average volume of rockfalls in different reefs.

Reef	Calculated average volume of fall (m^3)
Basal Reef	16,65
Carbon Leader Reef	68,07
Vaal Reef	17,51
VCR	25,38

The distribution of calculated fall volumes is shown in Figure 9.4.2.2-1, where it can be seen that the average rockfall volume can be misleading. The graph shows a modal value at approximately 1 m^3. A few very large falls tend to distort the average value.

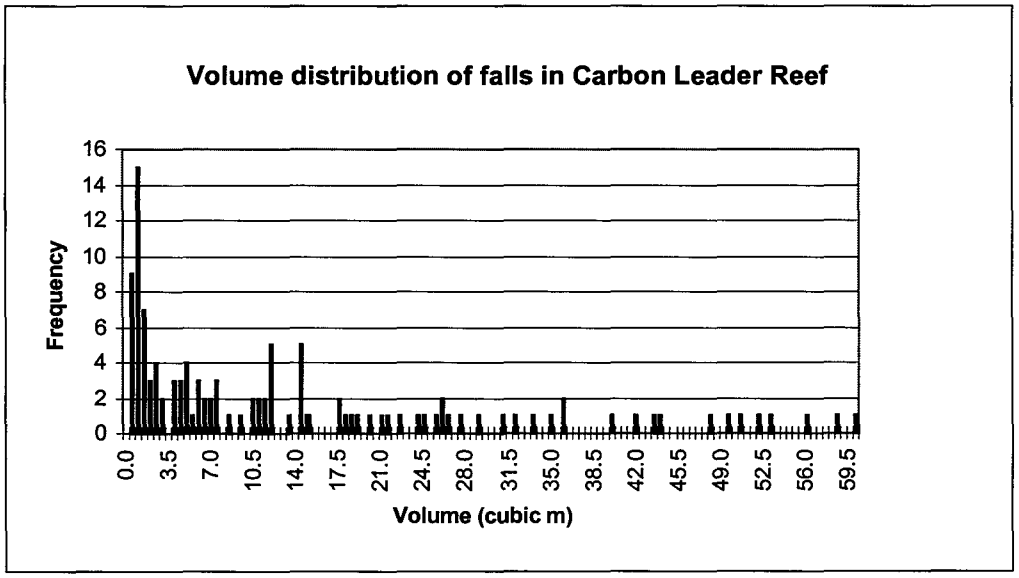

Figure 9.4.2.2-1 Distribution of rock fall volumes in the Carbon Leader Reef calculated from fall dimensions, (graph truncated at 60m^3).

9.4.2.3 Effect of rockbursts on rockfall dimensions

If rockfalls resulting from seismicity are compared to gravity driven rockfalls, it is clear that falls during seismic events are much larger than falls that are only gravity driven. This is likely to be the result of rockbursts dislodging rock blocks that would otherwise have been stable.

9.4.3 Collation of jointing and fracture data for analysis

9.4.3.1 Approach followed

Keyblock analysis requires that the spacing, orientation and trace length data of all discontinuities as well as the distribution of these parameters to be known. Since the literature did not provide sufficient data, it was necessary to obtain as much data as possible from previous studies of fracturing in gold mine stopes. The following sources of information were used:

- Discussions were held with researchers who have been closely involved with studying fractures in gold mines stopes, with the aim to obtaining best estimates of the required properties,
- Data were extracted from maps of fractures in the hangingwall,
- Mapping of discontinuities carried out as part of project GAP330 were used, and
- Records of discontinuities in preconditioning stopes were evaluated.

Based on these data and the information obtained from the literature study, descriptions of jointing and fractures in gold mine stopes were made.

9.4.3.2 Discussions with researchers

Keyblock analysis requires that the spacing, orientation and trace length data of all discontinuities, as well as the distribution of these parameters, to be known. Since the literature did not provide sufficient data, discussions were held with Mr AJ Jager and Mr N Reddy at CSIR Mining Technology, who have been closely involved in fracture mapping in gold mine stopes. The objective was to obtain best estimates of the required parameters. The results are summarised in Table 9.4.3.2-1. The Western Deep Levels site described by Reddy is in the Carbon Leader Reef and the reef is overlain by the Green Bar which is approximately 1,5 m above the reef. The immediate hangingwall is a fairly massive quartzite with poorly developed bedding planes. Natural quartz veins exist that strike NNE and minor faults striking at ENE. Falls of ground occur along the faults. The faults also locally affect the orientation of the stress fractures, which tend to swing parallel to the fault.

Table 9.4.3.2-1 Description of discontinuities at Western Deep Levels site after N Reddy (1998).

	Spacing (m)			**Strike Length (m)**			
Type*	Typical	Lower Limit	Upper Limit	Typical	Lower Limit	Upper Limit	Dip
1&2	0,1	0,05	0,5	3	0,4	6,0	75-90°
3	0,25	0,15	0,35	0,5	0,4	1,0	40-65°
5	1	0,8	2	12	10	30	80-90°
Bedding	1	0,8	2	4	2	6	20°

*Refer to Section 9.2.2

Discussions with Jager were based on general impressions of stress fractures in deep level stopes, and were not related to a specific site. The results are summarised in Table 9.4.3.2-2.

Table 9.4.3.2-2 Description of discontinuities in deep gold mine stope hangingwalls after AJ Jager (1998).

	Spacing			Length			
Type	Typical	Lower Limit	Upper Limit	Typical	Lower Limit	Upper Limit	**Dip**
1&2	0,07	0,05	0,5	1,5	0,8	4	60-80°
3	0,03	0,01	1	1,5	0,8	4	20-40°
4	0,3	0,1	0,5	0,3	0,1	0,5	0-20°
5	3	1	6	8	5	30	60-80°

With regard to bedding characteristics, Jager presented unpublished data on bedding in gold mines. Limited data on the length of bedding joints were recorded in the Basal Reef. The results showed that typically 50 per cent of the bedding joints in the hangingwall had lengths greater than 10,5 m and in one case 50 per cent of the bedding joints were longer than 23 m. With regard to the frequency of bedding joints, data was available as shown in Table 9.4.3.3-1. The data also showed that only in about 6 per cent of the observations were bedding joints absent in the immediate hangingwall and footwall.

9.4.3.3 Collation of previously mapped fracture data

The data described in the preceding sections provide insight into the general characteristics of stress fractures in deep mines. For the purpose of analysis it is, however, necessary to determine the spacing and length distributions. In the literature it is often found that joint spacing and trace lengths are described by negative exponential distributions. Sometimes a log-normal distribution is used. The objective of this study was to establish which distribution type to use. The work therefore focused on the length and spacing distributions. Sources of data were trace maps of discontinuities in Brummer & Rorke, (1984), and mapping of fractures by Reddy (1998) and Grodner (1997).

Table 9.4.3.3-1 Percentage of cases in which partings exist in hangingwall vs distance into hangingwall.

	Distance into hangingwall (m)				
Reef	0,2	0,4	0,6	0,8	1,0
Kimberley	30%	50%	66%	-	-
VCR	15%	20%	24%	26%	30%
Vaal Reef	32%	51%	55%	-	-
Carbon Leader	24%	30%	37%		

9.4.3.4 Discontinuity data from Brummer and Rorke (1984)

Brummer and Rorke used photographic techniques to map the hangingwall in the Carbon Leader Reef at Doornfontein gold mine and produced maps of all observed fractures. The maps were enlarged so that direct measurements of discontinuity spacings and trace lengths could be made. Scan lines were drawn onto the maps, spaced approximately 1 m apart (according to scale) to determine the fracture spacings. Eighteen scan lines were made resulting in 751 spacing measurements. Trace lengths were determined by measuring the length of each fracture on the map. A total of 1422 trace lengths were measured.

The results of the trace length data are summarised in Figure 9.4.3.4-1, which clearly shows that the trace lengths follow a negative exponential distribution. The average trace length was 0,62 m with a maximum of 12,3 m. Note that it was not possible to differentiate between the

different types of fractures on the maps. These values are the averages for all fractures observed.

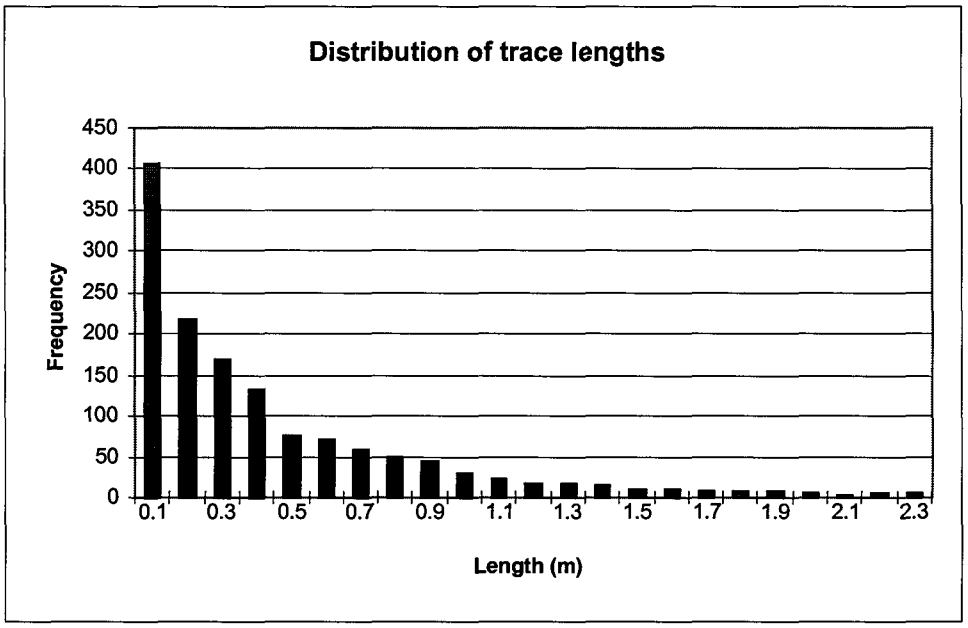

Figure 9.4.3.4-1 Distribution of trace lengths measured from maps of fractures in a Carbon Leader Reef stope.

The fracture spacing data is summarised in Figure 9.4.3.4-2 where the negative exponential form of the distribution is clearly seen. The average spacing was 0,17 m and the maximum spacing was 1,5 m.

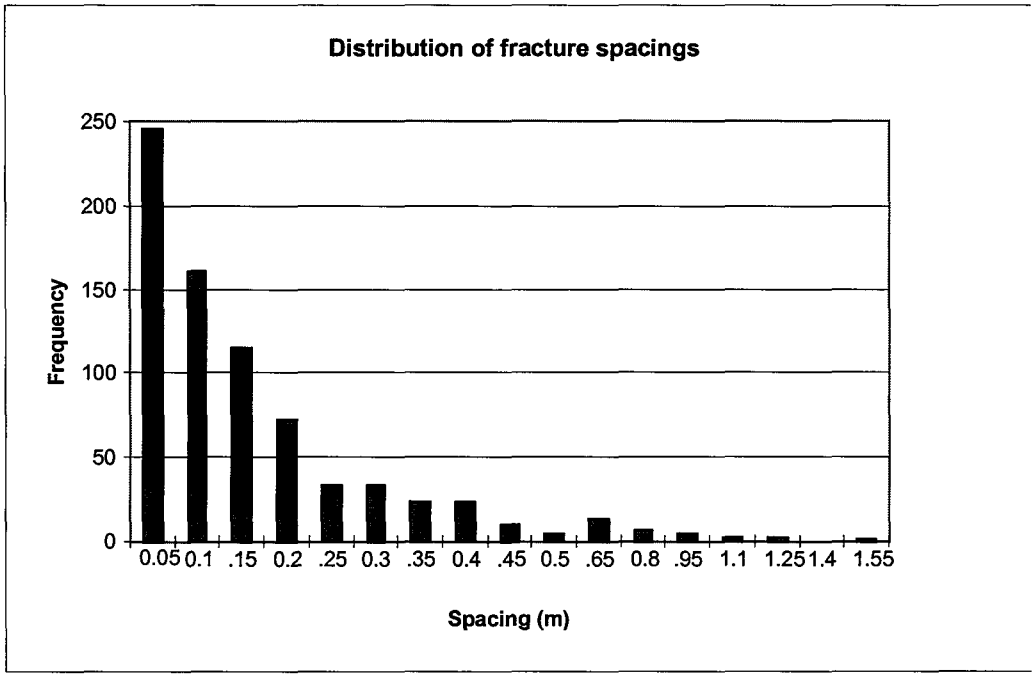

Figure 9.4.3.4-2 Distribution of spacings between fractures measured from maps of fractures in a Carbon Leader Reef stope.

9.4.3.5 Trace lengths from discontinuity data of Reddy (1998)

As part of the project GAP 300, Reddy (1998) mapped discontinuities along a gully in the 93 E4 bottom gully at Western Deep Levels mine. The site is also an experimental site where CSIR Mining Technology is carrying out detailed monitoring of the rock behaviour. Since mapping in a gully essentially truncates the data to the width of the gully, it was necessary to apply different mathematical techniques in an attempt to obtain the true trace length distribution. Two approaches were used, in the first the trace length data was assumed to follow a negative exponential distribution. Two methods by Priest (1993) were used, in which the truncated trace length data were used to estimate the true mean spacing. The results indicated mean trace lengths of 1,4 m and 1,7 m using the two methods. An alternative method of Pahl (1991) was also used and is distribution independent. This method provided a true mean trace length of 0,64 m. The latter result is similar to the mean spacing obtained from Brummers work, see Section 9.4.3.4. Reddy's data did not contain any trace lengths less than 0,75 m, which seems to indicate that the distribution independent method provided an incorrect estimate of the true mean trace length. The negative exponential distribution seems to provide a better estimate.

9.4.3.6 Joint spacings from discontinuity data of Grodner (1997)

Grodner (1997) logged discontinuities at an experimental pre-conditioning site at Blyvooruitzicht gold mine. The data were collected in such a manner that only the fracture frequency could be used for the purposes of this report . A total of 170 joints were used in the analysis. The joints were divided into four classes. The first three classes were for joints dipping towards the face and they were divided into shallow, intermediate and steeply dipping. A fourth class was identified, being the joints that dip away from the face. The average spacings of the four joint types were as follows.

Table 9.4.3.6-1 Average spacings of fractures at Blyvooruitzicht mine - from Grodner (1997).

Dip range	Shallow $0\text{-}30^0$	Intermediate $30\text{-}60^\circ$	Steep $60\text{-}90^0$	Other $90\text{-}180^0$
Average spacing (m)	0,32	0,49	0,44	0,43

The average spacings are larger than obtained from the results of Brummer and Rorke in Section 9.4.3.4. However, since Brummer and Rorke's results did not discern between the fracture types, one would expect a higher frequency of the combined fractures.

9.4.3.7 Discontinuities in lava

The results of mapping of discontinuities at a preconditioning site at Western Deep Levels South, where the hangingwall was lava, were presented in the GAP030 (1995) final project report. It was observed that the discontinuities could be described in five distinct groups as follows:

- Group I: Low angle face parallel fractures dipping at 0° to 30° towards the face, these are extensional features.
- Group II: Steeply dipping face parallel fractures some showing relative displacement. This is by far the most frequent set.
- Group III: Steeply dipping joints perpendicular to the face. They are filled with gouge and are not as frequent as the face parallel fractures.
- Group IV: Two groups of fractures at intermediate dips (40° to 60°) which dip towards and away from the face. They are parallel to the face and are infrequent.

It was observed that long slabs of rock, formed by the intersection of fractures from groups I and II, failed during seismic events. The data are summarised in Table 9.4.3.7-1. Note that the face advance direction was South (180°).

Table 9.4.3.7-1 Orientation data for joints and fractures in lava.

Fracture group	Dip	Dip direction	Scatter
Group I : Low angle face parallel	4°	170°	20°
Group II: Steep face parallel	84	178°	40°
Group III: Perpendicular to face	75°	99°	20°
Group IV: Face parallel, intermediate dip	41°	15°	20°
Group V: Face parallel, intermediate dip	60°	165°	20°
Reef plane	20°	178°	20°

9.4.3.8 Fracture and joint sets for keyblock analysis

For the purpose of analysing the formation of keyblocks, it was decided to set up a generic data set for quartzite hangingwalls, which could be modified to suit special cases. The five fracture sets identified by Gay and Jager (1986) were used as a basis for describing the jointing. Sets 1 and 2 were combined into a single set, as they are essentially the same type of fractures, the first set only being formed further ahead of the face.

The properties of geological discontinuities were summarised as follows:

- Steeply dipping geological structures may intersect the reef plane at any orientation.
- There are typically two steeply dipping joint sets that are approximately orthogonal.
- The average spacing of steeply dipping joints varies between 7 m and 10 m but may be as much as 30 m.
- Bedding joints are typically continuous over more than 10 m and may extend up to 30 m in both the strike and dip directions.

In setting up the data it was assumed that a stope face was advancing to the west (270^0) and the reef dips at 20^0 to the south (180^0). The joint orientation data and scatter is as shown in Table 9.4.3.8-1. In this table the scatter implies variations in orientations both in the dip and the dip direction. In the keyblock simulations, it was assumed that the joint orientations follow a normal distribution with equal scatter in the dip and the dip directions.

Table 9.4.3.8-1 Orientation data for joints and fractures in quartzite.

Fracture type after Gay & Jager	Dip	Dip direction	Scatter
1 & 2 Extension parallel to face	70°	270°	20°
3 Shallow parallel to face	30°	270°	20°
4 Bedding parallel	20°	180°	20°
5 Shear parallel to face	70°	90°	20°
Bedding	20°	180°	5°
Geological structures (usually two orthogonal sets)	70 - 90°	0 – 360°	10°

The spacing and trace length data for the above sets were based on the data presented in the previous sections and are summarised in Table 9.4.3.8-2. For the purpose of keyblock analysis

it is assumed that the joints spacings and trace lengths follow a negative exponential distribution. Truncation of the distribution is carried out at the minimum and maximum spacings.

Table 9.4.3.8-2 Spacing and trace length data for joints and fractures in quartzite.

Fracture type after Gay & Jager	Average spacing	Min spacing	Max spacing	Average length	Min Length	Max Length
1 & 2 Extension parallel to face	0,07	0,05	1,5	1,5	0,8	6
3 Shallow parallel to face	0,03	0,01	1	1,5	0,8	4
4 Bedding parallel	0,3	0,1	0,5	0,3	0,1	0,5
5 Shear parallel to face	1	0,7	5	8	5	30
Bedding	1	0,2	4	8	5	50
Geological structures	7	5	15	10	5	50

The above fracture data is valid only for typical quartzite hangingwalls in deep stopes. Generic models of the jointing in lava and shallow stopes are also required.

9.4.4 Calibration of keyblock software

Since the JBlock model had not been used to model gold mine stopes previously, it was necessary to establish whether it could produce realistic block sizes. The analyses were also aimed at determining the sensitivity of the software to variations in the input parameters.

9.4.4.1 Sensitivity of the model to joint combinations

The JBlock model was initially used to simulate a typical deep gold mine stope in order to assess the sensitivity of its results to variations in some of the important parameters. The initial runs were aimed at establishing whether JBlock would be able to generate similar block size distributions as found from the accident statistics. All blocks generated by the program with volumes of less than 0,01 m^3 were excluded from the calculation, since they were smaller than the smallest block in the accident statistics. The results of the model calculations were compared to the overall block volumes of all fall of ground fatalities in the accident database.

Two initial models were set up to simulate fractures and joints in lava, based on information from Western Deep Levels South VCR mining and Blyvooruitzicht Carbon Leader Reef mining. From these studies it was found that, if the closely spaced stress fractures (set 1 and 2 according to Jager & Gay) are assumed to take part in the formation of all the blocks, the block dimensions are much smaller than indicated by the accident statistics. This may be the result of two factors:

- Many small blocks may be unstable in a stope but they do not result in fatal accidents. This was partially accounted for by removing all blocks smaller than 0,01 m^3.
- Keyblocks are blocks that initiate failure, the size of a rockfall is likely to be larger than the initial keyblock dimensions.

The initial analyses did show the following:

- Simulated keyblocks showed a negative exponential distribution of volumes similar to the rockfall statistics.
- The average volume of simulated keyblocks (less than 1 m^3) was considerably smaller than the average volume of rockfalls (6 m^3).
- The length of joints has a significant effect on the simulated block sizes. The average volume of falls from the quartzite model, where the maximum joint length was 30 m, was

approximately five times larger than the lava model where the maximum joint length was 9 m.

- The volume of simulated keyblocks from combinations of different joint sets could vary significantly if the joint spacing and length varied. The minimum spacing played an important role in the distribution of volumes.

It was realised from the initial analyses that the JBlock software generated large numbers of very small keyblocks that were not present in the rockfall statistics. In order to obtain a good correlation between the simulated blocks and statistics, the issue small blocks would have to be addressed. In practice the small blocks (volumes less than 0,01 m^3, mass of less than 27 kg) would probably fallout during blasting or would not result in a fatal accident. This problem was addressed by applying the relationship between rockfall size and injuries, as described in section 9.4.1.4.

An alternative method of addressing the issue of small blocks could be to exclude the closely spaced fractures from the analysis. This could, however, result in unforeseen effects on other aspects of the analysis.

9.4.5 Sensitivity analyses

9.4.5.1 Number of keyblocks

Sensitivity analyses were initially conducted to establish what number of keyblocks should be used in analyses to ensure repeatability of the simulation results. Runs were conducted where between 1000 and 10 000 blocks were generated. It was found that if 5000 keyblocks were used in repeated simulations, the difference in the number of blocks in 0,3 m^3 intervals remained below 5 per cent, which was considered to be adequate.

9.4.5.2 Joint set orientation scatter

The scatter of orientations of joint sets is one of the input parameters that is required for JBlock simulations. Modelling 5000 blocks and changing the range (scatter) of orientations as follows tested the sensitivity to changes in the scatter of orientations: 5^0, 10^0 and 20^0.

It was found that the modal value of the blocks generated did not change significantly. A decrease in the average block size of about 30 per cent resulted when the scatter was changed from 10^0 to 5^0. This was partly the result of many smaller blocks being generated. The scatter in joint orientations is a factor that requires accurate input, if realistic block dimensions are to be generated.

9.4.5.3 Joint lengths

Following on the initial analyses, the sensitivity of block sizes to joint length was analysed. The effect of doubling both the average and the maximum joint length on the keyblock size distribution was investigated. The results showed that the average volume of the blocks increased by a factor of 2,4, while the modal value of the block volumes decreased slightly by about 20 per cent. This implies that the change in the average volume was the result of large blocks being formed, which did not affect the modal value. The increase in the average volume of the blocks is expected, since the volume of a block is related to the cube of the side dimensions. This is confirmed by the fact that the maximum keyblock size increased from 27,5 m^3 in the base case to 161,5 m^3 when the joint spacing was doubled. When attempting to simulate actual keyblocks it will be important to obtain accurate information on the trace lengths of the stress fractures and geological discontinuities.

9.4.5.4 Maximum Joint length

A further analysis of the joint length aspect was carried out to determine whether the change in joint volumes presented above was not related to the maximum length of the joints, rather than the average lengths. The effect of doubling and tripling the maximum joint length was therefore assessed. In these analyses the average joint length was held constant. The base case maximum length was between three and five times the average length. It was found that doubling or tripling the maximum joint length did not significantly affect the block size distribution. The average block dimensions remained essentially unchanged, while the distribution of block sizes changed in the lower block sizes (less than 1 m^3). The results indicate that, if the maximum joint lengths are greater than three to five times the average length, they have little effect on the resulting block size distributions.

9.4.5.5 Joint spacing

The effect of doubling the joint spacing was evaluated by doubling the average, minimum and maximum spacing of the joints. The results showed that if the spacings were doubled, the average keyblock dimension increases by 64 per cent. The modal value increases by about 20 per cent and the maximum keyblock size increases from 27,5 to 48 m^3. These results also indicate that the joint spacing affects the larger block sizes, and not the smaller blocks where the modal value lies. In terms of stability in a stope, changes in the joint spacing is therefore unlikely have a significant effect on the probability of failure of blocks between supports (the smaller blocks). The length of the joints, and not necessarily the spacing, ultimately affects larger block sizes. Changes in the lower limit of the spacing will have an effect on the smaller block sizes, which will be reflected in the average block size.

9.4.5.6 Orientation of geological discontinuities

In a deep gold mine stope the majority of the stress related fracturing is parallel to the stope face. The cut-off plane for keyblocks to form is usually provided by natural discontinuities, which are not parallel to the face. A number of analyses were carried out to determine the effect of a change in the orientation and spacing of natural discontinuities. These analyses were also intended to replicate the rockfall statistics.

The results showed the expected result, i.e. if the natural discontinuities strike perpendicular to the face, then the average volume of keyblocks is much larger than when they are approximately parallel to the face. The relationship between the average block sizes and the strike orientation of natural joints is shown in Figure 9.4.5.6-1.

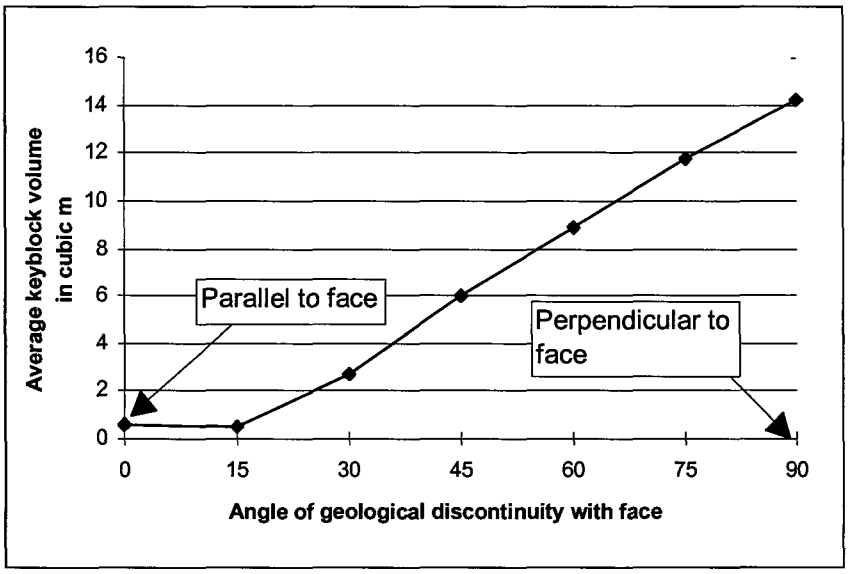

Figure 9.4.5.6-1 Graph showing the effect of the orientation of geological discontinuities on the average simulated keyblock size, assuming the geological discontinuities have an average spacing of 10 m.

This graph is based on an average spacing of the natural joints of 10 m, following a negative exponential distribution. In terms of safety, the larger blocks would be more likely to span between the support element, and provided the support elements do not fail, they are expected to result in a lower rockfall hazard. When the discontinuities are almost parallel to the face, the keyblocks are long slivers of rock, which may easily drop out between rows of support, resulting in a high rockfall hazard.

9.4.5.7 Calibration against rockfall statistics

All the results of simulated keyblocks, used in the initial analyses, were compared to actual rockfall dimensions as obtained from the accident statistics. In the initial analyses it was found that the JBlock software created many small blocks (volumes of less than 0,01 m^3) which did not reflect in the accident statistics, as they were too small to result in fatal fall of ground accidents. When comparing the results of the simulations to accident statistics, these small blocks were removed from the statistics.

For calibration with actual rockfall statistics, it was assumed that keyblocks would be formed by steeply dipping stress fractures, shallow dipping fractures, and steeply dipping geological discontinuities. The former two joint types are parallel to the face, while the geological discontinuities may have any orientation. The stress fractures were assumed to be spaced at an average of 0,3 m apart with a maximum of 1 m. The spacing of the geological discontinuities was varied between average values of 3 m and 10 m. The length of the geological discontinuities was set at 10 m with a maximum of 30 m.

The analyses produced considerably larger block sizes than the previous runs, where the joints were much shorter. If the geological discontinuities are perpendicular to the stope face, spaced at an average of 10 m apart, the average block size may be up to 16,9 m^3, which compares favourably with the 30 m^3 found from the accident statistics. When geological discontinuities strike at 75^0 to the stope face, the median value of the simulated keyblocks was 5,8 m^3 while the median value from the accident statistics was 5,4 m^3. Figure 9.4.5.7-1 shows an example of the results that were obtained from one of the runs. Note that the x-axis of the graph is logarithmic. Figure 9.4.5.7-2 indicates the results for smaller block sizes using a linear x-axis. Good correlation is indicated between the simulated block sizes and the block sizes reported in the accident data base.

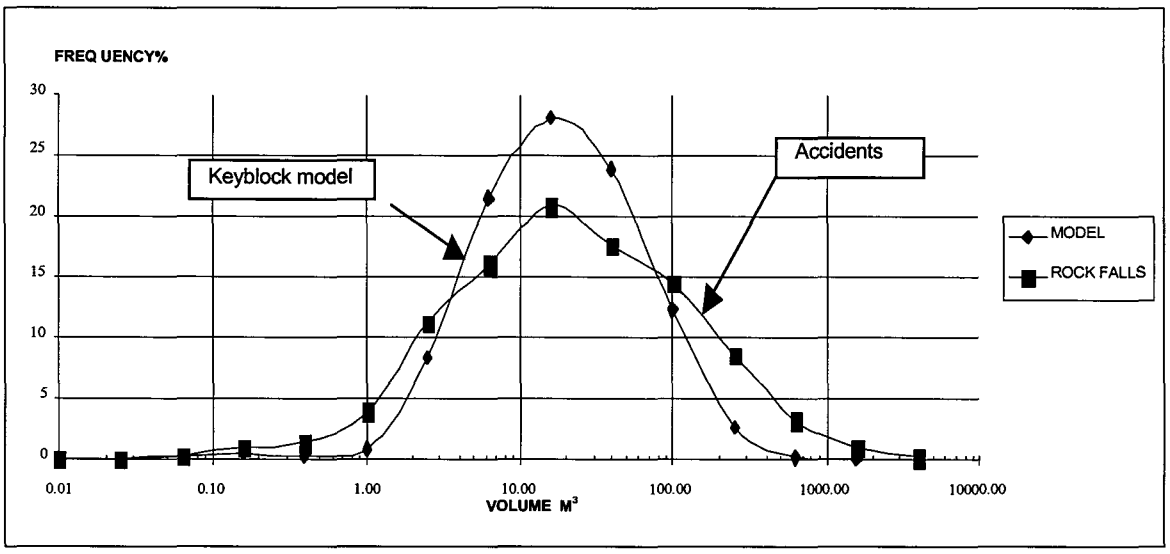

Figure 9.4.5.7-1 Graph with a logarithmic x-axis showing the frequency-size distribution of generated keyblocks and rockfalls from accident statistics.

The above results indicate that it is possible to simulate keyblocks that have a similar size distribution as the rockfalls reported in the fatal accident enquiries. The falls reported in enquiries do not necessarily consist of a single rock block, but may consist of a number of smaller blocks that fell out together. The JBlock software is able to model this type of failure by checking for combined blocks. A further problem with the accident statistics is that a few extremely large falls were recorded that distort the statistics. These extraordinary falls are difficult to simulate and are not representative of the typical rockfalls encountered frequently. The analyses did show, however, that the block size distributions were sensitive to the orientation of the geological discontinuities relative to the stress-induced fractures. An acute angle between the fractures and the discontinuities resulted in a much smaller average keyblock dimensions.

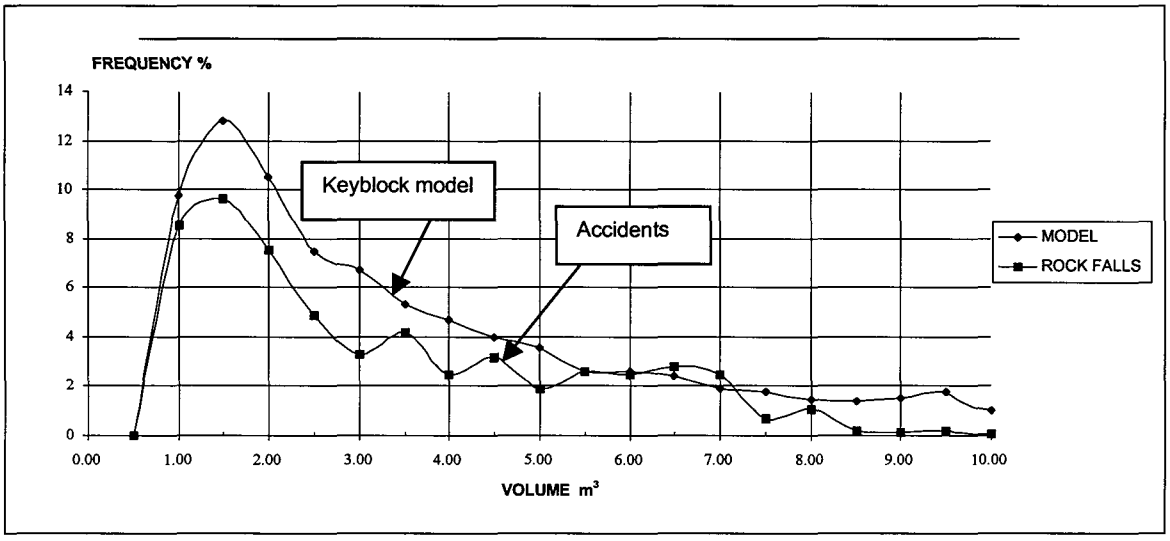

Figure 9.4.5.7-2 Graph with a linear x-axis showing the frequency-size distribution of generated keyblocks and rockfalls from accident statistics.

9.4.6 Analysis of geotechnical parameters on keyblock stability

9.4.6.1 Model parameters and evaluation method

The effect of variations of different geotechnical parameters on keyblock stability was evaluated using a base model in which a stope excavation was simulated, initially without any support. The objective was to determine how the keyblocks react to changes in parameters such as clamping stresses, dip of joints, spacing, and trace length. The parameters used in the base model were as shown in Table 9.4.6.1-1 and Table 9.4.6.1-2. In this model the stope face was modelled to advanced on breast in the direction 270° (west), so that the face is parallel to a line running north-south.

Table 9.4.6.1-1 Orientation data used in base keyblock analysis models.

Set	Dip	Dip direction	Scatter
1: Extension fractures	70°	270°	20°
2: Shear fractures	70°	90°	20°
3: Bedding	0°	180°	10°
4: Geological	90°	45°	10°
5: Stope hangingwall	0°	180°	10°

Table 9.4.6.1-2 Dimensions of discontinuities used in base models.

Set	Spacing (m)	Minimum spacing (m)	Maximum spacing (m)	Trace Length (m)	Minimum length (m)	Maximum length (m)
1: Extension fractures	0,15	0,05	1,0	5,0	3,0	20,0
2: Shear fractures	3,0	2,0	10,0	10,0	5,0	30,0
3: Bedding	1,0	0.3	3,2	10,0	3,0	30,0
4: Geological	1,0	0,2	3,0	10,0	3,0	30,0

The modelled fractures and jointing simulates the main features of a stope in a deep gold mine. The first set models closely spaced extension fractures that are face parallel dipping at 70°. The second set represents shear fractures that are less frequent and dip towards the back area of the stope. The third set was the bedding spaced at an average of 1 m apart parallel to the stope hangingwall. The fourth set was a set of geological discontinuities that are vertical and strike at right angles to the face.

The effects of the various parameters were evaluated by modelling 5000 keyblocks generated for each scenario and testing each one for stability. In the absence of any support or clamping stresses, a keyblock can only be stable if it is held in place by friction, as it attempts to slide out of the rock mass. If a keyblock is able to simply drop out of the rock mass, it will do so. If clamping stresses are present, they may cause a keyblock to be held in position by friction, even if it would otherwise have dropped out.

The results of the analyses were compared by considering the volume of unstable keyblocks per 1000 m^2 of hangingwall exposed. In this report, this is called the volume of failure. The failure volume is an indication of the amount of failure, and not the severity, in terms of risk or hazard. Other parameters such as the percentage of keyblocks that are unstable were also considered, but the results are not presented here.

9.4.6.2 Effect of the dip of geological structures

The role of the geological structures is important in the formation of keyblocks. Since all the stress related fractures are approximately parallel to the stope face, they cannot form keyblocks. A release surface is required, which defines the limits of the block. The initial studies were therefore directed to evaluating the effect of the geological structures. Note that in the base model only one set of geological structures was modelled.

The results in Figure 9.4.6.2-1 show how the volume of failure changes as the dip of the geological structures changes. In these runs the clamping stress was set to zero and no supports were present in the model. The results show that, when the geological structures are shallow dipping, the keyblocks are stable, as they must fail by sliding along the shallow dipping structures. As the dip increases, more of the keyblocks become unstable, as they are able to fail by sliding. A second contributing factor to the increase in failure volume is the increase in volume of the blocks. When the geological structures are shallow dipping, the keyblocks are flat blocks with small volumes, however, as the dip increases, the blocks are less flat and their volume increases.

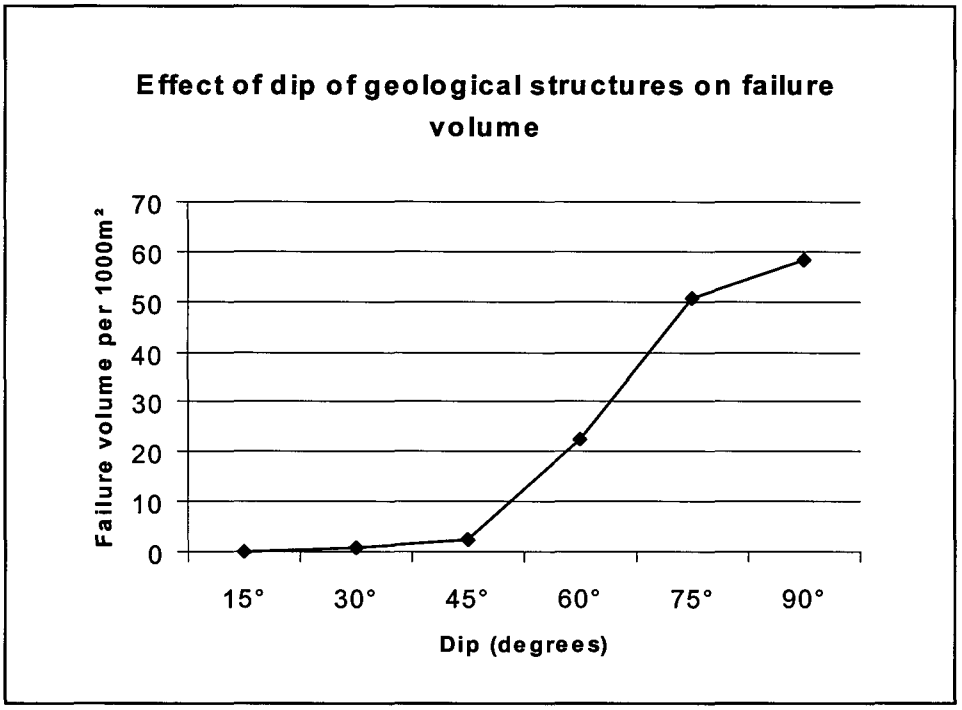

Figure 9.4.6.2-1 Graph showing the effect of the dip of geological structures on keyblock stability in the absence of clamping stresses.

When considering the results of Figure 9.4.6.2-1, it must be noted that the keyblocks formed by the joints all have two parallel cut-off planes, if viewed towards the stope face. The only way that these blocks can fail is by sliding along the lowermost of the two planes. The typical block shape and sliding mode is illustrated in Figure 9.4.6.2-2. It is therefore not surprising that the blocks are stable when the dip of the geological structure is shallower than the typical friction angle of 30°. The importance of the block shape on stability is illustrated clearly if wedge type blocks are formed, as illustrated in Figure 9.4.6.2-2, where the parallelepiped shaped blocks would fail by sliding, and the wedge shaped blocks are free to fall out of the rock mass. Although the geological structure has a similar dip in the two cases, the wedge block falls out and the parallelepiped is likely to be stabilised by friction. It is important therefore that the block types that can form be considered. This is automatically done in the Jblock software.

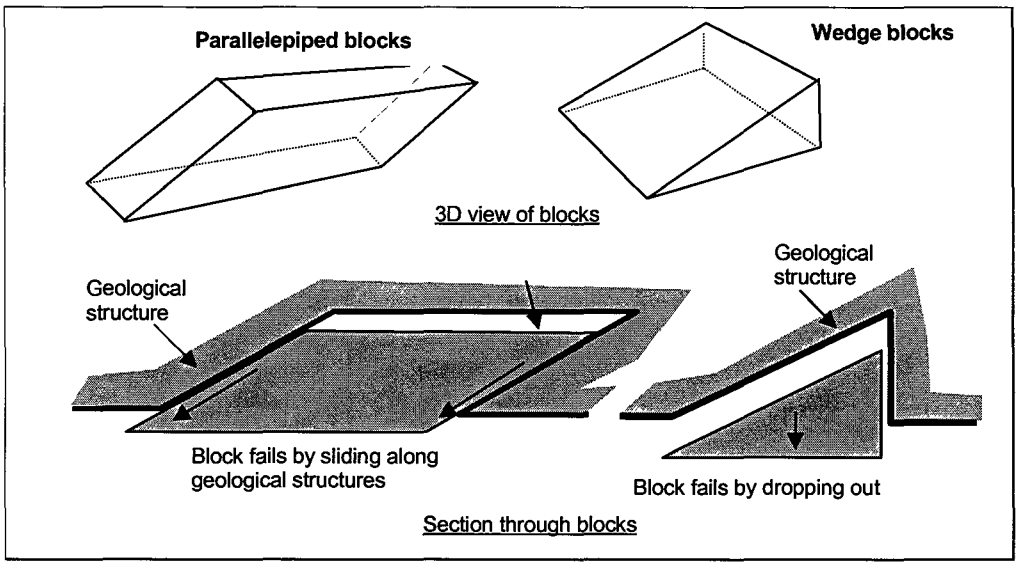

Figure 9.4.6.2-2 Sketch showing failure mode of two types of keyblocks.

A set of joint and fracture data were set up to investigate the effect of keyblock shape on stability. Four joint sets were selected so that they would be more likely to form wedge shaped keyblocks than parallelepiped shaped blocks. The difference in the stability of two rock masses was evaluated by generating 5000 keyblocks of each type and checking each keyblock for stability. The probability of the failure of the keyblocks was calculated as the ratio of unstable to stable keyblocks in each case. The results are presented in Figure 9.4.6.2-3.

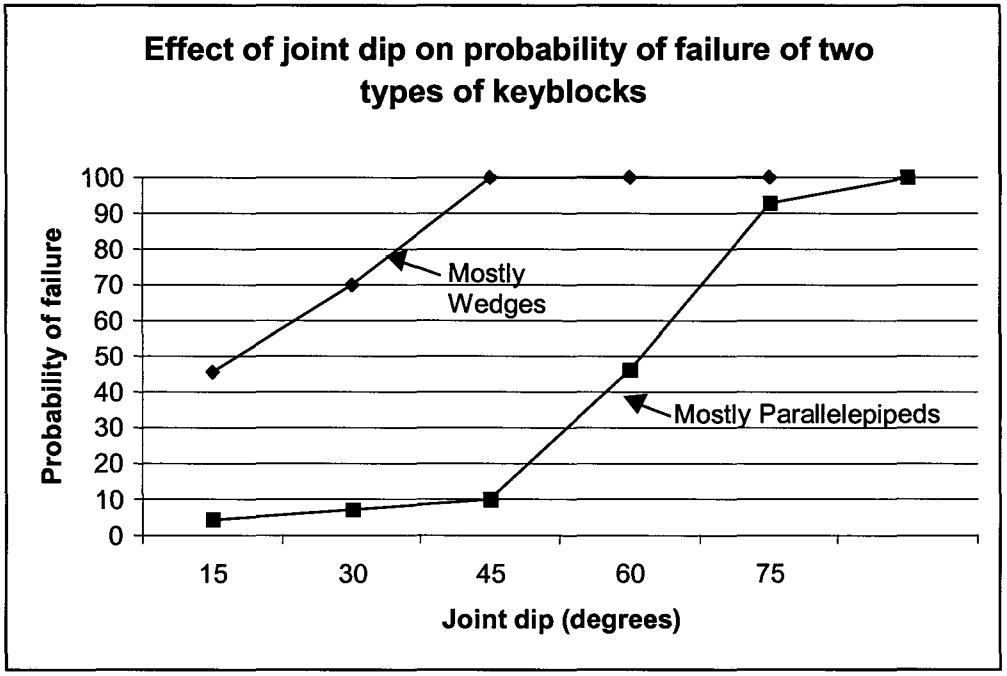

Figure 9.4.6.2-3 Graph showing the effect of keyblock shape on the failure probability of keyblocks in the absence of any support or clamping stresses.

The results clearly show that should the joints be such that mostly wedges are formed, the probability of failure of keyblocks is much higher than when mostly parallelepipeds are formed. For example, if the joints dip at 45° the wedge type keyblocks will have a 100 per cent probability of failure, while only about 10 per cent of the parallelepiped type keyblocks will be unstable. Note that both rock types contain keyblocks of both types, and that the joints were selected so that one type would dominate in each rock type.

9.4.6.3 The effect of clamping stresses on keyblock stability

In deep underground excavations, horizontal clamping stresses are present in the hangingwall of the stopes. The stability of the hangingwall is enhanced by preserving the horizontal clamping stresses. The magnitude of stress required to ensure that blocks remain in a clamped position in the hangingwall are small compared to the typical stresses in the rock. The effect of clamping stresses on wedge shaped blocks, similar to the wedge shown in Figure 9.4.6.2-2, was evaluated. The stability of a block with base dimensions of 2 m x 3 m was determined for different clamping stress conditions. The horizontal clamping stresses were equal in all directions. The dip of the geological discontinuity was varied between 15° and 75° and the clamping stress was increased from 0 to 2 MPa. The results are presented in Figure 9.4.6.3-1, which shows that clamping stresses of as low as 200 kPa are sufficient to stabilise most of the wedge shaped blocks. Only the flat wedges, where the geological feature dips at 15°, are unstable even when the clamping stresses are 2 MPa.

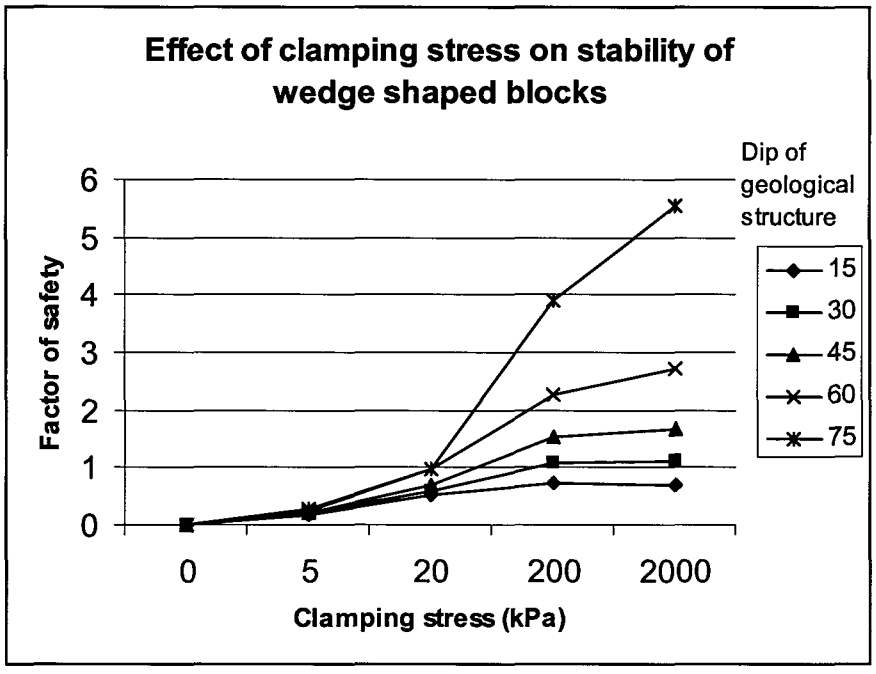

Figure 9.4.6.3-1 Graph showing the effect of clamping stresses on the factor of safety of wedge shaped blocks.

Further analyses of the effect of clamping stresses and geological features were carried out by generating 5000 keyblock that were tested for stability. Two types discontinuities were defined, with the one data set resulting mostly in parallelepipeds, and the other mostly in wedge shaped keyblocks. The analyses were all evaluated without any support. The results of the analyses are summarised in the following sets of graphs.

Figure 9.4.6.3-2 and Figure 9.4.6.3-3 show the effect of clamping stresses on the failure volume of the two data sets. It can be seen that when the clamping stress exceeds about 200 kPa in both cases the volume of failure becomes very low. However, at lower stress values the failure

volume of wedge shaped blocks is almost double that of the parallelepiped shaped blocks. It can also be seen that the flatter dip of the geological structures results in smaller blocks and, hence, lower volumes of failure.

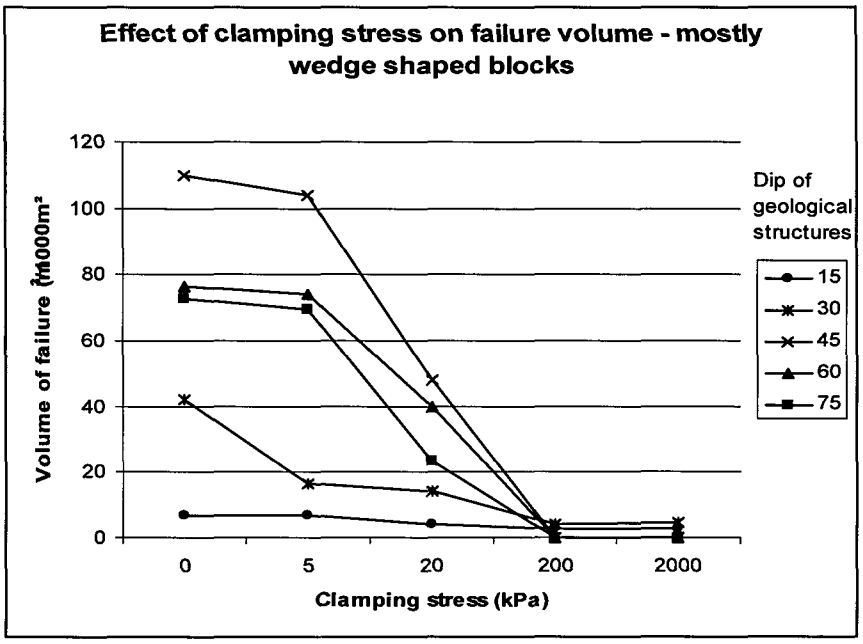

Figure 9.4.6.3-2 Effect of clamping stress on failure volume - mostly wedge shaped keyblocks.

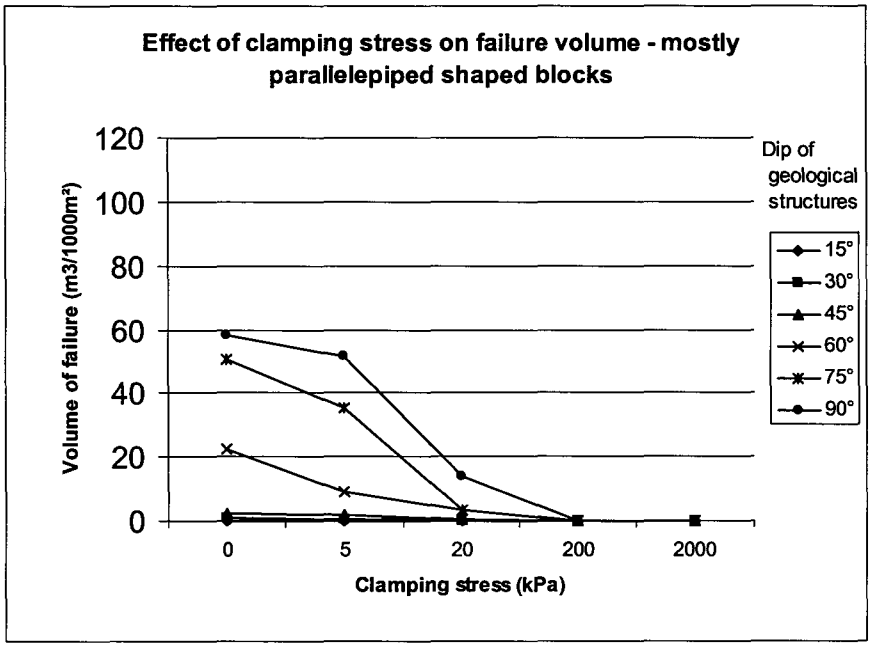

Figure 9.4.6.3-3 Effect of clamping stress on failure volume - mostly parallelepiped shaped keyblocks.

Since the volume of failure is affected by the shape of the individual blocks, a second set of graphs was prepared, in which the probability of failure of the keyblocks was determined. The probability was again expressed as the ratio of unstable to stable keyblocks. The results are shown in Figure 9.4.6.3-4 and Figure 9.4.6.3-5.

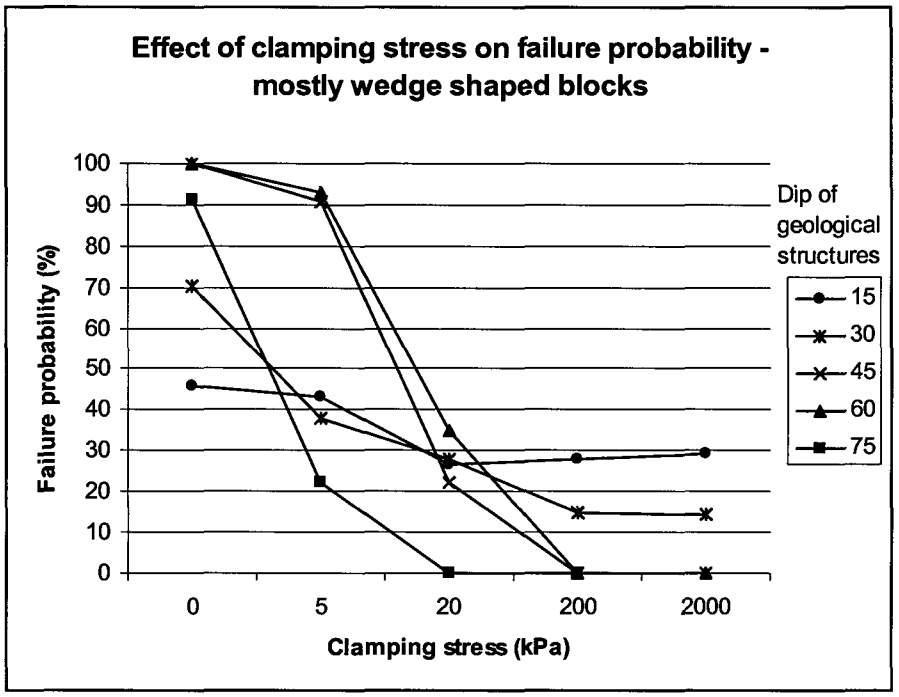

Figure 9.4.6.3-4 Graph showing the effect of clamping stresses and the dip of geological structures on failure probability - mostly wedge shaped keyblocks.

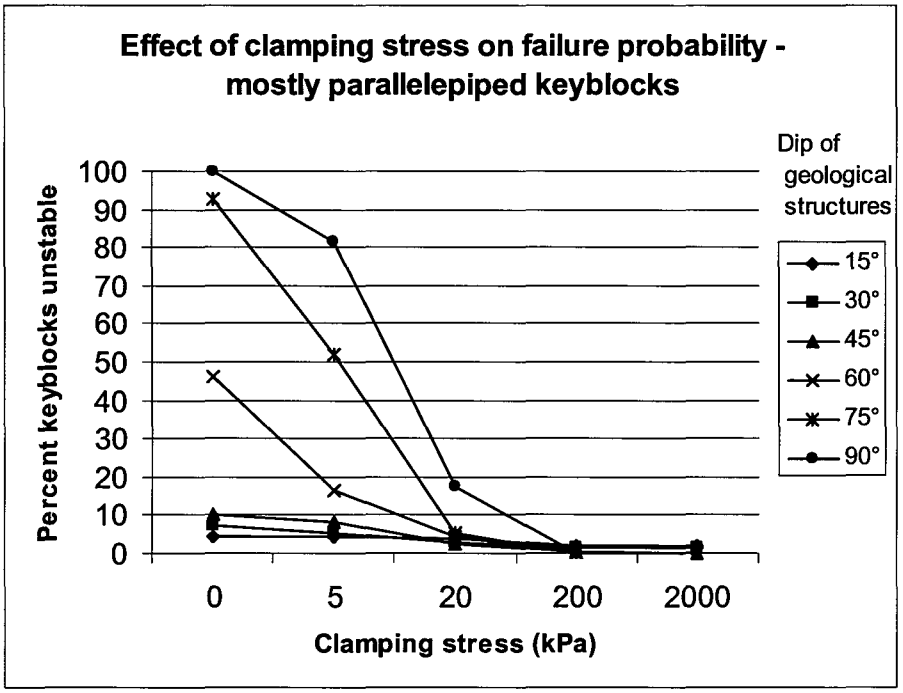

Figure 9.4.6.3-5 Graph showing the effect of clamping stresses and the dip of geological structures on failure probability - mostly parallelepiped shaped blocks.

The graphs show that in the case of the wedge shaped blocks, the probability of failure of the keyblocks with shallow dipping joints does not significantly reduce when the clamping stresses increase. When the joint dip is greater than 45 degrees, however, a clamping stress of 200 kPa or more is sufficient to hold all the keyblocks in place.

The results of these investigations show that clamping stresses need only be relatively low to stabilise keyblocks in the hangingwall. A objective of a support system should therefore be to preserve the horizontal clamping stresses in the hangingwall, because if they are maintained, most potential keyblocks will be stable. If the dip of the structures forming the keyblocks are shallow, it is possible that the clamping stresses will be unable to stabilise the blocks. An important result is that the shape of the blocks affects their stability. Blocks which approximate parallelepipeds are more stable than blocks that are wedge shaped. The number of parallelepiped or wedge shaped keyblocks formed by the jointing will, therefore, have a significant influence on the stability of the hangingwall.

9.4.6.4 Effect of dynamic loading on keyblock stability

Dynamic loading of stope hangingwalls during rockbursts is a major cause of falls of ground accidents in deep gold mines. The effect of dynamic loading on keyblock stability was investigated by modelling 5000 keyblocks at various orientations and clamping stress values. A set of results is shown in Figure 9.4.6.4-1, where the clamping stress was set to 200 kPa in the horizontal plane and the dip of the geological structures was allowed to vary between 15 degrees and 75 degrees. During a seismic event rock blocks in the hangingwall achieve high velocities, which may be arrested by support units or friction between blocks. The deceleration of the blocks requires a certain force, which must be generated by the support units or the friction between blocks. Deceleration values of between two and eight times the gravitational acceleration were considered. The direction of the deceleration was vertical. The results show that when the deceleration is equal to 1 g the keyblocks are all stable when the dip of the geological structures is greater than 45 degrees, however, as the seismic deceleration increases in magnitude, the keyblocks formed by steeper dipping joints also become unstable. When the deceleration is greater than 5 g all the keyblocks become unstable.

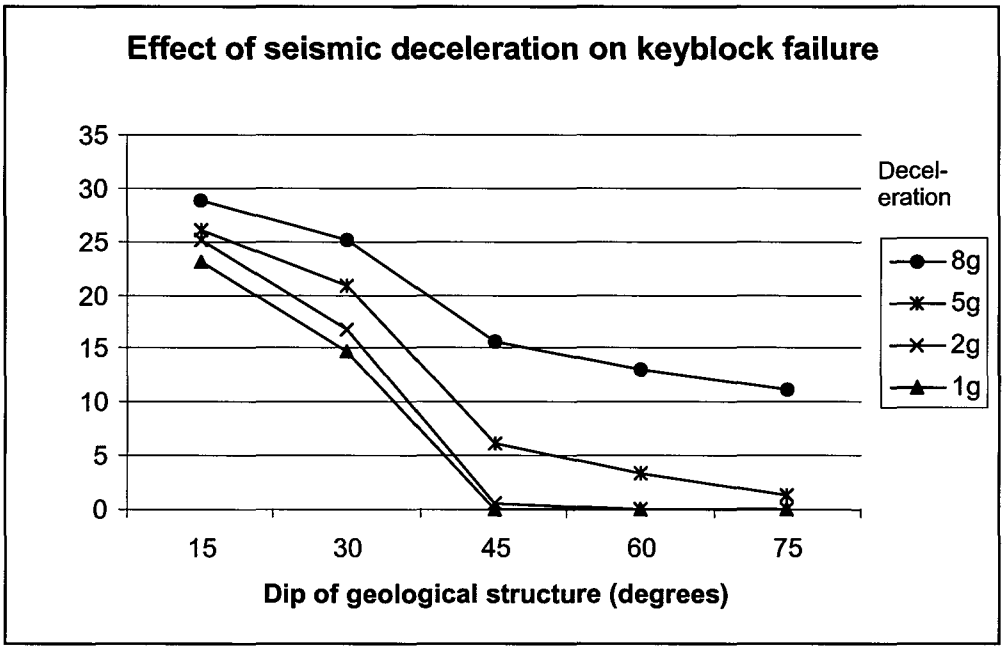

Figure 9.4.6.4-1 Graph showing the effect of seismic deceleration on keyblock stability, clamping stresses were 200 kPa.

It is interesting that the higher values of seismic acceleration do not have a significant effect on the keyblocks formed by the shallower dipping structures. A possible explanation is that the wedge shaped blocks fallout at low deceleration values anyway, and they make up about 25 to 30 per cent of the total number of blocks. The parallelepiped shaped blocks are intrinsically stable and are not dislodged, even when they are subject to dynamic loads of 8 g.

The effect of an increased clamping stress under seismic loading conditions was evaluated by increasing the clamping stresses to 2000 kPa. The results are shown in Figure 9.4.7.2-8 where it can be seen that a high clamping stress results in higher probability of failure of the keyblocks formed by very flat dipping geological structures, while the blocks formed by steeper dipping structures remain stable. However, a clamping stress of as high as 2000 kPa is unable to stabilise keyblocks formed by joints dipping at less than 45° when subject to seismic loads of 5 g.

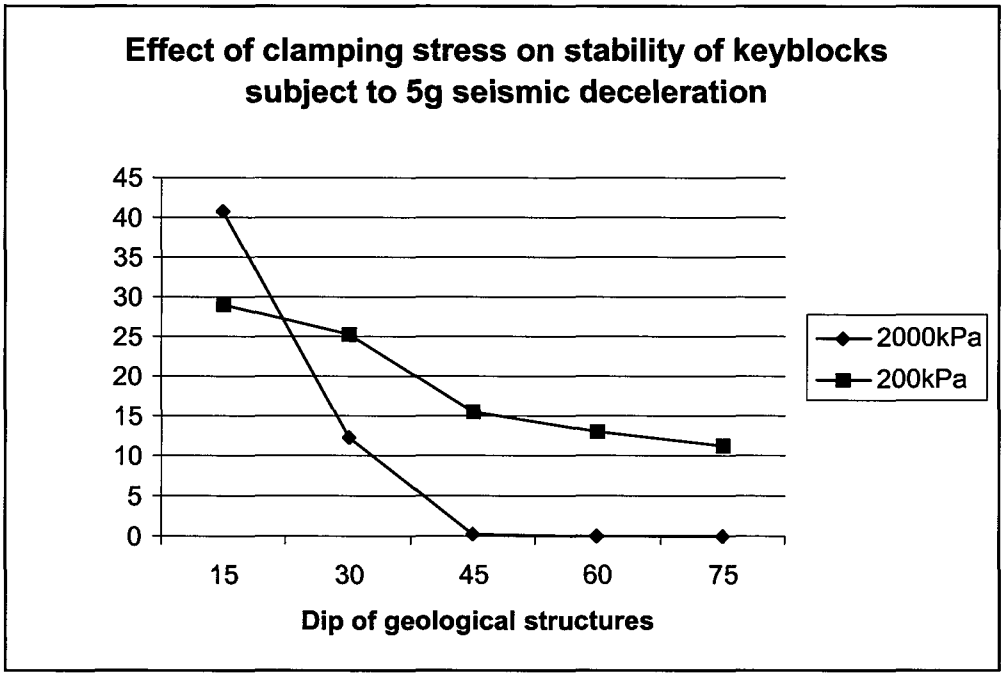

Figure 9.4.6.4-2 Graph showing the effect of clamping stresses on keyblock stability when subject to 5 g seismic deceleration, the clamping stresses were 2000 and 200 kPa.

These results show that dynamic loading of a stope hangingwall is able to dislodge keyblocks that would otherwise have been stable. The block shape appears to have an important effect on its stability. When designing support, it is necessary to note that the loss of a keyblock may result in the loss of horizontal clamping in the hangingwall, which would render more blocks unstable. Also, once a keyblock has failed, the surrounding keyblocks will become unstable and may be free to fail as well. This emphasises the importance of maintaining the horizontal clamping stresses to prevent keyblock failure.

9.4.7 Analysis of support parameters on keyblock stability

9.4.7.1 Approach used in analysis

The preceding sections of this report indicated that relatively low clamping stresses are able to stabilise most keyblocks in a stope hangingwall. It is only when shallow dipping joints or stress fractures exist that keyblock failure is possible in a clamped environment. When, however, the clamping stress is lost, the failure volume increases considerably and the efficiency of the support units in arresting keyblocks becomes important. In the analyses of the interaction between keyblocks and support it was assumed that no clamping stresses exist. The results, therefore, indicate the effectiveness of the supports if they were required to hold all the keyblocks in place. In reality this would represent the worst case, where control of the clamping stresses in the hangingwall is lost by, for example, a previous fall of ground within approximately 5 m of the face. This has implications for support design when undercutting in particular.

9.4.7.2 Area of influence of support types

The question of the effectiveness of different support types such as elongates and packs was investigated. Of particular interest was the "area of influence" concept. When designing support the support spacing is usually decided upon using energy absorption or support resistance criteria. The effectiveness of the support in arresting the individual blocks in the hangingwall has not been investigated before. The objective was therefore to determine how the area of influence varies under different geotechnical conditions and whether elongates at the same skin to skin spacing as packs are just as effective as packs in arresting potential roof falls.

Models were set up to evaluate the effectiveness of point supports, such as elongates, and area supports, such as packs. In these analyses the base discontinuity data set, described earlier in this report, was used. The runs were repeated for the base case and with variations in the orientation or dip of the fractures and discontinuities. A selected number of the results are shown below. The two figures, Figure 9.4.7.2-1 and Figure 9.4.7.2-2, show plan views of the probability of failure of keyblocks in the immediate vicinity of a point support (elongate) and an area support (pack). In these figures the stope face is parallel to the top of the figure, and the face parallel stress fractures run across the width of the page. In both cases the extension fracture set was modelled to dip at 45° and the geological structures dipped at 90° with a strike perpendicular to the stope face (i.e. running down the page). The strength of the support units was set to a high value in both cases, so that they would not fail. The results show that the area support unit is much more effective than the point support. If one looks at the area where the probability of failure of keyblocks is less than 50 per cent it can be seen that the effectiveness of the area support unit extends over a much greater area than for the point support unit. The area around the pack where the probability of failure is less than 50 per cent is equal to 8,5 m^2, while it is only 3,0 m^2 for the point support (both values exclude the area taken up by the support).

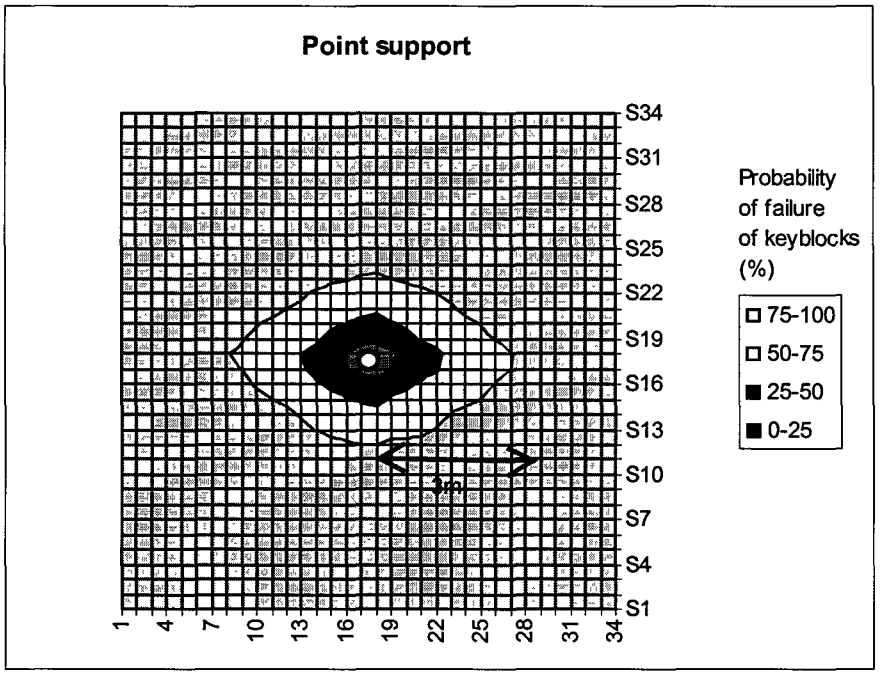

Figure 9.4.7.2-1 Plan view of a point support unit showing probability of failure contours of keyblocks, geological structures perpendicular to the face.

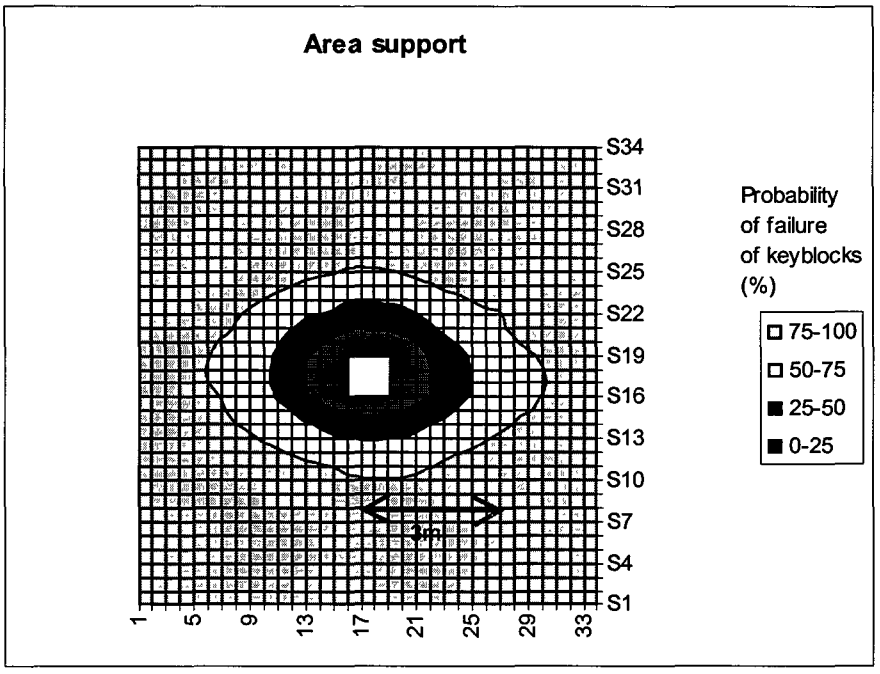

Figure 9.4.7.2-2 Plan view of an area support unit showing probability of failure contours of keyblocks, geological structures perpendicular to the face.

The above results are only valid for the particular set of discontinuity data. Two variations were modelled to demonstrate the effect of a change in the orientation of the geological structures and the effect of a change in the spacing of the geological structures. Figure 9.4.7.2-3 and Figure 9.4.7.2-4 show the failure probabilities associated with a point support and a pack support, where the geological structures strike at 45 degrees to the face direction (in the figure the geological structures would strike from the top left corner to the bottom right corner). These

results show, firstly, that the maximum failure percentage is now 60 per cent, where it went up to 100 per cent previously. This is owing to the fact that the sliding direction of the keyblocks becomes flatter as the geological structures are rotated. The orientation of the "area of influence" of the support units is also rotated to conform to the orientation of the geological structure, however, it does not rotate by 45 degrees.

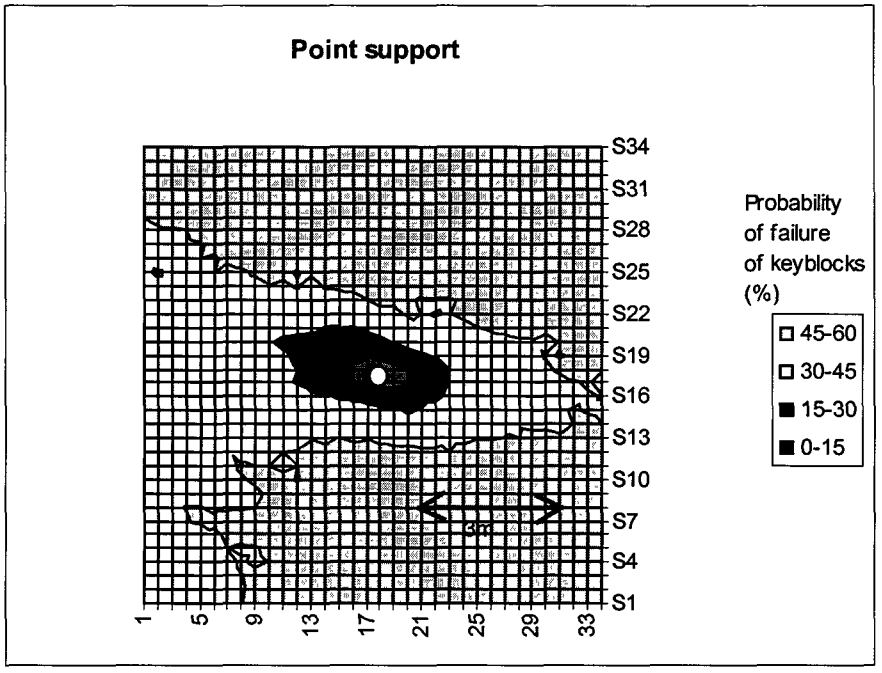

Figure 9.4.7.2-3 Plan view of a point support unit showing probability of failure contours of keyblocks – geological structures strike at 45° to the face.

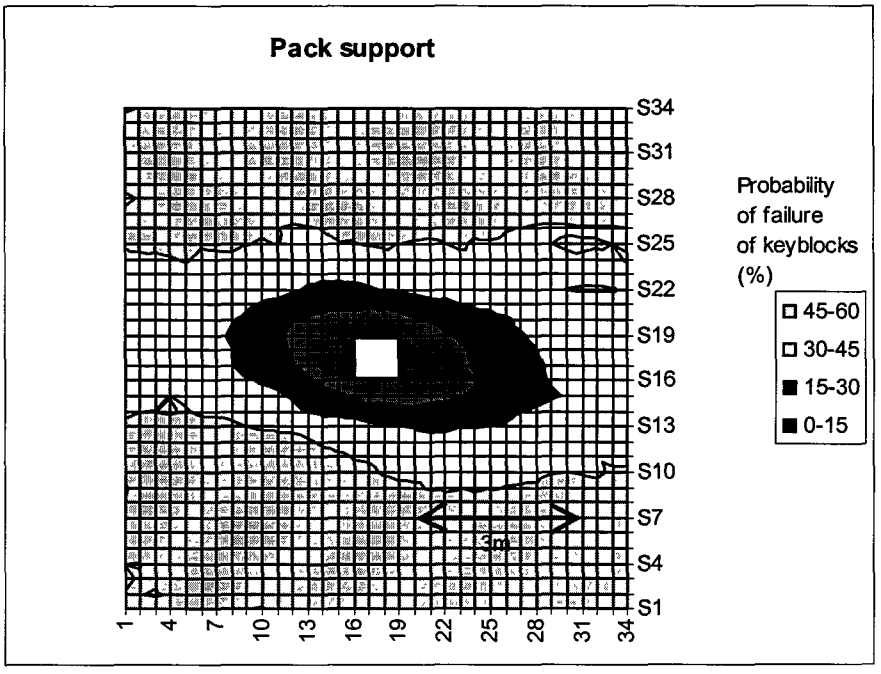

Figure 9.4.7.2-4 Plan view of an area support unit showing probability of failure contours of keyblocks – geological structures strike 45° to face.

The effect of a change in the spacing of geological structures is shown in Figure 9.4.7.2-5 and Figure 9.4.7.2-6. In these two models the extension stress fractures were set to dip at 70 degrees and the geological structures were modelled to strike at 45 degrees to the stope face. The spacing of the geological features was initially 2 m and changed to 5 m in the comparative case. It can be seen that when the spacing of the geological structures is decreased, the area of influence of the pack becomes slightly narrower. This reflects the fact that more small keyblocks are formed. The larger keyblocks are rather effected by the joint length than the spacing, and the overall area of influence is therefore only slightly affected.

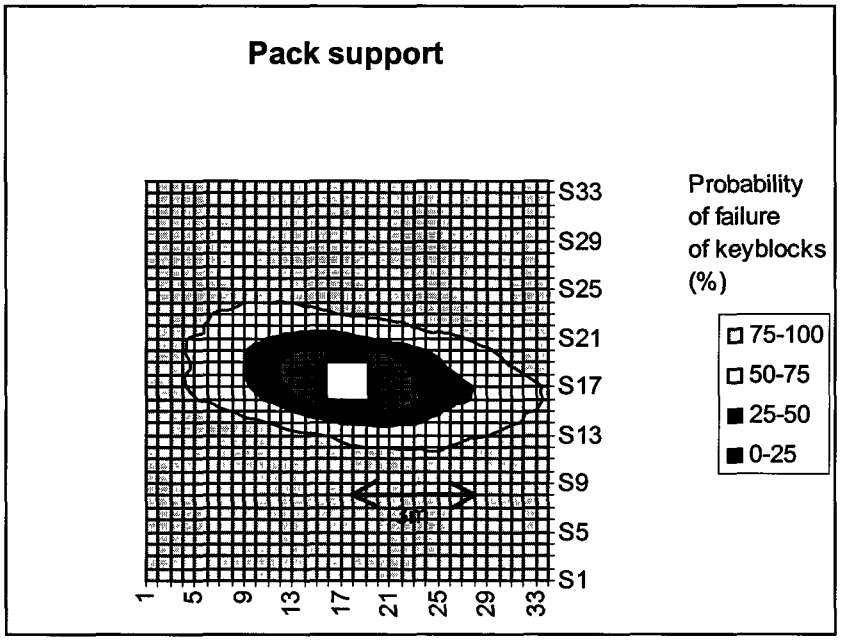

Figure 9.4.7.2-5 Plan view of an area support unit showing probability of failure contours of keyblocks – geological structures strike 45° to face, spacing 2 m.

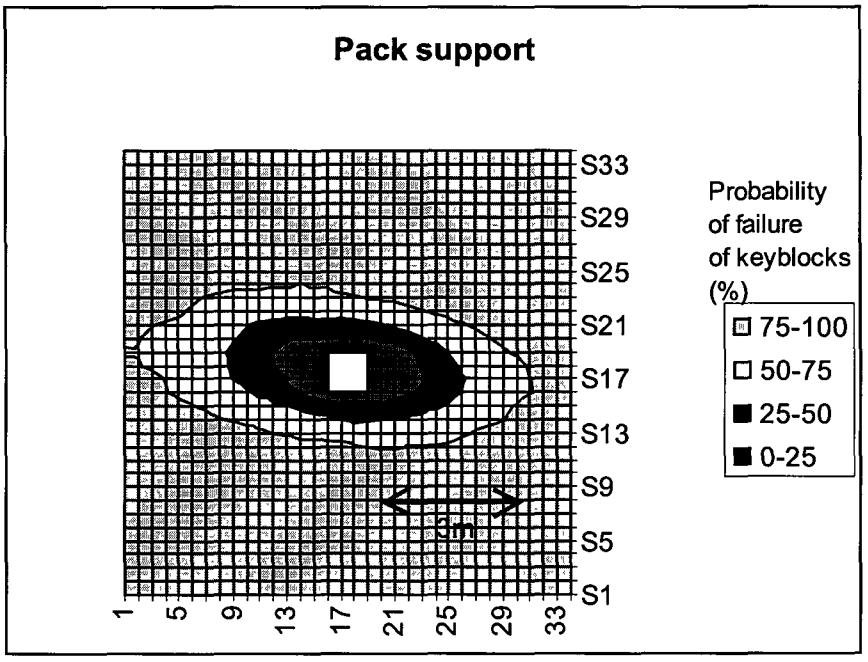

Figure 9.4.7.2-6 Plan view of an area support unit showing probability of failure contours of keyblocks – geological structures strike 45° to face, spacing 5 m.

The area of influence of the two types of support units can be compared by viewing the probability of failure along lines parallel to the strike and dip directions. Figure 9.4.7.2-7 and Figure 9.4.7.2-8 illustrate the results that show that a pack support is more effective in reducing keyblock failure in its immediate vicinity, compared to an elongate support. When viewed along dip, the pack support reduces the probability of failure to 50 per cent up to 1,8 m away from its edge, whilst the distance is 1,3 m for the elongate.

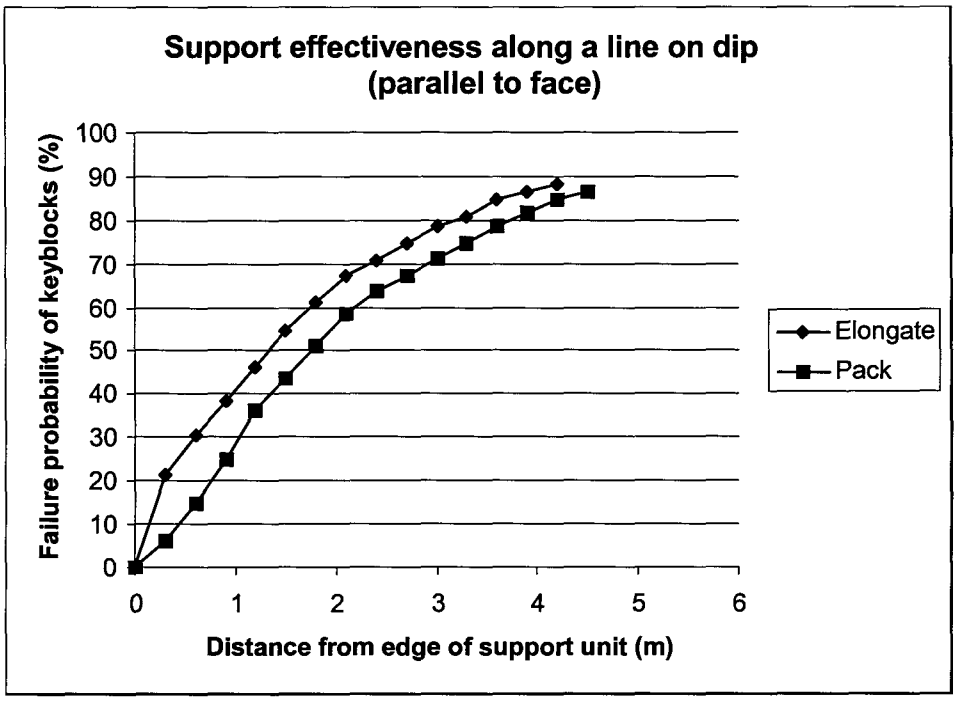

Figure 9.4.7.2-7 Graph showing the effectiveness of pack and elongate supports in reducing the probability of failure of keyblocks along dip.

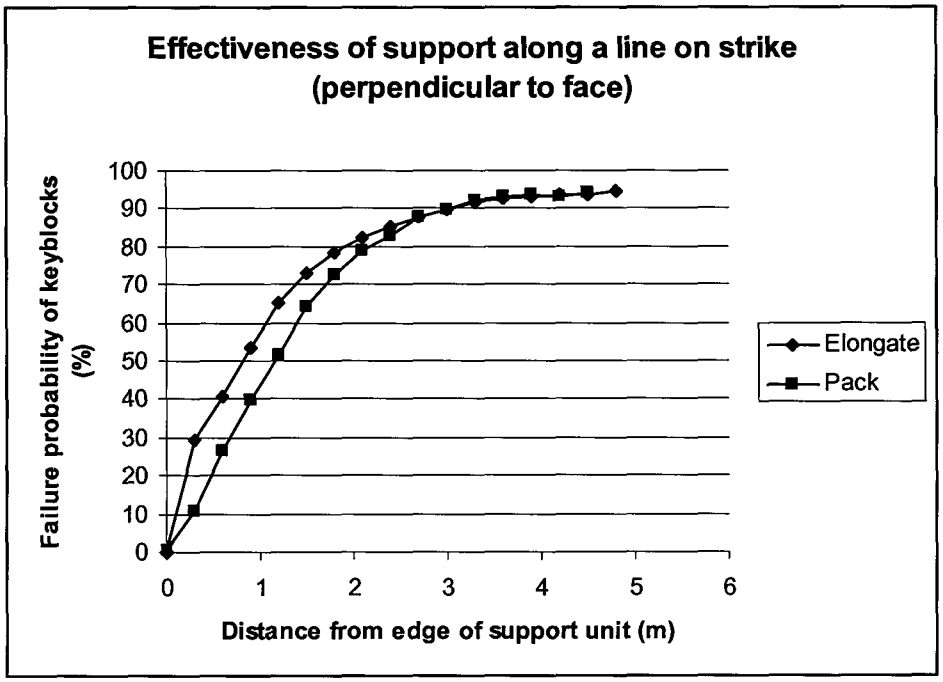

Figure 9.4.7.2-8 Graph showing the effectiveness of pack and elongate supports in reducing the probability of failure of keyblocks along strike.

When comparing the effectiveness of the supports along strike, as shown in Figure 9.4.7.2-8 the area of influence is much smaller, the pack reduces the failure probability of keyblocks to less than 50 per cent for a distance of only 1,1 m and the elongate for 0,9 m.

While the above results are applicable for the particular set of input data only, a similar trend was observed with other data sets. From the point of view of designing support, these results indicate that the area of influence of point supports (such as elongates) is much smaller than that for area supports (such as packs), even if the area covered by the support unit is excluded from the calculation. The effectiveness along dip and strike is different owing to the orientation of the closely spaced stress fractures parallel to the dip, in the models. When designing support it will be necessary to place support units closer to each other along strike, so that the effectiveness of the support is equal along dip and strike. The issue of support spacing is discussed in greater detail in the next section.

9.4.7.3 Support spacing

When designing support systems it is often difficult to decide on a support spacing. This is particularly true if strong support elements are used, that easily satisfy the energy absorption and support resistance criteria. The temptation exists to place the support units far apart, ignoring the potential for keyblocks to fail in-between the supports. The question of the effect of support spacing on keyblock failure probabilities is discussed in this section.

The effect of support spacing on the failure probability of keyblocks was evaluated using the base case data described earlier in this report. Point and area supports were modelled to simulate packs and elongate type supports. The strike skin to skin spacing of the supports was 2m and the dip spacing was varied from 0,5 m to 10 m. The spacings were selected so that the skin to skin spacing of both the packs and the elongates was the same in each case. A comparison was made of the maximum probability of failure for each case. The maximum value of the failure probability is found at the centre of the unsupported area between the supports. Several different orientations and dips of the geological structures were considered. Two sets of results are presented below, in which the effectiveness of the supports were evaluated for geological structures dipping at 90° and striking perpendicular to the face and 15° off parallel to the face. The results are presented in Figure 9.4.7.3-1 and Figure 9.4.7.3-2.

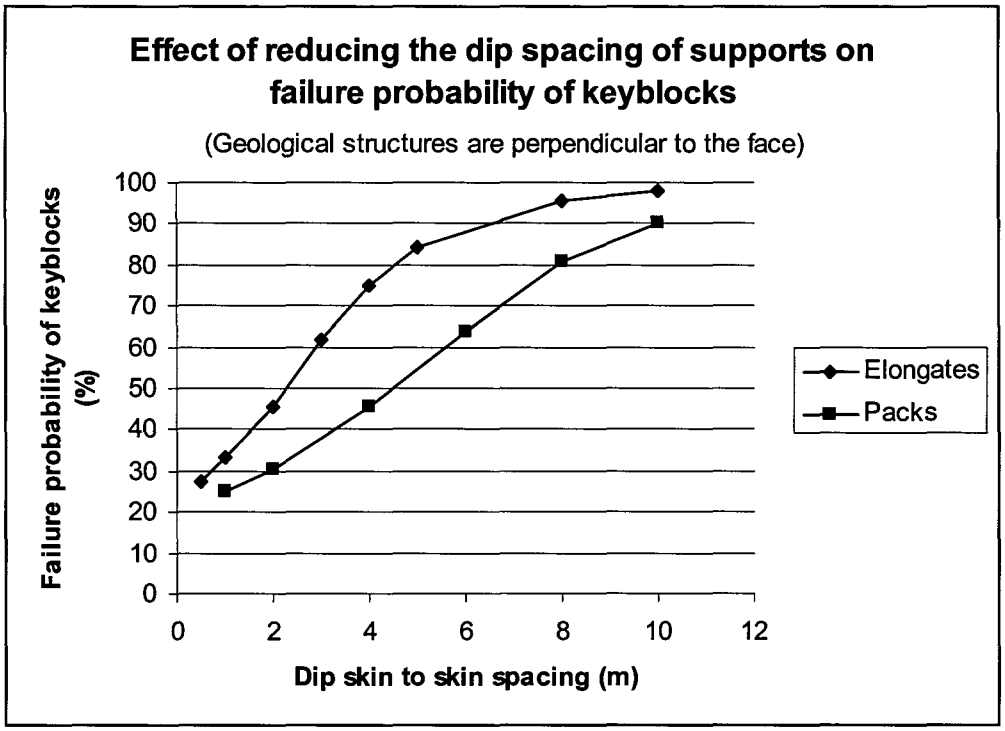

Figure 9.4.7.3-1 Graph showing the effect of changing the dip spacing of support units on failure probability of keyblocks, the strike spacing was 2 m and the geological structures strike perpendicular to the face.

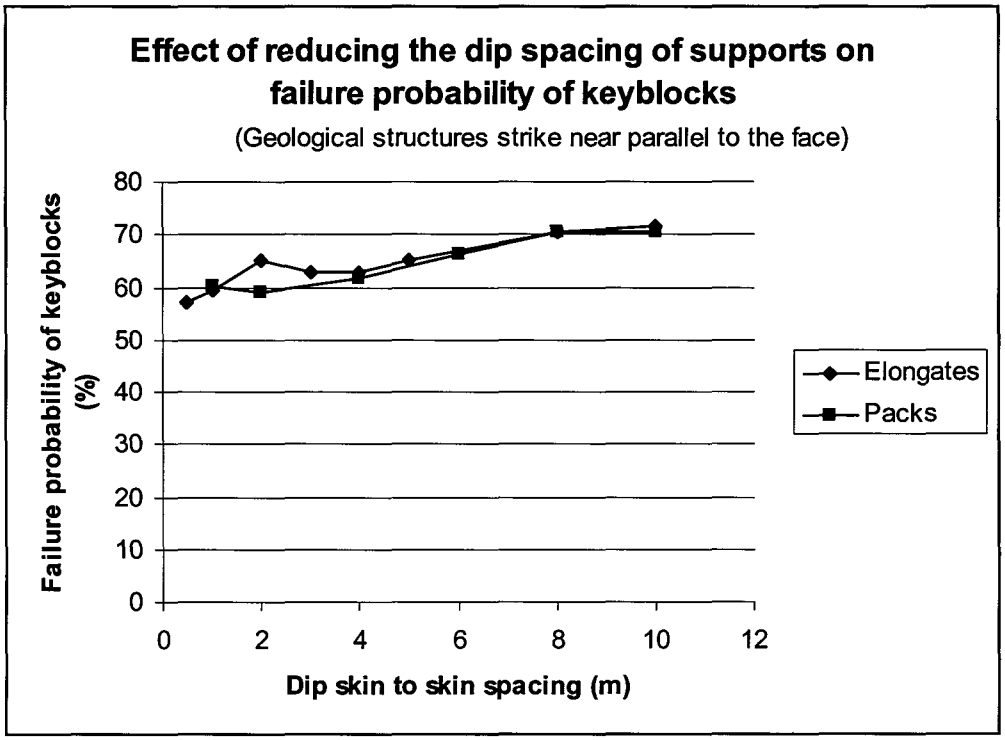

Figure 9.4.7.3-2 Graph showing the effect of changing the dip spacing of support units on failure probability of keyblocks, the strike spacing was 2 m and the geological structures strike near parallel (15 º) to the face.

The graphs show that when the geological structures are perpendicular to the face, the pack supports are much more effective than the elongates in preventing keyblock failure. For example, if the skin to skin spacing is 2 m x 2 m the packs result in a maximum failure probability of 30 per cent whilst the elongates result in a value of 48 per cent. If the orientation of the geological structures is nearly parallel to the face, the results are totally different, as shown in Figure 9.4.7.3-2, where it can be seen that the packs and elongates are equally ineffective in arresting the keyblocks. The reason is that the keyblocks are all long slivers of rock that are parallel to the face and they fallout between the rows of supports. The only way to reduce the failure probability would be to reduce the strike spacing of the support units.

Since the probability of failure of keyblocks is not directly related to the actual hazard of falls of ground, the hazard associated with each of the above sets of results was determined. The relationship between rockfall size and number of persons affected, presented in Section 9.4.1.4 was used to calculate the hazard. In this calculation, the total number of falls in an area of 10 m x 10 m was taken to conduct the comparison. The results were normalised to an area of 1000 m^2 . The effect of using the hazard as an indicator of support effectiveness is that blocks with a volume of less than 0,01 m^3 are ignored, since they did not result in any fatalities or injuries. The effect of the larger blocks is down rated.

The results for the case where the geological features are perpendicular to the stope face is shown in Figure 9.4.7.3-3, where it can be seen that the trend in Figure 9.4.7.3-1 is essentially repeated, except that the difference between packs and elongates is now greater, the packs being almost twice as effective as the elongates. In Figure 9.4.7.3-4, where the geological structures are nearly parallel to the stope face, the pack support system is again shown to be superior to the elongates.

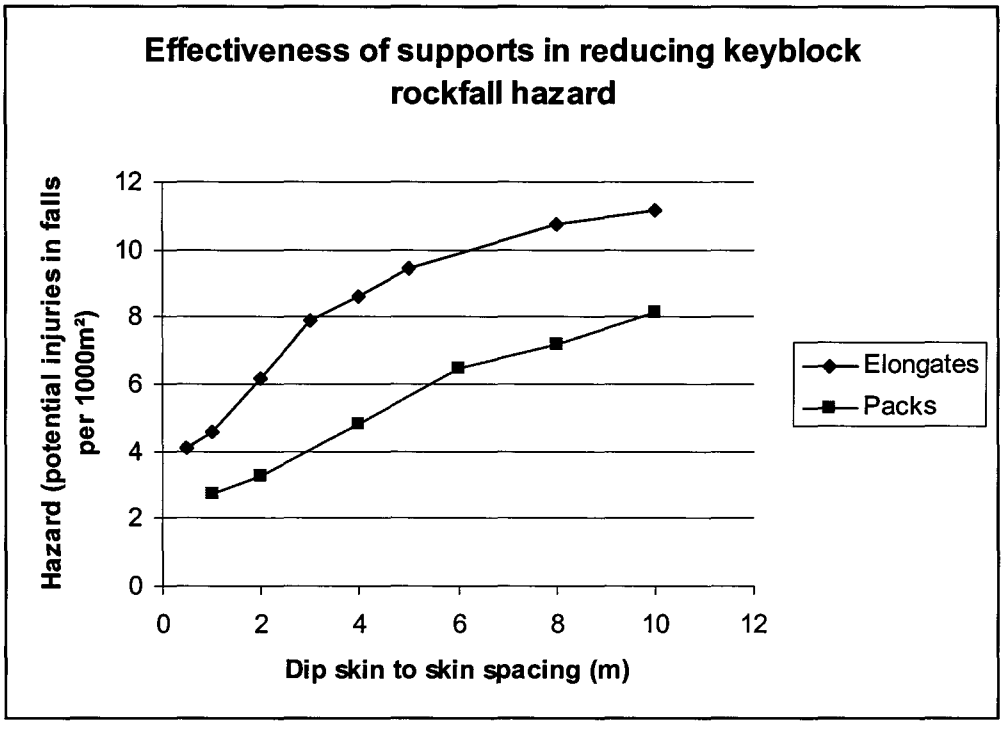

Figure 9.4.7.3-3 Graph showing the effect of support type and spacing on the hazard of keyblock failure, geological structures are perpendicular to the stope face, strike spacing is 2 m skin to skin.

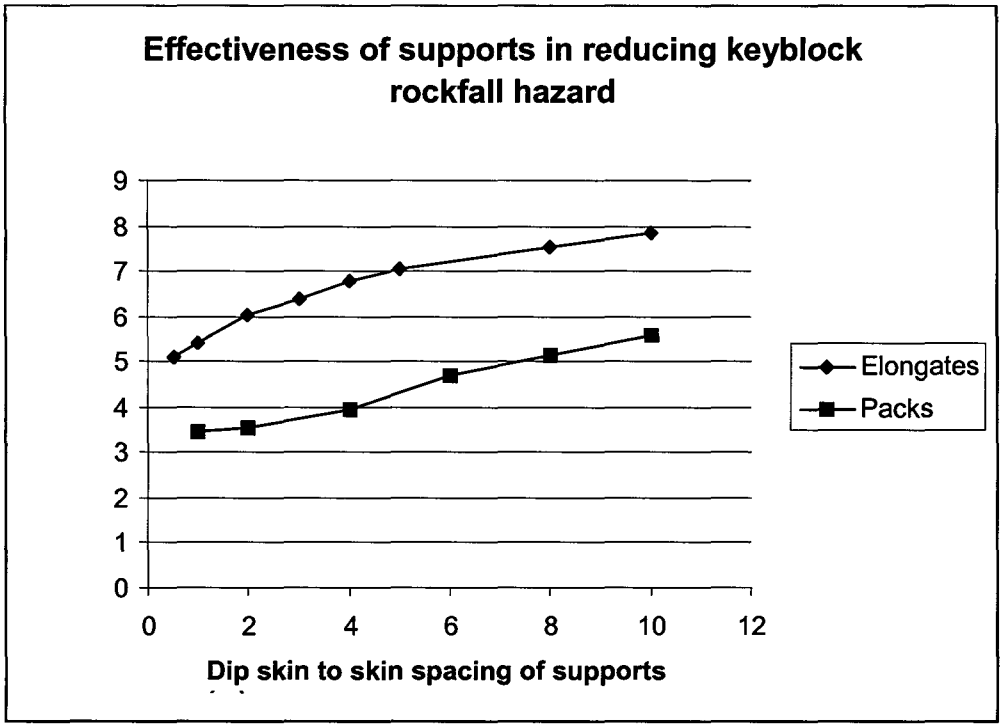

Figure 9.4.7.3-4 Graph showing the effect of support type and spacing on the hazard of keyblock failure, geological structures are 15° off parallel to the face, strike spacing is 2 m.

9.4.7.4 Dip and strike spacing of support

The question of dip and strike spacing of supports was further evaluated by considering the probability of failure of keyblocks in-line with the supports along strike and dip. The objective was to find the ratio of dip and strike spacings that would result in equal probabilities of failure in the two directions for different geotechnical situations. The locations used in the analyses are illustrated in Figure 9.4.7.4-1.

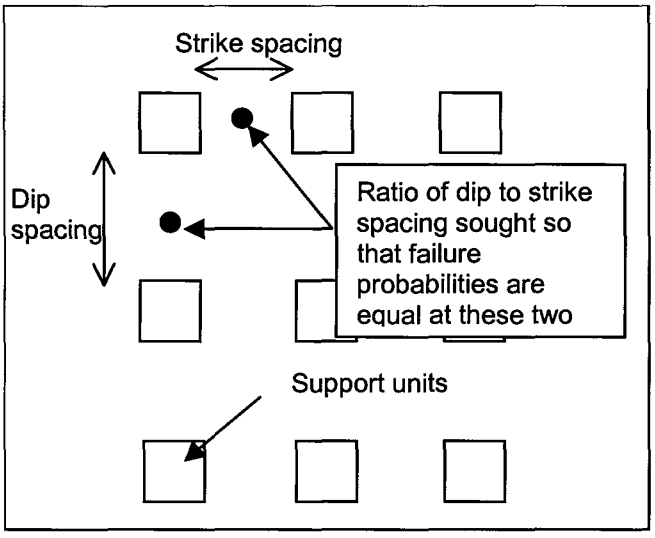

Figure 9.4.7.4-1 Sketch plan showing location of points to evaluate ratio of dip to strike spacing.

The standard discontinuity data set was again used in this analysis. The orientation of the geological structures was varied, as well as the dip of the stress fractures, to evaluate their effects on the failure probabilities. In the analyses the supports were maintained at a skin to skin spacing of 2,0 m in the strike direction. Only the dip spacing was varied. One set of results showing the ratio of dip to strike failure probabilities is presented in Figure 9.4.7.4-2.

The different sets of results were evaluated to obtain the support spacing ratio at which the failure probabilities were equal in the dip and strike directions. The analyses were repeated for point and area type supports. The results are summarised in Figure 9.4.7.4-3 and Figure 9.4.7.4-4. These results indicate that, for the standard data set, the spacing along dip may be at least 1,5 times the spacing on strike, resulting in an equal probability of failure at the points indicated in Figure 9.4.7.4-1. As the strike of the geological structures becomes more parallel to the face, the dip spacing may increase. In practice, however, other criteria of stability, such as support resistance, may no longer be met. A further aspect that is not assessed here is the maximum failure probability in the centre of the unsupported area between the support units.

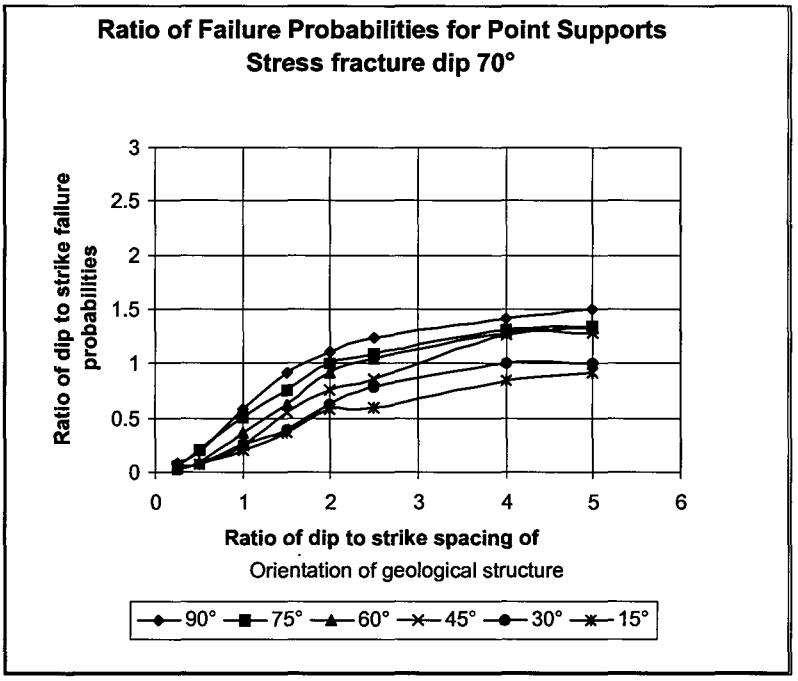

Figure 9.4.7.4-2 Graph showing ratio of dip:strike failure probabilities for point supports, the stress fractures dip at 70 °and the orientation of the geological structures varied as indicated (90 °being perpendicular to the face).

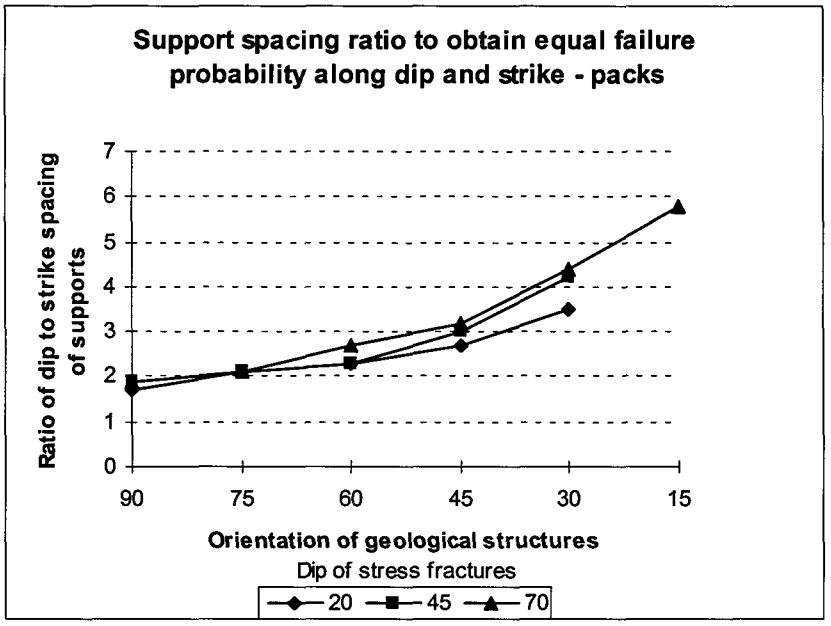

Figure 9.4.7.4-3 Graph showing the ratio of dip:strike spacing of support to achieve an equal probability of failure along dip and strike, for pack supports. Different dips of the stress fractures were considered as indicated.

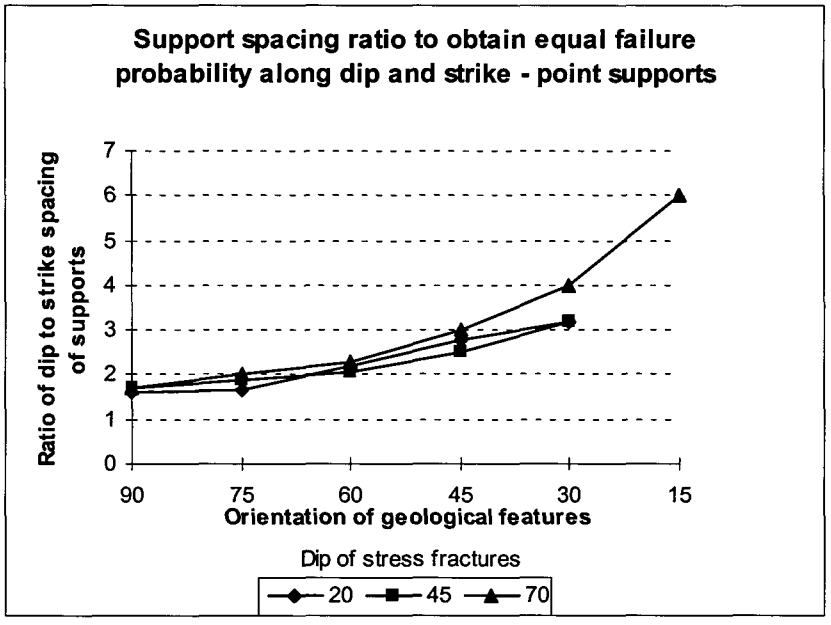

Figure 9.4.7.4-4 Graph showing the ratio of dip:strike spacing of support to achieve an equal probability of failure along dip and strike, for point supports. Different dips of the stress fractures were considered as indicated.

9.4.7.5 Effect of support pattern

It is possible to install supports in different patterns and still have the same number of supports per square metre of hangingwall. The effect of support patterns was evaluated by first studying the effect of using a square or a rectangular support pattern. The rectangular pattern results,

used in the preceding section of this report, were compared to results where the supports were installed in a square patter, i.e. the spacings were equal in both the dip and strike directions. The results were compared by normalising the support density to square metres per support unit. The analyses were carried out using exactly the same sets of keyblocks for the runs.

The results of the first analysis, where the geological structures are perpendicular to the face, are presented in Figure 9.4.7.5-1, where it can be seen that, except for the very high support densities, there is essentially no difference between the two support patterns. If the support densities are the same, the support effectiveness is essentially the same. The results do, however, show that elongate supports result in much higher hazard values than pack type supports. One reason is that the comparison made here includes the area taken up by the support unit, and not the skin-to-skin spacing used earlier. The results indicate, for example, that to reduce the hazard to four potential injuries per 1000 m^2 mined, would require 2 m^2 per elongate (spacing of 1 m x 2 m) and about 10 m^2 per pack (centre spacing of about 3,5 m x 3,5 m). These results are valid only if the geological structures are perpendicular to the stope face. These relative support spacings are remarkably similar to what is often used in the industry in deep mines.

An additional set of analyses was carried out in which the strike of the geological structures was set to 15° off parallel to the stope face. A similar procedure as above was followed to obtain the results shown in Figure 9.4.7.5-2. These results show an overall lower hazard compared to the previous set of results. The reason is that when the geological structures are near parallel to the face, the keyblocks become smaller and pose less of a hazard in terms of causing injuries. These results show that when the supports are closely spaced, the square pattern is more successful than the rectangular pattern in reducing keyblock failure. For example, the rectangular pattern is unable to reduce the fall hazard to below four units. Note that the strike spacing was constant at 2 m for the rectangular spacing runs.

Further analyses were carried out in which checkerboard and diamond support patterns were compared. The standard discontinuity data set was used and supports spaced at 2 m apart were modelled. The support pattern was modified in the different runs by setting the offset between supports to increasing values. An offset of zero results in a checkerboard pattern. As the offset increases the alternate rows of packs are moved in the dip direction so that a diamond shaped pattern is formed. Examples of the support patterns and failure probability distributions are shown in Figure 9.4.7.5-3.

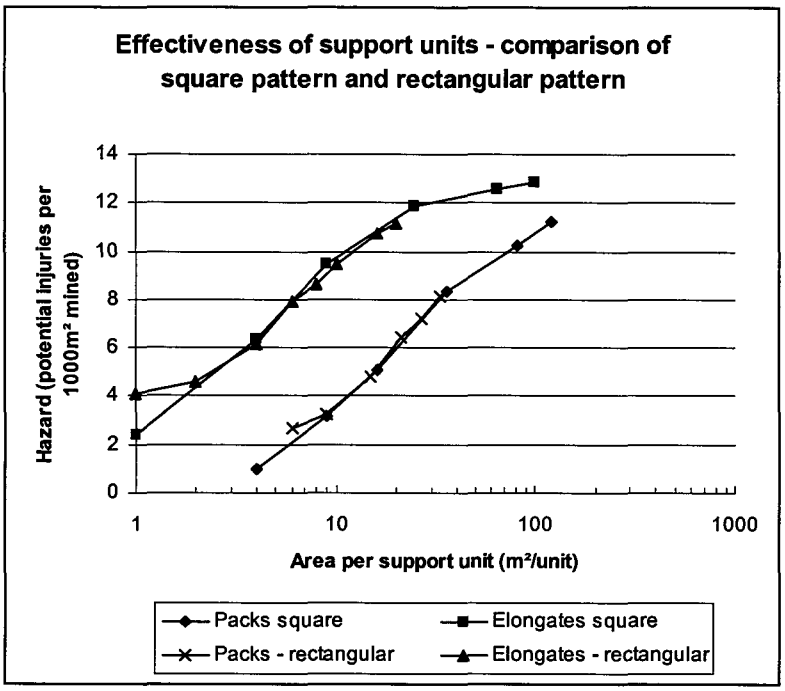

Figure 9.4.7.5-1 Graph showing a comparison of a square and rectangular support patterns in reducing keyblock failure, geological features strike perpendicular to the face.

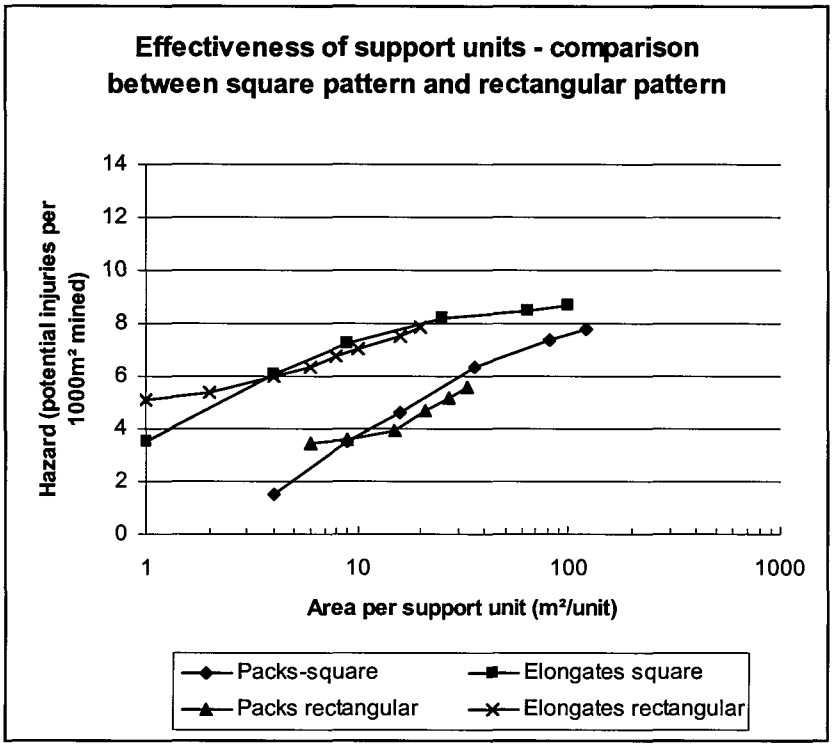

Figure 9.4.7.5-2 Graph showing a comparison of a square and rectangular support patterns in reducing keyblock failure, geological features strike 15° off parallel to the face.

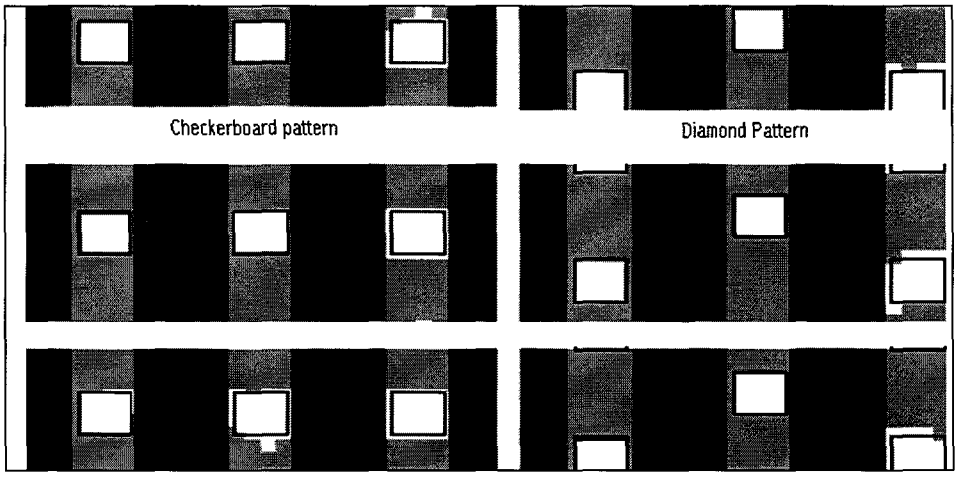

Figure 9.4.7.5-3 Plot showing a checkerboard and diamond support pattern with increasing failure probability of keyblocks indicated by darker shading (offset 0 m for checkerboard patter and 1m for diamond pattern).

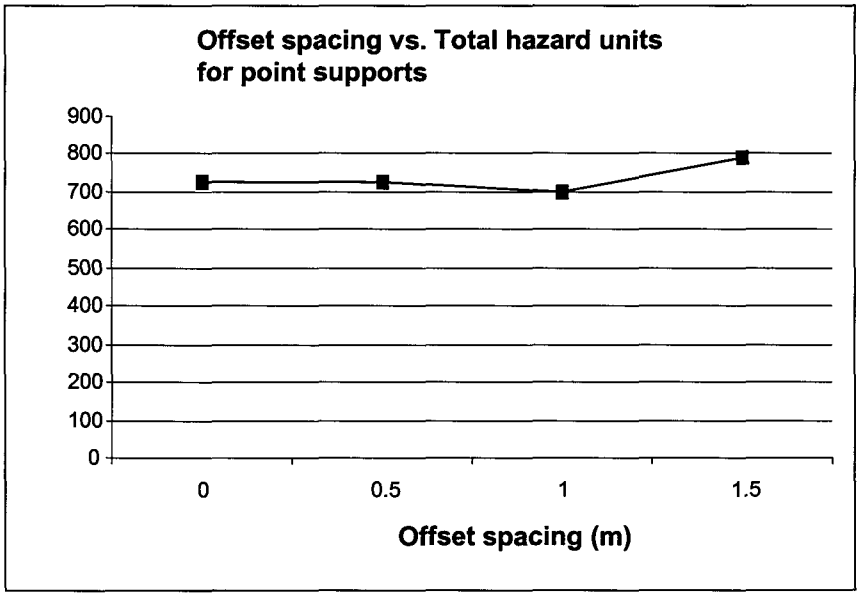

Figure 9.4.7.5-4 Effect of offset of alternate support rows on the potential hazard of keyblock failure, geological features strike 45 ° to the face.

It was found that the offset spacing of the supports had an almost negligible effect on the resulting failure probabilities and hazard values. In one set of results, shown in Figure 9.4.7.5-4, it can be seen that the total hazard units remain essentially unchanged as the support pattern changes.

9.4.7.6 Evaluation of support cycle

The support of stope excavations passes through several cycles as the stope advances. Accident statistics indicate that most fall of ground accidents occur in the face area. The potential for keyblock analysis to evaluate the relative hazard of the different stages of the support cycle was evaluated. A stope using pack supports and mechanical props as temporary

support was evaluated. The standard discontinuity data set was used, with geological structures perpendicular to the stope face. Five stages of the support cycle were modelled as follows:

- Stage 1: After blast – packs 4,5 m from face.
- Stage 2: Three lines of temporary support added after blast.
- Stage 3: One line of packs installed.
- Stage 4: Temporary supports removed to proceed with next blast.
- Stage 5: After next blast – packs 3 m from face.

The specifications of the supports were as follows:

- Temporary support: 100 kN mechanical props, spacing 1,5 m x 1,5 m.
- Permanent support: 1200 kN capacity packs 1 m x 1 m in plan, spacing 3 m x 3 m.

In the analysis of the stages of support, two areas were selected to assess the hazard. The first, called the working area, is an area from the face to a distance of 14 m behind the face. The second area, called the face area, was from the face to a distance of 5 m behind the face.

Results of the analyses, showing the relative hazard of rockfalls for the different stages of the support cycle, are presented in Figure 9.4.7.6-1 where increasing hazard of falls of ground are indicated by the darker shading. These results show the location of high and low failure probability of keyblocks. It is clear that after the blast the stope face area represents a highly dangerous situation, as the keyblock failure probability is high and any loss of clamping or the presence of shallow dipping discontinuities will result in a fall of ground in this area. Once the three rows of temporary supports have been installed, the failure probability is much lower, in spite of the low capacity of the supports. When the next line of packs is installed, the probability remains low. Just before and after the second blast the probability increases, but owing to the small distance of face to the first line of supports, the situation is relatively safer.

The different stages were compared to each other using the rockfall hazard and block size relationship as defined in Section 9.4.1.4. The sum of the hazard units in the working area, and the face area associated with each stage of mining was determined. The results for the working area, that is up to 14 m behind the face, are shown in Figure 9.4.7.6-1, which shows that stage 1, after the blast is about 30 per cent more hazardous than the other stages, where the hazard is essentially equal. For this case, mine support standards would have to be developed to minimise the risk associated with installing support immediately after the blast.

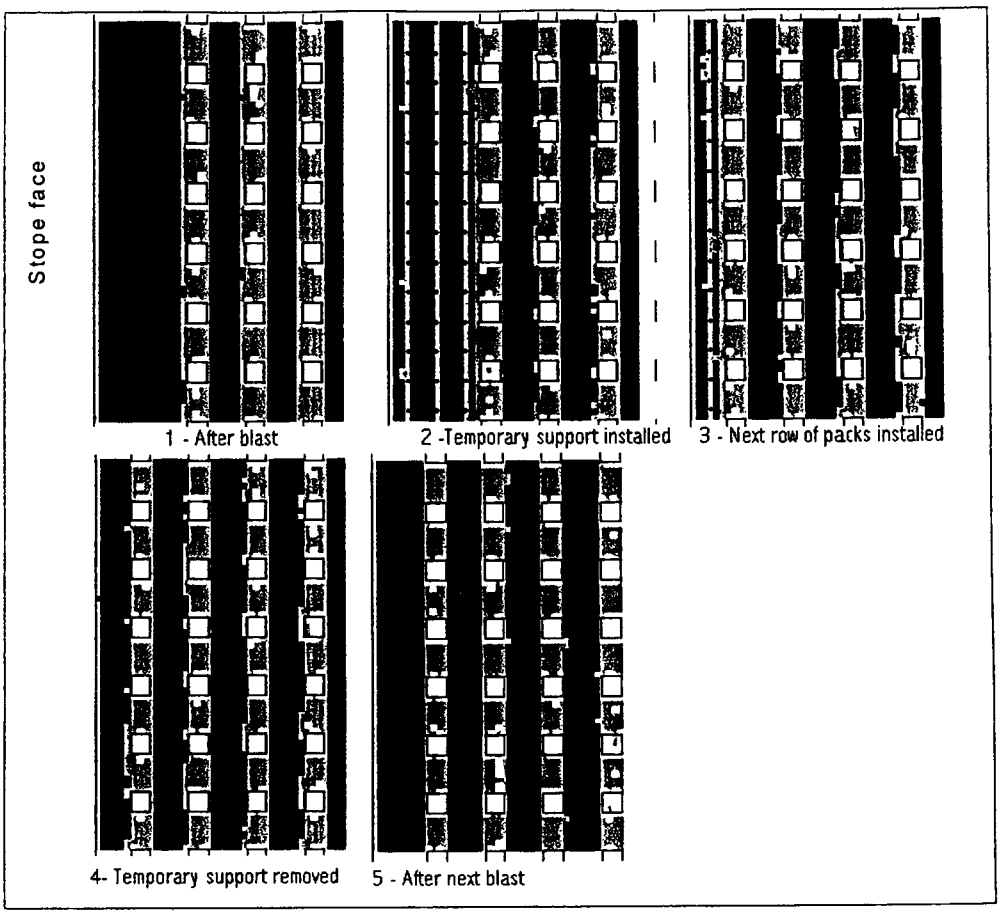

Figure 9.4.7.6-1 Results of keyblock analysis showing failure probabilities in the working area of a stope face through five stages of the support cycle.

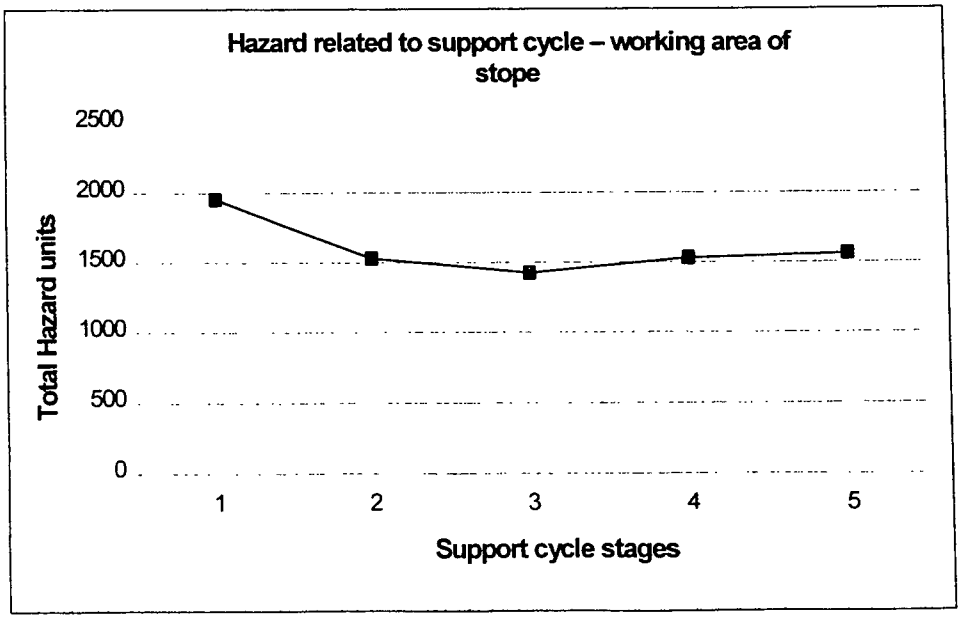

Figure 9.4.7.6-2 Graph showing the total hazard associated with potential keyblock failure in the working area of the stope, i.e. up to 14m behind the face.

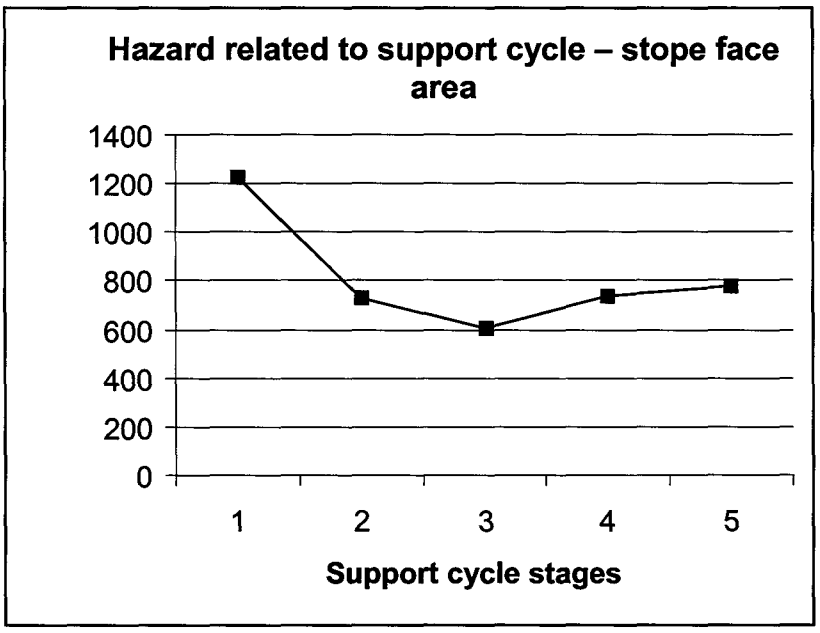

Figure 9.4.7.6-3 Graph showing the total hazard associated with potential keyblock failure in the stope face area of the stope, i.e. up to 4 m behind the face.

The hazard results for the face area show a different picture, as can be seen in Figure 9.4.7.6-3, where it is clear that the stope face area is twice as hazardous just after the blast, compared to the other stages of the cycle. It is also seen that after the packs have been installed near the face, and a single row of temporary supports remain near the face, the hazard of keyblock failure is minimised.

Although the results presented in this section are only applicable to the particular set of input data, they demonstrate how keyblock analysis may be used to evaluate support cycles. Changes to the support standard may easily be evaluated in terms of the change in the rockfall hazard. Areas of high rockfall hazard in the stope may be identified and appropriate changes made to the support standards.

9.4.8 Support design methodology using keyblock analysis

The preceding sections illustrated that the analysis of keyblock stability is able to provide insight into the effectiveness of support layouts in stabilising potential keyblocks. Although the results indicate that, if horizontal clamping stresses are maintained and the discontinuities are steeply dipping, keyblock failure is not possible. If seismic loading occurs, and clamping stresses are lost or shallow dipping discontinuities exist in the hangingwall, then keyblock failure is possible. A methodology to design support using keyblock analysis as part of the support optimisation process is presented in this section.

9.4.8.1 Approach when using keyblock analysis methods

Keyblock analysis should form part of an integrated approach to support design. It is important to remember that keyblock instability is only one of the potential modes of failure that should be evaluated. The requirements of support resistance, energy absorption, and hangingwall beam stability should not be ignored. The results of a keyblock study are able to indicate the relative merits of different support layouts, hazards associated with different stages of the support cycle and the hazard associated with particular geotechnical conditions. The results may be used to optimise support systems for safety and cost.

It is possible to use the keyblock analysis method in two ways:

- To conduct a site specific evaluation of hangingwall stability using localised geotechnical data, and
- to conduct a general assessment of stability using typical geotechnical data for an area of a mine.

The level of detail required for each type of analysis varies. The detailed evaluation may be relevant when an abnormal geological setting or high stress environment exists and it is necessary to modify the standard support system for those conditions. This general assessment may apply to a geotechnical area of a mine and would form the basis for drawing up support standards.

9.4.8.2 Data required for keyblock analysis

A keyblock analysis using the JBlock program requires the following geotechnical data:

- Dip and dip direction of discontinuity sets, as well as the scatter in orientations.
- The average, minimum and maximum spacing of each set of discontinuities.
- The average, minimum and maximum trace length of each set of discontinuities.
- The density of the rock.
- The friction angle of each discontinuity set.
- Clamping stresses in the hangingwall (if available).

Data regarding the stope and support system are as follows:

- The dip and dip direction of the stope excavation and orientation of the face relative to the dip.
- Support type and capacity
- Support dip and strike spacing.

When conducting a general analysis, typical values of the above parameters may be used. It will be necessary to make use of the knowledge of experienced rock engineers and geologists to set up a typical data set. The software does take into consideration variations of input parameters. If the variation is area bound, however, it will be necessary to conduct an analysis of each area separately.

A site specific analysis will require that geotechnical mapping of the different discontinuity sets be carried out to determine how they differ from the typical situation. Before collecting detailed data on the discontinuities, an initial analysis may be carried out using general impressions of an experienced rock engineer or geologist as input data. The most important observation required would be the dip and direction of discontinuities, as well as observations of trace lengths. The quality of the results would obviously be affected by the quality of the input data. Such a preliminary analysis may indicate whether the current support system is suitable or not. Should the preliminary analysis indicate that keyblock stability is a problem, a scan line survey or area mapping of discontinuities will be required.

9.4.8.3 Conducting a keyblock analysis

Once the input data has been collected, a keyblock analysis can be carried out. One of the important decisions is the number of keyblocks to run. From results obtained during this research it appears that at least 5000 keyblocks should be generated to ensure that repeatable keyblock size distributions are obtained. The program has the capability to generate and save a set of keyblocks, so that they can be re-used in different support scenarios. This ensures that each support scenario being evaluated is tested against the same set of keyblocks. Under these conditions it was found that 2000 keyblocks are sufficient. When conducting an analysis

the program automatically calculates the failure probabilities of keyblocks of different sizes, the hazard associated with the keyblock failures and the distribution of failure.

Different loading conditions should be investigated. A worst case scenario, assuming that all clamping stresses have been lost, should be done first. The worst case results should be used to optimise the support layout. The stabilising effect of clamping stresses may then be evaluated, followed by an assessment of the effect of seismic loading, if relevant.

The full support cycle should be assessed for each support layout. Since the hazard varies according to the layout of supports in each part of the cycle. Areas of high hazard should be identified and the support system modified accordingly.

A question that often arises when conducting a probabilistic type of study is "when is the design acceptable". In this regard it is best to make use of back analysis techniques, in which support systems that have been known to be successful in the past are evaluated and used as a reference. A new support system, or a system in changed geological conditions, should result in the same or lower failure probabilities. Ultimately, the results of a keyblock analysis should only be seen as a tool to assist the rock engineer in designing a support layout, as there are other factors, such as practicability and cost, that will affect the final support design.

The keyblock design process may be summarised in a flowchart, illustrated in Figure 9.4.8.4-1. The flowchart shows that keyblock analysis should form part of an overall support design process. Once a suitable support layout has been designed to reduce keyblock failure potential to acceptable levels, the design should be subject to other criteria, such as beam stability, energy absorption and support resistance.

9.4.8.4 Advantages and disadvantages of the keyblock method

The keyblock method of analysis, as embodied in the JBlock program, only considers one mode of hangingwall failure. It should be combined with other analysis techniques to provide a more comprehensive assessment of hangingwall stability. The advantages of using keyblock methods include the following:

- It is fully three dimensional, while most other stability analysis techniques are two dimensional. This means that insight can be obtained on such issues as support patterns, support spacing and failure in the unsupported areas between supports.
- The method is quick to use and provides meaningful results in terms of failure probabilities or fall of ground hazards.
- Except for the horizontal stresses in the hangingwall, the input parameters are easily obtained by visual observation.
- The results are displayed visually and are presented in failure or hazard units.

Some of the disadvantages of the keyblock approach are:

- At present keyblock rotation is not considered. All the forces are assumed to work through the centroid of the keyblock. This results in a non-conservative interpretation of the effectiveness of support units.
- Non-keyblocks are not considered in the analysis. The method only identifies the "first block" that will fail. Subsequent blocks that may be loosened are not considered.
- Combined blocks are, however, considered, that would include some of the non-keyblocks.

The output of the keyblock analysis software used in this research has not been fully verified against the actual performance of the hangingwall. This is a new analysis method and acceptable norms have yet to be developed.

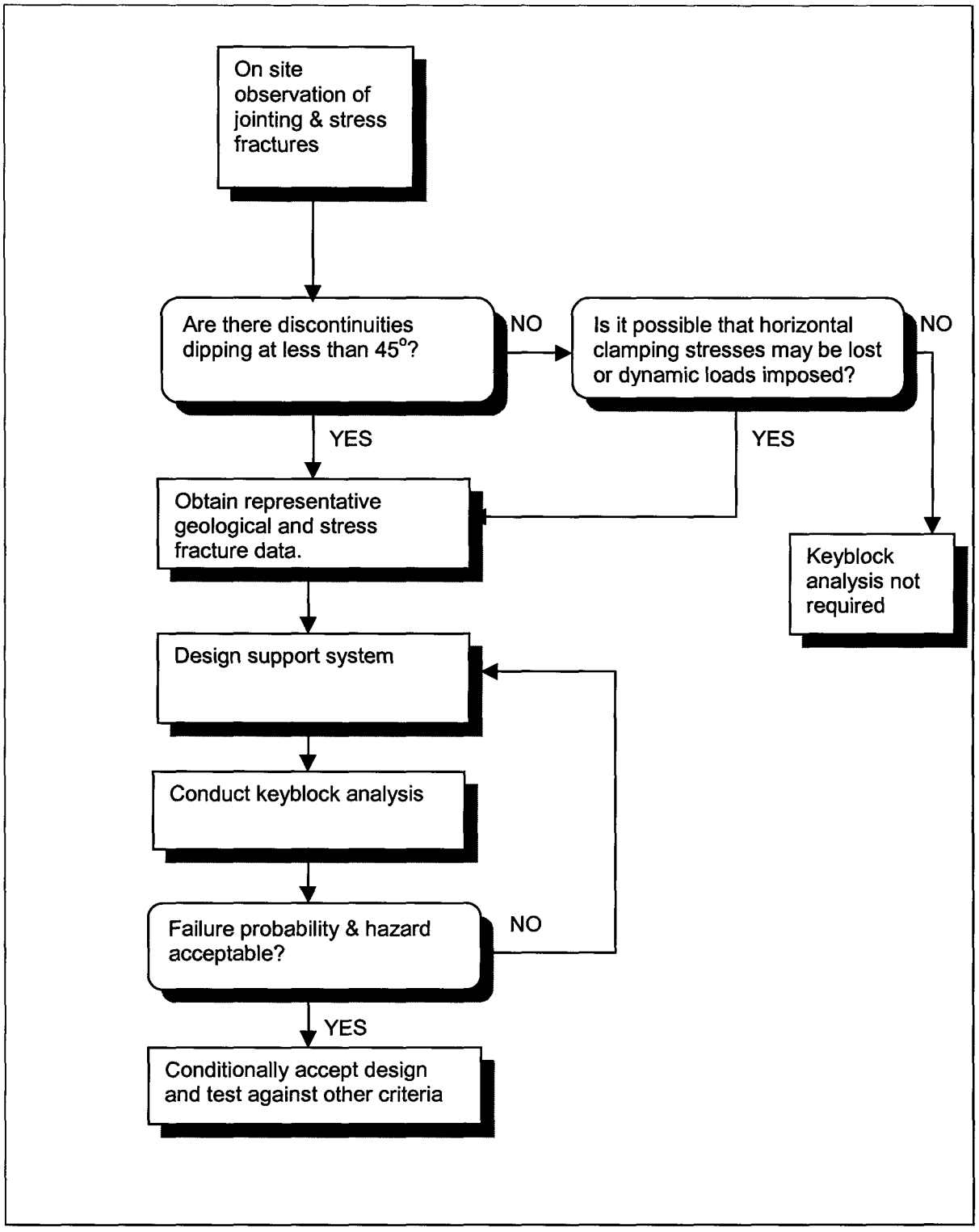

Figure 9.4.8.4-1 Flowchart showing methodology to follow when conducting a keyblock analysis.

9.5 Conclusions

The research into the application of keyblock methods in the design of support systems for deep gold mines has shown that:

- Under quasi-static conditions most keyblocks will be held in position by horizontal clamping stresses in the hangingwall. It is only when shallow dipping discontinuities exist or clamping stresses are lost, through falls of ground, that keyblock stability becomes a concern. When a stope hangingwall is subject to dynamic loading, the additional load may dislodge keyblocks that were previously stable.

- Slab shaped keyblocks are shown to be very stable even if clamping stresses are low. Wedge shaped keyblocks are the most likely to fail and their occurrence and stability may be evaluated using keyblock techniques. The ratio of slabs to wedges in a stope hangingwall may be an indication of its stability.

- The results of the investigation showed that, while the dominant stress fractures in stope hangingwalls are steeply dipping, shallow dipping fractures do occur and are likely to result in keyblock type failures. Geological structures, such as joints or depositional features, are often shallow dipping and may define keyblocks that are unstable.

- Keyblock analysis techniques are suitable for the analysis of the effect of stress fractures and geological structures on the stability of stope hangingwalls. The analysis technique provides realistic block size distributions. The results of such an analysis can assist in optimising support design for local geotechnical conditions.

- A methodology for applying keyblock analysis methods is proposed. It is noted, however, that further verification of the results of the keyblock method is required.

The investigation of the keyblock method has shown that keyblock analysis techniques are able to provide insight into the interaction between stope support units and the fractured hangingwall. The method may be used to account for site specific geological and stress fracturing conditions in support design. Application of keyblock analysis techniques will result in improved support design and hence improved safety in stoping excavations.

9.6 References

Adams, D. J. 1995. Final Report on the work covered during 1993 and 1994, *SIMRAC, CSIR Miningtek, Miningtek Information Centre, Project No GAP 034.*

Brummer, R. K. & Rorke, A. J. 1984. Mining induced fracturing around deep gold mine stopes, *Chamber of Mines research organisation, Project No GR3FO1, Research Report No 38/84, July 1984.*

Department of Mineral and Energy. 1996. Guidelines for the compilation of a mandatory code of practice to combat rockfall and rockburst accidents in metalliferous mines and mines other than coal mines, 1996.

Esterhuizen, G. S. 1996. JBlock user's manual and technical reference, Pretoria.

Esterhuizen, G. S. & Akermann, K. A. 1998. Stochastic keyblock analysis for stope support design, *Int J Rock Mech & Min Sci*, V 35 No 4 /5, p 397.

Eve, R. A., Mitchell, G. P. and Sellers, E. J. 1992. The behaviour of rock surrounding deep level excavations: Trends with increasing stope width, *Chamber of Mines of South Africa, Project No GR1S, Reference Report No 24/92, November 1992.*

Gay, N. C. & Jager, A. J. 1987. Stope support technology in South African gold mines - current status and future developments, *Chamber of Mines Research Organisation, Mining Timber - from stump to stope, CSIR, June 1987.*

Goodman, R.E. & Shi, G. 1985. Block theory and its application to rock engineering, Prentice Hall.

Grodner, M. 1997. *Interim report, SIMRAC Project GAP 330.*

Hagan, T. O. 1996. Stope Face Support Systems, *Interim report SIMRAC Project GAP 330, 14/11/96.*

Jager, A. J. & Turner, P. A. 1986. The influence of geological features and rock fracturing on mechanized mining systems in South African gold mines, *Chamber of Mines of South Africa Research Organization, GOLD 100. Proceedings of the Intern. Conference on Gold. Vol 1: Gold Mining Technology*, Johannesburg, SAIMM.

Joughin, N. C. & Jager, A. J. 1995. Fracture of rock at stope faces in South African gold mines, Research Report, *Chamber of Mines Research Organisation*

.

Priest, S. D. 1993. Discontinuity analysis in rock engineering. Chapman & Hall, London.

Reddy, N. 1998. Personal communication, CSIR Mining Technology, Johannesburg.

Van den Heever, P. 1982. *MSc Dissertation*, Rand Afrikaans University.

10 Review of principal findings and recommendations for further work

Work done under SIMRAC Project GAP 330, *Stope Face Support Systems*, has lead to a delineation of geotechnical areas across the gold and platinum mines, and forms the basis for future understanding of geotechnical area specific rock mass behaviour and support interaction, leading to improved site specific support systems for both static and dynamic loading. Nine enabling outputs have contributed towards this objective. Their findings can be broadly grouped into the following categories:

1. Increased understanding of the effect of support on the local behaviour of the rock mass and improved support design (enabling outputs 1, 4, 5, 6 and 9).

2. Analysis of existing support systems and rock related fatality statistics (enabling outputs 2 and 3).

3. Assessment of support performance (enabling output 8).

4. Identification of impediments to support implementation (enabling output 7).

The four categories, as well as the principal findings, conclusions and recommendations for further work of the associated enabling outputs, are reviewed below.

10.1 Improved understanding of the behaviour of the rock mass and support thereof

The combined findings of enabling outputs 1, 4, 5, 6 and 9 have contributed towards an improved understanding of the behaviour of the rock mass and support thereof. The main areas of progress are as follows:

10.1.1 Delineation of geotechnical areas

10.1.1.1 Summary

The objective of enabling output 1 is to delineate geotechnical areas across the gold and platinum mining industry. Geotechnical areas may be defined by fixed (geological) and variable (mining) parameters (see final project report of SIMGAP 416). In this investigation regional geotechnical area base maps that consider fixed parameters (predominantly footwall/hangingwall rock type assemblage, hangingwall partings, faults, joints and dykes) are compiled. These maps are then re-defined according to 'soft' and 'hard' footwall and hangingwall lithologies, using their uniaxial compressive strength (UCS) values. This aims to provide some indication with regard to the performance of regional and local support, such as footwall and hangingwall punching, or pillar foundation failure. It is expected that the compiled maps will form the basis for additional, detailed regional and local geotechnical subdivision. At this stage, however, they provide an indication of the complexity associated with an orebody, e.g. whether it is positioned in a low or high stress environment, as well as providing some insights with regard to the attitude and frequency of mining induced stress fracturing.

Eight Witwatersrand and two Bushveld orebodies were examined. The number of geotechnical areas, as per rock type assemblage and the distance of major parting planes to the orebody, and the number of re-defined geotechnical areas, using UCS values, are summarized as follows:

Table 10.1.1 Number of geotechnical areas delineated per reef type.

	Number of geotechnical areas (as per rock type)	Number of geotechnical areas (as per UCS)
Merensky Reef	6	-
UG2	4	-
Ventersdorp Contact Reef (VCR)	11	4
VS5	5	3
Witpan (8A)	2	1
Big Pebble Marker (BPM)	3	2
B-Reef	3	2
Leader Reef	1	1
Vaal Reef	7	4
Carbon Leader	6	4

Inspection of the above table reveals that the major orebodies of the West Wits Line (Carbon Leader, VCR) and the Klerksdorp Goldfield (Vaal Reef) formed in the most diverse geotechnical environments. Stope support strategies may, therefore, vary regionally for these orebodies. Partings appear to play a major role in determining hangingwall stability. Fallout thicknesses for the Carbon Leader, for example, can be correlated with the thicknesses of the siliceous hangingwall quartzite, separating the Carbon Leader from the Green Bar.

Orebodies of the Free State (Leader, B, BPM, Witpan) exhibit, except for the VS5, less geotechnical variability. Lithologies with relatively low UCS's predominate, and footwall and hangingwall punching of support or footwall bulging may occur.

Preliminary geotechnical areas have been defined for the platiniferous UG2 and Merensky Reef, with the Merensky Reef exhibiting a higher variability than the UG2. Further scope exists to classify the various footwall and hangingwall assemblages according to their UCS values. Norite and pyroxenite predominate as footwall and hangingwall lithologies, with potholes and domes representing hazardous mining conditions. Hangingwall partings are associated with both orebodies, and are especially prominent within a zone extending for six metres into the hangingwall. An especially pronounced hangingwall parting above the UG2 are three chromitite stringers (Triplets or Three Leaders), which part with ease from the surrounding rocks. They may rest immediately on top of the UG2, but can be several metres above the orebody.

10.1.1.2 Principal findings and conclusions

The compiled geotechnical area base maps provide an indication of the following rock engineering aspects that govern the rock mass behaviour and support thereof: stope stability (especially hangingwall stability, but also fall of ground characteristics and closure rate), attitude and frequency of mining-induced fracturing, seismicity, punching of support, footwall bulging and pillar strength. Areas such as rolls or faulting, where special support may be required, are also, to varying degrees, identified.

The importance of the rock type in determining the attitude and frequency of mining induced fracturing is illustrated. In further work (Section 6), dealing with support interaction with a discontinuous hangingwall beam, the implications of attitude and frequency of fractures on the hangingwall stability are illustrated. The geotechnical classification of the hangingwall and footwall rock types is thus important for the rock engineer to apply in a proposed support design methodology (given in Section 6) to design support systems, stipulate the spacing thereof, and gain insights into the hangingwall stability in various geotechnical areas.

Regional support performance is influenced by factors such as pillar strength and foundation failure, and hangingwall punching. Local support performance is governed in part by footwall and hangingwall punching of support, and areas are identified where the application of headboards is necessary.

The rock mass integrity in the stope vicinity is predominantly predicted through the delineation of major hangingwall partings that, to a large extent, control fall of ground characteristics (e.g. fall-out thickness) and soft footwall regions, were footwall bulging and high rates of closure may occur. The delineated competency of the footwall and hangingwall assemblages provides an indication of closure rate, as well as the attitude and frequency of mining-induced fracturing. These parameters are summarised for various reefs in Table 10.1.2, and are of immediate and practical importance for the rock engineer and design of support systems.

Table 10.1.2 Anticipated rock mass response as predicted for the defined geotechnical environments.

	Footwall soft[1]	Hangingwall Soft[2]	Competent FW/HW assemblage[3]	Incompetent FW/HW assemblage[4]	Pronounced HW partings[5]
Merensky Reef	tbd	tbd	tbd	tbd	✓
UG2	tbd	tbd	tbd	tbd	✓✓
Ventersdorp Contact Reef (hard lava)	(✓)	n/a	✓	n/a	✓
Ventersdorp Contact Reef (soft lava)	(✓)	✓	(✓)	(✓)	✓
VS5	✓	n/a	(✓)	(✓)	(✓)
Witpan (8a)	✓	✓	n/a	✓	✓
Big Pebble Marker	✓	✓	n/a	✓	(✓)
B-Reef	✓✓	✓	n/a	✓	(✓)
Leader Reef	✓	✓	n/a	✓	(✓)
Vaal Reef	(✓)	(✓)	(✓)	minor	✓
Carbon Leader	With increasing depth	n/a	✓	n/a	✓

✓✓ = occurs across the reef
✓ = occurs commonly
(✓) = occurs locally
tbd = to be determined
n/a = not applicable
1 = punching of support; pillar foundation failure; footwall bulging/ride
2 = punching of support; pillar stability
3 = relatively high frequency of mining induced fracturing; relative low closure rates
4 = relatively low frequency of mining induced fracturing; relatively high closure rates
5 = Height of falls of ground controlled by hangingwall parting

To conclude, this work has lead to the delineation of basic geotechnical areas across various reefs. Multiple rock engineering aspects, that need to be considered when designing and implementing support strategies, have been identified and are quantified. To the authors' knowledge, this work represents the most comprehensive regional geotechnical delineation study of South African gold and platinum reefs conducted to date. The delineation of geotechnical areas forms the basis for subsequent work conducted as part of GAP 330, as well as various other research projects currently underway.

10.1.1.3 Recommendations for further work

This study supports earlier observations that geological parameters have an important impact on the behaviour of the rockmass and the support thereof. Further work is, however, required to quantify the influence of geotechnical parameters on support requirements. Specifically, the following aspects are recommended as potential, future activities:

- Geotechnical area maps for the UG2 and Merensky Reef will contribute to the delineation and prediction of areas with varying rock mass behaviour.

- Future underground studies have to confirm and verify the predictions (see Table 10.1.2) as made during this investigation.

- A base map that shows depth contours, the location of major geological features, and rock types. This information can be gathered from boreholes drilled during the pre-production stage and historical data from areas of similar geological setting.

- Thickness contour (isopach) maps for both hangingwall and footwall strata should be compiled. In addition, dominant joint sets and orientations, and mean joint spacing and intensities associated with each rock type should be documented. This information can be deduced from stratigraphic studies and by tapping into experience of both mine geologists and rock mechanics personnel. It is then possible to extrapolate this information from mined out areas to solid ground.

- Isopach maps showing variations in reef thickness and pay width. This information can also be deduced from boreholes during the pre-production stage of the mine. This facilitates the adoption of correct support strategies that eventually improve support performance.

- The magnitude and orientation of the principal stresses should be determined. This will assist in estimating the k-ratio and, in deep mines, the direction of fracturing. Such information influences the correct choice of mining directions, approach angles and mining sequences in the vicinity of seismically active structures.

- Further investigations are required to quantify the relationship between competency contrast and fracture patterns.

- Deformation mechanisms associated with the reef horizons are complex and not well understood, requiring further investigations.

- Detailed rock engineering property studies could, in the future, define 'soft' / 'hard' thresholds that are orebody specific. This holds especially true for the UG2 and Merensky Reef.

- This study highlights the importance of hangingwall partings and their control on stope stability and support performance. A detailed investigation into the behaviour of parting planes will significantly contribute to a better understanding of the relationship between parting characteristics and associated rock mass behaviour.

- Characterisation of the quality of joints in various joint sets is urgently required to improve numerical modelling and identify the critical joint set in a particular geotechnical area. Quantification of joint friction angles, cohesion, shear strength and dilation properties are necessary.

10.1.2 Improved understanding of the rock mass / support interaction

10.1.2.1 Summary

Significant progress has been made in understanding and quantifying the rock mass / support interaction. Three approaches were used to investigate the support interaction, namely: (i) numerical models (enabling output 4), (ii) analytical models (enabling output 6), and (iii) a probabilistic study based on the keyblock approach (enabling output 9). A summary of the main progress associated with each model type follows.

Numerical models (enabling output 4)
Global models investigated the behaviour of bedded strata and their effect on closure mechanisms, as well as the influence of undulating bedding planes. Local models gave insights into hangingwall stability between adjacent support units, as well as zones of support influence.

Analytical models (enabling output 6)
Analytical models were used to quantify stable hangingwall spans between adjacent support units. Two failure modes were considered and parametric studies conducted to investigate the sensitivity to in-situ stresses, attitude and spacing of discontinuities, height of fallout thickness, friction angles, and hangingwall arrest distances following dynamic closure.

Probabilistic keyblock study (enabling output 9)
The University of Pretoria was subcontracted to conduct a detailed probabilistic evaluation of the support layout and geotechnical effects on keyblock failure. The investigation was based on statistical representations of discontinuity attitude, persistence and spacing data, as well as rockfall and rockburst fallout data obtained from the accident database.

10.1.2.2 Principal findings and conclusions

Numerical models
Numerical analyses modelling hangingwall beams have lead to the identification of three mechanisms resulting in stope closure, namely:

(i) The hangingwall beam is displaced into the stope due to gravitational forces.
(ii) Shear movement occurs on bedding planes ahead of the stope face. As a consequence, the hangingwall and footwall beams are subjected to bending moments, resulting in the hangingwall and footwall being displaced into the stope.
(iii) Slip on undulating bedding planes leads to bedding plane dilation and rock deformation into the stope. The dilation is cumulative, in other words the number of active bedding planes affect the total closure.

Effects associated with the various closure mechanisms have previously been identified underground. The closure mechanisms are important for understanding the rock mass behaviour surrounding stopes, and influence support design in terms of support yieldability and bedding plane separation. Associated with the issue of bedding plane separation is a particular stability problem associated with local support. Various numerical analyses were conducted to investigate support that is too stiff and strong, and parts of the immediate hangingwall may be punched through due to bed separation, thereby decreasing overall stability.

Numerical models are used to qualitatively investigate the stress transfer from the support units to the discontinuous hangingwall, thereby giving insights into zones of support influence. It is found that the stress is predominantly transmitted parallel to the discontinuity surfaces, and comparatively little stress (induced by support units) is transmitted across joints and fractures. Hence, from a conservative design point of view, it is assumed that the rock between adjacent support units is not directly supported, and that the stability thereof is governed by (i) shear failure at the abutments, or (ii) hangingwall beam buckling. The stability of the rock mass between adjacent support units, as governed by the two failure mechanisms, is further quantified by means of analytical models.

Analytical models
Analytical models were used to mathematically describe failure mechanism due to shear at the abutments and hangingwall beam buckling. This work has lead to quantified stable hangingwall spans between adjacent support units, and is suitable as a tool to maximise support spacing while maintaining rock mass stability.

On the basis of this work, a methodology is proposed to evaluate support systems catering for rockfall and rockburst conditions. The method consists of two stages: (i) a tributary area analysis determines the general support resistance requirements for the support system as a whole, and (ii) a stability analysis considering failure due to beam buckling and shear at the beam abutments gives maximum safe spacing of individual support units. The method is particularly suited to mines of intermediate and great depth, where, typically, the hangingwall is highly discontinuous due to face parallel mining induced fractures. Results of parametric studies show that with increasing in-situ compressive hangingwall stress, beam thickness and friction angle, hangingwall stability is increased, leading to wider stable hangingwall spans between adjacent support units.

Probabilistic keyblock study
The keyblock method was used to gain insights into the interaction between stope support units and the discontinuous hangingwall. The results agree with those obtained by means of numerical and analytical models, i.e. although separate solution paths were followed, the same general conclusions are found. The research into the mechanisms of supporting a discontinuous hangingwall has shown that:

- Horizontal clamping stresses in the hangingwall contribute significantly towards the rock mass stability. When the clamping stresses are reduced, through, for example, falls of ground, undercutting or irregular hangingwall profiles, the keyblock stability is compromised. Preliminary sensitivity analyses have shown that keyblock stability is significantly reduced when the compressive stresses decrease below $\approx 0{,}2$ MPa. It is therefore important to maintain hangingwall integrity in order to facilitate stress transfer along the hangingwall skin and maximise keyblock stability.
- Slab shaped keyblocks are shown to be very stable, even if clamping stresses are low. Wedge shaped keyblocks are the most likely to fail, and their occurrence and stability may be evaluated using keyblock techniques. The ratio of slabs to wedges in a stope hangingwall may be an indication of its stability.
- The results of the investigation showed that, while the dominant stress fractures in stope hangingwalls are steeply dipping, shallow dipping fractures do occur and are likely to result in keyblock type failures. Geological structures, such as joints or depositional features, are often shallow dipping and may define keyblocks that are unstable.
- Keyblock analyses have shown that, for typical discontinuity spacing and attitude as encountered in intermediate depth and deep gold mines, the support spacing in the dip direction can be increased by a factor of $\approx 1{,}5$ compared with the strike spacing, while maintaining the same probability of keyblock failure in the dip versus strike direction. This ratio is most commonly reversed in current support designs used on mines.

To conclude, substantial progress has been made in understanding and quantifying the mechanisms associated with supporting a discontinuous hangingwall. A new support design methodology, based on keyblock analyses and analytical descriptions thereof, is proposed, leading to optimised support spacing, improved hangingwall stability and, ultimately, safer working conditions.

10.1.2.3 Recommendations for further work

It is recommended to conduct underground examinations and back-analyses to verify the deformation mechanisms identified in this work. This is considered an essential extension of the research in order to calibrate the support design parameters and methodology, and optimise the design procedure.

10.1.3 Underground observations and measurements

10.1.3.1 Summary

As part of realising the objectives of enabling output 5, two underground sites were established and detailed measurements were taken in an attempt to quantify the quasi-static and dynamic rock mass behaviour associated with mining the Carbon Leader Reef. The following instruments were installed: closure-ride stations, extensometers, tiltmeters, crack gauges, a doorstopper and an uphole geophone array comprising five geophones spaced at 2 m intervals, as well as additional geophones placed on the hangingwall skin. Further measurements were taken to map discontinuities and hangingwall profiles.

10.1.3.2 Principal findings and conclusions

Quasi-static instrumentation
Data obtained by means of the instruments recording the quasi-static rock mass deformation were used to establish a conceptual model of the rock mass behaviour. Detailed geological investigations revealed a highly bedded, complex rock structure. New deformation mechanisms have been identified and the effect of blasting and seismicity on the behaviour of cracks and stope tilting investigated. Extensive closure data related to geotechnical area and support type were gathered at three sites and is documented in Appendix V.

At this stage it was found that it is not feasible to conduct numerical analyses modelling the full three dimensional behaviour of the rock mass. The underground measurements revealed highly complex and intricate deformation mechanisms, and preliminary numerical analyses indicated that current software is not capable of modelling such details. Some simplified numerical analyses were conducted, however, dealing with deformation mechanisms of bedded strata and this work is reported in Section 4.

Uphole geophone array
The uphole geophone array has shown a degradation of 'simple' waveforms in the solid to more complex waveforms in the excavation vicinity. Wave trapping, energy channeling and interface waves result in local site effects and velocity amplification. Understanding of site effects and particularly velocity amplification is important to design and quantify energy absorption requirements for effective rockburst resistant support systems.

An important finding of this work is that wave velocities for seismic energy sweeping through the three dimensional geophone array are very low compared to those measured in the solid rock. Previously, only estimates of wave velocities in discontinuous rock were available. This work has shown conclusively that wave velocities are typically an order of magnitude lower compared with wave velocities in solid rock. The low wave velocities are due to the rock mass properties being predominantly characterised by the joint stiffness, as opposed to the elasticity modulus, which, to a large extent, governs the wave speeds in intact rock. This confirms an important conclusion from the static modelling of the rock mass / support interaction, namely the rock behaviour is predominantly governed by discontinuities. This finding is especially important for the modelling of static and dynamic rock mass behaviour in the vicinity of stoping.

10.1.3.3 Recommendations for further work

The deformation mechanisms of the instrumented site were influenced and complicated by various geological features, such as a fault and roll, as well as a regional pillar in the vicinity of the instrumented stope. This has affected the results and complicated their interpretation and numerical back-analyses. It is therefore recommended that further intensive stope instrumentation programmes in geologically simpler and representative stopes be conducted, in order to gain further information focused on validating and obtaining additional data on results and concepts rendered by this project.

10.1.4 Seismic analysis

10.1.4.1 Summary

Further work conducted as part of enabling output 5 entailed an investigation of the seismicity associated with mining the Vaal Reef. The aim of the work was to determine if a correlation exists between the seismicity and the basic stratigraphic geotechnical classifications of the Klerksdorp Goldfield. Further work dealt with the temporal distribution of seismic events.

10.1.4.2 Principal findings and conclusions

The seismic analyses indicated two populations of seismic events, namely (i) low magnitude tremors associated with the formation of fractures at stope faces, i.e. face bursts, and (ii) larger events associated with major geological discontinuities.

It is found that there is some correlation between seismic parameters and geotechnical area. Somewhat higher levels of seismicity are associated with conditions where there is (i) a relatively large contrast in quartzite competency, and (ii) where competent siliceous quartzite occurs in both the hangingwall and footwall.

This preliminary work has shown that a decrease in the area mined for a particular mining step is often accompanied by an increase in the cumulative seismic moment for that step, and it is postulated that sudden changes in the rate of mining may initiate large magnitude seismic events. Further work, however, is required to investigate the influence on seismicity of time-dependent rock deformation, high extraction ratios, and the correlation of total ESS on faults and average ERRs of the area.

10.1.4.3 Recommendations for further work

Based on the findings and conclusions of this work, the following recommendations for further work are made:

- Future studies of this nature should be carried out in geotechnical areas where there is a marked competency contrast in hangingwall and footwall lithology. To overcome the subjectivity of the definition of the seismogenic volumes, it is suggested that the seismic parameters are contoured over the entire area of study, rather than computed for discrete volumes.

- The preliminary studies of the temporal variation of the seismic parameters with mining step have revealed some interesting results (i.e. the increase in cumulative seismic moment for a particular mining step with a decrease in the area mined; the correlation of high seismic moment with small area mined and *vice versa*). Further work investigating the potential triggering mechanisms could give some insights into where/when these phenomena occur. Such mechanisms could be the orientation of the geological features with respect to the regional stress field, rate of mining and mining geometry, and possibly the dewatering of the areas undergoing mining.

10.2 Analysis of existing support systems and rock related fatality statistics

10.2.1 Analysis of existing support usage

The aim of enabling output 2 is to review and quantify existing support usage and practices of the gold and platinum mining industry. The information is given in the form of an industry support database and provides totals for the industry, as well as individual information for the various gold and platinum mines according to shaft, reef types, depth ranges and stoping widths.

The industry support database is a valuable tool to monitor support usage and trends across the gold and platinum mining industry and to form a baseline from which future changes in industry support practices can be compared. It is shown that an expanded version of the support database, coupled with fatality statistics from the accident database, is a suitable tool for gaining further insights into the delineation of geotechnical areas, and for comparing the efficiency of existing support systems from one geotechnical area to another. Current data, giving a snapshot of the support usage in 1995 and 1997, is not sufficient to reach general conclusions regarding the efficacy of various support types in different geotechnical areas.

Mine support practices are changing on a regular basis, and it is recommended that the industry support database be updated on a yearly basis. This will ultimately result in a useful tool, comparable to the accident database, to direct and give insights into support systems requirements for various geotechnical areas.

10.2.2 Maintenance and expansion of accident database

The accident database has been maintained since 1990 and to date encompasses 1807 rock related fatalities. The objective of enabling output 3 is to continue maintaining and expanding the database, and to review and establish rock related fatality statistics and trends, which are associated with South African gold mines. The output of the work is the identification of potentially hazardous reefs and workplaces, and assist with focusing on problem areas and direct research needs.

It was found that of the total number of rock related fatalities associated with the gold mining industry, 56 per cent are due to rockfalls, while 44 per cent are due to rockbursts. Although most fatalities occur on the Ventersdorp Contact Reef, when the fatality data is normalised with respect to square metres mined, the Carbon Leader Reef is the most dangerous reef to mine, with a particularly large proportion of rockburst related fatalities (80 per cent).

Normalised data for all reefs indicates a mean annual decrease in rock related fatalities of 4,5 per cent per annum. The predominant reason for this decline is a significant decrease in the rockburst related fatalities associated with mining the Ventersdorp Contact Reef.

Most fatalities occur in stopes (55 per cent), and of these the majority are within 1,0 and 2,5 m of the stope face. This highlights the inadequacy of temporary support systems and/or their implementation in the immediate face area, and research effort is required to further elucidate this problem and reduce rock related hazards in face area.

It is recommended to continue maintaining and expanding the accident database. Furthermore, the quality of the database would be increased significantly by capturing additional information, such as the mine coordinates of the fatality positions, spacing of support units, descriptions of falls of ground, etc. To this end a new accident data capture form was submitted to the DME in 1996.

10.3 Assessment of support performance

10.3.1 Summary

Timber elongates are being used fairly widely in the gold and platinum mines as panel face area support. Initial testing of elongates has shown that pre-stressable, yielding varieties offer acceptable performance for rockfall and rockburst conditions, however, concern had been expressed that the performance consistency had not been fully evaluated.

The objective of enabling output 8 is to evaluate the quasi-static and dynamic performance characteristics of the 10 most widely used elongate support types, and to recommend a test procedure for quantifying the performance under rockfall and rockburst conditions.

10.3.2 Principal findings and conclusions

A preliminary testing procedure was applied to evaluate the 12 most widely used elongate types. The procedure entailed laboratory compression tests at various displacement rates to simulate rockfall and rockburst conditions, as well as underground tests to determine the in-situ force versus deformation behaviour.

Laboratory tests at various deformation rates showed that the force versus deformation characteristics of most elongate types are loading rate dependant, where timber based elongates generally carry higher loads at increased deformation rates, while frictional units typically carry lower loads at higher rates. Stepped platen tests, representing the effect of a rough hangingwall surface, resulted in lower load carrying abilities up to the point when the elongate had yielded sufficiently to negate the effect of the stepped platen.

During the course of this work the two underground test sites were severely damaged by seismic events, and hence only limited underground data is available. Generally the load carrying capability of particularly timber based elongates is downgraded underground by approximately 10 to 20 per cent. Steel based elongates, such as the Rocprop, showed similar behaviour underground as recorded by laboratory compression tests.

A statistical methodology is formulated to address the variability of elongate performance. The analysis is based on a normal distribution, and takes into account probabilities of exceeding statistically downgraded performance curves, as well as the influence of multiple support units on the average support load bearing capability. As an example of the applicability of the statistical methodology, the quasi-static and dynamic performance of various elongate types is investigated. By means of example evaluations, based on the performance of actual elongates, it is shown that, in order to meet the 90 per cent or 95 per cent probability curve, the design curve is adjusted within reasonable limits. For the 90 and 95 per cent probability curve of meeting the required elongate performance, the support spacing has to be reduced by an average (based on sample calculations using four elongate types) of 10 and 13 per cent, respectively, for the rockfall case, and 8 and 11 per cent, respectively, for the rockburst case.

It is shown that the extent of statistical downgrading of the performance curves depends on the sample size (n), which governs the mean behaviour of the support system. The rock engineer needs to assess the degree of interaction between adjacent support units, and choose the appropriate sample size (n). Typically in deep and intermediate mines the hangingwall is highly fractured, and interaction between adjacent support units is limited. In such a case the local rock mass stability is typically governed by the performance of a single support unit and hence $n = 1$ should be chosen. In shallow mines multiple support units can govern the stability of a larger hangingwall block, and thus sample size can typically range from $n = 2$ to $n = 5$. Until further expertise is developed in quantifying zones of support influence, it is not recommended to use $n > 5$.

10.3.3 Recommendations for further work

Based on the findings of the elongate evaluation programme the test procedure has been slightly modified. It is recommended to use the updated test procedure to quantify elongate performance and to provide standard, officially accepted, load / deformation curves to be used in support design. In addition, a quality assurance procedure needs to be applied in order to ensure consistent performance of existing support units.

It is recommended to use support performance curves that ensure a high probability, i.e. 90 per cent or 95 per cent, of exceeding the support capability. This specification aims for high levels of safety, while rationalising the support costs and practical difficulties associated with installing high-density support systems.

It is recommended to use different performance curves when designing support systems for seismic and non-seismic applications. In some cases the support bearing capacity of elongates increases during dynamic loading, while in certain cases the loading capacity decreases. Thus a single correction factor for various elongate types loaded under quasi-static and dynamic loading conditions is not applicable, and separate performance curves, based on laboratory and in-situ tests, are required.

10.4 Identification of impediments to support implementation.

10.4.1 Summary

Work done as part of enabling output 7 assesses the types of environmental, human and technical problems that can impede successful implementation of stope face support systems. Specifically, the three main objectives of this work were to (i) identify and assess impediments to the successful implementation of support systems, (ii) an assessment of how modifications to the mining/support cycle and mining methods could assist implementation of improved support systems, and (iii) identification of geotechnical areas where rockbolting would be an appropriate support system. A questionnaire was prepared to collect information from individual mines on their experiences with the introduction of new or improved support systems.

10.4.2 Principal findings and conclusions

It was found that the majority of impediments to successful support implementation fall into three categories. These are (i) *generic impediments*, where the most important impediments were cost, performance, and installation effort, (ii) *geotechnical impediments*, where jointing, variable stope widths and rolls were the most important geotechnical criteria, and (iii) *mining impediments*, where the rock breaking process and cleaning were identified as being critical. It has not been possible to establish a firm link between geotechnical area, support types and particular impediments. The prime reasons being that there are too many other factors that have a modifying influence.

The possibility of modifying mining methods to assist implementation of stope face support systems was investigated. It was found that, apart from using blast barricades to contain the rock against the face, thereby reducing cleaning time, and making use of alternative methods to scraping, such as water jetting, particularly for the sweepings, the possibility of modifying the

mining method to improve implementation appears limited. This highlights the limitations created by the explosive rock breaking process to improve support implementation.
Criteria under which rockbolts are being used as face supports on gold and platinum mines are identified. These criteria are extrapolated to indicate potential areas where rockbolts could (should) be considered as face support. It is recognised, however, that the ability to drill the desired length of hole to contain the correct length of rockbolt remains a major barrier in narrow stopes.

10.4.3 Recommendations for further work

It is recognised that, as mines go deeper, support densities are expected to increase, thus further adding to the physical effort required in narrow stopes. Long term solutions may be found in non-explosive mining systems and mechanical handling of support systems. In the short term support installation training and re-enforcement practices are essential. Research should consider alternatives to current technologies or systems to provide areal support at the required density. A system for drilling rockbolts in narrow stopes would also address problems of face access and workforce safety upon re-entry.

Safety in Mines Research Advisory Committee

Final Project Report

Stope Face Support Systems

Appendices

Research agency:	CSIR Mining Technology
Project number:	GAP 330
Date:	December 1998

GAP 330 – Stope Face Support Systems

List of Appendices:

Appendix A: Detailed results of numerical analyses modelling deformations in a layered rock mass.

Appendix B1: Closure data for Western Deep Levels East.

Appendix B2: Quasi-static instrumentation at Western Deep Levels East.

Appendix C: Temporal variation of seismic parameters for Hartebeestfontein G.M.

Appendix D: Laboratory and underground force versus deformation data of various elongate support types.

APPENDIX A

Detailed results of numerical analyses modelling deformations in a layered rock mass:

friction angle	dilation angle	number of layers	layer width	Gravity	mining steps	final span	mid-span stress	mid-span sag
15	10/0	18	2m	Yes	1	72m	8.55	227.11
15	0/0	18	2m	Yes	1	72m	8.52	203.47
15	0/0	18	2m	No	1	72m	6.77	146.07
15	10/0	18	2m	No	1	72m	2.12	162.38
15	45/45	18	2m	No	1	72m	13.85	>500.0
15	45/45	18	2m	Yes	1	72m	11.72	>500.0
15	30/0	18	2m	No	1	72m	7.12	242.57
15	30/0	18	2m	Yes	1	72m	13.32	321.56
15	20/20	1	2m	No	1	72m	11.70	120.38
15	20/20	1	2m	Yes	1	72m	12.12	120.71
15	0/0	1	2m	yes	1	72m	12.97	120.58
15	0/0	1	2m	no	1	72m	12.96	120.50
15	30/0	1	2m	no	1	72m	11.40	120.44
15	30/0	1	2m	yes	1	72m	11.93	120.94
15	45/0	1	2m	yes	1	72m	11.26	121.56
15	45/0	1	2m	no	1	72m	11.11	120.71
15	0/0	1	1m	no	1	72m	17.10	119.29
15	0/0	1	1m	yes	1	72m	16.98	119.31
15	45/0	1	1m	yes	1	72m	15.16	119.51
15	5/0	18	2m	no	4	16m	24.03	35.93
15	5/0	18	2m	no	10	36m	5.95	97.99
15	5/0	18	2m	no	14	52m	2.02	133.81
15	5/0	18	2m	no	18	72m	-0.04	163.32
15	5/5	18	2m	no	4	16m	24.30	35.98
15	5/5	18	2m	no	10	36m	5.95	99.13
15	5/5	18	2m	no	14	52m	1.78	135.97
15	5/5	18	2m	no	18	72m	-0.44	166.53
15	10/0	18	2m	no	4	16m	24.18	36.81
15	10/0	18	2m	no	10	36m	6.33	104.09
15	10/0	18	2m	no	14	52m	2.24	142.81
15	10/0	18	2m	no	18	72m	0.22	175.08
15	10/10	18	2m	no	4	16m	24.06	36.82
15	10/10	18	2m	no	10	36m	6.57	106.53
15	10/10	18	2m	no	14	52m	2.28	147.68
15	10/10	18	2m	no	18	72m	-0.20	181.36

friction angle	dilation angle	number of layers	layer width	gravity	mining steps	final span	mid-span stress	mid-span sag
15	10/0	18	2m	n0	4	16m	24.18	36.81
15	10/0	18	2m	no	10	36m	6.33	104.09
15	10/0	18	2m	no	14	52m	1.62	142.81
15	10/0	18	2m	no	18	72m	0.22	175.08
15	5/5	18	2m	no	4	16m	24.30	35.98
15	5/5	18	2m	no	10	36m	5.95	99.13
15	5/5	18	2m	no	14	52m	1.78	135.97
15	5/5	18	2m	no	18	72m	-0.44	166.53
15	20/0	18	2m	no	4	16m	25.62	39.31
15	20/0	18	2m	no	10	36m	8.45	120.85
15	20/0	18	2m	no	14	52m	3.96	168.00
15	20/0	18	2m	no	18	72m	1.17	205.94
15	20/20	18	2m	no	4	16m	25.80	39.45
15	20/20	18	2m	no	10	36m	9.04	125.27
15	20/20	18	2m	no	14	52m	4.08	177.25
15	20/20	18	2m	no	18	72m	1.10	220.86
15	20/20	18	2m	yes	4	16m	26.26	39.58
15	20/20	18	2m	yes	10	36m	11.60	130.17
15	20/20	18	2m	yes	14	52m	8.80	197.35
15	20/20	18	2m	yes	18	72m	5.38	262.05
15	30/0	18	2m	yes	4	16m	29.78	43.70
15	30/0	18	2m	yes	10	36m	15.67	157.32
15	30/0	18	2m	yes	14	52m	10.55	234.80
15	30/0	18	2m	yes	18	72m	6.65	307.67
15	30/30	18	2m	yes	4	16m	29.51	43.59
15	30/30	18	2m	yes	10	36m	16.09	161.90
15	30/30	18	2m	yes	14	52m	11.37	247.25
15	30/30	18	2m	yes	18	72m	6.01	324.53
15	45/0	18	2m	yes	4	16m	40.10	55.08
15	45/0	18	2m	yes	10	36m	29.49	218.91
15	45/0	18	2m	yes	14	52m	16.47	412.18
15	45/0	18	2m	yes	18	72m	8.14	>500.0
15	45/45	18	2m	yes	4	16m	39.84	54.96
15	45/45	18	2m	yes	10	36m	36.91	299.43
15	45/45	18	2m	yes	14	52m	24.36	477.57
15	45/45	18	2m	yes	18	72m	-10.97	>500.0

friction angle	dilation angle	number of layers	layer width	gravity	mining steps	final span	mid-span stress	mid-span sag
30	5/0	18	2m	no	4	16m	25.21	28.83
30	5/0	18	2m	no	10	40m	14.84	78.89
30	5/0	18	2m	no	14	56m	11.38	110.29
30	5/0	18	2m	no	18	72m	9.45	138.52
30	5/0	18	2m	yes	4	16m	25.30	28.84
30	5/0	18	2m	yes	10	40m	15.91	79.44
30	5/0	18	2m	yes	14	56m	14.70	118.17
30	5/0	18	2m	yes	18	72m	15.54	167.04
30	20/20	18	2m	no	4	16m	24.94	29.58
30	20/20	18	2m	no	10	40m	15.24	87.30
30	20/20	18	2m	no	14	56m	11.80	126.39
30	20/20	18	2m	no	18	72m	9.80	162.71
30	45/0	18	2m	yes	4	16m	28.98	32.74
30	45/0	18	2m	yes	10	40m	24.50	122.61
30	45/0	18	2m	yes	14	56m	22.36	197.05
30	45/0	18	2m	yes	18	72m	19.00	268.33
30	20/20	1	2m	no	4	16m	22.99	28.06
30	20/20	1	2m	no	10	40m	15.60	67.46
30	20/20	1	2m	no	14	56m	16.09	93.90
30	20/20	1	2m	no	18	72m	16.48	120.26
30	20/20	1	2m	yes	4	16m	23.33	28.18
30	20/20	1	2m	yes	10	40m	16.09	67.66
30	20/20	1	2m	yes	14	56m	17.04	94.20
30	20/20	1	2m	yes	18	72m	17.43	120.55
15	30/0	1	4m	no	1	72m	6.98	135.17
15	30/0	1	6m	no	1	72m	16.06	157.61
15	30/0	1	8m	no	1	72m	21.27	157.02
15	30/0	1	4m	no	18	72m	8.68	142.11
15	30/0	1	6m	no	18	72m	16.67	159.27
15	0/0	1	2m	yes	1	72m	12.97	120.58
15	0/0	1	4m	yes	1	72m	10.69	134.37
15	0/0	1	6m	yes	1	72m	17.49	145.18
15	0/0	1	8m	yes	1	72m	20.80	141.09
15	0/0	1	16m	yes	1	72m	28.69	130.98
30	0/0	1	4m	yes	1	72m	17.19	126.49
30	0/0	1	6m	yes	1	72m	22.20	132.13
30	0/0	1	8m	yes	1	72m	24.63	129.14

Appendix B1

Closure data for Western Deep Levels East.

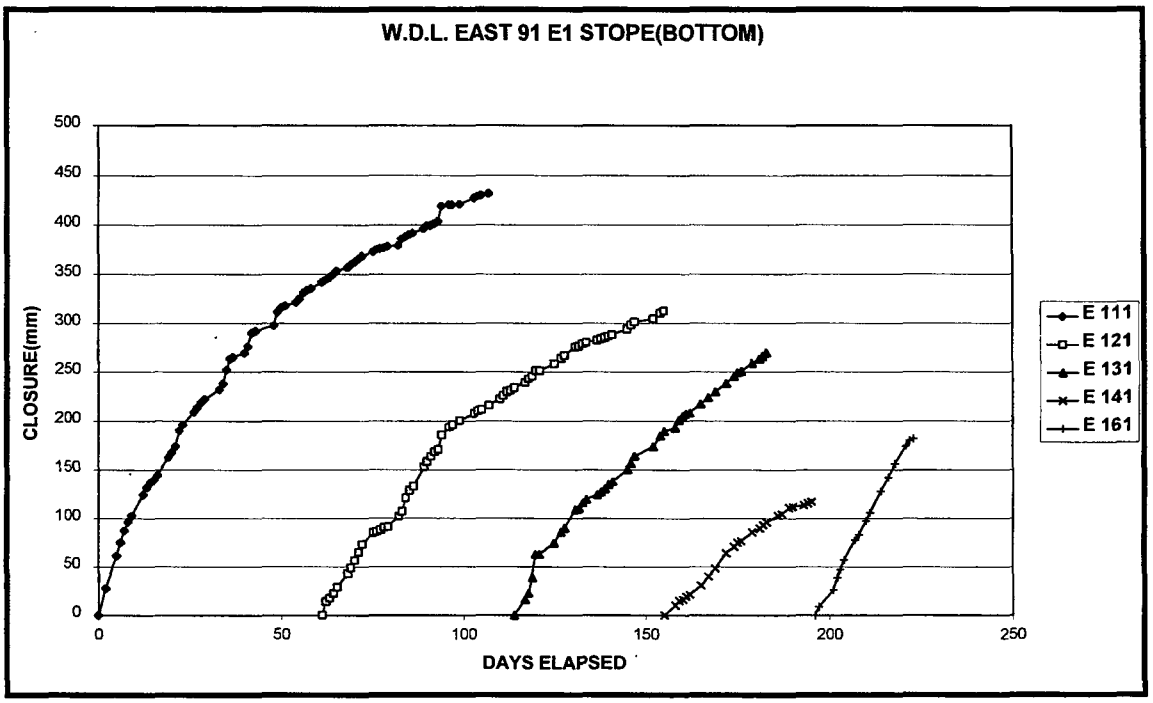

Figure B1-1 Closure data for 91 E1 stope bottom stations

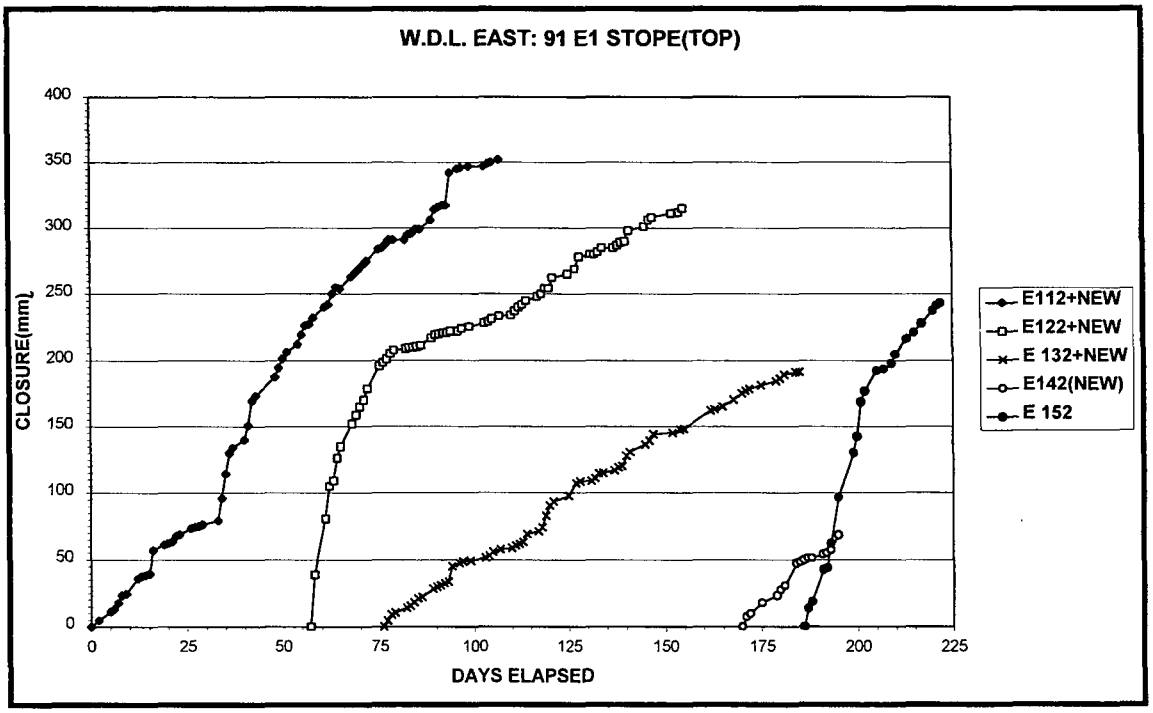

Figure B1-2 Closure data for 91 E1 stope top stations

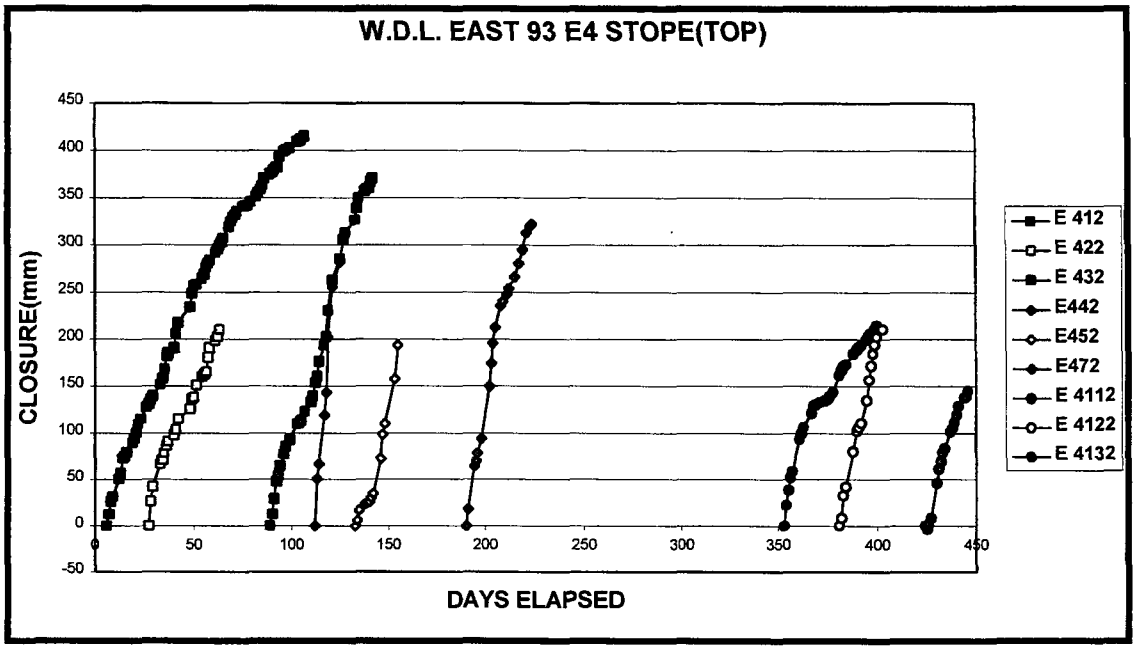

Figure B1-3 Closure data for 93 E4 stope top stations

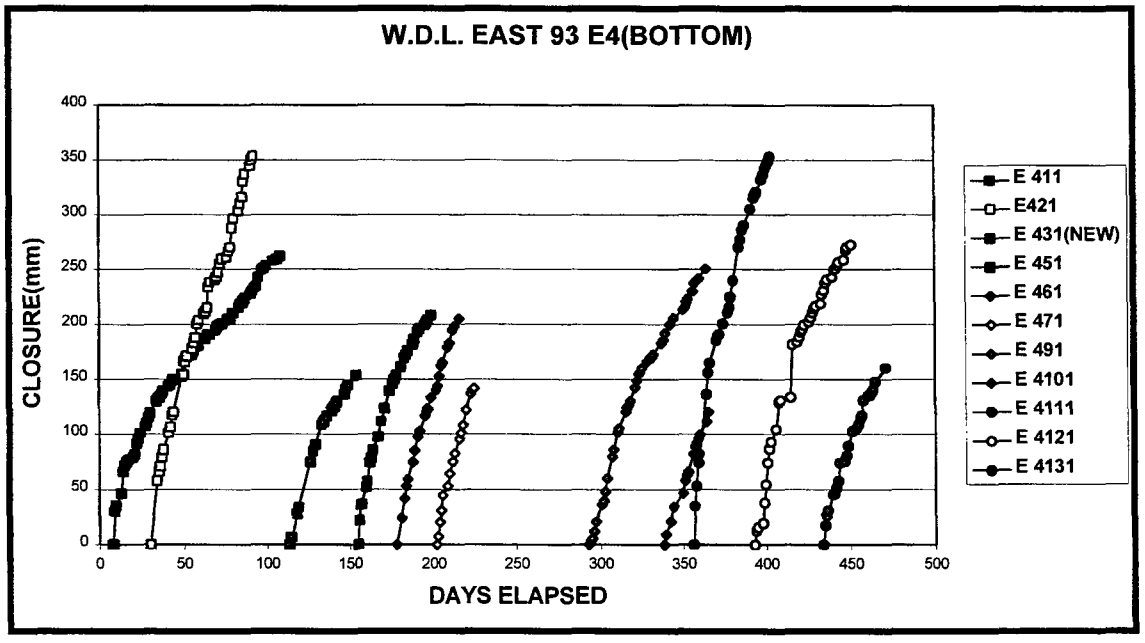

Figure B1-4 Closure data for 93 E4 stope bottom stations

APPENDIX B2

Quasi-static instrumentation at Western Deep Levels East, 93 E4 panel

Introduction

The continuous instrumentation and monitoring programme was undertaken to monitor the behaviour of the rock mass. Extensometers, crack gauges, tiltmeters, and closure-ride instruments were installed at pre-determined positions in the stope. The installed instrumentation was connected to a battery-operated data logger for the continuous recording of data. The test data was stored on a removable PCMCIA card. Data reduction was done on a PC with standard spreadsheet software.

System Requirements

The following measuring instruments were decided upon to measure the various parameters:

- *Doorstoppers* to measure the change in strain were installed and left in position to monitor strain changes in the hangingwall. The doorstoppers were constructed with a four-element strain gauge rosette.
- *Closure-ride* stations for recording the closure between the hangingwall and footwall of the stope were installed. Linear potentiometers with 300mm travel were used as the transducers in the closure-ride instruments.
- *Extensometers* were installed in vertical boreholes in the hangingwall to monitor movement between different rock layers. Linear potentiometers with 150 mm travel were used as the transducers in the extensometers.
- *Crack gauges* were installed over prominent cracks/joints in the hangingwall. Linear potentiometers with 50mm travel were used as the transducers in the crack gauges.
- *Tiltmeters* were attached to the hangingwall and footwall to monitor the tilt behaviour along dip and strike.

The different types and the total number of measuring transducers as well as the logging requirements dictated the overall requirements for the data logging system as follows:

- The logger must be battery operated and must be able to operate for at least three days on a battery.
- At least 30 channels input to the logger to accommodate all the instruments.
- The sensitivity of channels must be adjustable from volts to microvolts to ensure that the voltage output from all transducers can be measured.
- Data storage must be on a removable medium in an ASCII format to ensure compatibility with standard spreadsheet software.
- Data storage capacity must be big enough for the logger to operate for at least five days.
- Logger must be able to withstand the harsh underground environment.

Test site

The instruments were installed and measurements were carried out at WDL-East mine in panel 93E4. Extensometers and doorstoppers were installed in diamond drilled boreholes; closure-

ride and crack gauges were attached to special bolts installed in the hanging wall and footwall. A schematic layout of the test site is shown in Figure B2-1.

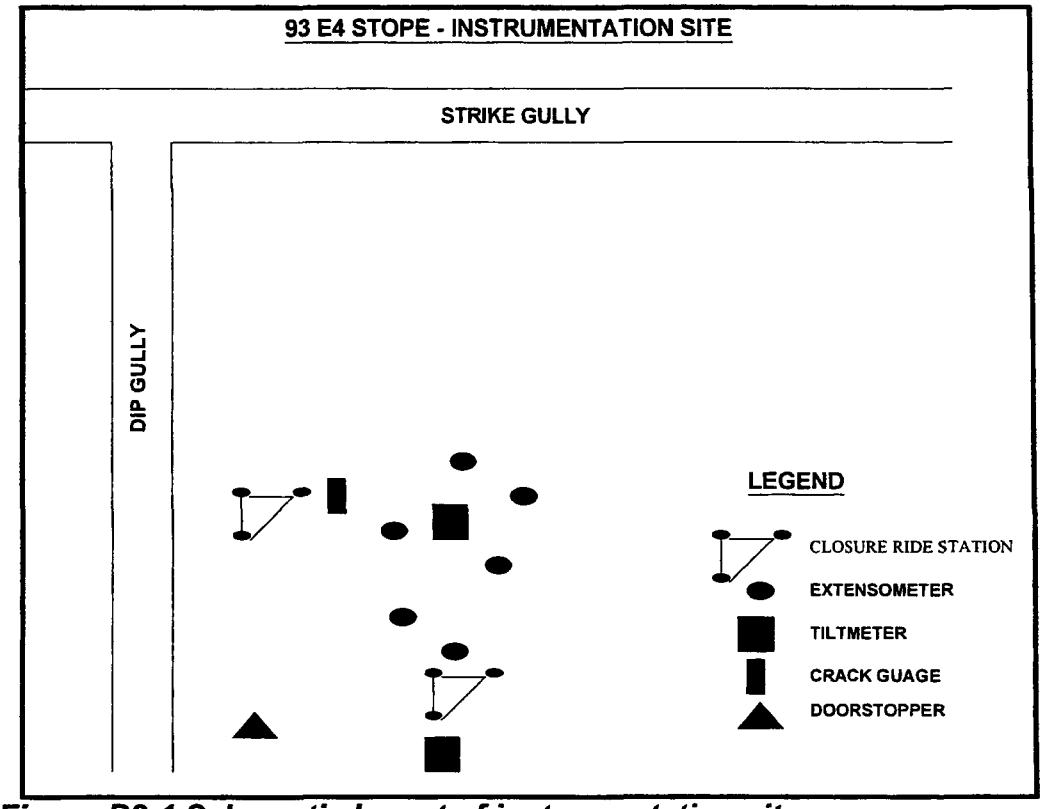

Figure B2-1 Schematic layout of instrumentation site

Measuring System

The measuring system consisted of transducers, wiring, battery, signal conditioning, signal measurement, calculations and data recording. The data logging software was developed on a personal computer. This dedicated software was downloaded into the datalogger to configure the logger for the different type of input signals and logging routines. Data was stored on a removable PCMCIA card. A flow diagram with the different components of the measuring system is shown in Figure B2-2.

Transducers

The various transducers used are presented in Table B2-1.

Doorstopper

Doorstoppers were modified with a four-core electrical cable permanently attached to the instrument as well as additional strain gauges to complete the strain gaugebridge. The modified instrument was cemented in position with a suitable strain gauge cement. The standard installation procedures for Doorstoppers were used to ensure reliable outputs. The strain gauges in the doorstopper are capable of measuring the induced strain in the rock directly in micro-strain units.

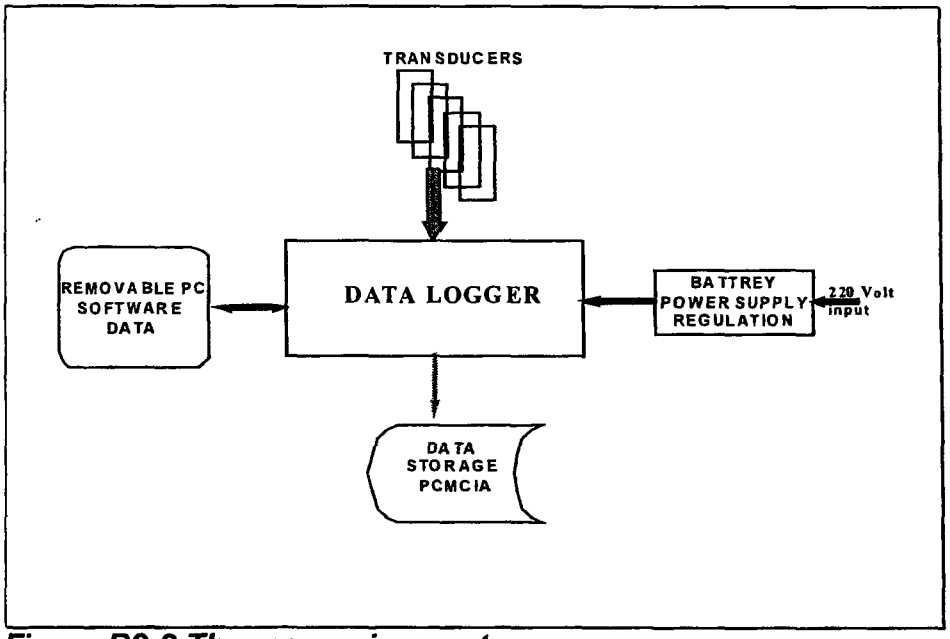

Figure B2-2 The measuring system

Table B2-1 Description of transducers used

TRANSDUCER	DESCRIPTION
Doorstopper	Strain gauge based instrument to measure change of strain in the rock in three directions.
Extensometer	Mechanical instrument with built in linear displacement transducer to measure displacement between collar of borehole and end of hole.
Tiltmeters	Bi-axial transducers to measure tilt of the hanging wall.
Closure-ride	Mechanical instrument with built in linear displacement transducer to measure displacement.
Crack meters	Mechanical instrument with built in linear displacement transducer for displacement measurements.

Extensometers

Mechanical extensometers to measure lengths of 0,5, 1,0 and 1,5 meters were designed and manufactured. Figure B2-3 shows the details of an assembled extensometer. The transducer in the extensometer measuring-head consists of a linear potentiometer with an internal resistance of 20kΩ and a measuring range of 100mm. A regulated stable voltage was applied over the potentiometer. Any changes in distance were measured as a change in output volts between the slider and one end of the resistor, which was connected, to the power source.

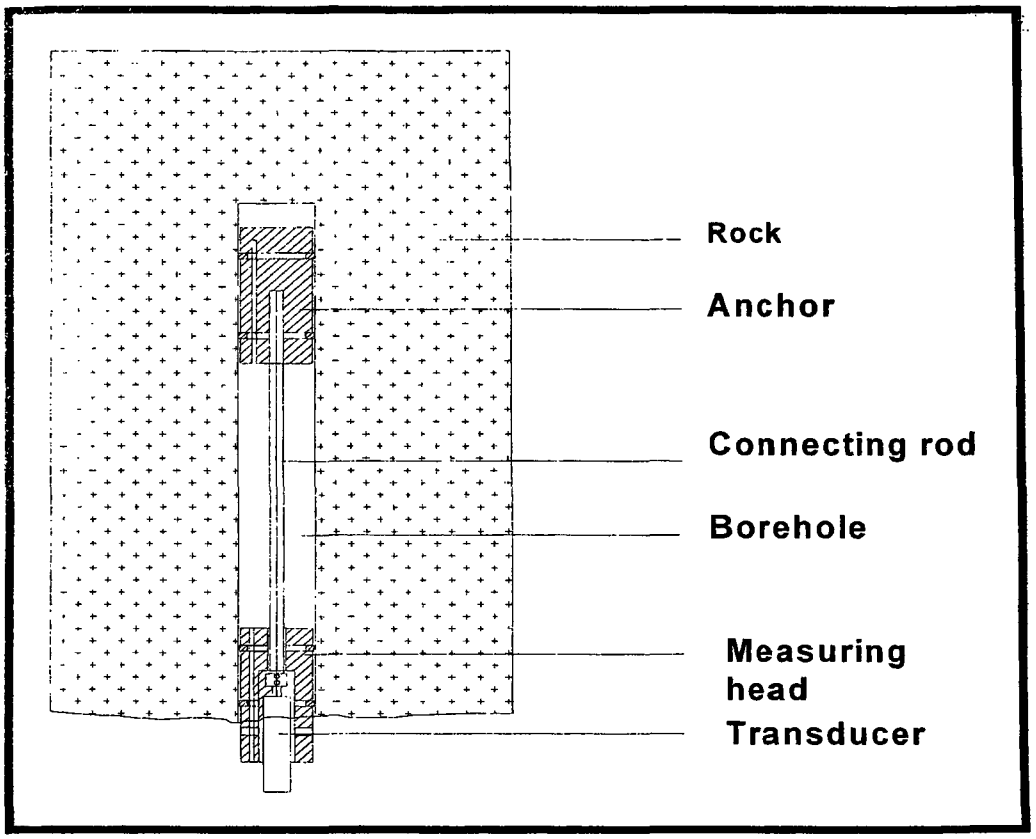

Figure B2-3 Extensometer configuration

Tiltmeters

A dual axis gravity reference clinometer was used to measure the tilt of the hangingwall and the footwall. The sensing element in the tiltmeter is a glass vial half-filled with a conductive liquid. When the sensor is level, fluid covers five internal electrodes to equal depths. When the sensor tilts, the depth of fluid on each electrode changes, altering the electrical resistance between matched pairs of electrodes. The electronic circuit measures these changes and converts them to DC (volt) outputs, which is proportional to the tilt angle.

Closure-ride

Closure-ride stations were installed between the hangingwall and footwall to measure the change in distance between the roof and floor of the excavation. Figure B2-4 shows the details of the measuring unit of a closure-ride instrument. The transducer (linear potentiometer) was used to measure changes in lengths. Closure-ride measuring stations consisted of three instruments, attached to different points, in a triangular configuration, on the hangingwall. The other ends were connected at the some point in the footwall.

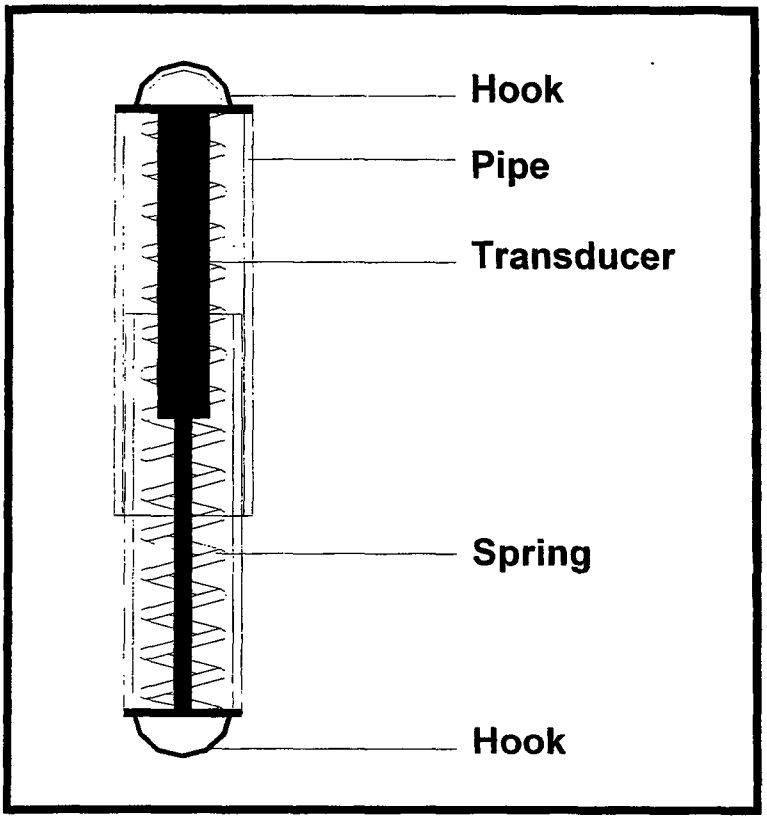

FIGURE B2-4 Closure-ride measuring system

Crack gauge

A crack gauge was installed over a large visible fault in the hangingwall. The instrument consisted of a linear displacement transducer (50 mm travel) with special spherical attachments on both ends of the transducer. The spherical attachments ensured easy fixing of the instrument to the rock surface as well as ensuring that no bending moments could be transmitted to the linear transducer.

Logging System

A Datataker 600 data logging system was selected to continuously monitor the instrumentation. The main features of the system were:

- Microprocessor based battery powered data logger
- Extender units can be added to system to increase the input channels
- Autocalibration and autoranging
- Resolution 15 bit plus sign, 1μVolt
- Sampling rate of 25 samples per second
- Time and date stamp with 1 second resolution
- Data storage internal 13 650 readings
- Removable memory card, store up to 340 000 readings
- ASCII data storage format
- Programming via RS232 port
- Compatible with computers (PC)
- Operating temperature –20 to 70 °C
- Humidity up to 95%

An external battery was connected to the logger to ensure that the system could continue to function for 150 hours in case of a power failure. The battery unit consisted of a 65 AH battery as well as a charger and a regulated 5-volt power output for transducer excitation.
The logger was built into an IP67 rating steel box (waterproof steel box). Cables from the measuring instruments were terminated in the box via cable glands.

Software

Software for data acquisition and logger control was developed to meet the specific requirements of the system. The software and data were stored on a removable PCMCIA card, which is compatible with the data logger. The strains, displacement and tilts were calculated from the voltages measured and stored as a spreadsheet file. Figure B2-5 shows a schematic diagram of data acquisition and control.

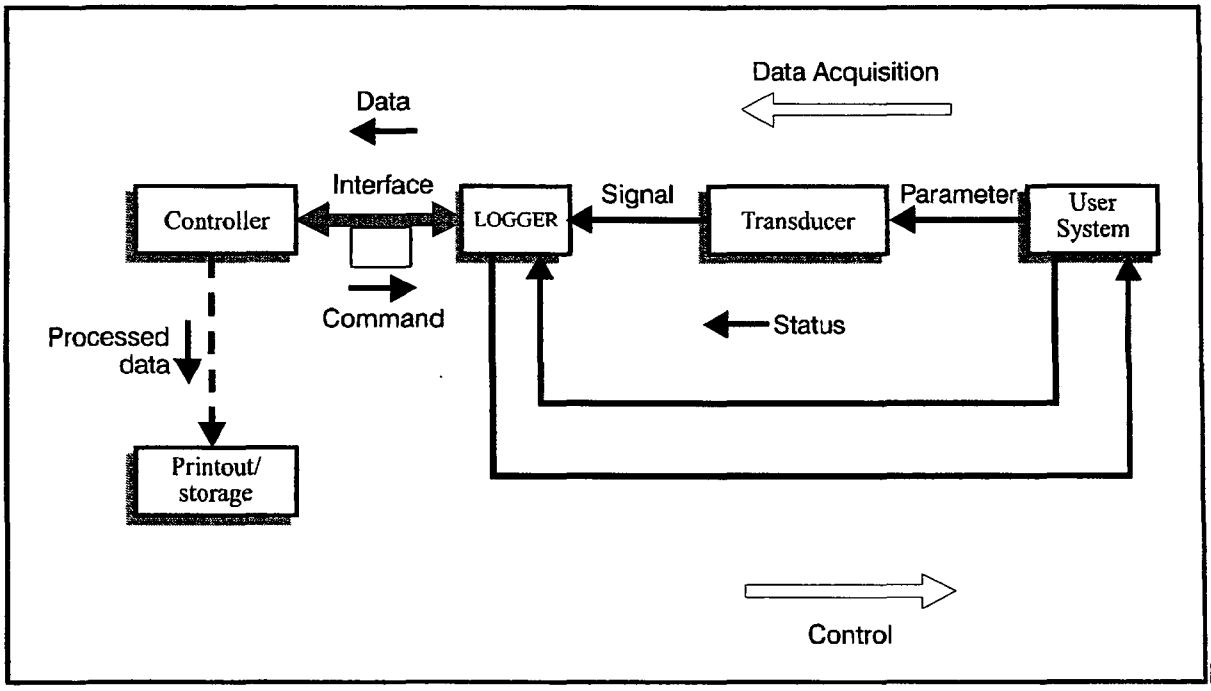

Figure B2-5 Data acquisition and control

Calculations

The data on the PCMIA cards were downloaded into a PC. Standard spreadsheet programmes were used to evaluate the data and to produce graphs of the various measurements.

Strain

The volt output of the doorstoppers was converted into strain. The following formula was used to calculate the strain from the voltage output of a strain gauge quarter bridge configuration.

vr = (Vout/Vin)-(Voutzero/Vinzero)
strain = (-4 * 1000000 * vr) / (k * (1 + 2 * vr))
Where:

vr	*- Relative voltage*	*V/V*
Vout	*- The output voltage of the bridge*	*V*
Vin	*- The input voltage to the bridge*	*V*
Voutzero	*- The output voltage of the bridge*	*V*
Vinzero	*- The input voltage to the bridge*	*V*

strain - *Strain*
k - *Gauge factor*

Displacement calculations

The following relationship was used to calculate the displacements from the linear potentiometers.

Displacement =(1000000 * (Output_Voltage - Zero_Voltage) * Cal_Factor)

Where:

Displacement - *mm*
Output_Voltage - *Volt*
Calibration_Factor - *mm/Volt*
Zero_Voltage - *Volt*

Tilt calculations

Tilt = (Gauge_Factor * (Voltage))

Where:

Tilt = *degrees*
Gauge_Factor = *unique calibration factor, supplied with transducer*
Voltage = *Volts (Output voltage from transducers)*

Calibration

Strain gauge calibration

Calibrations were done using an HBM strain gauge calibration unit. This calibration unit was calibrated by the SABS. The calibrator unit was connected to the strain gauges in the doorstopper. This was done to ensure that the effect of the length of the electrical leads and other errors had no effect on the calibrations. The calibrator simulates a known strain with its output connected to the voltmeter and A/D card. This known value is then compared to the measured and calculated strain.

Displacement transducers

The displacement transducers were calibrated in the laboratory against a mechanical micrometer with a resolution of 0,001 mm. The relationship between the displacement and output voltage was determined for each of the instruments. To ensure that any variations in the transducer excitation voltage could not influence the accuracy of the calibration, the calibration constants were expressed in V (out)/V (in)/mm.

Tiltmeter calibration

The calibration factors for the manufacturer supplied the tiltmeters. The factors were expressed in degrees/volt.

Data Processing

Before producing final data tables and graphs, error values in the data were removed by digital filtering and visual inspection. Some of the data points were suspect due to broken cable connections and were removed without loss of consistency.

Results

The results were presented in the form of data files on magnetic medium and as printed graphs. All the data sets were converted to ASCII text files. A separate file for each instrument was

created for the storage of the data. Graphs were generated from the ASCII data files using a standard spreadsheet program.

System Performance

- Sensitivity:

Sensitivity is the input to output ratio, or the smallest unit of measurement detectable by the instrumentation.
A sensitivity of three micro strains for the doorstopper measuring system, 0.2 degrees for the tiltmeters and .01 mm for the displacement transducers were observed.

- Repeatability :

Repeatability is the ability to give the same output for the same input if applied repeatedly.
For the duration of the monitoring, there were no observable changes in the system performance.

- Noise

Noise is all outputs that are not an effect of the input.
Some error levels were recorded at irregular intervals. The reason for these errors is still unclear but could be the result of weak electrical connections or moisture on the logger and transducers. These errors appeared to be severe but were significantly reduced by digital filtering and visual inspection of the results and graphs.

Evaluation

Doorstoppers

- As a result of the difficult conditions encountered at the instrumentation site, not all of the required boreholes could be drilled for the installation of the doorstoppers. Some boreholes collapsed immediately after drilling.
- The doorstopper functioned well during the monitoring cycle.
- Strains recorded from the doorstopper were accurate.

Extensometers

Not all of the required boreholes could be drilled for the installation of the extensometers because of the difficult conditions.

- The mechanical part of the extensometers proved to work well underground.
- Some problems with the electrical output of the transducers were experienced as a result of moisture.
- Extensometers were damaged during the blasting operations.
- Personnel moving through the instrumentation area with services such as air hoses and water supply hoses pulled extensometer cables out of the instruments.
- No useable results were obtained from the extensometers due to the above factors.

Tiltmeters

- Tiltmeters performed well during the monitoring cycle and gave continuos accurate data.
- Blasting during the mining process damaged a tiltmeter. Attention to the placement and protection of the tiltmeters was inadequate.
- Some section/blocks of rock with tiltmeters dislodged from the roof and crushed the instrument. Placement of instruments on the hangingwall must be done very carefully.

Closure-ride

- The design of the spring fixture system on the outside of the instrument failed on some installations. Modifications were made that proved to be successful.
- The fixing system of the instruments onto the hanging-wall andfootwall were also not robust enough. A standard rawlbolt and short section of a steel chain proved to be successful.
- Some transducers failed as a result of moisture penetrating the electrical cable plug.
- The positions of the anchor points in the roof and floor of the excavation were not as planned. Special attention must be given to the correct installation of closure-ride stations.

No useful results were obtained due to the above factors.

Crack gauges

- These instruments proved to work well under the conditions encountered underground. No modifications to the instruments were necessary.

Datalogger

- The data logger gave errors as a result of moisture. The instrumentation was sprayed with high-pressure water jetting during mining operations. Although the logger was installed in a waterproof, IP67 rating steel box, it could not withstand high pressure water jetting. The logger is supposed to operate under 95% humidity. Better protection from water is necessary for data loggers underground.
- Data was lost due to incorrect handling of the data storage medium (PCMCIA card). The utmost care must be given to the handling of sensitive electronic devices; some training must also be given to personnel handling these devices.
- Some wrong electrical connections were made underground, resulting in lost data from instruments and transducers.

Recommendations

- Mining personnel must be kept out of the instrumentation area. As an alternative, they must be made aware of the instruments and must take part in the underground instrumentation process. This will ensure that they are aware of the sensitivity of the instruments as well as the value of the data.
- Water jetting must not be allowed in the instrumentation area. High-pressure water jetting directly on instruments will cause some instruments to fail.
- Electrical connections to instruments and loggers must be kept to a minimum underground. The use of good quality waterproof plugs will minimise wrong connection and save on installation/commissioning time.
- Correct instrument installation procedures are essential for the optimum functioning of the instruments and accurate data.
- An accurate log of operations at the test site must be kept to monitor instrument performance. A daily log of mining activities as well as any in- situ repairs and modifications to logging equipment is essential for the successful completion of a logging programme.

References

Dunnicliff, J. 1993. Geotechnical Instrumentation for Monitoring Field Performance, A Wiley-Interscience publication, USA. pp. 37-55.

Wilson, A. and Holister, G. 1983. Strain Gauge Technology, Applied Science Publishers, London and New York. pp. 217-225.

APPENDIX C

Temporal variation of seismic parameters for Hartebeestfontein G.M.

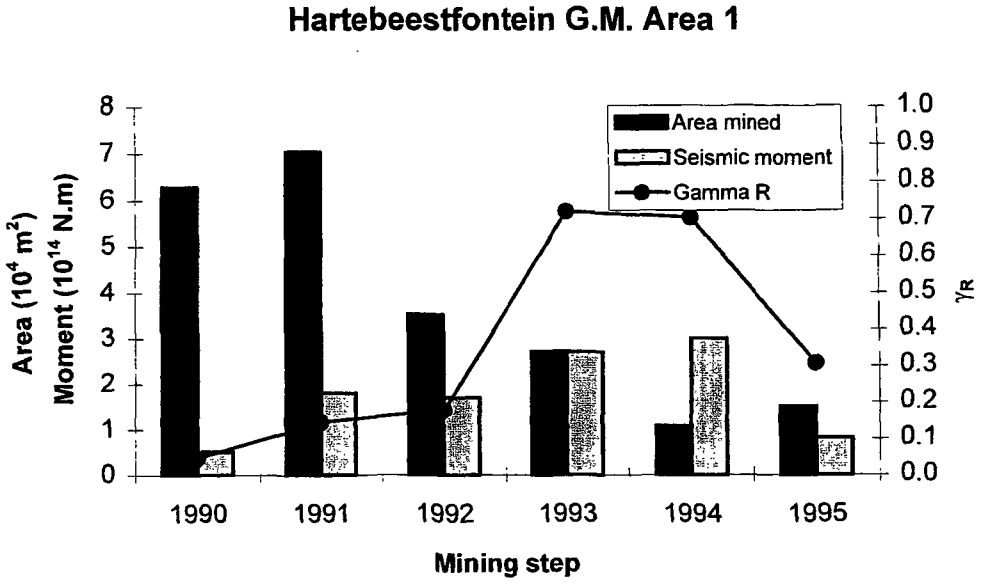

Figure C-1 Variation of area mined, seismic moment and γ_R with mining step for Area 1, Hartebeestfontein G.M.

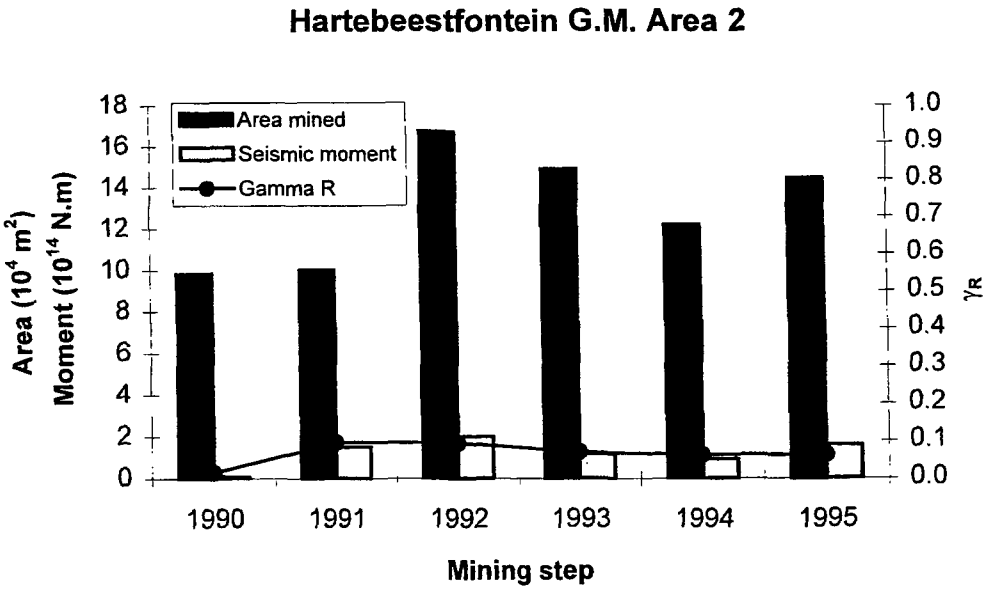

Figure C-2 Variation of area mined, seismic moment and γ_R with mining step for Area 2, Hartebeestfontein G.M.

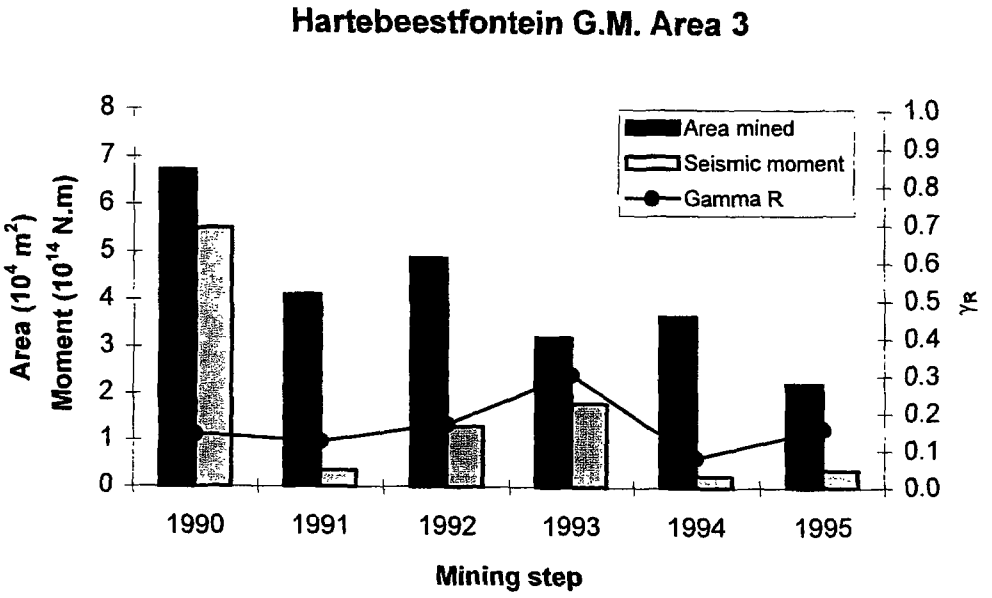

Figure C-3 Variation of area mined, seismic moment and γ_R with mining step for Area 3, Hartebeestfontein G.M.

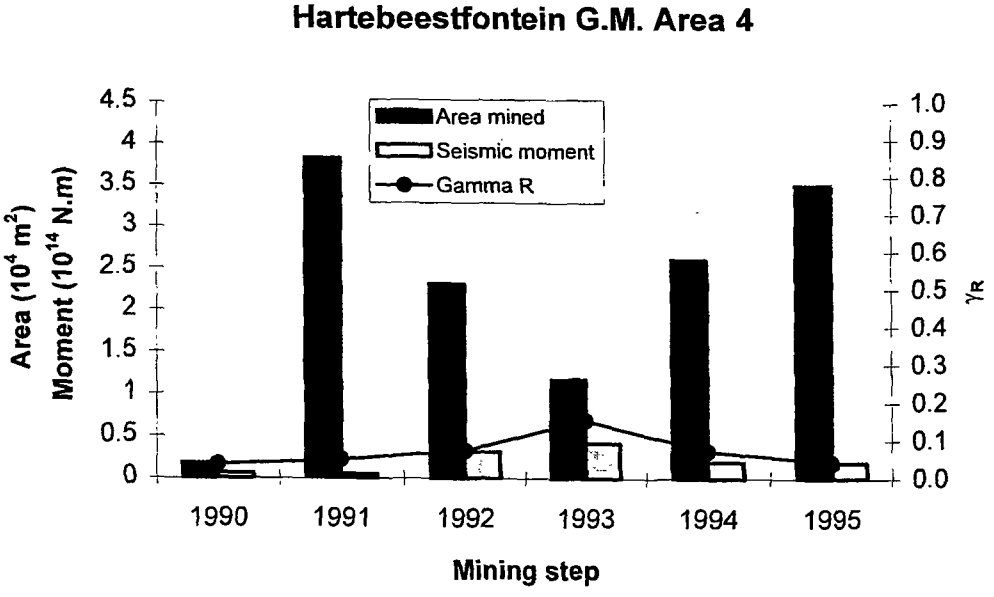

Figure C-4 Variation of area mined, seismic moment and γ_R with mining step for Area 4, Hartebeestfontein G.M.

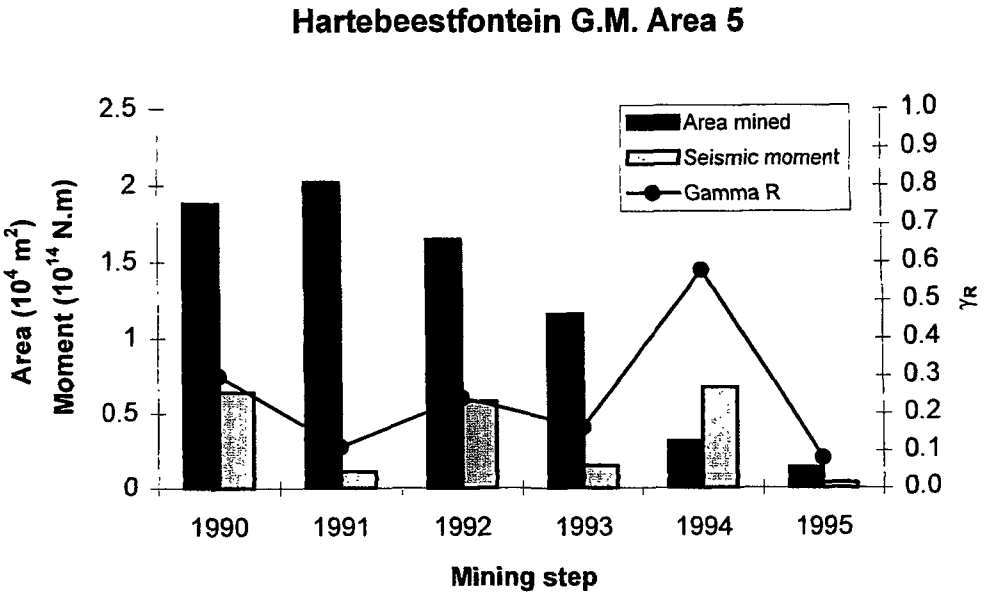

Figure C-5 Variation of area mined, seismic moment and γ_R with mining step for Area 5, Hartebeestfontein G.M.

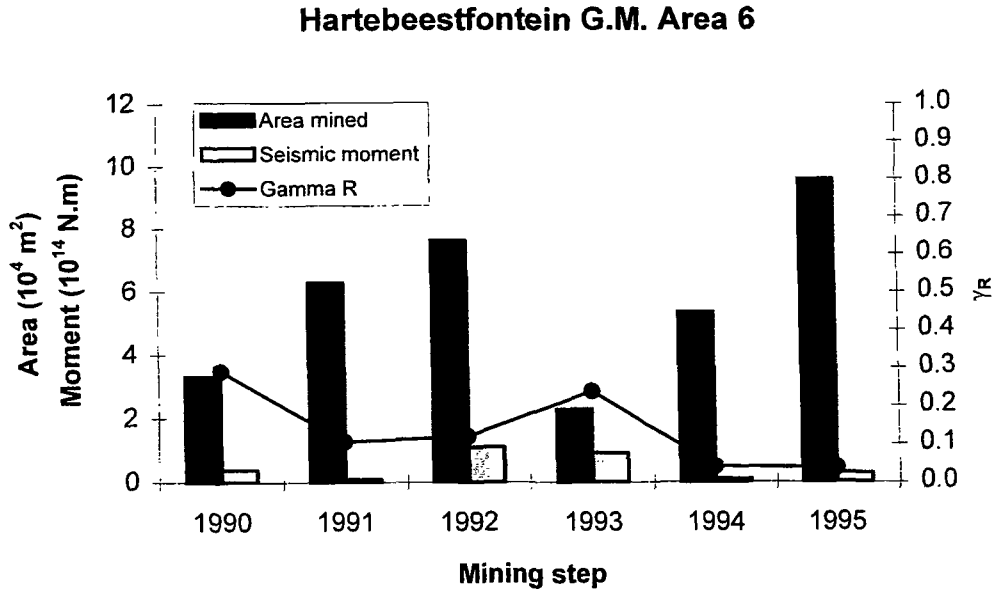

Figure C-6 Variation of area mined, seismic moment and γ_R with mining step for Area 6, Hartebeestfontein G.M.

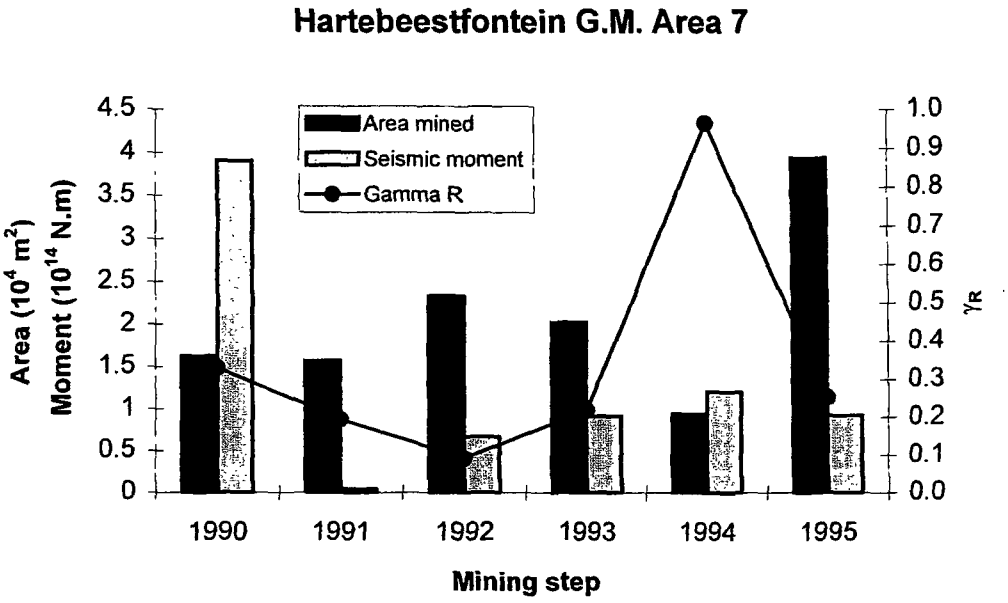

Figure C-7 Variation of area mined, seismic moment and γ_R with mining step for Area 7, Hartebeestfontein G.M.

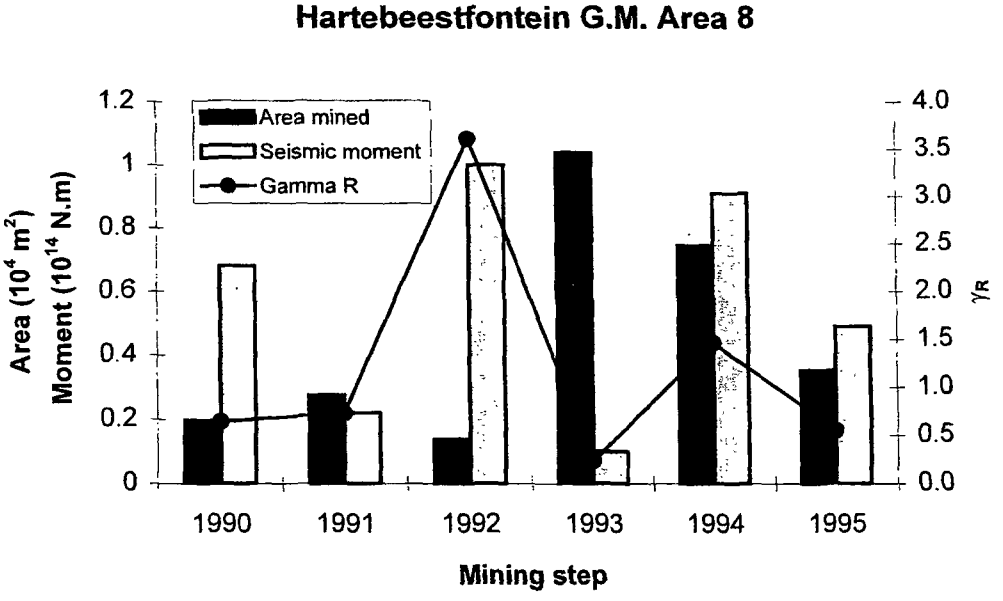

Figure C-8 Variation of area mined, seismic moment and γ_R with mining step for Area 8, Hartebeestfontein G.M.

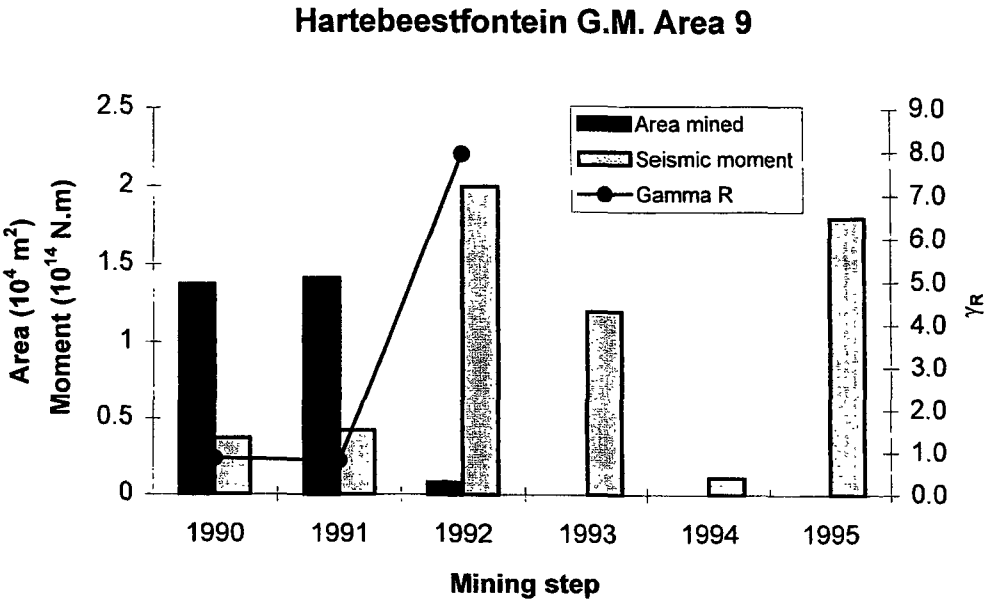

Figure C-9 Variation of area mined, seismic moment and γ_R with mining step for Area 9, Hartebeestfontein G.M.

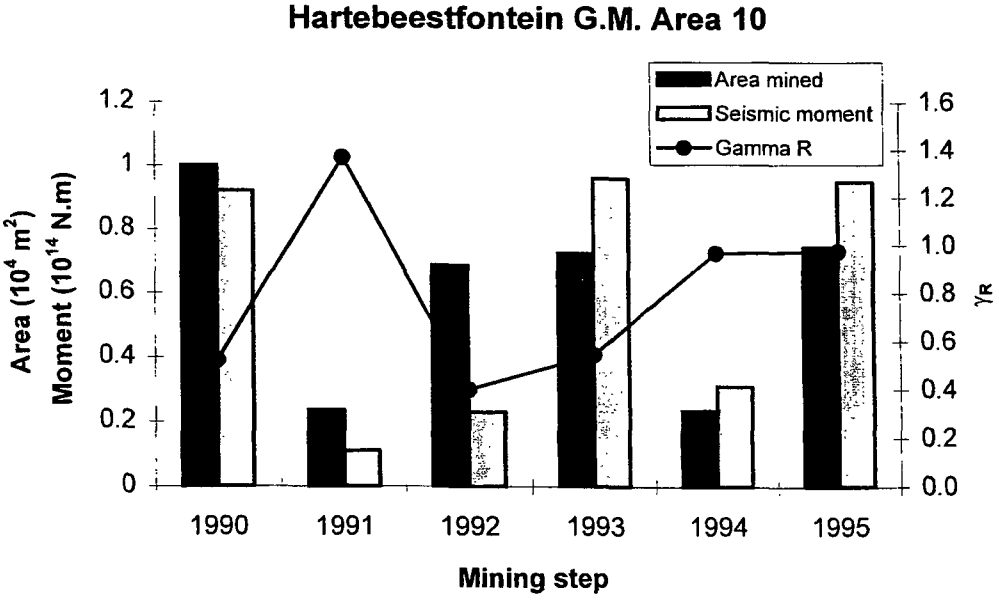

Figure C-10 Variation of area mined, seismic moment and γ_R with mining step for Area 10, Hartebeestfontein G.M.

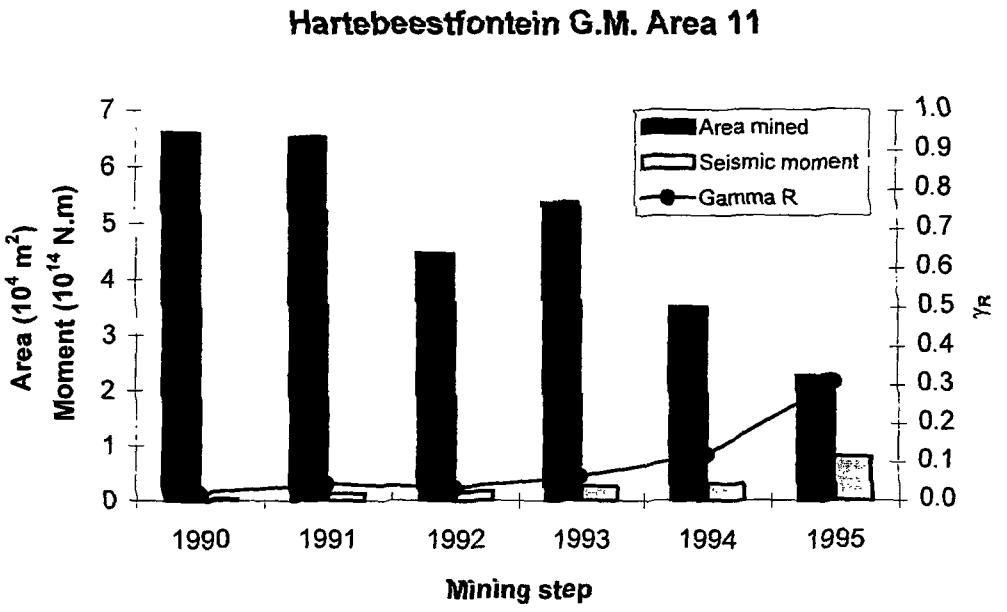

Figure C-11 Variation of area mined, seismic moment and γ_R with mining step for Area 11, Hartebeestfontein G.M.

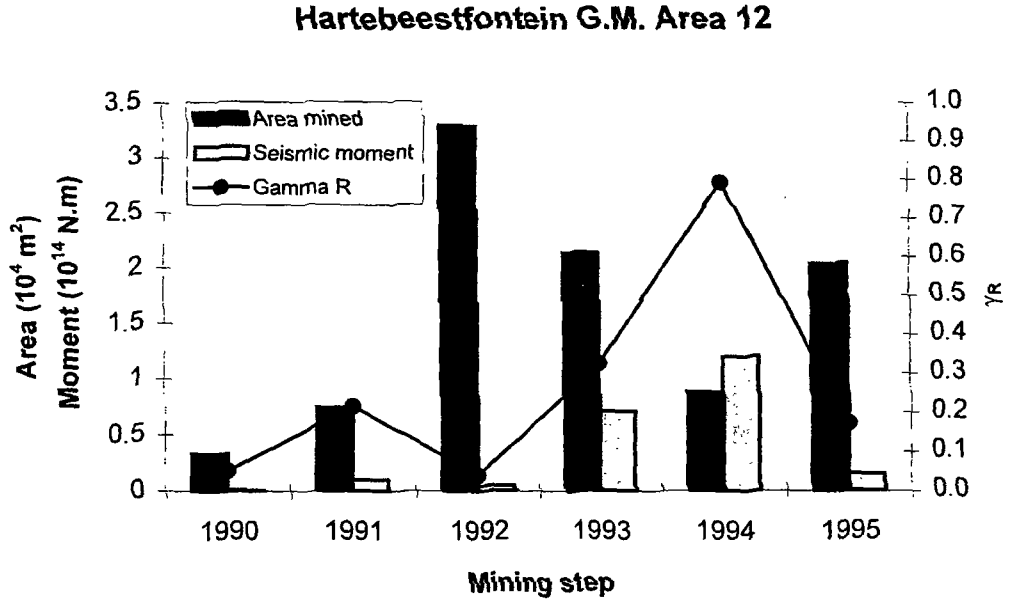

Figure C-12 Variation of area mined, seismic moment and γ_R with mining step for Area 12, Hartebeestfontein G.M.

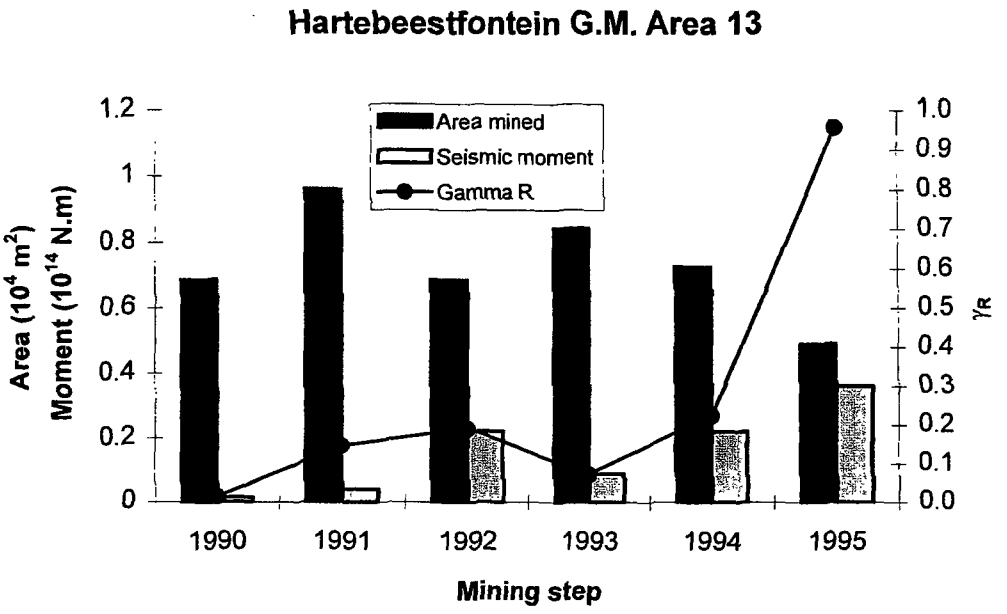

Figure C-13 Variation of area mined, seismic moment and γ_R with mining step for Area 13, Hartebeestfontein G.M.

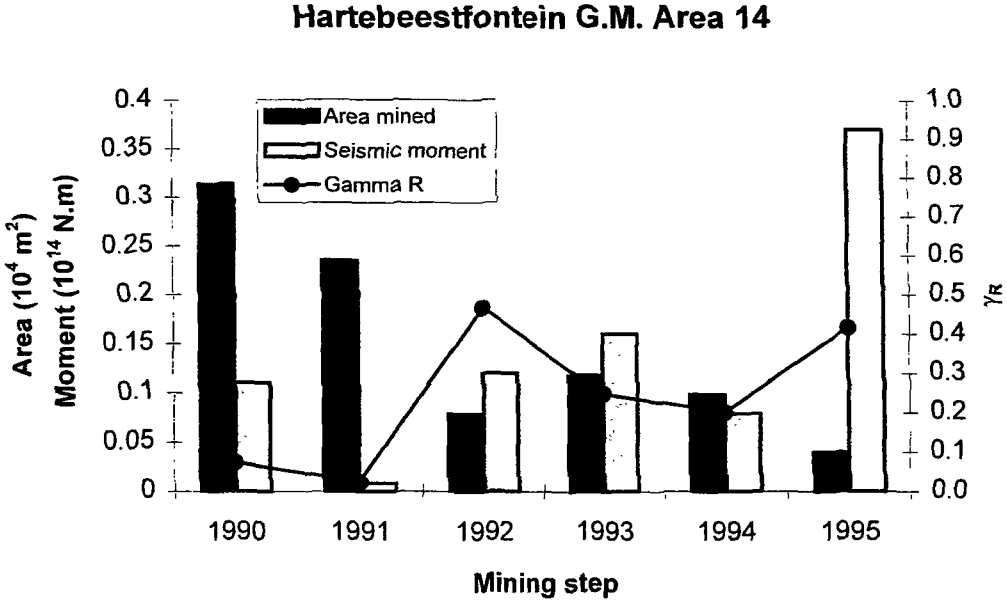

Figure C-14 Variation of area mined, seismic moment and γ_R with mining step for Area 14, Hartebeestfontein G.M.

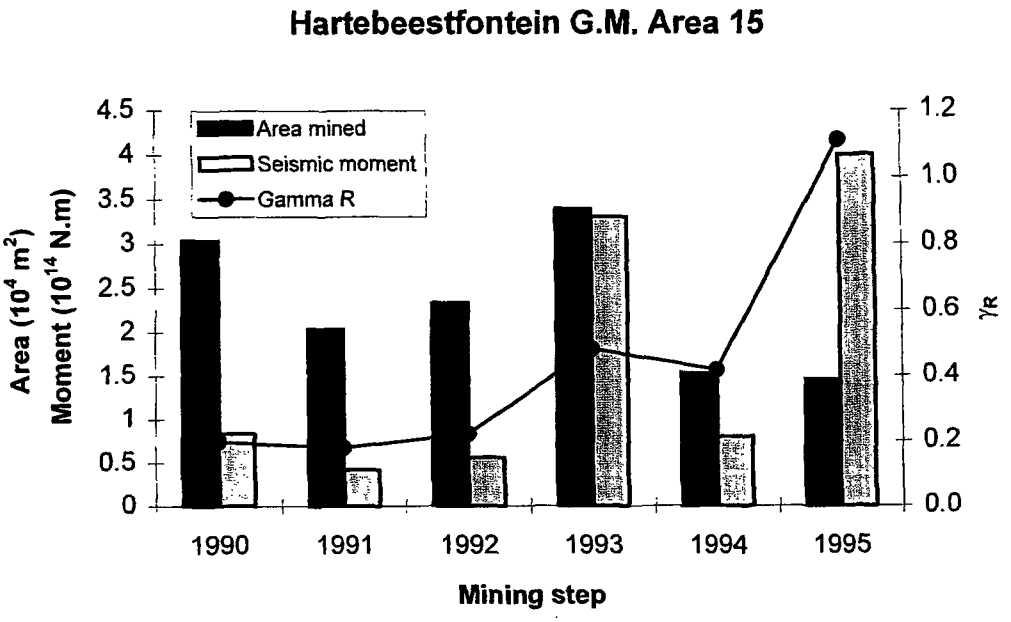

Figure C-15 Variation of area mined, seismic moment and γ_R with mining step for Area 15, Hartebeestfontein G.M.

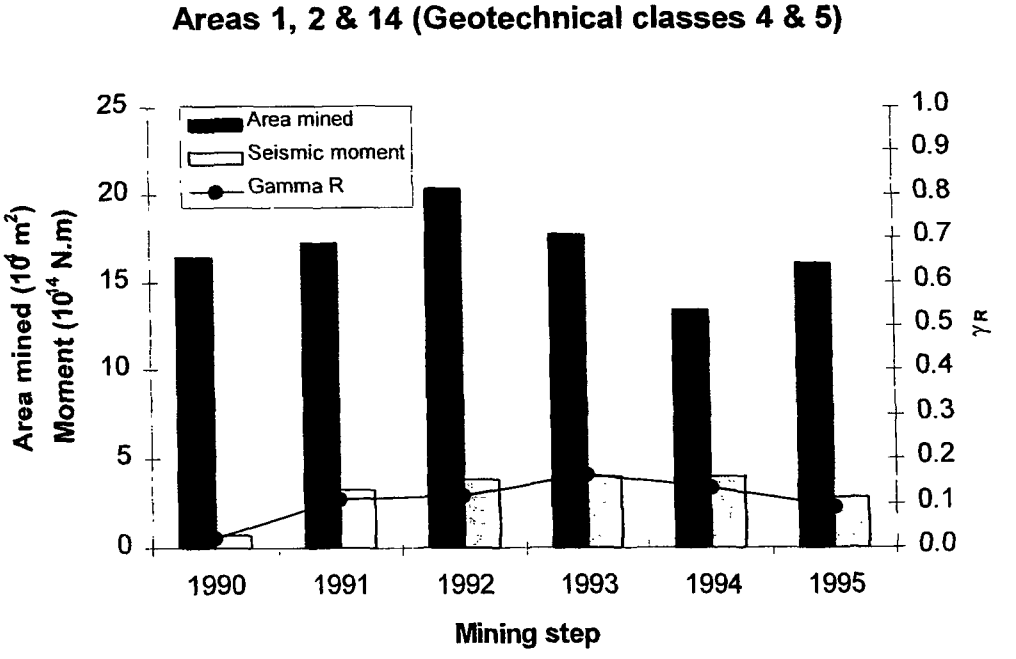

Figure C-16 Variation of area mined, seismic moment and γ_R with mining step for geotechnical classes 4 & 5, Hartebeestfontein G.M.

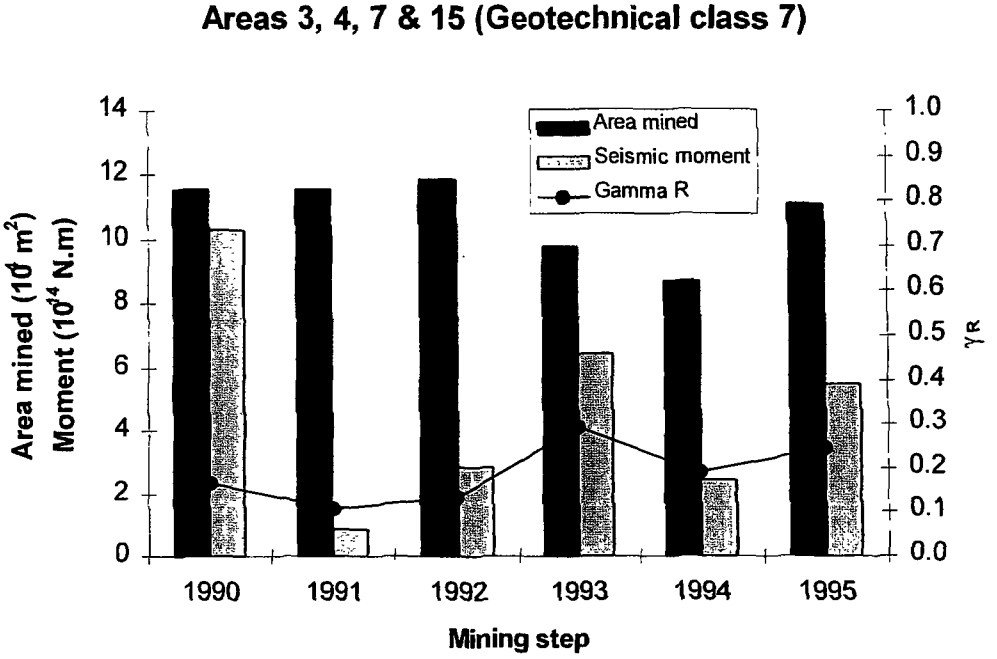

Figure C-17 Variation of area mined, seismic moment and γ_R with mining step for geotechnical class 7, Hartebeestfontein G.M.

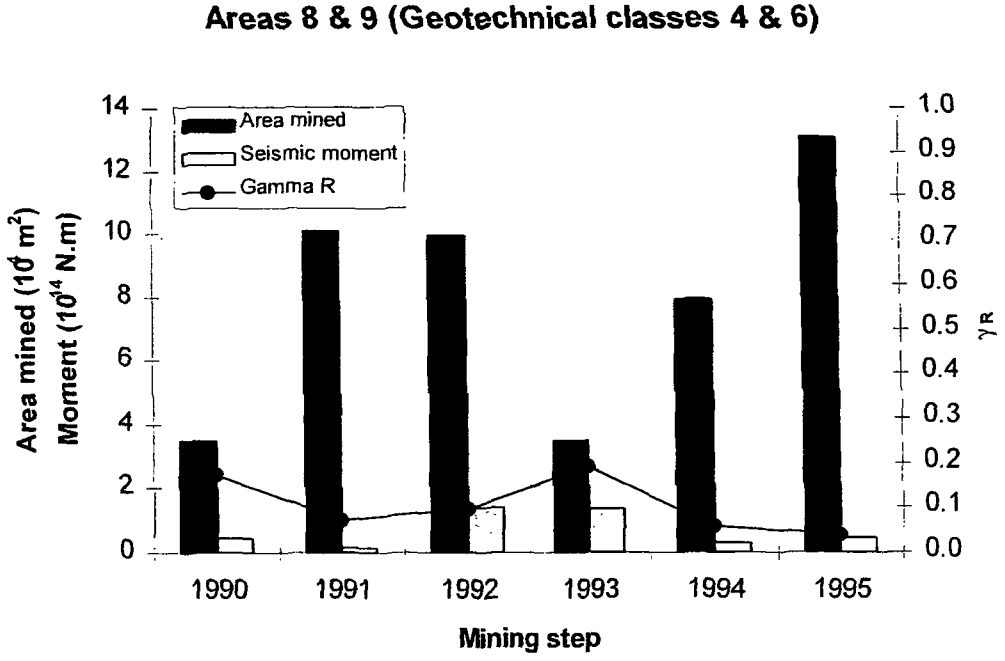

Figure C-18 Variation of area mined, seismic moment and γ_R with mining step for geotechnical classes 4 & 6, Hartebeestfontein G.M.

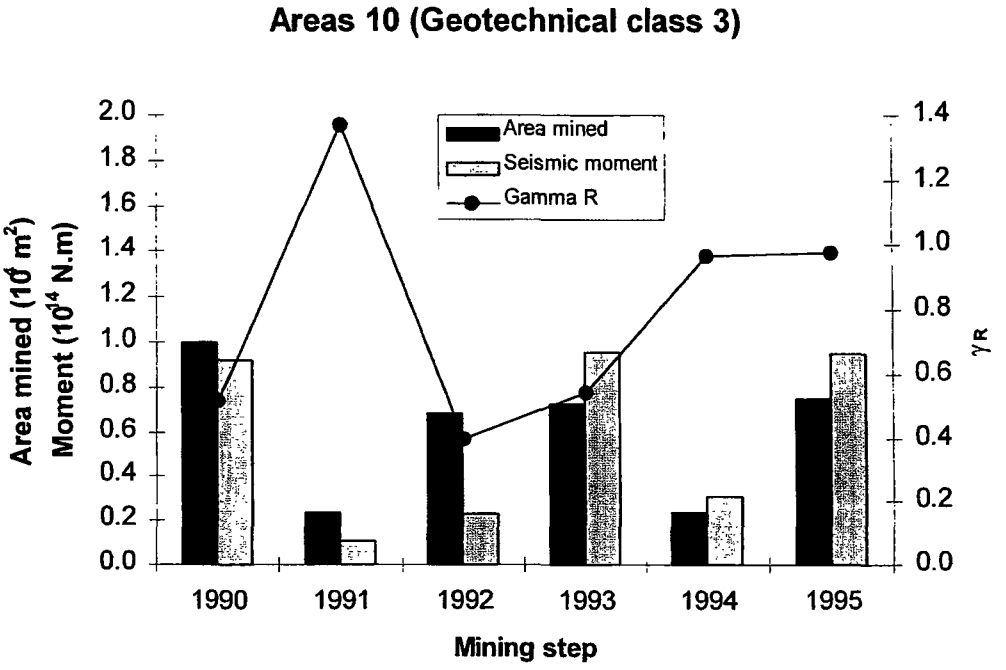

Figure C-19 Variation of area mined, seismic moment and γ_R with mining step for geotechnical class 3, Hartebeestfontein G.M.

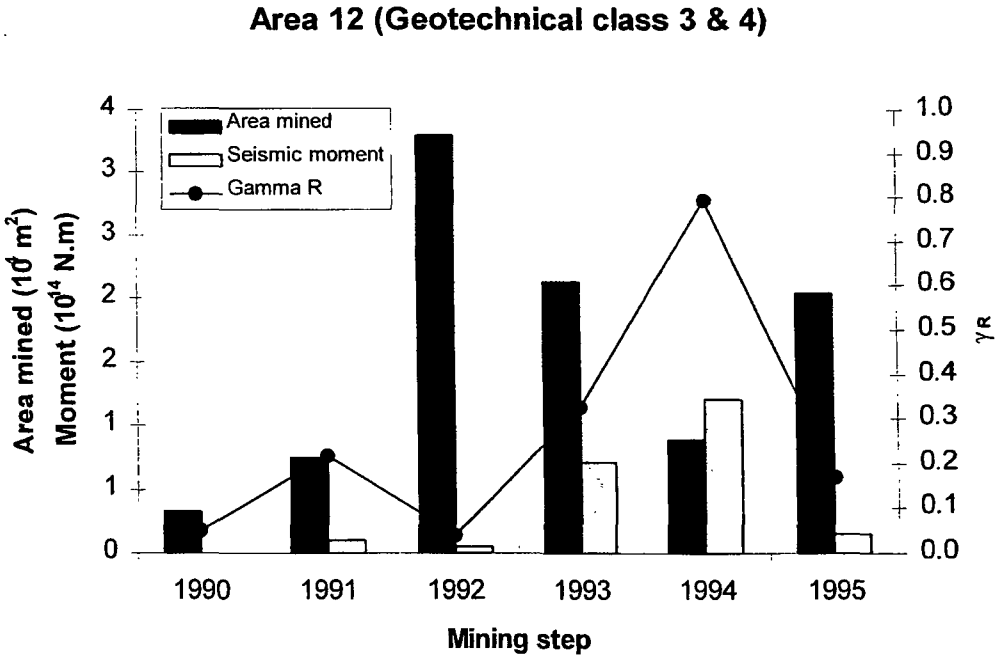

Figure C-20 Variation of area mined, seismic moment and γ_R with mining step for geotechnical classes 3 & 4, Hartebeestfontein G.M.

APPENDIX D

Laboratory and Underground Elongate Test Results

A series of laboratory and underground evaluations were conducted on a variety of elongates in order to determine the significant parameters affecting the performance of these elongates. Although it was initially intended that only the most commonly used elongates would be evaluated, in order to adequately develop a practical and meaningful testing procedure that could be applied without bias to all elongates, a wide spectrum of elongates were investigated. Units with a variety of yield mechanisms were selected for evaluation under the provisional procedure. A preliminary test procedure was drawn up in early 1997 and all elongate types were subjected to this series of tests.

The preliminary test procedure consisted of twenty-four tests as described below. This was applied to units suitable for 1,0 m and 1,6 m stoping widths.

- five rapid displacement tests at a rate of 3,0 m/s – the units are initially compressed slowly for 50 mm then subjected to 3,0 m/s for at least 200 mm and the test completed at the slow rate until failure
- ten slow displacement tests at a rate of 15 mm/minute
- one test at a deformation rate of 150 mm/min
- one test at 15 mm/min on a 10° inclined platen
- one test at 15 mm/min on a 20 mm stepped platen
- one test at 15 mm/min on a 50 mm stepped platen
- one slow test at a deformation rate of 10 mm/day for seven days
- one creep test for seven days
- three underground tests

Elongates that were not designed for use under rockburst conditions, were not tested under rapid displacement conditions.

Analyses and comparisons could then be made regarding the variability in performance under slow and dynamic loading conditions, effects of length and loading rate, stability under adverse loading conditions and how the laboratory performance compares with actual underground results.

A list of the different types of elongates (and suppliers where required) is given in the table below. As some of the units are generic, a supplier has not been listed. In the case of the pencil props, an unturned pre-stressed pencil was tested and then a turned, non pre-stressed pencil was tested. This was to provide an example of the range in performance that can be obtained from a generic elongate. Any such units tested in future must refer to the supplier including any details that may differentiate one generic elongate from another.

Elongate Type	Supplier	Nominal Diameter (mm)	Lengths Tested
Cone Prop	MM & E	190	1,0 m, 1,6 m
Disc Prop	Westeel Engineering	170	1,0 m, 1,6 m
Eben Haeser	Jan Woller Mining	200	1,0 m, 1,6 m
Eben Haeser MK 1	Jan Woller Mining	200	1,0 m, 1,6 m
Hard Gum Mine Pole	Generic	150	1,6 m
Load Stick	BMS Mining Supplies	160	1,0 m, 1,6 m
Loadmaster	BMS Mining Supplies	180	1,0 m, 1,6 m
Turned Pencil	Generic	200	1,0 m
Unturned Pencil, pre-stress	Generic	180	1,0 m, 1,6 m
Profile Prop	Mondi Timber	200	1,0 m
Rocprop	Mine Support Products	150	1,0 m, 1,6 m
Timber Splitter	Elbroc Strata Control	180	1,0 m, 1,6 m

This Appendix has been divided into three sections, each containing an explanation of tests and the graphed results:

- effect of unit length: comparison of performance for dynamic and slow test rates
- underground versus laboratory: comparison of performance
- summary of all test results

Effect of Elongate Length

Elongates have been tested at two lengths in order to evaluate the stability with increased length. The multiple tests were conducted at both dynamic (3 m/sec) and slow (15 mm/min) rates in order to account for variability (at least to some degree), preliminary comparisons can be made regarding effects of length at these two test rates. As at least two lengths were required, practical extremes were necessary. However, the controlled testing capabilities under dynamic conditions for the South African mining industry is limited to 1,6 m long elongates. Extreme lengths could therefore not be evaluated with the new generation yielding elongates.

Considering the limited testing that has been conducted of the various elongate types at two lengths, there does not appear to be a significant difference in the performance, at least within the design yield ranges, where engineered components dictate yield behaviour. Beyond this range, performance becomes less predicable and elongates may be more susceptible to buckling at greater lengths.

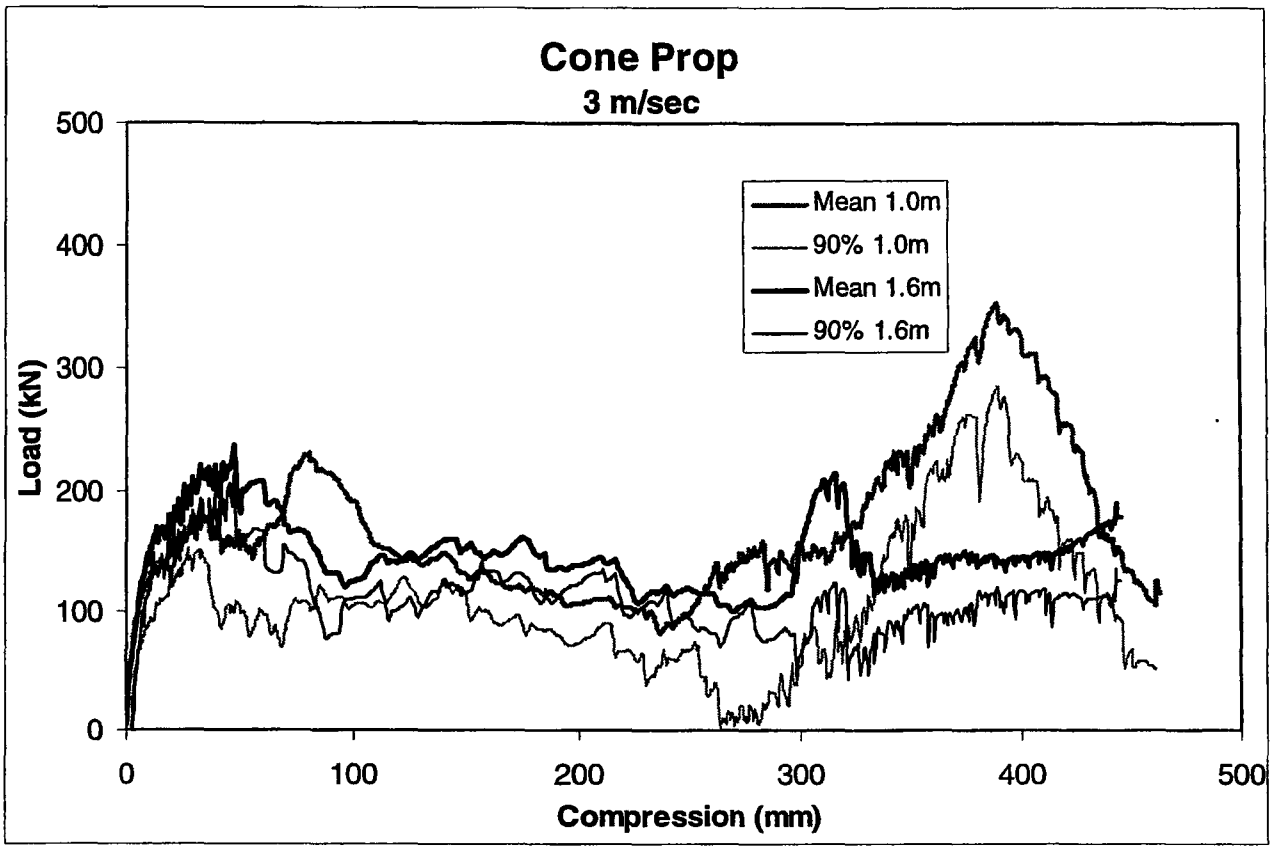
Cone Prop
3 m/sec
Mean 1.0m
90% 1.0m
Mean 1.6m
90% 1.6m
Load (kN)
0
100
200
300
400
500
Compression (mm)

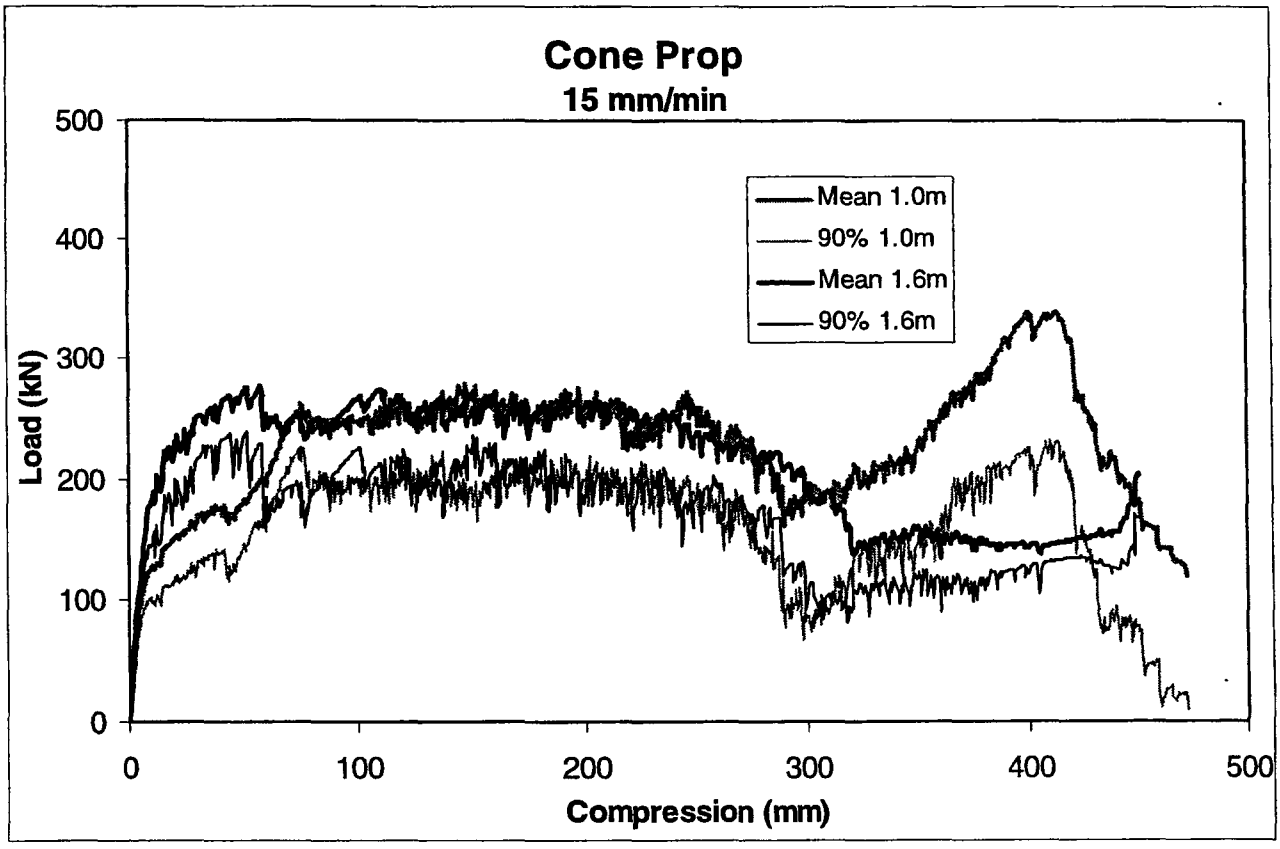
Cone Prop
15 mm/min
Mean 1.0m
90% 1.0m
Mean 1.6m
90% 1.6m
Load (kN)
0
100
200
300
400
500
Compression (mm)

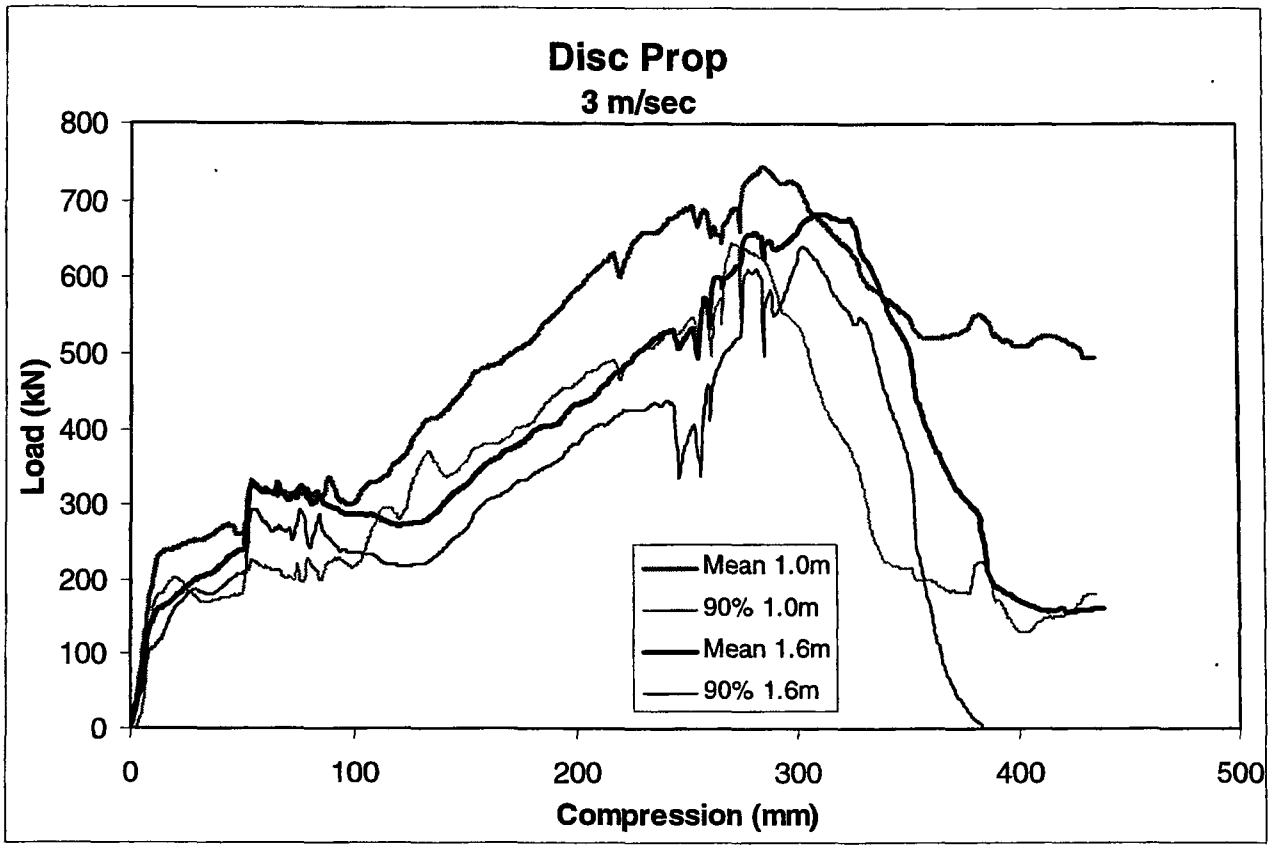
Disc Prop
3 m/sec
Load (kN)
800
700
600
500
400
300
200
100
0
0
100
200
300
400
500
Compression (mm)
Mean 1.0m
90% 1.0m
Mean 1.6m
90% 1.6m

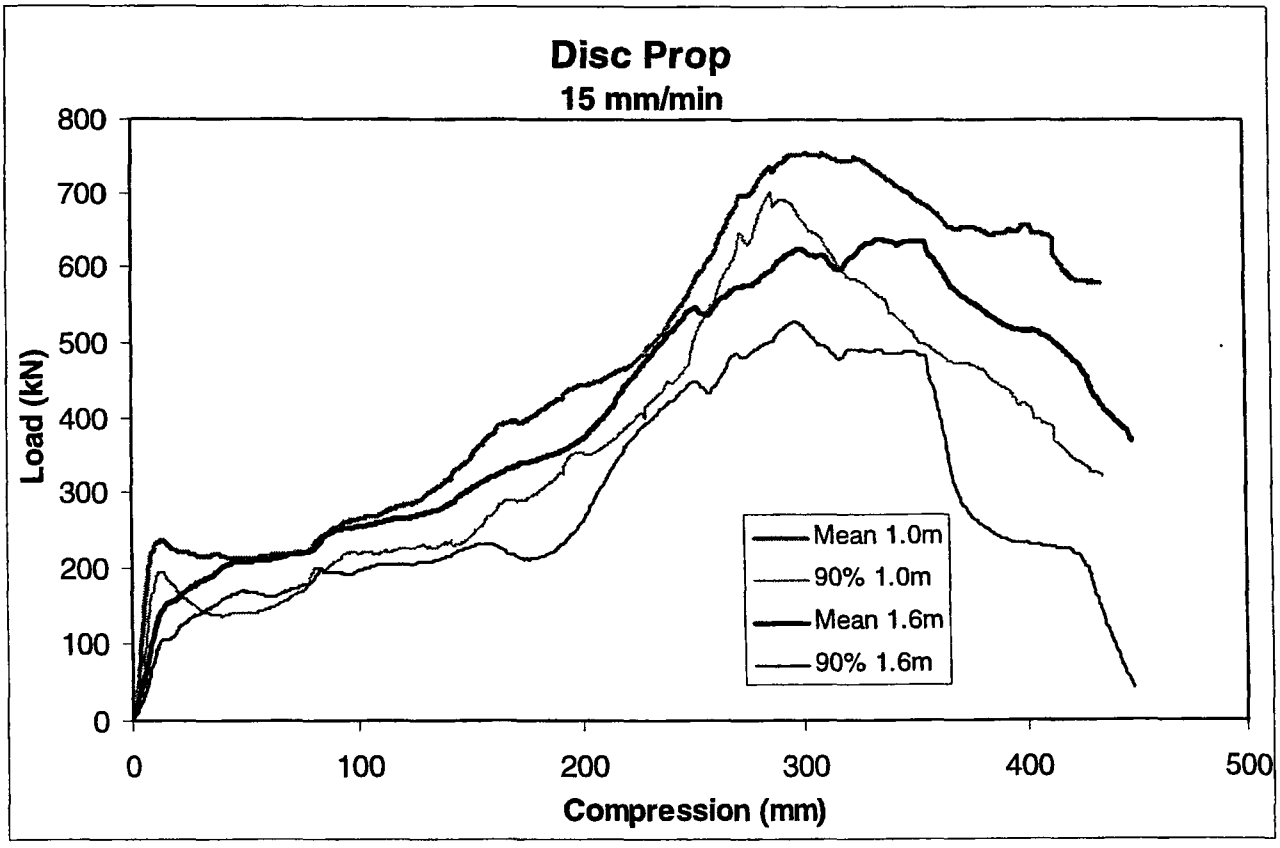
Disc Prop
15 mm/min
Load (kN)
800
700
600
500
400
300
200
100
0
0
100
200
300
400
500
Compression (mm)
Mean 1.0m
90% 1.0m
Mean 1.6m
90% 1.6m

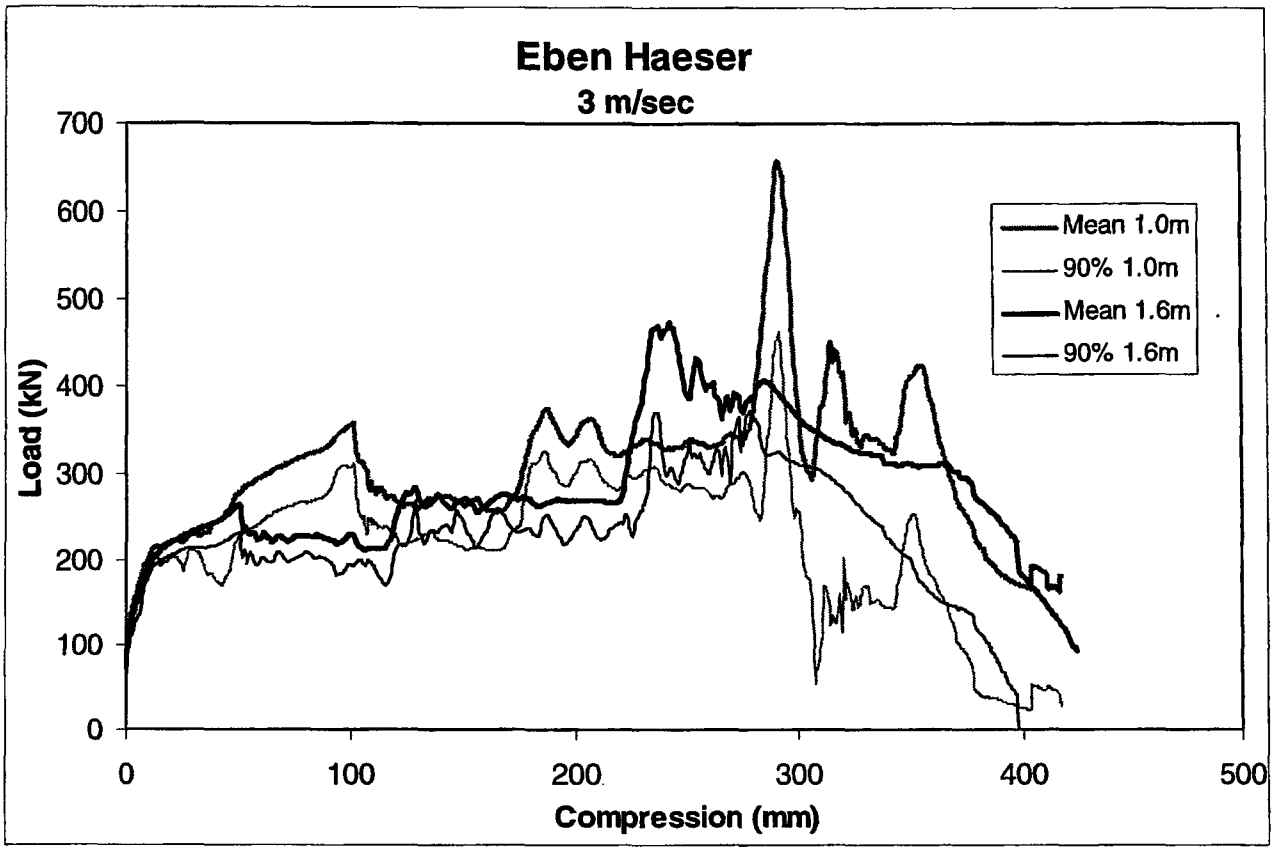
Eben Haeser
3 m/sec
Load (kN)
Compression (mm)
Mean 1.0m
90% 1.0m
Mean 1.6m
90% 1.6m
0
100
200
300
400
500
600
700

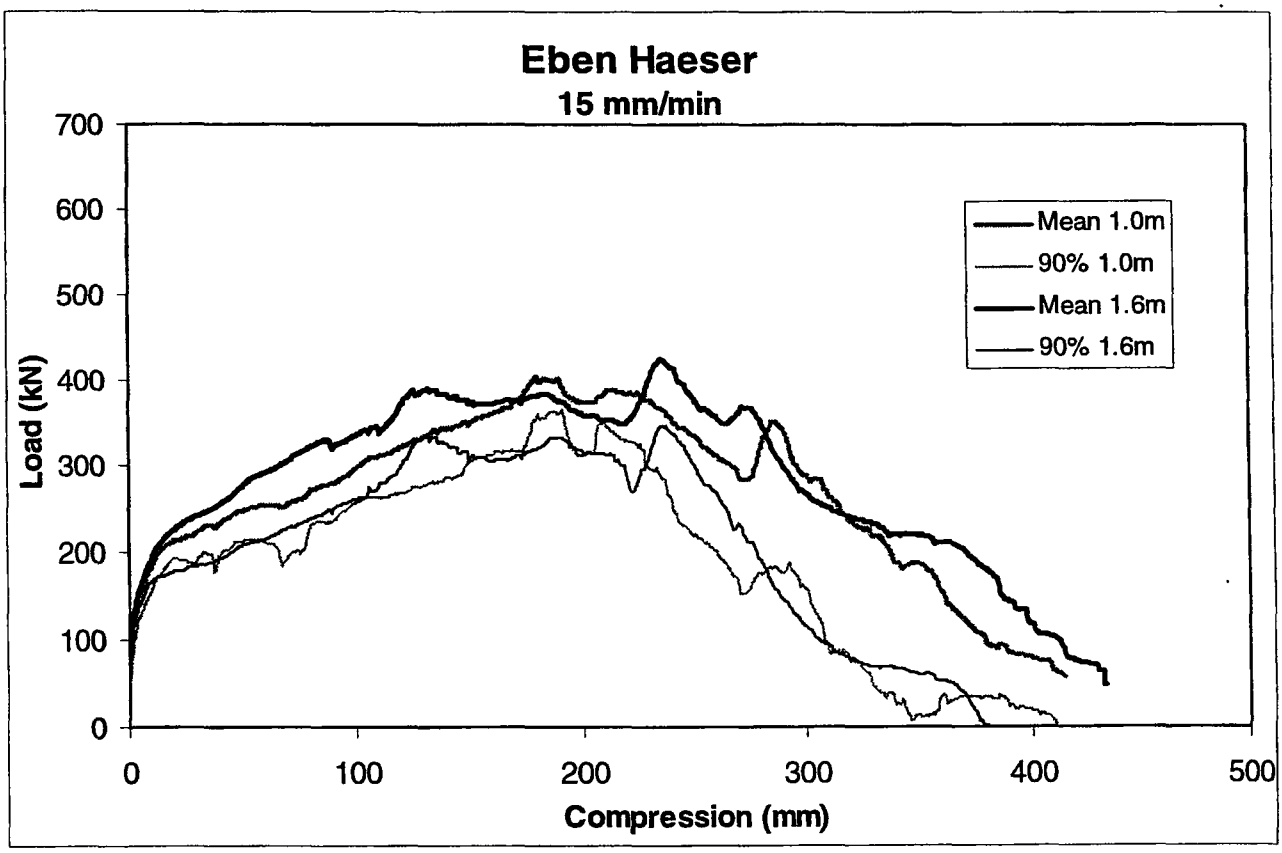
Eben Haeser
15 mm/min
Load (kN)
Compression (mm)
Mean 1.0m
90% 1.0m
Mean 1.6m
90% 1.6m
0
100
200
300
400
500
600
700

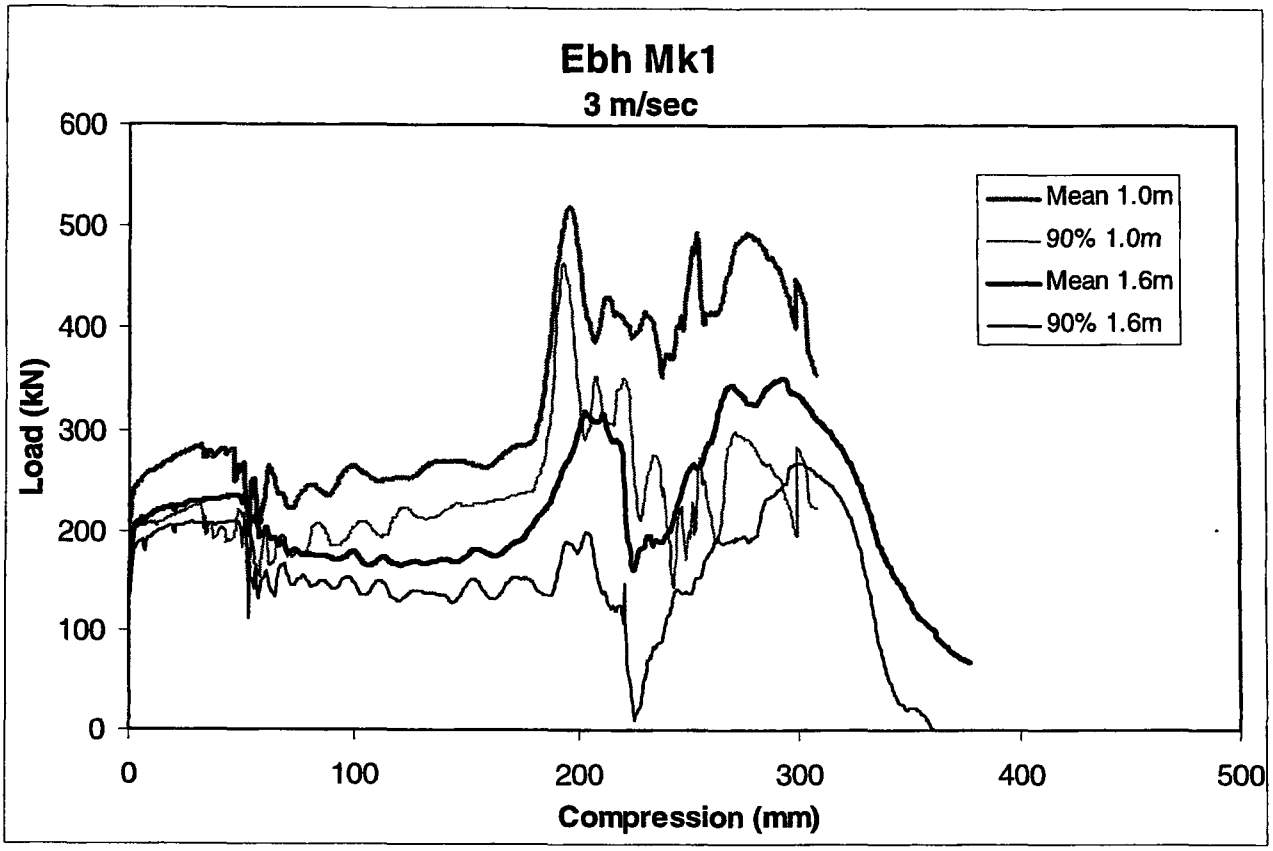
Ebh Mk1
3 m/sec
Load (kN)
Compression (mm)
Mean 1.0m
90% 1.0m
Mean 1.6m
90% 1.6m
0
100
200
300
400
500
600

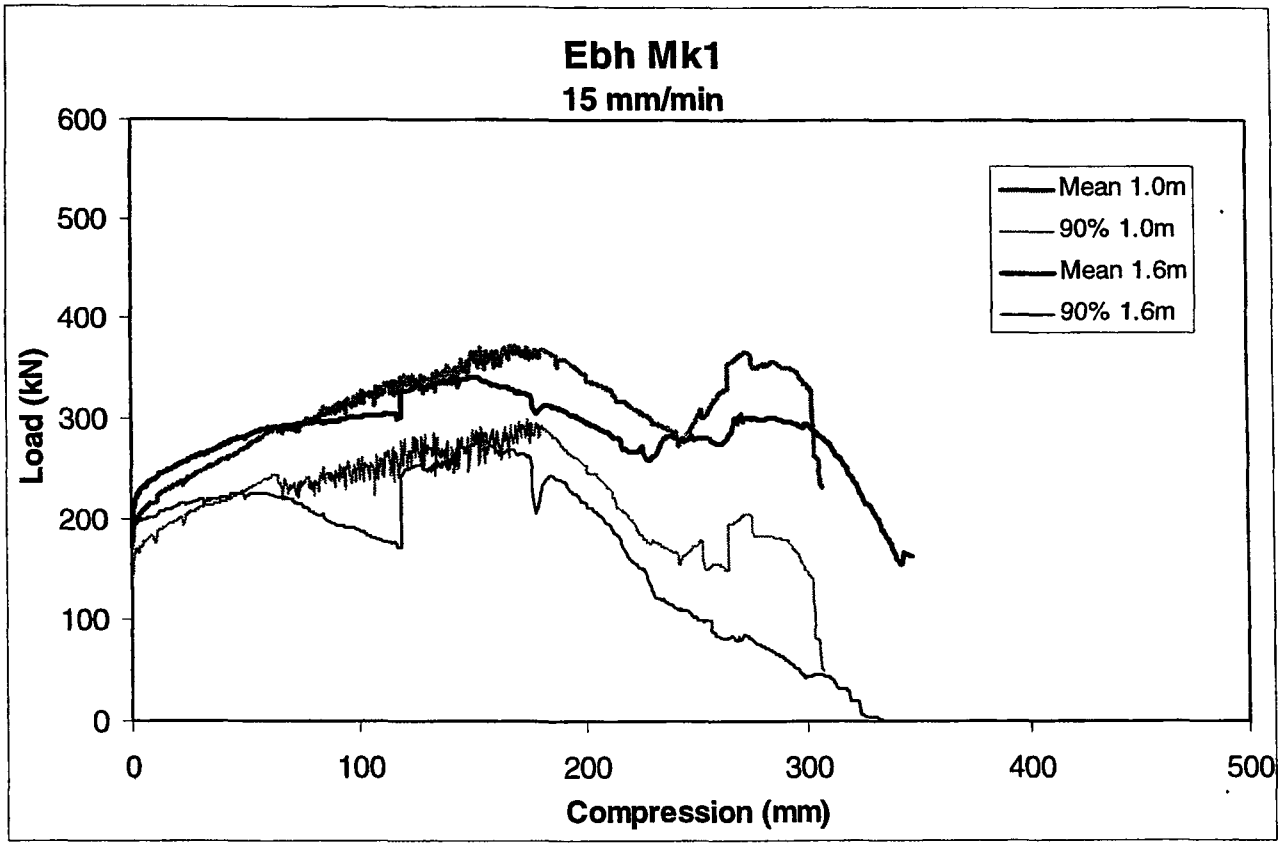
Ebh Mk1
15 mm/min
Load (kN)
Compression (mm)
Mean 1.0m
90% 1.0m
Mean 1.6m
90% 1.6m
0
100
200
300
400
500
600

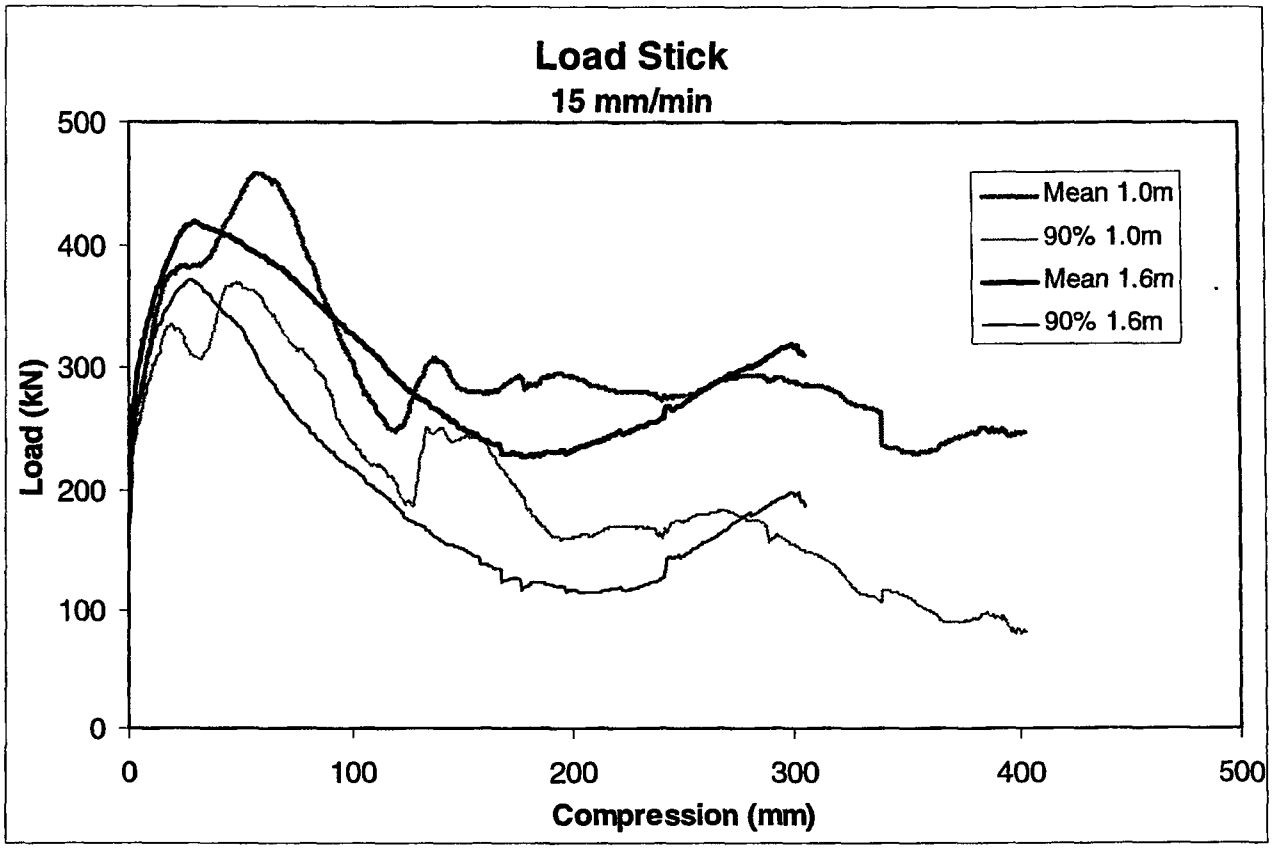
Load Stick
15 mm/min
Load (kN)
Compression (mm)
0
100
200
300
400
500
Mean 1.0m
90% 1.0m
Mean 1.6m
90% 1.6m

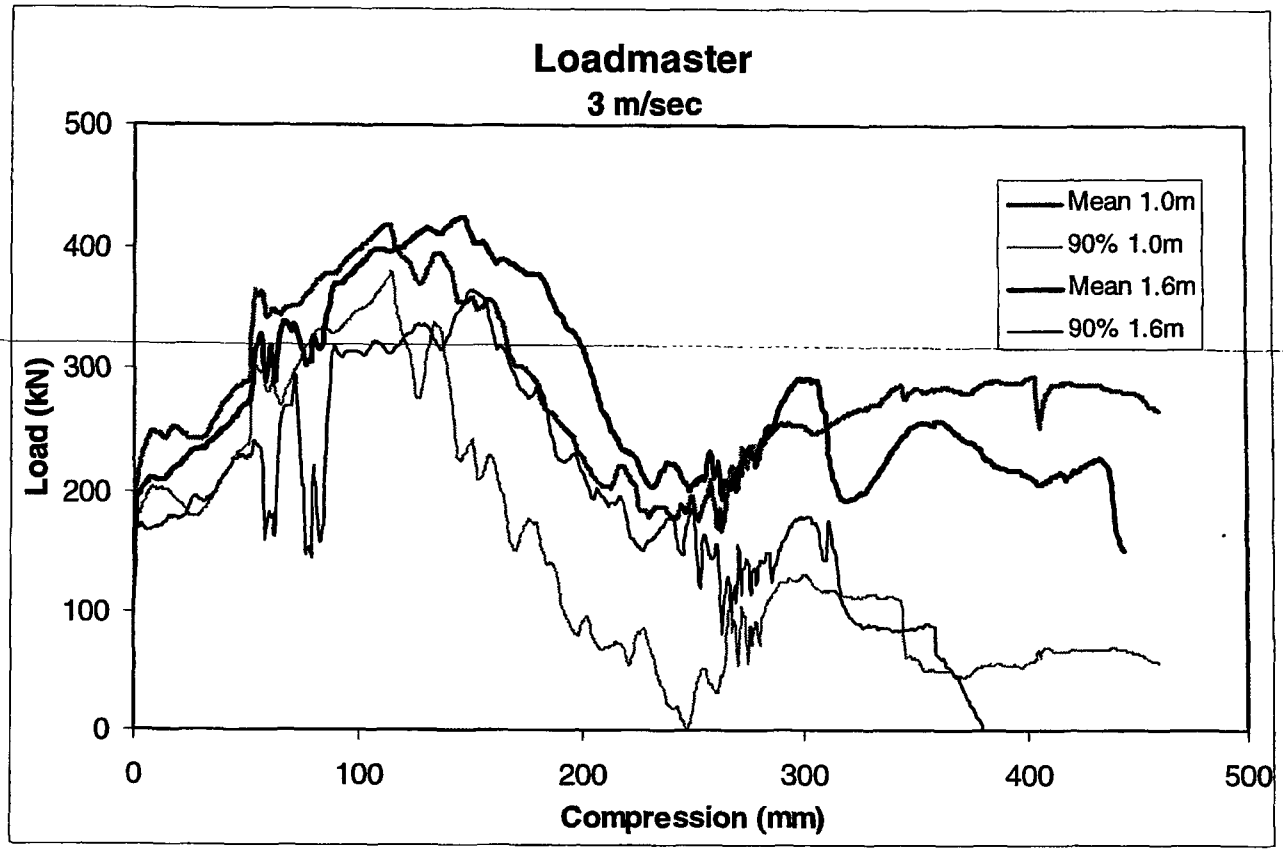
Loadmaster
3 m/sec
Load (kN)
Compression (mm)
Mean 1.0m
90% 1.0m
Mean 1.6m
90% 1.6m
0
100
200
300
400
500

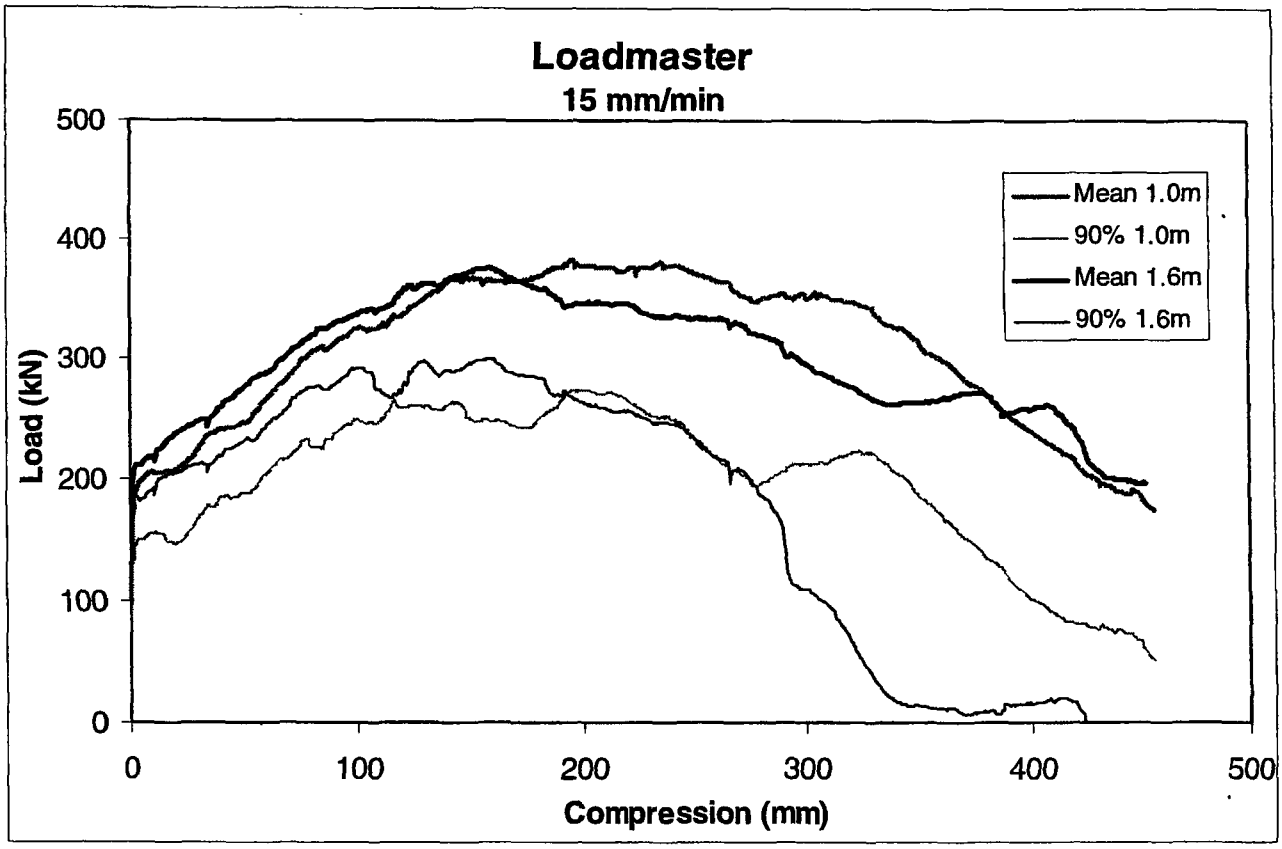
Loadmaster
15 mm/min
Load (kN)
Compression (mm)
Mean 1.0m
90% 1.0m
Mean 1.6m
90% 1.6m
0
100
200
300
400
500

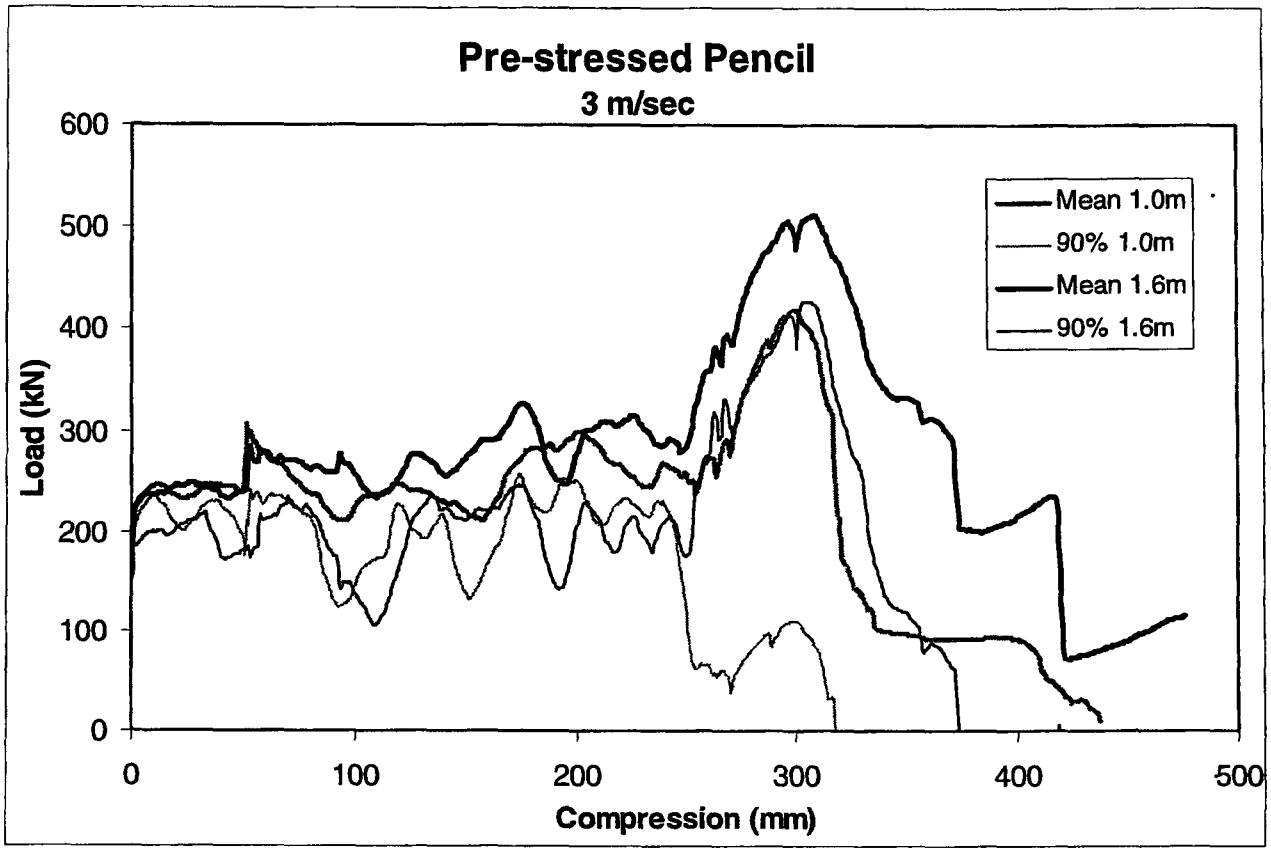
Pre-stressed Pencil
3 m/sec
Load (kN)
600
500
400
300
200
100
0
0
100
200
300
400
500
Compression (mm)
Mean 1.0m
90% 1.0m
Mean 1.6m
90% 1.6m

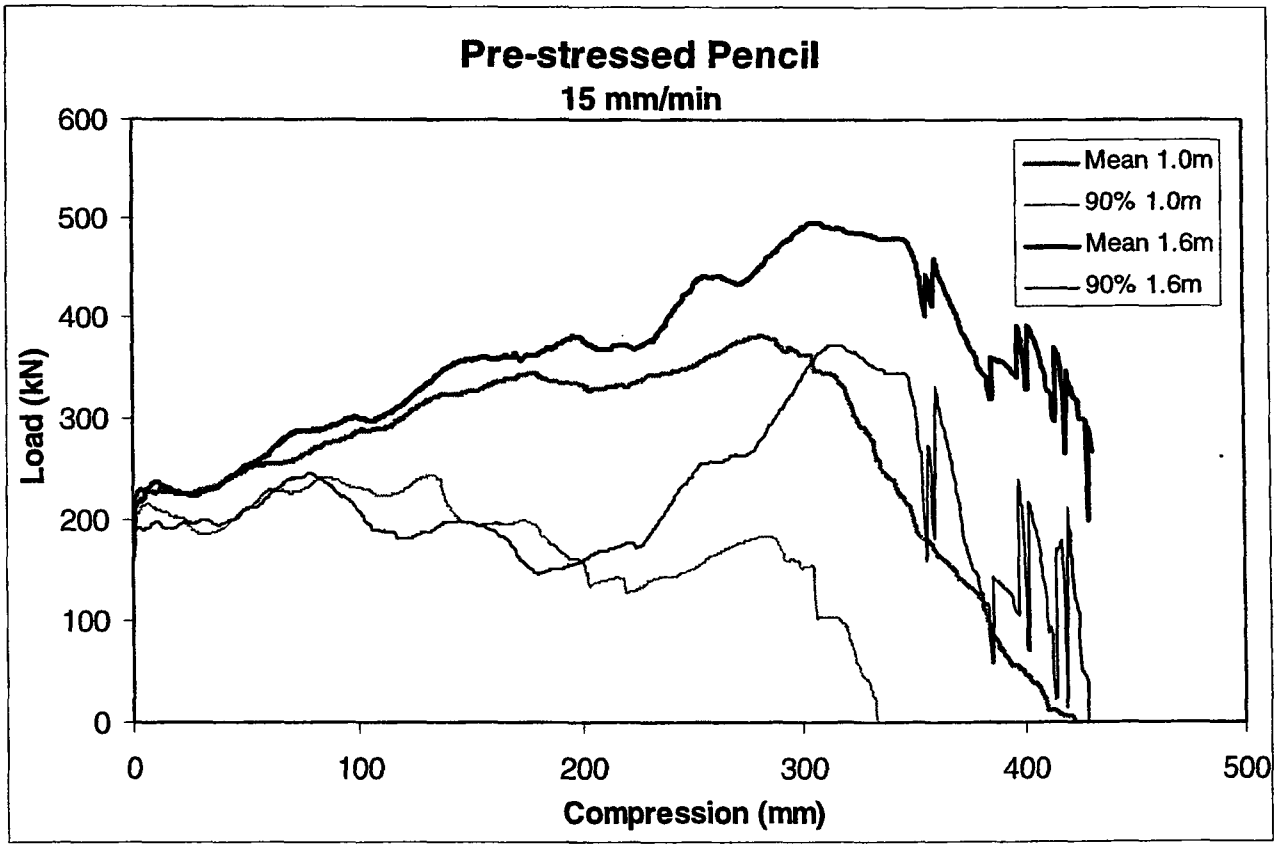
Pre-stressed Pencil
15 mm/min
Load (kN)
600
500
400
300
200
100
0
0
100
200
300
400
500
Compression (mm)
Mean 1.0m
90% 1.0m
Mean 1.6m
90% 1.6m

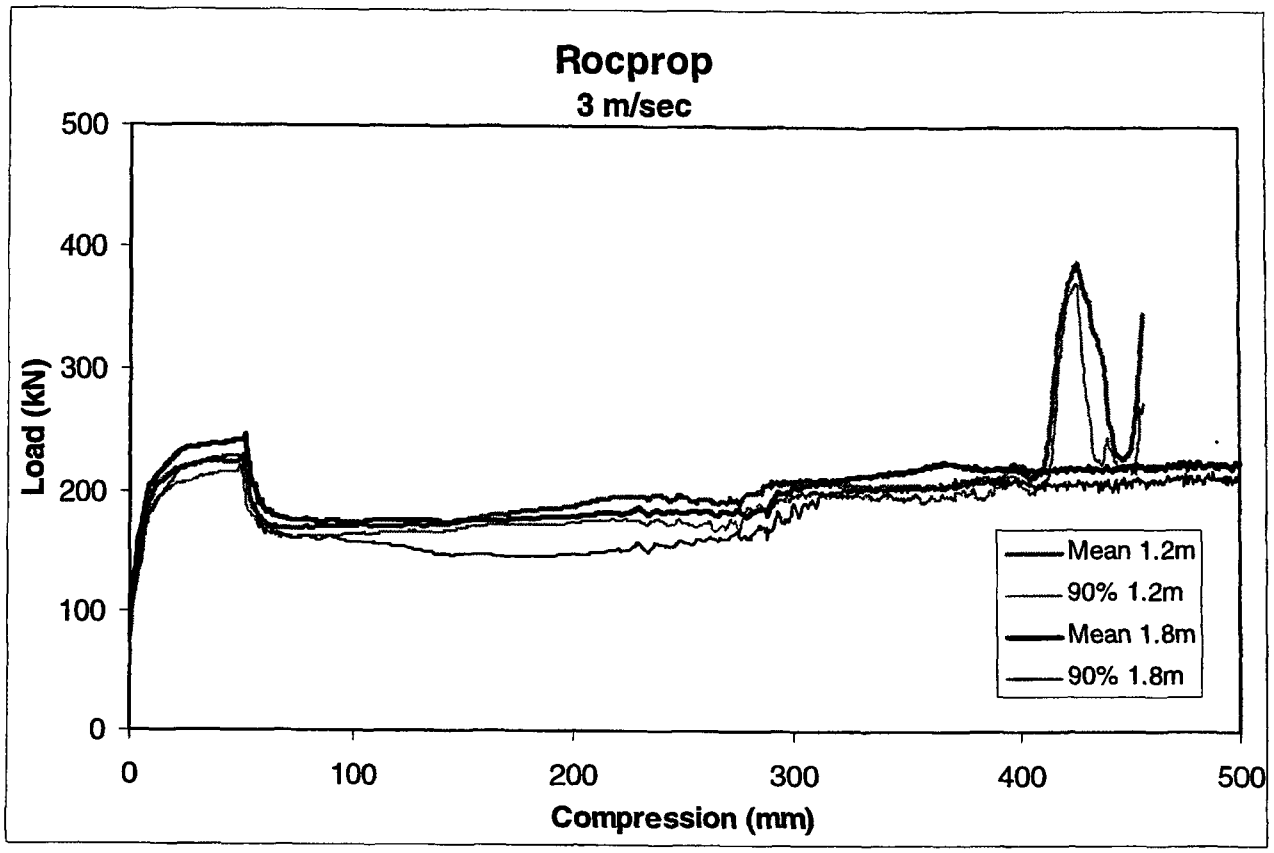
Rocprop
3 m/sec
Load (kN)
Compression (mm)
0
100
200
300
400
500
Mean 1.2m
90% 1.2m
Mean 1.8m
90% 1.8m

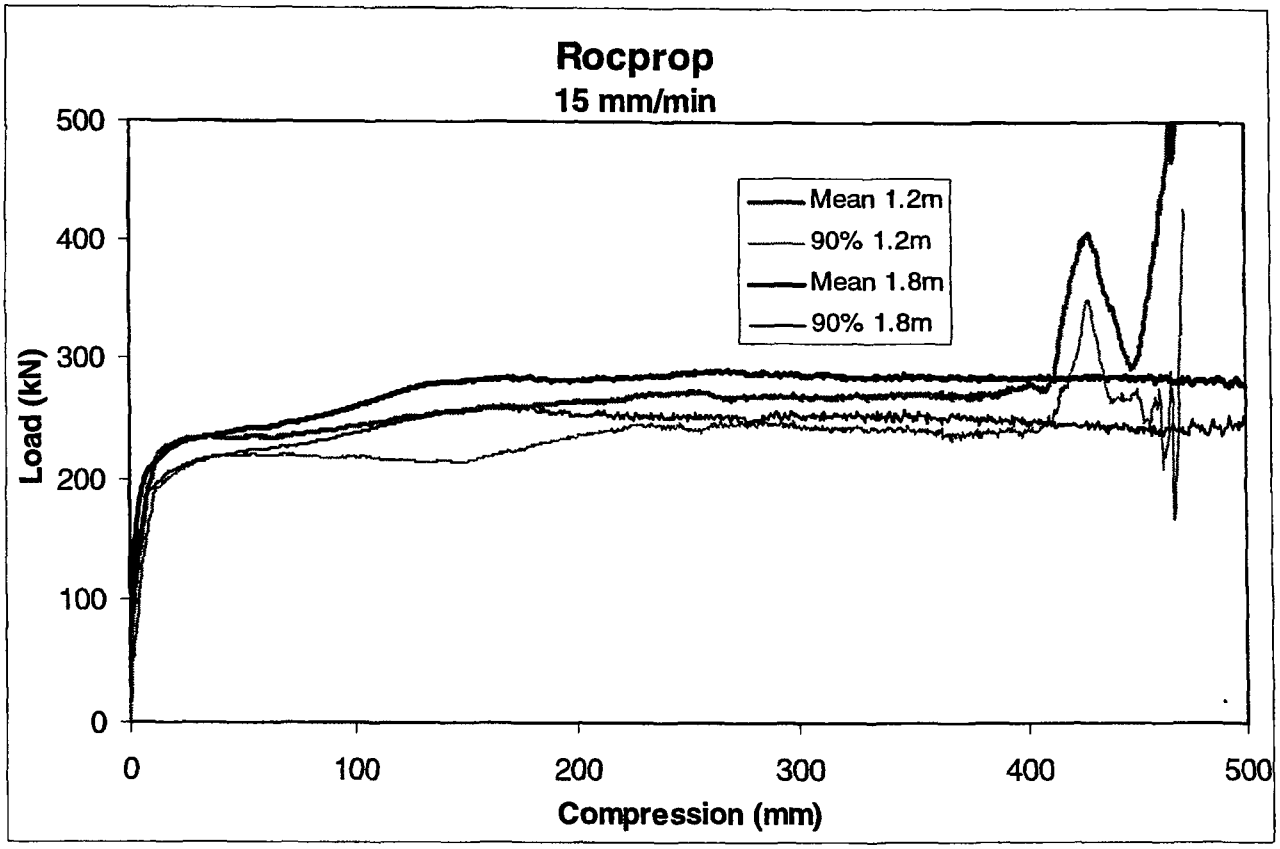
Rocprop
15 mm/min
Load (kN)
Compression (mm)
0
100
200
300
400
500
Mean 1.2m
90% 1.2m
Mean 1.8m
90% 1.8m

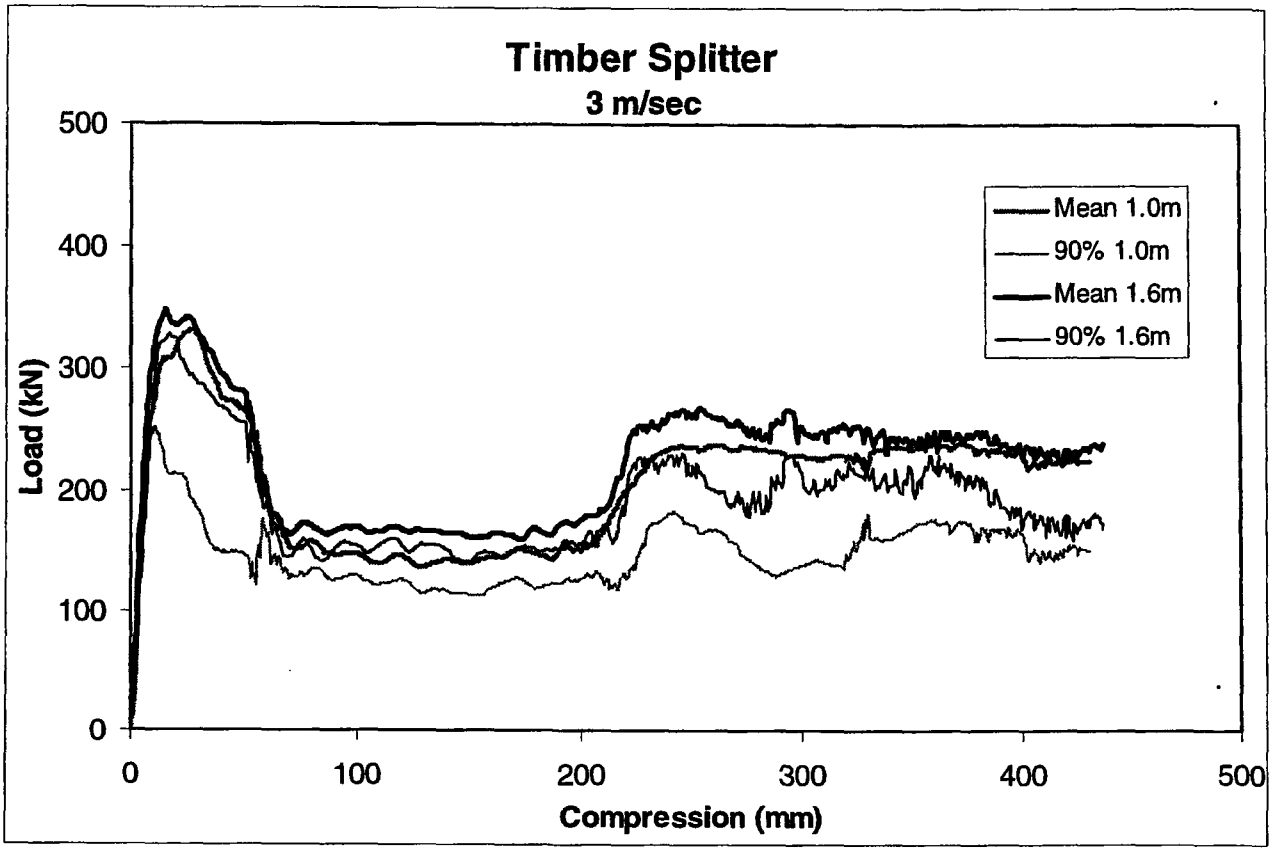
Timber Splitter
3 m/sec
Load (kN)
Compression (mm)
Mean 1.0m
90% 1.0m
Mean 1.6m
90% 1.6m
0
100
200
300
400
500

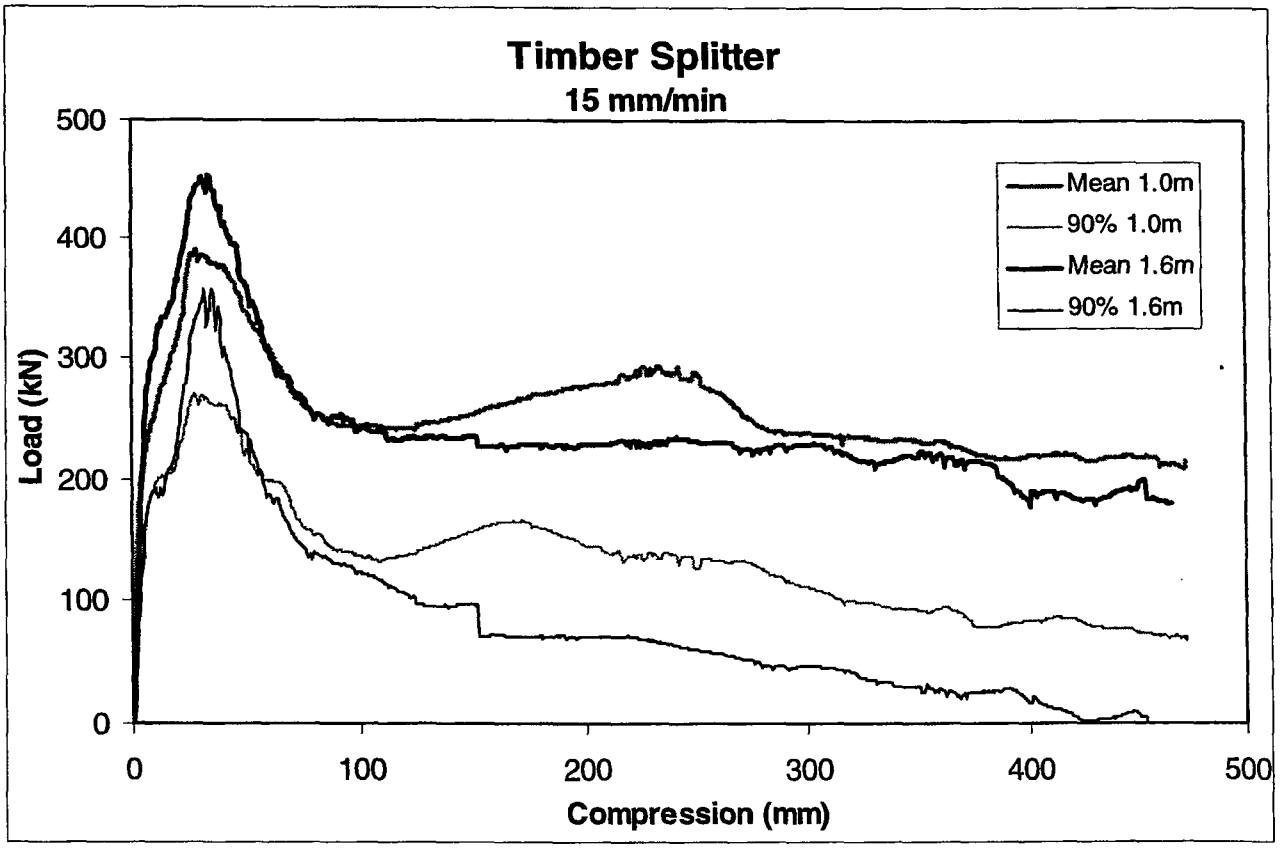
Timber Splitter
15 mm/min
Load (kN)
Compression (mm)
Mean 1.0m
90% 1.0m
Mean 1.6m
90% 1.6m
0
100
200
300
400
500

Comparision of Underground Results with Laboratory Results

The following graphs illustrate the comparison between underground and laboratory elongate performance. It has been recommended that in order to consider elongate variability, a 90 % lower confidence limit of unit performance be required for support design. For this reason, in situ performance is compared to the mean laboratory and 90 % limit performances. Since the in situ results are limited (one to three results per elongate type and length), an average in situ performance was considered only, providing at least a preliminary comparison.

These results indicate that the average laboratory performance would overestimate underground performance. In most cases, the 90 % performance limit of laboratory test results provides a good estimate of the expected undergound performance. Where the results do differ significantly, the underground units exhibit an increasing potential to buckling, which is likely to be the consequence of eccentric loading conditions resulting from non-parallel and uneven contact surfaces. Unfortunately, the eccentric loading laboratory tests (incline and step platens) do not show consistant results, and because these are essentially three one-off tests, conclusions or even indications of the effect on performance, cannot be drawn. For this reason, three identical eccentric loading tests have been recommended in the revised test procedure (see Section 8 of the main report).

The reduction in initial stiffness of the elongates noted in these graphs is a result of non-uniform loading conditions. This can also be seen on many of the eccentric loading tests conducted in the laboratory. Some elongates will be more susceptible to this lower stiffness than others as a result of their design and depending on which end of the elongate is subjected to this eccentricity.

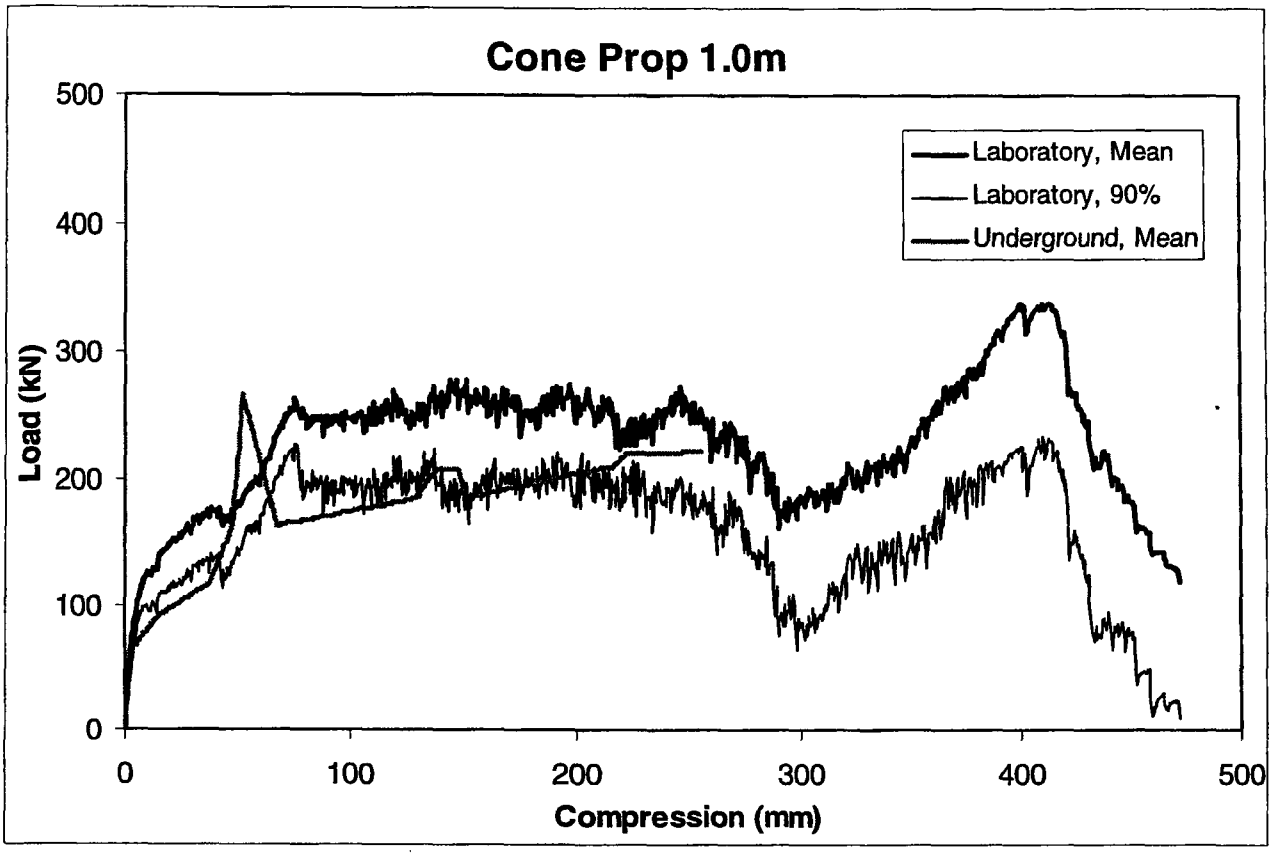
Cone Prop 1.0m
Load (kN)
Compression (mm)
Laboratory, Mean
Laboratory, 90%
Underground, Mean
0
100
200
300
400
500

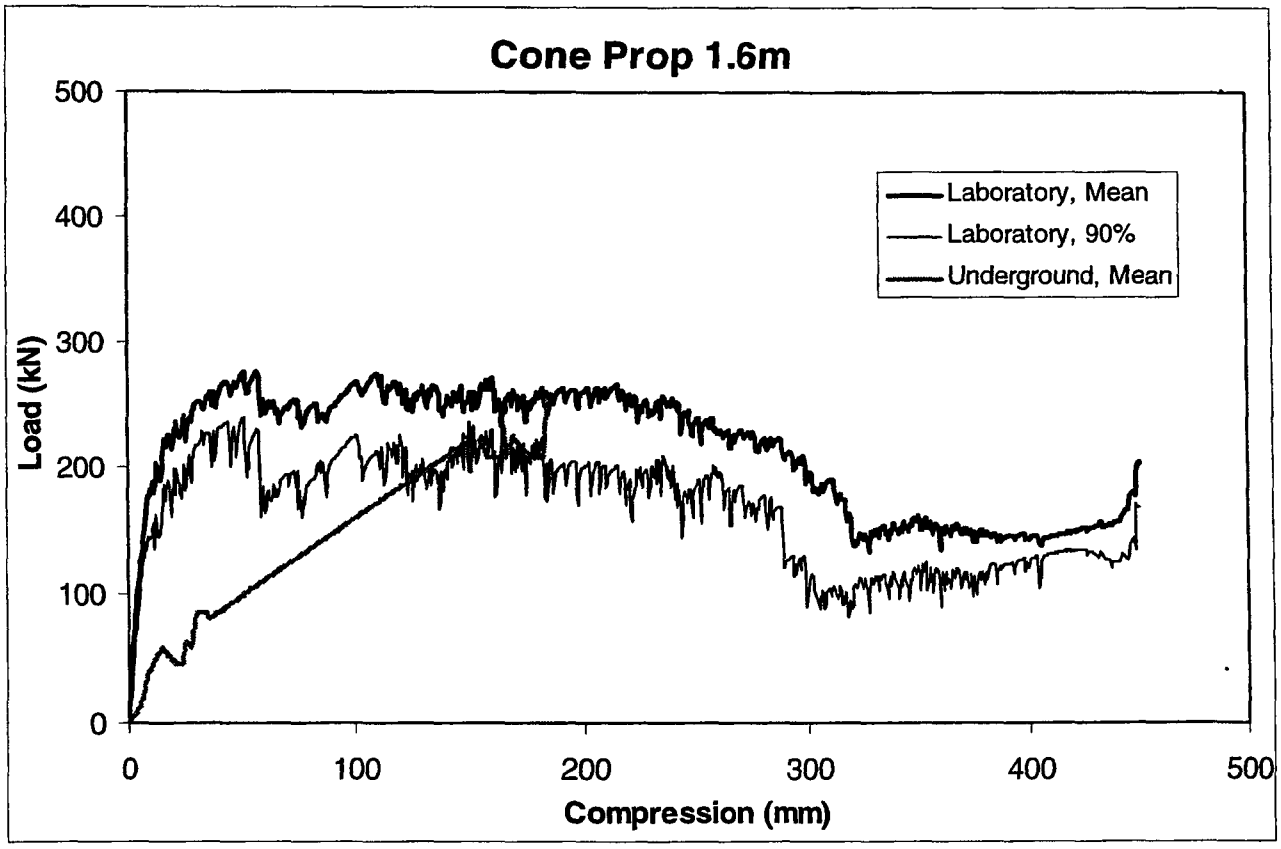
Cone Prop 1.6m
Load (kN)
Compression (mm)
Laboratory, Mean
Laboratory, 90%
Underground, Mean
0
100
200
300
400
500

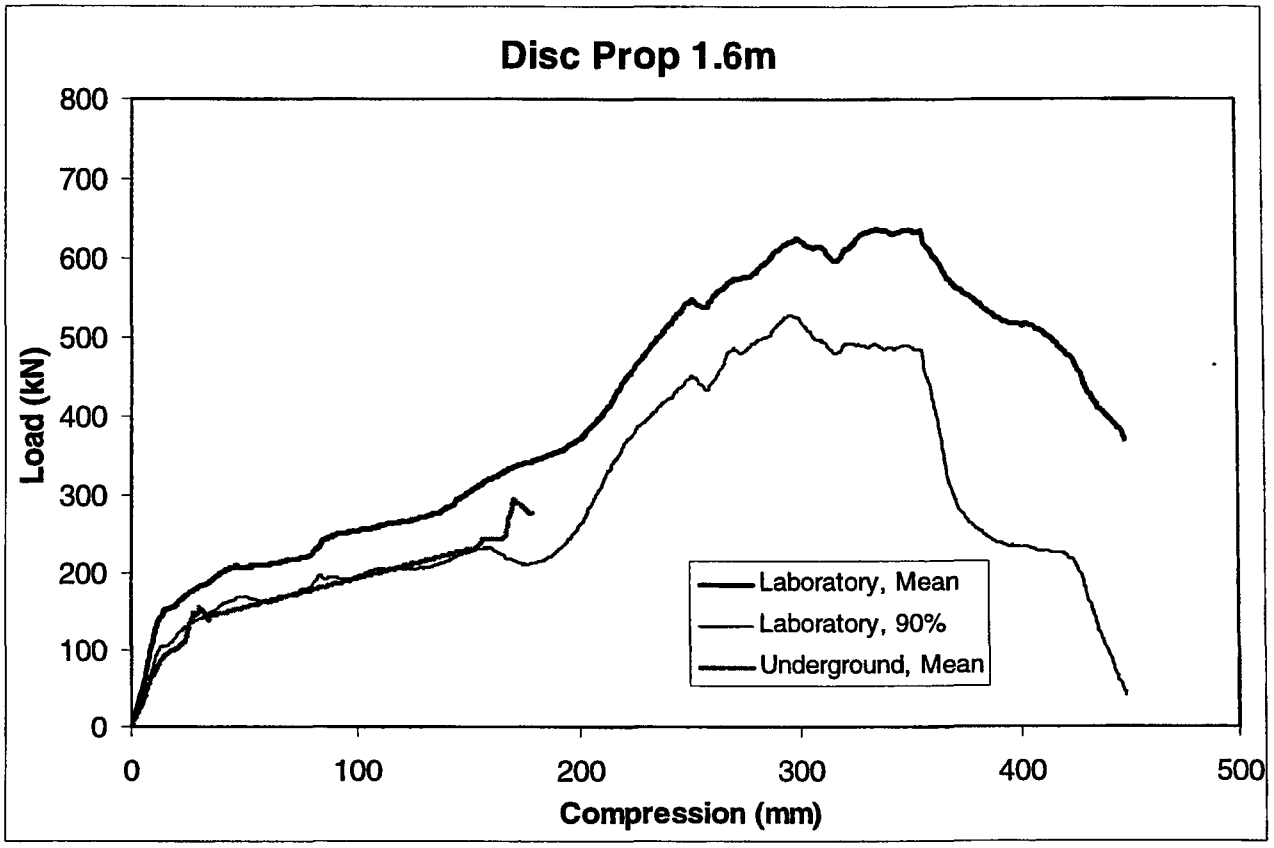
Disc Prop 1.6m
Load (kN)
800
700
600
500
400
300
200
100
0
0
100
200
300
400
500
Compression (mm)
Laboratory, Mean
Laboratory, 90%
Underground, Mean

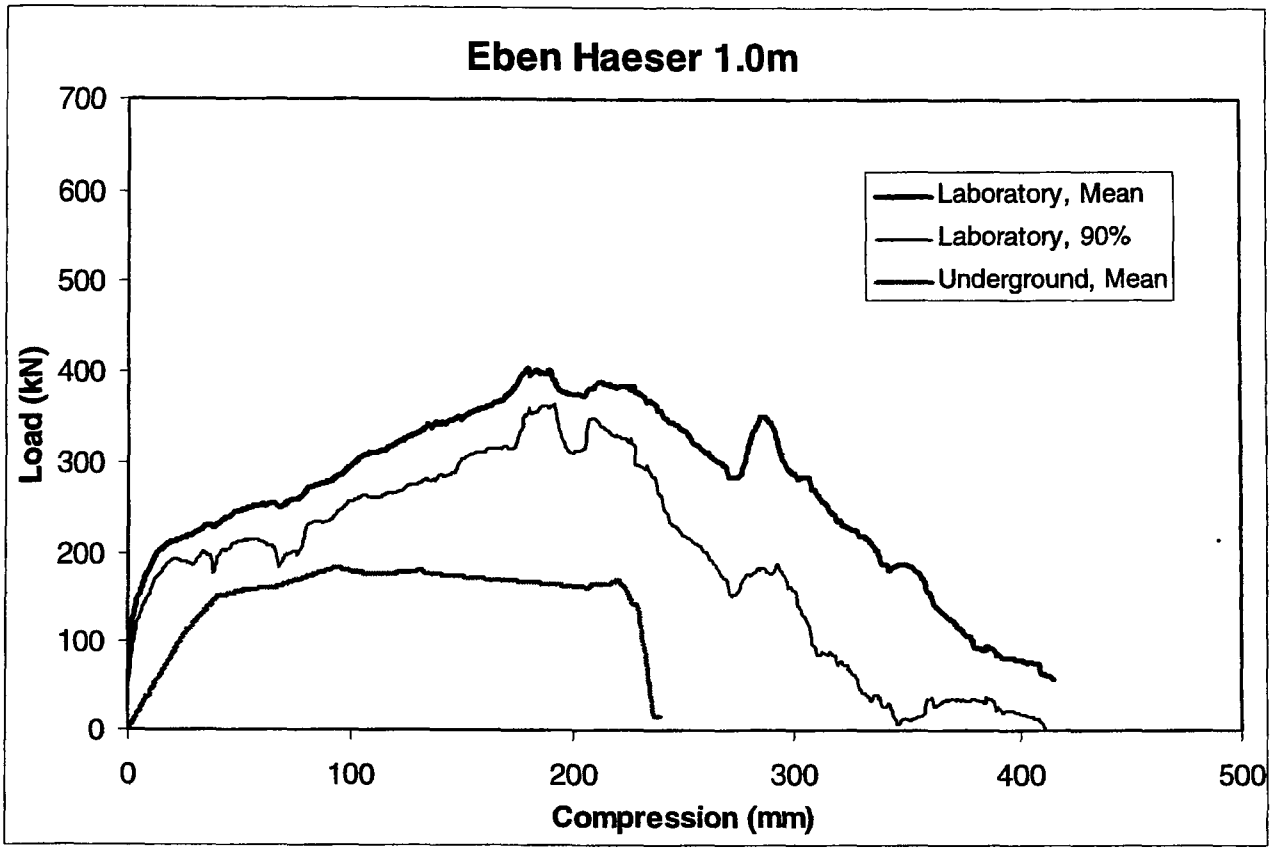
Eben Haeser 1.0m
Load (kN)
700
600
500
400
300
200
100
0
0
100
200
300
400
500
Compression (mm)
Laboratory, Mean
Laboratory, 90%
Underground, Mean

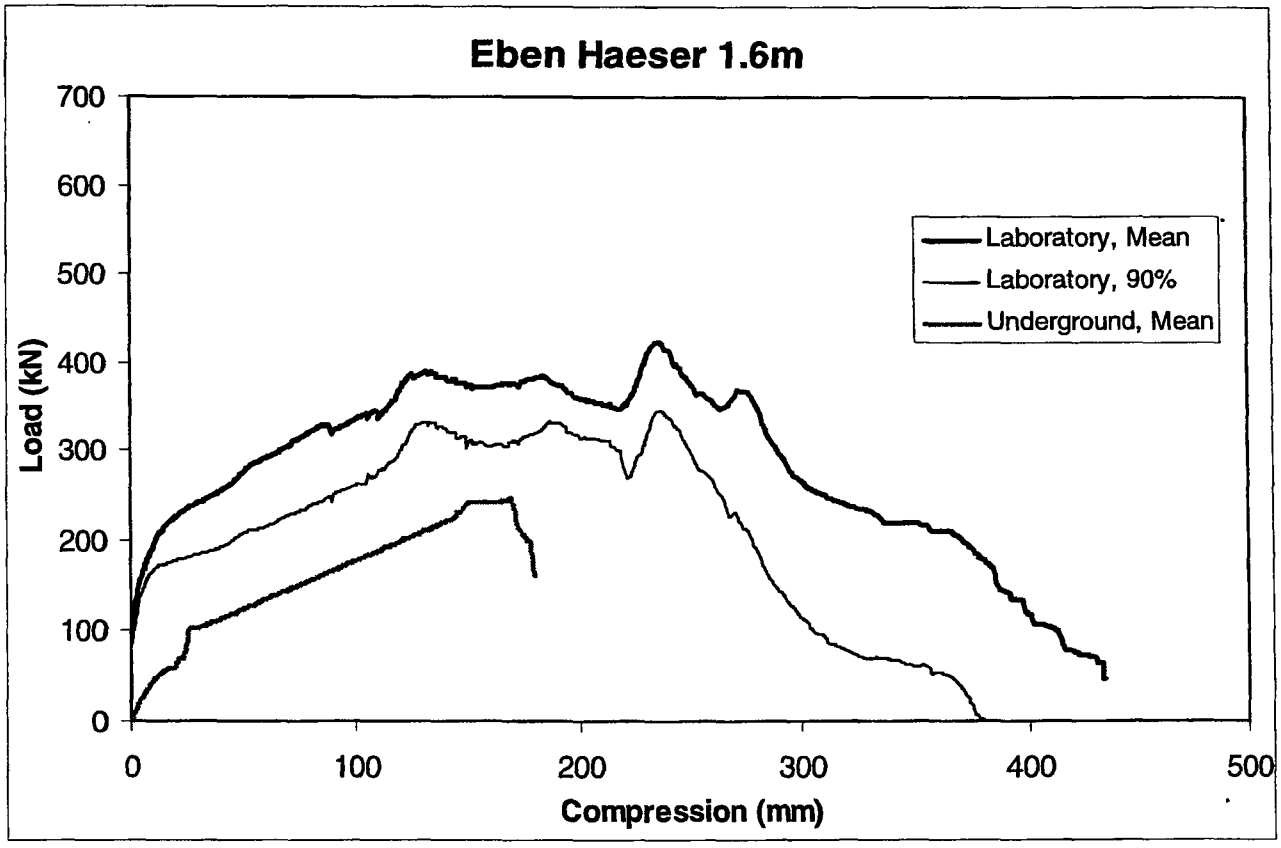
Eben Haeser 1.6m
Load (kN)
700
600
500
400
300
200
100
0
0
100
200
300
400
500
Compression (mm)
Laboratory, Mean
Laboratory, 90%
Underground, Mean

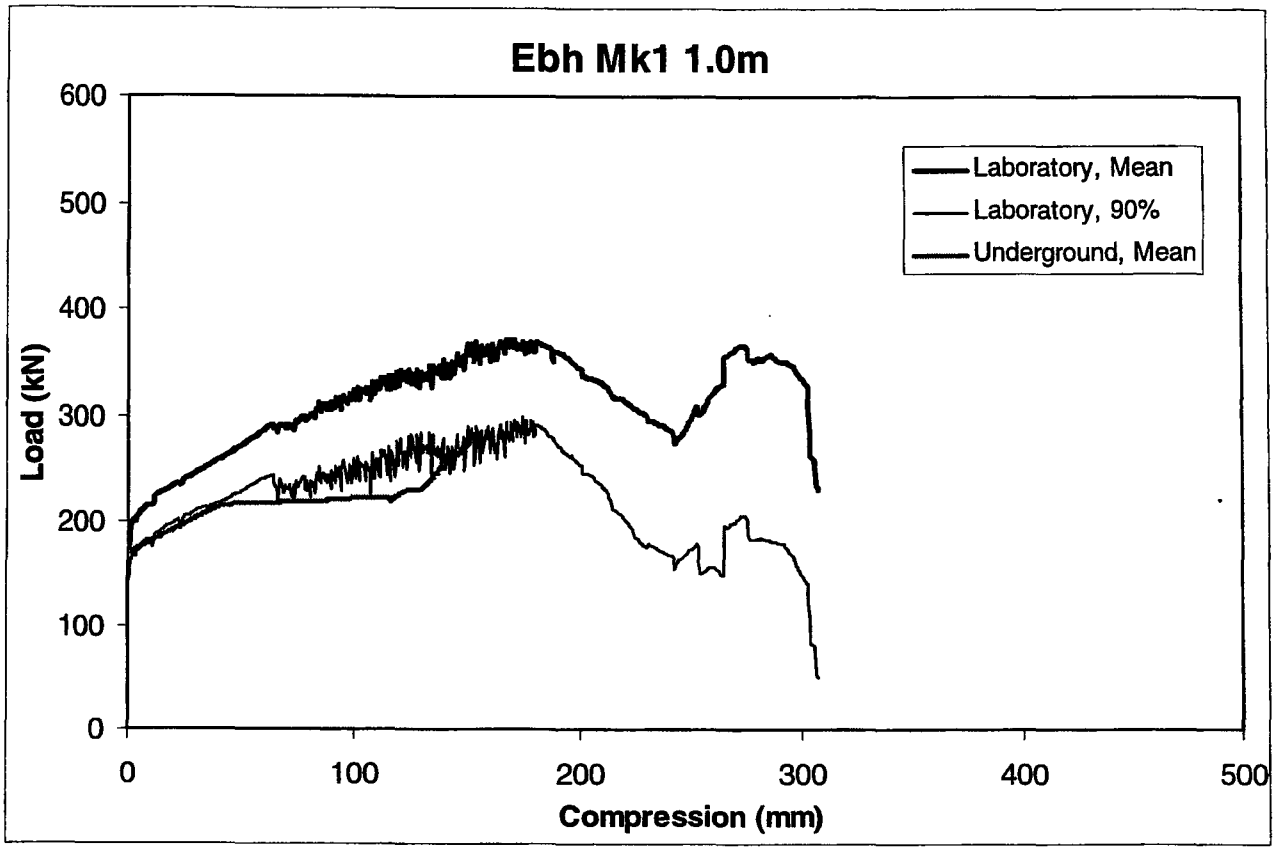
Ebh Mk1 1.0m
Load (kN)
600
500
400
300
200
100
0
0
100
200
300
400
500
Compression (mm)
Laboratory, Mean
Laboratory, 90%
Underground, Mean

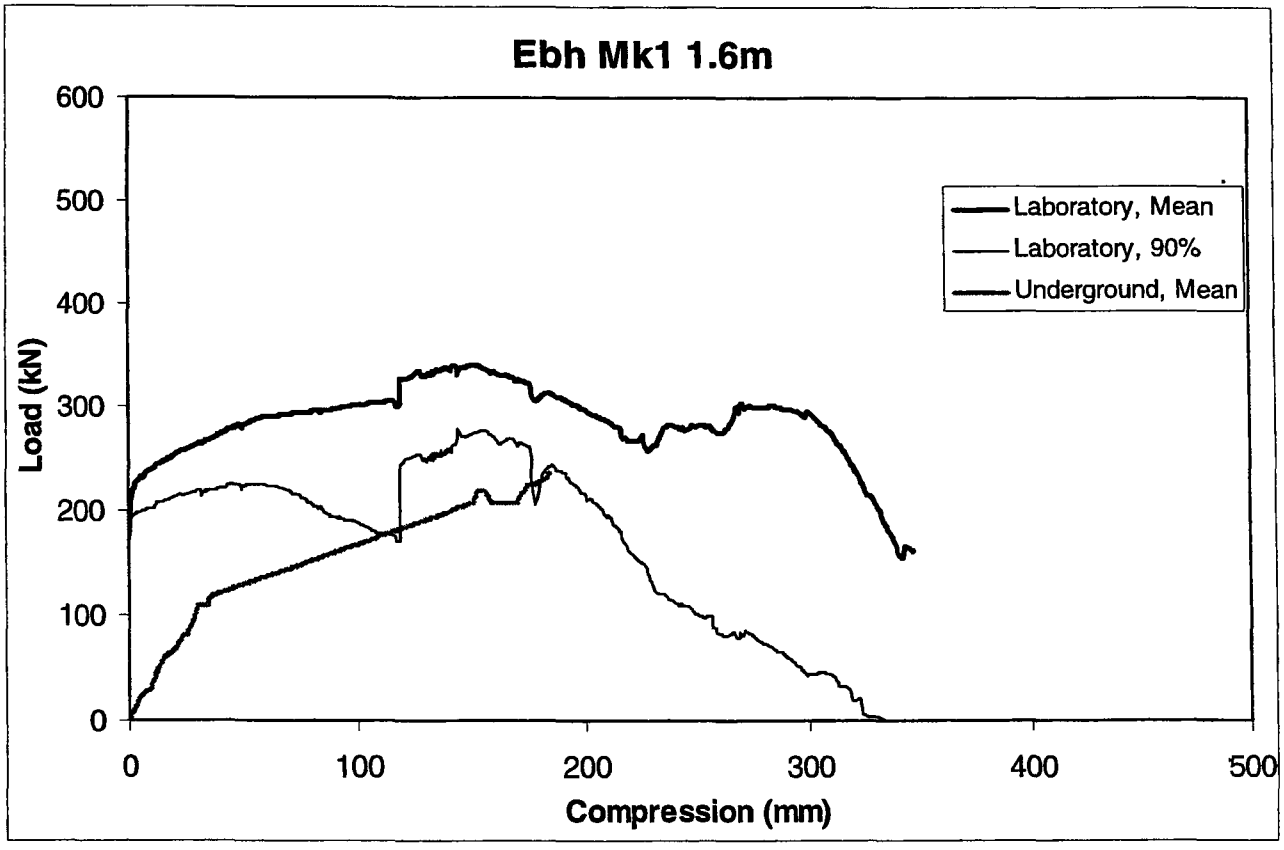
Ebh Mk1 1.6m
Load (kN)
600
500
400
300
200
100
0
0
100
200
300
400
500
Compression (mm)
Laboratory, Mean
Laboratory, 90%
Underground, Mean

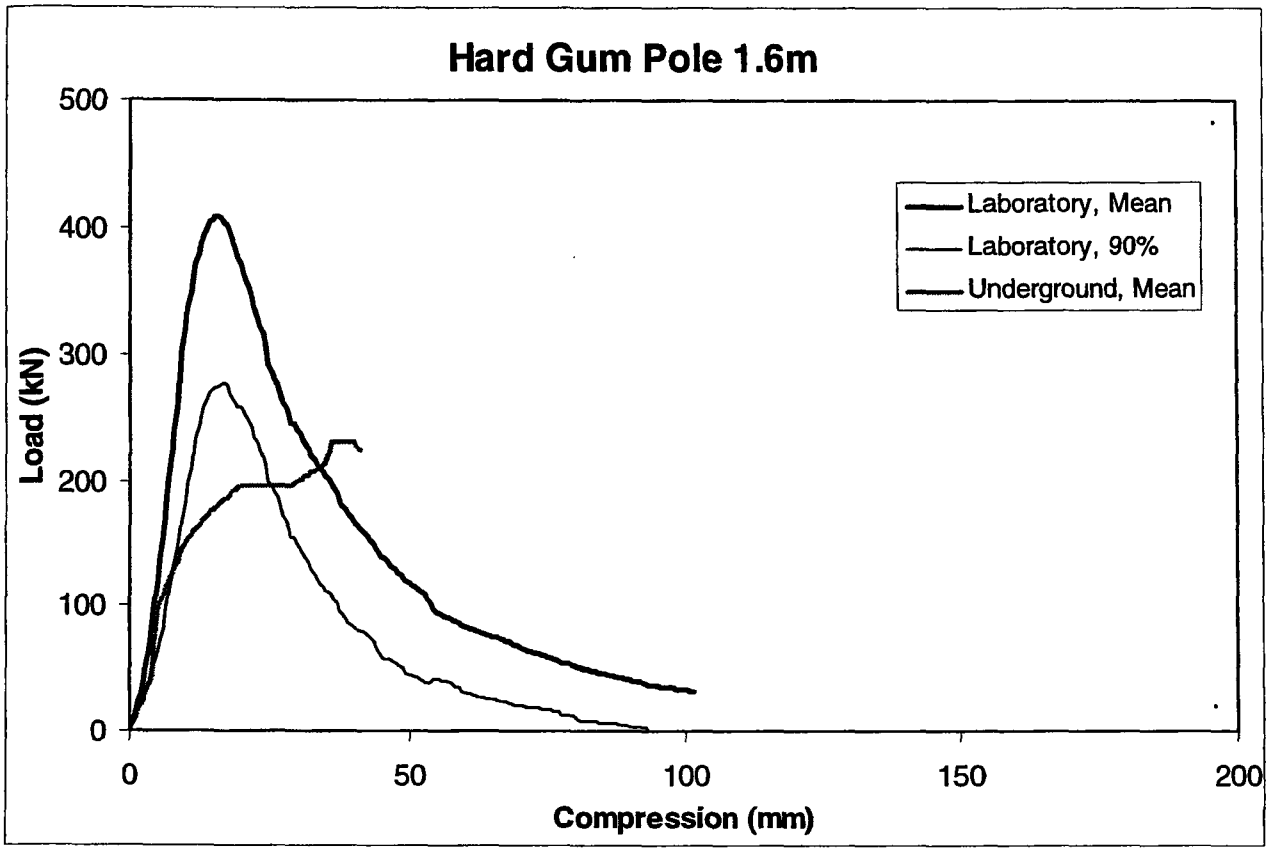
Hard Gum Pole 1.6m
500
400
300
200
100
0
Load (kN)
0
50
100
150
200
Compression (mm)
Laboratory, Mean
Laboratory, 90%
Underground, Mean

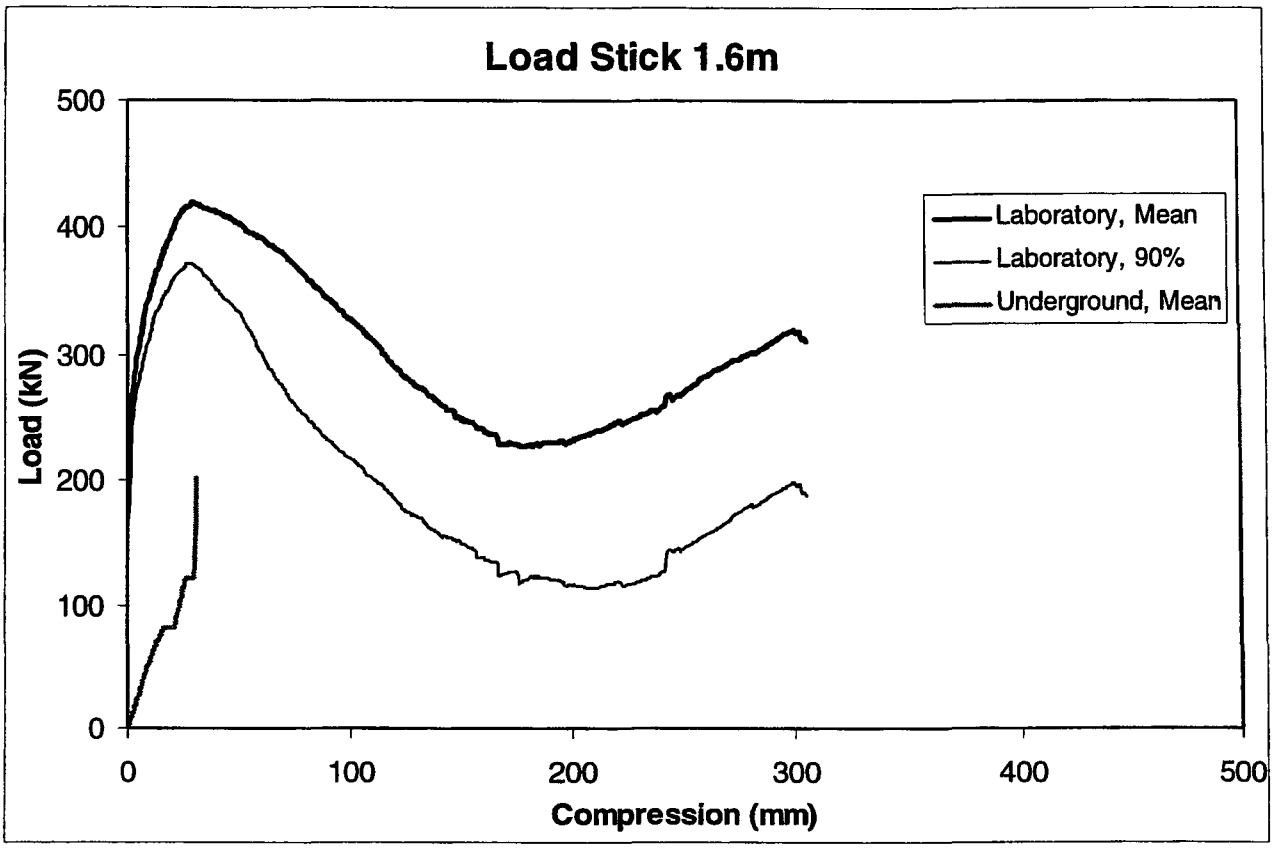
Load Stick 1.6m
500
400
300
200
100
0
Load (kN)
0
100
200
300
400
500
Compression (mm)
Laboratory, Mean
Laboratory, 90%
Underground, Mean

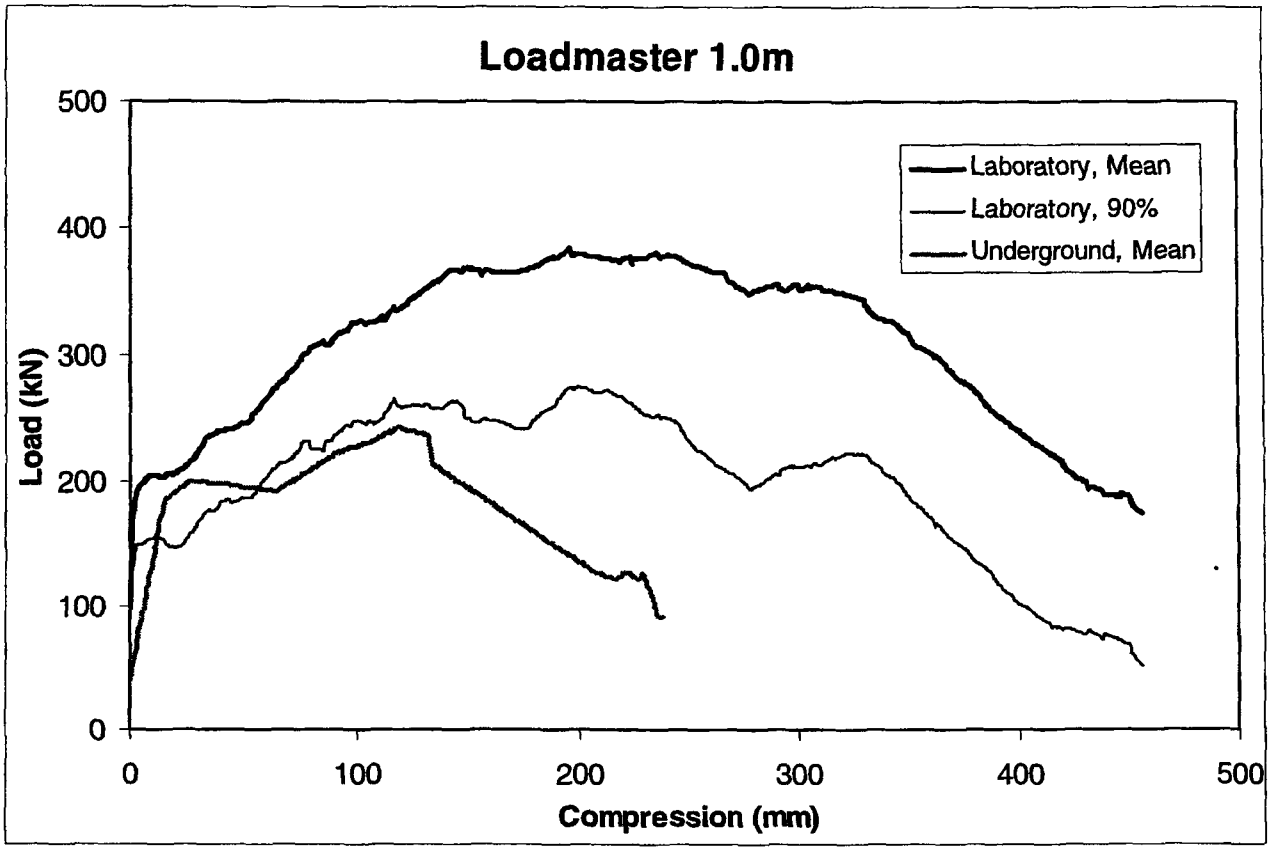
Loadmaster 1.0m
Load (kN)
Compression (mm)
Laboratory, Mean
Laboratory, 90%
Underground, Mean
0
100
200
300
400
500

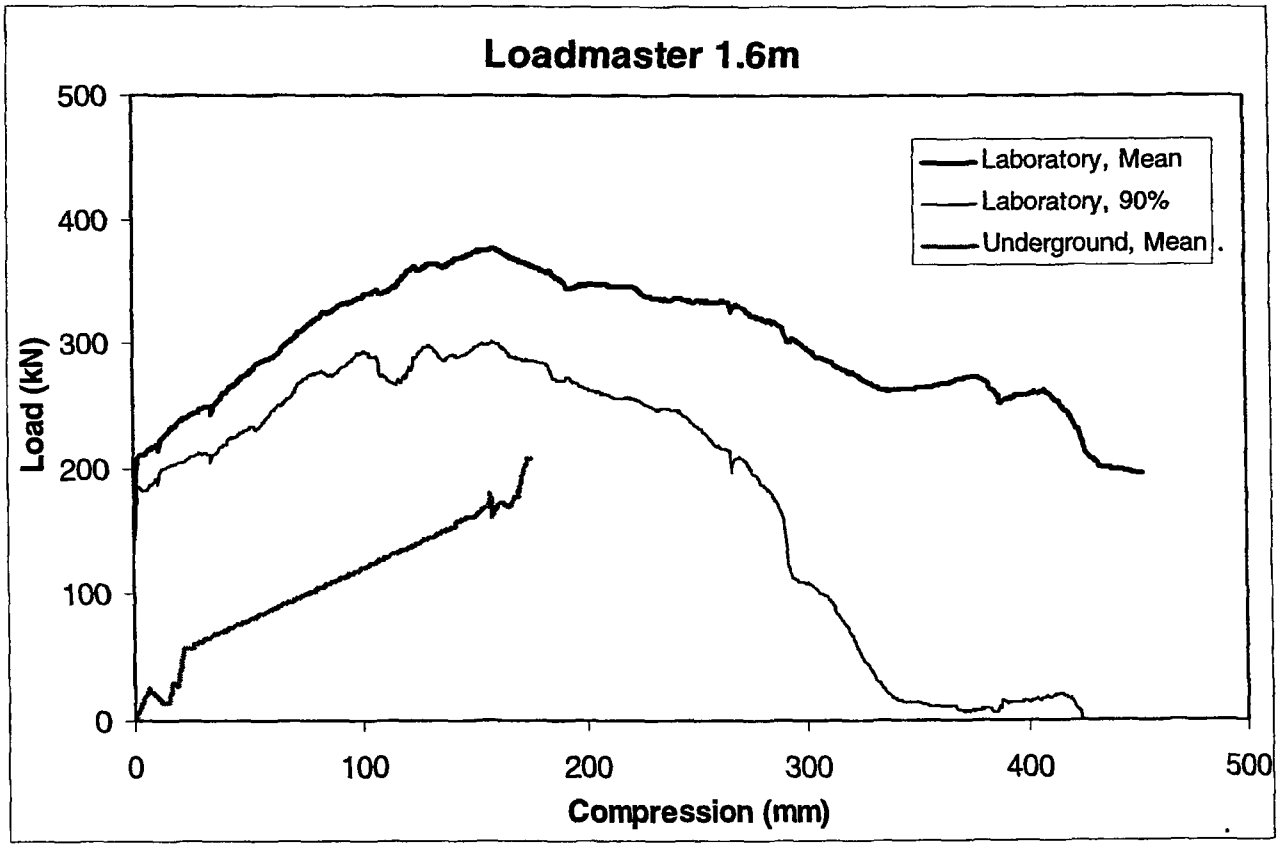
Loadmaster 1.6m
Load (kN)
Compression (mm)
Laboratory, Mean
Laboratory, 90%
Underground, Mean
0
100
200
300
400
500

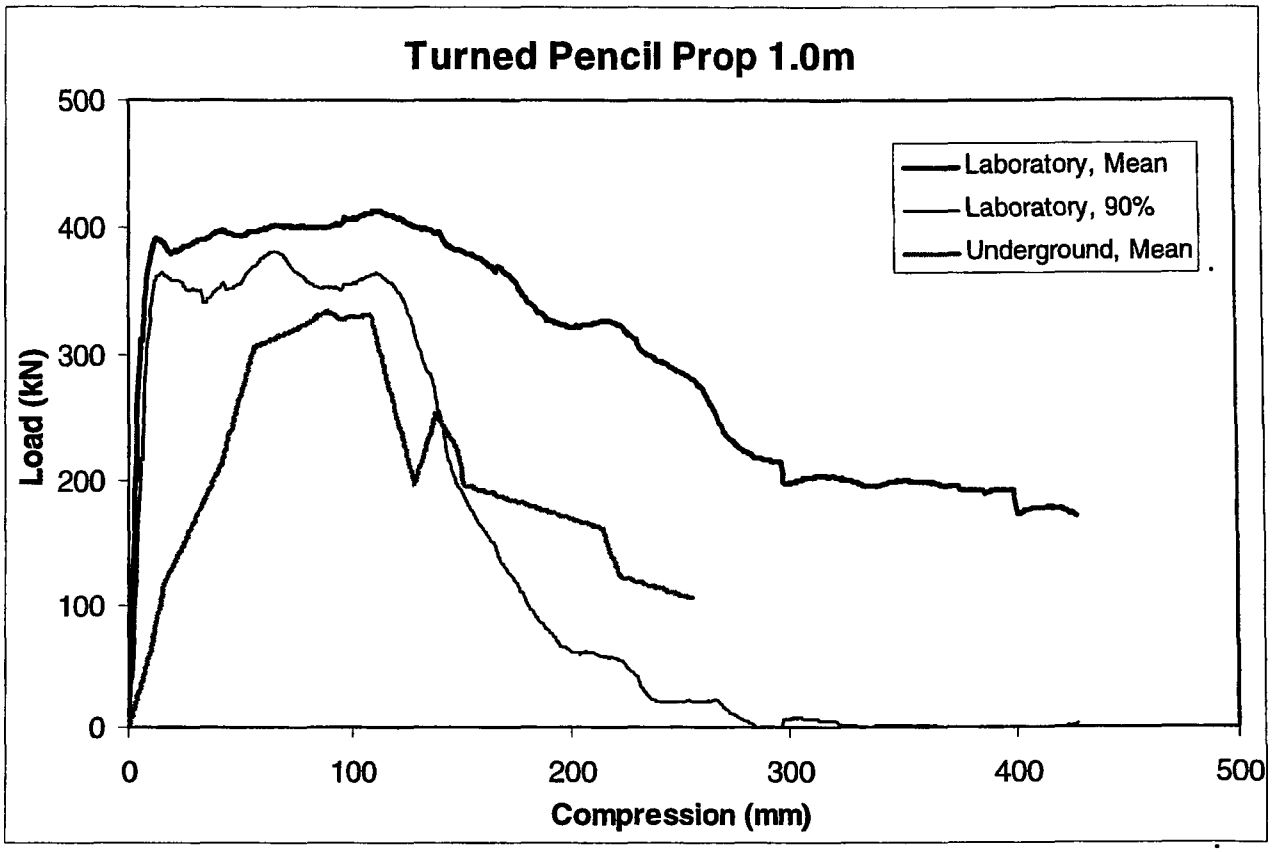
Turned Pencil Prop 1.0m
Load (kN)
Compression (mm)
Laboratory, Mean
Laboratory, 90%
Underground, Mean
0
100
200
300
400
500

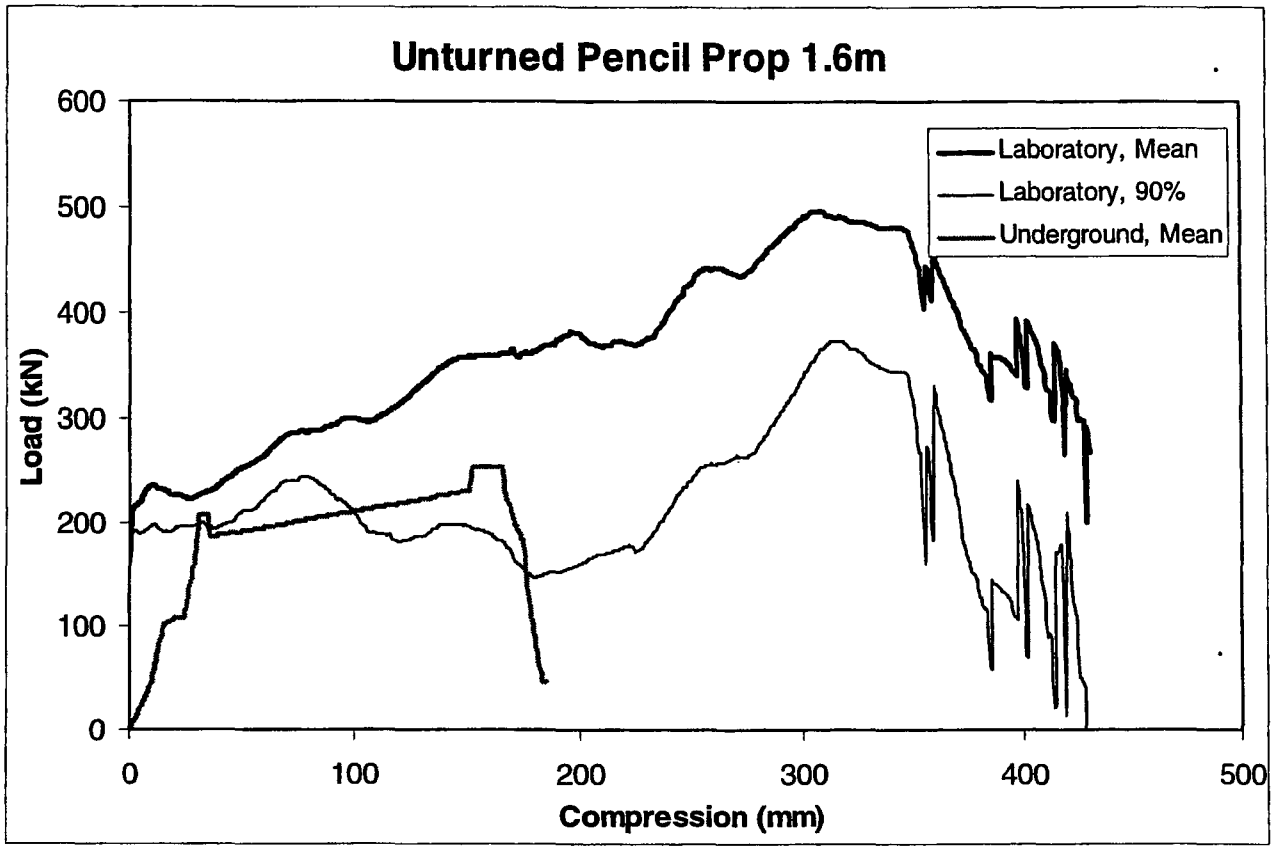
Unturned Pencil Prop 1.6m
Load (kN)
600
500
400
300
200
100
0
0
100
200
300
400
500
Compression (mm)
Laboratory, Mean
Laboratory, 90%
Underground, Mean

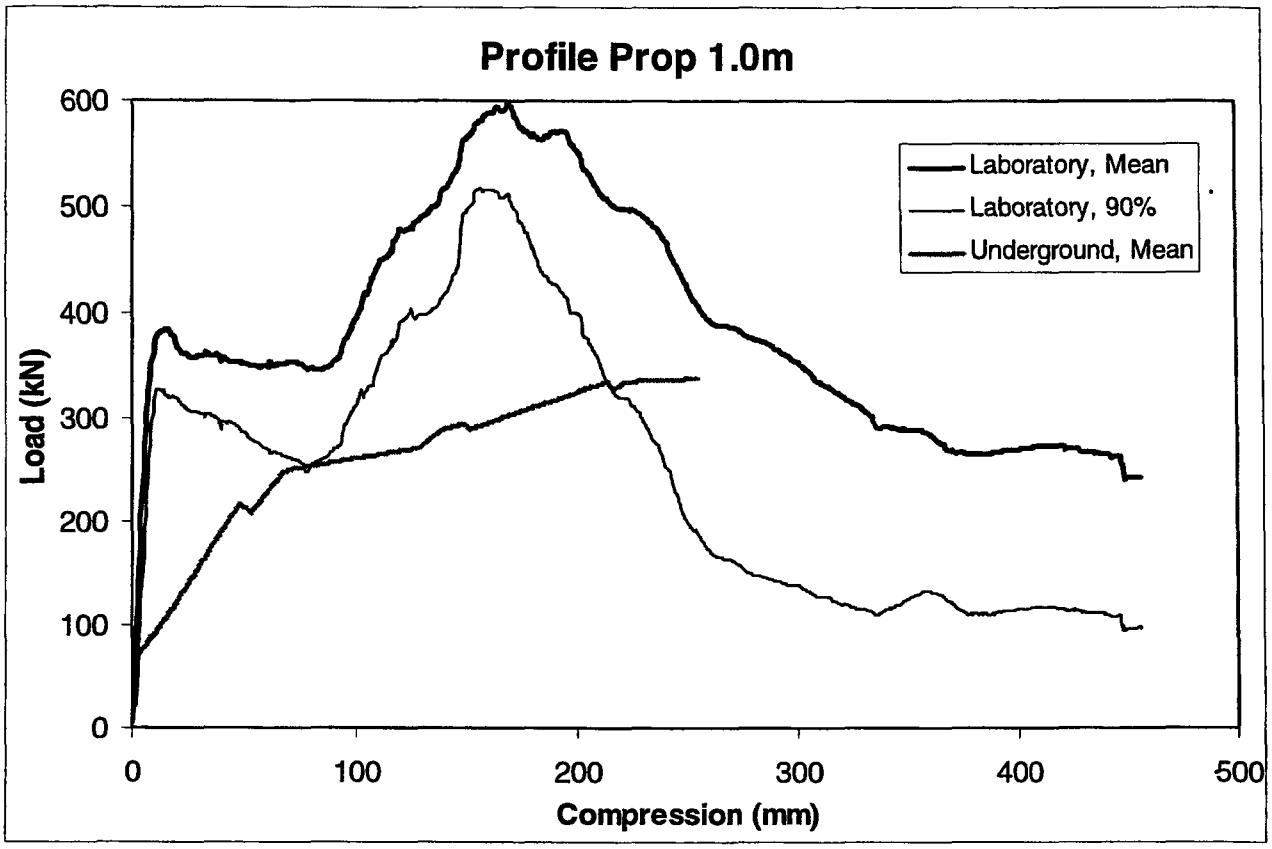
Profile Prop 1.0m
Load (kN)
600
500
400
300
200
100
0
0
100
200
300
400
500
Compression (mm)
Laboratory, Mean
Laboratory, 90%
Underground, Mean

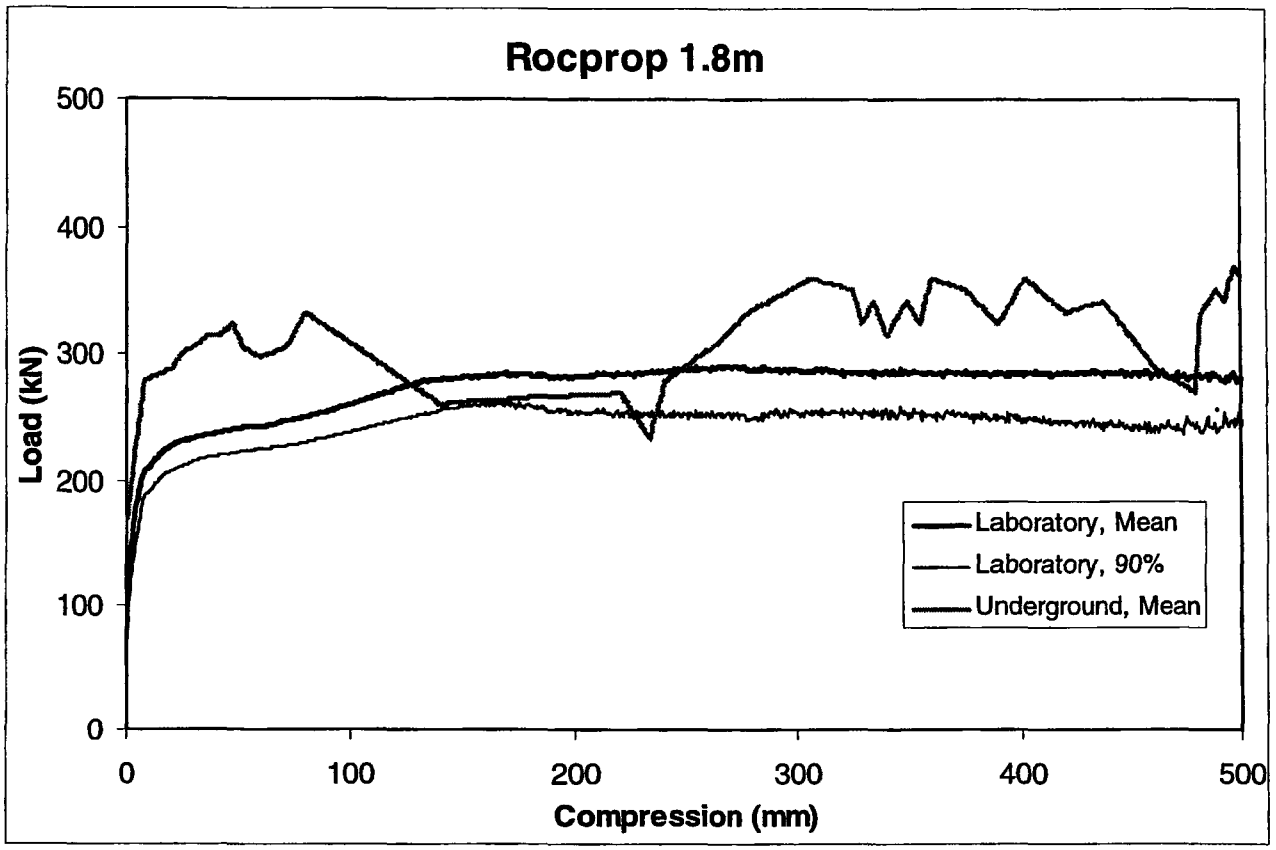
Rocprop 1.8m
Load (kN)
500
400
300
200
100
0
0
100
200
300
400
500
Compression (mm)
Laboratory, Mean
Laboratory, 90%
Underground, Mean

Summary of All Elongate Tests

The following graphs contain all test results (laboratory and underground) sorted according to elongate type and length. Summary statistical evaluations have been conducted on the slow and rapid test results and have been presented with the original test results. The graphs of the statistical evaluations show the mean values and measures of the variability of the limited number of units tested. These variability curves represent various lower confidence limits of the elongate performance. The mean – 1 standard deviation (or approximately 84 % lower limit), 90 % and 95 % limits are shown to illustrate the effects of increasing confidence of exceeding the design curve.

The graphs comparing of rate effects appear to indicate that little variation in performance exists between 15 and 150 mm/min, bearing in mind that only one test was conducted at 150 mm/min. As a whole however, there does appear to be enough information across all elongate types and at both lengths to imply that there is little difference (in most cases) between results from testing rates of 15 and 150 mm/min, certainly not when considering the variability obtained from ten slow tests. For this reason, a standard testing rate of 30 mm/min would be more practical, especially since many of the manufacturers / suppliers have used this rate in the past and their database is largely based on this test rate.

The use of the underground test results was somewhat subjective. Estimates had to be made regarding the accuracy of the load cells, especially following the large seismic events that both the short and load elongates were subjected to. Photographs of the installed units had to be reviewed in considerable detail in order to determine the validity of in situ results. The underground results shown in the following graphs have been formatted such that reliable results are shown with a dotted line unreliable or false results are shown with a dashed line. The average performance was determined from the reliable results.

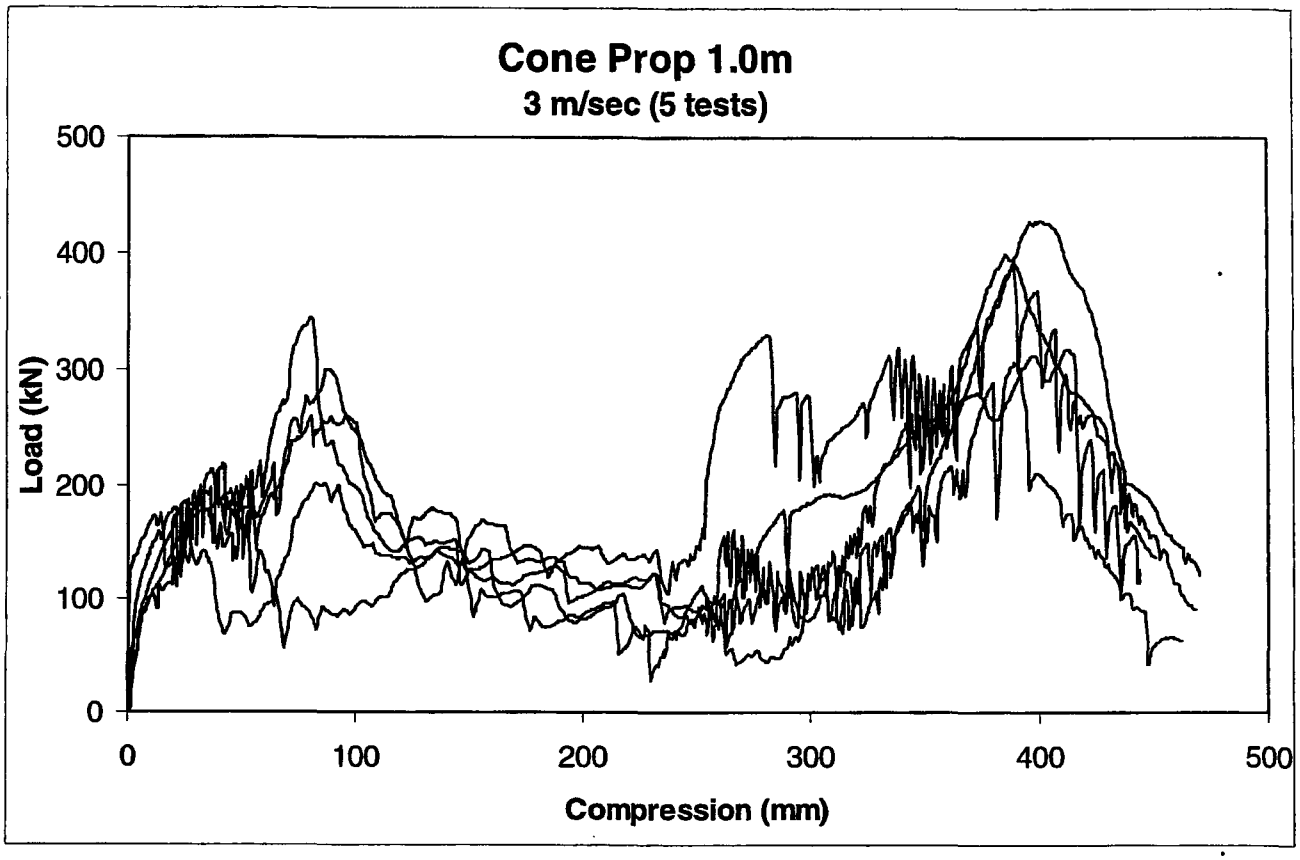
Cone Prop 1.0m
3 m/sec (5 tests)
Load (kN)
Compression (mm)
0
100
200
300
400
500

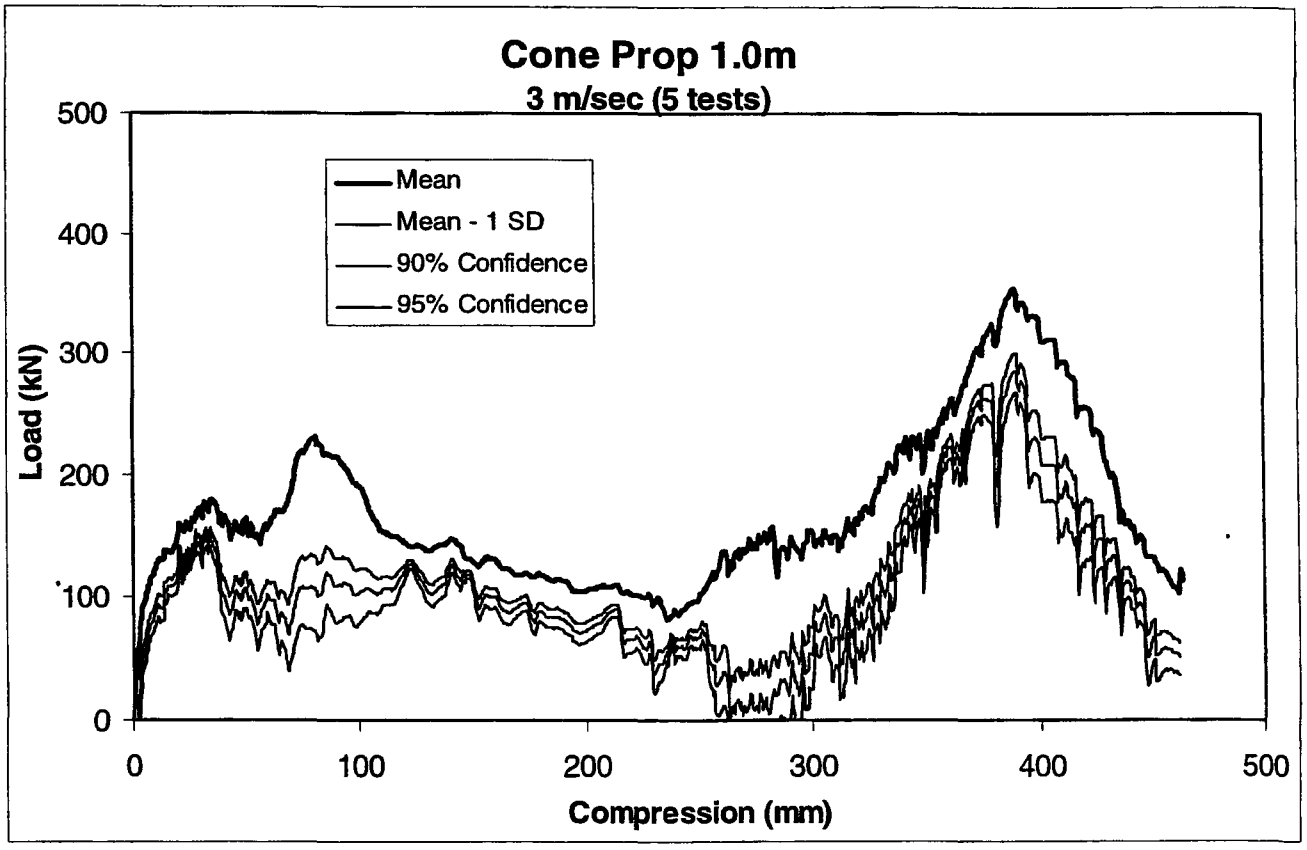
Cone Prop 1.0m
3 m/sec (5 tests)
Mean
Mean - 1 SD
90% Confidence
95% Confidence
Load (kN)
Compression (mm)
0
100
200
300
400
500

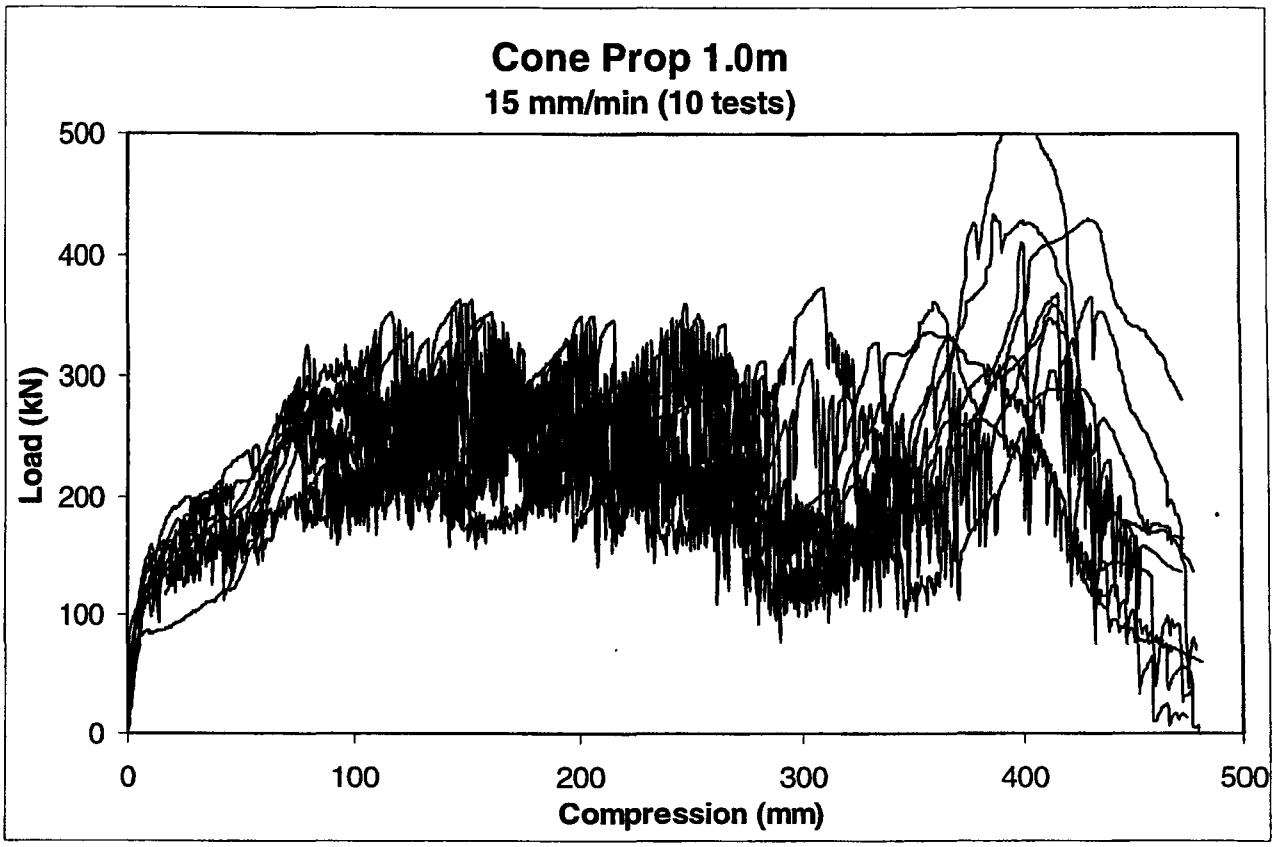
Cone Prop 1.0m
15 mm/min (10 tests)
Load (kN)
0
100
200
300
400
500
Compression (mm)

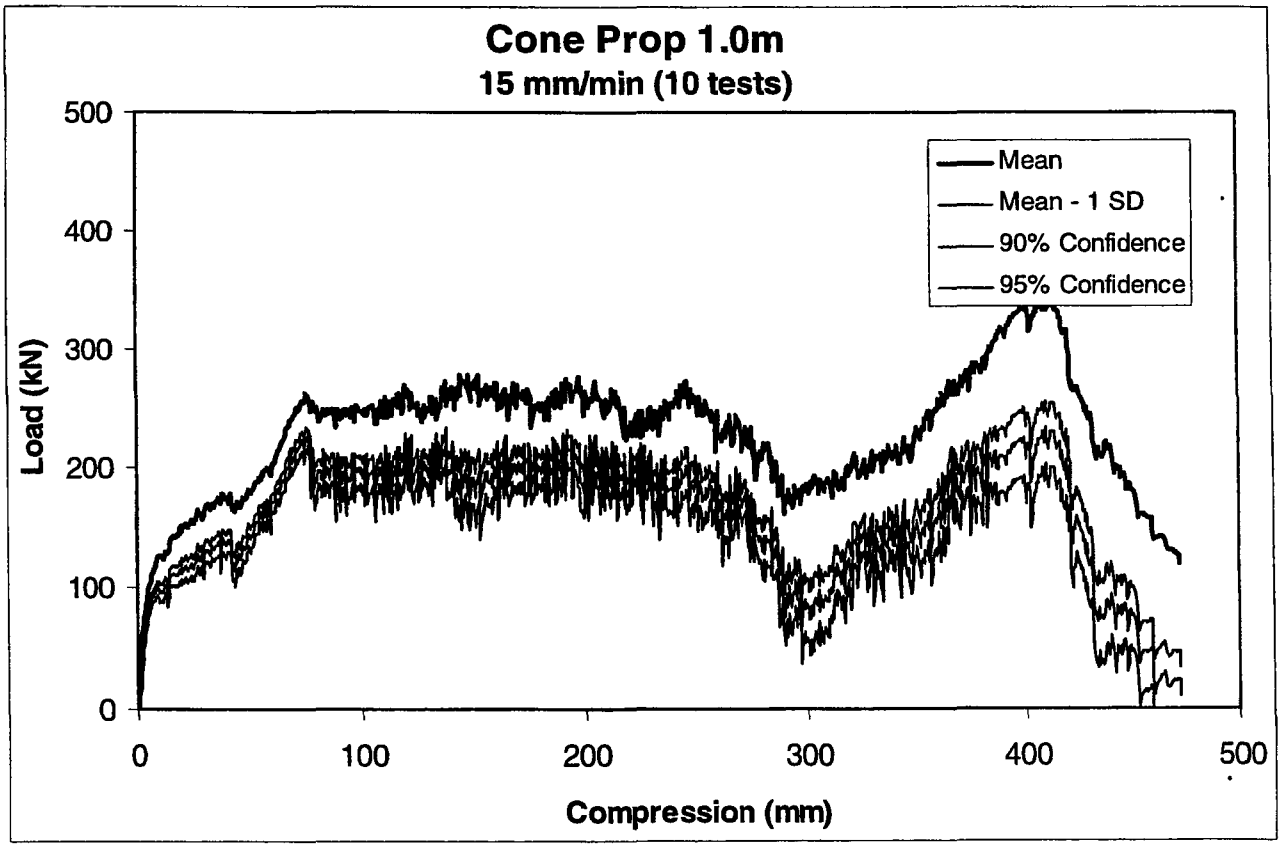
Cone Prop 1.0m
15 mm/min (10 tests)
Mean
Mean - 1 SD
90% Confidence
95% Confidence
Load (kN)
0
100
200
300
400
500
Compression (mm)

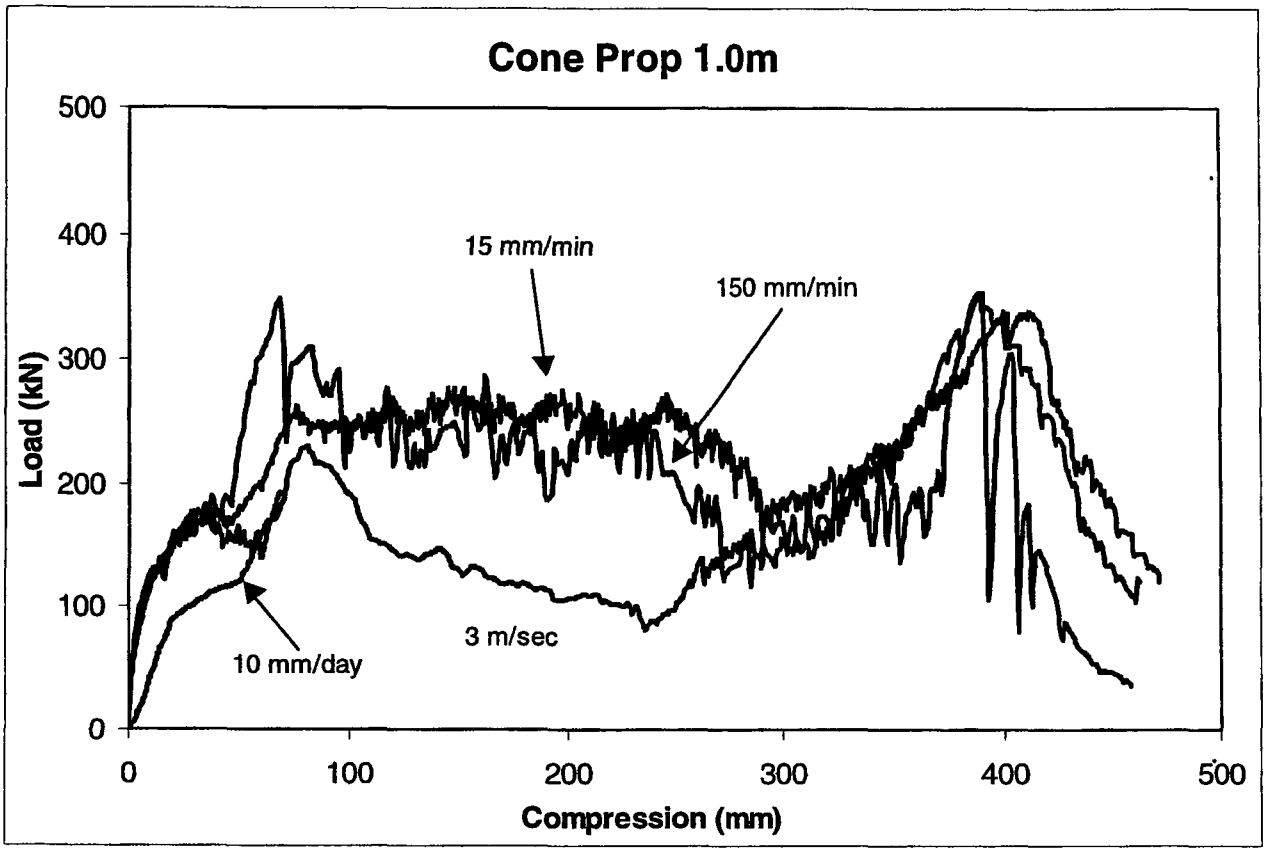
Cone Prop 1.0m
500
400
300
200
100
0
Load (kN)
15 mm/min
150 mm/min
3 m/sec
10 mm/day
0
100
200
300
400
500
Compression (mm)

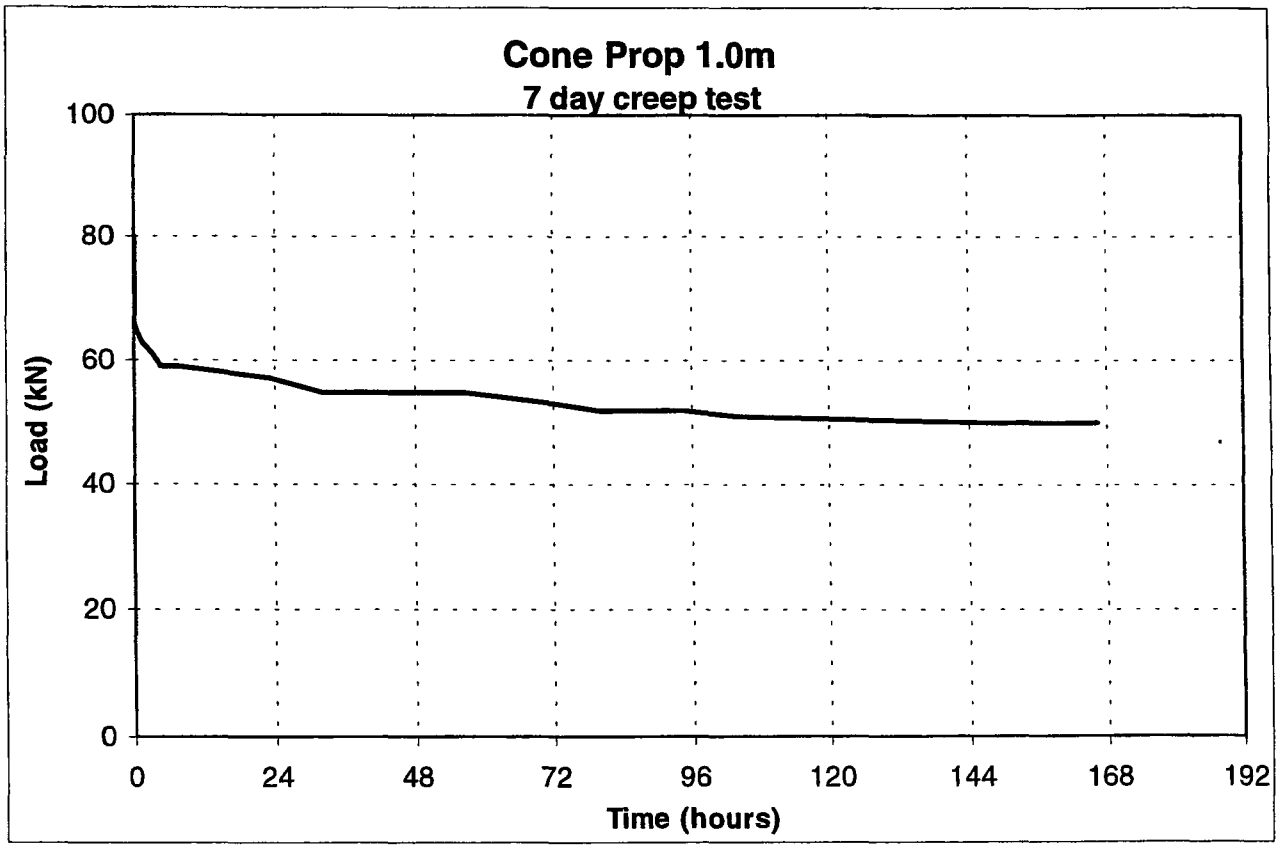
Cone Prop 1.0m
7 day creep test
100
80
60
40
20
0
Load (kN)
0
24
48
72
96
120
144
168
192
Time (hours)

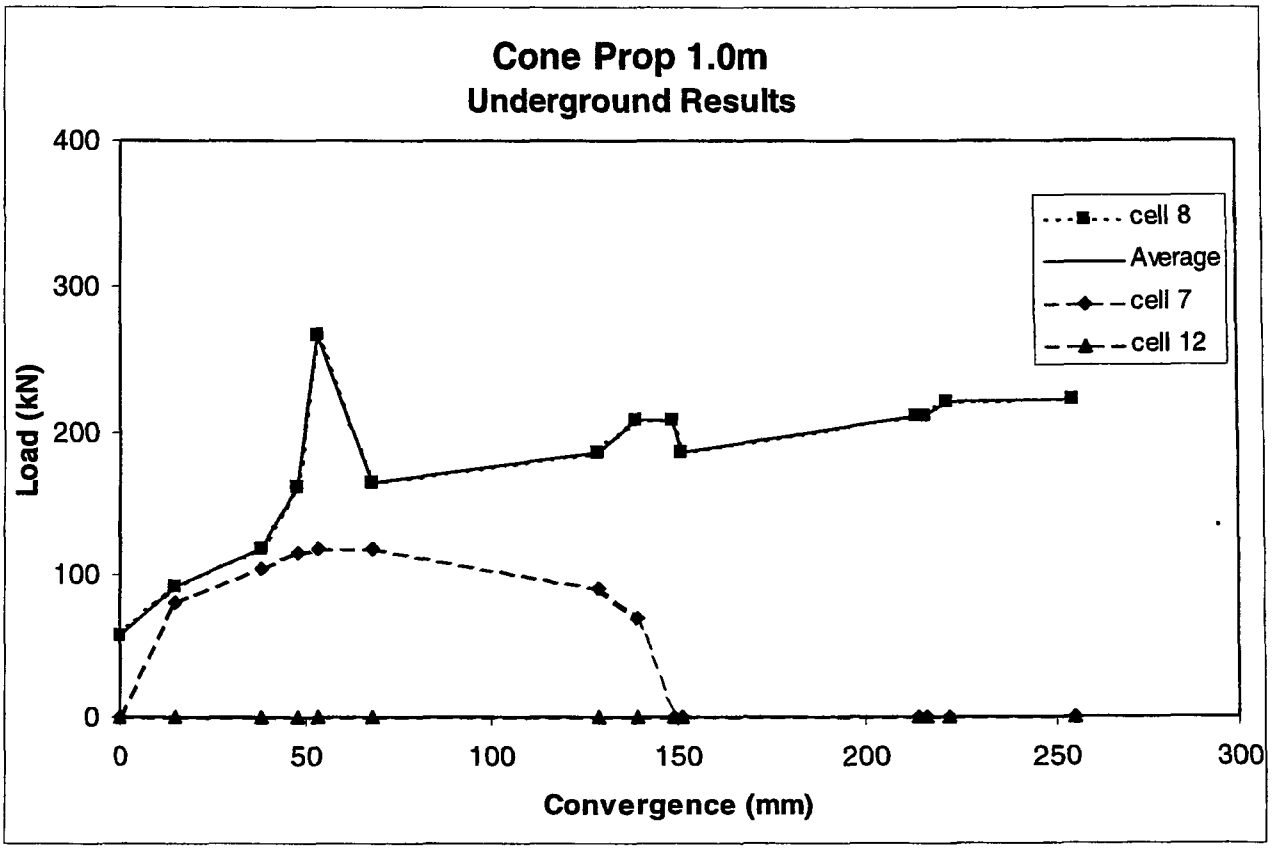
Cone Prop 1.0m
Underground Results
400
300
200
100
0
Load (kN)
0
50
100
150
200
250
300
Convergence (mm)
cell 8
Average
cell 7
cell 12

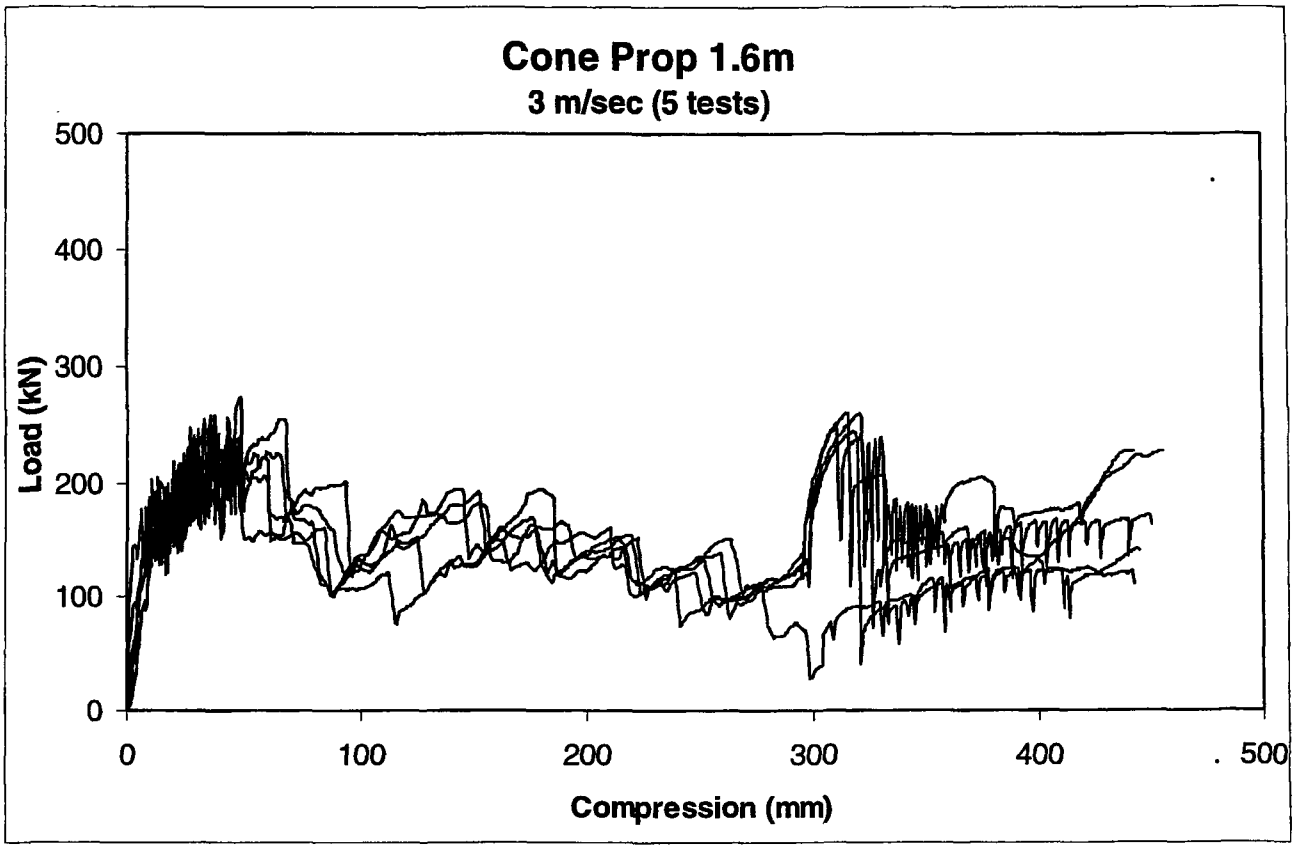
Cone Prop 1.6m
3 m/sec (5 tests)
Load (kN)
500
400
300
200
100
0
0
100
200
300
400
500
Compression (mm)

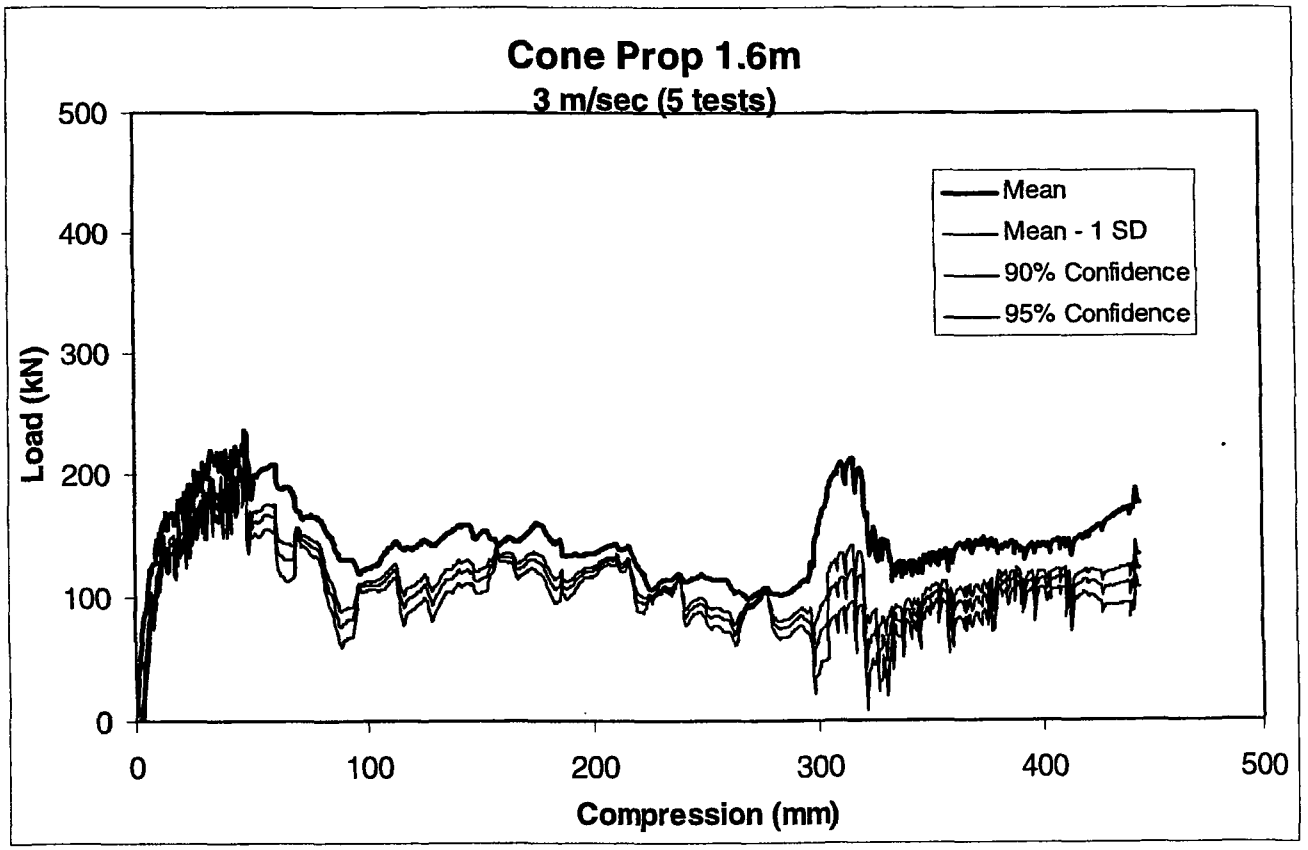
Cone Prop 1.6m
3 m/sec (5 tests)
Mean
Mean - 1 SD
90% Confidence
95% Confidence
Load (kN)
500
400
300
200
100
0
0
100
200
300
400
500
Compression (mm)

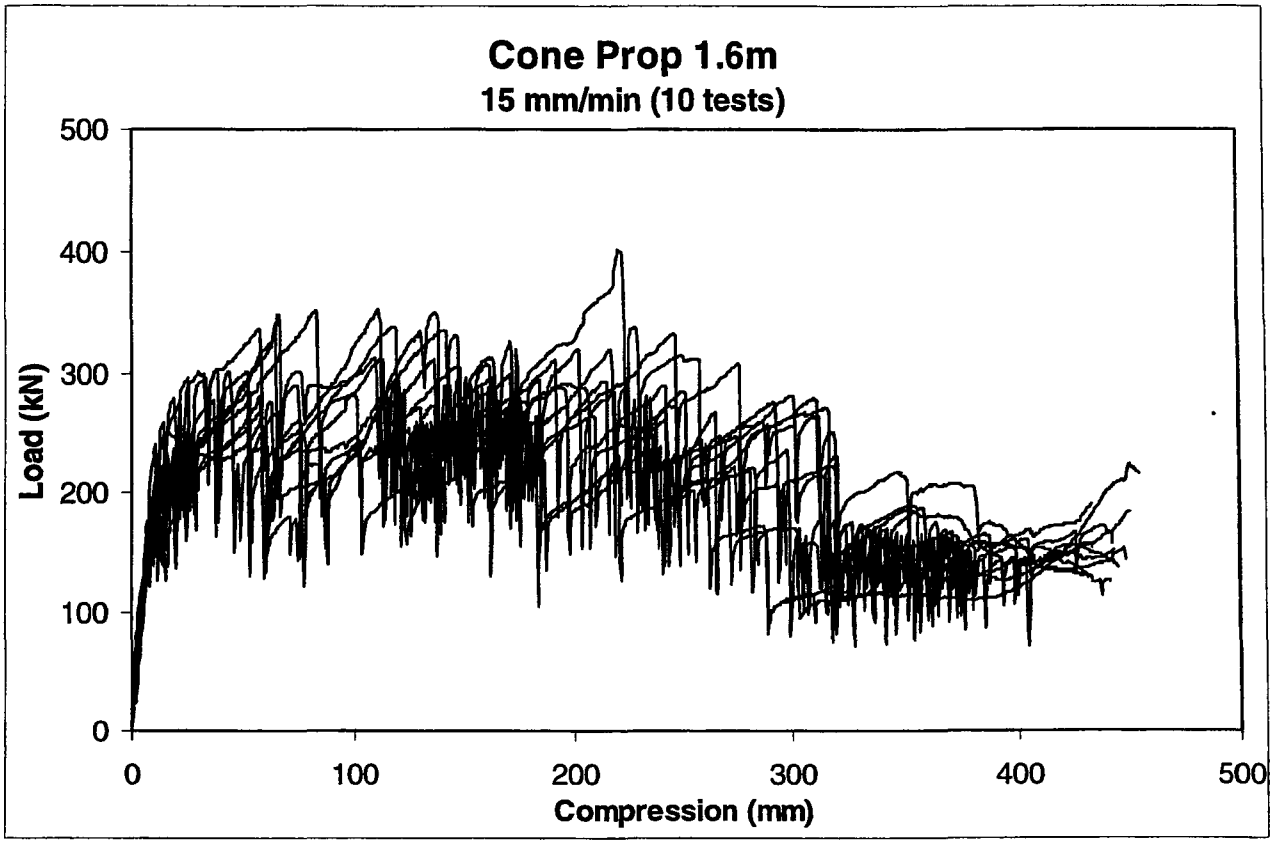
Cone Prop 1.6m
15 mm/min (10 tests)
Load (kN)
0
100
200
300
400
500
Compression (mm)

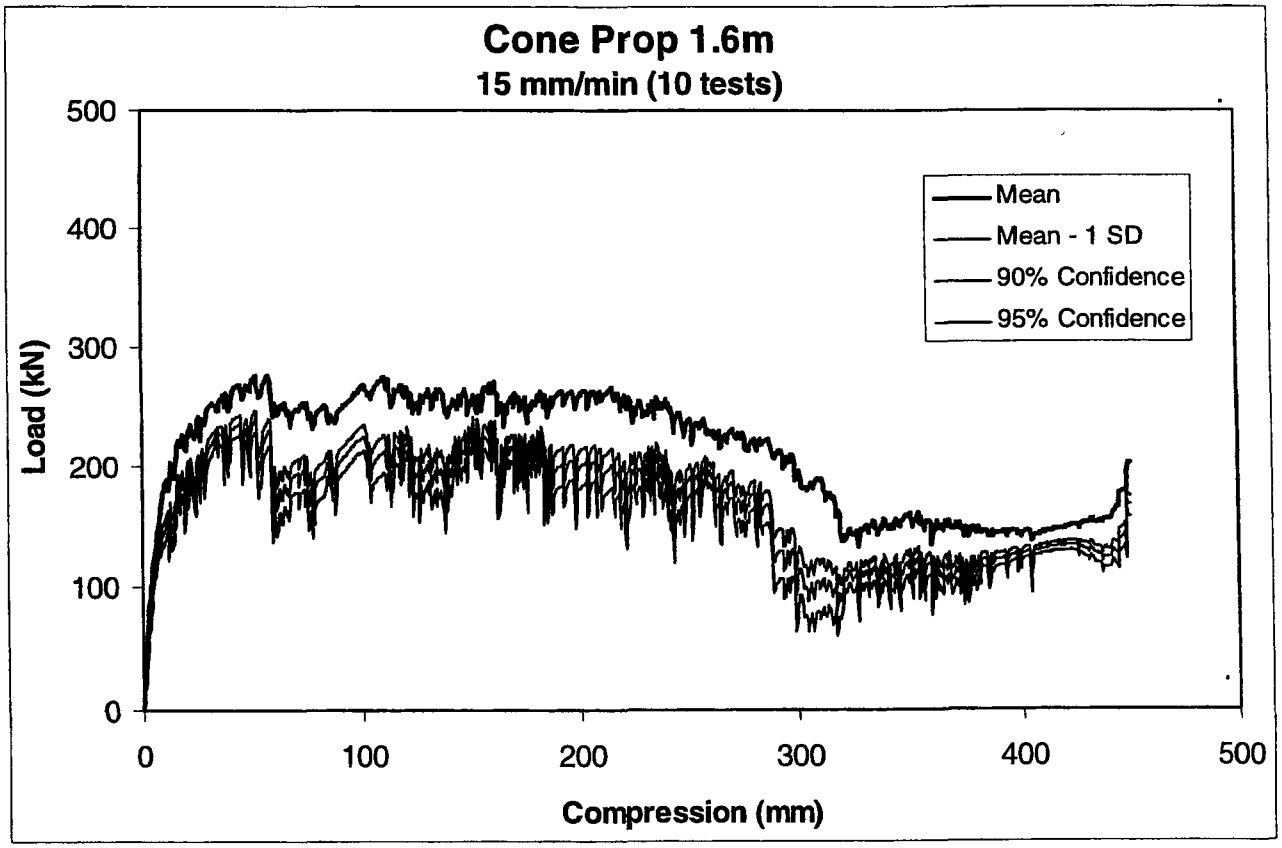
Cone Prop 1.6m
15 mm/min (10 tests)
Mean
Mean - 1 SD
90% Confidence
95% Confidence
Load (kN)
0
100
200
300
400
500
Compression (mm)

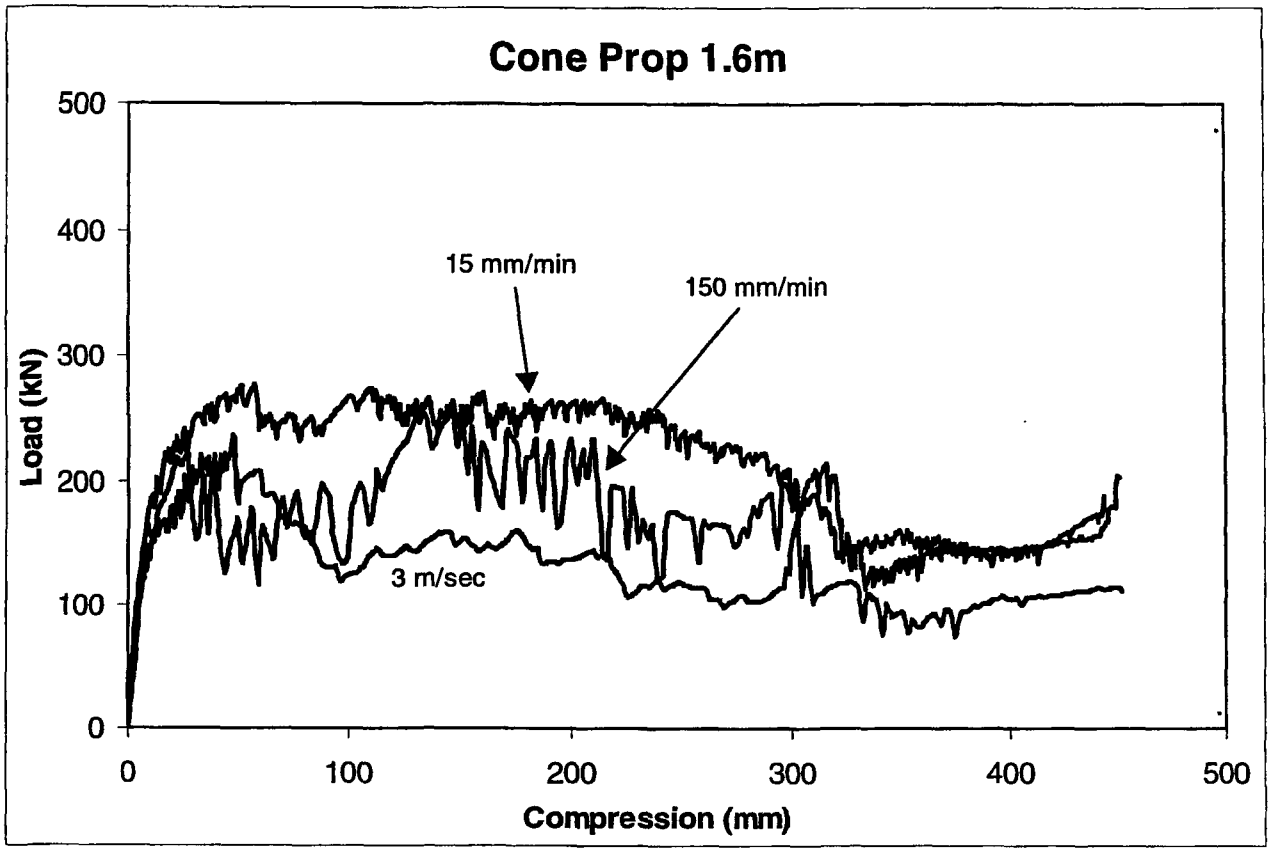
Cone Prop 1.6m
Load (kN)
Compression (mm)
15 mm/min
150 mm/min
3 m/sec
0
100
200
300
400
500

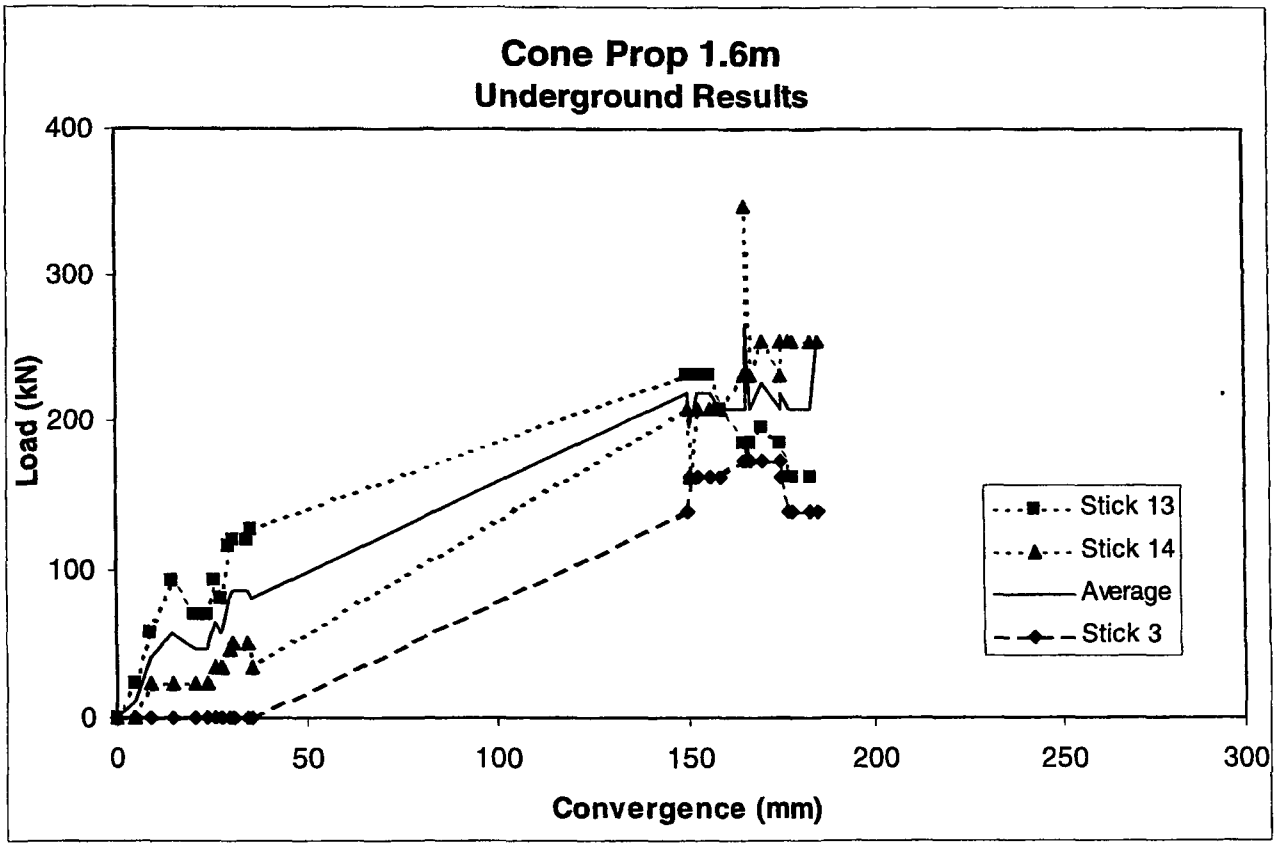
Cone Prop 1.6m
Underground Results
Load (kN)
Convergence (mm)
Stick 13
Stick 14
Average
Stick 3
0
50
100
150
200
250
300
400

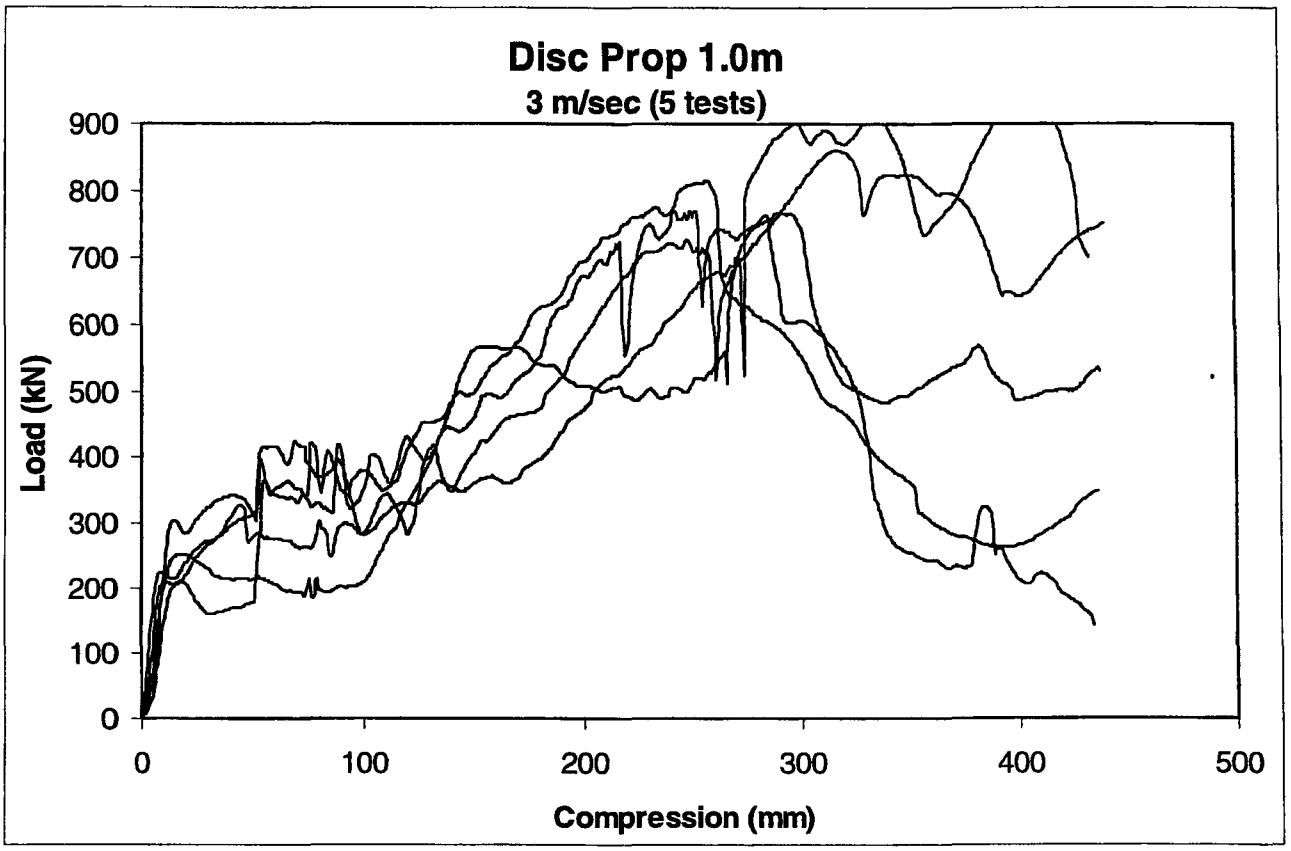
Disc Prop 1.0m
3 m/sec (5 tests)
Load (kN)
900
800
700
600
500
400
300
200
100
0
0
100
200
300
400
500
Compression (mm)

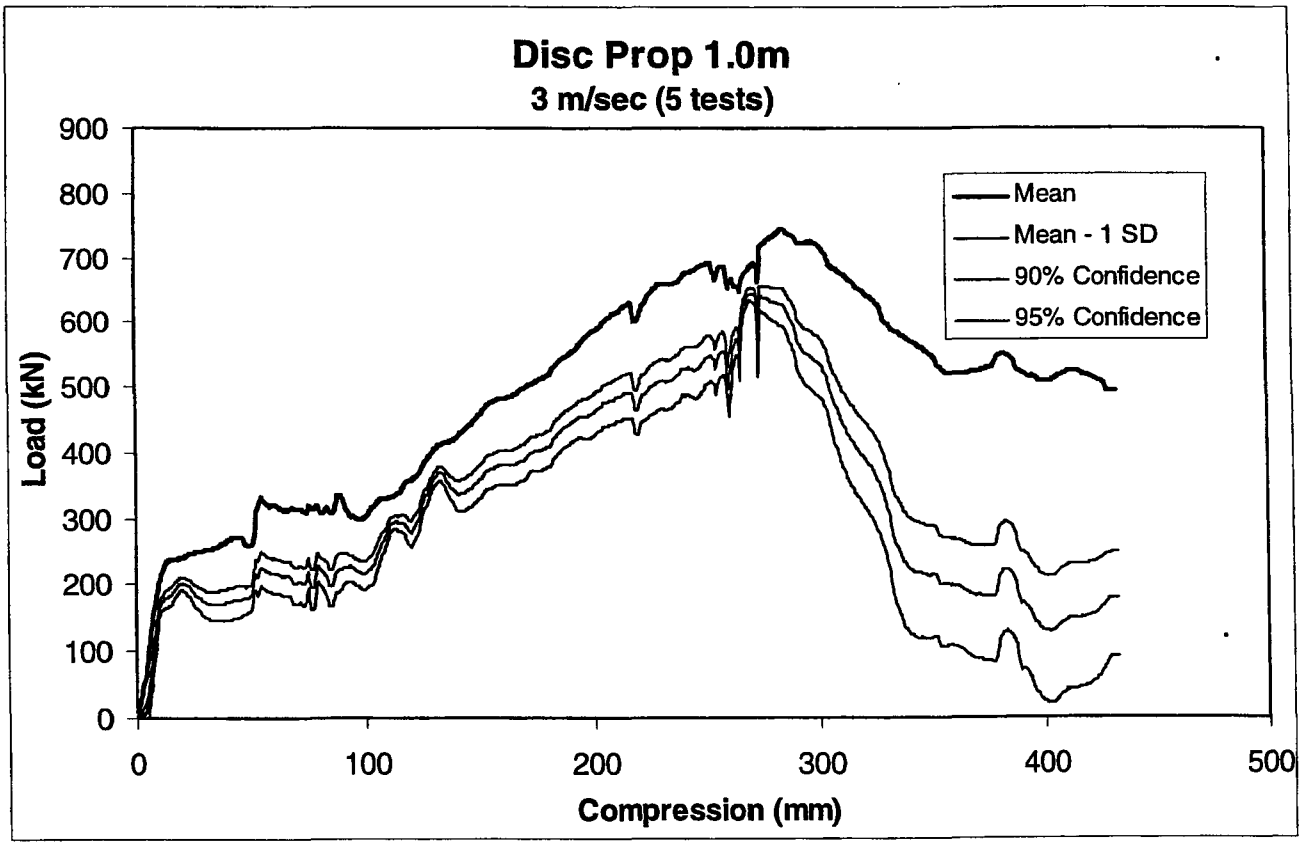
Disc Prop 1.0m
3 m/sec (5 tests)
Load (kN)
900
800
700
600
500
400
300
200
100
0
0
100
200
300
400
500
Compression (mm)
Mean
Mean - 1 SD
90% Confidence
95% Confidence

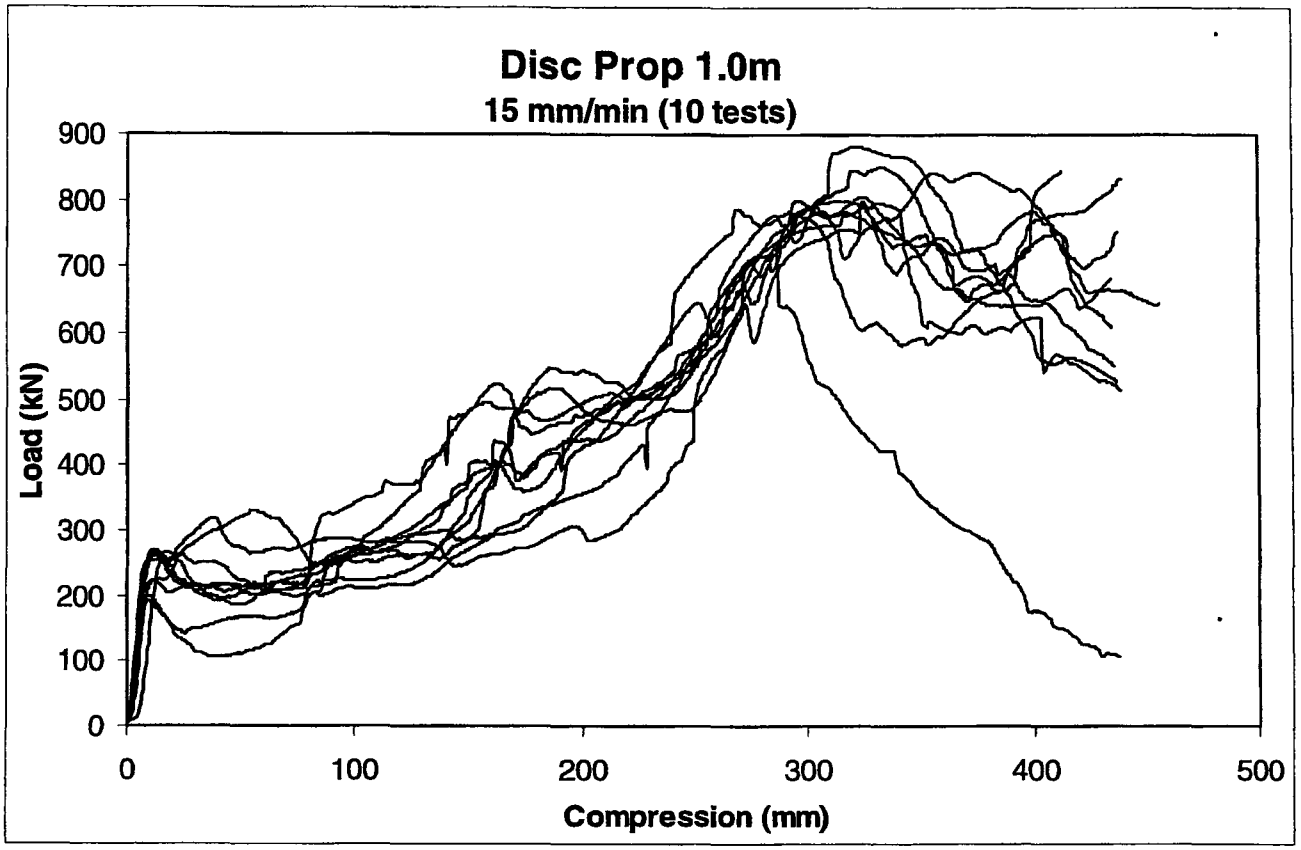
Disc Prop 1.0m
15 mm/min (10 tests)
Load (kN)
900
800
700
600
500
400
300
200
100
0
0
100
200
300
400
500
Compression (mm)

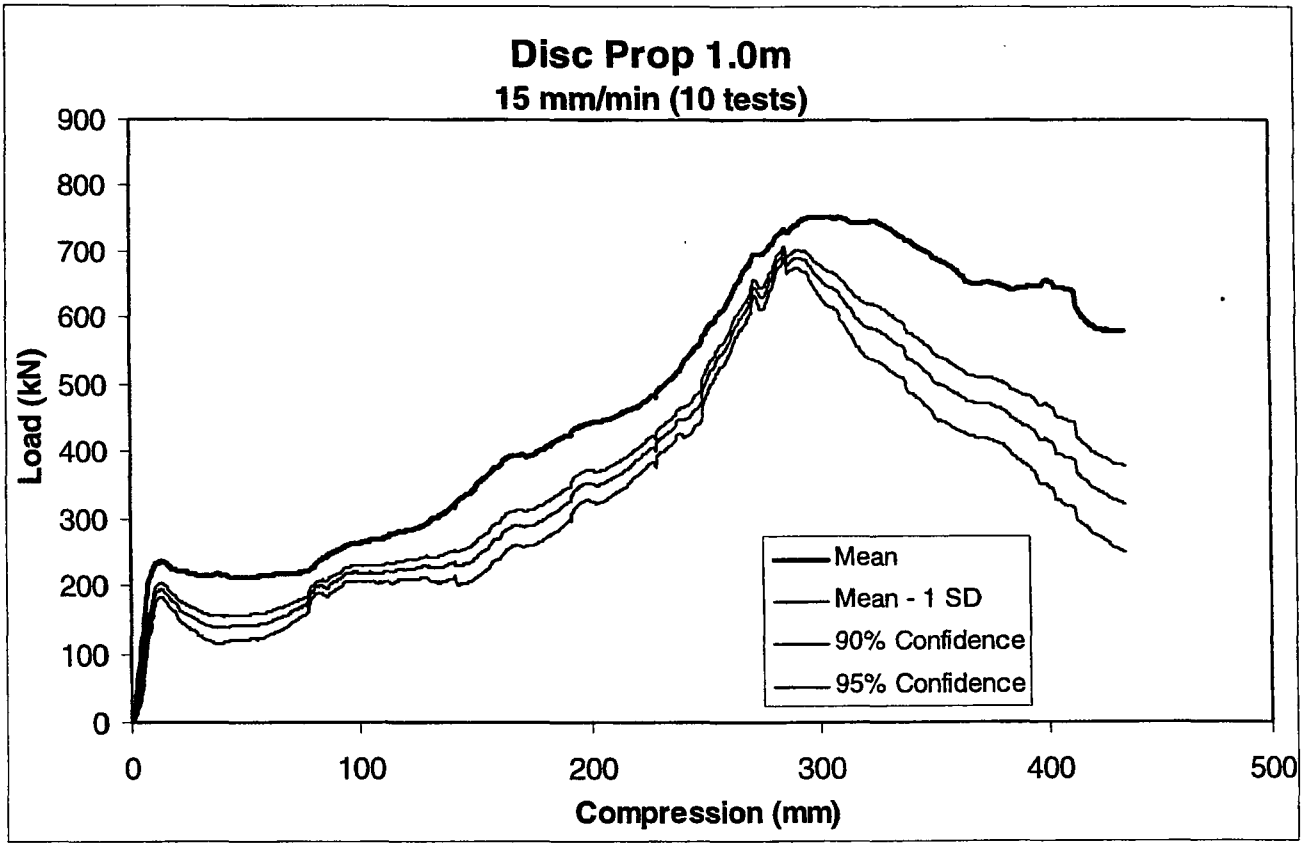
Disc Prop 1.0m
15 mm/min (10 tests)
Load (kN)
900
800
700
600
500
400
300
200
100
0
0
100
200
300
400
500
Compression (mm)
Mean
Mean - 1 SD
90% Confidence
95% Confidence

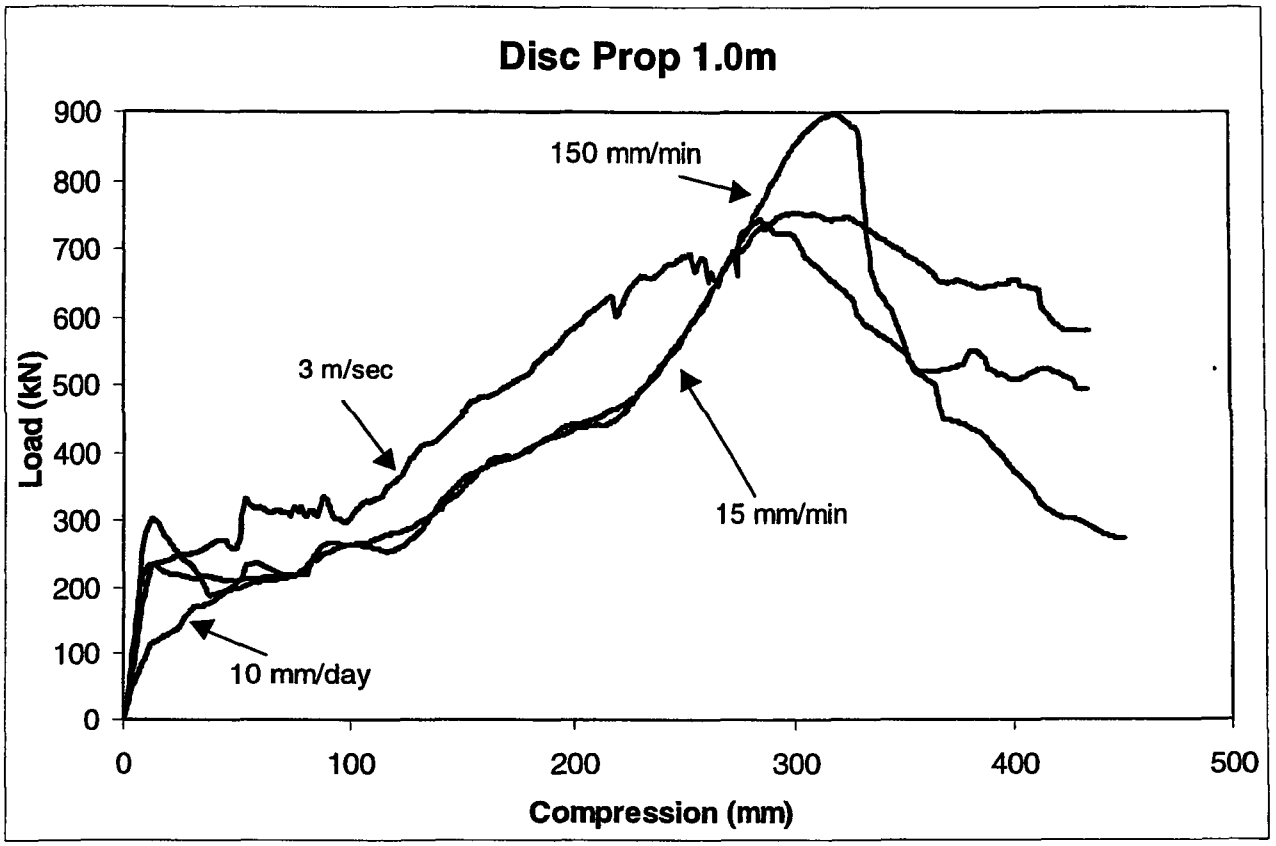
Disc Prop 1.0m
Load (kN)
900
800
700
600
500
400
300
200
100
0
0
100
200
300
400
500
Compression (mm)
150 mm/min
3 m/sec
15 mm/min
10 mm/day

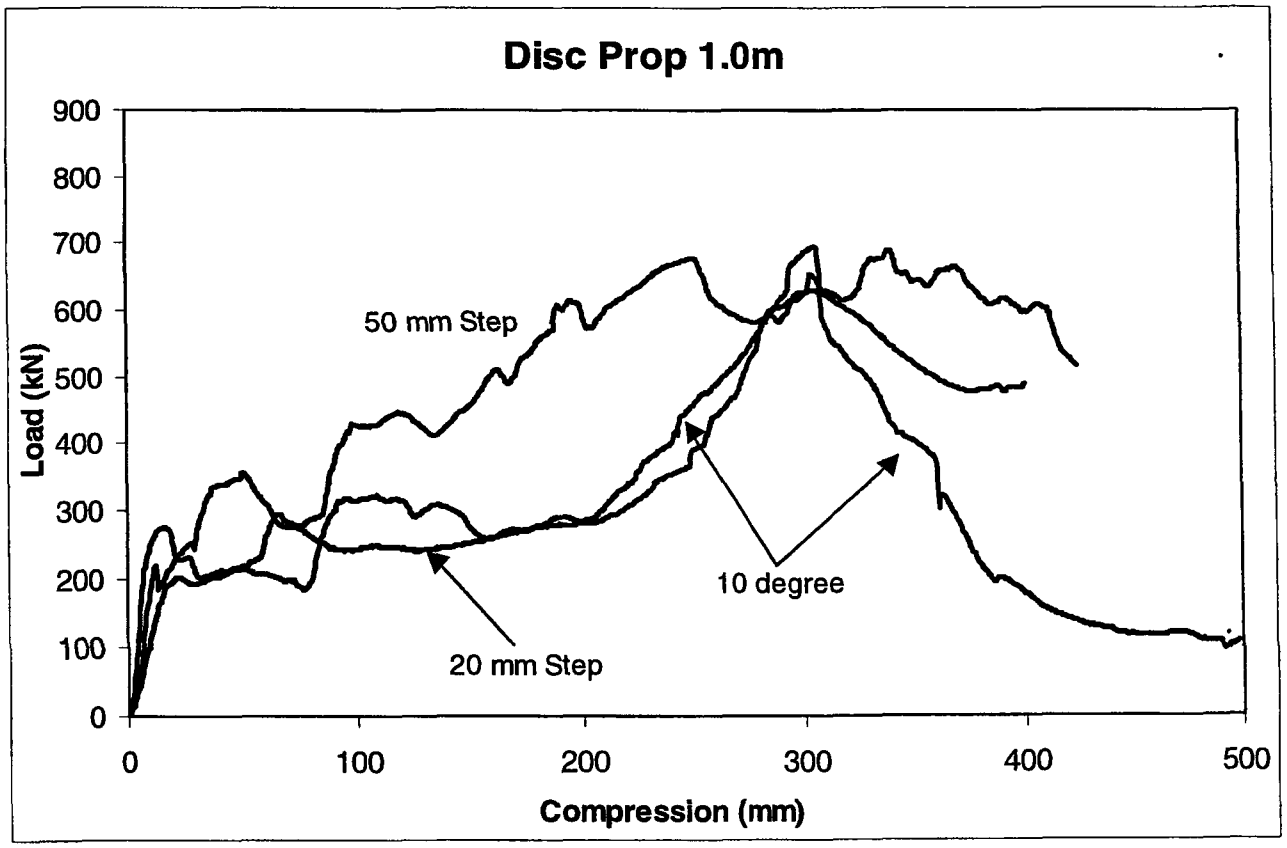
Disc Prop 1.0m
Load (kN)
900
800
700
600
500
400
300
200
100
0
0
100
200
300
400
500
Compression (mm)
50 mm Step
10 degree
20 mm Step

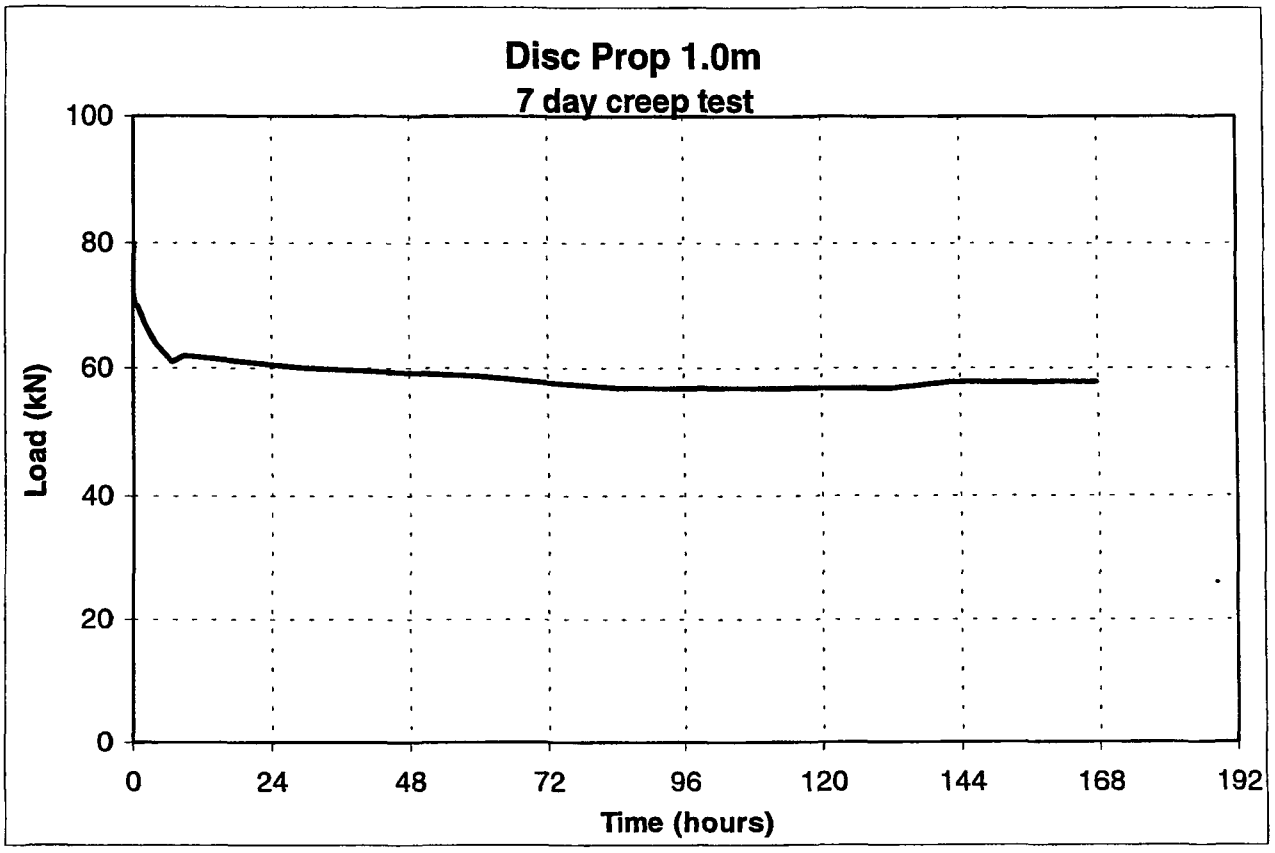
Disc Prop 1.0m
7 day creep test
Load (kN)
100
80
60
40
20
0
0
24
48
72
96
120
144
168
192
Time (hours)

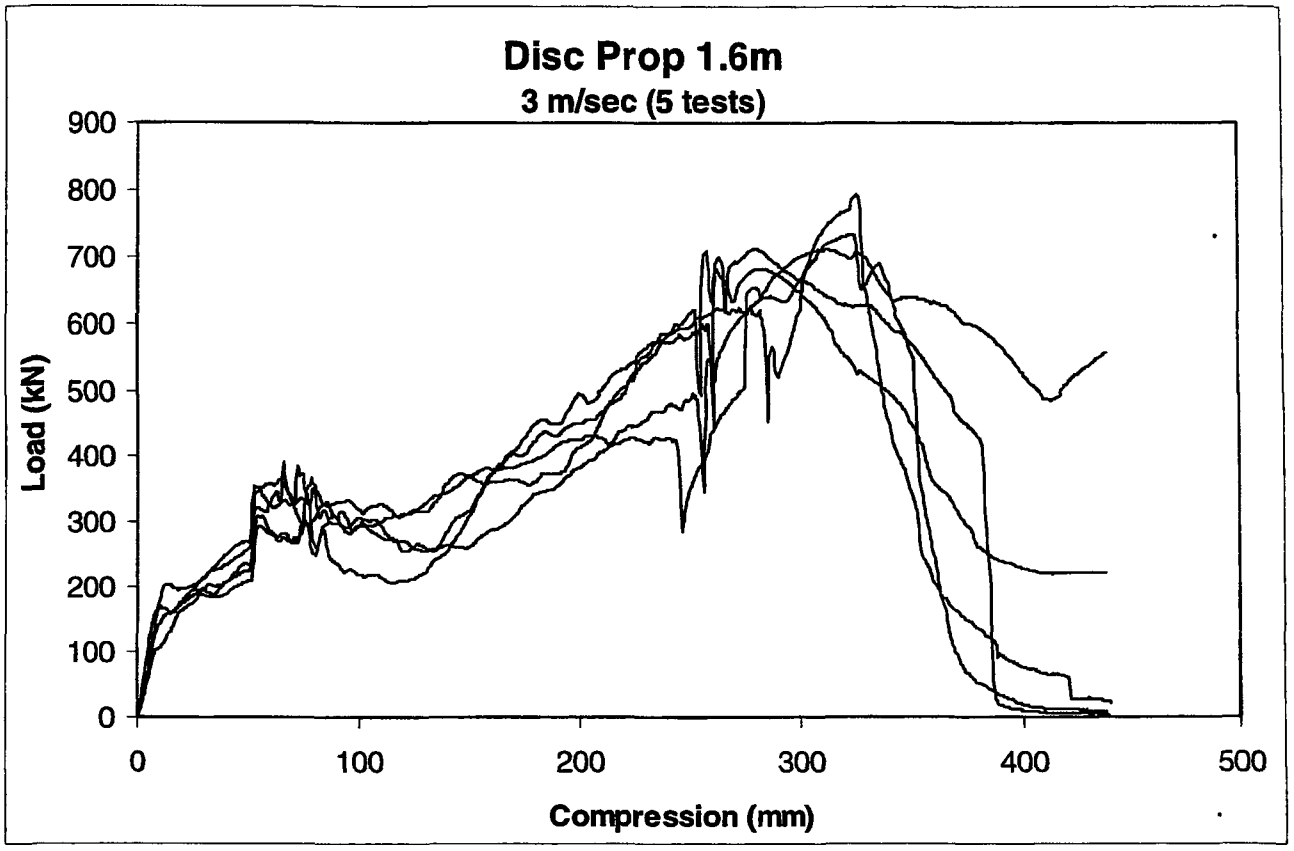
Disc Prop 1.6m
3 m/sec (5 tests)
Load (kN)
900
800
700
600
500
400
300
200
100
0
0
100
200
300
400
500
Compression (mm)

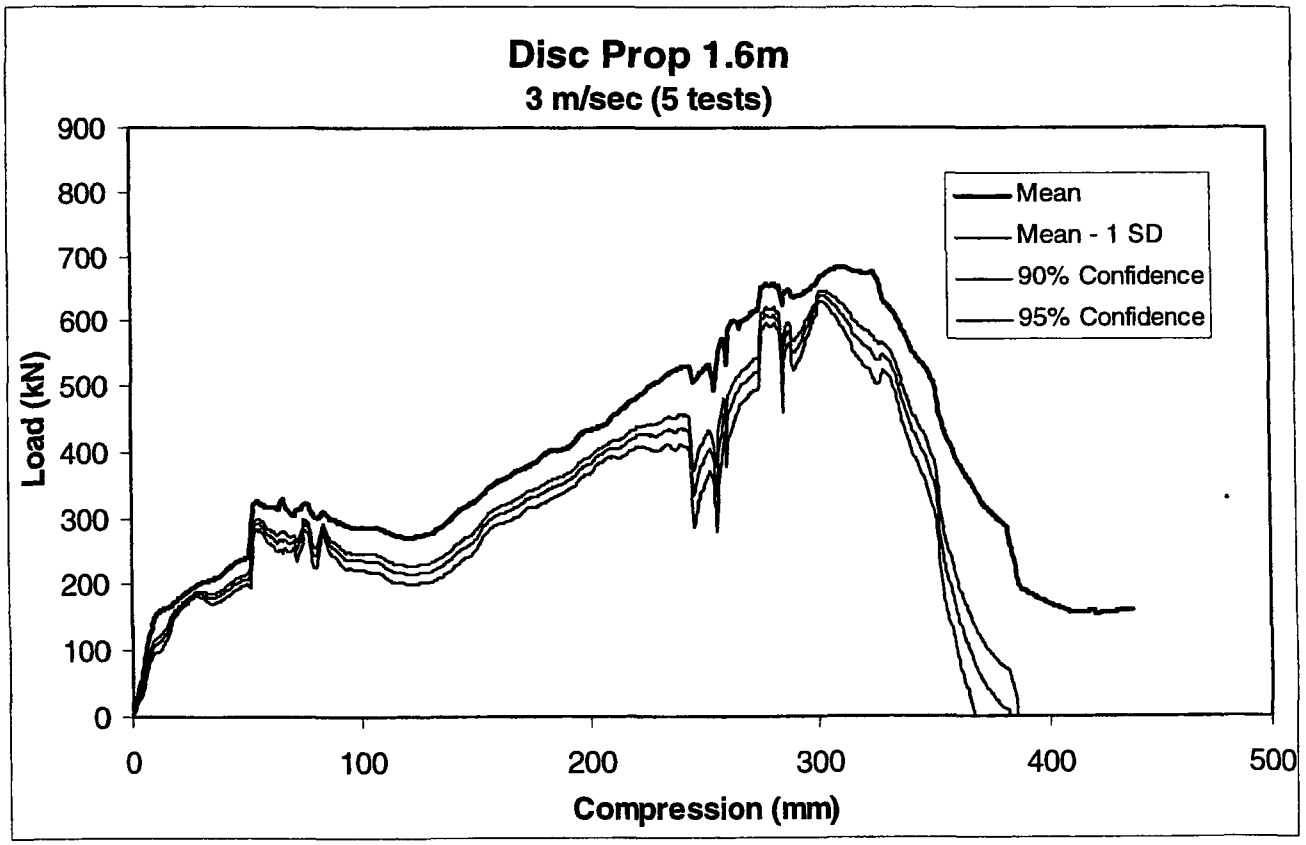
Disc Prop 1.6m
3 m/sec (5 tests)
Load (kN)
900
800
700
600
500
400
300
200
100
0
0
100
200
300
400
500
Compression (mm)
Mean
Mean - 1 SD
90% Confidence
95% Confidence

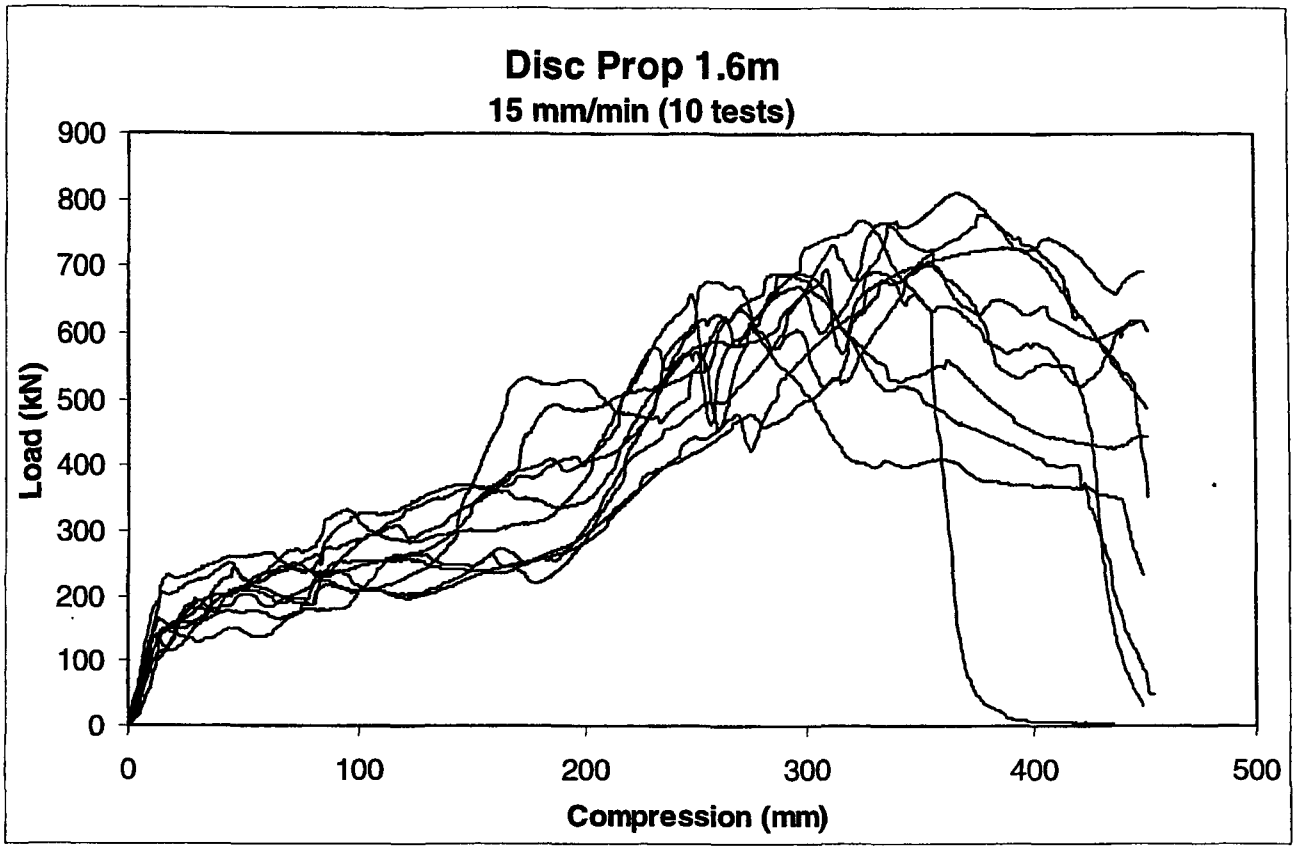
Disc Prop 1.6m
15 mm/min (10 tests)
Load (kN)
900
800
700
600
500
400
300
200
100
0
0
100
200
300
400
500
Compression (mm)

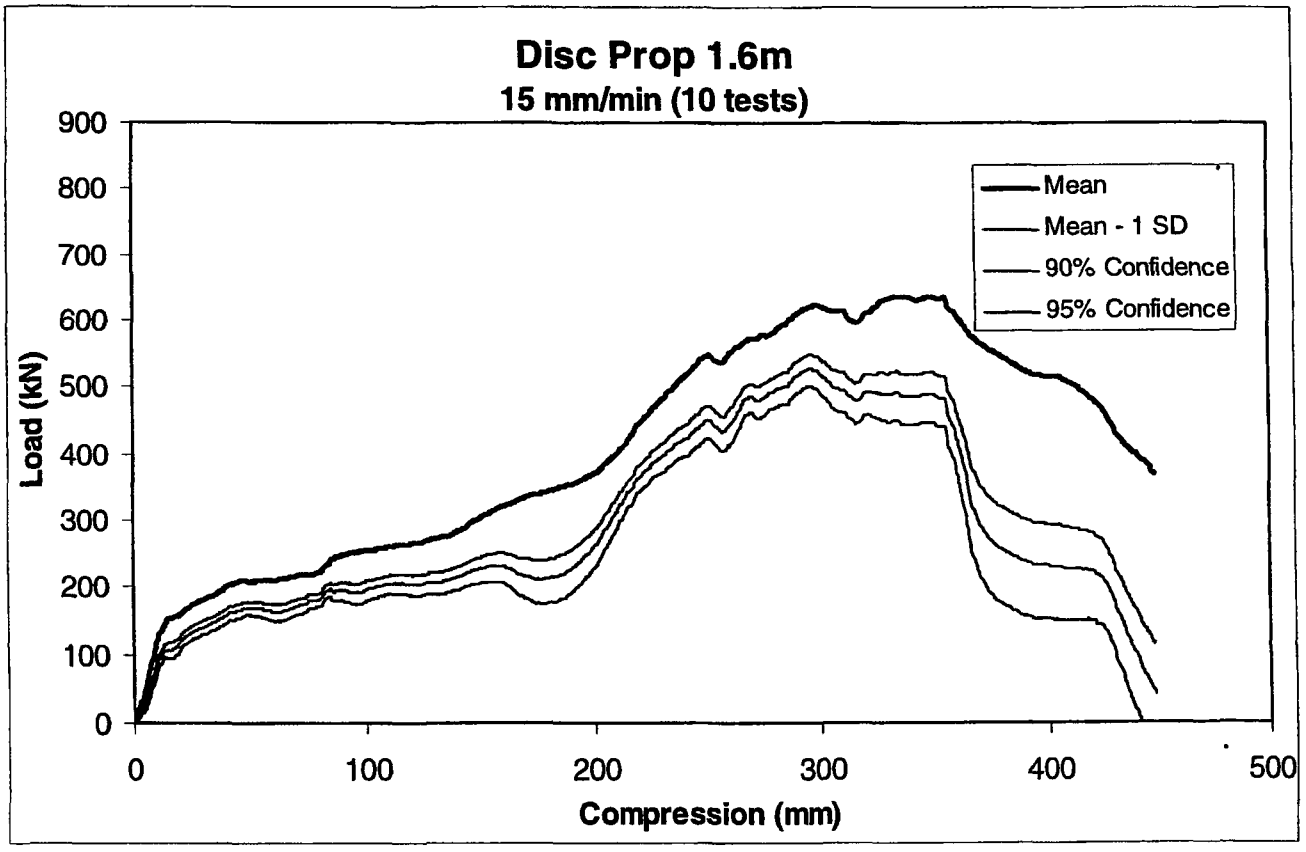
Disc Prop 1.6m
15 mm/min (10 tests)
Load (kN)
900
800
700
600
500
400
300
200
100
0
0
100
200
300
400
500
Compression (mm)
Mean
Mean - 1 SD
90% Confidence
95% Confidence

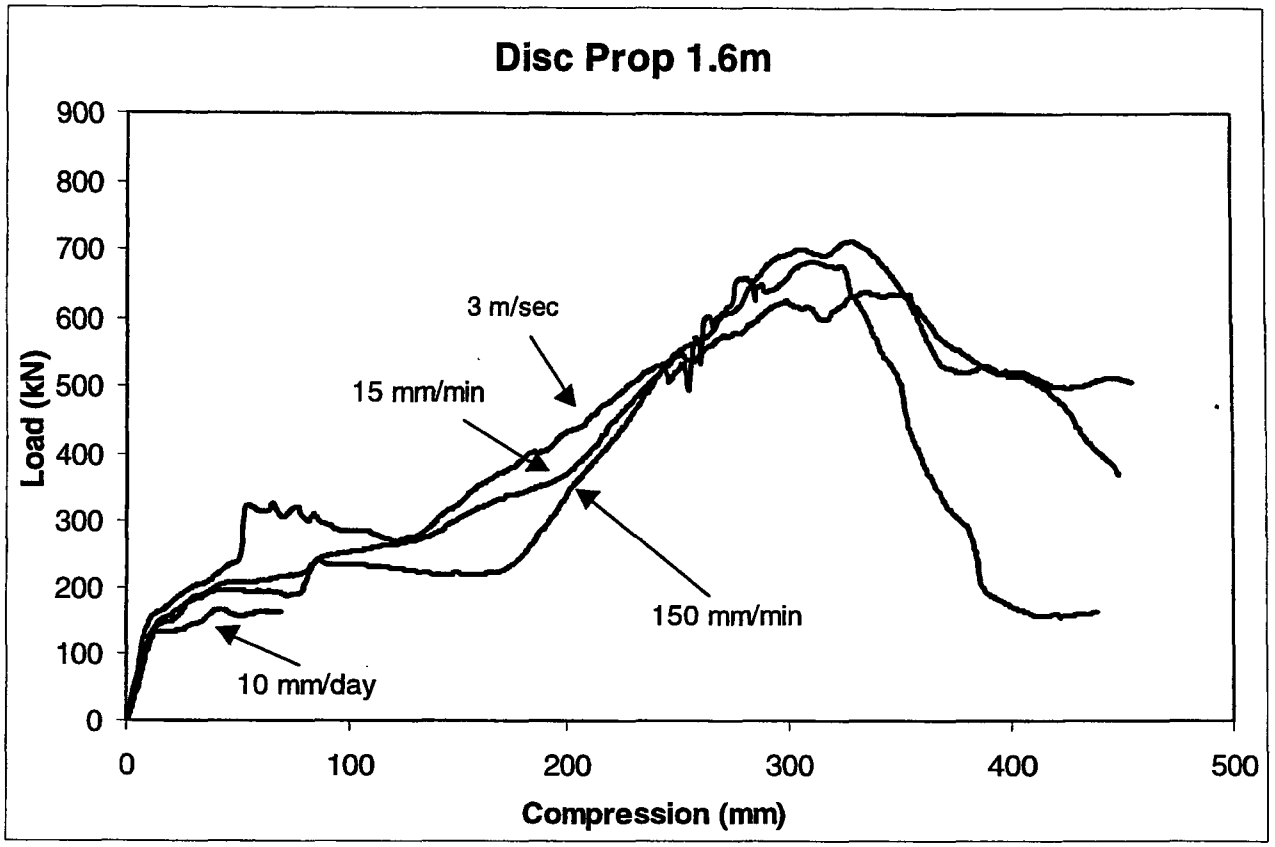
Disc Prop 1.6m
Load (kN)
900
800
700
600
500
400
300
200
100
0
0
100
200
300
400
500
Compression (mm)
3 m/sec
15 mm/min
150 mm/min
10 mm/day

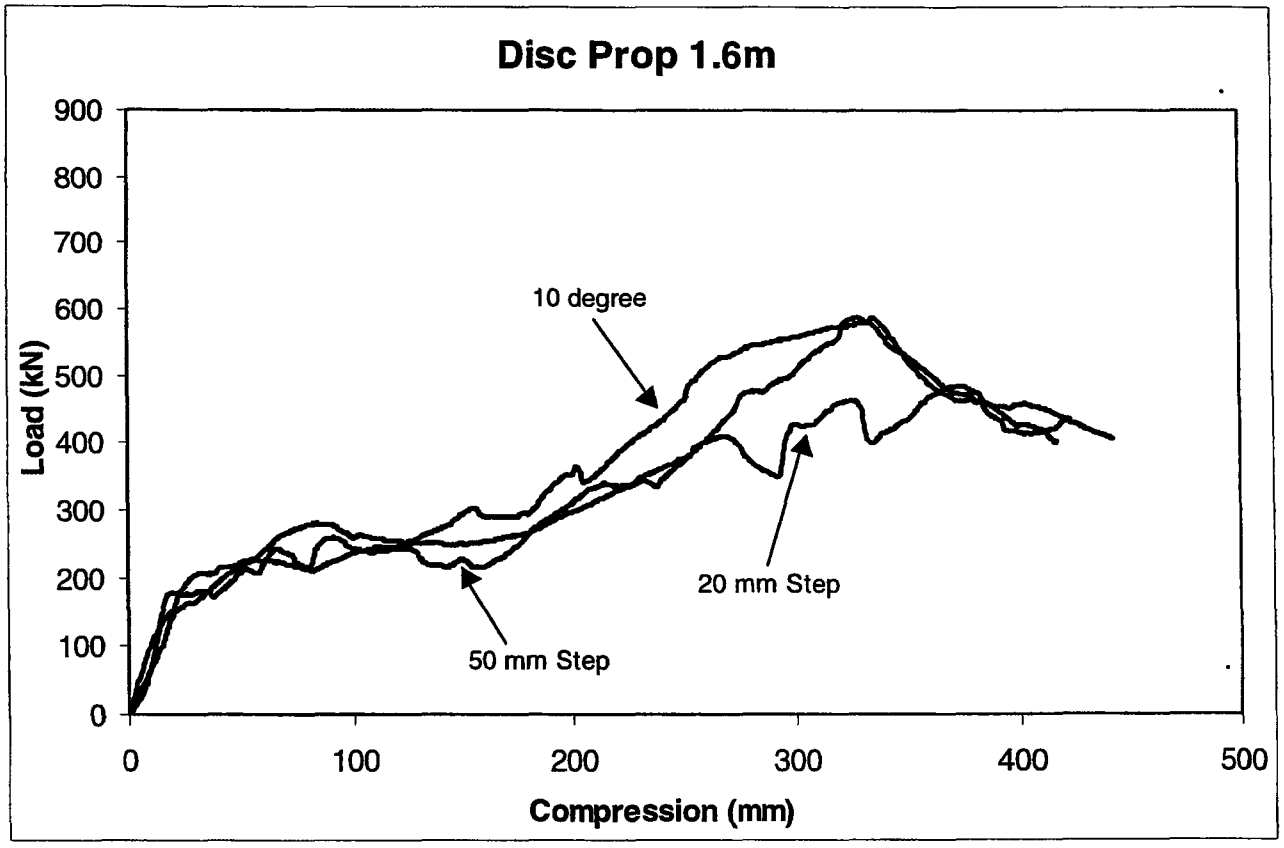
Disc Prop 1.6m
Load (kN)
900
800
700
600
500
400
300
200
100
0
0
100
200
300
400
500
Compression (mm)
10 degree
20 mm Step
50 mm Step

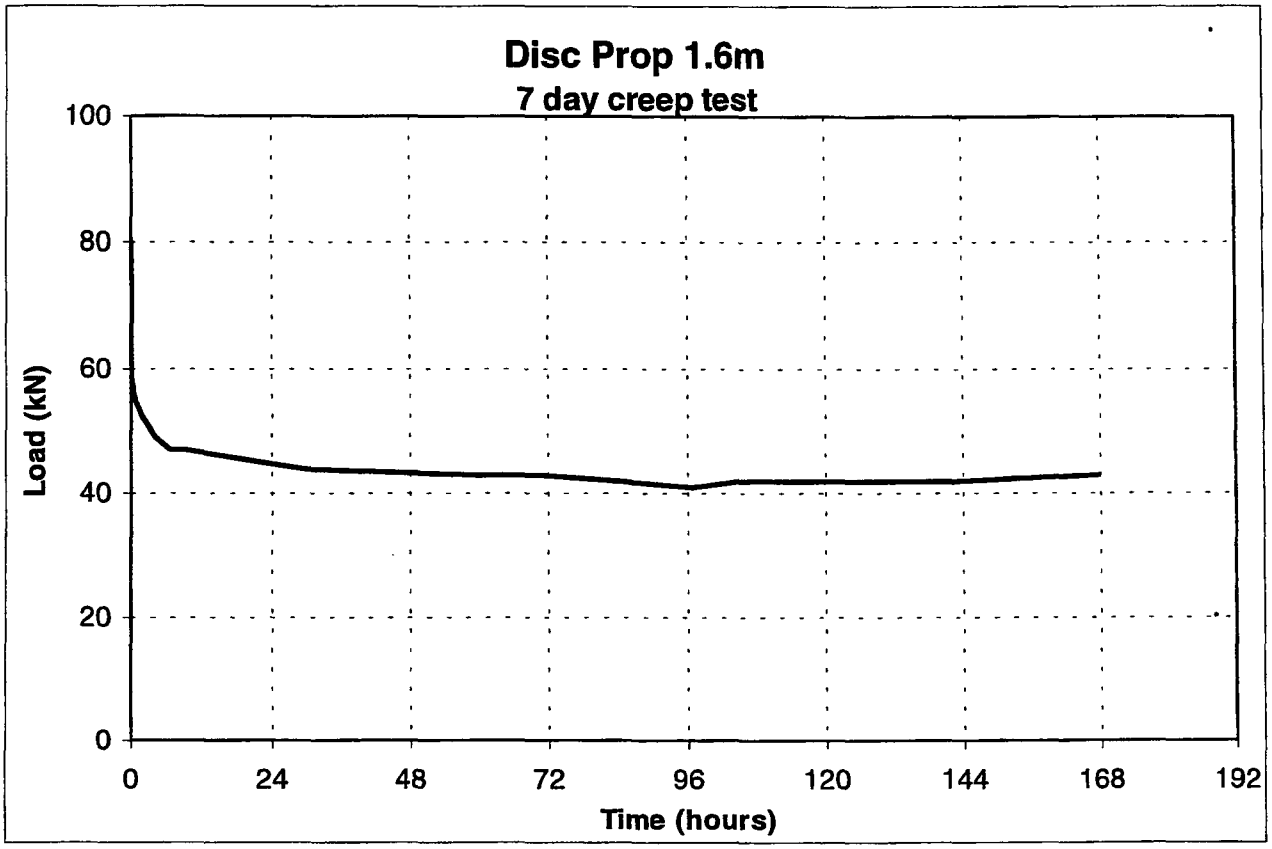
Disc Prop 1.6m
7 day creep test
Load (kN)
100
80
60
40
20
0
0
24
48
72
96
120
144
168
192
Time (hours)

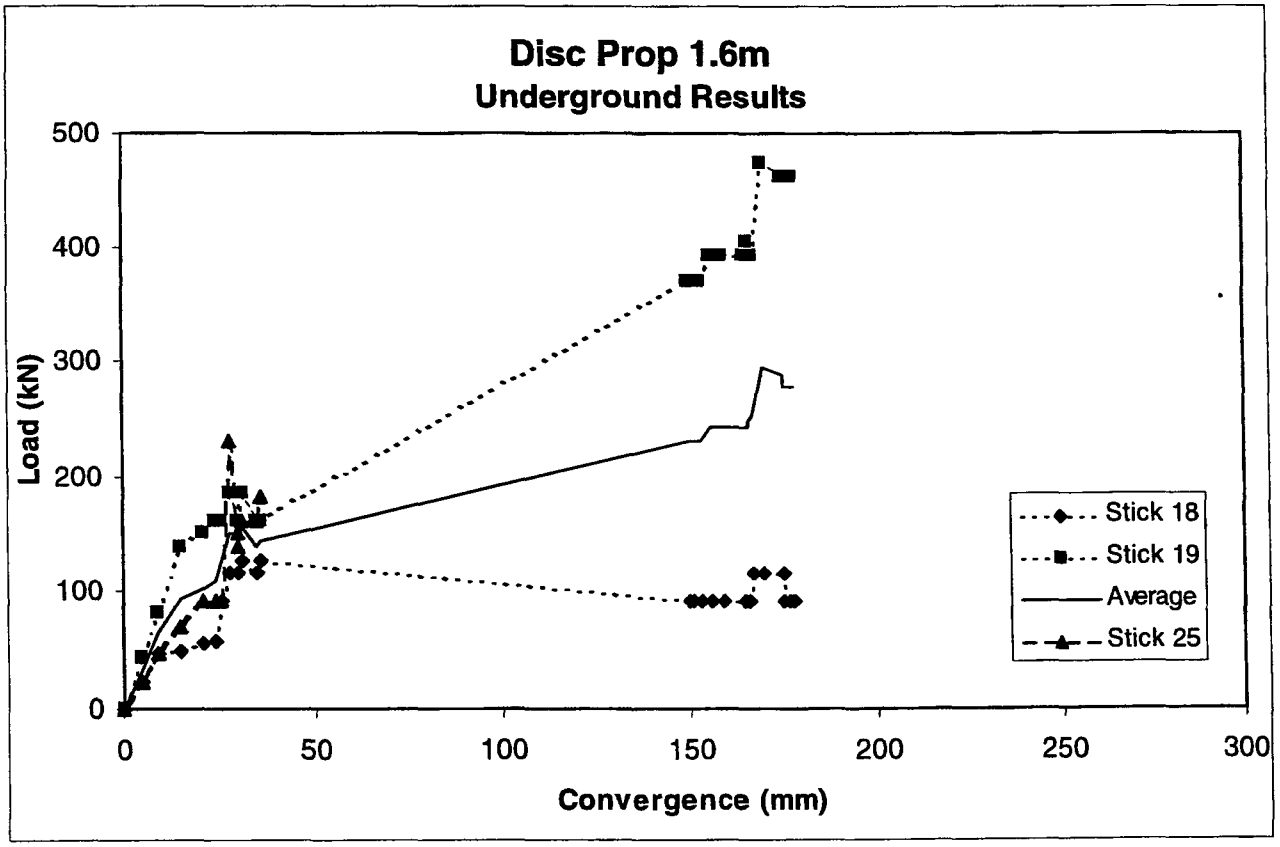
Disc Prop 1.6m
Underground Results
Load (kN)
500
400
300
200
100
0
0
50
100
150
200
250
300
Convergence (mm)
Stick 18
Stick 19
Average
Stick 25

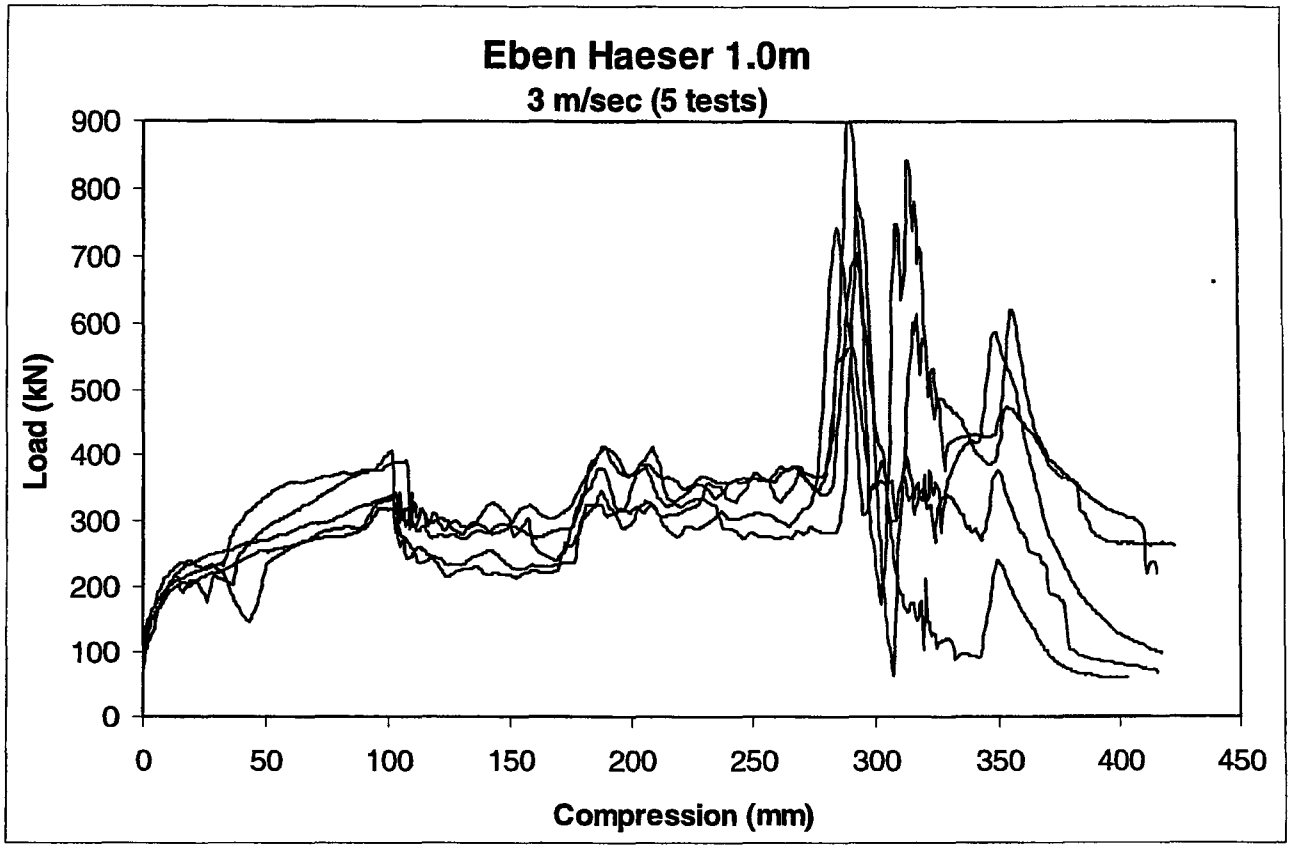
Eben Haeser 1.0m
3 m/sec (5 tests)
Load (kN)
900
800
700
600
500
400
300
200
100
0
0
50
100
150
200
250
300
350
400
450
Compression (mm)

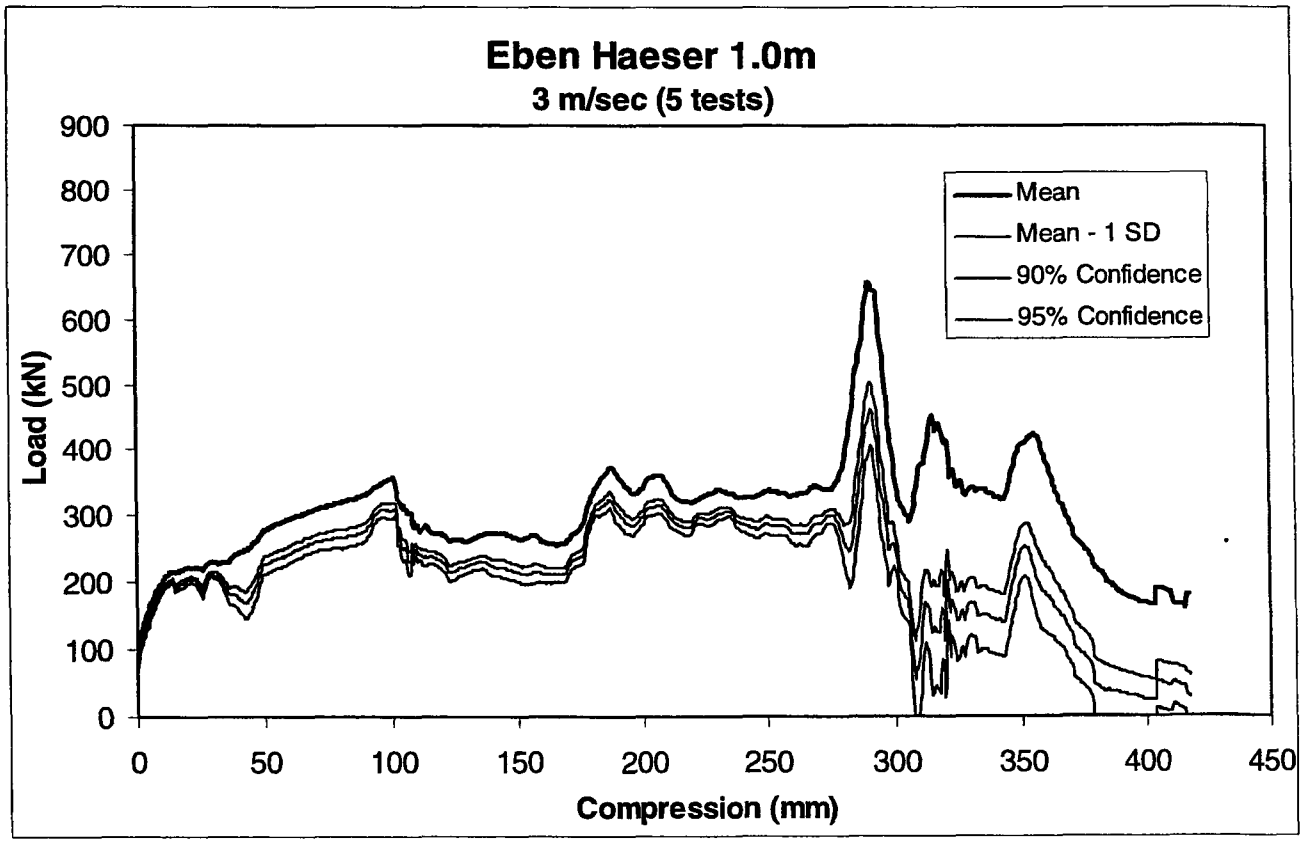
Eben Haeser 1.0m
3 m/sec (5 tests)
Load (kN)
900
800
700
600
500
400
300
200
100
0
0
50
100
150
200
250
300
350
400
450
Compression (mm)
Mean
Mean - 1 SD
90% Confidence
95% Confidence

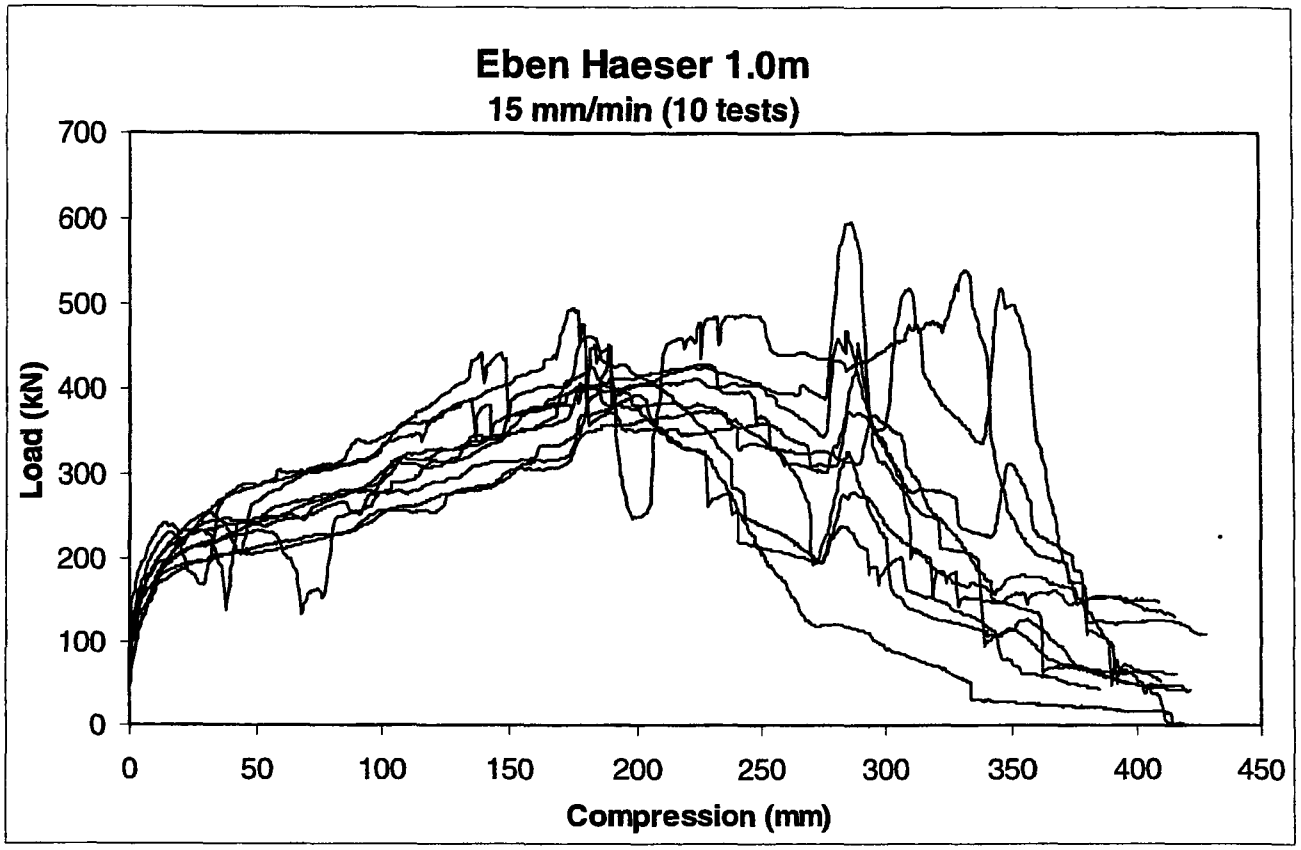
Eben Haeser 1.0m
15 mm/min (10 tests)
Load (kN)
700
600
500
400
300
200
100
0
0
50
100
150
200
250
300
350
400
450
Compression (mm)

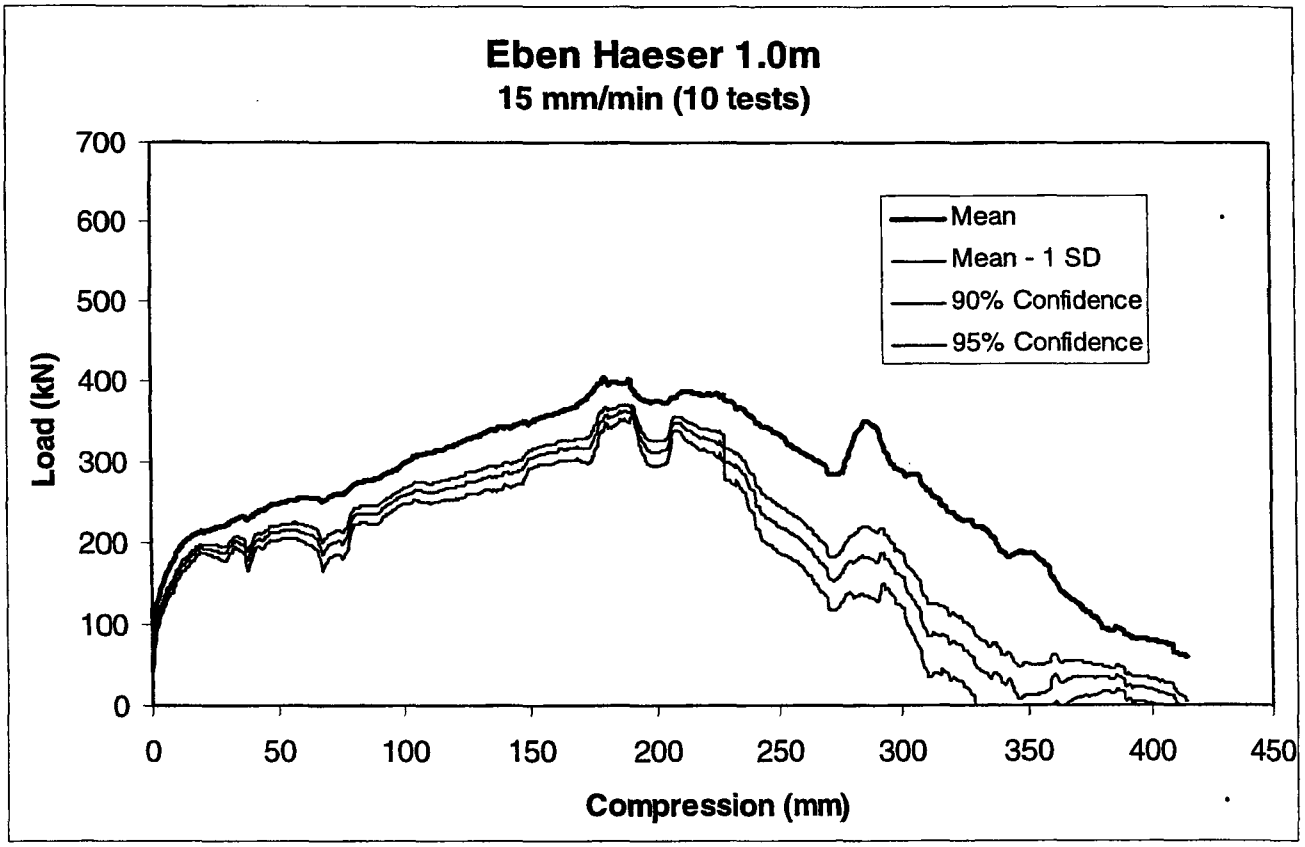
Eben Haeser 1.0m
15 mm/min (10 tests)
Load (kN)
700
600
500
400
300
200
100
0
0
50
100
150
200
250
300
350
400
450
Compression (mm)
Mean
Mean - 1 SD
90% Confidence
95% Confidence

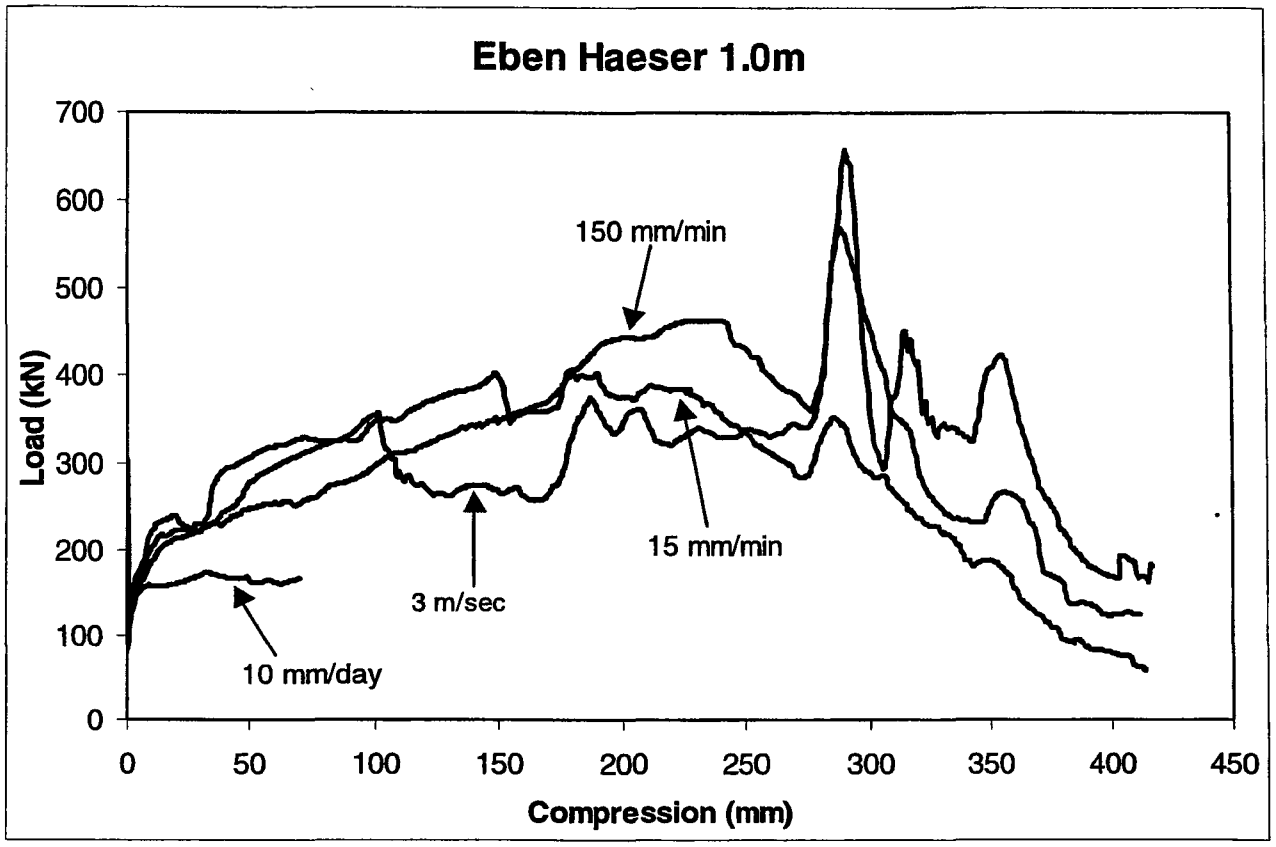
Eben Haeser 1.0m
Load (kN)
Compression (mm)
150 mm/min
15 mm/min
3 m/sec
10 mm/day
0
100
200
300
400
500
600
700
0
50
100
150
200
250
300
350
400
450

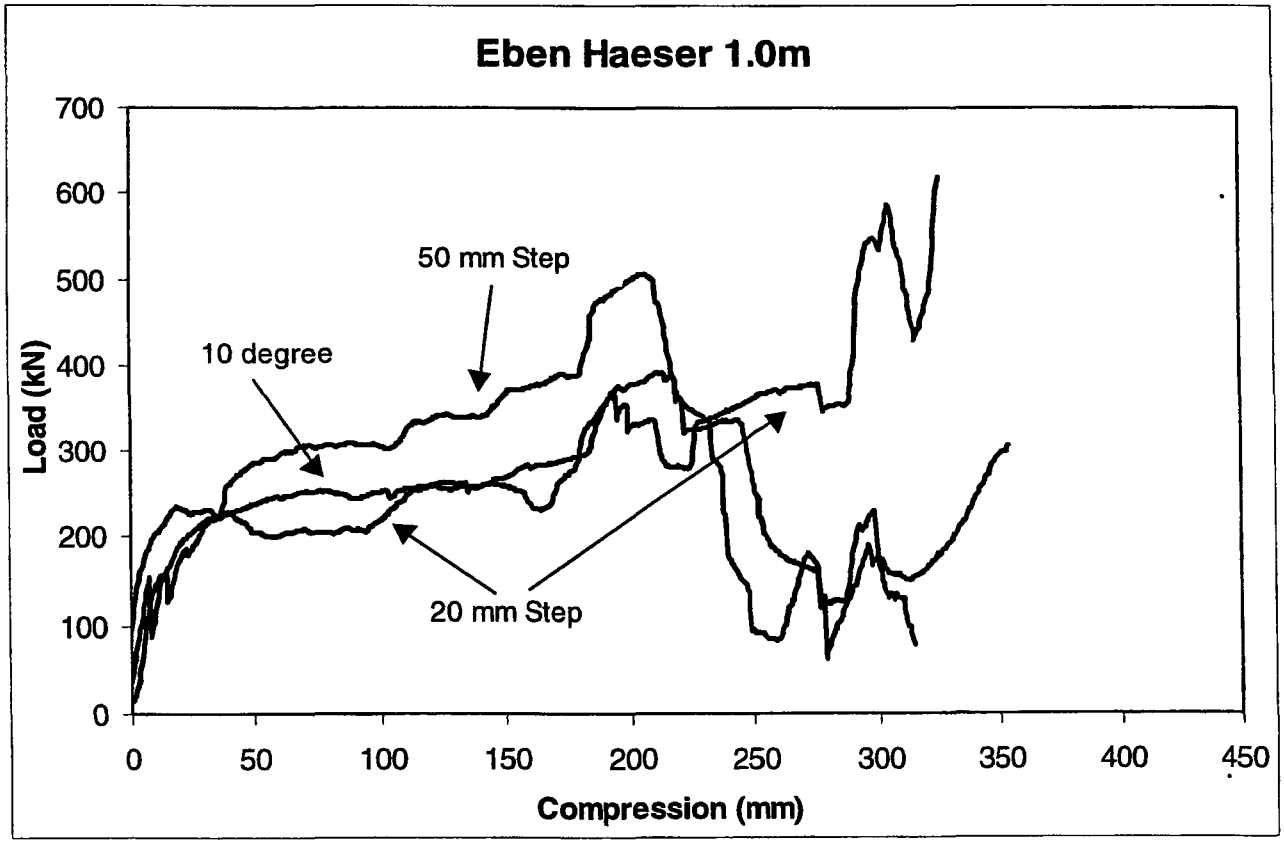
Eben Haeser 1.0m
Load (kN)
Compression (mm)
50 mm Step
10 degree
20 mm Step
0
100
200
300
400
500
600
700
0
50
100
150
200
250
300
350
400
450

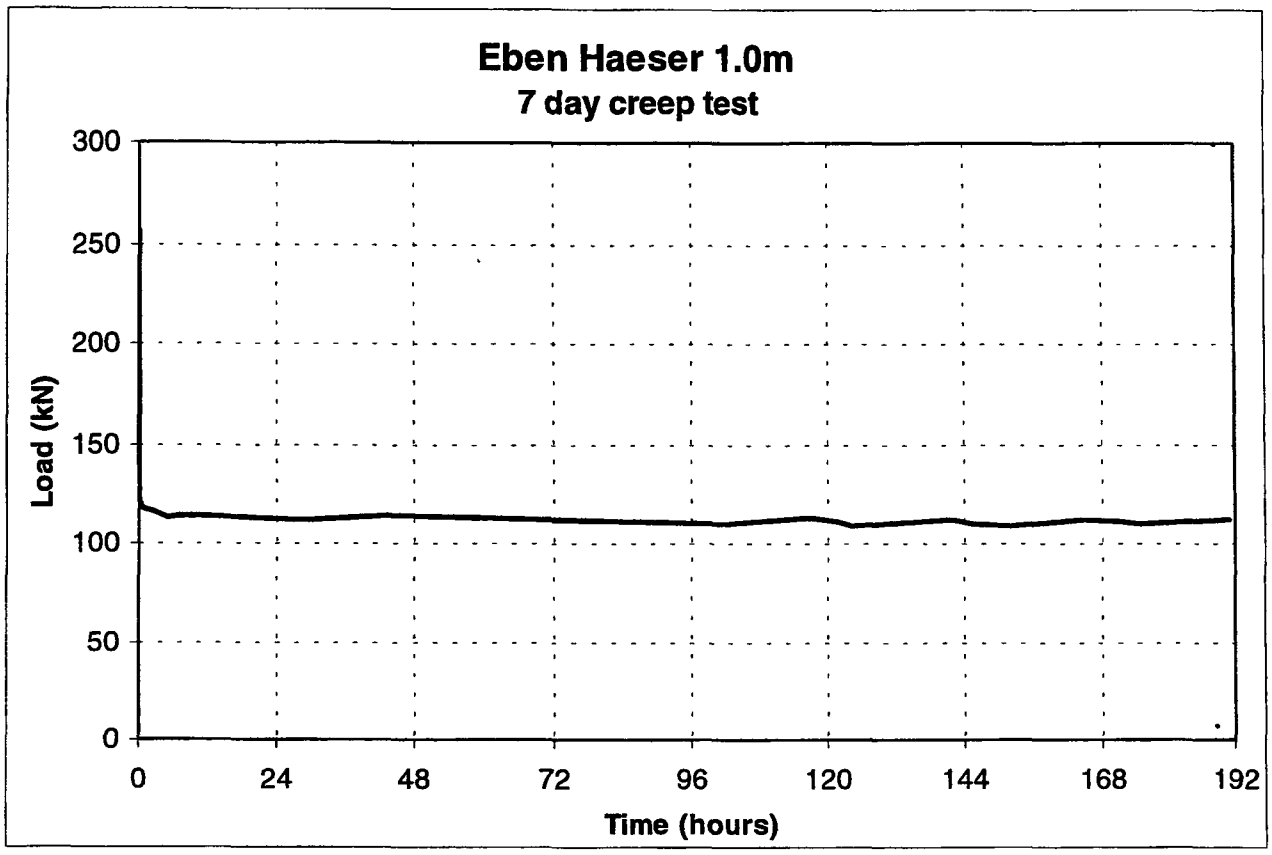
Eben Haeser 1.0m
7 day creep test
Load (kN)
300
250
200
150
100
50
0
0
24
48
72
96
120
144
168
192
Time (hours)

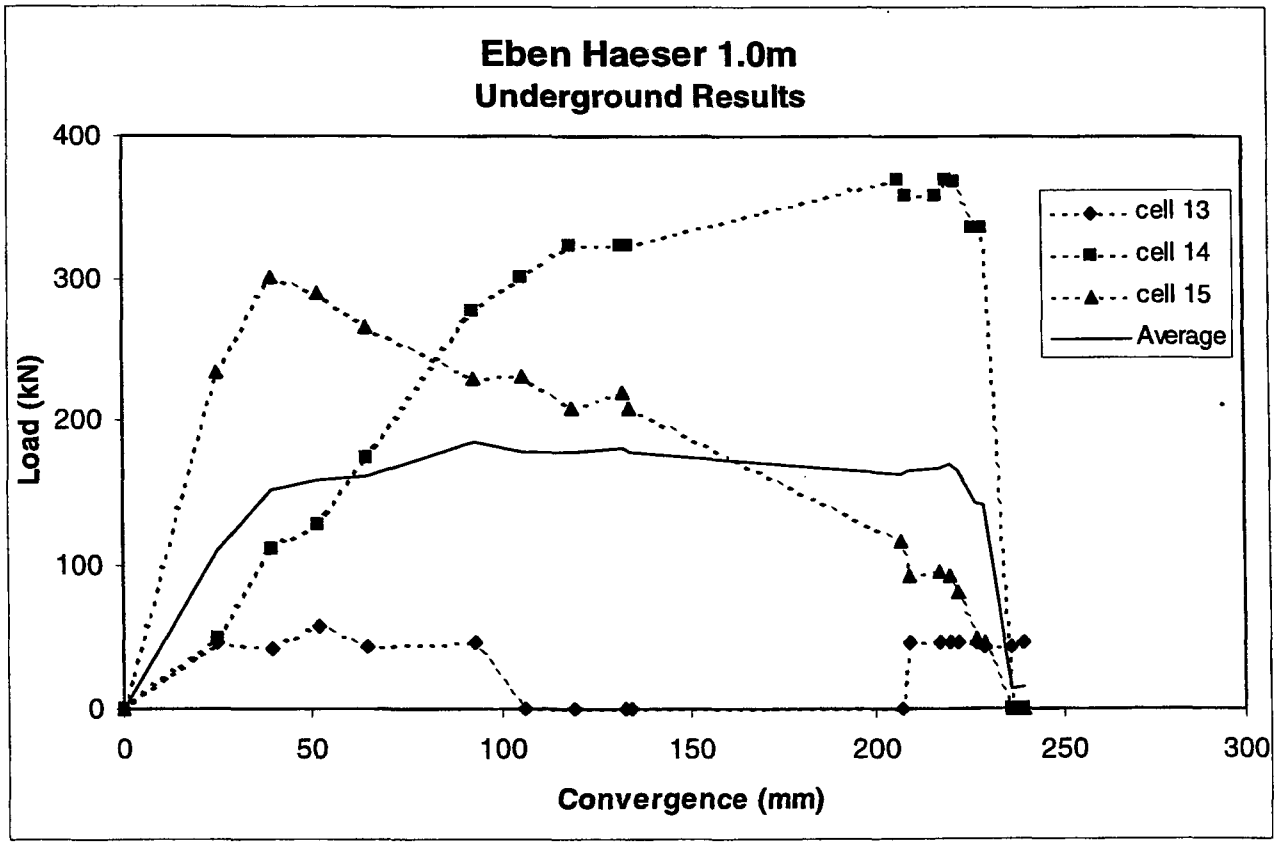
Eben Haeser 1.0m
Underground Results
Load (kN)
400
300
200
100
0
0
50
100
150
200
250
300
Convergence (mm)
cell 13
cell 14
cell 15
Average

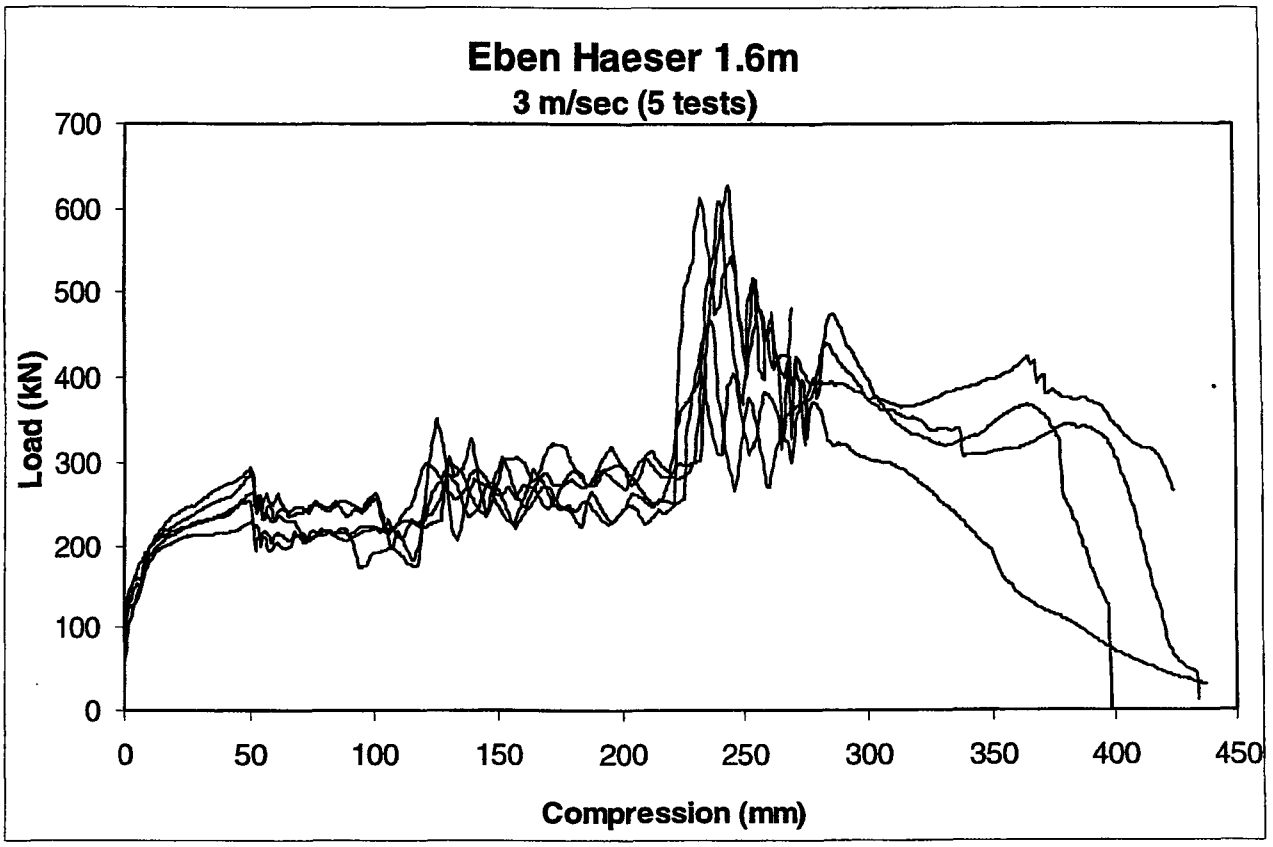
Eben Haeser 1.6m
3 m/sec (5 tests)
Load (kN)
700
600
500
400
300
200
100
0
0
50
100
150
200
250
300
350
400
450
Compression (mm)

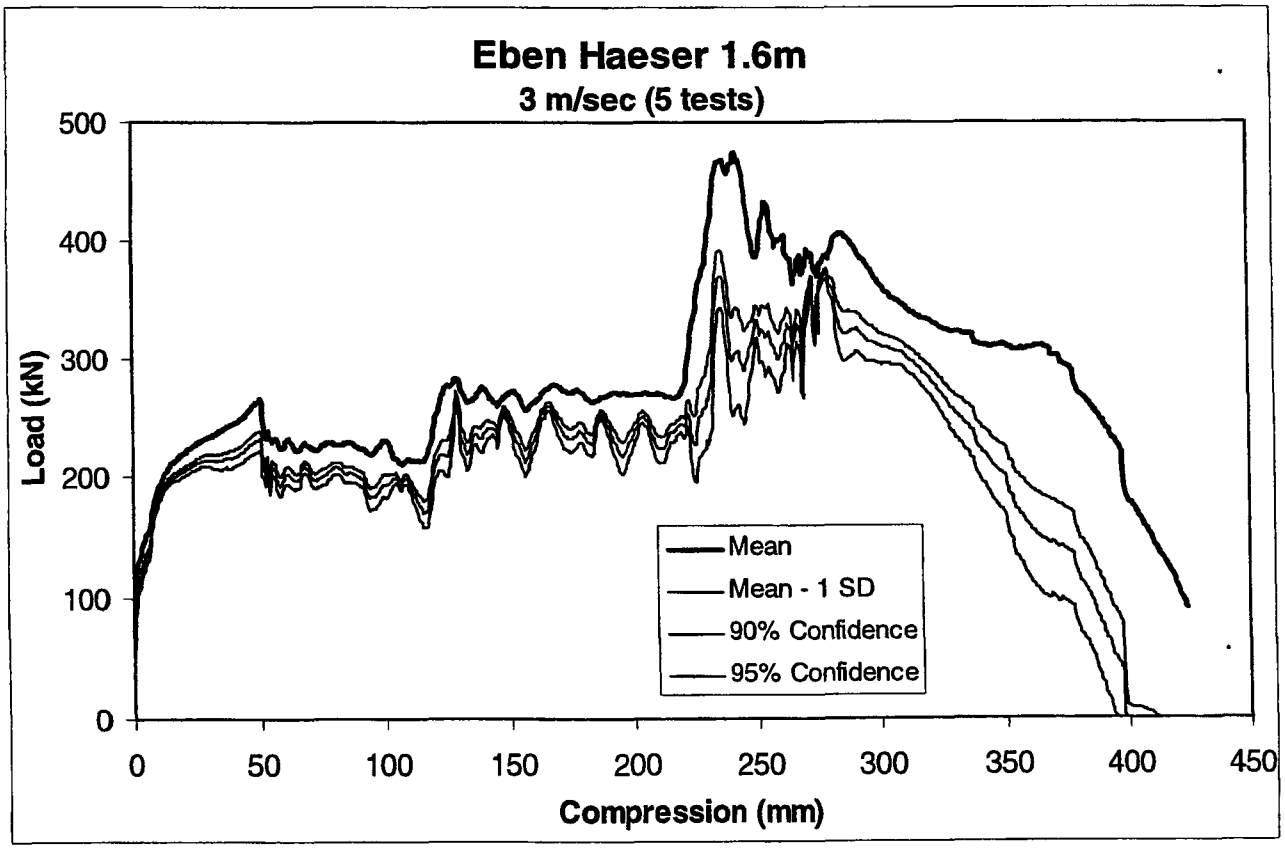
Eben Haeser 1.6m
3 m/sec (5 tests)
Load (kN)
500
400
300
200
100
0
0
50
100
150
200
250
300
350
400
450
Compression (mm)
Mean
Mean - 1 SD
90% Confidence
95% Confidence

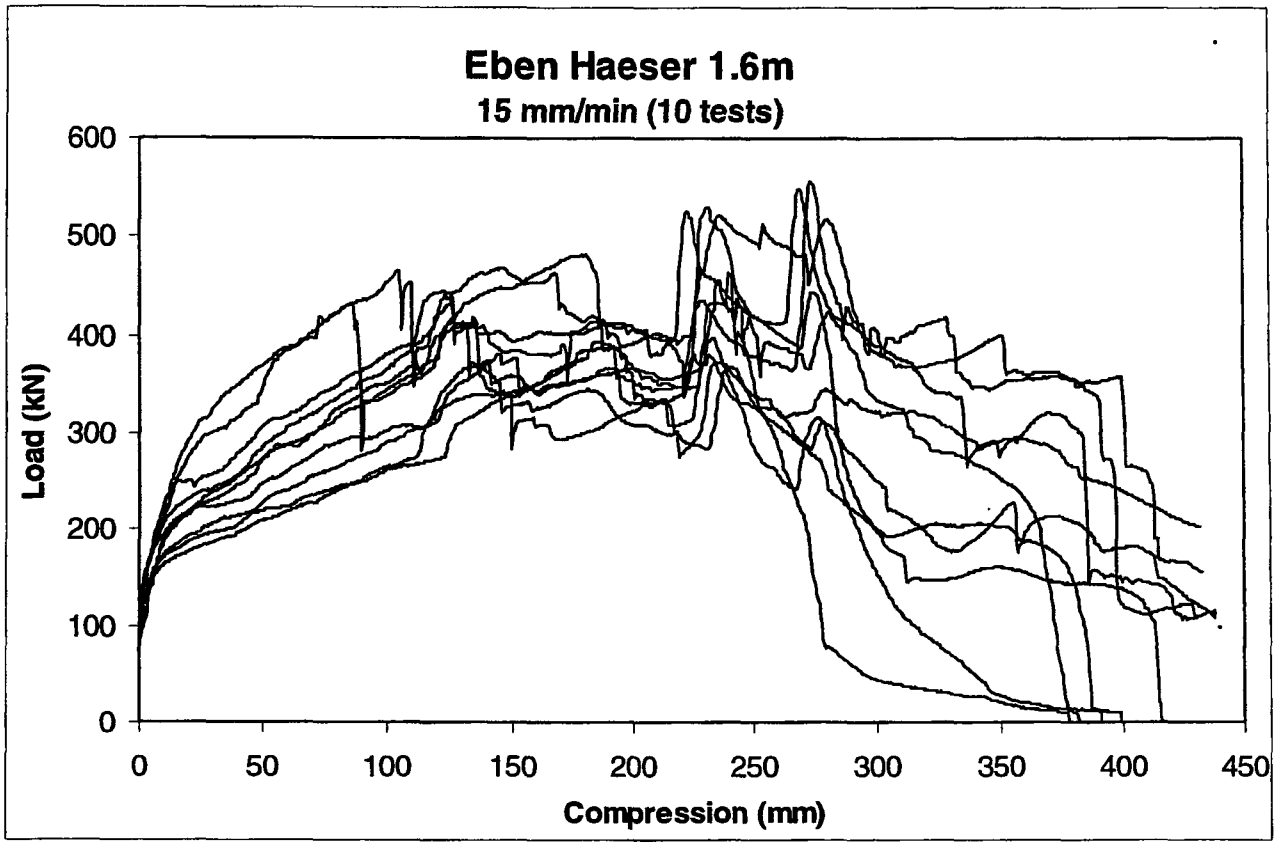
Eben Haeser 1.6m
15 mm/min (10 tests)
Load (kN)
600
500
400
300
200
100
0
0
50
100
150
200
250
300
350
400
450
Compression (mm)

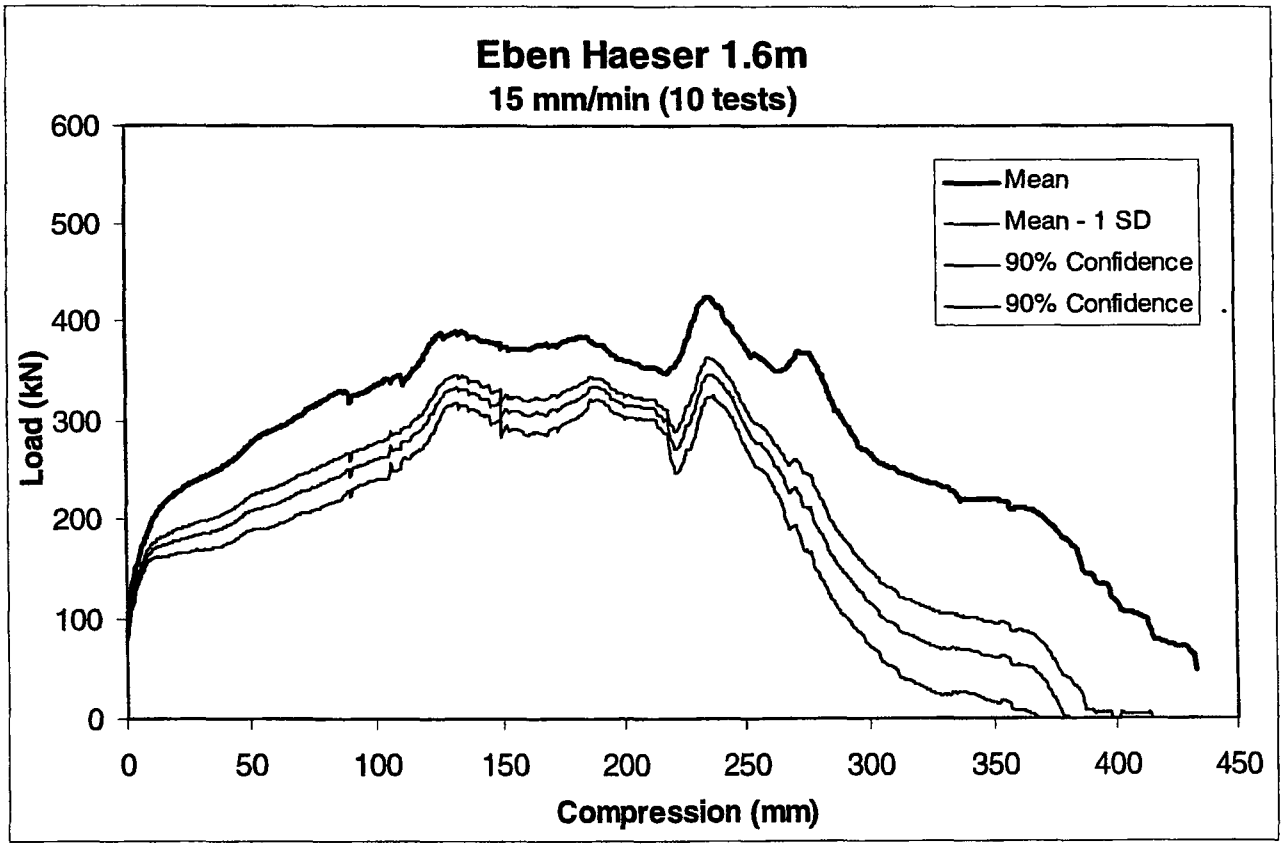
Eben Haeser 1.6m
15 mm/min (10 tests)
Mean
Mean - 1 SD
90% Confidence
90% Confidence
Load (kN)
600
500
400
300
200
100
0
0
50
100
150
200
250
300
350
400
450
Compression (mm)

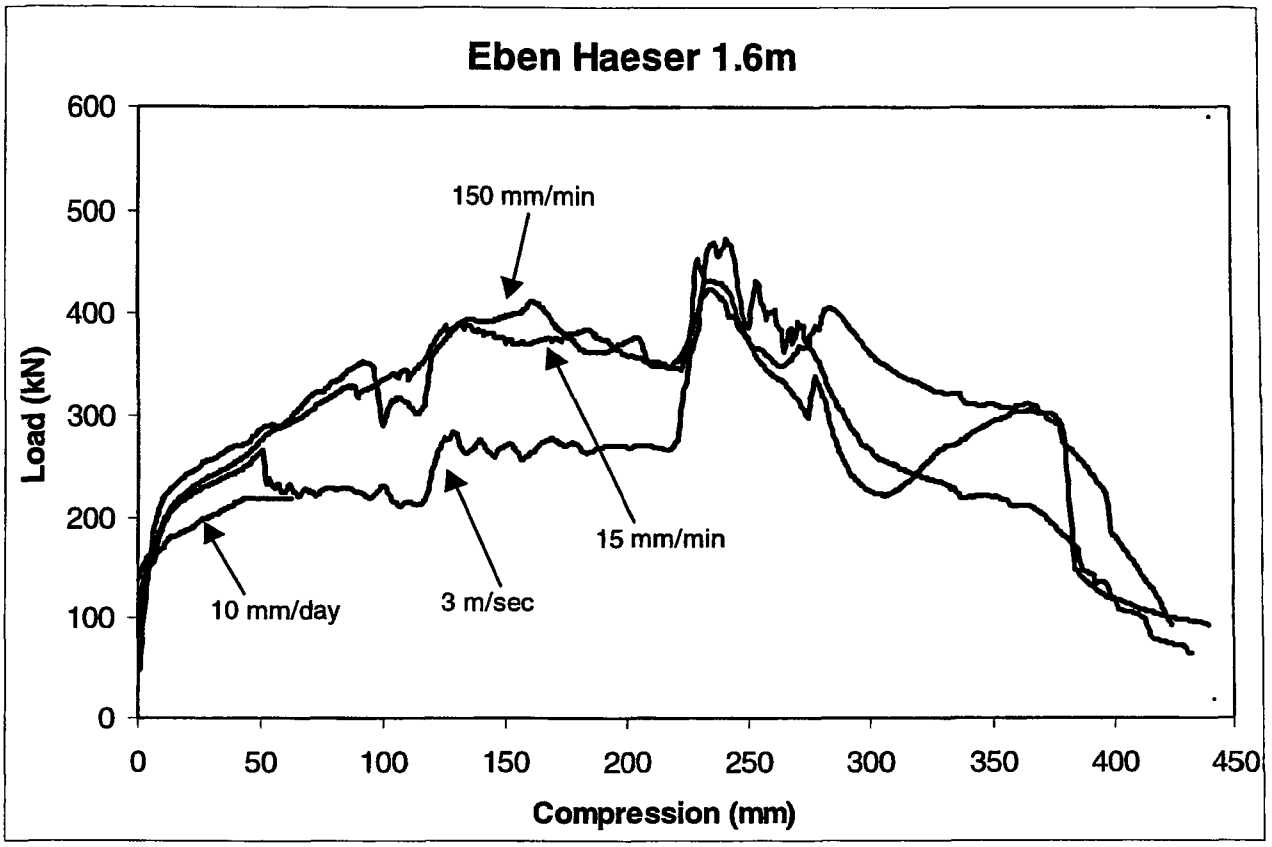
Eben Haeser 1.6m
Load (kN)
600
500
400
300
200
100
0
0
50
100
150
200
250
300
350
400
450
Compression (mm)
150 mm/min
15 mm/min
3 m/sec
10 mm/day

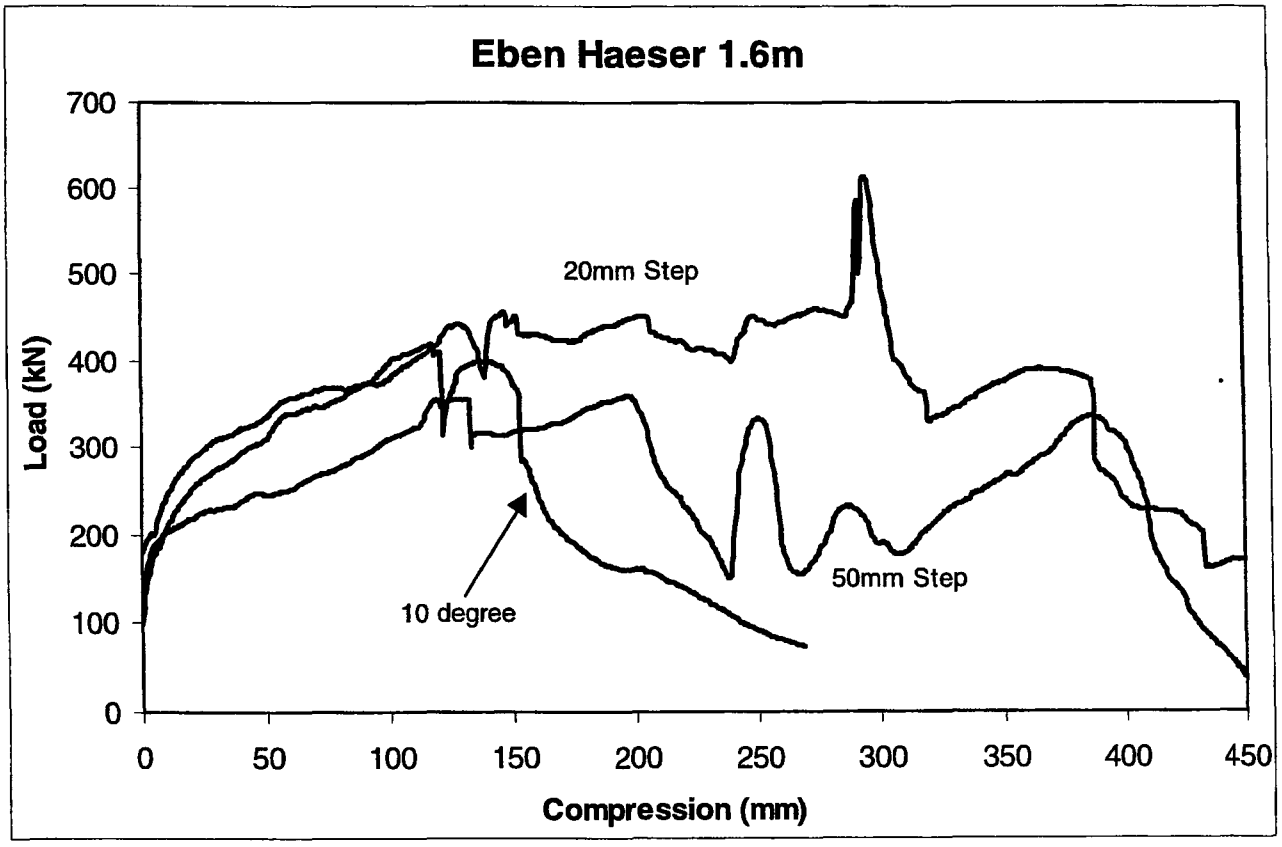
Eben Haeser 1.6m
Load (kN)
700
600
500
400
300
200
100
0
0
50
100
150
200
250
300
350
400
450
Compression (mm)
20mm Step
50mm Step
10 degree

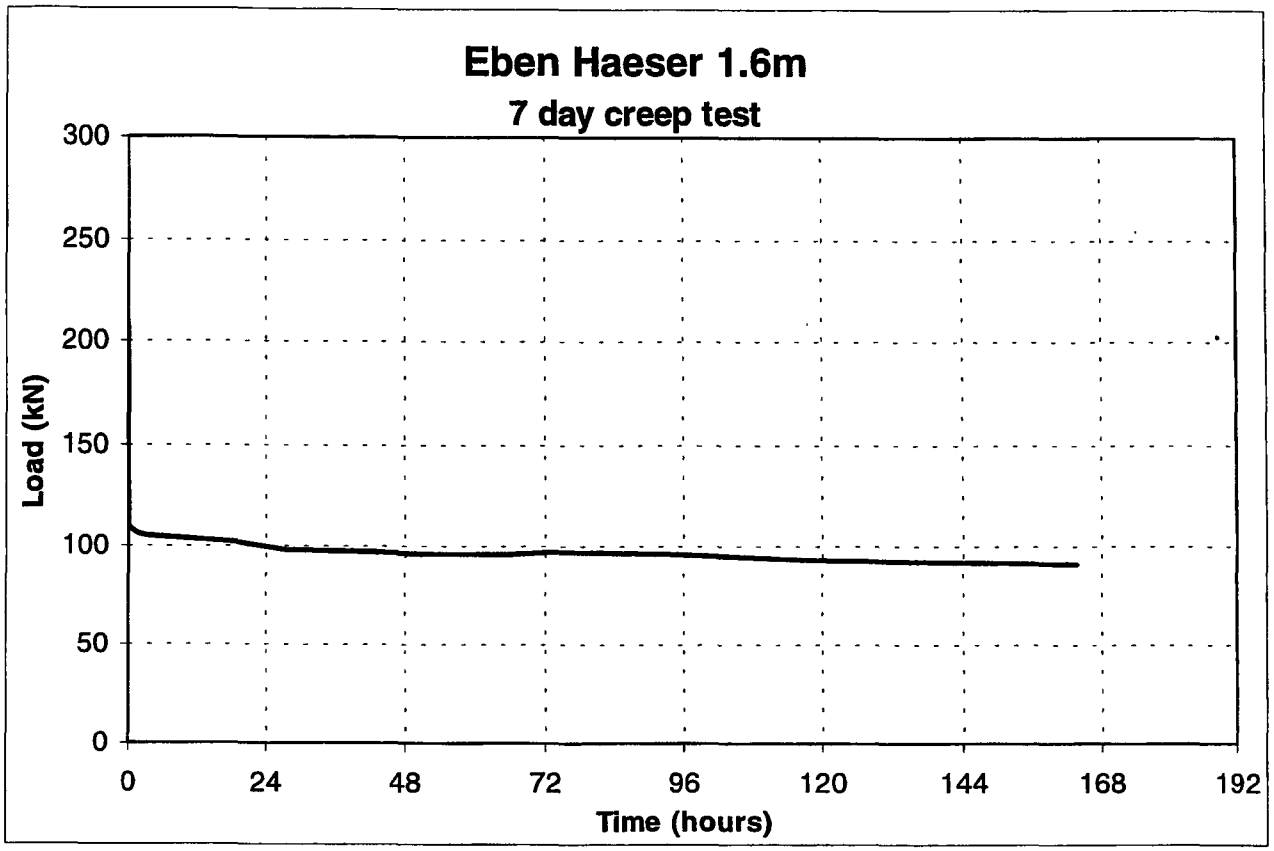
Eben Haeser 1.6m
7 day creep test
Load (kN)
300
250
200
150
100
50
0
0
24
48
72
96
120
144
168
192
Time (hours)

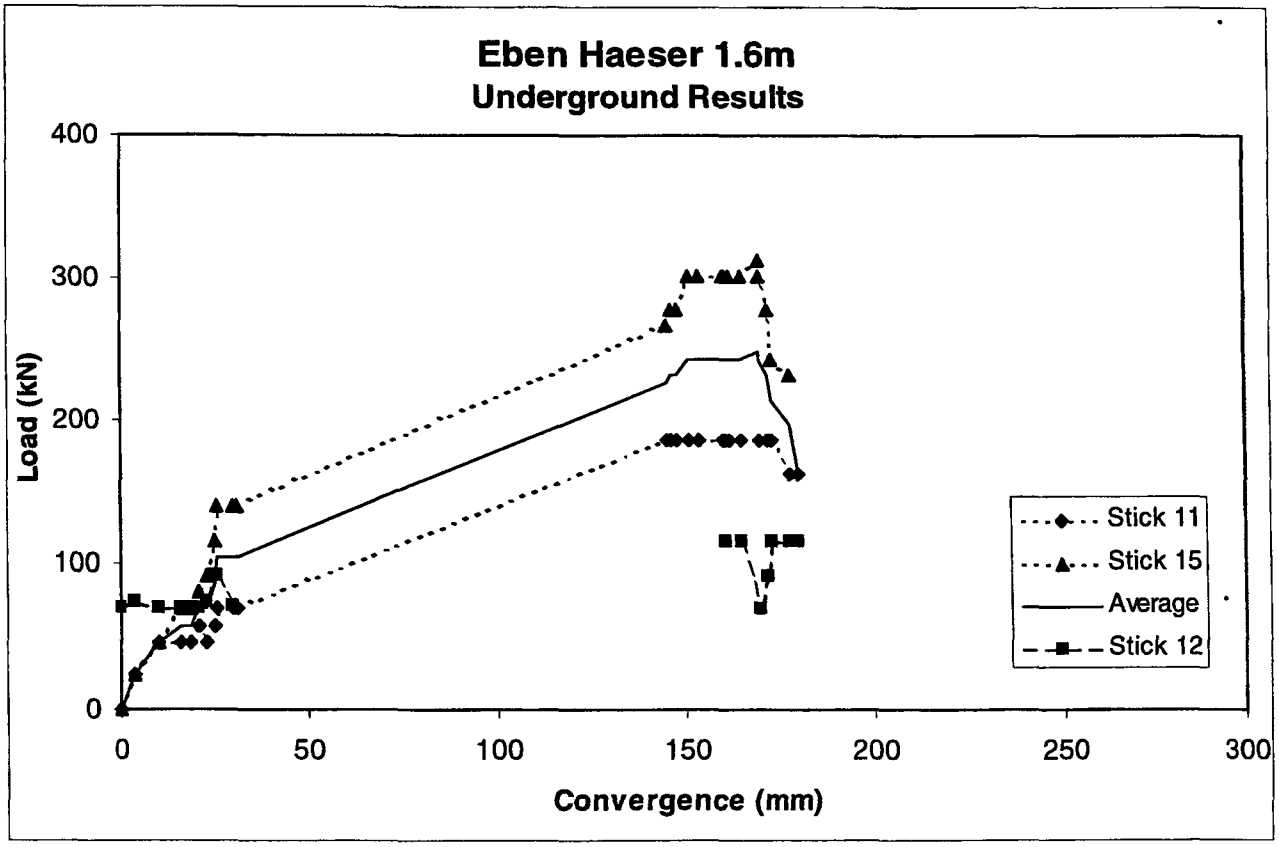
Eben Haeser 1.6m
Underground Results
Load (kN)
400
300
200
100
0
0
50
100
150
200
250
300
Convergence (mm)
Stick 11
Stick 15
Average
Stick 12

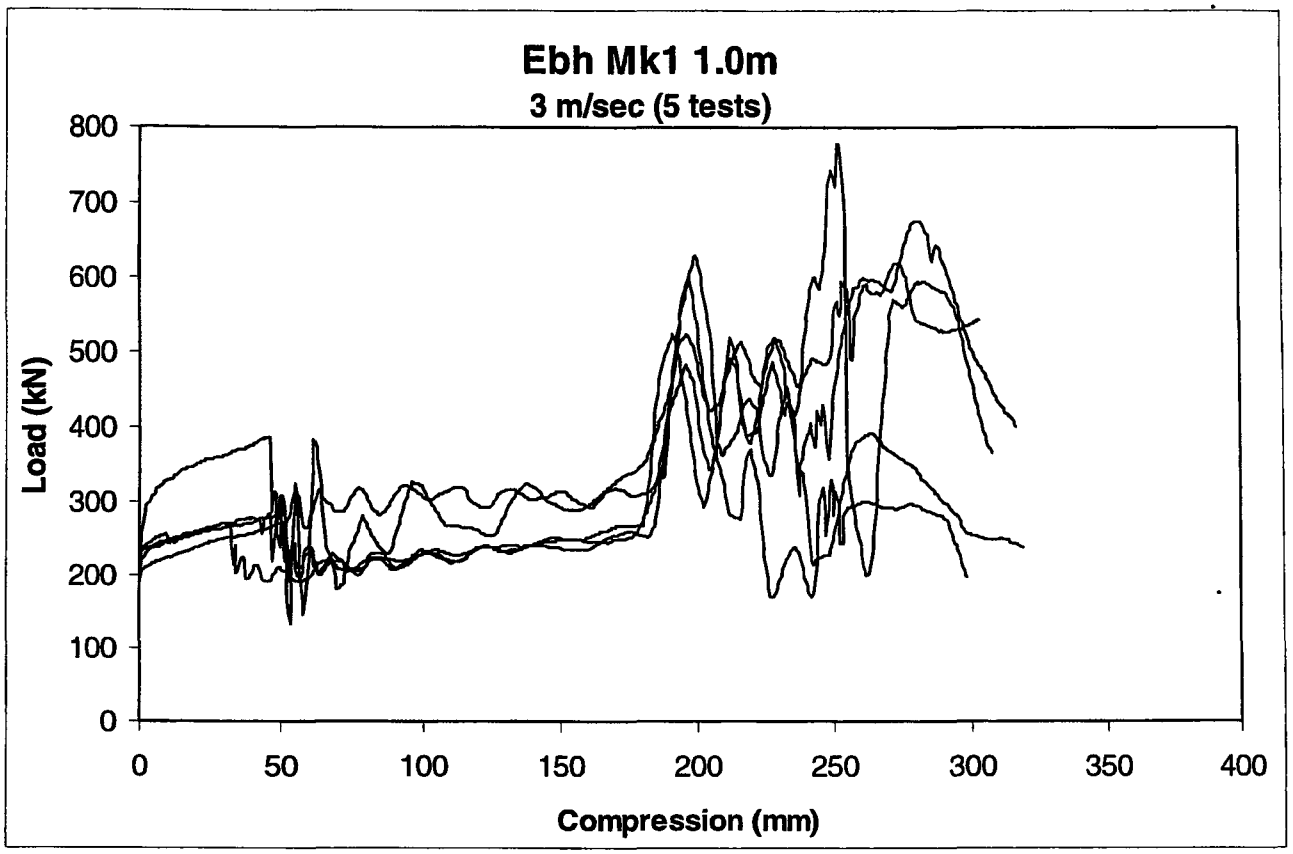
Ebh Mk1 1.0m
3 m/sec (5 tests)
Load (kN)
800
700
600
500
400
300
200
100
0
0
50
100
150
200
250
300
350
400
Compression (mm)

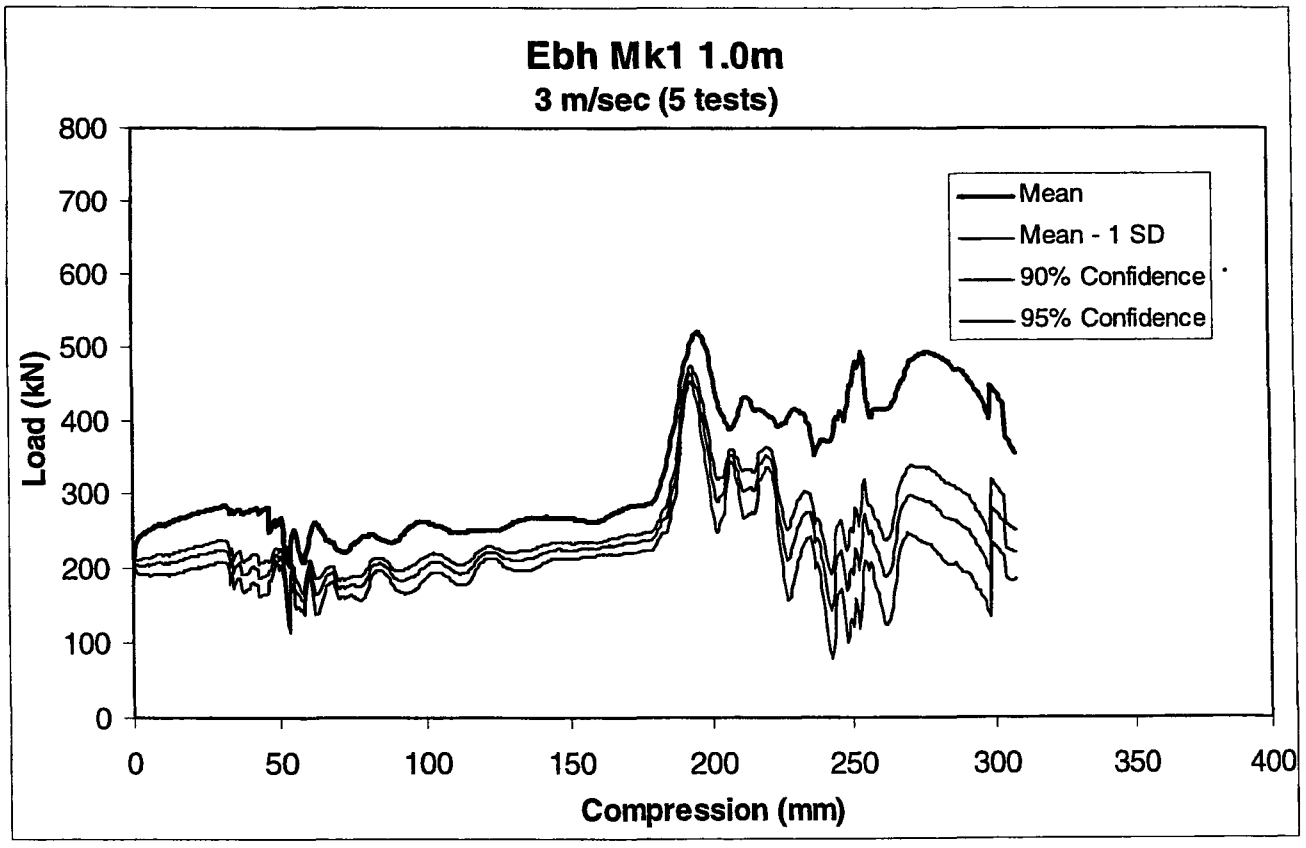
Ebh Mk1 1.0m
3 m/sec (5 tests)
Load (kN)
800
700
600
500
400
300
200
100
0
0
50
100
150
200
250
300
350
400
Compression (mm)
Mean
Mean - 1 SD
90% Confidence
95% Confidence

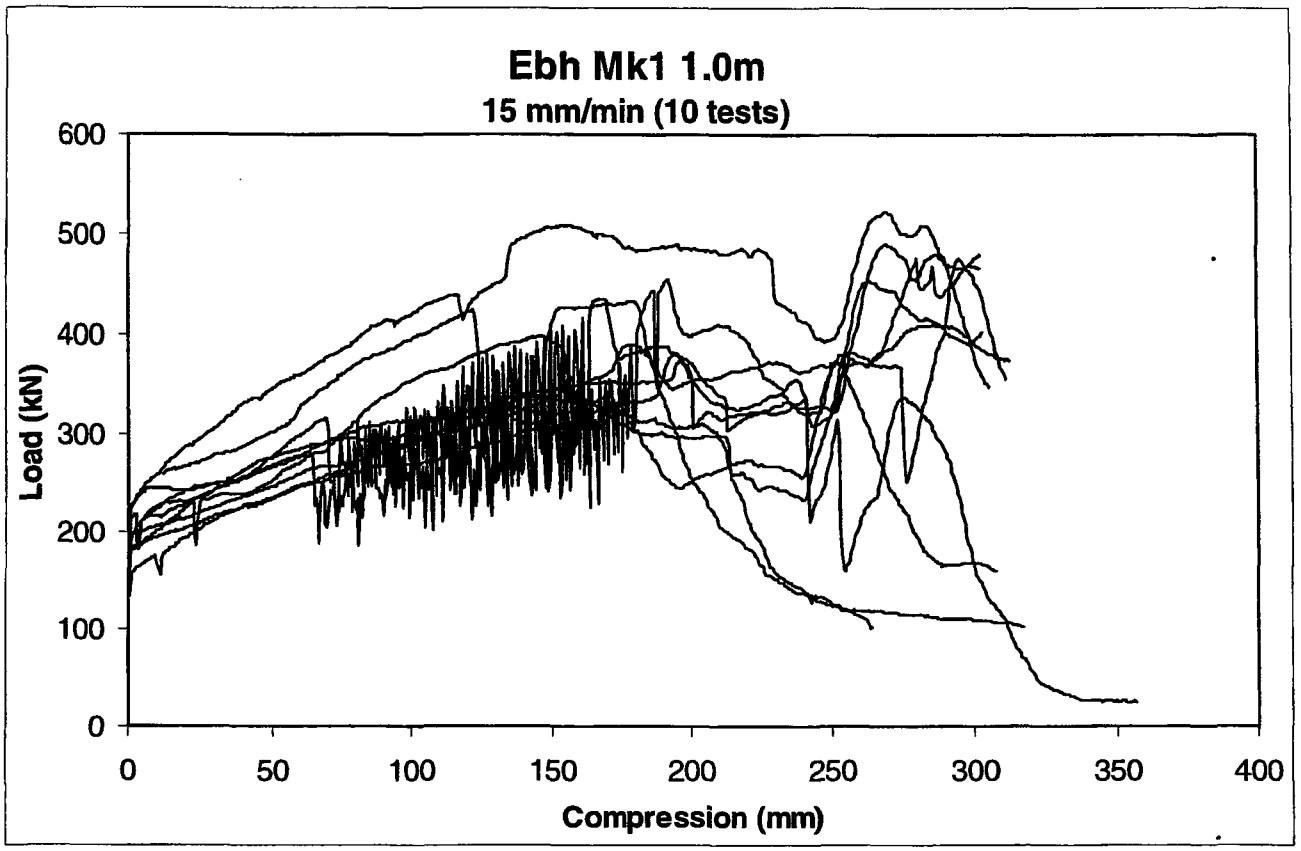
Ebh Mk1 1.0m
15 mm/min (10 tests)
Load (kN)
600
500
400
300
200
100
0
0
50
100
150
200
250
300
350
400
Compression (mm)

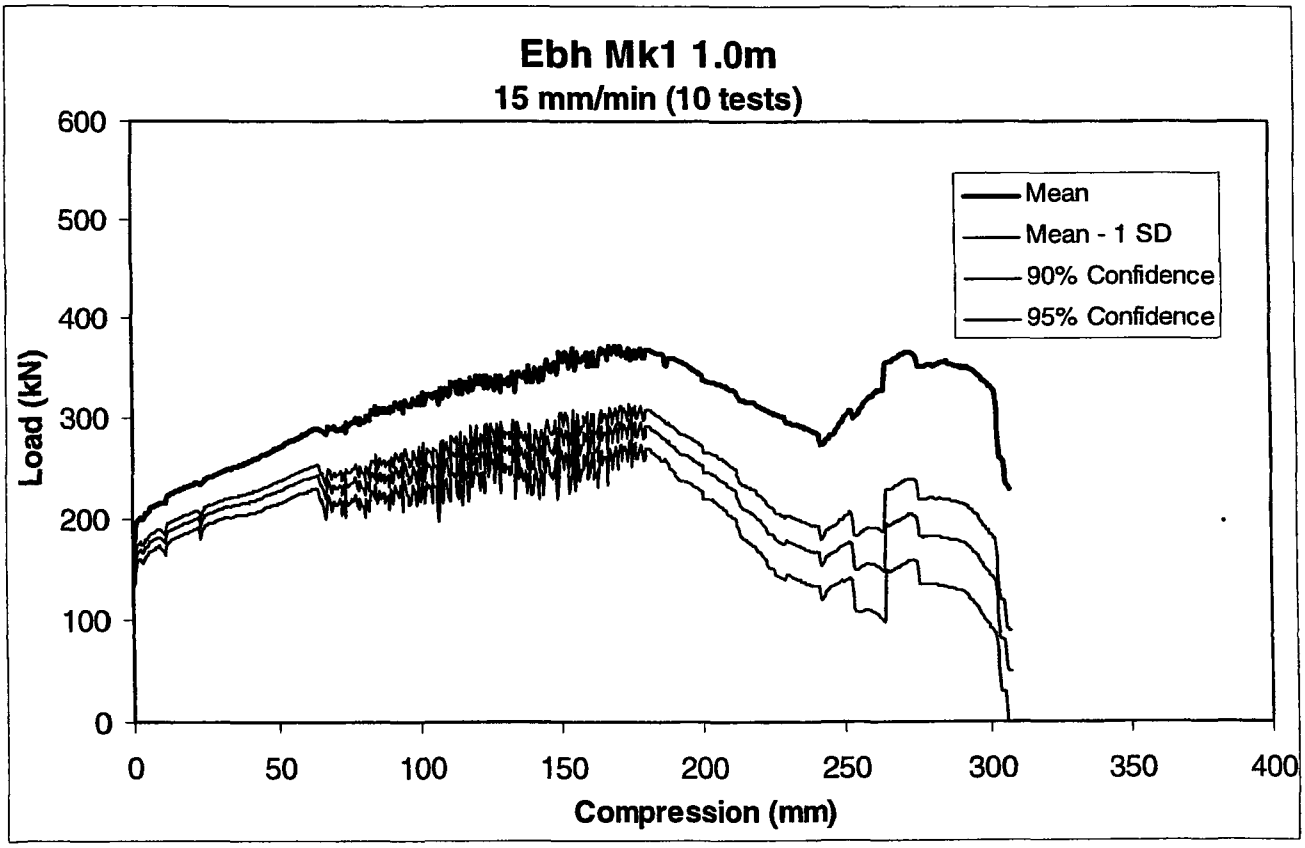
Ebh Mk1 1.0m
15 mm/min (10 tests)
Load (kN)
600
500
400
300
200
100
0
0
50
100
150
200
250
300
350
400
Compression (mm)
Mean
Mean - 1 SD
90% Confidence
95% Confidence

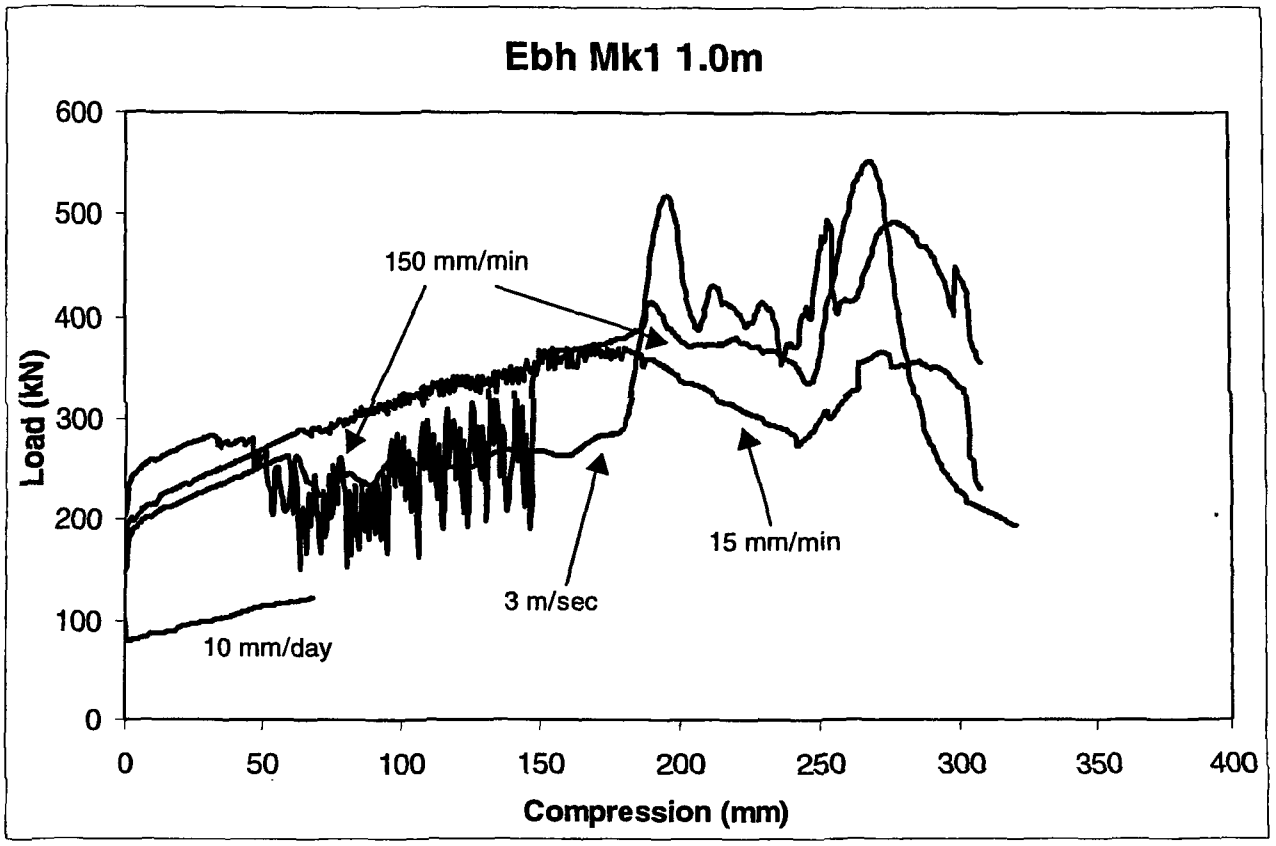
Ebh Mk1 1.0m
Load (kN)
600
500
400
300
200
100
0
150 mm/min
15 mm/min
3 m/sec
10 mm/day
0
50
100
150
200
250
300
350
400
Compression (mm)

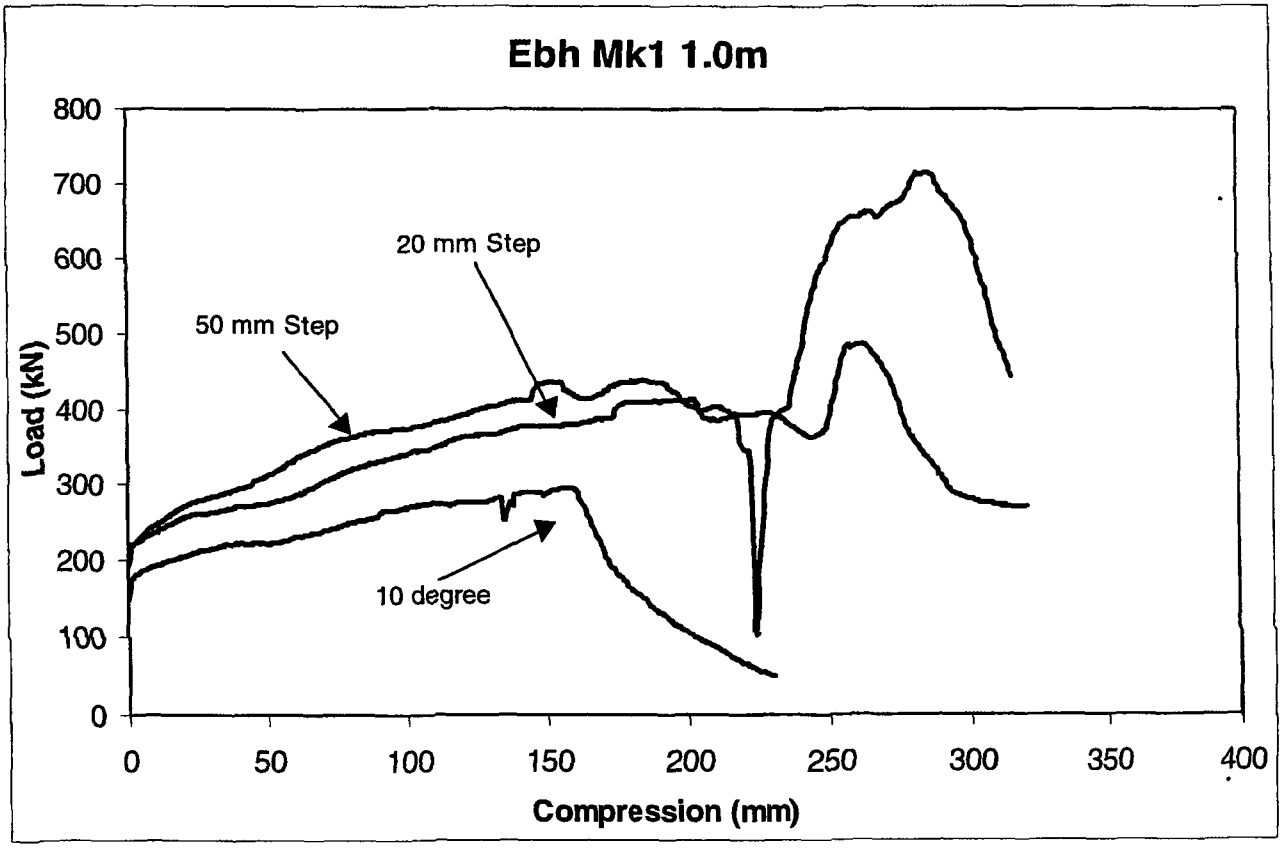
Ebh Mk1 1.0m
Load (kN)
800
700
600
500
400
300
200
100
0
20 mm Step
50 mm Step
10 degree
0
50
100
150
200
250
300
350
400
Compression (mm)

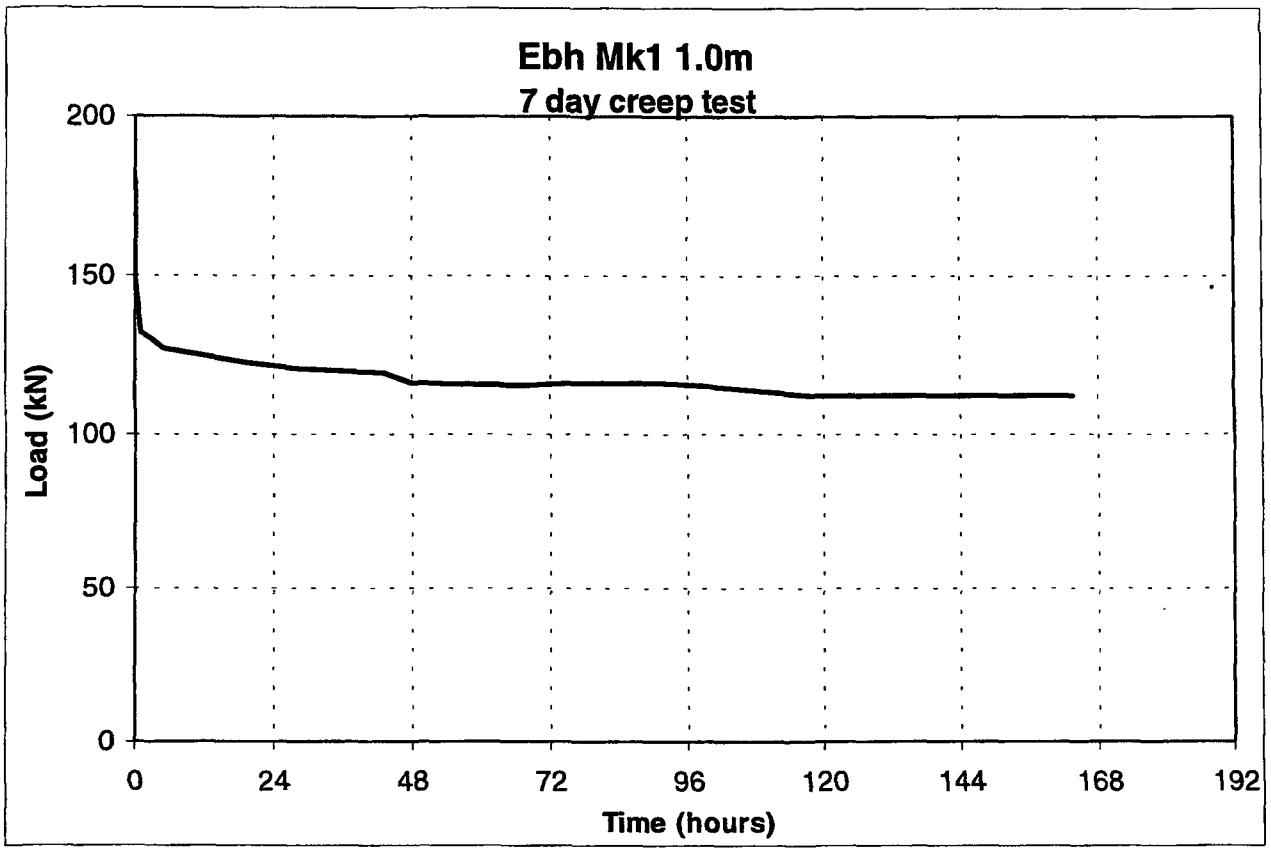
Ebh Mk1 1.0m
7 day creep test
Load (kN)
200
150
100
50
0
0
24
48
72
96
120
144
168
192
Time (hours)

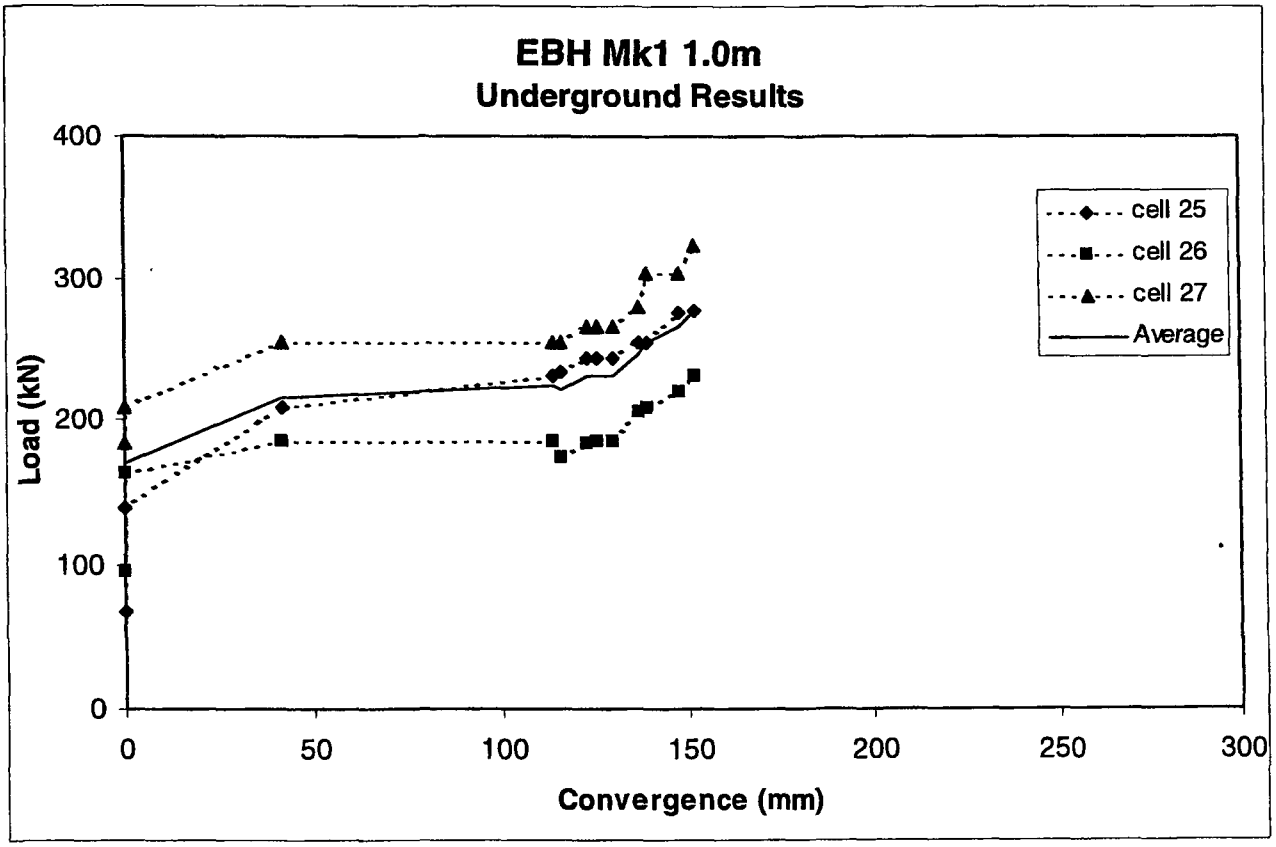
EBH Mk1 1.0m
Underground Results
Load (kN)
400
300
200
100
0
0
50
100
150
200
250
300
Convergence (mm)
cell 25
cell 26
cell 27
Average

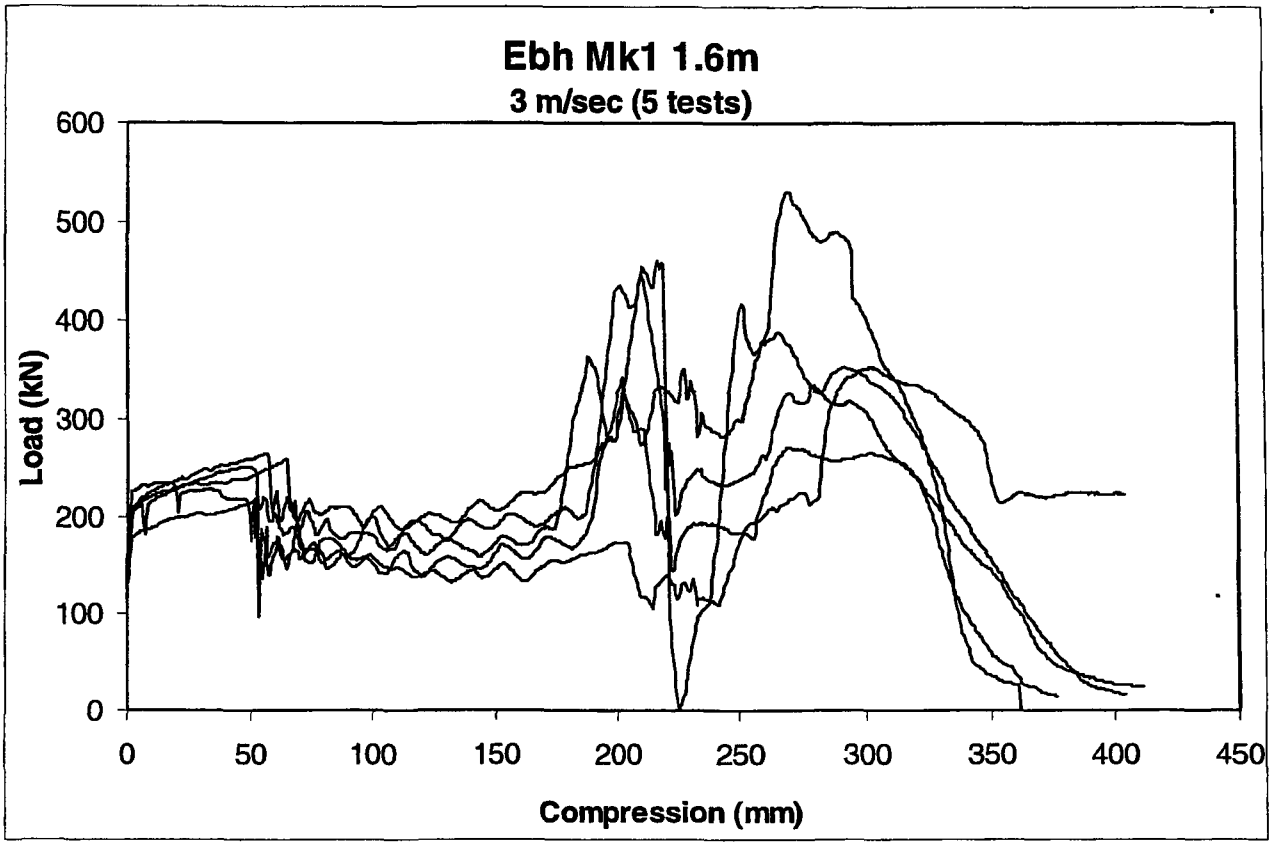
Ebh Mk1 1.6m
3 m/sec (5 tests)
Load (kN)
600
500
400
300
200
100
0
0
50
100
150
200
250
300
350
400
450
Compression (mm)

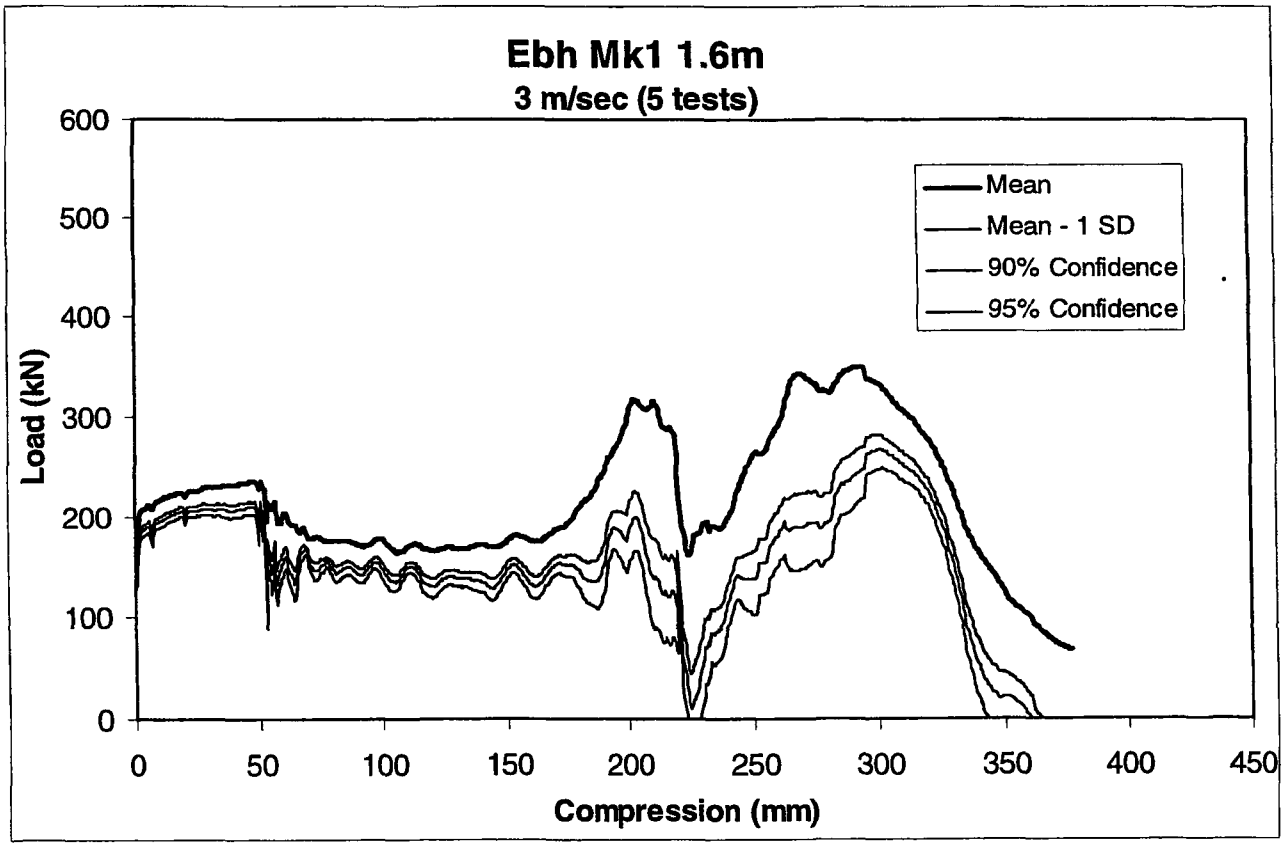
Ebh Mk1 1.6m
3 m/sec (5 tests)
Mean
Mean - 1 SD
90% Confidence
95% Confidence
Load (kN)
600
500
400
300
200
100
0
0
50
100
150
200
250
300
350
400
450
Compression (mm)

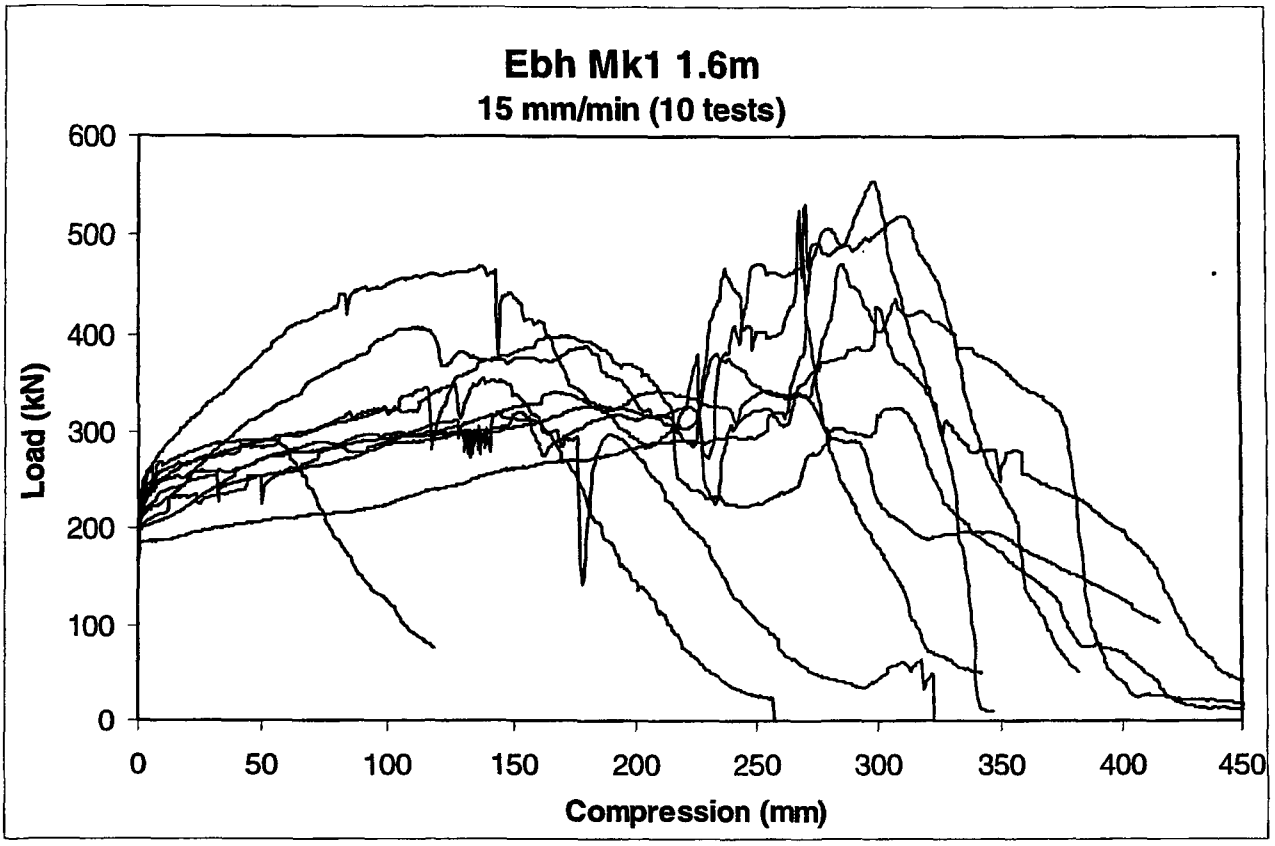
Ebh Mk1 1.6m
15 mm/min (10 tests)
Load (kN)
600
500
400
300
200
100
0
0
50
100
150
200
250
300
350
400
450
Compression (mm)

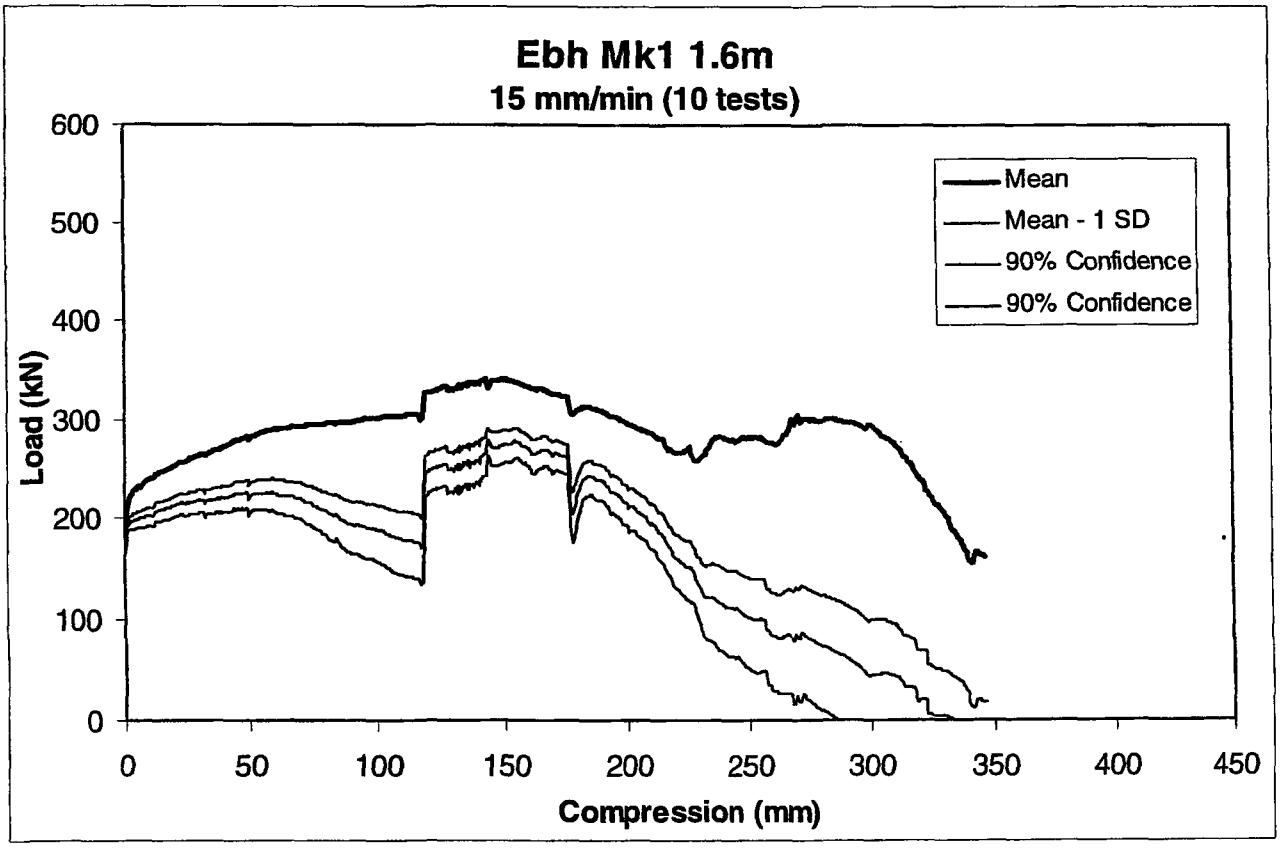
Ebh Mk1 1.6m
15 mm/min (10 tests)
Mean
Mean - 1 SD
90% Confidence
90% Confidence
Load (kN)
600
500
400
300
200
100
0
0
50
100
150
200
250
300
350
400
450
Compression (mm)

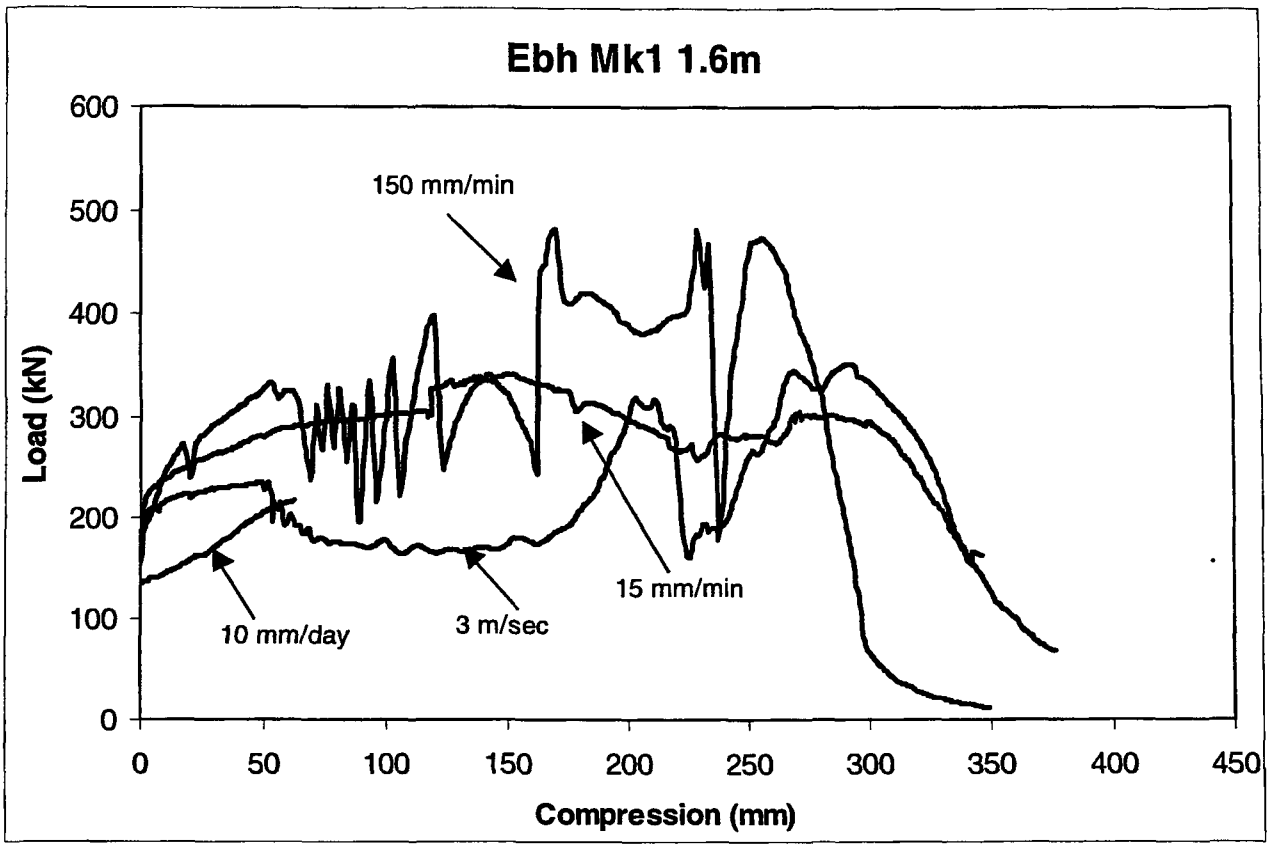
Ebh Mk1 1.6m
Load (kN)
Compression (mm)
150 mm/min
15 mm/min
10 mm/day
3 m/sec
0
100
200
300
400
500
600
0
50
100
150
200
250
300
350
400
450

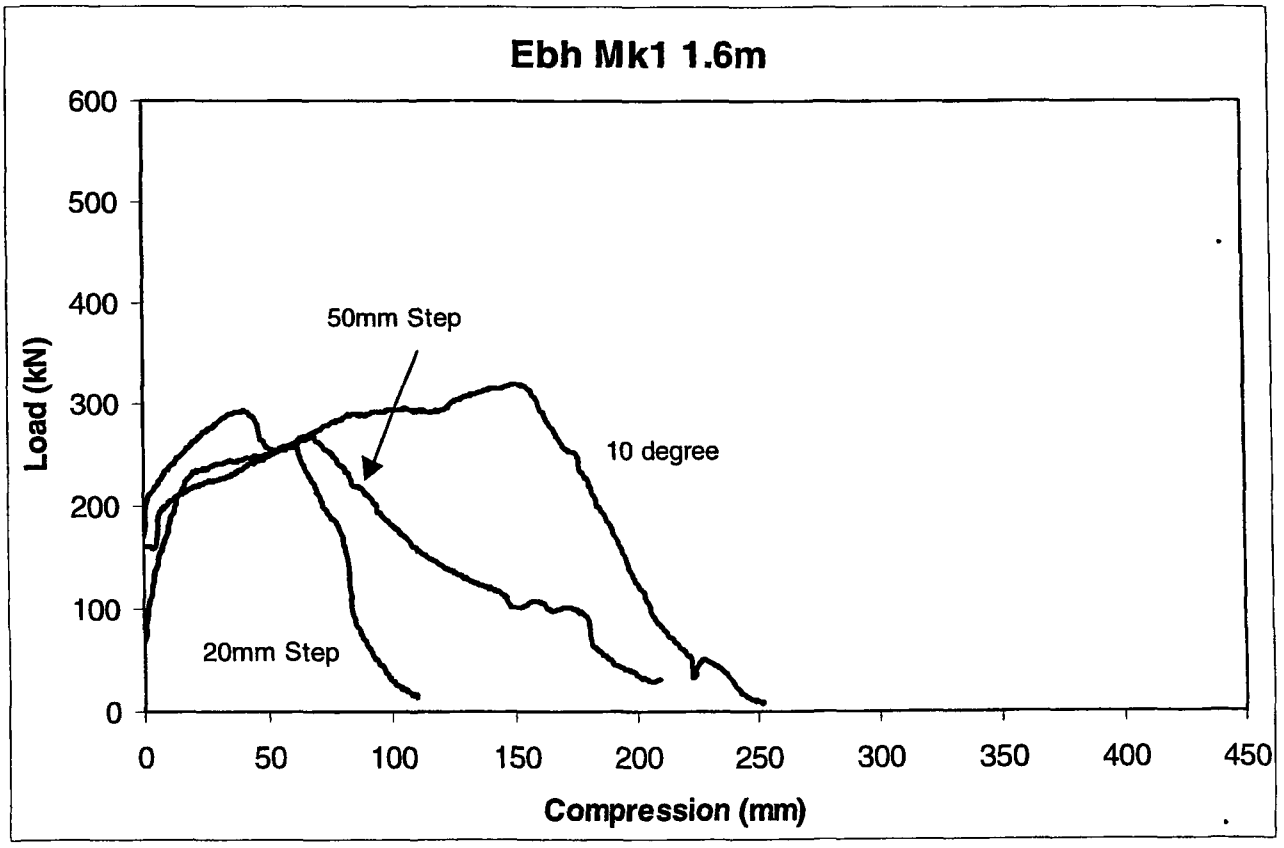
Ebh Mk1 1.6m
Load (kN)
Compression (mm)
50mm Step
10 degree
20mm Step
0
100
200
300
400
500
600
0
50
100
150
200
250
300
350
400
450

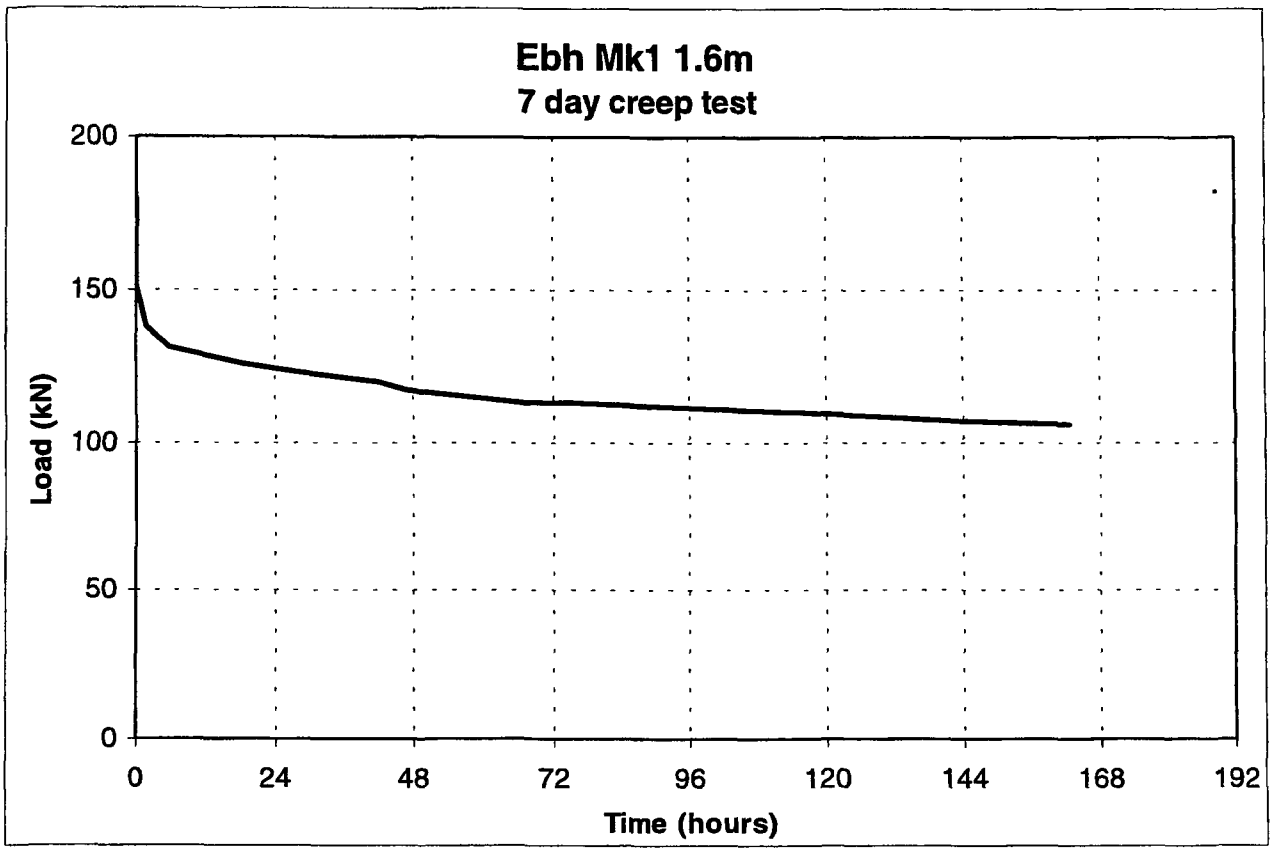
Ebh Mk1 1.6m
7 day creep test
Load (kN)
200
150
100
50
0
0
24
48
72
96
120
144
168
192
Time (hours)

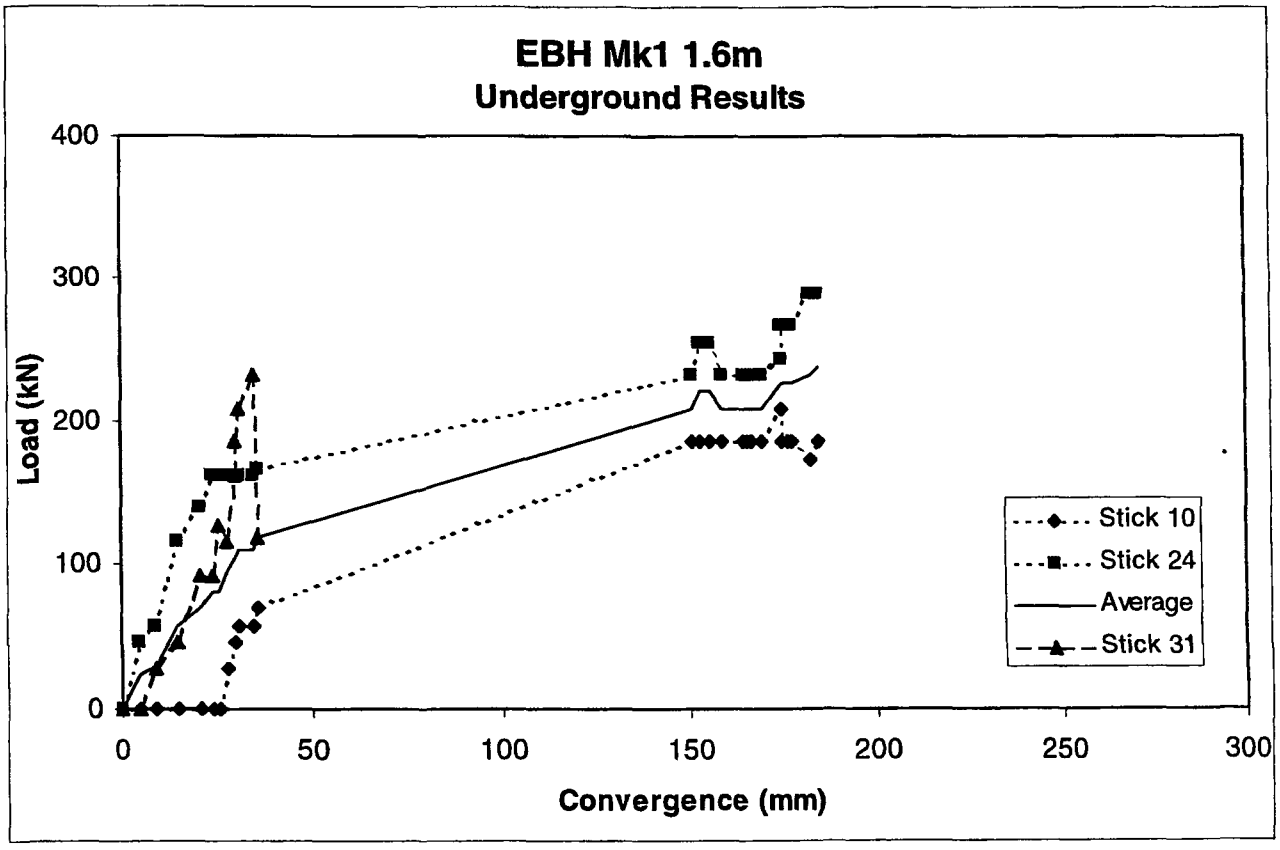
EBH Mk1 1.6m
Underground Results
Load (kN)
400
300
200
100
0
0
50
100
150
200
250
300
Convergence (mm)
Stick 10
Stick 24
Average
Stick 31

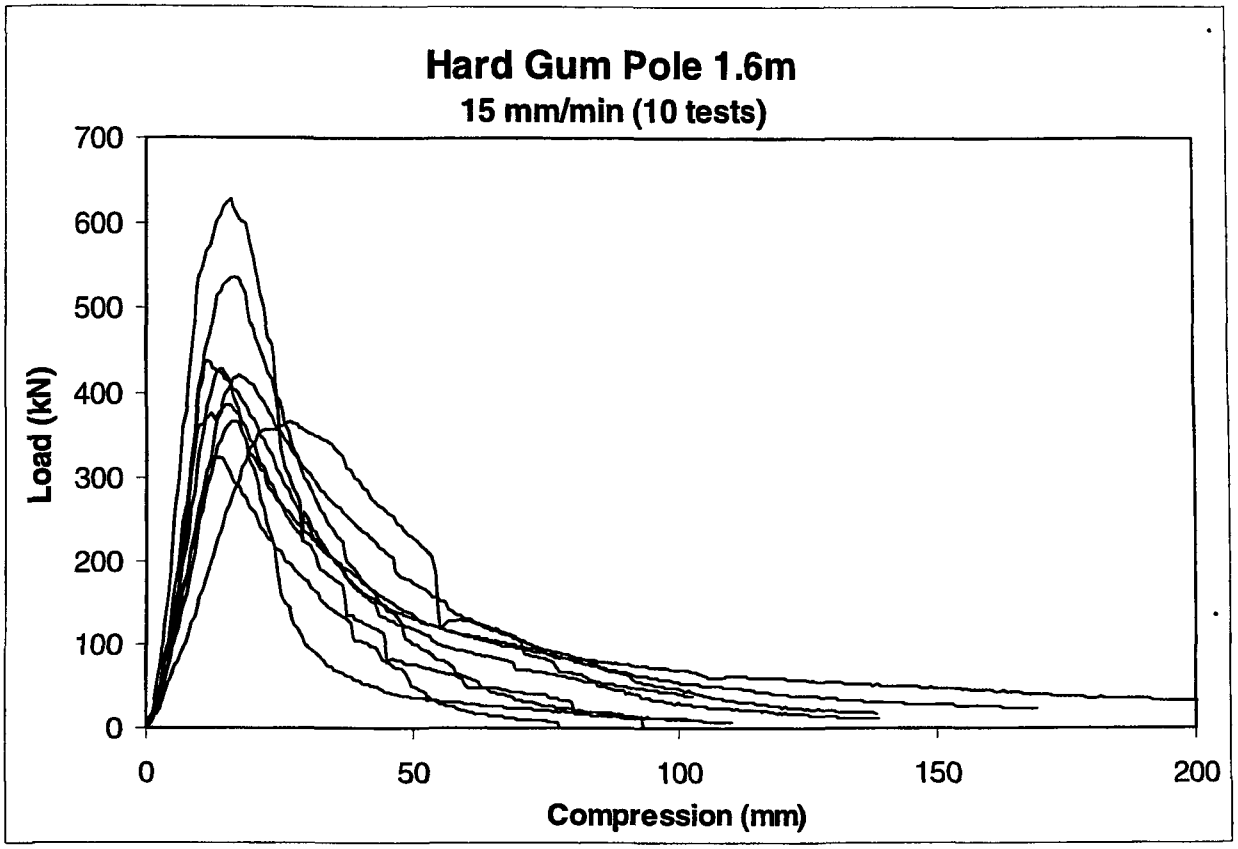
Hard Gum Pole 1.6m
15 mm/min (10 tests)
Load (kN)
700
600
500
400
300
200
100
0
0
50
100
150
200
Compression (mm)

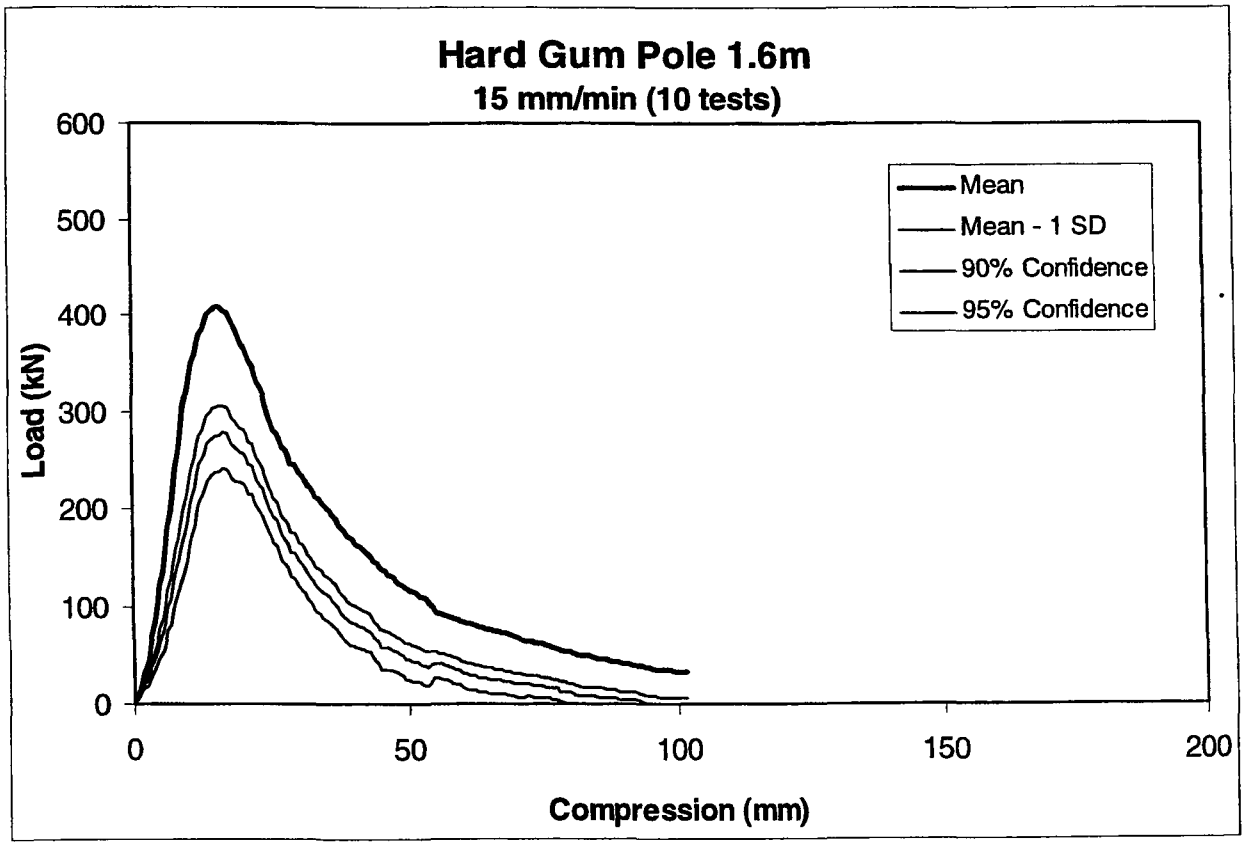
Hard Gum Pole 1.6m
15 mm/min (10 tests)
Load (kN)
600
500
400
300
200
100
0
0
50
100
150
200
Compression (mm)
Mean
Mean - 1 SD
90% Confidence
95% Confidence

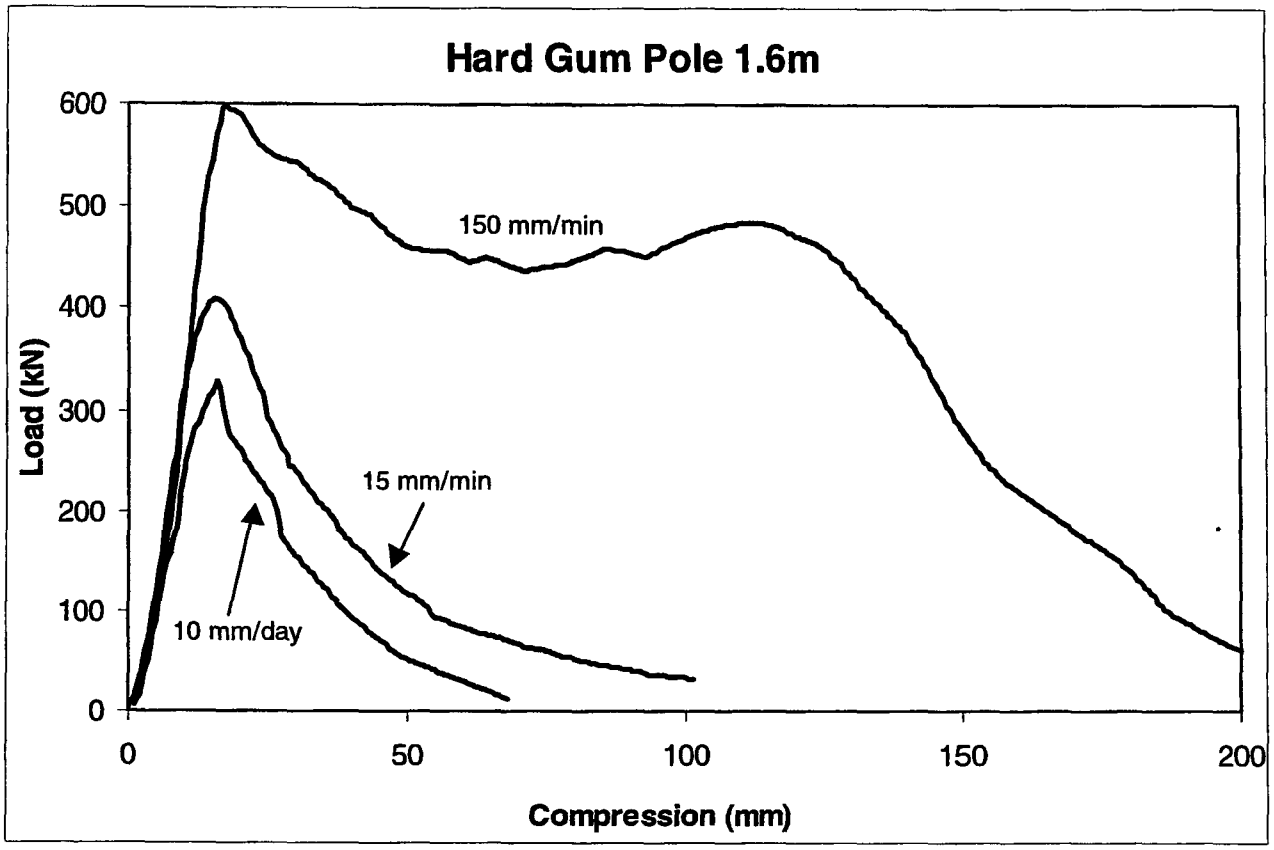
Hard Gum Pole 1.6m
Load (kN)
600
500
400
300
200
100
0
150 mm/min
15 mm/min
10 mm/day
0
50
100
150
200
Compression (mm)

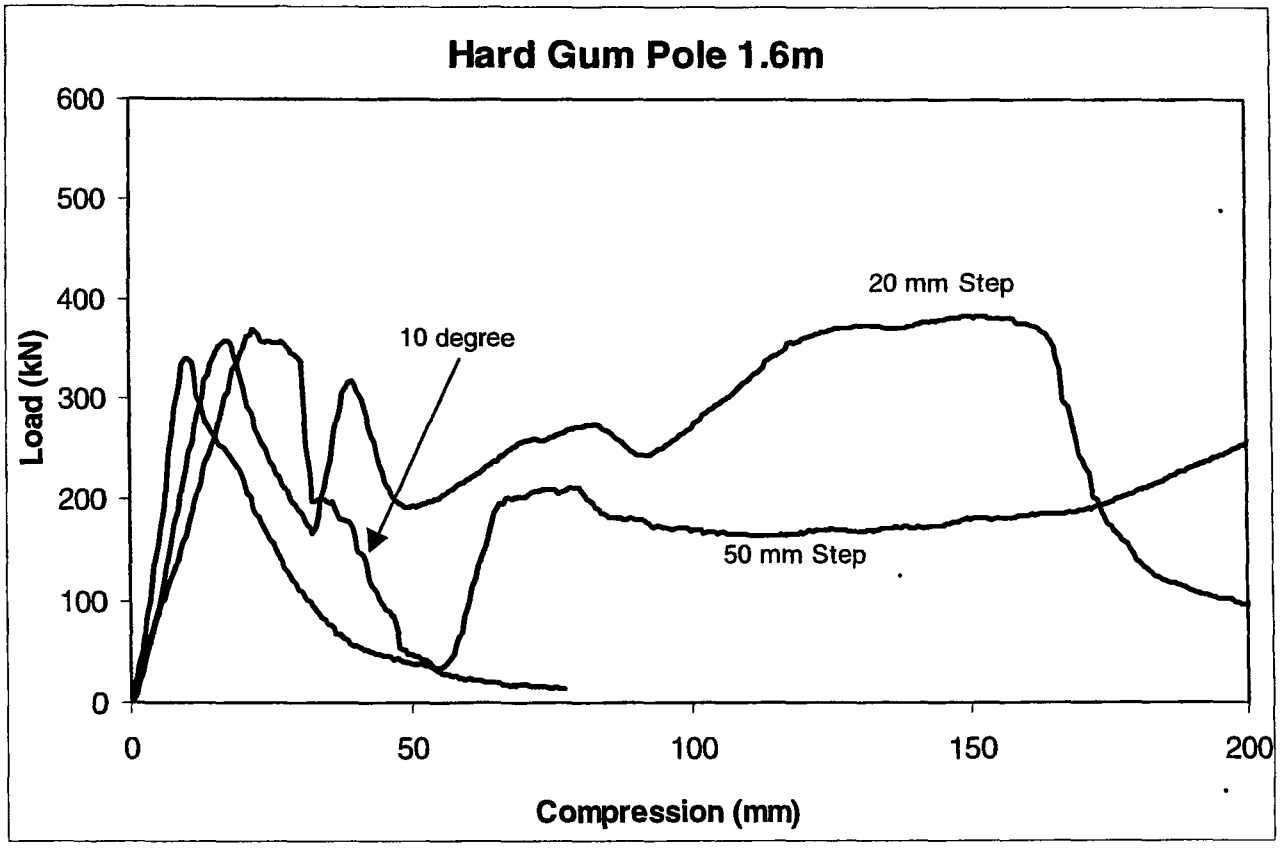
Hard Gum Pole 1.6m
Load (kN)
600
500
400
300
200
100
0
20 mm Step
10 degree
50 mm Step
0
50
100
150
200
Compression (mm)

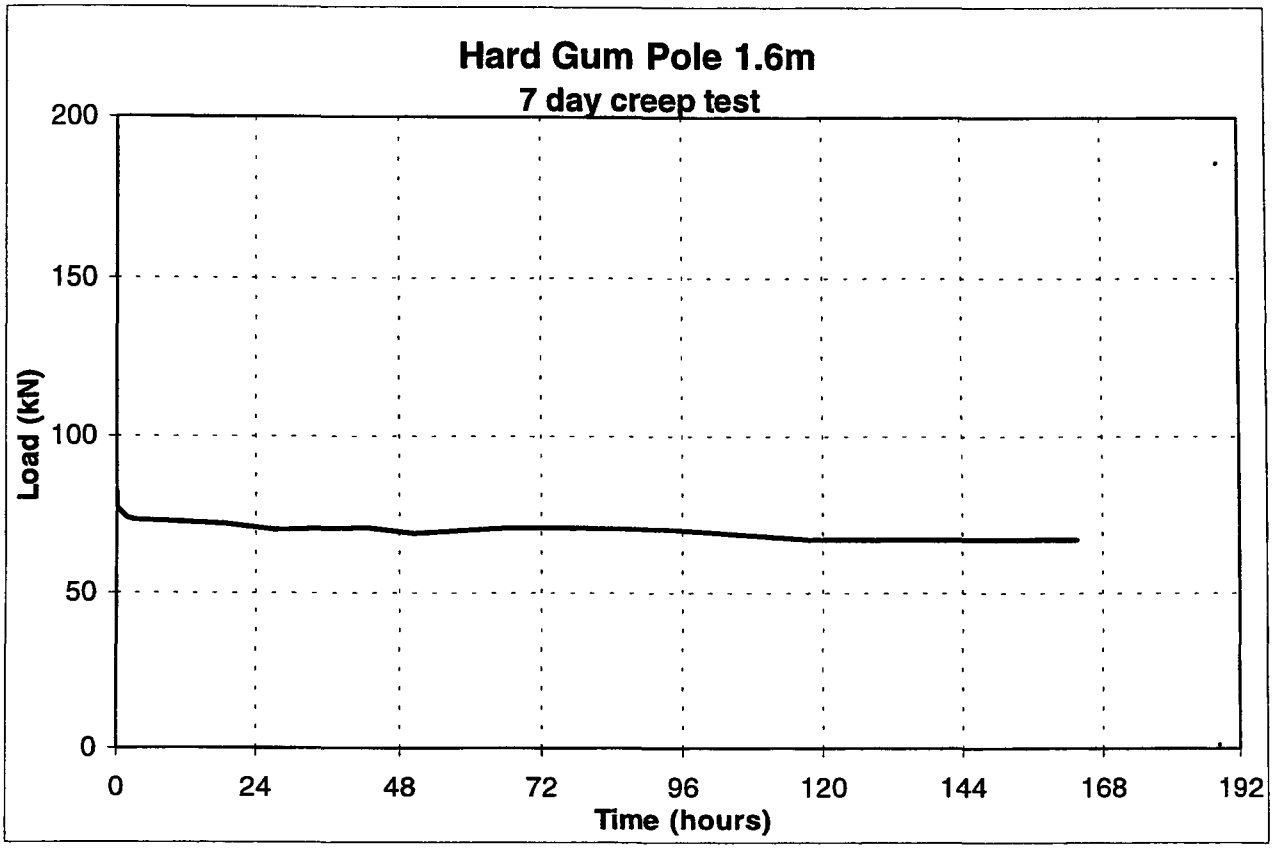
Hard Gum Pole 1.6m
7 day creep test
Load (kN)
200
150
100
50
0
0
24
48
72
96
120
144
168
192
Time (hours)

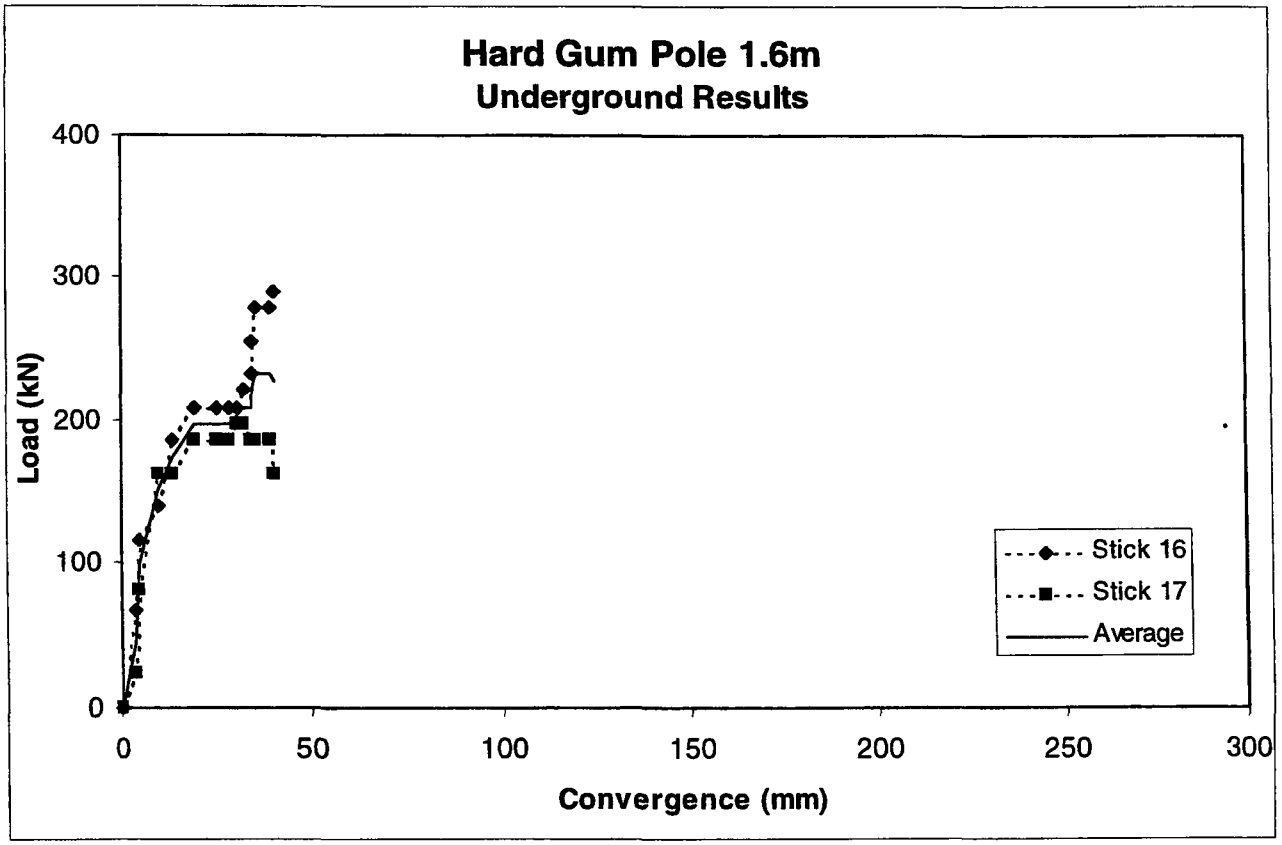
Hard Gum Pole 1.6m
Underground Results
Load (kN)
400
300
200
100
0
0
50
100
150
200
250
300
Convergence (mm)
Stick 16
Stick 17
Average

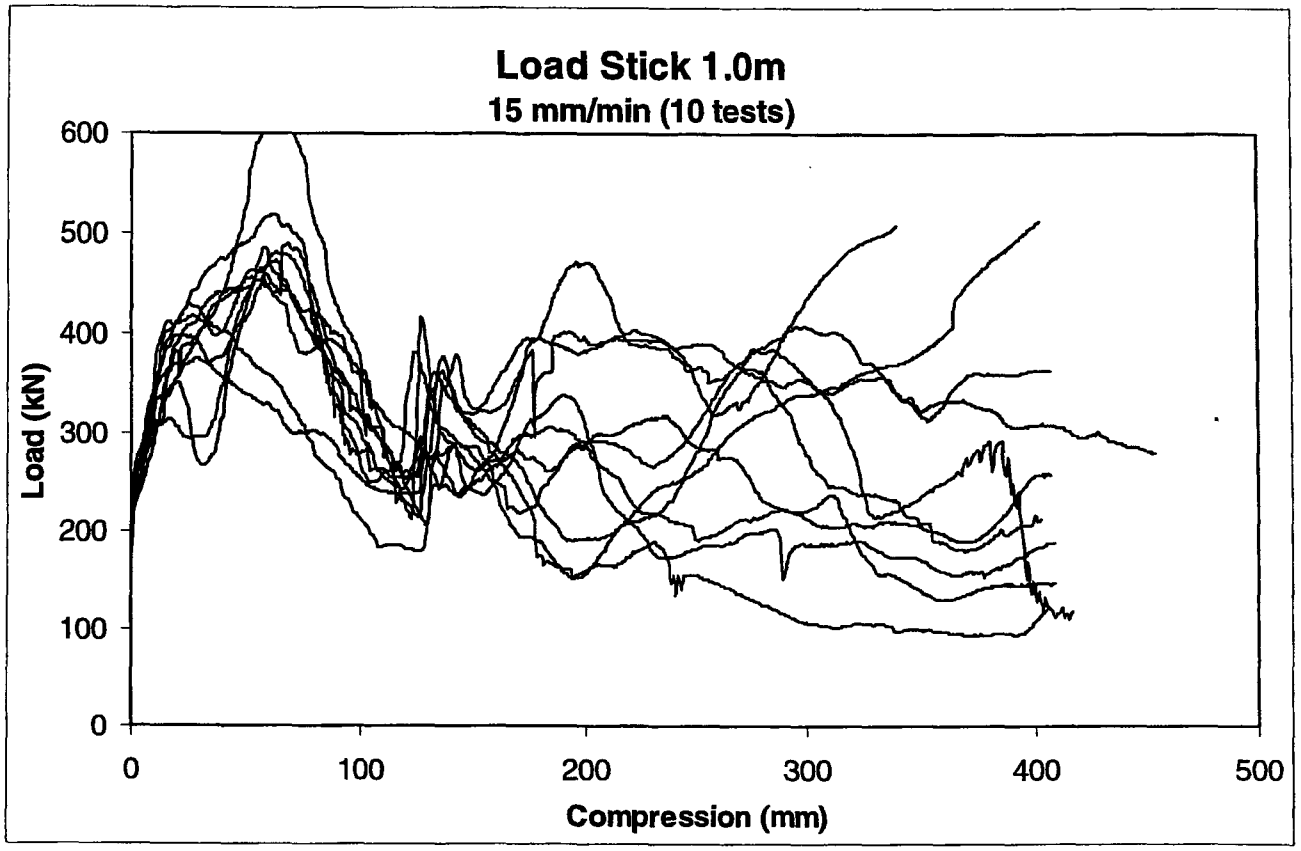
Load Stick 1.0m
15 mm/min (10 tests)
Load (kN)
600
500
400
300
200
100
0
0
100
200
300
400
500
Compression (mm)

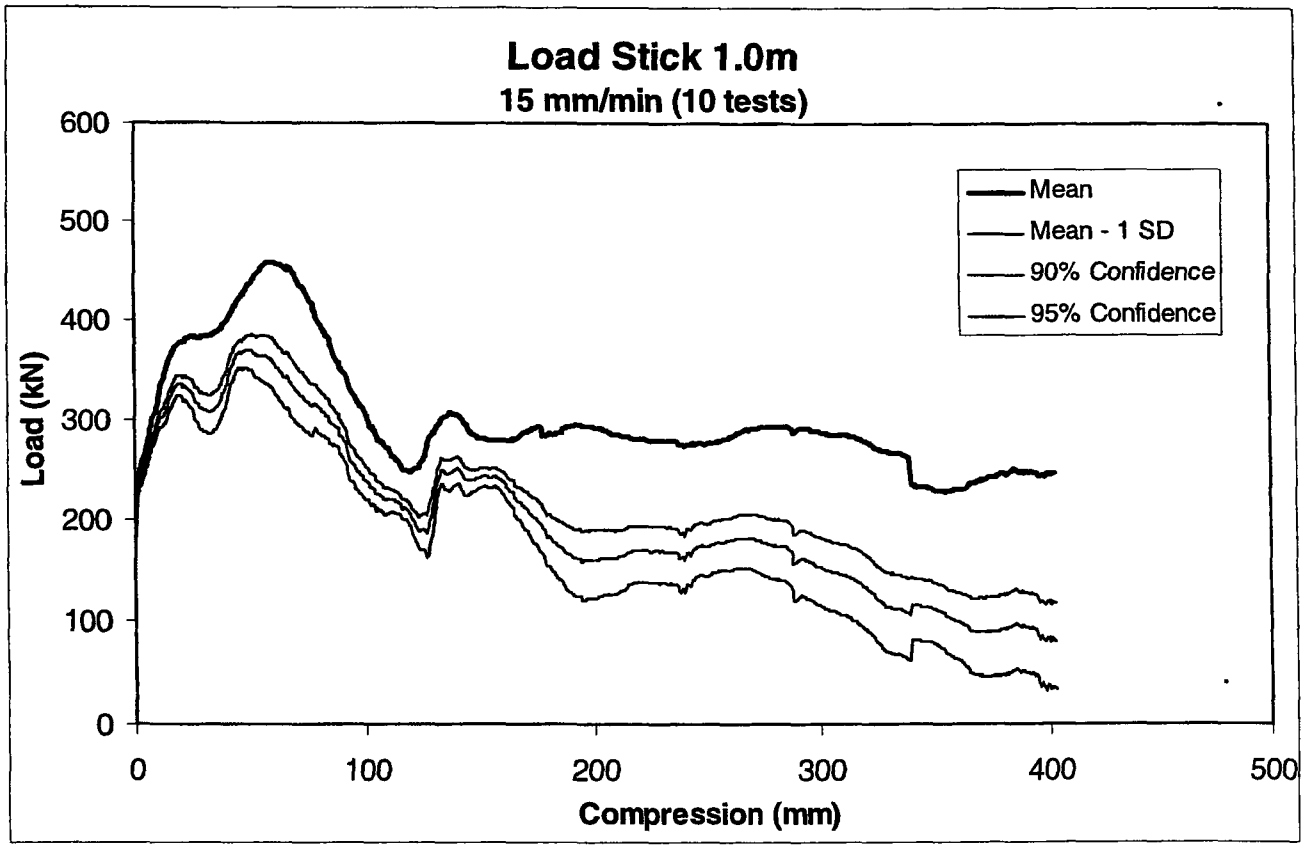
Load Stick 1.0m
15 mm/min (10 tests)
Load (kN)
600
500
400
300
200
100
0
0
100
200
300
400
500
Compression (mm)
Mean
Mean - 1 SD
90% Confidence
95% Confidence

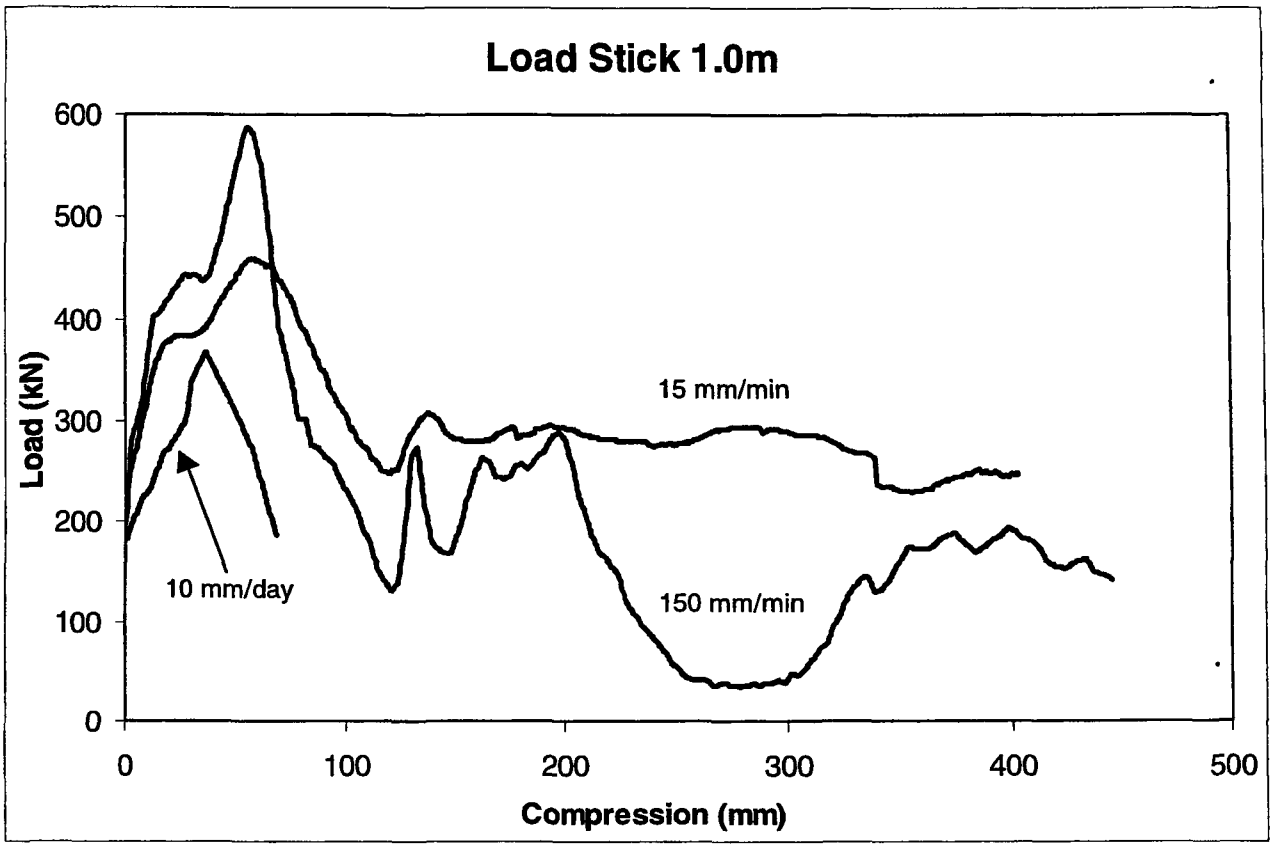
Load Stick 1.0m
600
500
400
300
200
100
0
Load (kN)
15 mm/min
10 mm/day
150 mm/min
0
100
200
300
400
500
Compression (mm)

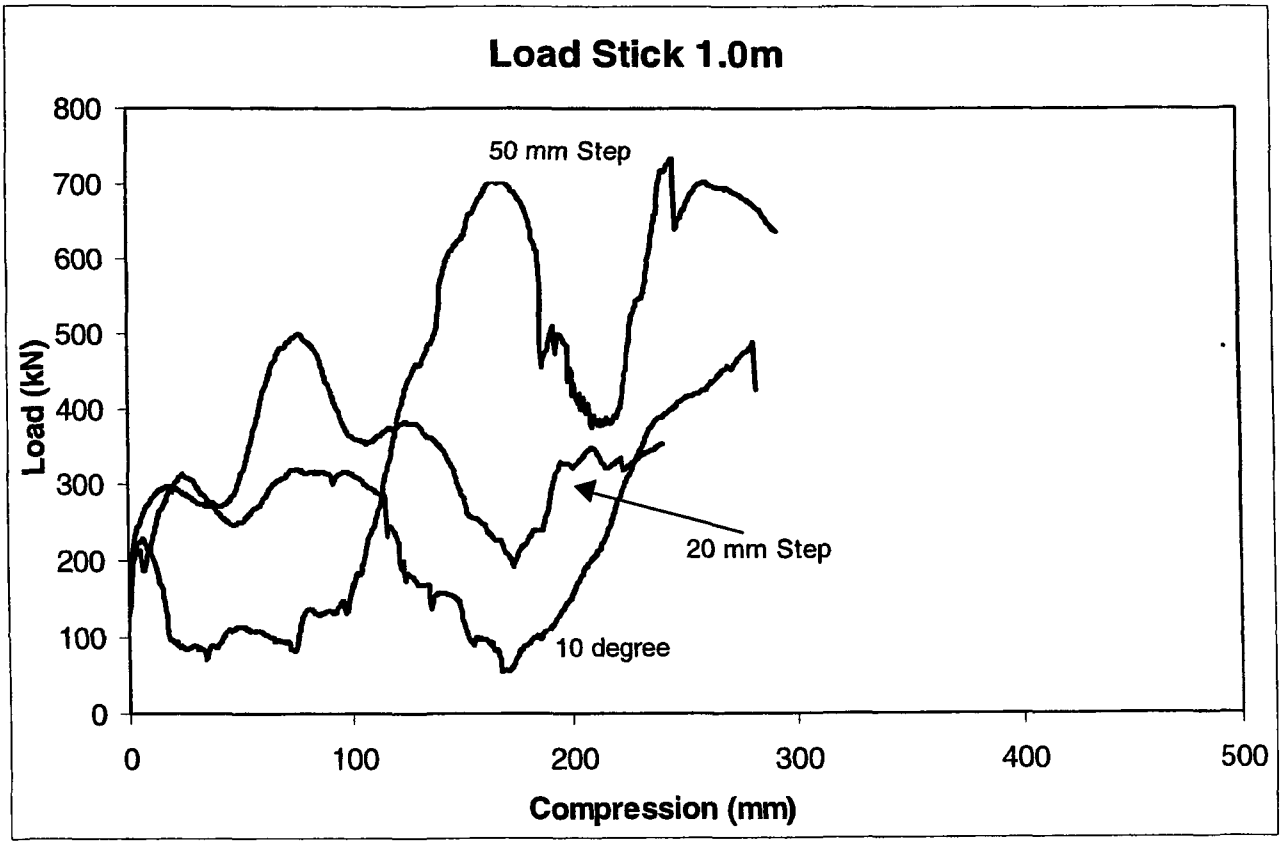
Load Stick 1.0m
800
700
600
500
400
300
200
100
0
Load (kN)
50 mm Step
20 mm Step
10 degree
0
100
200
300
400
500
Compression (mm)

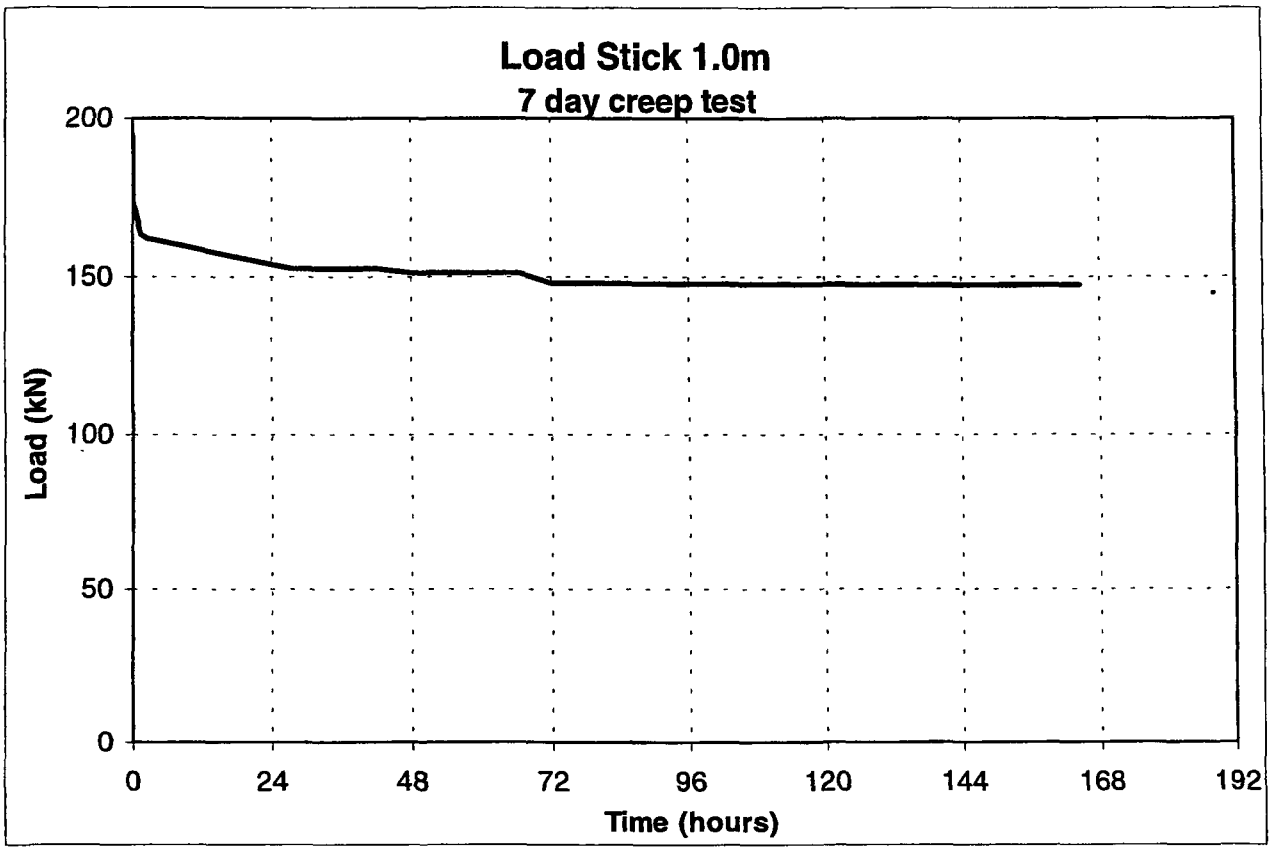
Load Stick 1.0m
7 day creep test
200
150
100
50
0
Load (kN)
0
24
48
72
96
120
144
168
192
Time (hours)

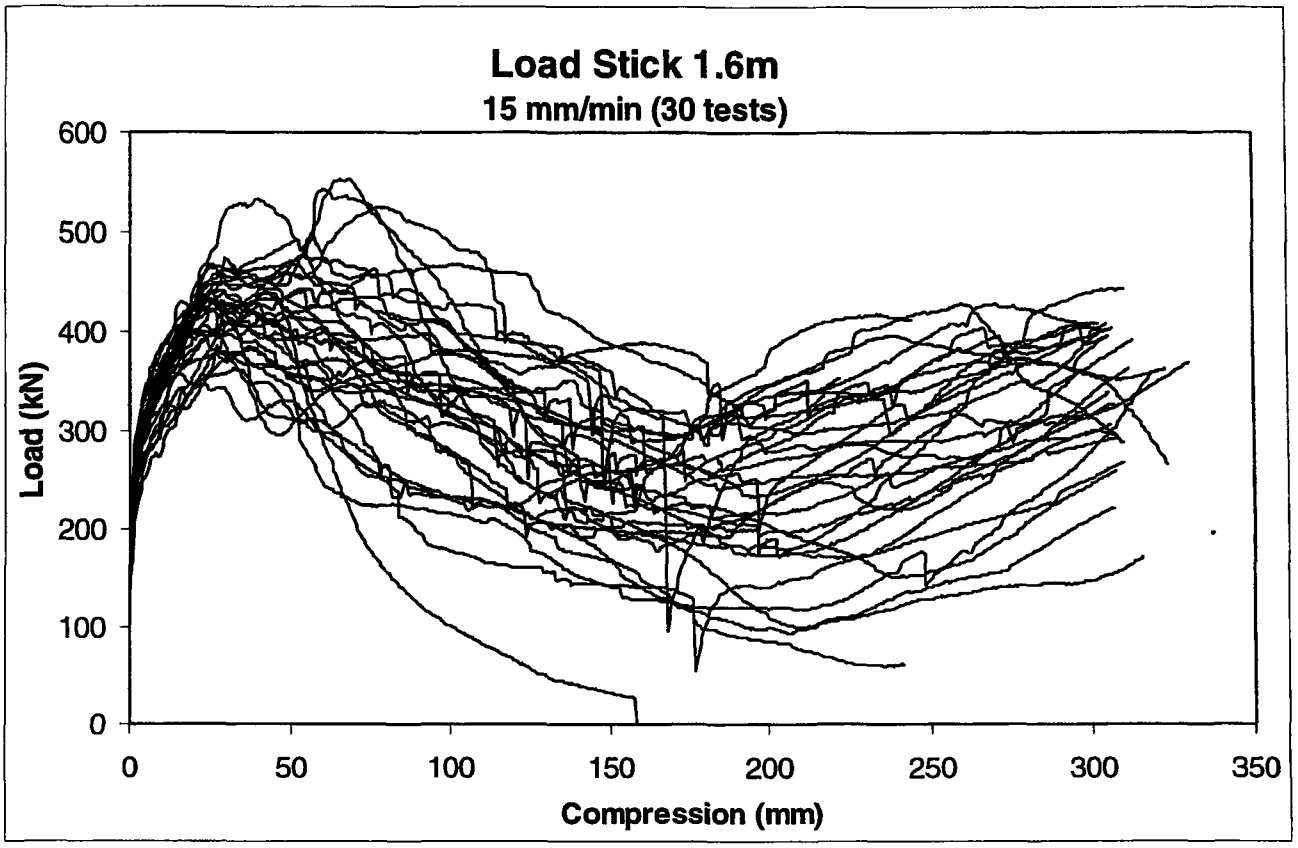
Load Stick 1.6m
15 mm/min (30 tests)
Load (kN)
600
500
400
300
200
100
0
0
50
100
150
200
250
300
350
Compression (mm)

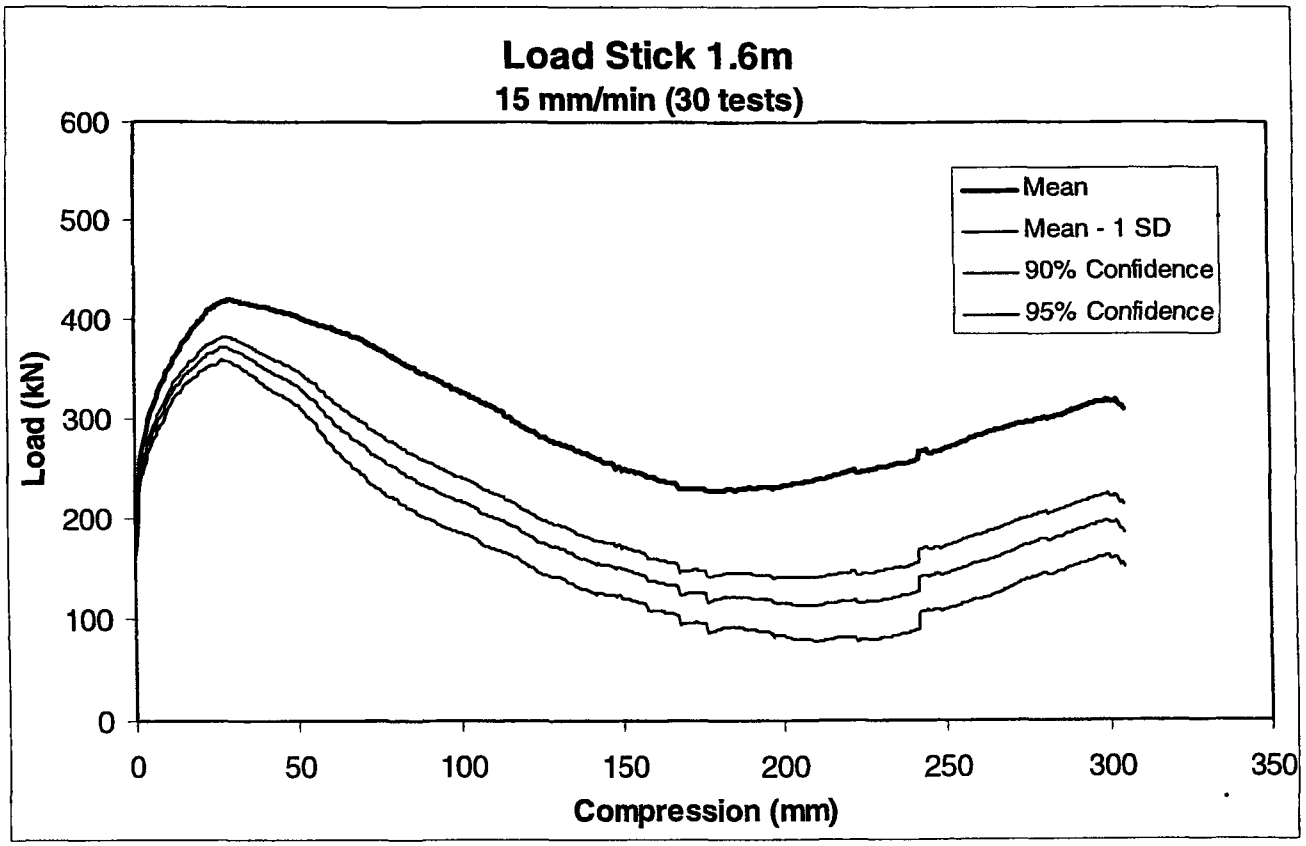
Load Stick 1.6m
15 mm/min (30 tests)
Load (kN)
600
500
400
300
200
100
0
0
50
100
150
200
250
300
350
Compression (mm)
Mean
Mean - 1 SD
90% Confidence
95% Confidence

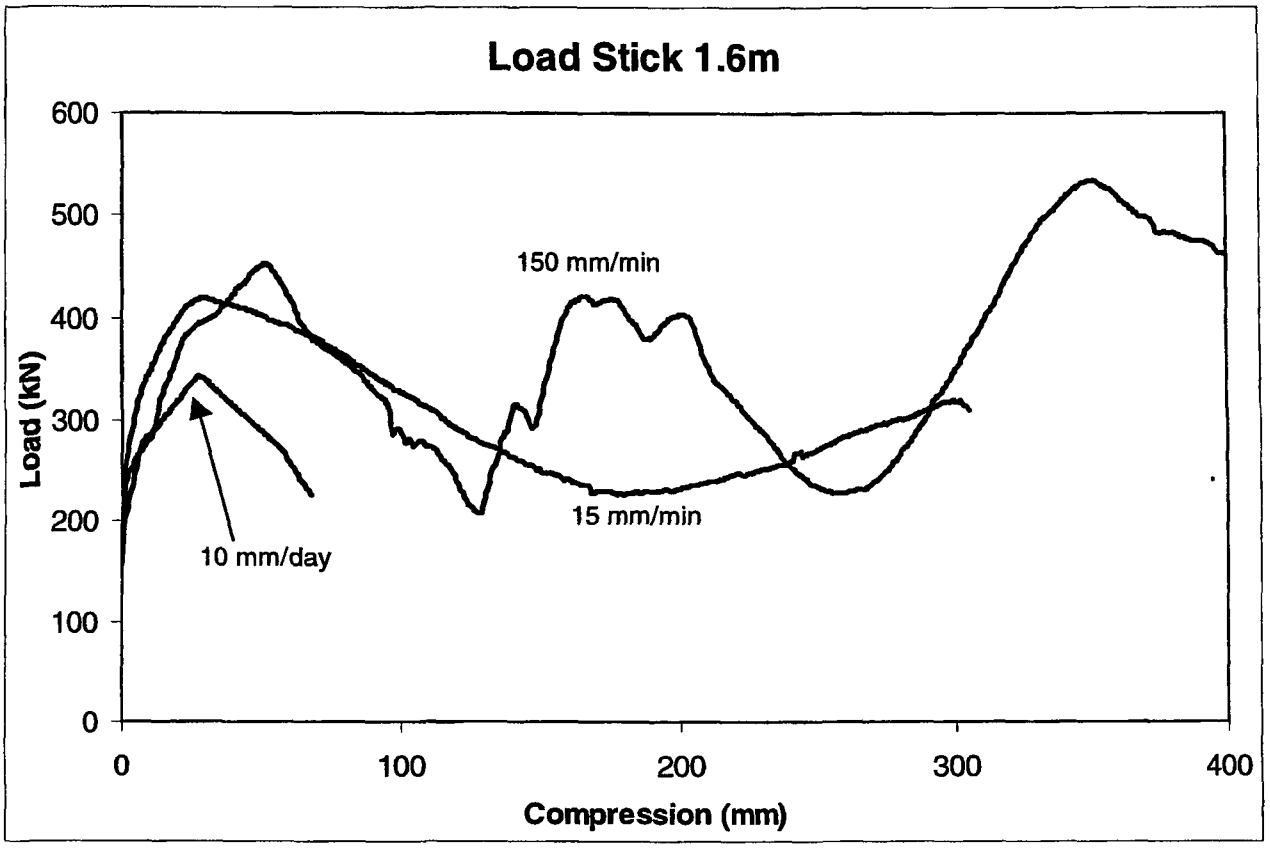
Load Stick 1.6m
600
500
400
300
200
100
0
Load (kN)
150 mm/min
15 mm/min
10 mm/day
0
100
200
300
400
Compression (mm)

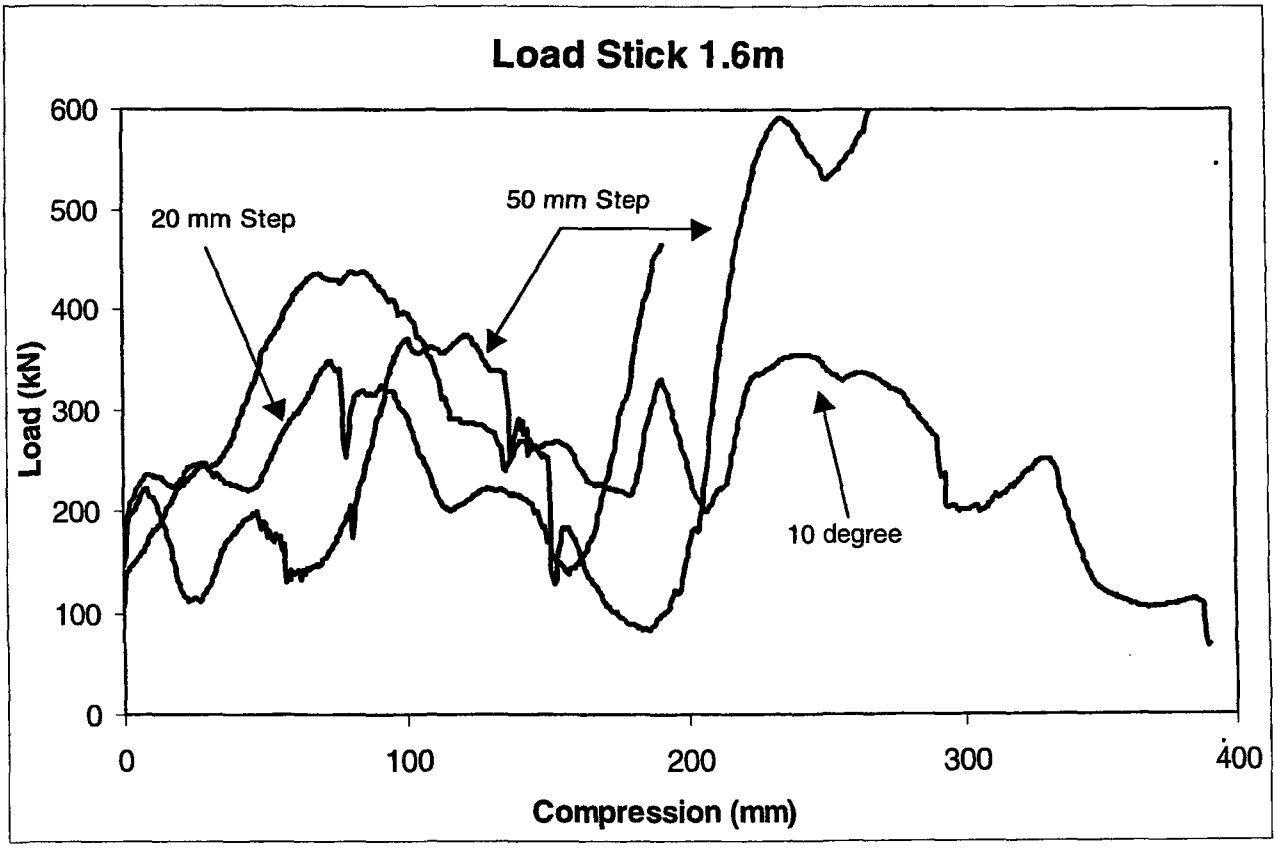
Load Stick 1.6m
600
500
400
300
200
100
0
Load (kN)
20 mm Step
50 mm Step
10 degree
0
100
200
300
400
Compression (mm)

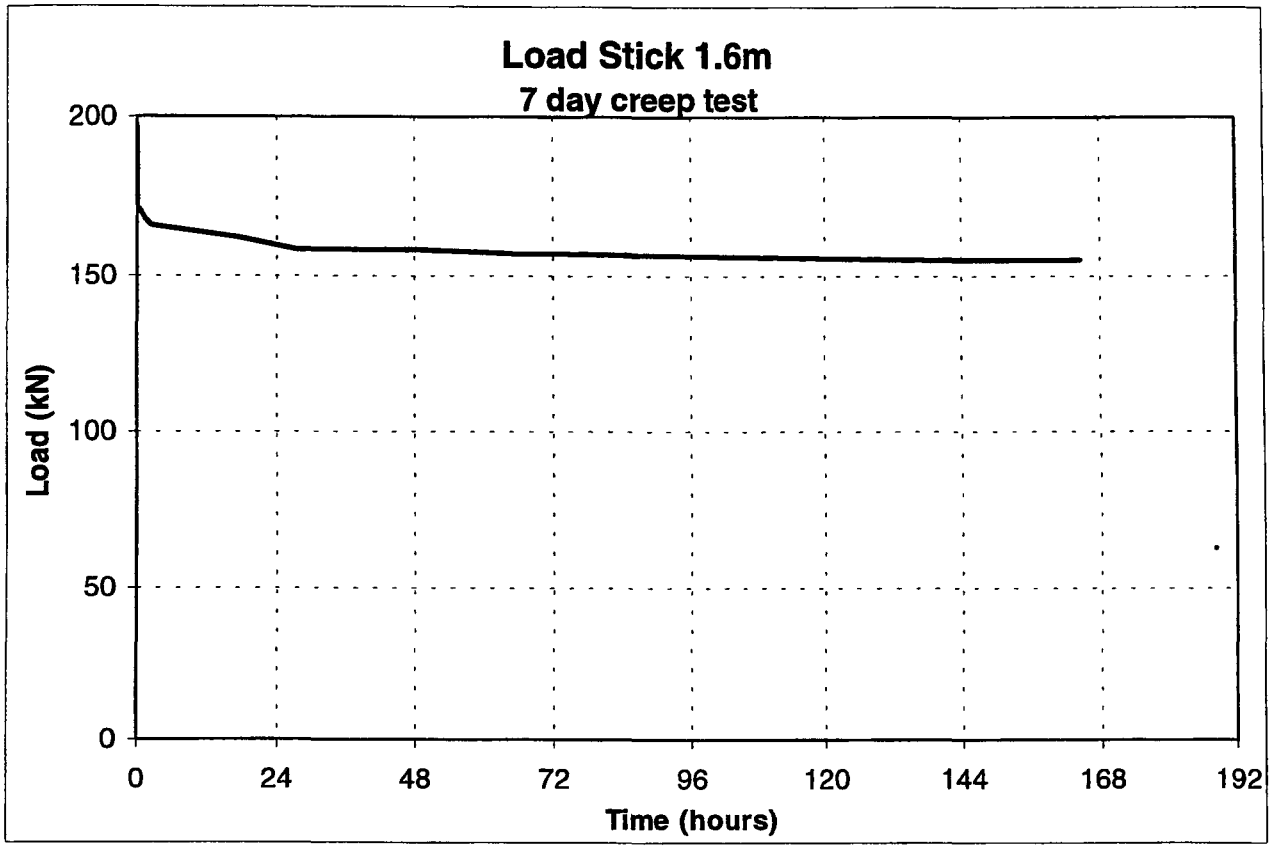
Load Stick 1.6m
7 day creep test
200
150
100
50
0
Load (kN)
0
24
48
72
96
120
144
168
192
Time (hours)

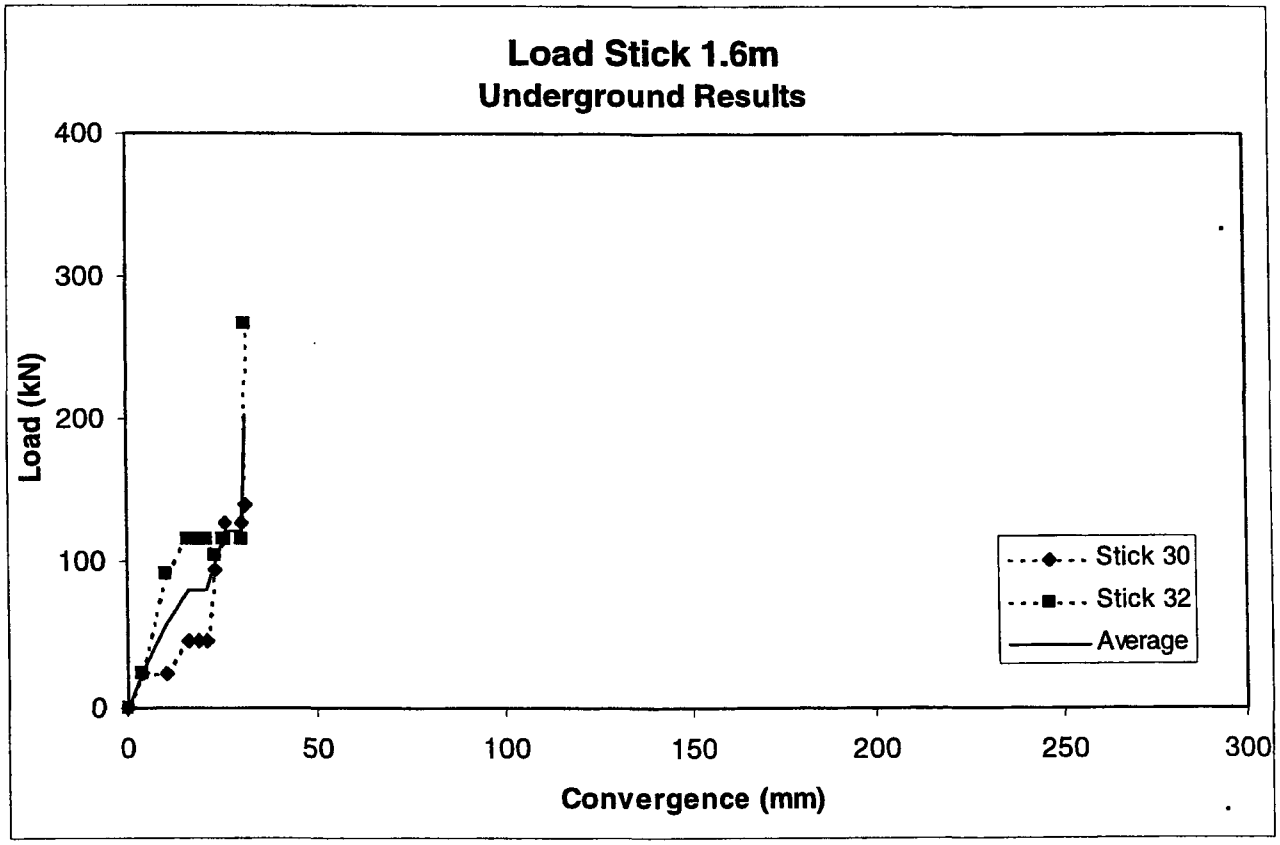
Load Stick 1.6m
Underground Results
400
300
200
100
0
Load (kN)
0
50
100
150
200
250
300
Convergence (mm)
Stick 30
Stick 32
Average

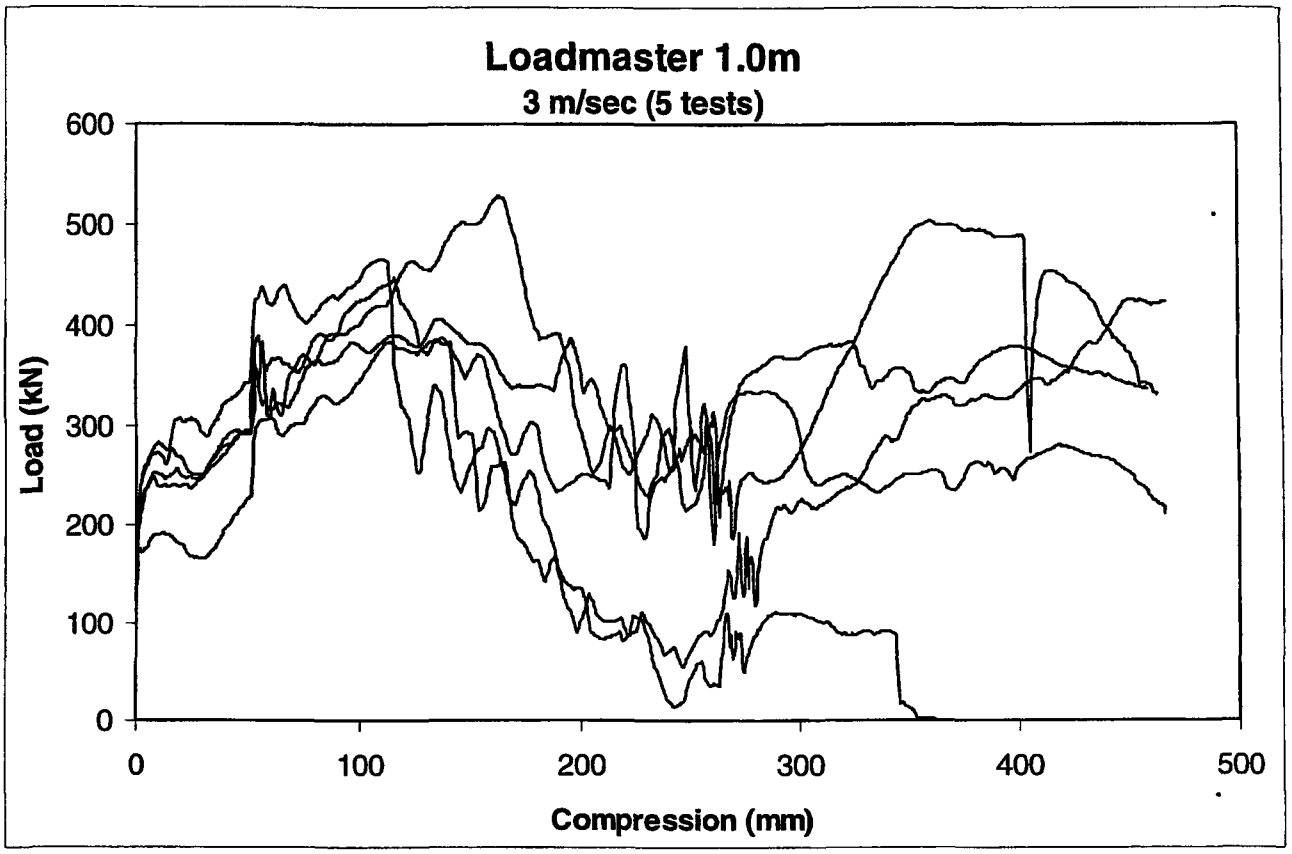
Loadmaster 1.0m
3 m/sec (5 tests)
Load (kN)
600
500
400
300
200
100
0
0
100
200
300
400
500
Compression (mm)

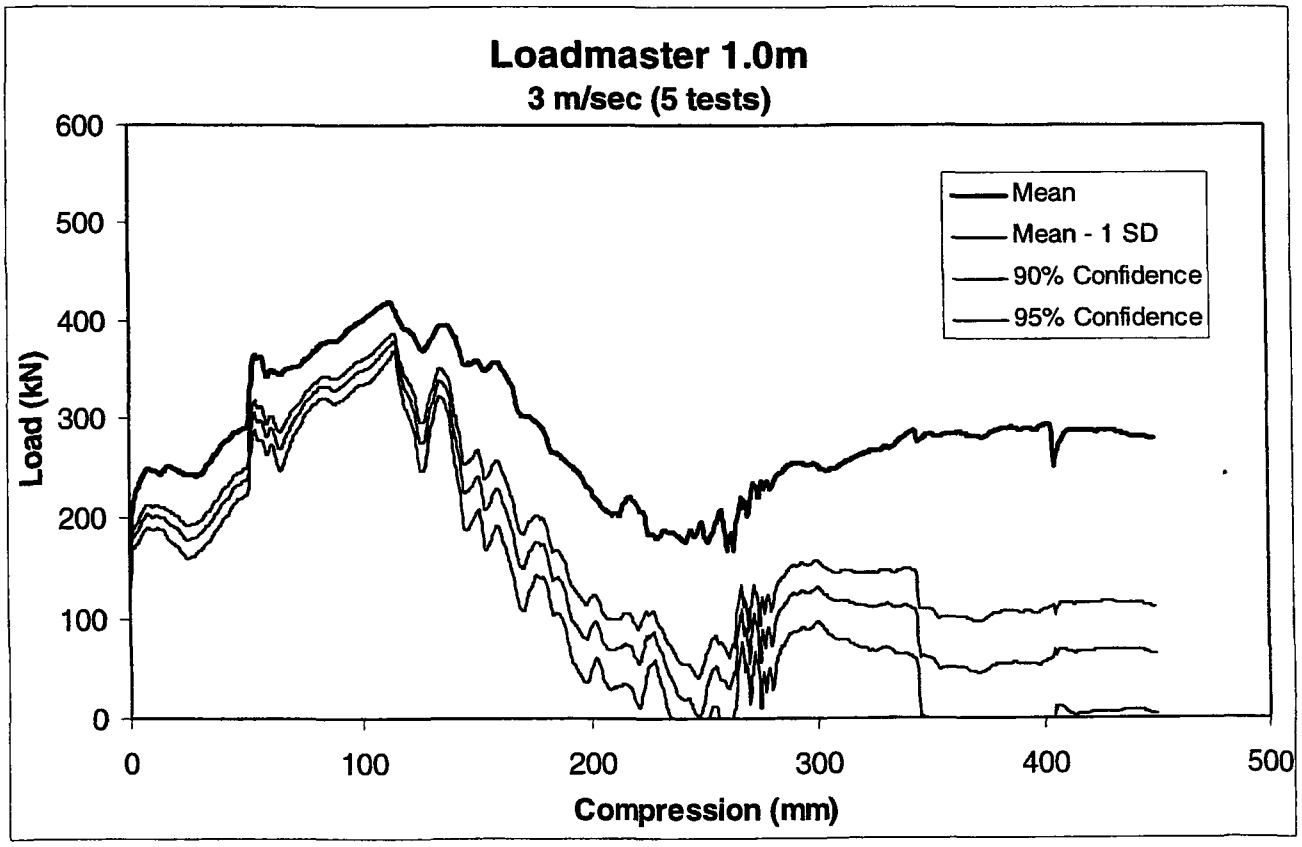
Loadmaster 1.0m
3 m/sec (5 tests)
Load (kN)
600
500
400
300
200
100
0
0
100
200
300
400
500
Compression (mm)
Mean
Mean - 1 SD
90% Confidence
95% Confidence

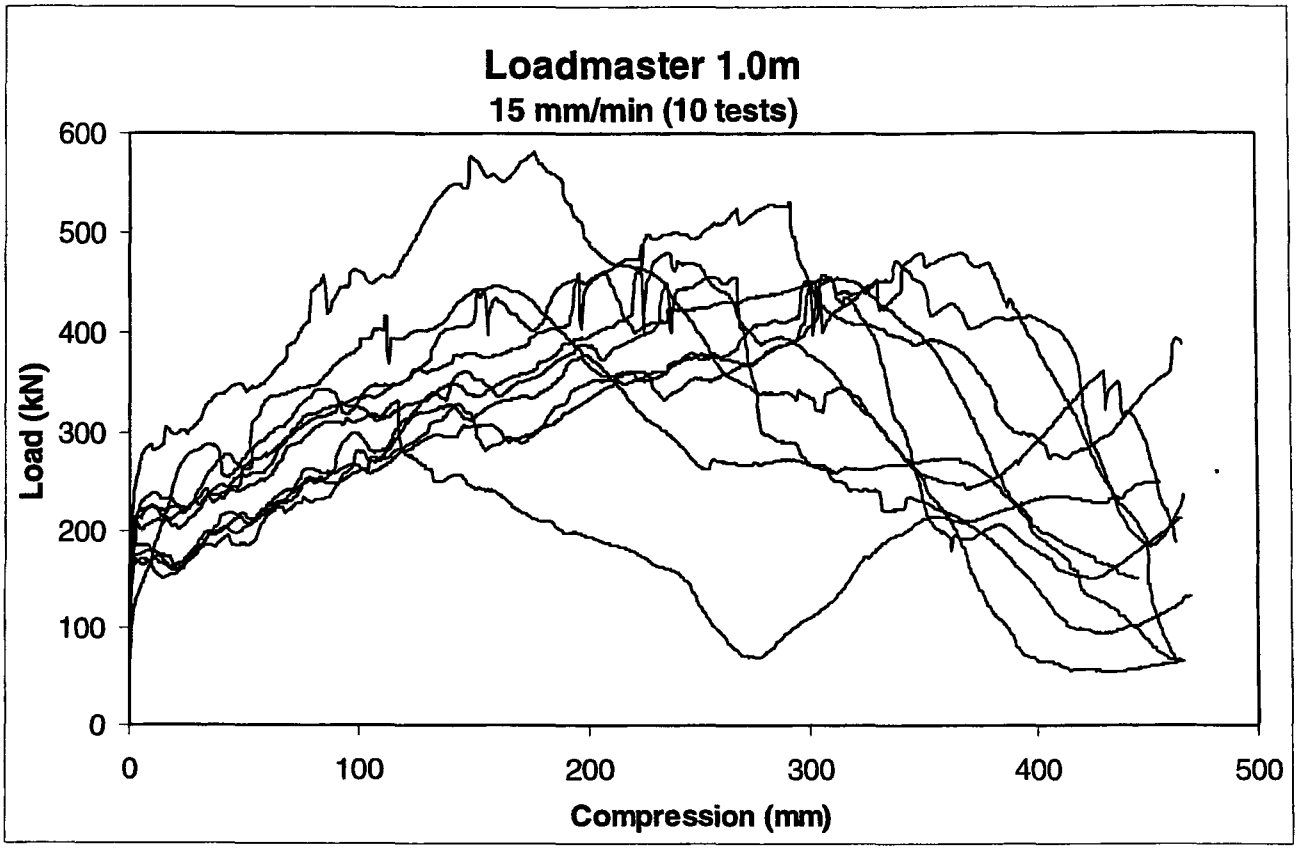
Loadmaster 1.0m
15 mm/min (10 tests)
Load (kN)
600
500
400
300
200
100
0
0
100
200
300
400
500
Compression (mm)

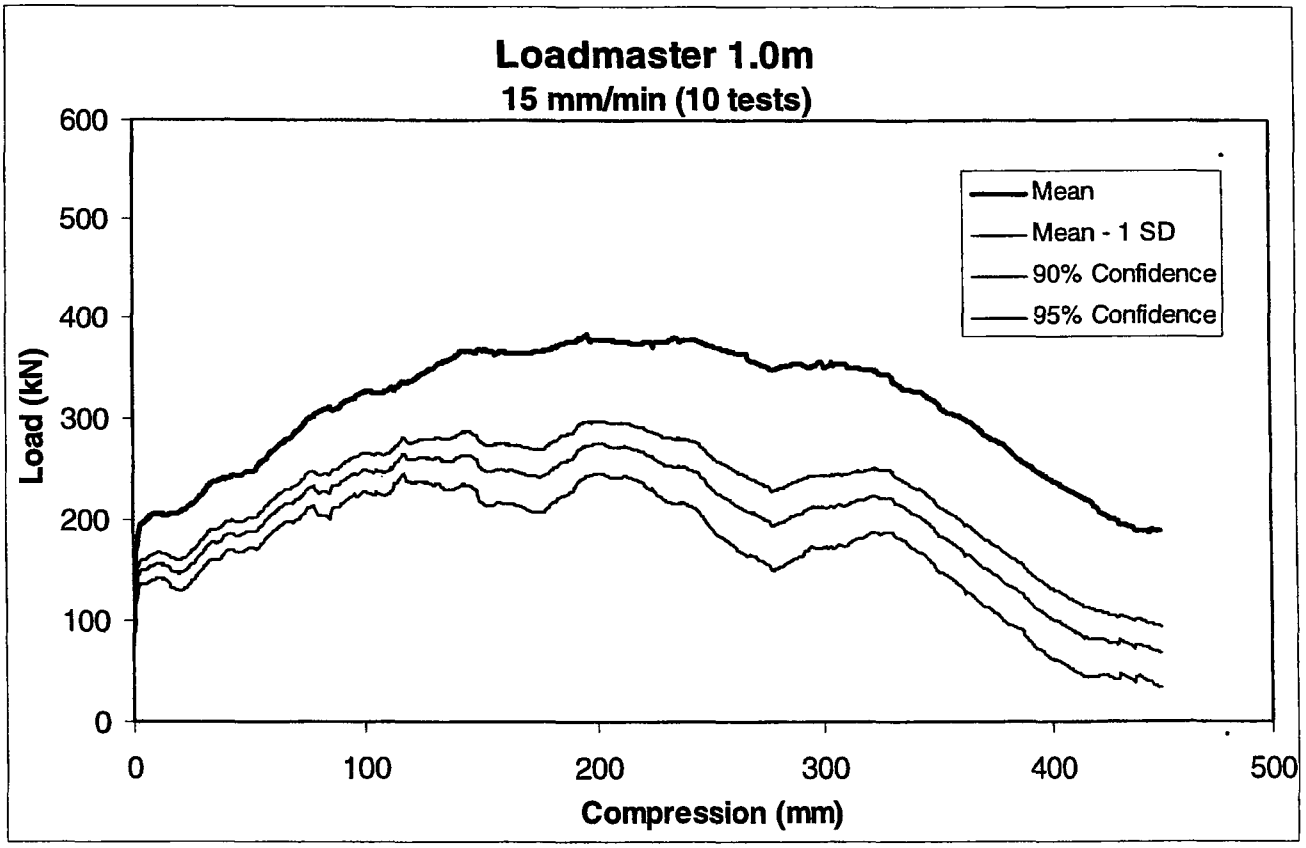
Loadmaster 1.0m
15 mm/min (10 tests)
Load (kN)
600
500
400
300
200
100
0
0
100
200
300
400
500
Compression (mm)
Mean
Mean - 1 SD
90% Confidence
95% Confidence

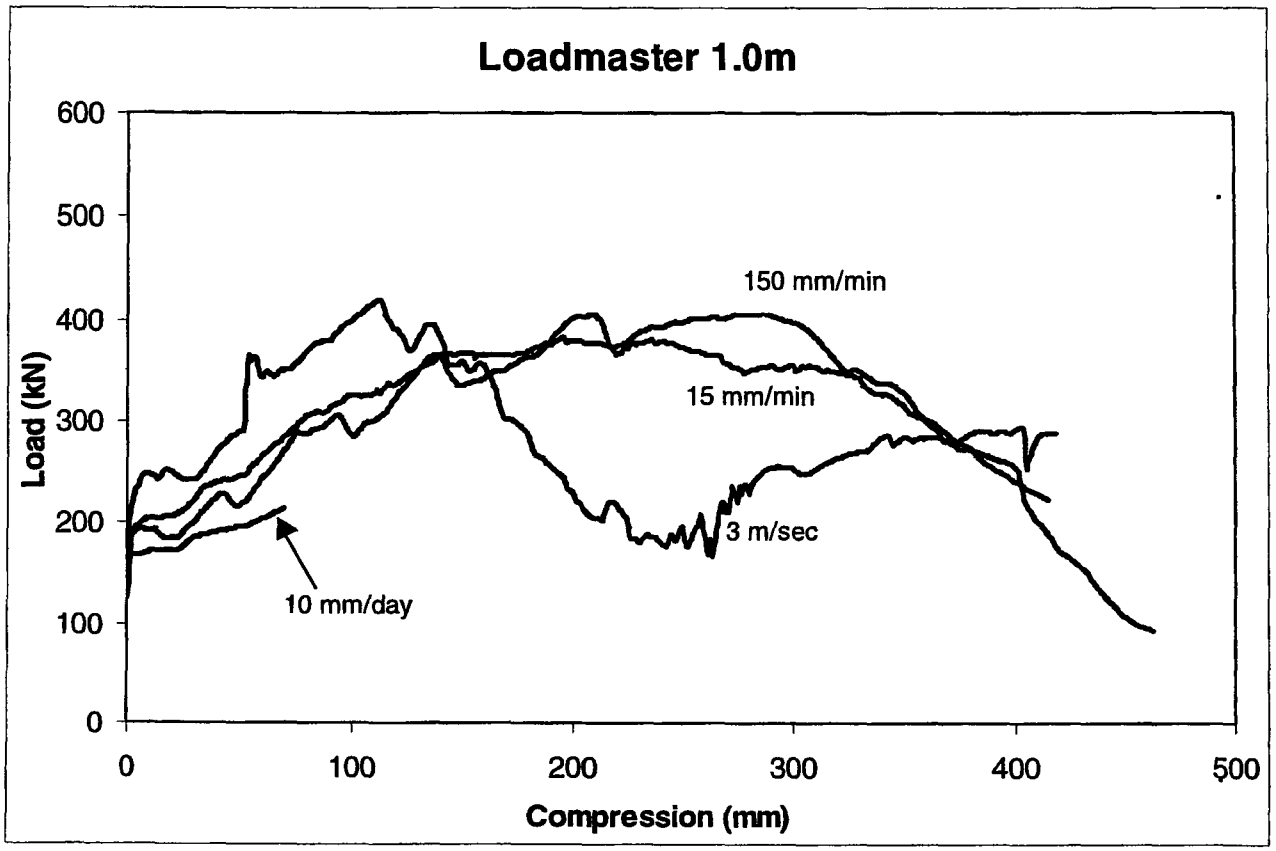
Loadmaster 1.0m
600
500
400
300
200
100
0
Load (kN)
150 mm/min
15 mm/min
3 m/sec
10 mm/day
0
100
200
300
400
500
Compression (mm)

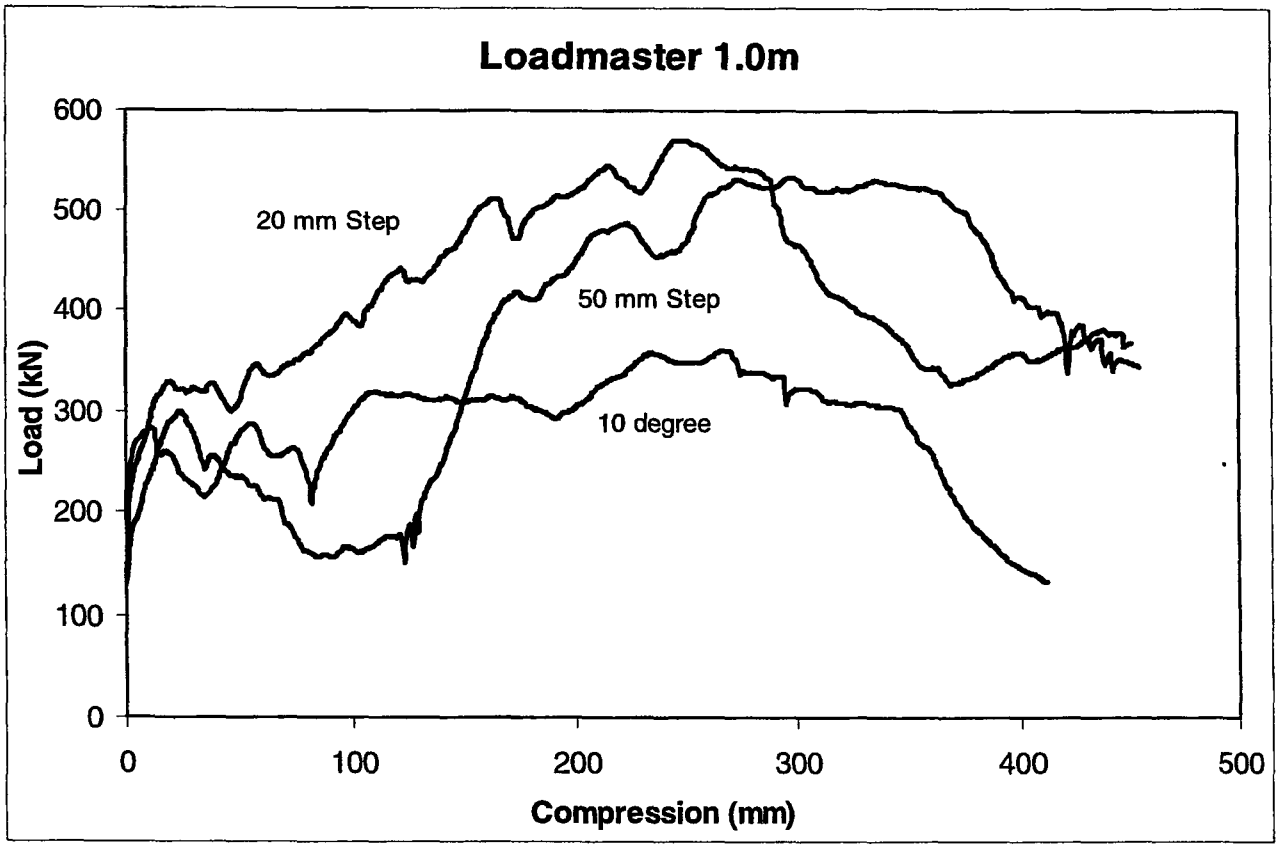
Loadmaster 1.0m
600
500
400
300
200
100
0
Load (kN)
20 mm Step
50 mm Step
10 degree
0
100
200
300
400
500
Compression (mm)

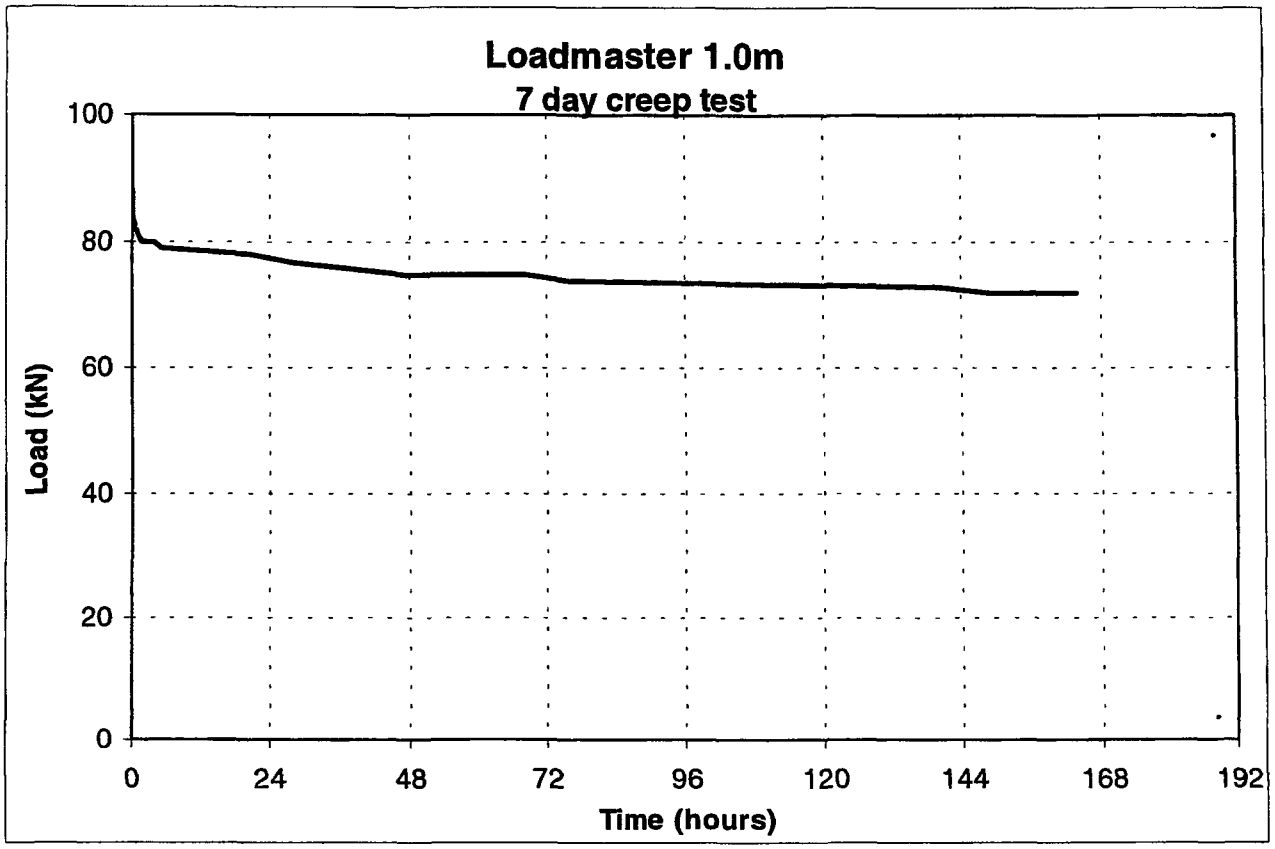
Loadmaster 1.0m
7 day creep test
Load (kN)
100
80
60
40
20
0
0
24
48
72
96
120
144
168
192
Time (hours)

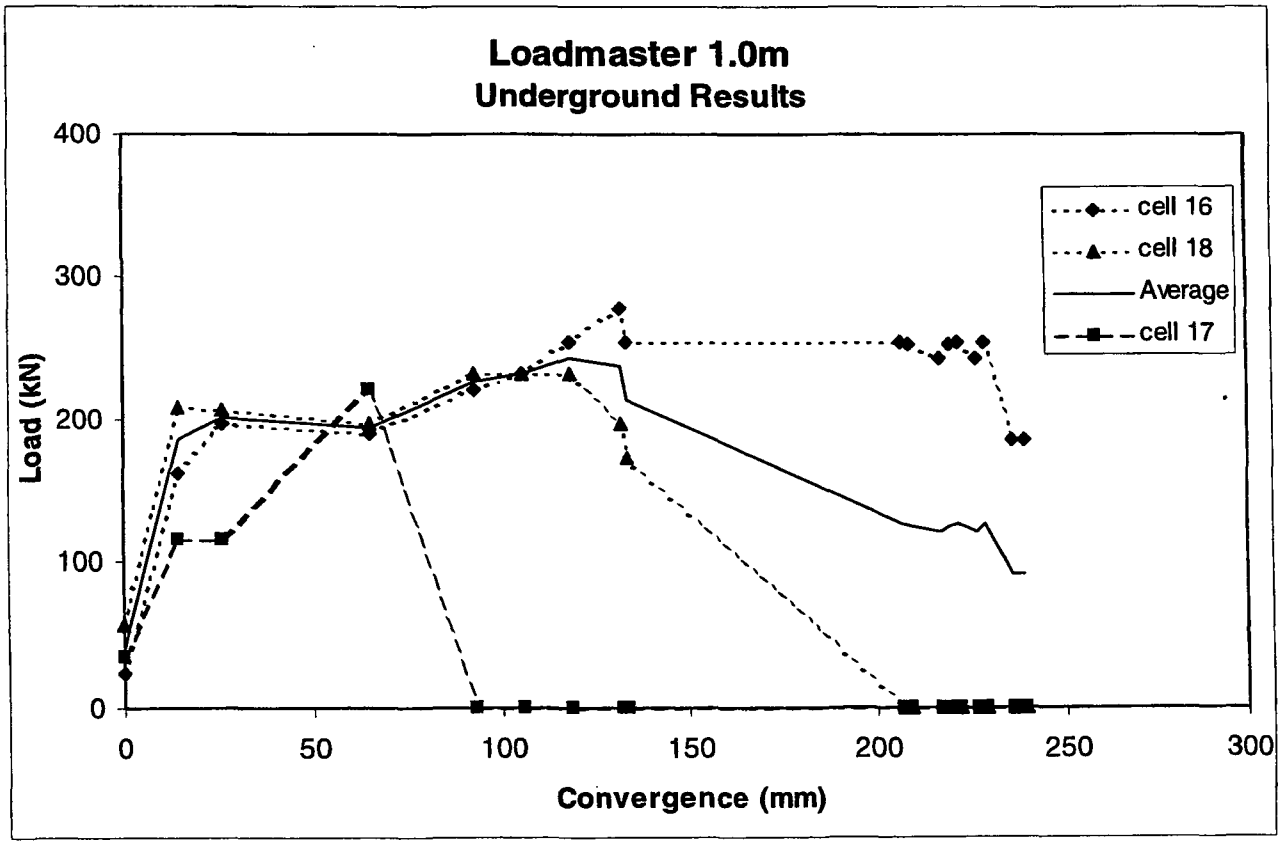
Loadmaster 1.0m
Underground Results
Load (kN)
400
300
200
100
0
0
50
100
150
200
250
300
Convergence (mm)
cell 16
cell 18
Average
cell 17

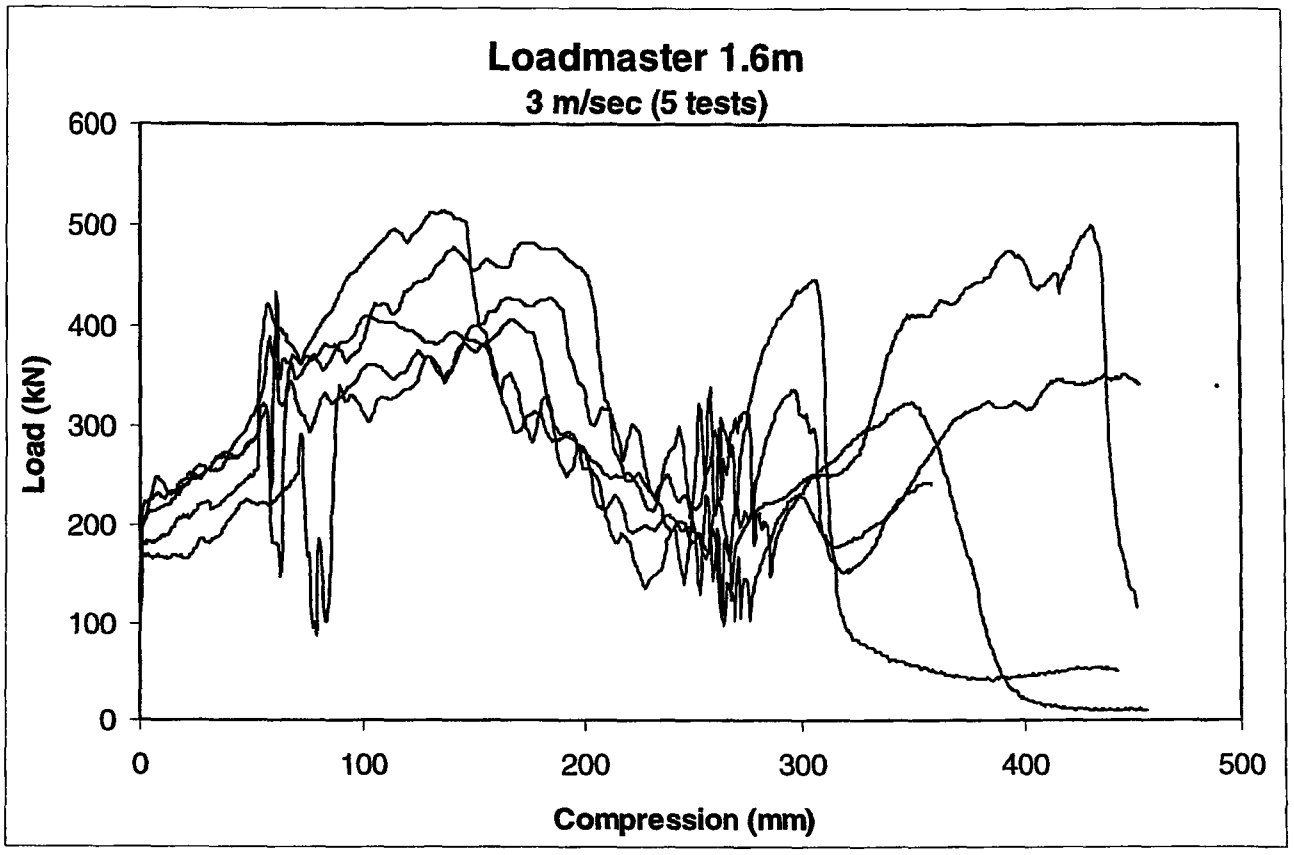
Loadmaster 1.6m
3 m/sec (5 tests)
Load (kN)
600
500
400
300
200
100
0
0
100
200
300
400
500
Compression (mm)

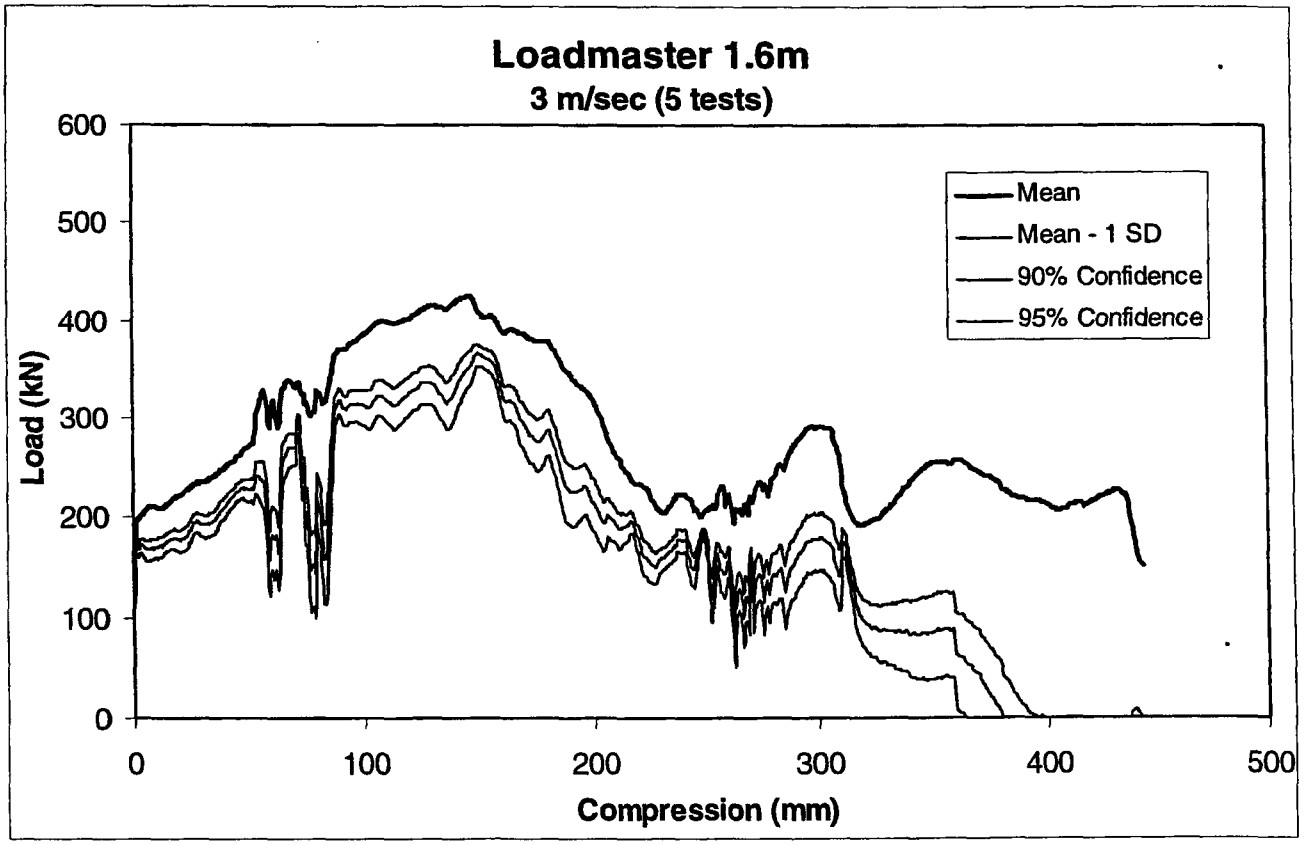
Loadmaster 1.6m
3 m/sec (5 tests)
Load (kN)
600
500
400
300
200
100
0
0
100
200
300
400
500
Compression (mm)
Mean
Mean - 1 SD
90% Confidence
95% Confidence

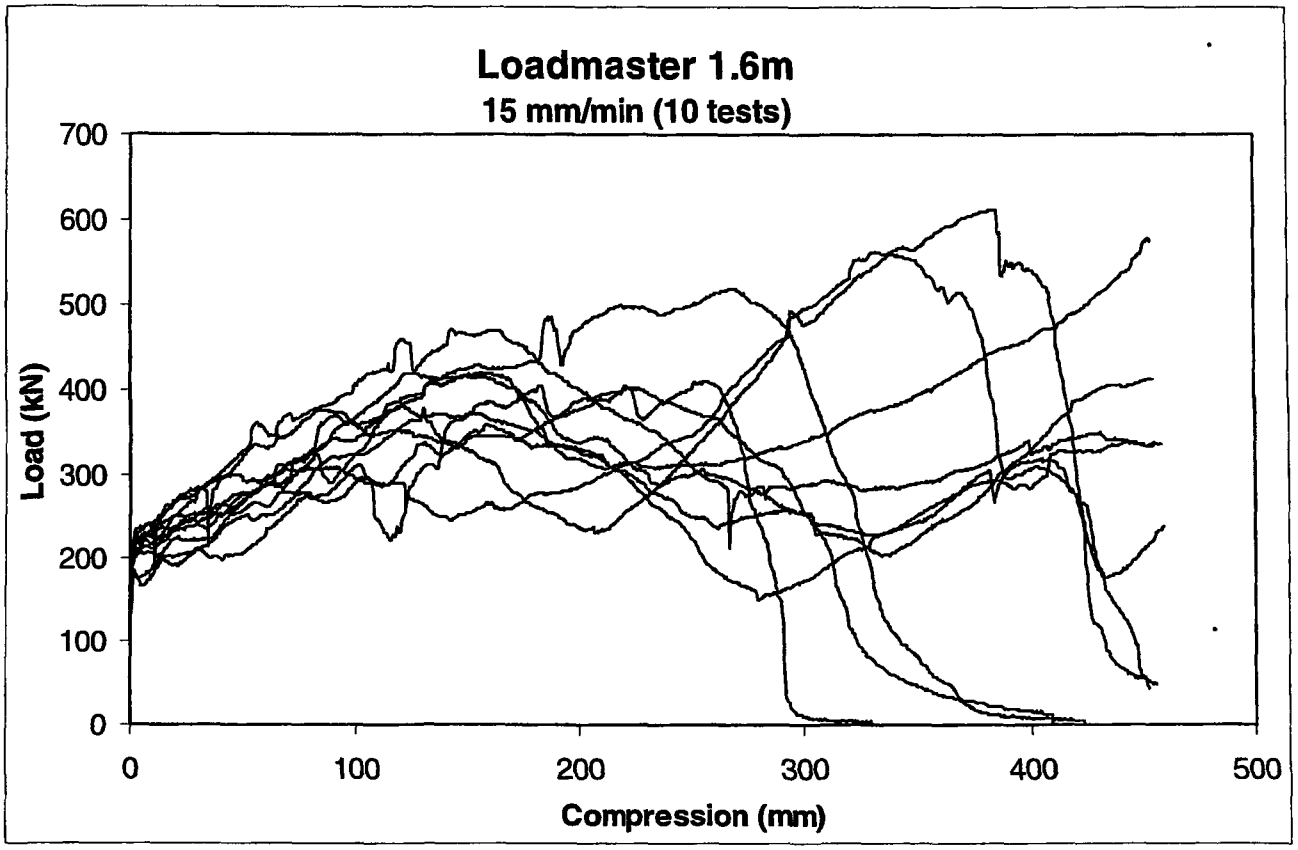
Loadmaster 1.6m
15 mm/min (10 tests)
Load (kN)
700
600
500
400
300
200
100
0
0
100
200
300
400
500
Compression (mm)

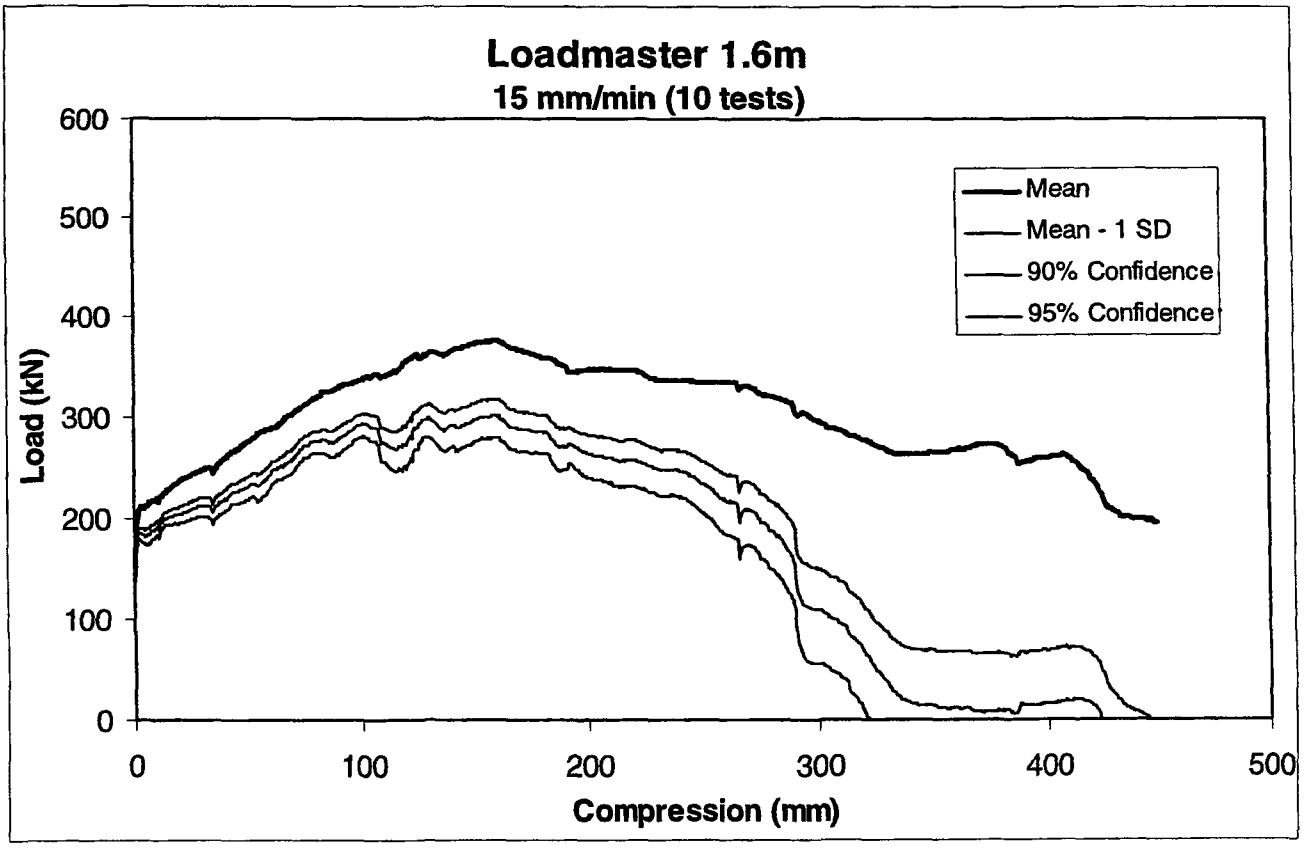
Loadmaster 1.6m
15 mm/min (10 tests)
Load (kN)
600
500
400
300
200
100
0
0
100
200
300
400
500
Compression (mm)
Mean
Mean - 1 SD
90% Confidence
95% Confidence

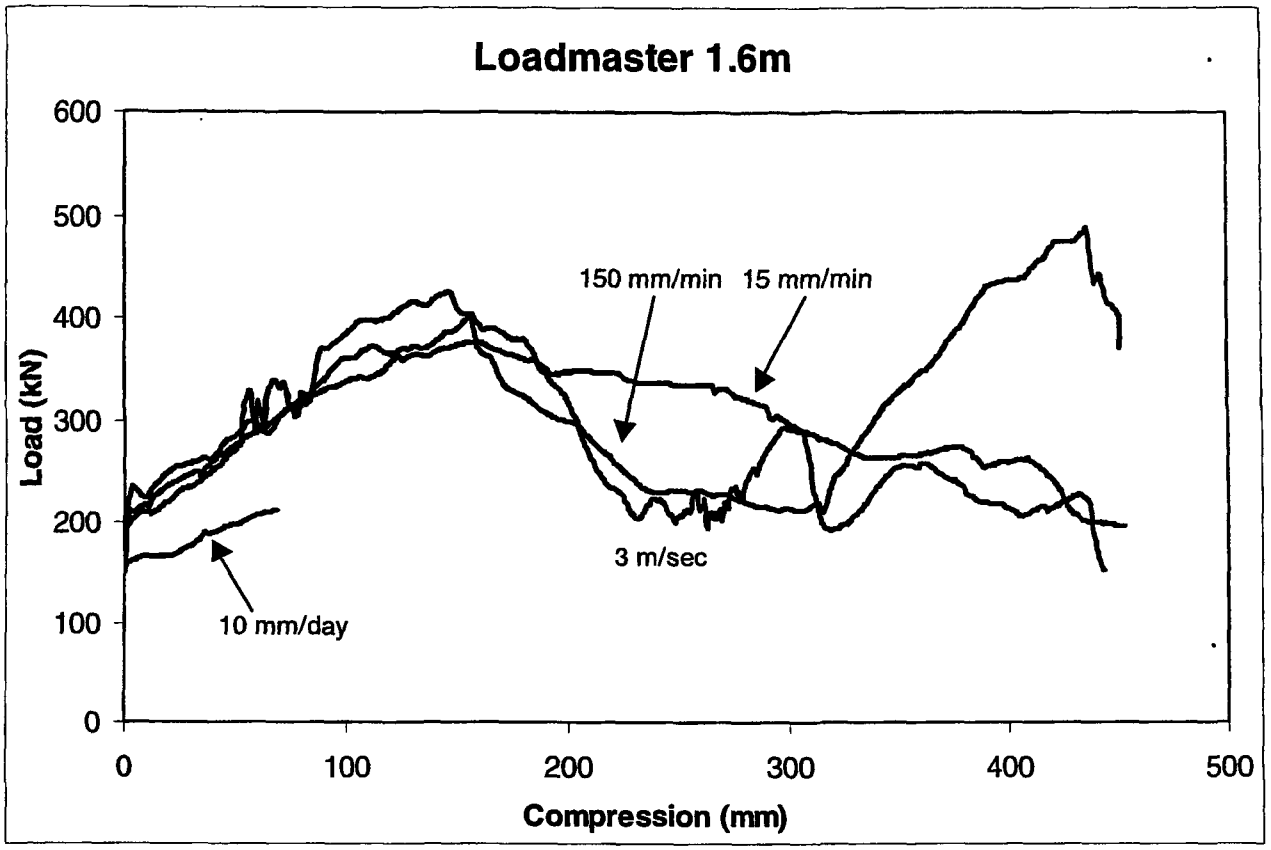
Loadmaster 1.6m
600
500
400
300
200
100
0
Load (kN)
150 mm/min
15 mm/min
3 m/sec
10 mm/day
0
100
200
300
400
500
Compression (mm)

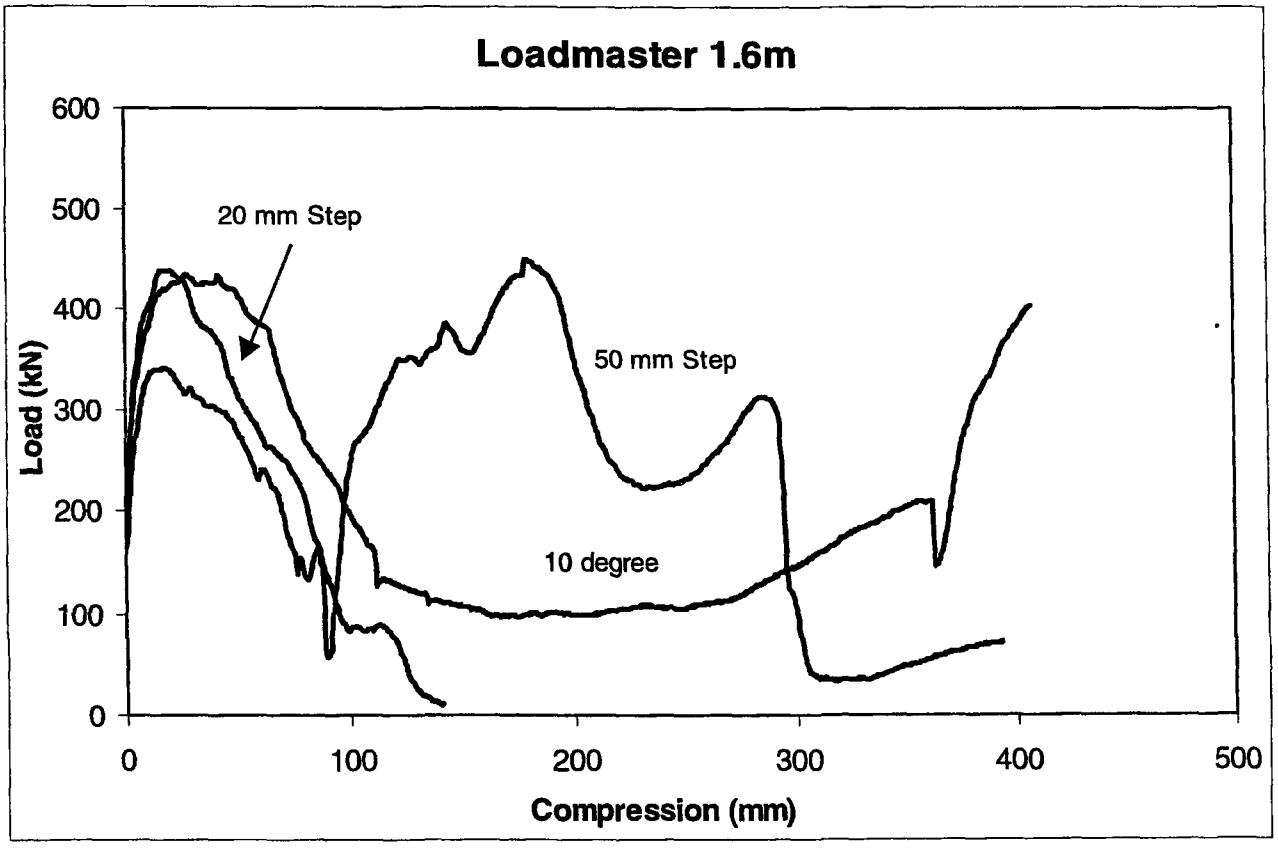
Loadmaster 1.6m
600
500
400
300
200
100
0
Load (kN)
20 mm Step
50 mm Step
10 degree
0
100
200
300
400
500
Compression (mm)

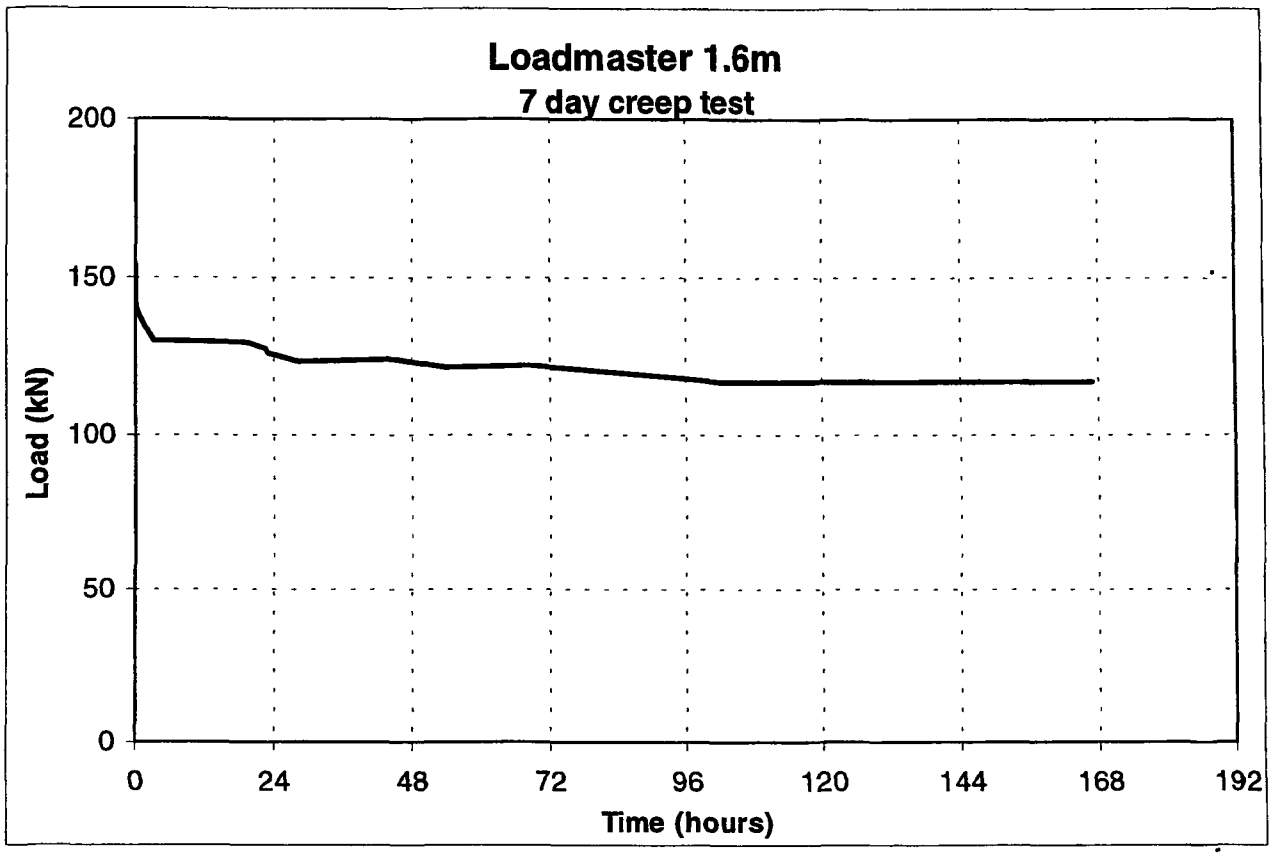
Loadmaster 1.6m
7 day creep test
Load (kN)
200
150
100
50
0
0
24
48
72
96
120
144
168
192
Time (hours)

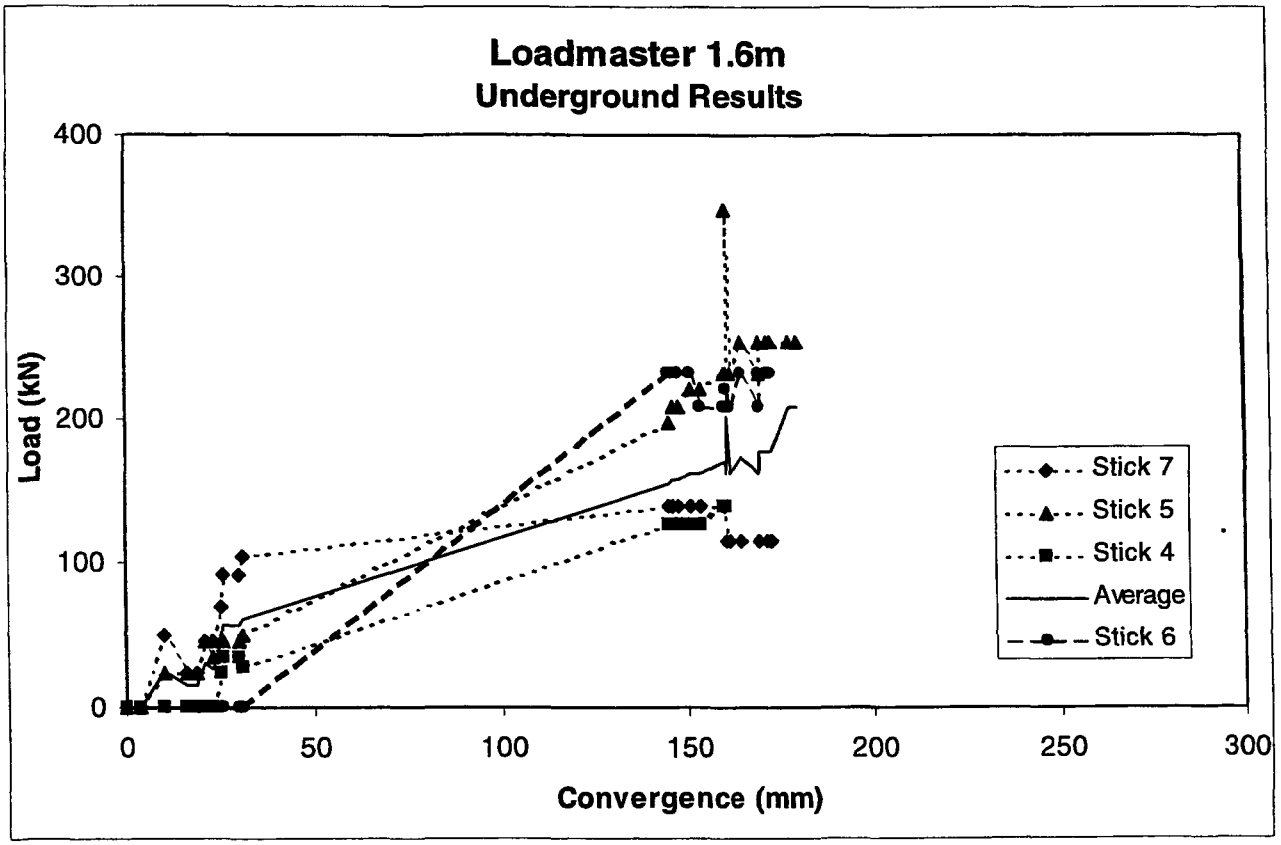
Loadmaster 1.6m
Underground Results
Load (kN)
400
300
200
100
0
0
50
100
150
200
250
300
Convergence (mm)
Stick 7
Stick 5
Stick 4
Average
Stick 6

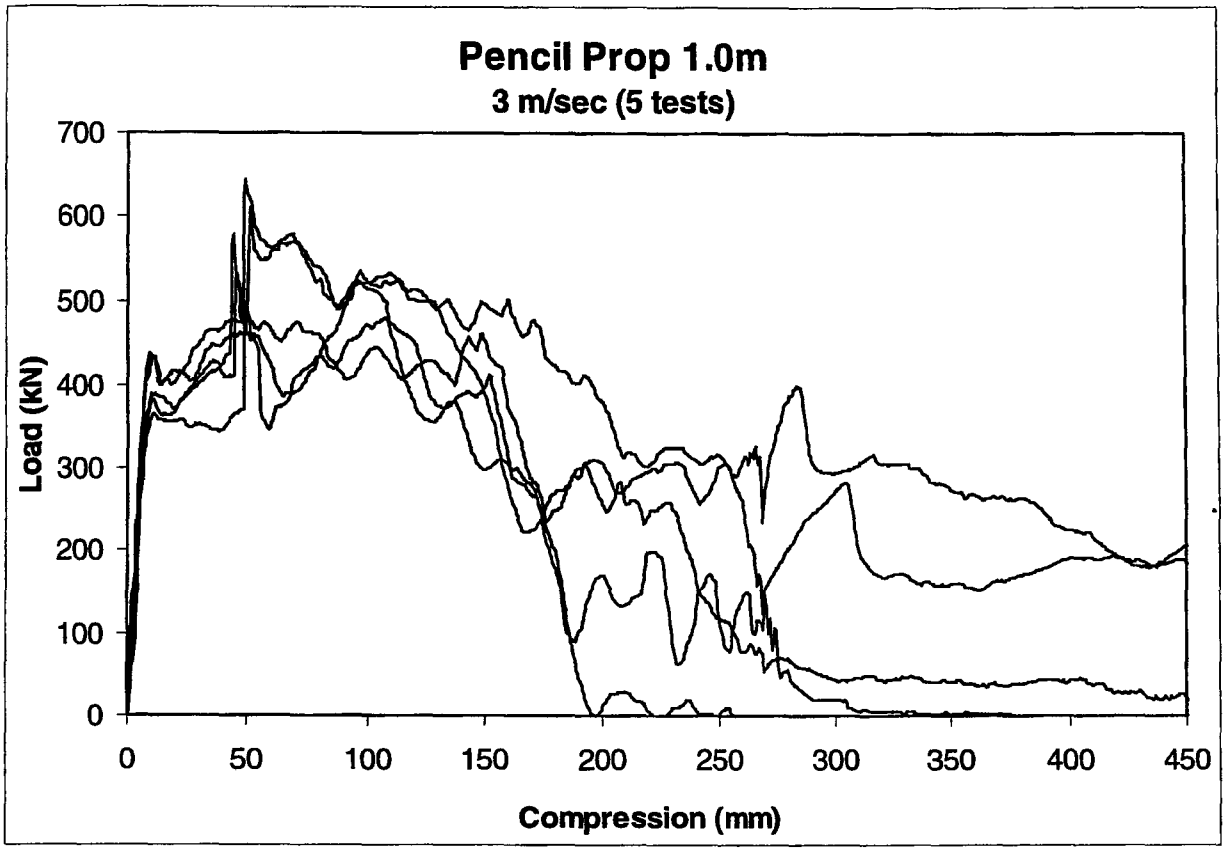
Pencil Prop 1.0m
3 m/sec (5 tests)
Load (kN)
700
600
500
400
300
200
100
0
0
50
100
150
200
250
300
350
400
450
Compression (mm)

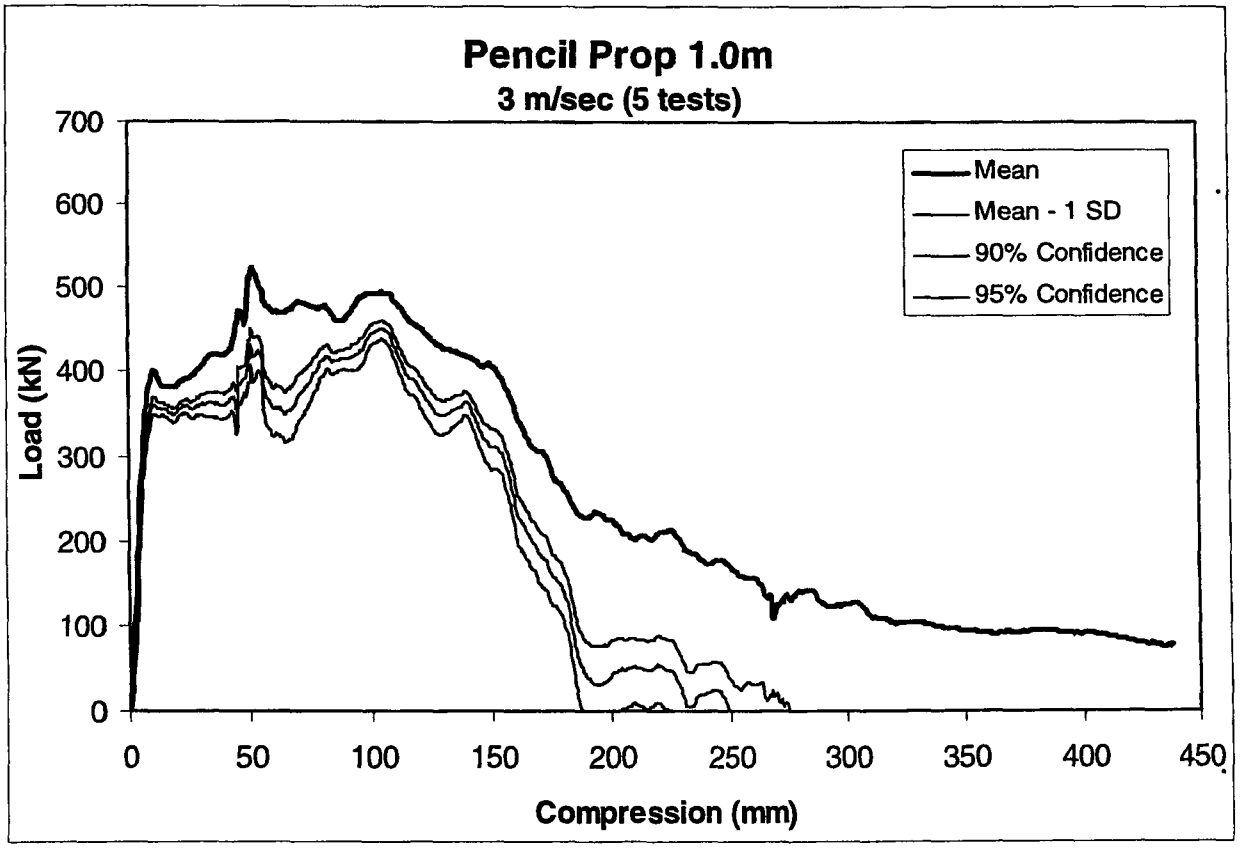
Pencil Prop 1.0m
3 m/sec (5 tests)
Mean
Mean - 1 SD
90% Confidence
95% Confidence
Load (kN)
700
600
500
400
300
200
100
0
0
50
100
150
200
250
300
350
400
450
Compression (mm)

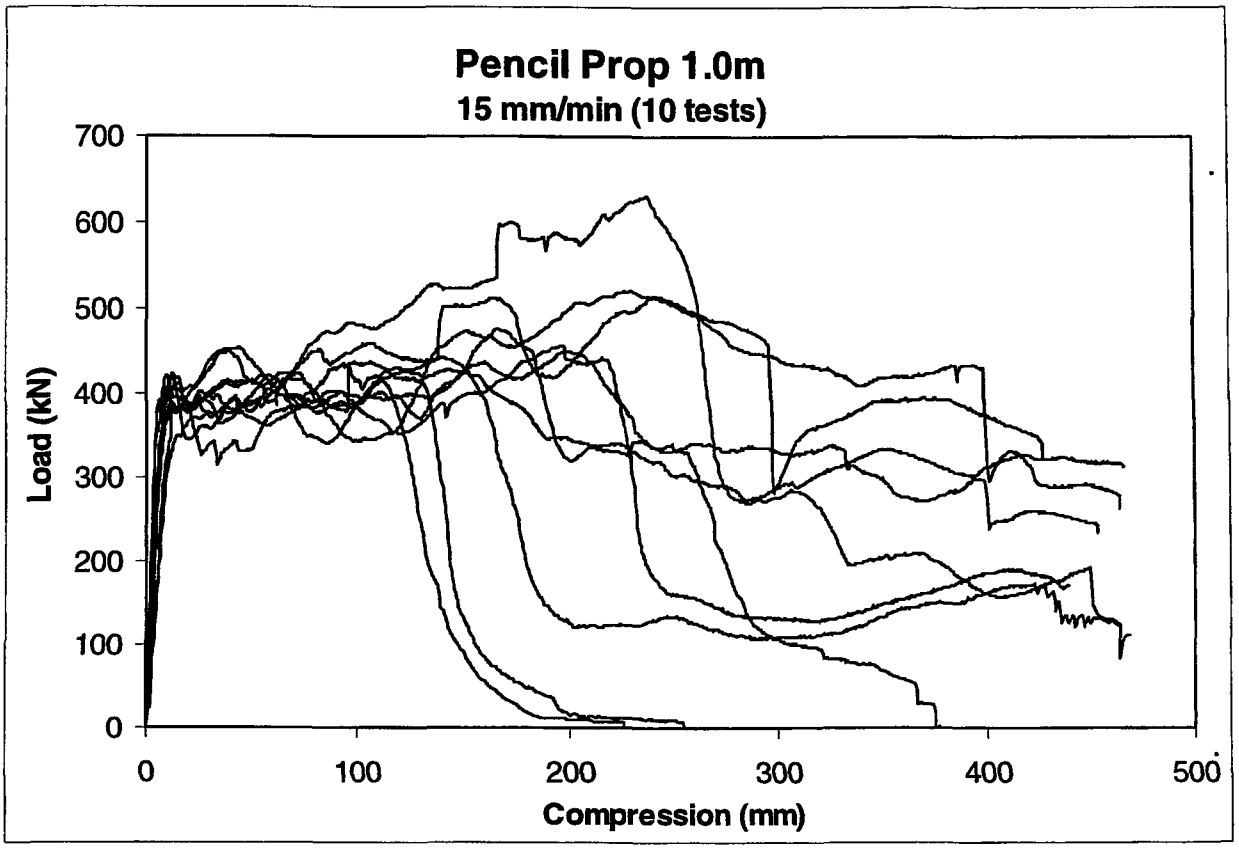
Pencil Prop 1.0m
15 mm/min (10 tests)
Load (kN)
Compression (mm)
0
100
200
300
400
500
600
700

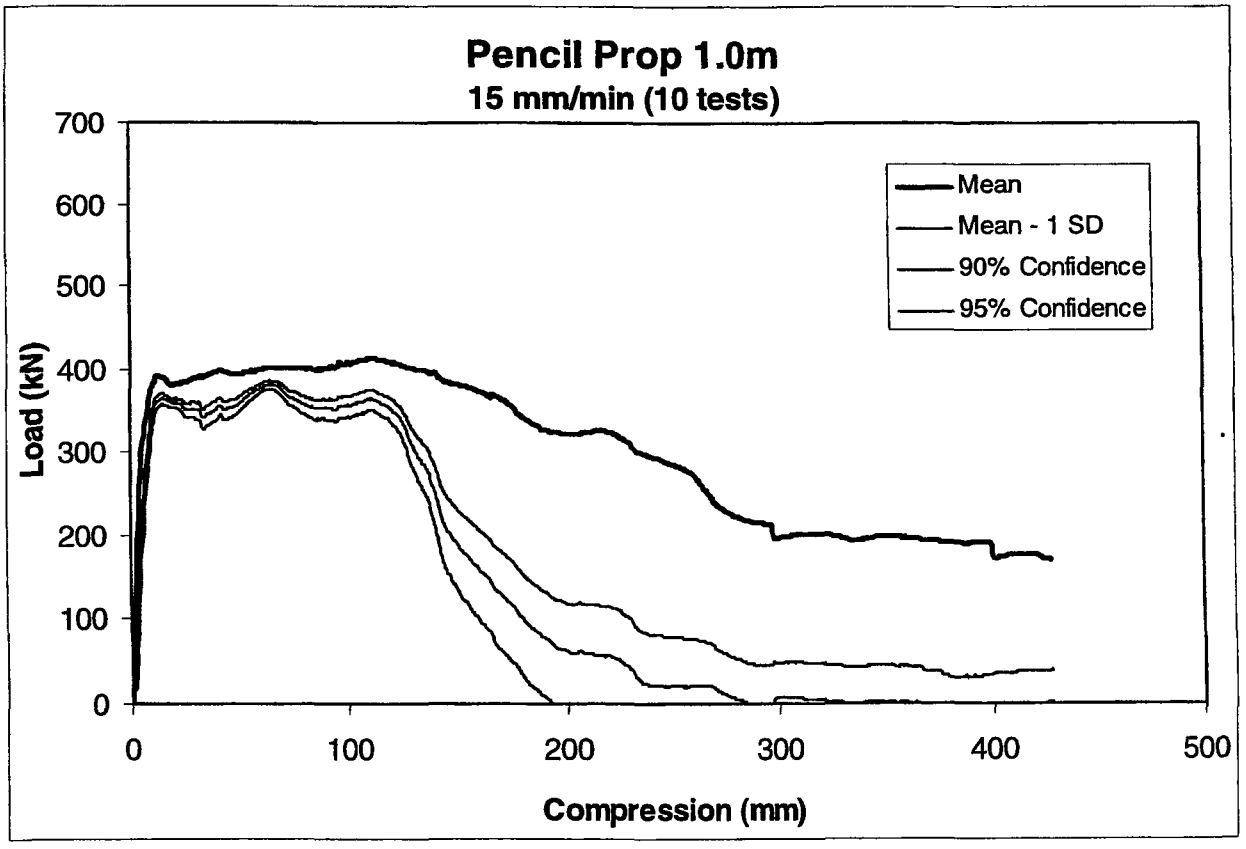
Pencil Prop 1.0m
15 mm/min (10 tests)
Mean
Mean - 1 SD
90% Confidence
95% Confidence
Load (kN)
Compression (mm)
0
100
200
300
400
500
600
700

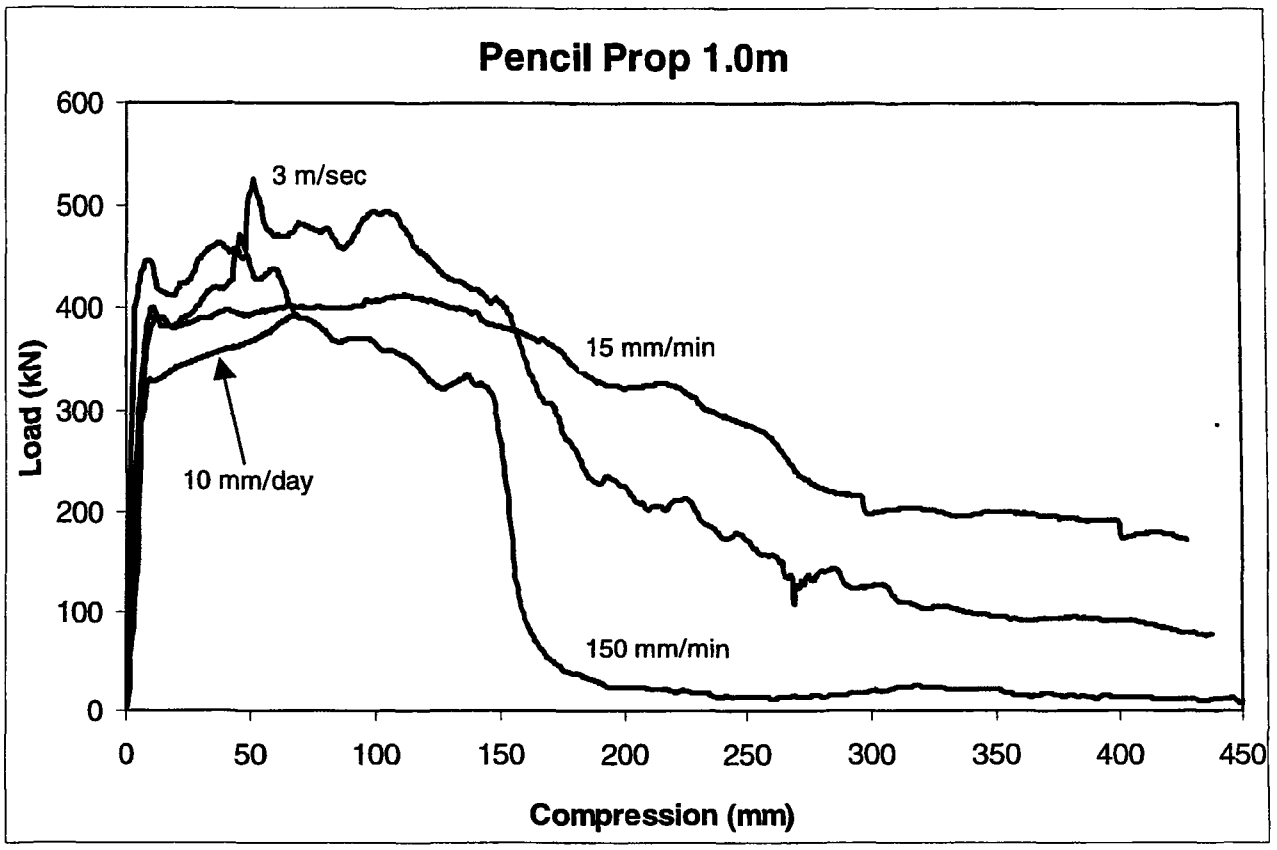
Pencil Prop 1.0m
600
500
400
300
200
100
0
Load (kN)
3 m/sec
15 mm/min
10 mm/day
150 mm/min
0
50
100
150
200
250
300
350
400
450
Compression (mm)

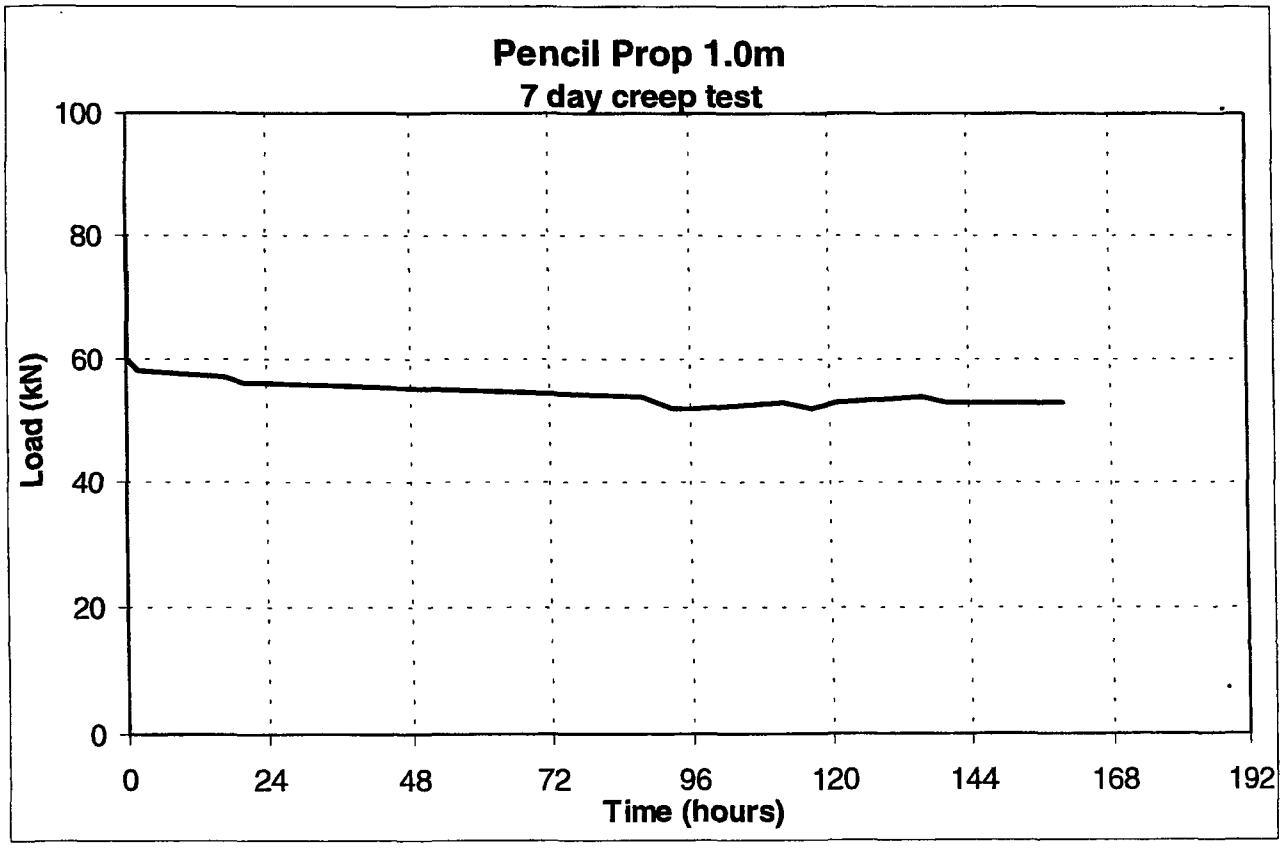
Pencil Prop 1.0m
7 day creep test
100
80
60
40
20
0
Load (kN)
0
24
48
72
96
120
144
168
192
Time (hours)

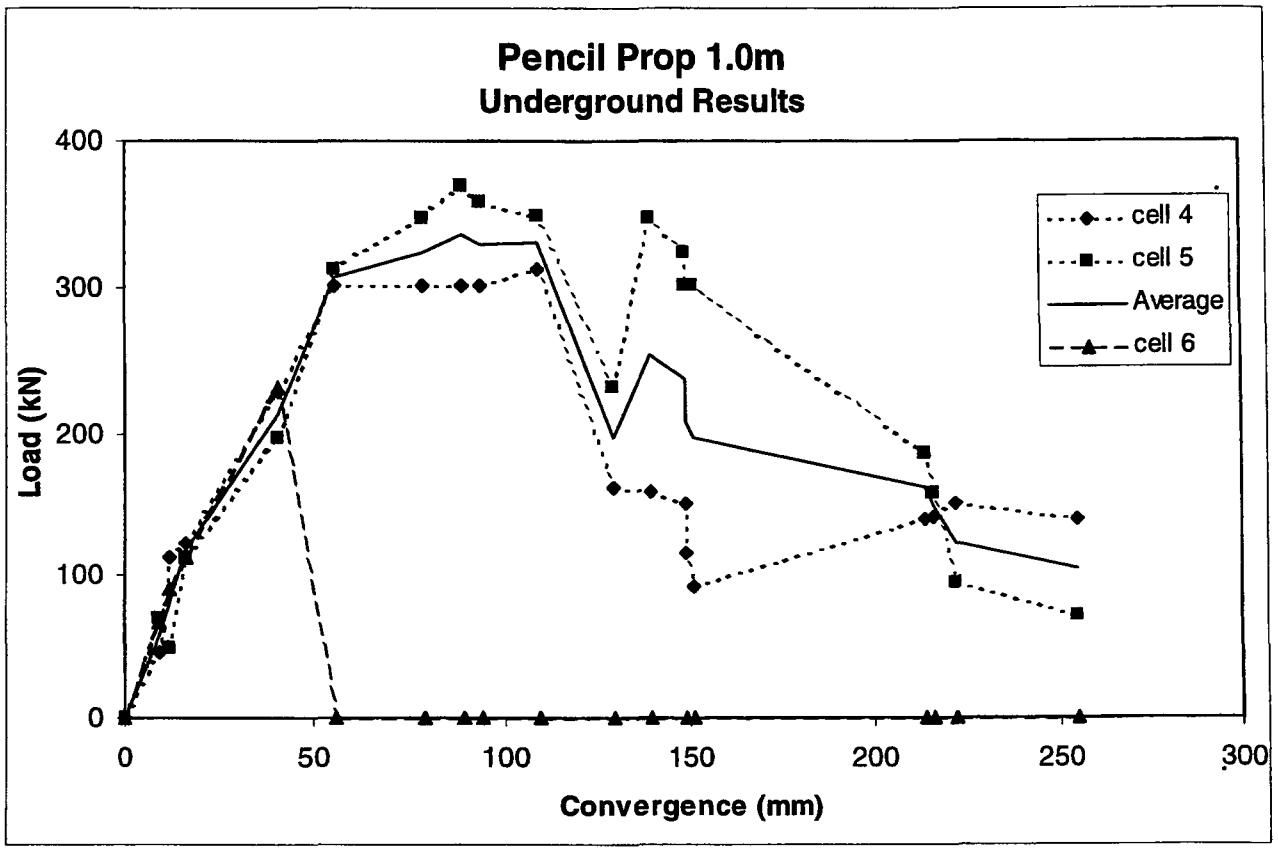
Pencil Prop 1.0m
Underground Results
Load (kN)
400
300
200
100
0
0
50
100
150
200
250
300
Convergence (mm)
cell 4
cell 5
Average
cell 6

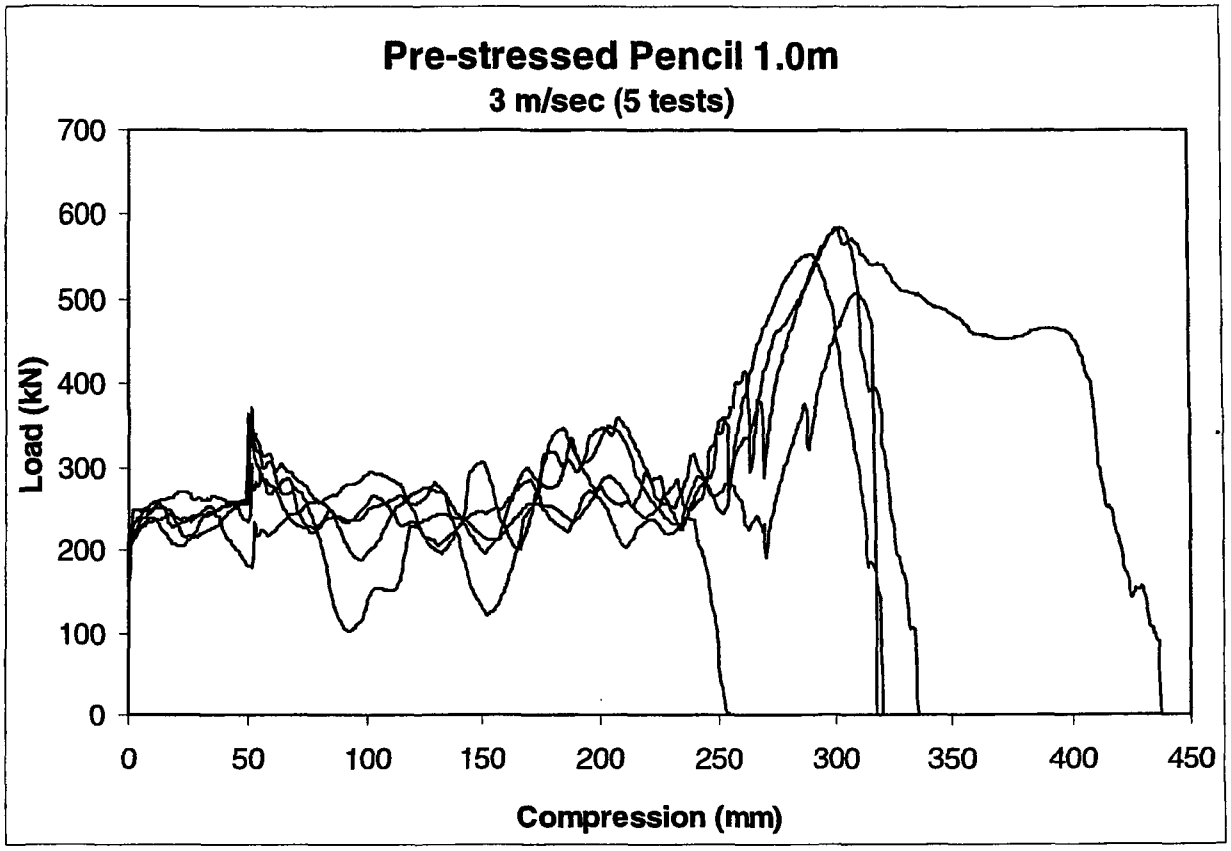
Pre-stressed Pencil 1.0m
3 m/sec (5 tests)
Load (kN)
700
600
500
400
300
200
100
0
0
50
100
150
200
250
300
350
400
450
Compression (mm)

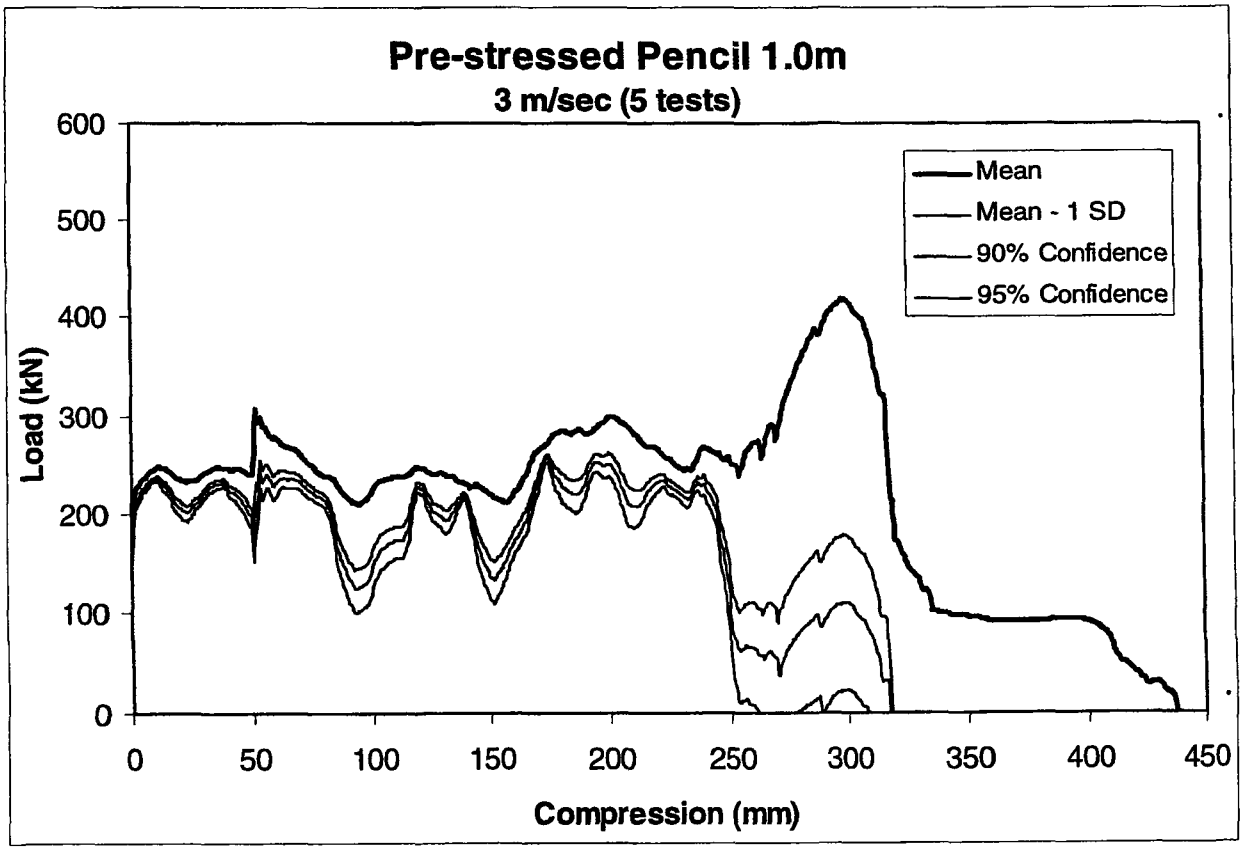
Pre-stressed Pencil 1.0m
3 m/sec (5 tests)
Mean
Mean - 1 SD
90% Confidence
95% Confidence
Load (kN)
600
500
400
300
200
100
0
0
50
100
150
200
250
300
350
400
450
Compression (mm)

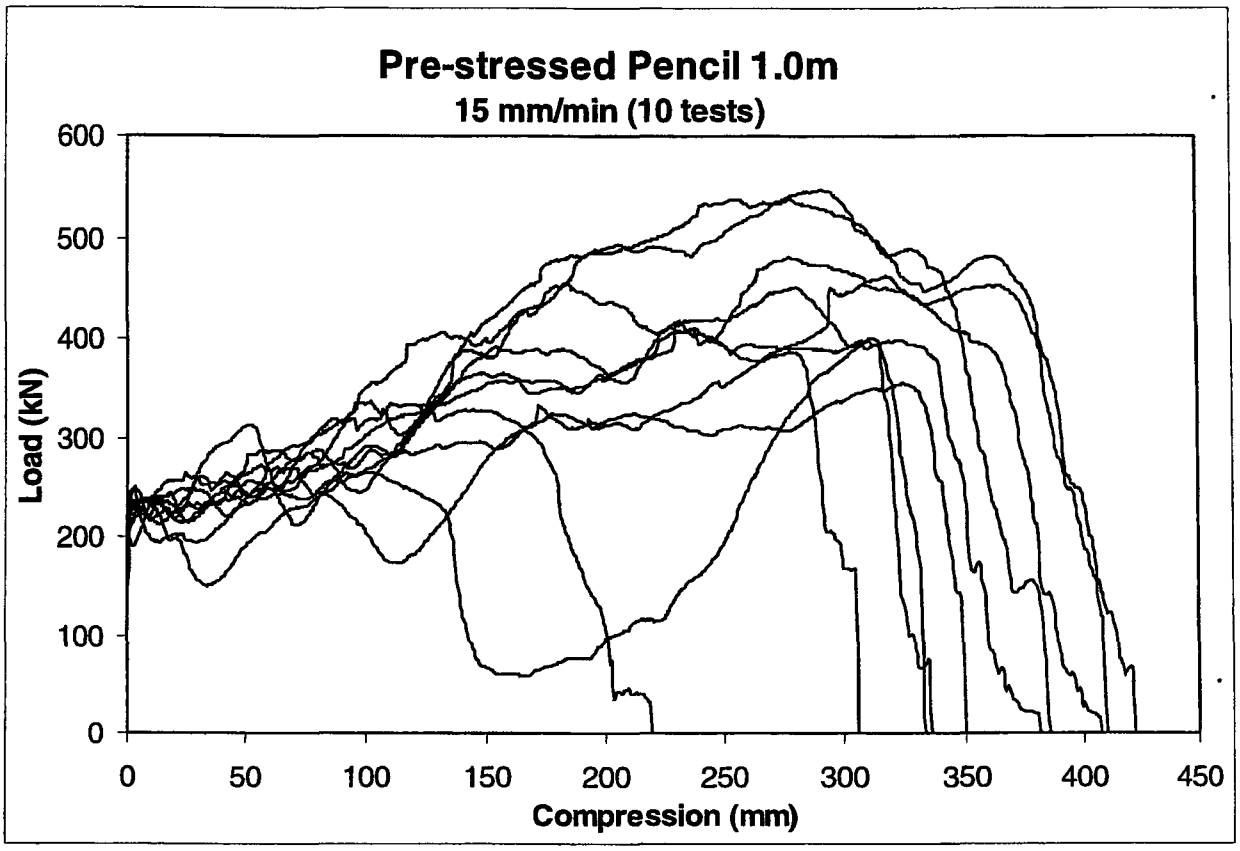
Pre-stressed Pencil 1.0m
15 mm/min (10 tests)
Load (kN)
600
500
400
300
200
100
0
0
50
100
150
200
250
300
350
400
450
Compression (mm)

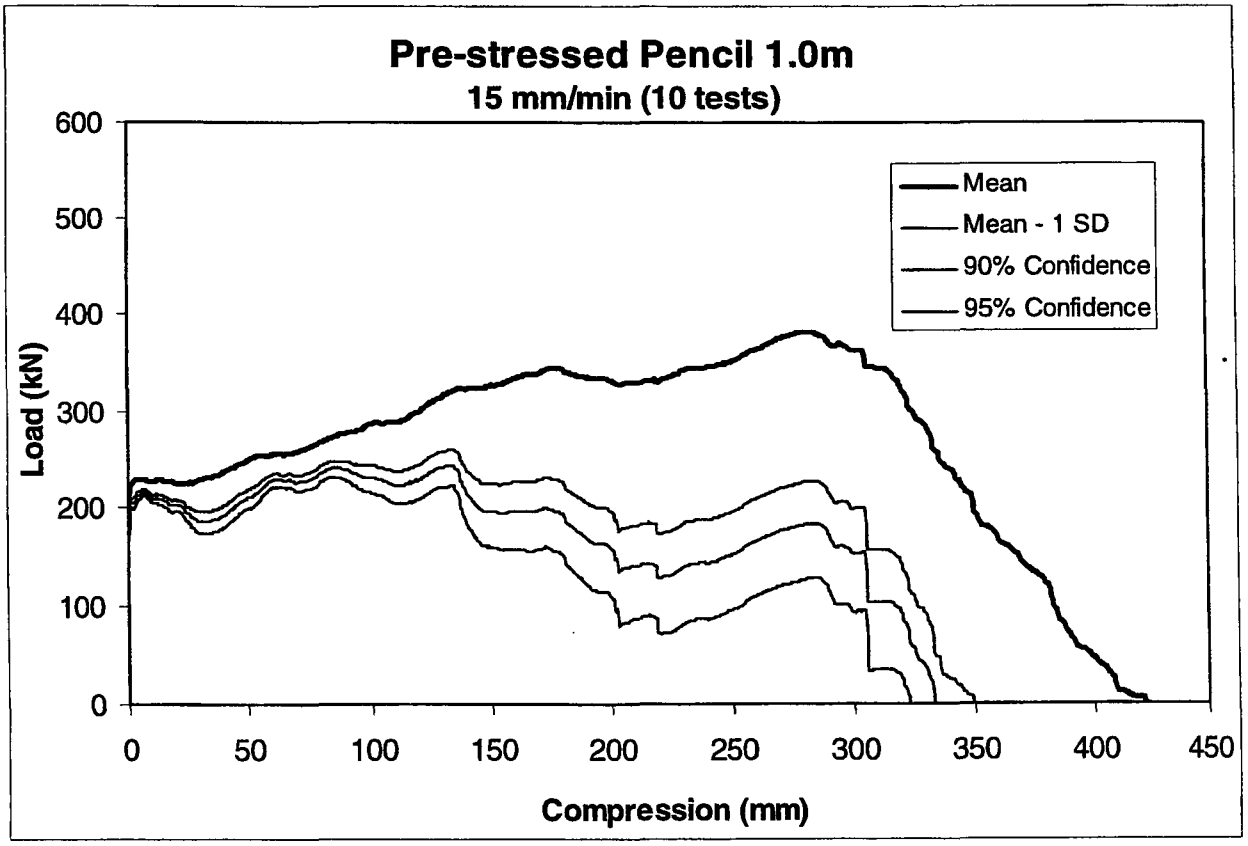
Pre-stressed Pencil 1.0m
15 mm/min (10 tests)
Mean
Mean - 1 SD
90% Confidence
95% Confidence
Load (kN)
600
500
400
300
200
100
0
0
50
100
150
200
250
300
350
400
450
Compression (mm)

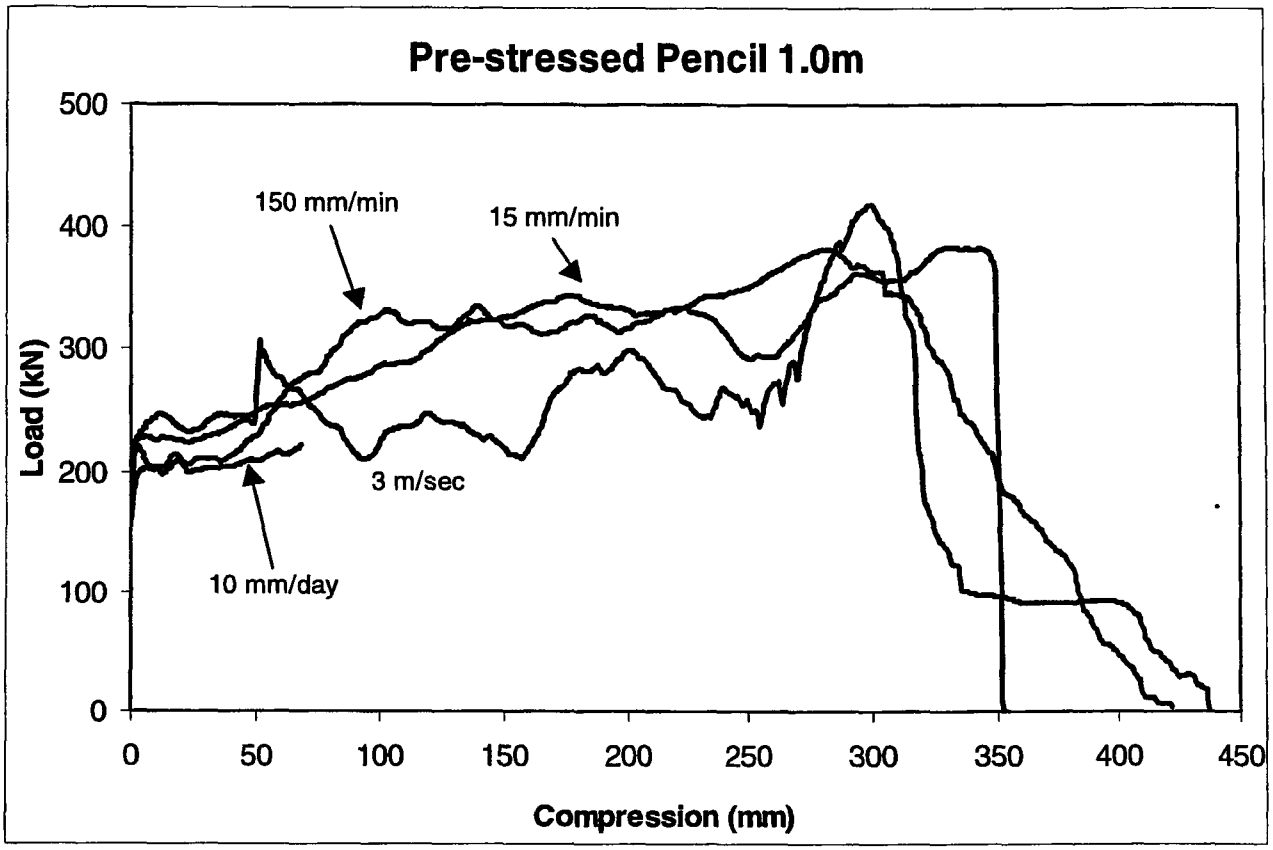
Pre-stressed Pencil 1.0m
Load (kN)
Compression (mm)
150 mm/min
15 mm/min
3 m/sec
10 mm/day
0
100
200
300
400
500
0
50
100
150
200
250
300
350
400
450

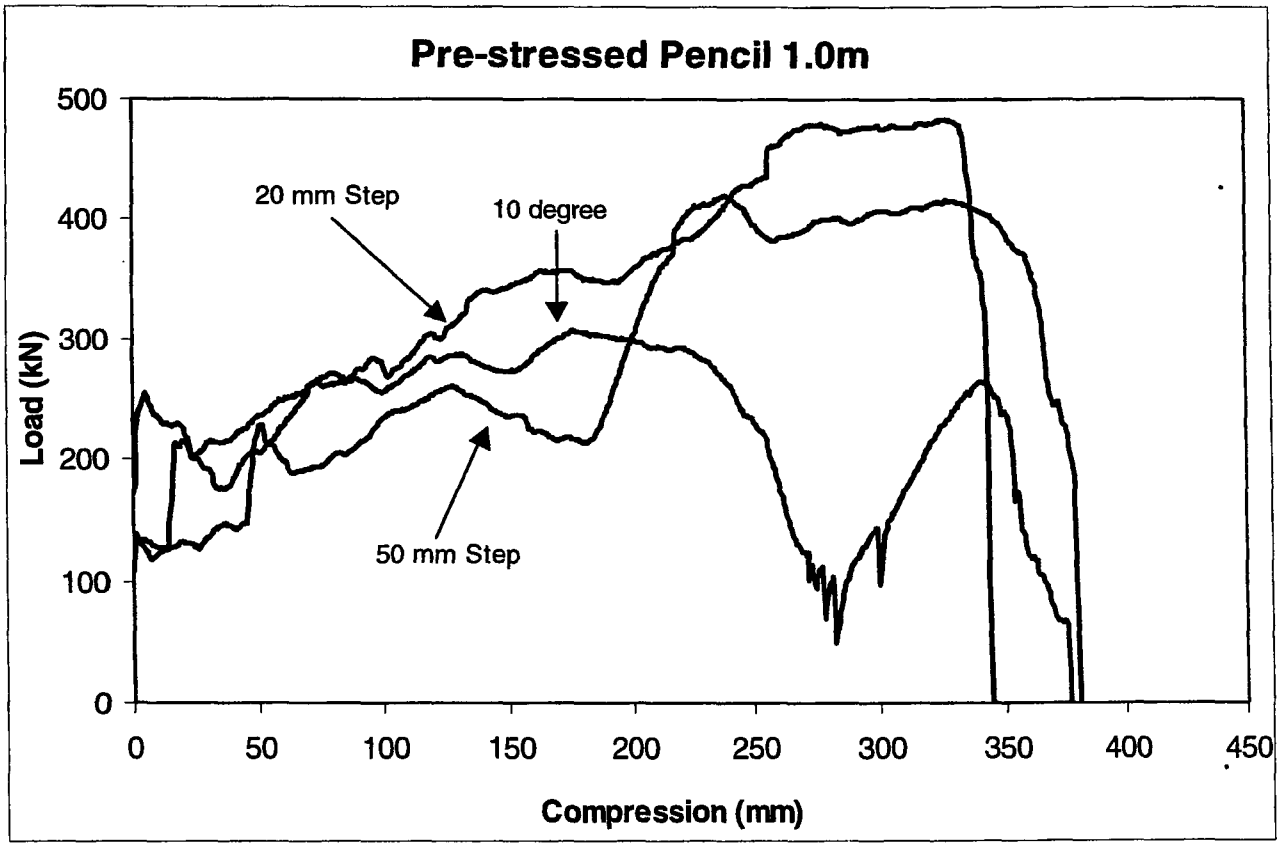
Pre-stressed Pencil 1.0m
Load (kN)
Compression (mm)
20 mm Step
10 degree
50 mm Step
0
100
200
300
400
500
0
50
100
150
200
250
300
350
400
450

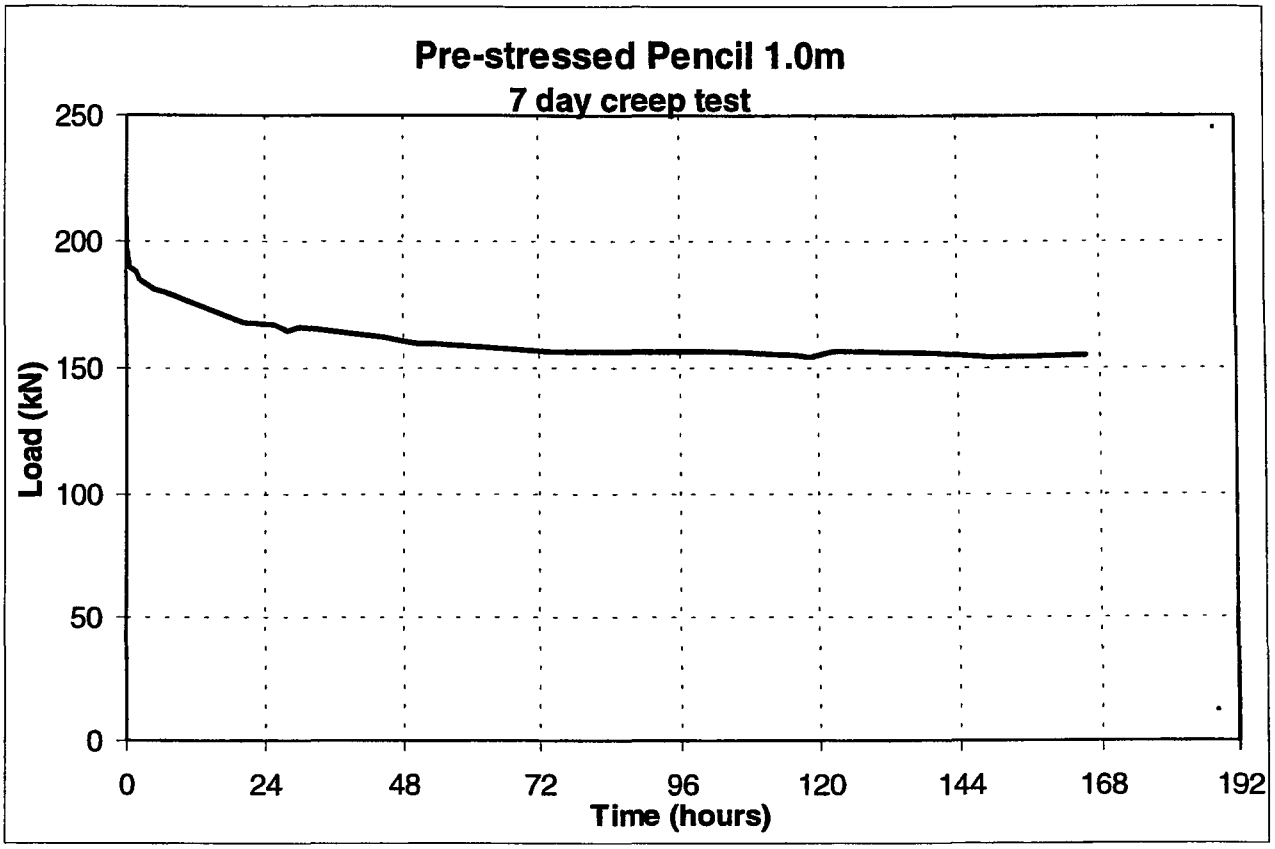
Pre-stressed Pencil 1.0m
7 day creep test
Load (kN)
250
200
150
100
50
0
0
24
48
72
96
120
144
168
192
Time (hours)

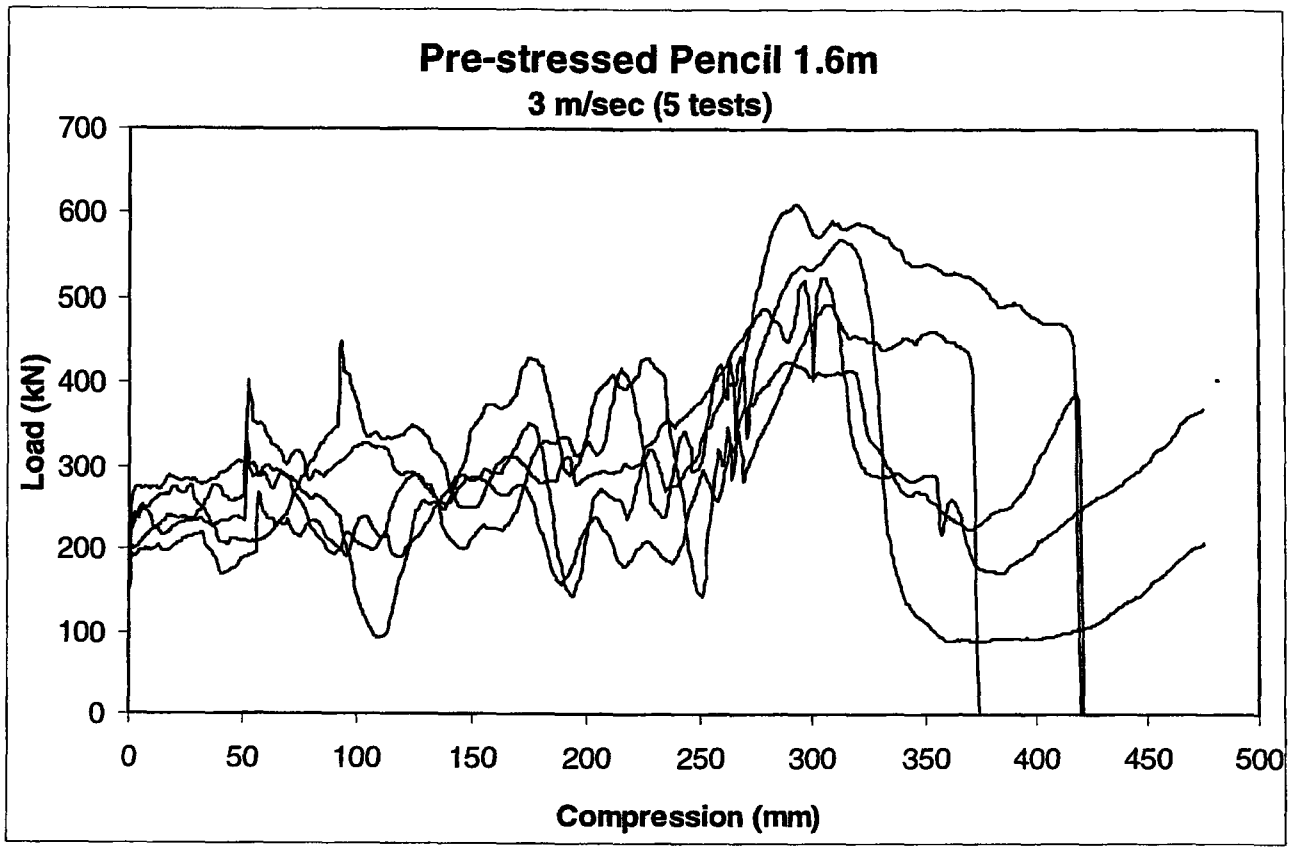
Pre-stressed Pencil 1.6m
3 m/sec (5 tests)
Load (kN)
700
600
500
400
300
200
100
0
0
50
100
150
200
250
300
350
400
450
500
Compression (mm)

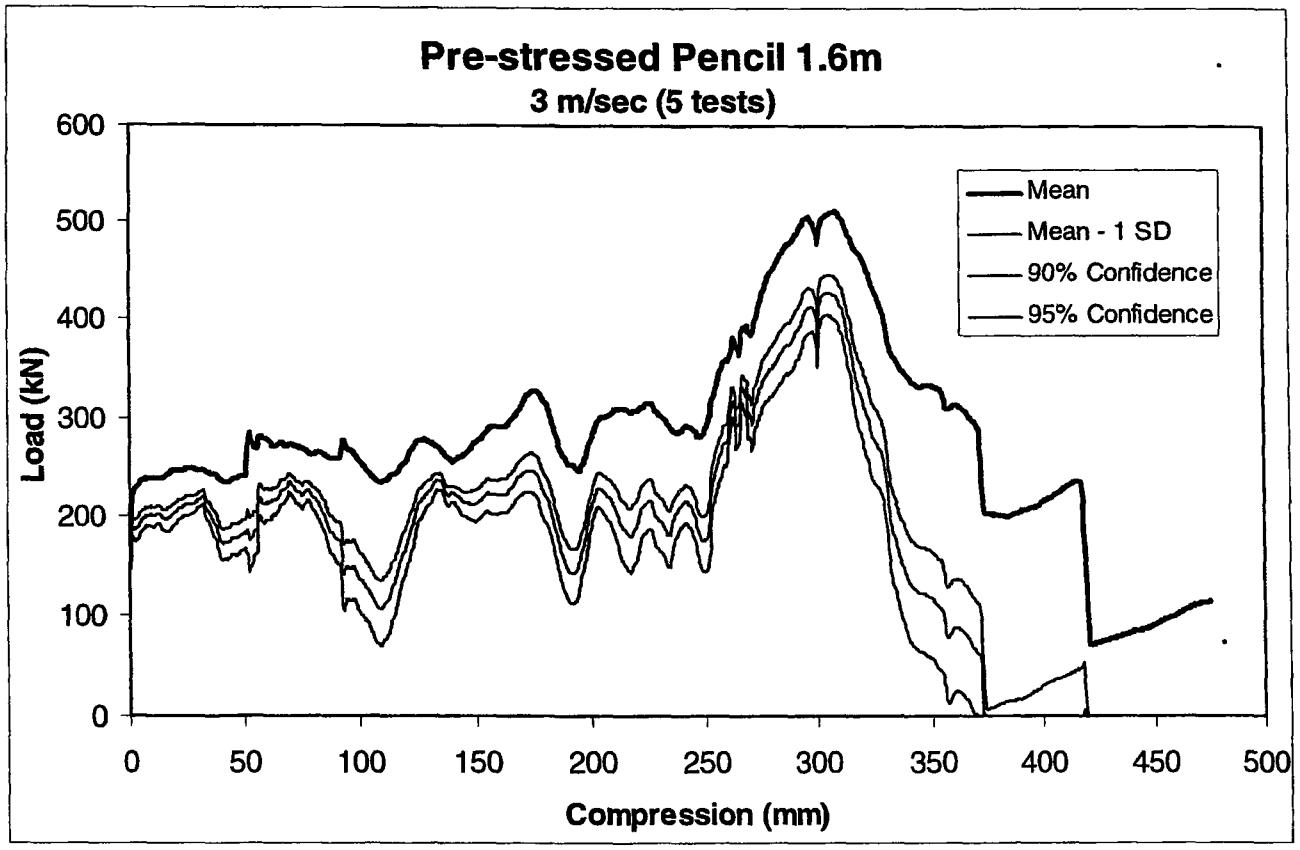
Pre-stressed Pencil 1.6m
3 m/sec (5 tests)
Load (kN)
600
500
400
300
200
100
0
0
50
100
150
200
250
300
350
400
450
500
Compression (mm)
Mean
Mean - 1 SD
90% Confidence
95% Confidence

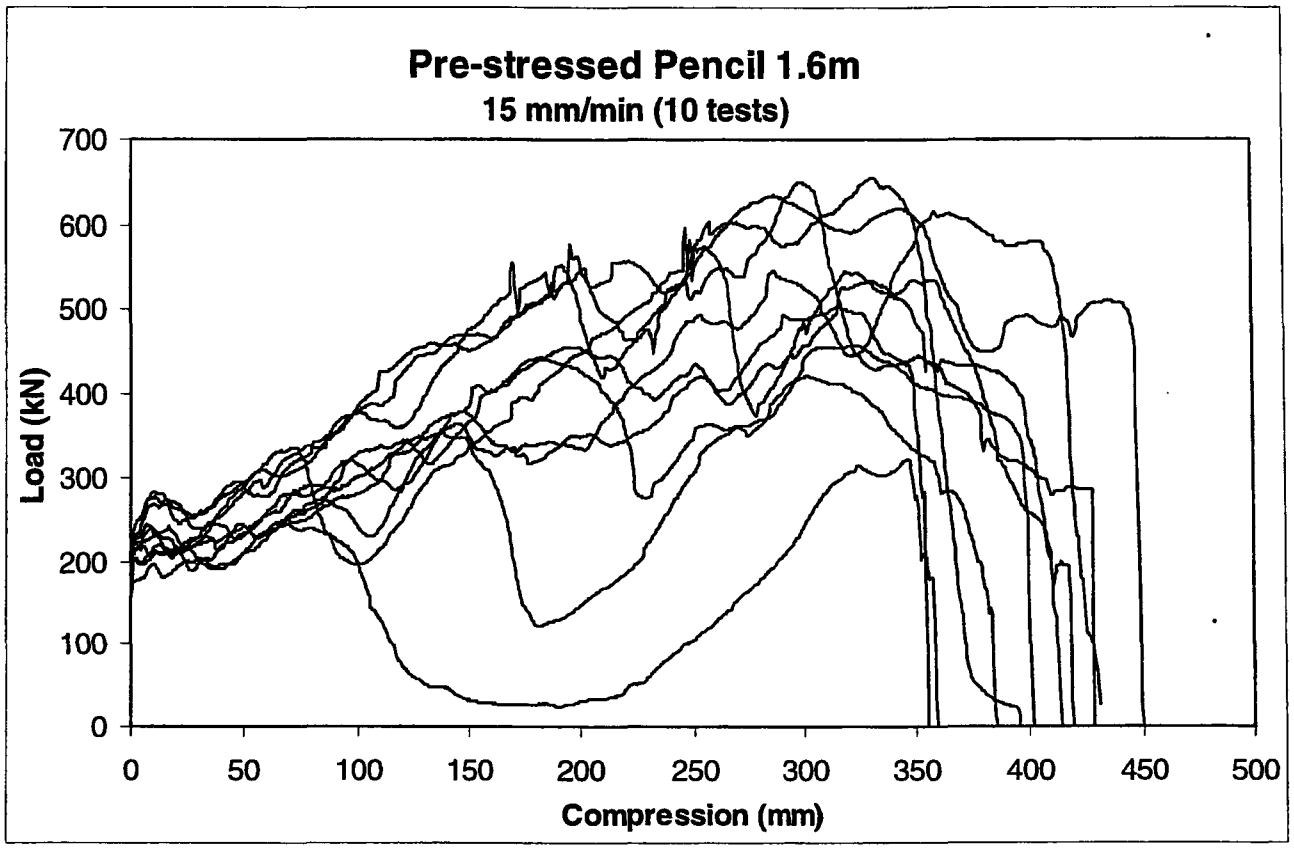
Pre-stressed Pencil 1.6m
15 mm/min (10 tests)
Load (kN)
700
600
500
400
300
200
100
0
0
50
100
150
200
250
300
350
400
450
500
Compression (mm)

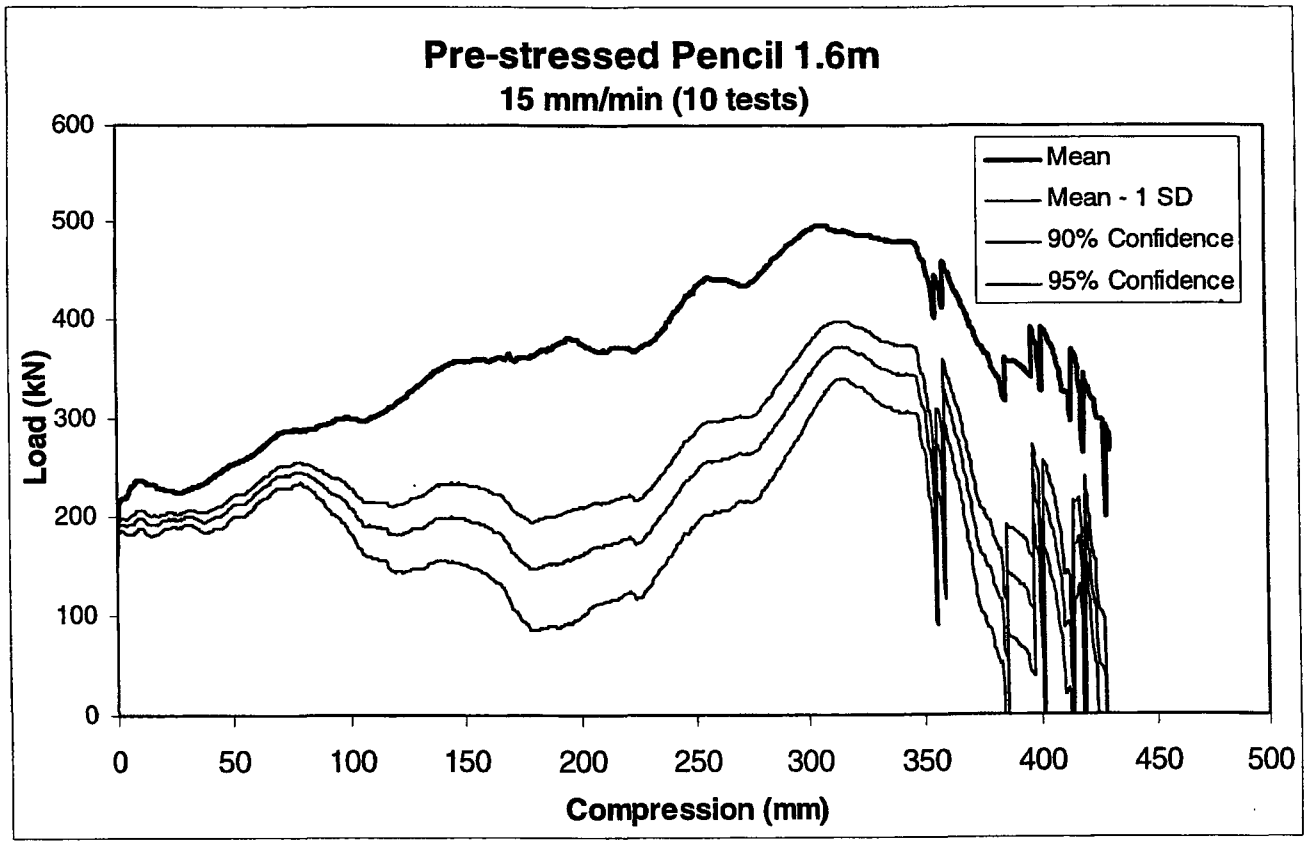
Pre-stressed Pencil 1.6m
15 mm/min (10 tests)
Load (kN)
600
500
400
300
200
100
0
0
50
100
150
200
250
300
350
400
450
500
Compression (mm)
Mean
Mean - 1 SD
90% Confidence
95% Confidence

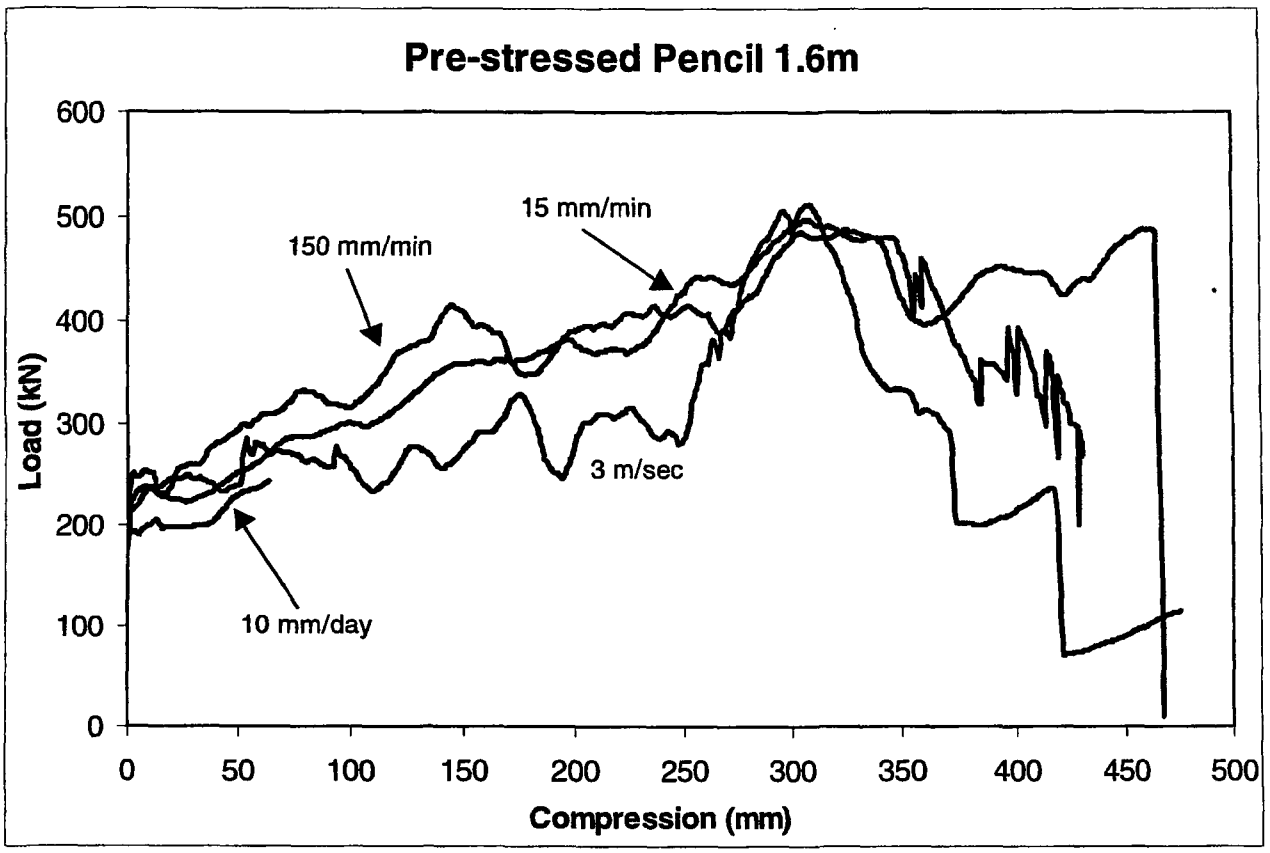
Pre-stressed Pencil 1.6m
Load (kN)
600
500
400
300
200
100
0
0
50
100
150
200
250
300
350
400
450
500
Compression (mm)
150 mm/min
15 mm/min
3 m/sec
10 mm/day

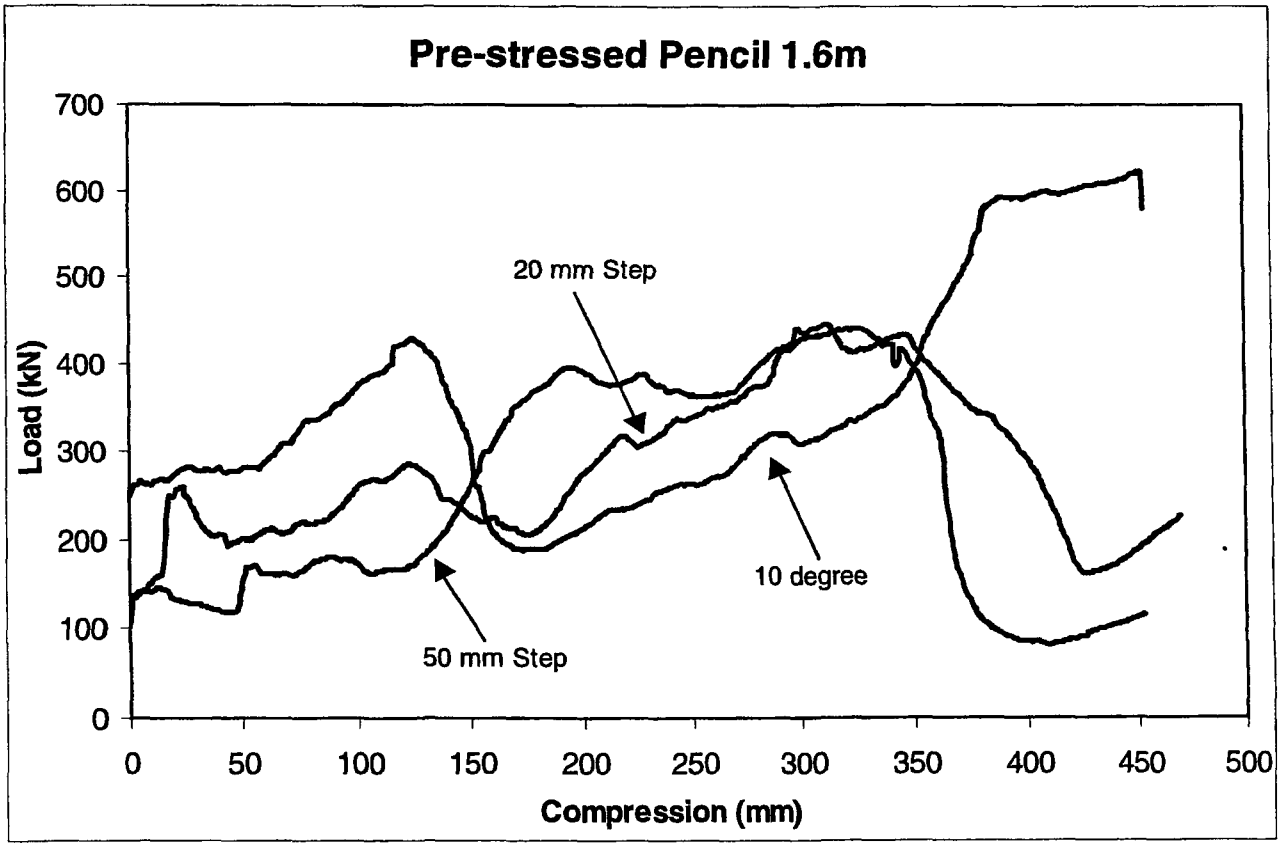
Pre-stressed Pencil 1.6m
Load (kN)
700
600
500
400
300
200
100
0
0
50
100
150
200
250
300
350
400
450
500
Compression (mm)
20 mm Step
10 degree
50 mm Step

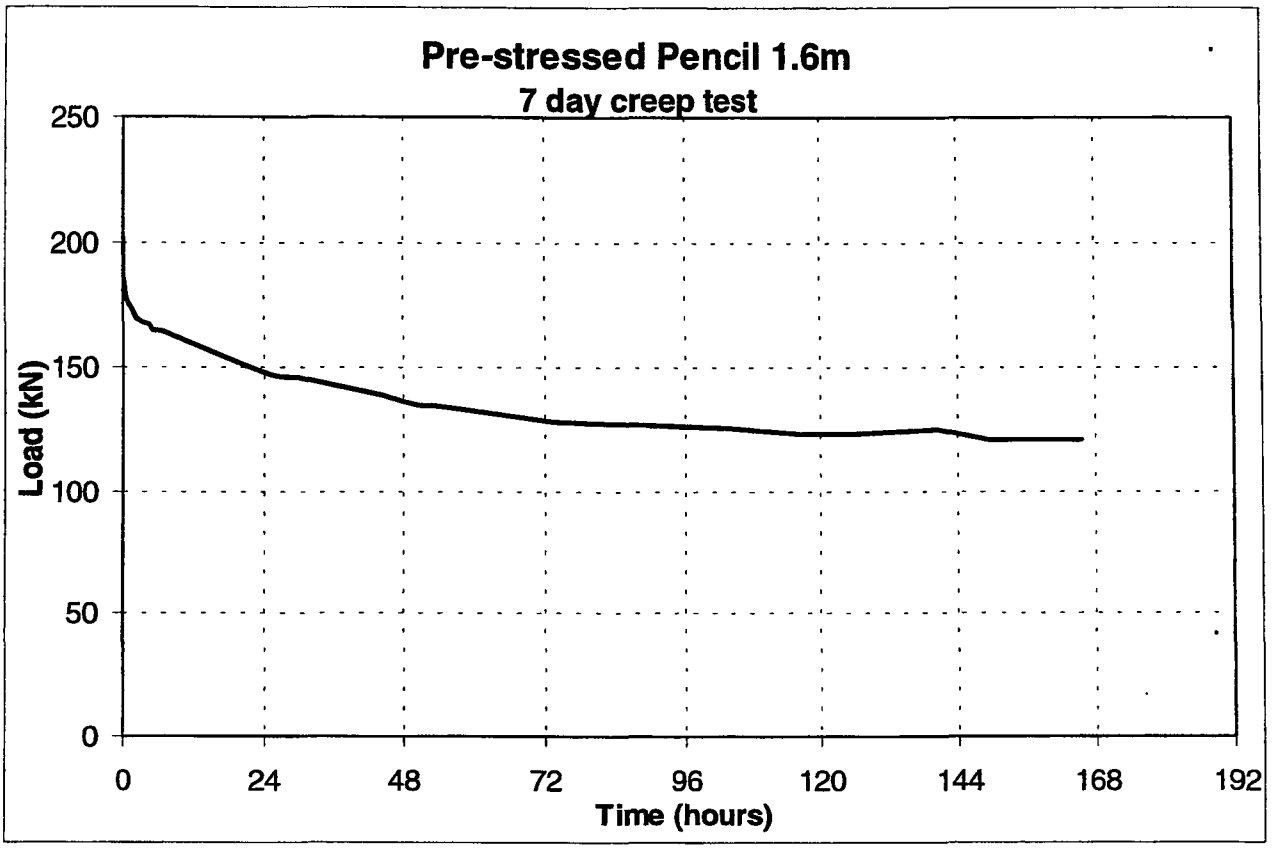
Pre-stressed Pencil 1.6m
7 day creep test
Load (kN)
250
200
150
100
50
0
0
24
48
72
96
120
144
168
192
Time (hours)

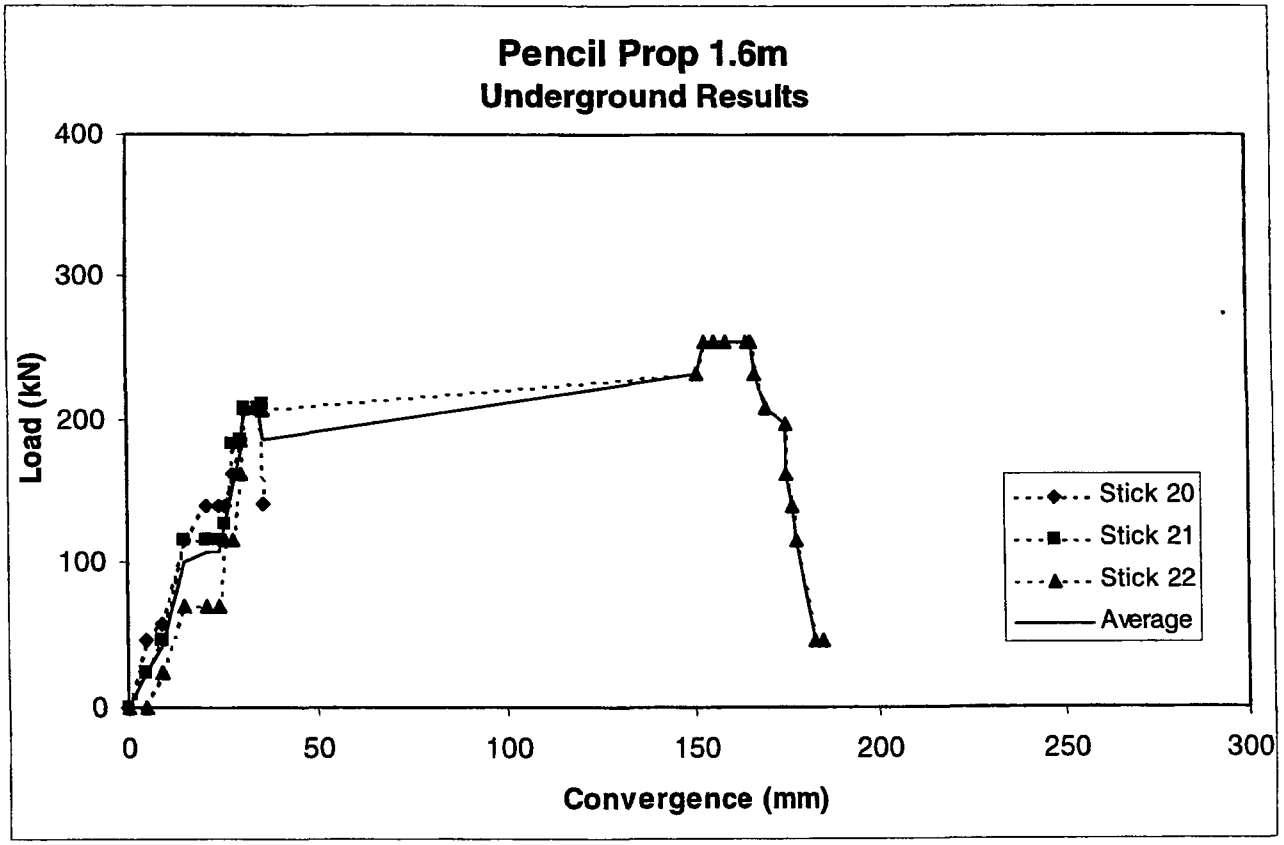
Pencil Prop 1.6m
Underground Results
Load (kN)
400
300
200
100
0
0
50
100
150
200
250
300
Convergence (mm)
Stick 20
Stick 21
Stick 22
Average

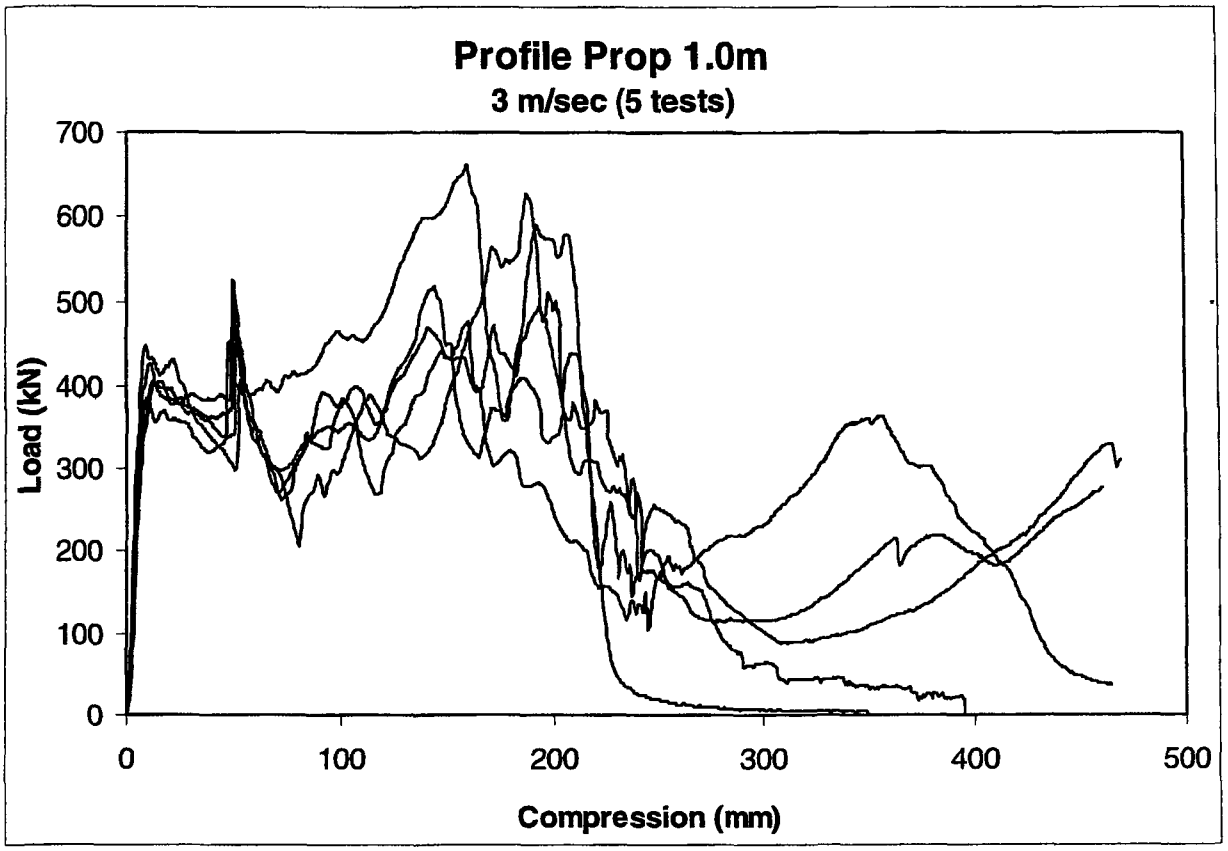
Profile Prop 1.0m
3 m/sec (5 tests)
Load (kN)
700
600
500
400
300
200
100
0
0
100
200
300
400
500
Compression (mm)

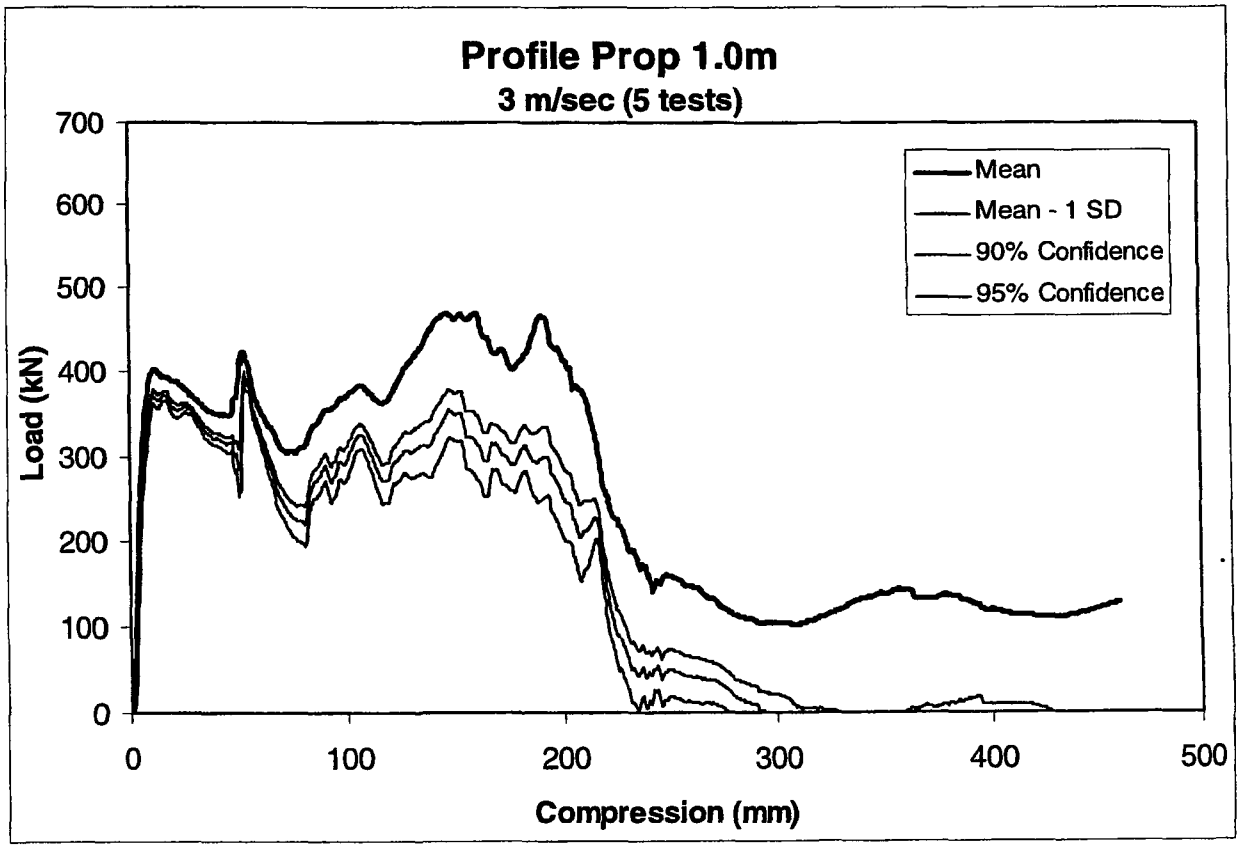
Profile Prop 1.0m
3 m/sec (5 tests)
Mean
Mean - 1 SD
90% Confidence
95% Confidence
Load (kN)
700
600
500
400
300
200
100
0
0
100
200
300
400
500
Compression (mm)

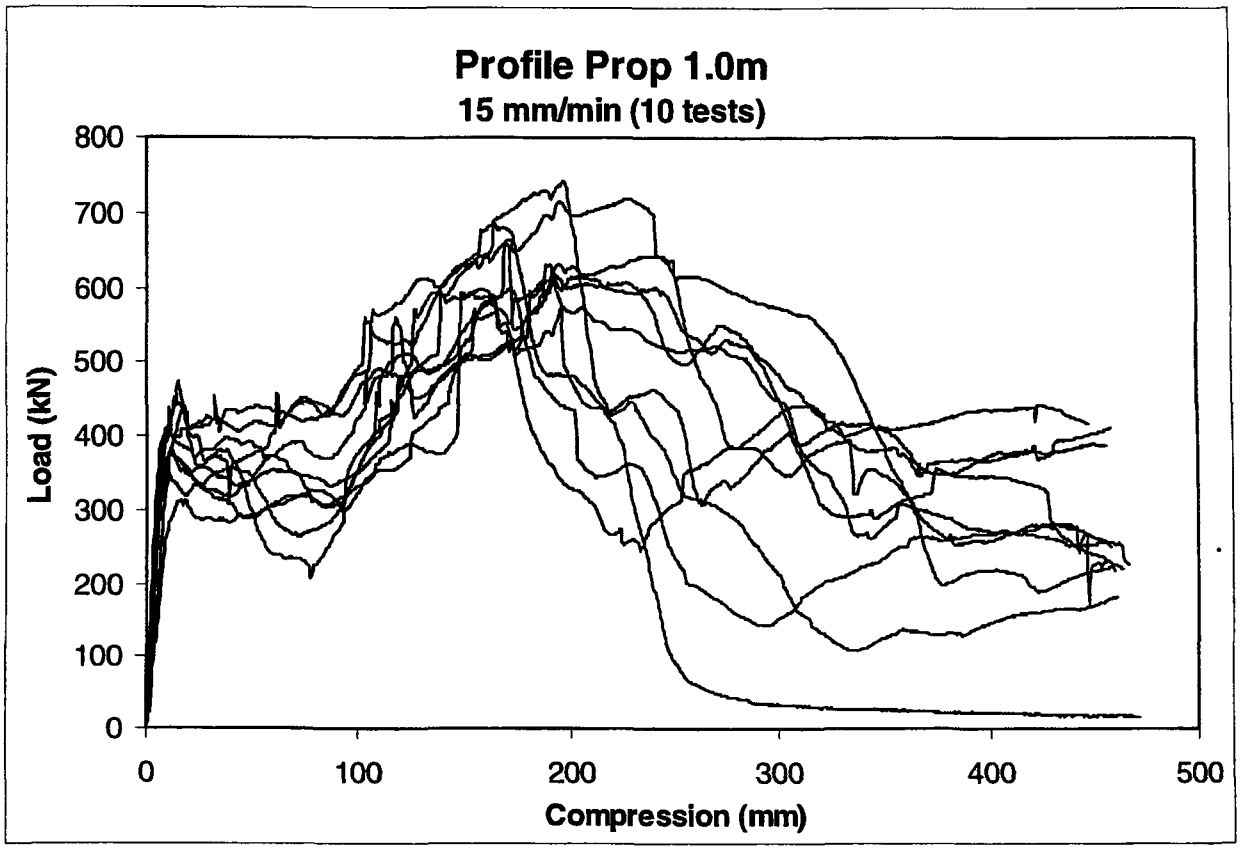
Profile Prop 1.0m
15 mm/min (10 tests)
Load (kN)
800
700
600
500
400
300
200
100
0
0
100
200
300
400
500
Compression (mm)

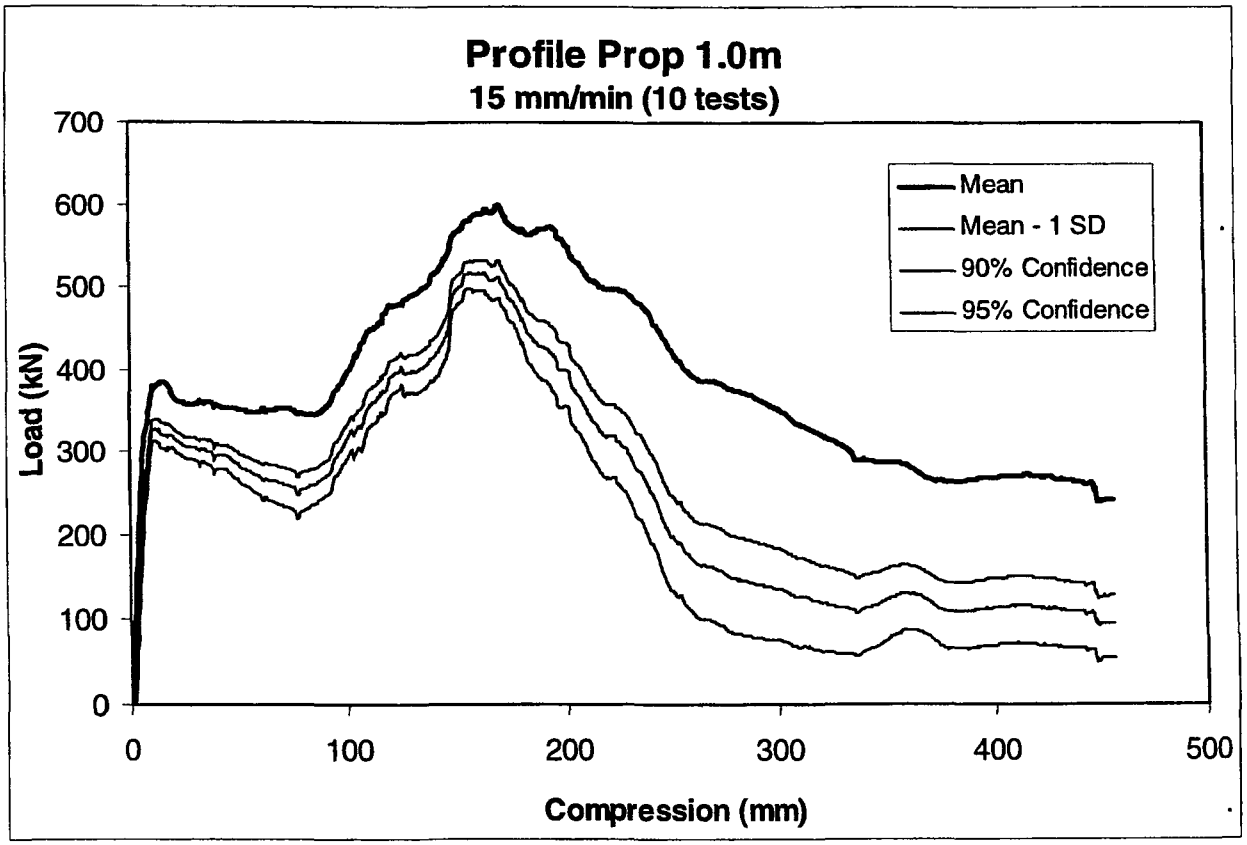
Profile Prop 1.0m
15 mm/min (10 tests)
Load (kN)
700
600
500
400
300
200
100
0
0
100
200
300
400
500
Compression (mm)
Mean
Mean - 1 SD
90% Confidence
95% Confidence

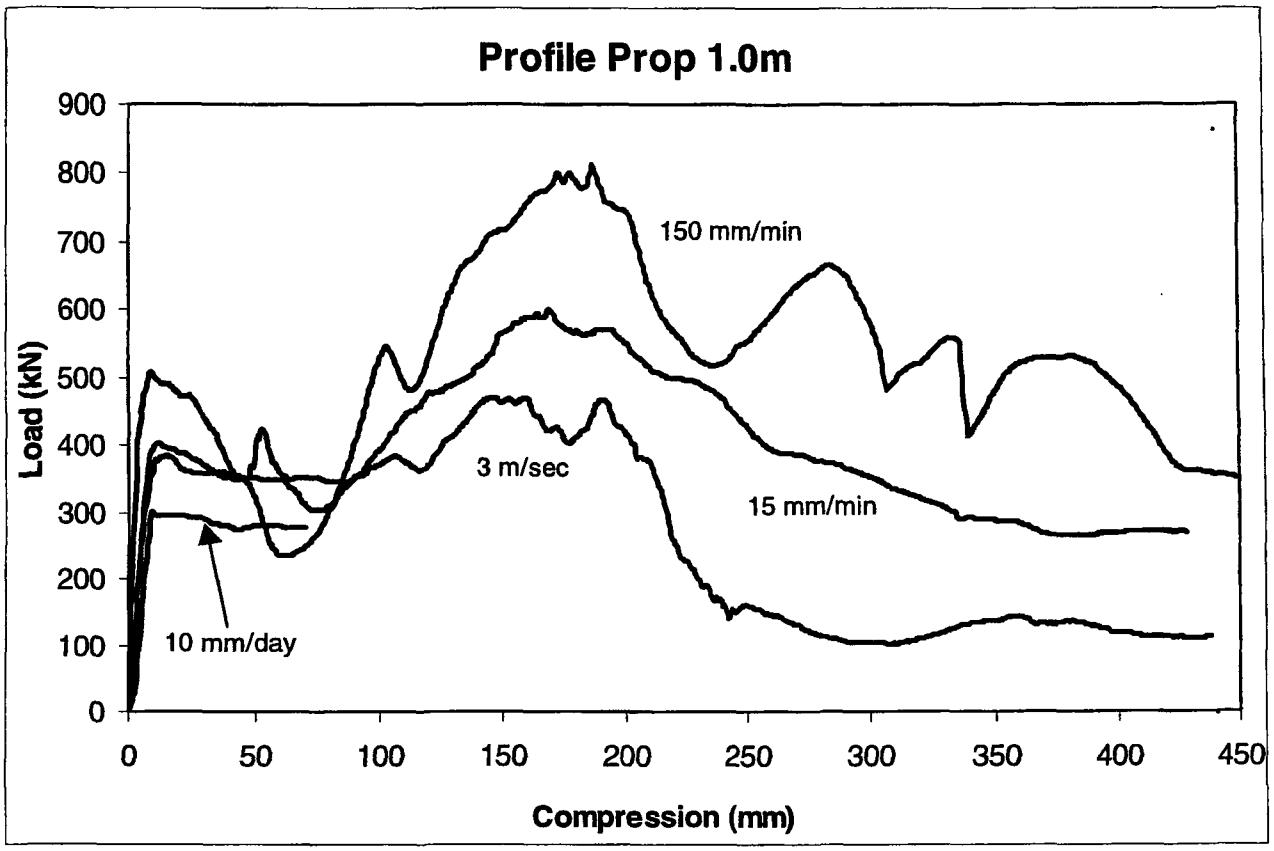
Profile Prop 1.0m
Load (kN)
900
800
700
600
500
400
300
200
100
0
0
50
100
150
200
250
300
350
400
450
Compression (mm)
150 mm/min
3 m/sec
15 mm/min
10 mm/day

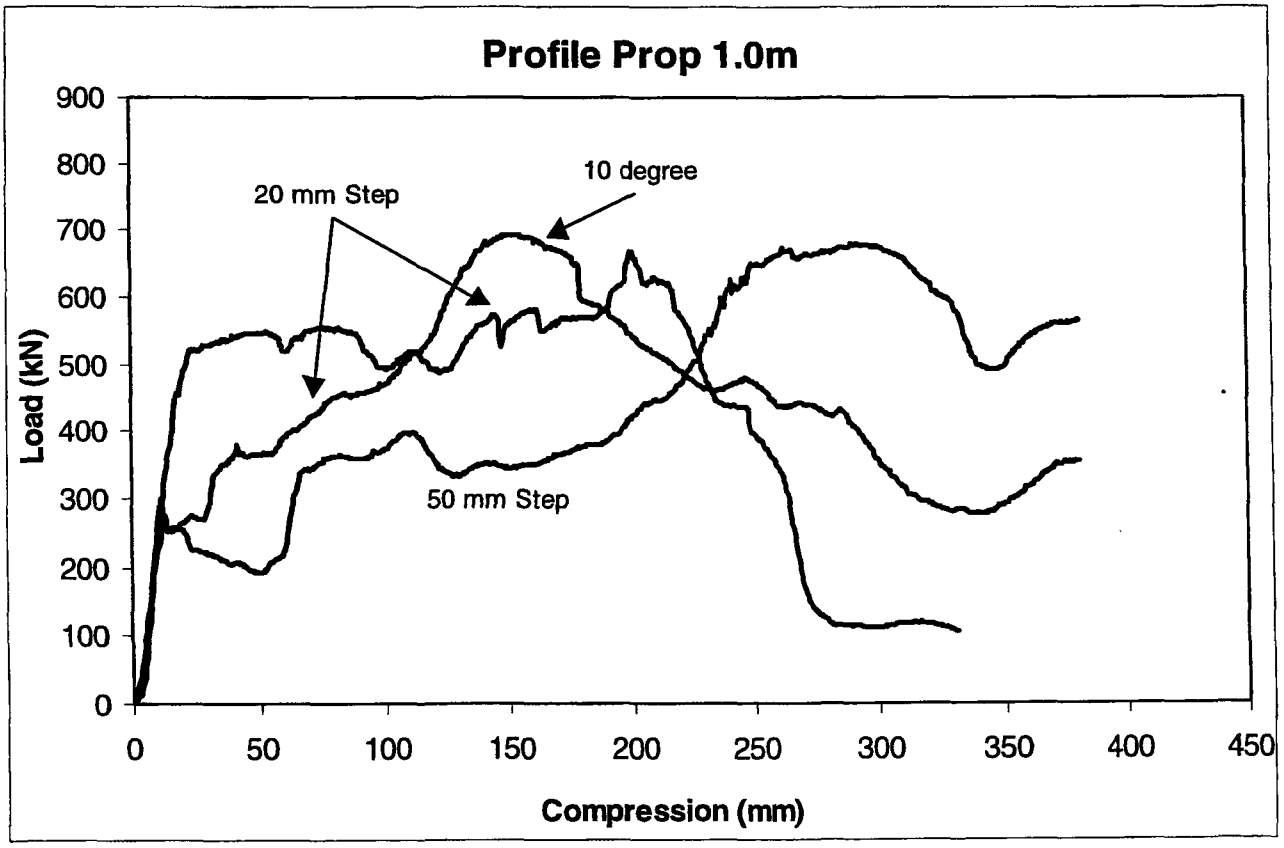
Profile Prop 1.0m
Load (kN)
900
800
700
600
500
400
300
200
100
0
0
50
100
150
200
250
300
350
400
450
Compression (mm)
20 mm Step
10 degree
50 mm Step

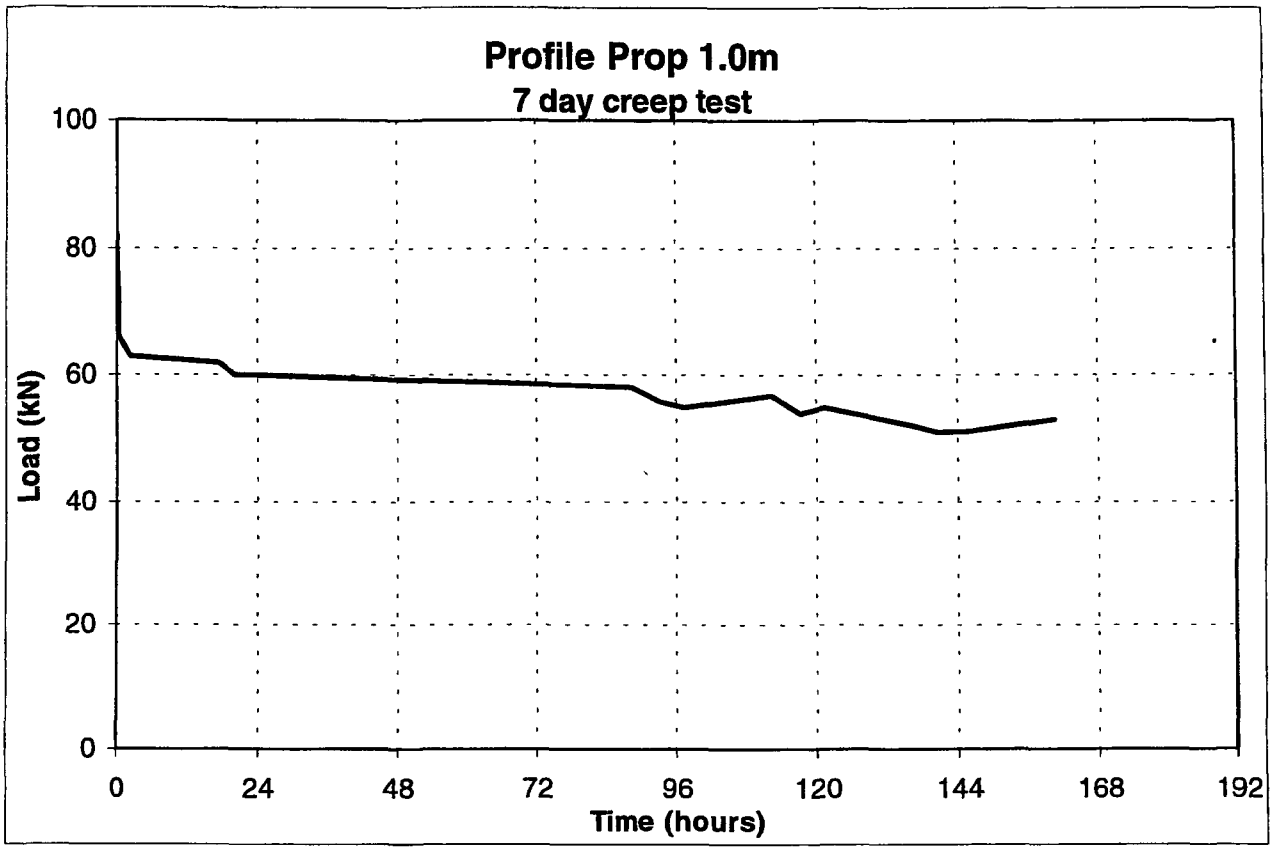
Profile Prop 1.0m
7 day creep test
Load (kN)
100
80
60
40
20
0
0
24
48
72
96
120
144
168
192
Time (hours)

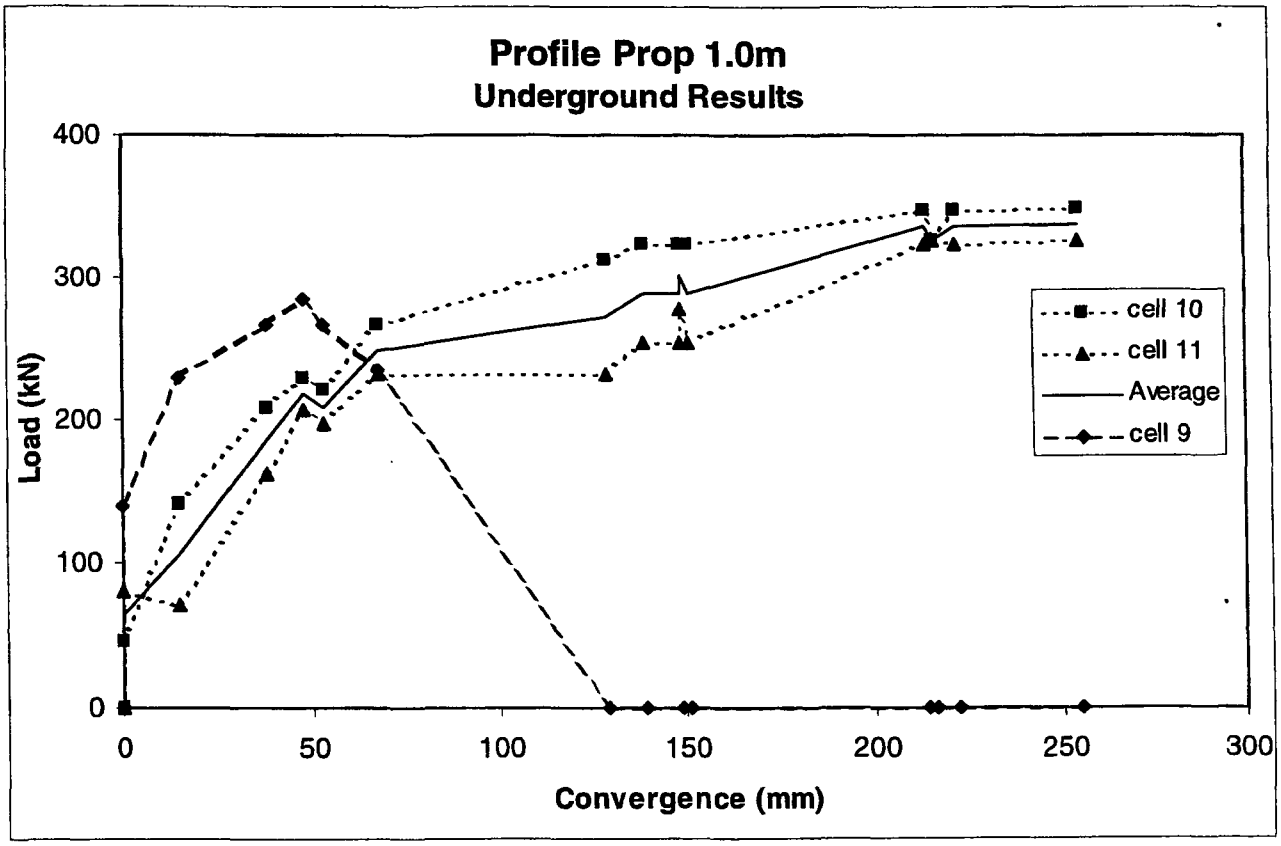
Profile Prop 1.0m
Underground Results
Load (kN)
400
300
200
100
0
0
50
100
150
200
250
300
Convergence (mm)
cell 10
cell 11
Average
cell 9

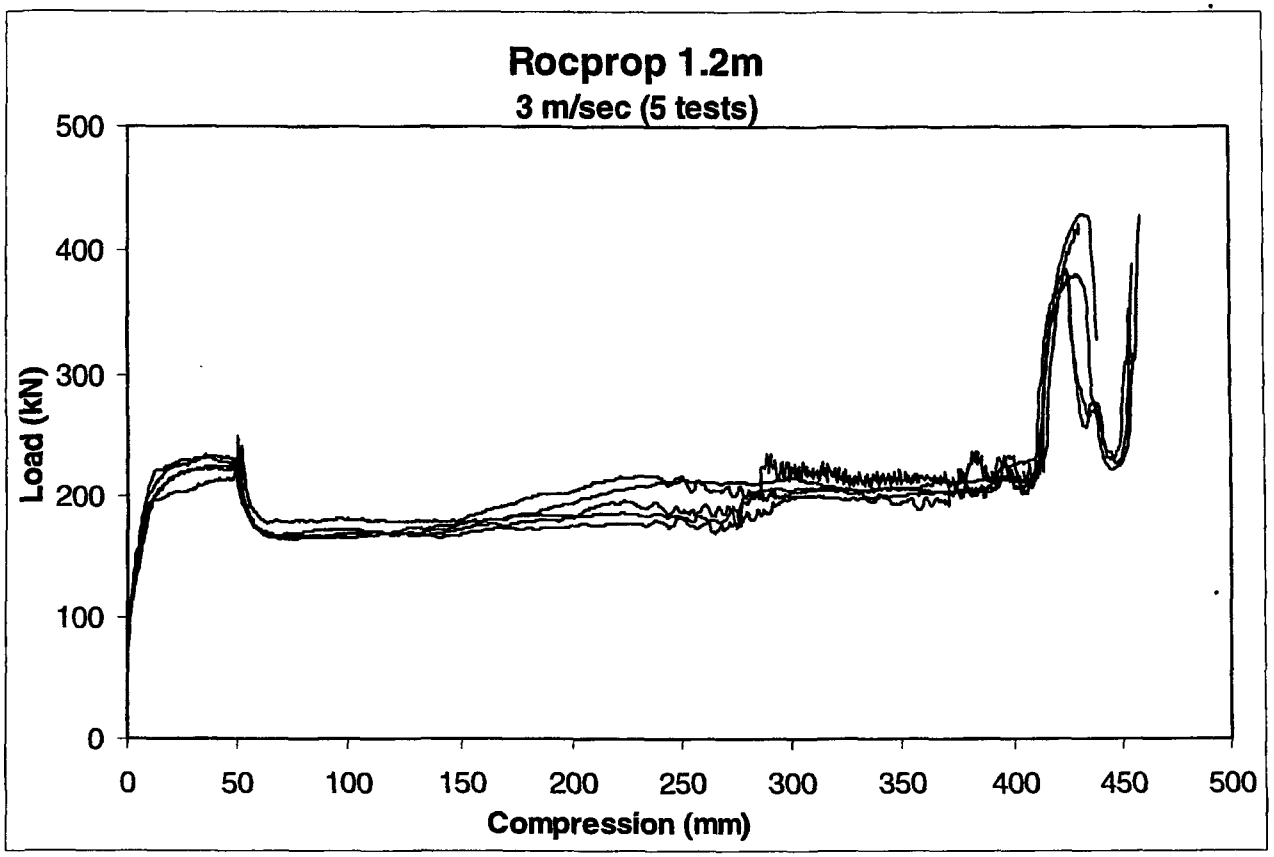
Rocprop 1.2m
3 m/sec (5 tests)
Load (kN)
0
100
200
300
400
500
0
50
100
150
200
250
300
350
400
450
500
Compression (mm)

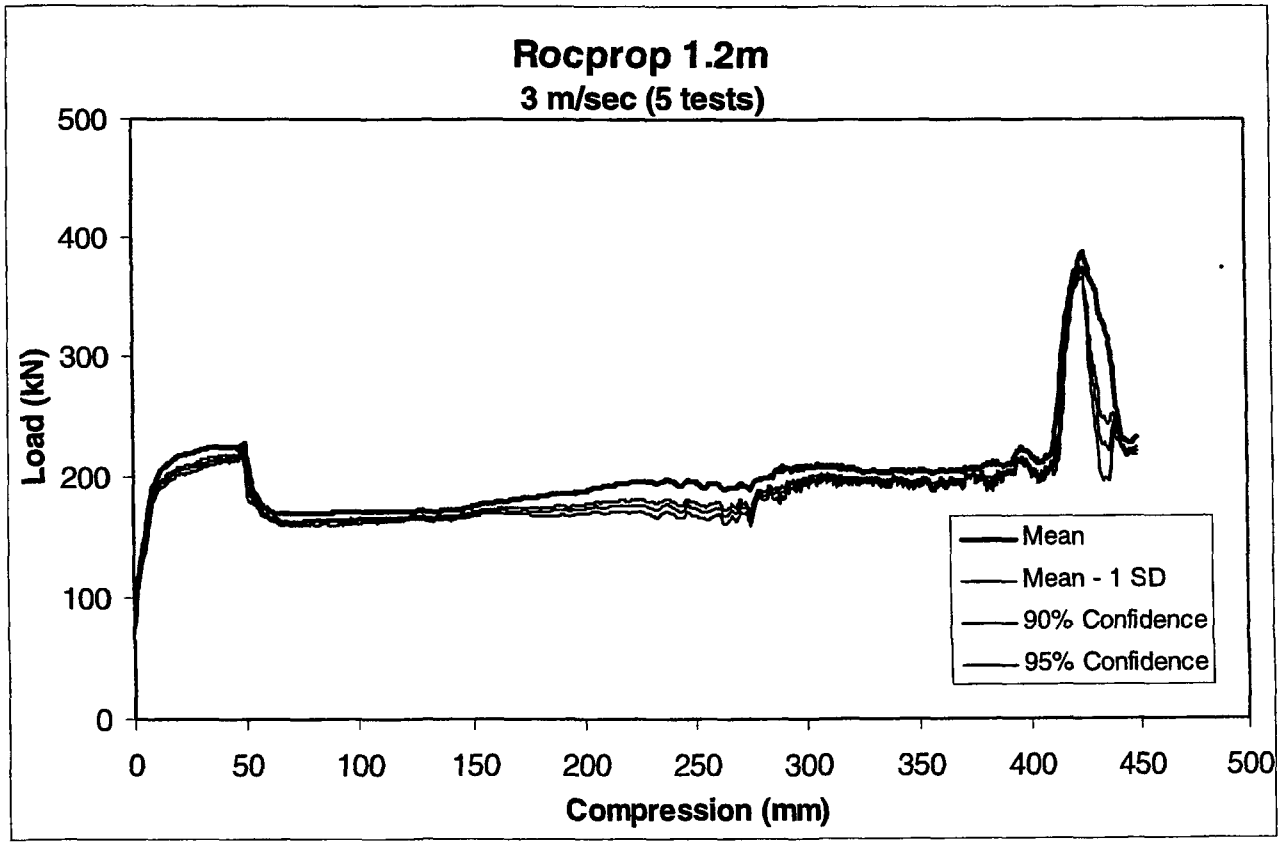
Rocprop 1.2m
3 m/sec (5 tests)
Load (kN)
0
100
200
300
400
500
0
50
100
150
200
250
300
350
400
450
500
Compression (mm)
Mean
Mean - 1 SD
90% Confidence
95% Confidence

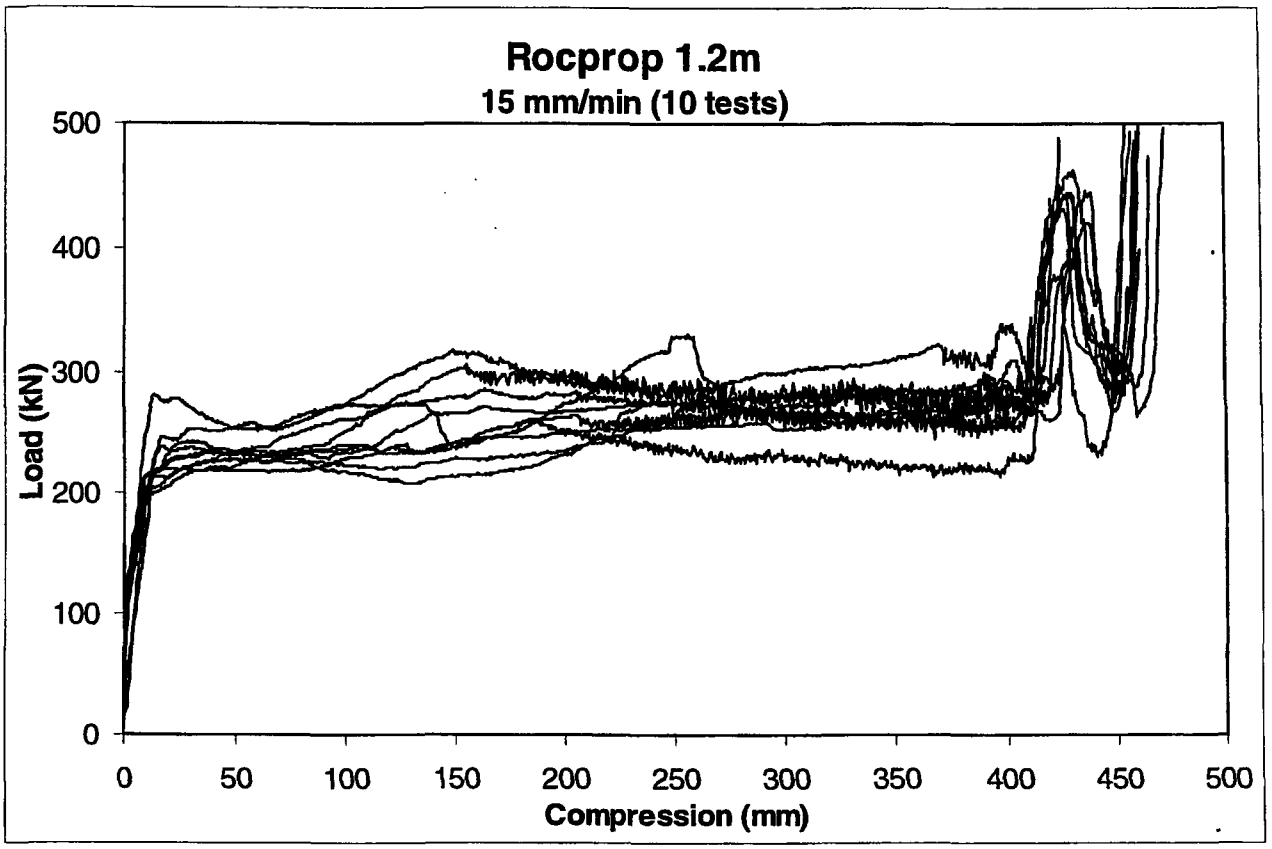
Rocprop 1.2m
15 mm/min (10 tests)
Load (kN)
0
100
200
300
400
500
0
50
100
150
200
250
300
350
400
450
500
Compression (mm)

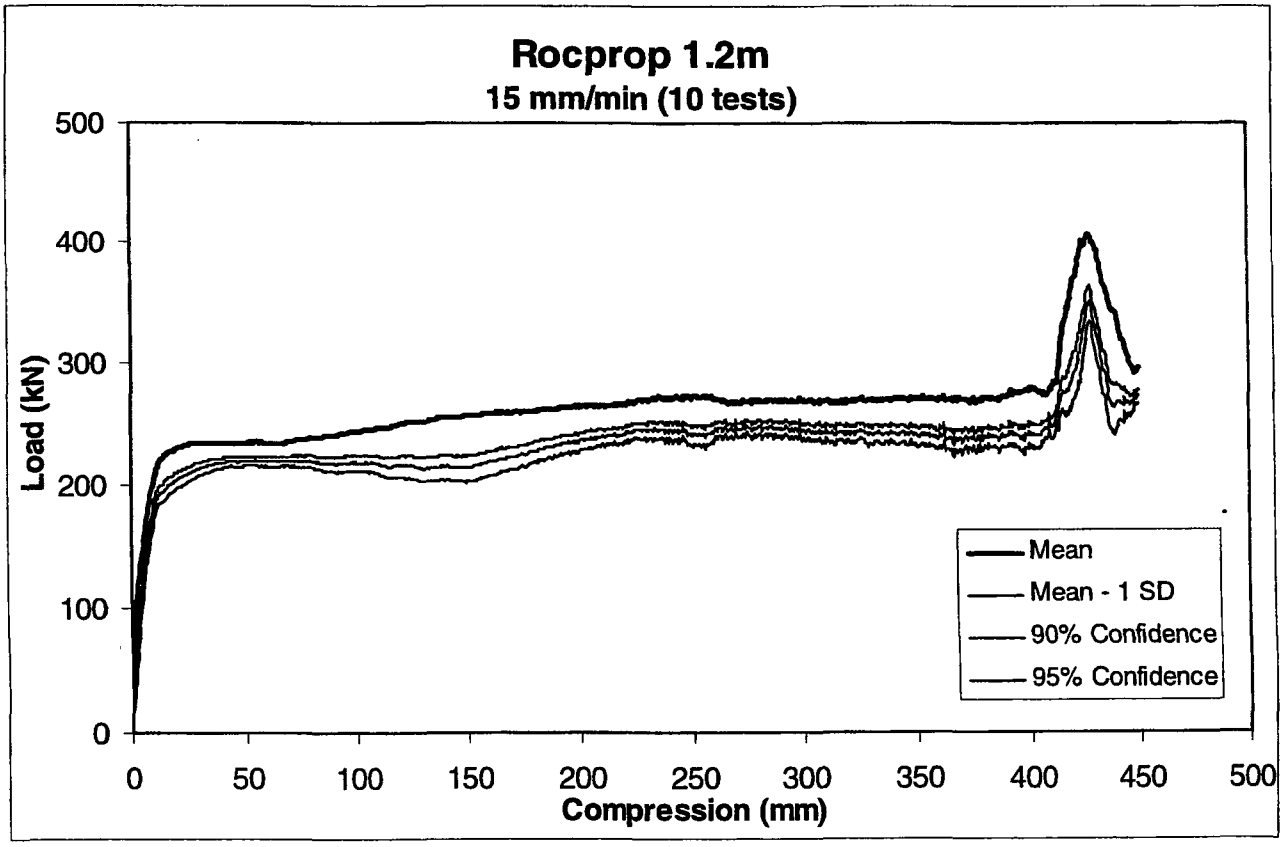
Rocprop 1.2m
15 mm/min (10 tests)
Load (kN)
0
100
200
300
400
500
0
50
100
150
200
250
300
350
400
450
500
Compression (mm)
Mean
Mean - 1 SD
90% Confidence
95% Confidence

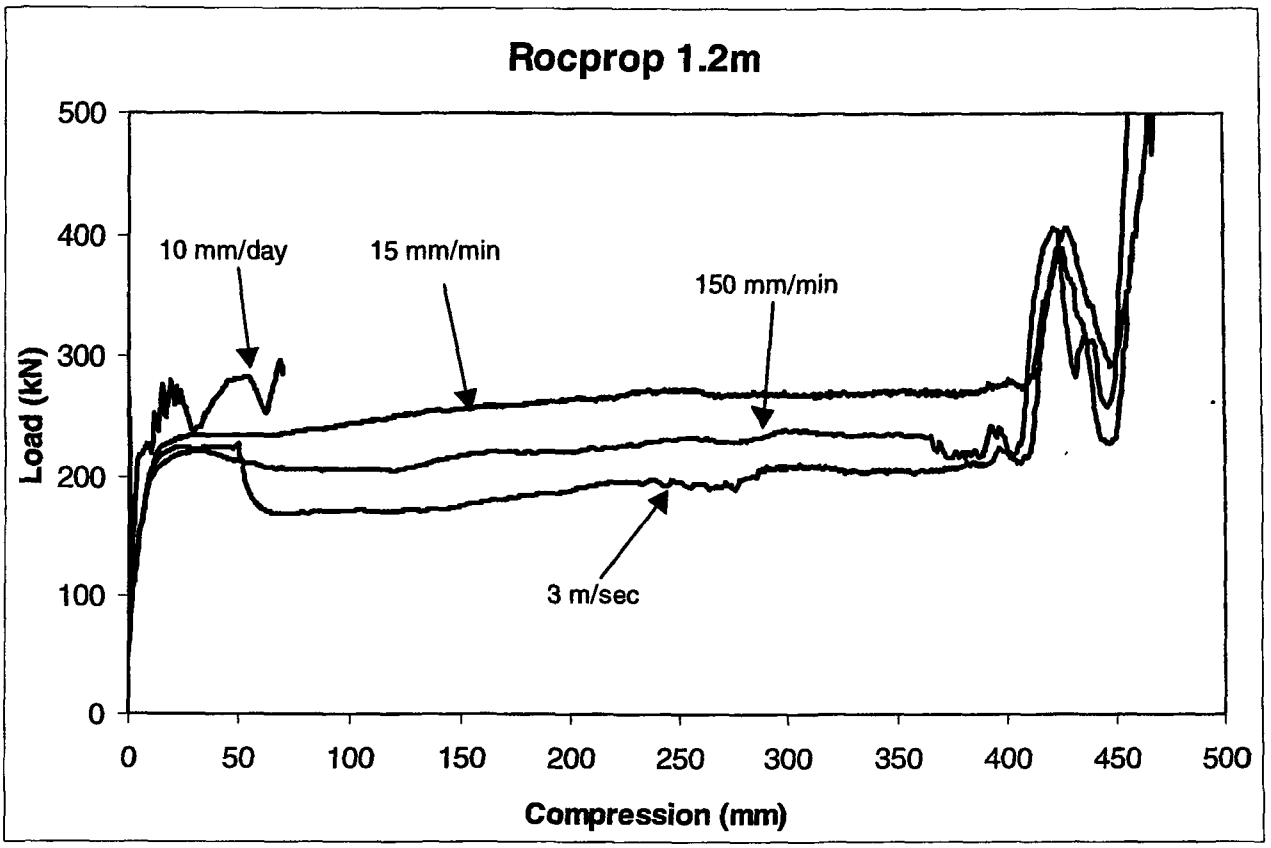
Rocprop 1.2m
500
400
300
200
100
0
Load (kN)
10 mm/day
15 mm/min
150 mm/min
3 m/sec
0
50
100
150
200
250
300
350
400
450
500
Compression (mm)

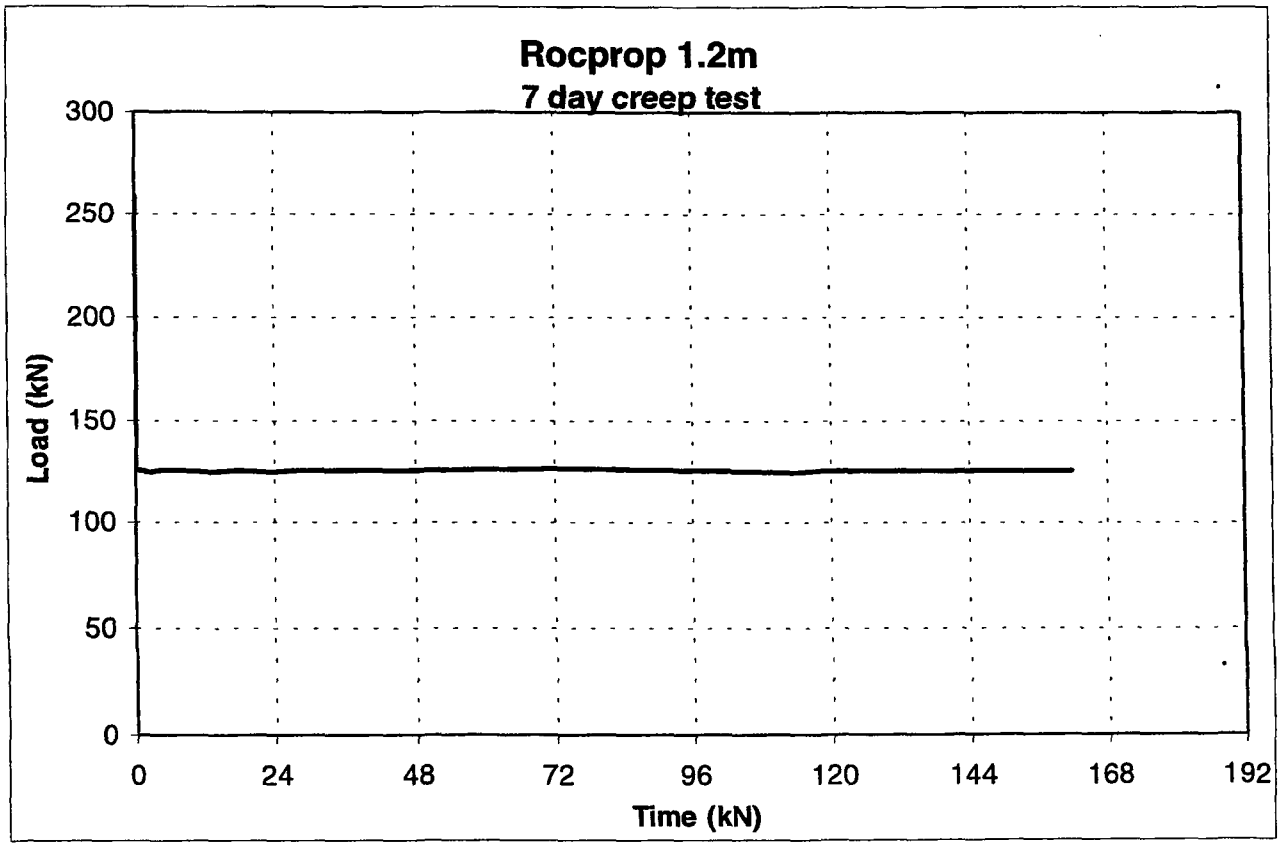
Rocprop 1.2m
7 day creep test
300
250
200
150
100
50
0
Load (kN)
0
24
48
72
96
120
144
168
192
Time (kN)

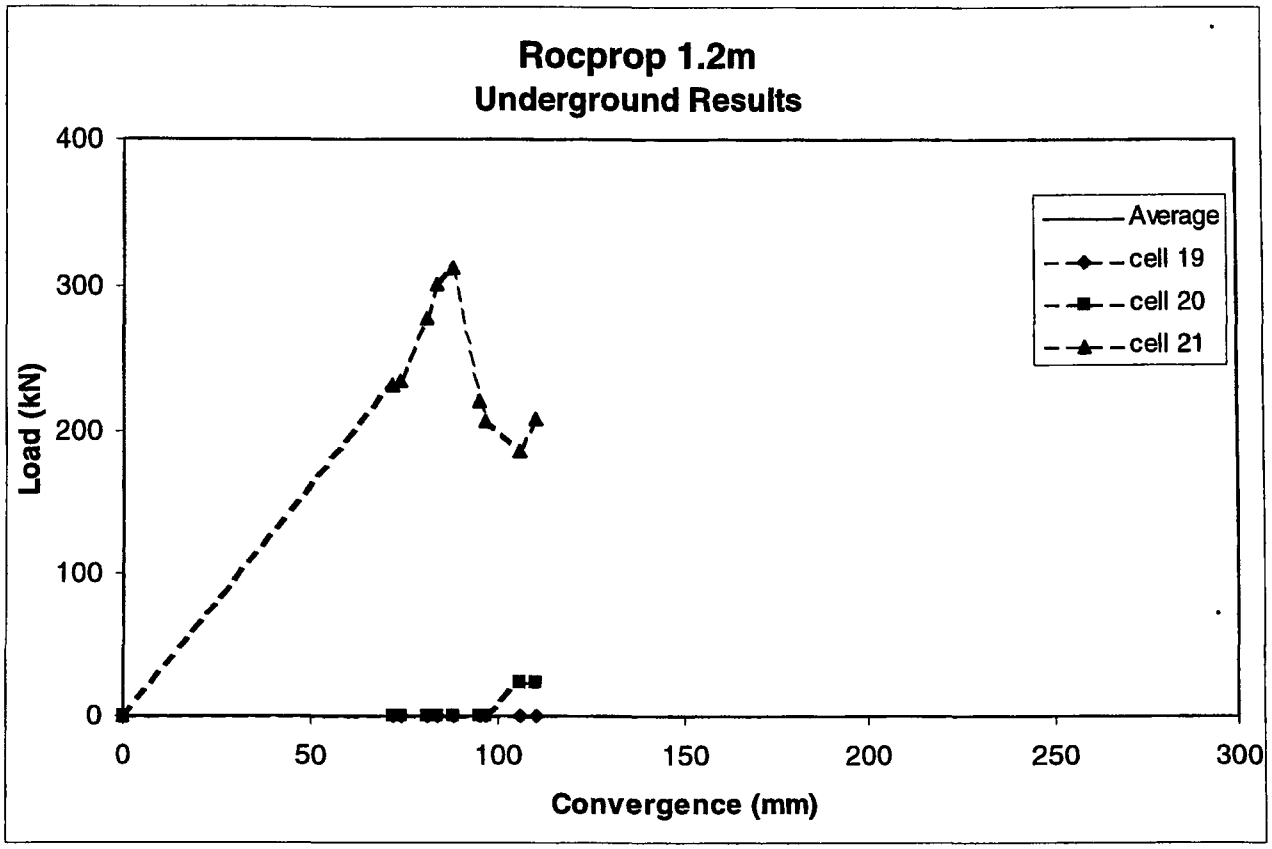
Rocprop 1.2m
Underground Results
Load (kN)
400
300
200
100
0
0
50
100
150
200
250
300
Convergence (mm)
Average
cell 19
cell 20
cell 21

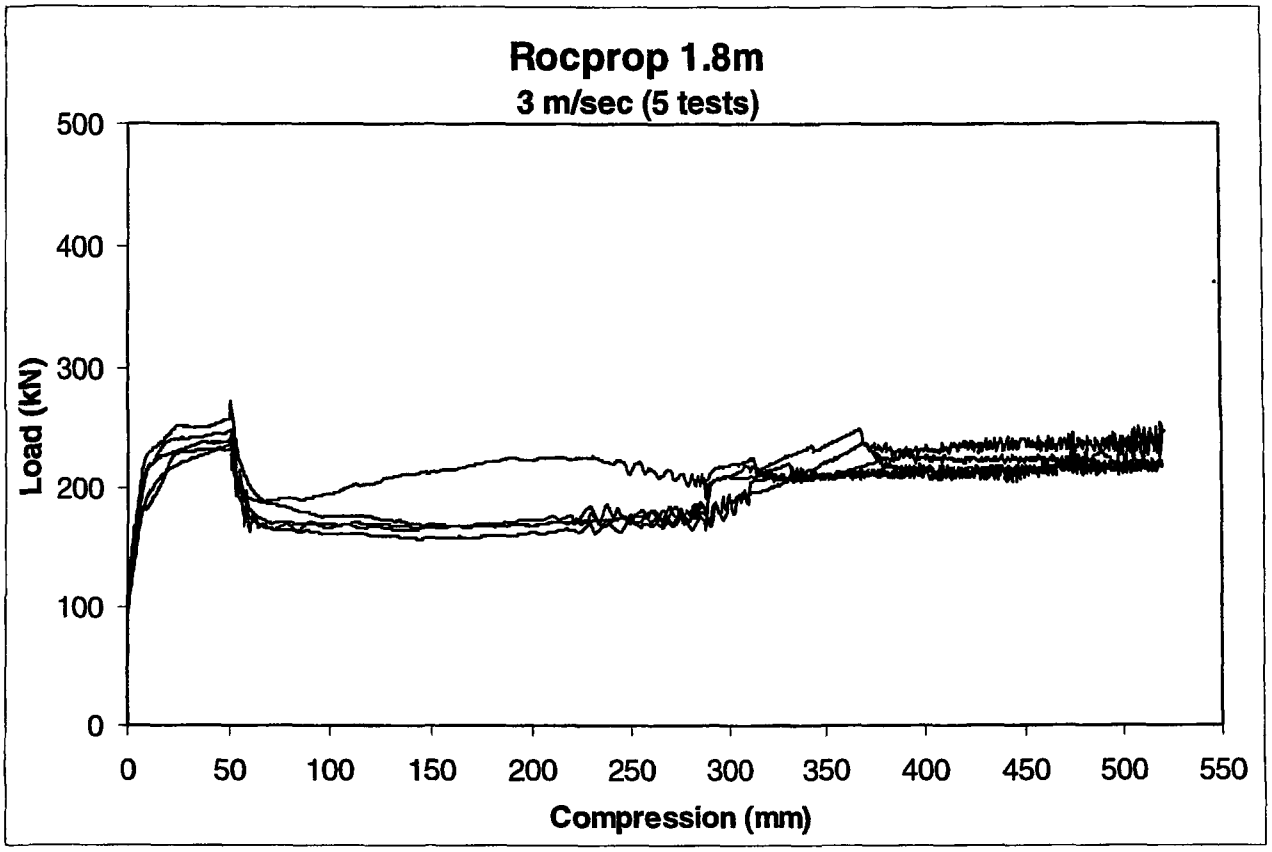
Rocprop 1.8m
3 m/sec (5 tests)
Load (kN)
500
400
300
200
100
0
0
50
100
150
200
250
300
350
400
450
500
550
Compression (mm)

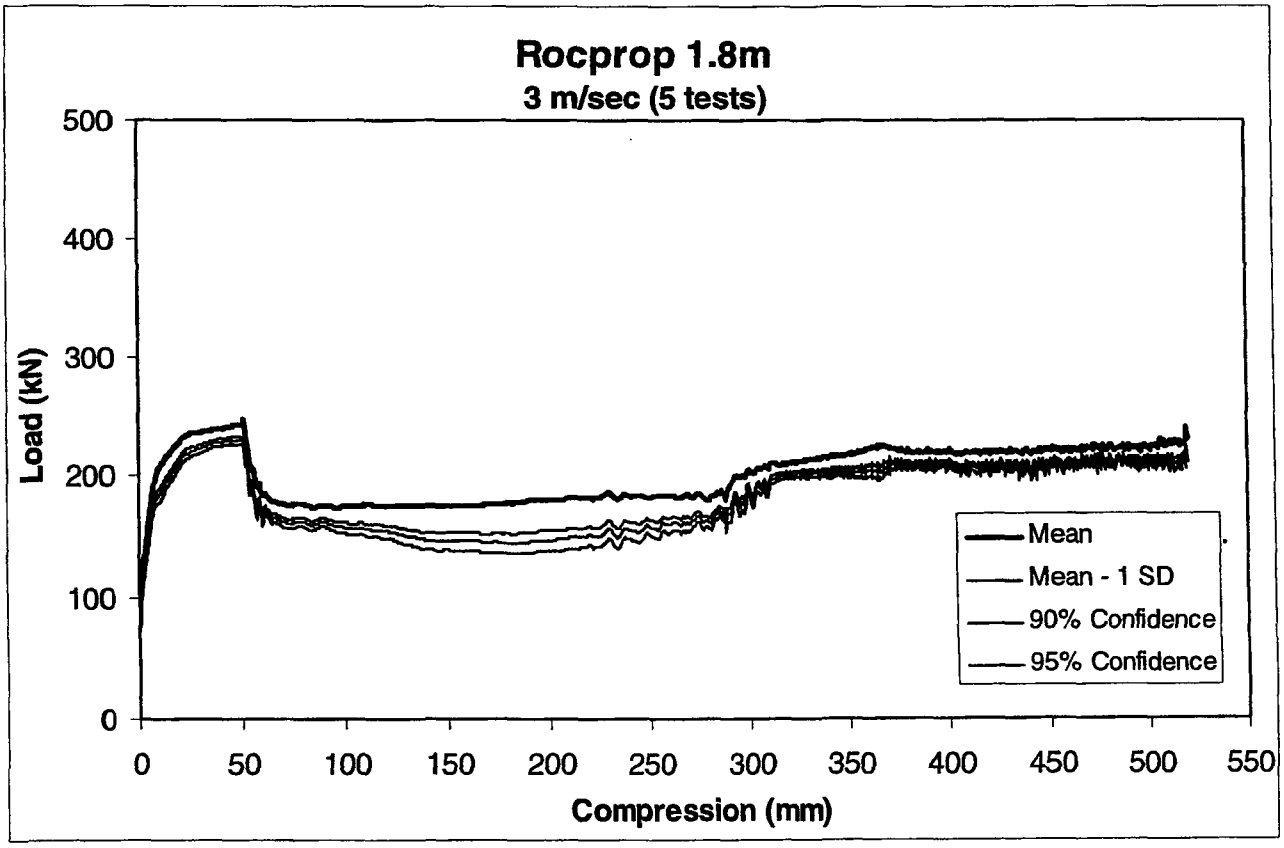
Rocprop 1.8m
3 m/sec (5 tests)
Load (kN)
500
400
300
200
100
0
0
50
100
150
200
250
300
350
400
450
500
550
Compression (mm)
Mean
Mean - 1 SD
90% Confidence
95% Confidence

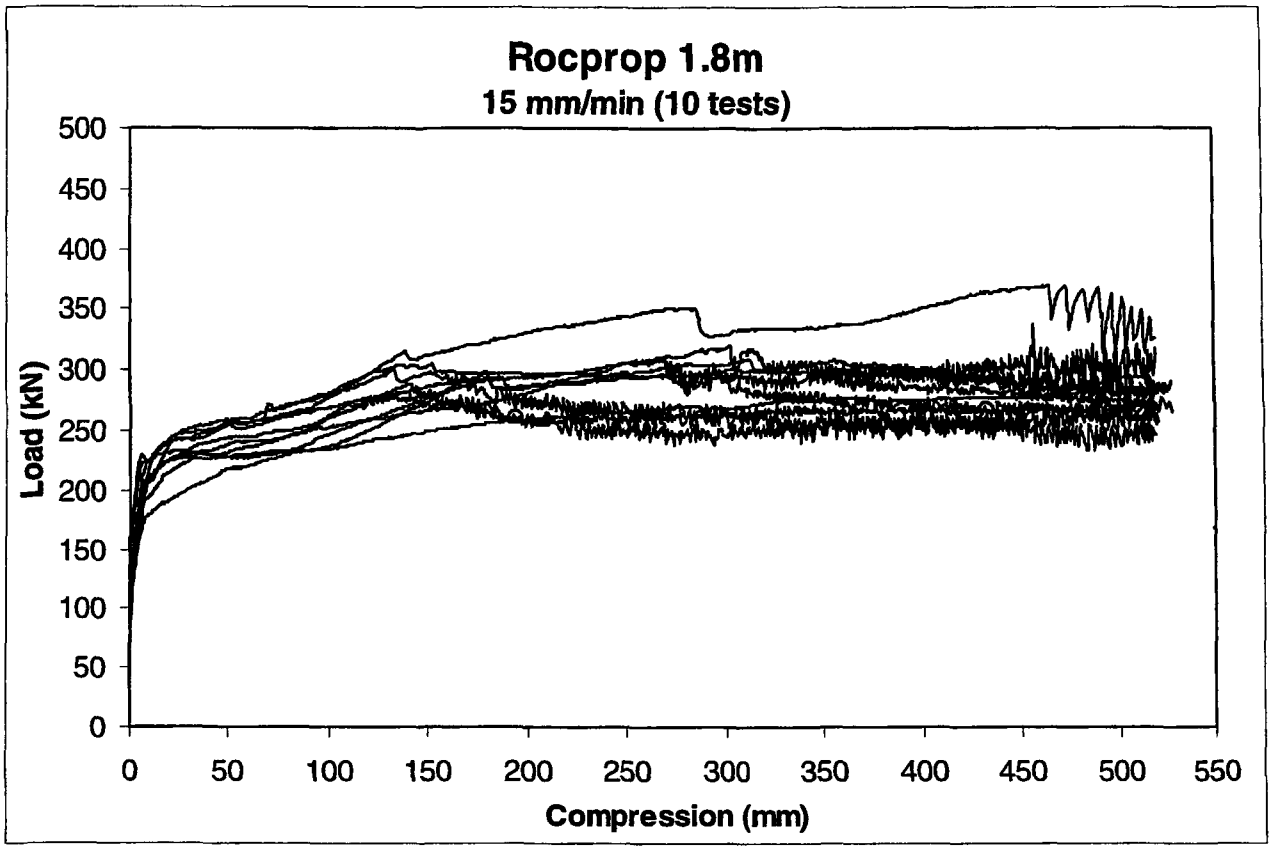
Rocprop 1.8m
15 mm/min (10 tests)
Load (kN)
500
450
400
350
300
250
200
150
100
50
0
0
50
100
150
200
250
300
350
400
450
500
550
Compression (mm)

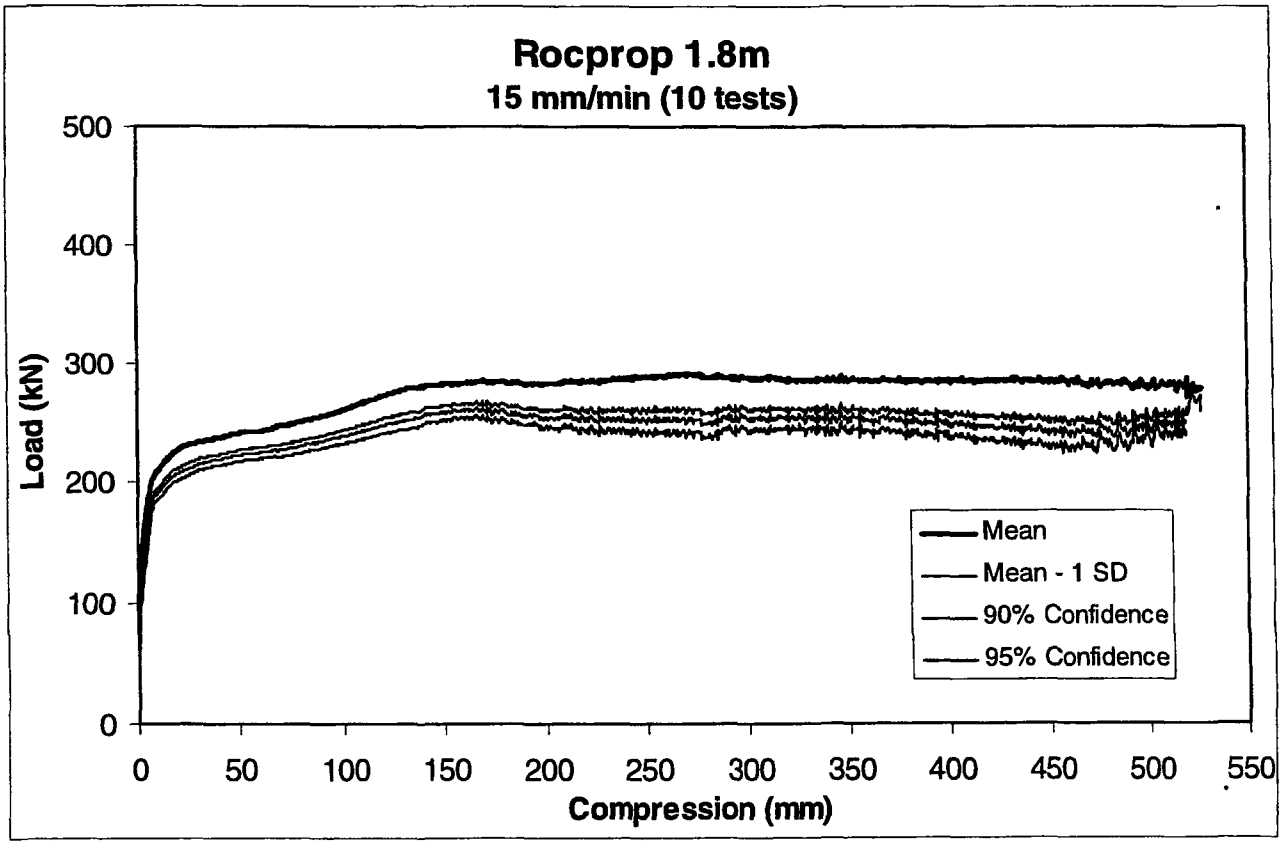
Rocprop 1.8m
15 mm/min (10 tests)
Load (kN)
500
400
300
200
100
0
0
50
100
150
200
250
300
350
400
450
500
550
Compression (mm)
Mean
Mean - 1 SD
90% Confidence
95% Confidence

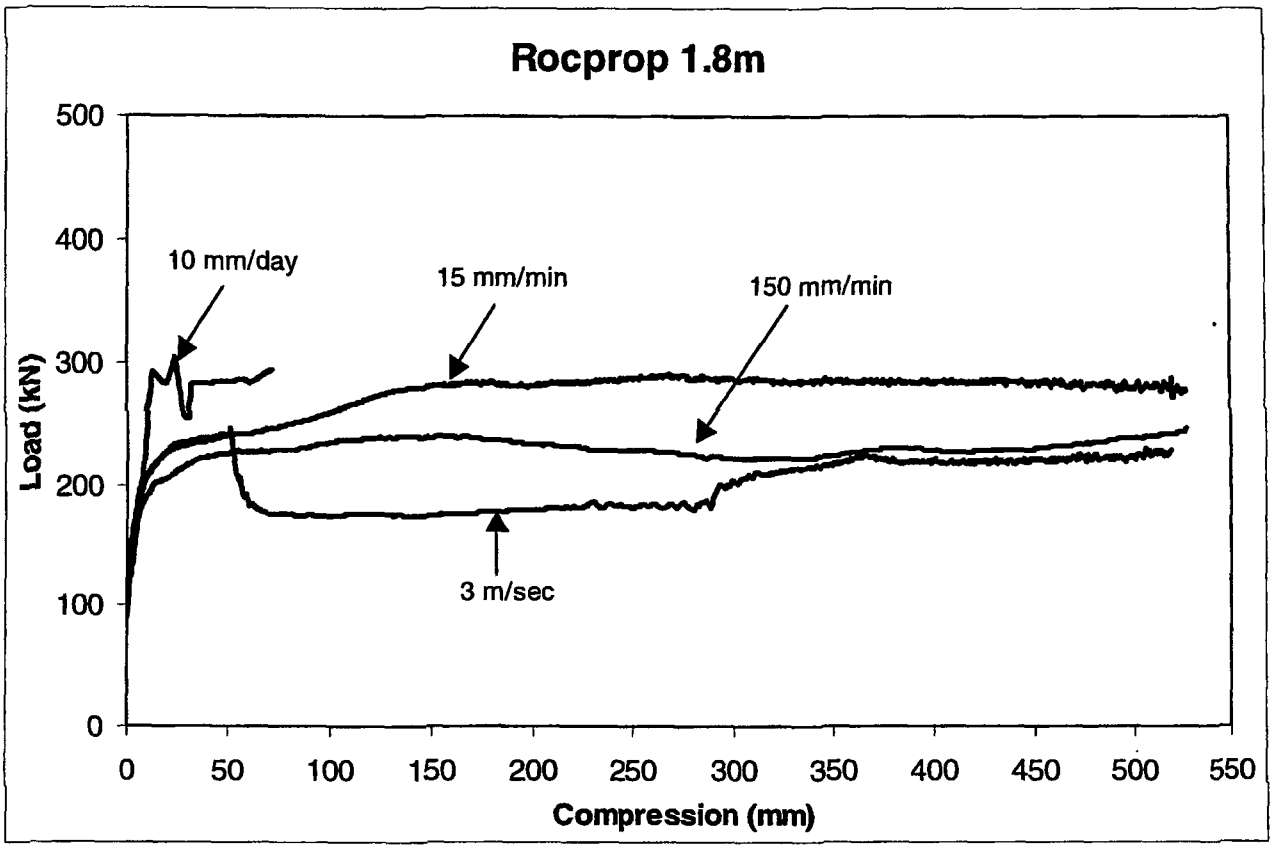
Rocprop 1.8m
500
400
300
200
100
0
Load (kN)
10 mm/day
15 mm/min
150 mm/min
3 m/sec
0
50
100
150
200
250
300
350
400
450
500
550
Compression (mm)

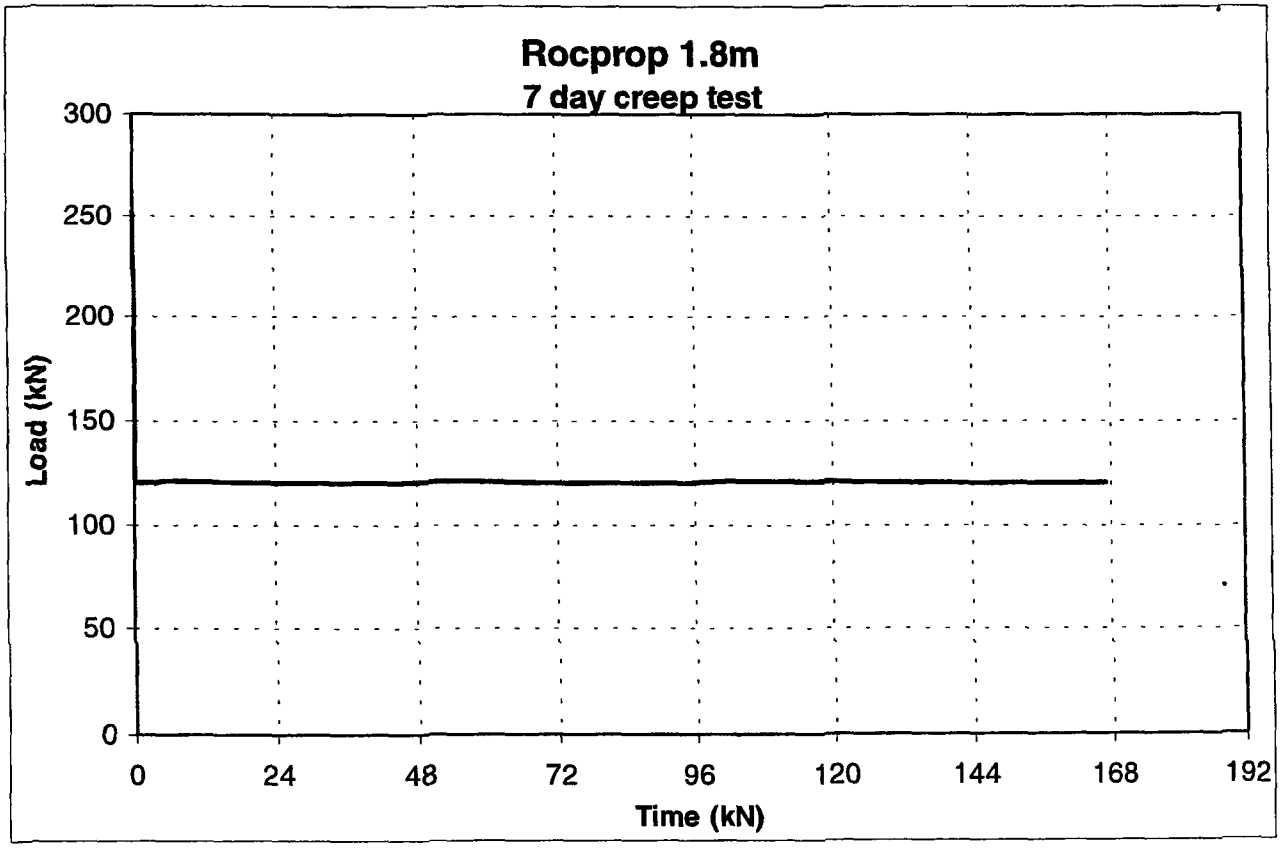
Rocprop 1.8m
7 day creep test
300
250
200
150
100
50
0
Load (kN)
0
24
48
72
96
120
144
168
192
Time (kN)

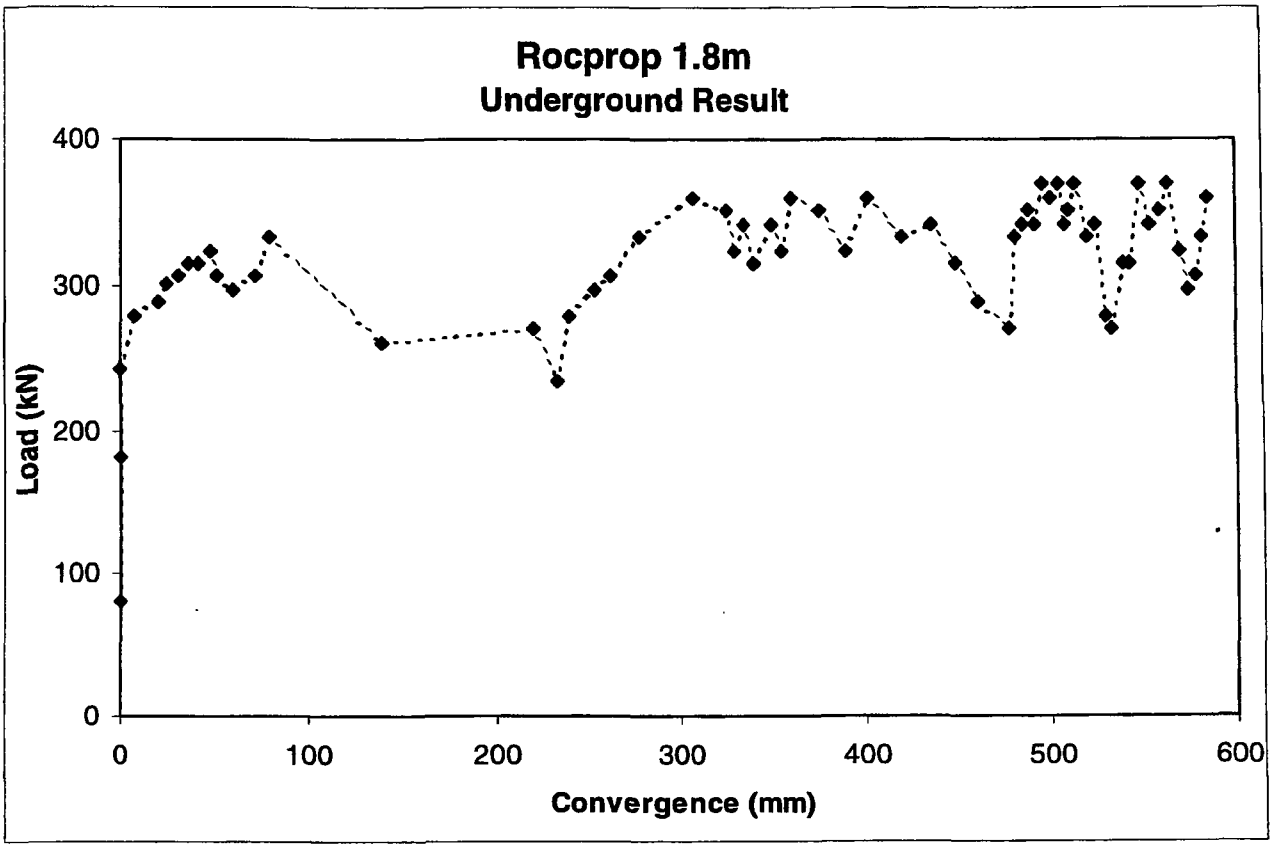
Rocprop 1.8m
Underground Result
Load (kN)
400
300
200
100
0
0
100
200
300
400
500
600
Convergence (mm)

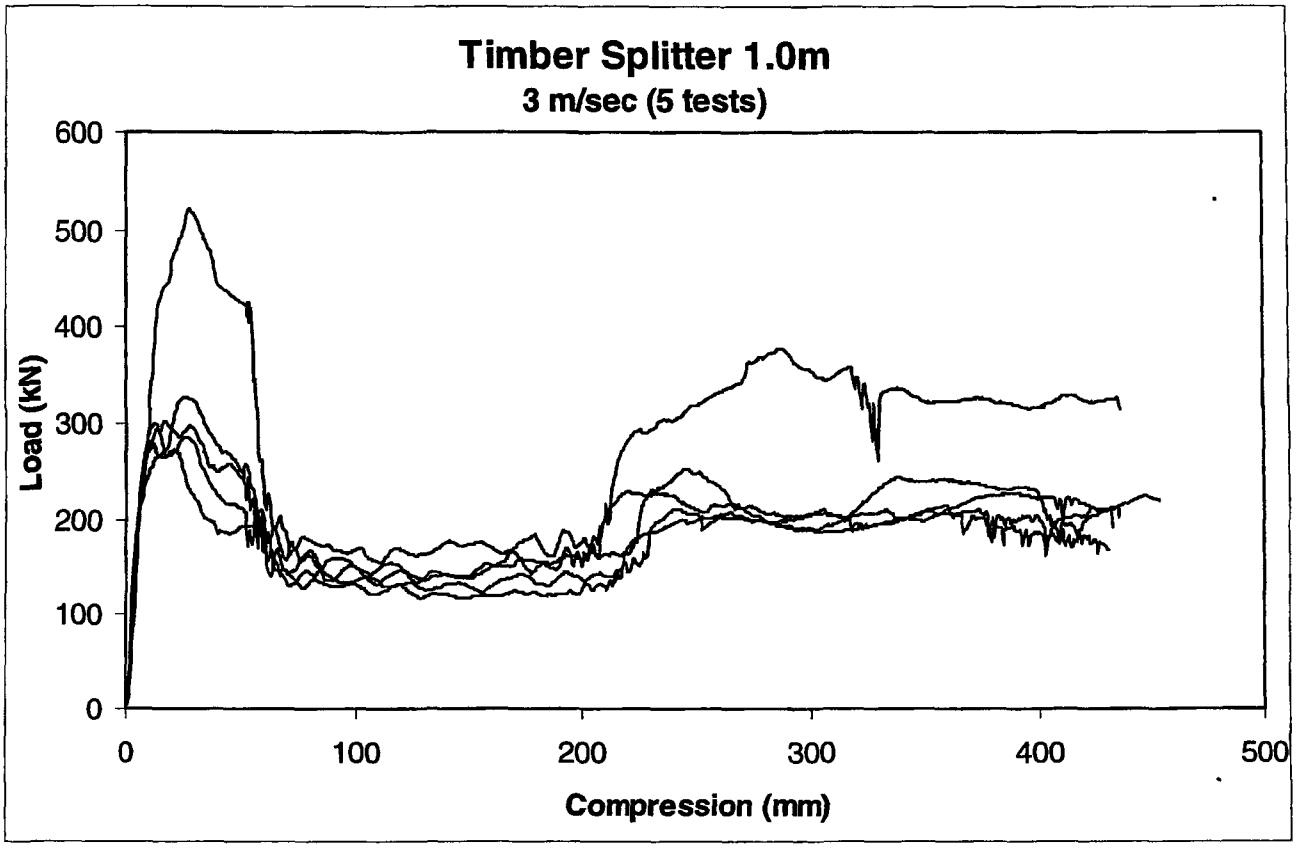
Timber Splitter 1.0m
3 m/sec (5 tests)
Load (kN)
600
500
400
300
200
100
0
0
100
200
300
400
500
Compression (mm)

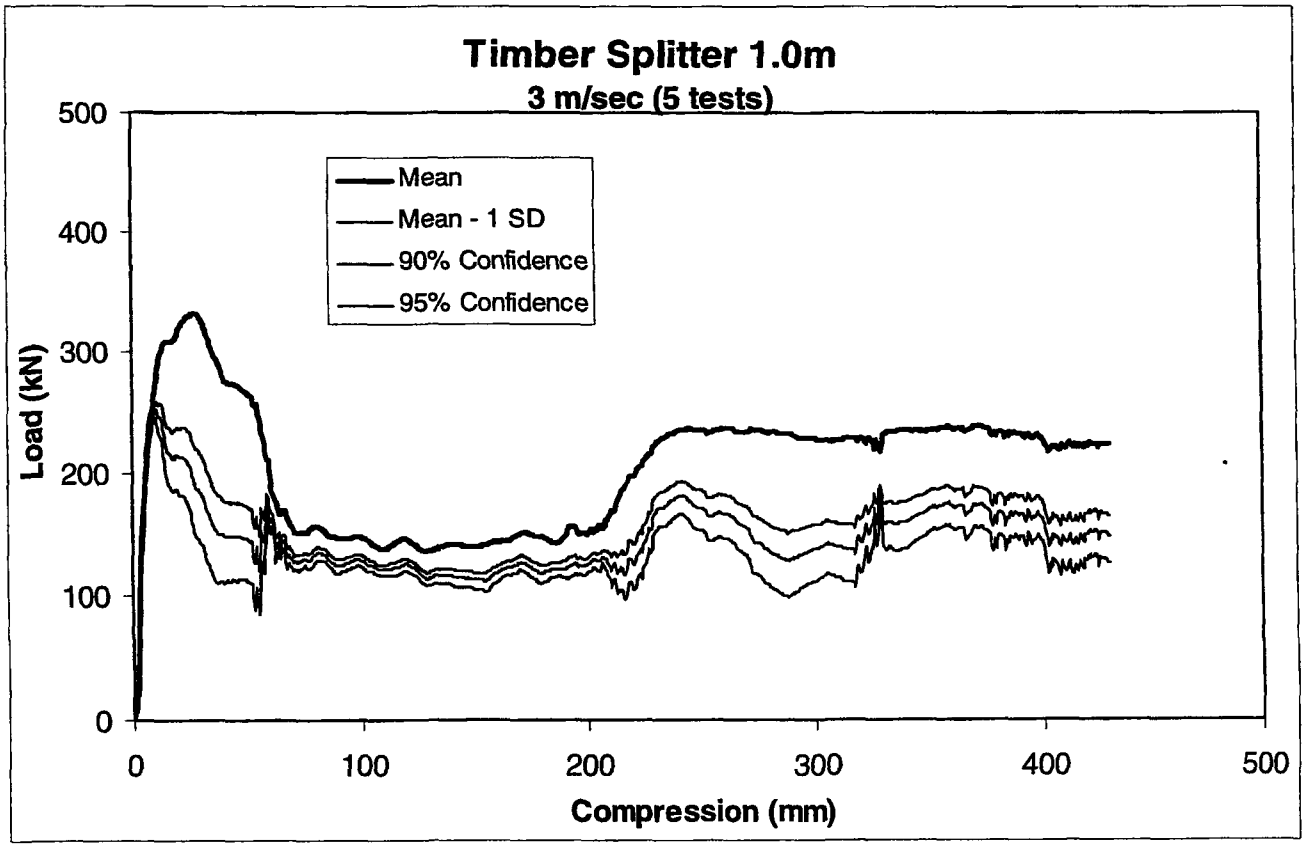
Timber Splitter 1.0m
3 m/sec (5 tests)
Mean
Mean - 1 SD
90% Confidence
95% Confidence
Load (kN)
500
400
300
200
100
0
0
100
200
300
400
500
Compression (mm)

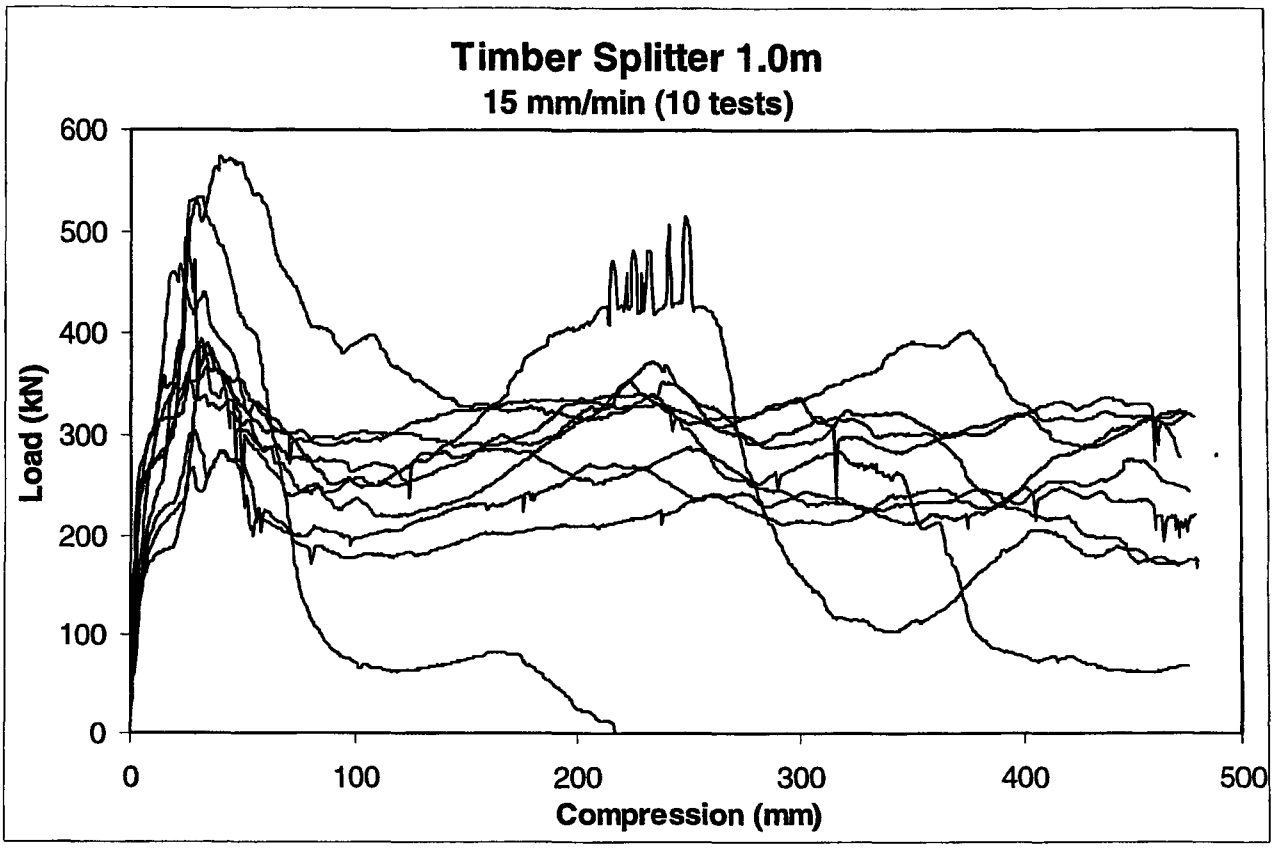
Timber Splitter 1.0m
15 mm/min (10 tests)
Load (kN)
600
500
400
300
200
100
0
0
100
200
300
400
500
Compression (mm)

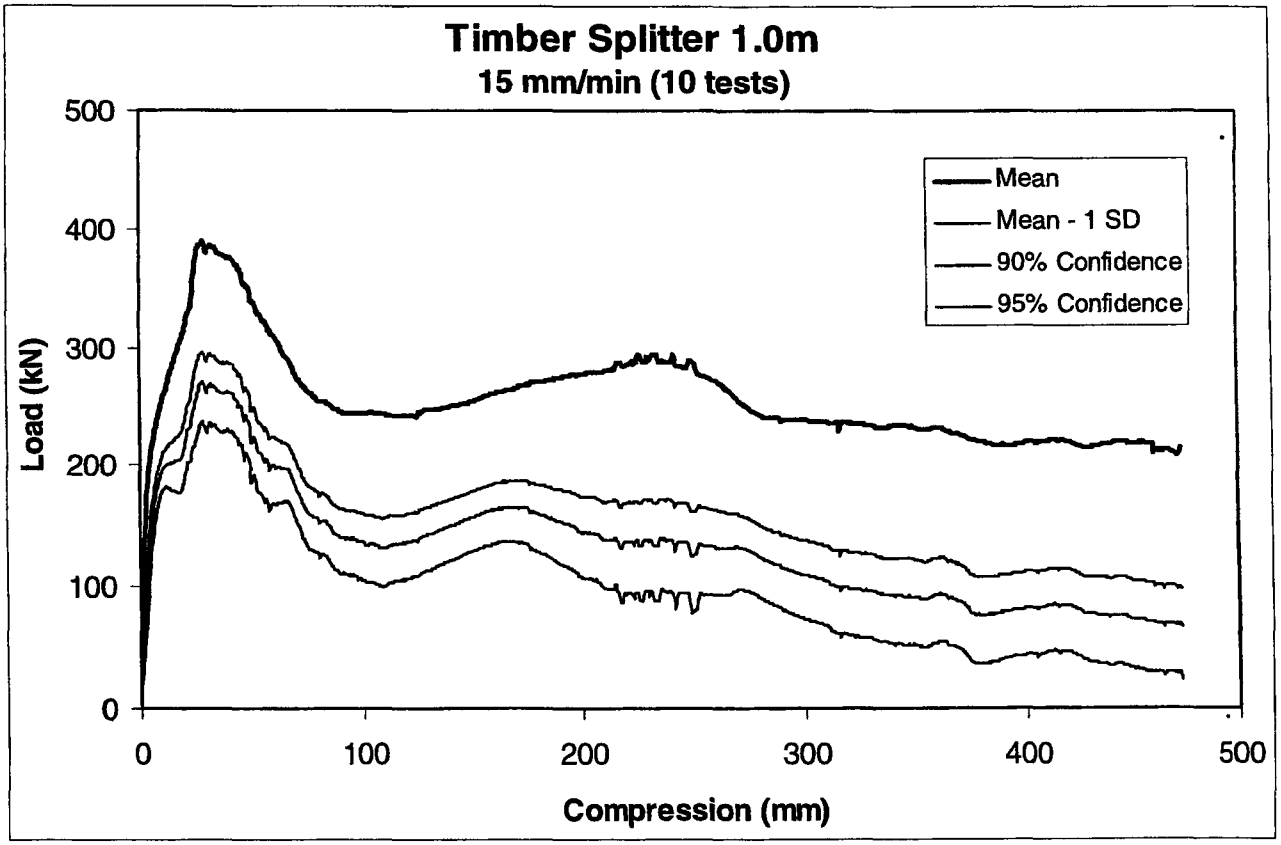
Timber Splitter 1.0m
15 mm/min (10 tests)
Load (kN)
500
400
300
200
100
0
0
100
200
300
400
500
Compression (mm)
Mean
Mean - 1 SD
90% Confidence
95% Confidence

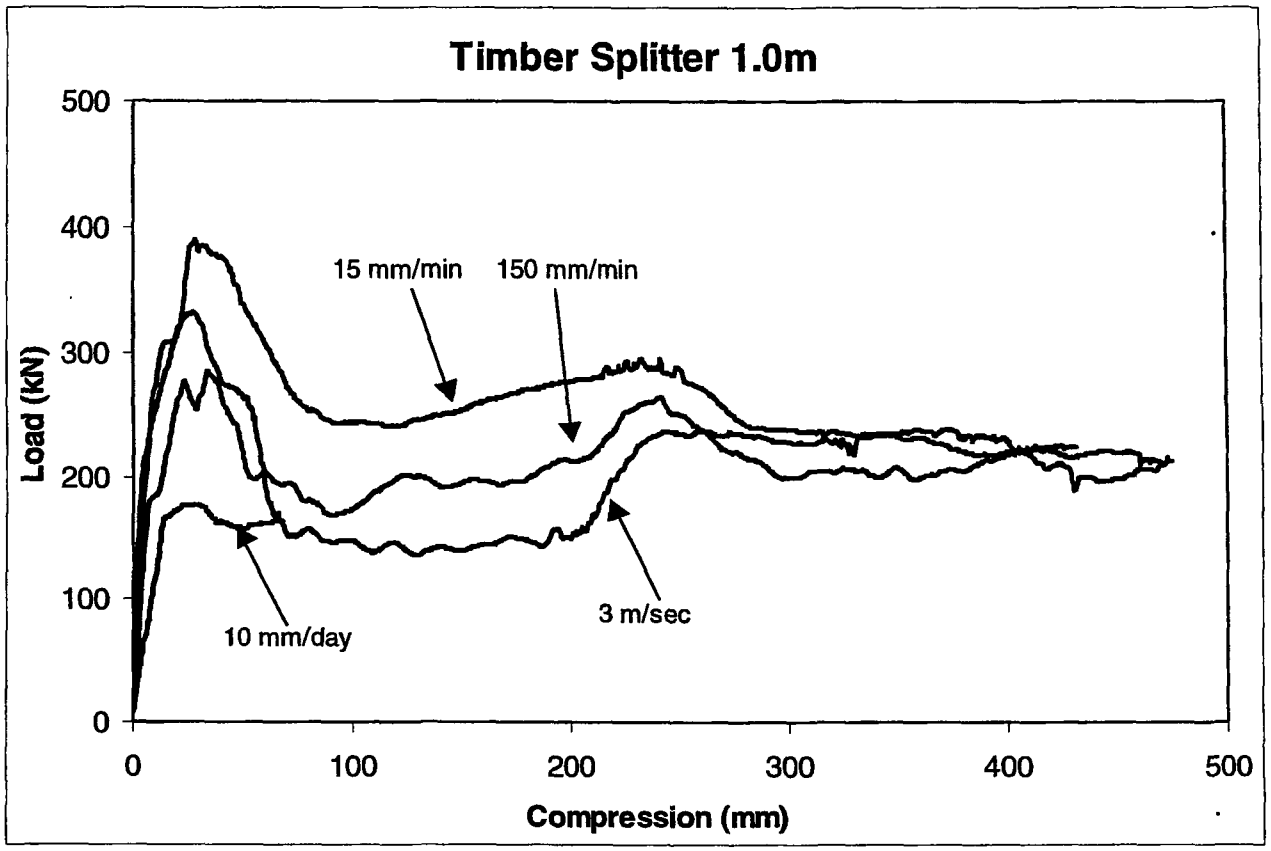
Timber Splitter 1.0m
Load (kN)
Compression (mm)
0
100
200
300
400
500
15 mm/min
150 mm/min
10 mm/day
3 m/sec

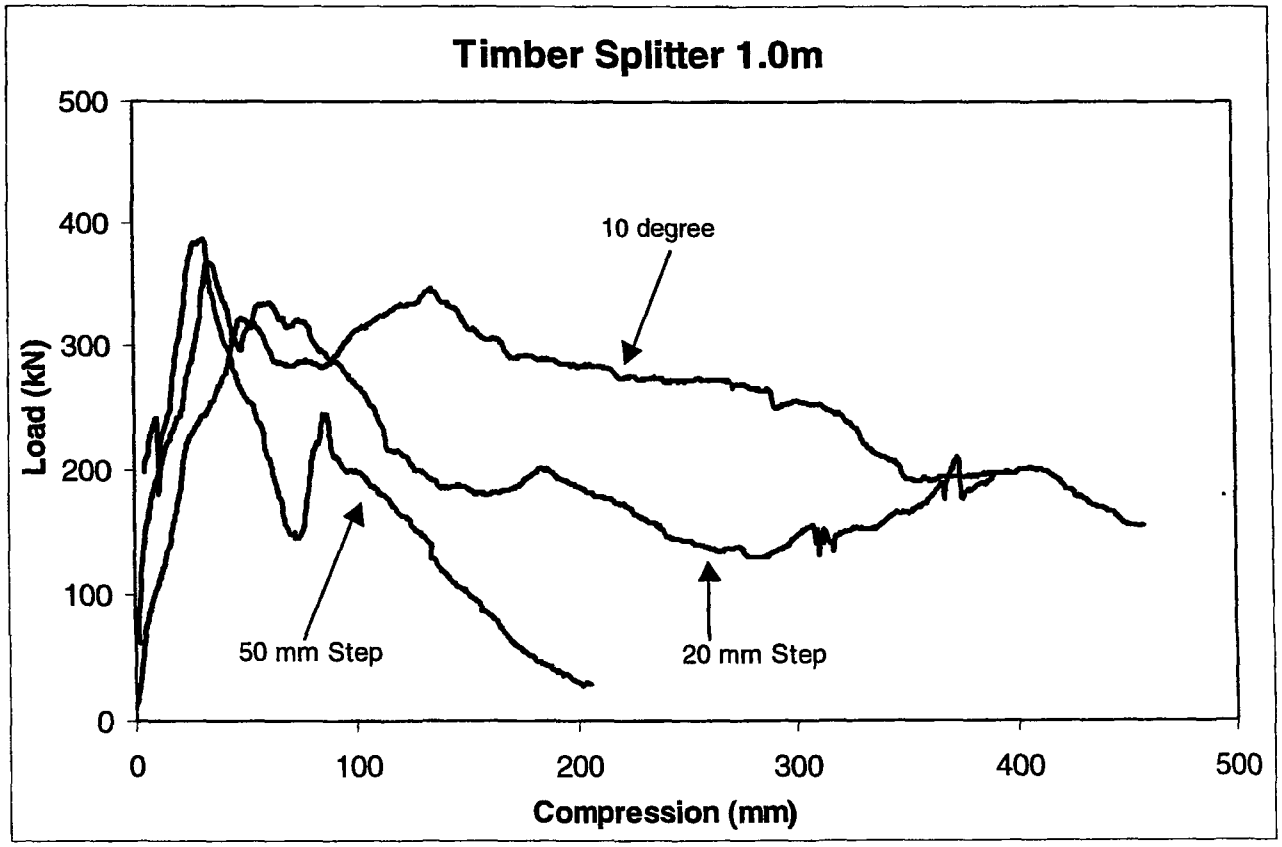
Timber Splitter 1.0m
Load (kN)
Compression (mm)
0
100
200
300
400
500
10 degree
50 mm Step
20 mm Step

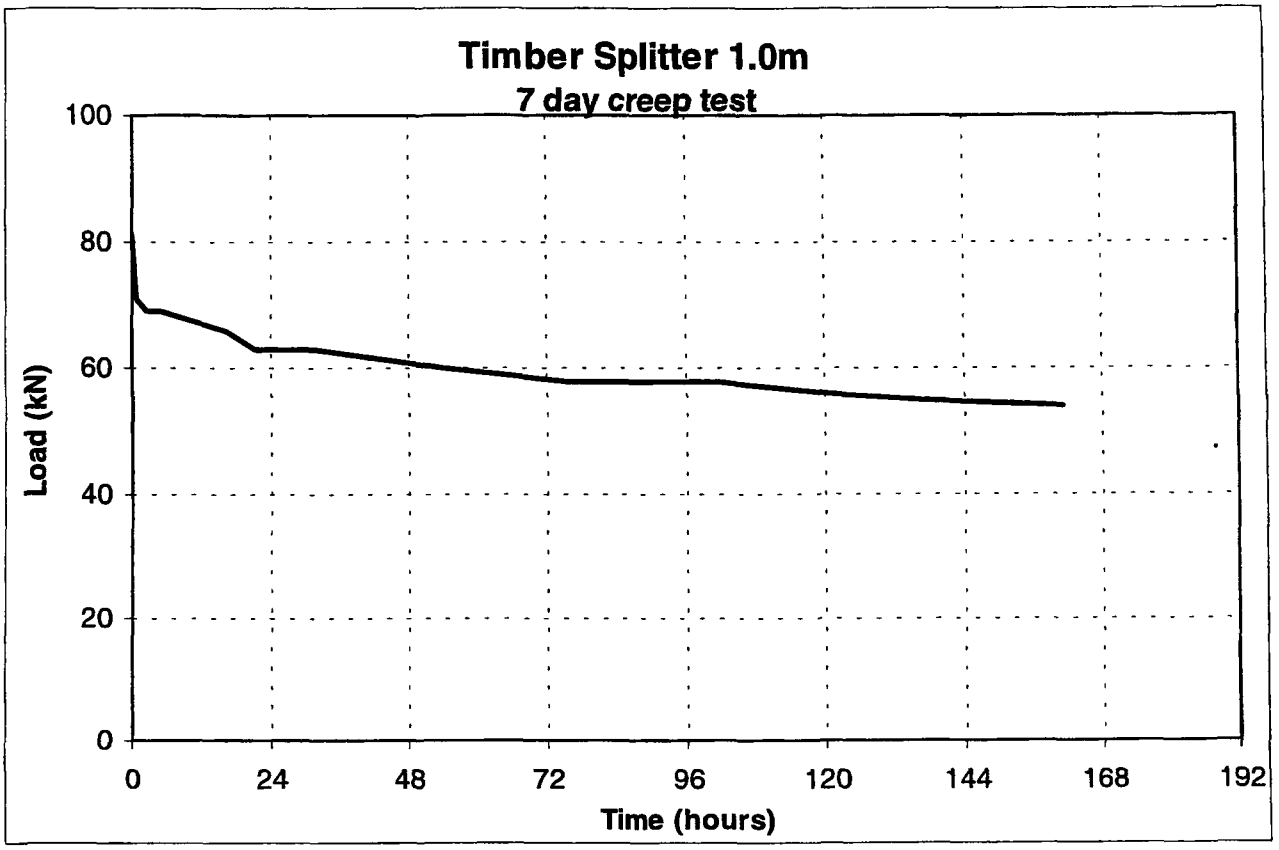
Timber Splitter 1.0m
7 day creep test
Load (kN)
100
80
60
40
20
0
0
24
48
72
96
120
144
168
192
Time (hours)

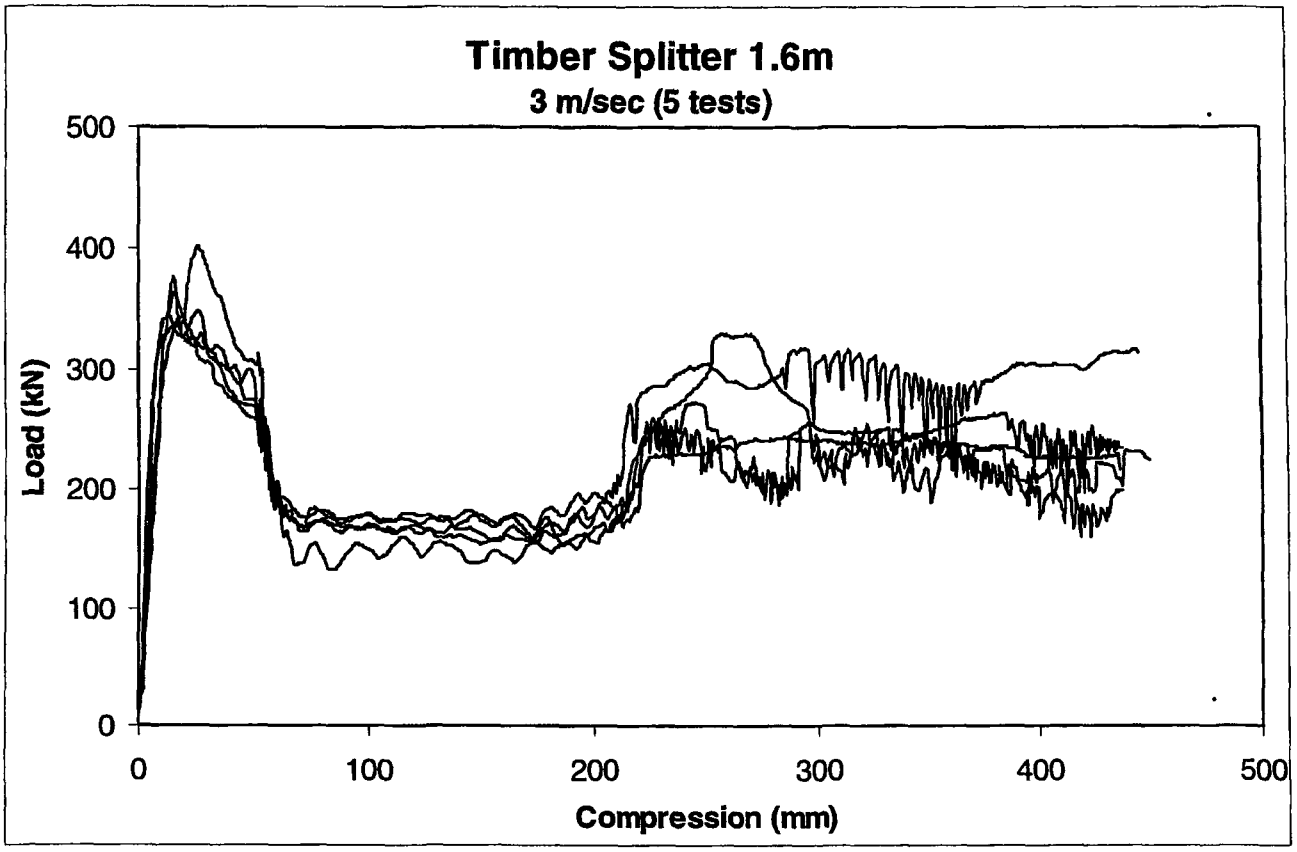
Timber Splitter 1.6m
3 m/sec (5 tests)
Load (kN)
500
400
300
200
100
0
0
100
200
300
400
500
Compression (mm)

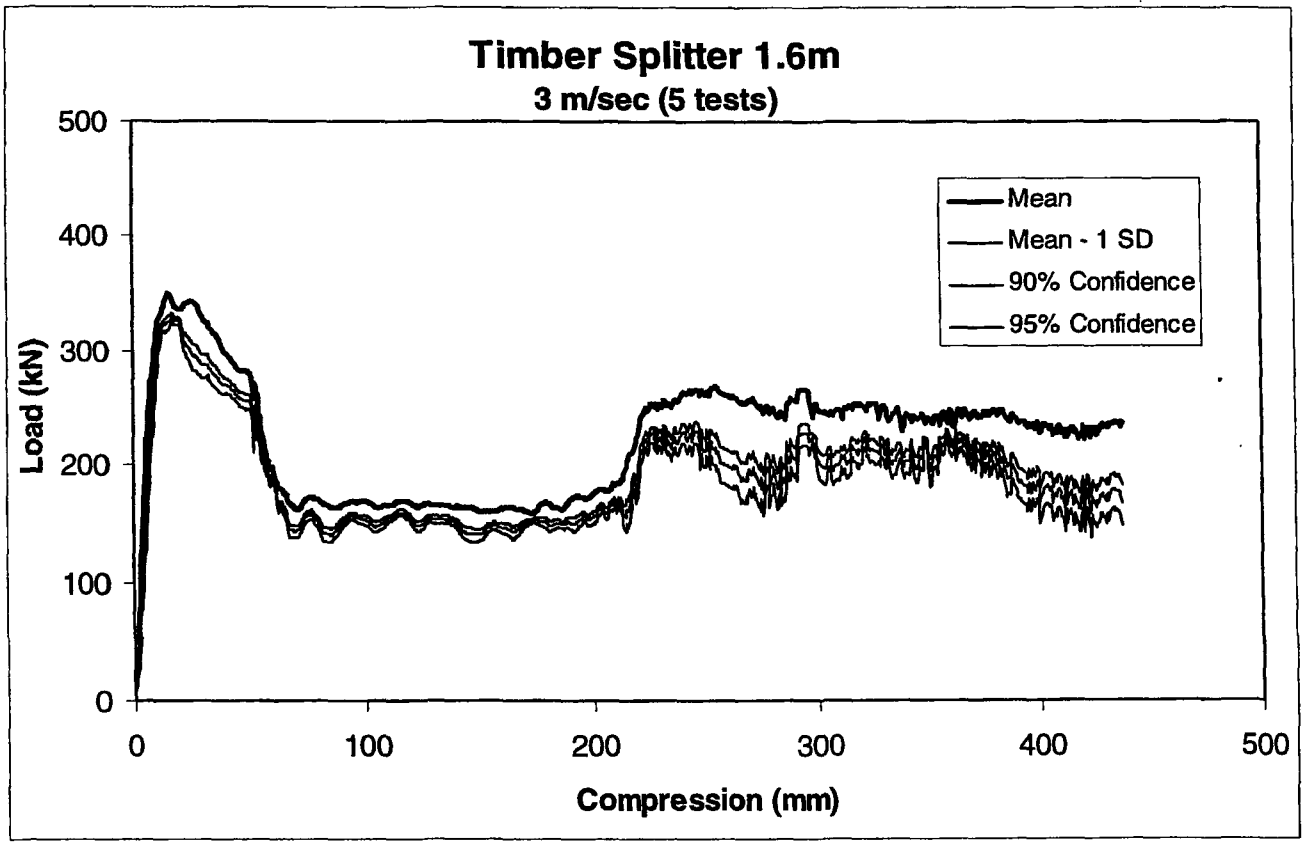
Timber Splitter 1.6m
3 m/sec (5 tests)
Load (kN)
500
400
300
200
100
0
0
100
200
300
400
500
Compression (mm)
Mean
Mean - 1 SD
90% Confidence
95% Confidence

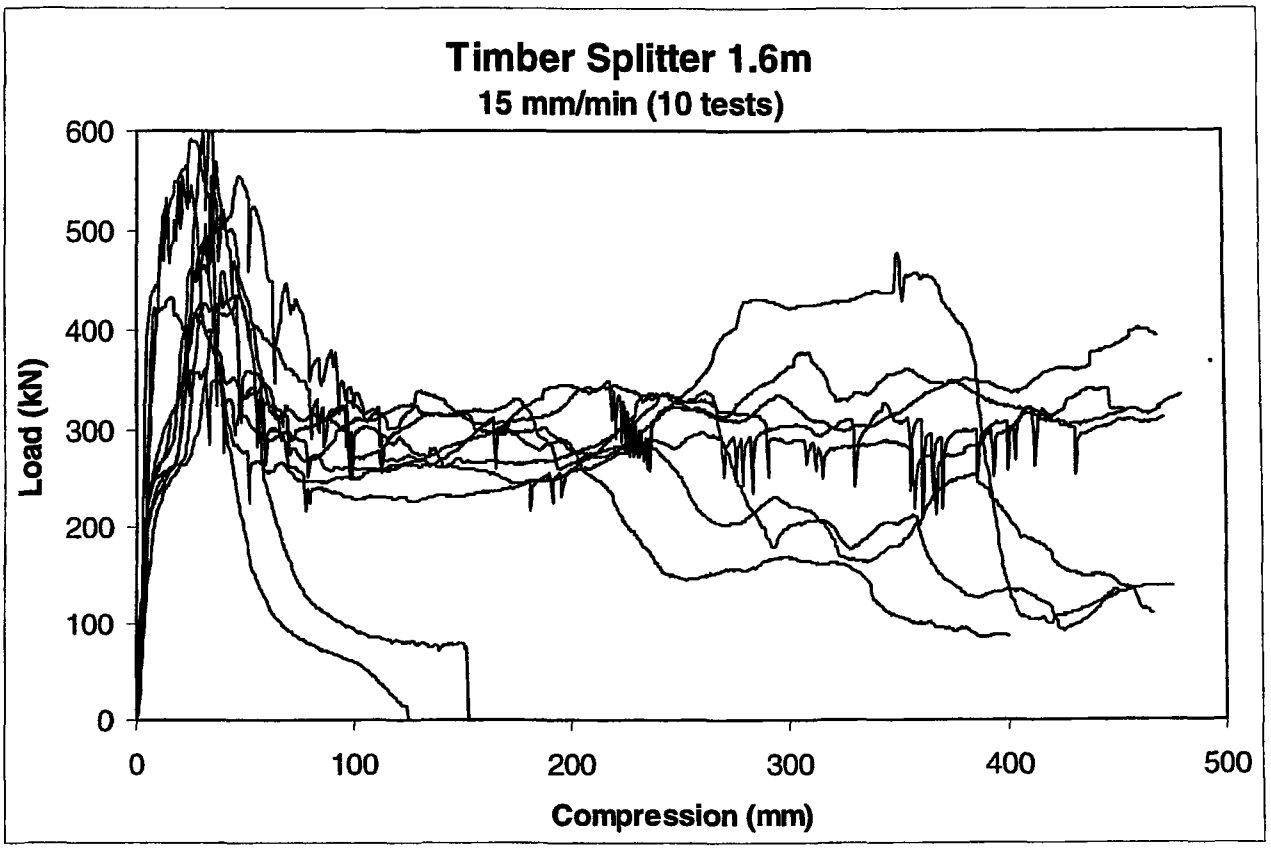
Timber Splitter 1.6m
15 mm/min (10 tests)
Load (kN)
600
500
400
300
200
100
0
0
100
200
300
400
500
Compression (mm)

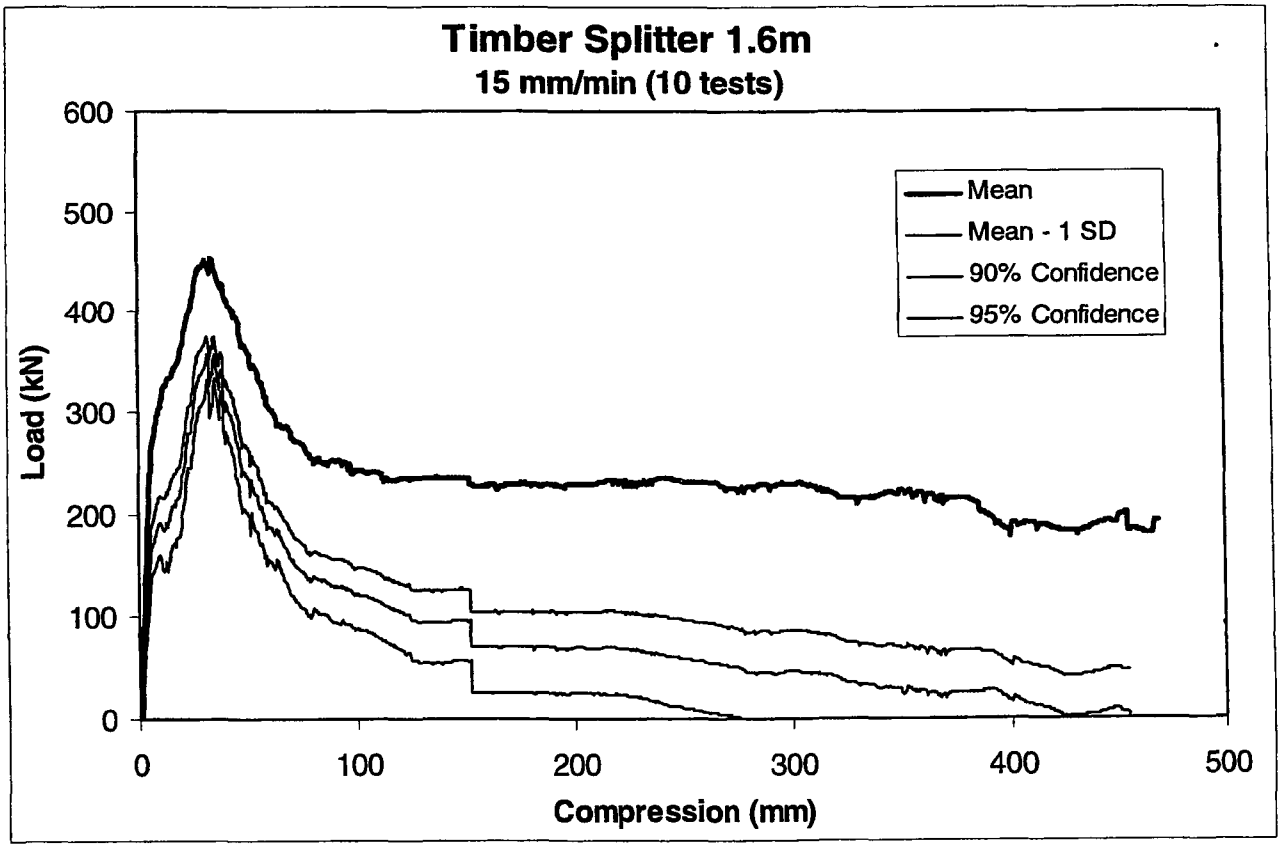
Timber Splitter 1.6m
15 mm/min (10 tests)
Load (kN)
600
500
400
300
200
100
0
0
100
200
300
400
500
Compression (mm)
Mean
Mean - 1 SD
90% Confidence
95% Confidence

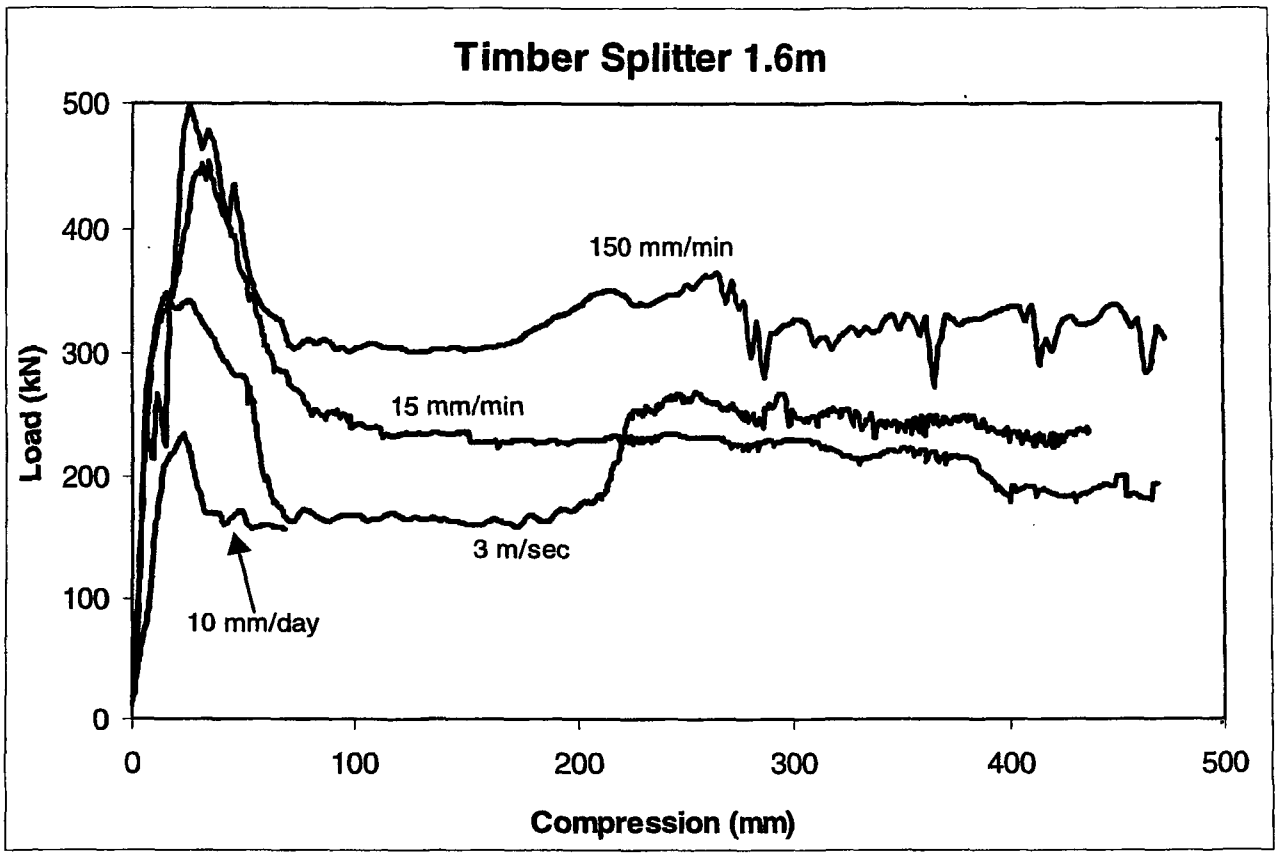
Timber Splitter 1.6m
Load (kN)
Compression (mm)
150 mm/min
15 mm/min
3 m/sec
10 mm/day
0
100
200
300
400
500

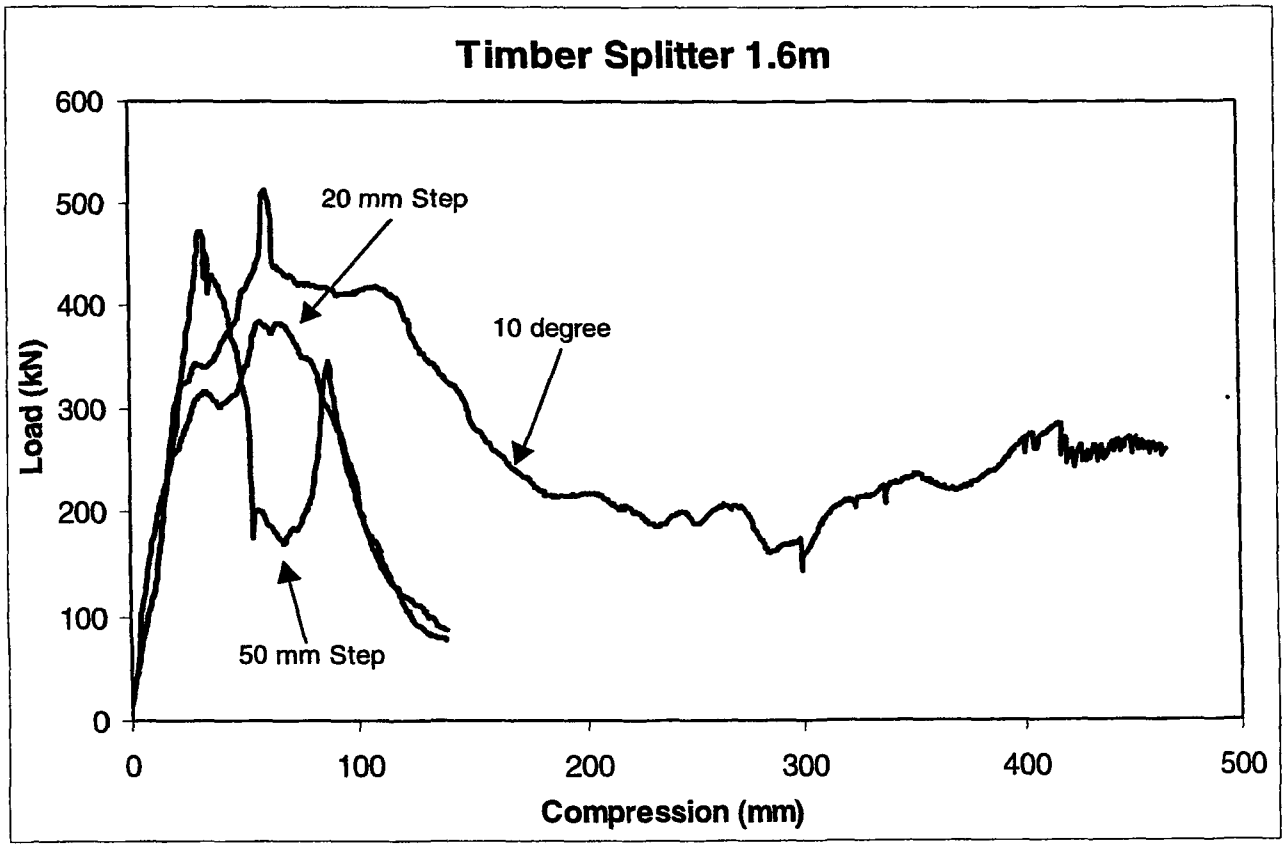
Timber Splitter 1.6m
Load (kN)
Compression (mm)
20 mm Step
10 degree
50 mm Step
0
100
200
300
400
500
600

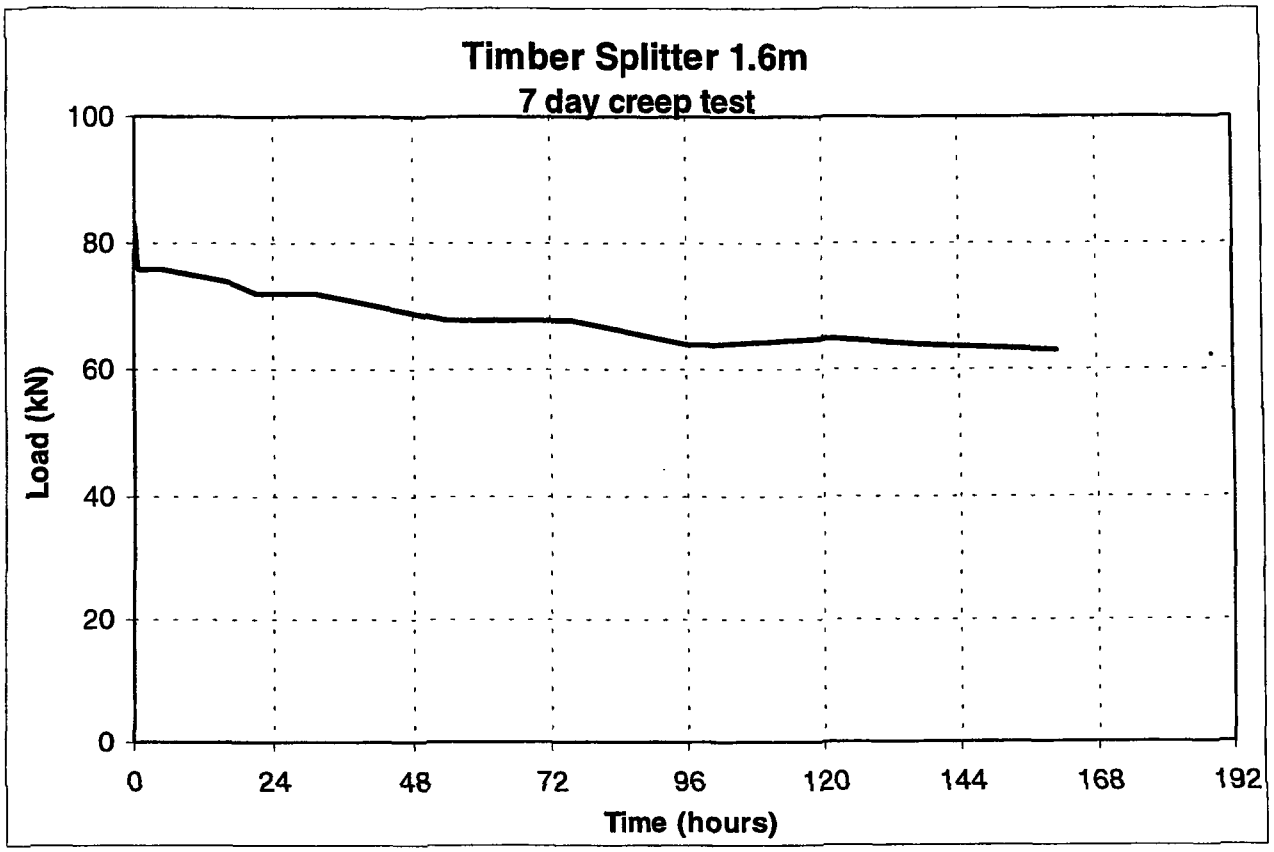
Timber Splitter 1.6m
7 day creep test
Load (kN)
100
80
60
40
20
0
0
24
48
72
96
120
144
168
192
Time (hours)